ADVANCES IN OSTEOIMMUNOLOGY

EDITED BY: Claudine Blin-Wakkach and Teun J. de Vries
PUBLISHED IN: Frontiers in Immunology

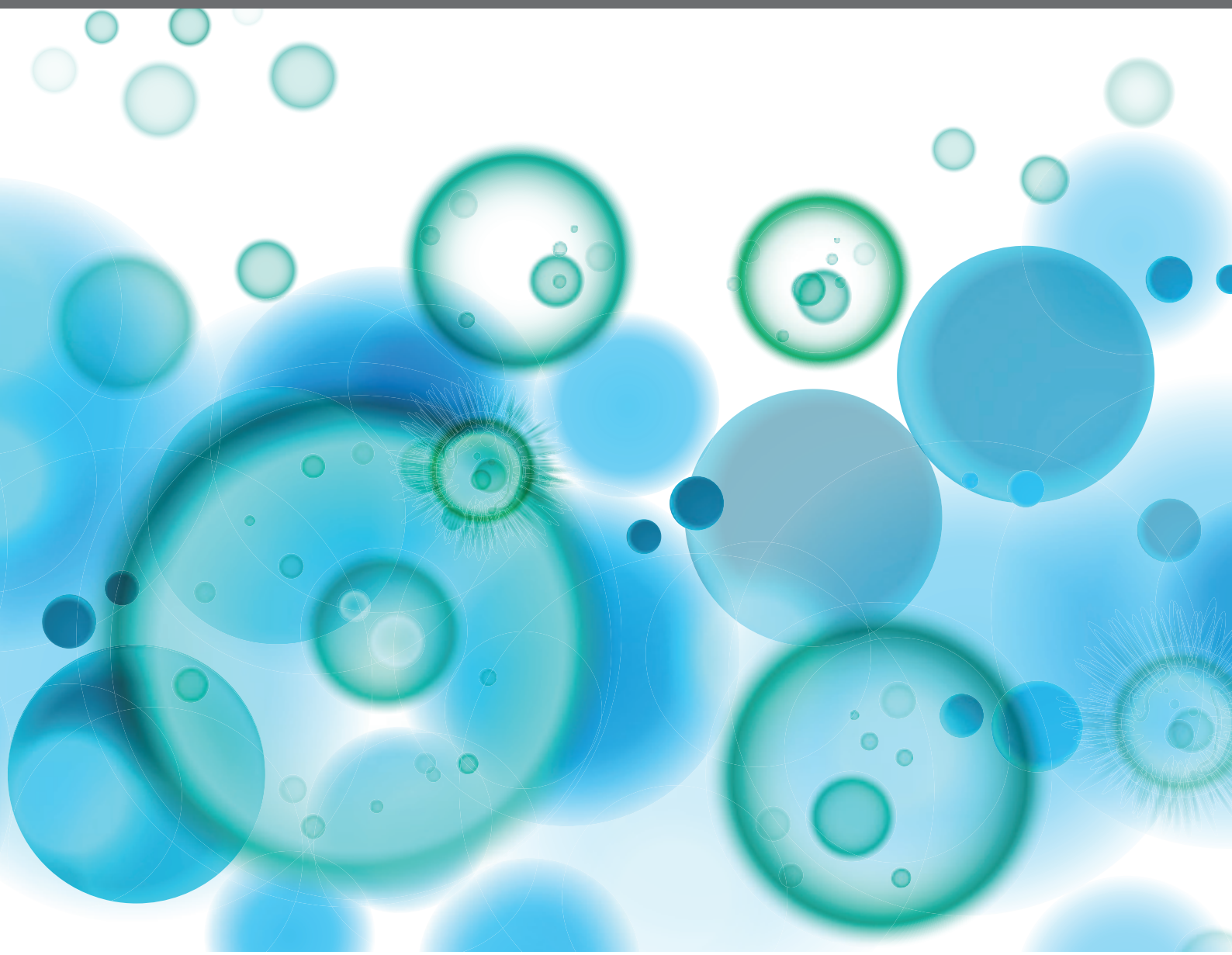

frontiers Research Topics

ISSN 1664-8714
ISBN 978-2-88963-324-1
DOI 10.3389/978-2-88963-324-1

About Frontiers

Frontiers is more than just an open-access publisher of scholarly articles: it is a pioneering approach to the world of academia, radically improving the way scholarly research is managed. The grand vision of Frontiers is a world where all people have an equal opportunity to seek, share and generate knowledge. Frontiers provides immediate and permanent online open access to all its publications, but this alone is not enough to realize our grand goals.

Frontiers Journal Series

The Frontiers Journal Series is a multi-tier and interdisciplinary set of open-access, online journals, promising a paradigm shift from the current review, selection and dissemination processes in academic publishing. All Frontiers journals are driven by researchers for researchers; therefore, they constitute a service to the scholarly community. At the same time, the Frontiers Journal Series operates on a revolutionary invention, the tiered publishing system, initially addressing specific communities of scholars, and gradually climbing up to broader public understanding, thus serving the interests of the lay society, too.

Dedication to Quality

Each Frontiers article is a landmark of the highest quality, thanks to genuinely collaborative interactions between authors and review editors, who include some of the world's best academicians. Research must be certified by peers before entering a stream of knowledge that may eventually reach the public - and shape society; therefore, Frontiers only applies the most rigorous and unbiased reviews.
Frontiers revolutionizes research publishing by freely delivering the most outstanding research, evaluated with no bias from both the academic and social point of view. By applying the most advanced information technologies, Frontiers is catapulting scholarly publishing into a new generation.

What are Frontiers Research Topics?

Frontiers Research Topics are very popular trademarks of the Frontiers Journals Series: they are collections of at least ten articles, all centered on a particular subject. With their unique mix of varied contributions from Original Research to Review Articles, Frontiers Research Topics unify the most influential researchers, the latest key findings and historical advances in a hot research area! Find out more on how to host your own Frontiers Research Topic or contribute to one as an author by contacting the Frontiers Editorial Office: researchtopics@frontiersin.org

ADVANCES IN OSTEOIMMUNOLOGY

Topic Editors:
Claudine Blin-Wakkach, Université Côte d'Azur, CNRS, Laboratoire de Physio Médecine Moléculaire (LP2M), France
Teun J. de Vries, Academic Centre for Dentistry Amsterdam (ACTA), University of Amsterdam and VU University, Netherlands

Citation: Blin-Wakkach, C., de Vries, T. J., eds. (2020). Advances in Osteoimmunology. Lausanne: Frontiers Media SA. doi: 10.3389/978-2-88963-324-1

Table of Contents

frontiers in Immunology

EDITORIAL
published: 13 November 2019
doi: 10.3389/fimmu.2019.02595

Editorial: Advances in Osteoimmunology

Claudine Blin-Wakkach[1,2]* *and Teun J. de Vries*[3]*

[1] Université Côte d'Azur, Nice, France, [2] CNRS UMR7370, Laboratoire de PhysioMédecine Moléculaire, Nice, France, [3] Academic Centre for Dentistry Amsterdam, University of Amsterdam and VU University, Amsterdam, Netherlands

Keywords: osteoimmunology, inflammation, osteoclast, T cell, bone marrow

Editorial on the Research Topic

Advances in Osteoimmunology

The association between chronic inflammation and bone destruction has long been recognized, but the molecular bases of the underlying mechanisms were identified only 20 years ago with the discovery of the essential role of the RANK/RANKL axis in bone and immune cell physiopathology [reviewed in (1)]. From this moment, the term "osteoimmunology" was proposed to define a new discipline covering the interplay between the bone and the immune system (2). Osteoimmunology has become an essential discipline for the study of a huge variety of inflammatory diseases such as rheumatic diseases, aging as manifested in osteoporosis, chronic inflammation such as inflammatory bowel disease, bone infection and bone healing such as is apparent in periodontitis and after surgery, as well as for cancer. Publications related to osteoimmunology are steadily increasing in number and cover fields as varied as immunology, endocrinology and metabolism, cell biology, biochemistry, rheumatology, experimental medicine, pharmacology, dentistry, biomaterials, and hematology (from Web of Science). This Research Topic brings together 24 contributions by 162 authors from all over the world, from North- (10) and South-America (21), Europe (113), Asia (3), and Australia (15). When summarizing all contributions, the topic has deepened our understanding on four topics in particular.

COMPONENTS OF THE IMMUNE SYSTEM CONTROLLING OSTEOCLAST OR OSTEOBLAST DIFFERENTIATION AND FUNCTION

The first major question in osteoimmunology has been to understand how the immune system controls the differentiation and activity of bone cells. Initially, an important role was attributed to Th17 cells that produce RANKL, IL-17, and TNF-α all increasing osteoclast formation, as reviewed in this topic in the context of arthritis (Coury et al.), inflammatory bowel disease (Madel et al.) and periodontal diseases (Alvarez et al.). Biphotonic microscopy became an important tool that enables visualization of the dynamic interaction between osteoclasts and T cells, as presented by Hasegawa et al.. The B cell lineage also plays an important role in controlling osteoclastogenesis. As reviewed by Coury et al., autoantibodies against citrullinated proteins (ACPA) mediate bone destruction in rheumatoid arthritis. The underlying mechanisms linking ACPA and osteoclastogenesis in arthritis were further explored in the review of Steffen et al.. The role of the adaptive immune system appears therefore essential in osteoimmunology. This was further emphasized in two papers from the group of Schmidt-Bleek. Bucher et al. demonstrated that, during aging in mice, the acquisition of a more experienced adaptive immune system alters the bone structure and mechanical properties and decreases the bone healing capacity of the mice. The same group (Wendler et al.) reported that

OPEN ACCESS

Edited and reviewed by:
Pietro Ghezzi,
Brighton and Sussex Medical School, United Kingdom

***Correspondence:**
Claudine Blin-Wakkach
blin@unice.fr
Teun J. de Vries
teun.devries@acta.nl

Specialty section:
This article was submitted to Inflammation, a section of the journal Frontiers in Immunology

Received: *16 October 2019*
Accepted: *21 October 2019*
Published: *13 November 2019*

Citation:
Blin-Wakkach C and de Vries TJ (2019) Editorial: Advances in Osteoimmunology. Front. Immunol. 10:2595. doi: 10.3389/fimmu.2019.02595

the immune suppressive drug Iloprost stimulates the osteogenic capacity of mesenchymal cells and bone healing by reducing the production of proinflammatory cytokines by $CD8^+$ T cells and modulating the M1/M2 balance in macrophages.

Nowadays, the effect of the immune system on bone cells appears much more complex, and beside T cells, many other immune cells also influence bone formation and/or resorption. Of course, myeloid cells greatly contribute to osteoimmune interactions mainly because some of them represent osteoclast progenitors. In a systematic literature review, de Vries et al. highlighted two common cell types participating in osteoclastogenesis in chronic diseases and bone metastasis: blood $CD16^+$ monocytes as major osteoclast progenitors, and T cells producing TNF-α that support pathological osteoclastogenesis. The origin of osteoclasts from myeloid cells was further reviewed by Madel et al.. They pointed out that dendritic cells contribute to osteoclast formation in pathological conditions related to chronic inflammation and cancer, always in the presence of high levels of IL-17, TNF-α, and RANK-L.

Two reviews present the importance of macrophages in osteoimmunology. Humbert et al. reassessed the reciprocal interactions between macrophages and mesenchymal stromal cells that modulate immune suppression and bone regeneration in bone healing after calcium-phosphate implant transplantation. Biguetti et al. demonstrated using Ti-implants that Damage Associated Molecular Patterns (DAMP) such as HMGB1 and Rage are essential for osteointegration by controlling the balance between M1 and M2 macrophages. As discussed by Pieters et al., macrophages produce extracellular vesicles (EVs) that mediate their interaction with bone cells. Among the various compounds carried by these EVs, alarmins, which are DAMPs released upon stress or inflammation, influence bone remodeling, decreasing or increasing bone resorption and formation depending on the content of the vesicles. EVs also carry miRNAs that are able to control bone cell differentiation. The role of miRNAs in osteoclastogenesis was further considered in a review by Lozano et al..

These data emphasize the importance of danger signals in osteoimmune interactions. This was further discussed by Souza and Lerner who, showed that Toll like receptors that recognize signals from bacteria and other microorganisms participate in the control of osteoclast, osteoblast, or MSC differentiation and function. In their review, Seebach and Kubatzky showed that implant-associated bone infection induces an immune-compromised environment where bacteria can persist, resulting in increased bone resorption. In this environment, different immune cells—including osteoclasts—may participate in an immune-suppressive environment that favors the chronicity of infection.

CONTROL OF INFLAMMATION AND IMMUNE CELLS BY BONE CELLS

The interaction between the bone and immune system is reciprocal. Mesenchymal stromal cells have an important immunosuppressive function that participates in regulating inflammatory responses (Xiao et al.) and in bone healing (Humbert et al.). In rheumatoid arthritis, Luque-Campos et al. analyzed the capacity of MSCs to restore the balance between inflammation and tolerance, which is of high interest for therapeutic purpose. Moreover, cells from the mesenchymal lineage are a major component of hematopoietic niches. Using lipodystrophic mouse models, Wilson et al. demonstrated that adipocytes are required for maintaining an environment that favors the retention of hematopoietic progenitors in the bone marrow.

An emerging field in osteoimmunology is the immune function of osteoclasts. Madel et al. provided the first review on this novel aspect of osteoclast activity. In line with the different origins of osteoclasts, they discussed the heterogeneity of mature osteoclasts as well as their function as innate immune cells. They showed that besides their bone resorption activity, osteoclasts are immuno-competent cells able to initiate T cell responses toward tolerance or inflammation depending on their context and origin (3). This opens new research avenues on the heterogeneity of osteoclasts in steady state and in chronic inflammatory conditions.

SIGNALING AND REGULATORY PATHWAYS IN OSTEOIMMUNOLOGY

At the molecular level, the topic has contributed in refining osteoclast signaling pathways in the context of the immune system and diseases with bone destruction. Sobacchi et al. updated us on the importance of RANK-RANKL signaling not only for osteoclast formation in bone (4), but also for T-cell maturation in the thymus. Using various TNF-α and RANKL knock-out, and overexpression mouse models, Papadaki et al. demonstrated that overall, arthritis was weakened in the absence of RANKL, but increased osteoclast formation at the pannus area was observed when TNF-α was overexpressed even in the absence of RANKL, confirming a RANKL-independent osteoclast formation (5). In contrast, overexpression of TNF-α was not able to compensate osteopetrosis in the absence of RANKL, indicating that disease-associated osteoclasts and turnover or physiological osteoclasts may have a different dependency on RANKL or TNF-α for their formation (as discussed in de Vries et al.; Madel et al.).

Cytokine signaling toward osteoblasts and osteoclasts has always been a key topic in osteoimmunology (6). Persson et al. interfered with family members of the gp130 receptor cytokine family in osteoblasts. When activating Shc1, Oncostatin M-mediated RANKL upregulation and subsequent osteoclastogenesis through interference with STAT3 signaling was achieved. Various studies suggest a role for inflammation in the onset of formation of heterotopic bone (7). In a model for spinal cord injury-induced heterotopic ossification, Alexander et al. showed that injured muscles display increased STAT3 signaling, activating JAK1/2 tyrosine kinases. When inhibiting this pathway, heterotopic ossification was diminished.

Two review articles described the importance of S1P-S1PR signaling in egression of immune cells to inflammatory bone

(Hasegawa et al.; Xiao et al.). One of the future challenges in the osteoimmunology field is to map the osteoclast-immune cell-interactions. When do and what kind of T cells interact with bone resorbing osteoclasts, and will these stimulate or inhibit their activity? The life cell imaging of bone-immune cell interactions (Hasegawa et al.) as developed by the group of Ishii (8, 9) will certainly assist herein. Syk is a non-receptor tyrosine kinase critically involved in signaling by various immune receptors. Mouse models where hematopoietic lineage or osteoclast specific knock-out of Syk is accomplished, develop osteopetrosis, demonstrating the role of Syk in osteoclasts (Csete et al.).

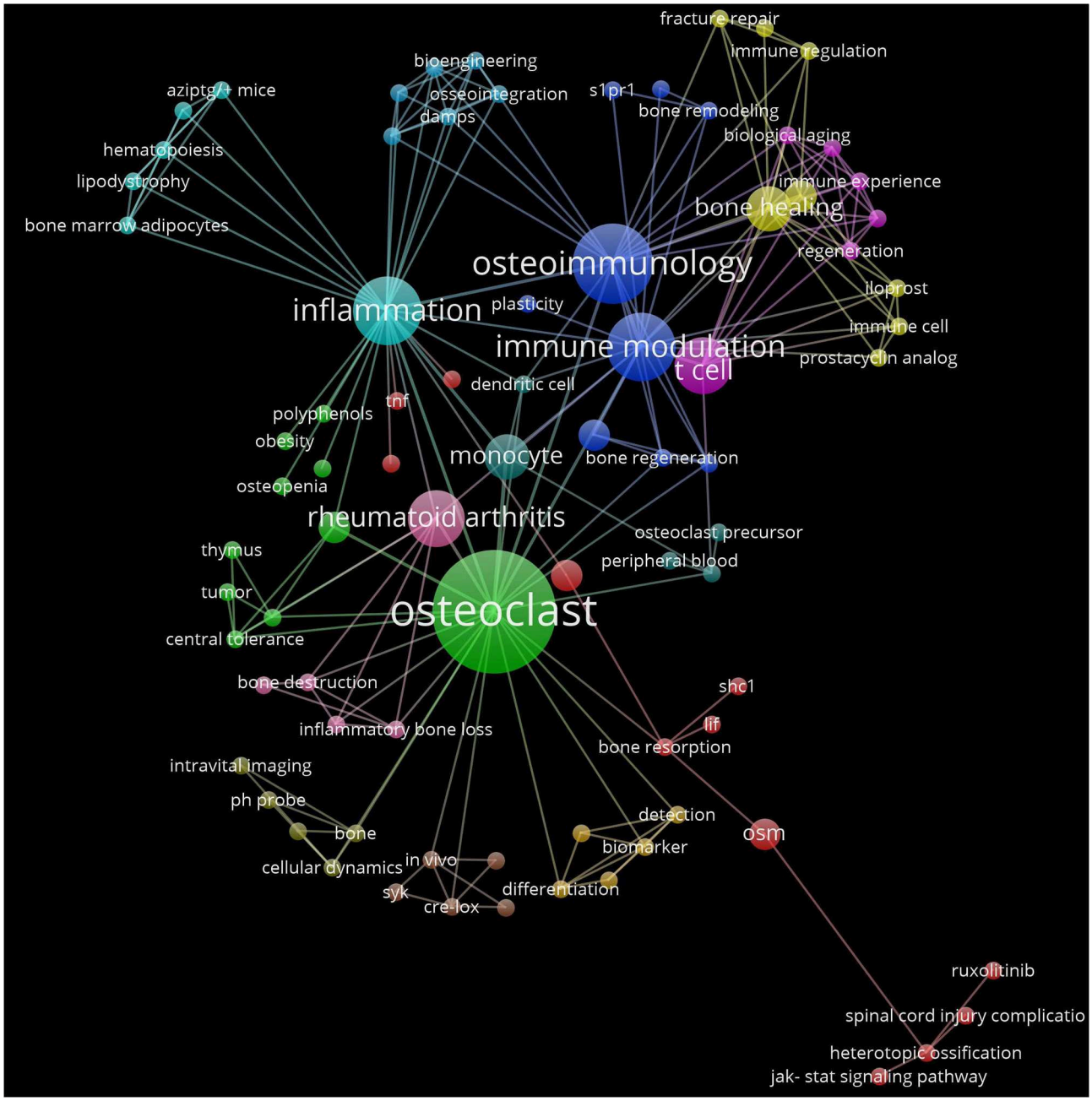

FIGURE 1 | Interaction network of articles from the Research Topic "Advances in Osteoimmuology". The network is built on the keywords from the 24 articles using VosViewer (http://www.vosviewer.com/) (ref https://doi.org/10.1007/s11192-009-0146-3). Keyword colors are determined by the cluster to which they belong. Each line represents an interaction among the keywords Distance between keywords approximately indicates their relatedness in network. The size of each keyword label and circle depends on the weight of the keyword.

PATHOLOGICAL IMPLICATIONS OF OSTEOIMMUNOLOGY

For the understanding of the pathophysiology of inflammatory bone diseases, our series of articles has contributed in highlighting the role of osteoimmunology in various diseases. First of all, possible common ground for the various inflammatory bone diseases in peripheral blood was found at the level of monocyte precursor type priming within the circulation by inflammatory cytokines such as TNF-α and a role for activated RANKL and/or TNF-α expressing T cells (de Vries et al.). Secondly, common osteoimmunology ground was searched for in diseases of the oral cavity such as periodontitis, oral cancer and degradation of the temporomandibular joint (Alvarez et al.).

For rheumatoid arthritis, our series had three review contributions, one general review (Coury et al.), and two more specialized ones describing a putative role for mesenchymal stem cells (Luque-Campos et al.) or autoantibodies (Steffen et al.) in disease modulation.

Obesity is a growing health care concern in Western society, a condition associated with an altered immune system (10, 11). Obese children display a deviant monocyte subpopulation distribution and concomitant increased osteoclast formation, which can be modulated with dietary substances such as sweet cherry polyphenols that reduce RANK-L and TNF-α production (Corbo et al.). At the other side of the spectrum, in two mouse models that lack adipocytes, hematopoiesis moved outside the bone marrow to the spleen and liver (Wilson et al.).

Bone infections, such as around implants or around teeth, may alter the immune system-driven osteoclast formation. Osteoclasts ultimately may contribute to implant or tooth loosening when not treated properly. Seebach and Kubatzky have investigated whether immune modulation could be a therapeutic target for chronic bone infections. Osteoclast precursors such as monocytes originate from the bone marrow or blood. Once at the site of a bacterial infection, they make a differentiation decision, either into macrophages, combating the infection, or into osteoclasts. These monocyte or osteoclast precursor cells respond with toll-like receptors to bacterial products. This toll on the route when egressing from the circulation determines the fate and can be both inhibitory and stimulatory (Souza and Lerner). Despite all attempts of cell biologists to mimic inflammation in a Petri dish, the influence of mechanical loading is often neglected. Fahy et al. have taken up the challenge to map the contribution of mechanical loading and found that mechanically loaded monocytes secrete a different repertoire of cytokines than the unloaded ones.

CONCLUDING REMARKS

Bone quality and bone healing are age-dependent, with a decreased osteogenesis and an increased osteoclastogenesis over time. Parallel to this, the immune system also changes over time and can be "learned" or "naïve." In order to dissect both components, bone strength and *in vitro* osteogenic capacity were analyzed in mice of various age, and the effect of learned and naïve immune system was analyzed. Supernatants of immune cells inhibited osteogenic capacity of mesenchymal stem cells, stronger so in older mice and in immune-stimulated mice (Bucher et al.). Suppression of inflammatory milieu at early stages of bone fracture may improve bone repair (Wendler et al.). Inflammatory processes also take place during early phases of implant osseointegration. Biguetti et al. have assessed the role of HGMB1 and RAGE in titanium osseointegration and demonstrated that activity of these immune modulators is essential for successful osseointegration. Many devices used for implantation are coated with calcium-phosphate. Humbert et al. reviewed the state-of-the-art of these implants in conjunction with co-transplantation of mesenchymal stem cells, which may provoke positive immune modulation.

For 20 years, osteoimmunology has more and more found its way into the field of immunology, even at the undergraduate level (12). The topic "Advances in Osteoimmunology" shows great diversity in the themes that were addressed. Relatively new is the attention for implants and the role of immune cells and bone cells. The key cell still seems to be the osteoclast (**Figure 1**). Concerning a deeper understanding in the pathophysiology of osteoclasts formed under the control of the immune system, specific markers, of for instance, osteoclast membrane markers such as CX3CR1 [Madel et al.; (3)] or blood-derived precursors such as miRNAs (Lozano et al.) could generate disease-specific fingerprints. However, one can never be certain about the fate of these latter circulating markers. Generation of osteoclasts from monocytes from patients will only partially provide fingerprint answers, since only very few cells turn into multinucleated osteoclasts in any *in vitro* experiment. Therefore, isolation and characterization of pure osteoclasts, such as which has recently been described (13) isolated from bone biopsies, may further advance the field. High-throughput technologies such as single cell RNAseq analysis (14) are bound to be successful in future research, deciphering the phenotypic and functional diversity of bone marrow cells (15) including for osteoclasts. This will pave the road for understanding of deregulated osteoimmune interactions and more specific targeting of cells participating in pathological bone loss.

AUTHOR CONTRIBUTIONS

CB-W and TV designed the project and wrote the manuscript.

REFERENCES

1. Walsh MC, Takegahara N, Kim H, Choi Y. Updating osteoimmunology: regulation of bone cells by innate and adaptive immunity. *Nat Rev Rheumatol.* (2018) 14:146–56. doi: 10.1038/nrrheum.2017.213
2. Arron JR, Choi Y. Osteoimmunology: bone versus immune system. *Nature.* (2000) 408:535–6. doi: 10.1038/35046196
3. Ibáñez L, Abou-Ezzi G, Ciucci T, Amiot V, Belaïd N, Obino D, et al. Inflammatory osteoclasts prime TNFα-producing CD4(+) T cells and express CX3 CR1. *J Bone Miner Res.* (2016) 31:1899–908. doi: 10.1002/jbmr.2868

4. Kong YY, Yoshida H, Sarosi I, Tan HL, Timms E, Capparelli C, et al. OPGL is a key regulator of osteoclastogenesis, lymphocyte development and lymph-node organogenesis. *Nature.* (1999) 397:315–23. doi: 10.1038/16852
5. Kim N, Kadono Y, Takami M, Lee J, Lee S-H, Okada F, et al. Osteoclast differentiation independent of the TRANCE–RANK–TRAF6 axis. *J Exp Med.* (2005) 202:589–95. doi: 10.1084/jem.20050978
6. Souza PPC, Lerner UH. The role of cytokines in inflammatory bone loss. *Immunol Invest.* (2013) 42:555–622. doi: 10.3109/08820139.2013.822766
7. Cholok D, Chung MT, Ranganathan K, Ucer S, Day D, Davis TA, et al. Heterotopic ossification and the elucidation of pathologic differentiation. *Bone.* (2018) 109:12–21. doi: 10.1016/j.bone.2017.09.019
8. Furuya M, Kikuta J, Fujimori S, Seno S, Maeda H, Shirazaki M, et al. Direct cell–cell contact between mature osteoblasts and osteoclasts dynamically controls their functions *in vivo*. *Nat Commun.* (2018) 9:300. doi: 10.1038/s41467-017-02541-w
9. Mizuno H, Kikuta J, Ishii M. *In vivo* live imaging of bone cells. *Histochem Cell Biol.* (2018) 149:417–22. doi: 10.1007/s00418-018-1638-0
10. Reilly SM, Saltiel AR. Adapting to obesity with adipose tissue inflammation. *Nat Rev Endocrinol.* (2017) 13:633–43. doi: 10.1038/nrendo.2017.90
11. Saltiel AR, Olefsky JM. Inflammatory mechanisms linking obesity and metabolic disease. *J Clin Invest.* (2017) 127:1–4. doi: 10.1172/JCI92035
12. de Vries TJ, Schoenmaker T, van Veen HA, Hogervorst J, Krawczyk PM, Moonen CGJ, et al. The Challenge of teaching essential immunology laboratory skills to undergraduates in one month—experience of an osteoimmunology course on TLR activation. *Front Immunol.* (2019) 10:1822. doi: 10.3389/fimmu.2019.01822
13. Madel M-B, Ibáñez L, Rouleau M, Wakkach A, Blin-Wakkach C. A novel reliable and efficient procedure for purification of mature osteoclasts allowing functional assays in mouse cells. *Front Immunol.* (2018) **9**:2567. doi: 10.3389/fimmu.2018.02567
14. Papalexi E, Satija R. Single-cell RNA sequencing to explore immune cell heterogeneity. *Nat Rev Immunol.* (2018) 18:35–45. doi: 10.1038/nri.2017.76
15. Tikhonova AN, Dolgalev I, Hu H, Sivaraj KK, Hoxha E, Cuesta-Domínguez Á, et al. The bone marrow microenvironment at single-cell resolution. *Nature.* (2019) 569:222–8. doi: 10.1038/s41586-019-1104-8

Conflict of Interest: The authors declare that the research was conducted in the absence of any commercial or financial relationships that could be construed as a potential conflict of interest.

frontiers in Immunology

ORIGINAL RESEARCH
published: 13 November 2018
doi: 10.3389/fimmu.2018.02573

Lack of Adipocytes Alters Hematopoiesis in Lipodystrophic Mice

Anne Wilson[1], He Fu[2], Mariano Schiffrin[2], Carine Winkler[2], Meriem Koufany[3], Jean-Yves Jouzeau[3], Nicolas Bonnet[4], Federica Gilardi[2†], François Renevey[5], Sanjiv A. Luther[5], David Moulin[3,6] and Béatrice Desvergne[2]**

[1] Department of Oncology, University of Lausanne, Epalinges, Switzerland, [2] Faculty of Biology and Medicine, Center for Integrative Genomics, Genopode, University of Lausanne, Lausanne, Switzerland, [3] IMoPA, UMR7365 CNRS-Université de Lorraine, Vandœuvre-lès-Nancy, France, [4] Division of Bone Diseases, Department of Internal Medicine Specialties, Faculty of Medicine, Geneva University Hospital, Geneva, Switzerland, [5] Department of Biochemistry, Center for Immunity and Infection, University of Lausanne, Epalinges, Switzerland, [6] CHRU de Nancy, Contrat d'interface, Vandœuvre-lès-Nancy, France

Adult hematopoiesis takes place in the perivascular zone of the bone cavity, where endothelial cells, mesenchymal stromal/stem cells and their derivatives such as osteoblasts are key components of bone marrow (BM) niches. Defining the contribution of BM adipocytes to the hematopoietic stem cell niche remains controversial. While an excess of medullar adiposity is generally considered deleterious for hematopoiesis, an active role for adipocytes in shaping the niche has also been proposed. We thus investigated the consequences of total adipocyte deletion, including in the BM niche, on adult hematopoiesis using mice carrying a constitutive deletion of the gene coding for the nuclear receptor peroxisome proliferator-activated receptor-γ (PPARγ). We show that *Pparg*$^{\Delta/\Delta}$ lipodystrophic mice exhibit severe extramedullary hematopoiesis (EMH), which we found to be non-cell autonomous, as it is reproduced when wild-type donor BM cells are transferred into *Pparg*$^{\Delta/\Delta}$ recipients. This phenotype is not due to a specific alteration linked to *Pparg* deletion, such as chronic inflammation, since it is also found in AZIP$^{tg/+}$ mice, another lipodystrophic mouse model with normal PPARγ expression, that display only very moderate levels of inflammation. In both models, the lack of adipocytes alters subpopulations of both myeloid and lymphoid cells. The CXCL12/CXCR4 axis in the BM is also dysregulated in an adipocyte deprived environment supporting the hypothesis that adipocytes are required for normal hematopoietic stem cell mobilization or retention. Altogether, these data suggest an important role for adipocytes, and possibly for the molecular interactions they provide within the BM, in maintaining the appropriate microenvironment for hematopoietic homeostasis.

Keywords: lipodystrophy, PPARγ null mice, AZIPtg/+ mice, bone marrow adipocytes, hematopoiesis, extramedullary hematopoiesis, inflammation, non-cell autonomous alteration of hematopoiesis in PPARγ null mice

OPEN ACCESS

Edited by:
Teun J. De Vries,
VU University Amsterdam,
Netherlands

Reviewed by:
Cristina Sobacchi,
CNR, Italy
Martina Rauner,
Technische Universität Dresden,
Germany
Miguel Luiz Batista Júnior,
University of Mogi das Cruzes, Brazil

****Correspondence:***
Anne Wilson
anne.wilson@unil.ch
Béatrice Desvergne
beatrice.desvergne@unil.ch

†Present Address:
Federica Gilardi,
Forensic Toxicology and Chemistry Unit, University Center of Legal Medicine, Lausanne University Hospital - Geneva University Hospitals, Geneva, Switzerland

Specialty section:
This article was submitted to Inflammation, a section of the journal Frontiers in Immunology

Received: *23 July 2018*
Accepted: *18 October 2018*
Published: *13 November 2018*

Citation:
Wilson A, Fu H, Schiffrin M, Winkler C, Koufany M, Jouzeau J-Y, Bonnet N, Gilardi F, Renevey F, Luther SA, Moulin D and Desvergne B (2018) Lack of Adipocytes Alters Hematopoiesis in Lipodystrophic Mice. Front. Immunol. 9:2573. doi: 10.3389/fimmu.2018.02573

INTRODUCTION

Bones and hematopoiesis are intimately linked. Adult hematopoiesis takes place in the bone cavity, where a variety of cells and molecular contacts create a niche allowing hematopoietic stem cells (HSCs) to undergo cell division and differentiation in a highly regulated manner. The concept of a stem cell niche was first coined by Schofield, who hypothesized that the cellular environment in the bone compartment creates multiple cell-cell contacts that are crucial for HSC function (1). Depending on the location in the bone cavity, the different cell types involved and different functions proposed, BM niches are described as endosteal, reticular, sinusoidal or perivascular, mainly involving osteoclast precursors, osteoblast and spindle-shaped osteoblast precursors (SNO), CXCL12-abundant-reticular (CAR) cells, Nestin+ mesenchymal stromal cells (MSCs), E-selectin+ endothelial cells, LeptinR+ perivascular stromal cells, and non-myelinating Schwann cells, respectively [reviewed in (2–4)].

The role of adipocytes, present in large numbers in the BM cavity, remains disputed. Adipocytes, which are the specialized cells of adipose tissue, store energy in the form of lipids, and release it when required by the organism. Adipocytes also secrete cytokines known as adipokines that participate in endocrine-mediated homeostasis (5). Both gain of adipose tissue, as in obesity, and the generalized lack of adipose tissue (generalized lipodystrophy), such as is seen in Berardinelli-Seip syndrome, causes metabolic disorders such as hypertriglyceridemia, metabolic syndrome, and type 2 diabetes (6, 7). While most adipocytes are found within depots forming the diverse adipose tissues, some of them are also found in substantial numbers in a less organized manner, particularly within the BM where their (local) role is less well characterized (8). The first link between adipocytes and the bone microenvironment is the fact that both adipocytes and osteoblasts are derived from a common mesenchymal progenitor, and their respective production is due to a balance between adipogenesis and osteoblastogenesis. A more direct contribution of adipocytes to the stem cell niche in the BM has been previously explored, albeit with contradictory results. First, using leptin deficient mice (*ob/ob* mice), Claycombe et al. showed that supplementation with leptin, a major adipokine secreted by adipocytes, rescued appropriate levels of lymphopoiesis and myelopoiesis in the BM (9). Second, a combination of *in vitro* and *in vivo* experiments has suggested that adiponectin, another adipokine expressed by adipocytes in the BM, is required for optimal HSC growth (10, 11). Third, BM adipocytes also secrete Stem Cell Factor, which contributes to restoring hematopoiesis after irradiation in the long bones but not in the vertebral bones (12). Finally, experiments performed in AZIP-F1 ($AZIP^{tg/+}$) transgenic mice carrying a C/EBP dominant negative transgene that induces deletion of mature adipocytes, showed improved marrow engraftment after irradiation, suggesting that in this specific context adipocytes are negative regulators of hematopoiesis (10, 13). A similar negative effect is also proposed when adipocytes overfill the medullary space upon BM failure in Fanconi Anemia (14).

In the present report, we reveal a novel aspect of the cross-talk between hematopoiesis and adipocytes, by exploiting a generalized lipodystrophic mouse model carrying a constitutive total-body deletion of the nuclear receptor peroxisome proliferator-activated receptor-γ (PPARγ) (15, 16). $Pparg^{\Delta/\Delta}$ mice show a complex phenotype including total lipoatrophy, increased lean mass, and hypermetabolism. They develop severe type 2 diabetes, characterized by hyperglycemia, hyperinsulinemia, polyuria, and polydipsia (personal communication, manuscript in preparation). Herein, we demonstrate that the total lack of adipocytes is accompanied by extramedullary hematopoiesis (EMH), which is defined as the production of blood cells occurring outside of the BM, mainly in the liver and spleen (17). We further evaluate the causes of this EMH and provide new insights in the role of adipocyte signaling in hematopoiesis.

MATERIALS AND METHODS

Mice

Genotype designations in this work follow the rules recommended by the Mouse Genome Database Nomenclature Committee. Procedures using mice were authorized by the Cantonal Commission for Animal Experimentation of the Canton of Vaud and carried out in accordance with the International Guiding Principles for Biomedical Research Involving Animals. *Sox2-Cre* transgenic mice (*Sox2-Cre* $^{tg/+}$; Tg(Sox2-cre)1Amc/J), CD45.1+ (B6.SJL-$Ptprc^{a}Pepc^{b}$/BoyJ) mice (Jackson Laboratory, Bar Harbour, MA), and *ob/ob* mice were kept in the University of Lausanne Animal Facility. Construction of the *Pparg* floxed (hereafter referred to as $Pparg^{fl}$) and *Pparg*-null alleles resulting from Cre recombination (hereafter referred to as $Pparg^{\Delta}$), as well as the mating strategy for the generation of *Sox2-Cre*$^{tg/+}$Pparg$^{em\Delta/\Delta}$ ($Pparg^{\Delta/\Delta}$) mice and their control littermates (CTL) with no *Sox2-Cre* transgene but two functional *Pparg* alleles ($Pparg^{fl/+}$) have been previously described (16, 18). This strategy ended up with a conditional epiblast-specific deletion of *Pparg* mediated by the *Sox2-Cre* transgene. The preservation of *Pparg* expression in the trophoblast (16) circumvented the embryonic-lethality of homozygous PPARγ knockout mice due to a placental defect (15, 16). Normal placental development allows *Sox2-Cre*$^{tg/+}$$Pparg^{em\Delta/\Delta}$ pups to be born, and as expected, these mice are totally deprived of any form of adipose tissue. Both male and female mice 12–22 weeks of age were used. AZIP/F1 mice on an FVB background [Tg(AZIP/F)1Vsn; hereafter referred to as $AZIP^{tg/+}$] and corresponding wild-type FVB controls were obtained from Charles Vinson and the colony was raised as previously described (19).

No *Pparg* expression could be detected in the long bones of $Pparg^{\Delta/\Delta}$ mice and the total lack of adipocytes in the BM in these two models, was confirmed by using Resistin, an adipokine specifically expressed by adipocytes and, herein, used as a surrogate marker for the presence of mature adipocytes. Expression of Resistin was indeed barely measurable

above the detection threshold in mRNA extracted from *Pparg*$^{\Delta/\Delta}$ bones, and at very low levels in AZIP$^{tg/+}$ bones (**Supplementary Figure S1**).

Flow Cytometry

BM cell suspensions from all mouse strains described above were prepared by crushing the long bones (2 femurs and 2 tibias per mouse) into DMEM/3% FCS. Bone fragments were removed by filtration through 40-μm filters. Splenocyte suspensions were obtained by mashing the organs through sieves into DMEM/3% FCS, washing by centrifugation and filtering through a 40-μm filter cap. Liver hematopoietic mononuclear cells were obtained by mashing entire livers through sieves, after which the cells were washed in DMEM/3% FCS and centrifuged using a Percoll (GE Healthcare) gradient (40% Percoll layered over 80% Percoll) for 30 mins at 2,000 rpm to remove hepatocytes and other non-hematopoietic cells. Cells localized at the interface were recovered, diluted in DMEM/3% FCS, centrifuged and filtered through 40-μm filter caps. Single-cell suspensions were stained as previously described (20). Monoclonal antibody conjugates used for flow cytometry are listed in **Supplementary Table S1**. Cells were analyzed on a 5-laser LSR II cytometer equipped with 355, 405, 488, 561, and 640-nm lasers (Becton Dickinson, San Jose, CA), and the data were analyzed with FlowJo V9 software (TreeStar, Ashland, OR).

Colony Forming Cell (CFC) Assay

Splenocyte cell suspensions were obtained by mashing the spleen through sieves into DMEM/3% FCS, washing by centrifugation then filtering through 70-μm filter caps. BM cells suspensions were obtained as described above. Splenocytes (3×10^5) and BM cells (2×10^4) were seeded into 35 mm dishes in Mouse Methylcellulose Complete Media containing cytokines/growth factors such as EPO, IL-3, IL-6, SCF, or the combination thereof according to the manufacturer's instructions (R&D Systems). After 10–12 days of culture at 37°C in 5% CO_2, Colonies were identified by eye with phase-contrast microscopy.

BM Transplantation

BM chimeras were prepared as previously described (21). Briefly, 12-week old host mice (CD45.1+) were lethally irradiated (1000 rads) and reconstituted with 10^7 T-depleted BM cells (CD45.2+) from either *Pparg*$^{\Delta/\Delta}$ mice or their littermate controls (CTL). For reverse chimeras, 12-week old host mice (*Pparg*$^{\Delta/\Delta}$ or CTL) were reconstituted with 10^7 T-depleted BM cells from CD45.1+ wild-type controls. Hematopoietic reconstitution was assessed by FACS staining of ficoll-purified peripheral blood cells 6 weeks after transfer as described above. Mice were euthanized and analyzed 12 weeks after transfer. Owing to variable reconstitution efficiency between animals, the BM chimera results were expressed as the percentage of donor-derived cells.

Quantitative RT-PCR

Total RNA was isolated from long bones (bone fragments and BM combined), liver, and spleen, using TRIzol LS reagent (ThermoFisher, Waltham, MA) and purified with the RNeasy kit (Qiagen, Hilden, Germany). RNA quality was verified by chip electrophoresis (Agilent 2100 Bioanalyzer; Santa Clara, CA), and the concentration was determined using Nanodrop (Wilmington, DE). Total RNA (500 ng to 1 μg) was reverse-transcribed using the iScript™ cDNA Synthesis Kit (Bio-Rad Laboratories, Hercules, CA) according to the manufacturer's instructions. Real-time PCR was performed with SYBR® Green PCR mastermix using an ABI PRISM® 7900 PCR machine (ThermoFisher). The results were normalized to the levels of Actin beta (*Actb*). For primer sequences, see **Supplementary Table S2**.

Histology

Spleen were fixed in 4% paraformaldehyde and paraffin embedded. Four micro meter paraffin sections were stained with hematoxylin and spleen area as well as white pulp (WP) area were calculated by measuring spleen or WP surface area, using ImageJ software (http://rsbweb.nih.gov/ij/). Red pulp (RP) area was calculated as total spleen area minus WP areas. One representative section per spleen and 3 spleens were analyzed per genotype.

Immunohistochemistry was performed on 8 μm-thick frozen sections of OCT-embedded spleen, which were fixed using acetone followed by primary and secondary antibodies or streptavidin (found in **Supplementary Table 1**), as described previously (22). Images were acquired with a Zeiss Axioplan microscope and treated with Photoshop (Adobe) or Image J opensource software.

Serum Levels of Parathyroid Hormone (PTH) and Inflammatory Markers

Blood was obtained by cardiac puncture immediately after euthanasia. After clotting and centrifugation, serum was collected and stored at −80°C until use. Parathyroid hormone (PTH) was measured by ELISA according to the manufacturer's protocol (Stoughton, MA; LifeSpan Biosciences, Inc., Seattle,WA). Serum levels of Serum Amyloid A (SAA), IL-1β and IL-6 were measured using commercial ELISA kits (Bio-techne, Abingdon, UK). Assays were run in duplicate using adequate dilution buffer (for SAA, sera were diluted between 1:200 and 1:2,000; for IL-1β and IL-6, sera were used pure or diluted 1:2), according to the manufacturer's protocol. A four-parameter logistic formula was used to calculate the sample concentrations from the standard curves. Limit of quantification was 0.022 ng/ml for SAA (manufacturer's data).

Statistical Analyses

The statistical analysis was performed using GraphPad Prism 6 software. Two-group comparisons were performed using Student's *t*-tests or Mann-Withney *U*-test for non-parametric data, as indicated. All data are presented as mean ± SEM.

RESULTS

Significant Increase in Hematopoietic Cells in the Spleen and Liver of Lipodystrophic *Pparg*$^{\Delta/\Delta}$ Mice

To explore both the systemic and local involvement of adipose tissue, we characterized the hematopoietic phenotype of mice carrying a constitutive deletion of the two *Pparg* alleles. We have previously shown that the ablation of PPARγ expression leads to the total absence of both white and brown adipose tissue (18) and the development of various metabolic disorders, which include the early onset of a type 2 diabetes [(23) and unpublished observations]. Adult *Pparg*$^{\Delta/\Delta}$ mice had significantly enlarged spleens and livers, both in volume and weight (**Figures 1A,B**). Histological analyses revealed an alteration of the red pulp of the spleen, with an increase in the red pulp compartment size (**Supplementary Figures S2A,B**) and the presence of numerous and large polynuclear cells corresponding to megakaryocytes (**Figure 1C**). The total surface occupied by the white pulp was similar in the spleen sections from control and *Pparg*$^{\Delta/\Delta}$ mice while the average white pulp cords were smaller (**Supplementary Figures S2A,B**). However, the overall perturbation might lead to an underestimation of the white pulp. Immunohistochemical characterization of the spleen further showed that the segregation of various immune cells into the red and white pulp compartment as well as into the B and T zone of the white pulp was not significantly altered in spleens of *Pparg*$^{\Delta/\Delta}$ mice. Similarly, only a mild reduction in splenic germinal centers was observed (**Supplementary Figures S2C–E**). During fetal life the liver and spleen are the major sites of hematopoiesis, and the perturbations observed, particularly the presence of numerous megakaryocytes, are suggestive of altered hematopoiesis.

Consistent with a perturbation of hematopoiesis, significant increases in total hematopoietic mononuclear cell numbers were observed in the liver and spleen of Pparg$^{\Delta/\Delta}$ mice (**Figure 1D**). Flow cytometric analysis of the major hematopoietic subsets in these organs showed significant increases (10-fold or more) in the numbers of granulocytes, macrophages and erythroblasts.

In contrast to these peripheral organs, the total numbers of hematopoietic cells in the BM of Pparg$^{\Delta/\Delta}$ mice were marginally decreased compared to the controls (**Figure 1D**). While the numbers of granulocytes and macrophages in the BM did not differ in Pparg$^{\Delta/\Delta}$ mice compared to the controls, lymphopoiesis was affected with numbers of B cells and T cells reduced 1.5-fold in Pparg$^{\Delta/\Delta}$ mice, and erythroblasts decreased ∼two-fold (**Figures 1E,F**). However, this hematopoietic cell dysregulation was associated with only minor changes in the peripheral blood counts (**Supplementary Figure S3**). Thus, while BM hematopoiesis is mildly altered in the absence of PPARγ, substantial increases in numbers of myeloid (granulocytes and macrophages) and erythroid (erythroblasts and RBCs) lineage cells are observed in peripheral hematopoietic organs such as the liver and spleen.

Lipodystrophic *Pparg*$^{\Delta/\Delta}$ Mice Exhibit Active Extra-Medullary Hematopoiesis

To determine whether the massive increase in hematopoietic cells observed in the peripheral organs was due to a local increase in their production, we assessed the number of HSCs and progenitor cells in these organs as well as in the BM. Under homeostatic conditions, adult hematopoiesis occurs almost exclusively in the BM, where mature hematopoietic lineages are normally produced from HSCs and progenitor cells (**Supplementary Figure S4**) located in specialized BM niches (24). However, under certain conditions (such as BM failure, myelostimulation, or inflammation), substantial numbers of HSCs and multi-potent progenitor cells (MPPs), as well as developing myeloid and erythroid lineages, can be found in peripheral organs such as the spleen and liver, contributing to an extramedullary hematopoiesis (EMH) [reviewed in (17)].

To evaluate and identify cells belonging to the different hematopoietic precursor populations, we analyzed by flow cytometry the LSK (Lin$^-$, Sca-1$^+$, cKit-r$^+$) and LK (Lin$^-$, Sca-1$^-$, cKit-r$^+$) populations. The LSK subset contains long-term (LT-) and short-term (ST-) HSCs, and several Multi-Potent Progenitors (MPPs) populations, while the LK subset contains the Common Myeloid Progenitors (CMPs), and gives rise to both Megakaryocyte Erythroid Progenitors (MEPs) and Granulocyte Monocyte Progenitors (GMPs; see also **Supplementary Figure S4**). Significant increases in both the relative proportion and total numbers of LSK and LK cells were observed in the spleen and liver of *Pparg*$^{\Delta/\Delta}$ mice compared to control mice. In contrast, the absolute and relative number of LSK and LK cells in the BM of *Pparg*$^{\Delta/\Delta}$ mice were modestly affected (**Figures 2A–C**).

To further identify subsets present in the LSK population, we analyzed the distribution of the markers CD34, CD48, and CD150, which define LT- and ST-HSCs as previously described [(20); **Supplementary Figure S4**]. Although LT-HSC (CD34$^-$ CD48$^-$ CD150$^+$) and MPP1 (ST-HSC; CD34$^+$ CD48$^+$ CD150$^+$) subsets were marginally decreased in the BM, the MPP2 (CD34$^+$ CD48$^-$ CD150$^+$) and MPP3/MPP4 (CD34$^+$ CD48$^+$ CD150$^-$ CD135$^{+/-}$) subsets were unchanged (**Figure 2C**). Thus, the HSC and MPP subsets were largely unaffected in the BM of mice lacking PPARγ. In contrast, a global 10- to 100-fold increase in LT-HSC and all MPP subsets (MPP1-4) was observed in the spleen and liver of *Pparg*$^{\Delta/\Delta}$ mice with no changes in their relative proportions compared to those seen in the BM of wild-type controls. These important increases were still observed when calculated as a % of the total cell number in these two organs (**Figures 2D,E**). The clonogenic potential of these hematopoietic precursor populations found in the spleen was also confirmed by performing a Colony Forming Unit assay on BM and spleen cells (**Supplementary Table S3**).

As B cells and T cells are derived from hematopoietic progenitors via a Common Lymphoid Precursor (CLP), which is defined as Lin$^-$, Sca-1^{lo}, cKit-r^{lo} and CD27$^+$, CD127$^+$, CD135$^+$(25), we quantified the proportion and number of CLPs in the BM and spleen of control and *Pparg*$^{\Delta/\Delta}$ mice. No significant changes were observed in the proportion or in the

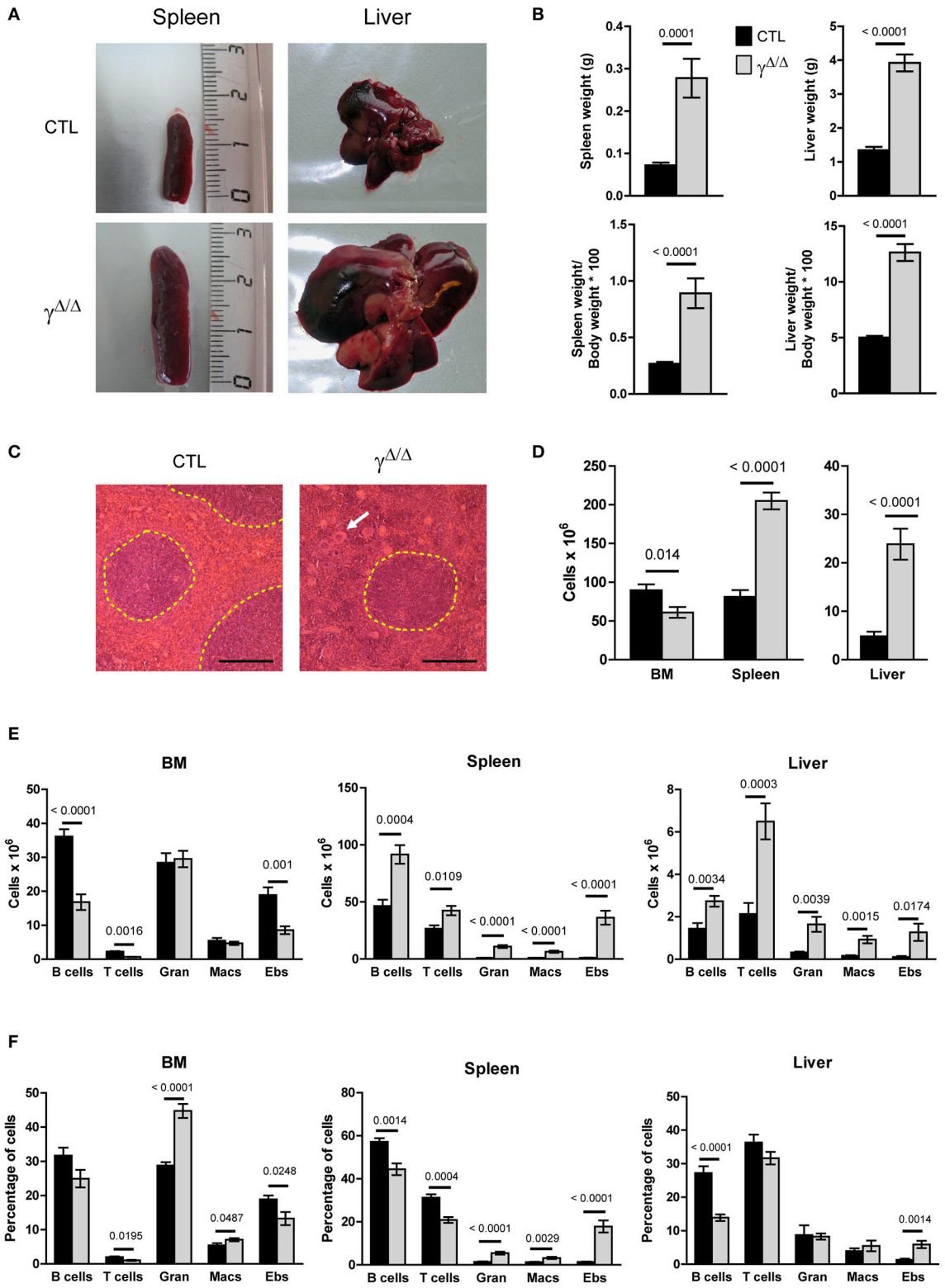

FIGURE 1 | Evaluation of hematopoiesis-derived cell populations in the bone marrow (BM) and peripheral organs of Pparg$^{\Delta/\Delta}$ mice. **(A)** Representative photographs of the spleens and livers of *Pparg*$^{\Delta/\Delta}$ ($\gamma^{\Delta/\Delta}$) mice (lower panels) and littermate control (CTL) mice (upper panels). **(B)** Spleen and liver weight in grams (top panels) and expressed as % of the body weight (bottom panels). **(C)** Hematoxylin & eosin staining of spleen sections; White pulp areas are circled by a dotted line. The white arrow indicates one of the numerous megakaryocytes present in the red pulp in *Pparg*$^{\Delta/\Delta}$ mice. The black bar indicates 200 micrometers. **(D)** Total hematopoietic cell

(Continued)

FIGURE 1 | numbers in the BM (2 tibias and 2 femurs from each mouse), spleen, and liver of control and *Pparg*$^{\Delta/\Delta}$ mice. Mean ± SEM, $n = 7$–8 mice per genotype. **(E)** Total numbers of mature hematopoietic cell subsets in the BM (left panel), spleen (middle panel) and liver (right panel) of control (dark bars) and *Pparg*$^{\Delta/\Delta}$ (light bars) mice. **(F)** Same as in **(E)**, with cell numbers expressed as a % of the total cell number in the corresponding organ. T cells (CD3$^+$); B cells (B220$^+$); Gran: granulocytes (Gr1$^+$CD11b$^+$), Macs: macrophages (Gr1$^-$CD11b$^+$), Ebs: erythroblasts (Ter119$^+$CD71$^+$); Mean ± SEM $n = 7$–8 mice per genotype. All significant *p*-values are indicated above the corresponding bars.

number of CLPs in the BM and spleen of Pparg$^{\Delta/\Delta}$ compared to control mice (data not shown).

Taken together, the increases observed in these HSC and progenitor cell subsets along with the increase in mature myeloid and erythroid subsets in peripheral organs are consistent with a significant EMH occurring in *Pparg*$^{\Delta/\Delta}$ mice.

The EMH Observed in *Pparg*$^{\Delta/\Delta}$ Mice Is Non-cell Autonomous

To determine whether the EMH observed in *Pparg*$^{\Delta/\Delta}$ mice was driven by a hematopoietic cell-autonomous mechanism or by a perturbation of the BM microenvironment, BM transplantation was performed. Lethally γ-irradiated CD45.1$^+$ wild-type recipient mice were reconstituted with either Pparg$^{\Delta/\Delta}$ or control littermate T-depleted BM cells (CD45.2$^+$). After 3 months, reconstitution from the donor was verified by staining peripheral blood lymphocytes (PBLs) for the allelic markers CD45.2 and CD45.1, and the mice were sacrificed for organ analyses. When wild-type recipients were reconstituted with donor BM from *Pparg*$^{\Delta/\Delta}$ or control mice, no significant difference was observed in either the number or proportions of most mature hematopoietic cell types (**Supplementary Figure S5A**). Furthermore, there was no evidence of EMH in these chimeras, as no increases in LSK or LK cells were observed in the spleen or the liver (**Figure 3A**).

We then performed the reciprocal experiment in which lethally irradiated *Pparg*$^{\Delta/\Delta}$ (CD45.2$^+$) recipients were reconstituted with wild-type BM from CD45.1$^+$ mice (reverse chimeras). In contrast to what we observed when using WT recipients, the EMH observed in the peripheral organs of *Pparg*$^{\Delta/\Delta}$ recipient mice was largely recapitulated (**Figure 3B**). Increased numbers and proportions of erythroblasts, granulocytes, lymphocytes, and macrophages were observed in the spleen (**Supplementary Figure S5B**), and liver (data not shown) in these reverse chimeras. Further evidence of EMH was provided by the increase in proportions of LSK and LK cells in the peripheral organs of *Pparg*$^{\Delta/\Delta}$ recipients, but not of control recipients, reconstituted with wild-type donor BM (**Figure 3B**).

Taken together, these results indicate that the EMH observed in *Pparg*$^{\Delta/\Delta}$ mice is non-cell autonomous. Although LT-HSCs (and other stem/progenitor subsets) appeared to home to and seed normally in the BM cavity in lethally irradiated *Pparg*$^{\Delta/\Delta}$ mice, they were also able to efficiently seed peripheral organs such as the spleen and liver and to mobilize to these organs. This suggests that the resulting EMH, rather than a defect of the hematopoietic cells themselves, was driven either by systemic cues or by changes in the microenvironment or factors produced by cells within the local microenvironment.

Respective Contributions of Inflammation and Lipodystrophy to EMH Onset

One important known systemic cause of EMH is inflammation. In a previous report, we showed that *Pparg*$^{\Delta/\Delta}$ mice have altered skin hair follicles, which with aging provoke an inflammatory response in the skin (18). To evaluate the contribution of these systemic disorders in the occurrence of EMH in *Pparg*$^{\Delta/\Delta}$ mice, we analyzed another mouse model that shares a similar phenotype with respect to lipodystrophy, but does not exhibit overt inflammation.

The AZIP$^{tg/+}$ mouse is a hemizygous transgenic mouse strain in which a dominant negative protein (A-ZIP) expressed under the control of the adipose tissue-specific aP2 enhancer/promoter inhibits expression of members of the C/EBP and Jun families of transcription factors. AZIP$^{tg/+}$ mice are born with no WAT and with severely decreased brown adipose tissue (19). One difference between *Pparg*$^{\Delta/\Delta}$ mice and AZIP$^{tg/+}$ mice is the presence of systemic inflammation, suggested in *Pparg*$^{\Delta/\Delta}$ mice by the high levels of Serum Amyloid A (SAA) protein, which is a highly sensitive marker for inflammation particularly in the acute phase, and moderate increased levels of IL-1β. In contrast, SAA, IL-1β, and IL-6 levels were not significantly increased in AZIP$^{tg/+}$ mice, indicating that the inflammation in these mice is very low, if not null (**Figure 4A** and data not shown).

We thus further analyzed the liver and the spleen of the lipodystrophic AZIP$^{tg/+}$ mice. While these animals also displayed enlarged spleens and a significant increase in total numbers of hematopoietic mononuclear cells, these increases were predominantly due to increased numbers of myeloid and erythroid cells (**Supplementary Figure S6**). Importantly, the EMH observed in the absence of PPARγ was recapitulated in AZIP$^{tg/+}$ mutants (**Figure 4B**), with a significant increase in the numbers of LSK cells in the spleen and the liver, and an increase of LK cells in the spleen and to a lesser extent in the liver (**Figure 4C**).

This observation demonstrated that even though inflammation likely contributes to the EMH observed in *Pparg*$^{\Delta/\Delta}$ mice, the lipodystrophy *per se* is responsible for the EMH.

Distinct Features of the EMH in *Pparg*$^{\Delta/\Delta}$ and in AZIP$^{tg/+}$ Mice

In the BM, inflammation provokes an increased demand on the granulocyte/macrophage lineage. This lineage is derived from one of the two cell populations that arise from the CMPs (defined as CD34$^+$, CD16/32$^-$): the MEPs (CD34$^-$, CD16/32$^+$) and the GMPs (CD34$^+$, CD16/32$^+$). We thus further analyzed the relative proportions of MEPs, GMPs, and CMPs found within the BM, according to these markers (see

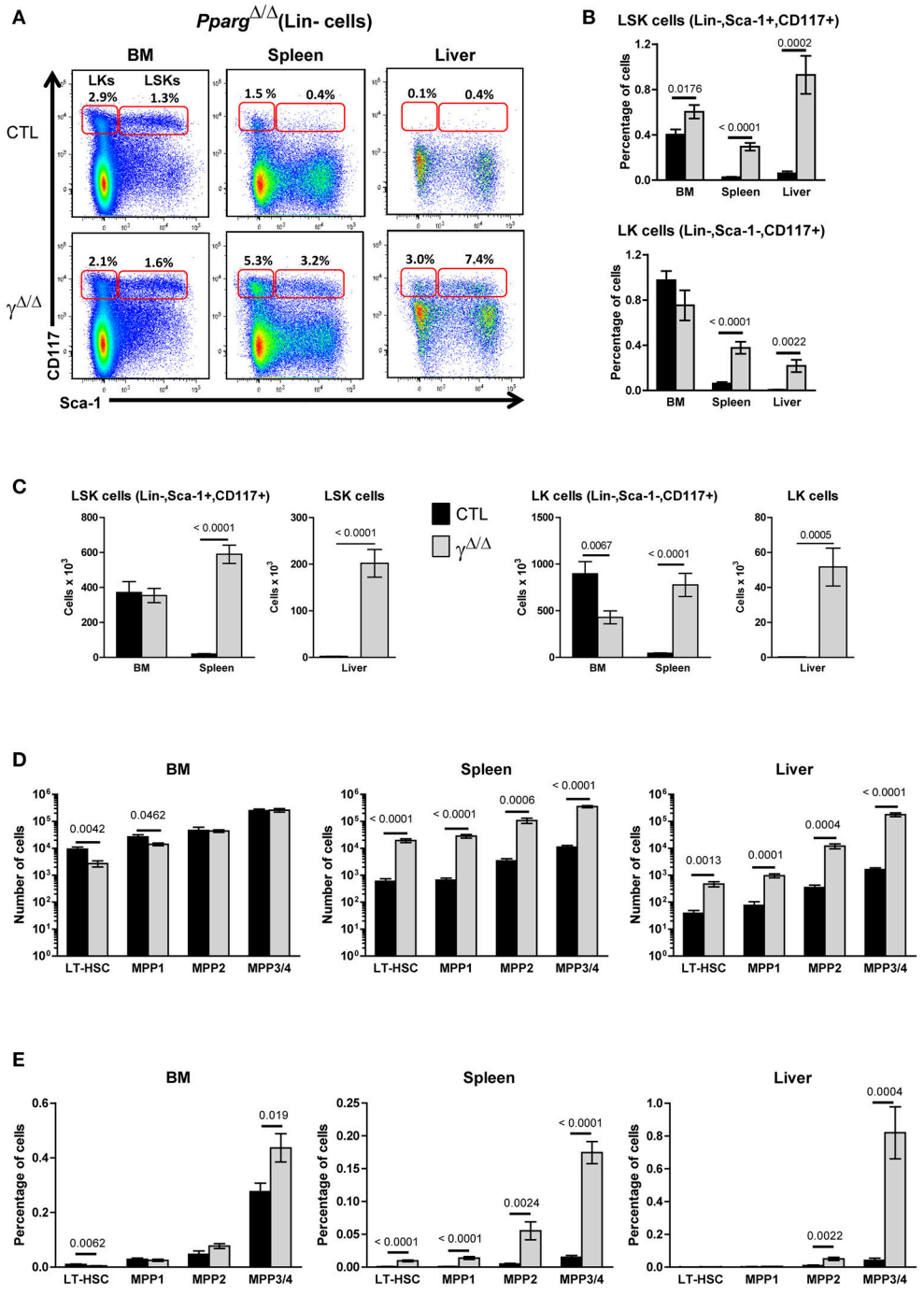

FIGURE 2 | Hematopoietic cell populations in the bone marrow (BM) and peripheral organs of Pparg$^{\Delta/\Delta}$ mice. **(A)** Representative FACS plots showing Sca-1 vs. CD117 staining on lineage-negative BM (left panels), spleen (middle panels), and liver (right panels) cells from littermate control (CTL, upper panels) or *Pparg*$^{\Delta/\Delta}$ (lower panels) mice. The red frames on the left and right of each plot indicate the gating and numbers of LK (Lineage-negative, Sca-1^{-}CD117^{+}) and LSK (Lineage-negative, Sca-1^{+}CD117^{+}) cells, respectively, as a percentage of lineage-negative cells from each organ. **(B)** Histograms showing the percentage of LSK (top panel) and LK (bottom panel) cells, with respect to the total cell numbers in the BM, spleen and liver of control (dark bars) and *Pparg*$^{\Delta/\Delta}$ (light bars) mice. Mean ± SEM, $n = 7$–8 mice per genotype. **(C)** Same as in **(B)**, expressed as absolute numbers of LSK (left panels) and LK cells (right panels). **(D)** Quantification of LT-HSC (CD34^{-}CD150^{+}CD48^{-}), MPP1 (CD34^{+}CD150^{+}CD48^{-}), MPP2 (CD34^{+}CD150^{+}CD48^{+}), and MPP3/4 (CD34^{+}CD150^{-}CD48^{+}) subsets in the LSK population of the BM, spleen, and liver from control (dark bars) and *Pparg*$^{\Delta/\Delta}$ (light bars) mice. Mean ± SEM, $n = 7$–8 mice per genotype. **(E)** Same as in **(D)**, expressed as a percentage of the total cell number in the corresponding organ. All significant *p*-values are indicated above the corresponding bars.

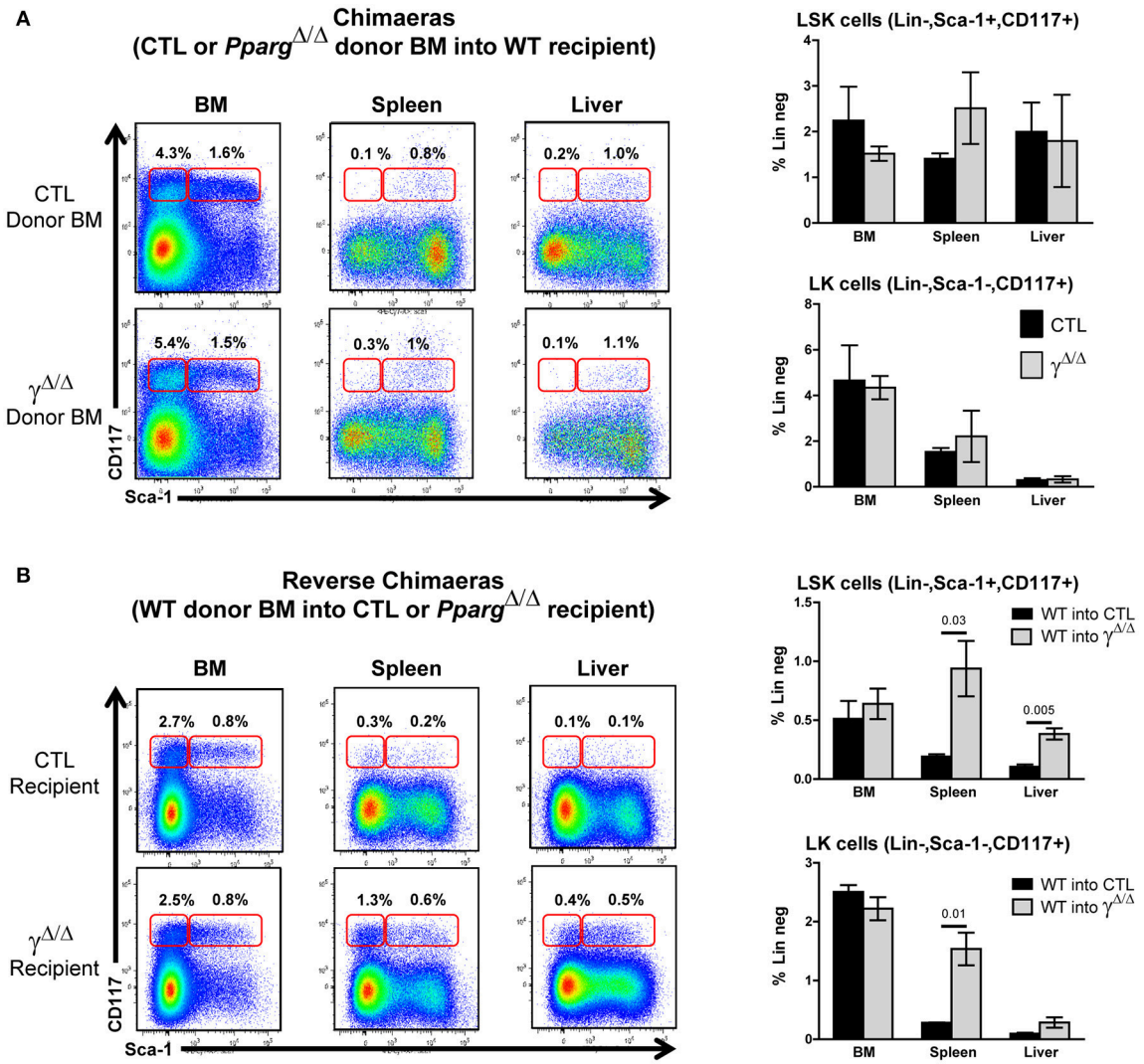

FIGURE 3 | Extramedullary hematopoiesis is non-cell autonomous. **(A)** Chimeras using wild-type recipient: Control or *Pparg*$^{\Delta/\Delta}$ donor BM (both CD45.2^{+}) was transferred into wild-type (WT) recipient CD45.1^{+} mice. Hematopoietic reconstitution was evaluated by FACS analysis 3 months after lethal γ-radiation and i.v. transfer of T-depleted BM. Left panels: representative FACS plots of Sca-1 vs. CD117 (cKit-r) on lineage-negative donor (CD45.2^{+}) BM (left), spleen (middle) or liver (right) cells from mice reconstituted with control BM (top row) or *Pparg*$^{\Delta/\Delta}$ BM (lower row). The red frames on the left and right of each plot indicate the gating and percentage of LK (Lineage-negative, Sca-1^{-}CD117^{+}) and LSK (Lineage-negative, Sca-1^{+}CD117^{+}) cells, respectively. Right panels: Relative proportions (in %) of LSK cells (top panel) and LK cells (bottom panel) over the total cell population of the BM, spleen, and liver. Dark bars represent donor control BM, and light bars represent donor *Pparg*$^{\Delta/\Delta}$ BM, both transplanted into WT host mice. Mean ± SEM, $n = 3$ mice per genotype. There are no significant p-values. **(B)** Reverse chimeras: Wild-type (WT) control donor BM (CD45.1^{+}) was transferred into CTL or *Pparg*$^{\Delta/\Delta}$ recipient CD45.2^{+} mice. Left panels: representative FACS plots of Sca-1 vs. CD117 (cKit-r) on lineage-negative donor (CD45.1^{+}) BM (left), spleen (middle), or liver (right) cells transferred into either CTL (upper row) or *Pparg*$^{\Delta/\Delta}$ (lower row) recipient mice. The red frames on the left and right of each plot indicate the gating and percentage of LK (Lineage-negative, Sca-1^{-}CD117^{+}) and LSK (Lineage-negative, Sca-1^{+}CD117^{+}) cells, respectively. Right panels: Relative proportions (in %) of LSK cells (top panel) and LK cells (bottom panel) over the total cell population of the BM, spleen, and liver. Dark bars represent donor control BM into CTL mice, and light bars represent donor control BM into *Pparg*$^{\Delta/\Delta}$ mice. Mean ± SEM, $n = 3$ mice per genotype. All significant p-values are indicated above the corresponding bars.

Supplementary Figure S4). In the BM, MEPs were decreased and GMPs increased, whereas CMPs were unchanged, resulting in a relatively lower proportion of MEPs and a higher proportion of granulocyte/macrophage progenitors in the BM of mice lacking PPARγ compared to wild-type controls (**Figures 5A,B**). These results were consistent with the gene expression profiles of their key regulators, with elevated levels of both *Sfpi/PU1* and *Gata2* in the long bones of *Pparg*$^{\Delta/\Delta}$ mice compared to control mice, whereas *Gata1* remained unchanged (**Figure 5D**). Thus, a bias in favor of myeloid over erythroid development in the BM was observed in the absence of PPARγ.

Importantly, the observed shift in the ratio of GMPs to MEPs within the LK subset in *Pparg*$^{\Delta/\Delta}$ mice was also recapitulated

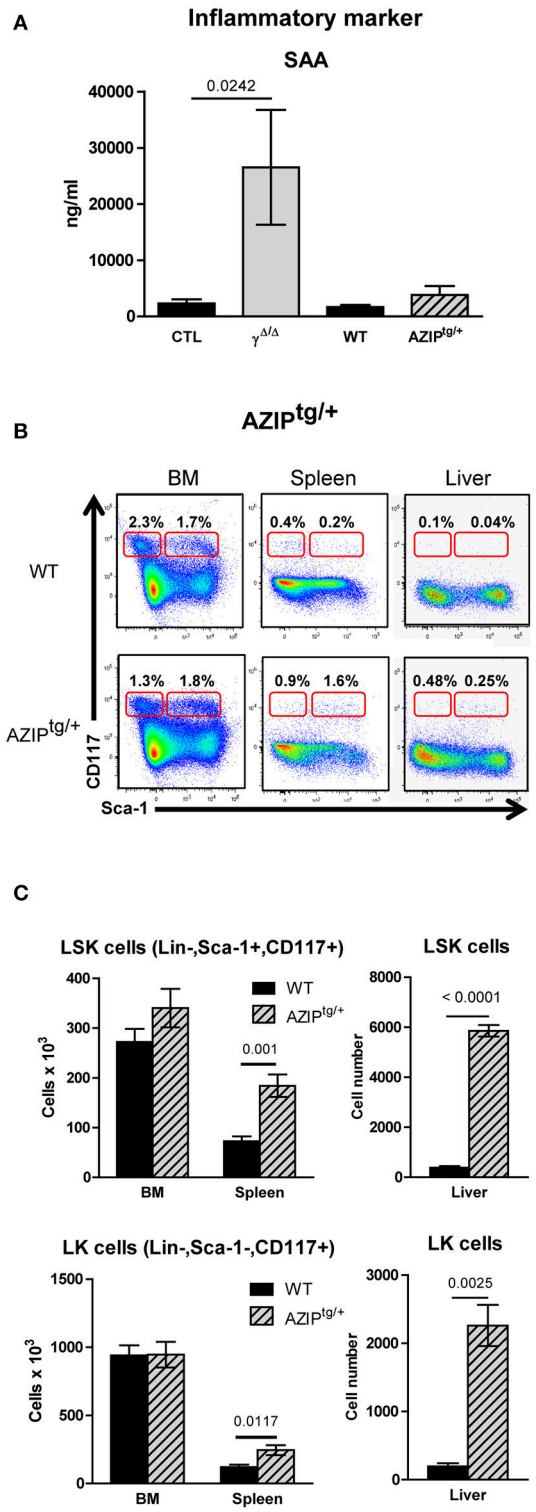

FIGURE 4 | Investigation of extramedullary hematopoiesis in AZIP$^{tg/+}$ mice. **(A)** Serum levels of the inflammatory marker Serum Amyloid A in *Pparg*$^{\Delta/\Delta}$ and in *AZIP*$^{tg/+}$, evaluated by ELISA. Mean ± SEM for 3 to 8 mice per genotype. **(B)** Representative FACS plots showing Sca-1 vs. CD117 staining on lineage-negative bone marrow (BM; left panels) and spleen (middle panels) and liver (right panels) cells from AZIP$^{tg/+}$ (lower row) mice and their wild-type (WT) littermates (upper row). The red frames on the left and right of each plot *(Continued)*

FIGURE 4 | indicate the gating and percentage of LK (Lineage-negative, Sca-1$^-$CD117$^+$) and LSK (Lineage-negative, Sca-1$^+$CD117$^+$) cells, respectively, expressed as a percentage of lineage-negative cells from each organ. **(C)** Histograms showing total numbers of LSK (left panel) and LK (right panel) cells in the BM, spleen and liver of WT control (dark bars) and AZIP$^{tg/+}$ (light hatched bars) mice. Mean ± SEM, $n = 3$–6 mice per genotype. All significant p-values are indicated above the corresponding bars.

in the reverse chimeras in the BM (**Figures 6A,B**), when wild-type cells were used to reconstitute the BM of irradiated *Pparg*$^{\Delta/\Delta}$ mice. However, in AZIP$^{tg/+}$ mice, which harbor no inflammation, increase of the LK cell population was observed in all progenitor subsets without alteration of the MEP to GMP ratio (**Figure 5C**). Consistent with this observation, mRNA expression levels of the myeloid-promoting transcription factor SFPI1/PU.1 were not increased in the bones of AZIP$^{tg/+}$ mice (**Figure 5D**). Altogether, these data suggest that the increased ratio of GMPs over MEPs is in part linked to the systemic inflammation, whereas the EMH is linked to the lipodystrophy context.

Another distinct feature between the phenotypes of *Pparg*$^{\Delta/\Delta}$ and AZIP$^{tg/+}$ mice is that no decrease is observed in the numbers of B lymphocytes in the BM of AZIP$^{tg/+}$ mice (**Supplementary Figures S6A,B**). Further analyses in *Pparg*$^{\boldsymbol{\Delta/\Delta}}$ mice demonstrated more specifically that while the early immature B cell subsets (PreProB, ProPreB, PreBI and large and small PreBII) were similar in control and *Pparg*$^{\boldsymbol{\Delta/\Delta}}$ mice, the numbers of later-stage B cells (IgM$^+$ immature and mature cells) were significantly decreased in the absence of PPARγ (data not shown). These observations, not seen in AZIP$^{tg/+}$ mice, are therefore unlikely to be directly due to the lack of adipocytes in the BM.

Altered HSC Retention in Lipodystrophic Mice BM Contributes to EMH in Peripheral Organs

The next question was therefore which common mechanism in these two models of lipodystrophy would promote EMH. One important systemic perturbation observed in these two models, which is directly due to the lack of adipose tissue, is a severe type 2 diabetes phenotype with hyperglycemia and hyperinsulinemia. To evaluate the possible impact of these metabolic disorders in the induction of EMH, we analyzed the occurrence of EMH in a well-characterized model of type 2 diabetes, the leptin-deficient *ob/ob* mice. In contrast to the *Pparg*$^{\boldsymbol{\Delta/\Delta}}$ and AZIP$^{tg/+}$ mice, no increase in spleen size was observed in *ob/ob* mice (data not shown). Moreover, normal numbers of LSK and LK cells were observed in the spleen of *ob/ob* mice (**Supplementary Figures S6C,D**), thus ruling out metabolic perturbation as a possible cause of EMH.

As the EMH observed in *Pparg*$^{\boldsymbol{\Delta/\Delta}}$ mice was not due to a cell autonomous defect in hematopoietic cells, and was reproduced in another model of lipodystrophy, we hypothesized that the lack of adipocytes or factors produced by adipocytes could be responsible for this phenomenon. Indeed, one mechanism by which peripheral organs such as the liver and the spleen harbor

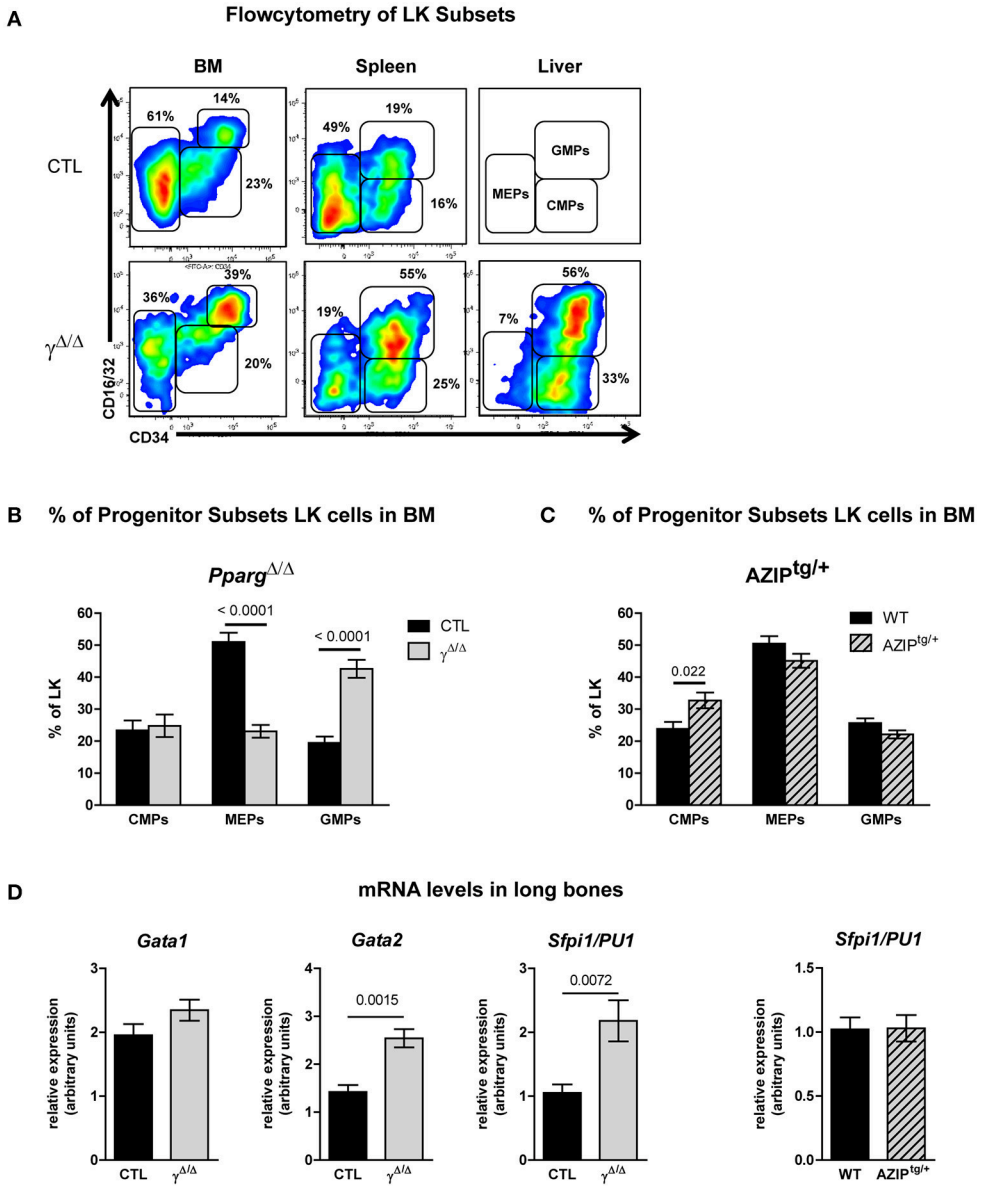

FIGURE 5 | FACS analyses of progenitor cell subsets in the LK population of the bone marrow (BM), spleen, and liver of Pparg$^{\Delta/\Delta}$ and AZIP$^{tg/+}$ mice. **(A)** Representative FACS plots of CD34 vs. CD16/32 expression in the LK subset of the BM (left panels), spleen (middle panels) and liver (right panels) of control (CTL, upper row) and *Pparg*$^{\Delta/\Delta}$ (lower row) mice. As there were insufficient liver cells to make a FACS plot for the CTL mice, the gating strategy for the progenitor subsets is indicated instead. The respective percentages of MEPs (CD34^{-}CD16/32^{-}), CMPs (CD34^{low}CD16/32^{-}), and GMPs (CD34^{+}CD16/32^{+}) are indicated in each plot. LK (Lineage-negative, Sca-1^{-},cKit-r /CD117^{+}); MEP (Megakaryocyte Erythroid Progenitor); CMP (Common Myeloid Progenitor); GMP (Granulocyte Monocyte Progenitor). **(B)** Histograms showing the proportion (%) of CMPs, MEPs and GMPs in the BM LK subset of control (dark bars) and *Pparg*$^{\Delta/\Delta}$ (light bars) mice. Mean ± SEM, $n = 7$–8 mice per genotype. **(C)** Histograms showing the proportion (%) of CMPs, MEPs, and GMPs in the BM LK subset of wild-type (dark bars) and AZIP$^{tg/+}$ (light hatched bars) mice. Mean ± SEM, $n = 7$ mice per genotype. **(D)** mRNA expression levels of the transcription factors *Gata1*, *Gata2, Sfpi1/PU1* evaluated by qRT-PCR in total cellular extracts from the long bones of control (dark bars) vs. *Pparg*$^{\Delta/\Delta}$ mice (light bars) or wild-type (dark bars) and AZIP$^{tg/+}$ (light hatched bars) mice. Mean ± SEM, $n = 5$–7 mice per genotype. All significant *p*-values are indicated above the corresponding bars.

HSC/progenitor cells is through egression of cells from the BM. This also occurs under normal homeostatic conditions, since small numbers of HSC/progenitor cells can be found, albeit at barely detectable levels, in the peripheral organs of normal mice (see for example **Figures 2A–C**).

The lack of adipocytes in the BM of *Pparg*$^{\Delta/\Delta}$ and AZIP$^{tg/+}$ mice may disrupt the local microenvironment. We thus explored whether the EMH observed in the absence of adipocytes resulted from an increase in cellular egress from the BM. As the CXCL12/CXCR4 axis is the main source of retention signals that

maintain hematopoietic stem and progenitor cells (HSPCs) in the BM (26), we evaluated the expression levels of this cytokine (*Cxcl12*) and its receptor (*Cxcr4*) in mRNA isolated from the long bones. These extracts included both stromal and hematopoietic cell niche components. In the two models we studied, the levels of *Cxcl12* remained unaffected, whereas a significant reduction of *Cxcr4* was observed. Albeit it remains speculative, these results suggest that the retention of HSPCs in the BM might be impaired, contributing to the EMH in $Pparg^{\Delta/\Delta}$ and in $AZIP^{tg/+}$ mice. In contrast, *Cxcl12* is decreased in the spleen, whereas *Cxcr4* expression is not affected, indicating that these signals do not contribute to retaining HSCs in the spleen (**Figure 7**). The Sphingosine kinase/sphingosine 1-phosphate (S1P)/S1P receptor axis as well as the Parathyroid hormone (PTH) and its receptor PTHRP, two signals that play a role in this context (27, 28) are not different between the two genotypes (**Figure 7**), excluding their contribution to the phenotype.

Altogether, these results highlight that the occurrence of EMH in lipodystrophic mouse models results from a lack of adipocytes and is aggravated when systemic inflammation occurs.

DISCUSSION

In this study, we explored the role of adipocytes in BM homeostasis and regulation of hematopoiesis and showed that the total lipodystrophy in $Pparg^{\Delta/\Delta}$ mice is accompanied by a severe EMH that impacts upon all hematopoietic lineages. After a thorough analysis of the cell lineages found in the spleen and liver, we first demonstrated that the EMH observed in $Pparg^{\Delta/\Delta}$ mice is not a direct consequence of the lack of PPARγ in hematopoietic cells that normally express PPARγ (29, 30). Indeed, the EMH was reproduced when WT cells were used to reconstitute lethally irradiated $Pparg^{\Delta/\Delta}$ mice. We then observed EMH in an independent model of lipodystrophy ($AZIP^{tg/+}$). Albeit, we cannot exclude a contribution of inflammation in $Pparg^{\Delta/\Delta}$ mice, data from both models indicate that the most likely causes of EMH are linked to the lipodystrophy with possible local alterations of the BM microenvironment. Thus, the combination of the two experimental models of lipodystrophy used, $Pparg^{\Delta/\Delta}$ and $AZIP^{tg/+}$, allowed us to reveal an important contribution of adiposity in setting the appropriate BM microenvironment required for normal hematopoiesis.

There are three main known causes of EMH in the clinics and in experimental settings. The first one is associated with myelofibrosis disorders, which trigger a compensation in hematopoietic organs such as the spleen and liver to maintain functional hematopoiesis (31). Primary myelofibrosis begins as a myeloproliferative disorder and leads to an altered marrow with cellular abnormalities. Along this line, EMH has also been observed in mice carrying hypomorphic *Pparg* alleles and was shown to result from structural changes in the bones and thus reduced numbers of BM cells (32). In contrast, we found here that the BM in $Pparg^{\Delta/\Delta}$ and $AZIP^{tg/+}$ mice exhibited close to normal cell numbers, with neither myeloproliferation nor dramatic changes in the HSC population, excluding myelofibrosis as the cause of EMH. The second main cause of EMH is hypoxia, in which the increased need of red blood cell production is the trigger. The stress response to hypoxia in the context of hemoglobinopathy (33) stimulates erythropoiesis and increases hematocrit. Again, neither increases in erythropoiesis nor increased hematocrit were observed in the absence of PPARγ or in $AZIP^{tg/+}$ mice, making this hypothesis also unlikely.

The third main cause of EMH is the presence of severe systemic inflammation, particularly in rodents, where it is associated with a marked increase in granulopoiesis (17). Local skin inflammation is indeed observed in $Pparg^{\Delta/\Delta}$ mice and was associated with PPARγ-dependent scarring alopecia (18). However, this feature is specific to $Pparg^{\Delta/\Delta}$ mice and not found in $AZIP^{tg/+}$ mice. In addition, the blood levels of the inflammatory markers are significantly increased in $Pparg^{\Delta/\Delta}$ mice but not in $AZIP^{tg/+}$ mice. Thus, although we cannot rule out a contribution of inflammation, particularly in the case of the $Pparg^{\Delta/\Delta}$ mice, it does not explain the presence of EMH in $AZIP^{tg/+}$ mice. These distinct features in terms of inflammation also provide an explanation for the biased development of CMPs toward the myeloid lineage at the expense of the erythroid and megakaryocyte lineages seen only in $Pparg^{\Delta/\Delta}$ and not in $AZIP^{tg/+}$ mice. The inflammation seen in the former and not in the latter likely contributes to this shift in CMP commitment. The resulting relative decrease in the number of erythroblasts in the BM of $Pparg^{\Delta/\Delta}$ mice might thus be compensated for by active EMH.

Finally, although the three mouse models described in this study ($Pparg^{\Delta/\Delta}$, $AZIP^{tg/+}$, and *ob/ob*) are all affected by type 2 diabetes, the fact that *ob/ob* mice did not exhibit EMH excludes this systemic metabolic disorder as a common causative factor. Thus in this context, the most likely hypothesis is that adipocytes function to contribute to hematopoietic homeostasis in the BM.

The BM transfer experiment that we performed clearly indicates that the bone cavity micro-environment was involved in the EMH observed in our experimental models. The BM stem cell niche concept was first defined as a local microenvironment that maintains and regulates the function of stem and progenitor cells (1), and many cell types have been shown to be involved in these processes [reviewed in (2–4)]. BM adipocytes may or may not be considered as part of the niche *per se,* but they are present in large numbers and could contribute to the microenvironment in several ways. First, they play a role in bone homeostasis, which may indirectly affect the BM stem cell niche. This is due to the fact that adipocytes and osteoblasts are linked *via* their common mesenchymal progenitors, resulting in a balance between adipogenesis and osteoblastogenesis. PPARγ is central in this balance since this nuclear factor is a crucial regulator of MSC orientation toward adipocytes, as it's *ex vivo* or *in vitro* activation using synthetic agonists results in an adipogenic MSC phenotype, whereas it's pharmacological blockade or genetic deletion result in the opposite phenotype i.e., an osteoblastic phenotype (34, 35). Moreover, leptin and adiponectin, which are secreted by adipocytes, also exert a local and systemic role in bone homeostasis [reviewed in (36)]. Second, a direct function for adipocytes in supporting the proliferation of hematopoietic cells has been proposed, albeit the nature of this support function is not well described. It could combine energy sources and specific

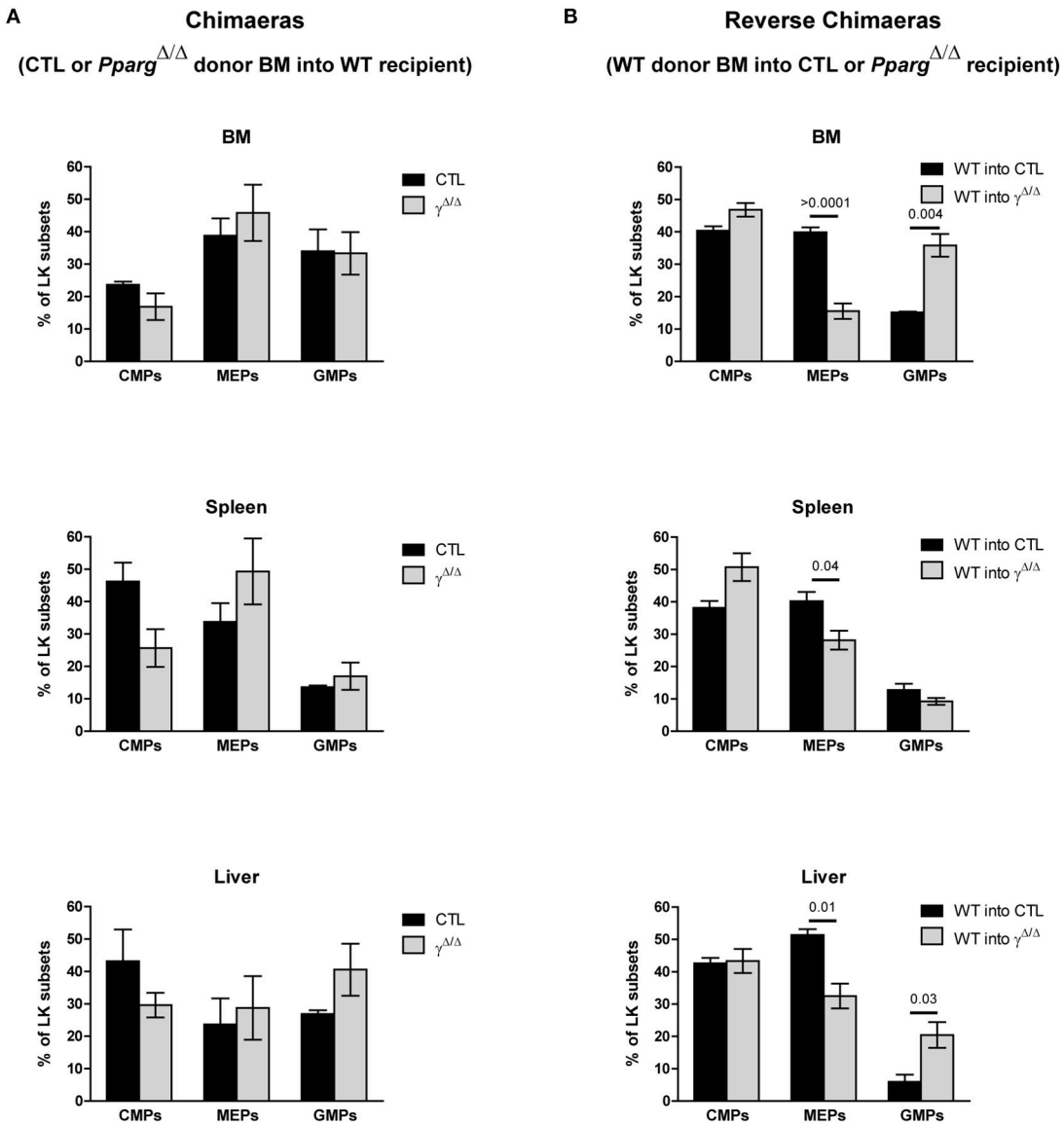

FIGURE 6 | FACS analyses of progenitor cell subsets in the LK population in chimeras and AZIP$^{tg/+}$ mice. **(A)** Chimeras using wild-type recipients and control or *Pparg*$^{\Delta/\Delta}$ donor BM. Hematopoietic reconstitution was evaluated by FACS analysis 3 months after the transfer (see also **Figure 3A**). The histograms show the proportion (%) of CMPs (CD34^{low}CD16/32^{-}), MEPs (CD34^{-}CD16/32^{-}), and GMPs (CD34^{+}CD16/32^{+}) in the LK cell subset, in the BM, the spleen and the liver of WT mice reconstituted with control (dark bars) or *Pparg*$^{\Delta/\Delta}$ (light bars) BM. Mean ± SEM, $n = 3$ mice per genotype. No significant p-value. **(B)** Reverse chimeras using wild-type (WT) control donor BM transferred into *Pparg*$^{\Delta/\Delta}$ or their littermate control (CTL) recipient. The histograms show the proportion (%) of CMPs, MEPs and GMPs in the LK cell subset in the BM, the spleen and the liver of control (dark bars) or *Pparg*$^{\Delta/\Delta}$ (light bars) mice reconstituted with wild-type donor BM. Mean ± SEM, $n = 3$ mice per genotype. All significant p-values are indicated above the corresponding bars.

adipokines, which have been proposed to mediate various aspects of HSC maintenance, quiescence and proliferation *in vitro* (9, 37, 38). In contrast, two reports have shown an anti-correlation between the number of adipocytes present in the bone cavity and the rapidity of recovery after BM irradiation (13, 39). One possible way to reconcile these conflicting observations is that the support provided by adipocytes may differ between *in vitro* and i*n vivo* conditions as proposed by Spindler et al. (40). In agreement with our results, it is tempting to speculate on a specific role for BM adipocytes in this phenotype. However, our experiments do not exclude the possibility of a systemic cue directly related to the generalized lipoatrophy.

A possible consequence of an altered BM microenvironment is a modification of the balance between active retention and mobilization of HSCs. We showed that in the absence of PPARγ, all hematopoietic lineages are increased. Thus, the most likely explanation for the observed EMH is reduced BM colonization at birth or an increase in egress of HSCs and early progenitors

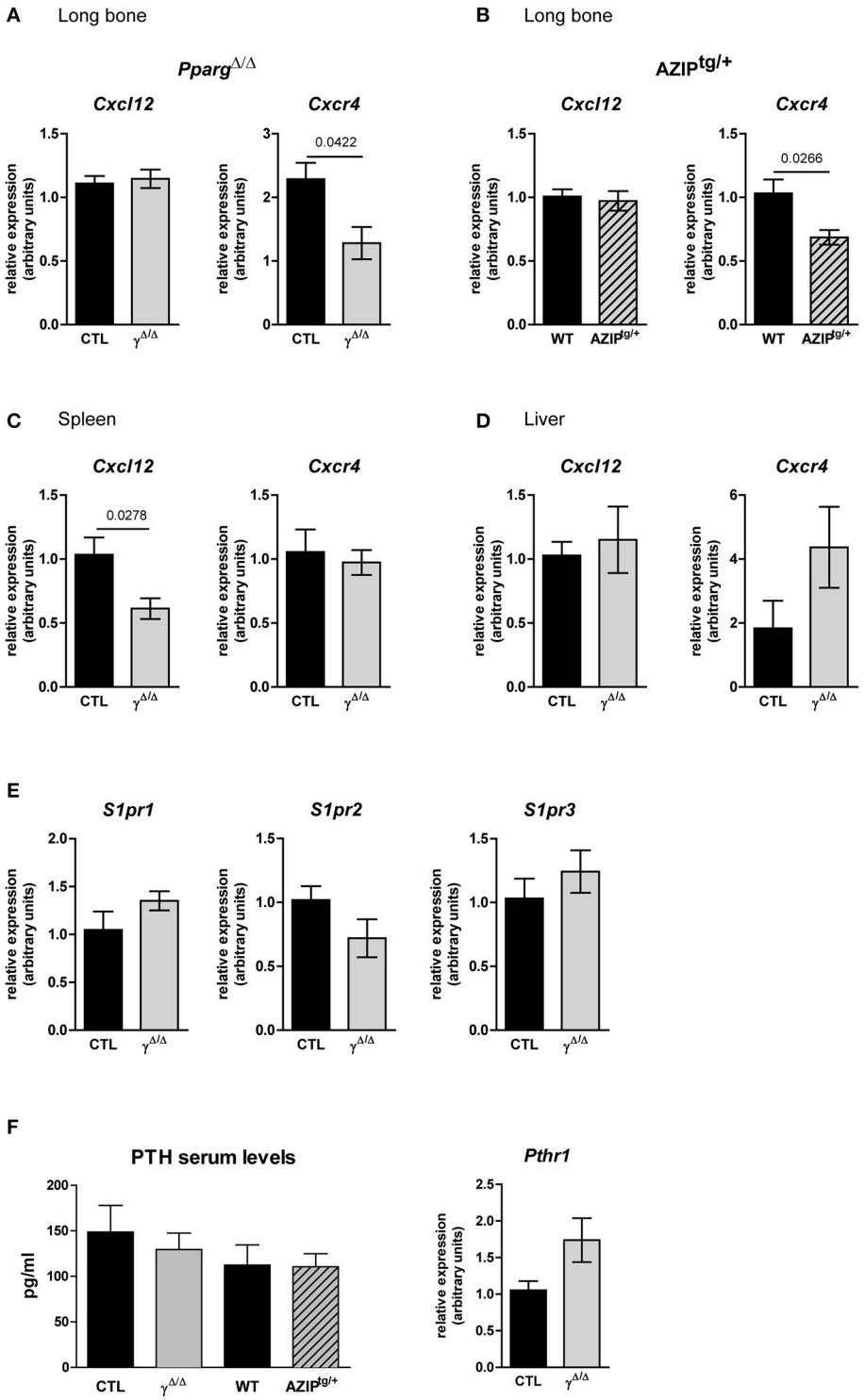

FIGURE 7 | Gene expression of key factors of cell egress from the BM in Pparg$^{\Delta/\Delta}$ and AZIP$^{tg/+}$ mice. **(A,B)** *Cxcl12* and *Cxcr4* mRNA expression in the long bones of *Pparg*$^{\Delta/\Delta}$ **(A)** and AZIP$^{tg/+}$ **(B)** mice and their controls, CTL and WT, respectively, as indicated. Mean ± SEM for 3 to 6 mice per genotype. **(C,D)** *Cxcl12* and *Cxcr4* mRNA expression in the spleen **(C**; Mean ± SEM for 5 mice per genotype) and the liver **(D**; Mean ± SEM for 6 to 7 mice per genotype) of *Pparg*$^{\Delta/\Delta}$ mice and their control. **(E)** Expression levels of Sphingosine Sphingosine kinase/sphingosine 1-phosphate receptors genes, *S1pr1, S1pr2, S1pr3*, in the long bone of *Pparg*$^{\Delta/\Delta}$ mice and their control. **(F)** Parathyroid hormone (PTH) serum levels and gene expression of its receptor PTHR1 in long bones of *Pparg*$^{\Delta/\Delta}$ mice and their control Mean ± SEM for 3 to 4 mice per genotype. All significant *p*-values are indicated above the corresponding bars.

from the BM. This is consistent with the fact that HSCs within the BM are very mobile cells, and that a small number of HSCs are constantly released into the circulation (41). Nevertheless, the best characterized mechanism of HSC and progenitor cell egress from the BM is the one provoked by pharmacological doses of G-CSF administered to patients for stem cell mobilization prior to autologous transplantation. This involves down-regulation of CXCL12, which is expressed by perivascular MSCs and CAR cells, as well as by osteoblast lineage cells. This decreased expression prevents interaction of CXCL12 with its receptor CXCR4 expressed by HSCs and progenitors, and the retention and survival of HSCs and progenitor cells in the BM (42, 43). In the models presented herein, *Cxcl12* expression levels in the BM were not altered, but gene expression of its receptor CXCR4 was significantly impaired. Pharmacological antagonists of CXCR4 are among the main recent innovations improving HSC mobilization in patients (44). Altogether, our observations are consistent with an alteration of the BM microenvironment due to the total lack of adipocytes, with loss of retention and/or increased egress of HSCs and progenitor cells from the BM to the peripheral organs, albeit this mechanistic hypothesis remains speculative. Nevertheless, we cannot completely exclude the contribution of an increased pool of splenic HSCs during development in both models of lipodystrophic mice. This could be due to reduced BM colonization at birth, when stem cell niches are being formed, or to an increased retention in spleen and liver, which are the primary sites of hematopoiesis before birth, although the decrease in CXCL12 expression in the spleen, does not favor this hypothesis.

The main limitation of the present study originates from the fact that mice, like most rodents, are more prone to develop EMH than humans. Nonetheless, our results strongly support the fact that lack or scarcity of adipocytes is deleterious for BM hematopoiesis. A deeper analysis of the adipocytes in the BM stem cell niche itself, more particularly with respect to their paracrine activity and cell-cell contacts may help to better define the role of adipocytes in cell retention/egress from the BM and highlight the importance of some key factors of interest for clinical situations of BM transfer. Alternately, and not exclusively, the search for a systemic cue linked to the generalized lipodystrophy might provide new avenues of research in hematopoiesis.

AUTHOR CONTRIBUTIONS

AW conceived the study, designed the experimental plan, performed all flow cytometry experiments, analyzed the data, wrote the manuscript, and acquired financial support for the project. HF designed the experimental plan, performed the experiments, analyzed the data, and contribute to the original draft preparation. MS, CW, and MK performed experiments, analyzed the data, and prepared the vizualisation. FG, NB, and J-YJ contributed to the conceptualization, analyzed the data, and reviewed/edited the manuscript. FR and SL performed histology experiments, analyzed the data, and prepared the figure for the spleen characterization. DM performed experiments, analyzed the data, contribute to the conceptualization, and reviewed/edited the manuscript. BD conceived the study, designed the experimental plan, supervised the study, analyzed the data, wrote the manuscript, and acquired financial support for the project. All authors read and edited the manuscript. AW and BD are the guarantors of this work and, as such, had full access to all the data in the study and take responsibility for the integrity of the data and the accuracy of the data analyses.

ACKNOWLEDGMENTS

We are indebted to Charles Vinson for providing the AZIP mouse line. The authors would like to thank Danny Labes of the University of Lausanne Flow Cytometry Facility. We warmly thank Professors Andreas Trump, Olaia Naveiras, Ping-Chih Ho, Serge Ferrari, Marie-Thérèse Rubio, and Doctor Cécile Pochon for helpful discussions. This work was supported by the Etat de Vaud (BD and AW) the FNRS (BD), the Région Grand Est (J-YJ), the Fondation Arthritis (DM) and by the french PIA project Lorraine Université d'Excellence, reference ANR-15-IDEX-04-LUE (J-YJ and DM).

SUPPLEMENTARY MATERIAL

The Supplementary Material for this article can be found online at: https://www.frontiersin.org/articles/10.3389/fimmu.2018.02573/full#supplementary-material

REFERENCES

1. Schofield R. The relationship between the spleen colony-forming cell and the haemopoietic stem cell. *Blood Cells* (1978) 4:7–25.
2. Kfoury Y, Scadden DT. Mesenchymal cell contributions to the stem cell niche. *Cell Stem Cell* (2015) 16:239–53. doi: 10.1016/j.stem.2015.02.019
3. Morrison SJ, Scadden DT. The bone marrow niche for haematopoietic stem cells. *Nature* (2014) 505:327–34. doi: 10.1038/nature12984
4. Nakamura-Ishizu A, Suda T. Hematopoietic stem cell niche: an interplay among a repertoire of multiple functional niches. *Biochim Biophys Acta* (2013) 1830:2404–9. doi: 10.1016/j.bbagen.2012.08.023
5. Rosen ED, Spiegelman BM. What we talk about when we talk about fat. *Cell* (2014) 156:20–44. doi: 10.1016/j.cell.2013.12.012
6. Luo L, Liu M. Adipose tissue in control of metabolism. *J Endocrinol.* (2016) 231:R77–99. doi: 10.1530/JOE-16-0211
7. Capeau J, Magre J, Caron-Debarle M, Lagathu C, Antoine B, Bereziat V, et al. Human lipodystrophies: genetic and acquired diseases of adipose tissue. *Endocr Dev*. (2010) 19:1–20. doi: 10.1159/000316893
8. Veldhuis-Vlug AG, Rosen CJ. Mechanisms of marrow adiposity and its implications for skeletal health. *Metabolism* (2017) 67:106–14. doi: 10.1016/j.metabol.2016.11.013
9. Claycombe K, King LE, Fraker PJ. A role for leptin in sustaining lymphopoiesis and myelopoiesis. *Proc Natl Acad Sci USA*. (2008) 105:2017–21. doi: 10.1073/pnas.0712053105
10. DiMascio L, Voermans C, Uqoezwa M, Duncan A, Lu D, Wu J, et al. Identification of adiponectin as a novel hemopoietic stem cell growth factor. *J Immunol.* (2007) 178:3511–20. doi: 10.4049/jimmunol.178.6.3511

11. Masamoto Y, Arai S, Sato T, Kubota N, Takamoto I, Kadowaki T, et al. Adiponectin enhances quiescence exit of murine hematopoietic stem cells and hematopoietic recovery through mTORC1 potentiation. *Stem Cells* (2017) 35:1835–48. doi: 10.1002/stem.2640
12. Zhou BO, Yu H, Yue R, Zhao Z, Rios JJ, Naveiras O, et al. Bone marrow adipocytes promote the regeneration of stem cells and haematopoiesis by secreting SCF. *Nat Cell Biol*. (2017) 19:891–903. doi: 10.1038/ncb3570
13. Naveiras O, Nardi V, Wenzel PL, Hauschka PV, Fahey F, Daley GQ. Bone-marrow adipocytes as negative regulators of the haematopoietic microenvironment. *Nature* (2009) 460:259–63. doi: 10.1038/nature08099
14. Sertorio M, Du W, Amarachintha S, Wilson A, Pang Q. *In vivo* RNAi screen unveils PPARgamma as a regulator of hematopoietic stem cell homeostasis. *Stem Cell Rep*. (2017) 8:1242–55. doi: 10.1016/j.stemcr.2017.03.008
15. Barak Y, Nelson MC, Ong ES, Jones YZ, Ruiz-Lozano P, Chien KR, et al. PPAR gamma is required for placental, cardiac, and adipose tissue development. *Mol Cell* (1999) 4:585–95. doi: 10.1016/S1097-2765(00)80209-9
16. Nadra K, Quignodon L, Sardella C, Joye E, Mucciolo A, Chrast R, et al. PPARgamma in placental angiogenesis. *Endocrinology* (2010) 151:4969–81. doi: 10.1210/en.2010-0131
17. Johns JL, Christopher MM. Extramedullary hematopoiesis: a new look at the underlying stem cell niche, theories of development, and occurrence in animals. *Vet Pathol*. (2012) 49:508–23. doi: 10.1177/0300985811432344
18. Sardella C, Winkler C, Quignodon L, Hardman JA, Toffoli B, Giordano Attianese GMP, et al. Delayed hair follicle morphogenesis and hair follicle dystrophy in a lipoatrophy mouse model of pparg total deletion. *J Invest Dermatol*. (2018) 138:500–10. doi: 10.1016/j.jid.2017.09.024
19. Moitra J, Mason MM, Olive M, Krylov D, Gavrilova O, Marcus-Samuels B, et al. Life without white fat: a transgenic mouse. *Genes Dev*. (1998) 12:3168–81. doi: 10.1101/gad.12.20.3168
20. Wilson A, Laurenti E, Oser G, van der Wath RC, Blanco-Bose W, Jaworski M, et al. Hematopoietic stem cells reversibly switch from dormancy to self-renewal during homeostasis and repair. *Cell* (2008) 135:1118–29. doi: 10.1016/j.cell.2008.10.048
21. Radtke F, Wilson A, Stark G, Bauer M, van Meerwijk J, MacDonald HR, et al. Deficient T cell fate specification in mice with an induced inactivation of Notch1. *Immunity* (1999) 10:547–58. doi: 10.1016/S1074-7613(00)80054-0
22. Link A, Vogt TK, Favre S, Britschgi MR, Acha-Orbea H, Hinz B, et al. Fibroblastic reticular cells in lymph nodes regulate the homeostasis of naive T cells. *Nat Immunol*. (2007) 8:1255–65. doi: 10.1038/ni1513
23. Toffoli B, Gilardi F, Winkler C, Soderberg M, Kowalczuk L, Arsenijevic Y, et al. Nephropathy in Pparg-null mice highlights PPARgamma systemic activities in metabolism and in the immune system. *PLoS ONE* (2017) 12:e0171474. doi: 10.1371/journal.pone.0171474
24. Wilson A, Trumpp A. Bone-marrow haematopoietic-stem-cell niches. *Nat Rev Immunol*. (2006) 6:93–106. doi: 10.1038/nri1779
25. Serwold T, Ehrlich LI, Weissman IL. Reductive isolation from bone marrow and blood implicates common lymphoid progenitors as the major source of thymopoiesis. *Blood* (2009) 113:807–15. doi: 10.1182/blood-2008-08-17ss3682
26. Karpova D, Bonig H. Concise review: CXCR4/CXCL12 signaling in immature hematopoiesis–lessons from pharmacological and genetic models. *Stem Cells* (2015) 33:2391–9. doi: 10.1002/stem.2054
27. Cyster JG, Schwab SR. Sphingosine-1-phosphate and lymphocyte egress from lymphoid organs. *Annu Rev Immunol*. (2012) 30:69–94. doi: 10.1146/annurev-immunol-020711-075011
28. Calvi LM, Adams GB, Weibrecht KW, Weber JM, Olson DP, Knight MC, et al. Osteoblastic cells regulate the haematopoietic stem cell niche. *Nature* (2003) 425:841–6. doi: 10.1038/nature02040
29. Choi JM, Bothwell AL. The nuclear receptor PPARs as important regulators of T-cell functions and autoimmune diseases. *Mol Cells*. (2012) 33:217–22. doi: 10.1007/s10059-012-2297-y
30. Ramon S, Bancos S, Thatcher TH, Murant TI, Moshkani S, Sahler JM, et al. Peroxisome proliferator-activated receptor gamma B cell-specific-deficient mice have an impaired antibody response. *J Immunol*. (2012) 189:4740–7. doi: 10.4049/jimmunol.1200956
31. Wolf BC, Neiman RS. Myelofibrosis with myeloid metaplasia: pathophysiologic implications of the correlation between bone marrow changes and progression of splenomegaly. *Blood* (1985) 65:803–9.
32. Cock TA, Back J, Elefteriou F, Karsenty G, Kastner P, Chan S, et al. Enhanced bone formation in lipodystrophic PPARgamma(hyp/hyp) mice relocates haematopoiesis to the spleen. *EMBO Rep*. (2004) 5:1007–12. doi: 10.1038/sj.embor.7400254
33. Tan TC, Tsao J, Cheung FC. Extramedullary haemopoiesis in thalassemia intermedia presenting as paraplegia. *J Clin Neurosci*. (2002) 9:721–5. doi: 10.1054/jocn.2001.1038
34. Rzonca SO, Suva LJ, Gaddy D, Montague DC, Lecka-Czernik B. Bone is a target for the antidiabetic compound rosiglitazone. *Endocrinology* (2004) 145:401–6. doi: 10.1210/en.2003-0746
35. Akune T, Ohba S, Kamekura S, Yamaguchi M, Chung UI, Kubota N, et al. PPARgamma insufficiency enhances osteogenesis through osteoblast formation from bone marrow progenitors. *J Clin Invest*. (2004) 113:846–55. doi: 10.1172/JCI200419900
36. Lecka-Czernik B, Stechschulte LA. Bone and fat: a relationship of different shades. *Arch Biochem Biophys*. (2014) 561:124–9. doi: 10.1016/j.abb.2014.06.010
37. Gimble JM, Robinson CE, Wu X, Kelly KA. The function of adipocytes in the bone marrow stroma: an update. *Bone* (1996) 19:421–8. doi: 10.1016/S8756-3282(96)00258-X
38. Glettig DL, Kaplan DL. Extending human hematopoietic stem cell survival *in vitro* with adipocytes. *Biores Open Access*. (2013) 2:179–85. doi: 10.1089/biores.2013.0006
39. Zhu RJ, Wu MQ, Li ZJ, Zhang Y, Liu KY. Hematopoietic recovery following chemotherapy is improved by BADGE-induced inhibition of adipogenesis. *Int J Hematol*. (2013) 97:58–72. doi: 10.1007/s12185-012-1233-4
40. Spindler TJ, Tseng AW, Zhou X, Adams GB. Adipocytic cells augment the support of primitive hematopoietic cells in vitro but have no effect in the bone marrow niche under homeostatic conditions. *Stem Cells Dev*. (2014) 23:434–41. doi: 10.1089/scd.2013.0227
41. Wright DE, Wagers AJ, Gulati AP, Johnson FL, Weissman IL. Physiological migration of hematopoietic stem and progenitor cells. *Science* (2001) 294:1933–6. doi: 10.1126/science.1064081
42. Foudi A, Jarrier P, Zhang Y, Wittner M, Geay JF, Lecluse Y, et al. Reduced retention of radioprotective hematopoietic cells within the bone marrow microenvironment in CXCR4-/- chimeric mice. *Blood* (2006) 107:2243–51. doi: 10.1182/blood-2005-02-0581
43. Sugiyama T, Kohara H, Noda M, Nagasawa T. Maintenance of the hematopoietic stem cell pool by CXCL12-CXCR4 chemokine signaling in bone marrow stromal cell niches. *Immunity* (2006) 25:977–88. doi: 10.1016/j.immuni.2006.10.016
44. Bonig H, Papayannopoulou T. Hematopoietic stem cell mobilization: updated conceptual renditions. *Leukemia* (2013) 27:24–31. doi: 10.1038/leu.2012.254

Conflict of Interest Statement: The authors declare that the research was conducted in the absence of any commercial or financial relationships that could be construed as a potential conflict of interest.

frontiers in Immunology

ORIGINAL RESEARCH
published: 05 February 2019
doi: 10.3389/fimmu.2019.00097

New Insights for RANKL as a Proinflammatory Modulator in Modeled Inflammatory Arthritis

Maria Papadaki[1,2], *Vagelis Rinotas*[1,2], *Foteini Violitzi*[1,2], *Trias Thireou*[1], *George Panayotou*[3], *Martina Samiotaki*[3] *and Eleni Douni*[1,2]*

[1] Laboratory of Genetics, Department of Biotechnology, Agricultural University of Athens, Athens, Greece, [2] Division of Immunology, Biomedical Sciences Research Center "Alexander Fleming", Athens, Greece, [3] Division of Molecular Oncology, Biomedical Sciences Research Center "Alexander Fleming", Athens, Greece

Receptor activator of nuclear factor-κB ligand (RANKL), a member of the Tumor Necrosis Factor (TNF) superfamily, constitutes the master regulator of osteoclast formation and bone resorption, whereas its involvement in inflammatory diseases remains unclear. Here, we used the human TNF transgenic mouse model of erosive inflammatory arthritis to determine if the progression of inflammation is affected by either genetic inactivation or overexpression of RANKL in transgenic mouse models. TNF-mediated inflammatory arthritis was significantly attenuated in the absence of functional RANKL. Notably, TNF overexpression could not compensate for RANKL-mediated osteopetrosis, but promoted osteoclastogenesis between the pannus and bone interface, suggesting RANKL-independent mechanisms of osteoclastogenesis in inflamed joints. On the other hand, simultaneous overexpression of RANKL and TNF in double transgenic mice accelerated disease onset and led to severe arthritis characterized by significantly elevated clinical and histological scores as shown by aggressive pannus formation, extended bone resorption, and massive accumulation of inflammatory cells, mainly of myeloid origin. RANKL and TNF cooperated not only in local bone loss identified in the inflamed calcaneous bone, but also systemically in distal femurs as shown by microCT analysis. Proteomic analysis in inflamed ankles from double transgenic mice overexpressing human TNF and RANKL showed an abundance of proteins involved in osteoclastogenesis, pro-inflammatory processes, gene expression regulation, and cell proliferation, while proteins participating in basic metabolic processes were downregulated compared to TNF and RANKL single transgenic mice. Collectively, these results suggest that RANKL modulates modeled inflammatory arthritis not only as a mediator of osteoclastogenesis and bone resorption but also as a disease modifier affecting inflammation and immune activation.

Keywords: RANKL, TNF, inflammation, arthritis, transgenic models, proteomics

OPEN ACCESS

Edited by:
Claudine Blin-Wakkach, UMR7370 Laboratoire de Physio Médecine Moléculaire (LP2M), France

Reviewed by:
Christopher G. Mueller, Center for the National Scientific Research (CNRS), France
João Eurico Fonseca, Universidade de Lisboa, Portugal

***Correspondence:**
Eleni Douni
douni@aua.gr

Specialty section:
This article was submitted to Inflammation, a section of the journal Frontiers in Immunology

Received: *28 November 2018*
Accepted: *14 January 2019*
Published: *05 February 2019*

Citation:
Papadaki M, Rinotas V, Violitzi F, Thireou T, Panayotou G, Samiotaki M and Douni E (2019) New Insights for RANKL as a Proinflammatory Modulator in Modeled Inflammatory Arthritis. Front. Immunol. 10:97. doi: 10.3389/fimmu.2019.00097

INTRODUCTION

Receptor Activator of Nuclear Factor κB Ligand (RANKL), a Tumor necrosis factor (TNF) superfamily member, is the master regulator of osteoclast-induced bone resorption (1), that is necessary for the lifelong process of bone remodeling where mature bone tissue is removed from the skeleton and new bone tissue is formed by osteoblasts. RANKL binds as a trimer to its

receptor RANK to promote osteoclast differentiation, activity and survival, which subsequently leads to bone resorption (2, 3). Osteoclasts derive from the myeloid lineage and have the unique ability to resorb bone through the decalcification and degradation of the bone matrix by hydrochloric acid and proteolysis, respectively (4). Genetic ablation of either RANKL or RANK results in severe osteopetrosis, a disease caused by osteoclast deficit, demonstrating that the RANKL/RANK system is indispensable for osteoclastogenesis (5–7). The function of RANKL is physiologically inhibited by the action of the decoy receptor osteoprotegerin (OPG) that binds to RANKL and prevents the process of osteoclastogenesis (8). An imbalance at the RANKL:OPG ratio caused by abundant RANKL levels is believed to be a major determinant in the development of bone loss diseases, including postmenopausal osteoporosis, a metabolic bone disease characterized by decreased bone density and increased fracture risk (9). The critical role of RANKL in osteoporosis is now well-established by the efficacy of denosumab, a human monoclonal anti-RANKL antibody, that specifically inhibits the interaction between RANKL and RANK, in postmenopausal osteoporosis (10). Although RANKL is best known for its function in osteoclastogenesis, it also plays multiple roles in the immune system (11), as it has been shown to enhance dendritic cell survival and regulates lymph node organogenesis. In addition, RANKL controls the development of autoimmune regulator $(AIRE)^{+}$ medullary thymic epithelial cells suggesting a key role of RANKL/RANK signals in the regulation of central tolerance. RANKL expression could also be detected in synovial fibroblasts and inflammatory cells isolated from the synovial fluid of Rheumatoid Arthritis (RA) patients, facilitating osteoclast maturation even in the absence of osteoblasts. Although the inhibition of RANKL effectively arrests progression of arthritic osteolysis, there are no evidence so far to support proinflammatory properties of RANKL (12). Thus, the role of RANKL in the progression of inflammation in RA remains unclear.

RA is a complex inflammatory disease characterized by synovial hyperplasia, cartilage damage, and bone erosions, leading to progressive disability. Inflammatory synovium, mainly including macrophage-like and fibroblast-like synoviocytes, leads to pannus formation that destroys the local articular structures through proteolytic digestion of the extracellular matrix (13). The destructive processes in RA involve a complex interplay between synovial fibroblasts, lymphocytes, macrophages, proinflammatory cytokines, and chemokines, inducing osteoclast-mediated bone resorption. TNF is a key proinflammatory cytokine in RA (14), as experimentally shown by the spontaneous development of chronic inflammatory polyarthritis upon TNF overexpression in transgenic mice (15, 16) and clinically by the efficacy of anti-TNF therapies in RA patients (17). Apart from its proinflammatory role, TNF also promotes bone resorption at sites of chronic inflammation, through the induction of osteoclastogenesis (18). Even though the RANK/RANKL signaling is also involved in local osteolysis induced by chronic inflammation, it remains unclear whether it is the absolute pathway. Previous studies have shown that proinflammatory cytokines such as TNF can compensate for RANKL during osteoclastogenesis *in vitro* (19–21), whereas it is unclear whether TNF can lead to osteoclastogenesis independently of RANKL, *in vivo*.

In the present study, we investigated the role of RANKL as a disease modifier in TNF-driven inflammatory arthritis employing two proprietary genetic models of RANKL-mediated pathologies; an osteopetrosis model caused by osteoclast absence due to a functional mutation in the *RANKL* gene (22) ($Rankl^{tles/tles}$ mice) and osteoporosis transgenic models that overexpress human RANKL (TgRANKL mice) displaying increased osteoclast activity and bone resorption (23). Our results showed that the onset and the progression of TNF-mediated arthritis is dramatically affected by deregulated RANKL expression, supporting an underestimated role of RANKL in inflammatory osteolytic diseases.

MATERIALS AND METHODS

Mouse Husbandry

Osteopetrotic $Rankl^{tles/tles}$ mice (22), osteoporotic Tg5516 and Tg5519 mice (23), and arthritic Tg197 mice (15) were maintained and bred under specific pathogen free conditions in the animal facility of Biomedical Sciences Research Center "Alexander Fleming." All animal procedures were approved and carried out in strict accordance with the guidelines of the Institutional Animal Care and Use Committee and the Region of Attica Veterinarian Office.

Arthritic Clinical Score

Arthritis was evaluated macroscopically weekly in ankle joints in a blinded manner using the following semi-quantitative arthritis score (24); 0: no arthritis (normal appearance and grip strength); (1) mild arthritis (joint swelling); (2) moderate arthritis (severe joint swelling and digit deformation, no grip strength); and (3) severe arthritis (ankylosis detected on flexion and severely impaired movement). Grip strength was evaluated as regards the ability of the mouse to grasp the cage grid cover.

Histological Processing and Scoring of Joints

Ankle joints and femurs were fixed in 10% formalin overnight at 4°C, decalcified in 13% EDTA for 14 days, and embedded in paraffin. Sections of 5 μm thickness were stained with hematoxylin and eosin, and the histopathologic score was evaluated microscopically, in a blinded manner using a modified scoring system (24) as follows; 0: no detectable pathology; 1: hyperplasia of the synovial membrane and presence of polymorphonuclear infiltrates; 2: pannus and fibrous tissue formation and focal subchondral bone erosion; 3: articular cartilage destruction and bone erosion; 4: extensive articular cartilage destruction and bone erosion, and 5: massive destruction of ankle joint with undefined structure. Osteoclasts were stained for TRAP (Tartrate Resistant Acid Phosphatase) activity using the leukocyte acid phosphatase kit 386A (Sigma-Aldrich), whereas cartilage was stained with Toluidine Blue (Sigma-Aldrich). TRAP staining was quantified as an osteoclast surface fraction (percentage of osteoclast surface in total bone surface, Oc.S/BS, %) focusing either in the bone marrow compartment area or the pannus-bone interface area using the

open source software for bone histomorphometry "TrapHisto" (25).

MicroCT Analysis

Bone samples (ankles and femurs) were fixed in 10% formalin overnight at 4°C and then washed and stored in PBS. Microarchitecture of the ankle joints and the distal femurs from 6 weeks old mice was evaluated using a high-resolution SkyScan1172 microtomographic (microCT) imaging system (Bruker). Images were acquired at 50 KeV, 100 μA with a 0.5 mm aluminum filter. Three-dimensional reconstructions (8.8 mm cubic resolution) were generated using NRecon software (Bruker) as previously described (26). For the trabecular area of the calcaneous bone, we assessed the bone volume fraction (BV/TV, %), and trabecular number (Tb.N, mm^{-1}). Calcaneous trabecular geometry was assessed using 75 continuous CT slides (300 μm) located at trabecular area underneath the growth plate of the calcaneous bone. For the trabecular area of the distal femur bone we assessed the bone volume fraction (BV/TV, %), and the trabecular number (Tb.N, mm^{-1}). Femoral trabecular geometry was assessed using 300 continuous CT slides (1,800 μm) located at the trabecular area underneath the growth plate. Femural cortical geometry was assessed using 100 continuous CT slides (600 μm) located at the femoral midshaft, where the bone volume fraction (BV/TV, %) and the bone volume (Ct.BV, mm^3) were measured.

Flow Cytometry

Mice were sacrificed, ankle joints were removed and cells were extracted from the synovium based on a modified protocol (27). In brief, synovial tissue from ankle joints was minced in RPMI medium containing 5% FBS, glutamine and freshly made Collagenase type II isolated from *Clostridium histolyticum* (Worthington) and incubated in a shaking waterbath for 90 min at 37°C. Single cell suspensions were generated through pushing the tissue on a size-40 metallic mesh disc (Sigma-Aldrich). Cells were filtered through a 100-μm sheet, centrifuged, resuspended in FACS buffer (1% FBS in PBS) and counted using a hematocytometer. 10^6 cells were plated in a 96 V-bottom well plate (Costar) and stained with antibodies against CD45-Alexa 700, CD11b-PE, Gr1-FITC, TCRα-APC/Cy7, and B220-PerCP (Biolegend). Cells were incubated for 30 min at 4°C, and then were washed and transferred to tubes for analysis. BD FACS Canto II Flow Cytometer (BD Biosciences) was used for processing the samples and results were analyzed with FlowJo v7.6 software.

Quantitative Expression Analysis

Total RNA was extracted from ankle joints using a monophasic solution of guanidine isothiocyanate and phenol according to the manufacturer's instructions (TRI Reagent, MRC). After removal of DNA remnants with DNase I treatment (Sigma-Aldrich), first strand cDNA was synthesized using 2 μg of total RNA and MMLV reverse transcriptase (Sigma-Aldrich). Templates were amplified with SsoFast EvaGreen Master Mix (Bio-Rad Laboratories) on the CFX96 real time PCR instrument (Bio-Rad Laboratories). Quantitative Real Time PCR (qPCR) was performed at 55°C for all genes (except: IL6 at 58°C) for 40 cycles. Specific primer pairs (Eurofins Genomics) were used for the quantitative expression as follows (sequences 5′ to 3′, sense and antisense): *human RANKL:* ACGCGTATT TACAGCCAGTG and CCCGTAATTGCTCCAATCTG; *mouse RANKL:* TGTACTTTCGAGCGCAGATG and AGGCTTGTT TCATCCTCCTG; *human TNF:* GAGGCCAAGCCCTGGTATG and CGGGCCGATTGATCTCAGC; *mouse TNF:* CAGGCG GTGCCTATGTCTC and CGATCACCCCGAAGTTCAGTAG; *mouse IL-1β:* ATCTTTTGGGGTCCGTCAACT and CCCTCA CACTCAGATCATCTTCT; and *mouse IL-6*: TAGTCCTTC CTACCCCAATTTCC and TTGGTCCTTAGCCACTCCTTC. The samples were normalized to GAPDH expression (TTA GCACCCCTGGCCAAGG and CTTACTCCTTGGAGGCCA TG). Relative expression was calculated as the fold difference compared with control values using BioRad CFX96^{TM}. For each experiment at least three biological and two technical replicates were used.

Proteomics

For the proteomic analysis, ankle joints were isolated from 6-week-old WT, Tg5519, Tg197 and Tg197/Tg5519 mice (6–8 mice per genotype).

Protein Extraction and Lysis

Ankle joints from the four different genotypes (WT, Tg5519, Tg197, and Tg197/Tg5519) were ground to powder in liquid nitrogen using a pestle and mortar and solubilized in 150 μl lysis buffer containing 100 mM Tris-HCl, pH 7.6, 4% SDS and freshly made 100 mM DTT. Samples were incubated for 3 min at 95°C, followed by 20 min incubation in a sonication water bath in order to shear the DNA. Finally, the samples were centrifuged at 17,000 × g for 30 min at 4°C and the supernatants were transferred to new tubes.

Protein Digestion

The protein extracts were processed according to the Filter Aided Sample Preparation (FASP) protocol using spin filter devices with 10 kDa cutoff (Sartorius, VN01H02). 40 μl lysate were diluted in 8 M Urea/100 mM Tris-HCl pH 8.5, the filters were extensively washed with the urea solution, covered with 10 mg/ml iodoacetamide in the urea solution and incubated for 30 min in the dark for the alkylation of cysteines. The proteins on the top of the filters were washed three times with 50 mM ammonium bicarbonate and finally the proteins were digested adding 1 μg trypsin/LysC mix in 80 μl 50 mM ammonium bicarbonate solution (Mass spec grade, Promega) and incubated overnight at 37°C. The peptides were eluted by centrifugation, followed by speed-vac-assisted solvent removal, reconstitution in 0.1% formic acid, 2% acetonitrile in water, and transferring to LC-MS glass sample vials. Peptide concentration was determined by nanodrop absorbance measurement at 280 nm.

Ultra High Pressure NanoLC

2.5 μg peptides were injected and pre-concentrated with a flow of 3 μl/ min for 10 min using a C18 trap column (Acclaim PepMap100, 100 μm × 2 cm, Thermo Scientific) and then loaded onto a 50 cm C18 column (75 μm ID, particle size 2 μm, 100 Å, Acclaim PepMap RSLC, Thermo Scientific). The binary pumps of the HPLC (RSLCnano, Thermo Scientific) consisted of solution A

(2% v/v ACN in 0.1% v/v formic acid) and solution B (80% ACN in 0.1% formic acid). The peptides were separated using a linear gradient of 4–40% B in 450 min at a flow rate of 300 nl/min. The column was placed in an oven operating at 35°C.

MS/MS

The purified peptides were ionized through nanoESI and analyzed by an LTQ Orbitrap XL Mass spectrometer (Thermo Fisher Scientific). Full scan MS spectra were acquired in the orbitrap (m/z 300–1,600) using profile mode with a data-dependent acquisition method were the resolution was set to 60,000 at m/z 400 and the automatic gain control target at 10^6 ions. The six most intense ions were sequentially isolated for collision-induced MS/MS fragmentation and their detection in the linear ion trap. Dynamic exclusion was set to 1 min and activated for 90 sec. Ions with single charge states were excluded. Lockmass of m/z 445.120025 was used for internal calibration. Xcalibur (Thermo Scientific) was used to control the system and acquire the raw files.

Data Analysis

The raw files were analyzed using MaxQuant (version 1.6.0.16), the complete Uniprot *Mus musculus (228 311 entries / Oct-2016)* and a common contaminants database by the Andromeda search engine. The search parameters used were strict trypsin specificity, allowing up to two missed cleavages. Oxidation of methionines, deamidation of asparagine and glutamine residues and N-terminal acetylation were set as variable modifications. Cysteine carbamidomethylation was set as a fixed modification. "Second peptide" option was enabled. The protein and peptide false discovery rate (FDR) was set to 0.01 for both proteins and peptides with a minimum length of seven amino acids that was determined by searching a reverse database. Protein abundance was calculated on the basis of the normalized spectral protein intensity as label free quantitation (LFQ intensity) enabling the "match between runs" option (set at 0.7 min). LFQ was performed with a minimum ratio count of 2.

Proteomics Statistical Analysis

The statistical analysis was performed using Perseus (version 1.6.1.3) (28). Proteins identified as contaminants, "reverse" and "only identified by site" were filtered out. The LFQ intensities were transformed to logarithmic values (log2(x)). The biological replicas were grouped together. The protein groups were filtered to obtain at least 4 valid values in at least one group. A total of 2,009 label free quantified proteins were subjected to statistical analysis with ANOVA test (permutation based FDR with 0.05 cutoff) for the comparison of all groups. The 1,019 statistically significant proteins were then Z-scored, visualized by Euclidean hierarchical clustering and grouped into three main clusters (I, II and III) consisting of 403, 179, and 437 proteins, respectively. Tukey's honestly significant difference (THSD) was performed on the ANOVA significant hits to determine in exactly which pairwise group comparisons, a given protein was differentially expressed. Enrichment analysis was performed with ClueGO (29) (version 3.6.1), a Cytoscape plug-in, using KEGG (30) pathways database. Only pathways that had p-value <0.05 (hypergeometric test with Benjamini–Hochberg correction) were considered and "is Specific" was set to 60%. Default values were used for the other parameters.

Statistical Analysis

All results are expressed as mean ± standard error mean (SEM). Statistical significance was calculated for two groups using Student's t-tests or the Mann-Whitney test for non-parametric distribution. The log-rank test was used for survival curve comparison. One-Way analysis of variance (ANOVA) and Tukey *post-hoc* test was performed to compare means of multiple groups. P-values <0.05 were considered significant; $^{*}p < 0.05$, $^{**}p < 0.01$, $^{***}p < 0.001$ when not otherwise specified.

RESULTS

Significant Attenuation of TNF-Mediated Inflammatory Arthritis in the Absence of Functional RANKL

To elucidate the role of RANKL in the progression of TNF-mediated inflammatory arthritis *in vivo*, we generated Tg197/Rankl$^{tles/tles}$ mice by crossing Tg197 arthritic mice overexpressing human TNF with Rankl$^{tles/tles}$ osteopetrotic mice carrying a functional mutation in the *RANKL* gene (22). The Tg197 transgenic mouse model spontaneously develops inflammatory arthritis characterized by swelling of the ankles, infiltration of inflammatory cells, synovial hyperplasia, articular cartilage destruction and bone erosion, closely resembling the human pathology of rheumatoid arthritis. Rankl$^{tles/tles}$ mice, expressing an inactive form of RANKL incapable of forming trimers, are osteopetrotic due to osteoclast absence (22). Tg197/Rankl$^{tles/tles}$ mice also displayed an osteopetrotic phenotype as shown by failure of tooth eruption, and growth retardation similarly to Rankl$^{tles/tles}$ mice, whereas an improvement was observed in their survival percentage compared to Rankl$^{tles/tles}$ mice even though not significant (**Figures 1A,B**). Macroscopically, arthritis appeared in Tg197 mice at 3 weeks of age as detected by mild swelling of the ankle joint, which progressed with severe joint swelling and distortion accompanied by movement deterioration by the 10th week of age, the end point of the study (**Figure 1C**). However, arthritis signs were not detected in Tg197/Rankl$^{tles/tles}$ mice throughout the study period (**Figure 1C**). Histological analysis at 10 weeks of age, when Tg197 control mice reached the peak of disease, demonstrated a dramatic attenuation of inflammatory arthritis in Tg197/Rankl$^{tles/tles}$ mice, as shown by moderate synovial hyperplasia (**Figures 1D,E**). These results indicate that RANKL loss significantly attenuates inflammatory arthritis onset and progression.

RANKL-Independent Formation of Osteoclasts in TNF-Driven Inflammatory Arthritis

So far, it has been shown that RANKL is necessary for the physiological process of bone remodeling. However, it is unclear whether osteoclasts can be formed in a TNF-driven inflammatory

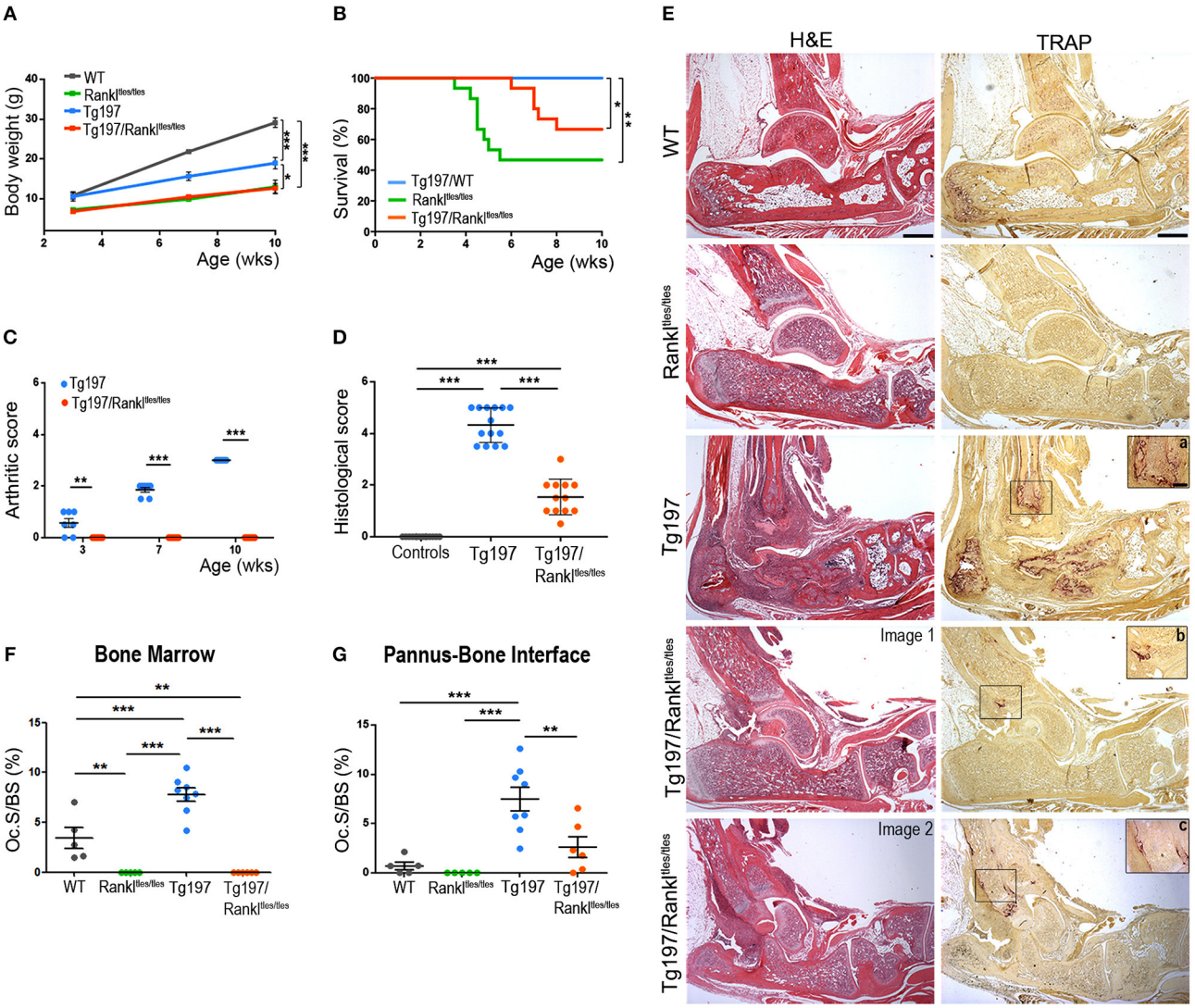

FIGURE 1 | Dramatic attenuation of TNF-driven arthritis upon RANKL genetic inactivation. Tg197/Rankl$^{tles/tles}$ mice and sex-matched control littermates WT (Rankl$^{tles/+}$), Tg197 (Tg197/Rankl$^{tles/+}$), and Rankl$^{tles/tles}$ were assessed until the 10th week of age for **(A)** body weight gain (n = 6–7 per genotype), **(B)** percent survival (n = 15 per genotype), **(C)** clinical arthritic score (from 0 to 3) in both ankles for each mouse (n = 7 per genotype), and **(D)** histological arthritic score (from 0 to 5) in both ankles for each mouse at 10 weeks of age (n = 12–14 per genotype). Control group includes Rankl$^{tles/+}$ and Rankl$^{tles/tles}$ mice. **(E)** Representative histological images of hematoxylin/eosin (H&E) and Tartrate-resistant acid phosphatase (TRAP) stained ankle joint sections from two Tg197/Rankl$^{tles/tles}$ mice, displaying either mild (Image 1), or moderate inflammatory arthritis (Image 2), and their littermate controls at 10 weeks of age. Boxed areas at TRAP staining show a higher magnification of regions harboring TRAP+ cells in Tg197 **(a)** and Tg197/Rankl$^{tles/tles}$ mice **(b,c)**. Scale bars: 300 μm at H&E and TRAP, 80 μm at boxed areas in TRAP. TRAP staining was measured as osteoclast surface fraction (Oc.S/BS, %) quantification in **(F)** the bone marrow compartment area, and **(G)** the pannus-bone interface (n = 5–8 per genotype). Data represent mean values ± SEM. One-Way ANOVA and Tukey *post-hoc* test was performed for statistical analysis of more than two groups and Mann-Whitney test was performed for statistical analysis between two groups. The log-rank test was used for survival curve comparison. Asterisks mark statistically significant difference (*$p < 0.05$, **$p < 0.01$, ***$p < 0.001$).

environment even without RANKL signaling *in vivo*. To investigate this possibility, we analyzed the hematoxylin/eosin stained sections for osteopetrosis and in parallel we stained serial sections from all experimental groups with Tartrate-resistant acid phosphatase (TRAP), which is an osteoclastic marker. As expected, Rankl$^{tles/tles}$ mice failed to develop TRAP+ osteoclasts and developed osteopetrosis, whereas enhanced osteoclastogenesis and bone resorption was identified in arthritic Tg197 mice at sites of pannus invasion into bone (**Figures 1E–G**). However, TNF overexpression failed to reverse the RANKL-mediated osteopetrotic phenotype in Tg197/Rankl$^{tles/tles}$ mice, which was further confirmed by the absence of osteoclastogenesis in the bone marrow compartment (**Figures 1E,F**). Instead, TRAP+ osteoclasts were identified in the inflamed synovium of Tg197/Rankl$^{tles/tles}$ mice (**Figures 1E,G**), indicating RANKL-independent mechanisms of osteoclastogenesis at sites of

TNF-induced inflammation *in vivo*. Notably, the extent of osteoclastogenesis, either limited or moderate, depended on arthritis severity in Tg197/Rankl$^{tles/tles}$ ankles (**Figures 1E,G**). Collectively, our results suggest that TNF overexpression can induce RANKL-independent osteoclastogenesis at sites of inflammatory invasion into the ankle joints but cannot compensate for RANKL in bone remodeling *in vivo* as the osteopetrotic phenotype is not affected.

RANKL Overexpression Exacerbates TNF-Driven Inflammatory Arthritis

We next investigated whether the progression of inflammatory arthritis in the TNF transgenic model was affected by human RANKL (huRANKL) overexpression. This was achieved by crossing Tg197 mice with the TgRANKL transgenic lines Tg5516 and Tg5519 that express huRANKL at a physiological relevant tissue-specific pattern. Tg5516 mice expressing huRANKL at

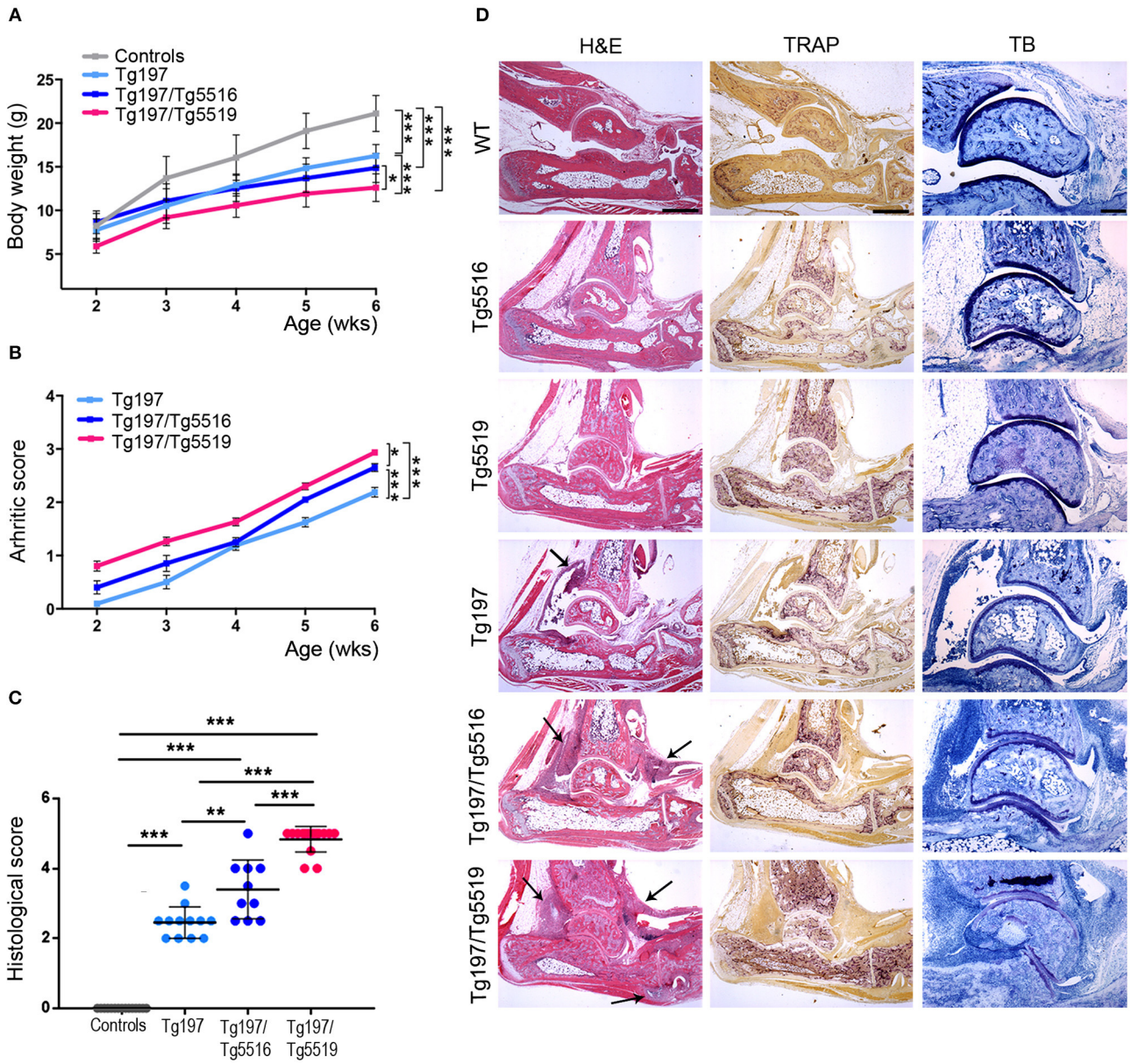

FIGURE 2 | RANKL overexpression exacerbates TNF-driven arthritis. Assessment of arthritis progression was conducted in Tg197/TgRANKL mice (Tg197/Tg5516, Tg197/Tg5519), Tg197 and sex-matched control littermates (WT, Tg5516, and Tg5519) till the 6th week of age. **(A)** Body weight curves ($n = 10$ per genotype), **(B)** clinical arthritic scores ($n = 10$–15 per genotype), **(C)** histological arthritic score ($n = 10$–15 per genotype), and **(D)** representative ankle joint sections from each genotype ($n = 10$–15) at the 6th week of age stained with hematoxylin/eosin (H&E), TRAP for osteoclasts and Toluidine Blue (TB) for articular cartilage destruction. Arrows at H&E indicate focal pannus invasion into subchondral bone regions. Scale bars: 300 μm at H&E and TRAP; 150 μm at TB. Data represent mean values ± SEM. One-Way ANOVA and Tukey *post-hoc* test was performed. Asterisks mark statistically significant difference (*$p < 0.05$, **$p < 0.01$, ***$p < 0.001$).

low levels develop mild trabecular bone loss, while a more severe osteoporotic phenotype is identified in the Tg5519 line overexpressing huRANKL with features of severe trabecular bone loss and cortical porosity (23). Simultaneous overexpression of RANKL and TNF in Tg197/TgRANKL mice resulted in an aggressive arthritic phenotype, characterized by earlier arthritis onset and exacerbated clinical symptoms, such as reduced body weight gain and increased arthritis scores compared to Tg197 arthritic control mice (**Figures 2A,B**). Histopathological analysis at 6 weeks of age, when arthritic manifestations in Tg197 mice were restricted on synovial hyperplasia and focal pannus formation, showed significantly increased arthritis progression in Tg197/Tg5519 mice characterized by aggravated inflammatory pannus formation, increased osteoclastogenesis, massive bone destruction and surface cartilage degradation as indicated by staining with hematoxylin/eosin, TRAP and Toluidine blue (**Figures 2C,D**). Similarly, Tg197/Tg5516 mice displayed an exacerbation of inflammatory arthritis compared to Tg197 mice but to a lesser extent as regards Tg197/Tg5519 mice, indicating a RANKL dose effect on arthritis progression (**Figures 2C,D**).

A hallmark of RA is the accumulation of inflammatory cells such as monocytes, neutrophils and lymphocytes in the proliferating synovium that penetrates the cartilage and the bone in the form of pannus causing aberrant joint destruction. So far, the role of RANKL in inflammation remains enigmatic. To examine whether the exacerbated arthritis phenotype developed in Tg197/TgRANKL mice correlates with an increased inflammatory profile, we analyzed the synovial tissue for inflammatory cells through flow cytometry (**Figure 3**). Our analysis showed a significant increase in the number of infiltrated cells extracted from Tg197/Tg5519 inflamed ankles compared to Tg197 mice (Tg197/Tg5519: $13.15 \pm 2.72 \times 10^6$ cells vs. Tg197: $4.39 \pm 0.16 \times 10^6$ cells), supporting arthritis exacerbation. More specifically, $CD45^+$ hematopoietic-derived cell infiltrates were increased 4 times in the synovium of Tg197/Tg5519 mice compared to Tg197 mice (Tg197/Tg5519: $9.59 \pm 2.2 \times 10^6$ cells vs. Tg197: $2.51 \pm 0.09 \times 10^6$ cells), while no statistical changes were identified between Tg5519 and WT mice (**Figure 3A**). The synovium of Tg197/Tg5519 mice was infiltrated by 2-fold more $CD11b^+Gr1^-$ monocytes/macrophages (Tg197/Tg5519: $2.91 \pm 0.28 \times 10^6$ cells vs. Tg197: $1.36 \pm 0.11 \times 10^6$ cells), and 5-fold more $CD11b^+Gr1^+$ granulocytes (Tg197/Tg5519: $2.4 \pm 0.73 \times 10^6$ cells vs. Tg197: $0.44 \pm 0.04 \times 10^6$ cells) than Tg197 mice, where monocytes and synovial macrophages are the dominant inflammatory cells (**Figure 3B**). The absolute numbers of B220+ B lymphocytes (Tg197/Tg5519: $0.98 \pm 0.11 \times 10^6$ cells vs. Tg197: $0.51 \pm 0.06 \times 10^6$ cells) and TCRα+ T lymphocytes (Tg197/Tg5519: $1.27 \pm 0.27 \times 10^6$ cells vs. Tg197: $0.5 \pm 0.05 \times 10^6$ cells) were also significantly increased in comparison to Tg197 mice, however to a lesser extent than myeloid cells (**Figure 3B**).

As regards the percentage of inflammatory cells in the arthritic synovium, flow cytometry revealed a statistical increase of the percentage of $CD45^+$ hematopoietic cells in Tg197/Tg5519 mice compared to Tg197, supporting exacerbation of inflammation (**Figure 3C**). Even though the percentages of B and T lymphocytes were rather low in the inflamed synovium of double transgenic mice (Tg197/Tg5519) and arthritic mice (Tg197), $CD11b^+/Gr1^-$ macrophages/monocytes were prevalent in Tg197, while $CD11b^+/Gr1^+$ granulocytes in Tg197/Tg5519 mice (**Figure 3D**), indicating probable differences in pathogenic mechanisms. Similarly, inflamed synovium from Tg197/Tg5516 mice also contained increased numbers and percentages of $CD45^+$ hematopoietic cells (Tg197/Tg5516: $72.4 \pm 1.2\%$ cells vs. Tg197: $59.02 \pm 0.37\%$) and $CD11b^+/Gr1^+$ granulocytes (Tg197/Tg5516: $15.63 \pm 0.62\%$ vs. Tg197: $10.9 \pm 1\%$) compared to Tg197. Collectively, the aberrant co-expression of TNF and RANKL, modifies the inflammatory profile in the inflamed ankles toward a massive accumulation of inflammatory cells mainly of myeloid origin.

Furthermore, the cytokine profile of the inflamed ankle joints was investigated through qPCR. Expression analysis for endogenous RANKL showed a progressive increase in Tg197 and Tg197/Tg5519 mice compared to control groups WT and Tg5519, indicating a positive correlation with arthritis severity (**Figure 3E**). Similarly, the expression levels of the huRANKL transgene were significantly increased in Tg197/Tg5519 mice compared to Tg5519 mice (**Figure 3F**), supporting an impact of the arthritic milieu in the regulation of the transgene's expression since it carries regulatory regions. In contrast, the expression levels of the endogenous TNF and those of the human TNF transgene were similar between Tg197 and Tg197/Tg5519 mice (**Figures 3E,F**), excluding their possible involvement in arthritis aggravation upon RANKL overexpression. We also investigated the expression of two proinflammatory cytokines, IL-6 and IL-1b in inflamed ankles (**Figures 3G–I**). Both cytokines were significantly upregulated in Tg197 mice compared to WT mice. The expression level of IL-6, a proinflammatory cytokine of the acute phase response that promotes neutrophil production, was further 1.5-fold increased in Tg197/Tg5519 mice compared to Tg197 (**Figure 3G**), in line with the granulocytic arthritic phenotype developed in such mice (**Figures 3B,D**). Instead, IL-1b, a proinflammatory cytokine expressed by activated macrophages, was 2-fold decreased in Tg197/Tg5519 compared to Tg197 mice (**Figure 3I**), which could be explained by the proportional decrease of macrophages in the inflamed synovium of Tg197/Tg5519 mice (**Figure 3D**).

Cooperative Effect of RANKL and TNF in Local and Systemic Bone Resorption

We further investigated whether the exacerbated arthritis phenotype identified in Tg197/TgRANKL mice affected bone erosion locally. Histological examination of the inflamed ankles from Tg197/TgRANKL mice showed pronounced inflammatory bone destruction. To quantify bone loss locally, we performed microcomputed tomography (microCT) at the trabecular region of the calcaneous bone, which is proximal to the inflamed synovium and contains an organized trabecular structure. Both TgRANKL osteoporotic mice and Tg197 arthritic mice showed trabecular bone loss in the calcaneous bone at 6 weeks of age (**Figure 4**), while the calcaneous bone loss was further exacerbated in Tg197/RANKL mice compared

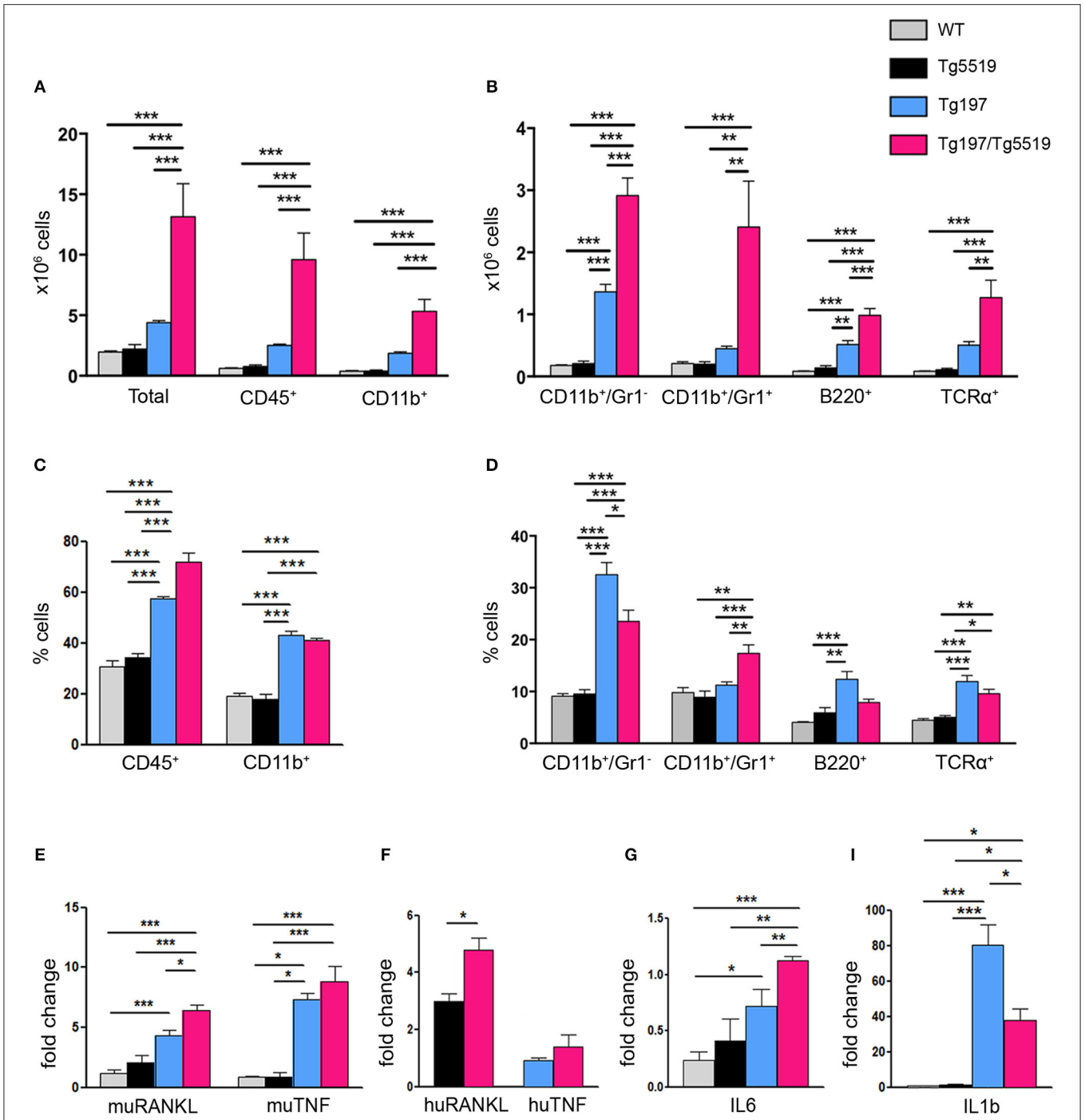

FIGURE 3 | Increased inflammatory cell infiltration in the synovium of Tg197/TgRANKL mice. **(A,B)** Absolute cell counts and **(C,D)** percentage of synovial subpopulations from 6 week-old Tg197/Tg5519 mice and sex-matched littermates (WT, Tg5519, Tg197) as determined by flow cytometry using antibodies against CD45 (hematopoietic cells), CD11b (myeloid cells), Gr1 (granulocytes), B220 (B lymphocytes) and TCRα (T lymphocytes) ($n = 4$–5 per genotype). qPCR analysis in inflamed ankles from 6 week-old Tg197/Tg5519 mice and littermate controls ($n = 3$–4) for **(E)** mouse RANKL and mouse TNF, **(F)** human RANKL and human TNF, **(G)** IL6 and **(I)** IL1b cytokine. Data represent mean values ± SEM. One-Way ANOVA and Tukey *post-hoc* test was performed for more than two groups and Student's *t*-test for two groups. Asterisks mark statistically significant difference (*$p < 0.05$, **$p < 0.01$, ***$p < 0.001$).

to the control littermate groups (WT, TgRANKL, Tg197). In the severe osteoporotic model Tg5519 the presence of the huTNF transgene promoted bone loss in an additive manner. Assessment of the trabecular bone volume fraction (BV/TV, %) demonstrated a 28% reduction in Tg5519, 46% in Tg197 and 73% in Tg197/Tg5519 compared to WT

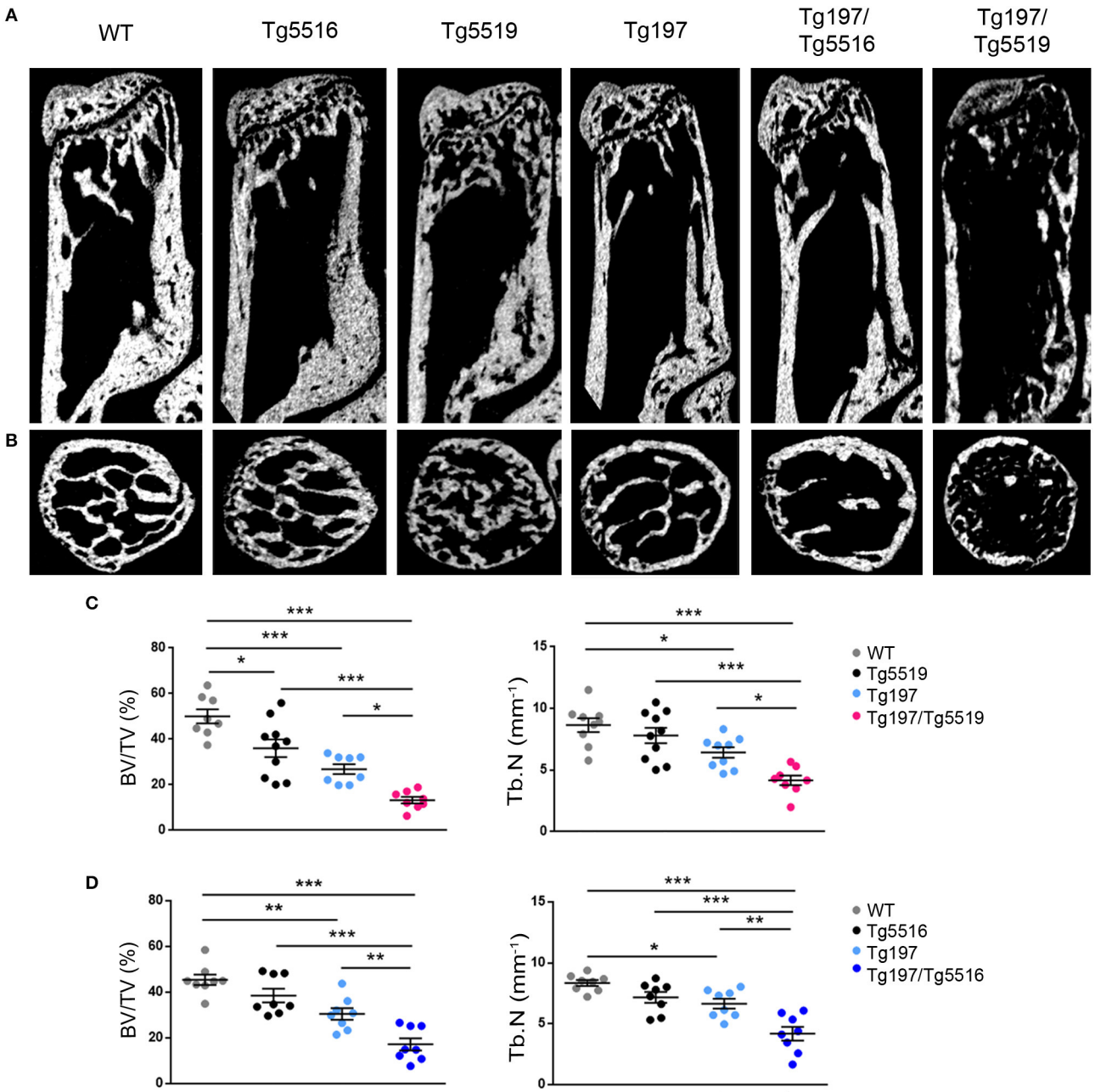

FIGURE 4 | Synergistic effect of RANKL and TNF in inflamed bone loss. MicroCT analysis in the trabecular region of the calcaneous bone from mice of each group at 6 weeks of age as shown by **(A)** representative longitudinal sections and **(B)** cross-sectional sections. Quantitative measurements with microCT in the trabecular area of the calcaneous bone for BV/TV (Bone Volume/Total Volume, %), and Tb.N (Trabecular Number per mm) in **(C)** Tg197/Tg5519 and littermates ($n = 8$–10, equal number of sexes per genotype), and **(D)** Tg197/Tg5516 and littermates ($n = 8$, equal number of sexes per genotype). Data represent mean values ± SEM. One-Way ANOVA and Tukey *post-hoc* test was performed for more than two groups. Asterisks mark statistically significant difference (*$p < 0.05$, **$p < 0.01$, ***$p < 0.001$).

group (**Figures 4A–C**). Furthermore, a synergistic effect was identified when huTNF was introduced in the mild osteoporosis model Tg5516, as Tg197/Tg5516 mice displayed a 62% reduction in BV/TV, while Tg5516 and Tg197 together reached a 48% reduction compared to WT (**Figure 4D**). These results indicate that the exacerbated arthritis developed in Tg197/TgRANKL mice coincides with a cooperative local bone loss.

To investigate whether simultaneous overexpression of RANKL and TNF also affected other skeletal sites outside of the inflamed ankles, we analyzed both metaphyseal and diaphyseal regions in distal femurs from Tg197, TgRANKL, and

Tg197/TgRANKL mice (**Figure 5**). Similarly to the calcaneous bone, both the trabecular and the cortical regions of the non-inflamed Tg197/TgRANKL femurs displayed exacerbated bone loss. The severe osteoporotic phenotype in Tg5519 was further aggravated, while mild osteoporosis in Tg5516 mice converted to severe osteoporosis upon huTNF expression, indicating that TNF and RANKL also cooperate in systemic bone loss.

Proteomic Analysis of Inflamed Joints

To identify altered biological processes and changes in the proteome at osteolytic inflammatory arthritis aggravated by the overexpression of RANKL, we utilized a comparative proteomic approach using LC-MS/MS and label free quantitation in ankles from 6 week-old Tg197/Tg5519 transgenic mice and control groups, including Tg197, Tg5519, and WT littermate mice. Analysis was performed on whole ankle joints in order to capture deregulated protein networks at the time of isolation while also maintaining all the populations and the potential interactions in inflamed ankles. For each ankle we quantified 2,009 proteins using label-free quantitation (LFQ) determined by the MaxQuant software (31, 32). We achieved high biological reproducibility as reflected by the unsupervised clustering of the genotypes in the composed heatmap (**Figure 6A**). To define significant regulated proteins, we performed one-way ANOVA analysis between the four genotypes and identified 1,019 significantly regulated proteins (**Figure 6A**). Hierarchical clustering of significantly regulated proteins revealed three major groups. Cluster I consists of 403 proteins, Cluster II of 179 and Cluster III of 437 proteins (**Figure 6A**). Bioinformatic "annotation enrichment analysis" in these clusters using ClueGO/CluePedia software (29) identified the main biological pathways (KEGG database) regulated by these proteins. Cluster I contained proteins involved in basic metabolic processes such as citrate cycle (TCA), oxidative phosphorylation or glycolysis/gluconeogenesis that were found specifically downregulated in arthritic groups Tg197 and Tg197Tg5519 (**Figure 6B** and **Supplementary Table 1**). Cluster II is composed mostly of ribosomal proteins which are enriched in huRANKL overexpressing mice Tg5519 and Tg197/Tg5519 (**Figure 6C** and **Supplementary Table 2**). Enrichment analysis in Cluster III revealed a high prevalence of proteins involved in phagosome, lysosome, proteasome, cytoskeleton regulation, leukocyte transendothelial migration and Fcγ-receptor-mediated phagocytosis in arthritic Tg197 and Tg197/Tg5519 mice compared to control groups Tg5519 and WT (**Figure 6D** and **Supplementary Table 3**), suggesting activation of immune responses.

To elucidate the most prominent proteins involved in RA aggravation by RANKL, Tukey's honestly significant difference was performed on the ANOVA significant hits. A total of 231 proteins, 120 downregulated and 111 upregulated, were found statistically altered in Tg197/Tg5519 compared to Tg197 mice. Enrichment analysis in downregulated proteins based on KEGG pathway database revealed classification to processes related with metabolism, and muscle contraction (**Figure 7A** and **Supplementary Table 4**). In contrast, the upregulated proteins were grouped to processes associated with RA, protein processing and amino acid metabolism (**Figure 7B** and **Supplementary Table 5**).

To exclude a possible involvement of the osteoporotic background in the deregulated proteins identified in Tg197/Tg5519 compared to Tg197, we examined which of the above mentioned 231 differentially expressed proteins were also statistically significant between Tg197/Tg5519 and Tg5519 mice. This analysis revealed 65 proteins downregulated (**Supplementary Table 6**) and 36 upregulated (**Figure 7C**, **Table 1**) in Tg197/Tg5519 compared to control groups Tg197 and Tg5519. Subcategorization of the 65 significantly downregulated proteins in Tg197/Tg5519 mice based on their biological function, showed that the majority of the proteins participated in metabolic processes of carbohydrates, lipids, amino acids and nucleotides as well as in mitochondrial function (**Supplementary Table 6**). On the other hand, the proteome of the inflamed ankles from Tg197/Tg5519 mice was enriched for proteins expressed in activated osteoclasts and vacuolar-type H+ ATPase subunits either osteoclast-specific or ubiquitous (**Figure 7C**, **Table 1**), indicating extended bone resorption. Similarly, upregulation was observed for proteins involved in DNA, RNA and protein processing, suggesting activation of chromatin remodeling and gene expression. Moreover, increased levels have been identified for proteins involved in intracellular signal transduction, vacuolar transport and cell migration. Many of the upregulated proteins have been implicated in inflammatory responses, and cell proliferation regulation that fully correlate with the aggressive inflammatory phenotype developed in the ankles of Tg197/Tg5519 mice.

DISCUSSION

The importance of the RANKL/RANK/OPG system in the development of bone destruction in RA has been recently established, since RANKL is highly expressed in the synovial tissue of RA patients (33–35) and inhibition of RANKL with denosumab results in amelioration of bone destruction in RA (36, 37). Paradoxically, there are limited clinical trials that inhibit RANKL in RA, and from the available ones an effectiveness has been demonstrated for bone resorption but not for inflammation during a short-term treatment period from 6 to 12 months (36–39). Thus, the role of RANKL in the progression of inflammation in RA remains unclear. Here, we investigated if the progression of TNF-mediated erosive inflammatory arthritis is affected either by genetic inactivation (22) or overexpression of RANKL in transgenic mouse models (23). Our previous studies have shown that the G278R substitution identified in Rankl$^{tles/tles}$ mice allows normal RANKL gene expression and protein production but abrogates RANKL trimer formation and subsequently receptor binding. Therefore, mutant RANKL lacks biological activity as it fails to induce osteoclastogenesis both *ex vivo* and *in vivo* leading to an osteopetrotic phenotype (22). Our results demonstrated that modeled arthritis was significantly attenuated in the absence of functional RANKL, as shown by the absence of clinical arthritis signs and significant decrease in synovial hyperplasia. The unexpected improvement of survival in Tg197/Rankl$^{tles/tles}$

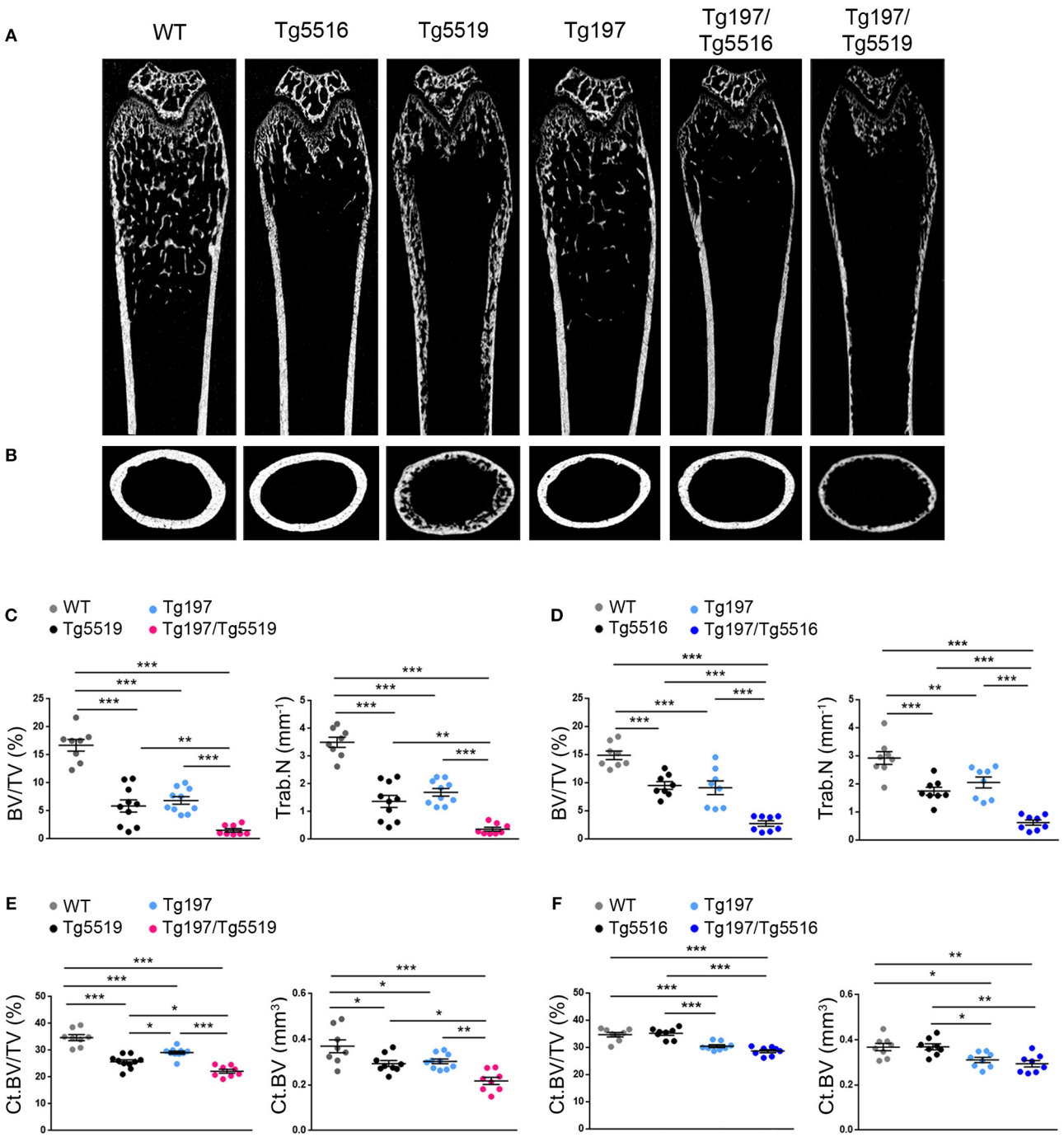

FIGURE 5 | Cooperative effect of RANKL and TNF in systemic bone loss. MicroCT analysis in the distal femur from mice of each genotype at 6 weeks of age as shown by **(A)** representative longitudinal sections and **(B)** cross-sectional sections at mid-diaphysis. Quantitative analysis with microCT of trabecular bone in the metaphyseal region of the distal femur of **(C)** Tg197/Tg5519 mice and their littermate controls ($n = 8$–10, equal number of sexes per genotype) and **(D)** Tg197/Tg5516 mice and their littermate controls ($n = 8$, equal number of sexes per genotype) for BV/TV (Bone Volume/Total Volume, %), and Tb.N (Trabecular Number per mm). Quantitative analysis with microCT of cortical bone in the mid-diaphyseal region of the femur of **(E)** Tg197/Tg5519 mice compared to their littermate controls ($n = 8$–10, equal number of sexes per genotype), and **(F)** Tg197/Tg5516 and their littermates ($n = 8$, equal number of sexes per genotype) for Ct.BV/TV (Cortical Bone Volume/Total Volume, %), and Ct. BV (Cortical Bone Volume, mm^3). Data represent mean values ± SEM. One-Way ANOVA and Tukey *post-hoc* test was performed for more than two groups. Asterisks mark statistically significant difference ($^*p < 0.05$, $^{**}p < 0.01$, $^{***}p < 0.001$).

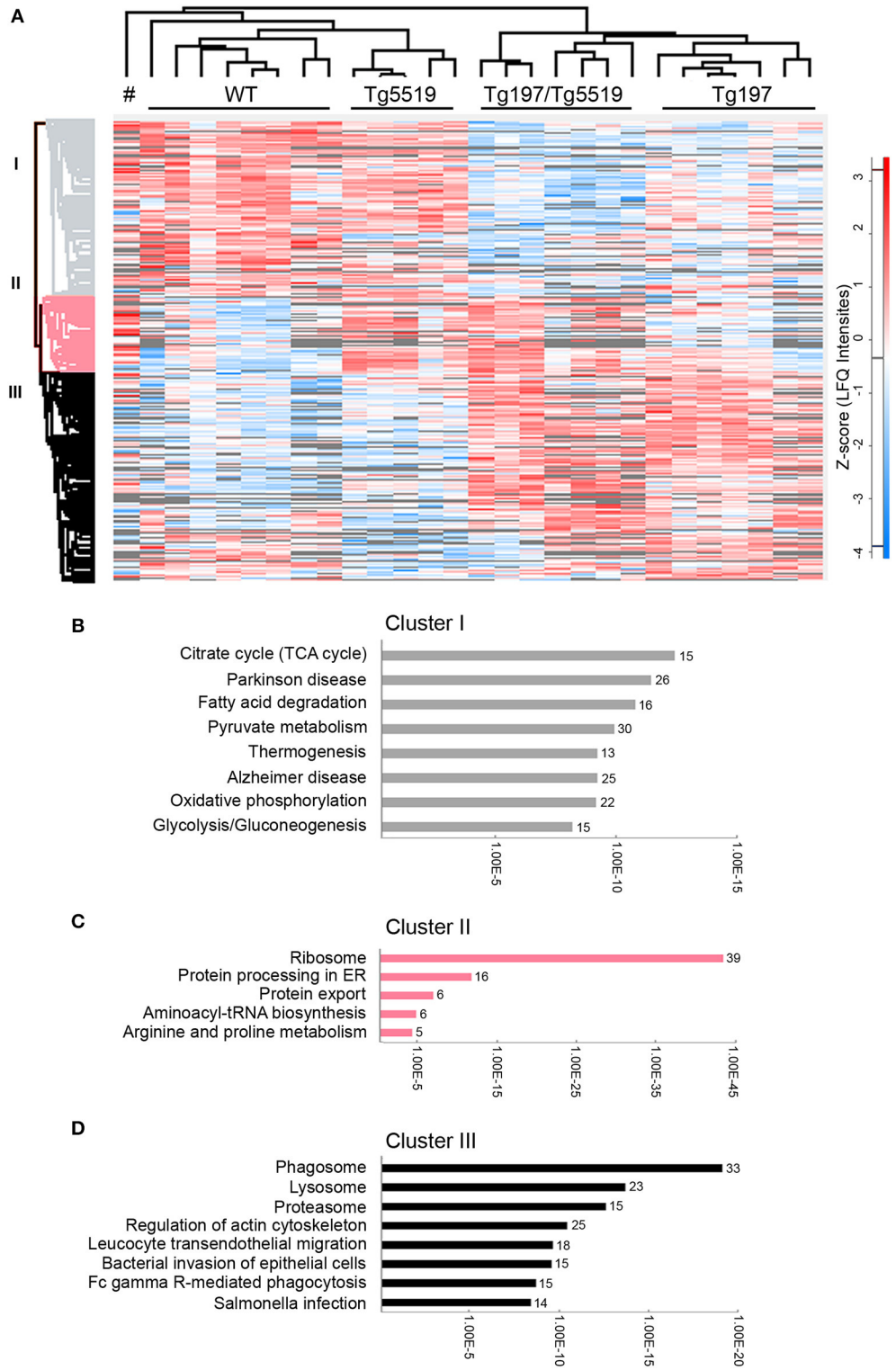

FIGURE 6 | Proteomic analysis in inflamed ankle joints of Tg197/TgRANKL mice. Comparative proteomic analysis using LC-MS/MS and label free quantitation in ankles from 6 week-old Tg197/Tg5519 mice and control groups including Tg197, Tg5519, and WT littermate mice ($n = 6–8$ biological replicas). **(A)** Heat map of statistical significant proteins (one-way ANOVA analysis). Columns represent each individual sample, labeled on top, and each row represents single proteins with an assigned color from blue (low expression) to red (high expression). Not detectable proteins are colored gray. Hierarchical Euclidean clustering created 3 protein clusters (gray, pink, and black). # indicates one Tg5519 mouse. Annotation enrichment analysis was performed using KEGG pathways database for **(B)** cluster I, **(C)** cluster II, and **(D)** cluster III.

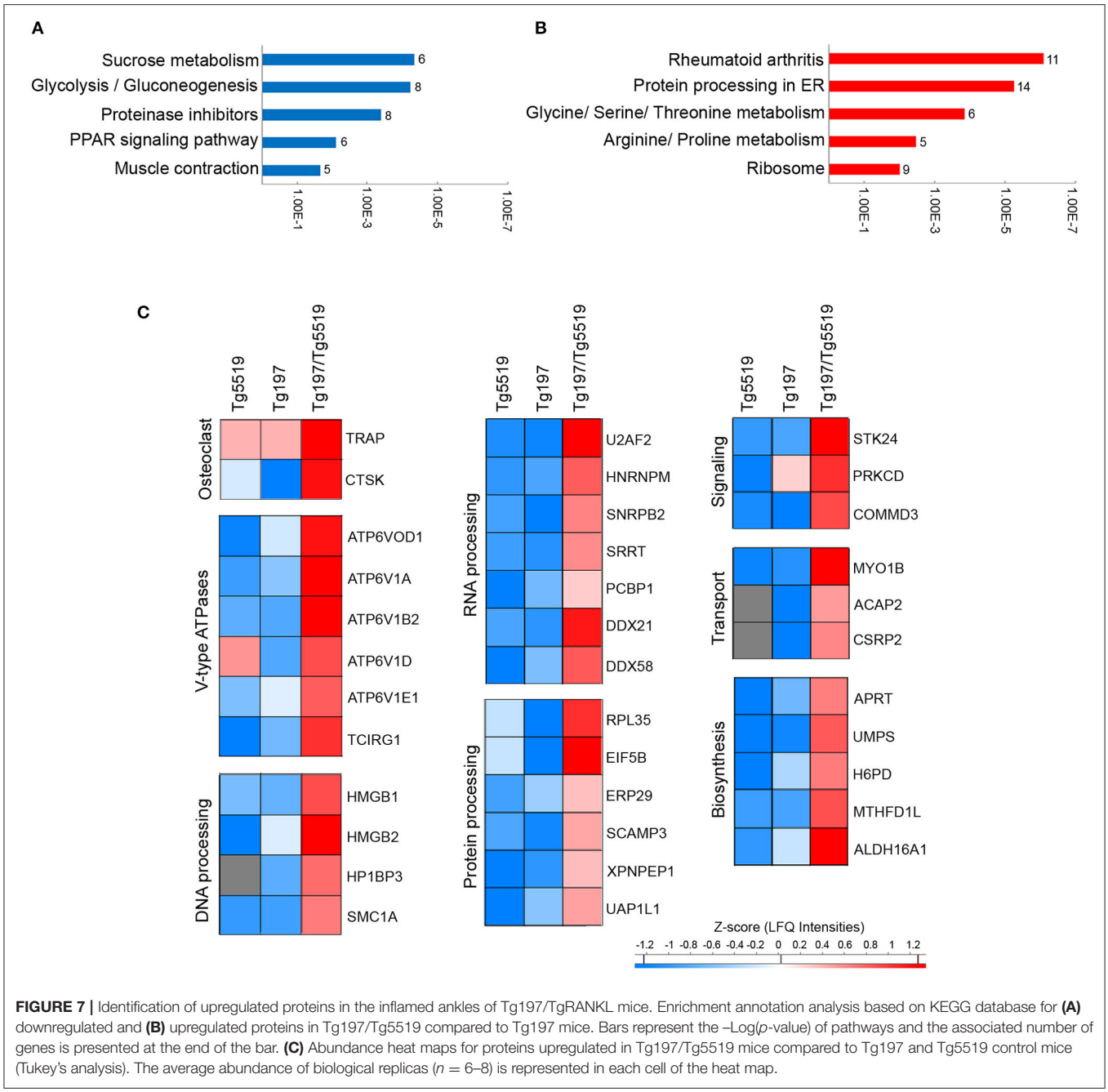

FIGURE 7 | Identification of upregulated proteins in the inflamed ankles of Tg197/TgRANKL mice. Enrichment annotation analysis based on KEGG database for **(A)** downregulated and **(B)** upregulated proteins in Tg197/Tg5519 compared to Tg197 mice. Bars represent the –Log(*p*-value) of pathways and the associated number of genes is presented at the end of the bar. **(C)** Abundance heat maps for proteins upregulated in Tg197/Tg5519 mice compared to Tg197 and Tg5519 control mice (Tukey's analysis). The average abundance of biological replicas ($n = 6–8$) is represented in each cell of the heat map.

mice compared to control Rankl$^{tles/tles}$ mice, could indicate a compensatory role for TNF in a RANKL-null background and needs further investigation. It is possible that the observed amelioration of arthritis is caused by the osteopetrotic phenotype rather than RANKL inactivation *per se*. In contrast, previous reports using c-fos deficient osteopetrotic mice crossed with TNF arthritic mice demonstrated that osteopetrosis is dispensable for TNF-mediated arthritis as synovial inflammation was not affected whereas bone resorption was blocked (40), supporting RANKL involvement in arthritis as shown in Tg197/Rankl$^{tles/tles}$ mice. Moreover, it is also possible that the attenuation of arthritis identified in Tg197/Rankl$^{tles/tles}$ mice is caused by the failure of RANKL deficient mice to develop a functional immune system (5, 6, 22).

Although several studies have revealed that TNF mediates osteoclastogenesis using *in vitro* cell culture systems (19, 20), there is still a central controversy of whether TNF can compensate for RANKL during osteoclastogenesis *in vivo*. Even though administration of high doses of exogenous TNF leads to the formation of osteoclast-like cells in RANK knockout mice at the site of calvarial injection (41), introduction of the Tg3647 TNF-expressing transgenic model displaying late

TABLE 1 | Proteins identified significantly overexpressed in the ankles from Tg197/Tg5519 mice compared to those isolated from their littermates Tg197, and Tg5519.

Gene Name	Protein ID	ANOVA *p*-value	WT	Tg5519	Tg197	Tg197/Tg5519
OSTEOCLAST ACTIVITY						
Acp5 (Trap)	Q05117	5.1E-08	18.46	21.24	21.24	22.73
Ctsk	P55097	2.2E-04	0.00	19.14	17.94	20.61
V-TYPE ATPASES						
Atp6v0d1	P51863	8.8E-07	18.26	19.14	19.52	20.05
Atp6v1a	P50516	7.0E-10	21.83	22.60	22.74	23.37
Atp6v1b2	P62814	1.2E-10	21.20	22.03	22.01	22.73
Atp6v1d	P57746	1.9E-08	17.95	19.33	18.78	19.47
Atp6v1e1	P50518	1.5E-08	20.34	21.33	21.50	21.85
Tcirg1	Q9JHF5	2.2E-08	18.13	19.23	19.59	20.57
DNA PROCESSING						
Hmgb1	P63158	9.5E-03	21.69	21.06	20.96	22.48
Hmgb2	P30681	8.3E-05	20.44	19.78	20.59	21.66
Hp1bp3	Q3TEA8	1.2E-03	17.51	0.00	17.47	18.22
Smc1a	Q9CU62	2.6E-02	17.38	17.11	17.13	17.75
RNA PROCESSING						
U2af2	P26369	2.7E-04	19.10	18.86	18.83	19.91
Hnrnpm	Q9D0E1	2.5E-03	21.95	22.03	22.06	22.46
Snrpd2	Q9CQI7	1.3E-02	19.58	19.11	18.96	19.68
Srrt	Q99MR6	5.3E-03	17.36	17.31	17.25	18.03
Pcbp1	P60335	1.3E-03	22.19	21.93	22.11	22.39
Ddx21	Q9JIK5	9.7E-04	18.70	18.82	18.76	19.64
Ddx58	Q6Q899	1.5E-03	17.00	17.40	17.77	18.56
PROTEIN PROCESSING						
Rpl35	Q6ZWV7	3.7E-03	20.45	21.16	20.43	22.08
Eif5b	Q05D44	9.0E-06	17.17	17.64	17.03	18.64
Erp29	P57759	7.5E-05	20.24	20.59	20.77	21.09
Scamp3	O35609	1.7E-03	18.44	18.62	18.54	18.95
Xpnpep1	Q6P1B1	9.1E-03	20.79	20.63	20.68	20.98
Uap1l1	Q3TW96	1.4E-05	20.54	20.69	20.96	21.34
SIGNAL TRANSDUCTION						
Stk24	Q99KH8	5.9E-04	17.66	17.96	18.02	19.43
Prkcd	P28867	7.6E-06	17.96	18.36	19.31	19.83
Commd3	Q63829	1.8E-02	0.00	17.98	17.91	18.70
VACUOLAR TRANSPORT, ENDOCYTOSIS, INVASIVENESS						
Myo1b	P46735	2.2E-03	17.84	18.23	18.27	19.08
Acap2	Q6ZQK5	7.8E-03	17.72	0.00	17.82	18.36
Csrp2	P97314	5.1E-05	18.22	0.00	18.37	19.36
BIOSYNTHETIC PROCESS						
Aprt	P08030	9.7E-06	19.19	19.41	19.72	20.38
Umps	P13439	2.3E-02	0.00	17.31	17.35	18.34
H6pd	Q8CFX1	6.2E-07	18.94	19.07	19.31	19.58
Mthfd1l	Q3V3R1	4.0E-04	19.55	19.73	19.75	20.25
Aldh6a1	Q9EQ20	7.2E-03	22.27	22.04	21.68	21.53

Logarithmic LFQ mean values are provided for each genotype.

onset arthritis in a RANK knockout background, showed that upon TNF overexpression osteoclastogenesis does not occur in the absence of RANKL/RANK signaling (42). Our results demonstrated that TNF overexpression could not compensate for RANKL-mediated osteopetrosis in Tg197/Rankl$^{tles/tles}$ mice, supported by the absence of osteoclasts in the bone marrow compartment. The fact that osteoclasts were identified between the pannus and bone interface in Tg197/Rankl$^{tles/tles}$ mice, indicates that this effect is driven by TNF-induced inflammation *in vivo*. However, the involvement of a subtle RANKL signaling

in TNF-driven osteoclastogenesis cannot be excluded and needs further investigation. Similarly, previous reports have shown that induction of K/BxN serum transfer arthritis in RANK-deleted mice, resulted in osteoclastogenesis in the inflamed synovium but not in the bone marrow, supporting RANKL-indepedent mechanisms for osteoclast formation *in vivo* in a sufficiently inflamed environment (43).

Following a similar approach, the effect of RANKL overexpression in arthritis progression was studied in Tg197/TgRANKL double transgenic mice that simultaneously overexpress TNF and RANKL. Our results demonstrated that abundance of RANKL accelerated TNF-driven arthritis onset and disease severity characterized by massive osteoclastogenesis and bone resorption, aggressive pannus expansion and immense infiltration of inflammatory cells mainly of myeloid origin. Even though in the inflamed ankles of Tg197 mice the dominant inflammatory cells were $CD11b^{+}Gr1^{-}$ monocytes and synovial macrophages, the synovium of Tg197/Tg5519 mice had a 5-fold increase in $CD11b^{+}Gr1^{+}$ granulocytes and 2-fold in $CD11b^{+}Gr1^{-}$ monocytes/macrophages. The percent composition of various infiltrated populations showed a clear prevalence of granulocytes in TNF-driven arthritis upon RANKL overexpression. Neutrophils, the most abundant type of granulocytes, are short-lived and highly motile cells that constitute an essential component in innate immune system, as they are among the first cells that arrive in inflamed tissues (44). They are involved in various chronic inflammatory diseases such as RA, where are found in synovial fluid and rheumatoid pannus. It has been previously demonstrated that the membrane-associated form of RANKL is expressed in healthy blood neutrophils as well as in SF neutrophils (45), suggesting a role for inflammatory neutrophils infiltrated at the hypertrophied synovium, in osteoclastogenesis and bone resorption. Apart from that, RANKL was recently demonstrated to potently activate human neutrophil degranulation (46) and treatment with anti-RANKL improved cardiac infarct size and function by potentially impacting on neutrophil-mediated injury and repair (47). Thus, the dramatic increase in the population of granulocytes in inflamed ankles from Tg197/Tg5519 mice could promote bone destruction.

Proteomics, the largescale study of the proteome, has emerged as a powerful technique to identify biomarkers for diagnosis, prognosis, disease monitoring and discovery of novel disease targets in RA (48). To identify proteome alterations in osteolytic inflammatory arthritis aggravated by the overexpression of RANKL, we utilized a comparative proteomic approach in inflamed ankles from Tg197/Tg5519 and control mice. Our analysis revealed 65 significantly downregulated proteins in Tg197/Tg5519 mice compared to Tg197 and Tg5519 mice, while their classification based on biological function, showed that the majority of the proteins participated in metabolic processes of carbohydrates, lipids, amino acids and nucleotides as well as in mitochondrial function. These results indicate that severe inflammation developed in the ankles of Tg197/Tg5519 mice is related to altered metabolic profile and probably mitochondria dysfunction as many mitochondrial proteins were downregulated (**Supplementary Table 6**). In RA the inflamed joint is profoundly hypoxic as a result of dysregulated angiogenesis, impaired mitochondrial function and inflammation, which leads to a bioenergetic crisis. Under these conditions synovial cells display adaptive survival responses, which in conjunction with altered metabolism, activate key transcriptional signaling pathways that further exacerbate inflammation (49). Notably, there is also downregulation of proteins functioning as protease inhibitors, such as Alpha-1-antitrypsin encoded by the *SERPINA1* gene, that protect tissues from enzymes of inflammatory cells, especially neutrophil elastase (50), suggesting extensive tissue damage in Tg197/Tg5519 mice. Moreover, downregulation of proteins involved in muscle contraction in Tg197/Tg5519 mice is indicative of muscle degeneration caused by movement impairment due to severe arthritis progression.

In contrast, the proteome of the inflamed ankles from Tg197/Tg5519 mice was enriched for proteins expressed in activated osteoclasts, including TRAP and cathepsin K (CTSK), and vacuolar-type H+ ATPase subunits. TRAP prompts the dephosphorylation of bone matrix phosphoproteins and allows osteoclast migration, and further resorption to occur (51), while Cathepsin K, a member of cysteine proteases, is involved in the degradation of bone matrix proteins, especially type I collagen (52). Apart from bone resorption, Cathepsin K plays an important role in the immune system as shown by suppression of experimental arthritis through its pharmacological inhibition (53). The vacuolar type H+ ATPases (V-ATPase) are ATP-driven proton pumps that establish and maintain the acidic environment of intracellular organelles, including secretory granules, endosomes, and lysosomes, as well as extracellular compartments by specialized cells (54). Within intracellular membranes, V-ATPases function in a variety of processes, including antigen processing in dendritic cells and lysosomal degradation, while their presence in the plasma membrane mediates extracellular acidification (55). The mammalian V-ATPase proton pump is a macromolecular complex composed of at least 14 subunits that are expressed and function in a tissue-specific manner. Genetic studies implicate a critical role for subunits ATP6V1B2, ATP6V1C1, ATPV0D2, and ATP6V0A3 (TCIRG1) in osteoclast activity as relevant mutations lead to osteopetrosis (56). Osteoclasts employ plasma membrane V-ATPases to release hydrogen ions (H+) into the resorption lacunae in order to dissolve the mineral component of bone and concomitantly to enhance the activity of enzymes that digest the organic matrix (56). The fact that Tg197/Tg5519 inflamed ankles overexpress various V-ATPase subunits either osteoclast specific such as ATP6V1B2, and TCIRG1 or ubiquitous ATP6V1A, ATP6V1E1, and ATPV0D1 indicates an overwhelming osteoclastic activity that causes massive joint destruction, which is also confirmed by the histological analysis. Upregulated V-ATPase subunits could also have an impact on inflammatory responses such as phagocytosis, cytokine secretion and exocytosis of neutrophil granules (57, 58). Notably, recent studies have shown that in inflammatory conditions, osteoclasts can differentiate from dendritic cells in the presence of RANKL and behave as antigen-presenting cells (59). Therefore, increased osteoclastogenesis identified in Tg197/TgRANKL mice could not only contribute to bone

destruction, but may also participate in perpetuating the inflammatory response.

In inflamed ankles from Tg197/Tg5519 mice there is also upregulated expression of proteins involved in DNA, RNA and protein processing, suggesting activation of chromatin remodeling and gene expression. Of special importance are DNA binding proteins, HMGB1 and HMGB2, members of the High-mobility group box (HMGB) family displaying two functions. In the nucleus, HMGB proteins bind to DNA in a DNA structure-dependent but nucleotide sequence-independent manner to function in chromatin remodeling. Extracellularly, HMGB proteins function as alarmins or damage-associated molecular pattern (DAMP) molecules, which are endogenous molecules released upon tissue damage to activate the immune system and drive inflammatory responses (60). Circulating HMGB1, the prototype member, has a crucial role in sterile inflammation caused by tissue injury or mitochondria damage, while its levels are increased in many human inflammatory diseases such as rheumatoid arthritis and their associated experimental models (61–63). Secreted HMGB1 binds to several immune receptors, principally toll-like receptors (TLRs) and through activation of NF-κB signaling (64) triggers inflammation by inducing cytokine release and recruitment of leucocytes. Thus, upregulation of HMGB1 and HMGB2 in inflamed ankles suggests extensive tissue damage and sustained inflammatory responses.

Moreover, proteomic analysis in Tg197/Tg5519 inflamed ankles identified high expression of RNA-binding proteins involved in mRNA splicing, and miRNA biogenesis. Among these proteins, U2AF2 (U2 Small Nuclear RNA Auxiliary Factor 2) is a central splicing complex member involved in pre-mRNA splicing and 3′-end processing (65) with an impact in the regulation of transcriptome in activated CD4 T lymphocytes (66). Moreover, HNRNPM (Heterogeneous nuclear ribonucleoprotein M), a component of the spliceosome machinery, promotes alternative spicing, cell proliferation and progression of breast cancer (67), while SRRT (Serrate, RNA Effector Molecule) participates to mRNA splicing and primary miRNA processing (68), it is involved in cell cycle progression at S phase, and its genetic deletion resulted in defective hematopoiesis in bone marrow and thymus (69). DDX21 and DDX58, as RNA helicases unwind their RNA substrates, and are involved in multiple biological processes related to RNA metabolism, including viral dsRNA sensing by innate cells, initiation of host antiviral responses and production of proinflammatory cytokines (70). Emerging evidence indicate that HMGBs bind to immunogenic nucleic acids (promiscuous sensing), which is required for subsequent recognition by specific pattern recognition receptors (discriminative sensing) such as DDXs to activate the innate immune responses. Such helicases also interact with endogenous RNAs regulating ribosome biogenesis (71) or translation of specific targets such as NF-κB1 (72). This category of nuclear RNA-binding proteins suggests increased transcription, RNA biogenesis and processing, while it remains unclear whether there is a specific correlation with regulation of inflammatory genes.

As regards intracellular signal transduction, there is abundance of protein kinases such as Serine/threonine kinase (STK24), and Protein kinase Cδ (PKCδ) in Tg197/T5519 ankles. STK24 plays an important role in controlling interleukin 17 (IL-17)-triggered inflammation and autoimmune diseases, since STK24 deficiency or knockdown markedly inhibited IL-17-induced phosphorylation of NF-κB and impaired IL-17-induced chemokines and cytokines expression (73). PKCδ, a signaling kinase with multiple downstream target proteins, is an essential regulator of peripheral B-cell development with a critical role in immune homeostasis. Among its main roles, PKCδ is responsible for the regulation of survival, proliferation, and apoptosis in a variety of cells including lymphocytes, while deficiency in PKCδ leads to systemic autoimmunity (74). Moreover, COMM domain-containing protein 3 (COMMD3) is an uncharacterised member of the COMMD family of proteins that interact with NF-κB and modulate its response (75).

Another group of proteins found upregulated in Tg197/Tg5519 ankles are involved in intracellular vesicular transport, endocytosis and invasiveness in extracellular matrix. MYO1B (Myosin IB) along with actin have been implicated in the control of secretory granule biogenesis and invagination of the plasma membrane during endocytosis (76). ACAP2 (ArfGAP With Coiled-Coil, Ankyrin Repeat And PH Domains 2), is a GTPase-activating protein that plays central role in endocytosis and FcγR-mediated phagocytosis (77), while CRP2 (Cysteine Rich Protein 2) is a new cytoskeletal component of invadopodia promoting breast cancer cell invasiveness and metastasis (78).

To our knowledge, this is the first study showing a proinflammatory role of RANKL in modeled arthritis apart from its well-established bone resorbing properties. A similar effect of RANKL has been identified in experimental periodontitis as RANKL antagonists inhibit both tissue inflammation and bone loss (79). Given that RA is a heterogeneous disease and so far the effect of denosumab in RA has been addressed only for a 12-month period, further studies are needed to investigate the inflammatory properties of RANKL in RA patients. Our results support that RANKL synergizes with TNF not only in local and systemic bone resorption but also in the inflammatory phenotype developed in modeled arthritis. Abundance of RANKL in TNF-driven arthritis worsens arthritis severity as shown by an increase in bone resorption, inflammatory cells and protein biomarkers indicative of extented osteoclastogenesis, tissue damage and activation of the immune system. Moreover, RANKL is essential for physiological and inflammation-induced bone remodeling, while TNF induces osteoclastogenesis *in vivo* at contact sites between synovium and bone. Therefore, RANKL provides an interesting candidate for resolution of inflammatory resorption in RA, whereas a dual inhibition of RANKL and TNF seems a promising therapeutic approach for severe inflammatory osteolytic arthritis.

AUTHOR CONTRIBUTIONS

ED conceived and designed the study, supervised experiments, and wrote the manuscript. MP performed and analyzed the majority of experiments and prepared the manuscript. VR

performed microCT analysis and edited the manuscript. FV and MS conducted proteomic analysis and edited the manuscript. TT performed statistic analysis in proteomics data. GP provided scientific insight and edited the manuscript.

FUNDING

This work was supported by the Seventh Framework Programme Marie Curie Initial Training Network Osteoimmune Grant FP7-PEOPLE-2011-ITN-289150 (to ED).

ACKNOWLEDGMENTS

We thank Professor George Kollias (Biomedical Sciences Research Center Alexander Fleming) for kindly providing Tg197 human TNF transgenic mice.

SUPPLEMENTARY MATERIAL

The Supplementary Material for this article can be found online at: https://www.frontiersin.org/articles/10.3389/fimmu.2019.00097/full#supplementary-material

REFERENCES

1. Fuller K, Wong B, Fox S, Choi Y, Chambers TJ. TRANCE is necessary and sufficient for osteoblast-mediated activation of bone resorption in osteoclasts. *J Exp Med*. (1998) 188:997–1001. doi: 10.1084/jem.188.5.997
2. Lacey DL, Timms E, Tan HL, Kelley MJ, Dunstan CR, Burgess T, et al. Osteoprotegerin ligand is a cytokine that regulates osteoclast differentiation and activation. *Cell* (1998) 93:165–76. doi: 10.1016/S0092-8674(00)81569-X
3. Yasuda H, Shima N, Nakagawa N, Yamaguchi K, Kinosaki M, Mochizuki S, et al. Osteoclast differentiation factor is a ligand for osteoprotegerin/osteoclastogenesis-inhibitory factor and is identical to TRANCE/RANKL. *Proc Natl Acad Sci USA*. (1998) 95:3597–602. doi: 10.1073/pnas.95.7.3597
4. Seeman E, Delmas PD. Bone quality–the material and structural basis of bone strength and fragility. *N Engl J Med*. (2006) 354:2250–61. doi: 10.1056/NEJMra053077
5. Kong YY, Yoshida H, Sarosi I, Tan HL, Timms E, Capparelli C, et al. OPGL is a key regulator of osteoclastogenesis, lymphocyte development and lymph-node organogenesis. *Nature* (1999) 397:315–23. doi: 10.1038/16852
6. Kim D, Mebius RE, MacMicking JD, Jung S, Cupedo T, Castellanos Y, Rho J, et al. Regulation of peripheral lymph node genesis by the tumor necrosis factor family member TRANCE. *J Exp Med*. (2000) 192:1467–78. doi: 10.1084/jem.192.10.1467
7. Dougall WC, Glaccum M, Charrier K, Rohrbach K, Brasel K, De Smedt T, et al. RANK is essential for osteoclast and lymph node development. *Genes Dev*. (1999) 13:2412–24. doi: 10.1101/gad.13.18.2412
8. Simonet WS, Lacey DL, Dunstan CR, Kelley M, Chang MS, Lüthy R, et al. Osteoprotegerin: a novel secreted protein involved in the regulation of bone density. *Cell* (1997) 89:309–19. doi: 10.1016/S0092-8674(00)80209-3
9. Darby AJ. Bone formation and resorption in postmenopausal osteoporosis. *Lancet* (1981) 2:536. doi: 10.1016/S0140-6736(81)90931-4
10. Cummings SR, San Martin J, McClung MR, Siris ES, Eastell R, Reid IR, et al. Denosumab for prevention of fractures in postmenopausal women with osteoporosis. *N Engl J Med*. (2009) 361:1914. doi: 10.1056/NEJMoa0809493
11. Leibbrandt A, Penninger JM. Novel functions of RANK(L) signaling in the immune system. *Adv Exp Med Biol*. (2010) 658:77–94. doi: 10.1007/978-1-4419-1050-9_9
12. Tanaka Y. Clinical immunity in bone and joints. *J Bone Miner Metab* (2018). doi: 10.1007/s00774-018-0965-5. [Epub ahead of print].
13. Firestein GS. Evolving concepts of rheumatoid arthritis. *Nature* (2003) 423:356–61. doi: 10.1038/nature01661
14. Feldmann M, Brennan FM, Foxwell BM, Maini RN. The role of TNF alpha and IL-1 in rheumatoid arthritis. *Curr Dir Autoimmun*. (2001) 3:188–99. doi: 10.1159/000060522)
15. Keffer J, Probert L, Cazlaris H, Georgopoulos S, Kaslaris E, Kioussis D, et al. Transgenic mice expressing human tumour necrosis factor: a predictive genetic model of arthritis. *EMBO J*. (1991) 10:4025–31. doi: 10.1002/J.1460-2075.1991.TB04978.X
16. Kontoyiannis D, Pasparakis M, Pizarro TT, Cominelli F, Kollias G. Impaired on/off regulation of TNF biosynthesis in mice lacking TNF AU- rich elements: implications for joint and gut-associated immunopathologies. *Immunity* (1999) 10:387–98. doi: 10.1016/S1074-7613(00)80038-2
17. Elliott MJ, Maini RN, Feldmann M, Long-Fox A, Charles P, Bijl H, et al. Repeated therapy with monoclonal antibody to tumour necrosis factor alpha (cA2) in patients with rheumatoid arthritis. *Lancet* (1994) 344:1125–7. doi: 10.1016/S0140-6736(94)90632-7
18. Boyce BF, Li P, Yao Z, Zhang Q, Badell IR, Schwarz EM, et al. TNF-alpha and pathologic bone resorption. *Keio J Med*. (2005) 54:127–31. doi: 10.2302/kjm.54.127
19. Azuma Y, Kaji K, Katogi R, Takeshita S, Kudo A. Tumor necrosis factor-alpha induces differentiation of and bone resorption by osteoclasts. *J Biol Chem*. (2000) 275:4858–64. doi: 10.1074/jbc.275.7.4858
20. Kobayashi K, Takahashi N, Jimi E, Udagawa N, Takami M, Kotake S, et al. Tumor necrosis factor stimulates osteoclast differentiation by a mechanism independent of the Odf/rankl-rank interaction. *J Exp Med*. (2000) 191:275–86. doi: 10.1084/jem.191.2.275
21. Fuller K, Murphy C, Kirstein B, Fox SW, Chambers TJ. TNFα potently activates osteoclasts, through a direct action independent of and strongly synergistic with RANKL. *Endocrinology* (2002) 143:1108–18. doi: 10.1210/en.143.3.1108
22. Douni E, Rinotas V, Makrinou E, Zwerina J, Penninger JM, Eliopoulos E, et al. A RANKL G278R mutation causing osteopetrosis identifies a functional amino acid essential for trimer assembly in RANKL and TNF. *Hum Mol Genet*. (2012) 21:784–98. doi: 10.1093/hmg/ddr510
23. Rinotas V, Niti A, Dacquin R, Bonnet N, Stolina M, Han CY, et al. Novel genetic models of osteoporosis by overexpression of human RANKL in transgenic mice. *J Bone Miner Res*. (2014) 29:1158–69. doi: 10.1002/jbmr.2112
24. Douni E, Sfikakis PP, Haralambous S, Fernandes P, Kollias G. Attenuation of inflammatory polyarthritis in TNF transgenic mice by diacerein: comparative analysis with dexamethasone, methotrexate and anti-TNF protocols. *Arthritis Res Ther*. (2004) 6:R65–72. doi: 10.1186/ar1028
25. van 't Hof RJ, Rose L, Bassonga E, Daroszewska A. Open source software for semi-automated histomorphometry of bone resorption and formation parameters. *Bone* (2017) 99:69–79. doi: 10.1016/j.bone.2017.03.051
26. Bouxsein ML, Boyd SK, Christiansen BA, Guldberg RE, Jepsen KJ, Müller R. Guidelines for assessment of bone microstructure in rodents using micro-computed tomography. *J Bone Miner Res*. (2010) 25:1468–86. doi: 10.1002/jbmr.141
27. Armaka M, Gkretsi V, Kontoyiannis D, Kollias G. A standardized protocol for the isolation and culture of normal and arthritogenic murine synovial fibroblasts. *Protoc Exch* (2009). doi: 10.1038/nprot.2009.102
28. Tyanova S, Cox J. Perseus: a bioinformatics platform for integrative analysis of proteomics data in cancer research. *Methods Mol Biol*. (2018) 1711:133–48. doi: 10.1007/978-1-4939-7493-1_7
29. Bindea G, Mlecnik B, Hackl H, Charoentong P, Tosolini M, Kirilovsky A, et al. ClueGO: a cytoscape plug-in to decipher functionally grouped gene ontology and pathway annotation networks. *Bioinformatics* (2009) 25:1091–3. doi: 10.1093/bioinformatics/btp101
30. Ogata H, Goto S, Sato K, Fujibuchi W, Bono H, Kanehisa M. KEGG: kyoto encyclopedia of genes and genomes. *Nucleic Acids Res*. (1999) 27:29–34. doi: 10.1093/nar/27.1.29
31. Cox J, Mann M. Maxquant enables high peptide identification rates, individualized p.p.b.-range mass accuracies and proteome-wide protein quantification. *Nat Biotechnol*. (2008) 26:1367–72. doi: 10.1038/nbt.1511

32. Cox J, Hein MY, Luber CA, Paron I, Nagaraj N, Mann M. Accurate proteome-wide label-free quantification by delayed normalization and maximal peptide ratio extraction, termed maxlfq. *Mol Cell Proteomics* (2014) 13:2513–26. doi: 10.1074/mcp.M113.031591
33. Gravallese EM, Manning C, Tsay A, Naito A, Pan C, Amento E, et al. Synovial tissue in rheumatoid arthritis is a source of osteoclast differentiation factor. *Arthritis Rheum*. (2000) 43:250–8. doi: 10.1002/1529-0131(200002)43:2<250::AID-ANR3>3.0.CO;2-P
34. Shigeyama Y, Pap T, Kunzler P, Simmen BR, Gay RE, Gay S. Expression of osteoclast differentiation factor in rheumatoid arthritis. *Arthritis Rheum*. (2000) 43:2523–30. doi: 10.1002/1529-0131(200011)43:11<2523::AID-ANR20>3.0.CO;2-Z
35. Takayanagi H, Iizuka H, Juji T, Nakagawa T, Yamamoto A, Miyazaki T, et al. Involvement of receptor activator of nuclear factor κB ligand/osteoclast differentiation factor in osteoclastogenesis from synoviocytes in rheumatoid arthritis. *Arthritis Rheum*. (2000) 43:259–69. doi: 10.1002/1529-0131(200002)43:2<259::AID-ANR4>3.0.CO;2-W
36. Cohen SB, Dore RK, Lane NE, Ory PA, Peterfy CG, Sharp JT, et al. Denosumab treatment effects on structural damage, bone mineral density, and bone turnover in rheumatoid arthritis: a twelve-month, multicenter, randomized, double-blind, placebo-controlled, phase II clinical trial. *Arthritis Rheum*. (2008) 58:1299–309. doi: 10.1002/art.23417
37. Takeuchi T, Tanaka Y, Ishiguro N, Yamanaka H, Yoneda T, Ohira T, et al. Effect of denosumab on Japanese patients with rheumatoid arthritis: a dose-response study of AMG 162 (Denosumab) in patients with rheumatoid arthritis on methotrexate to validate inhibitory effect on bone erosion (DRIVE) - A 12-month, multicentre, randomi. *Ann Rheum Dis*. (2016) 75:983–90. doi: 10.1136/annrheumdis-2015-208052
38. Sharp JT, Tsuji W, Ory P, Harper-Barek C, Wang H, Newmark R. Denosumab prevents metacarpal shaft cortical bone loss in patients with erosive rheumatoid arthritis. *Arthritis Care Res*. (2010) 62:537–44. doi: 10.1002/acr.20172
39. Deodhar A, Dore RK, Mandel D, Schechtman J, Shergy W, Trapp R, et al. Denosumab-mediated increase in hand bone mineral density associated with decreased progression of bone erosion in rheumatoid arthritis patients. *Arthritis Care Res*. (2010) 62:569–74. doi: 10.1002/acr.20004
40. Redlich K, Hayer S, Ricci R, David J, Tohidast-Akrad M, Kollias G, et al. Osteoclasts are essential for TNF-alpha-mediated joint destruction. *J Clin Invest*. (2002) 110:1419–27. doi: 10.1172/JCI15582
41. Li J, Sarosi I, Yan XQ, Morony S, Capparelli C, Tan HL, et al. RANK is the intrinsic hematopoietic cell surface receptor that controls osteoclastogenesis and regulation of bone mass and calcium metabolism. *Proc Natl Acad Sci USA*. (2000) 97:1566–71. doi: 10.1073/pnas.97.4.1566
42. Li P, Schwarz EM, O'Keefe RJ, Ma L, Boyce BF, Xing L. RANK signaling is not required for TNFalpha-mediated increase in CD11(hi) osteoclast precursors but is essential for mature osteoclast formation in TNFalpha-mediated inflammatory arthritis. *J Bone Miner Res*. (2004) 19:207–13. doi: 10.1359/JBMR.0301233
43. O'Brien W, Fissel BM, Maeda Y, Yan J, Ge X, Gravallese EM, et al. RANK-independent osteoclast formation and bone erosion in inflammatory arthritis. *Arthritis Rheumatol*. (2016) 68:2889–900. doi: 10.1002/art.39837
44. Lipsky PE, Davis LS, Cush JJ, Oppenheimer-Marks N. The role of cytokines in the pathogenesis of rheumatoid arthritis. *Springer Semin Immunopathol*. (1989) 11:123–62. doi: 10.1007/BF00197186
45. Poubelle PE, Chakravarti A, Fernandes MJ, Doiron K, Marceau AA. Differential expression of RANK, RANK-L, and osteoprotegerin by synovial fluid neutrophils from patients with rheumatoid arthritis and by healthy human blood neutrophils. *Arthritis Res Ther*. (2007) 9:R25. doi: 10.1186/ar2137
46. Quercioli A, Mach F, Bertolotto M, Lenglet S, Vuilleumier N, Galan K, et al. Receptor activator of NF-κB ligand (RANKL) increases the release ofneutrophil products associated with coronary vulnerability. *Thromb Haemost*. (2012) 107:124–39. doi: 10.1160/TH11-05-0324
47. Carbone F, Crowe LA, Roth A, Burger F, Lenglet S, Braunersreuther V, et al. Treatment with anti-RANKL antibody reduces infarct size and attenuates dysfunction impacting on neutrophil-mediated injury. *J Mol Cell Cardiol*. (2016) 94:82–94. doi: 10.1016/j.yjmcc.2016.03.013
48. Park Y-J, Chung MK, Hwang D, Kim W-U. Proteomics in rheumatoid arthritis research. *Immune Netw*. (2015) 15:177–85. doi: 10.4110/in.2015.15.4.177
49. Fearon U, Canavan M, Biniecka M, Veale DJ. Hypoxia, mitochondrial dysfunction and synovial invasiveness in rheumatoid arthritis. *Nat Rev Rheumatol*. (2016) 12:385–97. doi: 10.1038/nrrheum.2016.69
50. Potempa J, Korzus E, Travis J. The serpin superfamily of proteinase inhibitors: structure, function, and regulation. *J Biol Chem*. (1994) 269:15957–60. doi: 10.1021/ed056pA86.2
51. Ek-Rylander B, Flores M, Wendel M, Heinegard D, Andersson G. Dephosphorylation of osteopontin and bone sialoprotein by osteoclastic tartrate-resistant acid phosphatase. Modulation of osteoclast adhesion *in vitro*. *J Biol Chem*. (1994) 269:14853–6. doi: 10.1111/j.1095-8649.2004.00473.x
52. Bossard MJ, Tomaszek TA, Thompson SK, Amegadzie BY, Hanning CR, Jones C, et al. Proteolytic activity of human osteoclast cathepsin K: expression, purification, activation, and substrate identification. *J Biol Chem*. (1996) 271:12517–24. doi: 10.1074/jbc.271.21.12517
53. Asagiri M, Hirai T, Kunigami T, Kamano S, Gober HJ, Okamoto K, et al. Cathepsin K-dependent toll-like receptor 9 signaling revealed in experimental arthritis. *Science* (2008) 319:624–7. doi: 10.1126/science.1150110
54. Cotter K, Stransky L, McGuire C, Forgac M. Recent insights into the structure, regulation, and function of the V-ATPases. *Trends Biochem Sci*. (2015) 40:611–22. doi: 10.1016/j.tibs.2015.08.005
55. Trombetta ES, Ebersold M, Garrett W, Pypaert M, Mellman I. Activation of lysosomal function during dendritic cell maturation. *Science* (2003) 299:1400–3. doi: 10.1126/science.1080106
56. Qin A, Cheng TS, Pavlos NJ, Lin Z, Dai KR, Zheng MH. V-ATPases in osteoclasts: structure, function and potential inhibitors of bone resorption. *Int J Biochem Cell Biol*. (2012) 44:1422–35. doi: 10.1016/j.biocel.2012.05.014
57. Gilman-Sachs A, Tikoo A, Akman-Anderson L, Jaiswal M, Ntrivalas E, Beaman K. Expression and role of a2 vacuolar-ATPase (a2V) in trafficking of human neutrophil granules and exocytosis. *J Leukoc Biol*. (2015) 97:1121–31. doi: 10.1189/jlb.3A1214-620RR
58. Scherer O, Steinmetz H, Kaether C, Weinigel C, Barz D, Kleinert H, et al. Targeting V-ATPase in primary human monocytes by archazolid potently represses the classical secretion of cytokines due to accumulation at the endoplasmic reticulum. *Biochem Pharmacol*. (2014) 91:490–500. doi: 10.1016/j.bcp.2014.07.028
59. Ibáñez L, Abou-Ezzi G, Ciucci T, Amiot V, Belaïd N, Obino D, et al. Inflammatory Osteoclasts Prime TNFα-Producing CD4+T Cells and Express CX3CR1. *J Bone Miner Res*. (2016) 31:1899–908. doi: 10.1002/jbmr.2868
60. Lotze MT, Tracey KJ. High-mobility group box 1 protein (HMGB1): nuclear weapon in the immune arsenal. *Nat Rev Immunol*. (2005) 5:331–42. doi: 10.1038/nri1594
61. Yanai H, Ban T, Wang Z, Choi MK, Kawamura T, Negishi H, et al. HMGB proteins function as universal sentinels for nucleic-acid-mediated innate immune responses. *Nature* (2009) 462:99–103. doi: 10.1038/nature08512
62. Andersson U, Tracey KJ. HMGB1 is a therapeutic target for sterile inflammation and infection. *Annu Rev Immunol*. (2011) 29:139–62. doi: 10.1146/annurev-immunol-030409-101323
63. Taniguchi N, Kawakami Y, Maruyama I, Lotz M. HMGB proteins and arthritis. *Hum Cell* (2018) 31:1–9. doi: 10.1007/s13577-017-0182-x
64. Park JS, Svetkauskaite D, He Q, Kim JY, Strassheim D, Ishizaka A, et al. Involvement of toll-like receptors 2 and 4 in cellular activation by high mobility group box 1 protein. *J Biol Chem*. (2004) 279:7370–7. doi: 10.1074/jbc.M306793200
65. Millevoi S, Loulergue C, Dettwiler S, Karaa SZ, Keller W, Antoniou M, et al. An interaction between U2AF 65 and CF Imlinks the splicing and 3′ end processing machineries. *EMBO J*. (2006) 25:4854–64. doi: 10.1038/sj.emboj.7601331
66. Whisenant TC, Peralta ER, Aarreberg LD, Gao NJ, Head SR, Ordoukhanian P, et al. The activation-induced assembly of an RNA/protein interactome centered on the splicing factor U2AF2 regulates gene expression in human CD4 T cells. *PLoS ONE* (2015) 10:e0144409. doi: 10.1371/journal.pone.0144409
67. Yang W-H, Ding M-J, Cui G-Z, Yang M, Dai D-L. Heterogeneous nuclear ribonucleoprotein M promotes the progression of breast cancer by regulating the axin/β-catenin signaling pathway. *Biomed Pharmacother*. (2018) 105:848–55. doi: 10.1016/j.biopha.2018.05.014

68. Gruber JJ, Zatechka DS, Sabin LR, Yong J, Lum JJ, Kong M, et al. Ars2 Links the nuclear cap-binding complex to RNA interference and cell proliferation. *Cell* (2009) 138:328–39. doi: 10.1016/j.cell.2009.04.046
69. Elahi S, Egan SM, Holling GA, Kandefer RL, Nemeth MJ, Olejniczak SH. The RNA binding protein Ars2 supports hematopoiesis at multiple levels. *Exp Hematol*. (2018) 64:45–58.e9. doi: 10.1016/j.exphem.2018.05.001
70. Steimer L, Klostermeier D. RNA helicases in infection and disease. *RNA Biol*. (2012) 9:751–71. doi: 10.4161/rna.20090
71. Xing YH, Yao RW, Zhang Y, Guo CJ, Jiang S, Xu G, et al. SLERT regulates DDX21 rings associated with Pol I transcription. *Cell* (2017) 169:664–78.e16. doi: 10.1016/j.cell.2017.04.011
72. Zhang H-X, Liu Z-X, Sun Y-P, Zhu J, Lu S-Y, Liu X-S, et al. Rig-I regulates NF-B activity through binding to Nf- b1 3′-UTR mRNA. *Proc Natl Acad Sci USA*. (2013) 110:6459–64. doi: 10.1073/pnas.1304432110
73. Jiang Y, Tian M, Lin W, Wang X, Wang X. Protein kinase serine/threonine kinase 24 positively regulates interleukin 17-induced inflammation by promoting IKK complex activation. *Front Immunol*. (2018) 9:1–16. doi: 10.3389/fimmu.2018.00921
74. Salzer E, Santos-Valente E, Keller B, Warnatz K, Boztug K. Protein kinase C δ: a gatekeeper of immune homeostasis. *J Clin Immunol*. (2016) 36:631–40. doi: 10.1007/s10875-016-0323-0
75. Bartuzi P, Hofker MH, van de Sluis B. Tuning NF-κB activity: a touch of COMMD proteins. *Biochim Biophys Acta* (2013) 1832:2315–21. doi: 10.1016/j.bbadis.2013.09.014
76. Delestre-Delacour C, Carmon O, Laguerre F, Estay-Ahumada C, Courel M, Elias S, et al. Myosin 1b and F-actin are involved in the control of secretory granule biogenesis. *Sci Rep*. (2017) 7:5172. doi: 10.1038/s41598-017-05617-1
77. Egami Y, Fujii M, Kawai K, Ishikawa Y, Fukuda M, Araki N. Activation-inactivation cycling of Rab35 and ARF6 is required for phagocytosis of zymosan in RAW264 macrophages. *J Immunol Res*. (2015) 2015:429439. doi: 10.1155/2015/429439
78. Hoffmann C, Mao X, Dieterle M, Moreau F, Absi A Al, Steinmetz A, et al. CRP2, a new invadopodia actin bundling factor critically promotes breast cancer cell invasion and metastasis. *Oncotarget* (2016) 7:13688–705. doi: 10.18632/oncotarget.7327
79. Yuan H, Gupte R, Zelkha S, Amar S. Receptor activator of nuclear factor kappa B ligand antagonists inhibit tissue inflammation and bone loss in experimental periodontitis. *J Clin Periodontol*. (2011) 38:1029–36. doi: 10.1111/j.1600-051X.2011.01780.x

Conflict of Interest Statement: The authors declare that the research was conducted in the absence of any commercial or financial relationships that could be construed as a potential conflict of interest.

frontiers in Immunology

ORIGINAL RESEARCH
published: 05 March 2019
doi: 10.3389/fimmu.2019.00383

Shear and Dynamic Compression Modulates the Inflammatory Phenotype of Human Monocytes *in vitro*

*Niamh Fahy, Ursula Menzel, Mauro Alini and Martin J. Stoddart**

AO Research Institute Davos, Davos, Switzerland

Monocytes and their derived macrophages are found at the site of remodeling tissue, such as fracture hematoma, that is exposed to mechanical forces and have been previously implicated in the reparative response. However, the mechanoresponsive of monocytes and macrophages to skeletal tissue-associated mechanical forces and their subsequent contribution to skeletal repair remains unclear. The aim of this study was to investigate the potential of skeletal tissue-associated loading conditions to modulate human monocyte activation and phenotype. Primary human monocytes or the human monocyte reporter cell line, THP1-Blue, were encapsulated in agarose and exposed to a combination of shear and compressive loading for 1 h a day for 3 consecutive days. Exposure of monocytes to mechanical loading conditions increased their pro-inflammatory gene and protein expression. Exposure of undifferentiated monocytes to mechanical loading conditions significantly upregulated gene expression levels of interleukin(IL)-6 and IL-8 compared to free swelling controls. Additionally, multiaxial loading of unstimulated monocytes resulted in increased protein secretion of TNF-α (17.1 ± 8.9 vs. 8 ± 7.4 pg/ml) and MIP-1α (636.8 ± 471.1 vs. 124.1 ± 40.1 pg/ml), as well as IL-13 (42.1 ± 19.8 vs. 21.7 ± 13.6) compared monocytes cultured under free-swelling conditions. This modulatory effect was observed irrespective of previous activation with the M1/pro-inflammatory differentiation stimuli lipopolysaccharide and interferon-γ or the M2/anti-inflammatory differentiation factor interleukin-4. Furthermore, mechanical shear and compression were found to differentially regulate nitric oxide synthase 2 (NOS2) and IL-12B gene expression as well as inflammatory protein production by THP1-Blue monocytes. The findings of this study indicate that human monocytes are responsive to mechanical stimuli, with a modulatory effect of shear and compressive loading observed toward pro-inflammatory mediator production. This may play a role in healing pathways that are mechanically regulated. An in depth understanding of the impact of skeletal tissue-associated mechanical loading on monocyte behavior may identify novel targets to maximize inflammation-mediated repair mechanisms.

Keywords: osteoimmunology, immune regulation, fracture repair, mechanoregulation, bone healing, macrophage

OPEN ACCESS

Edited by:
Claudine Blin-Wakkach, UMR7370 Laboratoire de Physio Médecine Moléculaire (LP2M), France

Reviewed by:
Melanie Haffner-Luntzer, University of Ulm, Germany
Valérie Trichet, University of Nantes, France
Emeline Groult, UMS3760 Institut de Biologie et Chimie des Protéines (IBCP), France

****Correspondence:***
Martin J. Stoddart
martin.stoddart@aofoundation.org

Specialty section:
This article was submitted to Inflammation, a section of the journal Frontiers in Immunology

Received: *08 November 2018*
Accepted: *14 February 2019*
Published: *05 March 2019*

Citation:
Fahy N, Menzel U, Alini M and Stoddart MJ (2019) Shear and Dynamic Compression Modulates the Inflammatory Phenotype of Human Monocytes in vitro. Front. Immunol. 10:383. doi: 10.3389/fimmu.2019.00383

INTRODUCTION

The repair process following traumatic injury to the musculoskeletal system is known to be influenced by the mechanical environment. The natural course of bone healing can be intramembranous ossification resulting from stable fracture fixation and subsequent low interfragmentary motion, or endochondral ossification which is associated with moderate interfragmentary movement (1). In addition to driving fracture healing responses, mechanical forces of an appropriate magnitude are also key to maintaining cartilage homeostasis within the articulating joint (2).

A wound healing response is initiated during the process of bone fracture repair, as well as marrow stimulation techniques applied in cartilage repair strategies where the subchondral bone is penetrated. This involves inflammatory cell exudation or infiltration to the site of injury, followed by coagulation activation and fibrin clot formation, which is known to regulate monocyte chemotaxis and proliferation (3, 4). Monocytes and monocyte-derived macrophages are key immune effector cells playing a vital role in host defense, as well as contributing to tissue remodeling and repair (5). Macrophages are associated with a high degree of plasticity having the potential to change phenotype in response to environmental cues, and may be classified according to pro-inflammatory (M1) or anti-inflammatory (M2) subsets (5). Pro-inflammatory macrophages are associated with high production of pro-inflammatory cytokines and increased microbicidal activity, whereas anti-inflammatory macrophages are associated with wound healing and immunoregulatory functions (3, 6).

Infiltrating monocytes and macrophages may influence the success of musculoskeletal tissue repair processes. Macrophage depletion has been previously demonstrated to negatively impact endochondral ossification and subsequently delay bone fracture healing (7–9). Furthermore, monocyte and macrophage associated inflammatory cytokines such as IL-6 and TNF-α are known to promote bone repair, with inhibition of TNF-α signaling shown to delay both intramembranous and endochondral bone formation (10, 11). In contrast to bone healing, pro-inflammatory factors such as IL-1β and TNF-α produced by both activated monocytes and M1 polarized macrophages, induce destructive processes in cartilage tissue including catabolic enzyme expression and reduced extracellular matrix deposition (12–14). However, recruitment of anti-inflammatory macrophages to the site of subchondral drill holes within osteochondral defects using chitosan-glycerol phosphate composites was reported enhance subchondral bone repair and improve cartilage resurfacing, further highlighting the impact of macrophages on skeletal tissue repair (15). Monocytes and macrophages are found at the site of remodeling tissue that is exposed to mechanical forces and have been previously implicated in the reparative response (16–18). As the area of osteoimmunology gains in importance, the influence of mechanical stimulation on immune cell phenotype needs to be investigated in greater detail. However, the responsiveness of macrophages and monocytes, their lineage precursors, to mechanical forces that are native to skeletal tissues and the effect of such mechanical stimuli on macrophage phenotype requires further elucidation. Therefore, the aim of this study was to investigate the impact of mechanical shear and compressive loading on monocyte activation and phenotype. Unstimulated, M1 or M2-stimulated primary human monocytes as well as the human monocyte reporter cell line, THP1-Blue, were exposed to a combination of shear and compressive loading *in vitro*. Gene expression levels of inflammatory mediators and inflammatory protein secretion was assessed following 3 days of mechanical stimulation.

MATERIALS AND METHODS

Human Monocyte Isolation

Human monocytes were isolated from buffy coats left over from voluntary whole blood donations after informed consent of the donors according to the regulations of Swiss Red Cross Blood Service. Buffy coats were processed within 23 h after blood donation by centrifugation at 5,000 g for 15 min and subsequent separation on Compomat G5 (Fresenius, Oberdorf, Switzerland) using top-and-bottom 450 ml blood bag systems pre-filled with Citrate-Dextrose-Phosphate Solution (Fresenius). Buffy coats were anonymized prior to delivery from the Blood Service to AO Institute in line with the ethics code provided by the Swiss Drug Law (Heilmittelgesetz). For the isolation of peripheral blood mononuclear cells (PBMCs), each buffy coat was diluted at a 1:5 ratio with 0.1% bovine serum albumin (BSA) in phosphate buffered saline (PBS). Thirty milliliter of diluted buffy coat was layered on 15 ml of Ficoll and centrifuged at 1,000 g for 15 min without brake. Following centrifugation, the interphase layer containing PBMCs was removed and washed with 0.5% BSA/PBS containing 2 mM EDTA. Isolated PBMCs were labeled with 100 μl of anti-CD14 magnetic bead solution (Miltenyi Biotec Bergisch Gladbach, Germany) in the dark at 4°C for 20 min. Monocytes were isolated utilizing MACS LS Separation columns and a MidiMACS™ Separator (Miltenyi Biotec), according to manufacturer's instructions. Purity of isolated CD14+ cells was assessed by fluorescence activated cell sorting (FACS) analysis. 1×10^5 monocytes were incubated with APC-Cy7-conjugated anti-human CD14 antibody (BD pharmingen) for 20 min in the dark at 4°C. FACS analysis was performed using a BD Aria III machine, and data analyzed using BD FACS Diva 6.1.3 software (BD Biosciences). The average purity of CD14+ monocytes from all donors was found to be 95% (data not shown). Monocytes were isolated from two individual buffy coat donors and pooled per experiment.

THP1-Blue™ Cell Culture

The human monocyte reporter cell line THP1-Blue™ (InvivoGen, CA, USA) which expresses an NF-κB and AP-1-inducible secreted embryonic alkaline phosphatase (SEAP) reporter gene, was cultured in RPMI-1640 medium (2 mM L-glutamine; Gibco, Carlsbad, USA) supplemented with 1% penicillin/streptomycin (Gibco) and 10% heat inactivated fetal bovine serum (FBS; Pan Biotech, Aidenbach, Germany). Monocyte suspension cultures were maintained at a density of at 3–8 × 100,000 cells/ml.

Agarose Gel Seeding and Culture

To evaluate the effect of mechanical loading on monocyte phenotype, human primary monocytes and THP1-Blue cells were encapsulated in 2% low melting temperature agarose (Lonza) at a cell density of 3×10^6 monocytes per gel. In brief, a 4% agarose solution was prepared by dissolving low melting temperature agarose in sterile phosphate buffered saline and heated. The 4% agarose solution was cooled and mixed with an equal volume of cells suspended in pre-warmed culture media, composed of RPMI-1640 medium supplemented with 2 mM L-glutamine, 1% penicillin/streptomycin and 10% heat inactivated FBS. Two hundred and fifty microliters of cells/agarose suspension was added to a sterile cap of an Eppendorf tube and gels were allow to set at 37°C for 20 min. All agarose constructs were carefully removed from the Eppendorf cap, placed in a sterile PEEK sample holder and cultured with 2.5 ml of culture medium. To investigate the effect of mechanical loading on macrophage phenotype, CD14+ monocytes were stimulated with 10 ng/ml IFN-γ (PeproTech, Rocky Hill, NJ, USA) and 100 ng/ml lipopolysaccharide to induce differentiation toward a pro-inflammatory/M1 phenotype, 10 ng/ml IL-4 (PeproTech) for an anti-inflammatory/M2 phenotype or unstimulated for 72 h prior to loading. Agarose gels containing THP1-Blue monocytes were prepared 24 h prior to loading.

Mechanical Loading

CD14+ monocyte seeded agarose gels were mechanically loaded using a custom built multi-axial load bioreactor based on a 32 mm ceramic hip ball that can apply compression, shear or a combination of the two, to the sample as previously described (19, 20). Shear (±25° ball rotation at 1 Hz) and compression (10% compression superimposed on top of a 10% pre-strain at 1 Hz) loading was applied for 1 h a day for 3 consecutive days. This protocol was chosen as it has been shown to direct osteochondral differentiation of human MSCs and therefore we aimed to investigate similar loading patterns on the modulation of macrophage phenotype (21). Control gels were maintained in free-swelling conditions for the duration of the experiment. To investigate the effect of shear or compression alone on monocyte phenotype, THP1-Blue monocytes were stimulated with shear or compression alone as well as multiaxial loading for 1 h a day for 3 consecutive days. Control gels were maintained in free-swelling conditions for the duration of the experiment. Cell culture media was refreshed every 24 h prior to loading.

Reverse Transcription and PCR

Monocyte-seeded agarose gels were homogenized in 1 ml TRI reagent (Molecular Research Center Inc., Cincinnati, OH, USA). Homogenized samples were supplemented with 100 μl of 1-Bromo-3-chloropropane (Sigma-Aldrich) and processed according to manufacturer's instructions to achieve phase separation. Following phase separation the aqueous phase was removed, supplemented with an equal volume of 70% ethanol (Sigma-Aldrich) and transferred to a RNeasy spin column (Qiagen, Hilden, Germany). RNA was extracted using RNeasy mini spin columns according to manufacturer's instructions. The purity of isolated RNA was assessed using a NanoDrop spectrophotometer (Fisher Scientific, Delaware, USA) based on the absorbance ratios 260/280 nm and 260/230 nm. Reverse transcription was performed using random hexamer primers and TaqMan reverse transcription reagents (Applied Biosystems, Carlsbad, CA, USA). Quantitative real time PCR was performed in 10 μl reactions on cDNA using the Applied Biosystems QuantStudio 6 Flex Real Time PCR system (Applied Biosystems). Primers for cyclooxygenase(COX)-2 (*PTGS2*) were synthesized by Microsynth AG (Balgach, SG, Switzerland; **Table 1**). Gene expression assays for 18S ribosomal RNA (*18S*), interleukin(IL)-6 (*IL6*), IL-8 (*IL8*), IL-10 (*IL10*), tumor necrosis factor (TNF)-α (*TNF*), chemokine (C-C motif) ligand 18 (*CCL18*), mannose receptor CD206 (*MRC1*), nitric oxide synthase 2 (*NOS2*), and monocyte chemoattractant protein 1 (*CCL2*) were purchased from Applied Biosystems, Switzerland (**Table 1**). Gene expression levels were normalized to 18S rRNA, and relative expression calculated via a ΔΔCT comparison.

Cytokine Assays

Levels of IL-6, IL-8, and CCL18 in cell culture supernatant were quantified utilizing commercially available human IL-6 and CCL18 DuoSet ELISA kits according to manufacturer's instructions (R&D Systems, Minneapolis, Minnesota). Levels of IL-10, IL-13, IL-1β, C-X-C motif chemokine 10 (IP-10), macrophage-derived chemokine (MDC), monocyte chemoattractant protein-1 (MCP-1), macrophage inflammatory protein-1α (MIP-1α), and TNF-α were measured utilizing a Meso Scale Development multiplex assay according to manufacturer's instructions (Meso Scale Discovery, Maryland, USA).

Secreted Alkaline Phosphatase Assay

Secreted embryonic alkaline phosphatase (SEAP) levels were detected in cell culture supernatant using a QUANTI-Blue™ enzymatic assay (InvivoGen) according to manufacturer's instructions. SEAP levels were determined qualitatively following spectrophotometric measurement at 620 nm.

Statistical Analysis

IBM SPSS Statistics 21.0 (IBM, New York, USA) and GraphPad Prism software version 6 (GraphPad Software Inc., La Jolla, USA) were used for all statistical analysis. To take donor variability into account between primary monocyte donors, mixed models analysis was applied to test for statistical differences between loaded and free-swelling groups with monocyte donor considered a random factor. THP1-Blue monocyte data sets were analyzed using a Kruskal–Wallis test followed by Dunn's multiple comparisons test. For all analyses, differences were considered statistically significant at $P < 0.05$.

RESULTS

Pro-inflammatory Gene and Protein Expression by Differentially Activated Primary Human Monocytes Following Multiaxial Loading

Monocytes encapsulated in 2% agarose gel were unstimulated, LPS and IFN-γ or IL-4-stimulated for 3 days, prior to subjection

TABLE 1 | Gene expression assays utilized for quantitative real time PCR.

Gene name	Alias	Assay ID/Primer sequence
Human 18S rRNA (*18S)*	18S ribosomal RNA (18S rRNA)	Hs99999901_s1
Human interleukin-8 (*IL8)*	C-X-C motif chemokine ligand 8 (CXCL8)	Hs00174103_m1
Human interleukin-10 (*IL10)*	Cytokine Synthesis Inhibitory Factor (CSIF)	Hs00961622_m1
Human interleukin-6 (*IL6)*	B-Cell Stimulatory Factor (BSF)- 2	Hs00985639_m1
Human tumor necrosis factor (*TNF)*	Tumor Necrosis Factor (TNF)-α	Hs01113624_g1
Human chemokine (C-C motif) ligand 18 (*CCL18)*	Macrophage Inflammatory Protein (MIP)-4	Hs00268113_m1
Human mannose receptor, C type 1 (*MRC1)*	Macrophage Mannose Receptor (MMR, CD206)	Hs00267207_m1
Human C-C motif chemokine ligand 2 (*CCL2)*	Monocyte Chemoattractant Protein (MCP)-1	Hs00234140_m1
Human nitric oxide synthase 2 (*NOS2)*	Inducible Nitric Oxide Synthase (INOS)	Hs01075529_m1
Human interleukin 12B (*IL12B)*	Natural Killer Cell Stimulatory Factor	Hs01011518_m1
Human Prostaglandin-Endoperoxide Synthase 2 (*PTGS2)*	Cyclooxygenase (COX)-2	**Forward:** 5′-TTG TAC CCG GAC AGG ATT CTA TG-3′ **Reverse:** 5′-TGT TTG GAG TGG GTT TCA GAA ATA-3′ **Probe(5′FAM/3′ TAMRA):** 5′-GAA AAC TGC TCA ACA CCG GAA TTT TTG ACA A-3′

to multiaxial loading or free-swelling conditions and analysis of inflammatory gene and protein expression. Monocytes stimulated with LPS and IFN-γ had significantly higher gene expression levels of the pro-inflammatory genes *IL8* and *CCL2* under free-swelling conditions compared to IL-4 stimulated monocytes (10.3- and 28.3-fold increases, respectively), confirming their pro-inflammatory phenotype (**Figure 1A**). Additionally, IL-4 stimulated monocytes were associated with significantly higher *CCL18* expression compared to LPS and IFN-γ stimulated monocytes (41.5-fold increase), confirming their polarization toward an M2-like phenotype. Unstimulated primary human monocytes significantly upregulated gene expression levels of the pro-inflammatory genes *IL6* (5.9-fold change) and *IL8* (2.8-fold change) following 3 days of mechanical loading compared to monocytes cultured in free-swelling conditions (**Figure 1B**). Additionally, expression of the anti-inflammatory macrophage marker *IL10* was decreased in all four donors compared to free-swell controls, with gene expression levels undetectable in donors 1 and 3 following loading. No significant difference was observed in the expression levels of inflammatory mediators *CCL18*, *TNF*, and *CCL2*. Although a similar trend was observed toward inflammatory gene expression by LPS and IFN-γ activated monocytes following mechanical loading, larger variation was observed between donors and these findings were not statistically significant (**Figure 1C**). However, expression of *CCL2* was significantly decreased (1.9-fold decrease). Additionally, gene expression levels of *IL10* were also undetectable in LPS and IFN-γ stimulated monocytes from donors 1 and 3 following loading. In a similar manner to unstimulated monocytes, IL-4 activated cells were also associated with a significant increase in *IL6* (8.9-fold change) and decrease of *IL10* (3.1-fold) expression (**Figure 1D**).

Compared to free-swelling controls, mechanical loading of unstimulated monocytes significantly increased production of the pro-inflammatory mediators TNF-α (17.1 ± 8.9 vs. 8 ± 7.4 pg/ml) and MIP-1α (636.8 ± 471.1 vs. 124.1 ± 40.1 pg/ml), as well as IL-13 (42.1 ± 19.8 vs. 21.7 ± 13.6) (**Figure 2**). Protein levels of IL-10, CCL18, IP-10, MCP-1, MDC, and IL-1β produced by loaded unstimulated monocytes did not significantly differ from free-swelling controls. In a similar manner to gene expression levels, a trend toward an increase in IL-6 production was observed in response to loading of unstimulated monocytes. However, large donor variation was observed and this finding was not statically significant. Mechanical stimulation of LPS and IFN-γ stimulated monocytes significantly increased MDC levels in addition to TNF-α, MIP-1α, and IL-13 (**Figure 2**). In a similar manner to gene expression data, IL-4 activated monocytes were associated with significantly increased production of pro-inflammatory factors IL-6, IL-8, TNF-α, MIP-1α, IP-10, IL-13, IL-1β as well as IL-10 in response to mechanical loading, and decreased expression of CCL18 and MDC (**Figure 2**).

Inflammatory Gene and Protein Expression by THP1-Blue Monocytes Following Mechanical Shear or Compression

To evaluate the potential of mechanical shear or compression to differentially regulate inflammatory gene and protein expression by human monocytes, unstimulated THP1-Blue monocytes were subjected to multiaxial loading conditions, or mechanical shear or compression alone. THP1-Blue monocytes significantly upregulated gene expression levels of the pro-inflammatory markers *NOS2* and *IL12B* in response to compression alone compared to the combination of compression and shear, as well as shear alone following 3 days of loading (**Figure 3**). Gene expression levels of *IL6*, *IL-8*, *TNF-α*, *PTGS2*, *IL-10*, *CCL2*, and *CCL18* did not significantly differ between loading conditions, or compared to free-swelling controls at this time point. However, significantly increased levels of TNF-α, IL-10, IL-8, IL-13, and MDC were detected in the cell culture media

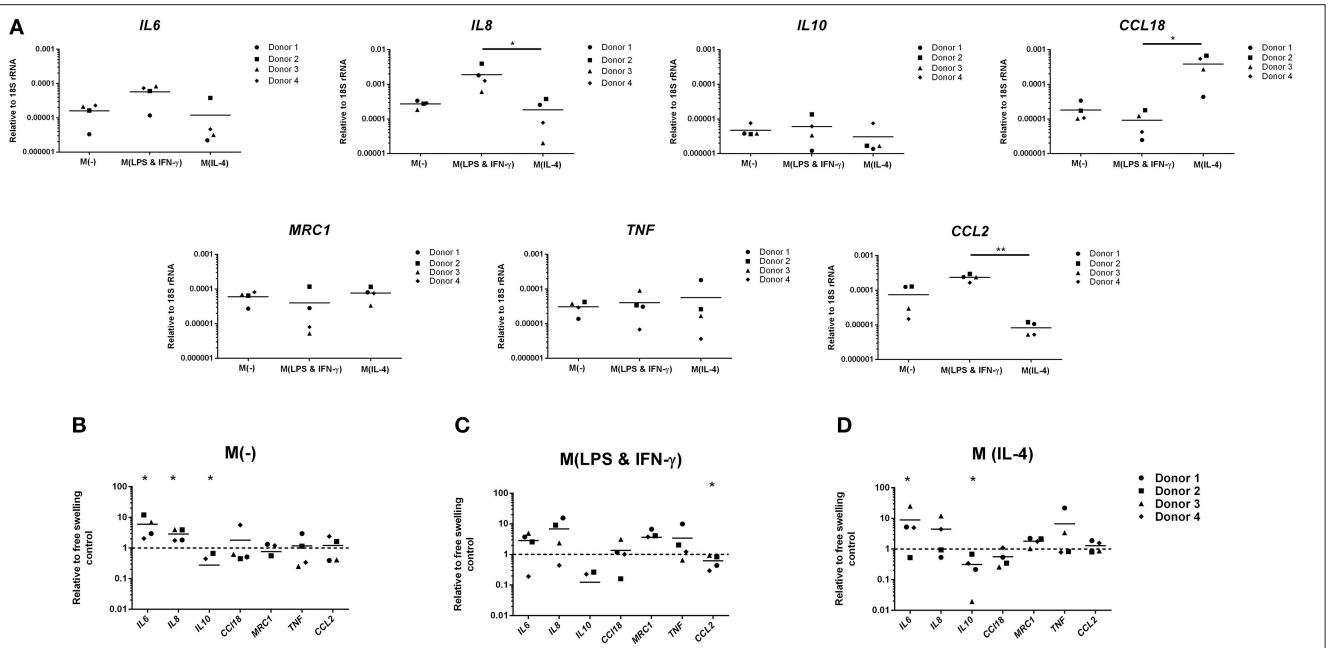

FIGURE 1 | Inflammatory gene expression by differentially activated primary human monocytes following multiaxial loading. **(A)** Gene expression by primary monocytes cultured for 6 days under free-swelling conditions as measured by real-time PCR. Gene expression levels were normalized to the housekeeper gene 18S rRNA. **(B)** Gene expression levels by unstimulated primary human monocytes, or LPS & IFN-γ **(C)** or IL-4 **(D)** stimulated monocytes following 3 days of multiaxial loading. Gene expression levels were normalized to the free swelling control, represented by the dashed line. Data is represented as dot plots including the median for 4 monocyte donors, each assessed in experimental triplicate. Missing points indicate undetectable gene expression. Statistical significance was determined utilizing a mixed model analysis, $^*P < 0.05$.

harvested from gels subjected to the combination of compression and shear, as well as compression and shear alone for 3 days compared to control (**Figure 4A**). Additionally, the application of compressive loading alone significantly upregulated IL-1β production by monocytes, whereas shear alone increased the release of MCP-1 compared to all other culture conditions. Levels of IL-6 and IP-10 did not significantly differ in response to any loading condition compared to free-swelling cultures. In addition to modulating inflammatory cytokine production, the application of both compression and shear or shear alone induced the release of secreted alkaline phosphatase by THP1-Blue monocytes, indicative of NF-κB and AP-1 transcription factor activation (**Figure 4B**).

DISCUSSION

Monocytes and their derived macrophages are considered key players in tissue remodeling and repair processes. Mechanical loading has been previously shown to influence the levels or pro and anti-inflammatory macrophages in a model of tendon healing (18). Additionally, cyclic strain has been reported to modulate macrophage polarization state toward a reparative phenotype which promoted extracellular matrix synthesis (22). Monocytes are found at the site of skeletal tissue injuries resulting from either traumatic bone fractures, or microdrilling of the subchondral bone to facilitate microfracture-mediated cartilage repair (23). However, the mechanoresponsive of monocytes and their derived macrophages to skeletal tissue-associated mechanical forces, and their subsequent contribution to skeletal repair remains unclear. The aim of this study was to investigate the potential of shear and compressive forces to modulate human monocyte activation and phenotype. In the present study, exposure of monocytes to mechanical loading conditions increased their production of pro-inflammatory mediators. Furthermore, mechanical loading modulated the production of inflammatory factors produced by monocytes irrespective of previous activation with the M1/pro-inflammatory differentiation stimuli LPS and IFN-γ or the M2/anti-inflammatory differentiation factor IL-4.

Bone fractures associated with less mechanical stability are known to heal via the process of endochondral ossification, involving inflammation, callus formation and tissue remodeling processes (1). Infiltration of macrophages into the fracture callus occurs at an early stage of fracture healing, and inhibition of macrophage recruitment impairs vascularization, decreases callus formation and delays repair (24). Macrophages are associated with a high degree of plasticity and can change phenotype according to environmental cues, encompassing both pro-inflammatory/M1 and anti-inflammatory/M2 phenotypes (5). In an experimental osteotomy model, M1-polarized macrophages were identified as the primary macrophage phenotype in the osteotomy area 24 h post-surgery (7). Interestingly, M1 polarized macrophages have also been reported to promote the osteogenic differentiation of bone

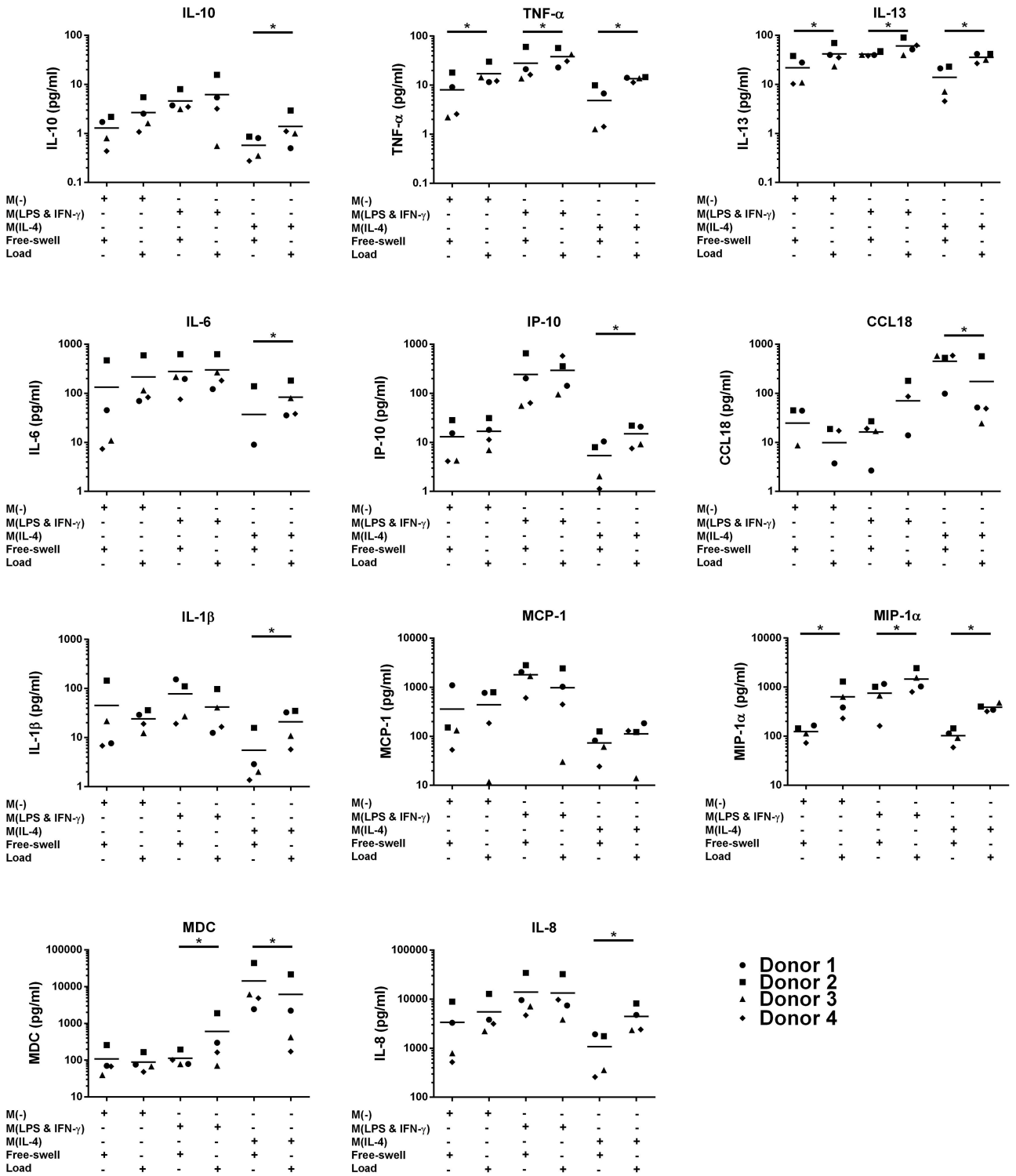

FIGURE 2 | Inflammatory mediator production by primary human monocytes following multiaxial loading. Levels of inflammatory mediators produced by primary monocytes following 3 days of multiaxial loading as quantified by ELISA and multiplex assay. Data is represented as dot plots including the median for 4 monocyte donors, each assessed in experimental triplicate. Missing points indicate undetectable protein levels. Statistical significance was determined utilizing a mixed model analysis, $^*P < 0.05$. IL-6, Interleukin-6; IL-10, Interleukin-10; CCL18, chemokine (C-C motif) ligand 18; TNF-α, Tumor necrosis factor-α; MIP-1α, Macrophage inflammatory protein-1α; IP-10, C-X-C motif chemokine 10; MCP-1, Monocyte chemoattractant protein-1; IL-13, Interleukin-13; MDC, Macrophage-derived chemokine; IL-1β, Interleukin-1β; IL-8, Interleukin-8.

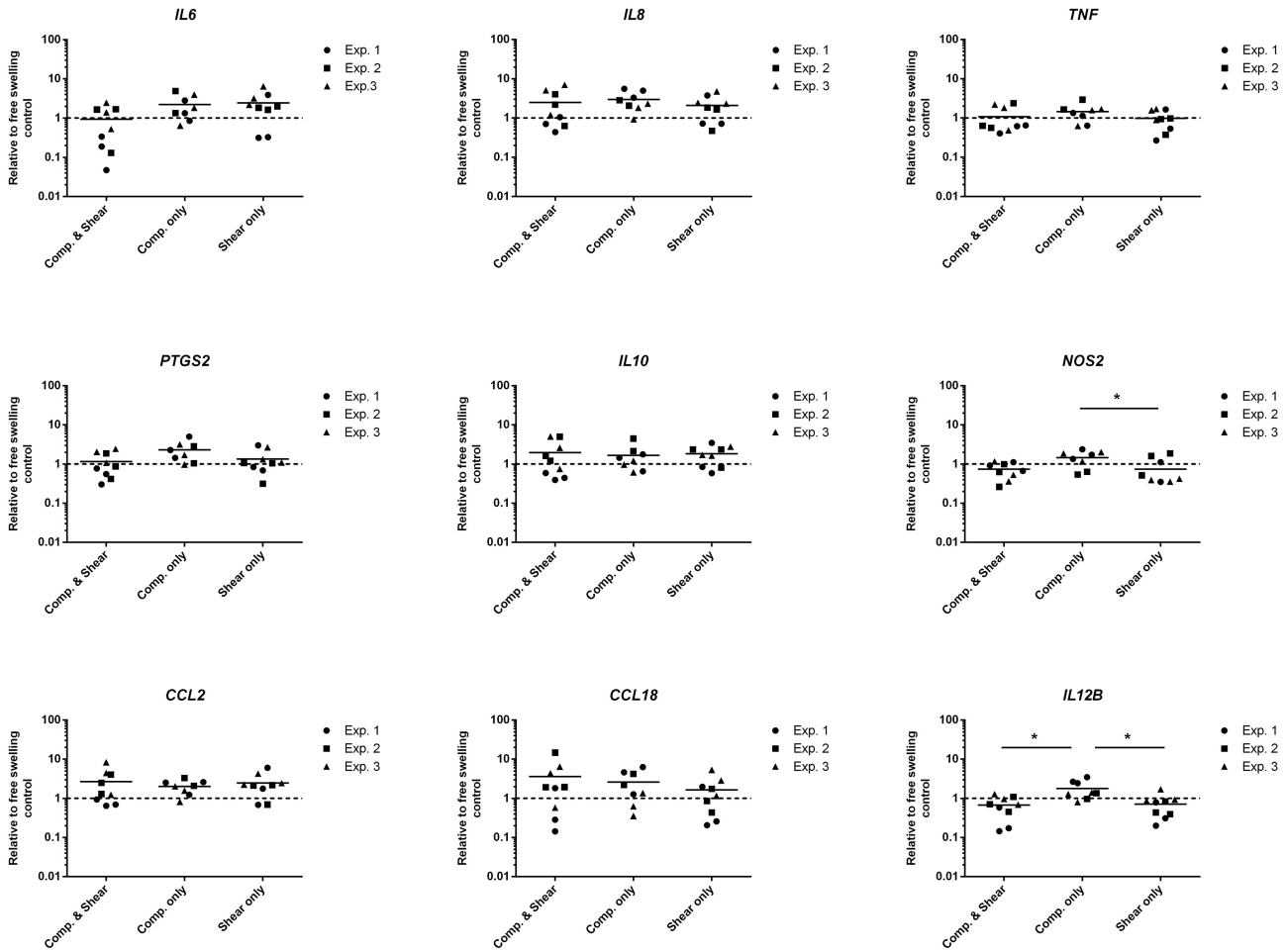

FIGURE 3 | Levels of inflammatory genes expressed by THP1-Blue monocytes in response to multiaxial loading, shear or compression alone. Gene expression by THP1-Blue monocytes following 3 days of multiaxial loading, shear, or compression alone as measured by real-time PCR. Gene expression levels were normalized to the free-swelling control, represented by the dashed line. Data is represented as dot plots including the median for three separate experiments, each assessed in experimental triplicate except for experiment 2 compression only group, which was assessed in duplicate. Statistical significance was determined by a Kruskal–Wallis test followed by Dunn's multiple comparisons test. *$P < 0.05$. Comp, Compression.

marrow-derived mesenchymal stem cells (MSCs) (25). Furthermore, macrophage infiltration and prevalence of a M1-like phenotype has been observed in association with MSC-mediated bone repair *in vivo* (26, 27). In the present study, we have observed a skewing of monocyte activation toward a M1-like phenotype following 3 days of shear and compressive loading, highlighting the responsiveness of human monocytes to mechanical stimuli. These findings may shed some light on how the biomechanical environment may play a role in guiding monocyte/macrophage polarization, and potentially contribute to skeletal tissue repair.

In the present study, we have observed an increase in TNF-α, MIP-1α, and IL-13 protein production by unstimulated as well as LPS and IFN-γ and IL-4 activated monocytes following mechanical shear and compression. Two of four donors in the unstimulated group also substantially increased IL-6 production upon loading. Furthermore, levels of the pro-inflammatory cytokines IL-1β, IL-8, and IL-6 produced by IL-4 activated monocytes were increased following loading. Additionally, gene expression levels of IL-8 and IL-6 were increased by unstimulated primary human monocytes subjected to the combination of mechanical compression and shear. This could indicate that these factors would be induced within an unstable fracture. Previous reports have highlighted an influence of mechanical stimuli resulting from fracture fixation stability upon gene expression of matrix metalloproteinase (MMP)-9 and MMP-13 by fracture hematoma in rats (28). Both MMP-9 and MMP-13 are known to play a key role during the process of endochondral bone formation, facilitating extracellular matrix and cell migration (29). Additional studies have demonstrated an upregulation in the expression of genes involved in cartilage and skeletal development by callus tissue following mechanical stimulation, in a rat osteotomy model (30). However, the impact of mechanical stimuli upon the induction of inflammatory

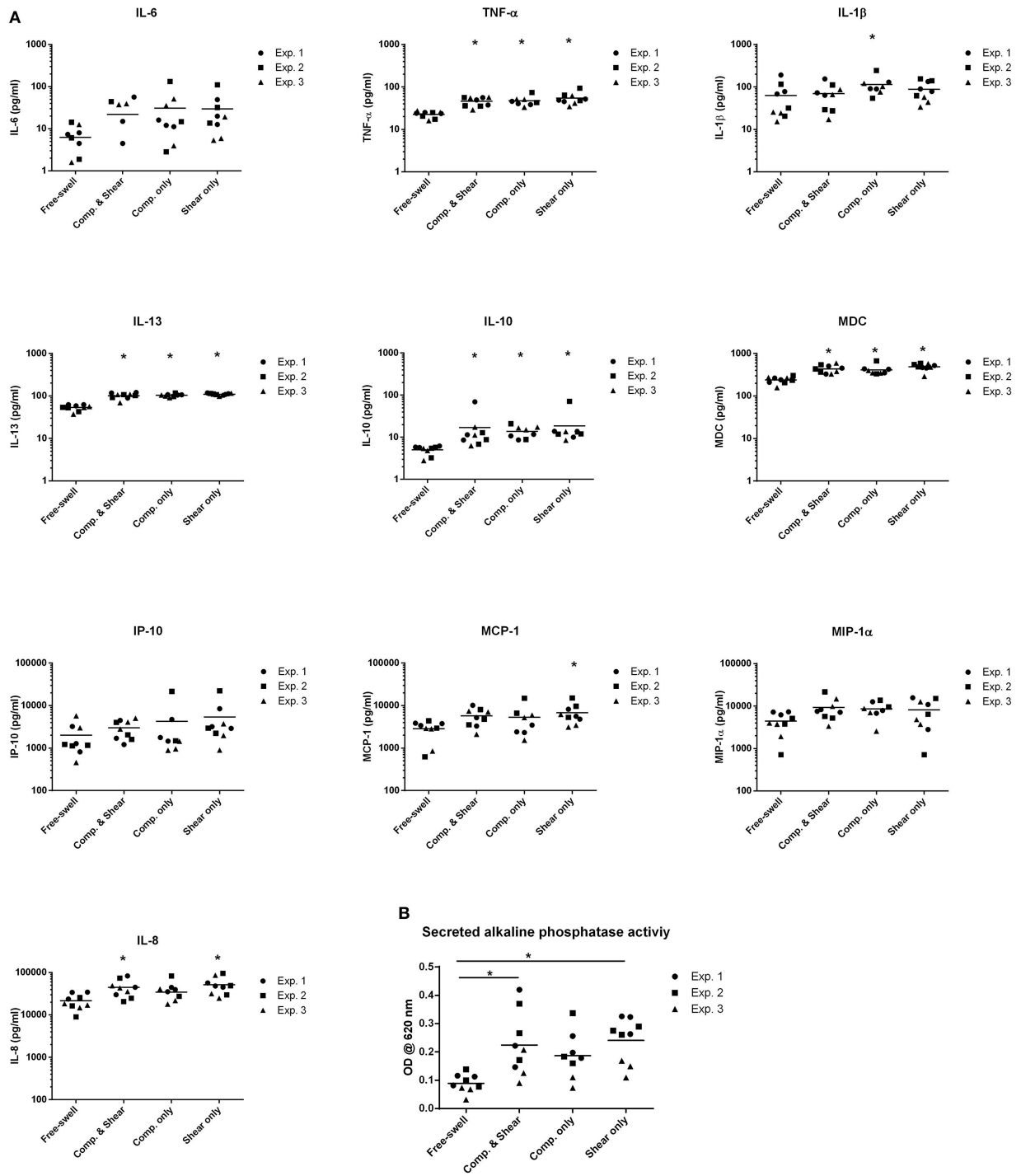

FIGURE 4 | Shear and compression differentially regulate inflammatory mediator expression by THP1-Blue monocytes. **(A)** Levels of inflammatory mediators produced by THP1-Blue monocytes following 3 days of multiaxial loading, shear or compression alone as measured by ELISA and multiplex assay. Protein levels were normalized to the free-swelling control, represented by the dashed line. Data is represented as dot plots including the median for 3 separate experiments, each assessed in experimental triplicate except for experiment 2 compression only group, which was assessed in duplicate. **(B)** SEAP levels detected in cell culture supernatant following 3 days of loading, as measured by spectrophotometric measurement. Statistical significance was determined by a Kruskal–Wallis test followed by Dunn's multiple comparisons test. *$P < 0.05$. IL-6, Interleukin-6; IL-10, Interleukin-10; CCL18, chemokine (C-C motif) ligand 18; TNF-α, Tumor necrosis factor-α; MIP-1α, Macrophage inflammatory protein-1α; IP-10, C-X-C motif chemokine 10; MCP-1, Monocyte chemoattractant protein-1; IL-13, Interleukin-13; MDC, Macrophage-derived chemokine; IL-1β, Interleukin-1β; IL-8, Interleukin-8; Comp, Compression.

gene expression by fracture hematoma *in vivo* requires further investigation. Production of IL-6 and TNF-α is characteristic of activated monocytes and pro-inflammatory M1 macrophages (5, 31). Both IL-6 and TNF-α signaling are known to play a key role in bone fracture healing (32, 33). Additionally, TNF-α is involved in osteoclastic bone resorption (34). Interestingly, in addition to acting as a chemotactic cytokine for monocytes and neutrophils, IL-8 has been reported by Ringe et al. to induce migration of human MSCs (35, 36). Furthermore, IL-8 is known to promote angiogenesis (37, 38). Mechanical stimulation of early human fracture hematoma has also been previously reported to result in increased production of the pro-angiogenic protein vascular endothelial growth factor (VEGF) (39). MIP-1α, also known as CCL3, has been previously implicated in the recruitment of macrophages to the site of injury during bone repair (40). In contrast to the observed upregulation of pro-inflammatory mediators by monocytes in response to mechanical loading, we also detected increased levels of IL-13 protein irrespective of cell activation with LPS and IFN-γ or IL-4. The pleiotropic cytokine IL-13 is known to polarize macrophages toward an M2 phenotype, encompassing anti-inflammatory and tissue repair subsets (41). Additionally, IL-13 is a key mediator of tissue fibrosis, reported to stimulate transforming growth factor (TGF)-β1 production by monocytes and macrophages, as well as increasing TGF-β1 activation (42, 43). TGF-β signaling may promote extracellular matrix deposition and tissue remodeling (44, 45). In addition to mediating tissue fibrosis and macrophage polarization, a role for IL-13 in osteoclast differentiation and bone resorption has been previously highlighted (46). Macrophages have been previously reported to change their phenotype throughout the course of bone healing, with a more predominant role of the M2 subset identified at later stages of repair (7). Given that in the current study loading of monocytes also resulted in production of the M2-polarization factor IL-13, whether a longer duration of loading may switch the balance from M1/M2 requires further investigation.

Having identified an influence of mechanical loading upon the phenotype of M1 or M2-differentiated as well as undifferentiated primary human monocytes, we next sought to investigate whether shear forces or compression alone may be responsible for this effect. In addition to compressive loading, cartilage in the articulating joint and fractures that have not been rigidly fixated, are also subjected to shear. Therefore, we next sought to examine whether shear or compression alone may exert differential effects on undifferentiated monocytes, to gain further insight into whether loading associated with various skeletal tissues may differentially modulate monocyte activation. The human monocyte cell line THP1-Blue^{TM} was utilized to assess the effect of shear, compression or the combination of both on inflammatory mediator expression by monocytes. THP1-Blue^{TM} cells are a reporter cell line, which express secreted embryonic alkaline phosphatase (SEAP) following activation of the transcription factors NF-κB and AP-1. Both NF-κB and AP-1 are activated in monocytes following toll-like receptor 4 (TLR4) stimulation and are involved in the induction of inflammatory gene expression (47). In a similar manner to primary human monocytes, the application of both compression and shear increased expression of inflammatory mediators TNF-α, IL-13, macrophage-derived chemokine (MDC), and IL-10. Interestingly, IL-10 is an anti-inflammatory cytokine but is also produced by monocytes in response to pro-inflammatory stimulation a part of a regulatory feedback mechanism (48). Furthermore, IL-10 is a factor also known to induce the differentiation of macrophages toward an anti-inflammatory phenotype (5). MDC is chemotactic for monocytes and is also considered a marker of M2 macrophages (49, 50). Additionally, we observed differential effects of compression or shear alone on monocyte phenotype. Application of compression alone increased expression of the pro-inflammatory genes *IL12B* and *NOS2* compared to shear alone or the combination of both stimuli. Interestingly, inducible nitric oxide synthase, which is encoded by the gene *NOS2*, has been previously shown to be expressed the initial phase of bone fracture repair (51). Compression alone also significantly increased IL-1β production compared to control, whereas shear alone was found to increase MCP-1. Furthermore, stimulation with both compression and shear or shear alone significantly increased SEAP expression compared to free-swelling controls, suggestive of potential TLR4 activation by monocytes in response to shear force (47). TLR4 has been previously implicated in the pro-inflammatory response of chondrocytes to high fluid shear, and increasing evidence highlights a role of TLR4 activation in inflammatory and catabolic processes associated with osteoarthritis pathogenesis (52–54). Our present findings may provide further insight to the mechanism of the effect of mechanical loading on monocyte activation, however further investigation is required to evaluate the effect of such mechanical stimuli directly on monocyte TLR expression and activation. These mechanically induced changes suggest that the initial monocyte containing hematoma would respond to mechanical motion by upregulating pro-inflammatory cytokines. This could be a danger signal that recruits cells to the site of damage and regulates their response. Rigid fixation would reduce this inflammatory signal leading to a different response. However, further investigation is required to fully determine the impact of mechanical stimuli resulting from fracture fixation stability upon monocyte behavior *in vivo*, and the subsequent influence of mechanically-stimulated monocytes upon skeletal tissue repair.

The findings of the present study highlight the mechanical sensitivity of human monocytes to skeletal tissue-associated loading conditions. Monocyte-derived macrophages have been previously shown to respond to mechanical strain *in vitro*, with an observed upregulation of MMP-1 and MMP-3 expression as well as the transcription factors c-fos and c-jun (55). Furthermore, Yang et al. highlighted a potential role of mechanical strain in the induction of monocyte to macrophage differentiation, mediated by upregulation of the monocyte differentiation-associated transcription factor PU.1 (55). In line with our findings, shear stress has also been shown to promote macrophage differentiation toward a pro-inflammatory M1-like phenotype in a model of atherosclerosis (56). Interestingly, extracellular physical cues resulting from surface stiffness have been reported to modulate TLR signaling by macrophages (57). However, whether these signaling pathways play a role

in the responsiveness of monocytes and monocyte-derived macrophages to shear and compressive forces native to skeletal tissue requires further elucidation. This study has several limitations. Primary peripheral blood monocytes treated with LPS and IFN-γ or IL-4 were used as a model *in vitro* culture system to evaluate the effect of loading on M1 or M2-polarized cells, respectively. Investigation of the effect of mechanical loading on M1 and M2 pre-differentiated macrophages and a longer duration of study may be required to specifically examine the modulatory effect of mechanical loading on macrophage polarization state. Additionally, 2% agarose was used in this study as a cell-carrier system in our *in vitro* model to investigate the short-term response of human monocytes to skeletal tissue-associated mechanical stimuli. However, previous studies have highlighted an impact of different scaffold materials toward the cellular mechanical response (58). Therefore, further investigation may be required to determine whether monocyte interactions with different scaffold materials such as fibrin gels, as a more specific model of the wound healing phase of tissue repair, may determine their response to such mechanical stimuli. Furthermore, additional examination utilizing *in vivo* models of fracture healing is required to relate this observed induction of inflammatory mediators by mechanical loaded monocytes to skeletal tissue repair.

In conclusion, the findings of the present study indicate that human monocytes are responsive to mechanical stimuli, with a modulatory effect of shear and compressive loading observed toward pro-inflammatory mediator production. An in depth understanding of the impact of skeletal tissue-associated mechanical loading on monocyte behavior and their subsequent influence on local cellular responses and tissue repair processes, may identify novel strategies to maximize inflammation-mediated repair mechanisms. Furthermore, the findings of this study may provide insights for the development of novel rehabilitation medicine strategies to improve therapeutic outcome for skeletal tissue repair.

DATA AVAILABILITY

The datasets generated for this study are available on request to the corresponding author.

AUTHOR CONTRIBUTIONS

NF performed the experiments, processed samples, analyzed, and interpreted the data. UM processed samples and analyzed the data. MA supported in data analysis and interpretation. MS conceived and designed the study, and interpreted the data. NF, UM, MA, and MS drafted and critically revised the manuscript for important intellectual content. All authors have approved the final submitted manuscript.

FUNDING

This work was supported by the AO Foundation and the Swiss National Science Foundation (Grant no. 31003a_146375/1).

ACKNOWLEDGMENTS

We acknowledge the technical support of Dr. Reinhard Henschler and the team of Swiss Red Cross Blood Service Graubünden, CH-7000 Chur with buffy coats from whole blood donations.

REFERENCES

1. Claes L, Recknagel S, Ignatius A. Fracture healing under healthy and inflammatory conditions. *Nat Rev Rheumatol.* (2012) 8:133–43. doi: 10.1038/nrrheum.2012.1
2. Sanchez-Adams J, Leddy HA, McNulty AL, O'Conor CJ, Guilak F. The mechanobiology of articular cartilage: bearing the burden of osteoarthritis. *Curr Rheumatol Rep.* (2014) 16:451. doi: 10.1007/s11926-014-0451-6
3. Johnson K, Aarden L, Choi Y, De Groot E, Creasey A. The proinflammatory cytokine response to coagulation and endotoxin in whole blood. *Blood.* (1996) 87:5051–60.
4. Altieri DC. Proteases and protease receptors in modulation of leukocyte effector functions. *J Leukocyte Biol.* (1995) 58:120–7. doi: 10.1002/jlb.58.2.120
5. Mosser DM, Edwards JP. Exploring the full spectrum of macrophage activation. *Nat Rev Immunol.* (2008) 8:958–69. doi: 10.1038/nri2448
6. Murray PJ, Allen JE, Biswas SK, Fisher EA, Gilroy DW, Goerdt S, et al. Macrophage activation and polarization: nomenclature and experimental guidelines. *Immunity.* (2014) 41:14–20. doi: 10.1016/j.immuni.2014.06.008
7. Schlundt C, El Khassawna T, Serra A, Dienelt A, Wendler S, Schell H, et al. Macrophages in bone fracture healing: their essential role in endochondral ossification. *Bone.* (2018) 106:78–89. doi: 10.1016/j.bone.2015.10.019
8. Raggatt LJ, Wullschleger ME, Alexander KA, Wu AC, Millard SM, Kaur S, et al. Fracture healing via periosteal callus formation requires macrophages for both initiation and progression of early endochondral ossification. *Am J Pathol.* (2014) 184:3192–204. doi: 10.1016/j.ajpath.2014.08.017
9. Vi L, Baht GS, Whetstone H, Ng A, Wei Q, Poon R, et al. Macrophages promote osteoblastic differentiation *in-vivo*: implications in fracture repair and bone homeostasis. *J Bone Miner Res.* (2015) 30:1090–102. doi: 10.1002/jbmr.2422
10. Gerstenfeld LC, Cullinane DM, Barnes GL, Graves DT, Einhorn TA. Fracture healing as a post-natal developmental process: molecular, spatial, and temporal aspects of its regulation. *J Cell Biochem.* (2003) 88:873–84. doi: 10.1002/jcb.10435
11. Gerstenfeld LC, Cho TJ, Kon T, Aizawa T, Cruceta J, Graves BD, et al. Impaired intramembranous bone formation during bone repair in the absence of tumor necrosis factor-alpha signaling. *Cells Tissues Organs.* (2001) 169:285–94. doi: 10.1159/000047893
12. Westacott CI, Barakat AF, Wood L, Perry MJ, Neison P, Bisbinas I, et al. Tumor necrosis factor alpha can contribute to focal loss of cartilage in osteoarthritis. *Osteoarthr Cartil.* (2000) 8:213–21. doi: 10.1053/joca.1999.0292
13. Shakibaei M, John T, Schulze-Tanzil G, Lehmann I, Mobasheri A. Suppression of NF-kappaB activation by curcumin leads to inhibition of expression of cyclo-oxygenase-2 and matrix metalloproteinase-9 in human articular chondrocytes: implications for the treatment of osteoarthritis. *Biochem Pharmacol.* (2007) 73:1434–45. doi: 10.1016/j.bcp.2007.01.005
14. Johnson K, Hashimoto S, Lotz M, Pritzker K, Terkeltaub R. Interleukin-1 induces pro-mineralizing activity of cartilage tissue transglutaminase and factor XIIIa. *Am J Pathol.* (2001) 159:149–63. doi: 10.1016/S0002-9440(10)61682-3
15. Hoemann CD, Chen G, Marchand C, Tran-Khanh N, Thibault M, Chevrier A, et al. Scaffold-guided subchondral bone repair: implication

of neutrophils and alternatively activated arginase-1+ macrophages. *Am J Sports Med.* (2010) 38:1845–56. doi: 10.1177/0363546510369547
16. Hibino N, Yi T, Duncan DR, Rathore A, Dean E, Naito Y, et al. A critical role for macrophages in neovessel formation and the development of stenosis in tissue-engineered vascular grafts. *FASEB J.* (2011) 25:4253–63. doi: 10.1096/fj.11-186585
17. Arras M, Ito WD, Scholz D, Winkler B, Schaper J, Schaper W. Monocyte activation in angiogenesis and collateral growth in the rabbit hindlimb. *J Clin Invest.* (1998) 101:40–50. doi: 10.1172/JCI119877
18. Blomgran P, Blomgran R, Ernerudh J, Aspenberg P. A possible link between loading, inflammation and healing: immune cell populations during tendon healing in the rat. *Sci Rep.* (2016) 6:29824. doi: 10.1038/srep29824
19. Wimmer MA, Grad S, Kaup T, Hanni M, Schneider E, Gogolewski S, et al. Tribology approach to the engineering and study of articular cartilage. *Tissue Eng.* (2004) 10:1436–45. doi: 10.1089/ten.2004.10.1436
20. Neumann AJ, Gardner OF, Williams R, Alini M, Archer CW, Stoddart MJ. Human articular cartilage progenitor cells are responsive to mechanical stimulation and adenoviral-mediated overexpression of bone-morphogenetic protein 2. *PLoS ONE.* (2015) 10:e0136229. doi: 10.1371/journal.pone.0136229
21. Li Z, Kupcsik L, Yao SJ, Alini M, Stoddart MJ. Mechanical load modulates chondrogenesis of human mesenchymal stem cells through the TGF-beta pathway. *J Cell Mol Med.* (2010) 14:1338–46. doi: 10.1111/j.1582-4934.2009.00780.x
22. Ballotta V, Driessen-Mol A, Bouten CV, Baaijens FP. Strain-dependent modulation of macrophage polarization within scaffolds. *Biomaterials.* (2014) 35:4919–28. doi: 10.1016/j.biomaterials.2014.03.002
23. Hoff P, Gaber T, Strehl C, Schmidt-Bleek K, Lang A, Huscher D, et al. Immunological characterization of the early human fracture hematoma. *Immunol Res.* (2016) 64:1195–206. doi: 10.1007/s12026-016-8868-9
24. Xing Z, Lu C, Hu D, Yu YY, Wang X, Colnot C, et al. Multiple roles for CCR2 during fracture healing. *Dis Models Mech.* (2010) 3:451–8. doi: 10.1242/dmm.003186
25. Guihard P, Danger Y, Brounais B, David E, Brion R, Delecrin J, et al. Induction of osteogenesis in mesenchymal stem cells by activated monocytes/macrophages depends on oncostatin M signaling. *Stem Cells.* (2012) 30:762–72. doi: 10.1002/stem.1040
26. Tour G, Wendel M, Tcacencu I. Bone marrow stromal cells enhance the osteogenic properties of hydroxyapatite scaffolds by modulating the foreign body reaction. *J Tissue Eng Regen Med.* (2014) 8:841–9. doi: 10.1002/term.1574
27. Gamblin AL, Brennan MA, Renaud A, Yagita H, Lezot F, Heymann D, et al. Bone tissue formation with human mesenchymal stem cells and biphasic calcium phosphate ceramics: the local implication of osteoclasts and macrophages. *Biomaterials.* (2014) 35:9660–7. doi: 10.1016/j.biomaterials.2014.08.018
28. Ode A, Duda GN, Geissler S, Pauly S, Ode JE, Perka C, et al. Interaction of age and mechanical stability on bone defect healing: an early transcriptional analysis of fracture hematoma in rat. *PLoS ONE.* (2014) 9:e106462. doi: 10.1371/journal.pone.0106462
29. Ortega N, Behonick D, Stickens D, Werb Z. How proteases regulate bone morphogenesis. *Ann N Y Acad Sci.* (2003) 995:109–16. doi: 10.1111/j.1749-6632.2003.tb03214.x
30. Salisbury Palomares KT, Gerstenfeld LC, Wigner NA, Lenburg ME, Einhorn TA, Morgan EF. Transcriptional profiling and biochemical analysis of mechanically induced cartilaginous tissues in a rat model. *Arthritis Rheum.* (2010) 62:1108–18. doi: 10.1002/art.27343
31. Agbanoma G, Li C, Ennis D, Palfreeman AC, Williams LM, Brennan FM. Production of TNF-alpha in macrophages activated by T cells, compared with lipopolysaccharide, uses distinct IL-10-dependent regulatory mechanism. *J Immunol.* (2012) 188:1307–17. doi: 10.4049/jimmunol.1100625
32. Gerstenfeld LC, Cho TJ, Kon T, Aizawa T, Tsay A, Fitch J, et al. Impaired fracture healing in the absence of TNF-alpha signaling: the role of TNF-alpha in endochondral cartilage resorption. *J Bone Miner Res.* (2003) 18:1584–92. doi: 10.1359/jbmr.2003.18.9.1584
33. Yang X, Ricciardi BF, Hernandez-Soria A, Shi Y, Pleshko Camacho N, Bostrom MP. Callus mineralization and maturation are delayed during fracture healing in interleukin-6 knockout mice. *Bone.* (2007) 41:928–36. doi: 10.1016/j.bone.2007.07.022
34. Bertolini DR, Nedwin GE, Bringman TS, Smith DD, Mundy GR. Stimulation of bone resorption and inhibition of bone formation *in vitro* by human tumour necrosis factors. *Nature.* (1986) 319:516–8. doi: 10.1038/319516a0
35. Mukaida N. Pathophysiological roles of interleukin-8/CXCL8 in pulmonary diseases. *Am J Physiol Lung Cell Mol Physiol.* (2003) 284:L566–77. doi: 10.1152/ajplung.00233.2002
36. Ringe J, Strassburg S, Neumann K, Endres M, Notter M, Burmester GR, et al. Towards *in situ* tissue repair: human mesenchymal stem cells express chemokine receptors CXCR1, CXCR2 and CCR2, and migrate upon stimulation with CXCL8 but not CCL2. *J Cell Biochem.* (2007) 101:135–46. doi: 10.1002/jcb.21172
37. Brat DJ, Bellail AC, Van Meir EG. The role of interleukin-8 and its receptors in gliomagenesis and tumoral angiogenesis. *Neuro Oncol.* (2005) 7:122–33. doi: 10.1215/S1152851704001061
38. Li A, Dubey S, Varney ML, Dave BJ, Singh RK. IL-8 directly enhanced endothelial cell survival, proliferation, and matrix metalloproteinases production and regulated angiogenesis. *J Immunol.* (2003) 170:3369–76. doi: 10.4049/jimmunol.170.6.3369
39. Groothuis A, Duda GN, Wilson CJ, Thompson MS, Hunter MR, Simon P, et al. Mechanical stimulation of the pro-angiogenic capacity of human fracture haematoma: involvement of VEGF mechano-regulation. *Bone.* (2010) 47:438–44. doi: 10.1016/j.bone.2010.05.026
40. Kawao N, Tamura Y, Horiuchi Y, Okumoto K, Yano M, Okada K, et al. The tissue fibrinolytic system contributes to the induction of macrophage function and CCL3 during bone repair in mice. *PLoS ONE.* (2015) 10:e0123982. doi: 10.1371/journal.pone.0123982
41. Van Dyken SJ, Locksley RM. Interleukin-4- and interleukin-13-mediated alternatively activated macrophages: roles in homeostasis and disease. *Ann Rev Immunol.* (2013) 31:317–43. doi: 10.1146/annurev-immunol-032712-095906
42. Fichtner-Feigl S, Strober W, Kawakami K, Puri RK, Kitani A. IL-13 signaling through the IL-13alpha2 receptor is involved in induction of TGF-beta1 production and fibrosis. *Nat Med.* (2006) 12:99–106. doi: 10.1038/nm1332
43. Lee CG, Homer RJ, Zhu Z, Lanone S, Wang X, Koteliansky V, et al. Interleukin-13 induces tissue fibrosis by selectively stimulating and activating transforming growth factor beta(1). *J Exp Med.* (2001) 194:809–21. doi: 10.1084/jem.194.6.809
44. Burns WC, Twigg SM, Forbes JM, Pete J, Tikellis C, Thallas-Bonke V, et al. Connective tissue growth factor plays an important role in advanced glycation end product-induced tubular epithelial-to-mesenchymal transition: implications for diabetic renal disease. *J Am Soc Nephrol.* (2006) 17:2484–94. doi: 10.1681/ASN.2006050525
45. Zhu Z, Homer RJ, Wang Z, Chen Q, Geba GP, Wang J, et al. Pulmonary expression of interleukin-13 causes inflammation, mucus hypersecretion, subepithelial fibrosis, physiologic abnormalities, and eotaxin production. *J Clin Invest.* (1999) 103:779–88. doi: 10.1172/JCI5909
46. Palmqvist P, Lundberg P, Persson E, Johansson A, Lundgren I, Lie A, et al. Inhibition of hormone and cytokine-stimulated osteoclastogenesis and bone resorption by interleukin-4 and interleukin-13 is associated with increased osteoprotegerin and decreased RANKL and RANK in a STAT6-dependent pathway. *J Biol Chem.* (2006) 281:2414–29. doi: 10.1074/jbc.M510160200
47. Guha M, Mackman N. LPS induction of gene expression in human monocytes. *Cell Signal.* (2001) 13:85–94. doi: 10.1016/S0898-6568(00)00149-2
48. Donnelly RP, Freeman SL, Hayes MP. Inhibition of IL-10 expression by IFN-gamma up-regulates transcription of TNF-alpha in human monocytes. *J Immunol.* (1995) 155:1420–7.
49. Godiska R, Chantry D, Raport CJ, Sozzani S, Allavena P, Leviten D, et al. Human macrophage-derived chemokine (MDC), a novel chemoattractant for monocytes, monocyte-derived dendritic cells, and natural killer cells. *J Exp Med.* (1997) 185:1595–604. doi: 10.1084/jem.185.9.1595
50. Jaguin M, Houlbert N, Fardel O, Lecureur V. Polarization profiles of human M-CSF-generated macrophages and comparison of M1-markers in classically activated macrophages from GM-CSF and M-CSF origin. *Cell Immunol.* (2013) 281:51–61. doi: 10.1016/j.cellimm.2013.01.010
51. Zhu W, Diwan AD, Lin JH, Murrell GA. Nitric oxide synthase isoforms during fracture healing. *J Bone Miner Res.* (2001) 16:535–40. doi: 10.1359/jbmr.2001.16.3.535

52. Wang P, Zhu F, Tong Z, Konstantopoulos K. Response of chondrocytes to shear stress: antagonistic effects of the binding partners Toll-like receptor 4 and caveolin-1. *FASEB J.* (2011) 25:3401–15. doi: 10.1096/fj.11-184861
53. Kim HA, Cho ML, Choi HY, Yoon CS, Jhun JY, Oh HJ, et al. The catabolic pathway mediated by Toll-like receptors in human osteoarthritic chondrocytes. *Arthritis Rheum.* (2006) 54:2152–63. doi: 10.1002/art.21951
54. Bobacz K, Sunk IG, Hofstaetter JG, Amoyo L, Toma CD, Akira S, et al. Toll-like receptors and chondrocytes: the lipopolysaccharide-induced decrease in cartilage matrix synthesis is dependent on the presence of toll-like receptor 4 and antagonized by bone morphogenetic protein 7. *Arthritis Rheum.* (2007) 56:1880–93. doi: 10.1002/art.22637
55. Yang JH, Sakamoto H, Xu EC, Lee RT. Biomechanical regulation of human monocyte/macrophage molecular function. *Am J Pathol.* (2000) 156:1797–804. doi: 10.1016/S0002-9440(10)65051-1
56. Seneviratne AN, Cole JE, Goddard ME, Park I, Mohri Z, Sansom S, et al. Low shear stress induces M1 macrophage polarization in murine thin-cap atherosclerotic plaques. *J Mol Cell Cardiol.* (2015) 89(Pt B):168–72. doi: 10.1016/j.yjmcc.2015.10.034
57. Gruber E, Heyward C, Cameron J, Leifer C. Toll-like receptor signaling in macrophages is regulated by extracellular substrate stiffness and Rho-associated coiled-coil kinase (ROCK1/2). *Int Immunol.* (2018) 30:267–78. doi: 10.1093/intimm/dxy027
58. Hunter CJ, Mouw JK, Levenston ME. Dynamic compression of chondrocyte-seeded fibrin gels: effects on matrix accumulation and mechanical stiffness. *Osteoarthr Cartil.* (2004) 12:117–30. doi: 10.1016/j.joca.2003.08.009

Conflict of Interest Statement: The authors declare that the research was conducted in the absence of any commercial or financial relationships that could be construed as a potential conflict of interest.

frontiers in Immunology

ORIGINAL RESEARCH
published: 07 March 2019
doi: 10.3389/fimmu.2019.00377

Inhibition of JAK1/2 Tyrosine Kinases Reduces Neurogenic Heterotopic Ossification After Spinal Cord Injury

Kylie A. Alexander[1†], Hsu-Wen Tseng[1†], Whitney Fleming[1], Beulah Jose[1], Marjorie Salga[1,2], Irina Kulina[1], Susan M. Millard[1], Allison R. Pettit[1], François Genêt[2,3] and Jean-Pierre Levesque[1]*

[1] Mater Research Institute – The University of Queensland, Translational Research Institute, Woolloongabba, QLD, Australia, [2] CIC-IT 1429, Service de Médecine Physique et de Réadaptation, Raymond Poincaré University Hospital, AP-HP, Garches, France, [3] Université de Versailles Saint Quentin en Yvelines, END:ICAP Inserm U1179, Montigny le Bretonneux, France

OPEN ACCESS

Edited by:
Claudine Blin-Wakkach,
UMR7370 Laboratoire de Physio Médecine Moléculaire (LP2M), France

Reviewed by:
Frederic Blanchard,
INSERM U1238 Sarcomes Osseux et Remodelage des Tissus Calcifiés, France
Florent Elefteriou,
Baylor College of Medicine, United States
Nicole Horwood,
University of Oxford, United Kingdom

***Correspondence:**
Jean-Pierre Levesque
jp.levesque@mater.uq.edu.au

[†]These authors share first authorship

Specialty section:
This article was submitted to Inflammation, a section of the journal Frontiers in Immunology

Received: 30 November 2018
Accepted: 14 February 2019
Published: 07 March 2019

Citation:
Alexander KA, Tseng H-W, Fleming W, Jose B, Salga M, Kulina I, Millard SM, Pettit AR, Genêt F and Levesque J-P (2019) Inhibition of JAK1/2 Tyrosine Kinases Reduces Neurogenic Heterotopic Ossification After Spinal Cord Injury. Front. Immunol. 10:377. doi: 10.3389/fimmu.2019.00377

Neurogenic heterotopic ossifications (NHO) are very incapacitating complications of traumatic brain and spinal cord injuries (SCI) which manifest as abnormal formation of bone tissue in periarticular muscles. NHO are debilitating as they cause pain, partial or total joint ankylosis and vascular and nerve compression. NHO pathogenesis is unknown and the only effective treatment remains surgical resection, however once resected, NHO can re-occur. To further understand NHO pathogenesis, we developed the first animal model of NHO following SCI in genetically unmodified mice, which mimics most clinical features of NHO in patients. We have previously shown that the combination of (1) a central nervous system lesion (SCI) and (2) muscular damage (via an intramuscular injection of cardiotoxin) is required for NHO development. Furthermore, macrophages within the injured muscle play a critical role in driving NHO pathogenesis. More recently we demonstrated that macrophage-derived oncostatin M (OSM) is a key mediator of both human and mouse NHO. We now report that inflammatory monocytes infiltrate the injured muscles of SCI mice developing NHO at significantly higher levels compared to mice without SCI. Muscle infiltrating monocytes and neutrophils expressed OSM whereas mouse muscle satellite and interstitial cell expressed the OSM receptor (OSMR). *In vitro* recombinant mouse OSM induced tyrosine phosphorylation of the transcription factor STAT3, a downstream target of OSMR:gp130 signaling in muscle progenitor cells. As STAT3 is tyrosine phosphorylated by JAK1/2 tyrosine kinases downstream of OSMR:gp130, we demonstrated that the JAK1/2 tyrosine kinase inhibitor ruxolitinib blocked OSM driven STAT3 tyrosine phosphorylation in mouse muscle progenitor cells. We further demonstrated *in vivo* that STAT3 tyrosine phosphorylation was not only significantly higher but persisted for a longer duration in injured muscles of SCI mice developing NHO compared to mice with muscle injury without SCI. Finally, administration of ruxolitinib for 7 days post-surgery significantly reduced STAT3 phosphorylation in injured muscles *in vivo* as well as NHO volume at all analyzed time-points up to 3 weeks post-surgery. Our results identify the JAK/STAT3 signaling pathway as a potential therapeutic target to reduce NHO development following SCI.

Keywords: spinal cord injury complications, heterotopic ossification, JAK- STAT signaling pathway, ruxolitinib, oncostatin M receptor

INTRODUCTION

Neurogenic heterotopic ossification (NHO) is the abnormal formation of extra-skeletal bones in muscles (1), mostly periarticular (2), and is a frequent and very incapacitating complication in patients with spinal cord injury (SCI) (15–25%) and traumatic brain injuries (5–12%) (3, 4). NHO prevalence is higher in combat-inflicted trauma particularly in victims of explosive blasts with associated SCI or TBI where NHO prevalence is over 60% (5, 6). NHOs are debilitating due to their size (up to 2 kg), causing significant pain and gradual reduction in the range of motion of affected limbs, often progressing to complete joint ankylosis. This exacerbates functional disabilities by increasing difficulty in sitting, eating and dressing (7). NHO growth can also cause nerve, blood vessel compression, and irreversibly damage the affected joint further increasing patient morbidity (8). Despite knowing this pathology for 100 years, treatment is currently limited to surgical resection after NHO have matured and become symptomatic (2, 7, 9–11). The surgical procedure is challenging, particularly when ossifications entrap joints, large blood vessels and nerves. Furthermore, even after resection, NHO recurrence is observed in at least 6% patients (1, 2, 9, 12). The development of improved treatments for NHO has been slow and trials of pharmacological interventions have continued to show limited effectiveness, reflecting the current limited knowledge on the etiology and pathophysiology of NHO. Identification of therapeutic targets to block NHO development in SCI/TBI patients remains a priority in order to decrease the prevalence and morbidity of this pathology (5).

We have developed the first clinically relevant animal model of NHO following SCI in genetically unmodified mice (13). In this model the combination of two injuries is necessary to trigger NHO development in the muscle: a severe lesion of the central nervous system such as a SCI in combination with a muscle injury (13). Development of NHO following spinal cord transection in this model was triggered by macrophages infiltrating damaged muscles exclusively in the context of a complete SCI (13, 14). More recently we established that the inflammatory cytokine oncostatin M (OSM) secreted in part by macrophages infiltrating the inflamed muscle contribute to both human and mouse NHO development (15). This is consistent with the pleiotropic role of OSM in regulating skeletal bone formation and resorption (16, 17) and the previous demonstration that macrophage-derived OSM can promote mesenchymal stem cell osteogenic differentiation (18) and intramembranous bone formation (19). OSM was shown to be elevated in the serum of patients developing NHO and OSM produced by activated macrophages isolated from NHO biopsies promoted osteoblastic differentiation and mineralization of human muscle-derived stromal cells extracted from NHOs (15). Likewise in mice, SCI caused the abnormal and persistent expression of OSM in the injured muscles. Importantly, mice defective for the OSM receptor (OSMR) α chain gene *Osmr* had significantly reduced NHO volumes in response to SCI and muscle injury (15). Overall our results provide strong evidence that macrophages contribute to NHO formation in part through the osteogenic action of OSM on muscle cells suggesting that OSM/OSMR signaling could be a suitable therapeutic target for NHO.

OSM is a member of the interleukin (IL)-6 family of cytokines which include IL-6, IL-11, leukemia inhibitory factor (LIF), cardiotrophin-1, and ciliary neurotrophic factor. These cytokines bind to diverse heteromeric receptors with a common glycoprotein 130 (Gp130) chain. Binding of IL-6 family cytokines to their cognate receptors, all of which comprise a common gp130 subunit, causes the activation of Janus tyrosine kinase (JAK)-1 and JAK2 which in turn tyrosine phosphorylate signal transducer and activator of transcription (STAT)-1 and STAT3 (20, 21). Once tyrosine phosphorylated (p), pSTAT1, and pSTAT3 translocate to the nucleus and activate the transcription of a large array of genes depending on the cell type. Mouse OSM binds with a strong affinity to the OSMR:gp130 complex and with a 30-fold lower affinity to the leukemia inhibitory factor receptor (LIFR):gp130 complex (22). Typically, OSM binding to the OSMR:gp130 complex causes the phosphorylation and activation of both STAT1 and STAT3 via JAK1/2 (23, 24) which in turns leads the transcription of a large range of genes that include suppressor of cytokine signaling (SOCS)-3. A negative feed-back loop is triggered by SOCS3, which binds to both gp130 and activated JAKs, suppressing this signaling cascade and STAT1 and STAT3 activation (25, 26).

Since OSM and OSMR play an important role in NHO pathogenesis following SCI (15), we further examined STAT3 activation status in mouse muscles during NHO development. We confirmed that muscle satellite and interstitial cells isolated from mouse muscles express OSMR, with JAK1/2-dependant tyrosine phosphorylation of STAT3 in response to OSM. In addition, we found higher and persistent STAT3 tyrosine phosphorylation in injured muscles of SCI mice developing NHO. We show that this persistent STAT3 phosphorylation and activation in the injured muscle is an important driver of NHO as administration of ruxolitinib, a small synthetic inhibitor of JAK1/2 tyrosine kinases used to treat myelofibrosis and polycythemia vera caused by activating mutations of JAK2 (27, 28), significantly reduced STAT3 phosphorylation in the injured muscles of mice. Importantly, ruxolitinib administration also significantly reduced NHO development following SCI.

MATERIALS AND METHODS

Animals

C57BL/6 mice were obtained from Animal Resource Center (Perth, Australia). All mouse procedures were approved by the Health Sciences Animal Ethics Committee of The University of Queensland and performed in accordance with the Australian Code of Practice for the Care and Use of Animals for Scientific Purposes.

NHO Mouse Model

NHO mouse model was carried out as previously described (15) by performing a spinal cord transection between T11 and T13 together with intramuscular injection (i.m.) of cardiotoxin (CDTX) purified from the venom of Naja pallida (Latoxan) at 0.32 mg/kg in the hamstring muscles under general anesthesia

(100 mg/kg Ketamine, 10 mg/kg xylazine, and 1% isofluorane). Control mice underwent sham-surgery and/or intramuscular injection of equal volume of phosphate buffered saline (PBS). In this model, NHO develop in the CDTX-injected muscle within 1–3 weeks (13, 15). Post-surgery, mice were administered ruxolitinib phosphate (LC Laboratories) 60 mg/kg by oral gavage twice daily from day 0 to day 7 post-surgery. Ruxolitinib phosphate powder was first dissolved as a 4X stock in dimethyl sulfoxide (DMSO) then diluted to 1X in vehicle (5 mg/ml hydroxypropyl methylcellulose, 0.1% Tween 20 in water). Control mice were gavaged with 25% DMSO in vehicle.

Tissue Collection

At 1–3 weeks post-surgery mice were euthanized by CO_2 asphyxiation. For histological analysis, the hind limbs were fixed in PBS with 4% paraformaldehyde as previously described (15). For western blots, muscle samples were harvested at specified time points and immediately placed in ice-cold protein extraction buffer (300 mM NaCl, 30 mM Tris-HCl, 1% Triton-X 100) containing a house made cocktail of phosphatase inhibitors (10 mM EDTA, 0.1% NaN_3, 20 mM NaF, 1 mM Na_3VO_4, 10 mM β-glycerophosphate, 10 mM levamisole) buffered at pH 7.4 and supplemented with 1X protease inhibitor cocktail (Complete™ ULTRA Tablets, Roche) and snap frozen in liquid nitrogen until extraction.

Muscle Cell Isolation, Sorting, and Culture

Isolation, sorting and culture of muscle $CD45^-Ter119^-CD31^-CD34^+Sca1^-$ satellite cells and $CD45^-Ter119^-CD31^-CD34^+Sca1^+$ interstitial cells was carried out as previously described (15). For pSTAT3 phos-flow analysis, cultured muscle satellite cells, interstitial cells, and the mouse mesenchymal progenitor cell line Kusa4b10 cells (29, 30) were detached by incubating cell monolayers in PBS plus 4 mM EDTA for 5 min at 37°C. Once in suspension, cells were washed in Dulbecco modified essential medium (DMEM, Gibco, Life Technologies), centrifuged and resuspended in DMEM. Cell aliquots (1×10^6) were then preincubated with or without 1 μM ruxolitinib (LC Laboratories), for 30 min at 37°C and subsequently stimulated by addition of 25 ng/mL recombinant mouse OSM (R&D Systems) for 10 min. Cells were then immediately washed in 10 mL ice cold Tris-buffered saline pH 7.4 containing 1 mM Na_3VO_4, centrifuged, and cell pellets resuspended for fixation and permeabilization (BD Cytofix, Perm buffer IV, BD Biosciences) for 10 and 30 min respectively, cells were then stained with AlexaFluor647-conjugated mouse anti-pSTAT3 (pY705) monoclonal antibody (BD Biosciences, catalog # 557815) for 30 min on ice, cells were then washed and subsequently run on a LSR Fortessa x20 flow cytometer (BD Biosciences). Files were subsequently analyzed with Flow Jo software version 10.4.

Protein Extraction and Western Blot

Frozen muscle samples were thawed and homogenized using a TissueRuptor (Qiagen), in ice cold protein extraction buffer for 3 rounds of 20 s at top speed, incubated on a horizontal rotator at 4°C for 15 min. Tissue debris were removed by centrifugation at 15,000 g at 4°C for 20 min. Supernatants were taken and protein concentrations measured using a BCA assay (ThermoFisher). Muscle lysates (25 μg protein per lane, one separate mouse per lane) were loaded on a 4–12% acrylamide Bis-Tris pre-cast gel (ThermoFisher), and subsequently wet transferred onto a Hybond C Extra membrane (Amersham Biosciences) and blocked with Odyssey Blocking Buffer. Primary antibodies included an anti-total-STAT3 rabbit monoclonal antibody (mAb) clone 79D7 diluted at 1/2,000 (Cell Signaling), anti-phospho-STAT3 (Tyr705) XP® rabbit mAb clone D3A7 (Cell Signaling) diluted 1/1,000. IRDye® 800CW-conjugated donkey anti-rabbit IgG (H+L) (LI-COR Biosciences) was used to detect primary antibodies using an Odyssey scanner (LI-COR Biosciences). Western blot zip files were uploaded onto Image Studio Lite Software (Version 5.2). Boxes were drawn around the bands with background boarder width set at 2 value for above and below the box. Intensity values minus background of pSTAT3 were divided by the values obtained for total STAT3, normalized to the average value obtained in control mice (SHAM+PBS) at the defined time-point, plotted, and significance calculated.

Mouse Muscle Monocyte Isolation

All leukocytes were isolated from either SHAM-operated or SCI mice with an intramuscular injection of CDTX as described above. Injected hamstrings were harvested at 4 days post-surgery and muscle monocyte populations were isolated using a skeletal muscle dissociation kit (Miltenyi Biotech). In brief, hamstrings were cut into 1 mm pieces and up to 0.5 g of tissue was used per dissociation sample as per manufactures instructions. Total muscle leukocytes were subsequently separated into multiple populations using a Beckman Coulter Life Sciences CytoFLEX benchtop flow cytometer using the following antibodies (Biolegend); PerCP/Cyanine (CY) 5.5 anti-mouse/human CD11b (clone M1/70), FITC anti-mouse CD48 (clone HM48-1), APC anti-mouse F4/80 (clone BM8), Pacific Blue™ anti-mouse Ly-6C (clone HK1.4), APC/Cy7 anti-mouse Ly-6G (clone 1A8), and Zombie Aqua™ Fixable Viability Kit. Subsequently total muscle leukocytes were also sorted into multiple populations using a BD FACS Aria Fusion using the following antibodies (Biolegend): Brilliant Violet 785™ anti-mouse CD45 (clone 30-F11), FITC anti-mouse TER-119/Erythroid Cells (clone TER-119), FITC anti-mouse/human CD45R/B220 (clone RA3-6B2), FITC anti-mouse CD3ε (clone 145-2C11), APC anti-mouse F4/80 (clone BM8), Brilliant Violet 510™ anti-mouse/human CD11b (clone M1/70), PE anti-mouse Ly-6G (clone 1A8), APC/Cy7 anti-mouse CD48 (clone HM48-1), Pacific Blue™ anti-mouse Ly-6C (clone HK1.4), and 7-aminoactinomycin D (Life Technologies). Files were subsequently analyzed with Flow Jo software version 10.4. Muscle monocyte populations were sorted directly into trizol LS (ThermoFisher) and frozen until extraction.

mRNA Extraction and qRT-PCR Analysis

For RNA isolation, frozen muscle was homogenized using a TissueRuptor (Qiagen), directly in Trizol (Life Technologies). After chloroform separation, RNA was isolated from aqueous

phase. mRNA of sorted and cultured cells was isolated using chloroform separation followed by GeneJET RNA cleanup and concentration micro kit (ThermoFisher). Reverse transcription was performed using the iScript cDNA kit (BioRad) as per manufacturer's instructions. Analysis of mRNA expression for *Osm, Osmr, and Hprt* and was carried out using the Taqman Fast Advanced Master Mix and primer / probe sets (ThermoFisher): *Osmr* (Mm01307326_m1), *Osm* (Mm01193966_m1), and *Hprt* (Mm03024075_m1) on ViiA 7 Real-Time PCR System (Life Technologies) with PCR setting: 20 s at 95°C, then 40 cycles of 95°C (1 s) and 60°C (20 s). Results were normalized relative to *Hprt* mRNA expression.

Micro-Computerized Tomography (μCT) and NHO Volume Quantification

NHO volume was measured *in vivo* or *ex vivo* using the Inveon positron emission tomography/computed tomography (PET-CT) multimodality system (Siemens Medical Solutions Inc.) as previously described (15). In brief, parameters were as follows: 360° rotation, 180 projections, 500 ms exposure time, 80 kV voltage, 500 μA current, and effective pixel size 36 μm. 3D reconstitutions were performed with the Inveon Research Workplace (Siemens Medical Solutions). To calculate NHO volumes, the region of interest (ROI) was drawn around the muscles containing NHO, and was carefully checked from three dimensions. After defining the ROI, the NHO region was defined by setting the threshold Hounsfield units (HU) to 450 HU.

Histology

Fixed hind limbs were decalcified and processed as previously described (15). Five μm sections were cut and stained using Masson's Trichrome. In brief sections were deparaffinized and rehydrated then stained for 10 min in Weigert's iron hematoxylin, rinsed under tap water for 10 min, differentiated in 1% acid alcohol (1% hydrochloric acid) for 15–30 s, rinsed in tap water (3 min) then distilled water, followed by staining in Biebrich scarlet-acid fuchsine solution for 10–15 min (Biebrich scarlet, 1% aqueous, Acid fuchsine, 1% aqueous, glacial acetic acid), slides are then washed in distilled water and differentiated in 5% phosphomolybdic −5% phosphotungstic acid solution for 10–15 min or until collagen is not red. Slides were transferred into aniline blue solution for 5–10 min and rinsed in 1% acetic acid for 2–5 min, dehydrated, and mounted in resinous mounting medium. Immunohistochemistry was performed as previously described (15). Primary antibodies used were: rat anti-mouse F4/80 mAb (clone CI:A3-1, Abcam), rabbit anti-mouse Osterix/Sp7 polyclonal IgG (ab22552, Abcam), rabbit anti-mouse collagen type 1 polyclonal IgG (C7510-13, US Biological), or relevant isotype control antibodies; ratIgG2b (400602, Biolegend), or rabbit IgG (ab27478, Abcam). A 3-step procedure was employed using biotinylated F(ab)2 secondary antibodies (biotinylated goat anti-rat IgG and goat anti-rabbit IgG antibodies, Vector Labs) and VECTASTAIN Elite ABC -Peroxidase Kit (Vector Labs), was used to detect primary antibodies. Slides were viewed using an Olympus BX50 microscope with an attached DP26 camera and imaged using Olympus CellSens standard 1.7 imaging software (Olympus).

Quantification of F4/80 Immunohistochemistry

Immunohistochemistry staining for the pan macrophage marker F4/80 was imaged using an Olympus VS120 (Olympus) at 40X magnification. Automated digital image analysis was subsequently performed using the Visiopharm Integrator System (Visiopharm, Hoersholm, Denmark). In each sample, at each sectional depth (4 depths analyzed with each depth at least 50 μm apart), ROIs were generated which contained all damaged muscle. Automated analysis was performed from the ROIs and the data was calculated as percent of $F4/80^+$ staining per total area of injured muscle. All cases were visually reviewed to ensure accuracy. Data was represented separately at each sectional depth as the area of damaged tissue is not uniform throughout each hamstring.

Statistical Analysis

Statistically significant differences were determined using ANOVA with *post-hoc* Tukey's multiple comparison test or Mann-Whitney test using PRISM 6 or 7 (GraphPad software, La Jolla, CA, USA).

RESULTS

Increased $Ly6C^{high}$ Monocyte Infiltration in Injured Muscles of Mice Following SCI

We have previously reported that systemic depletion of phagocytic macrophages and monocytes by injections of clodronate-loaded liposomes significantly reduces NHO development (13). Therefore, we further characterized the macrophage/monocyte populations present within the muscles of mice developing NHO by flow cytometry. In this model, only mice that undergo both SCI + i.m. CDTX injection develop NHO exclusively in the CDTX injected muscle (13, 15). Mice underwent SCI or SHAM surgery followed by an intramuscular injection of CDTX to cause muscle injury or a control PBS injection. At 4 days post-surgery leukocytes were extracted from the hamstrings of all mice and isolated into four subsets based on forward scatter, side scatter as well as zombie aqua negativity (viable cells), F4/80, Ly6G, CD11b, and Ly6C expression (**Figure 1A**). Preliminary flow cytometry analysis confirmed that CDTX-induced intramuscular injury caused a large and significant accumulation of total $F4/80^+$ monocyte/macrophages (**Figure 1B**i $p < 0.0001$) in SCI+CDTX and SHAM+CDTX groups compared to control groups (SCI+PBS and SHAM+PBS). When the total $F4/80^+$ population was sub-gated based on expression of Ly6C, we observed a significantly higher frequency of $Ly6C^{high}$ 'inflammatory monocytes/macrophages' ($CD11b^+F4/80^+Ly6G^-Ly6C^{hi}$) in the mice that develop NHO (SCI+CDTX), compared to SHAM+CDTX mice (**Figure 1B**ii $p = 0.0002$). Minimal $Ly6C^{hi}$ monocyte/macrophages were noted in the SCI+PBS and SHAM+PBS groups. The frequencies of $Ly6C^{mid/lo}$ monocyte/macrophages ($CD11b^+F4/80^+Ly6G^-Ly6C^{mid/lo}$) was unchanged between SCI+CDTX and SHAM+CDTX groups (**Figure 1B**iii). We also observed the presence of

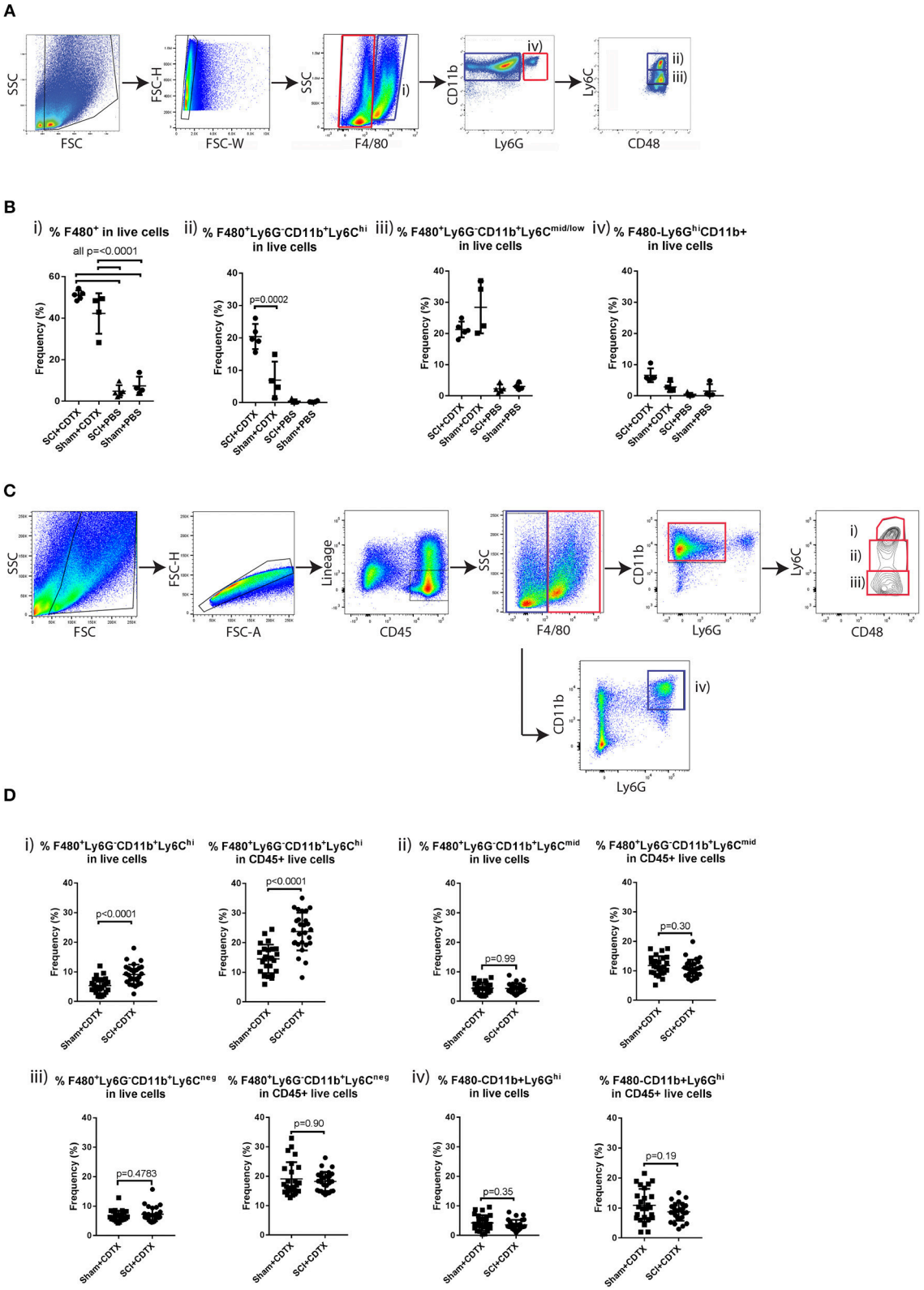

FIGURE 1 | Increased inflammatory monocyte infiltration in injured muscles of mice developing NHO. **(A)** C57BL/6 mice underwent either SCI or Sham surgery followed by an intra muscular injection of CDTX or PBS. Muscle leukocytes were extracted from hamstrings at day 4 post-surgery and isolated into four subsets

(Continued)

FIGURE 1 | based on forward scatter, side scatter as well as zombie aqua negativity (viable cells), F4/80, Ly6G, CD11b, and Ly6C expression. **(B)** Frequencies of each leukocyte population relative to total live muscle cells using the gating strategy outlined: (i) "Total F4/80$^+$ cells" (CD11b$^+$F4/80$^+$, blue gates in **A**), (ii) "Ly6C^{hi} inflammatory monocytes" (F4/80$^+$CD11b$^+$Ly6G$^-$ CD48$^+$Ly6C^{hi}, blue gates in **A**), (iii) "Ly6C$^{mid/lo}$ monocytes/macrophages" (F4/80$^+$ CD11b$^+$ Ly6G$^-$CD48$^+$ Ly6C$^{mid/lo}$, blue gates in **A**), and (iv) "granulocytes" (F4/80$^-$CD11b$^+$Ly6G$^+$, red gates in **A**). The frequency of Ly6C^{hi} inflammatory monocytes (relative to total live muscle cells) in mice developing NHO (SCI+CDTX), compared to all other treatment groups was significantly higher ($p = 0.0002$ ANOVA $n = 3$–5/group). Each dot represents an individual mouse. Bars represent as mean ± SD. **(C)** Muscle leukocytes were extracted from hamstrings at day 4 post surgery, and 4 separate leukocyte populations were identified by flow cytometry using the following gating strategy: (i) "Ly6C^{hi} inflammatory monocytes" as CD45$^+$ lineage (Ter119,CD3ε,B220)-negative F4/80$^+$ CD11b$^+$ Ly6G$^-$ CD48$^+$Ly6C^{hi}, red gates, (ii) "Ly6C^{mid} monocytes/macrophages" CD45$^+$ Lin$^-$ F4/80$^+$ CD11b$^+$ Ly6G$^-$CD48$^+$ Ly6C^{mid}, red gates, (iii) "Ly6C^{neg} monocytes" CD45$^+$ Lin$^-$ F4/80$^+$ CD11b$^+$ Ly6G$^-$ CD48$^+$ Ly6C^{neg} red gates, and (iv) "granulocytes" CD45$^+$ Lin$^-$ F4/80^{neg} CD11b$^+$ Ly6G$^+$, blue gates. **(D)** Frequencies of each myeloid subset relative to total live muscle cells and to total live CD45$^+$ muscle leukocytes. There was a significant increase in frequency of Ly6C^{hi} monocytes relative to total live muscle cells (Di, $p < 0.0001$ Mann-Whitney test) and to CD45$^+$ live muscle leukocytes (Di, $p < 0.0001$ Mann-Whitney test) after SCI+CDTX compared to Sham+CDTX. Each dot represents an individual mouse, $n = 25$–27/treatment group. Bars represent mean ± SD.

granulocytes (CD11b$^+$F4/80$^-$Ly6G^{hi}) (**Figure 1B**iv**),** albeit with lower frequencies compared to monocyte/macrophage subsets. In view of these preliminary results, we focused our subsequent analysis on leukocyte populations infiltrating the CDTX-injured muscles in SCI+CDTX and SHAM+CDTX groups in a larger cohort of mice to achieve higher statistical power. Leukocytes were isolated into 4 separate populations based on forward scatter, side scatter as well as 7-actinomycin D-negativity (7AAD$^-$ viable cells), CD45, lineage (Ter119, CD3ε, B220), F4/80, Ly6G, CD11b, Ly6C expression (**Figure 1C**). Although we initially wanted to incorporate antibodies specific for CD169, Mer tyrosine kinase and VCAM-1 which clearly identifies macrophages from monocytes (31), preliminary experiments on bone marrow cells where macrophages and monocytes are abundant confirmed this was not possible as these antigens are cleaved from the cell surface by the protease cocktail used to extract leukocytes from skeletal muscles (data not shown). Despite this limitation, we again observed that the frequency of "Ly6C^{hi} inflammatory monocytes/macrophages" (CD45$^+$Lin$^-$CD11b$^+$F4/80$^+$Ly6G$^-$Ly6C^{hi}) in live muscle cells was significantly higher in mice that develop NHO (SCI+CDTX) mice compared to SHAM+CDTX mice (**Figure 1D**i, left panel $p < 0.0001$). When the frequency of Ly6C^{hi} monocytes was calculated relative to all CD45$^+$ leukocytes present, the frequency of these inflammatory monocytes was also significantly increased (**Figure 1D**i, right panel $p < 0.0001$). The frequencies of other monocyte/macrophage subsets identified as CD45$^+$Lin$^-$CD11b$^+$F4/80$^+$Ly6G$^-$Ly6C^{mid} monocytes (**Figure 1D**ii), CD45$^+$Lin$^-$CD11b$^+$F4/80$^+$Ly6G$^-$Ly6C^{neg} monocytes (**Figure 1D**iii), as well as CD45$^+$Lin$^-$CD11b$^+$F4/80$^-$Ly6G$^+$ neutrophils (**Figure 1D**iv) were not significantly different in SCI+CDTX compared to SHAM+CDTX mice.

Expression of OSM and OSMR in Muscle Cell Populations

We have previously confirmed by qRT-PCR, that *Osm* mRNA is significantly upregulated in the whole muscles of mice developing NHO (15). As there is no commercial monoclonal antibody specific for mouse OSMR that works by flow cytometry, we isolated RNA from the sorted myeloid populations described in **Figure 1D** at 4 days post-surgery, as well as whole skeletal muscle from naïve mice and mouse muscle progenitor cell populations; CD45$^-$Ter119$^-$CD31$^-$CD34$^+$Sca1$^-$ satellite cells and CD45$^-$Ter119$^-$CD31$^-$CD34$^+$Sca1$^+$ interstitial cells [also known as fibro-adipogenic progenitors or FAP (32)] freshly sorted from naïve skeletal muscle, to establish which cell types express *Osm* and *Osmr* mRNA. *Osm* mRNA was detected in all myeloid populations infiltrating the SCI+CDTX-injured muscle with the highest abundance in granulocytes **(Figure 2A**), whereas no *Osm* was detected in whole naïve skeletal muscle. These results are consistent with the tissue expression profile of mouse *Osm* mRNA in the BioGPS database (http://biogps.org). In sharp contrast, *Osmr* mRNA was undetectable in myeloid populations in the muscle but was expressed by both muscle satellite cells and interstitial cells (**Figure 2B**). This suggests that OSM can act directly on muscle progenitor cells that express its receptor OSMR rather than indirectly via infiltrating myeloid cells.

OSM Induces STAT3 Y705 Phosphorylation in Cultured Mouse Muscle Cells

Given that both muscle satellite cells and interstitial cells expressed *Osmr* mRNA, we further investigated OSM/OSMR signaling in these cells. The OSMR/gp130 receptor complex is known to activate both JAK1 and JAK2 tyrosine kinases following OSM binding (23, 24). Once activated, JAK1 and JAK2 tyrosine phosphorylate STAT1 and STAT3 (23) which enable their nuclear translocation to initiate transcription of OSM responsive genes. In preliminary experiments, we were unable to detect phosphorylated JAK1 and JAK2 by immunoprecipitation and western-blot of whole muscle lysates because the very low levels of total JAK1 and JAK2 proteins (data not shown). Instead, we measured the tyrosine phosphorylation status of the JAK1/2 substrate STAT3 in response to recombinant mouse OSM in satellite and interstitial cells sorted from the muscles of naïve mice. The mouse mesenchymal progenitor cell line Kusa4b10 (29, 30) was used as a positive control. By flow cytometry with a mAb specific for STAT3 phosphorylation on tyrosine 705 (pSTAT3 Y705), we confirmed that recombinant mouse OSM caused a rapid phosphorylation of STAT3 Y705 on all cell types tested (**Figure 2C**), confirming that OSMR is functional on mouse muscle satellite and interstitial cells. To confirm that STAT3 Y705 phosphorylation was mediated by JAK1/2, we also preincubated cells for 30 min with the small synthetic JAK1/2 inhibitor ruxolitinib (27, 28). Ruxolitinib completely inhibited phosphorylation of STAT3 Y705 in response to mouse OSM in all three cell types (**Figure 2C**). Together these results suggest that OSMR expressed by satellite and interstitial cells are able

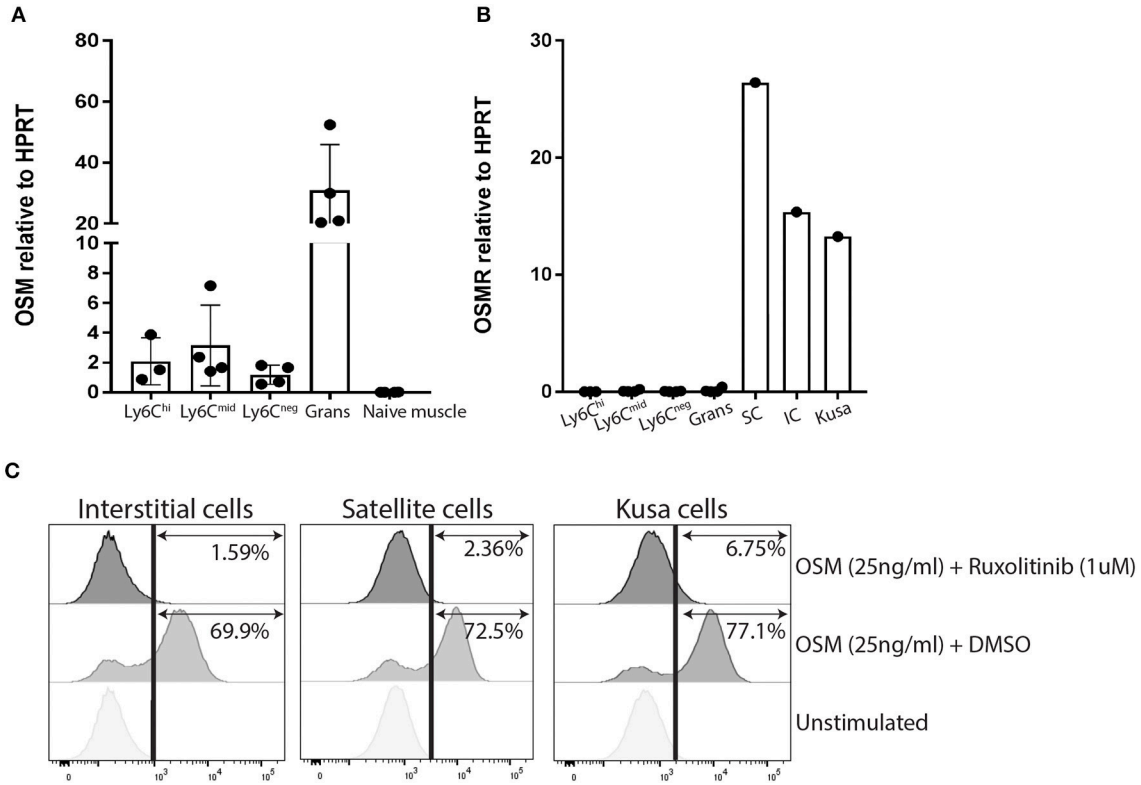

FIGURE 2 | OSM and OSMR expression and signaling in muscle cells. **(A)** *Osm* mRNA expression by qRT-PCR. *Osm* is expressed by all sorted infiltrating myeloid populations but absent in whole naïve skeletal muscle. Each dot represents an individual mouse (n = 3–4/group). Bars represent mean ± SD. **(B)** *Osmr* mRNA expression is only present in sorted mouse muscle satellite and interstitial cells, not in any sorted myeloid population infiltrating the injured muscle **(C)** Phos-flow of pSTAT3 Y705 phosphorylation in cultured CD45$^-$Ter119$^-$CD31$^-$CD34$^+$Sca1$^+$ muscle interstitial cells (IC), CD45$^-$Ter119$^-$CD31$^-$CD34$^+$Sca1$^-$ muscle satellite cells (SC), and Kusa4b10 cells. Cells were incubated for 10 min at 37°C with medium alone (unstimulated), or 25 ng/ml recombinant mouse OSM plus DMSO or of 25 ng/ml OSM plus 1 μM ruxolitinib. Cell were then fixed and permeabilized before staining with AlexaFluor647-conjugated mouse mAb anti-pSTAT3 (Y705) and analyzed by flow cytometry. Representative figures were one of two independent experiments.

to respond to upregulated OSM in muscle and activate downstream JAK1/2-STAT3 signaling pathway.

Persistence of STAT3 Tyrosine Phosphorylation in the Injured Muscle Following SCI

Next, we examined STAT3 Y705 phosphorylation in the muscles of mice developing NHO. Western blots for pSTAT3 Y705 and total STAT3 were performed using whole muscle lysates from hamstrings of mice that underwent either (1) SCI+CDTX, (2) SCI+PBS, (3) SHAM+CDTX, or (4) SHAM+PBS at day 4, 7, and 14 days post-surgery. At 4 days post-surgery there was a clear increase in STAT3 Y705 phosphorylation in muscle injured with CDTX (**Figure 3A**). Importantly the ratio of pSTAT3 Y705 vs. total STAT3 normalized to the pSTAT3/STAT3 ratio measured in control mice (SHAM+PBS), was significantly higher in SCI+CDTX mice compared to SHAM+CDTX mice (**Figure 3A**). Seven days post-injury, STAT3 Y705 phosphorylation persisted in the injured muscles from the SCI+CDTX group while it was resolving in the SHAM+CDTX group (**Figure 3B**). This pattern of persistent STAT3 Y705 phosphorylation in the injured muscles of the SCI+CDTX group that developed NHO was noted up to 14 days post-surgery (**Figure 3C**) whereas in SHAM+CDTX, pSTAT3 Y705 had returned to levels not significantly different from those observed in controls without muscle injury as expected from previous reports showing that without a SCI, CDTX-injured muscles are mostly repaired 14 post-injury (33). These data establish that the combination of SCI with muscle injury, compared to all other control treatments, caused enhanced STAT3 signaling in the injured muscle which persisted for an extended period of time after the initial injury. Overall these data establish that in the context of a SCI, STAT3 phosphorylation is exaggerated and persists over a longer period of time in injured muscles developing NHO.

JAK1/2 Inhibition Significantly Reduced NHO Development Following SCI

From this we hypothesized that exaggerated and persistent STAT3 tyrosine phosphorylation and activation by JAK1/2 in injured muscles of SCI mice is functionally important in NHO pathogenesis. To test this, we treated mice that underwent

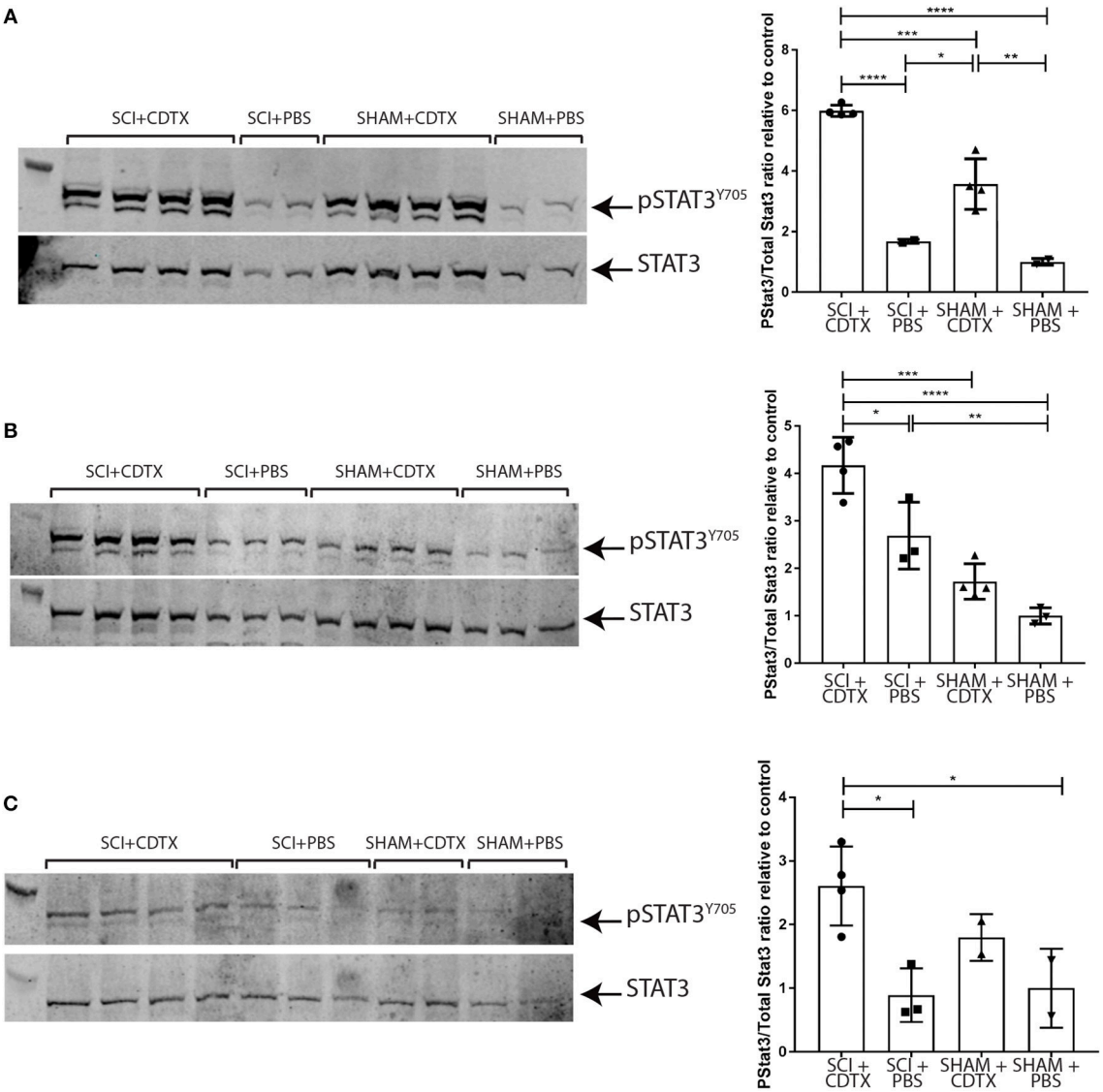

FIGURE 3 | Persistence of STAT3 tyrosine phosphorylation in injured muscles following spinal cord injury. Western-blots of whole muscle lysates collected from mice that underwent either SCI or SHAM surgery together with an intramuscular injection of either CDTX or PBS. Western blot of whole muscle lysates from individual mice taken on day 4 **(A)**, 7 **(B),** or 14 **(C)** post-injury. Each membrane was probed with rabbit anti-pSTAT3 Y705 mAb, stripped and then re-probed with rabbit anti-total STAT3 mAb. Band fluorescence intensity was quantified and ratio of signal intensity of pSTAT3 vs. total STAT3 calculated for each individual mouse and normalized relative to the average pSTAT3/STAT3 ratio in control mice (SHAM+PBS) at each time-point. Each lane and each dot represents a separate mouse, $n = 2$–4 mice/treatment/time-point. Bars represent mean ± SD. *P* values were calculated by ANOVA, $^{*}p < 0.05$, $^{**}p < 0.01$, $^{***}p < 0.001$, $^{****}p < 0.0001$.

SCI+CDTX with ruxolitinib bi-daily for the first 7 days post-surgery. Ruxolitinib treatment significantly reduced STAT3 Y705 phosphorylation at 7 days post-surgery (**Figure 4A** $^{*}p = 0.03$). Micro CT (μCT) confirmed a significant reduction in NHO bone volume at day 7, 14, and 23 post surgery in mice treated with ruxolitinib for the first 7 days post-injury (**Figure 4B**i,ii $^{**}p = 0.0076$, $^{*}p = 0.031$, and $^{*}p = 0.015$). Visual representation of collagen^{+} NHO by Masson's trichrome staining at 3 weeks post-surgery was consistent with μCT quantification and confirmed the presence of collagen^{+} NHO foci in the muscles of vehicle treated SCI+CDTX mice (**Figure 4C,** crosshatches). Collagen^{+} NHO foci were reduced after ruxolitinib treatment. As previously described by us (13, 15) and others (33), in SHAM+CDTX mice at 3 weeks post-surgery, no NHO and little collagen deposition was observed, with reformation of muscle fibers confirming that in the absence of SCI, the CDTX-injured muscle repairs within 7–14 days post-injury (33). Immunohistochemistry with anti-collagen type I or anti-osterix/SP7 antibodies were consistent with both μCT and Masson's trichrome staining and confirmed that in vehicle treated SCI+CDTX mice the

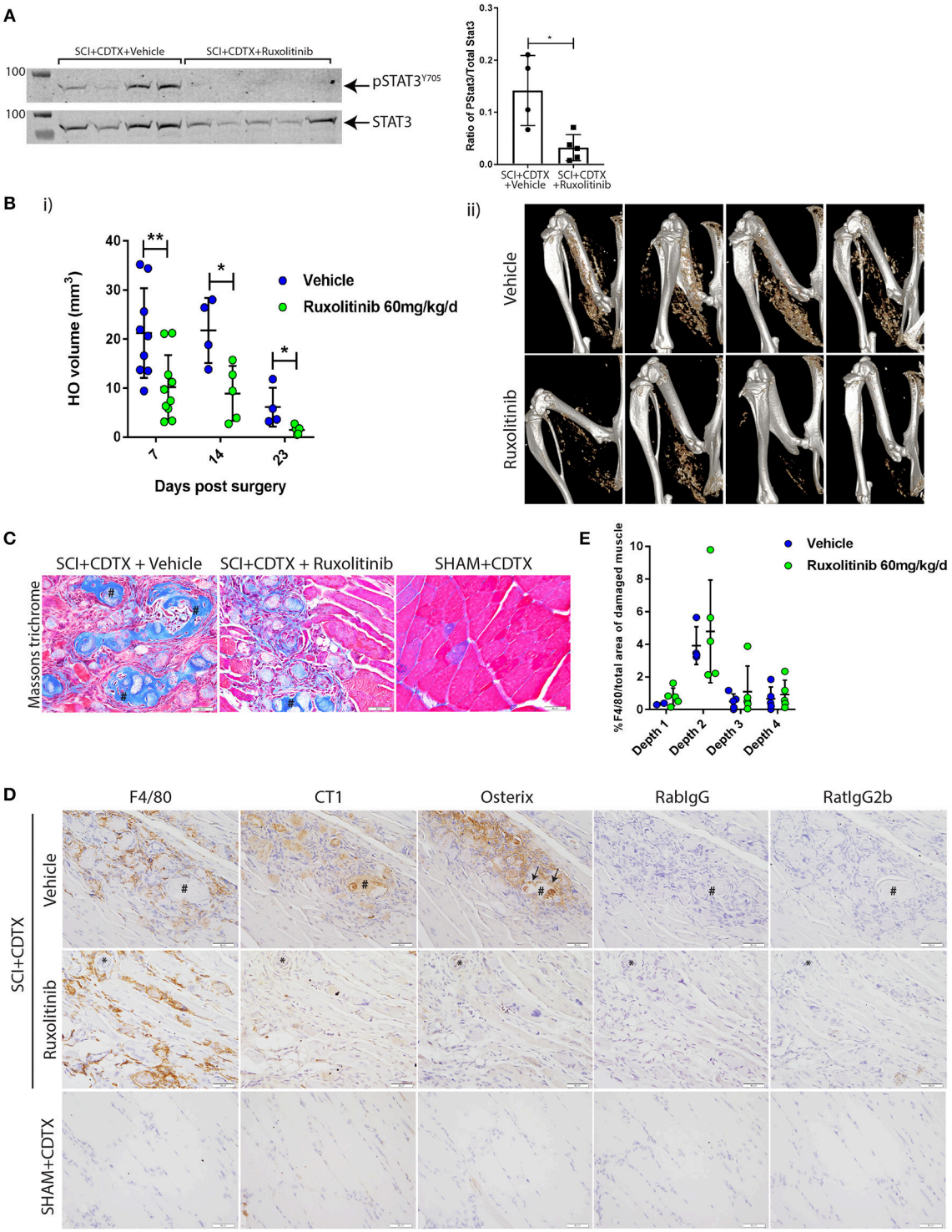

FIGURE 4 | Inhibition of JAK1/2 kinases with ruxolitinib reduces NHO development after SCI *in vivo*. **(A)** Western-blots of whole muscle lysates collected at day 7 from SCI+CDTX mice that were treated with either vehicle control or ruxolitinib (60 mg/kg bi-daily) from day 0–7 post surgery. Western-blots of whole muscle lysates were probed with rabbit anti-pSTAT3 Y705 mAb, and rabbit anti-total STAT3 mAb, then band fluorescence was quantified and ratio of signal intensity of pSTAT3 versus total STAT3 calculated for each individual mouse. Each lane and each dot represents a separate mouse, $n = 4$–5/treatment group. Data represented as mean ± SD, $^*p = 0.03$ by Mann-Whitney test. **(B)** Measurement of NHO volume by micro CT (μCT) in mice which received SCI+CDTX and treated with either vehicle control or ruxolitinib (60 mg/kg bi-daily) from day 0–7 post surgery. (i) NHO volumes were quantified *in vivo* by μCT at indicated time points post-surgery illustrating the

(Continued)

FIGURE 4 | reduction in NHO development. Each dot represents a separate mouse, $n = 4$–10 mice/treatment/time point. Data represented as mean ± SD, $^{**}p = 0.0076$, $^{*}p = 0.031$, and $p = 0.015$ respectively by Mann-Whitney test. (ii) Representative μCT images at 7 days post-surgery **(C)** Masson's trichrome staining 3 weeks post-surgery confirming the development of multiple NHO bone and collagen+ foci (crosshatches) within the muscle in vehicle treated mice, which are reduced after ruxolitinib treatment, and absent in control mice (SHAM+CDTX) **(D)** Immunohistochemistry staining of serial sections from SCI+CDTX mice 3 weeks post-surgery (top and middle panels). Mice were treated with vehicle or ruxolitinib (60 mg/kg bi-daily) from day 0–7 post surgery. Stains were performed with either rat anti-F4/80 mAb, rabbit anti-collagen I (CT1), or anti-osterix antibodies. Isotype control (rat IgG2b for F4/80; Rabbit IgG for CT1, and Osterix) are also shown to confirm specificity of staining. In vehicle treated mice $CT1^+$ NHO foci are present within the damaged muscle (crosshatch), these foci are surrounded by $F4/80^+$ macrophages and have $Osterix^+$ cells lining the NHO foci surface (arrows). After ruxolitinib treatment there are still $F4/80^+$ macrophages within the damaged muscle, however there are less $CT1^+$ NHO foci with $Osterix^+$ cells lining the surface. *symbols denote the same anatomical landmark in each image. NHO development is absent in SHAM+CDTX mice 3 weeks post-surgery, with no CT1, and Osterix expression (bottom panel). **(E)** Quantification of F4/80 expression via IHC confirmed that ruxolitinib treatment did not change $F4/80^+$ macrophage expression within the hamstrings of vehicle vs. ruxolitinib treated mice, 7 days post-surgery. Each dot represents a separate mouse, $n = 2$–5/treatment group/sectional depth. Four different depths were analyzed for each sample with at least 50 μm between each depth. Data represented as mean ± SD. All images taken at 40X magnification, scale bar represents 50 μm.

collagen type I^+ NHO foci were lined with $osterix^+$ osteo-lineage cells (**Figure 4D,** top panel, arrows). Reduced osterix-positive osteo-lineage cells and type 1 collagen deposition was noted after ruxolitinib treatment (**Figure 4D,** middle panel). In SHAM+CDTX mice there was little expression of collagen type I and osterix (**Figure 4D,** bottom panel). Ruxolitinib treatment had minimal impact on the density of $F4/80^+$ macrophages within the injured muscles 7 days post-surgery (**Figure 4E**).

DISCUSSION

The inflammatory component that frequently accompanies severe trauma of the central nervous system and the spine has been suggested to be a key factor in NHO development (5, 34, 35). We have previously established in a mouse model of SCI-induced NHO in which macrophages infiltrate the damaged muscles was critical for NHO development (13–15). Our current study demonstrates that SCI causes an increased infiltration of $Ly6C^{hi}$ inflammatory monocytes/macrophages into injured muscles. Furthermore, we show that myeloid cells infiltrating the injured muscle express the pro-inflammatory cytokine OSM. Binding of OSM to OSMR, which is expressed by satellite cells and interstitial cells isolated from muscle, activates JAK1/2 tyrosine kinases with subsequent STAT3 tyrosine phosphorylation and activation *in vitro*. *In vivo* we established that SCI with accompanying muscle injury caused an increase in STAT3 phosphorylation in injured muscles which persisted for up to 2 weeks only in the muscles that develop NHO. Finally, *in vivo* inhibition of JAK1/2 with ruxolitinib reduced STAT3 phosphorylation in injured muscles and most importantly reduced NHO volume subsequent to SCI combined with muscle injury.

OSM has been recently reported to induce muscle satellite cell quiescence *in vivo*, and conditional deletion of the *Osmr* gene specifically in satellite cells led to reduced myofiber regeneration in response to injury (36). In agreement with this, STAT3, which is activated by JAK1/2 immediately downstream of the OSMR:gp130 complex, has been implicated in controlling satellite cell expansion and muscle repair after muscle injury (37). In addition, STAT3 knock-down or conditional *Stat3* gene deletion in satellite cells increased satellite cell proliferation following muscle injury but impaired muscle repair, suggesting that STAT3 activation is required for accelerated muscle repair (37, 38). In contrast, OSM is known to promote osteogenic differentiation of mesenchymal stromal cells *in vitro* (18, 39) and osteoblast differentiation and bone formation *in vivo* (16, 17, 19). Therefore, OSM plays an important role in both muscle repair and osteogenic differentiation and activity. This is consistent with our observations that (1) OSMR is expressed in skeletal muscles by both satellite cells, which regenerate myoblasts following muscle injury (40), and by interstitial cells which are of mesenchymal origin (32), and (2) that OSM causes STAT3 phosphorylation in both cell types *in vitro*. A limitation of our study is that we were unable to demonstrate STAT3 phosphorylation specifically in muscle satellite cells or interstitial cells *in vivo*. The extended enzymatic digestion of muscles at 37°C required to obtain single cell suspension amenable for flow cytometry, removes OSM protein from the extracellular milieu thus disrupting OSMR ligation on satellite and interstitial cells and downstream JAK/STAT signaling. Further immunohistological experiments using reporter mice in which muscle satellite cells or mesenchymal cells are specifically labeled with a fluorescent reporter will be required to definitively prove STAT3 activation *in vivo* in these two cell types.

It is also important to note that in our experiments, ruxolitinib may also block STAT activation in additional cell types particularly myeloid cells that infiltrate the injured muscle. Indeed, these myeloid cells express receptors for other inflammatory cytokines such as IL-6 (41), granulocyte colony-stimulating factor (G-CSF) (42) and granulocyte macrophage colony-stimulating factors (GM-CSF) (43) which also activate STATs via JAK1/2. Although it remains to be determined whether IL-6, G-CSF, and GM-CSF contribute to NHO pathogenesis (44), the ruxolitinib-mediated inhibition of JAK1/2 in both muscle progenitor cells and infiltrating myeloid cells may also contribute to the overall inhibition of NHO in our model.

Intriguingly, while STAT3 inhibition has been reported to improve muscle repair in mice without SCI (37, 38), we did not note improved muscle repair following JAK1/2 inhibitor administration in mice that underwent SCI as macrophage infiltration and collagen deposits remained in the injured muscles even after ruxolitinib treatment. A few hypotheses can be formulated to explain this divergent outcome in terms of muscle repair. Firstly, the SCI may cause a dramatic change in the function of macrophages orchestrating muscle repair (33) and in muscle satellite and interstitial cells, such that inhibition of either

STAT3 or JAK1/2 is not sufficient to re-establish coordinated muscle regeneration. A second possibility is that the JAK1/2 inhibitor used in our study also inhibits the activation of other STAT proteins such as STAT1 and STAT5 which may be activated in response to OSM (16) as well as STAT activation in response to other cytokines such IL-6, IL-12, G-CSF, or GM-CSF in muscle cells and macrophages which orchestrate muscle regeneration as discussed above.

It is also important to note that despite the significant effect of ruxolinitib in reducing STAT3 phosphorylation in muscles of mice developing NHO, and the reduction in NHO volume after ruxolitinib treatment, while pronounced was only partial (**Figure 4**). Herein we find that SCI and muscle injury caused an exaggerated infiltration of Ly6C^{hi} inflammatory monocytes into the injured muscles consistent with our previous observation that *in vivo* depletion of phagocytes with clodronate-loaded liposomes markedly inhibited NHO formation (13). Because of this increased inflammatory monocyte infiltration, it is likely that other pro-inflammatory cytokines and mediators are released within the injured muscle and participate to NHO development. For instance we have previously reported in this model of SCI-induced NHO that substance P may contribute to NHO development (13). Others have reported in a rat model of multi-trauma, that the retinoic acid receptor-γ agonist Palovarotene also partially decreased heterotopic ossification (45). In a similar rat model of multi-trauma, rapamycin was also found to partially decrease heterotopic ossification, suggesting that mammalian targets of rapamycin (mTOR) may also play an important role (46). Altogether these findings suggest that many other pathways could be abnormally activated in injured muscles in the context of a SCI. Indeed since NHO is driven by two different insults, it is unlikely that the pathogenesis converges to a single pathway. Therefore, a highly effective therapy is likely to require a combined approach. We are currently undertaking transcriptome analyses on injured muscles with and without SCI to elucidate the molecular pathways that could potentially promote NHO development.

Although ruxolitinib caused a pronounced but still partial reduction in NHO development, inhibitors of JAK1/2 or STAT3 may represent a new therapeutic approach to decrease NHO development in patients or perhaps to avoid NHO re-occurrence after surgical resection, which is observed in 6% of NHO patients (2, 9, 12). However, the roles of STAT3 and JAK1/2 in spinal cord recovery will need to be carefully evaluated. In a rat model of SCI, treatment with a STAT3 inhibitor post-surgery promoted neural stem cell differentiation (47). In other studies, augmentation of IL-6 after SCI resulted in enhanced infiltration of neutrophils and macrophages with a subsequent increase in lesion size and reduction in axonal growth, suggesting that balanced IL-6 signaling is required for efficient repair after SCI (48). However, other studies have demonstrated that conditional deletion of STAT3 in reactive astrocytes leads to the limited migration of astrocytes, higher infiltration of inflammatory cells, demyelination, and more severe loss of motor function following SCI (49, 50). The SCI-NHO model used in our studies involves a complete spinal cord transection and further analysis on neurological recovery was not possible in this model. Therefore, further studies in a SCI-NHO model where neurological recovery is achievable are necessary to effectively determine whether ruxolitinib treatment to reduce NHO development has any beneficial or negative impact on neurological recovery following SCI.

In conclusion our experiments suggest that STAT3 activation persists in the muscles of mice that are developing NHO following SCI and that targeting STAT3 activation via transient JAK1/2 inhibition immediately following SCI may be a possible therapeutic approach to reduce NHO development in patients.

DATA AVAILABILITY

The datasets generated for this study are available on request to the corresponding author.

ETHICS STATEMENT

This study was carried out in accordance with the Australian Code of Animal Experimentations. All protocols and experiments were approved by the Animal Experimentation Committee of the University of Queensland, Saint Lucia, Queensland, Australia.

AUTHOR CONTRIBUTIONS

KA, H-WT, WF, BJ, MS, IK, and SM performed the experiments. KA, H-WT, and J-PL conceived the experiments and the work. KA, H-WT, and J-PL wrote the manuscript. KA, H-WT, FG, ARP, and J-PL edited the manuscript.

FUNDING

This research was supported by Project Grant 1101620 from the National Health and Medical Research Council of Australia (NHMRC) to J-PL, ARP and FG, and award W81XWH-15-1-0606 from the Congressionally Approved Spinal Cord Injury Research Program of the US Department of Defense to J-PL, ARP, and FG, and by funds from the Mater Foundation. J-PL is supported by Research Fellowship 1136130 from the NHMRC. ARP is supported by an Australian Research Council Future Fellowship ARP FT150500335. The Translational Research Institute is partly funded by the Federal Government of Australia.

ACKNOWLEDGMENTS

The authors also acknowledge the scientific and technical assistance of the UQ biological resources TRI facility, histology facility, flow cytometry facility, microscopy facility, and the preclinical Imaging Facility, Translational Research Institute, which is supported by Therapeutic Innovation Australia (TIA). TIA is supported by the Australian Government through the National Collaborative Research Infrastructure Strategy (NCRIS) program.

REFERENCES

1. Ohlmeier M, Suero EM, Aach M, Meindl R, Schildhauer TA, Citak M. Muscle localization of heterotopic ossification following spinal cord injury. *Spine J.* (2017) 17:1519–22. doi: 10.1016/j.spinee.2017.04.021
2. Genet F, Jourdan C, Schnitzler A, Lautridou C, Guillemot D, Judet T, et al. Troublesome heterotopic ossification after central nervous system damage: a survey of 570 surgeries. *PLoS ONE.* (2011) 6:e16632. doi: 10.1371/journal.pone.0016632
3. Dizdar D, Tiftik T, Kara M, Tunc H, Ersoz M, Akkus S. Risk factors for developing heterotopic ossification in patients with traumatic brain injury. *Brain Inj.* (2013) 27:807–11. doi: 10.3109/02699052.2013.775490
4. Reznik JE, Biros E, Marshall R, Jelbart M, Milanese S, Gordon S, et al. Prevalence and risk-factors of neurogenic heterotopic ossification in traumatic spinal cord and traumatic brain injured patients admitted to specialised units in Australia. *J Musculoskelet Neuronal Interact.* (2014) 14:19–28.
5. Brady RD, Shultz SR, McDonald SJ, O'Brien TJ. Neurological heterotopic ossification: current understanding and future directions. *Bone.* (2018) 109:35–42. doi: 10.1016/j.bone.2017.05.015
6. Forsberg JA, Pepek JM, Wagner S, Wilson K, Flint J, Andersen RC, et al. Heterotopic ossification in high-energy wartime extremity injuries: prevalence and risk factors. *J Bone Joint Surg Am.* (2009) 91:1084–91. doi: 10.2106/JBJS.H.00792
7. Vanden Bossche L, Vanderstraeten G. Heterotopic ossification: a review. *J Rehabil Med.* (2005) 37:129–36. doi: 10.1080/16501970510027628
8. Salga M, Jourdan C, Durand MC, Hangard C, Denormandie P, Carlier RY, et al. Sciatic nerve compression by neurogenic heterotopic ossification: use of CT to determine surgical indications. *Skeletal Radiol.* (2015) 44:233–40. doi: 10.1007/s00256-014-2003-6
9. Genet F, Chehensse C, Jourdan C, Lautridou C, Denormandie P, Schnitzler A. Impact of the operative delay and the degree of neurologic sequelae on recurrence of excised heterotopic ossification in patients with traumatic brain injury. *J Head Trauma Rehabil.* (2012) 27:443–8. doi: 10.1097/HTR.0b013e31822b54ba
10. Genet F, Marmorat JL, Lautridou C, Schnitzler A, Mailhan L, Denormandie P. Impact of late surgical intervention on heterotopic ossification of the hip after traumatic neurological injury. *J Bone Joint Surg Br.* (2009) 91:1493–8. doi: 10.1302/0301-620X.91B11.22305
11. Genêt F, Denormandie P, Keenan MA. Orthopaedic surgery for patients with central nervous system lesions: concepts and techniques. *Ann Phys Rehabil Med.* (2018) doi: 10.1016/j.rehab.2018.09.004
12. Genet F, Jourdan C, Lautridou C, Chehensse C, Minooee K, Denormandie P, et al. The impact of preoperative hip heterotopic ossification extent on recurrence in patients with head and spinal cord injury: a case control study. *PLoS ONE.* (2011) 6:e23129. doi: 10.1371/journal.pone.0023129
13. Genet F, Kulina I, Vaquette C, Torossian F, Millard S, Pettit AR, et al. Neurological heterotopic ossification following spinal cord injury is triggered by macrophage-mediated inflammation in muscle. *J Pathol.* (2015) 236:229–40. doi: 10.1002/path.4519
14. Levesque J-P, Sims NA, Pettit AR, Alexander KA, Tseng H-W, Torossian F, et al. Macrophages driving heterotopic ossification: convergence of genetically-driven and trauma-driven mechanisms. *J Bone Miner Res.* (2018) 33:365–6. doi: 10.1002/jbmr.3346
15. Torossian F, Guerton B, Anginot A, Alexander KA, Desterke C, Soave S, et al. Macrophage-derived oncostatin M contributes to human and mouse neurogenic heterotopic ossifications. *JCI Insight.* (2017) 2:e96034. doi: 10.1172/jci.insight.96034
16. Walker EC, McGregor NE, Poulton IJ, Solano M, Pompolo S, Fernandes TJ, et al. Oncostatin M promotes bone formation independently of resorption when signaling through leukemia inhibitory factor receptor in mice. *J Clin Invest.* (2010) 120:582–92. doi: 10.1172/JCI40568
17. Sims NA, Quinn JM. Osteoimmunology: oncostatin M as a pleiotropic regulator of bone formation and resorption in health and disease. *Bonekey Rep.* (2014) 3:527. doi: 10.1038/bonekey.2014.22
18. Guihard P, Danger Y, Brounais B, David E, Brion R, Delecrin J, et al. Induction of osteogenesis in mesenchymal stem cells by activated monocytes/macrophages depends on oncostatin M signaling. *Stem Cells.* (2012) 30:762–72. doi: 10.1002/stem.1040
19. Guihard P, Boutet MA, Brounais-Le Royer B, Gamblin AL, Amiaud J, Renaud A, et al. Oncostatin M, an inflammatory cytokine produced by macrophages, supports intramembranous bone healing in a mouse model of tibia injury. *Am J Pathol.* (2015) 185:765–75. doi: 10.1016/j.ajpath.2014.11.008
20. Gerhartz C, Heesel B, Sasse J, Hemmann U, Landgraf C, Schneider-Mergener J, et al. Differential activation of acute phase response factor/STAT3 and STAT1 via the cytoplasmic domain of the interleukin 6 signal transducer gp130: I. Definition of a novel phosphotyrosine motif mediating STAT1 activation. *J Biol Chem.* (1996) 271:12991–8. doi: 10.1074/jbc.271.22.12991
21. Heinrich PC, Behrmann I, Muller-Newen G, Schaper F, Graeve L. Interleukin-6-type cytokine signalling through the gp130/Jak/STAT pathway. *Biochem J.* (1998) 334:297–314. doi: 10.1042/bj3340297
22. Ichihara M, Hara T, Kim H, Murate T, Miyajima A. Oncostatin M and leukemia inhibitory factor do not use the same functional receptor in mice. *Blood.* (1997) 90:165–73.
23. Levy JB, Schindler C, Raz R, Levy DE, Baron R, Horowitz MC. Activation of the JAK-STAT signal transduction pathway by oncostatin-M cultured human and mouse osteoblastic cells. *Endocrinology.* (1996) 137:1159–65. doi: 10.1210/endo.137.4.8625884
24. Hermanns HM, Radtke S, Haan C, Schmitz-Van de Leur H, Tavernier J, Heinrich PC, et al. Contributions of leukemia inhibitory factor receptor and oncostatin M receptor to signal transduction in heterodimeric complexes with glycoprotein 130. *J Immunol.* (1999) 163:6651–8.
25. Magrangeas F, Boisteau O, Denis S, Jacques Y, Minvielle S. Negative regulation of onconstatin M signaling by suppressor of cytokine signaling (SOCS-3). *Eur Cytokine Netw.* (2001) 12:309–15.
26. Ehlting C, Böhmer O, Hahnel MJ, Thomas M, Zanger UM, Gaestel M, et al. Oncostatin M regulates SOCS3 mRNA stability via the MEK–ERK1/2-pathway independent of p38MAPK/MK2. *Cell Signal.* (2015) 27:555–67. doi: 10.1016/j.cellsig.2014.12.016
27. Quintás-Cardama A, Vaddi K, Liu P, Manshouri T, Li J, Scherle PA, et al. Preclinical characterization of the selective JAK1/2 inhibitor INCB018424: therapeutic implications for the treatment of myeloproliferative neoplasms. *Blood.* (2010) 115:3109–17. doi: 10.1182/blood-2009-04-214957
28. Verstovsek S, Mesa RA, Gotlib J, Levy RS, Gupta V, DiPersio JF, et al. A double-blind, placebo-controlled trial of ruxolitinib for myelofibrosis. *N Engl J Med.* (2012) 366:799–807. doi: 10.1056/NEJMoa1110557
29. Allan EH, Häusler KD, Wei T, Gooi JH, Quinn JM, Crimeen-Irwin B, et al. EphrinB2 regulation by PTH and PTHrP revealed by molecular profiling in differentiating osteoblasts. *J Bone Miner Res.* (2008) 23:1170–81. doi: 10.1359/jbmr.080324
30. Allan EH, Ho PWM, Umezawa A, Hata JI, Makishia F, Gillespie MT, et al. Differentiation potential of a mouse bone marrow stromal cell line. *J Cell Biochem.* (2003) 90:158–69. doi: 10.1002/jcb.10614
31. Kaur S, Raggatt LJ, Millard SM, Wu AC, Batoon L, Jacobsen RN, et al. Self-repopulating recipient bone marrow resident macrophages promote long-term hematopoietic stem cell engraftment. *Blood.* (2018) 132:735–49. doi: 10.1182/blood-2018-01-829663
32. Joe AWB, Yi L, Natarajan A, Le Grand F, So L, Wang J, et al. Muscle injury activates resident fibro/adipogenic progenitors that facilitate myogenesis. *Nat Cell Biol.* (2010) 12:153. doi: 10.1038/ncb2015
33. Mounier R, Théret M, Arnold L, Cuvellier S, Bultot L, Göransson O, et al. AMPKα1 regulates macrophage skewing at the time of resolution of inflammation during skeletal muscle regeneration. *Cell Metab.* (2013) 18:251–64. doi: 10.1016/j.cmet.2013.06.017
34. Banovac K, Williams JM, Patrick LD, Haniff YM. Prevention of heterotopic ossification after spinal cord injury with indomethacin. *Spinal Cord.* (2001) 39:370–4. doi: 10.1038/sj.sc.3101166
35. Banovac K, Williams JM, Patrick LD, Levi A. Prevention of heterotopic ossification after spinal cord injury with COX-2 selective inhibitor (rofecoxib). *Spinal Cord.* (2004) 42:707–10. doi: 10.1038/sj.sc.3101628
36. Sampath SC, Sampath SC, Ho ATV, Corbel SY, Millstone JD, Lamb J, et al. Induction of muscle stem cell quiescence by the secreted niche factor Oncostatin M. *Nat Commun.* (2018) 9:1531. doi: 10.1038/s41467-018-03876-8
37. Tierney MT, Aydogdu T, Sala D, Malecova B, Gatto S, Puri PL, et al. STAT3 signaling controls satellite cell expansion and skeletal muscle repair. *Nat Med.* (2014) 20:1182–6. doi: 10.1038/nm.3656

38. Price FD, von Maltzahn J, Bentzinger CF, Dumont NA, Yin H, Chang NC, et al. Inhibition of JAK-STAT signaling stimulates adult satellite cell function. *Nat Med.* (2014) 20:1174–81. doi: 10.1038/nm.3655
39. Song HY, Jeon ES, Kim JI, Jung JS, Kim JH. Oncostatin M promotes osteogenesis and suppresses adipogenic differentiation of human adipose tissue-derived mesenchymal stem cells. *J Cell Biochem.* (2007) 101:1238–51. doi: 10.1002/jcb.21245
40. Sambasivan R, Yao R, Kissenpfennig A, Van Wittenberghe L, Paldi A, Gayraud-Morel B, et al. Pax7-expressing satellite cells are indispensable for adult skeletal muscle regeneration. *Development.* (2011) 138:3647–56. doi: 10.1242/dev.067587
41. Jenkins BJ, Roberts AW, Najdovska M, Grail D, Ernst M. The threshold of gp130-dependent STAT3 signaling is critical for normal regulation of hematopoiesis. *Blood.* (2005) 105:3512–20. doi: 10.1182/blood-2004-09-3751
42. Panopoulos AD, Zhang L, Snow JW, Jones DM, Smith AM, El Kasmi KC, et al. STAT3 governs distinct pathways in emergency granulopoiesis and mature neutrophils. *Blood.* (2006) 108:3682–90. doi: 10.1182/blood-2006-02-003012
43. Mui AL, Wakao H, O'Farrell AM, Harada N, Miyajima A. Interleukin-3, granulocyte-macrophage colony stimulating factor and interleukin-5 transduce signals through two STAT5 homologs. *Embo J.* (1995) 14:1166–75. doi: 10.1002/j.1460-2075.1995.tb07100.x
44. Wright CR, Ward AC, Russell AP. Granulocyte colony-stimulating factor and its potential application for skeletal muscle repair and regeneration. *Mediators Inflamm.* (2017) 2017:7517350. doi: 10.1155/2017/7517350
45. Pavey GJ, Qureshi AT, Tomasino AM, Honnold CL, Bishop DK, Agarwal S, et al. Targeted stimulation of retinoic acid receptor-γ mitigates the formation of heterotopic ossification in an established blast-related traumatic injury model. *Bone.* (2016) 90:159–67. doi: 10.1016/j.bone.2016.06.014
46. Qureshi AT, Dey D, Sanders EM, Seavey JG, Tomasino AM, Moss K, et al. Inhibition of mammalian target of rapamycin signaling with rapamycin prevents trauma-induced heterotopic ossification. *Am J Pathol.* (2017) 187:2536–45. doi: 10.1016/j.ajpath.2017.07.010
47. Cui M, Ma X, Sun J, He J, Shen L, Li F. Effects of STAT3 inhibitors on neural functional recovery after spinal cord injury in rats. *Biosci Trends.* (2017) 10:460–6. doi: 10.5582/bst.2016.01160
48. Lacroix S, Chang L, Rose-John S, Tuszynski MH. Delivery of hyper-interleukin-6 to the injured spinal cord increases neutrophil and macrophage infiltration and inhibits axonal growth. *J Comp Neurol.* (2002) 454:213–28. doi: 10.1002/cne.10407
49. Okada S, Nakamura M, Katoh H, Miyao T, Shimazaki T, Ishii K, et al. Conditional ablation of Stat3 or Socs3 discloses a dual role for reactive astrocytes after spinal cord injury. *Nat Med.* (2006) 12:829–34. doi: 10.1038/nm1425
50. Faulkner JR, Herrmann JE, Woo MJ, Tansey KE, Doan NB, Sofroniew MV. Reactive astrocytes protect tissue and preserve function after spinal cord injury. *J Neurosci.* (2004) 24:2143–55. doi: 10.1523/JNEUROSCI.3547-03.2004

Conflict of Interest Statement: The authors declare that the research was conducted in the absence of any commercial or financial relationships that could be construed as a potential conflict of interest.

frontiers in Immunology

REVIEW
published: 07 March 2019
doi: 10.3389/fimmu.2019.00375

MicroRNAs: Key Regulators to Understand Osteoclast Differentiation?

*Claire Lozano[1,2], Isabelle Duroux-Richard[1], Hüseyin Firat[3], Eric Schordan[3] and Florence Apparailly[1]**

[1] IRMB, Univ Montpellier, INSERM, CHU Montpellier, Montpellier, France, [2] Immunology Department, CHU Montpellier, Montpellier, France, [3] Firalis SA, Molecular Diagnostics, Huningue, France

MicroRNAs (miRNAs) are small non-coding single-stranded RNAs that represent important posttranscriptional regulators of protein-encoding genes. In particular, miRNAs play key roles in regulating cellular processes such as proliferation, migration, and cell differentiation. Recently, miRNAs emerged as critical regulators of osteoclasts (OCs) biology and have been involved in OCs pathogenic role in several disorders. OCs are multinucleated cells generated from myeloid precursors in the bone marrow, specialized in bone resorption. While there is a growing number of information on the cytokines and signaling pathways that are critical to control the differentiation of osteoclast precursors (OCPs) into mature OCs, the connection between OC differentiation steps and miRNAs is less well-understood. The present review will first summarize our current understanding of the miRNA-regulated pathways in the sequential steps required for OC formation, from the motility and migration of OCPs to the cell-cell fusion and the final formation of the actin ring and ruffled border in the functionally resorbing multinucleated OCs. Then, considering the difficulty of working on primary OCs and on the generation of robust data we will give an update on the most recent advances in the detection technologies for miRNAs quantification and how these are of particular interest for the understanding of OC biology and their use as potential biomarkers.

Keywords: microRNA, osteoclast, differentiation, regulation, detection, biomarker

OPEN ACCESS

Edited by:
Teun J. De Vries, VU University Amsterdam, Netherlands

Reviewed by:
Toshio Kukita, Kyushu University, Japan
Frédéric Velard, Université de Reims Champagne-Ardenne, France
Jeroen Van De Peppel, Erasmus University Rotterdam, Netherlands

***Correspondence:**
Florence Apparailly
florence.apparailly@inserm.fr

Specialty section:
This article was submitted to Inflammation, a section of the journal Frontiers in Immunology

Received: *08 December 2018*
Accepted: *14 February 2019*
Published: *07 March 2019*

Citation:
Lozano C, Duroux-Richard I, Firat H, Schordan E and Apparailly F (2019) MicroRNAs: Key Regulators to Understand Osteoclast Differentiation? Front. Immunol. 10:375. doi: 10.3389/fimmu.2019.00375

INTRODUCTION

MicroRNAs (miRNAs) are key regulatory molecules that control cellular processes such as proliferation, migration and cell differentiation small. As shown in **Figure 1**, in the canonical pathway, miRNAs are transcribed by RNA polymerase II as large RNA precursors called primary (pri-) miRNAs that will be cleaved in the nucleus by the microprocessors complex into short hairpin precursors (pre-miRNAs) of about 70-nucleotides in length (1, 2). Pre-miRNAs are subsequently exported to the cytoplasm to be processed by DICER and yield mature miRNA duplexes (∼22 nucleotides long) prior their loading onto the Argonaute-containing RNA-induced silencing complex (RISC). They bind through imperfect complementarity, mostly to the 3′-UTR regions of their target mRNAs, and lead to translation inhibition or degradation (3). These single-stranded RNAs thus modulate gene expression mostly at a posttranscriptional level. Current database describes more than 1,917 miRNA genes, which can contain 3 and 5p miRNAs. MiRNAs are recognized as crucial regulators of the expression of more than 60% of mammalian genes. The

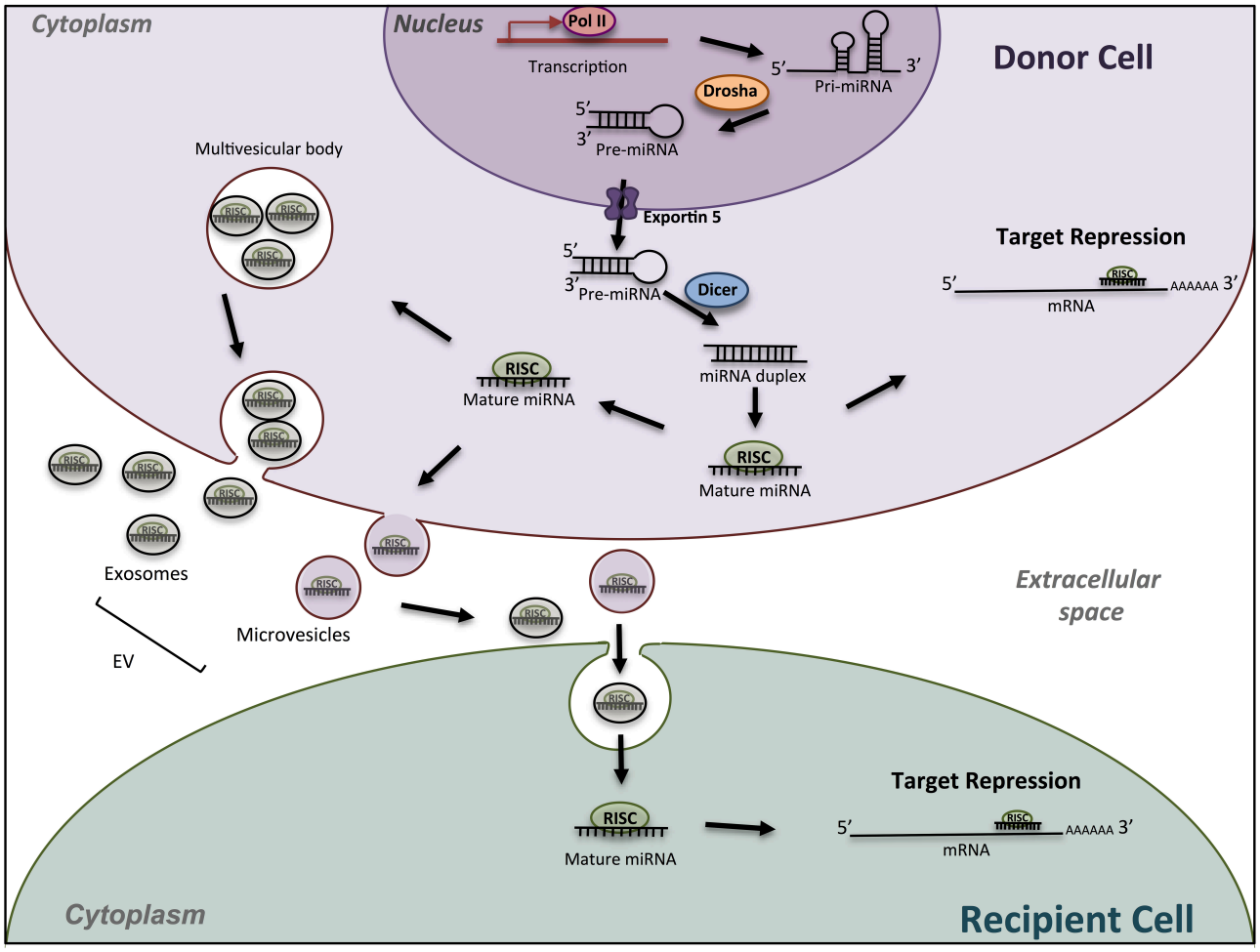

FIGURE 1 | Schematic miRNA biogenesis and mode of action. miRNA biogenesis begins in the nucleus with transcription of miRNA gene into a pri-miRNA, followed by the action of the enzyme Drosha to produce pre-miRNA hairpins. After exportation into the cytosol, pre-miRNA, are processed into an intermediary miRNA duplex by Dicer. One miRNA strand is loaded onto the RNA-induced silencing complex (RISC) to form mature miRNA, which can regulate the expression of target mRNAs. The miRNA/RISC complex can also be incorporated into extracellular vesicles such as exosomes or microvesicle bodies, to be released into extracellular space. Then, miRNAs can be found in body fluids and travel across the entire body till elimination, or can be incorporated into a recipient cell and specifically regulate the expression of target genes into this new cell. Drosha, RNase III-type endonuclease family protein; Dicer, endoribonuclease; RISC; RNA- used silencing complex; EV, extracellular vesicles.

number of encoded miRNAs is limited compared to mRNAs and proteins expressed; however, one miRNA may regulate hundreds of mRNAs/lncRNAs and, as a result, may have substantial effects on gene expression networks. Although a lot of miRNAs have conserved sequences between species, the targeted mRNA sequences may be poorly conserved and biological effects are difficult to predict. *In silico* analyses using updated databases are thus useful to screen for putative targets according to the species and to find the miRNA sequence homology. *In vitro* functional studies are however needed to validate the miRNA targets, which may provide clues on the biological effects of the miRNA. In addition, available and freely accessible algorithms have been designed to identify potential miRNA-promoter interactions conserved between species that could represent additional clues to further push toward experimental validation (4). *In vivo* studies add indeed robustness to the biological role of miRNA-mediated regulation in pathophysiological conditions.

As to many other biological processes, miRNAs act as fine modulators to maintain bone homeostasis. Key evidence that miRNAs are essential to osteoclastogenesis is provided by genetic studies deleting one enzyme essential for their biogenesis, DICER1. DICER deficient mouse and osteoclast-specific DICER gene deficiency both lead to impaired osteoclast (OC) formation and activity (5, 6). Since then, the field of bone biology has regularly reviewed the role of miRNAs in OC biology or bone remodeling, mostly in the context of osteoporosis (7–13). A growing interest in miRNA-based therapeutic strategies has also emerged in bone-related disorders [for review see (14)]. Although

the role of miRNAs in the OC lineage and ontogeny is a current hot topic, it remains poorly studied.

OCs are multinucleated cells specialized in bone resorption and derived from myeloid precursors that differentiate *in situ* in the bone marrow (15). The commitment of myeloid precursors in osteoclastic differentiation is controlled by micro-environmental factors to maintain bone homeostasis. Among them, osteoblasts, osteocytes and bone marrow stromal cells stimulate OC differentiation through the production of receptor activator of nuclear factor kappa-B ligand (RANKL), which binds to its receptor RANK. The growth factor macrophage colony-stimulating factor (MCSF) is also required to initiate the differentiation of osteoclastic precursors by binding its receptor CSF1R (colony stimulating factor 1 receptor). The Wnt-5a ligand is another pro-osteoclastic factor secreted by osteoblasts and OCs themselves (16, 17). In addition to these pro-osteoclastogenic factors, there are several inhibitory regulators including the osteoprotegerin (OPG), a soluble protein secreted by stromal cells that binds soluble and membrane forms of RANKL, thus preventing the activation of the RANK/RANKL signaling pathway. Indirectly, estrogens repress bone resorption by stimulating the production of OPG. Other environmental factors such as cytokines and lipid mediators impact on the osteoclastogenesis (18, 19). In addition to these well-known regulatory mechanisms, other elements could influence the commitment of myeloid precursors to the osteoclastic lineage. Instead of being differentiated into OCs, the myeloid precursors can also be differentiated into macrophages, especially in the presence of MCSF. Indeed, the osteoclastic and macrophagic lineages are thought to originate from an immediate bipotent precursor (20), demonstrating their close proximity. OCs retain the phagocytic potential and the ability to present the antigen of macrophages (21) but are the only cells capable of bone resorption. Among critical regulators of the polarization toward the OC vs. macrophage lineage, the mitochondrial metabolism has been involved (22). Although the role of miRNAs in the commitment of hematopoietic (23) and osteoblastic (24) lineages has been reviewed, only few studies have addressed the involvement of miRNAs in the commitment of the osteoclastic lineage.

The initiation of osteoclastogenesis requires the major signaling pathways RANK/RANKL and CSF1R/MCSF. The transcription factor NFATC1 (nuclear factor of activated T cells 1) is the cornerstone of the early phase of osteoclastogenesis. An amplification loop of NFATC1 induces the expression of many genes of the late phase, such as ACP5 (acid phosphatase 5, tartrate resistant), CTSK (Cathepsin K), and DCSTAMP (dendrocyte expressed seven transmembrane protein) [reviewed in (25)].

Under physiological conditions, the selective expression of miRNAs promoting and repressing the generation of OCs relies on the regulation of their own promoter (a shared promoter in case of miRNA clusters) and is thus closely linked to the sequential signaling pathways involved in the different steps of OC differentiation. MiRNAs are thus essential in a lot of biological feedback loops, including in the regulation of the OC biology.

Our present review will focus on the miRNA-mediated regulation of the sequential steps of OC formation. We will also report on the most recent advances in technologies used for the quantification of miRNAs. Finally, we will discuss the contribution of these technologies to the field of OC biology and the questions that remain to be asked.

miRNAs AND THE COMMITMENT OF PROGENITORS TOWARD OCs

There are very few studies available on the miRNA-mediated regulation of OC commitment. Osteoclastogenesis is repressed by miR-155-mediated control of the transcription factor MITF (melanocyte inducing transcription factor) that is involved in the differentiation of monocytes toward macrophages (26). Conversely, miR-29 family (miR-29a, b, c) guides the commitment of bone marrow precursors toward the OC lineage by inhibiting GPR85 and CD93, two molecules involved in macrophage engagement (27). Authors showed that the transfection of the mouse monocytic cell line RAW264.7 with an inhibitor of miR-29 promotes macrophage differentiation, as evidenced by an up-regulation of the F4/80 surface marker and of the phagocytosis, even in presence of the major pro-osteoclastogenic cytokine RANKL.

miRNAs IN THE EARLY PHASE OF OCs GENERATION

Majority of the studies have described the global impact of miRNAs on the terminal OC formation, as evidenced by OC number and bone resorption activity. Few studies addressed beyond this final step which cellular processes are impacted. In **Figure 2**, we have summarized the miRNAs involved in the functional steps paving the generation of OCs, including cell survival, proliferation and motility of OC precursors. We also provide an updated list of their validated target genes (**Table 1**).

Pro-Osteoclastogenic miRNAs

In addition to its role in the OC commitment of precursors, miR-29 family may promote migration of precursors since miR-29 neutralization inhibits the migration RAW264.7 cells (27). Furthermore, miR-29 family is involved in early phase of osteoclastogenesis by targeting NFIA (nuclear factor I A), a negative regulator of CSF1R (27). CSF1R is also indirectly induced by miR-223 through NFIA targeting as a positive feedback loop enhanced by the transcription factor PU.1 induced downstream of the MCSF/CSF1R (5). Same authors however previously reported contradictory findings using the same RAW264.7 cell line, as overexpression of miRNA-223 suppressed TRAP-positive OC formation (28). These later data were in agreement with a work performed on human peripheral blood mononuclear cells (PBMCs) (29). Bone loss is enhanced in arthritic condition due to activation of OC differentiation, and miR-223 is intensely expressed in rheumatoid arthritis (RA) synovium, particularly in monocyte/macrophage and $CD4^+$ T-cell subsets (29). All these findings suggest an important role of

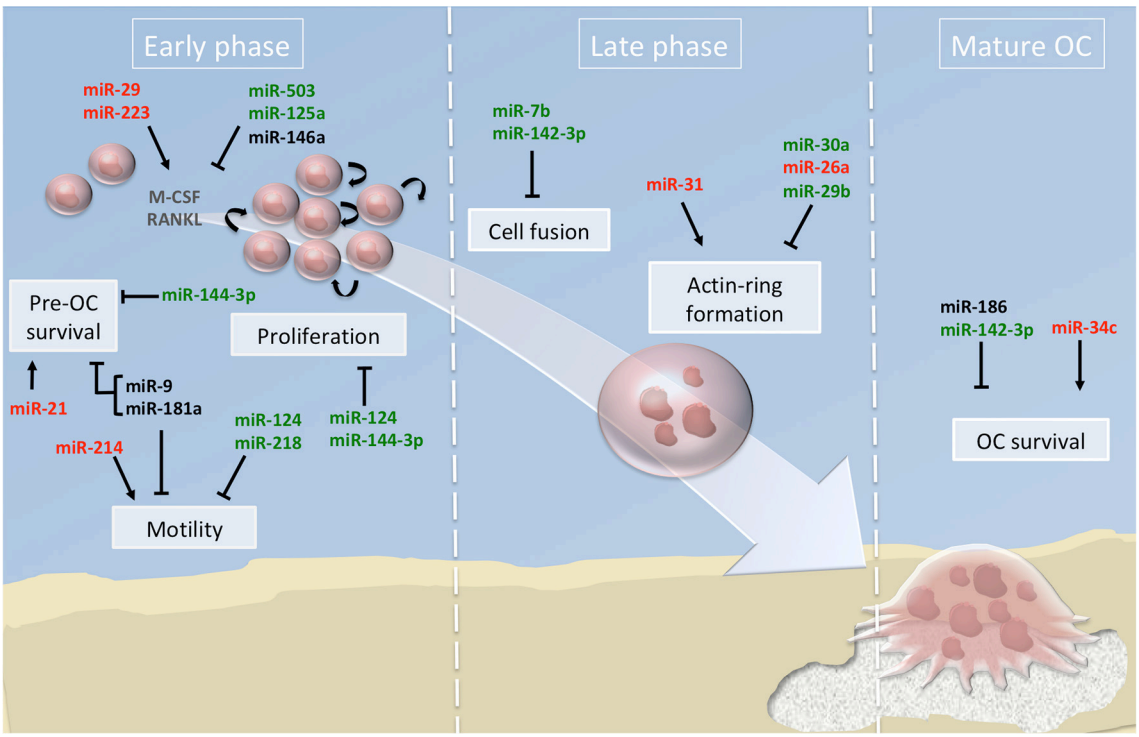

FIGURE 2 | miRNA regulation of osteoclast differentiation. Illustration of the 3 phases of osteoclastogenesis. The early phase is associated with pre-osteoclast (OC) survival, motility, and proliferation; the late phase focused on pre-OC cell fusion and OC acting-ring formation; and the mature OC phase consists in the degradation of the mineralized matrix by mature OC. Green, red and black colors indicate down, up and normal miRNA expression, respectively. Arrows and bars indicate positive or negative effects on osteoclastogenesis respectively. M-CSF, macrophage colony-stimulating factor; RANKL, Receptor activator of NF-κB ligand.

miR-223 in the early phase of osteoclastogenesis, but an in-depth evaluation of the expression level of miR-223 under physiological osteoclastogenesis requires further studies.

The early phase of OC generation triggers increased NFATC1 expression, together with reduced expression of its three negative regulators MAFB (MAF bZIP transcription factor B), IRF8 (interferon regulatory factor 8), and BCL6 (BCL6, transcription repressor) (25). MAFB is a relevant target of miRNAs in OC precursors. Up-regulation of miR-199a-5p and miR-148a promotes the amplification loop of NFATC1 and the formation of resorbing OCs by targeting MAFB in RAW264.7 cells (30) and in $CD14^+$ PBMCs (31), respectively. MiR-9718 is a newly described miRNA specifically expressed in the OC lineage, which promotes OC differentiation by targeting PIAS3 (protein inhibitor of activated STAT3) (32), another negative modulator of NFATC1 (33). Finally, the injection of molecules neutralizing miR-148a or miR-9718 in ovariectomy-induced osteoporotic mice increases total bone mass and decreases the OC number and activity (31, 32).

Among the other miRNAs up-regulated in OCs, the pro-osteoclastogenic role of miR-21 was demonstrated *in vivo* using the miR-21 KO mouse that display a slight increase in the trabecular bone mass and a reduced OC number and bone resorption (34). The expression of miR-21 is induced by c-Fos, which activation upon RANKL treatment of mouse bone marrow-derived macrophages (BMMs) operates a positive feedback loop by targeting the programmed cell death protein 4 (PDCD4) (35). The binding of c-Fos to miR-21 promoter is strikingly diminished by estrogen E2 treatment in RANKL-induced osteoclastogenesis. Estrogen attenuate miR-21 biogenesis, leading to increased FasL protein level and caspase-3 activity in mouse BMMs precursors (36). These results suggest that miR-21 expression is important in the development of OCs, particularly by controlling pre-osteoclast survival.

The activation of mitogen activated protein kinases (MAPKs) downstream of the early RANKL pro-osteoclastogenic signaling cascade is supported by the reactive oxygen species (ROS) produced by RANK-NADPH oxidase 1-dependant pathway (25). ROS production by mouse BMMs is regulated by heme oxygenase 1 (HMOX1), which attenuates osteoclastogenesis, specifically during the early phase of OC formation (37). MiR-183 is up-regulated by RANKL and targets HMOX1, thus promoting the early phase of osteoclastogenesis (38).

The PI3K/AKT pathway is induced by RANKL signaling and promotes cell survival (39). By reversing the action of PI3K (phosphoinositide 3-kinase), PTEN (phosphatase and tensin homolog) negatively impacts on OC precursor motility in the early phase of osteoclastogenesis (40). It was shown that miR-214 enhances the OC precursor differentiation via the PTEN/PI3K/AKT pathway, downstream of RANK signaling in RAW264.7 and primary mouse BMMs. *In vivo*, OC-specific miR-214 transgenic mice exhibit reduced expression of PTEN,

TABLE 1 | MiRNAs involved in the early phase of OC generation.

miRNAs	Species	Up/Down	Overall impact	Targets	Early steps impacted	References
miR-21	Mouse[a,b]	Up	Positive	PDCD4 FASLG	Survival	(34–36)
miR-29 family	Mouse[a]	Up	Positive	NFIA CDC42 SRGAP2	ND	(27)
miR-148a	Human[a] Mouse [a,b]	Up	Positive	MAFB	ND	(31)
miR-183	Mouse[a]	Up	Positive	HMOX1	ND	(38)
miR-199a-5p	Mouse[a]	Up	Positive	MAFB	ND	(30)
miR-214	Mouse[a,b]	Up	Positive	PTEN	Motility	(41)
miR-223	Mouse[a,b]	Up	Pos/neg	NFIA	ND	(5)
miR-9718	Mouse[a,b]	Up	Positive	PIAS3	ND	(32)
miR-34a	Mouse[a,b] Human [a]	Down	Negative	TGIF2	NS (survival, proliferation)	(54)
miR-124	Mouse[a] Rat [a,b]	Down	Negative	NFATC1	Proliferation, motility	(67, 68)
miR-125a	Human[a]	Down	Negative	TRAF6	ND	(48)
miR-141	Monkey[a,b]	Down	Negative	EPHA2 CALCR	ND	(56)
miR-144-3p	Human[a]	Down	Negative	RANK	Survival, proliferation	(47)
miR-145	Mouse[a,b]	Down	Negative	SMAD3	ND	(58)
miR-155	Mouse[a]	Down	Negative	SOCS1 MITF	ND	(61)
miR-155	Mouse[a]	Down	Positive	TAB2	ND	(63)
miR-218	Mouse[a]	Down	Negative	ND	Motility	(52)
miR-218	Mouse[a]	Down	Negative	TNFRSF1A	ND	(53)
miR-340	Mouse[a]	Down	Negative	MITF	ND	(65)
miR-503	Human[a] Mouse [a,b]	Down	Negative	RANK	ND	(46)
miR-9; miR-181a	Mouse[a]	ND	Negative	CBL	Survival, motility	(45)
miR-146a	Human[a] Mouse [a,b]	ND	Negative	TRAF6	ND	(50, 51)

Species and experimental context of the model used are indicated (a, in vitro). Up- or down-regulation of respective miRNAs during OC generation and the overall impact on OC differentiation are given. We detailed steps impacted in OC precursors (pre-OC) such as cell survival, proliferation and motility. Validated targets are also listed. PDCD4, programmed cell death protein 4; FASLG, Fas ligand; NFIA, nuclear factor I A; CDC42, cell division cycle 42; SRGAP2, SLIT-ROBO Rho GTPase activating protein 2; MAFB, MAF bZIP transcription factor B; HMOX1, heme oxygenase 1; PTEN, phosphatase and tensin homolog; PIAS3, protein inhibitor of activated STAT3; TGIF2, TGFB induced factor homeobox 2; NFATC1, nuclear factor of activated T cells 1; TRAF6, TNF receptor associated factor 6; EphA2: EPH receptor A2; CALCR, calcitonin receptor; RANK, receptor activator of nuclear factor kappa-B; SMAD3, SMAD family member 3; SOCS1, suppressor of cytokine signaling 1; MITF, melanocyte inducing transcription factor; TAB2, TGF-beta activated kinase 1 binding protein 2; TNFRSF1A, TNF receptor superfamily member 1A; CBL, Cbl proto-oncogene. ND, not determined; NS, not significant.

increased OC resorption activity, and reduced bone mineral density (41). Since a miR-214/PTEN axis has been involved in cell proliferation and invasion of various cancer cells (42–44), it would be of particular interest to investigate the specific role of miR-214 on cell proliferation, survival and motility in the context of OC lineage.

The over-expression of miR-9 and miR-181a diminishes the migration of RAW264.7 cells and primary mouse OC survival by repressing the expression of the proto-oncogene Cbl, which enhances the amount of the pro-apoptotic protein Bim (45). This was the first study reporting a functional role for miR-9 and miR-181a by targeting proteins belonging to the apoptosis pathway. Further experiments are needed to confirm the potential role of these miRNAs on the precursor survival during osteoclastogenesis.

miRNAs With an Inhibitory Role on OC Precursors

The initiation of the OC precursor differentiation is largely mediated by RANK/RANKL signaling. The expression density of RANK at the cell surface conditions the efficacy of RANK trimerization and downstream signal transduction. In human $CD14^+$ precursors, miR-503 targets RANK mRNA in the coding sequence (CDS) region, leading to reduced RANK protein level, OC numbers and cell density *in vitro* (46). *In vivo*, treatment of OVX mice with anti-miR-503 reduced bone resorption (46). The 3′ untranslated region (UTR) of RANK is also targeted by miR-144-3p in $CD14^+$ precursors, controlling OC formation, proliferation and survival of OC precursors (47).

The binding of RANKL to RANK induces the recruitment of the adaptor protein TRAF6 (TNF Receptor Associated

Factor 6). This important signaling adaptor for RANK is targeted by miR-125a and miR-146a in human PBMCs (48, 49). The expression of miR-125a is controlled by NFATC1, which directly binds to the promoter of miR-125a during osteoclastogenesis and reduces its expression (48). MiR-146a has been extensively studied in monocytes in pathological conditions, including pathologies associated with bone erosion such as RA. The expression of miR-146a is induced by LPS, TNFα, or IL1β signaling cascades, through the activation of NF-κB (nuclear factor kappa B), which directly binds to the miR-146 promoter (49). It was shown that miR-146a inhibits OC formation from human PBMCs in a dose-dependent manner and that the treatment of collagen-induced arthritic mice with miR-146 mimics attenuates bone resorption (50). We recently demonstrated that the reduced expression of miR-146a in the $Ly6C^{high}$ monocyte subset of arthritic mice is involved in the pathogenic bone erosion, and that it can be rescued by specific delivery of miR-146 mimics to $Ly6C^{high}$ monocytes (51). Taken together, these findings evidence a negative regulation of osteoclastogenesis by NFκB-induced miR-146a to partly counterbalance the deregulated differentiation of OC precursors in inflammatory disorders.

The RANK/TRAF6 signaling cascade activates the NFκB and MAPK pathways, which may represent additional miRNA targets. Indeed, miR-218 over-expression inhibits osteoclastogenesis by controling the p38MAPK pathway in mouse BMMs (52). Interestingly, miR-218 negatively impacts on the migration of RANKL-treated BMMs. Although authors also reported a decrease of actin-ring formation, it was most probably a consequence than a cause of the decreased OC number. The putative targets of miR-218 were not explored in this study. A recent study confirmed the negative regulation of osteoclastogenesis by miR-218, and show that it was mediated by targeting TNFRSF1A (TNF receptor superfamily member 1A), which leads to the inhibition of the NFκB pathway activation in RAW264.7 cells (53). Overall, miR-218 may act on both NFκB and MAPK pathways in OC precursors to control OC precursor differentiation, and further studies are required to unravel the molecular mechanisms involved.

The early RANKL signaling is mediated by two transcription factors, NFκB and AP1, which are essential to the initiation of the NFATC1 amplification loop. AP1 components such as c-Jun and c-Fos could be critical targets to modulate NFATC1 activation in OC precursors. The transcriptional regulator TGIF2 (TGFB induced factor homeobox 2) is induced by NFATC1, c-Fos and c-Jun and potentiates the activity of NFATC1 and c-Jun in turn, promoting the osteoclastogenesis in a positive feedback loop (54). Interestingly, TGIF2 is a direct target of miR-34a, and OC-specific miR-34a transgenic mice exhibit lower bone resorption and higher bone mass, with no alteration of OC precursor survival and proliferation (54). Finally, miR-34a seems to negatively regulate the NFATC1 pathway during OC differentiation, mostly in the early phase upon RANKL signaling.

RANKL signaling enhances another co-stimulatory signal mediated by the ephrinA2-EphA2 interaction at the cell surface of OC precursors. EphrinA2 expression is rapidly induced in a c-Fos-dependent manner and cleaved by metalloproteinases to release an active soluble form able to interact with its receptor EphA2, enhancing osteoclastogenesis (55). In rhesus monkey BMMs EphA2 is a potential target of miR-141 (56). OC differentiation and bone resorption are suppressed *in vitro* by miR-141, and *in vivo* using repeated injections of an OC-targeted delivery system into aged monkeys (56). The calcitonin receptor (CALCR) is also a target of miR-141 in rhesus OCs. A down-regulation of CALCR is however expected to suppress the negative effect of calcitonin on OC differentiation and to enhance bone resorption, whereas miR-141 globally inhibits OC differentiation and activity, both *in vitro* and *in vivo*. One can speculate that the targeting of CALCR by miR-141 may represent a minor part of the effects of miR-141 functions in rhesus OCs.

Another critical interaction in RANKL-induced osteoclast ogenesis is the cooperation between Smad complex and c-Fos, which leads to NFATC1 transcription (57). Recently, miR-145 was shown to target Smad3, thus reducing the formation of p-Smad2/3 complex, repressing c-Fos and NFATC1 transcription in mouse OC precursors, and decreasing OC number (58). Smad proteins are induced by members of the transforming growth factor beta (TGFβ) super family, and Smad pathway has become of particular interest in inflammatory disorders [reviewed in (59)]. TGFβ1/Smad4 signaling directly induces miR-155 expression, a negative regulator of osteoclastogenesis (60). In addition, miR-155 is induced by interferon (IFN)-β and mediates its suppressive effect on OC differentiation by targeting the pro-osteoclastogenic gene SOCS1 (suppressor of cytokine signaling 1) in OC precursors (61). These data were suggestive of a suppressive role of miR-155 in osteoclastogenesis. In physiological condition, miR-155 is downregulated during osteoclastogenesis. Nevertheless, miR-155 is up-regulated in activated immune cells, such as lymphocyte B-cells, T-cells and dendritic cells, promoting the inflammatory response and thus aggravating the inflammatory-induced arthritis and bone erosion *in vivo* through the indirect immune-mediated activation of OCs [reviewed in (62)]. In lipopolysaccharide (LPS)-induced inflammatory condition, miR-155 directly induces autophagy in OCs as well as OC differentiation and activity by targeting TGFβ-activated kinase 1-binding protein 2 (TAB2) (63). A fine modulation of the TAB2 expression level may promote the destabilization of the inactive complex TAB2/Beclin1, leading to (i) the release of Beclin1 and induction of autophagy and (ii) the interaction of the adaptor proteins TAB2 and TAK1 that activates the RANK/TRAF6/NFκB pathway. These findings illustrate the variable role of miR-155 in osteoclastogenesis depending on the microenvironment, i.e., according to the presence of LPS, IFNβ, or TGFβ-mediated inflammatory signals. To make things even more complex, miR-155 also targets the transcription factor MITF that is up-regulated upon RANKL signaling (60, 61). MITF plays a critical role in the OC differentiation by collaborating with NFATC1 in the early phase of osteoclastogenesis (64). In summary, miR-155 seems to globally inhibit the OC generation in physiological condition by acting both in the commitment of myeloid precursors (26) and in osteoclastogenesis (61) through

TABLE 2 | MiRNAs involved in the late phase of OC generation.

miRNAs	Species	Up/Down	Overall impact	Targets	Late steps impacted	References
miR-26a	Mouse[a]	Up	Negative	CTGF	Actin ring formation	(82)
miR-31	Mouse[a]	Up	Positive	RHOA	Actin ring formation	(70)
miR-34c	Mouse[a]	Up	Positive	LGR4	OC survival	(74)
miR-7b	Mouse[a]	Down	Negative	DCSTAMP	Cell fusion	(79)
miR-29b	Human[a]	Down	Negative	FOS MMP2	Actin ring formation	(77)
miR-30a	Mouse[a]	Down	Negative	DCSTAMP	Actin ring formation	(80)
miR-124	Mouse[a]	Down	Negative	RAB27A	ND	(69)
miR-142-3p	Human[a]	Down	Negative	PRKCA	Cell fusion, OC survival	(83)
miR-186	Mouse[a]	ND	Negative	CTSK	OC survival	(84)

Species of model used are indicated; whether experiments were performed in vitro (a) or in vivo (b) is specified with superscript letters. Up- or down-regulation of respective miRNAs during OC generation and the overall impact on OC differentiation are given. We detailed steps impacted in the late phase such as cell fusion, actin ring formation and the survival of mature OCs. Validated targets are also listed. CTGF, connective tissue growth factor; RHOA, ras homolog family member A; LGR4, leucine rich repeat containing G protein-coupled receptor 4; DCSTAMP, dendrocyte expressed seven transmembrane protein; FOS, Fos proto-oncogene, AP-1 transcription factor subunit; MMP2, matrix metallopeptidase 2; RAB27A, RAB27A, member RAS oncogene family; PRKCA, protein kinase C alpha; CTSK, cathepsin K. ND, not determined; NS, not significant.

the regulation of MITF expression. MITF is also targeted by miR-340, which inhibits the OC differentiation of mouse BMMs (65). This reinforces the idea that MITF is a key target for miRNAs in osteoclastogenesis.

Finally, NFATC1 has hardly been described as a direct target of miRNAs so far. The activity of NFATC1 is regulated by phosphorylation, which retains NFATC1 in the cytosol compartment and inhibits its translocation into the nucleus. Epigenetic controls of the NFATC1 gene have been reported [reviewed in (66)]. To date, only miR-124 is predicted to bind NFATC1 in its 3′ UTR in OC precursors (67). The targeting of the 3′UTR of both rat and human NFATC1 mRNAs by miR-124 was confirmed using luciferase reporter assays (68). Functionally, miR-124 represses NFATC1 expression in mouse BMMs and diminishes the migration and proliferation of OC precursors (67), without impact on their survival (69).

miRNAs IN THE LATE PHASE OF OC GENERATION

To achieve OC maturation, the key transcription factors MITF, PU.1, and NFATC1 lead to the expression of several osteoclastogenic genes involved in the cytoskeleton organization, the cell fusion and actin-ring formation. MiRNAs also regulate the late stage of OC formation by targeting Rho GTPases, DCSTAMP, CSTK, and the RANKL-receptor inhibitor LGR4 (**Table 2**).

Pro-Osteoclastogenic miRNAs

One of the most up-regulated miRNAs during osteoclastogenesis in mouse BMMs is miR-31. It specifically acts on the actin-ring formation (70). Neutralization of miR-31 impairs the matrix resorption and the ring-shaped OC formation, while cell-fusion is conserved. Increased RhoA activity and protein expression level are also observed in miR-31-deficient OC precursors, suggesting that RhoA is targeted by miR-31 in the OC lineage (70). Small GTPases of the Rho family (Rac1, Rac2, CDC42, RhoA, and RhoU) play important roles in the cell-fusion of OC precursors, podosome organization, migration, and polarization of mature OCs [reviewed in (71)]. RhoA controls the polymerization of actin, the turnover of podosomes, and the migration of OCs through the bone matrix (72). While a moderate level of RhoA activity is required to allow both stability of the sealing zone and bone resorption, RhoA over-activation or inhibition cause disassembly of the podosomes and thus impair the OC activity [reviewed in (73)]. Finally, miR-31 seems essential to OC maturation by finely modulating RhoA activity.

Another relevant miRNA in mature OC biology is miR-34c, which promotes the OC survival at the end of maturation by targeting the R-spondins receptor LGR4 (leucine rich repeat containing G protein-coupled receptor 4), also known as GPR48 (74). During the OC maturation, NFATC1 induces the expression of LGR4 at the cell surface to negatively regulate RANK/RANKL-signaling by a direct competition with RANK. The binding of RANKL to LGR4 activates the NFκB-inhibitor GSK3β, which results in OC apoptosis (75). These data suggest that miR-34c sustains the OC formation.

miRNAs Displaying an Inhibitory Role in OC Maturation

Based on the study of Franceschetti et al. (27), we reviewed above the role of miR-29 family in the OC commitment and in the early phase of OC generation. The authors however also showed a late up-regulation of miR-29 (a, b, c) family members at the third day of RANKL-induced OC differentiation of mouse BMMs, suggesting another predominant role of miR-29 in the late phase of osteoclastogenesis. They found two targets involved in the cytoskeleton organization, CDC42 and SRGAP2 (SLIT-ROBO Rho GTPase Activating Protein 2), which present opposite effects. Indeed, SRGAP2 belongs to GAP family, which inactivates Rho GTPases such as CDC42 by increasing the intrinsic GTPase activity of Rho proteins (76). Rho GTPases are essential in the polarization and the podosome belt/sealing zone formation of functional OCs [reviewed in (17, 71)].The neutralization of miR-29 family has no effect on the formation of the actin-ring in mature RAW-derived OCs. A role for miR-29 family in the OC maturation remains thus questionable. Another study showed a down-regulation of miR-29b during OC

generation, and demonstrated an inhibitory role of miR-29b in resorption and actin-ring formation in human $CD14^+$-derived OCs (77). Considering only the multinucleated cells for their analysis, authors observed disarranged nodular actin spots in OCs over-expressing miR-29b, leading to a failure to form actin-rings. Although the authors did not perform a validation of the known targets of miR-29b in the OC lineage, they observed a significant down-regulation of c-Fos and MMP2 expression in miR-29b-transfected OCs at the end of the differentiation. The apparent discrepancies on the role of miR-29 family members and miR-29b could be partially explained by the chosen approach in the different studies, which rely either on gain-of function of miR-29b (77) or loss-of function of miR-29 family (27), as well as on the nature of OC precursors used (cell line vs. primary cells).

In addition to its negative effect on cell proliferation and motility in the early phase of osteoclatogenesis (67), miR-124 seems to act on the late phase of the differentiation by targeting Rab27a (69), a protein belonging to the small Rab GTPase family and involved in vesicle trafficking and resorbing activity of OCs (78). Notably, miR-124 is under-expressed in the OVX mouse model, which displays a deregulated resorbing activity (69).

DCSTAMP is a key protein involved in cell fusion. DCSTAMP is targeted by miR-7b and miR-30a in mouse BM precursors (79, 80). Mimics of miR-7b and miR-30a repress the expression level of DCSTAMP, decrease the OC number and inhibit matrix resorption. Conversely, anti-miR-7b promotes the OC formation and increase nuclei number in mature OC, suggesting an increase of cell fusion events (79). By measuring the membrane merge rate, the authors confirmed that overexpression of miR-7b in mouse BMMs significantly abrogates OC fusion (81). Anti-miR-30a enhances the actin-ring formation (80). Similarly, miR-26a attenuates the actin-ring formation and resorption in mouse BMMs. MiR-26a targets the connective tissue growth factor (CTGF), which induces and interacts with DCSTAMP (82). Contrary to miR-7b and miR-30a, miR-26a is upregulated in the late phase of osteoclastogenesis, suggesting a physiological regulation of multinucleation in the OC lineage. Thus, it will be of particular interest to evaluate the role of miR-30a and miR-26a on cell fusion.

During OC formation from human $CD14^+$ progenitors, the enforced expression of miR-142-3p inhibits cell-to-cell contact, clustering and fusion events associated with the induction of OC apoptosis upon RANKL stimulation (83). The negative effect of miR-142-3p on OC fusion could be partially explained by the silencing of PKCα. Indeed, PKCα is involved in the microtubule and actin networks and is predicted as a putative target of miR-142-3p by prediction software. A decreased expression of anti-apoptotic factors downstream of PKCα might also explain the induction of cell death (83), however it has not been functionally explored yet.

Finally, miR-186 was newly described as a negative regulator of mature OC survival. Mimics of miR-186 induce caspase-3/7 activity and OC apoptosis in transfected RAW264.7-derived mature OCs (84). Moreover, miR-186 targets the CTSK gene (84) and probably represses the resorbing function of OCs, although it remains to be explored in functional assays.

ADVANCES IN TECHNOLOGIES FOR THE QUANTIFICATION OF miRNAs IN BIOLOGICAL TISSUES

MiRNAs are classically studied from the total mRNA (including small RNAs) extracted from the tissue of interest. As miRNAs are expressed in various cell types and tissues, it is necessary to well define the targeted sample and to control the purity of the elicited source of miRNAs. The study of miRNAs in primary OCs is challenging because of the localization of OCs into bone cavities, and thus a purified extract of primary OCs is very hard. Finally, primary OC precursors from blood sample or bone marrow are used to derive OCs in *in vivo* experiments. Nevertheless, the OC differentiation in culture is only partial without reaching a pure OC population. The obtained population includes all stages from the precursor to the mature OC. The study of miRNAs in such heterogeneous cell culture is not satisfactory and gives a lot of variations between samples that could impact on the reliability of the results, particularly in "end-point" studies without a kinetic expression of miRNAs during the OC differentiation. Some studies are based on purified OCs using chemical methods to eliminate non- and poor-adherent cells, as mature OCs are extremely adherent. Very recently, a novel method of purification based on the OC sorting has been described, allowing a standardized approach to better characterize the miRNA profiling in mature OCs (85).

Other biological tissues are become novel sources of study in the OC biology and the bone remodeling. Indeed, miRNAs can be exported from a donor cell to a recipient *via* exosomes and microvesicles (**Figure 1**), and thus participate to the cell communication between osteocytes, osteoblasts and osteoclasts in the bone micro-environment (86–89). Circulating miRNAs can also be used as biomarkers in pathophysiological conditions, reaching liquid biopsies as potential interesting samples in clinical application.

Molecular technologies are used to detect and quantify miRNAs, and some panels were developed to determine the miRNA profiling. Here we provide a global and detailed view of these technologies and their application in the quantification of miRNAs in biological tissues.

Screening Methods for the miRNA Profiling

In recent years, technological advances in research tools including qPCR, microarrays, and next generation sequencing (NGS), have enabled sensitive detection of miRNAs. Typically, miRNA biomarkers are measured with quantitative polymerase chain reaction (qPCR) after RNA extraction and conversion into complementary DNA (cDNA). Many other methods are available for large screening of the miRNome to understand pathologies or discovery of biomarkers. Mestdagh et al., have extensively analyzed analytical parameters of many solutions available for miRNA measurement based on qPCR, hybridization platforms and sequencing technologies (90). Recently, new technologies for miRNAs measurement or optimization of existing methods have emerged. Currently, the miRbase 22 includes 1917 miRNA genes. With the constant evolution of the miRbase, the different miRNA detection platforms need to adapt their product. This flexibility

however depends on the technic used. New technologies that are more sensitive, or extraction free chemistry, are definitively modifying the miRNA measurement landscape (**Table 3**).

Among these technologies, we will focus on the most innovative technologies for miRNA detection. These technologies provide real advance and alternative with the direct use of matrices avoiding preprocessing step or optimized library preparation for RNA-Seq method for the profiling of miRNAs. For the measurement of single miRNAs, new methods using microfluidic detection by laminar flow (91) or absolute quantification of signal by RCA-FRET technology (92) are in development. These last technologies may simplify the adoption of miRNA testing in clinical laboratories.

Screening methods such as the microarrays of Affymetrix (version 4.1) and Agilent (v21) now include 2,578 and 2,549 miRNAs, respectively, thus offering a more comprehensive dataset. In addition to these updated microarray versions, the company Takara Bio have recently developed the SMARTer miRNA-Seq kit, which uses Mono-Adapter ligation and Intramolecular Circularization (MAGIC) technology to efficiently capture miRNA species with reduced bias inherent to other approaches. Measurement of equimolar mixture of 963 miRNAs shows that >70% of the miRNAs are accurately represented, whereas other competitors have 49–79% of the miRNAs underrepresented Nevertheless, besides having less bias than the competitors (including TruSeq and NEXTFlex), this kit also produces large amounts of side products and as a result did not perform better for the detection of biological miRNAs (93). Since several years now, a new technology of HTG Molecular (High Throughput Genomic) called EdgeSeq provides miRNAs measurement without RNA extraction. The technology is a combination of hybridization with nuclease protection assay and next generation sequencing. Based on an extraction free chemistry, the technology[1] allows the direct measurement of miRNAs from as little as 15 μl of body fluid. This last critical point avoids biases associated to the extraction protocols (94) and increases the sensitivity of the measure. Correlation between replicates is very similar to those shown previously (90) for hybridization and sequencing technologies, whereas accuracy of the gradient of miRNA measure is superior to other hybridization and sequencing platform[2]. Nevertheless, cross reactivity is higher compared to qPCR assays[2]. It has been shown that HTG EdgeSeq results were closest to the RNASeq results with >95% concordance on tissue samples (95). The technology also shows very good correlation with the PCR on plasma samples, with Pearson's coefficient of 0.93 and 0.94 for qPCR and digital PCR (dPCR) data, respectively (96).

Circulating miRNAs as Biomarkers

In the past decade, the search for circulating miRNA for functional studies and biomarkers research has yielded numerous associations between miRNAs and different types of disease. However, many of these relations could not be replicated in subsequent studies under similar experimental conditions. Although this lack of reproducibility may be explained by variations in experimental design and analytical methods, guidelines of the most appropriate design and methods of analysis are scarce. MiRNAs have significant promise as biomarkers for diseases, due to their regulatory role in many cellular processes, and their stability in samples such as plasma and serum. Circulating miRNAs are moreover easily accessible. Biomarker experiments generally consist of a discovery phase and a validation phase. In the discovery phase, typically hundreds of miRNAs are simultaneously measured to identify candidates. Because of the costs of such high-throughput experiments, numbers of subjects are often too small, which can lead to false positives and negatives. In validation phase, a small number of identified candidates are measured in a large cohort, generally using quantitative PCR (qPCR). Although qPCR is a sensitive method to measure miRNAs in the circulation, experimental design, and qPCR data analysis remain challenging with many sources of biases. The MIQE guidelines are useful to stress on the most important biases in qPCR experiments and to give some elements to improve experimental practice (97). There is still a need for standardization or development of new methods to reach the clinic. Thus, choosing the right tools is critical for a successful miRNA-based experiment.

Despite new advances and evolution of technologies, many challenges remain unmet. For example, the impact of RNA isolation, which is known to induce biases (94), but also the lack of standardization of miRNA measurement or normalization of miRNAs data from plasma/serum samples, are key factors of variation, making more challenging the translation of biomarker discovery to diagnostic tool. Indeed, while many reports are describing miRNAs as potential biomarkers since many years, miRNA-based diagnostics have many difficulties to enter to the clinic and to get IVD approval. Moreover, these kinds of tests are likely best suited to a companion role. In contrast to RNA or DNA-based tests, especially that indicate the presence of SNP or a specific expression profile (98), miRNA tests produce results that are more difficult to interpret. While many miRNAs were reported as biomarkers in many reports (99), most miRNAs are expressed widely in a non-cell-specific manner, and their levels of expression are not differing drastically between patients' group and controls. For liquid biopsies such as blood, urine, or other body fluids, miRNA levels are very sensitive to pre-processing and post-processing factors. As a result, despite being very stable, miRNA-based tests are often based on a combination of miRNAs associated with an algorithm, and strict standardization of the entire process, from obtaining and processing the sample to results reporting, is mandatory and is key for reproducible results, no matter what technology is used.

Point of care diagnostics requires short detection time, small sample volume and portability of the device. These requests are often not compatible with miRNA measurement technologies since they are requesting many steps and devices. New methods based on microfluidic chip and laminar flow assisted dentritic amplification is currently under development, with a promise of time to result of only 20 min (91). Sensitivity and accuracy have still to be increased, but this attractive solution could potentially allow the compatibility of miRNAs to short diagnostic

[1]From www.takarabio.com/learning-centers/next-generation-sequencing/technical-notes/accurate-mirna-representation-in-microrna-seq,2018

[2]From the poster presented at ESHG, 2017, available on https://www.htgmolecular.com/assets/htg/publications/PO-17-Aissaoui-EHSG-miRNA-Metrics.pdf

TABLE 3 | Technologies of miRNA profiling.

	Exiqon qiagen LNA	Open array (Taqman)	Takara smarter microRNA-Seq kit	Illumina TruSeq	IonTorrent	Affymetrix miRNA 4.1	Agilent miRNA microarray (21.0)	Nanostring ncounter	HTG molecular
Technology	qPCR	qPCR	NGS	NGS	NGS	Hybrid.	Hybrid.	Hybrid.	Hybrid. and NGS
Input RNA	40 ng	100 ng	100 ng	1000 ng	1000 ng	130 ng	100 ng	100 ng	15 μl/25 ng
Extraction	Yes	Yes	Yes	Yes	Yes	Yes	Yes	Yes	No
miRNAs in the assay	752	754	miRNome*	miRNome*	miRNome*	2,578	2,549	800	2,083

LNA, locked nucleic acid; HTG, high throughput genomic; qPCR, quantitative polymerase chain reaction; NGS, next generation sequencing; Hybrid, hybridization.
**Based on current database miRBase 22 with 1,917 entries.*

delay. Without such solution able to reduce time to results, use of miRNAs in diagnostic is only possible for non-urgent test. Most used platforms remain qPCR, with various technologies available such as LNA/Taqman/SybrGreen PCR, which request high level of standardization to provide accurate and stable results. Another novel technology that could facilitate miRNA transfer to clinic is called RCA-FRET, which is a combination of rolling circle amplification (RCA) and Förster resonance energy transfer (FRET) (92). Key advantage of the technology is a simple workflow, device needed and material for absolute quantification results. This last point is of key importance since normalization of miRNA data is a true hurdle.

Indeed, accurate quantification of miRNAs using qPCR is largely dependent on proper normalization techniques, the absence of which can lead to misinterpretation of data and incorrect conclusions (100). The goal of most miRNA experiments using qPCR is to identify differences in expression between two groups of samples. In this case, cell-free miRNAs from biofluids are emerging as important noninvasive biomarkers because of their stability. Many works are describing miRNAs as potential blood biomarkers. One challenge in studying miRNAs from serum and plasma is their relatively low abundance and lack of reliable endogenous controls. It has been shown that hsa-miR-24, hsamiR-126, hsa-miR-484 (101), hsa-miR-16-5p, hsa-miR-93-5p (102), hsamiR-484, and hsa-miR-191-5p (103) are stable normalizers in serum. Nevertheless, some reports indicate also these miRNAs not as normalizers but as biomarkers, as for miR-16-5p described in the progression of gastric cancer for example (104). In the absence of reliable endogenous controls in serum/plasma, exogenous or spike-in controls can be used to normalize miRNA expression data. Exogenous controls can also be used to monitor extraction efficiency or sample input amount for difficult samples (e.g., serum, plasma, or other biofluids).

In addition to most common used matrices, extracellular vesicles (EVs) are emerging and even more challenging to get reliable results. EVs are nanometer-scale particles, which include exosomes, microvesicles, and apoptotic bodies. EVs are intercellular communicators released by most cell types with key functions in physiological and pathological processes (86, 105). EVs deliver specific proteins, microRNAs and other cellular components. One of the most important aspects of EV research is analyzing their nucleic acid cargo, particularly miRNAs. These are commonly quantified by RT-qPCR or, increasingly, by comprehensive transcriptomic profiling using NGS or hybridization technologies. One critical issue is the methods for RNA extraction that can influence downstream analyses by yielding non-identical, kit-specific results. This is of particular challenge since typical concentration of this type of sample is low, RNA integrity is decreased and associated to high individual variability. Several kits are on the market and tested (106) but optimal isolation methodology is mainly dependent on the respective research setting and downstream analyses.

Overall, it is not easy to give a simple answer to a complex problem. Many methods are available for miRNAs measurement and generate complex data that need to be validated. Real efforts have to be done on standardization and analytical validation until one can consider to successfully translate biomarker discovery to the clinic.

CONCLUSION

In the present review we have shown the complexity of understanding OC biology and pointed out key miRNAs that have been involved in OC differentiation as key regulators, with very specific roles in the different phases progressing from early progenitors toward fully mature OC. We also stressed the challenge to get reliable data from miRNA measurement either for supporting the knowledge of OC regulation or the translation into biomarker tools for clinical application.

DATA AVAILABILITY

All datasets generated for this study are included in the manuscript and/or the supplementary files.

AUTHOR CONTRIBUTIONS

CL, ID-R, HF, ES, and FA wrote the review. CL, ID-R, and ES designed the figures and tables.

FUNDING

INSERM, ANR-16-CE14-0030-02, ANR-15-RAR3-0013-05, University of Montpellier, and H2020 project RABIOPRED (#666798).

REFERENCES

1. Fire A, Xu S, Montgomery MK, Kostas SA, Driver SE, Mello CC. Potent and specific genetic interference by double-stranded RNA in *Caenorhabditis elegans*. *Nature*. (1998) 391:806–11. doi: 10.1038/35888
2. Winter J, Jung S, Keller S, Gregory RI, Diederichs S. Many roads to maturity: microRNA biogenesis pathways and their regulation. *Nat Cell Biol.* (2009) 11:228–34. doi: 10.1038/ncb0309-228
3. Ha M, Kim VN. Regulation of microRNA biogenesis. *Nat Rev Mol Cell Biol.* (2014) 15:509–24. doi: 10.1038/nrm3838
4. Piriyapongsa J, Bootchai C, Ngamphiw C, Tongsima S. microPIR2: a comprehensive database for human-mouse comparative study of microRNA-promoter interactions. *Database*. (2014) 2014:bau115. doi: 10.1093/database/bau115
5. Sugatani T, Hruska KA. Impaired Micro-RNA pathways diminish osteoclast differentiation and function. *J Biol Chem.* (2009) 284:4667–78. doi: 10.1074/jbc.M805777200
6. Mizoguchi F, Izu Y, Hayata T, Hemmi H, Nakashima K, Nakamura T, et al. Osteoclast-specific Dicer gene deficiency suppresses osteoclastic bone resorption. *J Cell Biochem.* (2010) 109:866–75. doi: 10.1002/jcb.22228
7. Xia Z, Chen C, Chen P, Xie H, Luo X. MicroRNAs and their roles in osteoclast differentiation. *Front Med.* (2011) 5:414–9. doi: 10.1007/s11684-011-0168-0
8. Tang P, Xiong Q, Ge W, Zhang L. The role of microRNAs in osteoclasts and osteoporosis. *RNA Biol.* (2014) 11:1355–63. doi: 10.1080/15476286.2014.996462
9. Chen J, Qiu M, Dou C, Cao Z, Dong S. MicroRNAs in bone balance and osteoporosis. *Drug Dev Res.* (2015) 76:235–45. doi: 10.1002/ddr.21260
10. Sun M, Zhou X, Chen L, Huang S, Leung V, Wu N, et al. The regulatory roles of MicroRNAs in bone remodeling and perspectives as biomarkers in osteoporosis. *Biomed Res Int.* (2016) 2016:1652417. doi: 10.1155/2016/1652417
11. Ji X, Chen X, Yu X. MicroRNAs in osteoclastogenesis and function: potential therapeutic targets for osteoporosis. *Int J Mol Sci.* (2016) 17:349. doi: 10.3390/ijms17030349
12. Gennari L, Bianciardi S, Merlotti D. MicroRNAs in bone diseases. *Osteoporos Int.* (2017) 28:1191–13. doi: 10.1007/s00198-016-3847-5
13. Feng Q, Zheng S, Zheng J. The emerging role of microRNAs in bone remodeling and its therapeutic implications for osteoporosis. *Biosci Rep.* (2018) 38:BSR20180453. doi: 10.1042/BSR20180453
14. Yang Y, Fang S. Small non-coding RNAs-based bone regulation and targeting therapeutic strategies. *Mol Cell Endocrinol.* (2017) 456:16–35. doi: 10.1016/j.mce.2016.11.018
15. Boyle WJ, Simonet WS, Lacey DL. Osteoclast differentiation and activation. *Nature*. (2003) 423:337–42. doi: 10.1038/nature01658
16. Maeda K, Kobayashi Y, Udagawa N, Uehara S, Ishihara A, Mizoguchi T, et al. Wnt5a-Ror2 signaling between osteoblast-lineage cells and osteoclast precursors enhances osteoclastogenesis. *Nat Med.* (2012) 18:405–12. doi: 10.1038/nm.2653
17. Uehara S, Udagawa N, Kobayashi Y. Non-canonical Wnt signals regulate cytoskeletal remodeling in osteoclasts. *Cell Mol Life Sci.* (2018) 75:3683–92. doi: 10.1007/s00018-018-2881-1
18. Oikawa T, Kuroda Y, Matsuo K. Regulation of osteoclasts by membrane-derived lipid mediators. *Cell Mol Life Sci.* (2013) 70:3341–53. doi: 10.1007/s00018-012-1238-4
19. Amarasekara DS, Yun H, Kim S, Lee N, Kim H, Rho J. Regulation of osteoclast differentiation by cytokine networks. *Immune Netw.* (2018) 18:e8. doi: 10.4110/in.2018.18.e8
20. Xiao Y, Palomero J, Grabowska J, Wang L, de Rink I, van Helvert L, et al. Macrophages and osteoclasts stem from a bipotent progenitor downstream of a macrophage/osteoclast/dendritic cell progenitor. *Blood Adv.* (2017) 1:1993–2006. doi: 10.1182/bloodadvances.2017008540
21. Li H, Hong S, Qian J, Zheng Y, Yang J, Yi Q. Cross talk between the bone and immune systems: osteoclasts function as antigen-presenting cells and activate CD4+ and CD8+ T cells. *Blood*. (2010) 116:210–7. doi: 10.1182/blood-2009-11-255026
22. Jin Z, Wei W, Yang M, Du Y, Wan Y. Mitochondrial complex I activity suppresses inflammation and enhances bone resorption by shifting macrophage-osteoclast polarization. *Cell Metab.* (2014) 20:483–98. doi: 10.1016/j.cmet.2014.07.011
23. Undi RB, Kandi R, Gutti RK. MicroRNAs as haematopoiesis regulators. *Adv Hematol.* (2013) 2013:695754. doi: 10.1155/2013/695754
24. Valenti MT, Dalle Carbonare L, Mottes M. Role of microRNAs in progenitor cell commitment and osteogenic differentiation in health and disease (Review). *Int J Mol Med.* (2018) 41:2441–9. doi: 10.3892/ijmm.2018.3452
25. Park JH, Lee NK, Lee SY. Current understanding of RANK signaling in osteoclast differentiation and maturation. *Mol Cells*. (2017) 40:706–13. doi: 10.14348/molcells.2017.0225
26. Mann M, Barad O, Agami R, Geiger B, Hornstein E. miRNA-based mechanism for the commitment of multipotent progenitors to a single cellular fate. *Proc Natl Acad Sci USA*. (2010) 107:15804–9. doi: 10.1073/pnas.0915022107
27. Franceschetti T, Kessler CB, Lee S-K, Delany AM. miR-29 promotes murine osteoclastogenesis by regulating osteoclast commitment and migration. *J Biol Chem.* (2013) 288:33347–60. doi: 10.1074/jbc.M113.484568
28. Sugatani T, Hruska KA. MicroRNA-223 is a key factor in osteoclast differentiation. *J Cell Biochem.* (2007) 101:996–9. doi: 10.1002/jcb.21335
29. Shibuya H, Nakasa T, Adachi N, Nagata Y, Ishikawa M, Deie M, et al. Overexpression of microRNA-223 in rheumatoid arthritis synovium controls osteoclast differentiation. *Mod Rheumatol.* (2013) 23:674–85. doi: 10.3109/s10165-012-0710-1
30. Guo K, Zhang D, Wu H, Zhu Q, Yang C, Zhu J. MiRNA-199a-5p positively regulated RANKL-induced osteoclast differentiation by target Mafb protein. *J Cell Biochem.* (2018). doi: 10.1002/jcb.27968. [Epub ahead of print].
31. Cheng P, Chen C, He H-B, Hu R, Zhou H-D, Xie H, et al. miR-148a regulates osteoclastogenesis by targeting V-maf musculoaponeurotic fibrosarcoma oncogene homolog B. *J Bone Miner Res.* (2013) 28:1180–90. doi: 10.1002/jbmr.1845
32. Liu T, Qin A-P, Liao B, Shao H-G, Guo L-J, Xie G-Q, et al. A novel microRNA regulates osteoclast differentiation via targeting protein inhibitor of activated STAT3 (PIAS3). *Bone*. (2014) 67:156–65. doi: 10.1016/j.bone.2014.07.004
33. Kim K, Lee J, Kim JH, Jin HM, Zhou B, Lee SY, et al. Protein inhibitor of activated STAT 3 modulates osteoclastogenesis by down-regulation of NFATc1 and osteoclast-associated receptor. *J Immunol.* (2007) 178:5588–94. doi: 10.4049/jimmunol.178.9.5588
34. Hu C-H, Sui B-D, Du F-Y, Shuai Y, Zheng C-X, Zhao P, et al. miR-21 deficiency inhibits osteoclast function and prevents bone loss in mice. *Sci Rep.* (2017) 7:43191. doi: 10.1038/srep43191
35. Sugatani T, Vacher J, Hruska KA. A microRNA expression signature of osteoclastogenesis. *Blood*. (2011) 117:3648–57. doi: 10.1182/blood-2010-10-311415
36. Sugatani T, Hruska KA. Down-regulation of miR-21 biogenesis by estrogen action contributes to osteoclastic apoptosis. *J Cell Biochem.* (2013) 114:1217–22. doi: 10.1002/jcb.24471
37. Florczyk-Soluch U, Józefczuk E, Stępniewski J, Bukowska-Strakova K, Mendel M, Viscardi M, et al. Various roles of heme oxygenase-1 in response of bone marrow macrophages to RANKL and in the early stage of osteoclastogenesis. *Sci Rep.* (2018) 8:10797. doi: 10.1038/s41598-018-29122-1
38. Ke K, Sul O-J, Rajasekaran M, Choi H-S. MicroRNA-183 increases osteoclastogenesis by repressing heme oxygenase-1. *Bone*. (2015) 81:237–46. doi: 10.1016/j.bone.2015.07.006
39. Teitelbaum SL, Ross FP. Genetic regulation of osteoclast development and function. *Nat Rev Genet.* (2003) 4:638–49. doi: 10.1038/nrg1122
40. Sugatani T, Alvarez U, Hruska KA. PTEN regulates RANKL- and osteopontin-stimulated signal transduction during osteoclast differentiation and cell motility. *J Biol Chem.* (2003) 278:5001–8. doi: 10.1074/jbc.M209299200
41. Zhao C, Sun W, Zhang P, Ling S, Li Y, Zhao D, et al. miR-214 promotes osteoclastogenesis by targeting Pten/PI3k/Akt pathway. *RNA Biol.* (2015) 12:343–53. doi: 10.1080/15476286.2015.1017205

42. Penna E, Orso F, Taverna D. miR-214 as a key hub that controls cancer networks: small player, multiple functions. *J Invest Dermatol.* (2015) 135:960–9. doi: 10.1038/jid.2014.479
43. Xin R, Bai F, Feng Y, Jiu M, Liu X, Bai F, et al. MicroRNA-214 promotes peritoneal metastasis through regulating PTEN negatively in gastric cancer. *Clin Res Hepatol Gastroenterol.* (2016) 40:748–54. doi: 10.1016/j.clinre.2016.05.006
44. Liu J, Chen W, Zhang H, Liu T, Zhao L. miR-214 targets the PTEN-mediated PI3K/Akt signaling pathway and regulates cell proliferation and apoptosis in ovarian cancer. *Oncol Lett.* (2017) 14:5711–8. doi: 10.3892/ol.2017.6953
45. Wang S, Tang C, Zhang Q, Chen W. Reduced miR-9 and miR-181a expression down-regulates Bim concentration and promote osteoclasts survival. *Int J Clin Exp Pathol.* (2014) 7:2209–18.
46. Chen C, Cheng P, Xie H, Zhou H-D, Wu X-P, Liao E-Y, et al. MiR-503 regulates osteoclastogenesis via targeting RANK. *J Bone Miner Res.* (2014) 29:338–47. doi: 10.1002/jbmr.2032
47. Wang C, He H, Wang L, Jiang Y, Xu Y. Reduced miR-144-3p expression in serum and bone mediates osteoporosis pathogenesis by targeting RANK. *Biochem Cell Biol.* (2018) 96:627–35. doi: 10.1139/bcb-2017-0243
48. Guo L-J, Liao L, Yang L, Li Y, Jiang T-J. MiR-125a TNF receptor-associated factor 6 to inhibit osteoclastogenesis. *Exp Cell Res.* (2014) 321:142–52. doi: 10.1016/j.yexcr.2013.12.001
49. Taganov KD, Boldin MP, Chang K-J, Baltimore D. NF-kappaB-dependent induction of microRNA miR-146, an inhibitor targeted to signaling proteins of innate immune responses. *Proc Natl Acad Sci USA.* (2006) 103:12481–6. doi: 10.1073/pnas.0605298103
50. Nakasa T, Shibuya H, Nagata Y, Niimoto T, Ochi M. The inhibitory effect of microRNA-146a expression on bone destruction in collagen-induced arthritis. *Arthritis Rheum.* (2011) 63:1582–90. doi: 10.1002/art.30321
51. Ammari M, Presumey J, Ponsolles C, Roussignol G, Roubert C, Escriou V, et al. Delivery of miR-146a to Ly6C ^{high} monocytes inhibits pathogenic bone erosion in inflammatory arthritis. *Theranostics.* (2018) 8:5972–85. doi: 10.7150/thno.29313
52. Qu B, Xia X, Yan M, Gong K, Deng S, Huang G, et al. miR-218 is involved in the negative regulation of osteoclastogenesis and bone resorption by partial suppression of p38MAPK-c-Fos-NFATc1 signaling: potential role for osteopenic diseases. *Exp Cell Res.* (2015) 338:89–96. doi: 10.1016/j.yexcr.2015.07.023
53. Wang W, Yang L, Zhang D, Gao C, Wu J, Zhu Y, et al. MicroRNA-218 negatively regulates osteoclastogenic differentiation by repressing the nuclear factor-κB signaling pathway and targeting tumor necrosis factor receptor 1. *Cell Physiol Biochem.* (2018) 48:339–47. doi: 10.1159/000491740
54. Krzeszinski JY, Wei W, Huynh H, Jin Z, Wang X, Chang T-C, et al. miR-34a blocks osteoporosis and bone metastasis by inhibiting osteoclastogenesis and Tgif2. *Nature.* (2014) 512:431–5. doi: 10.1038/nature13375
55. Irie N, Takada Y, Watanabe Y, Matsuzaki Y, Naruse C, Asano M, et al. Bidirectional signaling through ephrinA2-EphA2 enhances osteoclastogenesis and suppresses osteoblastogenesis. *J Biol Chem.* (2009) 284:14637–44. doi: 10.1074/jbc.M807598200
56. Yang S, Zhang W, Cai M, Zhang Y, Jin F, Yan S, et al. Suppression of bone resorption by miR-141 in aged rhesus monkeys. *J Bone Miner Res.* (2018) 33:1799–812. doi: 10.1002/jbmr.3479
57. Omata Y, Yasui T, Hirose J, Izawa N, Imai Y, Matsumoto T, et al. Genomewide comprehensive analysis reveals critical cooperation between Smad and c-Fos in RANKL-induced osteoclastogenesis. *J Bone Miner Res.* (2015) 30:869–77. doi: 10.1002/jbmr.2418
58. Yu F, Xie C, Sun J, Peng W, Huang X. Overexpressed miR-145 inhibits osteoclastogenesis in RANKL-induced bone marrow-derived macrophages and ovariectomized mice by regulation of Smad3. *Life Sci.* (2018) 202:11–20. doi: 10.1016/j.lfs.2018.03.042
59. Fennen M, Pap T, Dankbar B. Smad-dependent mechanisms of inflammatory bone destruction. *Arthritis Res Ther.* (2016) 18:279. doi: 10.1186/s13075-016-1187-7
60. Zhao H, Zhang J, Shao H, Liu J, Jin M, Chen J, et al. Transforming growth factor β1/Smad4 signaling affects osteoclast differentiation via regulation of miR-155 expression. *Mol Cells.* (2017) 40:211–21. doi: 10.14348/molcells.2017.230
61. Zhang J, Zhao H, Chen J, Xia B, Jin Y, Wei W, et al. Interferon-β-induced miR-155 inhibits osteoclast differentiation by targeting SOCS1 and MITF. *FEBS Lett.* (2012) 586:3255–62. doi: 10.1016/j.febslet.2012.06.047
62. Su L-C, Huang A-F, Jia H, Liu Y, Xu W-D. Role of microRNA-155 in rheumatoid arthritis. *Int J Rheum Dis.* (2017) 20:1631–7. doi: 10.1111/1756-185X.13202
63. Sul O-J, Sung Y-B, Rajasekaran M, Ke K, Yu R, Back S-H, et al. MicroRNA-155 induces autophagy in osteoclasts by targeting transforming growth factor β-activated kinase 1-binding protein 2 upon lipopolysaccharide stimulation. *Bone.* (2018) 116:279–89. doi: 10.1016/j.bone.2018.08.014
64. Lu S-Y, Li M, Lin Y-L. Mitf regulates osteoclastogenesis by modulating NFATc1 activity. *Exp Cell Res.* (2014) 328:32–43. doi: 10.1016/j.yexcr.2014.08.018
65. Zhao H, Zhang J, Shao H, Liu J, Jin M, Chen J, et al. miRNA-340 inhibits osteoclast differentiation via repression of MITF. *Biosci Rep.* (2017) 37:BSR20170302. doi: 10.1042/BSR20170302
66. Kim JH, Kim N. Regulation of NFATc1 in osteoclast differentiation. *J Bone Metab.* (2014) 21:233–41. doi: 10.11005/jbm.2014.21.4.233
67. Lee Y, Kim HJ, Park CK, Kim Y-G, Lee H-J, Kim J-Y, et al. MicroRNA-124 regulates osteoclast differentiation. *Bone.* (2013) 56:383–9. doi: 10.1016/j.bone.2013.07.007
68. Nakamachi Y, Ohnuma K, Uto K, Noguchi Y, Saegusa J, Kawano S. MicroRNA-124 inhibits the progression of adjuvant-induced arthritis in rats. *Ann Rheum Dis.* (2016) 75:601–8. doi: 10.1136/annrheumdis-2014-206417
69. Tang L, Yin Y, Liu J, Li Z, Lu X. MiR-124 attenuates osteoclastogenic differentiation of bone marrow monocytes via targeting Rab27a. *Cell Physiol Biochem.* (2017) 43:1663–72. doi: 10.1159/000484027
70. Mizoguchi F, Murakami Y, Saito T, Miyasaka N, Kohsaka H. miR-31 controls osteoclast formation and bone resorption by targeting RhoA. *Arthritis Res Ther.* (2013) 15:R102. doi: 10.1186/ar4282
71. Strzelecka-Kiliszek A, Mebarek S, Roszkowska M, Buchet R, Magne D, Pikula S. Functions of Rho family of small GTPases and Rho-associated coiled-coil kinases in bone cells during differentiation and mineralization. *Biochim Biophys Acta Gen Subj.* (2017) 1861:1009–23. doi: 10.1016/j.bbagen.2017.02.005
72. Chellaiah MA, Soga N, Swanson S, McAllister S, Alvarez U, Wang D, et al. Rho-A is critical for osteoclast podosome organization, motility, and bone resorption. *J Biol Chem.* (2000) 275:11993–2002. doi: 10.1074/jbc.275.16.11993
73. Georgess D, Machuca-Gayet I, Blangy A, Jurdic P. Podosome organization drives osteoclast-mediated bone resorption. *Cell Adh Migr.* (2014) 8:191–204. doi: 10.4161/cam.27840
74. Cong F, Wu N, Tian X, Fan J, Liu J, Song T, et al. MicroRNA-34c promotes osteoclast differentiation through targeting LGR4. *Gene.* (2017) 610:1–8. doi: 10.1016/j.gene.2017.01.028
75. Luo J, Yang Z, Ma Y, Yue Z, Lin H, Qu G, et al. LGR4 is a receptor for RANKL and negatively regulates osteoclast differentiation and bone resorption. *Nat Med.* (2016) 22:539–46. doi: 10.1038/nm.4076
76. Heasman SJ, Ridley AJ. Mammalian Rho GTPases: new insights into their functions from *in vivo* studies. *Nat Rev Mol Cell Biol.* (2008) 9:690–701. doi: 10.1038/nrm2476
77. Rossi M, Pitari MR, Amodio N, Di Martino MT, Conforti F, Leone E, et al. miR-29b negatively regulates human osteoclastic cell differentiation and function: implications for the treatment of multiple myeloma-related bone disease. *J Cell Physiol.* (2013) 228:1506–15. doi: 10.1002/jcp.24306
78. Shimada-Sugawara M, Sakai E, Okamoto K, Fukuda M, Izumi T, Yoshida N, Tsukuba T. Rab27A regulates transport of cell surface receptors modulating multinucleation and lysosome-related organelles in osteoclasts. *Sci Rep.* (2015) 5:9620. doi: 10.1038/srep09620
79. Dou C, Zhang C, Kang F, Yang X, Jiang H, Bai Y, et al. MiR-7b directly targets DC-STAMP causing suppression of NFATc1 and c-Fos signaling during osteoclast fusion and differentiation. *Biochim Biophys Acta.* (2014) 1839:1084–96. doi: 10.1016/j.bbagrm.2014.08.002
80. Yin Y, Tang L, Chen J, Lu X. MiR-30a attenuates osteoclastogenesis via targeting DC-STAMP-c-Fos-NFATc1 signaling. *Am J Transl Res.* (2017) 9:5743–53.

81. Dou C, Ding N, Luo F, Hou T, Cao Z, Bai Y, et al. Graphene-based MicroRNA transfection blocks preosteoclast fusion to increase bone formation and vascularization. *Adv Sci.* (2018) 5:1700578. doi: 10.1002/advs.201700578
82. Kim K, Kim JH, Kim I, Lee J, Seong S, Park Y-W, et al. MicroRNA-26a regulates RANKL-induced osteoclast formation. *Mol Cells*. (2015) 38:75–80. doi: 10.14348/molcells.2015.2241
83. Fordham JB, Guilfoyle K, Naqvi AR, Nares S. MiR-142-3p is a RANKL-dependent inducer of cell death in osteoclasts. *Sci Rep.* (2016) 6:24980. doi: 10.1038/srep24980
84. Ma Y, Yang H, Huang J. Icariin ameliorates dexamethasone-induced bone deterioration in an experimental mouse model via activation of microRNA-186 inhibition of cathepsin K. *Mol Med Rep*. (2018) 17:1633–41. doi: 10.3892/mmr.2017.8065
85. Madel M-B, Ibáñez L, Rouleau M, Wakkach A, Blin-Wakkach C. A novel reliable and efficient procedure for purification of mature osteoclasts allowing functional assays in mouse cells. *Front Immunol.* (2018) 9:2567. doi: 10.3389/fimmu.2018.02567
86. Liu M, Sun Y, Zhang Q. Emerging role of extracellular vesicles in bone remodeling. *J Dent Res.* (2018) 97:859–68. doi: 10.1177/0022034518764411
87. Xie Y, Chen Y, Zhang L, Ge W, Tang P. The roles of bone-derived exosomes and exosomal microRNAs in regulating bone remodelling. *J Cell Mol Med.* (2017) 21:1033–41. doi: 10.1111/jcmm.13039
88. Yuan F-L, Wu Q-Y, Miao Z-N, Xu M-H, Xu R-S, Jiang D-L, et al. Osteoclast-derived extracellular vesicles: novel regulators of osteoclastogenesis and osteoclast-osteoblasts communication in bone remodeling. *Front Physiol.* (2018) 9:628. doi: 10.3389/fphys.2018.00628
89. Tao S-C, Guo S-C. Extracellular vesicles in bone: "dogrobbers" in the "eternal battle field." *Cell Commun Signal*. (2019) 17:6. doi: 10.1186/s12964-019-0319-5
90. Mestdagh P, Hartmann N, Baeriswyl L, Andreasen D, Bernard N, Chen C, et al. Evaluation of quantitative miRNA expression platforms in the microRNA quality control (miRQC) study. *Nat Methods*. (2014) 11:809–15. doi: 10.1038/nmeth.3014
91. Ishihara R, Hasegawa K, Hosokawa K, Maeda M. Multiplex MicroRNA detection on a power-free microfluidic chip with laminar flow-assisted dendritic amplification. *Anal Sci.* (2015) 31:573–6. doi: 10.2116/analsci.31.573
92. Wu X, Zhu S, Huang P, Chen Y. Highly specific quantification of microRNA by coupling probe-rolling circle amplification and Förster resonance energy transfer. *Anal Biochem.* (2016) 502:16–23. doi: 10.1016/j.ab.2016.03.001
93. Dard-Dascot C, Naquin D, d'Aubenton-Carafa Y, Alix K, Thermes C, van Dijk E. Systematic comparison of small RNA library preparation protocols for next-generation sequencing. *BMC Genomics*. (2018) 19:118. doi: 10.1186/s12864-018-4491-6
94. Rice J, Roberts H, Burton J, Pan J, States V, Rai SN, et al. Assay reproducibility in clinical studies of plasma miRNA. *PLoS ONE*. (2015) 10:e0121948. doi: 10.1371/journal.pone.0121948
95. Yeri A, Courtright A, Danielson K, Hutchins E, Alsop E, Carlson E, et al. Evaluation of commercially available small RNASeq library preparation kits using low input RNA. *BMC Genomics*. (2018) 19:331. doi: 10.1186/s12864-018-4726-6
96. Songia P, Chiesa M, Valerio V, Moschetta D, Myasoedova VA, D'Alessandra Y, et al. Direct screening of plasma circulating microRNAs. *RNA Biol.* (2018) 15:1268–72. doi: 10.1080/15476286.2018.1526538
97. Bustin SA, Benes V, Garson JA, Hellemans J, Huggett J, Kubista M, et al. The MIQE guidelines: minimum information for publication of quantitative real-time PCR experiments. *Clin Chem.* (2009) 55:611–22. doi: 10.1373/clinchem.2008.112797
98. Deng MC. The AlloMap^{TM} genomic biomarker story: 10 years after. *Clin Transplant*. (2017) 31:e12900. doi: 10.1111/ctr.12900
99. Haider BA, Baras AS, McCall MN, Hertel JA, Cornish TC, Halushka MK. A critical evaluation of microRNA biomarkers in non-neoplastic disease. *PLoS ONE*. (2014) 9:e89565. doi: 10.1371/journal.pone.0089565
100. Peltier HJ, Latham GJ. Normalization of microRNA expression levels in quantitative RT-PCR assays: identification of suitable reference RNA targets in normal and cancerous human solid tissues. *RNA*. (2008) 14:844–52. doi: 10.1261/rna.939908
101. Marabita F, de Candia P, Torri A, Tegnér J, Abrignani S, Rossi RL. Normalization of circulating microRNA expression data obtained by quantitative real-time RT-PCR. *Brief Bioinform.* (2016) 17:204–12. doi: 10.1093/bib/bbv056
102. Song J, Bai Z, Han W, Zhang J, Meng H, Bi J, et al. Identification of suitable reference genes for qPCR analysis of serum microRNA in gastric cancer patients. *Dig Dis Sci.* (2012) 57:897–904. doi: 10.1007/s10620-011-1981-7
103. Hu Z, Dong J, Wang L-E, Ma H, Liu J, Zhao Y, et al. Serum microRNA profiling and breast cancer risk: the use of miR-484/191 as endogenous controls. *Carcinogenesis*. (2012) 33:828–34. doi: 10.1093/carcin/bgs030
104. Zhang J, Song Y, Zhang C, Zhi X, Fu H, Ma Y, et al. Circulating MiR-16-5p and MiR-19b-3p as two novel potential biomarkers to indicate progression of gastric cancer. *Theranostics*. (2015) 5:733–45. doi: 10.7150/thno.10305
105. Luo H, Li X, Li T, Zhao L, He J, Zha L, et al. Exosomes/microvesicles microRNA-423-3p derived from cardiac fibroblasts mediates the cardioprotective effects of ischemic postconditioning. *Cardiovasc Res.* (2018) doi: 10.1093/cvr/cvy231. [Epub ahead of print].
106. Buschmann D, Kirchner B, Hermann S, Märte M, Wurmser C, Brandes F, et al. Evaluation of serum extracellular vesicle isolation methods for profiling miRNAs by next-generation sequencing. *J Extracell Vesicles*. (2018) 7:1481321. doi: 10.1080/20013078.2018.1481321

Conflict of Interest Statement: The authors declare that the research was conducted in the absence of any commercial or financial relationships that could be construed as a potential conflict of interest.

frontiers in Immunology

REVIEW
published: 19 March 2019
doi: 10.3389/fimmu.2019.00505

What Are the Peripheral Blood Determinants for Increased Osteoclast Formation in the Various Inflammatory Diseases Associated With Bone Loss?

Teun J. de Vries[1], Ismail el Bakkali[1], Thomas Kamradt[2], Georg Schett[3], Ineke D. C. Jansen[1] and Patrizia D'Amelio[4]*

[1] Department of Periodontology, Academic Centre for Dentistry Amsterdam (ACTA), University of Amsterdam and Vrije Universiteit Amsterdam, Amsterdam, Netherlands, [2] Institute of Immunology, Universitätsklinikum Jena, Jena, Germany, [3] Department of Internal Medicine III, Friedrich-Alexander University Erlangen-Nürnberg and Universitatsklinikum Erlangen, Erlangen, Germany, [4] Gerontology and Bone Metabolic Diseases Division, Department of Medical Science, University of Turin, Turin, Italy

OPEN ACCESS

Edited by:
Takayuki Yoshimoto, Tokyo Medical University, Japan

Reviewed by:
Guillaume Mabilleau, Université d'Angers, France
Francesca Salamanna, Rizzoli Orthopedic Institute, Italy

****Correspondence:***
Teun J. de Vries
teun.devries@acta.nl

Specialty section:
This article was submitted to Inflammation, a section of the journal Frontiers in Immunology

Received: *29 November 2018*
Accepted: *25 February 2019*
Published: *19 March 2019*

Citation:
de Vries TJ, el Bakkali I, Kamradt T, Schett G, Jansen IDC and D'Amelio P (2019) What Are the Peripheral Blood Determinants for Increased Osteoclast Formation in the Various Inflammatory Diseases Associated With Bone Loss? Front. Immunol. 10:505. doi: 10.3389/fimmu.2019.00505

Local priming of osteoclast precursors (OCp) has long been considered the main and obvious pathway that takes place in the human body, where local bone lining cells and RANKL-expressing osteocytes may facilitate the differentiation of OCp. However, priming of OCp away from bone, such as in inflammatory tissues, as revealed in peripheral blood, may represent a second pathway, particularly relevant in individuals who suffer from systemic bone loss such as prevalent in inflammatory diseases. In this review, we used a systematic approach to review the literature on osteoclast formation in peripheral blood in patients with inflammatory diseases associated with bone loss. Only studies that compared inflammatory (bone) disease with healthy controls in the same study were included. Using this core collection, it becomes clear that experimental osteoclastogenesis using peripheral blood from patients with bone loss diseases in prevalent diseases such as rheumatoid arthritis, osteoporosis, periodontitis, and cancer-related osteopenia unequivocally point toward an intrinsically increased osteoclast formation and activation. In particular, such increased osteoclastogenesis already takes place without the addition of the classical osteoclastogenesis cytokines M-CSF and RANKL *in vitro*. We show that T-cells and monocytes as OCp are the minimal demands for such unstimulated osteoclast formation. In search for common and disease-specific denominators of the diseases with inflammation-driven bone loss, we demonstrate that altered T-cell activity and a different composition—such as the CD14+CD16+ vs. CD14+CD16– monocytes—and priming of OCp with increased M-CSF, RANKL, and TNF- α levels in peripheral blood play a role in increased osteoclast formation and activity. Future research will likely uncover the barcodes of the OCp in the various inflammatory diseases associated with bone loss.

Keywords: peripheral blood, osteoclast formation, T-cells, CD14+CD16+, osteoclast precursor priming, inflammatory bone diseases

INTRODUCTION

Close inspection of skeletons as seen in anatomy museums may show signs of inflammatory bone loss, present as joint erosions and bone degradation of the tooth sockets that surround teeth. This betrays an evoked activity of bone degradation by inflammation steered osteoclasts, so different from turn-over osteoclasts that in fact leave the rest of the skeleton seemingly normal. The different bone cells, osteoclasts, bone-lining cells, osteoblasts and osteocytes are responsible for a lifelong balanced remodeling process. When this process becomes unbalanced, such as during inflammatory diseases with bone-loss, it may result in severe bone loss, locally, or systemically. The key cell-type in this disturbed bone balance is the osteoclast, the multinucleated cell responsible for breaking down bone tissue (1).

Osteoclasts derive from cells of the monocyte/macrophage lineage (2–4) present in bone marrow (5), but also present in peripheral blood (6). Osteoclasts play a key role in diseases that are associated with increased bone loss (7). Such diseases include common diseases such as the rheumatic diseases, osteoporosis, periodontitis, cancers that metastasize to bone and Crohn's disease. Less common diseases that also give rise to bone loss are chronic liver disease, Gaucher's disease, Turner's syndrome, and phenylketonuria. Bone loss is also frequently observed in patients with chronic kidney disease. In nearly all of these diseases, excessive osteoclast generation and activation, with a key contribution to the altered immune system plays a dominant role. All these diseases are discussed in detail below.

Growth factors and cytokines that can be produced by a wide range of cells in the human body regulate the activity and formation of osteoclasts. The principle differentiation factors for osteoclast differentiation are macrophage colony-stimulating factor (M-CSF), receptor activator of nuclear factor kappa-B ligand (RANKL) (8) and the inhibitor of osteoclast differentiation, the "protector of bone," osteoprotegerin (OPG) (9). These cytokines are produced by osteocytes and bone lining cells/osteoblasts (10). However, RANKL can also be produced by T-cells (11, 12), by synovial fibroblasts from inflamed joints (13) and by tooth-associated fibroblasts (14). Apart from this classical pathway, it was demonstrated by Kim et al. using RANK-/- mouse models, that osteoclasts may also form through stimulation with inflammatory cytokines such as tumor necrosis factor-α (TNF-α) (15).

Apart from the common culture methods of osteoclasts using M-CSF and RANKL, there are strong indications that osteoclast precursors may differentiate into multinucleated osteoclasts in the absence of added osteoclastogenesis stimulating factors M-CSF and RANKL. This is referred to as "spontaneous" or unstimulated osteoclast formation (16, 17), recently excellently reviewed by Salamanna et al. (7). A better term for this could be self-stimulatory osteoclastogenesis, where the combination of T-cells that may provide the osteoclastogenesis signals with primed OCp may give rise to osteoclast formation. Here, and experimental evidence is provided below, cells from peripheral blood, such as T-cells, may provide the necessary differentiation factors for the monocytic, CD14+ osteoclast precursor cells in blood. These studies are based on experimental *in vitro* studies which suggest an activation of the OCp by inflammatory mediators present in the plasma of patients with inflammatory bone disease or an intrinsic change of cells toward more osteoclastic differentiation. Examples include periodontitis, osteoporosis, Crohn's disease, rheumatoid arthritis, and bone metastatic cancer and will be further described later on in this review.

The aim of this systematic literature review is to provide an overview and an interpretation of experimental *in vitro* studies involving osteoclast formation from peripheral blood of patients with inflammatory diseases that lead to bone loss compared to the osteoclast formation from peripheral blood of healthy controls. This will gain insight into the various mechanisms that play a role in the activation of osteoclasts from peripheral blood in these inflammatory bone diseases. The similarities and differences in peripheral blood-mediated osteoclast formation between the various inflammatory diseases associated with bone loss will be examined and discussed.

LITERATURE SEARCH

The methodological approach of systematic review was used. The PRISMA (Preferred Reporting Items for Systematic Reviews and Meta-Analyses) was used to reduce the bias in the selection of publications for this review.

Search strategy

Search Query

#1 Peripheral blood

#2 Osteoclast OR osteoclasts

#3 Osteoclast formation OR osteoclast differentiation OR osteoclastogenesis

#4 (Periodontitis OR periodontal disease) OR rheumatoid arthritis OR psoriatic arthritis OR inflammatory bowel disease OR Crohn's disease OR osteoporosis OR bone metastatic cancer

#5 (#1 AND #2 AND #3 AND #4) AND ("2002/01/01"[PDat]: "2018/07/31"[PDat])

The electronic search for relevant studies was carried out in the three databases Pubmed, Embase, and Web of science. The keywords used for the search were "peripheral blood," "osteoclast," "osteoclasts," "osteoclast formation," "osteoclast differentiation," "osteoclastogenesis," "periodontitis," "periodontal disease," "rheumatoid arthritis," "psoriatic arthritis," "inflammatory bowel disease," "Crohn's disease," "osteoporosis," "bone metastatic cancer." In terms of time and language, articles published from 2002 until 2018 were assessed and only publications in English were included in this study.

SCREENING AND SELECTION

A set of inclusion and exclusion criteria were used to retrieve relevant *in vitro* studies. All *in vitro* studies involving exogenously added cytokine driven and spontaneous osteoclast formation from peripheral blood from patients with periodontitis or

rheumatoid arthritis or psoriatic arthritis or osteoporosis or Crohn's disease or bone metastatic cancer were included for further examination.

The titles and abstracts of all publications identified by the electronic search were manually screened and discussed by two reviewers (IB and TdV). When the suitability of an article for this review could not be determined based on the title and abstract, the full text was read and examined by one reviewer (IB) and reported and discussed (IB and TdV). Outcomes of *in vitro* studies included comparison between osteoclast formation from peripheral blood of patients with one of the diseases listed above and healthy controls. All articles that did not meet with the primary outcome of interest, (spontaneous) osteoclast formation from PBMCs or monocytes of diseased patients compared to healthy controls were excluded, leaving 29 papers in the core-collection (**Figure 1**).

Apart from the systematic approach on the common diseases osteoporosis, periodontitis and rheumatoid arthritis, literature on less frequent diseases (Turner, Gaucher, chronic liver disease, Crohn's disease, and phenylketonuria) that was found with this search strategy was incorporated.

PERIPHERAL BLOOD OSTEOCLAST FORMATION IS INCREASED IN A WIDE SPECTRUM OF BONE DISEASES

Overall it can be concluded that osteoclast formation from peripheral blood cells is increased in a wide range of diseases (**Table 1**). Results per disease or group of diseases are discussed in detail below.

Rheumatic Diseases

Rheumatoid Arthritis

Rheumatoid arthritis is a chronic inflammatory joint disease that is characterized by chronic synovitis and exaggerated local and systemic bone loss. It was established by Gravallese et al., that osteoclasts accumulate in the joints of RA patients (44) and that RANKL, the key osteoclastogenic mediator, is expressed locally in the joints of RA patients (45). Systemically, increased circulating osteoclast precursors have been reported in RA, which express key osteoclastogenic molecules on their surface (46, 47). Notably, when exposing similar numbers of peripheral CD14+ cells to osteoclastogenic conditions, more osteoclasts form in RA patients than in healthy controls (20), which is a strong argument that these peripheral osteoclast precursors are primed in the circulation. Moreover, elevated osteoclast formation in RA was shown to be correlated to local and systemic bone loss in RA (23). In addition, data showed that RA affects the longevity of osteoclasts, with a significantly lower number of osteoclasts undergoing apoptosis in RA compared to the healthy controls (22).

Enhanced osteoclastogenesis in RA essentially depends on T cells (48). Thus, in T-cell (CD3+ cells) depleted cultures, osteoclast precursors from RA patients show significantly lower spontaneous differentiation. Addition of exogenous RANKL to these cultures resulted in partial recovery of osteoclast formation. Together, these data indicate a crucial role for T-cells in osteoclast formation in RA, in line with earlier studies that demonstrated the activating role of T-cells in osteoclast formation (8, 49) which initiated osteoimmunology research. Miranda-Carus et al. (21) showed that T-cells present in peripheral blood play a major role in the formation of osteoclasts in RA patients. They interact with the osteoclast precursors of the monocyte/ macrophage lineage *in vitro*. An increased level of TNF-α, IL-1, IL-17, and RANKL was also found in the autologous T-cell/monocyte co-cultures derived from patients with early RA and established RA compared with controls (21) suggesting that these cytokines drive osteoclast differentiation in RA. Especially CD4+ T-cells play a role in osteoclastogenesis. OPG, anti-TNF-α and anti-IL-1 in this study, were shown to inhibit osteoclast formation (21).

Psoriatic Arthritis

Psoriatic arthritis (PsA) is a chronic inflammatory joint disease, which develops in about 30% of patients with psoriasis and is characterized by local bone erosions and systemic bone loss. TNFa and the interleukins 17 and −23 are key mediators of bone loss in PsA (50). In 2003, Ritchlin et al. (18) showed that the number of osteoclast precursors is increased in patients with PsA. In part, the development of osteoclasts in PsA could be independent from M-CSF or RANKL. This could be explained by a higher number of circulating OC precursors or by the ability of maturation of osteoclast precursors without supplementation with exogenous levels of M-CSF or RANKL. Ritchlin et al., also showed strong RANKL expression in synovial tissue of PsA patients as well as strong RANK expression in osteoclasts at areas with bone erosion. Fewer osteoclasts formed from blood of PsA patients after anti-tumor necrosis factor-α (TNF-α) treatment, indicating that TNF-α primes OC precursors in PsA (16). The original findings of Ritchlin et al., were also corroborated by Colucci et al., who showed that more TRAP+ multinucleated cells formed in cultures from PsA patients. Interestingly, supplementation of inflammatory cytokines abrogated these differences between PsA patients and controls (**Table 1**). This finding indicates an intrinsically higher osteoclastogenesis potential of blood from PsA patients. Increased osteoclast formation in PBMCs appears to be T-cell dependent, since the formation of osteoclasts was absent in T-cell-depleted PBMC cultures, which implies that T-cells are responsible for osteoclast formation. These results also suggest that blockade of RANKL and TNF-α might be used as an effective strategy for inhibiting enhanced osteoclastogenesis in PsA patients (19). Indeed such concept is supported by data on TNF inhibitors, which effectively inhibit osteoclast formation (51). Notably, aside from inflammation, PsA is strongly linked to obesity and the metabolic syndrome. In this context it is interesting that Xue et al., found an elevated value of certain adipokines, cytokines derived from adipose tissues, in the circulation of patients with PsA (52). Adipokines like leptin, adiponectin, chemerin, and omentin may not only play a role in inflammation but also in osteoclastogenesis in patients with PsA. Higher levels of leptin and omentin, for instance, positively correlated with the number of osteoclast precursors found in

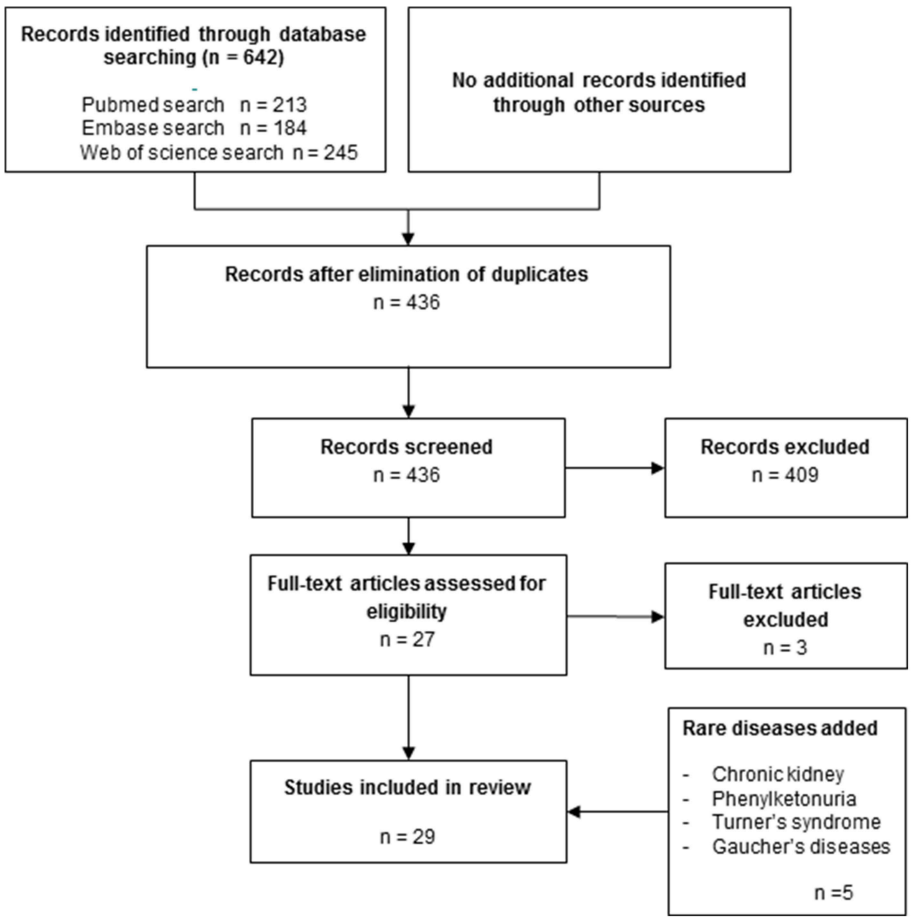

FIGURE 1 | Flow chart of the literature search strategy.

PsA patients, while adiponectin was negatively correlated with osteoclast precursors.

Osteoarthritis

In osteoarthritis (OA) (24), the key degenerative joint disease, it was found that the number of TRACP+ multinucleated osteoclasts is higher than in healthy controls providing an explanation for the sometimes bone erosive phenotype of OA. No significant difference was found between OA and healthy controls regarding the number of circulating CD14+ cells. However, osteoclasts from the OA patients were found capable of resorbing a significantly larger (4 times) area than the osteoclasts from the healthy controls. The higher number of osteoclast-like cells formed by the PBMCs from the osteoarthritis group compared to the PBMCs from the control group could be responsible for enhanced local bone resorption in OA.

Though strictly speaking not a rheumatoid disease, Charcot's arthropathy that is associated with diabetes co-incides with joint erosions, in particular of the foot (53). Charcot's arthropathy is associated with increased peripheral blood osteoclast formation, with more osteoclasts than in matched diabetes patients without Charcot's arthropathy is or healthy controls (26). A later study from the same group showed that higher numbers of CD14+ cells prevail in blood of patients with Charcot foot, concomitant with higher peripheral blood TNF-α levels (53).

Acroosteolysis

Also patients suffering from acroosteolysis, which is part of the systemic sclerosis disease spectrum, show increased osteoclast formation compared to healthy controls. In this context, the increased osteoclast formation is associated with higher VEGF levels in the peripheral blood (27). VEGF can substitute for M-CSF in driving osteoclast differentiation (54).

Ankylosing Spondylitis

Ankylosing spondylitis is an inflammatory rheumatic disease of the spine, which is characterized by loss of trabecular bone but periosteal apposition of cortical bone leading to bony spur formation sometimes leading to fusion of vertebra (55). Interestingly, ankylosing spondylitis is the only rheumatic disease where data showed that less osteoclasts form *in vitro* and where data on serum CTX levels show that lower overall bone resorption happens. Lower osteoclast numbers correlated with lower RANKL/OPG ratios. Furthermore, osteoclasts from

TABLE 1 | Unstimulated and stimulated osteoclast formation is increased in peripheral blood from patients with bone loss.

	Unstimulated [without cytokines]			Stimulated [M-CSF + RANKL]		
Disease, study	**Disease**	**Healthy control**	**Resorption?**	**Disease**	**Healthy control**	**Resorption?**
REUMATOID DISEASES						
PsA, Ritchlin et al. (18)	168	3.7*	D>C	N.D.	N.D.	D>C
PsA, Colocci et al. (19)	49	0 [n.t.]*	D>C	55	50 [n.t.]	N.D.
PsA, Ikic et al. (20)	N.D.	N.D.	N.D.	120	40*	N.D.
RA, Miranda-Carus et al. (21)	100	5*	D>C	N.D.	N.D.	N.D.
RA and OA, Durand et al. (22)	N.D.	N.D.	N.D.	450*	350	N.S
RA, Ikic et al. (20)	N.D.	N.D.	N.D.	360*	40	N.D.
RA, Shang et al. (23)	N.D.	N.D.	N.D.	125*	75	N.S.
OA, Durand et al. (24)	N.D.	N.D.	N.D.	248*	210	D>C
AS, Caparbo et al. (25)	N.D.	N.D.	N.D.	700	750*	
Charcot's osteoarthropathy, Mabilleau et al. (26)	N.D.	N.D.	N.D.	96*	56 (diabetes) 21 (HC)	D>C
Acroosteolysis, Park et al. (27)	ND	ND	ND	142	18*	D>C
OSTEOPOROSIS						
Jevon et al. (28)	9	7	D>C	ND	ND	ND
D'Amelio et al. (17)	48	15*	D>C	50	40	N.D.
D'Amelio et al. (29)	145	5*	D>C	180	140	N.D.
Koek et al. (30)	N.D.	N.D.	N.D.	28	27	N.S.
PERIODONTITIS						
Brunetti et al. (12)	59	5*	D>C	70	62	N.D.
Tjoa et al. (31)	14	8	N.D.	14	15	
Herrera et al. (32)	17	8*	D>C	ns	ns	N.S.
CANCER						
Solid tumors, Roato et al. (33)	172	48*	D>C	161	132 [n.s.]	N.S.
Solid tumors, Roato et al. (34)	60	20*				
Prostate cancer, Roato et al. (35)	216	73*	N.D.	N.D.	N.D.	N.D.
Gastric, D'Amico et al. (36)	N.D.	N.D.	N.D.	90	40	N.S.
CHRONIC LIVER DISEASE						
Olivier et al. (37)	35	20*		45	37	D>C
CROHN'S DISEASE						
Oostlander et al. (38)	380	50*	0	ND	ND	
CHRONIC KIDNEY DISEASE						
Cafiero et al. (39)	20	1*	D>C	±40	40	N.D.
TURNER'S SYNDROME						
Faienza et al. (40)	49	5*	D>C	±42	±50	N.D.
GAUCHER						
Mucci et al. (41)	N.D.	N.D.	N.D.	±140	±75*	D>C
Reed et al. (42)	N.D.	N.D.	N.D.	±120	±40*	D>C
PHENYLKETONURIA						
Roato et al. (43)	149	91*	D>C	189	124*	ND

*N.D., not determined; *, significantly different from disease; N.N., not significantly different from disease; D, Disease; C, control. Numbers of osteoclasts formed between studies are not comparable, since culture conditions differed between the studies.*

ankylosing spondylitits patients were less prone to apoptosis (25) which has also been observed in other rheumatic diseases (24).

Osteoporosis

Osteoporosis is a skeletal disease characterized by lower bone mass and micro-architectural deterioration of bone leading to an increased risk of fractures (56). Several indications show that this phenomenon is caused by a higher activity of osteoclasts due to an imbalance of the osteoclasts and osteoblasts, postmenopausal bone loss is triggered by estrogen deficiency that increased osteoclastogenesis through several pathways, and in particular by the activation of T cells that produce higher level of pro-inflammatory and pro-osteoclastogenic cytokines as TNFα and RANKL (57). Bone fractures are the severe consequence of osteoporosis and represent a major health problem in the increasingly older (58). Old patients experiencing a femoral fracture have a decreased life expectancy and may become care-dependent in half the survivors. The presence of a fragility

fracture increases the risk of new fractures creating a "domino effect": one vertebral fracture doubles the risk of subsequent femoral fracture within a year, the presence of vertebral fractures as well as of femoral fracture impair patients' quality of life and increase mortality.

In a first study comparing the peripheral blood osteoclast formation from patients and controls, similar numbers of osteoclasts formed, but the resorptive capacity was higher in osteoclasts from osteoporosis patients (28), suggesting that the peripheral OCp had the same osteoclastogenic potential, but were somehow primed to form more active osteoclasts (28). D'Amelio et al. (17, 57) investigated the osteoclast formation in osteoporosis. The first study compared the osteoclast formation in osteoporotic women compared to healthy controls, without adding M-CSF, TNF-α, or RANKL to the cultures (17). A higher number of osteoclasts was formed in the cultures from osteoporosis blood compared to healthy controls. After supplementation of M-CSF and RANKL the numbers of osteoclasts reached a same level in controls and patients. A significantly higher level of TNF-α and RANKL was found in the PBMC cultures of the osteoporotic group. Adding 1,25-OH vitamin D3 to the PBMCs cultures resulted in both groups in lower numbers of osteoclasts, but higher resorption. The lacunar resorption area was significantly higher in the osteoporotic patients group compared to the healthy subjects with and without the addition of 1,25-OH vitamin D3. Comparable results were reported in the second paper by the same group (29): higher levels of TNF-α and RANKL in the PBMC cultures and higher osteoclast formation in the osteoporotic group compared to the healthy subjects. Antibodies against TNF-α and RANKL decreased spontaneous osteoclast formation strongest in the osteoporotic group. Additionally this study demonstrated that the T-cells of osteoporosis patients play a key role in the osteoclastogenesis by increasing the TNF-α and RANKL production. It was shown that osteoclast formation was severely suppressed when depleting the T-cells from the PBMCs cultures. This indicates that T-cells play a crucial role in osteoclast formation and that they secrete cytokines necessary for osteoclast formation in osteoporosis. In a fourth study, no differences in osteoclast formation were found between controls and osteoporotic patients (30), but in this case only M-CSF and RANKL stimulated cultures were studied. This was in line with the previous studies (17, 28, 57) regarding the stimulated osteoclastogenesis, where addition of M-CSF and RANKL may shield possible differences.

Periodontitis

Periodontitis is the inflammatory bone-destructive disease affecting the alveolar bone between teeth. It's individual susceptibility is driven by an oral bacterial dysbiosis, genetic factors (59) and life style (60). Currently, it is estimated that no <46% of Americans adults have moderate to severe periodontitis (61). When peripheral blood mononuclear cells (PBMC) from chronic periodontitis patients were cultured in the absence of M-CSF and RANKL, more osteoclast-like cells form from chronic periodontitis patients (12). Osteoclast-like cells in the control group were fewer and smaller. The addition of stimulating factors M-CSF and RANKL resulted in comparable numbers of osteoclast-like cells in control and periodontitis group. M-CSF and RANKL only triggered osteoclast formation in the control group, osteoclast numbers of the periodontitis group did not increase after cytokine treatment. The osteoclasts formed spontaneously from the PBMC cultures from the periodontitis patients and showed a significantly higher resorbtive activity compared to the controls. A T-cell dependent osteoclastogenesis was shown in this study, since the number of osteoclasts was low in the T-cell depleted unstimulated PBMCs cultures from the periodontitis patients. Addition of stimulating factors M-CSF and RANKL to these cultures led to a significantly higher formation of numerous large osteoclasts. An explanation for this finding is the overexpression of RANKL and TNF-α by T-cells, which was shown to be higher by the T-cells from the patient group. Addition of anti-RANKL and anti-TNF-α antibodies induced a dose dependent inhibition of the osteoclast formation in the periodontitis group (12). Also Tjoa et al., aimed to determine if there was a difference in osteoclast formation between the PBMC from patients suffering from chronic periodontitis and matched healthy controls (31). In this study, no differences were observed in unstimulated osteoclast formation between controls and periodontitis patients. A significant difference was shown however after the stimulation with M-CSF between control and diseased group. Larger and more multinucleated cells were found in the control group, whereas the patient group was insensitive to stimulation with M-CSF (31), suggesting that the OCp in this group were already primed in the circulation. In another study, it was shown that peripheral blood monocytes from periodontitis patients are more prone to differentiate into mature multinucleated osteoclasts (32). In other words, this study shows that these monocytes were primed in peripheral blood and prepared here for enhanced osteoclast formation. Only the stimulation with RANKL and not with M-CSF and RANKL gave significant differences between the periodontitis group and healthy controls regarding the osteoclast-like cells formed. A significantly higher level of M-CSF was found in the periodontitis group (32). This could be an explanation for the insensitive response of PBMC from periodontitis patients to stimulation with M-CSF in the study of Tjoa et al. (31), since the osteoclast precursors could be already pre-activated by higher M-CSF levels present in serum.

Cancer That Metastasizes to Bone

Hematological Cancers

B cell multiple myeloma was studied by Colucci et al. who cultured 10 times more osteoclasts in the absence of added cytokines from myeloma blood than from control blood. As described repetitively above, this difference was no longer seen when the M-CSF and RANKL was added to these cultures. Colluci et al., found that peripheral blood contained upregulated OPG and RANKL levels. OPG co-precipitated with TRAIL, by which more RANKL became available. Autologous T-cells added to these osteoclasts, prolonged survival of osteoclasts (11).

Solid Tumor

Using blood from patients with bone metastasis from diverse primary tumors such as melanoma, lung, prostate, kidney, breast, and colon, it was found that these cultures gave rise to more osteoclast compared to controls when no cytokines were added (33). Addition of M-CSF and RANKL nullified this effect. OCp from tumor patients were further characterized and apart from CD14 and CD11, these precursors, and not in the control group, also expressed the osteoclast marker the vitronectin receptor αvβ3, which could be typical for precursors that are a bit further differentiated, indicating that the OCp in peripheral blood of cancer patients are already a step further in differentiation. Addition of OPG did not inhibit unstimulated osteoclast formation (33). It was shown that anti-TNF blocked osteoclast formation (33), which was recently confirmed in a separate study (51) Only T-cells from osteolysis patients expressed TNF-α, and also osteoclasts derived from cancer patients expressed TNF-α (33). The same group showed in subsequent years with a relatively large cohort of heterogeneous tumors (34) and in a group of prostate cancer (35) that most osteoclasts are formed without stimulation in patients with bone metastasis, compared to cancer patients without metastasis, and least osteoclasts formed from blood from controls. In both studies, a role of IL-7 was described. IL-7 serum levels were high in patients with metastasis, lower in sera from patients without and lower in control sera. T-lymphocytes could be identified as the source for IL-7, antibodies against IL-7 significantly inhibited osteoclast formation (34, 35). In a group of gastric cancer patients, no differences were observed in numbers of osteoclasts that differentiation from blood from patients with metastases, from patients without metastases and controls (36). An important difference with the other solid tumor studies was that only cytokine stimulated conditions were considered.

Rarer Bone Diseases Associated With Increased Bone Loss

Diseases Associated With Osteopenia: Chronic Liver Disease, Crohn's Disease and Chronic Kidney Disease

Chronic liver disease can lead to osteoporosis, but not in all individuals with chronic liver disease. In attempt to explain this phenomenon, osteoclasts were cultured from blood of chronic liver disease patients with osteopenia, without osteopenia and matched healthy controls. More osteoclasts formed without adding osteoclastic cytokines M-CSF and RANKL from blood of osteopenic patients compared to non-osteopenic and healthy controls (37). Interestingly, and in line with what was found in the periodontitis study from the same group (31), only controls responded with higher osteoclast numbers when stimulated with M-CSF, whereas both osteopenic and non-osteopenic patients did not respond to addition of M-CSF. Serum levels M-CSF of both patient groups were significantly higher than controls, suggesting M-CSF priming of OCp in peripheral blood. Furthermore, number of osteoclasts cultured *in vitro*, correlated negatively with the lumbar spine density score (37).

Though Crohn's disease is an intestinal disease, it is associated with inflammatory flair-ups periods. Some of the patients develop osteoporosis, including those who are not on high levels of corticosteroids. In a study with patients in a quiescent disease stage, Oostlander et al. (38) were the first to describe the pre-stages of unstimulated osteoclast formation. It was shown that the formation of osteoclasts is preceded with a stage of cell clusters, the number of which correlate with the numbers of osteoclasts that form (38). In a similar approach as in a previous study (57), OCp were either cultured with purified autologous B-cells, T-cells or the combination or without. Osteoclasts only formed in combinations where T-cells were present, which also made part of the cell clusters that preceded osteoclast formation. More osteoclasts formed from OCp:T-cell cultures from Crohn's disease than from controls and correlated to IL-17 levels *in vitro*. TNF-α levels were highest in OCp+ T-cells, compared to T-cells alone (no secretion) or monocytes only (lower levels), indicating that the T-cell:OCp interaction induces TNF-expression (36), later confirmed by Moonen et al. (3). Interestingly, the diverse combinations of T-cells, B-cells, or T-Cells + B-cells did not affect control monocytes, indicating that the osteoclastogenesis driving T-cell activity is increased in Crohn's disease.

Bone disease in patients with chronic kidney disease (CKD) is a major clinical concern due to its prevalence and consequences that greatly impact patients quality of life (62). CKD patients may be affected by both higher and lower bone turnover disease, in patients with high bone turnover disease increased osteoclastogenesis is sustained by both increased in inflammatory and pro-osteoclastogenic cytokines and by increased PTH due to the decreased ability of kidney to hydroxylate vitamin D into its active form 1,25OHvitamin D. Patients with terminal kidney failure who are on dialysis, experience a chronically inflammatory state with often skeletal complications. Osteoclast formation was studied both without and cytokine stimulation (39). Osteoclast formation was lowest in controls, and higher in early chronic patients and higher in late chronic patients and highest in hemodialysis patients, similar correlations were seen with resorptive capacity. RANKL was expressed on T-lymphocytes in renal patients, not in controls. RANK-Fc can inactive RANKL, and when added it dose dependently decreased osteoclastogenesis, demonstrating that osteoclast formation was RANKL dependent (39).

Rare Diseases Associated With Bone Loss: Turner's Syndrome, Gaucher's Disease and Phenylketonuria

Patients with Turner's syndrome may present with decreased bone due to hypergonadism associated with the disease. Estrogen deficiency could be the course for such bone loss (40). Unstimulated osteoclast formation resulted in more osteoclasts that were more active, both in the group with high levels of follicle stimulating hormone (FSH) and with low levels. These osteoclasts resorbed more calcium phosphate. Osteoclast numbers from monocytes with addition of M-CSF and RANKL were similar between controls and patients. The increased unstimulated osteoclast formation in Turner's syndrome correlated with a lower percentage of osteoclastogenesis inhibitory CD4+CD25+ cells and a higher percentage of CD3+

NKT cells. The CD8+TNF-α+ cells were higher in Turner's syndrome, as well as the CD14+TNF-α+ monocytes. This skewness could contribute and be responsible for the increased osteoclast formation (40).

Gaucher's disease is a heritable disease with deficiency of the lysomal enzyme glucocerebrosidase, resulting in excess of glycosylceramide, which is then stored in high quantities in macrophages, concomitant with a disturbed immunological balance and cytokine secretion profiles (42). Approximately 3-fold more osteoclasts formed from Gaucher patient's PBMC cultured with M-CSF and RANKL. These osteoclasts were larger in size and number of nuclei and resorbed larger areas of bone. When distinguishing between active and non- active bone disease, the Gaucher patients with active bone disease formed more osteoclasts. Especially the Gaucher cultures were relatively independent of M-CSF (42), in line with data from periodontitis (31) and chronic liver disease patients (37). When control PBMC were cultured with inhibitors of glucocerebrosidase, increased numbers of osteoclast formed (42), indicating that this enzyme plays a key role in tempering osteoclast numbers. The increased osteoclast formation in Gaucher's disease was confirmed by Mucci et al. (41). Here, it was shown that Gaucher's disease blood contained a higher percentage of non-classical/inflammatory CD14+CD16+ cells compared to the classical CD14+CD16– monocytes. When culturing with an enzyme that replenishes the missing glucocerebrosidase, osteoclast numbers decreased only in Gaucher patients cultures, again indicating that glucocerebrosidase tempers osteoclast formation. T-cells from Gaucher's disease express more RANKL (41). Osteoclast cultures from controls were insensitive to OPG or anti-TNF-α treatment, whereas osteoclast numbers went significantly down in Gaucher's PBMC cultures that were treated with OPG or anti-TNF-α (41).

Phenylketonuria (PKU) is a rare, inherited disease with a defect in the synthesis of the amino acid phenylalanine. These patients have a hitherto not understood progressive bone impairment. Also with this disease, increased osteoclasts were cultured both without osteoclastogenesis stimulating cytokines and with these cytokines (43). As shown for Gaucher (41), the blood of PKU also contains a higher proportion of CD14+CD16+ monocytes, which co-express CD51/CD61, or αvβ3 integrin, that is typical for osteoclasts (63). The unstimulated osteoclastogenesis cultures contained increased levels of TNF-α and RANKL in PKU patients. Only RANK-Fc, that blocks RANKL activity, decreased osteoclast numbers in PKU cultures. PKU patients contained activated T- cells of the CD4+CD25+CD69+ signature, a cell type that was absent in controls.

GENERAL OSTEOCLASTOGENESIS FEATURES OF INFLAMMATORY BONE DISEASES

When summarizing the osteoclastogenesis capacity of the various inflammatory bone disease, several features become apparent (**Table 1**). Firstly, when taking together all 29 summarized studies, more osteoclasts formed, be it unstimulated or stimulated with M-CSF and RANKL. This was the case for 24 of the 29 studies. Secondly, in all cases where resorptive activity was determined, the osteoclasts from bone loss diseases were more active. Thirdly, osteoclasts can be cultured without exogenous addition of M-CSF and RANKL, only when cultured from PBMC or at least the addition of T-cells to OCp. These osteoclasts often displayed lytic activity of calcium phosphate coatings, but also bone resorption activity has been reported. Fourthly, those studies that have compared unstimulated and M-CSF and RANKL stimulated osteoclast formation, often found increased osteoclast formation in unstimulated cultures, whereas these differences were often not found any more when cultured with M-CSF and RANKL. This accounted for a variety of diseases, such as psoriatic arthritis (19), osteoporosis (17, 57), periodontitis (12, 31), multiple myeloma (11), solid tumors (33), chronic liver disease (37), kidney disease (39), and Turner's syndrome (40). This suggests that stimulation with unphysiological levels of M-CSF and RANKL may hide the intrinsically increased osteoclastogenic activities present in peripheral blood. Especially these studies with self-stimulatory osteoclastogenesis cocktails of T-cells and OCp can give us clues of common and disease specific determinants of increased osteoclast formation. Below, three common denominators which stood out when comparing the various inflammatory bone diseases, being (1) inflammatory mediators in serum, (2) the role of T-cells and (3) differential priming or skewness in monocyte distribution are worked out for the inflammatory bone diseases.

Common Inflammatory Mediators in Serum Prepares OCp in the Circulation

A different priming whilst in the circulation by increased levels of pro-osteoclastogenic mediators could make monocytes more equipped to differentiate into osteoclasts. Most commonly described is the increased presence of TNF-α, see the above paragraph where it's presence is discussed in the context of T-cells, but also in serum from patients with Charcot's disease, where it co-incides with increased numbers of CD14+ cells (53). Another such pro-osteoclastogenic cytokine is M-CSF. Higher levels of M-CSF in the circulation have been described for periodontitis (32) and chronic liver disease (37). This could make PBMC from these patients less responsive to exogenous M-CSF (31, 37).

A Common Role for T-Cells in Osteoclast Formation in the Various Inflammatory Bone Diseases

The general role of T- cells in osteoclast regulation (64), the role of osteoclast activating T-cells such as Th17 (65) and the regulatory role of Treggs (66) have been reviewed elsewhere. Here, we describe the T-cell findings in the context of inflammatory diseases with bone loss in the context of the core collection used for this review. When reviewing the above literature it is clear that T-cells are indispensable for spontaneous osteoclastogenesis: without T-cells, no osteoclasts form. This has been investigated for psoriatic arthritis (19, 48),

osteoporosis (57), periodontitis (12) and Crohn's disease (38). The mechanism by which they adhere and stimulate OCp is likely by LFA-1: ICAM-1 interaction, since antibodies against LFA-1 interfere both with cell cluster formation and with osteoclast formation (38). TNF-α is most commonly reported as the cytokine secreted by T-cells in the various diseases. T-cells from patients with inflammatory bone loss diseases secrete more TNF-α, as shown for psoriatic arthritis (19), osteoporosis (57), periodontitis (12), and Turner's syndrome (40). Exclusively the T-cells from peripheral blood from patients with osteolytic solid tumors and not those without osteolytic tumors were reported to express detectable levels of TNF-α (34). Treating unstimulated osteoclastogenesis cultures with anti TNF-α agent infliximab reduces both cell cluster formation and osteoclast formation (51). Anti-TNF-α treatment also decreased osteoclast formation in patients with RA (18), periodontitis (12), and Gaucher's disease (41). T-cells from inflammatory bone diseases express more RANKL, as reported for RA (21), osteoporosis (57), and chronic kidney disease (39). Anti RANKL reduced osteoclast formation in Gaucher's disease more than in controls (41), and also in phenylketonuria patients (43), chronic kidney disease (39). Studies with RANKL-independent osteoclast formation were also reported (33, 37). In these studies, OPG or RANK-Fc did not affect osteoclast formation. Two osteoclastogenesis studies from solid tumors report spontaneous osteoclastogenesis stimulated by T-cell secreted IL-7 (34, 35). This has not been studied in the other inflammatory bone loss diseases. Finally, it has been reported for myeloma derived osteoclasts that autologous T-cells added to osteoclast cultures may prolong osteoclast survival (11).

A Different Distribution of Monocytes Subtypes and Different Monocyte Priming in Inflammatory Diseases

A third commonality between the different diseases is that due to the inflammatory disease, a skewed distribution of monocytes that is better equipped to differentiate into osteoclasts populate the peripheral blood. The existence of different monocyte populations (2, 67) which distributions are then different between disease and controls, is indeed a very attractive explanation for the outcome of more osteoclasts in inflammatory disease. One way to achieve a relatively crude and likely heterogeneous populations of OCp is with CD14+ positive isolation. Studies that show more osteoclasts as outcome, where equal numbers of purified CD14+ monocytes were uses in disease vs. healthy controls, provide a first indication for a better equipment of these cells for osteoclast differentiation. This has been shown for RA and psoriatic arthritis (20) and for periodontitis (32). When comparing monocyte heterogeneity, two different criteria have been used in the articles assessed in this review: an approach based on CD14, CD11b, and the vitronectin receptor (VNR) expression and the more commonly used CD14/CD16 expression of monocytes. One study that has used CD14+ in conjunction with CD11b and the vitronectin receptor or αvβ3 showed that peripheral blood of osteolytic cancers contained more VNR+ monocytes, which correlated to higher osteoclast formation (33).

The much more commonly used classification of monocytes is based on their CD14 and CD16 expression. The CD14+CD16– are the classical monocytes that become the phagocytic cells in tissues and comprise the majority of blood monocytes, intermediate monocytes are CD14+CD16+ and are pro-inflammatory and play a role in wound healing, and the CD14+CD16++ cells are the non-classical monocytes that play a role in patrolling and fibrosis (2, 67). Initial description on either CD16– and CD16+, before the subsequent refinement of CD16+ monocytes into intermediate and non-classical monocytes (68) and also recent literature on the transcriptome of the classical and non-classical monocytes (69) suggest that the physiological osteoclasts derive from classical, CD14+CD16– monocytes. This was refined recently by Sprangers et al., who found that all three monocyte subtypes differentiate equally well on plastic, but that only the classical and intermediate ones form resorbing osteoclasts on bone (6). On bone slices, non-classical monocytes hardly differentiated and no resorption was observed. For some of the inflammatory bone loss diseases, however, several studies indicate that likely the CD16+ monocytes are important for osteoclast formation. A skew distribution compared to healthy controls was demonstrated for several inflammatory bone loss diseases. It was demonstrated for multiple myeloma, that CD14+CD16+ monocytes are predominant in active disease

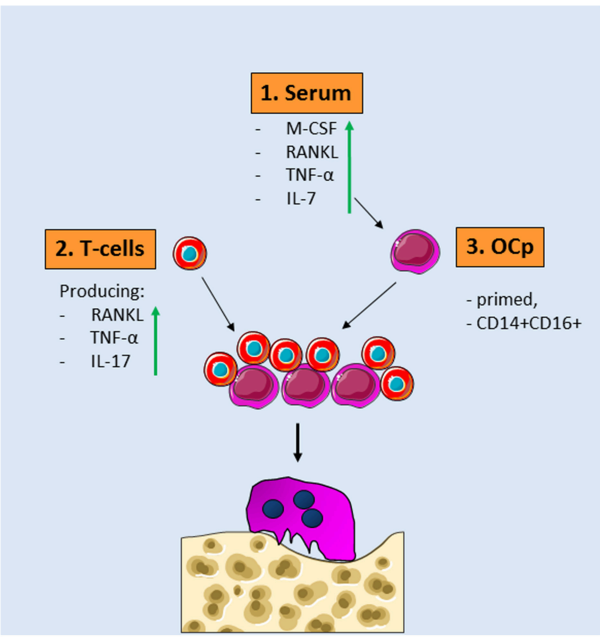

FIGURE 2 | Common denominators for osteoclast formation in diseases with inflammatory bone loss. **1**. Serum of patients with inflammatory bone loss diseases contains more osteoclastogenesis stimulating factors such as RANKL, TNF-α, IL-7, and M-CSF. **2**. These serum factors prime OCp present in peripheral blood. These OCp are skewed toward more CD14+CD16+ cells. **3**. T-cells from patients with inflammatory bone diseases express more IL-17, RANKL, and TNF-α. When these different OCp and T-cells—both of them different from controls—are added together, more osteoclasts are formed that are more active in bone resorption.

compared to smoldering disease. These cells gave rise to larger osteoclasts (70). Also in kidney disease, more CD14+CD16+ monocytes were found in peripheral blood, and exclusively more "inflammatory" monocytes expressed RANKL, providing the possibility for auto-stimulation (39). Patients with Gaucher's disease (41) and patients with phenylketonuria (43) have more CD14+CD16+ monocytes in peripheral blood than matched controls. All the above studies are association studies, where a higher percentage of CD14+CD16+ in blood of patients is associated with increased osteoclast formation. To prove that these cells indeed give rise to more osteoclasts, Chiu et al., have sorted the three subtypes of OCp from psoriatic arthritis patients and healthy controls (71). Interestingly, the CD16+ monocytes from controls gave rise to low levels of osteoclasts, whereas the CD16+ monocytes from patients gave rise to high numbers of osteoclasts. This suggests that apart from the common distinction of OCp with the CD14 and CD16 markers, other features have been acquired by psoriatic arthritis patients, making them more equipped to differentiate into osteoclasts. An experiment with healthy control OCps confirmed the relative inertness of CD16+ monocytes in healthy controls. When adding increasing numbers of CD16+ monocytes to a constant number of CD14+CD16– monocytes in an osteoclastogenesis experiment, there was no increase in osteoclast numbers, suggesting that under these conditions, only the CD14+CD16– monocytes contributed to the formation of a syncytium (72).

Concluding Remarks on the Common Denominators for Increased Osteoclast Formation in Patients With Inflammation Related Bone Loss

In summary, this core collection of studies with well-matched bone-loss patient—healthy controls, unequivocally shows an increased osteoclast formation and activity in patients with inflammatory bone loss. In search for the conditions that give rise to this, several factors that are shared between diseases can be identified. First of all, the serum that surrounds OCp in the circulation is beneficiary for the differentiation of OCp. Second, T-cells that secrete TNF-α and RANKL are present in the circulation of patients. In light of the fact that inflammatory bone loss diseases may occur simultaneously, anti-TNF-α treatment could benefit more than one disease, as was shown for instance in rheumatoid arthritis patients receiving anti-TNF-α medication infliximab, who had lower periodontal indices. Finally, the patient blood may contain more OCp and differently primed OCp, probably containing the CD14+CD16+ phenotype rather than CD14+CD16–. On top of that, either disease specific or a general immunological stimulus has given the OCp from bone loss patients a profile to facilitate enhance osteoclast formation (**Figure 2**). Future research will likely uncover the barcodes of the OCps in the various inflammatory diseases associated with bone loss. This knowledge of the biological mechanisms underlying the alterations of monocytes and osteoclasts will likely reveal future therapeutic targets that will specifically target the immune system-steered osteoclast formation.

AUTHOR CONTRIBUTIONS

TV wrote most of the manuscript and coordinated feedback. IB performed literature search and drafted the initial parts of the manuscript. TK commented on earlier versions of the manuscript. GS critically evaluated the rheumatology part. IJ critically evaluated all stages of the manuscript. GS and PD put the manuscript in a clinical context. PD wrote the sections on osteoporosis.

REFERENCES

1. Boyce BF, Yao Z, Xing L. Osteoclasts have multiple roles in bone in addition to bone resorption. *Crit Rev Eukaryot Gene Expr.* (2009) 19:171–80. doi: 10.1615/CritRevEukarGeneExpr.v19.i3.10
2. Sprangers S, de Vries TJ, Everts V. Monocyte heterogeneity: consequences for monocyte-derived immune cells. *J Immunol Res.* (2016) 2016:1475435. doi: 10.1155/2016/1475435
3. Moonen CGJ, Alders ST, Bontkes HJ, Schoenmaker T, Nicu EA, Loos BG, et al. Survival, retention, and selective proliferation of lymphocytes is mediated by gingival fibroblasts. *Front Immunol.* (2018) 9:1725. doi: 10.3389/fimmu.2018.01725
4. Mbalaviele G, Novack DV, Schett G, Teitelbaum SL. Inflammatory osteolysis: a conspiracy against bone. *J Clin Invest.* (2017) 127:2030–9. doi: 10.1172/jci93356
5. De Vries TJ, Schoenmaker T, Hooibrink B, Leenen PJ, Everts V. Myeloid blasts are the mouse bone marrow cells prone to differentiate into osteoclasts. *J Leukoc Biol.* (2009) 85:919–27. doi: 10.1189/jlb.0708402
6. Sprangers S, Schoenmaker T, Cao Y, Everts V, de Vries TJ. Different blood-borne human osteoclast precursors respond in distinct ways to IL-17A. *J Cell Physiol.* (2016) 231:1249–60. doi: 10.1002/jcp.25220
7. Salamanna F, Maglio M, Borsari V, Giavaresi G, Aldini NN, Fini M. Peripheral blood mononuclear cells spontaneous osteoclastogenesis: mechanisms driving the process and clinical relevance in skeletal disease. *J Cell Physiol.* (2016) 231:521–30. doi: 10.1002/jcp.25134
8. Kong YY, Feige U, Sarosi I, Bolon B, Tafuri A, Morony S, et al. Activated T cells regulate bone loss and joint destruction in adjuvant arthritis through osteoprotegerin ligand. *Nature.* (1999) 402:304–9. doi: 10.1038/46303
9. Yasuda H, Shima N, Nakagawa N, Mochizuki SI, Yano K, Fujise N, et al. Identity of osteoclastogenesis inhibitory factor (OCIF) and osteoprotegerin (OPG): a mechanism by which OPG/OCIF inhibits osteoclastogenesis *in vitro*. *Endocrinology.* (1998) 139:1329–37. doi: 10.1210/endo.139.3.5837
10. Xiong J, Onal M, Jilka RL, Weinstein RS, Manolagas SC, O'Brien CA. Matrix-embedded cells control osteoclast formation. *Nat Med.* (2011) 17:1235–41. doi: 10.1038/nm.2448
11. Colucci S, Brunetti G, Rizzi R, Zonno A, Mori G, Colaianni G, et al. T cells support osteoclastogenesis in an *in vitro* model derived from human multiple myeloma bone disease: the role of the OPG/TRAIL interaction. *Blood.* (2004) 104:3722–30. doi: 10.1182/blood-2004-02-0474
12. Brunetti G, Colucci S, Pignataro P, Coricciati M, Mori G, Cirulli N, et al. Grano. T cells support osteoclastogenesis in an *in vitro* model derived from human periodontitis patients. *J Periodontol.* (2005) 76:1675–80. doi: 10.1902/jop.2005.76.10.1675
13. Takayanagi H, Iizuka H, Juji T, Nakagawa T, Yamamoto A, Miyazaki T, et al. Involvement of receptor activator of nuclear factor kappaB

ligand/osteoclast differentiation factor in osteoclastogenesis from synoviocytes in rheumatoid arthritis. *Arthritis Rheum*. (2000) 43:259–69. doi: 10.1002/1529-0131(200002)43:2<259::Aid-anr4>3.0.Co;2-w
14. Sokos D, Everts V, De Vries TJ. Role of periodontal ligament fibroblasts in osteoclastogenesis: a review. *J Periodontal Res*. (2015) 50:152–9. doi: 10.1111/jre.12197
15. Kim N, Kadono Y, Takami M, Lee J, Lee S, H, Okada F, et al. Osteoclast differentiation independent of the TRANCE-RANK-TRAF6 axis. *J Exp Med*. (2005) 202:589–95. doi: 10.1084/jem.20050978
16. Anandarajah AP, Schwarz EM, Totterman S, Monu J, Feng CY, Shao T, et al. The effect of etanercept on osteoclast precursor frequency and enhancing bone marrow oedema in patients with psoriatic arthritis. *Ann Rheum Dis*. (2008) 67:296–301. doi: 10.1136/ard.2007.076091
17. D'Amelio P, Grimaldi A, Pescarmona GP, Tamone C, Roato I, Isaia G. Spontaneous osteoclast formation from peripheral blood mononuclear cells in postmenopausal osteoporosis. *FASEB J*. (2005) 19, 410–2. doi: 10.1096/fj.04-2214fje
18. Ritchlin CT, Haas-Smith SA, Li P, Hicks DG, Schwarz EM. Mechanisms of TNF-alpha- and RANKL-mediated osteoclastogenesis and bone resorption in psoriatic arthritis. *J Clin Invest*. (2003) 111:821–31. doi: 10.1172/JCI200316069
19. Colucci S, Brunetti G, Cantatore FP, Oranger A, Mori G, Quarta L, et al. Lymphocytes and synovial fluid fibroblasts support osteoclastogenesis through RANKL, TNFalpha, and IL-7 in an *in vitro* model derived from human psoriatic arthritis. *J Pathol*. (2007) 212:47–55. doi: 10.1002/path.2153
20. Ikic M, Jajic Z, Lazic E, Ivcevic S, Grubisic F, Marusic A, et al. Association of systemic and intra-articular osteoclastogenic potential, pro-inflammatory mediators and disease activity with the form of inflammatory arthritis. *Int Orthop*. (2014) 38:183–92. doi: 10.1007/s00264-013-2121-0
21. Miranda-Carus ME, Benito-Miguel M, Balsa A, Cobo-Ibanez T, Perez DA, Pascual-Salcedo D, et al. Peripheral blood T lymphocytes from patients with early rheumatoid arthritis express RANKL and interleukin-15 on the cell surface and promote osteoclastogenesis in autologous monocytes. *Arthritis Rheum*. (2006) 54:1151–64. doi: 10.1002/art.21731
22. Durand M, Boire G, Komarova SV, Dixon SJ, Sims SM, Harrison RE, et al. The increased *in vitro* osteoclastogenesis in patients with rheumatoid arthritis is due to increased percentage of precursors and decreased apoptosis—the In Vitro Osteoclast Differentiation in Arthritis (IODA) study. *Bone*. (2011) 48:588–96. doi: 10.1016/j.bone.2010.10.167
23. Shang W, Zhao LJ, Dong XL, Zhao ZM, Li J, Zhang BB, et al. Curcumin inhibits osteoclastogenic potential in PBMCs from rheumatoid arthritis patients via the suppression of MAPK/RANK/c-Fos/NFATc1 signaling pathways. *Mol Med Rep*. (2016) 14:3620–6. doi: 10.3892/mmr.2016.5674
24. Durand M, Komarova SV, Bhargava A, Trebec-Reynolds DP, Li K, Fiorino C, et al. Monocytes from patients with osteoarthritis display increased osteoclastogenesis and bone resorption: the *In Vitro* Osteoclast Differentiation in Arthritis study. *Arthritis Rheum*. (2013) 65:148–58. doi: 10.1002/art.37722
25. Caparbo VF, Saad CGS, Moraes JC, de Brum-Fernandes AJ, Pereira RMR. Monocytes from male patients with ankylosing spondylitis display decreased osteoclastogenesis and decreased RANKL/OPG ratio. *Osteoporos Int*. (2018) 29:2565–73. doi: 10.1007/s00198-018-4629-z
26. Mabilleau G, Petrova NL, Edmonds ME, Sabokbar A. Increased osteoclastic activity in acute Charcot's osteoarthropathy: the role of receptor activator of nuclear factor-kappaB ligand. *Diabetologia*. (2008) 51:1035–40. doi: 10.1007/s00125-008-0992-1
27. Park JK, Fava A, Carrino J, Del Grande F, Rosen A, Boin F. Association of acroosteolysis with enhanced osteoclastogenesis and higher blood levels of vascular endothelial growth factor in systemic sclerosis. *Arthritis Rheumatol*. (2016) 68:201–9. doi: 10.1002/art.39424
28. Jevon M, Hirayama T, Brown MA, Wass JA, Sabokbar A, Ostelere S, et al. Osteoclast formation from circulating precursors in osteoporosis. *Scand J Rheumatol*. (2003) 32:95–100. doi: 10.1080/03009740310000102
29. D'Amelio P, Grimaldi A, Di Bella S, Tamone C, Brianza SZ, Ravazzoli MG, et al. Risedronate reduces osteoclast precursors and cytokine production in postmenopausal osteoporotic women. *J Bone Miner Res*. (2008) 23:373–9. doi: 10.1359/jbmr.071031
30. Koek WNH, van der Eerden BCJ, Alves R, van Driel M, Schreuders-Koedam M, Zillikens MC, et al. Osteoclastogenic capacity of peripheral blood mononuclear cells is not different between women with and without osteoporosis. *Bone*. (2017) 95:108–14. doi: 10.1016/j.bone.2016.11.010
31. Tjoa STS, De Vries TJ, Schoenmaker T, Kelder A, Loos BG, Everts V. Formation of osteoclast-like cells from peripheral blood of periodontitis patients occurs without supplementation of M-CSF. *J Clin Periodontol*. (2008) 35:568575. doi: 10.1111/j.1600-051X.2008.01241.x
32. Herrera BS, Bastos AS, Coimbra LS, Teixeira SA, Rossa C Jr, Van Dyke TE, et al. Peripheral blood mononuclear phagocytes from patients with chronic periodontitis are primed for osteoclast formation. *J Periodontol*. (2014) 85:e72–81. doi: 10.1902/jop.2013.130280
33. Roato I, Grano M, Brunetti G, Colucci S, Mussa A, Bertetto O, et al. Mechanisms of spontaneous osteoclastogenesis in cancer with bone involvement. *FASEB J*. (2005) 19:228–30. doi: 10.1096/fj.04-1823fje
34. Roato I, Gorassini E, Brunetti G, Grano M, Ciuffreda L, Mussa A, et al. IL-7 modulates osteoclastogenesis in patients affected by solid tumors. *Ann N Y Acad Sci*. (2007) 1117:377–84. doi: 10.1196/annals.1402.002
35. Roato I, D'Amelio P, Gorassini E, Grimaldi A, Bonello L, Fiori C, et al. Osteoclasts are active in bone forming metastases of prostate cancer patients. *PLoS ONE*. (2008) 3:e3627. doi: 10.1371/journal.pone.0003627
36. D'Amico L, Satolli MA, Mecca C, Castiglione A, Ceccarelli M, D'Amelio P, et al. Bone metastases in gastric cancer follow a RANKL-independent mechanism. *Oncol Rep*. (2013) 29:1453–8. doi: 10.3892/or.2013.2280
37. Olivier BJ, Schoenmaker T, Mebius RE, Everts V, Mulder CJ, van Nieuwkerk KM, et al. Increased osteoclast formation and activity by peripheral blood mononuclear cells in chronic liver disease patients with osteopenia. *Hepatology*. (2008) 47, 259–67. doi: 10.1002/hep.21971
38. Oostlander A, Everts V, Schoenmaker T, Bravenboer N, van Vliet SJ, van Bodegraven AA, et al. T cell-mediated increased osteoclast formation from peripheral blood as a mechanism for Crohn's disease-associated bone loss. *J Cell Biochem*. (2012) 113:260–8. doi: 10.1002/jcb.23352
39. Cafiero C, Gigante M, Brunetti G, Simone S, Chaoul N, Oranger A, et al. Inflammation induces osteoclast differentiation from peripheral mononuclear cells in chronic kidney disease patients: crosstalk between the immune and bone systems. *Nephrol Dial Transplant*. (2018) 33:65–75. doi: 10.1093/ndt/gfx222
40. Faienza MF, Brunetti G, Ventura A, Piacente L, Messina MF, De Luca F, et al. Mechanisms of enhanced osteoclastogenesis in girls and young women with Turner's Syndrome. *Bone*. (2015) 81:228–36. doi: 10.1016/j.bone.2015.07.021
41. Mucci JM, Cuello MF, Kisinovsky I, Larroude M, Delpino MV, Rozenfeld PA. Proinflammatory and proosteoclastogenic potential of peripheral blood mononuclear cells from Gaucher patients: implication for bone pathology. *Blood Cells Mol Dis*. (2015) 55:134–43. doi: 10.1016/j.bcmd.2015.05.009
42. Reed M, Baker RJ, Mehta AB, Hughes DA. Enhanced differentiation of osteoclasts from mononuclear precursors in patients with Gaucher disease. *Blood Cells Mol Dis*. (2013) 51:185–94. doi: 10.1016/j.bcmd.2013.04.006
43. Roato I, Porta F, Mussa A, D'Amico L, Fiore L, Garelli D, et al. Bone impairment in phenylketonuria is characterized by circulating osteoclast precursors and activated T cell increase. *PLoS ONE*. (2010) 5:e14167. doi: 10.1371/journal.pone.0014167
44. Gravallese EM, Goldring SR. Cellular mechanisms and the role of cytokines in bone erosions in rheumatoid arthritis. *Arthritis Rheum*. (2000) 43:2143–51. doi: 10.1002/1529-0131(200010)43:10<2143::Aid-anr1>3.0.Co;2-s
45. Gravallese EM, Manning C, Tsay A, Naito A, Pan C, Amento E, et al. Synovial tissue in rheumatoid arthritis is a source of osteoclast differentiation factor. *Arthritis Rheum*. (2000) 43:250–8. doi: 10.1002/1529-0131(200002)43:2<250::AID-ANR3>3.0.CO;2-P
46. Herman S, Muller RB, Kronke G, Zwerina J, Redlich K, Hueber AJ, et al. Induction of osteoclast-associated receptor, a key osteoclast costimulation molecule, in rheumatoid arthritis. *Arthritis Rheum*. (2008) 58:3041–50. doi: 10.1002/art.23943
47. Gengenbacher M, Sebald HJ, Villiger PM, Hofstetter W, Seitz M. Infliximab inhibits bone resorption by circulating osteoclast precursor cells in patients with rheumatoid arthritis and ankylosing spondylitis. *Ann Rheum Dis*. (2008) 67:620–4. doi: 10.1136/ard.2007.076711
48. Vandooren B, Melis L, Veys EM, Tak PP, Baeten D. *In vitro* spontaneous osteoclastogenesis of human peripheral blood mononuclear cells is not

crucially dependent on T lymphocytes. *Arthritis Rheum*. (2009) 60:1020–5. doi: 10.1002/art.24413
49. Horwood NJ, Kartsogiannis V, Quinn JM, Romas E, Martin TJ, Gillespie MT. Activated T lymphocytes support osteoclast formation *in vitro*. *Biochem Biophys Res Commun*. (1999) 265:144–50. doi: 10.1006/bbrc.1999.1623
50. Gravallese EM, Schett G. Effects of the IL-23-IL-17 pathway on bone in spondyloarthritis. *Nat Rev Rheumatol*. (2018) 14:631–40. doi: 10.1038/s41584-018-0091-8
51. de Vries TJ, Yousovich J, Schoenmaker T, Scheres N, Everts V. Tumor necrosis factor-alpha antagonist infliximab inhibits osteoclast formation of peripheral blood mononuclear cells but does not affect periodontal ligament fibroblast-mediated osteoclast formation. *J Periodontal Res*. (2016) 51:186–95. doi: 10.1111/jre.12297
52. Xue Y, Jiang L, Cheng Q, Chen H, Yu Y, Lin Y, et al. Adipokines in psoriatic arthritis patients: the correlations with osteoclast precursors and bone erosions. *PLoS ONE*. (2012) 7:e46740. doi: 10.1371/journal.pone.0046740
53. Mabilleau G, Petrova N, Edmonds ME, Sabokbar A. Number of circulating CD14-positive cells and the serum levels of TNF-α are raised in acute charcot foot. *Diabetes Care*. (2011) 34:e33. doi: 10.2337/dc10-1695
54. Niida S, Kaku M, Amano H, Yoshida H, Kataoka H, Nishikawa S, et al. Vascular endothelial growth factor can substitute for macrophage colony-stimulating factor in the support of osteoclastic bone resorption. *J Exp Med*. (1999) 190:293–8. doi: 10.1084/jem.190.2.293
55. Watad A, Bridgewood C, Russell T, Marzo-Ortega H, Cuthbert R, McGonagle D. The early phases of ankylosing spondylitis: emerging insights from clinical and basic science. *Front Immunol*. (2018) 9:2668. doi: 10.3389/fimmu.2018.02668
56. Tella SH, Gallagher JC. Prevention and treatment of postmenopausal osteoporosis. *J Steroid Biochem Mol Biol*. (2014) 142:155–70. doi: 10.1016/j.jsbmb.2013.09.008
57. D'Amelio P, Grimaldi A, Di Bella S, Brianza SZ, Cristofaro MA, Tamone C, et al. Estrogen deficiency increases osteoclastogenesis up-regulating T cells activity: a key mechanism in osteoporosis. *Bone*. (2008) 43:92–100. doi: 10.1016/j.bone.2008.02.017
58. Drake MT, Clarke BL, Lewiecki EM. The pathophysiology and treatment of osteoporosis. *Clin Ther*. (2015) 37:1837–50. doi: 10.1016/j.clinthera.2015.06.006
59. de Vries TJ, Andreotta S, Loos BG, Nicu EA. Genes critical for developing periodontitis: lessons from mouse models. *Front Immunol*. (2017) 8:1395. doi: 10.3389/fimmu.2017.01395
60. Loos BG, Papantonopoulos G, Jepsen S, Laine ML. What is the contribution of genetics to periodontal risk? *Dent Clin N Am*. (2015) 59:761–80. doi: 10.1016/j.cden.2015.06.005
61. Bakri Y, Sarrazin S, Mayer UP, Tillmanns S, Nerlov C, Boned A, et al. Balance of MafB and PU.1 specifies alternative macrophage or dendritic cell fate. *Blood*. (2005) 105:2707–16. doi: 10.1182/blood-2004-04-1448
62. Nitta K, Yajima A, Tsuchiya K. Management of osteoporosis in chronic kidney disease. *Intern Med*. (2017) 56:3271–6. doi: 10.2169/internalmedicine.8618-16
63. Horton MA, Taylor ML, Arnett TR, Helfrich MH. Arg-Gly-Asp (RGD) peptides and the anti-vitronectin receptor antibody 23C6 inhibit dentine resorption and cell spreading by osteoclasts. *Exp Cell Res*. (1991) 195:368–75. doi: 10.1016/0014-4827(91)90386-9
64. D'Amico L, Roato I. Cross-talk between T cells and osteoclasts in bone resorption. *Bonekey Rep*. (2012) 1:82. doi: 10.1038/bonekey.2012.82
65. Wakkach A, Rouleau M, Blin-Wakkach C. Osteoimmune interactions in inflammatory bowel disease: central role of bone marrow Th17 TNFalpha cells in osteoclastogenesis. *Front Immunol*. (2015) 6:640. doi: 10.3389/fimmu.2015.00640
66. Bozec A, Zaiss MM. T regulatory cells in bone remodelling. *Curr Osteoporos Rep*. (2017) 15:121–5. doi: 10.1007/s11914-017-0356-1
67. Ziegler-Heitbrock L, Ancuta P, Crowe S, Dalod M, Grau V, Hart DN, et al. Nomenclature of monocytes and dendritic cells in blood. *Blood*. (2010) 116:74–80. doi: 10.1182/blood-2010-02-258558
68. Geissmann F, Jung S, Littman DR. Blood monocytes consist of two principal subsets with distinct migratory properties. *Immunity*. (2003) 19:71–82. doi: 10.1016/S1074-7613(03)00174-2
69. Anbazhagan K, Duroux-Richard I, Jorgensen C, Apparailly F. Transcriptomic network support distinct roles of classical and non-classical monocytes in human. *Int Rev Immunol*. (2014) 33:470–89. doi: 10.3109/08830185.2014.902453
70. Bolzoni M, Ronchetti D, Storti P, Donofrio G, Marchica V, Costa F, et al. IL21R expressing $CD14^{+}CD16^{+}$ monocytes expand in multiple myeloma patients leading to increased osteoclasts. *Haematologica*. (2017) 102:773–84. doi: 10.3324/haematol.2016.153841
71. Chiu YG, Shao T, Feng C, Mensah KA, Thullen M, Schwarz EM, et al. CD16 (FcRgammaIII) as a potential marker of osteoclast precursors in psoriatic arthritis. *Arthritis Res Ther*. (2010) 12:R14. doi: 10.1186/ar2915
72. Komano Y, Nanki T, Hayashida K, Taniguchi K, Miyasaka N. Identification of a human peripheral blood monocyte subset that differentiates into osteoclasts. *Arthritis Res Ther*. (2006) 8:R152. doi: 10.1186/ar2046

Conflict of Interest Statement: The authors declare that the research was conducted in the absence of any commercial or financial relationships that could be construed as a potential conflict of interest.

frontiers in Immunology

PERSPECTIVE
published: 26 March 2019
doi: 10.3389/fimmu.2019.00596

Imaging the Bone-Immune Cell Interaction in Bone Destruction

Tetsuo Hasegawa[1,2], *Junichi Kikuta*[1,3] *and Masaru Ishii*[1,3]*

[1] *Department of Immunology and Cell Biology, Graduate School of Medicine and Frontier Biosciences, Osaka University, Osaka, Japan,* [2] *Division of Rheumatology, Department of Internal Medicine, Keio University School of Medicine, Tokyo, Japan,* [3] *WPI-Immunology Frontier Research Center, Osaka University, Osaka, Japan*

Bone is a highly dynamic organ that is continuously being remodeled by the reciprocal interactions between bone and immune cells. We have originally established an advanced imaging system for visualizing the *in vivo* behavior of osteoclasts and their precursors in the bone marrow cavity using two-photon microscopy. Using this system, we found that the blood-enriched lipid mediator, sphingosine-1-phosphate, controlled the migratory behavior of osteoclast precursors. We also developed pH-sensing chemical fluorescent probes to detect localized acidification by bone-resorbing osteoclasts on the bone surface *in vivo*, and identified two distinct functional states of differentiated osteoclasts, "bone-resorptive" and "non-resorptive." Here, we summarize our studies on the dynamics and functions of bone and immune cells within the bone marrow. We further discuss how our intravital imaging techniques can be applied to evaluate the mechanisms of action of biological agents in inflammatory bone destruction. Our intravital imaging techniques would be beneficial for studying the cellular dynamics in arthritic inflammation and bone destruction *in vivo* and would also be useful for evaluating novel therapies in animal models of bone-destroying diseases.

Keywords: intravital imaging, two-photon microscopy, cellular dynamics, bone, osteoclast, pH probe

OPEN ACCESS

Edited by:
Claudine Blin-Wakkach, UMR7370 Laboratoire de Physio Médecine Moléculaire, France

Reviewed by:
Vincent Everts, Academic Centre for Dentistry Amsterdam (ACTA), Netherlands
Jenny A. F. Vermeer, University of Oxford, United Kingdom
Dominique Heymann, INSERM U1232 Centre de Recherche en Cancérologie et Immunologie Nantes Angers, France

***Correspondence:**
Masaru Ishii
mishii@icb.med.osaka-u.ac.jp

Specialty section:
This article was submitted to Inflammation, a section of the journal Frontiers in Immunology

Received: *13 December 2018*
Accepted: *05 March 2019*
Published: *26 March 2019*

Citation:
Hasegawa T, Kikuta J and Ishii M (2019) Imaging the Bone-Immune Cell Interaction in Bone Destruction. Front. Immunol. 10:596. doi: 10.3389/fimmu.2019.00596

INTRODUCTION

The interdisciplinary research field focusing on the crosstalk between the bone and immune systems, termed "osteoimmunology," has revealed extensive reciprocal interplay between the two systems (1–3). Over the past two decades, a number of molecules, including cytokines, receptors, and transcription factors, have been shown to link the two systems, leading to successful translation of research into therapeutic approaches in osteoimmune diseases, such as rheumatoid arthritis (RA) (4). Bone and immune cells are in close contact with each other, and mechanisms of cell migration play a key role in their interplay. The development of an intravital imaging system using two-photon microscopy, combined with an increasing variety of fluorescent reporter mouse strains and fluorescence probes, has provided insight into the dynamic behavior of osteoclasts, osteoblasts, macrophages, and T cells in the bone marrow of living mice. This approach facilitates investigation of cellular dynamics in the pathogenesis of osteoimmune diseases and enables direct observation of complex biological phenomena *in vivo*. In this review, we discuss how the advances of imaging methods in living mice have contributed to our understanding of the bone–immune cell interaction in bone destruction. Furthermore, we introduce our recent studies, including evaluation of the interaction between osteoclasts and osteoblasts, and our novel approach for evaluating the mechanisms of action of different biological agents used for the treatment of bone-destructive diseases.

TABLE 1 | Comparison of different modalities used for bone research.

Modalities	Advantages	Disadvantages
Multi-photon microscopy (MPM)	√ Efficient light detection √ Reduced phototoxicity √ Penetrates deeper into tissues √ Detection of bone by second harmonic generation (SHG)	√ Higher cost √ Artifacts caused by autofluorescence √ Difficult to image more than four colors
Confocal microscopy	√ Easy to perform simultaneous, multicolor imaging √ High spatial and temporal resolutions	√ High phototoxicity and photobleaching √ Not suitable for thick tissues because of light scattering √ Artifacts caused by autofluorescence
MicroCT	√ Three-dimensional visualization of bone architecture √ Rapid	√ No cellular information √ No molecular information
Histochemistry	√ Inexpensive √ Highly specific for individual molecules	√ No vital cell information √ Enzymatic stains cannot be easily combined

INTRAVITAL TWO-PHOTON IMAGING OF BONE TISSUE

Bone is the hardest tissue in the body. It is technically difficult to visualize interactions between bone and immune cells in the bone marrow cavities of living animals. Although conventional methods such as micro-computed tomography, histomorphological analyses, and flow cytometry, can yield information on the bone structures and molecular expression patterns, *in vivo* information on dynamic cell movements and cellular interactions is not available (**Table 1**). Fluorescent microscopy imaging allows us to better understand the cellular dynamics of organs *in vivo* (5, 6), and we have established an imaging system to visualize living bone tissue using intravital two-photon microscopy (7–10).

Two-photon excitation-based laser microscopy affords several advantages compared to conventional confocal microscopy. In the latter technique, a fluorophore absorbs energy from a single photon and subsequently releases that energy as an emitted photon. In contrast, in the former technique, a fluorophore simultaneously absorbs two photons but only in the region of the focal plane where the photon density is high. Thus, all images are of high resolution. Second, excitation by a laser operating at near-infrared wavelength reduces phototoxic tissue damage, which is essential to yield reliable results. Third, light of near-infrared wavelengths penetrates deeper into tissue (to 100–1,000 μm) compared to confocal microscopy, which yields data to only a depth of <100 μm. Thus, two-photon excitation microscopy affords efficient light detection, reduces phototoxicity, and penetrates deeper into tissues, which makes it an important imaging tool for intravital visualization of the dynamic cellular behavior of deep tissues (5, 6).

Bone marrow is surrounded by calcium phosphate crystals of the bone matrix, which can readily scatter light of near-infrared wavelengths. However, in parietal bones of mice, the distance from the bone surface to the bone marrow cavity is only 80–120 μM, which is sufficiently thin to permit controlled fluorophore excitation within the cavity. Intravital two-photon imaging of skull bone tissue allows *in vivo* visualization of the real-time behavior of bone and immune cells in bone marrow cavities, such as osteoclasts, osteoblasts, macrophages, and lymphocytes. Moreover, such imaging may be useful when it is desirable to evaluate the effects of novel drugs targeting skeletal disease.

MIGRATORY CONTROL OF OSTEOCLAST PRECURSORS

Osteoclasts develop from cells of the monocyte/macrophage lineage. However, the means by which osteoclast precursor cells migrate to bony surfaces remain elusive. In previous work, intravital two-photon imaging of skull bone tissue allowed us to define the *in vivo* behavior of osteoclast precursor macrophages in the bone marrow (**Figure 1A**). We found that a blood-enriched mediator of lipid metabolism, sphingosine-1-phosphate (S1P), controlled the migratory behavior of osteoclast precursors in combination with several chemokines (7, 8).

S1P is a bioactive sphingolipid metabolite that regulates various biological activities, including cell proliferation, motility, and survival (11). S1P signaling is involved in T cell egress from lymphoid organs to circulatory fluids (12). Fingolimod (FTY720), a modulator of S1P receptor activity, was the first US Food and Drug Administration-approved oral therapy for relapsing forms of multiple sclerosis (MS) (13). S1P signaling involves five receptors, designated S1PR1 to S1PR5 (14, 15); osteoclast precursors in the bone marrow express both S1PR1 and S1PR2. S1PR1 is extremely sensitive to low S1P concentrations, promoting cell movement toward higher S1P concentrations in circulatory fluids, whereas S1PR2 requires a higher S1P concentration for activation and negatively regulates the S1PR1 response. When macrophages enter a low-S1P environment, such as the bone marrow, S1PR1 is transported to the cell surface and then osteoclast precursor macrophages move from bone tissue into the blood vessels, reflecting positive chemotaxis along an S1P gradient. Thus, the number of osteoclast precursor macrophages on bone surfaces is determined by bidirectional exchange of osteoclast precursors with the circulation. Many preclinical studies of S1P receptor modulators have been performed on autoimmune diseases (16), with an emphasis on the roles they play in inhibiting T cell migration, but their combined effects on cells of the monocyte/macrophage lineage require further exploration.

We have also showed that vitamin D controls the migratory behavior of osteoclast precursor macrophages by suppressing S1PR2 expression (10). In that study, intravital two-photon microscopy of bone marrow revealed that the motility of osteoclast precursor macrophages was significantly increased in mice treated with active vitamin D derivatives, suggesting that

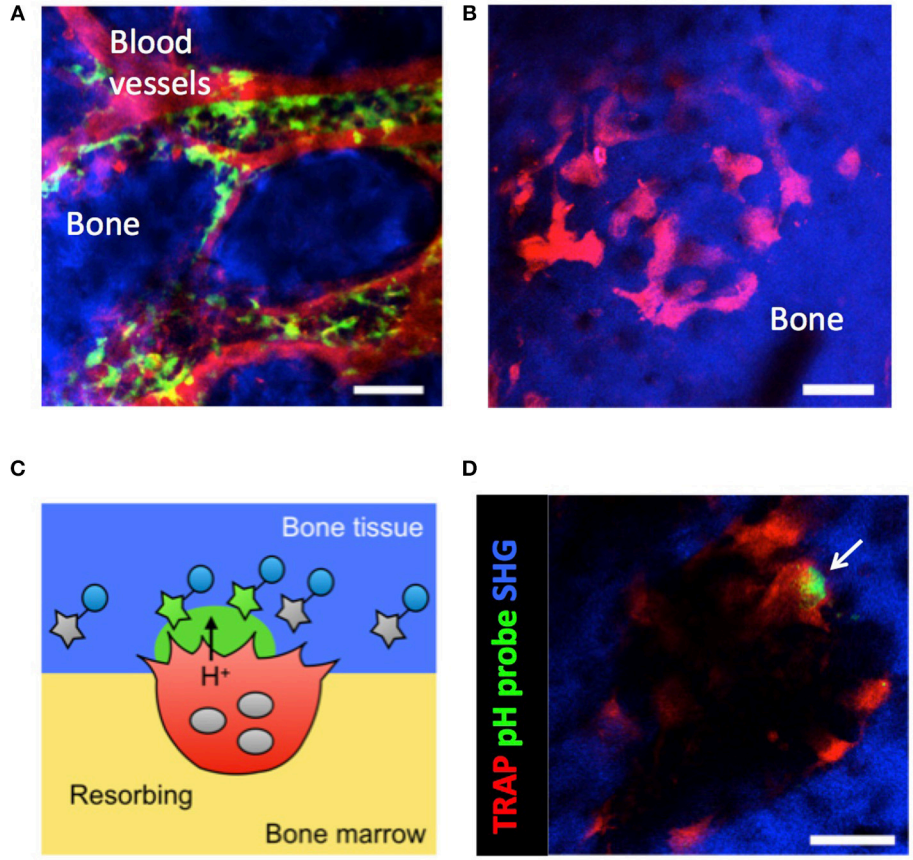

FIGURE 1 | Intravital imaging of CX_3CR1^+ osteoclast precursors and mature osteoclasts in the bone marrow. **(A)** Image of the calvaria of CX_3CR1-EGFP knock-in mice taken by two-photon microscopy. Osteoclast precursors are CX_3CR1-$EGFP^+$ (green). Blood vessels were stained via intravenous injection of Texas Red-conjugated dextran (red). Scale bar: 50 μm. The maximum intensity projections (MIPs) of two-dimensional image stacks of vertical calvarial slices are shown. **(B)** Images of the calvaria of TRAP-tdTomato transgenic mice taken by two-photon microscopy. Mature osteoclasts are $tdTomato^+$ (red). Scale bar: 50 μm. Second harmonic fluorescence generated from two-photon excitation of collagen fibers defines the bone matrix (blue). The maximum intensity projections (MIPs) of two-dimensional image stacks of vertical calvarial slices are shown. **(C)** Schematic diagram of osteoclast localization and activity evaluation using a pH-sensing fluorescent probe. **(D)** Representative intravital two-photon images of the bone marrow of heterozygous TRAP-tdTomato transgenic mice treated with a pH-sensing fluorescent probe. Mature osteoclasts expressing TRAP-tdTomato signals (red), fluorescent signals from high H^+ concentration (green), and second harmonic generation (SHG) defining the bone matrix. Some green fluorescent signal (arrow) could be detected along the bone surfaces near to osteoclasts. Scale bars: 50 μm. A two-dimensional image of the calvaria is shown.

in vivo administration of active vitamin D suppresses both S1PR2 expression and mobilization of osteoclast precursor macrophages from the blood to the bone marrow. This results in suppression of osteoclastic bone resorption *in vivo* and it is the principal effect of active vitamin D. Thus, elucidation of the migratory behavior of osteoclast precursor macrophages to the bone surface has led to a better understanding of the mechanism of conventionally used medications.

REGULATION OF BONE RESORBING CAPACITY OF MATURE OSTEOCLASTS

Mature osteoclasts must be fluorescently labeled to allow their visualization by fluorescence microscopy. Fully differentiated osteoclasts form a tight attachment zone (a "sealing zone") via interactions between integrin αvβ3 on the osteoclast membrane and bone matrix components (17). A number of vacuolar type H^+-ATPases (V-ATPase) are specifically expressed along the ruffled border membrane to maintain highly acidic conditions in the resorption pit (18). V-ATPase is composed of multiple subunits, each of which has several isoforms. Of these, the a3 isoform of the a-subunit is preferentially and abundantly expressed in mature osteoclasts (19, 20). To fluorescently label mature osteoclasts, we generated mice expressing a3 subunit-GFP fusion proteins under the control of the original promoter of the a3 subunit (a3-GFP knock-in mice).

We also generated pH-sensing chemical fluorescent probes capable of detecting localized acidification by bone-resorbing osteoclasts on the bone surface *in vivo* (**Figures 1C,D**). These probes are based on the boron-dipyrromethene (BDPM) dye combined with a bisphosphonate group. BDPM dyes are used

in several applications because of their environmental stability, large molar absorption coefficients, and high fluorescence quantum yields (21). The bisphosphonate group replaces the phosphate ion of hydroxyapatite (the principal component of bone tissue) to forms a tight bond with the bone matrix. Therefore, the bisphosphonate group facilitates probe delivery and fixation to bone in living animals (22). When mature osteoclasts secrete H^+ for bone resorption, the probe detects the fall in local pH and emits a green fluorescent signal from the bone surface (9).

Our system that allows imaging of mature osteoclasts and bone-resorbing lesion *in vivo* via intravital two-photon microscopy has enabled us to identify two distinct functional states of osteoclasts; bone-resorbing (R) cells that are firmly adherent to bones and dissolve the bone matrix by secreting acids, and non-resorbing (N) cells that are relatively loosely attached to bones and moved laterally along bone surfaces (9). Treatment with recombinant RANKL, an essential osteoclastogenic cytokine under both homeostatic and arthritic conditions (23–28), changes the composition of these populations and the total number of mature osteoclasts. We have found that RANKL not only promotes osteoclast differentiation but also regulates the bone-resorptive function of fully differentiated mature osteoclasts (9).

Furthermore, $CD4^+$ T helper 17 (Th17) cells, but not Th1, preferentially adhere to mature osteoclasts, although both T cell types migrate into bone marrow cavities to the same extent (9). Th17 cells express RANKL on the surface (29) and intravital bone imaging has shown that RANKL-bearing Th17 cells stimulate osteoclastic bone destruction by directly contacting N-state osteoclasts, converting such cells into the R-state (9). Pretreatment of Th17 cells with anti-RANKL neutralizing antibody or osteoprotegerin (OPG) reduces the interactions of such cells with the osteoclasts, but anti-RANKL antibody does not affect the mobility of Th1 cells. Thus, Th17 cells play a novel role, interacting with mature osteoclasts during inflammatory bone destruction.

CROSSTALK BETWEEN OSTEOCLASTS AND OSTEOBLASTS

Bone is a dynamic tissue that undergoes continuous remodeling by bone-resorbing osteoclasts and bone-forming osteoblasts (30). Tight control of bone remodeling through a complex communication network between osteoblast and osteoclast lineage cells is critical for maintenance of bone homeostasis in response to structural and metabolic demands. In addition, the functional balance between these two cell types determines the final clinical manifestations of arthritic diseases, such as RA and psoriatic arthritis (PsA). In RA, pathological osteoclasts on the outer surface of the periarticular bone trigger devastating bone erosion, whereas PsA is characterized by inflammation of the connective tissue between tendon and bone, leading to new bone formation at enthesial sites created by osteoblasts. Therefore, it is essential to understand the spatiotemporal relationships and interactions between mature osteoblasts and osteoclasts *in vivo*.

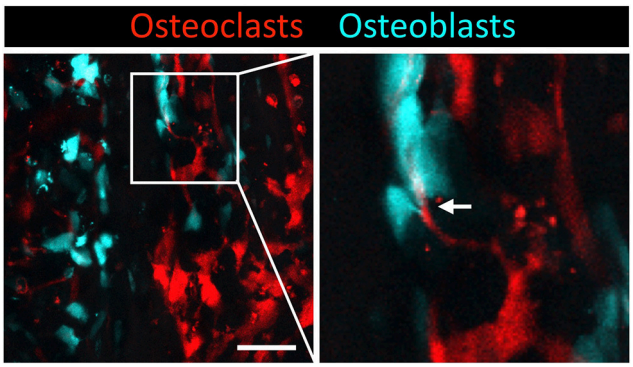

FIGURE 2 | Intravital imaging of mature osteoclasts and osteoblasts in the bone marrow. Images of the calvaria of TRAP-tdTomato/Col2.3-ECFP double fluorescently labeled mice taken via two-photon microscopy. Scale bar: 50 μm. Maximum intensity projections (MIPs) of two-dimentional image stacks of vertical calvarial slices. Mature osteoclasts express TRAP-tdTomato signals (red) and mature osteoblasts express Col2.3-ECFP signals (cyan). Arrowhead indicates the direct osteoclast-osteoblast interaction.

To visualize mature osteoclasts, we generated transgenic reporter mice expressing tdTomato (a red fluorescent protein) in the cytosol of osteoclasts (TRAP-tdTomato mice) (**Figure 1B**) (9). To visualize mature osteoblasts, we recently generated mice expressing enhanced cyan fluorescent protein (ECFP) in the cytosol of osteoblasts (Col2.3-ECFP mice) (31). To visualize communications between osteoclasts and osteoblasts, we crossed TRAP-tdTomato mice with Col2.3-ECFP mice to generate TRAP-tdTomato/Col2.3-ECFP doubly fluorescent mice (**Figure 2**). Using intravital two-photon microscopy, we successfully visualized the *in vivo* behaviors of living osteoclasts and osteoblasts on the bone surface; imaging revealed direct interactions between osteoclasts and osteoblasts *in vivo*. In wide-field views of skull bones obtained under normal conditions, the osteoclasts and osteoblasts appeared to be separately distributed, although some direct osteoclast-osteoblast interactions were identified (**Figure 2**). Time-lapse images showed that several osteoclasts that were in contact with osteoblasts developed dendritic shapes and projected synapse-like structures toward the osteoblasts. Use of our imaging technique to visualize the osteoclasts and osteoblasts of animal models of arthritis may allow us to (at least in part) define why arthritis triggers osteolysis in certain disorders (such as RA) and osteogenesis in others (such as PsA).

In addition, a pH-sensing fluorescence probe revealed that osteoclasts secrete H^+ for bone resorption when they are not in contact with osteoblasts, whereas osteoclasts in contact with osteoblasts are non-resorptive, suggesting that osteoblasts inhibit the bone resorption capacity of osteoclasts in a contact-dependent manner. Intermittent administration of parathyroid hormone led to a mixed distribution of osteoblasts and osteoclasts, thus increasing cell–cell contact to induce bone anabolic effects. The precise molecular mechanisms involved in the direct cell–cell contact should be explored in detail.

An earlier study used another mouse line featuring an osteoblast reporter, the Col2.3–GFP reporter line, to explore

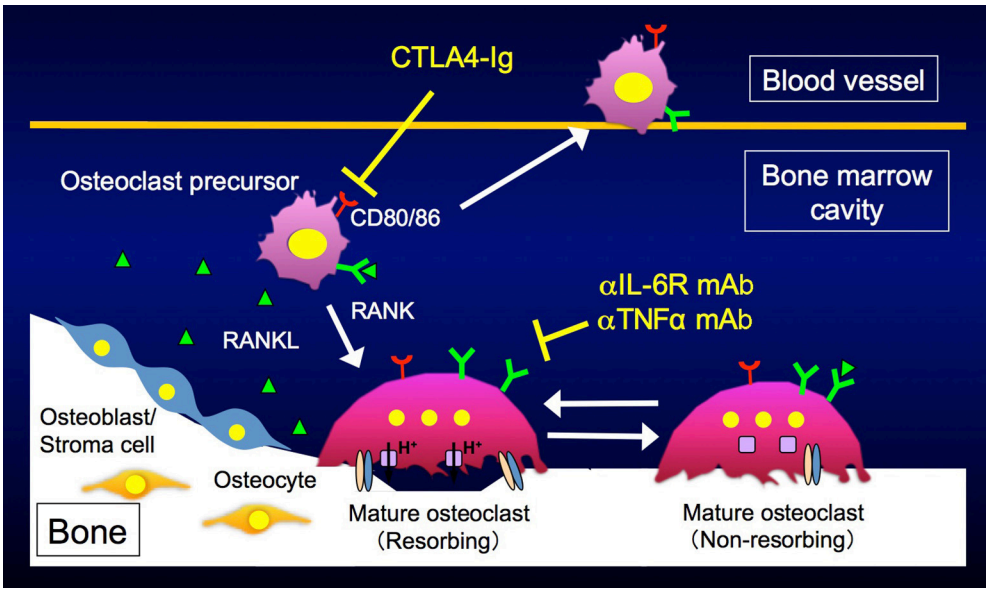

FIGURE 3 | Different modes of action of biological disease-modifying antirheumatic drugs (DMARDs). Anti-IL6R and anti-TNFα monoclonal antibodies affect mature osteoclasts and switch bone-resorbing osteoclasts to non-resorbing cells. CTLA4 mobilizes osteoclast precursors, eliminating their attachment to bone surfaces.

the interactions between T-cell acute leukemia and bone marrow microenvironment via two-photon microscopy (32). Further technical improvement in terms of bone marrow microenvironment imaging may reveal the detailed interplay between bone and the immune system not only in autoimmune diseases, but also in bone metastases and infectious diseases.

VISUALIZATION OF THE EFFECTS OF BIOLOGICAL AGENTS ON MACROPHAGE DYNAMICS DURING INFLAMMATORY BONE DESTRUCTION

Arthritic bone erosion in RA has been a major research topic in osteoimmunology. Works on the interplay between the immune and bone systems have suggested many useful drug development strategies. For example, proinflammatory cytokines, such as interleukin (IL) 6 and tumor necrosis factor α (TNFα), promote osteoclast differentiation by inducing RANKL in mesenchymal cells, and may directly stimulate both osteoclastogenesis and the bone-resorbing capacity of mature osteoclasts (33–37). Biological agents, such as monoclonal antibodies (mAbs) against IL-6 receptor (IL-6R) and TNFα, and CTLA4, have markedly improved the therapeutic outcomes of RA. Despite the differences in the molecular targets of these drugs, they equivalently suppress bone erosion in patients with RA and little is known about the differences in their modes of actions.

Using the LPS injection model, we directly visualized the *in vivo* behavior of mature osteoclasts and their precursors during inflammatory bone destruction, and explored how different biological agents affect the dynamics of these cells *in vivo* (38). We found that anti-IL-6R and anti-TNFα mAbs affected mature osteoclasts and switched bone-resorbing osteoclasts to non-resorbing cells. On the other hand, CTLA4 had no effect on mature osteoclasts but mobilized osteoclast precursor macrophages, eliminating the firm attachment of such cells to bone surfaces. In agreement with these results, CD80/86, the target molecules of CTLA4, were prominently expressed in osteoclast precursor macrophages, but were suppressed during osteoclast maturation (**Figure 3**). Taken together, these data indicate that various biological agents acted at specific therapeutic points in states of inflammatory bone destruction, and these new findings may enable us to optimize treatment efficacy for each patient by adjusting therapeutic regimens and doses, representing an important step toward personalized medicine. The development of intravital bone imaging techniques for other inflammatory bone destruction models, such as collagen-induced arthritis, will allow us to better understand the modes of action of biologics within arthritic joints.

In addition, macrophages of osteal tissues are reported to be involved in the regulation of osteoblast function, and subsequently bone dynamics (39). The additive role played of CTLA4 in bone remodeling through mobilizing osteal tissue macrophages should be further examined in the future.

CONCLUSION

Considerable progress has been made in clarifying the interplay between bone and immune cells under both physiological and inflammatory conditions. However, their dynamic crosstalk within living animals is still largely obscure. Intravital two-photon imaging provides unbiased spatiotemporal information on the biological phenomena in living organisms, which are often

much more complex than we may have hypothesized. Therefore, it is important to incorporate technical developments in imaging, such as two-photon microscopy, to directly observe the biological phenomena *in vivo* and determine the precise interplay between bone and immune systems in future studies.

AUTHOR CONTRIBUTIONS

TH, JK, and MI contributed to the discussion and wrote and reviewed the manuscript.

ACKNOWLEDGMENTS

This work was supported in part by CREST, Japan Science and Technology Agency; Grants-in-Aid for Scientific Research (A) from the Japan Society for the Promotion of Science (JSPS to MI); grants from the Uehara Memorial Foundation (to MI); from the Kanae Foundation for the Promotion of Medical Sciences (to MI); from Mochida Memorial Foundation (to MI); and from the Takeda Science Foundation (to MI).

REFERENCES

1. Takayanagi H. Osteoimmunology: shared mechanisms and crosstalk between the immune and bone systems. *Nat Rev Immunol.* (2007) 7:292–304. doi: 10.1038/nri2062
2. Takayanagi H. Osteoimmunology in 2014: two-faced immunology—from osteogenesis to bone resorption. *Nat Rev Rheumatol.* (2015) 11:74–6. doi: 10.1038/nrrheum.2014.219
3. Greenblatt MB, Shim J. Osteoimmunology: a brief introduction. *Immune Netw.* (2013) 13:111–5. doi: 10.4110/in.2013.13.4.111
4. Okamoto K, Nakashima T, Shinohara M, Negishi-koga T, Komatsu N, Terashima A, et al. Osteoimmunology: the conceptual framework unifying the immune and skeletal systems. *Physiol Rev.* (2017) 97:1295–349. doi: 10.1152/physrev.00036.2016
5. Cahalan MD, Parker I, Wei SH, Miller MJ. Two-photon tissue imaging: seeing the immune system in a fresh light. *Nat Rev Immunol.* (2002) 2:872–81. doi: 10.1038/nri935
6. Germain RN, Miller MJ, Dustin ML, Nussenzweig MC. Dynamic imaging of the immune system: progress, pitfalls and promise. *Nat Rev Immunol.* (2006) 6:497–507. doi: 10.1038/nri1884
7. Ishii M, Egen JG, Klauschen F, Meier-Schellersheim M, Saeki Y, Vacher J, et al. Sphingosine-1-phosphate mobilizes osteoclast precursors and regulates bone homeostasis. *Nature.* (2009) 458:524–8. doi: 10.1038/nature07713
8. Ishii M, Kikuta J, Shimazu Y, Meier-Schellersheim M, Germain RN. Chemorepulsion by blood S1P regulates osteoclast precursor mobilization and bone remodeling *in vivo*. *J Exp Med.* (2010) 207:2793–8. doi: 10.1084/jem.20101474
9. Kikuta J, Wada Y, Kowada T, Wang Z, Sun-Wada GH, Nishiyama I, et al. Dynamic visualization of RANKL and Th17-mediated osteoclast function. *J Clin Invest.* (2013) 123:866–73. doi: 10.1172/JCI65054
10. Kikuta J, Kawamura S, Okiji F, Shirazaki M, Sakai S, Saito H, et al. Sphingosine-1-phosphate-mediated osteoclast precursor monocyte migration is a critical point of control in antibone-resorptive action of active vitamin D. *Proc Natl Acad Sci USA.* (2013) 110:7009–13. doi: 10.1073/pnas.1218799110
11. Cyster JG. Chemokines, sphingosine-1-phosphate, and cell migration in secondary lymphoid organs. *Annu Rev Immunol.* (2005) 23:127–59. doi: 10.1146/annurev.immunol.23.021704.115628
12. Baeyens A, Fang V, Chen C, Schwab SR. Exit strategies: S1P signaling and T Cell migration. *Trends Immunol.* (2015) 36:778–87. doi: 10.1016/j.it.2015.10.005
13. Chun J, Kihara Y, Jonnalagadda D, Blaho VA. Fingolimod: lessons learned and new opportunities for treating multiple sclerosis and other disorders. *Annu Rev Pharmacol Toxicol.* (2019) 59:149–70. doi: 10.1146/annurev-pharmtox-010818-021358
14. Rosen H, Goetzl EJ. Sphingosine 1-phosphate and its receptors: an autocrine and paracrine network. *Nat Rev Immunol.* (2005) 5:560–70. doi: 10.1038/nri1650
15. Rivera J, Proia RL, Olivera A. The alliance of sphingosine-1-phosphate and its receptors in immunity. *Nat Rev Immunol.* (2008) 8:753–63. doi: 10.1038/nri2400
16. Huwiler A, Zangemeister-wittke U. The sphingosine 1-phosphate receptor modulator fingolimod as a therapeutic agent: recent findings and new perspectives. *Pharmacol Ther.* (2018) 185:34–49. doi: 10.1016/j.pharmthera.2017.11.001
17. Teitelbaum SL, Ross FP. Genetic regulation of osteoclast development and function. *Nat Rev Genet.* (2003) 4:638–49. doi: 10.1038/nrg1122
18. Blair HC, Teitelbaum SL, Ghiselli R, Gluck S. Osteoclastic bone resorption by a polarized vacuolar proton pump. *Science.* (1989) 810:855–8.
19. Toyomura T, Oka T, Yamaguchi C, Wada Y, Futai M. Three subunit a isoforms of mouse vacuolar H^+-ATPase. preferential expression of the a3 isoform during osteoclast differentiation. *J Biol Chem.* (2000) 275:8760–5. doi: 10.1074/jbc.275.12.8760
20. Toyomura T, Murata Y, Yamamoto A, Oka T, Wada Y, Futai M. From lysosomes to the plasma membrane. *J Biol Chem.* (2003) 278:22023–30. doi: 10.1074/jbc.M302436200
21. Loudet A, Burgess K. Bodipy dyes and their derivatives : syntheses and spectroscopic properties. *Chem Rev.* (2007) 107:4891–932. doi: 10.1021/cr078381n
22. Kozloff KM, Volakis LI, Marini JC, Caird MS. Near-infrared fluorescent probe traces bisphosphonate. *J Bone Miner Res.* (2010) 25:1748–58. doi: 10.1002/jbmr.66
23. Zaheer S, Leboff M, Lewiecki EM. Denosumab for the treatment of osteoporosis. *Expert Opin Drug Metab Toxicol.* (2015) 11:461–70. doi: 10.1517/17425255.2015.1000860
24. Boleto G, Dramé M, Lambrecht I, Eschard J. Disease-modifying anti-rheumatic drug effect of denosumab on radiographic progression in rheumatoid arthritis: a systematic review of the literature. *Clin Rheumatol.* (2017) 36:1699–706. doi: 10.1007/s10067-017-3722-6
25. Hasegawa T, Kaneko Y, Izumi K, Takeuchi T. Efficacy of denosumab combined with bDMARDs. *Jt Bone Spine.* (2017) 84:379–80. doi: 10.1016/j.jbspin.2016.05.010
26. Cohen SB, Dore RK, Lane NE, Ory PA, Peterfy CG, Sharp JT. Denosumab treatment effects on structural damage, bone mineral density, and bone turnover in rheumatoid arthritis. *Arthritis Rheum.* (2008) 58:1299–309. doi: 10.1002/art.23417
27. Walsh MC, Choi Y. Biology of the RANKL–RANK–OPG system in immunity, bone, and beyond. *Front Immunol.* (2014) 5:1–11. doi: 10.3389/fimmu.2014.00511
28. Yasuda H, Shima N, Nakagawa N, Yamaguchi K, Masahiko K, Suda T. Osteoclast differentiation factor is a ligand for osteoprotegerin /osteoclastogenesis-inhibitory factor and is identical to TRANCE/RANKL. *Proc Natl Acad Sci USA.* (1998) 95:3597–602. doi: 10.1073/pnas.95.7.3597
29. Sato K, Suematsu A, Okamoto K, Yamaguchi A, Morishita Y, Kadono Y, et al. Th17 functions as an osteoclastogenic helper T cell subset that links T cell activation and bone destruction. *J Exp Med.* (2006) 203:2673–82. doi: 10.1084/jem.20061775
30. Sims NA, Martin TJ. Coupling the activities of bone formation and resorption: a multitude of signals within the basic multicellular unit. *Bonekey Rep.* (2014) 481:1–10. doi: 10.1038/bonekey.2013.215
31. Furuya M, Kikuta J, Fujimori S, Seno S, Maeda H, Shirazaki M, et al. Direct cell–cell contact between mature osteoblasts and osteoclasts dynamically controls their functions *in vivo*. *Nat Commun.* (2018) 9:300. doi: 10.1038/s41467-017-02541-w

32. Hawkins E, Duarte D, Akinduro O, Khorshed R, Passaro D, Nowicka M, et al. T-cell acute leukaemia exhibits dynamic interactions with bone marrow microenvironments. *Nature*. (2016) 538:518–22. doi: 10.1038/nature19801
33. Lam J, Ross FP, Teitelbaum SL, Lam J, Takeshita S, Barker JE, et al. TNF-α induces osteoclastogenesis by direct stimulation of macrophages exposed to permissive levels of RANK ligand. *J Clin Invest*. (2000) 106:1481–8. doi: 10.1172/JCI11176
34. Fuller K, Murphy C, Kirstein B, Fox SW, Chambers TJ. TNFα potently activates osteoclasts, through a direct action independent of and strongly synergistic with RANKL. *Endocrinology*. (2002) 143:1108–18. doi: 10.1210/endo.143.3.8701
35. Li P, Schwarz EM, Boyce BF, Xing L. RANK signaling is not required for TNFα-mediated increase in $CD11b^{hi}$ osteoclast precursors but is essential for mature osteoclast formation in TNFα-mediated inflammatory arthritis. *J Bone Miner Res*. (2004) 19:207–13. doi: 10.1359/JBMR.0301233
36. Tamura T. Soluble interleukin-6 receptor triggers osteoclast formation by interleukin 6. *Proc Natl Acad Sci USA*. (1993) 90:11924–8. doi: 10.1073/pnas.90.24.11924
37. Factor LI, Palmqvist P, Persson E, Conaway HH, Lerner H. IL-6, leukemia inhibitory factor, and oncostatin m stimulate bone resorption and regulate the expression of receptor activator of NF-κB ligand, osteoprotegerin, and receptor activator of NF-κB in mouse calvariae. *J Immunol*. (2002) 169:3353–62. doi: 10.4049/jimmunol.169.6.3353
38. Matsuura Y, Kikuta J, Kishi Y, Hasegawa T, Okuzaki D, Hirano T, et al. *In vivo* visualisation of different modes of action of biological DMARDs inhibiting osteoclastic bone resorption. *Ann Rheum Dis*. (2018) 77:1220–6. doi: 10.1136/annrheumdis-2017-212880
39. Chang MK, Raggatt L, Alexander KA, Kuliwaba JS, Fazzalari NL, Schroder K, et al. Osteal tissue macrophages are intercalated throughout human and mouse bone lining tissues and regulate osteoblast function *in vitro* and *in vivo*. *J Immunol*. (2008) 181:1232–44. doi: 10.4049/jimmunol.181.2.1232

Conflict of Interest Statement: The authors declare that the research was conducted in the absence of any commercial or financial relationships that could be construed as a potential conflict of interest.

frontiers in Immunology

MINI REVIEW
published: 29 March 2019
doi: 10.3389/fimmu.2019.00629

The RANKL-RANK Axis: A Bone to Thymus Round Trip

Cristina Sobacchi[1,2], *Ciro Menale*[1,2] *and Anna Villa*[1,3]*

[1] Milan Unit, Institute for Genetic and Biomedical Research (CNR-IRGB), Milan, Italy, [2] Humanitas Clinical and Research Center IRCCS, Rozzano, Italy, [3] San Raffaele Telethon Institute for Gene Therapy (SR-Tiget), IRCCS San Raffaele Scientific Institute, Milan, Italy

The identification of Receptor activator of nuclear factor kappa B ligand (RANKL) and its cognate receptor Receptor activator of nuclear factor kappa B (RANK) during a search for novel tumor necrosis factor receptor (TNFR) superfamily members has dramatically changed the scenario of bone biology by providing the functional and biochemical proof that RANKL signaling via RANK is the master factor for osteoclastogenesis. In parallel, two independent studies reported the identification of mouse RANKL on activated T cells and of a ligand for osteoprotegerin on a murine bone marrow-derived stromal cell line. After these seminal findings, accumulating data indicated RANKL and RANK not only as essential players for the development and activation of osteoclasts, but also for the correct differentiation of medullary thymic epithelial cells (mTECs) that act as mediators of the central tolerance process by which self-reactive T cells are eliminated while regulatory T cells are generated. In light of the RANKL-RANK multi-task function, an antibody targeting this pathway, denosumab, is now commonly used in the therapy of bone loss diseases including chronic inflammatory bone disorders and osteolytic bone metastases; furthermore, preclinical data support the therapeutic application of denosumab in the framework of a broader spectrum of tumors. Here, we discuss advances in cellular and molecular mechanisms elicited by RANKL-RANK pathway in the bone and thymus, and the extent to which its inhibition or augmentation can be translated in the clinical arena.

Keywords: osteoclasts, denosumab, thymus, central tolerance, rheumatoid arthritis, osteoporosis, tumor

OPEN ACCESS

Edited by:
Claudine Blin-Wakkach, UMR7370 Laboratoire de Physio Médecine Moléculaire (LP2M), France

Reviewed by:
Frederic Lezot, INSERM UMR957, France
Magali Irla, Institut National de la Santé et de la Recherche Médicale (INSERM), France
Eleni Douni, Agricultural University of Athens, Greece

***Correspondence:**
Anna Villa
villa.anna@hsr.it

Specialty section:
This article was submitted to Inflammation, a section of the journal Frontiers in Immunology

Received: *11 January 2019*
Accepted: *08 March 2019*
Published: *29 March 2019*

Citation:
Sobacchi C, Menale C and Villa A (2019) The RANKL-RANK Axis: A Bone to Thymus Round Trip. Front. Immunol. 10:629. doi: 10.3389/fimmu.2019.00629

INTRODUCTION

Receptor activator of nuclear factor kappa B (RANK) and its ligand (RANKL), encoded, respectively, by the *Tumor necrosis factor receptor superfamily member 11A* (*Tnfrsf11a*) and the *Tumor necrosis factor ligand superfamily member 11* (*Tnfsf11*) genes, constitute a receptor-ligand pair initiating a signaling pathway of paramount relevance in many pathophysiological contexts (1). They have been described in the context of T cell-dendritic cell interactions (2), in bone and in the immune system (3, 4), thus triggering the start of the osteoimmunology era. This axis has revealed an unexpected role in the thermoregulation by the central nervous system (5) and in mammary epithelium development during pregnancy and progesterone-driven breast cancer (3, 6). The RANKL-RANK axis has also been involved in diverse immune-mediated diseases affecting the bone (7–9) as well as other tissues (10), and in cancer settings (11). Overall, this pathway has emerged as a potential target of therapy in a wide range of conditions; which at the same time implies monitoring many different physiological functions when interfering with this axis.

As schematically depicted in **Figure 1**, here we focus on advances in cellular and molecular mechanisms elicited by RANKL-RANK signaling in two functionally related compartments: the bone and the thymus. Moreover, we review novel perspectives to translate inhibition or enhancement of this pathway in the clinic.

RANKL-RANK AXIS IN THE BONE

The identification of RANKL-RANK signaling in bone represents a milestone in bone biology (12, 13). Its indispensable role in osteoclast formation is clearly demonstrated by the complete absence of osteoclasts in the *Rankl*$^{-/-}$ and *Rank*$^{-/-}$ murine models (3, 4, 14, 15), as well as in their human counterpart, i.e., patients affected by RANKL-deficient and RANK-deficient osteoclast-poor Autosomal Recessive Osteopetrosis (16, 17). Nonetheless, the possibility of RANKL-independent osteoclastogenesis, particularly in pathologic conditions, has been a matter of a long-lasting debate (18–22) and a general consensus in the field has not been reached, yet.

RANKL is mainly produced by stromal cells in bone, in normal conditions, and primarily by osteocytes (23–25). RANKL is mostly membrane-bound and can be shed to form a soluble protein; the former is sufficient for most functions, while the latter contributes to physiological bone remodeling, as recently demonstrated in mice expressing a sheddase-resistant form of RANKL (26).

The membrane functional receptor RANK is mainly expressed by cells of hematopoietic origin, including also osteoclasts and their precursors, and has been recently detected also in Mesenchymal Stem Cells (MSCs) (27, 28), raising the intriguing hypothesis of an autocrine/paracrine loop in these cells (**Figure 1A**).

The RANKL-RANK signaling pathway in the osteoclast lineage comprises a plethora of molecules (29). Essentially, upon engagement by its ligand, RANK recruits a number of adaptors (most importantly, TNF Receptor-Associated Factor 6, TRAF6) (30), which converge on kinases activation, including Phosphoinositide-3-Kinase (PI3K) and Mitogen Activated Protein (MAP) kinases. This promotes nuclear translocation and activation of transcription factors, Nuclear Factor of Activated T cell 1 (NFATc1) (31), c-fos (32), and Nuclear Factor kappa B (NF-κB) (33), comprising the master regulator of the osteoclast-specific transcriptional program. The RANKL-RANK pathway interacts with costimulatory signals from immunoreceptor tyrosine based activation (ITAM)-motif containing proteins, further regulating NFATc1 activation (34, 35).

RANKL signaling during osteoclastogenesis results in the generation of reactive oxygen species (ROS), which further stimulate osteoclast formation and bone resorption (36). On the other hand, a variety of antioxidant mechanisms monitors ROS levels and the reciprocal control between these opposite functions (i.e., ROS production and scavenging) importantly impacts on bone homeostasis (37–39).

The RANKL-RANK axis is counterbalanced by the soluble decoy receptor osteoprotegerin (OPG) (40), which is itself controlled by many ligands, including the TNF-Related Apoptosis Inducing Ligand (TRAIL), von Willebrand factor (vWF), and glycosaminoglycans (GAGs) (41). Moreover, the Leucine-rich repeat-containing G protein-coupled receptor 4 (LGR4) is an additional membrane receptor for RANKL, competing with RANK for ligand binding and negatively regulating osteoclastogenesis through the inhibition of NFATc1 activation (42). LGR4 acts also as an R-spondin receptor in bone marrow MSCs and has been recently demonstrated as a key molecule in mesoderm-derived tissue development and MSC differentiation (43), whether RANKL might be involved in this specific context has to be investigated (**Figure 1A**).

The recognition of the crucial role of RANKL-RANK signaling in osteoclast biology led to the development of the anti-RANKL antibody denosumab, a fully human Immunoglobulin (Ig) G2 monoclonal antibody with high affinity and specificity for human soluble and membrane-bound RANKL (44). Specifically, denosumab binds to the DE loop region of the ligand, which is one of the surface loop structures interacting with the functional receptor on responding cells (44). Denosumab is used as an antiresorptive drug for diverse indications, such as osteoporosis (45), primary bone tumors (46), and osteolytic bone metastases (47). Its use is under evaluation also in other fields, such as solid tumors (11) and Rheumatoid Arthritis (48), and has been very recently proposed in the prevention of BRCA1-associated breast cancer (49). Finally, denosumab administration has been considered in the field of rare diseases too, for example for the treatment of persistent severe hypercalcemia after hematopoietic stem cell transplantation in patients affected by Autosomal Recessive Osteopetrosis (50), in patients affected by Fibrous Dysplasia (51), or by Osteogenesis Imperfecta, even though

Abbreviations: ACPA, Anti-Citrullinated Protein Antibodies; AIRE, Auto Immune Regulator; anti-CarP, anti-Carbamylated Protein; anti-CCP2, anti-Cyclic Citrullinated Peptide 2; Bcl-xl, B-cell lymphoma-extra-large; CCL20, C-C Motif Chemokine Ligand 20; CCR5, C-C chemokine receptor type 5; CCR6, C-C chemokine receptor type 6; cTEC, cortical Thymic Epithelial Cell; CXCR3, C-X-C Motif Chemokine Receptor 3; CXCR4, C-X-C Motif Chemokine Receptor 4; bDMARDs, biological Disease-Modifying Anti-Rheumatic Drugs; DETC, dendritic epidermal T cell; DP, Double Positive; FTOC, fetal thymic organ culture; GAGs, glycosaminoglycans; IL-1, Interleukin 1; IL-6, Interleukin 6; IL-17, Interleukin 17; IFNβ, Interferon beta; IFNAR, Interferon-α/β receptor; IRF7, Interferon Regulatory Factor 7; ITAM, Immunoreceptor Tyrosine-based Activation Motif; LGR4, Leucine Rich Repeat Containing G Protein-Coupled Receptor 4; LTα Lymphotoxin α; LTi, Lymphoid Tissue inducer cells; MAP kinase, Mitogen Activated Protein kinase; MHC, Major Histocompatibility Complex; MSCs, Mesenchymal Stem Cells; mTEC, medullary Thymic Epithelial Cell; NFATc1, Nuclear Factor Of Activated T Cells 1; NF-κB, Nuclear Factor kappa B; OPG, Osteoprotegerin; OVX, ovariectomized; PI3K, Phosphoinositide 3-kinase; RA, Rheumatoid Arthritis; RANK, Receptor Activator of Nuclear Factor kappa B; RANKL, Receptor Activator of Nuclear Factor kappa B Ligand; RF, Rheumatoid Factor; ROS, Reactive Oxygen Species; SP, Single Positive; STAT1, Signal Transducer and Activator of Transcription 1; TCR, T Cell Receptor; Th1, T helper 1 cells; Th17, T helper 17 cells; TNFα, Tumor Necrosis Factor α; TNFR, Tumor Necrosis Factor Receptor; TNFRSF11A, Tumor Necrosis Factor Receptor Superfamily Member 11A; TNFSF11, Tumor Necrosis Factor Ligand Superfamily Member 11; TRAF6, TNF Receptor-Associated Factor 6; TRAIL, TNF-Related Apoptosis Inducing Ligand; TRAs, Tissue Restricted Antigens; Treg, T regulatory cells; vWF, von Willebrand factor; XCL-1, X-C Motif Chemokine Ligand 1; ZAP-70, Zeta Chain Of T Cell Receptor Associated Protein Kinase 70.

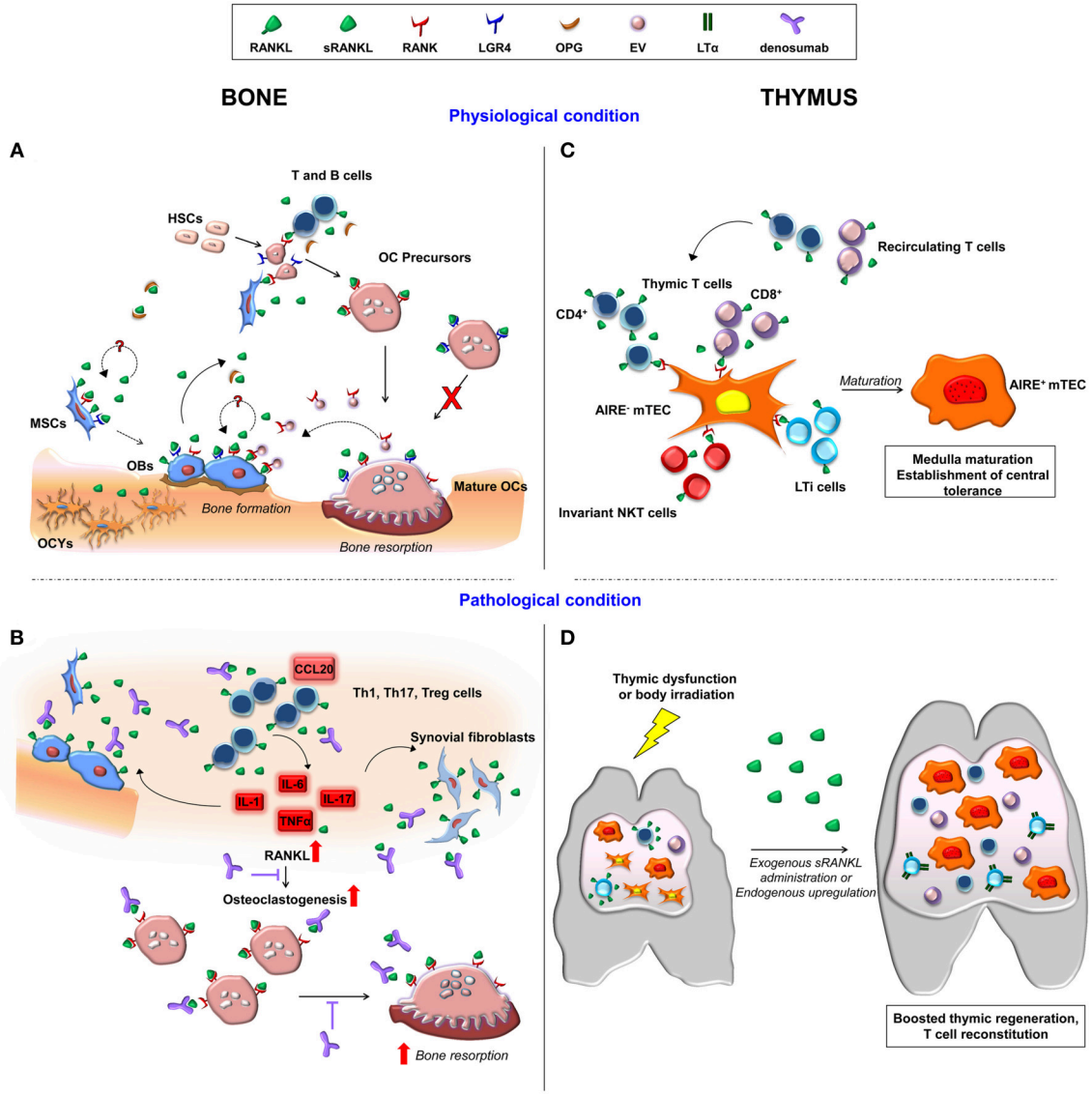

FIGURE 1 | Schematic representation of cellular and molecular players involved in RANKL-RANK signaling axis in the bone and thymus in physiological and in pathological conditions. **(A)** Membrane-bound and soluble RANKL produced by cells of the osteoblast lineage and by immune cells induce osteoclastogenesis upon its binding to RANK on osteoclast precursors. OPG is the soluble decoy receptor for RANKL. Moreover, RANKL binding to LGR4 on osteoclasts hinders their maturation. RANK expression by MSC and osteoblasts points to a potential RANKL autoregulatory mechanism affecting bone formation. In addition, osteoclast-derived RANK-expressing extracellular vesicles (EV) trigger a reverse signaling on osteoblast. **(B)** The inflammatory bone environment in pathological condition, such as osteoporosis and rheumatoid arthritis, results in increased production of RANKL by immune cells, osteoblastic cells and synovial fibroblasts. This exacerbates osteoclast generation and bone loss, which are target of denosumab treatment. **(C)** In the thymus, RANKL produced by resident and recirculating T cells, invariant NKT and LTi cells fosters mTEC AIRE expression and maturation via RANK receptor, allowing correct establishment of central tolerance. **(D)** In the presence of thymic dysfunction, pharmacological sRANKL administration boosts thymic regeneration, and T cell reconstitution. Similarly, in the early phases of thymic regeneration after body irradiation, $CD4^+$ and LTi cells upregulate RANKL. This results in increased expression of LTα in LTi cells. OBs, osteoblasts; OCs, osteoclasts; OCYs, osteocytes.

some variability in the clinical outcome has been reported (52) (**Figure 1B**).

Clinical case series and a recent analysis of the FREEDOM and FREEDOM Extension Trials about osteoporosis treatment with the anti-RANKL antibody have pointed to an increased risk of multiple vertebral fractures after denosumab discontinuation due to a rebound in bone resorption (53, 54), thus raising a note of caution. In an attempt to identify potential alternative antiresorptive therapies, scientific interest about natural compounds possibly interfering with the RANKL-RANK axis (e.g., flavonoids, alkaloid compounds, triterpenoids, polysaccharides as well as monomeric sugars) has been growing exponentially, as demonstrated by the number of publications evaluating this kind of approach (55–58).

In parallel, recent papers pointed to an unexpected osteogenic function of RANKL through (at least) two different, not mutually exclusive mechanisms: an autocrine-paracrine loop activated by RANKL binding to its receptor(s) on MSCs (27); and a reverse signaling elicited by osteoclast-derived RANK-expressing extracellular vesicles, which might induce membrane-RANKL clustering on osteoblasts (59, 60). This might represent an additional means for osteoblast-osteoclast crosstalk. As a perspective, it might be exploited by means of a new drug with two simultaneous activities: dampening of bone resorption by preventing RANKL binding to RANK receptors on the osteoclasts, and stimulating osteogenesis by triggering RANKL signaling in the osteoblasts (**Figure 1A**).

Actually, the biological relevance of these new findings in the framework of the overall bone homeostasis has to be clearly defined; for the sake of completeness, opposite results have been reported by others (28). Nevertheless, the possibility of an osteogenic function of RANKL is worth further investigations since it could pave the way to the development of new therapeutic strategies, thus fulfilling a medical need.

RANKL-RANK AXIS IN THE THYMUS

The thymus is a primary lymphoid organ responsible for the development of T lymphocytes expressing a T cell repertoire capable of responding to a diverse array of foreign antigens but tolerant to self-antigens (61, 62). Migrant lymphoid progenitors, arising in the liver during embryonic life and in the bone marrow in postnatal life, enter the thymus where they undergo different phases of differentiation throughout a complex journey from the cortical region to the medullary compartment (63). The early phases of thymocyte differentiation strictly depend on stromal derived signals mediated by the interaction of $CD4^+CD8^+$ double positive (DP) T cell precursors with cortical thymic epithelial cells (cTECs) and indirectly by the production of soluble factors (**Figure 1C**). cTECs foster lineage commitment during the early stages of T cell differentiation (double negative, DN, stage) through the expression of Notch ligand Delta-like 4 (64, 65) and mediate positive selection of DP T cells by presenting a broad array of self-peptides via major histocompatibility complex (MHC) class I and II molecules. This process results in the survival of thymocytes, which migrate into the thymic medulla where T cells are negatively selected to single positive (SP) $CD4^+CD8^-$ and $CD8^+CD4^-$ T cells (66). Mature medullary thymic epithelial cells (mTECs) mediate central tolerance process by expressing the transcriptional coactivator AutoImmune Regulator (AIRE), which drives the expression of self-antigens, including tissue restricted antigens (TRAs) leading to the clonal deletion of autoreactive T cells, while inducing the generation of regulatory T cells (67, 68), and the intra-thymic positioning of X-C Motif Chemokine Ligand 1 $(XCL1)^+$ dendritic cells (69).

Various factors modulate the development and maturation of the thymic epithelial compartment, including several signal transducers regulating NF-κB pathway and the NF-κB family member RelB (70–76). Signaling mediated by four receptors of the tumor necrosis factor family [RANK, OPG, CD40, and lymphotoxin (LT) β receptor] acts as important modulator of thymic microenvironment along with the cross talk between thymocytes and TECs (77–79). In addition, the Ets transcription factor family member Spi-B, which was found to be associated with autoimmune phenomena (80), mediates OPG expression via a negative feedback regulatory loop thus limiting the development of mature TECs (81). RANKL is mainly produced by $CD4^+$ cells, a small subset of $CD8^+$ cells, invariant (Natural Killer T) NKT cells and $CD4^+CD3^-$ lymphoid tissue inducer (LTi) cells (82, 83). Of note, during embryonic life at the initial stages of thymus development, invariant $V\gamma5^+$ dendritic epidermal T cells (DETCs) and $V\gamma5^+$ γδ T cells T cells contribute to central tolerance establishment by promoting $CD80^-Aire^-$ mTECs to become $CD80^+Aire^+$ mTECs (84–86) thus supporting a critical role for RANK signaling in the interaction between fetal γδ T cell progenitors and mTECs (87, 88). Of note, these immune cell subsets provide different physiological levels of RANKL and CD40 Ligand (CD40L) during ontogeny. During fetal life, mTEC development is controlled by the expression of RANKL by LTi and invariant $V\gamma5^+$ DETC progenitors, while after birth is controlled by RANKL and CD40L produced by αβ T Cell Receptor $(TCR)^{high}$ $CD4^+$ thymocytes (89).

Transgenic mice expressing Venus, a fluorescent protein to track RANK expression, showed that this receptor is mainly expressed by mTECs at different stages of differentiation (90). Moreover, activated T cells recirculating to the thymus further contribute to the production of RANKL (91). Thus, it is tempting to speculate that the increased production of RANKL may support the skewing toward mTEC lineage, with consequent maturation of T cells leading to the exhaustion of the progenitor pool. These observations might explain the age-related changes observed in thymic epithelium during aging or thymic dysmorphology found in some pathological conditions (92, 93).

Extensive *in vitro* and *in vivo* studies have further confirmed the relevant role of the RANKL-RANK axis in the establishment and maintenance of the central tolerance process. *In vitro* stimulation of fetal thymic organ culture (FTOC) with recombinant RANKL or agonistic anti-RANK antibody results in the upregulation of CD80 and Aire expression by mTECs (87, 94). In parallel, mice deficient in TCRα or murine models with a reduced number of $CD4^+$ T cells for instance lacking molecules of the MHC II complex have a dramatic reduction in $Aire^+$ cells and decreased mTEC compartment (95, 96). Other molecular players contribute to TEC differentiation and among them a peculiar role is played by the interferon regulatory factor 7/interferon β/ interferon-α/β receptor/signal transducer and activator of transcription 1 (IRF7/IFNβ/IFNAR/STAT1) pathway (97). During embryonic life, the absence of RANK or RANKL severely affects mTEC maturation resulting in the complete loss of $Aire^+$ mTECs (87, 94, 98). However, after birth other factors compensate the absence of RANK signaling allowing the maturation of few $Aire^+$ mTECs (94). Furthermore, OPG is expressed by mTECs and genetically deletion in mice causes enlargement of the medulla area (82, 90). Overall, these data indicate that the RANKL-RANK axis is essential for the correct differentiation and development of mTECs and for the formation of the thymic medulla and consequent establishment of self-tolerance (**Figure 1C**). Consistently with the role of

RANKL as a potent mTEC inducer and indirectly as a key player in the control of central tolerance, systemic administration of soluble RANKL (sRANKL) can be considered to treat primary or secondary thymic dysfunction (99). Transgenic mice constitutively overexpressing human sRANKL displayed thymic medulla enlargement (100) and increased number of $Aire^+$ mTECs (101). Interestingly, during *in vivo* administration of recombinant soluble RANKL (sRANKL) to cure the bone defect in $Rankl^{-/-}$ mice, we observed a dramatic effect of the cytokine on thymic architecture (102) further confirming data reported in literature. Pharmacological sRANKL treatment induced expansion of the medulla in $Rankl^{-/-}$ mice and increase of $Aire^+$ mTECs. Improvement of thymic epithelium resulted in higher frequency of $CD4^+$ and $CD8^+$ SP and reduction of double positive thymocytes (102). These data suggest that the exogenous administration of RANKL may be a new therapeutic strategy to boost thymic regeneration. In line with this, compelling evidence indicate that upon body irradiation $CD4^+$ cells and LTi cells up-regulate RANKL in the early phase of thymic regeneration. Upon tissue damage, RANKL mediates the increased expression of LTα by LTi cells and reduces the expression of pro-apoptotic genes while increases the expression of the B-cell lymphoma-extra large (Bcl-xl) anti-apoptotic gene (103). The administration of RANKL to wild-type animals confirmed its crucial role in thymic recovery by enhancing TECs, thymocyte numbers, and in parallel increasing vasculature. Improved T cell reconstitution is also mediated by the increased expression of adhesion molecules and chemokines, which foster thymus homing of lymphoid progenitors. Remarkably, since RANKL is the master gene of osteoclastogenesis, it is tempting to speculate that the increased osteoclast activity may also boost hematopoiesis and consequent migration of thymic progenitors. Overall, these *in vivo* findings confirm the therapeutic effect of RANKL suggesting its putative use to boost immune reconstitution in transplanted elderly patients or in patients affected by primary thymic epithelial defects (104–106) (**Figure 1D**). Conversely, transient inhibition of RANKL in murine models indicate its effect on thymic negative selection of self-reactive T cells specific for tumor antigens, and resulting in an improvement of antitumor immune response (107, 108). However, *in vivo* inhibition of RANKL during prenatal life in rats and mice or long-life inhibition after birth did not show gross effects on innate or humoral immune response (109), thus supporting a possible repurposing of denosumab as anti-tumoral agent in combinatorial treatments and extending its use in the clinical arena.

T CELLS AND RANKL-RANK SIGNALING IN BONE PATHOLOGY

The overall picture described highlighted the importance of the RANKL-RANK axis in the bone and thymus compartments: in the former, RANKL-RANK signaling influences the bone remodeling process regulating bone cells activities; in the latter, it is pivotal in thymic cell development and T cell maturation and functioning.

After maturation, T cells exert their function centrally and in all the other peripheral organs, going back also to the bone. Although T cell levels represent about 3–8% of total nucleated bone marrow cells in homeostatic conditions (110), in pathological settings T cell recruitment from the periphery may occur and induce molecular and metabolic changes in bone cells, contributing to the bone loss phenotype associated with various conditions such as post-menopausal osteoporosis and Rheumatoid Arthritis (RA) (**Figure 1B**).

In post-menopausal osteoporotic patients an increase in RANKL production by activated T cells (and B cells, too), alone or in combination with TNFα, has been reported (111, 112). A similar finding has been shown in surgically ovariectomized (OVX) pre-menopausal women (113), further confirming the causative link between estrogen deprivation, T cell activation and RANKL-mediated bone loss previously observed in the murine model (114). Accordingly, 17β-estradiol inhibits thymic expansion after OVX in mice and T cell development, and protects against bone loss, while selective estrogen receptor modulators exhibit agonistic activity on bone but do not affect T lymphopoiesis (115). Of note, a study in thymectomized pre-menopausal women showed a drop in T cell counts after surgery, as expected, with enhanced activation and production of osteoclastogenic factors by the remaining T cells (116). On the other hand, the authors of the study hypothesized that the establishment of not clarified compensatory mechanisms could be responsible for maintaining bone density at levels similar to euthymic age-matched controls.

Another example of bone-thymus interplay is RA, a chronic inflammatory autoimmune disease characterized by joint inflammation, involving mainly synovial membranes, and bone and cartilage destruction (117, 118). In this condition, the synovium and articular tissues are highly enriched in inflammatory leukocytes, likely due to cell recruitment in the inflamed tissue (119), sustained by resident stromal cells of mesenchymal origin (120). The inflammatory process in the joints is suggested to enhance bone loss in patients with RA, in particular when Anti-Citrullinated Protein Antibodies (ACPA), Rheumatoid Factor (RF) and anti-Carbamylated Protein Antibodies (anti-CarP) are present (121, 122). Most of the T cells recruited from the circulation are T helper 1 (Th1), Th17, and Treg cells (123), which express C-X-C Motif Chemokine Receptor 3 (CXCR3), CXCR4, C-C chemokine receptor type 5 (CCR5), and CCR6 (mainly on Th17 cells) receptors that permit their entry into the inflammatory site upon attraction by the high levels of chemokines (e.g., CCL20) found in arthritic joints (124–126). The relevant presence of these cells exacerbates bone erosion by osteoclasts located at the interface between the synovial membrane and bone (48). The pathological bone loss is not compensated by osteoblast-repairing activity since this process is inhibited by synovial inflammation (127). Pro-inflammatory cytokines, such as IL-1, IL-6, and more importantly TNFα and IL-17 are produced in the inflamed synovium and strongly induce RANKL production through the activation of NF-κB pathway in synovial cells and T cells, which in turn massively activate osteoclasts (22, 48, 128). In patients with early RA, RANKL plasma levels have

been associated with bone destruction and with radiological progression of the disease after 24 months of follow-up (129). Moreover, the combined presence of increased RANKL levels and the positivity for anti-Cyclic Citrullinated Peptide 2 (anti-CCP2) antibodies correlated with a more destructive process. These data were confirmed in a case-control study conducted in RA pre-symptomatic patients, where RANKL plasma levels were higher in pre-symptomatic individuals as compared to control subjects, increased over time until the onset of RA symptoms and were associated with levels of inflammatory cytokines. However, the positivity for ACPA/RF/anti-CarP preceded the rise of RANKL plasma levels (129).

Based on this, preventing bone erosion by targeting RANKL-RANK axis could be an effective strategy for intervention (130). In fact, taking into account that RANKL-RANK axis is a pivotal immune modulator in DC development and function, in memory B cells, Th17, and Treg cells (131), RANKL blockade might modulate the immune response thus contributing to limit pathological bone erosion and joint damage occurring in RA.

In a phase II trial (Denosumab in patients with RheumatoId arthritis on methotrexate to Validate inhibitory effect on bone Erosion -DRIVE- study) on Japanese RA patients treated with methotrexate, denosumab significantly inhibited the progression of bone erosion at 12 months, and preserved the bone mineral density (132). In addition, in a retrospective cohort trial, the decrease of bone erosion in patients treated with denosumab in combination with biological disease-modifying anti-rheumatic drugs (bDMARDs), at 12 months was significantly higher as compared to denosumab alone, with no adverse effects. Therefore, blocking RANKL-RANK signaling in RA patients by the addition of denosumab to conventional treatment agents may represent a potential new therapeutic option for patients to limits RA pathological outcome (**Figure 1B**).

Importantly, RA is primarily an autoimmune disease, in which defects in central and peripheral T cell tolerance are involved. Altered intra-thymic selection for the removal of autoreactive T cells may have a great impact on the onset of T cell mediated autoimmune disease (133). In the SKG strain murine model of autoimmune arthritis, bearing a spontaneous point mutation in Zeta Chain of T Cell Receptor Associated Protein Kinase 70 (ZAP-70), alterations in αβ TCR signaling in the thymus have been linked to the escape of autoreactive T cells from negative selection, playing an essential role in immune response in the periphery (134). In turn, the onset of RA may be due to impaired peripheral tolerance mechanisms, mainly elicited by Treg cells, in controlling autoreactive T cells (135, 136). In addition, recirculation of peripheral T cells back to the thymus has been described, and the re-entering cells (mainly Treg cells) might alter central tolerance and induce the deletion of thymic antigen presenting cell populations. This could be considered a mechanism for silencing autoreactive T cells in an RA setting where impaired thymic functions are present (133). Whether alteration of this process may be linked to T cell mediated autoimmunity is still not clear and how T cell production in the thymus and their effector functions in the periphery regulate tolerance maintenance needs further investigation from a therapeutic point of view.

Overall, although targeting RANKL-RANK axis in RA with a RANKL antagonist can improve bone and joints pathological features, it remains to be defined whether an effect on central tolerance and autoimmune reactions is achieved too, because of RANKL requirement for the correct thymic development and production of functional T cells.

Finally, interest has recently grown in another field, i.e., regarding the possibility to exploit immune-related mechanisms based on RANKL-RANK signaling in cancer settings for therapeutic purposes (11). In malignancies with enhanced RANKL expression, such as Multiple Myeloma, denosumab alone is well-known to be effective in terms of overall survival and skeletal-related events (137). In different tumor types that usually have low expression of RANKL, denosumab treatment combined with immune check-point inhibitors might lead to a cross-modulation of antitumor immunity (138, 139). The mechanisms proposed are various: denosumab might act on RANKL-expressing tumor infiltrating lymphocytes and relieve their anticancer activity that is otherwise blocked by engagement of the ligand with RANK receptor on cells of the tumor microenvironment (138, 139). Moreover, RANKL antagonists might put a break on central tolerance by transiently inhibiting negative selection in the thymus, resulting in the release of self-specific T cells in the periphery (108). Finally, the activation of reverse-signaling pathways might be proposed (140, 141), in line with mechanisms described in bone (142). At present, all these possibilities require further investigations; their elucidation might shed light on novel therapeutic perspectives.

CONCLUSIONS

The RANKL-RANK axis exerts pleiotropic effects and consistently involves an ever-increasing number of molecular and cellular players. In the bone and thymus compartments, where the crucial role of RANKL signaling was recognized first, novel functions have recently been discovered. This extends our understanding of the basic biology of these tissues and has translational implications in terms of current therapies monitoring. In particular, opposite effects are expected in the case of blocking or activating the RANKL-RANK pathway on bone and immune tolerance: while used as an antiresorptive drug, the anti-RANKL antibody denosumab might have adverse effects on the establishment of central tolerance, which would deserve attention. On the other hand, recent advances might support efforts toward drug repurposing strategies and development of new medicines, based on limitations of those currently available.

AUTHOR CONTRIBUTIONS

All authors listed have made a substantial, direct and intellectual contribution to the work, and approved it for publication.

FUNDING

The original work was supported by the Italian Telethon Grant C5, the European Community's Seventh Framework

Program (FP7/2007-2013, SYBIL Project), PRIN Project (2015F3JHMB_004), and by Programma Nazionale per la Ricerca-Consiglio Nazionale delle Ricerche Aging Project to AV. CM is recipient of an ECTS Basic Research Fellowship.

ACKNOWLEDGMENTS

We acknowledge the many authors whose original contribution in the field has not been cited in this mini review for the sake of brevity.

REFERENCES

1. Rao S, Cronin SJF, Sigl V, Penninger JM. RANKL and RANK: from mammalian physiology to cancer treatment. *Trends Cell Biol.* (2018) 28:213–23. doi: 10.1016/j.tcb.2017.11.001
2. Anderson DM, Maraskovsky E, Billingsley WL, Dougall WC, Tometsko ME, Roux ER, et al. A homologue of the TNF receptor and its ligand enhance T-cell growth and dendritic-cell function. *Nature.* (1997) 390:175–9. doi: 10.1038/36593
3. Kong YY, Yoshida H, Sarosi I, Tan HL, Timms E, Capparelli C, et al. OPGL is a key regulator of osteoclastogenesis, lymphocyte development and lymph-node organogenesis. *Nature.* (1999) 397:315–23. doi: 10.1038/16852
4. Kim N, Odgren PR, Kim DK, Marks SC Jr, Choi Y. Diverse roles of the tumor necrosis factor family member TRANCE in skeletal physiology revealed by TRANCE deficiency and partial rescue by a lymphocyte-expressed TRANCE transgene. *Proc Natl Acad Sci USA.* (2000) 97:10905–10. doi: 10.1073/pnas.200294797
5. Hanada R, Leibbrandt A, Hanada T, Kitaoka S, Furuyashiki T, Fujihara H, et al. Central control of fever and female body temperature by RANKL/RANK. *Nature.* (2009) 462:505–9. doi: 10.1038/nature08596
6. Schramek D, Leibbrandt A, Sigl V, Kenner L, Pospisilik JA, Lee HJ, et al. Osteoclast differentiation factor RANKL controls development of progestin-driven mammary cancer. *Nature.* (2010) 468:98–102. doi: 10.1038/nature09387
7. Hofbauer LC, Schoppet M. Clinical implications of the osteoprotegerin/RANKL/RANK system for bone and vascular diseases. *JAMA.* (2004) 292:490–5. doi: 10.1001/jama.292.4.490
8. Han YK, Jin Y, Miao YB, Shi T, Lin XP. Improved RANKL production by memory B cells: a way for B cells promote alveolar bone destruction during periodontitis. *Int Immunopharmacol.* (2018) 64:232–7. doi: 10.1016/j.intimp.2018.08.033
9. Tanaka S, Tanaka Y, Ishiguro N, Yamanaka H, Takeuchi T. RANKL: a therapeutic target for bone destruction in rheumatoid arthritis. *Mod Rheumatol.* (2018) 28:9–16. doi: 10.1080/14397595.2017.1369491
10. Guerrini MM, Okamoto K, Komatsu N, Sawa S, Danks L, Penninger JM, et al. Inhibition of the TNF family cytokine RANKL prevents autoimmune inflammation in the central nervous system. *Immunity.* (2015) 43:1174–85. doi: 10.1016/j.immuni.2015.10.017
11. Ahern E, Smyth MJ, Dougall WC, Teng MWL. Roles of the RANKL-RANK axis in antitumour immunity - implications for therapy. *Nat Rev Clin Oncol.* (2018) 15:676–93. doi: 10.1038/s41571-018-0095-y
12. Nakagawa N, Kinosaki M, Yamaguchi K, Shima N, Yasuda H, Yano K, et al. RANK is the essential signaling receptor for osteoclast differentiation factor in osteoclastogenesis. *Biochem Biophys Res Commun.* (1998) 253:395–400. doi: 10.1006/bbrc.1998.9788
13. Yasuda H, Shima N, Nakagawa N, Yamaguchi K, Kinosaki M, Mochizuki S, et al. Osteoclast differentiation factor is a ligand for osteoprotegerin/osteoclastogenesis-inhibitory factor and is identical to TRANCE/RANKL. *Proc Natl Acad Sci USA.* (1998) 95:3597–602. doi: 10.1073/pnas.95.7.3597
14. Dougall WC, Glaccum M, Charrier K, Rohrbach K, Brasel K, De Smedt T, et al. RANK is essential for osteoclast and lymph node development. *Genes Dev.* (1999) 13:2412–24. doi: 10.1101/gad.13.18.2412
15. Li J, Sarosi I, Yan XQ, Morony S, Capparelli C, Tan HL, et al. RANK is the intrinsic hematopoietic cell surface receptor that controls osteoclastogenesis and regulation of bone mass and calcium metabolism. *Proc Natl Acad Sci USA.* (2000) 97:1566–71. doi: 10.1073/pnas.97.4.1566
16. Sobacchi C, Frattini A, Guerrini MM, Abinun M, Pangrazio A, Susani L, et al. Osteoclast-poor human osteopetrosis due to mutations in the gene encoding RANKL. *Nat Genet.* (2007) 39:960–2. doi: 10.1038/ng2076
17. Guerrini MM, Sobacchi C, Cassani B, Abinun M, Kilic SS, Pangrazio A, et al. Human osteoclast-poor osteopetrosis with hypogammaglobulinemia due to TNFRSF11A (RANK) mutations. *Am J Hum Genet.* (2008) 83:64–76. doi: 10.1016/j.ajhg.2008.06.015
18. Kobayashi K, Takahashi N, Jimi E, Udagawa N, Takami M, Kotake S, et al. Tumor necrosis factor alpha stimulates osteoclast differentiation by a mechanism independent of the ODF/RANKL-RANK interaction. *J Exp Med.* (2000) 191:275–86. doi: 10.1084/jem.191.2.275
19. Kim N, Kadono Y, Takami M, Lee J, Lee SH, Okada F, et al. Osteoclast differentiation independent of the TRANCE-RANK-TRAF6 axis. *J Exp Med.* (2005) 202:589–95. doi: 10.1084/jem.20050978
20. O'Brien W, Fissel BM, Maeda Y, Yan J, Ge X, Gravallese EM, et al. RANK-independent osteoclast formation and bone erosion in inflammatory arthritis. *Arthritis Rheumatol.* (2016) 68:2889–900. doi: 10.1002/art.39837
21. Tsukasaki M, Hamada K, Okamoto K, Nagashima K, Terashima A, Komatsu N, et al. LOX fails to substitute for RANKL in osteoclastogenesis. *J Bone Miner Res.* (2017) 32:434–9. doi: 10.1002/jbmr.2990
22. Mbalaviele G, Novack DV, Schett G, Teitelbaum SL. Inflammatory osteolysis: a conspiracy against bone. *J Clin Invest.* (2017) 127:2030–9. doi: 10.1172/JCI93356
23. Nakashima T, Hayashi M, Fukunaga T, Kurata K, Oh-Hora M, Feng JQ, et al. Evidence for osteocyte regulation of bone homeostasis through RANKL expression. *Nat Med.* (2011) 17:1231–4. doi: 10.1038/nm.2452
24. Xiong J, Onal M, Jilka RL, Weinstein RS, Manolagas SC, O'Brien CA. Matrix-embedded cells control osteoclast formation. *Nat Med.* (2011) 17:1235–41. doi: 10.1038/nm.2448
25. Fujiwara Y, Piemontese M, Liu Y, Thostenson JD, Xiong J, O'Brien CA. RANKL (receptor activator of NFkB ligand) produced by osteocytes is required for the increase in B cells and bone loss caused by estrogen deficiency in mice. *J Biol Chem.* (2016) 291:24838–50. doi: 10.1074/jbc.M116.742452
26. Xiong J, Cawley K, Piemontese M, Fujiwara Y, Zhao H, Goellner JJ, et al. Soluble RANKL contributes to osteoclast formation in adult mice but not ovariectomy-induced bone loss. *Nat Commun.* (2018) 9:2909. doi: 10.1038/s41467-018-05244-y
27. Schena F, Menale C, Caci E, Diomede L, Palagano E, Recordati C, et al. Murine Rankl(-/-) mesenchymal stromal cells display an osteogenic differentiation defect improved by a RANKL-expressing lentiviral vector. *Stem Cells.* (2017) 35:1365–77. doi: 10.1002/stem.2574
28. Chen X, Zhi X, Wang J, Su J. RANKL signaling in bone marrow mesenchymal stem cells negatively regulates osteoblastic bone formation. *Bone Res.* (2018) 6:34. doi: 10.1038/s41413-018-0035-6
29. Okamoto K, Nakashima T, Shinohara M, Negishi-KOGA T, Komatsu N, Terashima A, et al. Osteoimmunology: the conceptual framework unifying the immune and skeletal systems. *Physiol Rev.* (2017) 97:1295–349. doi: 10.1152/physrev.00036.2016
30. Kobayashi N, Kadono Y, Naito A, Matsumoto K, Yamamoto T, Tanaka S, et al. Segregation of TRAF6-mediated signaling pathways clarifies its role in osteoclastogenesis. *EMBO J.* (2001) 20:1271–80. doi: 10.1093/emboj/20.6.1271
31. Kim K, Lee SH, Ha Kim J, Choi Y, Kim N. NFATc1 induces osteoclast fusion via up-regulation of Atp6v0d2 and the dendritic cell-specific transmembrane protein (DC-STAMP). *Mol Endocrinol.* (2008) 22:176–85. doi: 10.1210/me.2007-0237
32. Matsuo K, Owens JM, Tonko M, Elliott C, Chambers TJ, Wagner EF. Fosl1 is a transcriptional target of c-Fos during osteoclast differentiation. *Nat Genet.* (2000) 24:184–7. doi: 10.1038/72855
33. Abu-Amer Y. NF-kappaB signaling and bone resorption. *Osteoporos Int.* (2013) 24:2377–86. doi: 10.1007/s00198-013-2313-x
34. Kim HS, Kim DK, Kim AR, Mun SH, Lee SK, Kim JH, et al. Fyn positively regulates the activation of DAP12 and FcRgamma-mediated costimulatory

signals by RANKL during osteoclastogenesis. *Cell Signal.* (2012) 24:1306–14. doi: 10.1016/j.cellsig.2012.02.014
35. Li S, Miller CH, Giannopoulou E, Hu X, Ivashkiv LB, Zhao B. RBP-J imposes a requirement for ITAM-mediated costimulation of osteoclastogenesis. *J Clin Invest.* (2014) 124:5057–73. doi: 10.1172/JCI71882
36. Lee NK, Choi YG, Baik JY, Han SY, Jeong DW, Bae YS, et al. A crucial role for reactive oxygen species in RANKL-induced osteoclast differentiation. *Blood.* (2005) 106:852–9. doi: 10.1182/blood-2004-09-3662
37. Gambari L, Lisignoli G, Cattini L, Manferdini C, Facchini A, Grassi F. Sodium hydrosulfide inhibits the differentiation of osteoclast progenitor cells via NRF2-dependent mechanism. *Pharmacol Res.* (2014) 87:99–112. doi: 10.1016/j.phrs.2014.06.014
38. Tan P, Guan H, Xie L, Mi B, Fang Z, Li J, et al. FOXO1 inhibits osteoclastogenesis partially by antagnozing MYC. *Sci Rep.* (2015) 5:16835. doi: 10.1038/srep16835
39. Kim HS, Nam ST, Mun SH, Lee SK, Kim HW, Park YH, et al. DJ-1 controls bone homeostasis through the regulation of osteoclast differentiation. *Nat Commun.* (2017) 8:1519. doi: 10.1038/s41467-017-01527-y
40. Simonet WS, Lacey DL, Dunstan CR, Kelley M, Chang MS, Luthy R, et al. Osteoprotegerin: a novel secreted protein involved in the regulation of bone density. *Cell.* (1997) 89:309–19. doi: 10.1016/S0092-8674(00)80209-3
41. Baud'huin M, Duplomb L, Teletchea S, Lamoureux F, Ruiz-Velasco C, Maillasson M, et al. Osteoprotegerin: multiple partners for multiple functions. *Cytokine Growth Factor Rev.* (2013) 24:401–9. doi: 10.1016/j.cytogfr.2013.06.001
42. Luo J, Yang Z, Ma Y, Yue Z, Lin H, Qu G, et al. LGR4 is a receptor for RANKL and negatively regulates osteoclast differentiation and bone resorption. *Nat Med.* (2016) 22:539–46. doi: 10.1038/nm.4076
43. Sun P, Jia K, Zheng C, Zhu X, Li J, He L, et al. Loss of Lgr4 inhibits differentiation, migration and apoptosis, and promotes proliferation in bone mesenchymal stem cells. *J Cell Physiol.* (2018). doi: 10.1002/jcp.27927. [Epub ahead of print].
44. Lacey DL, Boyle WJ, Simonet WS, Kostenuik PJ, Dougall WC, Sullivan JK, et al. Bench to bedside: elucidation of the OPG-RANK-RANKL pathway and the development of denosumab. *Nat Rev Drug Discov.* (2012) 11:401–19. doi: 10.1038/nrd3705
45. Lewiecki EM. New and emerging concepts in the use of denosumab for the treatment of osteoporosis. *Ther Adv Musculoskelet Dis.* (2018) 10:209–23. doi: 10.1177/1759720X18805759
46. Savvidou OD, Bolia IK, Chloros GD, Papanastasiou J, Koutsouradis P, Papagelopoulos PJ. Denosumab: current use in the treatment of primary bone tumors. *Orthopedics.* (2017) 40:204–10. doi: 10.3928/01477447-20170627-04
47. Zheng H, Li W, Kang Y. Tumor-stroma interactions in bone metastasis: molecular mechanisms and therapeutic implications. *Cold Spring Harb Symp Quant Biol.* (2016) 81:151–61. doi: 10.1101/sqb.2016.81.030775
48. Tanaka Y, Ohira T. Mechanisms and therapeutic targets for bone damage in rheumatoid arthritis, in particular the RANK-RANKL system. *Curr Opin Pharmacol.* (2018) 40:110–9. doi: 10.1016/j.coph.2018.03.006
49. Sigl V, Jones LP, Penninger JM. RANKL/RANK: from bone loss to the prevention of breast cancer. *Open Biol.* (2016) 6:160230. doi: 10.1098/rsob.160230
50. Shroff R, Beringer O, Rao K, Hofbauer LC, Schulz A. Denosumab for post-transplantation hypercalcemia in osteopetrosis. *N Engl J Med.* (2012) 367:1766–7. doi: 10.1056/NEJMc1206193
51. Rotman M, Hamdy NAT, Appelman-Dijkstra NM. Clinical and translational pharmacological aspects of the management of fibrous dysplasia of bone. *Br J Clin Pharmacol.* (2018). doi: 10.1111/bcp.13820. [Epub ahead of print].
52. Li G, Jin Y, Levine MAH, Hoyer-Kuhn H, Ward L, Adachi JD. Systematic review of the effect of denosumab on children with osteogenesis imperfecta showed inconsistent findings. *Acta Paediatr.* (2018) 107:534–7. doi: 10.1111/apa.14154
53. Tsourdi E, Langdahl B, Cohen-Solal M, Aubry-Rozier B, Eriksen EF, Guanabens N, et al. Discontinuation of Denosumab therapy for osteoporosis: a systematic review and position statement by ECTS. *Bone.* (2017) 105:11–7. doi: 10.1016/j.bone.2017.08.003
54. Roux S, Massicotte MH, Huot Daneault A, Brazeau-Lamontagne L, Dufresne J. Acute hypercalcemia and excessive bone resorption following anti-RANKL withdrawal: case report and brief literature review. *Bone.* (2019) 120:482–6. doi: 10.1016/j.bone.2018.12.012
55. An J, Hao D, Zhang Q, Chen B, Zhang R, Wang Y, et al. Natural products for treatment of bone erosive diseases: the effects and mechanisms on inhibiting osteoclastogenesis and bone resorption. *Int Immunopharmacol.* (2016) 36:118–31. doi: 10.1016/j.intimp.2016.04.024
56. Hong G, Zhou L, Shi X, He W, Wang H, Wei Q, et al. Bajijiasu abrogates osteoclast differentiation via the suppression of RANKL signaling pathways through NF-kappaB and NFAT. *Int J Mol Sci.* (2018) 18:E203. doi: 10.3390/ijms18010203
57. Wang Q, Yao L, Xu K, Jin H, Chen K, Wang Z, et al. Madecassoside inhibits estrogen deficiency-induced osteoporosis by suppressing RANKL-induced osteoclastogenesis. *J Cell Mol Med.* (2019) 23:380–94. doi: 10.1111/jcmm.13942
58. Xu Q, Chen G, Liu X, Dai M, Zhang B. Icariin inhibits RANKL-induced osteoclastogenesis via modulation of the NF-kappaB and MAPK signaling pathways. *Biochem Biophys Res Commun.* (2019) 508:902–6. doi: 10.1016/j.bbrc.2018.11.201
59. Ikebuchi Y, Aoki S, Honma M, Hayashi M, Sugamori Y, Khan M, et al. Coupling of bone resorption and formation by RANKL reverse signalling. *Nature.* (2018) 561:195–200. doi: 10.1038/s41586-018-0482-7
60. Sone E, Noshiro D, Ikebuchi Y, Nakagawa M, Khan M, Tamura Y, et al. The induction of RANKL molecule clustering could stimulate early osteoblast differentiation. *Biochem Biophys Res Commun.* (2018) 509:435–40. doi: 10.1016/j.bbrc.2018.12.093
61. Koch U, Radtke F. Mechanisms of T cell development and transformation. *Annu Rev Cell Dev Biol.* (2011) 27:539–62. doi: 10.1146/annurev-cellbio-092910-154008
62. Shah DK, Zuniga-Pflucker JC. An overview of the intrathymic intricacies of T cell development. *J Immunol.* (2014) 192:4017–23. doi: 10.4049/jimmunol.1302259
63. Petrie HT, Zuniga-Pflucker JC. Zoned out: functional mapping of stromal signaling microenvironments in the thymus. *Annu Rev Immunol.* (2007) 25:649–79. doi: 10.1146/annurev.immunol.23.021704.115715
64. Koch U, Fiorini E, Benedito R, Besseyrias V, Schuster-Gossler K, Pierres M, et al. Delta-like 4 is the essential, nonredundant ligand for Notch1 during thymic T cell lineage commitment. *J Exp Med.* (2008) 205:2515–23. doi: 10.1084/jem.20080829
65. Hirano K, Negishi N, Yazawa M, Yagita H, Habu S, Hozumi K. Delta-like 4-mediated Notch signaling is required for early T-cell development in a three-dimensional thymic structure. *Eur J Immunol.* (2015) 45:2252–62. doi: 10.1002/eji.201445123
66. Rodrigues PM, Peterson P, Alves NL. Setting up the perimeter of tolerance: insights into mTEC physiology. *Trends Immunol.* (2018) 39:2–5. doi: 10.1016/j.it.2017.11.001
67. Aschenbrenner K, D'Cruz LM, Vollmann EH, Hinterberger M, Emmerich J, Swee LK, et al. Selection of Foxp3+ regulatory T cells specific for self antigen expressed and presented by Aire+ medullary thymic epithelial cells. *Nat Immunol.* (2007) 8:351–8. doi: 10.1038/ni1444
68. Anderson G, Takahama Y. Thymic epithelial cells: working class heroes for T cell development and repertoire selection. *Trends Immunol.* (2012) 33:256–63. doi: 10.1016/j.it.2012.03.005
69. Lei Y, Ripen AM, Ishimaru N, Ohigashi I, Nagasawa T, Jeker LT, et al. Aire-dependent production of XCL1 mediates medullary accumulation of thymic dendritic cells and contributes to regulatory T cell development. *J Exp Med.* (2011) 208:383–94. doi: 10.1084/jem.20102327
70. Burkly L, Hession C, Ogata L, Reilly C, Marconi LA, Olson D, et al. Expression of relB is required for the development of thymic medulla and dendritic cells. *Nature.* (1995) 373:531–6. doi: 10.1038/373531a0
71. Weih F, Carrasco D, Durham SK, Barton DS, Rizzo CA, Ryseck RP, et al. Multiorgan inflammation and hematopoietic abnormalities in mice with a targeted disruption of RelB, a member of the NF-kappa B/Rel family. *Cell.* (1995) 80:331–40. doi: 10.1016/0092-8674(95)90416-6
72. Kajiura F, Sun S, Nomura T, Izumi K, Ueno T, Bando Y, et al. NF-kappa B-inducing kinase establishes self-tolerance in a thymic stroma-dependent manner. *J Immunol.* (2004) 172:2067–75. doi: 10.4049/jimmunol.172.4.2067
73. Akiyama T, Maeda S, Yamane S, Ogino K, Kasai M, Kajiura F, et al. Dependence of self-tolerance on TRAF6-directed development

of thymic stroma. *Science.* (2005) 308:248–51. doi: 10.1126/science.1105677
74. Nitta T, Ohigashi I, Nakagawa Y, Takahama Y. Cytokine crosstalk for thymic medulla formation. *Curr Opin Immunol.* (2011) 23:190–7. doi: 10.1016/j.coi.2010.12.002
75. Sun L, Luo H, Li H, Zhao Y. Thymic epithelial cell development and differentiation: cellular and molecular regulation. *Protein Cell.* (2013) 4:342–55. doi: 10.1007/s13238-013-3014-0
76. Bichele R, Kisand K, Peterson P, Laan M. TNF superfamily members play distinct roles in shaping the thymic stromal microenvironment. *Mol Immunol.* (2016) 72:92–102. doi: 10.1016/j.molimm.2016.02.015
77. Lkhagvasuren E, Sakata M, Ohigashi I, Takahama Y. Lymphotoxin beta receptor regulates the development of CCL21-expressing subset of postnatal medullary thymic epithelial cells. *J Immunol.* (2013) 190:5110–7. doi: 10.4049/jimmunol.1203203
78. Danzl NM, Jeong S, Choi Y, Alexandropoulos K. Identification of novel thymic epithelial cell subsets whose differentiation is regulated by RANKL and Traf6. *PLoS ONE.* (2014) 9:e86129. doi: 10.1371/journal.pone.0086129
79. Fujihara C, Williams JA, Watanabe M, Jeon H, Sharrow SO, Hodes RJ. T cell-B cell thymic cross-talk: maintenance and function of thymic B cells requires cognate CD40-CD40 ligand interaction. *J Immunol.* (2014) 193:5534–44. doi: 10.4049/jimmunol.1401655
80. Liu X, Invernizzi P, Lu Y, Kosoy R, Lu Y, Bianchi I, et al. Genome-wide meta-analyses identify three loci associated with primary biliary cirrhosis. *Nat Genet.* (2010) 42:658–60. doi: 10.1038/ng.627
81. Akiyama N, Shinzawa M, Miyauchi M, Yanai H, Tateishi R, Shimo Y, et al. Limitation of immune tolerance-inducing thymic epithelial cell development by Spi-B-mediated negative feedback regulation. *J Exp Med.* (2014) 211:2425–38. doi: 10.1084/jem.20141207
82. Hikosaka Y, Nitta T, Ohigashi I, Yano K, Ishimaru N, Hayashi Y, et al. The cytokine RANKL produced by positively selected thymocytes fosters medullary thymic epithelial cells that express autoimmune regulator. *Immunity.* (2008) 29:438–50. doi: 10.1016/j.immuni.2008.06.018
83. White AJ, Lucas B, Jenkinson WE, Anderson G. Invariant NKT cells and control of the thymus medulla. *J Immunol.* (2018) 200:3333–9. doi: 10.4049/jimmunol.1800120
84. Zuklys S, Balciunaite G, Agarwal A, Fasler-Kan E, Palmer E, Hollander GA. Normal thymic architecture and negative selection are associated with Aire expression, the gene defective in the autoimmune-polyendocrinopathy-candidiasis-ectodermal dystrophy (APECED). *J Immunol.* (2000) 165:1976–83. doi: 10.4049/jimmunol.165.4.1976
85. White AJ, Withers DR, Parnell SM, Scott HS, Finke D, Lane PJ, et al. Sequential phases in the development of Aire-expressing medullary thymic epithelial cells involve distinct cellular input. *Eur J Immunol.* (2008) 38:942–7. doi: 10.1002/eji.200738052
86. Montero-Herradon S, Garcia-Ceca J, Zapata AG. Altered maturation of medullary TEC in EphB-deficient Thymi is recovered by RANK signaling stimulation. *Front Immunol.* (2018) 9:1020. doi: 10.3389/fimmu.2018.01020
87. Rossi SW, Kim MY, Leibbrandt A, Parnell SM, Jenkinson WE, Glanville SH, et al. RANK signals from CD4(+)3(−) inducer cells regulate development of Aire-expressing epithelial cells in the thymic medulla. *J Exp Med.* (2007) 204:1267–72. doi: 10.1084/jem.20062497
88. Roberts NA, White AJ, Jenkinson WE, Turchinovich G, Nakamura K, Withers DR, et al. Rank signaling links the development of invariant gammadelta T cell progenitors and Aire(+) medullary epithelium. *Immunity.* (2012) 36:427–37. doi: 10.1016/j.immuni.2012.01.016
89. Desanti GE, Cowan JE, Baik S, Parnell SM, White AJ, Penninger JM, et al. Developmentally regulated availability of RANKL and CD40 ligand reveals distinct mechanisms of fetal and adult cross-talk in the thymus medulla. *J Immunol.* (2012) 189:5519–26. doi: 10.4049/jimmunol.1201815
90. Mccarthy NI, Cowan JE, Nakamura K, Bacon A, Baik S, White AJ, et al. Osteoprotegerin-mediated homeostasis of rank+ Thymic epithelial cells does not limit Foxp3+ regulatory T cell development. *J Immunol.* (2015) 195:2675–82. doi: 10.4049/jimmunol.1501226
91. Yin C, Pei XY, Shen H, Gao YN, Sun XY, Wang W, et al. Thymic homing of activated CD4(+) T cells induces degeneration of the thymic epithelium through excessive RANK signaling. *Sci Rep.* (2017) 7:2421. doi: 10.1038/s41598-017-02653-9
92. Shanley DP, Aw D, Manley NR, Palmer DB. An evolutionary perspective on the mechanisms of immunosenescence. *Trends Immunol.* (2009) 30:374–81. doi: 10.1016/j.it.2009.05.001
93. Sato K, Kato A, Sekai M, Hamazaki Y, Minato N. Physiologic thymic involution underlies age-dependent accumulation of senescence-associated CD4(+) T cells. *J Immunol.* (2017) 199:138–48. doi: 10.4049/jimmunol.1602005
94. Akiyama T, Shimo Y, Yanai H, Qin J, Ohshima D, Maruyama Y, et al. The tumor necrosis factor family receptors RANK and CD40 cooperatively establish the thymic medullary microenvironment and self-tolerance. *Immunity.* (2008) 29:423–37. doi: 10.1016/j.immuni.2008.06.015
95. Irla M, Hugues S, Gill J, Nitta T, Hikosaka Y, Williams IR, et al. Autoantigen-specific interactions with CD4+ thymocytes control mature medullary thymic epithelial cell cellularity. *Immunity.* (2008) 29:451–63. doi: 10.1016/j.immuni.2008.08.007
96. Irla M, Guerri L, Guenot J, Serge A, Lantz O, Liston A, et al. Antigen recognition by autoreactive CD4(+) thymocytes drives homeostasis of the thymic medulla. *PLoS ONE.* (2012) 7:e52591. doi: 10.1371/journal.pone.0052591
97. Otero DC, Baker DP, David M. IRF7-dependent IFN-beta production in response to RANKL promotes medullary thymic epithelial cell development. *J Immunol.* (2013) 190:3289–98. doi: 10.4049/jimmunol.1203086
98. Mouri Y, Yano M, Shinzawa M, Shimo Y, Hirota F, Nishikawa Y, et al. Lymphotoxin signal promotes thymic organogenesis by eliciting RANK expression in the embryonic thymic stroma. *J Immunol.* (2011) 186:5047–57. doi: 10.4049/jimmunol.1003533
99. Lin J, Yang L, Silva HM, Trzeciak A, Choi Y, Schwab SR, et al. Increased generation of Foxp3(+) regulatory T cells by manipulating antigen presentation in the thymus. *Nat Commun.* (2016) 7:10562. doi: 10.1038/ncomms10562
100. Mizuno A, Kanno T, Hoshi M, Shibata O, Yano K, Fujise N, et al. Transgenic mice overexpressing soluble osteoclast differentiation factor (sODF) exhibit severe osteoporosis. *J Bone Miner Metab.* (2002) 20:337–44. doi: 10.1007/s007740200049
101. Ohigashi I, Nitta T, Lkhagvasuren E, Yasuda H, Takahama Y. Effects of RANKL on the thymic medulla. *Eur J Immunol.* (2011) 41:1822–7. doi: 10.1002/eji.201141480
102. Lo Iacono N, Blair HC, Poliani PL, Marrella V, Ficara F, Cassani B, et al. Osteopetrosis rescue upon RANKL administration to Rankl(-/-) mice: a new therapy for human RANKL-dependent ARO. *J Bone Min Res.* (2012) 27:2501–10. doi: 10.1002/jbmr.1712
103. Lopes N, Vachon H, Marie J, Irla M. Administration of RANKL boosts thymic regeneration upon bone marrow transplantation. *Embo Mol Med.* (2017) 9:835–51. doi: 10.15252/emmm.201607176
104. Poliani PL, Vermi W, Facchetti F. Thymus microenvironment in human primary immunodeficiency diseases. *Curr Opin Allergy Clin Immunol.* (2009) 9:489–95. doi: 10.1097/ACI.0b013e3283327e5c
105. Toubert A, Glauzy S, Douay C, Clave E. Thymus and immune reconstitution after allogeneic hematopoietic stem cell transplantation in humans: never say never again. *Tissue Antigens.* (2012) 79:83–9. doi: 10.1111/j.1399-0039.2011.01820.x
106. Da Rocha LKA, De Barros SF, Bandeira F, Bollini A, Testa LHD, Simione AJ, et al. Thymopoiesis in pre- and post-hematopoietic stem cell transplantation. *Front Immunol.* (2018) 9:1889. doi: 10.3389/fimmu.2018.01889
107. Khan IS, Mouchess ML, Zhu ML, Conley B, Fasano KJ, Hou Y, et al. Enhancement of an anti-tumor immune response by transient blockade of central T cell tolerance. *J Exp Med.* (2014) 211:761–8. doi: 10.1084/jem.20131889
108. Bakhru P, Zhu ML, Wang HH, Hong LK, Khan I, Mouchess M, et al. Combination central tolerance and peripheral checkpoint blockade unleashes antimelanoma immunity. *JCI Insight.* (2017) 2:93265. doi: 10.1172/jci.insight.93265
109. Stolina M, Dwyer D, Ominsky MS, Corbin T, Van G, Bolon B, et al. Continuous RANKL inhibition in osteoprotegerin transgenic mice and rats suppresses bone resorption without impairing lymphorganogenesis or functional immune responses. *J Immunol.* (2007) 179:7497–505. doi: 10.4049/jimmunol.179.11.7497

110. Di Rosa F, Gebhardt T. Bone marrow T cells and the integrated functions of recirculating and tissue-resident memory T cells. *Front Immunol.* (2016) 7:51. doi: 10.3389/fimmu.2016.00051
111. Eghbali-Fatourechi G, Khosla S, Sanyal A, Boyle WJ, Lacey DL, Riggs BL. Role of RANK ligand in mediating increased bone resorption in early postmenopausal women. *J Clin Invest.* (2003) 111:1221–30. doi: 10.1172/JCI200317215
112. D'Amelio P, Grimaldi A, Di Bella S, Brianza SZM, Cristofaro MA, Tamone C, et al. Estrogen deficiency increases osteoclastogenesis up-regulating T cells activity: a key mechanism in osteoporosis. *Bone.* (2008) 43:92–100. doi: 10.1016/j.bone.2008.02.017
113. Adeel S, Singh K, Vydareny KH, Kumari M, Shah E, Weitzmann MN, et al. Bone loss in surgically ovariectomized premenopausal women is associated with T lymphocyte activation and thymic hypertrophy. *J Investig Med.* (2013) 61:1178–83. doi: 10.2310/JIM.0000000000000016
114. Toraldo G, Roggia C, Qian WP, Pacifici R, Weitzmann MN. IL-7 induces bone loss *in vivo* by induction of receptor activator of nuclear factor kappa B ligand and tumor necrosis factor alpha from T cells. *Proc Natl Acad Sci USA.* (2003) 100:125–30. doi: 10.1073/pnas.0136772100
115. Bernardi AI, Andersson A, Stubelius A, Grahnemo L, Carlsten H, Islander U. Selective estrogen receptor modulators in T cell development and T cell dependent inflammation. *Immunobiology.* (2015) 220:1122–8. doi: 10.1016/j.imbio.2015.05.009
116. D'Amelio P, Grimaldi A, Bernabei P, Pescarmona GP, Isaia G. Immune system and bone metabolism: does thymectomy influence postmenopausal bone loss in humans? *Bone.* (2006) 39:658–65. doi: 10.1016/j.bone.2006.03.009
117. Takayanagi H. New developments in osteoimmunology. *Nat Rev Rheumatol.* (2012) 8:684–9. doi: 10.1038/nrrheum.2012.167
118. Smolen JS, Aletaha D, Barton A, Burmester GR, Emery P, Firestein GS, et al. Rheumatoid arthritis. *Nat Rev Dis Primers.* (2018) 4:18001. doi: 10.1038/nrdp.2018.1
119. Mcinnes IB, Schett G. The pathogenesis of rheumatoid arthritis. *N Engl J Med.* (2011) 365:2205–19. doi: 10.1056/NEJMra1004965
120. Dakin SG, Coles M, Sherlock JP, Powrie F, Carr AJ, Buckley CD. Pathogenic stromal cells as therapeutic targets in joint inflammation. *Nat Rev Rheumatol.* (2018) 14:714–26. doi: 10.1038/s41584-018-0112-7
121. Harre U, Georgess D, Bang H, Bozec A, Axmann R, Ossipova E, et al. Induction of osteoclastogenesis and bone loss by human autoantibodies against citrullinated vimentin. *J Clin Invest.* (2012) 122:1791–802. doi: 10.1172/JCI60975
122. Bugatti S, Bogliolo L, Vitolo B, Manzo A, Montecucco C, Caporali R. Anti-citrullinated protein antibodies and high levels of rheumatoid factor are associated with systemic bone loss in patients with early untreated rheumatoid arthritis. *Arthritis Res Ther.* (2016) 18:226. doi: 10.1186/s13075-016-1116-9
123. Komatsu N, Takayanagi H. Immune-bone interplay in the structural damage in rheumatoid arthritis. *Clin Exp Immunol.* (2018) 194:1–8. doi: 10.1111/cei.13188
124. Hirota K, Yoshitomi H, Hashimoto M, Maeda S, Teradaira S, Sugimoto N, et al. Preferential recruitment of CCR6-expressing Th17 cells to inflamed joints via CCL20 in rheumatoid arthritis and its animal model. *J Exp Med.* (2007) 204:2803–12. doi: 10.1084/jem.20071397
125. Komatsu N, Okamoto K, Sawa S, Nakashima T, Oh-Hora M, Kodama T, et al. Pathogenic conversion of Foxp3+ T cells into TH17 cells in autoimmune arthritis. *Nat Med.* (2014) 20:62–8. doi: 10.1038/nm.3432
126. Nevius E, Gomes AC, Pereira JP. Inflammatory cell migration in rheumatoid arthritis: a comprehensive review. *Clin Rev Allergy Immunol.* (2016) 51:59–78. doi: 10.1007/s12016-015-8520-9
127. Baum R, Gravallese EM. Bone as a target organ in rheumatic disease: impact on osteoclasts and osteoblasts. *Clin Rev Allergy Immunol.* (2016) 51:1–15. doi: 10.1007/s12016-015-8515-6
128. Hayer S, Bauer G, Willburger M, Sinn K, Alasti F, Plasenzotti R, et al. Cartilage damage and bone erosion are more prominent determinants of functional impairment in longstanding experimental arthritis than synovial inflammation. *Dis Model Mech.* (2016) 9:1329–38. doi: 10.1242/dmm.025460
129. Boman A, Kokkonen H, Arlestig L, Berglin E, Rantapaa-Dahlqvist S. Receptor activator of nuclear factor kappa-B ligand (RANKL) but not sclerostin or gene polymorphisms is related to joint destruction in early rheumatoid arthritis. *Clin Rheumatol.* (2017) 36:1005–12. doi: 10.1007/s10067-017-3570-4
130. Chiu YG, Ritchlin CT. Denosumab: targeting the RANKL pathway to treat rheumatoid arthritis. *Expert Opin Biol Ther.* (2017) 17:119–28. doi: 10.1080/14712598.2017.1263614
131. Walsh MC, Choi Y. Biology of the RANKL-RANK-OPG System in Immunity, Bone, and Beyond. *Front Immunol.* (2014) 5:511. doi: 10.3389/fimmu.2014.00511
132. Takeuchi T, Tanaka Y, Ishiguro N, Yamanaka H, Yoneda T, Ohira T, et al. Effect of denosumab on Japanese patients with rheumatoid arthritis: a dose-response study of AMG 162 (Denosumab) in patients with RheumatoId arthritis on methotrexate to Validate inhibitory effect on bone Erosion (DRIVE)-a 12-month, multicentre, randomised, double-blind, placebo-controlled, phase II clinical trial. *Ann Rheum Dis.* (2016) 75:983–90. doi: 10.1136/annrheumdis-2015-208052
133. Cosway E, Anderson G, Garside P, Prendergast C. The thymus and rheumatology: should we care? *Curr Opin Rheumatol.* (2016) 28:189–95. doi: 10.1097/BOR.0000000000000251
134. Tanaka S, Maeda S, Hashimoto M, Fujimori C, Ito Y, Teradaira S, et al. Graded attenuation of TCR signaling elicits distinct autoimmune diseases by altering thymic T cell selection and regulatory T cell function. *J Immunol.* (2010) 185:2295–305. doi: 10.4049/jimmunol.1000848
135. Flores-Borja F, Jury EC, Mauri C, Ehrenstein MR. Defects in CTLA-4 are associated with abnormal regulatory T cell function in rheumatoid arthritis. *Proc Natl Acad Sci USA.* (2008) 105:19396–401. doi: 10.1073/pnas.0806855105
136. Cribbs AP, Kennedy A, Penn H, Read JE, Amjadi P, Green P, et al. Treg cell function in rheumatoid arthritis is compromised by ctla-4 promoter methylation resulting in a failure to activate the indoleamine 2,3-dioxygenase pathway. *Arthritis Rheumatol.* (2014) 66:2344–54. doi: 10.1002/art.38715
137. Raje N, Terpos E, Willenbacher W, Shimizu K, Garcia-Sanz R, Durie B, et al. Denosumab versus zoledronic acid in bone disease treatment of newly diagnosed multiple myeloma: an international, double-blind, double-dummy, randomised, controlled, phase 3 study. *Lancet Oncol.* (2018) 19:370–81. doi: 10.1016/S1470-2045(18)30072-X
138. Ahern E, Harjunpaa H, Barkauskas D, Allen S, Takeda K, Yagita H, et al. Co-administration of RANKL and CTLA4 antibodies enhances lymphocyte-mediated antitumor immunity in mice. *Clin Cancer Res.* (2017) 23:5789–801. doi: 10.1158/1078-0432.CCR-17-0606
139. Ahern E, Harjunpaa H, O'Donnell JS, Allen S, Dougall WC, Teng MWL, et al. RANKL blockade improves efficacy of PD1-PD-L1 blockade or dual PD1-PD-L1 and CTLA4 blockade in mouse models of cancer. *Oncoimmunology.* (2018) 7:e1431088. doi: 10.1080/2162402X.2018.1431088
140. Chen NJ, Huang MW, Hsieh SL. Enhanced secretion of IFN-gamma by activated Th1 cells occurs via reverse signaling through TNF-related activation-induced cytokine. *J Immunol.* (2001) 166:270–6. doi: 10.4049/jimmunol.166.1.270
141. Secchiero P, Corallini F, Barbarotto E, Melloni E, Di Iasio MG, Tiribelli M, et al. Role of the RANKL/RANK system in the induction of interleukin-8 (IL-8) in B chronic lymphocytic leukemia (B-CLL) cells. *J Cell Physiol.* (2006) 207:158–64. doi: 10.1002/jcp.20547
142. Zhang S, Wang X, Li G, Chong Y, Zhang J, Guo X, et al. Osteoclast regulation of osteoblasts via RANKRANKL reverse signal transduction *in vitro*. *Mol Med Rep.* (2017) 16:3994–4000. doi: 10.3892/mmr.2017.7039

Conflict of Interest Statement: The authors declare that the research was conducted in the absence of any commercial or financial relationships that could be construed as a potential conflict of interest.

frontiers in Immunology

REVIEW
published: 02 April 2019
doi: 10.3389/fimmu.2019.00663

Immune Modulation by Transplanted Calcium Phosphate Biomaterials and Human Mesenchymal Stromal Cells in Bone Regeneration

Paul Humbert[1], *Meadhbh Á. Brennan*[1,2], *Noel Davison*[3,4], *Philippe Rosset*[1,5], *Valérie Trichet*[1], *Frédéric Blanchard*[1]* *and Pierre Layrolle*[1]

[1] Laboratory Phy-Os, Inserm UMR1238, University of Nantes, Nantes, France, [2] Harvard School of Engineering and Applied Sciences, Harvard University, Cambridge, MA, United States, [3] MERLN Institute for Technology-Inspired Regenerative Medicine, Maastricht University, Maastricht, Netherlands, [4] Instructure Labs, B.V., The Hague, Netherlands, [5] Centre Hospitalier Universitaire de Tours, Tours, France

OPEN ACCESS

Edited by:
Claudine Blin-Wakkach, UMR7370 Laboratoire de Physio Médecine Moléculaire (LP2M), France

Reviewed by:
Catarina R. Almeida, University of Aveiro, Portugal
Yasser Mohamed El-Sherbiny, Nottingham Trent University, United Kingdom
Aisling Dunne, Trinity College Dublin, Ireland

***Correspondence:**
Frédéric Blanchard
frederic.blanchard@univ-nantes.fr

Specialty section:
This article was submitted to Inflammation, a section of the journal Frontiers in Immunology

Received: *11 December 2018*
Accepted: *11 March 2019*
Published: *02 April 2019*

Citation:
Humbert P, Brennan MÁ, Davison N, Rosset P, Trichet V, Blanchard F and Layrolle P (2019) Immune Modulation by Transplanted Calcium Phosphate Biomaterials and Human Mesenchymal Stromal Cells in Bone Regeneration. Front. Immunol. 10:663. doi: 10.3389/fimmu.2019.00663

A wide variety of biomaterials have been developed as both stabilizing structures for the injured bone and inducers of bone neoformation. They differ in chemical composition, shape, porosity, and mechanical properties. The most extensively employed and studied subset of bioceramics are calcium phosphate materials (CaPs). These materials, when transplanted alongside mesenchymal stem cells (MSCs), lead to ectopic (intramuscular and subcutaneous) and orthotopic bone formation in preclinical studies, and effective fracture healing in clinical trials. Human MSC transplantation in pre-clinical and clinical trials reveals very low engraftment in spite of successful clinical outcomes and their therapeutic actions are thought to be primarily through paracrine mechanisms. The beneficial role of transplanted MSC could rely on their strong immunomodulatory effect since, even without long-term engraftment, they have the ability to alter both the innate and adaptive immune response which is critical to facilitate new bone formation. This study presents the current knowledge of the immune response to the implantation of CaP biomaterials alone or in combination with MSC. In particular the central role of monocyte-derived cells, both macrophages and osteoclasts, in MSC-CaP mediated bone formation is emphasized. Biomaterial properties, such as macroporosity and surface microstructure, dictate the host response, and the ultimate bone healing cascade. Understanding intercellular communications throughout the inflammation, its resolution and the bone regeneration phase, is crucial to improve the current therapeutic strategies or develop new approaches.

Keywords: osteoimmunology, mesenchymal stromal cell, calcium phosphate biomaterial, bone regeneration, osteoclast, immune modulation

INTRODUCTION

Bone regeneration strategies remain a critical challenge in the treatment of delayed union and non-union fractures (1), bone loss due to tumor resection (2), metabolic bone diseases, or to heritable skeletal dysplasia such as *osteogenesis imperfecta*. Autologous bone grafting is the current clinical gold standard to repair large bone defects. This entails harvesting the patient's own bone

fragments, and transplanting them to the site of injury (3). There are ∼2.2 million bone graft procedures performed annually worldwide, including 1 million procedures in Europe (4). Indeed, after blood, bone is the most frequently transplanted tissue. The significant disadvantages of bone grafting, including the severe pain and morbidity endured by patients as a consequence of the bone harvest site, have prompted advances in the development of synthetic biomaterials targeting bone repair. Human bone comprises ∼70% of calcium phosphate (CaP) mineral; therefore CaPs are the biomaterials of choice to heal injured bone. They were first introduced in the 1920s as materials to facilitate bone repair (5) and have since undergone intense chemical and physical developments aimed at optimizing porosity, surface architecture, resorption rates, and mechanical strength in order to improve their bone healing capacities. Despite these advances in biomaterial design, CaPs still lack adequate osteogenecity to heal large, critical sized bone defects, and thus cell therapy has been employed for bone defect treatment with biomaterial bone substitutes such as CaPs to increase bone regeneration efficiency. Mesenchymal stromal stem cells (MSCs), derived primarily from the bone marrow and isolated by adherence to plastic, show great capacity for bone healing in unison with CaPs (6, 7). Although it is yet to be adopted into standard clinical practice, this state-of-the-art cell therapy is currently the most promising regenerative medicine strategy and has demonstrated successful bone healing in patients in clinical trials (8). The initial premise that MSCs, through cellular differentiation, regenerated damaged tissue was largely disregarded following observations that very few transplanted cells survive and engraft (9–11). Few children with severe *osteogenesis imperfecta* have received allogenic bone marrow transplant or allogenic MSC and showed faster growth, higher bone mineral content and less bone fracture than before transplant (12–16). Such growth and mineralization improvements were associated with <5% of donor cell engraftment. Consequently, it is proposed that the therapeutic benefit of transplanted MSCs is largely through a paracrine mechanism that stimulates recruitment of host cells, which ultimately form the new bone tissue. The underlying mechanisms involved have yet to be delineated, however evidence to date reveals that roles of MSCs and their secretions such as modulating immune responses (17), attenuating inflammation, and promoting angiogenesis (18), together act to ultimately ameliorate healing and restore function. The host immune-modulatory response to both CaPs and MSCs, encompassing both innate and adaptive immunity, and how this contributes to bone healing in the context of tissue engineered implants is the focus of the current review.

OSTEOIMMUNOLOGY OF CALCIUM PHOSPHATE CERAMICS IN BONE REGENERATION

A wide variety of CaP biomaterials have been developed to fill bone defects as alternatives to autologous bone grafting. Synthetically synthesized ceramics mainly comprise sintered CaPs in order to achieve higher mechanical strength, including β-tricalcium phosphate (β -TCP), hydroxyapatite (HA), or their mixtures (biphasic calcium phosphate: BCP). These CaPs are therefore widely described in terms of their interactions with cells and tissues following implantation, as well as in relation to their bone forming abilities. Synthetic CaPs bioceramics are used successfully to fill bone defects in various clinical indications since they are considered biocompatible, bioactive and osteoconductive, thereby permitting guidance of the bone healing process (19). *In vivo*, the chemical and physical properties of the biomaterial dictate the host response and the ultimate bone healing cascade and osteoinduction has been achieved by various CaP ceramics, which demonstrate ectopic bone formation when implanted in the muscles or subcutaneously in animals [reviewed in (13)].While the interactions of these CaP materials with body fluids, cells, and tissues have been investigated at both the microscopic and ultrastructural levels, there is still a lack of understanding of the potential mechanisms leading to osteoinduction. Early on, the dissolution and precipitation of an apatite layer on CaP materials was identified as a potential major trigger for bone formation (20). It was further proposed that concentration of bone growth factors from body fluids, especially BMPs onto the biomaterial surface, attracts circulating stem cells to form bone tissue (21). The geometry of the biomaterial is certainly a critical parameter for bone induction. Studies demonstrate that in order for CaPs to exhibit osteoinductive properties, both a macroporous structure and surface microporosity are prerequisites. Micro- and macro-porous BCP biomaterials demonstrated the ability to induce mature lamellar bone tissue after 6 months without the addition of osteogenic cells or bone growth factors when implanted ectopically in sheep (22). Macro pores are introduced into CaPs by the addition of pore makers during the fabrication process. The importance of macrostructure in efficient osteoinduction is highlighted as bone formation occurs primarily in concavities (23). Microporosity is controlled by the sintering temperature, with lower sintering temperatures resulting in higher surface microporosity. Interestingly, the microporous CaPs bioceramics exhibited higher bone growth in critical size bone defects in goats compared with autologous bone grafts or the same CaPs bearing larger surface micropores and lower specific surface area (higher sintering temperature) (24). Increasing the microporosity increases the surface area thus possibly enhancing the dissolution/reprecipitation phenomenon (21). Further to biomaterial geometry, it has been speculated that low oxygen tension in the central region of the implants might provoke dedifferentiation of pericytes from blood vessels into osteoblasts (25). Most recently, Bohner and Miron added the idea that depletion of calcium and/or phosphate ions in the center of an implanted material could induce bone formation *via* the calcium-sensing of immune and bone cells (26).

In early reports, bone induction by CaPs ceramics was thought to be limited to the muscles of large animals such as rabbits, sheep, goats, dogs, and baboon, until Barradas et al. screened various different mouse strains and found osteoinduction by CaPs ceramics in FVB/NCrl mice (27). This study was a major step for further understanding the biological mechanisms of osteoinduction by these ceramics because there are abundant

immunohistochemistry protocols available for mice compared to large animals, not to mention their ease of handling and low cost.

Innate Immune Response to Calcium Phosphate Biomaterials

Various innate immune cells participate in the host-cell response to the implantation of CaP materials including mast cells, neutrophils, monocytes, macrophages, and multinucleated giant cells (MNGCs) (28). In addition to their role in the innate immune response, macrophages have tissue-specific functions. Osteal macrophages (so called OsteoMacs), a specific type of specialized macrophages residing in the periosteum and endosteum, are an important cell type for the regulation of bone healing (29) but less is known about their relationship with implanted biomaterials (30). Depletion of OsteoMacs in mice demonstrates their key role in regulating bone regeneration in normal bone healing in a bone injury model (31, 32), suggesting that resident macrophages may also possess the phenotypic capability to instruct bone regeneration upon implantation of biomaterials used for bone repair. Previous studies have documented that resident or infiltrating monocyte-derived macrophages present at early time points after tissue trauma or the implantation of a biomaterial are characterized as pro-inflammatory (M1 macrophages), typified by their secretion of inflammatory cytokines such as TNFα, IL-1, IL-6, and IL-12, while macrophages present at later time points exhibit a predominantly anti-inflammatory profile (M2 subtype) and promote healing by secretion of cytokines such as IL-10 and TGF-β, stimulating angiogenesis, and recruiting cells for tissue repair (33–36). Importantly, macrophage polarization can be switched between M1 and M2, rendering them highly sensitive and adaptive to their environment. Moreover, mounting evidence suggests that macrophage polarization occurs over a continuous spectrum, rendering the M1/M2 classification paradigm too simple to accurately characterize their dynamic phenotypic changes and plasticity *in vivo*. In any case, macrophages are among the first cells present at the site of CaP implantation and play an integral role in MSC migration and bone formation (**Table 1**). The infiltration of macrophages and the subsequent homing of MSCs and ectopic bone formation was observed after CaP implantation in mice (44). Interestingly, MSCs migration and osteogenic differentiation was significantly enhanced by conditioned media (CM) from macrophages cultured on BCP, compared to CM from macrophages cultured on tissue culture plastic (43, 44). Furthermore, it was shown that macrophage-secreted MCP-1 and MIP-1α were the effectors of enhanced MSC migration.

Osteoclasts, which originate from the same hematopoietic precursor as macrophages, are multi-nucleated cells capable of efficiently degrading both the organic and inorganic fractions of bone. Activated osteoclasts have a characteristic morphology including a ruffle border by which they secrete proteases, such as cathepsin K and matrix metalloproteinases, and release hydrogen ions by proton pumps to acidify the resorptive pit. Histologically, osteoclasts can be identified by intensely positive tartrate-resistant acid phosphatase (TRAP) activity, which relates to their functional activity in resorbing bone or mineralized substrates such as CaPs (45). Osteoclastogenesis is essentially regulated, both *in vivo* and *in vitro*, by the macrophage colony-stimulating factor (M-CSF) and the tripartite system constituted by the receptor activator of nuclear factor κB (RANK), its ligand (RANKL) and osteoprotegerin (OPG). M-CSF permits survival and proliferation of osteoclast-precursors, also allowing them to respond efficiently to RANKL stimulation. RANKL triggers differentiation into osteoclasts by binding RANK, while OPG can prevent the interaction as a decoy receptor for RANKL (46). Osteoclasts are important players in the bone healing cascade. Several studies have documented that osteoclast presence at the site of CaP implantation precedes new bone formation (39). Evidence to demonstrate the crucial interplay between osteoclasts and osteoblasts, in association with CaPs, was highlighted by several studies (**Table 1**). Bisphosphonates are a class of drug employed to inhibit bone resorption by induced osteoclast apoptosis (47). The first-line medical management for *osteogenesis imperfecta* is based on bisphosphonates to inhibit osteoclasts, while the disease relies on osteoblast dysfunction. Bisphosphonates allow an increase of bone mineral density and a 20% decrease of fractures in long-bone in the pediatric *osteogenesis imperfecta* population (48, 49). However, in CaP-mediated bone formation, several osteoclast depletion strategies including the administration of bisphosphonates highlight the important role of osteoclasts, suggesting that coupling mechanisms linking osteoclast resorption to osteogenesis may be involved (50). Of note, Takeshita et al. convincingly showed that osteoclasts in association with CaP or bone secrete CTHRC1, which enhances osteoblastogenesis, thereby coupling bone resorption to formation. CTHRC1-triggered bone turnover was attenuated when resorption was inhibited by bisphosphonate (alendronate) treatment, and OC-specific CTHRC1 KO mice led to reduced bone formation and lower bone mass (37). This concurs with findings by other groups that bisphosphonates inhibited osteoclasts and osteoinduction by CaPs in baboons (38) or rabbits (41). Furthermore, depletion of osteoclasts by local injection of liposome-encapsulated clodronate impeded heterotopic bone formation by intrinsically osteoinductive microstructured CaPs after subcutaneous implantation in mice (42). Surface microstructure stimulates osteoclastogenesis and therefore may be a primary trigger for subsequent *de novo* bone formation for certain CaPs which do not require the addition of MSCs or growth factors to induce bone formation (40). The biological mechanism by which osteoclasts stimulate subsequent osteogenesis in response to these microstructured CaPs is still not understood. Even more interesting, non-microstructured CaPs, which possess no intrinsic osteoinduction potential, have been show to induce heterotopic bone formation when first seeded with osteoclasts prior to implantation. Taken together, OC depletion and enrichment strategies combined with implanted CaPs points to an essential role of this cell type in inducing new bone formation

Distinct from osteoclasts, MNGCs are observed in human histological samples around various CaP bone substitutes and their presence correlates with a higher maintenance of bone

TABLE 1 | Implication of macrophages and osteoclasts in the bone formation induced by calcium phosphate biomaterials.

CaP biomaterial	*In vitro* and *in vivo* models	Outcome	References
Hydroxyapatite (HA)	*In vitro:* Osteoclasts (OCs) were differentiated from bone marrow monocytes from C57BL/6 mice. Primary osteoblasts (OBs) were derived from the calvaria. *Ex vivo:* Organ culture of explanted calvaria. *In vivo model:* C57BL/6mice	CTHRC1 protein is secreted by mature OCs. CTHRC1 mRNA expression is elevated in OCs cultured on HA compared to tissue culture plastic (TCP). CTHRC1 stimulates osteoblastogenesis (gene expression and mineralized matrix deposition). CTHRC1 expression and bone turnover *in vivo* was increased by RANKL injections and conversely decreased by alendronate treatment. OC-specific CTHRC1 KO mice led to reduced bone formation and lower bone mass.	(37)
Coral derived calcium carbonate (CC)/ HA constructs	*In vivo model:* Intramuscular implantation in Chacma baboons	Osteoinduction of biomaterials was inhibited by preloading constructs with the bisphosphonate zoledronate.	(38)
β-TCP	*In vivo model:* Intramuscular implantation in female beagle dogs	CaP induces the formation of TRAP and Cathepsin K positive, multinucleated cells on the biomaterial, and their presence precedes ectopic bone formation	(39)
β-TCP with different surface microstructures	*In vitro:* Osteoclasts were differentiated from a murine macrophage cell line RAW264.7 Human MSCs were isolated from bone marrow harvested from femoral heads. *In vivo model:* Intramuscular implantation in male mongrel dogs	*In vitro*, CaPs with submicron-scale surfaces lead to increased differentiation of OCs and higher secretions of factors that induced osteogenic differentiation of MSCs. *In vivo*, submicro-structured CaPs formed bone and OCs presence was significant, whereas micro-structured CaPs formed no bone and OC presence was spare.	(40)
β-TCP	*In vivo model:* Rabbit femoral condyles	Loading of Alendronate (bisphosphonate) onto β-TCP inhibited the presence of TRAP-positive cells on the surface of the biomaterial and abrogated the CaP-mediated bone formation.	(41)
β-TCP	*In vivo model:* FVB/NCrl strain mice	CaPs induced osteoclastogenesis and ectopic bone formation. Depletion of osteoclasts by local injection of liposome-encapsulated clodronate impeded bone formation by CaPs.	(42)
Biphasic calcium phosphate (BCP) HA/ β-TCP composite	*In vitro:* Mouse macrophage cell line RAW264.7. Mouse bone marrow-derived MSCs.	Macrophages upregulated gene expression of inflammatory factors (IL-1, IL-6, MCP-1) and growth factors (EGF, PDGF, and VEGF) as a consequence of their CaP substrate. This macrophage conditioned media (CM) increased MSC migration and osteogenic differentiation (osteogenic gene expression and mineralized matrix deposition).	(43)
BCP (HA/ β-TCP)	*In vitro:* Mouse macrophage cell line RAW264.7. Mouse bone marrow-derived MSCs. *In vivo model:* Implantation into thigh muscle of male BALB/c mice.	BCP implantation *in vivo* caused infiltration of macrophages to the site, followed by homing of MSCs and subsequent ectopic bone formation. BMSCs migrated significantly faster under stimulation by CM from macrophages cultured on BCP, compared to CM from macrophages cultured on TCP. Secretion of MCP-1 and MIP- 1α by macrophages was increased by culture on BCP and were shown to be the effectors of enhanced migration since blocking these in macrophage CM had inhibited MSC migration.	(44)

mass in grafted sites (51). Such MNGCs are formed by fusion of monocytes/macrophages on various bone substitutes not surrounded by bone. Histologically, they are slightly TRAP positive and occasionally associated with small resorption lacunae, indicating a potential osteoclast-like activity. *In vitro*, they can be obtained by stimulation of monocytes with IL-4 and IL-13 (52, 53). These *in vitro* generated MNGCs can dissolve hydroxyapatite, although not as efficiently as osteoclasts, but they cannot digest the bone matrix (54). The case *in vivo* may however be more complex, particularly since mononucleated and fused macrophages found at the surface of implanted biomaterials or wounds may express a variety of markers spanning both classical M1 and alternatively activated M2 phenotypes.

Dendritic cells (DC) have been described as the scavenging sentinel cells also responsible for identifying foreign materials and organisms in the host. Although 25% of monocytes present at the site of injury or inflammation differentiate into DCs, the current knowledge of how DCs interact with biomaterials is incomplete—particularly whether they interact with the foreign body distinctly or in concert with macrophages and MNGCs (55). This is compounded by the heterogeneity of DC subsets, similar to macrophages (56). Still, it is clear that DCs also possess

phagocytic ability and can readily internalize CaP particles or polymeric beads. Such particle internalization causes DCs to secrete inflammatory cytokines as well as migrate back to the lymph nodes and instruct the adaptive immune response through T cell priming (55, 57). Because these cells interrogate and recognize foreign bodies as well as prolifically express surface antigens, DCs represent an important bridge between the innate and adaptive immune system and may mediate the polarization or transition between inflammatory or anti-inflammatory adaptive immunity. Illustrating this immune-modulatory role, DCs have been implicated with suppression of a chronic inflammatory response to implanted biomaterials and thus may play a key role in mediating the transition from fibrous encapsulation to functional tissue regeneration, and as the case may be with CaPs implanted in bony locations, the regeneration of bone tissue. Similar to macrophages, DCs have been shown to distinctly respond to biomaterial surface chemistry, hydrophobicity, and topography which direct activated vs. suppressive states of DCs (58). Some work has been conducted to explore the role of DCs in mediating the innate and adaptive immune response to subcutaneously implanted polymeric materials *in vivo* (59), but less is known about how DCs may interact with resorbable biomaterials such as calcium phosphates, particularly those that are too large to phagocytose.

These studies emphasize the crucial role of the innate immune system and osteoclastogenesis in modulating and facilitating bone healing and how CaP biomaterial properties such as surface microporosity significantly affect such responses. It should be noted that the combination of CaP biomaterial and natural (collagen, fibrinogen etc.) or synthetic polymers are also developed to influence the osteoinductive capacities of the implant (60) and could therefore influence the immune response. In spite of the significant improvements in CaPs, yielding well tolerated, osteoconductive biomaterials with some osteoinductive capability, most CaPs still lack adequate osteoinduction capacity for regenerating large bone defects. Therefore, they are generally employed for treating small bone defects, to supplement autologous bone grafting, or, increasingly, as scaffolds to deliver cells or growth factors targeting bone repair (61, 62).

OSTEOIMMUNOMODULATION AND OSTEOINDUCTION BY MSC/CaP COMBINATIONS

Bone marrow derived mesenchymal stromal cells may overcome the challenges of autologous bone grafting for the regeneration of large defects. Transplanted in unison with CaP bioceramics, MSCs achieve ectopic (intramuscular and subcutaneous) (7, 9, 63) and orthotopic bone formation and critical-sized defect healing in preclinical studies, and efficient fracture healing and bone augmentation in clinical trials (64, 65). The key role of implanted MSCs was initially thought to be their differentiation into bone forming osteoblast cells and studies observing transplanted MSCs within osteocyte lacunae of newly formed bone support this hypothesis (6, 66–68). However, in general, cell engraftment of transplanted MSCs is very low or completely absent, in spite of successful outcomes (10, 11, 69), leading to the contention that the therapeutic benefit of transplanted MSCs is largely through a paracrine mechanism. These conflicting observations of the fate of transplanted MSCs is present throughout the literature and could be caused by a multitude of reasons such as initial cell dosage, biomaterial scaffold employed, implantation site, and host immune response. In our own hands, we have observed instances of some, albeit a small proportion, transplanted MSCs present in newly formed bone (9), and others where cell engraftment was not detected (10), while both resulted in ectopic bone formation. Although not quantified, it appears the transplanted MSCs persisted in outcomes of abundant bone formation and interestingly human MSCs resided in osteocyte lacunae in the vicinity of host (mice) osteocytes, with host osteocytes representing the larger proportion (9). MSCs secrete a vast array of paracrine factors into their conditioned media (MSC-CM) *in vitro* and interestingly, administration of MSC-CM *in vivo*, induces healing in many tissues including bone (70–72) providing evidence that the MSC secretome can initiate the bone tissue regeneration cascade. The MSC secretome comprises all factors secreted by MSCs, including soluble secretions (cytokines, growth factors, chemokines, and hormones) as well as vesicular secretions, or extracellular vesicles (EVs), which encompass exosomes, microvesicles, and apoptotic bodies. EVs are nanoparticles (ranging in size from 30 to 1,000 nm) that are secreted by all cells and carry bioactive cargo from the parental cells including lipids, proteins, RNA, and DNA (73, 74). It was recently reported that EVs secreted by MSCs have therapeutic potential in preclinical studies targeting bone repair (75–78). While not yet investigated in the context of bone regeneration, it has been observed in other settings that EVs secreted from MSCs mimic the immune-regulatory function of MSCs (79).

The Immune System Influences MSC-Based Bone Regeneration

Several studies have observed that MSCs enhance bone repair by modulating the foreign body response to CaPs. Macrophages are an important innate immune cell population for the regulation of MSC-based bone regeneration. Interestingly, it was observed that the mobilization of macrophages to the site of CaP implantation was significantly enhanced by MSC transplantation prior to MSC-mediated ectopic bone formation (10, 17). Early studies indicated that inflammatory macrophages suppressed osteoblastogenesis, through secretion of TNFα and IL1b [reviewed in (50)]. However, in contrast to this, both Tour et al. (17) and Gamblin et al. (10) independently observed that transplanted MSCs led to a M1 dominant macrophage phenotype, which was followed by bone formation. In line with these *in vivo* studies, several *in vitro* studies have demonstrated the impact of M1 macrophages on enhancing the osteogenic differentiation of MSCs. We previously demonstrated that inflammatory M1 macrophages secrete Oncostatin M (OSM) to improve osteoblastogenesis *in vitro* (80). In addition, OSM production by macrophages

sustained bone regeneration in a mouse model of tibia injury (81). Furthermore, MSCs treated with conditioned media (CM) from lipopolysaccharide (LPS) stimulated monocytes exhibited increased osteogenic differentiation (82), an effect partially imparted by extracellular vesicles secreted by the activated monocytes (83). Conversely, other *in vitro* studies have reported that M2, and not M1 macrophages, enhanced osteogenic differentiation of MSCs (84). The exact role of resident vs. monocyte-derived macrophages or of M1 vs. M2 alternatively activated macrophages in response to transplanted MSCs are still not clear. The M1/M2 paradigm is certainly a key for successful bone regeneration, since resolution of inflammation and tissue repair are tightly linked (85). Interestingly, M1 and M2 macrophages were both recently demonstrated to modulate MSC osteogenic differentiation but in disparate manners, whereby M1 macrophages enhanced early osteogenic differentiation without any effect on matrix mineralization, which was subsequently enhanced by M2 macrophages (86). In addition, it was demonstrated that macrophages preferentially recruit fibroblasts over MSCs. Pre-incubation of macrophages with immunomodulatory MSCs impairs fibroblast recruitment (87). Taken together, these studies indicate that macrophage polarization is important for distinct roles in the bone healing cascade by MSCs in association with CaPs, much like how normal tissue repair encompasses a transition from a pro-inflammatory status to a pro-reparative status.

Osteoclasts also play a central role in the regulation of MSC-based bone regeneration. It was demonstrated *in vitro* that osteoclasts secrete factors (S1P, BMPs, WNTs etc.) which induce MSC migration and osteogenic differentiation (88, 89). Interestingly, MSCs transplanted with BCP were shown to positively influence the foreign body reaction by attracting circulating monocytes and inducing their differentiation into osteoclasts, thus favoring bone formation. Importantly, depletion of osteoclasts by local injection of clodronate or injection of neutralizing anti-RANKL antibodies impeded bone formation, highlighting the imperative role of osteoclasts in MSC-mediated bone formation (10).

The adaptive immune system also plays an important role in MSC-modulated bone regeneration, which was elegantly shown by Liu et al. (90) and is discussed in detail in **Table 2**. Briefly, MSCs together with CaP particles induced ectopic bone formation in immuno-deficient mice but failed to do so in immune competent C57BL/6 mice (90). Moreover, infusion of CD4+ T cells in nude mice blocked ectopic bone formation through secretion of TNFα and IFNγ, which inhibited MSC differentiation and induced MSC apoptosis (90, 92). Interestingly, infusion of CD4+ CD25+ Treg abolished TNFα and IFNγ production and improved MSC-mediated bone regeneration in critical-sized calvarial bone defects in C57BL/6 mice (90). These observations were corroborated by findings that MSC from immune-competent mice formed ectopic bone in immune deficient mice, but much less in syngenic mice with the initiation of an inflammatory reaction involving Th1, Th2, and cytotoxic T-cell responses (91). Collectively these data demonstrate that modulation of both the innate and adaptive host immune response facilitates MSC-based bone regeneration.

IMPACT OF MSC STRESS ON IMMUNOMODULATION

As indicated above, implantation of MSCs with CaP results in the local recruitment of various innate immune cells including mast cells, neutrophils, monocytes, macrophages, and several types of multinucleated giant cells. An exhaustive overview of how MSC influence the innate and adaptive immune system is outside the scope of this review. Rather, we focus on how transplanted MSCs in association with CaPs may modulate the immune system by focusing on the conditions that MSCs encounter following transplantation and the potential impact that these cell stresses can have on MSCs immunomodulation.

MSC Influence the Innate and Adaptive Immune System

Since MSCs express low levels of MHC-II and costimulatory molecules (CD40, CD80, CD86), but substantial amount of the tolerogenic HLA-G molecule, they are considered as immunoprivileged cells, and thus would be ideal for tissue repair even in allogeneic transplantation (92, 93). Moreover, the discovery of the immunomodulatory roles of MSCs fostered their therapeutic use to suppress inflammation and limit pathogenic immune responses in graft-vs-host and auto-immune diseases such as multiple sclerosis, diabetes, and rheumatoid arthritis. Indeed, MSCs tend to limit macrophage polarization to M1, favoring M2 polarization. They also favor the generation of regulatory dendritic cells. They inhibit mast cells degranulation and NK cell effector functions (**Figure 1**). MSC production of PGE2, IL-6, TGFβ, and IDO for example has a key role in these suppressive effects on innate immune cells (93, 94). With regard to adaptive immune cells, MSCs favor the development of Th2 and Treg cells, with suppression of CD4+ T cells proliferation and polarization toward Th1 and Th17 cells. They also inhibit B cell activation, proliferation, and differentiation into plasma cells. These suppressive effects depend on MSCs production of NO, TGFβ, PGE2, IL-10, and ligation of PD-1/PD-L1 for example (93, 94). Interestingly, culture of MSC on BCP did not impair their suppressive effect toward T, B, and Natural Killer (NK) cells (95). Extracellular vesicles produced by MSC are also implicated in immunomodulation (96). It is important to note that the immunosuppressive effect of MSCs when delivered systemically is well documented, but the possible role of MSCs in regulating the innate and adaptive immune responses when delivered locally to regenerate bone remains elusive.

Impact of Stressful Conditions on MSCs Phenotype/Secretome

Because MSCs disappear shortly after implantation with CaP, it is important to consider the impact of cell stress or cell death on MSCs immunomodulation activity. The primary factors responsible for the large cell death of transplanted BMSCs include the ischemic environment and the lack of glucose that the BMSCs encounter (97–100). It is unclear the exact means of MSCs death after implantation with CaP

TABLE 2 | Osteoimmunology of mesenchymal stem cells transplantation with calcium phosphate biomaterials.

CaP Biomaterial	MSC origin	*In vitro* and *In vivo* models	Outcome	References
BCP (HA/β-TCP)	Human bone marrow derived MSCs	*In vivo model:* Intramuscular implantation in immunocompromised nude NMRI Nu/Nu female mice	Both macrophage and osteoclast presence at the CaP site was significantly enhanced by MSC transplantation. Their presence preceded MSC-mediated ectopic bone formation. Depletion of osteoclasts by local injection of clodronate impeded bone formation, highlighting the imperative role of osteoclasts in MSC-mediated bone formation	(10)
HA	Rat (Lewis) bone marrow derived MSCs	*In vivo model:* Rat calvaria critical-sized defects	MSCs increase bone formation by modulating (both up- and down-regulation) the foreign body reaction. MSCs increased macrophage presence at the CaP implantation site and enhanced bone healing. However, MSCs reduced the immune cell presence (macrophages and eosinophils at the site when the scaffold was delivered with extracellular matrix produced by fibroblasts (dermis of Sprague-Dawley rats), indicating that MSCs modulate the host immune response depending on the environment with the aim of positively influencing the tissue healing cascade.	(17)
BCP (HA/β-TCP)	Bone marrow MSCs C57BL/6-Tg (CAG-EGFP)1Osb/J mice	*In vivo model:* Subcutaneous and calvaria implants. Female C3H/HeJ, C57BL6J, B6.129S7-Ifng^{tm1Ts}/J, C57BL/6-Tg(CAG-EGFP)1Osb/J, B6.MRL-Fas^{lpr}/J, immunocompromised nude mice (Beige nude/nudeXIDIII).	Firstly, MSC transplantation with CaP formed ectopic bone in nude mice but not in C57BL/6 mice. Interestingly CD8+ T cells, and CD4+ T cell infusion into nude mice partially and totally blocked bone formation, respectively. Inhibition of MSC-mediated bone formation in C57BL/6 was caused by interferon (IFN)-γ induced down-regulation of the runt-related transcription factor 2 (Runx-2) pathway and tumor necrosis factor (TNF)-α-induced MSC apoptosis. Treatment with IFN-γ and TNF-α also inhibited MSC-mediated bone formation in nude mice and interestingly antibodies to neutralize IFN-γ and TNF-α, as well as infusion of Treg cells rescued bone formation by transplanted MSCs in C57BL/6 mice. Together, this reveals that pro-inflammatory T cells inhibit transplanted MSC-mediated bone repair.	(90)
BCP (HA/β-TCP)	Bone marrow MSCs from C57BL/6 mice	*In vivo model:* Subcutaneous implantation in C57BL/6 and immunocompromised nude mice (NMRI Nu/Nu)	MSC transplantation into nude mice led to abundant ectopic bone and bone marrow formation, whereas MSC transplantation into syngenic C57BL/6 mice resulted in only minor quantities of ectopic bone formation and significant quantities of multinucleated giant cells (MNGCs). MSCs survived for a shorter duration in immune-competent mice and the implant site was characterized by Th1, Th2, and cytotoxic T-lymphocyte activation, highlighting the benefit T-lymphocyte absence in nude mice for bone formation.	(91)

but senescence, apoptosis, necrosis, or other types of cell death could presumably be implicated which can have a profound effect on MSC-mediated immunomodulation. MSCs are considered relatively resistant to programmed apoptosis and prefer senescent growth arrest or autophagy to cell death (101). In general, necrotic (necroptotic, pyroptotic) cell death is associated with inflammation and exacerbated immune responses, whereas apoptosis avoids an inflammatory response and rather contributes to its resolution. For example, Laing et al. demonstrated that systemic injection of H_2O_2-induced apoptotic MSCs is more efficient than injection of live MSCs to induce a robust immune suppressive reaction in an ovalbumin induced model of allergic airway inflammation (102). Similarly, Galleu et al. showed that after infusion of apoptotic MSCs in a murine model of graft-vs-host disease, recipient phagocytes engulf apoptotic MSCs and produce IDO, which is ultimately necessary for effecting immunosuppression (103). The authors also observed that cytotoxic cells, such as CD8+ T lymphocytes and NK cells, induce MSCs apoptosis through perforin, granzyme B, and FasL, and that PBMCs from patients that responded to MSC therapy had more cytotoxic activity against MSCs. Another level of complexity is that when apoptotic cells are not cleared in an efficient and timely manner, they progress to secondary necrosis and lose their membrane integrity. This results in a leakage of immunostimulatory, danger associated molecular patterns (DAMPs) such as HMGB1 and nucleosomes (104, 105). They induce an inflammatory response which can become chronic and even induce an adaptive immune response, a situation that would

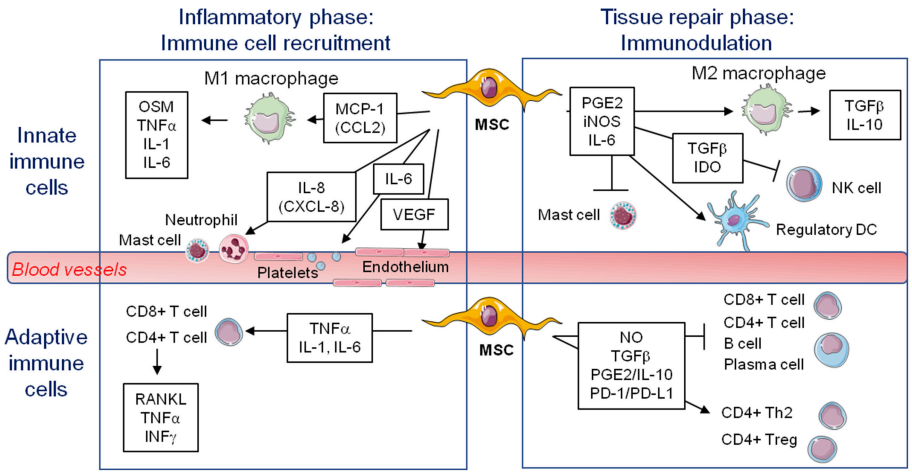

FIGURE 1 | Known immunomodulatory secretions from mesenchymal stem cells favoring (↑) or inhibiting (-) various cells potentially involved in bone formation on a biomaterial during early inflammation or the later stage of tissue repair. MSC, mesenchymal stem cell; M1, pro-inflammatory macrophages; M2, alternatively activated macrophages; NK, natural killer; DC, dendritic cell; OSM, oncostatin M; TNFα, tumor necrosis factor alpha; IL, interleukin; VEGF, vascular endothelial growth factor; PGE2, prostaglandin E2; iNOS, inducible nitric oxide synthase; TGFβ, transforming growth factor beta; IDO, indoleamine 2,3-dioxygenase; RANKL, receptor activator of nuclear factor kappa-B ligand; IFNγ, interferon gamma; NO, nitric oxide; PD-1/PD-L1, programmed cell death protein 1/programmed cell death-ligand 1.

presumably preclude local bone formation. Additional studies are mandatory in the context of bone regeneration induced by MSC-CaP combination.

Upon aging and in age-related deficiencies, compromised MSC-mediated immunological responses have been observed and attributed to MSC senescence. Senescence by replicative exhaustion or genotoxic stress during *ex vivo* culturing was also demonstrated (69). Acute, transient senescence induced by cell stresses such as hypoxia is presumably beneficial, because senescent cells secrete a plethora of molecules as part of the senescence-associated secretory phenotype (SASP), leading to rapid MSC clearance by immune cells, modulation of innate and adaptive immune cells, followed by tissue healing and regeneration (106). However, when chronic senescence occurs, for example upon aging, it impacts on the SASP, the local microenvironment and causes local and/or systemic inflammation.

The modifications of the secretome of MSCs induced by various stimuli, either mimicking physiological situations such as hypoxia and inflammatory stress or specific *in vitro* culture conditions to enhance the immunomodulatory properties of the cells, were previously widely reviewed (107–109). Those stresses could also alter the production and composition of EVs (110–112). Hypoxia is a main characteristic of the natural environment of MSCs and a major difference with *in vitro* culture. Overall, culture under low-oxygen atmosphere results in higher proliferation rate, survival, differentiation potential, and immune modulating secretions (113). For example, Paquet et al. (114) reported an upregulation of proangiogenic and chemotactic mediators (VEGF-A/-C, IL-8, MCP-1, and RANTES) and a downregulation of inflammatory mediators (IL-1b, IL-6, IL-15, IL-1Ra) with close to anoxic conditions (0.1% O_2). An artificial overexpression of the hypoxia-inducible factor 1 (HIF-1) in dental stem cells leads to an improved resistance to NK cells, an upregulation of CXCL12, CCL5, and IL-6 as well as a downregulation of CXCL10 (115).

Inflammatory stress is also characteristic of an implantation site and is mimicked *in vitro* by exogenous addition of LPS, TNFα, and/or IFNγ, usually termed MSC priming. When primed with inflammatory cytokines, MSCs increase their suppressive capacities (95). MSCs express constitutively many mitogenic growth factors, chemokines and matrix metalloproteinases at various levels. They are sensors and modulators of their microenvironment; i.e., MSC response to TNFα by increasing expression of some growth factor receptors, growth factors, chemokines, and matrix metalloproteases (116). Just as hypoxia, MSCs stimulated with LPS or TNFα produced more VEGF and FGF2 but also more HGF and IGF-1 via the activation of NFκB (117). Stimulation with IFNγ increases the expression of anti-inflammatory and regenerative molecules such as IDO, TGFβ or PGE2 for example (60). The addition of hypoxia to a TNFα and IFNγ stimulation on adipose-derived stem cells did not impair their higher secretion of immunomodulatory molecules IDO and PD-L1 (118).

PROPOSED MECHANISM OF BONE FORMATION AFTER MSC-CAP IMPLANTATION

It has been shown in many studies that only the combination of CaP and MSCs has the ability to induce abundant bone formation. MSCs have numerous, complex, and sometimes antagonist effects on the immune system depending on the physiological context. Their role in bone regeneration on CaP biomaterials remains unclear but evidence indicate that their immunomodulatory properties are involved. We previously highlighted the crucial role that osteoclasts seem to play and

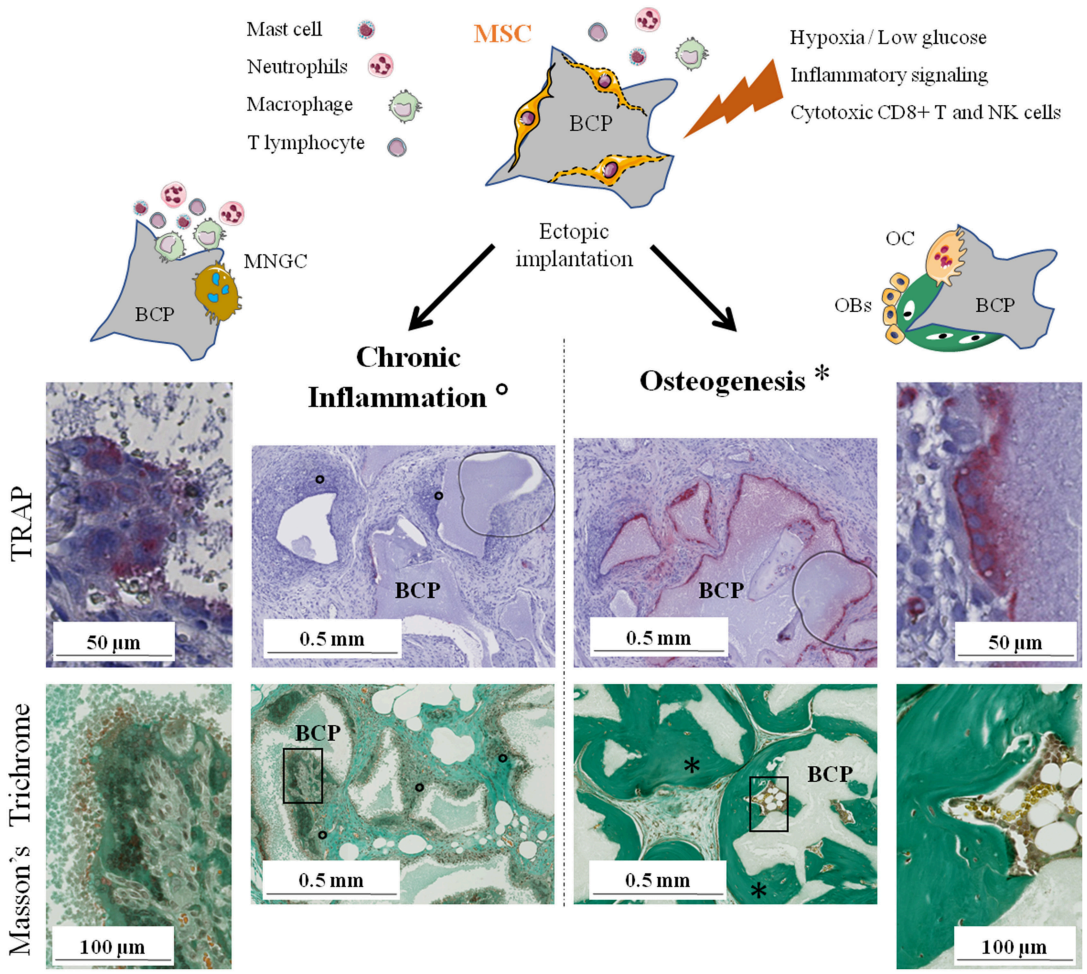

FIGURE 2 | The two possible outcomes of subcutaneous implantation of mesenchymal stem cells on calcium phosphate ceramic in mice. Histology of the implants: TRAP staining for osteoclasts detection after 4 weeks and Masson's trichrome to evaluate bone formation after 8 weeks. On the left, chronic inflammation (o) with formation of TRAP negative MNGCs followed by fibrous encapsulation and no sign of bone formation. On the right, osteoclastogenesis on the biomaterial followed by abundant bone formation (*). NK, natural killer; BCP, biphasic calcium phosphate; MNGC, multi-nucleated giant cell; OC, osteoclast; OBs, osteoblasts; TRAP, tartrate-resistant acid phosphatase.

the rapid disappearance of implanted MSCs before new bone is formed. Therefore, we hypothesize that MSCs, through their dialogue with various cells of the immune system, favor osteoclastogenesis on lieu of MNGCs formation, i.e., inducing a switch from chronic inflammation and fibrous encapsulation to bone formation via the recruitment and differentiation of new MSCs or skeletal stem cells in the bone remodeling process (**Figure 2**).

In detail, the environment just after implantation consists of the biomaterial exhibiting specific properties (chemical composition, micro-/macro-porosity, topography) and the MSCs adhering and reacting to it. Neutrophils, mast cells and macrophages are the first immune cells in contact with the implant, the latter mostly polarizing toward the inflammatory M1 phenotype (28). Therefore, inflammatory cytokines, ions released by the biomaterial, lack of O_2 (98), and nutrients (97), presence of cytotoxic CD8+ T and NK cells are all environmental factors influencing MSCs' behavior in the early stages of implantation. Most of those stresses were individually found to increase the production of pro- or anti-inflammatory molecules by MSCs (107–109). Given the osteogenic effect of the biomaterial (119) and the M1 population of macrophages (86), implanted MSCs might also express some markers of early osteoblast precursors. Eventually, MSCs will disappear by senescence, apoptosis and/or necrosis, releasing novel pro- and anti-inflammatory signals. Clearance of dead MSC by immune cells would also modulate the innate and adaptive immune system.

We believe that the secretions from those highly stimulated MSCs directly or indirectly (through modulation of innate and adaptive immune cells) favor the formation of osteoclasts at the expense of MNGCs. Indeed, MSC-based bone formation was significantly altered by anti-RANKL mAB (10) or clodronate (42) administration. While clodronate also affects MNGCs, the

anti-RANKL mAB is specifically restricting osteoclastogenesis. Due to their common origin and similar morphology, osteoclasts, and MNGCs are difficult to distinguish. Theoretically, both osteoclasts and MNGCs can arise from the fusion of circulating monocytes, M1/M2 macrophages or even of dendritic cells. An in depth description of the known differences between osteoclasts and MNGCs have already been well reviewed (120). Both cell types share a lot of markers but they can be differentiated by expression of the calcitonin receptor and RANK only in osteoclasts, or CD86 (B7-2), CD206, and HLA-DR only present in MNGCs. Interestingly, MNGCs are able to express low levels of TRAP a few days after formation (both *in vitro* and *in vivo*) while there seem to be two distinct populations expressing or not Cathepsin K (121, 122). Miron et al. also discussed the polarization potential of MNGCs, in parallel with the polarization of macrophages, with a proposed distinction between pro-inflammatory M1-MNGCs that were also called foreign body giant cells (FBGCs) and wound-healing M2-MNGCs. It is impossible to state whether the suggested M2-MNGCs are the MNGCs observed in close contact to the CaP materials leading to bone formation or if M2-MNGCs can differentiate further into true osteoclasts even if this last statement seems unlikely due to their unresponsiveness to RANKL *in vitro* (54). In our hypothesis, M2-MNGCs are likely to be involved in late stages of chronic inflammation, leading to fibrous encapsulation. In any case, there is an urgent need to better characterize those MNGCs and to discover the cell communications involved in their formation.

Preliminary results showed that conditioned media from MSC culture could have a positive direct impact on osteoclastogenesis (123). This effect of MSCs could rely on enhanced secretion or membrane expression of RANKL. Activated T cells were also reported to increase osteoclastogenesis *in vitro* (124) but they cannot be the main source of RANKL in MSC-based bone formation as many successful experiments were carried out in Nude mice. Also, a number of factors are known to influence osteoclastogenesis, primarily by modifying RANKL/RANK signaling (125). *In vitro*, TGFβ (a known product of MSC but also Treg) promote osteoclast formation from RANKL stimulated precursors but also decreases RANKL expression in osteoblasts resulting in fewer osteoclasts in co-culture (126). In mice, activation of the non-canonical Wnt pathway by Wnt5a in osteoclast precursors increases the production of RANK (127). These are only few examples of molecules that could be implicated in the MSC-osteoclast communications and future studies will certainly better delineate this key step toward MSC-CaP induced bone formation.

As the newly formed bone comes mostly from host osteoblasts, it entails recruitment and differentiation of new MSCs or the newly characterized subset of skeletal stem cells [SSC, (128)]. We hypothesize that osteoclasts might be the essential attractor for those cells, setting off a local bone remodeling cycle. The basic mechanisms and the major signaling molecules involved in the osteoclast-osteoblast crosstalk during the physiological coupling of bone resorption and formation are well described (129, 130). Osteoclasts are known to release growth factors from the degradation of bone matrix and, most importantly in our case, to express chemotactic and osteogenic coupling factors toward cell of the osteoblastic lineage such as BMP6, WNT10b, and S1P (131). The CTHRC1 protein, expressed by mature osteoclasts, promote osteoblastic differentiation *in vitro* and an osteoclast-specific KO induce

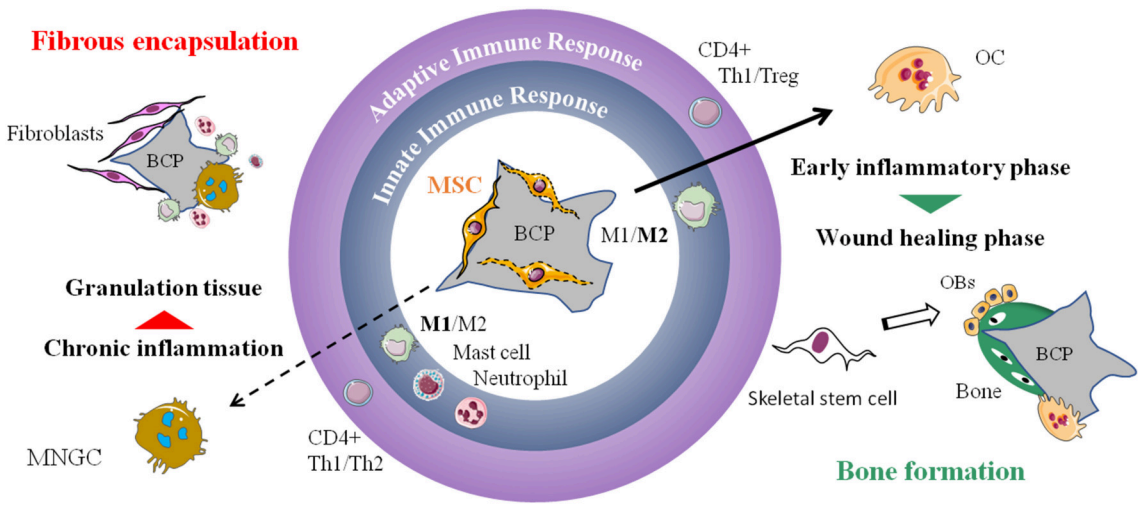

FIGURE 3 | Proposed mechanism of MSC-CaP immune modulation leading to bone formation. The local innate and adaptive immune response will determine the fate of the implanted biomaterial (central part of the drawing). On the left, is displayed the classical foreign body reaction characterized by activation of M1 macrophages, mast cells, neutrophils, Th1, and Th2 CD4+ lymphocytes. It leads to the formation of MNGCs, chronic inflammation and subsequent fibrous encapsulation of the implant. On the right, adjunction of MSCs to the biomaterial favor M2 macrophages, Th1, Treg, and osteoclastogenesis followed by recruitment of new stem cells, likely from the skeletal subtype, that differentiate into bone forming osteoblasts. MSC, mesenchymal stem cell; BCP, biphasic calcium phosphate; M1, pro-inflammatory macrophages; M2, alternatively activated macrophages; Th1/Th2/Treg, type 1 helper/type 2 helper/regulatory T cells; MNGC, multi-nucleated giant cell; OC, osteoclast; OBs, osteoblasts.

a low bone mass phenotype in mice (37). More recently, an important study unveiled a reverse signaling mechanism whereby osteoclasts secrete extracellular vesicles expressing RANK which are able to stimulate membrane RANKL on the surface of osteoblasts to induce bone formation (132). Also, as osteoclasts can degrade the biomaterial, they modulate the local calcium and phosphate concentrations, thus influencing the deposition of the apatite layer and the calcium sensing of other cell types (26, 133).

Simultaneously to this main phenomenon, MSCs are likely to induce a switch from M1 macrophages to the M2 phenotype, the formation of regulatory dendritic cells and the suppression of B, NK, CD4+, and CD8+ T cells while promoting Th2 and Treg cells. The timing of activation of the various cells is critical as the initial acute inflammation is necessary to recruit all the immune cells but is detrimental if it becomes chronic and favors the formation of MNGCs. The M1/M2 balance of macrophages phenotype has a key role in this switch to resolve inflammation and move on to bone formation (85, 134). Moreover, the M2 phenotype favored by MSCs is thought to help in late stages of osteoblastic differentiation and mineralization (86). The stressful conditions and, eventually, the apoptosis of implanted MSCs might increase their inherent immunomodulatory properties.

CONCLUSION

The implantation of CaP biomaterials in combination with MSCs emphasizes the central role of the host immune system in bone regeneration. It is important to consider that the cellular events hypothesized here may only occur on an osteoconductive CaP material. The implanted MSCs potentiate the effect of the biomaterial allowing ectopic bone formation by creating a bone-like microenvironment. We highlighted here the pivotal role that macrophages and osteoclasts play in the multistep process of bone formation induced by MSC-CaP implantation (**Figure 3**) but this complex mechanism is just beginning to be explored. Over the course of several weeks, multiples cells types and molecules appear implicated in a coordinated manner before bone is formed. Any dysregulation would lead to unwanted chronic inflammation and fibrosis. A better comprehension of these spatiotemporal cell communications is mandatory to reach more efficient bone healing and develop better cell-free approaches.

AUTHOR CONTRIBUTIONS

All authors participated in the literature search, organization, writing, reviewing, and proofreading of the manuscript. PH, ND, VT, and FB designed the figures. MB and PL created the tables.

FUNDING

This work is financially supported by the European Commission through the H2020 project ORTHOUNION (Grant Agreement: 733288). PH receives a PhD fellowship from the Regional Council Pays de la Loire and the ORTHOUNION project. MB benefits from a Marie Skłodowska-Curie Individual Fellowships from the European Commission through the H2020 project PARAGEN (Project ID: 708711).

REFERENCES

1. Stanovici J, Le Nail L-R, Brennan MA, Vidal L, Trichet V, Rosset P, et al. Bone regeneration strategies with bone marrow stromal cells in orthopaedic surgery. *Curr Res Transl Med.* (2016) 64:83–90. doi: 10.1016/j.retram.2016.04.006
2. Abe K, Yamamoto N, Hayashi K, Takeuchi A, Miwa S, Igarashi K, et al. The usefulness of wide excision assisted by a computer navigation system and reconstruction using a frozen bone autograft for malignant acetabular bone tumors: a report of two cases. *BMC Cancer*. (2018) 18:1036. doi: 10.1186/s12885-018-4971-8
3. Ahlmann E, Patzakis M, Roidis N, Shepherd L, Holtom P. Comparison of anterior and posterior iliac crest bone grafts in terms of harvest-site morbidity and functional outcomes. *J Bone Joint Surg Am*. (2002) 84–A:716–20. doi: 10.2106/00004623-200205000-00003
4. Giannoudis PV, Dinopoulos H, Tsiridis E. Bone substitutes: an update. *Injury*. (2005) 36:S20–7. doi: 10.1016/j.injury.2005.07.029
5. Albee FH. Studies in bone growth triple calcium phosphate as a stimulus to osteogenesis. *Ann Surg*. (1920) 71:32–9.
6. Mankani MH, Kuznetsov SA, Wolfe RM, Marshall GW, Robey PG. *In vivo* bone formation by human bone marrow stromal cells: reconstruction of the mouse calvarium and mandible. *Stem Cells*. (2006) 24:2140–9. doi: 10.1634/stemcells.2005-0567
7. Mankani MH, Kuznetsov SA, Robey PG. Formation of hematopoietic territories and bone by transplanted human bone marrow stromal cells requires a critical cell density. *Exp Hematol*. (2007) 35:995–1004. doi: 10.1016/J.EXPHEM.2007.01.051
8. Granchi D, Gómez-Barrena E, Rojewski M, Rosset P, Layrolle P, Spazzoli B, et al. Changes of bone turnover markers in long bone nonunions treated with a regenerative approach. *Stem Cells Int*. (2017) 2017:1–11. doi: 10.1155/2017/3674045
9. Brennan MÁ, Renaud A, Amiaud J, Rojewski MT, Schrezenmeier H, Heymann D, et al. Pre-clinical studies of bone regeneration with human bone marrow stromal cells and biphasic calcium phosphate. *Stem Cell Res Ther*. (2014) 5:114. doi: 10.1186/scrt504
10. Gamblin A-L, Brennan MA, Renaud A, Yagita H, Lézot F, Heymann D, et al. Bone tissue formation with human mesenchymal stem cells and biphasic calcium phosphate ceramics: the local implication of osteoclasts and macrophages. *Biomaterials*. (2014) 35:9660–7. doi: 10.1016/j.biomaterials.2014.08.018
11. Giannoni P, Scaglione S, Daga A, Ilengo C, Cilli M, Quarto R. Short-time survival and engraftment of bone marrow stromal cells in an ectopic model of bone regeneration. *Tissue Eng Part A*. (2010) 16:489–99. doi: 10.1089/ten.tea.2009.0041
12. Otsuru S, Gordon PL, Shimono K, Jethva R, Marino R, Phillips CL, et al. Transplanted bone marrow mononuclear cells and MSCs impart clinical benefit to children with osteogenesis imperfecta through different mechanisms. *Blood*. (2012) 120:1933–41. doi: 10.1182/blood-2011-12-400085
13. Götherström C, Westgren M, Shaw SWS, Åström E, Biswas A, Byers PH, et al. Pre- and postnatal transplantation of fetal mesenchymal stem cells in osteogenesis imperfecta: a two-center experience. *Stem Cells Transl Med*. (2014) 3:255–64. doi: 10.5966/sctm.2013-0090
14. Le Blanc K, Götherström C, Ringdén O, Hassan M, McMahon R, Horwitz E, et al. Fetal mesenchymal stem-cell engraftment in bone after *in utero* transplantation in a patient with severe osteogenesis imperfecta. *Transplantation*. (2005) 79:1607–14. doi: 10.1097/01.TP.0000159029.48678.93

15. Horwitz EM, Gordon PL, Koo WKK, Marx JC, Neel MD, McNall RY, et al. Isolated allogeneic bone marrow-derived mesenchymal cells engraft and stimulate growth in children with osteogenesis imperfecta: implications for cell therapy of bone. *Proc Natl Acad Sci USA*. (2002) 99:8932–7. doi: 10.1073/pnas.132252399
16. Horwitz EM, Prockop DJ, Fitzpatrick LA, Koo WWK, Gordon PL, Neel M, et al. Transplantability and therapeutic effects of bone marrow-derived mesenchymal cells in children with osteogenesis imperfecta. *Nat Med*. (1999) 5:309–13. doi: 10.1038/6529
17. Tour G, Wendel M, Tcacencu I. Bone marrow stromal cells enhance the osteogenic properties of hydroxyapatite scaffolds by modulating the foreign body reaction. *J Tissue Eng Regen Med*. (2014) 8:841–9. doi: 10.1002/term.1574
18. Qi X, Zhang J, Yuan H, Xu Z, Li Q, Niu X, et al. Exosomes secreted by human-induced pluripotent stem cell-derived mesenchymal stem cells repair critical-sized bone defects through enhanced angiogenesis and osteogenesis in osteoporotic rats. *Int J Biol Sci*. (2016) 12:836–49. doi: 10.7150/ijbs.14809
19. Barradas AMCA, Yuan H, van Blitterswijk CAC, Habibovic P. Osteoinductive biomaterials: current knowledge of properties, experimental models and biological mechanisms. *Eur Cells Mater*. (2011) 21:407–29. doi: 10.22203/eCM.v021a31
20. Daculsi G, Legeros RZ, Nery E, Lynch K, Kerebel B. Transformation of biphasic calcium phosphate ceramics *in vivo*: ultrastructural and physicochemical characterization. *J Biomed Mater Res*. (1989) 23:883–94. doi: 10.1002/jbm.820230806
21. Habibovic P, Yuan H, van der Valk CM, Meijer G, van Blitterswijk CA, de Groot K. 3D microenvironment as essential element for osteoinduction by biomaterials. *Biomaterials*. (2005) 26:3565–75. doi: 10.1016/j.biomaterials.2004.09.056
22. Le Nihouannen D, Daculsi G, Saffarzadeh A, Gauthier O, Delplace S, Pilet P, et al. Ectopic bone formation by microporous calcium phosphate ceramic particles in sheep muscles. *Bone*. (2005) 36:1086–93. doi: 10.1016/j.bone.2005.02.017
23. Ripamonti U, Roden LC, Ferretti C, Klar RM. Biomimetic matrices self-initiating the induction of bone formation. *J Craniofac Surg*. (2011) 22:1859–70. doi: 10.1097/SCS.0b013e31822e83fe
24. Fellah BH, Gauthier O, Weiss P, Chappard D, Layrolle P. Osteogenicity of biphasic calcium phosphate ceramics and bone autograft in a goat model. *Biomaterials*. (2008) 29:1177–88. doi: 10.1016/j.biomaterials.2007.11.034
25. Diaz-Flores L, Gutierrez R, Lopez-Alonso A, Gonzalez R, Varela H. Pericytes as a supplementary source of osteoblasts in periosteal osteogenesis. *Clin Orthop Relat Res*. (1992)280–6.
26. Bohner M, Miron RJ. A proposed mechanism for material-induced heterotopic ossification. *Mater Today*. (2018) 22:132–41. doi: 10.1016/j.mattod.2018.10.036
27. Barradas AMC, Yuan H, van der Stok J, Le Quang B, Fernandes H, Chaterjea A, et al. The influence of genetic factors on the osteoinductive potential of calcium phosphate ceramics in mice. *Biomaterials*. (2012) 33:5696–705. doi: 10.1016/j.biomaterials.2012.04.021
28. Anderson JM, Rodriguez A, Chang DT. Foreign body reaction to biomaterials. *Semin Immunol*. (2008) 20:86–100. doi: 10.1016/j.smim.2007.11.004
29. Batoon L, Millard SM, Raggatt LJ, Pettit AR. Osteomacs and bone regeneration. *Curr Osteoporos Rep*. (2017) 15:385–95. doi: 10.1007/s11914-017-0384-x
30. Miron RJ, Bosshardt DD. OsteoMacs: key players around bone biomaterials. *Biomaterials*. (2016) 82:1–19. doi: 10.1016/j.biomaterials.2015.12.017
31. Alexander KA, Chang MK, Maylin ER, Kohler T, Müller R, Wu AC, et al. Osteal macrophages promote *in vivo* intramembranous bone healing in a mouse tibial injury model. *J Bone Miner Res*. (2011) 26:1517–32. doi: 10.1002/jbmr.354
32. Batoon L, Millard SM, Wullschleger ME, Preda C, Wu AC-K, Kaur S, et al. CD169 + macrophages are critical for osteoblast maintenance and promote intramembranous and endochondral ossification during bone repair. *Biomaterials*. (2017) 2017:33. doi: 10.1016/j.biomaterials.2017.10.033
33. Mantovani A, Sica A, Sozzani S, Allavena P, Vecchi A, Locati M. The chemokine system in diverse forms of macrophage activation and polarization. *Trends Immunol*. (2004) 25:677–86. doi: 10.1016/j.it.2004.09.015
34. Mantovani A, Sozzani S, Locati M, Allavena P, Sica A. Macrophage polarization: tumor-associated macrophages as a paradigm for polarized M2 mononuclear phagocytes. *Trends Immunol*. (2002) 23:549–55. doi: 10.1016/S1471-4906(02)02302-5
35. Jones JA, Chang DT, Meyerson H, Colton E, Kwon IK, Matsuda T, et al. Proteomic analysis and quantification of cytokines and chemokines from biomaterial surface-adherent macrophages and foreign body giant cells. *J Biomed Mater Res Part A*. (2007) 83A:585–96. doi: 10.1002/jbm.a.31221
36. Badylak SF, Valentin JE, Ravindra AK, McCabe GP, Stewart-Akers AM. Macrophage phenotype as a determinant of biologic scaffold remodeling. *Tissue Eng Part A*. (2008) 14:1835–42. doi: 10.1089/ten.tea.2007.0264
37. Takeshita S, Fumoto T, Matsuoka K, Park K, Aburatani H, Kato S, et al. Osteoclast-secreted CTHRC1 in the coupling of bone resorption to formation. *J Clin Invest*. (2013) 123:3914–24. doi: 10.1172/JCI69493
38. Ripamonti U, Klar RM, Renton LF, Ferretti C. Synergistic induction of bone formation by hOP-1, hTGF-β3 and inhibition by zoledronate in macroporous coral-derived hydroxyapatites. *Biomaterials*. (2010) 31:6400–10. doi: 10.1016/j.biomaterials.2010.04.037
39. Kondo N, Ogose A, Tokunaga K, Umezu H, Arai K, Kudo N, et al. Osteoinduction with highly purified β-tricalcium phosphate in dog dorsal muscles and the proliferation of osteoclasts before heterotopic bone formation. *Biomaterials*. (2006) 27:4419–27. doi: 10.1016/j.biomaterials.2006.04.016
40. Barrère-de Groot F, de Bruijn, Everts V, Davison N, Yuan H, Luo X, et al. Submicron-scale surface architecture of tricalcium phosphate directs osteogenesis *in vitro* and *in vivo*. *Eur Cells Mater*. (2016) 27:281–97. doi: 10.22203/ecm.v027a20
41. Tanaka T, Saito M, Chazono M, Kumagae Y, Kikuchi T, Kitasato S, et al. Effects of alendronate on bone formation and osteoclastic resorption after implantation of beta-tricalcium phosphate. *J Biomed Mater Res A*. (2010) 93:469–74. doi: 10.1002/jbm.a.32560
42. Davison NL, Gamblin A-L, Layrolle P, Yuan H, de Bruijn JD, Barrère-de Groot F. Liposomal clodronate inhibition of osteoclastogenesis and osteoinduction by submicrostructured beta-tricalcium phosphate. *Biomaterials*. (2014) 35:5088–97. doi: 10.1016/j.biomaterials.2014.03.013
43. Wang J, Liu D, Guo B, Yang X, Chen X, Zhu X, et al. Role of biphasic calcium phosphate ceramic-mediated secretion of signaling molecules by macrophages in migration and osteoblastic differentiation of MSCs. *Acta Biomater*. (2017) 51:447–60. doi: 10.1016/j.actbio.2017.01.059
44. Wang M, Chen F, Wang J, Chen X, Liang J, Yang X, et al. Calcium phosphate altered the cytokine secretion of macrophages and influenced the homing of mesenchymal stem cells. *J Mater Chem B*. (2018) 6:4765–74. doi: 10.1039/C8TB01201F
45. Hayman AR. Tartrate-resistant acid phosphatase (TRAP) and the osteoclast/immune cell dichotomy. *Autoimmunity*. (2008) 41:218–23. doi: 10.1080/08916930701694667
46. Feng W. Osteoclastogenesis and osteoimmunology. *Front Biosci*. (2014) 19:758. doi: 10.2741/4242
47. Drake MT, Clarke BL, Khosla S. Bisphosphonates: mechanism of action and role in clinical practice. *Mayo Clin Proc*. (2008) 83:1032–45. doi: 10.4065/83.9.1032
48. Shi CG, Zhang Y, Yuan W. Efficacy of bisphosphonates on bone mineral density and fracture rate in patients with osteogenesis imperfecta: a systematic review and meta-analysis. *Am J Ther*. (2016) 23:e894-904. doi: 10.1097/MJT.0000000000000236
49. Biggin A, Munns CF. Long-term bisphosphonate therapy in osteogenesis imperfecta. *Curr Osteoporos Rep*. (2017) 15:412–8. doi: 10.1007/s11914-017-0401-0
50. Sims NA, Martin TJ, Quinn JMW. Coupling: the influences of immune and bone cells. In: Lorenzo J, Horowitz MC, Choi Y, Takayanagi H, Schett G, editors. *Osteoimmunology: Interactions of the Immune and Skeletal Systems*. London: Academic Press. p. 169–85. Available online at: https://www.sciencedirect.com/science/article/pii/B9780128005712000219 doi: 10.1016/B978-0-12-800571-2.00010-4
51. Jensen SS, Gruber R, Buser D, Bosshardt DD. Osteoclast-like cells on deproteinized bovine bone mineral and biphasic calcium phosphate: light

and transmission electron microscopical observations. *Clin Oral Implants Res*. (2015) 26:859–64. doi: 10.1111/clr.12376
52. DeFife KM, Jenney CR, McNally AK, Colton E, Anderson JM. Interleukin-13 induces human monocyte/macrophage fusion and macrophage mannose receptor expression. *J Immunol*. (1997) 158:3385–90.
53. McNally AK, Jones JA, MacEwan SR, Colton E, Anderson JM. Vitronectin is a critical protein adhesion substrate for IL-4-induced foreign body giant cell formation. *J Biomed Mater Res Part A*. (2008) 86A:535–43. doi: 10.1002/jbm.a.31658
54. ten Harkel B, Schoenmaker T, Picavet DI, Davison NL, de Vries TJ, Everts V. The foreign body giant cell cannot resorb bone, but dissolves hydroxyapatite like osteoclasts. *PLoS ONE. (*2015) 10:e0139564. doi: 10.1371/journal.pone.0139564
55. Randolph GJ, Inaba K, Robbiani DF, Steinman RM, Muller WA. Differentiation of phagocytic monocytes into lymph node dendritic cells *in vivo*. *Immunity*. (1999) 11:753–61. doi: 10.1016/S1074-7613(00)80149-1
56. Merad M, Sathe P, Helft J, Miller J, Mortha A. The dendritic cell lineage: ontogeny and function of dendritic cells and their subsets in the steady state and the inflamed setting. *Annu Rev Immunol*. (2013) 31:563–604. doi: 10.1146/annurev-immunol-020711-074950
57. Sokolova V, Knuschke T, Kovtun A, Buer J, Epple M, Westendorf AM. The use of calcium phosphate nanoparticles encapsulating Toll-like receptor ligands and the antigen hemagglutinin to induce dendritic cell maturation and T cell activation. *Biomaterials*. (2010) 31:5627–33. doi: 10.1016/j.biomaterials.2010.03.067
58. Keselowsky BG, Lewis JS. Dendritic cells in the host response to implanted materials. *Semin Immunol*. (2017) 29:33–40. doi: 10.1016/j.smim.2017.04.002
59. Vasilijić S, Savić D, Vasilev S, Vučević D, Gašić S, Majstorović I, et al. Dendritic cells acquire tolerogenic properties at the site of sterile granulomatous inflammation. *Cell Immunol*. (2005) 233:148–57. doi: 10.1016/J.CELLIMM.2005.04.007
60. Michel J, Penna M, Kochen J, Cheung H. Recent advances in hydroxyapatite scaffolds containing mesenchymal stem cells. *Stem Cells Int*. (2015) 2015:305217. doi: 10.1155/2015/305217
61. Miron RJ, Zhang YF. Osteoinduction. *J Dent Res*. (2012) 91:736–44. doi: 10.1177/0022034511435260
62. García-Gareta E, Coathup MJ, Blunn GW. Osteoinduction of bone grafting materials for bone repair and regeneration. *Bone*. (2015) 81:112–21. doi: 10.1016/J.BONE.2015.07.007
63. Brennan MA, Renaud A, Guilloton F, Mebarki M, Trichet V, Sensebé L, et al. Inferior *in vivo* osteogenesis and superior angiogeneis of human adipose-derived stem cells compared with bone marrow-derived stem cells cultured in xeno-free conditions. *Stem Cells Transl Med*. (2017) 6:2160–72. doi: 10.1002/sctm.17-0133
64. Gjerde C, Mustafa K, Hellem S, Rojewski M, Gjengedal H, Yassin MA, et al. Cell therapy induced regeneration of severely atrophied mandibular bone in a clinical trial. *Stem Cell Res Ther*. (2018) 9:213. doi: 10.1186/s13287-018-0951-9
65. Gómez-Barrena E, Rosset P, Gebhard F, Hernigou P, Baldini N, Rouard H, et al. Feasibility and safety of treating non-unions in tibia, femur and humerus with autologous, expanded, bone marrow-derived mesenchymal stromal cells associated with biphasic calcium phosphate biomaterials in a multicentric, non-comparative trial. *Biomaterials*. (2018) 196:100–8. doi: 10.1016/j.biomaterials.2018.03.033
66. Fang D, Seo B-M, Liu Y, Sonoyama W, Yamaza T, Zhang C, et al. Transplantation of mesenchymal stem cells is an optimal approach for plastic surgery. *Stem Cells*. (2007) 25:1021–8. doi: 10.1634/stemcells.2006-0576
67. Hasegawa N, Kawaguchi H, Hirachi A, Takeda K, Mizuno N, Nishimura M, et al. Behavior of transplanted bone marrow–derived mesenchymal stem cells in periodontal defects. *J Periodontol*. (2006) 77:1003–7. doi: 10.1902/jop.2006.050341
68. Oshima Y, Watanabe N, Matsuda K, Takai S, Kawata M, Kubo T. Behavior of transplanted bone marrow-derived GFP mesenchymal cells in osteochondral defect as a simulation of autologous transplantation. *J Histochem Cytochem*. (2005) 53:207–16. doi: 10.1369/jhc.4A6280.2005
69. Tasso R, Augello A, Boccardo S, Salvi S, Caridà M, Postiglione F, et al. Recruitment of a host's osteoprogenitor cells using exogenous mesenchymal stem cells seeded on porous ceramic. *Tissue Eng Part A*. (2009) 15:2203–12. doi: 10.1089/ten.tea.2008.0269
70. Ando Y, Matsubara K, Ishikawa J, Fujio M, Shohara R, Hibi H, et al. Stem cell-conditioned medium accelerates distraction osteogenesis through multiple regenerative mechanisms. *Bone*. (2014) 61:82–90. doi: 10.1016/j.bone.2013.12.029
71. Xu J, Wang B, Sun Y, Wu T, Liu Y, Zhang J, et al. Human fetal mesenchymal stem cell secretome enhances bone consolidation in distraction osteogenesis. *Stem Cell Res Ther*. (2016) 7:134. doi: 10.1186/s13287-016-0392-2
72. Osugi M, Katagiri W, Yoshimi R, Inukai T, Hibi H, Ueda M. Conditioned media from mesenchymal stem cells enhanced bone regeneration in rat calvarial bone defects. *Tissue Eng Part A*. (2012) 18:1479–89. doi: 10.1089/ten.tea.2011.0325
73. Skog J, Würdinger T, van Rijn S, Meijer DH, Gainche L, Curry WT, et al. Glioblastoma microvesicles transport RNA and proteins that promote tumour growth and provide diagnostic biomarkers. *Nat Cell Biol*. (2008) 10:1470–6. doi: 10.1038/ncb1800
74. Valadi H, Ekström K, Bossios A, Sjöstrand M, Lee JJ, Lötvall JO. Exosome-mediated transfer of mRNAs and microRNAs is a novel mechanism of genetic exchange between cells. *Nat Cell Biol*. (2007) 9:654–9. doi: 10.1038/ncb1596
75. Furuta T, Miyaki S, Ishitobi H, Ogura T, Kato Y, Kamei N, et al. Mesenchymal stem cell-derived exosomes promote fracture healing in a mouse model. *Stem Cells Transl Med*. (2016) 5:1620–30. doi: 10.5966/sctm.2015-0285
76. Xie H, Wang Z, Zhang L, Lei Q, Zhao A, Wang H, et al. Extracellular vesicle-functionalized decalcified bone matrix scaffolds with enhanced pro-angiogenic and pro-bone regeneration activities. *Sci Rep*. (2017) 7:45622. doi: 10.1038/srep45622
77. Zhang J, Liu X, Li H, Chen C, Hu B, Niu X, et al. Exosomes/tricalcium phosphate combination scaffolds can enhance bone regeneration by activating the PI3K/Akt signaling pathway. *Stem Cell Res Ther*. (2016) 7:136. doi: 10.1186/s13287-016-0391-3
78. Otsuru S, Desbourdes L, Guess AJ, Hofmann TJ, Relation T, Kaito T, et al. Extracellular vesicles released from mesenchymal stromal cells stimulate bone growth in osteogenesis imperfecta. *Cytotherapy*. (2018) 20:62–73. doi: 10.1016/j.jcyt.2017.09.012
79. Burrello J, Monticone S, Gai C, Gomez Y, Kholia S, Camussi G. Stem cell-derived extracellular vesicles and immune-modulation. *Front Cell Dev Biol*. (2016) 4:83. doi: 10.3389/fcell.2016.00083
80. Guihard P, Danger Y, Brounais B, David E, Brion R, Delecrin J, et al. Induction of osteogenesis in mesenchymal stem cells by activated monocytes/macrophages depends on oncostatin M signaling. *Stem Cells*. (2012) 30:762–72. doi: 10.1002/stem.1040
81. Guihard P, Boutet M-A, Brounais-Le Royer B, Gamblin A-L, Amiaud J, Renaud A, et al. Oncostatin M, an inflammatory cytokine produced by macrophages, supports intramembranous bone healing in a mouse model of tibia injury. *Am J Pathol*. (2015) 185:765–75. doi: 10.1016/J.AJPATH.2014.11.008
82. Omar OM, Granéli C, Ekström K, Karlsson C, Johansson A, Lausmaa J, et al. The stimulation of an osteogenic response by classical monocyte activation. *Biomaterials*. (2011) 32:8190–204. doi: 10.1016/j.biomaterials.2011.07.055
83. Ekström K, Omar O, Granéli C, Wang X, Vazirisani F, Thomsen P. Monocyte exosomes stimulate the osteogenic gene expression of mesenchymal stem cells. *PLoS ONE.* (2013) 8:e75227. doi: 10.1371/journal.pone.0075227
84. Gong L, Zhao Y, Zhang Y, Ruan Z. The macrophage polarization regulates MSC osteoblast differentiation *in vitro*. *Ann Clin Lab Sci*. (2016) 46:65–71.
85. Pajarinen J, Lin T, Gibon E, Kohno Y, Maruyama M, Nathan K, et al. Mesenchymal stem cell-macrophage crosstalk and bone healing. *Biomaterials*. (2018) 196:80–9. doi: 10.1016/j.biomaterials.2017.12.025
86. Zhang Y, Böse T, Unger RE, Jansen JA, Kirkpatrick CJ, van den Beucken JJJP. Macrophage type modulates osteogenic differentiation of adipose tissue MSCs. *Cell Tissue Res*. (2017) 369:273–86. doi: 10.1007/s00441-017-2598-8
87. Caires HR, Barros da Silva P, Barbosa MA, Almeida CR. A co-culture system with three different primary human cell populations reveals that biomaterials and MSC modulate macrophage-driven fibroblast recruitment. *J Tissue Eng Regen Med*. (2018) 12:e1433–40. doi: 10.1002/term.2560

88. Quint P, Ruan M, Pederson L, Kassem M, Westendorf JJ, Khosla S, et al. Sphingosine 1-phosphate (S1P) receptors 1 and 2 coordinately induce mesenchymal cell migration through S1P activation of complementary kinase pathways. *J Biol Chem*. (2013) 288:5398–406. doi: 10.1074/jbc.M112.413583
89. Pederson L, Ruan M, Westendorf JJ, Khosla S, Oursler MJ. Regulation of bone formation by osteoclasts involves Wnt/BMP signaling and the chemokine sphingosine-1-phosphate. *Proc Natl Acad Sci*. (2008) 105:20764–9. doi: 10.1073/pnas.0805133106
90. Liu Y, Wang L, Kikuiri T, Akiyama K, Chen C, Xu X, et al. Mesenchymal stem cell–based tissue regeneration is governed by recipient T lymphocytes via IFN-γ and TNF-α. *Nat Med*. (2011) 17:1594–601. doi: 10.1038/nm.2542
91. Bouvet-Gerbettaz S, Boukhechba F, Balaguer T, Schmid-Antomarchi H, Michiels J-F, Scimeca J-C, et al. Adaptive immune response inhibits ectopic mature bone formation induced by BMSCs/BCP/plasma composite in immune-competent mice. *Tissue Eng Part A*. (2014) 20:2950–62. doi: 10.1089/ten.tea.2013.0633
92. Su Y, Shi S, Liu Y. Immunomodulation regulates mesenchymal stem cell-based bone regeneration. *Oral Dis*. (2014) 20:633–6. doi: 10.1111/odi.12248
93. Najar M, Raicevic G, Crompot E, Fayyad-Kazan H, Bron D, Toungouz M, et al. The immunomodulatory potential of mesenchymal stromal cells. *J Immunother*. (2016) 39:45–59. doi: 10.1097/CJI.0000000000000108
94. Glenn JD. Mesenchymal stem cells: emerging mechanisms of immunomodulation and therapy. *World J Stem Cells*. (2014) 6:526. doi: 10.4252/wjsc.v6.i5.526
95. Bassi G, Guilloton F, Menard C, Di Trapani M, Deschaseaux F, Sensebé L, Schrezenmeier H, et al. Effects of a ceramic biomaterial on immune modulatory properties and differentiation potential of human mesenchymal stromal cells of different origin. *Tissue Eng Part A*. (2015) 21:767–81. doi: 10.1089/ten.tea.2014.0269
96. Giebel B, Kordelas L, Börger V. Clinical potential of mesenchymal stem/stromal cell-derived extracellular vesicles. *Stem Cell Investig*. (2017) 4:84. doi: 10.21037/sci.2017.09.06
97. Deschepper M, Manassero M, Oudina K, Paquet J, Monfoulet L-E, Bensidhoum M, et al. Proangiogenic and prosurvival functions of glucose in human mesenchymal stem cells upon transplantation. *Stem Cells*. (2013) 31:526–35. doi: 10.1002/stem.1299
98. Becquart P, Cambon-Binder A, Monfoulet L-E, Bourguignon M, Vandamme K, Bensidhoum M, et al. Ischemia is the prime but not the only cause of human multipotent stromal cell death in tissue-engineered constructs *in vivo*. *Tissue Eng Part A*. (2012) 18:2084–94. doi: 10.1089/ten.tea.2011.0690
99. Potier E, Ferreira E, Meunier A, Sedel L, Logeart-Avramoglou D, Petite H. Prolonged hypoxia concomitant with serum deprivation induces massive human mesenchymal stem cell death. *Tissue Eng*. (2007) 13:1325–31. doi: 10.1089/ten.2006.0325
100. Moya A, Paquet J, Deschepper M, Larochette N, Oudina K, Denoeud C, et al. Human mesenchymal stem cell failure to adapt to glucose shortage and rapidly use intracellular energy reserves through glycolysis explains poor cell survival after implantation. *Stem Cells*. (2018) 36:363–76. doi: 10.1002/stem.2763
101. Nicolay NH, Perez RL, Saffrich R, Huber PE, Nicolay NH, Perez RL, et al. Radio-resistant mesenchymal stem cells: mechanisms of resistance and potential implications for the clinic. *Oncotarget*. (2015) 6:19366–80. doi: 10.18632/oncotarget.4358
102. Laing AG, Riffo-Vasquez Y, Sharif-Paghaleh E, Lombardi G, Sharpe PT. Immune modulation by apoptotic dental pulp stem cells *in vivo*. *Immunotherapy*. (2018) 10:201–11. doi: 10.2217/imt-2017-0117
103. Galleu A, Riffo-Vasquez Y, Trento C, Lomas C, Dolcetti L, Cheung TS, et al. Apoptosis in mesenchymal stromal cells induces *in vivo* recipient-mediated immunomodulation. *Sci Transl Med*. (2017) 9:eaam7828. doi: 10.1126/scitranslmed.aam7828
104. Sachet M, Liang YY, Oehler R. The immune response to secondary necrotic cells. *Apoptosis*. (2017) 22:1189–204. doi: 10.1007/s10495-017-1413-z
105. Bianchi ME, Crippa MP, Manfredi AA, Mezzapelle R, Rovere Querini P, Venereau E. High-mobility group box 1 protein orchestrates responses to tissue damage via inflammation, innate and adaptive immunity, and tissue repair. *Immunol Rev*. (2017) 280:74–82. doi: 10.1111/imr.12601
106. Lunyak VV, Amaro-Ortiz A, Gaur M. Mesenchymal stem cells secretory responses: senescence messaging secretome and immunomodulation perspective. *Front Genet*. (2017) 8:1–21. doi: 10.3389/fgene.2017.00220
107. Madrigal M, Rao KS, Riordan NH. A review of therapeutic effects of mesenchymal stem cell secretions and induction of secretory modification by different culture methods. *J Transl Med*. (2014) 12:260. doi: 10.1186/s12967-014-0260-8
108. Sisakhtnezhad S, Alimoradi E, Akrami H. External factors influencing mesenchymal stem cell fate *in vitro*. *Eur J Cell Biol*. (2017) 96:13–33. doi: 10.1016/j.ejcb.2016.11.003
109. Silva LHA, Antunes MA, Dos Santos CC, Weiss DJ, Cruz FF, Rocco PRM. Strategies to improve the therapeutic effects of mesenchymal stromal cells in respiratory diseases. *Stem Cell Res Ther*. (2018) 9:45. doi: 10.1186/s13287-018-0802-8
110. Xue C, Shen Y, Li X, Li B, Zhao S, Gu J, et al. Exosomes derived from hypoxia-treated human adipose mesenchymal stem cells enhance angiogenesis through the PKA signaling pathway. *Stem Cells Dev*. (2018) 27:456–65. doi: 10.1089/scd.2017.0296
111. Ban J-J, Lee M, Im W, Kim M. Low pH increases the yield of exosome isolation. *Biochem Biophys Res Commun*. (2015) 461:76–9. doi: 10.1016/j.bbrc.2015.03.172
112. Eldh M, Ekström K, Valadi H, Sjöstrand M, Olsson B, Jernås M, et al. Exosomes communicate protective messages during oxidative stress; possible role of exosomal shuttle RNA. *PLoS ONE*. (2010) 5:e15353. doi: 10.1371/journal.pone.0015353
113. Ejtehadifar M, Shamsasenjan K, Movassaghpour A, Akbarzadehlaleh P, Dehdilani N, Abbasi P, et al. The effect of hypoxia on mesenchymal stem cell biology. *Adv Pharm Bull*. (2015) 5:141–9. doi: 10.15171/apb.2015.021
114. Paquet J, Deschepper M, Moya A, Logeart-Avramoglou D, Boisson-Vidal C, Petite H. Oxygen tension regulates human mesenchymal stem cell paracrine functions. *Stem Cells Transl Med*. (2015) 4:809–21. doi: 10.5966/sctm.2014-0180
115. Martinez VG, Ontoria-Oviedo I, Ricardo CP, Harding SE, Sacedon R, Varas A, et al. Overexpression of hypoxia-inducible factor 1 alpha improves immunomodulation by dental mesenchymal stem cells. *Stem Cell Res Ther*. (2017) 8:208. doi: 10.1186/s13287-017-0659-2
116. Ponte AL, Marais E, Gallay N, Langonné A, Delorme B, Hérault O, et al. The *in vitro* migration capacity of human bone marrow mesenchymal stem cells: comparison of chemokine and growth factor chemotactic activities. *Stem Cells*. (2007) 25:1737–45. doi: 10.1634/stemcells.2007-0054
117. Crisostomo PR, Wang Y, Markel TA, Wang M, Lahm T, Meldrum DR. Human mesenchymal stem cells stimulated by TNF-α, LPS, or hypoxia produce growth factors by an NFκB- but not JNK-dependent mechanism. *Am J Physiol Physiol*. (2008) 294:C675–82. doi: 10.1152/ajpcell.00437.2007
118. Roemeling-van Rhijn M, Mensah FKF, Korevaar SS, Leijs MJ, van Osch GJVM, IJzermans JNM, et al. Effects of hypoxia on the immunomodulatory properties of adipose tissue-derived mesenchymal stem cells. *Front Immunol*. (2013) 4:1–8. doi: 10.3389/fimmu.2013.00203
119. Cordonnier T, Layrolle P, Gaillard J, Langonné A, Sensebé L, Rosset P, et al. 3D environment on human mesenchymal stem cells differentiation for bone tissue engineering. *J Mater Sci Mater Med*. (2010) 21:981–7. doi: 10.1007/s10856-009-3916-9
120. Miron RJ, Zohdi H, Fujioka-Kobayashi M, Bosshardt DD. Giant cells around bone biomaterials: osteoclasts or multi-nucleated giant cells? *Acta Biomater*. (2016) 46:15–28. doi: 10.1016/j.actbio.2016.09.029
121. Ahmed GJ, Tatsukawa E, Morishita K, Shibata Y, Suehiro F, Kamitakahara M, et al. Regulation and biological significance of formation of osteoclasts and foreign body giant cells in an extraskeletal implantation model. *Acta Histochem Cytochem*. (2016) 49:97–107. doi: 10.1267/ahc.16007
122. Khan UA, Hashimi SM, Bakr MM, Forwood MR, Morrison NA. Foreign body giant cells and osteoclasts are TRAP positive, have podosome-belts and both require OC-STAMP for cell fusion. *J Cell Biochem*. (2013) 114:1772–8. doi: 10.1002/jcb.24518
123. Ogata K, Katagiri W, Hibi H. Secretomes from mesenchymal stem cells participate in the regulation of osteoclastogenesis *in vitro*. *Clin Oral Investig*. (2017) 21:1979–88. doi: 10.1007/s00784-016-1986-x

124. Horwood NJ, Kartsogiannis V, Quinn JMW, Romas E, Martin TJ, Gillespie MT. Activated T lymphocytes support osteoclast formation *in vitro*. *Biochem Biophys Res Commun*. (1999) 265:144–50. doi: 10.1006/bbrc.1999.1623
125. Martin TJ, Sims NA. RANKL/OPG; critical role in bone physiology. *Rev Endocr Metab Disord*. (2015) 16:131–9. doi: 10.1007/s11154-014-9308-6
126. Quinn JMW, Itoh K, Udagawa N, Häusler K, Yasuda H, Shima N, et al. Transforming growth factor β affects osteoclast differentiation via direct and indirect actions. *J Bone Miner Res*. (2001) 16:1787–94. doi: 10.1359/jbmr.2001.16.10.1787
127. Maeda K, Kobayashi Y, Udagawa N, Uehara S, Ishihara A, Mizoguchi T, et al. Wnt5a-Ror2 signaling between osteoblast-lineage cells and osteoclast precursors enhances osteoclastogenesis. *Nat Med*. (2012) 18:405–12. doi: 10.1038/nm.2653
128. Chan CKF, Gulati GS, Sinha R, Tompkins JV, Lopez M, Carter AC, et al. Identification of the human skeletal stem cell. *Cell*. (2018) 175:43–56.e21. doi: 10.1016/J.CELL.2018.07.029
129. Sims NA, Martin TJ. Coupling the activities of bone formation and resorption: a multitude of signals within the basic multicellular unit. *Bonekey Rep*. (2014) 3:1–10. doi: 10.1038/bonekey.2013.215
130. Matsuo K, Irie N. Osteoclast–osteoblast communication. *Arch Biochem Biophys*. (2008) 473:201–9. doi: 10.1016/j.abb.2008.03.027
131. Henriksen K, Karsdal MA, John Martin T. Osteoclast-derived coupling factors in bone remodeling. *Calcif Tissue Int*. (2014) 94:88–97. doi: 10.1007/s00223-013-9741-7
132. Ikebuchi Y, Aoki S, Honma M, Hayashi M, Sugamori Y, Khan M, et al. Coupling of bone resorption and formation by RANKL reverse signalling. *Nature*. (2018) 561:195–200. doi: 10.1038/s41586-018-0482-7
133. Cianferotti L, Gomes AR, Fabbri S, Tanini A, Brandi ML. The calcium-sensing receptor in bone metabolism: from bench to bedside and back. *Osteoporos Int*. (2015) 26:2055–71. doi: 10.1007/s00198-015-3203-1
134. Chen Z, Klein T, Murray RZ, Crawford R, Chang J, Wu C, et al. Osteoimmunomodulation for the development of advanced bone biomaterials. *Mater Today*. (2016) 19:304–21. doi: 10.1016/j.mattod.2015.11.004

Conflict of Interest Statement: ND is employed by Instructure Labs, B.V.

The remaining authors declare that the research was conducted in the absence of any commercial or financial relationships that could be construed as a potential conflict of interest.

frontiers in Immunology

MINI REVIEW
published: 03 April 2019
doi: 10.3389/fimmu.2019.00679

Osteoimmunology of Bone Loss in Inflammatory Rheumatic Diseases

Fabienne Coury[1,2,3], *Olivier Peyruchaud*[1,2] *and Irma Machuca-Gayet*[1,2]*

[1] INSERM, UMR1033 LYOS, Lyon, France, [2] University Claude Bernard Lyon I, Lyon, France, [3] Department of Rheumatology, Lyon Sud Hospital, Lyon, France

Over the past two decades, the field of osteoimmunology has emerged in response to a range of evidence demonstrating the reciprocal relationship between the immune system and bone. In particular, localized bone loss, in the form of joint erosions and periarticular osteopenia, as well as systemic osteoporosis, caused by inflammatory rheumatic diseases including rheumatoid arthritis, the prototype of inflammatory arthritis has highlighted the importance of this interplay. Osteoclast-mediated resorption at the interface between synovium and bone is responsible for the joint erosion seen in patients suffering from inflammatory arthritis. Clinical studies have helped to validate the impact of several pathways on osteoclast formation and activity. Essentially, the expression of pro-inflammatory cytokines as well as Receptor Activator of Nuclear factor κB Ligand (RANKL) is, both directly and indirectly, increased by T cells, stimulating osteoclastogenesis and resorption through a crucial regulator of immunity, the Nuclear factor of activated T-cells, cytoplasmic 1 (NFATc1). Furthermore, in rheumatoid arthritis, autoantibodies, which are accurate predictors both of the disease and associated structural damage, have been shown to stimulate the differentiation of osteoclasts, resulting in localized bone resorption. It is now also evident that osteoblast-mediated bone formation is impaired by inflammation both in joints and the skeleton in rheumatoid arthritis. This review summarizes the substantial progress that has been made in understanding the pathophysiology of bone loss in inflammatory rheumatic disease and highlights therapeutic targets potentially important for the cure or at least an alleviation of this destructive process.

Keywords: inflammatory rheumatic diseases, rheumatoid arthritis, spondyloarthritis, bone erosion, inflammatory bone loss, osteoclast

OPEN ACCESS

Edited by:
Claudine Blin-Wakkach, UMR7370 Laboratoire de Physio Médecine Moléculaire (LP2M), France

Reviewed by:
Patrizia D'Amelio, University of Turin, Italy
Yong-Gil Kim, University of Ulsan College of Medicine, South Korea
Mascha Koenen, University of Ulm, Germany

***Correspondence:**
Irma Machuca-Gayet
irma.machuca-gayet@inserm.fr
orcid.org/0000-0002-3010-9774

Specialty section:
This article was submitted to Inflammation, a section of the journal Frontiers in Immunology

Received: *08 January 2019*
Accepted: *12 March 2019*
Published: *03 April 2019*

Citation:
Coury F, Peyruchaud O and Machuca-Gayet I (2019) Osteoimmunology of Bone Loss in Inflammatory Rheumatic Diseases. Front. Immunol. 10:679. doi: 10.3389/fimmu.2019.00679

INTRODUCTION

The close relationship between the immune and bone systems has long been noted since pioneering work on soluble immune cell-derived osteoclast-activating factors performed in the early 1970s (1, 2) and was termed osteoimmunology (3). The most significant osteoimmunological example arose from the observation of osteoclast-mediated bone loss in inflammatory rheumatic diseases. Inflammatory rheumatic diseases encompass more than 100 heterogeneous multisystem disorders which can affect joints and lead to disability. However, rheumatoid arthritis (RA) and the spondyloarthritis group (SpA) are the most common inflammatory rheumatic diseases that preferentially affect joints and cause tenderness, swelling, and destruction of joints. Consequently, in this review, we will confine the term "inflammatory rheumatic diseases" to these particular

diseases. SpA, also termed "seronegative" as they do not produce rheumatoid factor nor the anti-citrullinated peptide antibodies (ACPA) observed in RA, represent a group of diseases with common genetic and clinical features, including ankylosing spondylitis (AS), reactive arthritis, psoriatic arthritis (PsA), and SpA associated with inflammatory bowel disease.

RA is considered to be the prototype of destructive inflammatory arthritis with bone loss at sites of articular and peri-articular inflammation. SpA also causes inflammation of the axial skeleton and extra-articular entheses leading to not only bone degradation but also to ectopic bone formation—which in some cases can even lead to bony ankylosis of the joint. Genetic and experimental evidence has associated the activation of IL23-IL17 axis with inflammation and entheseal new bone. The ectopic bone formation aspect of SpA will not be discussed further, as herein review focus is restricted to bone loss, formation is reviewed elsewhere (4). This dissimilarity in the anatomical sites of bone affected and in bone formation patterns highlights the differences in pathophysiological mechanisms involved in these conditions.

Herein, we briefly highlight the key concepts and recent advances in the osteoimmunology field within the context of bone loss in inflammatory rheumatic diseases.

DIFFERENTIAL BONE LOSS IN INFLAMMATORY RHEUMATIC DISEASES

Three forms of bone loss have been identified in patients with inflammatory rheumatic diseases: localized bone loss with erosion, periarticular osteopenia, and generalized bone loss (**Table 1**).

Although cortical bone erosion revealed by radiography is commonly considered to be a hallmark of RA, it can also be observed in SpA as well as other rheumatic diseases such as gout or osteoarthritis—with a distinct radiographic appearance and location. Erosion begins early in inflammatory rheumatic diseases, even prior to the clinical onset of arthritis: erosion has been described in ACPA-positive healthy subjects (5). For long considered as being less destructive than RA, PsA is much more aggressive than previously thought. Essentially, about 20% of PsA patients develop a mutilating form of arthritis and 40–60% of PsA patients develop erosions in the first 2 years of the disease (6). Usually considered to be irreversible, bone erosion is a key outcome in inflammatory rheumatic diseases and correlates with disease severity and functional deterioration. The radiographic assessment of bone erosion is the ≪ gold standard ≫ for diagnosis, in daily clinical practice as well as in randomized controlled clinical trials of disease-modifying antirheumatic drugs, but is challenging. The development of more sensitive and reproducible analysis using ultrasound, magnetic resonance imaging or high-resolution peripheral quantitative computer tomography would be a promising development for erosion detection and monitoring in daily clinical practice. Periarticular trabecular bone is also altered in RA likely with similar mechanisms involved in generalized bone loss. Radiographic periarticular osteopenia is one of the earliest radiological manifestations and may precede bone erosion or joint space narrowing in RA (7). In contrast, it appears that there is no periarticular bone loss in early PsA (8).

TABLE 1 | Common features and differences in bone loss between SpA and RA.

	SpA (AS, PsA, reactive arthritis)	RA
Erosions	• DIP, PIP joints	• MTP, MCP, PIP, and wrist joints
	• Evenly distributed	• Radial sites
	• Small, Ω or tubule-shaped	• U-shaped
	• Poorly demarcated	• Neatly demarcated
	• Periarticular site	• Joint margins
	• Association with enthesitis and bone formation	• No association with enthesitis and bone formation
Periarticular osteopenia	• absent	• May precede bone erosion
Generalized bone loss	• Axial skeleton	• Axial and appendicular skeleton
	• Vertebral fractures	• Vertebral and non-vertebral fractures
	• Association with ectopic new bone formation	• No association with ectopic new bone formation
Bone remodeling	• ↑ Bone resorption	• ↑ Bone resorption
		• ↓ bone formation

DIP, distal interphalangeal; MTP, metatarsophalangeal; MCP, metacarpophalangeal; PIP, proximal interphalangeal. RA erosions, Neatly demarcated and located at joint margins where the inflamed synovium is in direct contact with bone, erosions in RA are U-shaped and observed predominantly in metacarpophalangeal / metatarsophalangeal and proximal interphalangeal joints with a strong preponderance for radial sites; PsA erosion, Poorly demarcated, smaller in size and depth, Ω or tubule-shaped, and are more evenly distributed. They are located in the periarticular site in proximal and distal interphalangeal joints and are closely associated with bone formation.

Secondary systemic osteopenia or osteoporosis involving the axial and appendicular skeleton remote from synovial inflammation is an important co-morbidity in inflammatory rheumatic diseases. In effect, the prevalence of densitometric osteoporosis in RA patients is increased about two fold compared with the general population and is responsible for a risk of both vertebral and non-vertebral fractures (9). Although patients with SpA have radiographic evidence of ectopic new bone formation, many present evidences of marked osteopenia, and osteoporosis in the spine that is associated with a high prevalence of vertebral fractures—even in early axial SpA (10, 11). Inflammation is the major mechanism involved in bone loss in inflammatory rheumatic diseases. Proinflammatory cytokines increase osteoclast activation and subsequent bone resorption in both rheumatic disease types (12) but inhibit bone formation only in RA (13, 14). As a consequence, treatment with TNF-blockers both in RA and SpA has been shown to improve skeletal remodeling (15, 16). Apart from inflammation, others factors play a role such as the adverse skeletal effects of corticosteroids used to treat these diseases and immobility, due to painful joints, muscle weakness, and spine ankylosis—although

bone loss is observed well-before the development of spinal immobility (17–19).

OSTEOCLAST DIFFERENTIATION AND FUNCTION IN INFLAMMATORY RHEUMATIC DISEASES

Osteoclasts are responsible for bone erosion and have been identified at sites of focal erosion at the pannus-bone interface both in RA patients (20, 21) and animal models of arthritis (22–26). This role was definitively demonstrated by osteoclast-deficient mouse models of arthritis which were shown to be fully protected from bone erosion (25, 26). Osteoclasts are multinucleated bone resorbing cells which originate from the fusion of mononucleated cells belonging to the myeloid lineage in the presence of macrophage colony-stimulating factor (M-CSF) and Receptor Activator of Nuclear factor-κB Ligand (RANKL). Osteoclast formation is governed by a regulatory triad, the receptor activator of NF-κB (RANK), its ligand RANKL and a decoy receptor osteoprotegerin (OPG) also known as osteoclastogenesis inhibitory factor. OPG binds to RANKL hampering RANK-RANKL interaction, though RANKL/OPG ratio determines osteoclast number, lifespan and activity. Activation of RANK on mononuclear osteoclast precursors initiates a transcriptional cascade culminating in osteoclast differentiation. Interestingly, transcription factors important for osteoclast differentiation are key regulators of immune responses—such as NF-κB and nuclear factor of activated T cells cytoplasmic 1 (NFATc1). RANKL signaling in osteoclasts is strengthened by the synergistic activation of Immunoreceptor tyrosine-based activation motif (ITAM)-containing proteins, DNAX-activating protein of 12 kDa (DAP12) and Fc gamma receptor (FcRγ) (27, 28).

RANKL expression is high in synovial tissue from RA, PsA, and SpA peripheral joint disease patients (29–32). Treatment with non-biologic disease-modifying anti-rheumatic drugs (DMARDs) or glucocorticoids decreases the RANKL/OPG ratio in RA synovium and is satisfyingly associated with improved radiographic scores (17, 33). In addition, pharmacological inhibition of osteoclasts either by bisphosphonate zolendronic acid, or denosumab, a RANKL-specific monoclonal blocking antibody, also demonstrated some efficacy in impairing the progression of bone erosion in both arthritic mice and RA patients (34–38). However, these anti-resorptive drugs targeting osteoclasts are inadequate because they also alter physiological bone remodeling, necessitating the discovery of new targets.

ROLE OF T CELLS IN OSTEOCLASTOGENESIS

T cells have emerged as primary players through both direct and indirect mechanisms in the pathogenesis of bone loss in arthritis (39). Although osteoblasts, osteocytes and T cells express RANKL, the major RANKL-expressing cell subset in arthritic joints has been shown to be synovial fibroblasts [(39), (**Figure 1**)]. However, these cells express RANKL under the effect of interleukin-17 (IL-17) produced by T helper (Th) 17 cells (40). Congruent with this result, IL-17A promotes osteoclast precursor increase, bone resorption biomarker induction, and bone erosion (41, 42); its inhibition leads to improvement of inflammatory arthritis animal models (24, 43). Nevertheless, while IL-17A inhibition has demonstrated robust efficacy in SpA including PsA (44–46), it has shown only limited effect in the treatment of active RA (47–51).

IL-17-producing Th17 cells are the exclusive pro-osteoclastogenic Tcell subset while Th1 and Th2 subsets inhibit osteoclastogenesis through their respective canonical cytokines IFN-γ and IL-4 (52). Similarly, regulatory T cells inhibit osteoclastogenesis through anti-inflammatory cytokines such as IL-10 and through cytotoxic T lymphocyte antigen 4 (CTLA4) signaling, a negative regulator of T cell activation (47, 49, 50). The anti-erosive effect of abatacept, a CTLA4-Ig fusion protein efficacious in patients with RA and active PsA, underlines this effect. Deficiencies in regulatory T cell function and Th17/regulatory T cell imbalance have been identified in RA and psoriasis (53, 54). However, data on the presence and distribution of regulatory T cells in inflamed synovial tissue and on the effects of abatacept on regulatory T cell function are both limited and conflicting (8, 55–57).

ACPA-MEDIATED BONE EROSION

ACPA targets are citrullinated proteins—mainly fibrinogen, α-enolase, and vimentin. Citrullination, a posttranslational conversion of arginine residues to citrulline performed by peptidylarginine deiminases, is a physiological process which can be pathologically triggered by smoking, a well-known risk factor for RA (58).

ACPA currently constitute the most specific serological marker for the diagnosis of RA and have been thereby included in the American College of Rheumatology (ACR)/European League Against Rheumatism (EULAR) 2010 RA classification criteria (59). ACPA are also a strong predictive factor for the development of bone erosion (60, 61) and can emerge long before the onset of synovitis during an initial pre-clinical phase of autoimmunity, which is either asymptomatic or only associated with arthralgia (62–65). Remarkably, the hypothesis that bone damage in RA precedes the clinical onset of disease is supported by the discovery of systemic bone loss and cortical bone erosion in a cohort of healthy ACPA-positive individuals (5), suggesting that ACPA directly trigger bone loss.

ACPA mainly belong to the IgG subtype and thus are recognized by FcγR on immune cells. It was therefore originally proposed that ACPA indirectly mediate bone loss through the enhanced production of TNF by monocytes / macrophages (66), but in recent years two groups have shown that ACPA also bind directly to citrullinated proteins on the surface of osteoclast precursors and directly enhance osteoclastogenesis

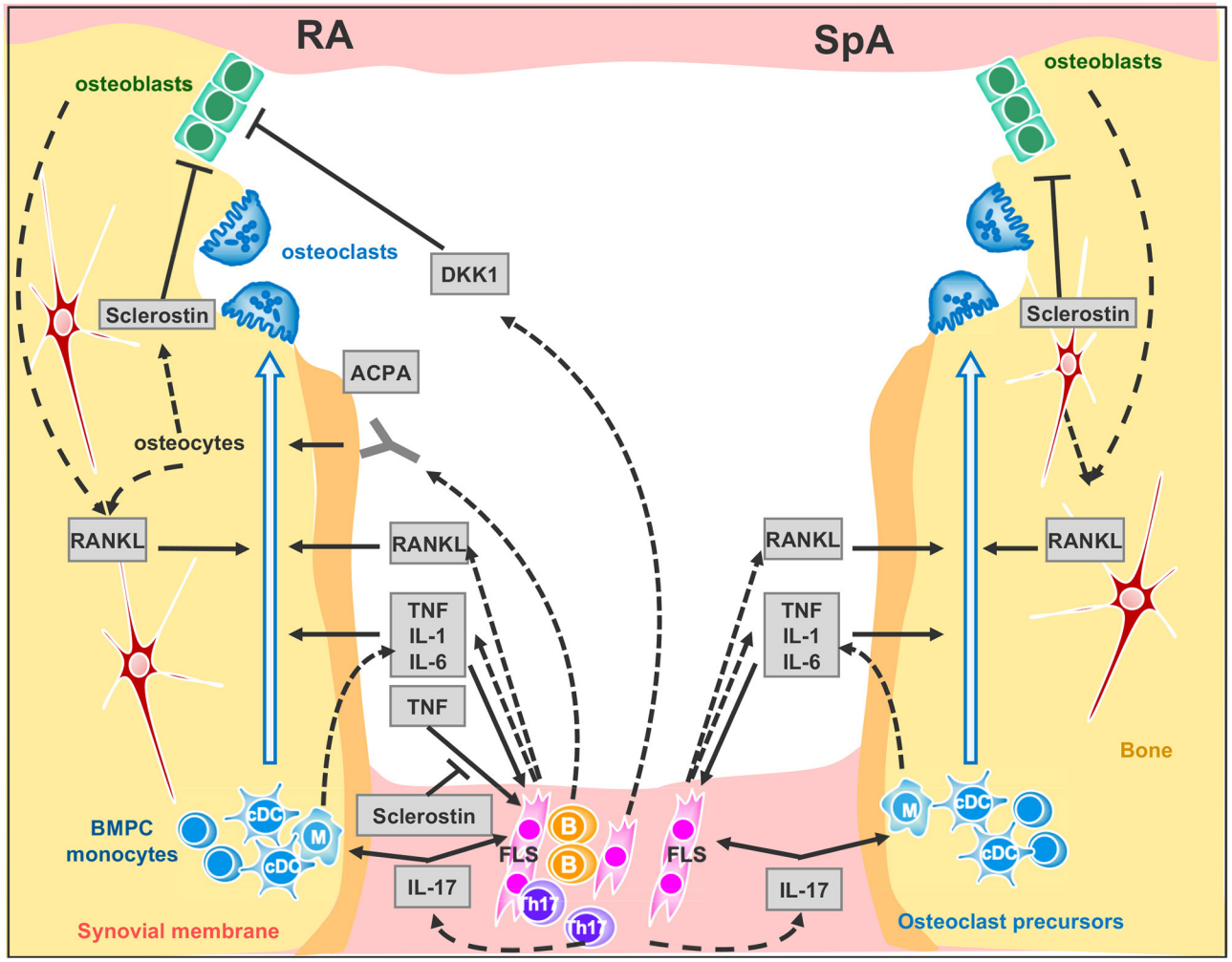

FIGURE 1 | Signaling network between synovial membrane and bone in inflammatory rheumatic disease. Left panel RA and right panel SpA cytokine signaling at inflamed joint. Plain arrows indicate an action of the cytokine, factor or auto-antibodies on the cells. Dotted arrows indicate cytokine, factor or auto-antibody production by the cells. ACPA, anti-citrullinated peptide antibodies; BMPC, bone marrow progenitor cells; DKK-1, Dickkopf-1; FLS, Fibroblast-like synoviocytes. B, B cells; Th17, Th17-cells; cDC, circulating dendritic cells. M, Macrophages.

(67, 68) (**Figure 1**). Remarkably, ACPA glycosylation patterns shift the change toward a more pro-inflammatory phenotype only within the 3 months prior to the onset of RA (69, 70). Furthermore, in newly differentiating antibody-producing cells, β-galactoside α2,6-sialyltransferase expression is regulated by Th17 cells in an IL-22- and IL-21- dependent manner, determining the glycosylation profile of IgG produced by plasma cells (70). Consequently, while IL-17 inhibition has a limited effect in the treatment of active RA, it may have a role when instituted at the early stages. Moreover, insofar as ACPA can promote bone resorption and some biologic DMARDs such as abatacept and rituximab (a monoclonal antibody against B cell CD20) can decrease ACPA levels in RA patients, the goal of achieving immunological remission with these treatments is enticing (71). However, the real value of reducing ACPA in RA patients still needs to be determined.

Taken together, these studies support a pathogenic role for ACPA in mediating bone loss in RA. In contrast, PsA is not frequently associated with circulating autoantibodies, including ACPA (72). This is probably the reason why rituximab, is effective in RA and not in PsA. However, when ACPA are present in PsA, titers are usually low but the disease phenotype is more severe with polyarticular involvement and erosive disease (73).

PROINFLAMMATORY CYTOKINE-MEDIATED BONE RESORPTION

Bone loss correlates well with disease activity and severity, supporting the current therapeutic strategy in inflammatory rheumatic diseases of targeting the best control of synovitis

and the biological inflammatory syndrome. Indeed, conventional DMARDs, such as methotrexate, enable protection from bone erosion simply by their ability to reduce synovitis (74). However, some RA patients in sustained clinical remission or low disease activity still continue to accrue bone erosions (38, 75), likely because of subclinical synovial inflammation (76). This evolution is probably similar in SpA, but it has not yet been clearly demonstrated in the absence of well-defined remission criteria.

TNF overexpression is sufficient to induce arthritis in mice (77). TNF operates by several mechanisms: it promotes bone resorption indirectly in conjunction with IL-6 by up-regulating RANKL expression in synovial fibroblasts (78, 79) and directly by aiding the differentiation of osteoclasts from mononuclear precursors in synovial tissues in synergy with RANKL (80) (**Figure 1**). Recent evidence suggests that combinations of cytokines, such as TNF plus IL-6, may drive RANK/RANKL-independent osteoclast formation (81) but this process still needs confirmation using other models. TNF also expands the pool of osteoclast precursor cells (82). Additionally, IL-1 is a mediator of TNF-induced osteoclastogenesis (83) while IL-6 is an important factor for Th17 differentiation. Accordingly, clinical trials—only in RA—with TNF blockers (16) and the Il-6 receptor blockade (84), have confirmed the impact of pro-inflammatory cytokines on osteoclastogenesis as they can retard or arrest the occurrence of bone erosion. As for the IL-1 blockade, despite having a limited effect on swelling, it protects from bone erosion in RA (85).

OSTEOFORMATION AND EROSION REPAIR

In RA only, the inflammatory milieu also impairs bone formation and erosion repair. TNF is the instrumental cytokine that unbalances bone homeostasis, blocking osteoblast differentiation and maturation through Wingless (Wnt) ligand signaling (86). Bone formation is governed by Wnt pathways which are critical for the osteoblast transcriptional differentiation program through the canonical β catenin-dependent activation. The Wnt ligands interact with the membrane-bound co-receptor frizzled and the low–density lipoprotein receptor-related proteins LRP-5 or LRP-6. This activated receptor complex stabilizes β catenin transcription factor, allowing its translocation to the nucleus to directly coactivate Runx2 and OPG (87, 88). In inflammatory rheumatic diseases, bone erosion repair is scarcely observed, even under biologic therapies such as TNF or IL-6 receptor blockers, and manifests only as apposition of new bone (sclerosis) at the base of the erosion (89, 90). Paradoxically, analysis of histological sections of arthritic samples, either from humans or from murine models, has shown the presence of osteoblast lineage cells close to the eroded bone once inflammation resolves (21, 91). In addition, intermittent parathyroid hormone (PTH) treatment - an anabolic agent for bone- used for treatment of osteoporosis, fails to reduce erosion volume in patients with established RA with disease activity controlled by TNF blockers (92). By contrast to humans, treatment of hTNFtg mice with a combined therapy consisting of anti-TNF together with intermittent PTH led to regression of local bone erosion and bone repair, demonstrating new bone formation (93). An alternative to anabolic treatment aiming at increasing bone formation and repair, is to block bone formation antagonists. Indeed, Wnt pro-osteogenic function is controlled and tempered by several physiological antagonists: Dickkopf proteins (DKK-1 and 2), soluble frizzled-related proteins (sFRPs) (94, 95) and sclerostin that—in the presence of Wnt ligands—antagonizes LRP-6 internalization (96, 97). In RA, TNF lessens osteoformation by up-regulating DKK-1 expression, for instance DKK-1 level is found to be elevated in RA patients' sera and in hTNFtg mice, CIA, and GPI-induced arthritis mice, (98, 99). In hTNFtg mice only, DKK-1 inhibition is able to prevent bone erosion and to promote bone formation, generating osteophytes around inflamed joints (99). Soluble frizzled-related proteins sFRP1 and sFRP2 are Wnt antagonist that sequestrate Wnt ligands, preventing them to activate frizzle/Lpr5 receptors, were also found elevated in synovial fluids of KBxN serum transfert inflammation induced mice model (91). Among the Wnt ligand antagonists, sclerostin is an attractive therapeutic target for bone loss pathologies. Sclerostin-neutralizing antibodies have been shown to have strong bone-building effects in mice, rats, monkeys, and humans (97–101). This treatment prevents the decrease of bone mineral density and bone volume at axial and appendicular sites in Collagen-Induced Arthritis mice but does not protect from erosion on the periarticular bone and fails to repair focal erosions (102). On the other hand, in hTNFtg mice, TNF induced sclerostin expression in inflammatory synoviocytes, unexpectedly, the absence of sclerostin in hTNFtg/ $Sost^{-/-}$ mice, instead of reversing the inflammatory bone destruction, elicited exacerbation of the disease. These observations suggest that sclerostin may be involved in regulating other pathways besides Wnt signaling or has an anti-osteoclastogenic effect in TNF-dependent chronic arthritis (103). In line with this paradigm of uncovered sclerostin functions, recent findings surprisingly show that overexpressing sclerostin in murine skeletal stem cells forms overgrown bones when engrafted. This observation indicates that sclerostin could have an osteoforming effect on skeletal stem cells (104). Moreover, a recent study using non-inflammatory bone loss mouse models, unveiled a compensatory mechanism leading to increased expression of sclerostin when DKK-1 is inhibited. It would therefore perhaps be prudent before embarking upon anti-sclerostin treatments for RA, to conduct further studies in animal models of RA using *Sost* tissue-specific ablation to help obtain a better understanding of the precise role of sclerostin in chronic inflammatory diseases.

In contrast to RA, bone formation is observed in SpA at entheseal sites, resulting in endochondral bone formations. IL32γ, among others pro-inflammatory cytokines, is found elevated in SpA synovial fluid, it is proposed that IL32γ enhances osteoblast differentiation via DKK-1 suppression, thereafter promoting abnormal bone formation (105). Indeed, lower levels of DKK-1 in AS and PsA patients and sclerostin in AS patients have been reported, potentially explaining the non-impediment of osteoblast activity (99, 106, 107). In conflict with the above report, a recent meta-analysis showed no significant difference in sclerostin serum levels in AS and RA

patients vs. healthy controls which suggests that sclerostin may not be associated with the pathogenesis of AS and RA (108). Last, a recent and challenging study revealed that vesicular RANK produced by mature osteoclasts stimulate early osteoblast differentiation through osteoblastic RANKL reverse signaling (109). Consequently, the development of a biological compound to trigger RANKL reverse signaling in osteoblast would be a new promising lead to promote bone formation.

CONCLUSIONS

In inflammatory rheumatic diseases, systemic and local bone loss constitute a common key outcome in terms of functional capacity and reflects the tight interaction between the immune system and bone, leading to an increase in osteoclast activity and a consequent uncoupling of bone resorption from formation. Once established, bone erosions are at present, still irreversible. It is to be hoped that a better future understanding of the molecular pathways involved in bone loss and bone formation—particularly in the context of inflammation—will enable the development of new therapies that can selectively and directly halt, or even repair, bone erosion.

AUTHOR CONTRIBUTIONS

All authors listed have made a substantial, direct and intellectual contribution to the work, and approved it for publication.

FUNDING

This work was supported by grants from INSERM and the University Claude Bernard Lyon-1 (OP), the Comité Départemental de la Loire de la Ligue Contre le Cancer (OP), the ANR grant LYSBONE (OP) (Grant n°. ANR-15-CE14-0010-01).

REFERENCES

1. Horton JE, Raisz LG, Simmons HA, Oppenheim JJ, Mergenhagen SE. Bone resorbing activity in supernatant fluid from cultured human peripheral blood leukocytes. *Science*. (1972) 177:793–5.
2. Mundy GR, Raisz LG, Cooper RA, Schechter GP, Salmon SE. Evidence for the secretion of an osteoclast stimulating factor in myeloma. *N Engl J Med*. (1974) 291:1041–6. doi: 10.1056/NEJM197411142912001
3. Arron JR, Choi Y. Bone versus immune system. *Nature*. (2000) 408:535–6. doi: 10.1038/35046196
4. Gravallese EM, Schett G. Effects of the IL-23-IL-17 pathway on bone in spondyloarthritis. *Nat Rev Rheumatol*. (2018) 14:631–40. doi: 10.1038/s41584-018-0091-8
5. Kleyer A, Finzel S, Rech J, Manger B, Krieter M, Faustini F, et al. Bone loss before the clinical onset of rheumatoid arthritis in subjects with anticitrullinated protein antibodies. *Ann Rheum Dis*. (2014) 73:854–60. doi: 10.1136/annrheumdis-2012-202958
6. Gladman DD, Antoni C, Mease P, Clegg DO, Nash P. Psoriatic arthritis: epidemiology, clinical features, course, and outcome. *Ann Rheum Dis*. (2005) 64 Suppl 2:ii14–7. doi: 10.1136/ard.2004.032482
7. Brower AC. Use of the radiograph to measure the course of rheumatoid arthritis. The gold standard versus fool's gold. *Arthritis Rheum*. (1990) 33:316–24.
8. Szentpetery A, Heffernan E, Haroon M, Kilbane M, Gallagher P, McKenna MJ, et al. Striking difference of periarticular bone density change in early psoriatic arthritis and rheumatoid arthritis following anti-rheumatic treatment as measured by digital X-ray radiogrammetry. *Rheumatology*. (2016) 55:891–6. doi: 10.1093/rheumatology/kev443
9. Haugeberg G, Uhlig T, Falch JA, Halse JI, Kvien TK. Bone mineral density and frequency of osteoporosis in female patients with rheumatoid arthritis: results from 394 patients in the Oslo County Rheumatoid Arthritis register. *Arthritis Rheum*. (2000) 43:522–30. doi: 10.1002/1529-0131(200003)43:3<522::AID-ANR7>3.0.CO;2-Y
10. van der Weijden MA, van Denderen JC, Lems WF, Heymans MW, Dijkmans BA, van der Horst-Bruinsma IE. Low bone mineral density is related to male gender and decreased functional capacity in early spondylarthropathies. *Clin Rheumatol*. (2011) 30:497–503. doi: 10.1007/s10067-010-1538-8
11. van der Weijden MA, van der Horst-Bruinsma IE, van Denderen JC, Dijkmans BA, Heymans MW, Lems WF. High frequency of vertebral fractures in early spondylarthropathies. *Osteoporos Int*. (2012) 23:1683–90. doi: 10.1007/s00198-011-1766-z
12. Redlich K, Smolen JS. Inflammatory bone loss: pathogenesis and therapeutic intervention. *Nat Rev Drug Discov*. (2012) 11:234–50. doi: 10.1038/nrd3669
13. Bultink IE, Vis M, van der Horst-Bruinsma IE, Lems WF. Inflammatory rheumatic disorders and bone. *Curr Rheumatol Rep*. (2012) 14:224–30. doi: 10.1007/s11926-012-0252-8
14. Gao Y, Grassi F, Ryan MR, Terauchi M, Page K, Yang X, et al. IFN-gamma stimulates osteoclast formation and bone loss *in vivo* via antigen-driven T cell activation. *J Clin Invest*. (2007) 117:122–32. doi: 10.1172/JCI30074
15. Allali F, Breban M, Porcher R, Maillefert JF, Dougados M, Roux C. Increase in bone mineral density of patients with spondyloarthropathy treated with anti-tumour necrosis factor alpha. *Ann Rheum Dis*. (2003) 62:347–9. doi: 10.1136/ard.62.4.347
16. Vis M, Havaardsholm EA, Haugeberg G, Uhlig T, Voskuyl AE, van de Stadt RJ, et al. Evaluation of bone mineral density, bone metabolism, osteoprotegerin and receptor activator of the NFkappaB ligand serum levels during treatment with infliximab in patients with rheumatoid arthritis. *Ann Rheum Dis*. (2006) 65:1495–9. doi: 10.1136/ard.2005.044198
17. Hartmann K, Koenen M, Schauer S, Wittig-Blaich S, Ahmad M, Baschant U, et al. Molecular actions of glucocorticoids in cartilage and bone during health, disease, and steroid therapy. *Physiol Rev*. (2016) 96:409–47. doi: 10.1152/physrev.00011.2015
18. Mandl P, Kainberger F, Friberg Hitz M. Imaging in osteoporosis in rheumatic diseases. *Best Pract Res Clin Rheumatol*. (2016) 30:751–65. doi: 10.1016/j.berh.2016.08.010
19. Boling EP. Secondary osteoporosis: underlying disease and the risk for glucocorticoid-induced osteoporosis. *Clin Ther*. (2004) 26:1–14.
20. Bromley M, Woolley DE. Chondroclasts and osteoclasts at subchondral sites of erosion in the rheumatoid joint. *Arthritis Rheum*. (1984) 27:968–75.
21. Gravallese EM, Harada Y, Wang JT, Gorn AH, Thornhill TS, Goldring SR. Identification of cell types responsible for bone resorption in rheumatoid arthritis and juvenile rheumatoid arthritis. *Am J Pathol*. (1998) 152:943–51.
22. Kong YY, Feige U, Sarosi I, Bolon B, Tafuri A, Morony S, et al. Activated T cells regulate bone loss and joint destruction in adjuvant arthritis through osteoprotegerin ligand. *Nature*. (1999) 402:304–9. doi: 10.1038/46303
23. Romas E, Sims NA, Hards DK, Lindsay M, Quinn JW, Ryan PF, et al. Osteoprotegerin reduces osteoclast numbers and prevents bone erosion in collagen-induced arthritis. *Am J Pathol*. (2002) 161:1419–27. doi: 10.1016/S0002-9440(10)64417-3
24. Lubberts E, Koenders MI, Oppers-Walgreen B, van den Bersselaar L, Coenen-de Roo CJ, Joosten LA, et al. Treatment with a neutralizing anti-murine interleukin-17 antibody after the onset of collagen-induced arthritis reduces joint inflammation, cartilage destruction, and bone erosion. *Arthritis Rheum*. (2004) 50:650–9. doi: 10.1002/art.20001

25. Pettit AR, Ji H, von Stechow D, Muller R, Goldring SR, Choi Y, et al. TRANCE/RANKL knockout mice are protected from bone erosion in a serum transfer model of arthritis. *Am J Pathol*. (2001) 159:1689–99. doi: 10.1016/S0002-9440(10)63016-7
26. Redlich K, Hayer S, Ricci R, David JP, Tohidast-Akrad M, Kollias G, et al. Osteoclasts are essential for TNF-alpha-mediated joint destruction. *J Clin Invest*. (2002) 110:1419-27. doi: 10.1172/JCI15582
27. Mocsai A, Humphrey MB, Van Ziffle JA, Hu Y, Burghardt A, Spusta SC, et al. The immunomodulatory adapter proteins DAP12 and Fc receptor gamma-chain (FcRgamma) regulate development of functional osteoclasts through the Syk tyrosine kinase. *Proc Natl Acad Sci USA*. (2004) 101:6158–63. doi: 10.1073/pnas.0401602101
28. Koga T, Inui M, Inoue K, Kim S, Suematsu A, Kobayashi E, et al. Costimulatory signals mediated by the ITAM motif cooperate with RANKL for bone homeostasis. *Nature*. (2004) 428:758–63. doi: 10.1038/nature02444
29. Crotti TN, Smith MD, Weedon H, Ahern MJ, Findlay DM, Kraan M, et al. Receptor activator NF-kappaB ligand (RANKL) expression in synovial tissue from patients with rheumatoid arthritis, spondyloarthropathy, osteoarthritis, and from normal patients: semiquantitative and quantitative analysis. *Ann Rheum Dis*. (2002) 61:1047–54. doi: 10.1136/ard.61.12.1047
30. Ritchlin CT, Haas-Smith SA, Li P, Hicks DG, Schwarz EM. Mechanisms of TNF-alpha- and RANKL-mediated osteoclastogenesis and bone resorption in psoriatic arthritis. *J Clin Invest*. (2003) 111:821–31. doi: 10.1172/JCI16069
31. Haynes DR, Barg E, Crotti TN, Holding C, Weedon H, Atkins GJ, et al. Osteoprotegerin expression in synovial tissue from patients with rheumatoid arthritis, spondyloarthropathies and osteoarthritis and normal controls. *Rheumatology*. (2003) 42:123–34. doi: 10.1093/rheumatology/keg047
32. van Tuyl LH, Voskuyl AE, Boers M, Geusens P, Landewe RB, Dijkmans BA, et al. Baseline RANKL:OPG ratio and markers of bone and cartilage degradation predict annual radiological progression over 11 years in rheumatoid arthritis. *Ann Rheum Dis*. (2010) 69:1623–8. doi: 10.1136/ard.2009.121764
33. Haynes D, Crotti T, Weedon H, Slavotinek J, Au V, Coleman M, et al. Modulation of RANKL and osteoprotegerin expression in synovial tissue from patients with rheumatoid arthritis in response to disease-modifying antirheumatic drug treatment and correlation with radiologic outcome. *Arthritis Rheum*. (2008) 59:911–20. doi: 10.1002/art.23818
34. Jarrett SJ, Conaghan PG, Sloan VS, Papanastasiou P, Ortmann CE, O'Connor PJ, et al. Preliminary evidence for a structural benefit of the new bisphosphonate zoledronic acid in early rheumatoid arthritis. *Arthritis Rheum*. (2006) 54:1410–4. doi: 10.1002/art.21824
35. Herrak P, Gortz B, Hayer S, Redlich K, Reiter E, Gasser J, et al. Zoledronic acid protects against local and systemic bone loss in tumor necrosis factor-mediated arthritis. *Arthritis Rheum*. (2004) 50:2327–37. doi: 10.1002/art.20384
36. Sims NA, Green JR, Glatt M, Schlict S, Martin TJ, Gillespie MT, et al. Targeting osteoclasts with zoledronic acid prevents bone destruction in collagen-induced arthritis. *Arthritis Rheum*. (2004) 50:2338–46. doi: 10.1002/art.20382
37. Deodhar A, Dore RK, Mandel D, Schechtman J, Shergy W, Trapp R, et al. Denosumab-mediated increase in hand bone mineral density associated with decreased progression of bone erosion in rheumatoid arthritis patients. *Arthritis Care Res*. (2010) 62:569–74. doi: 10.1002/acr.20004
38. Cohen G, Gossec L, Dougados M, Cantagrel A, Goupille P, Daures JP, et al. Radiological damage in patients with rheumatoid arthritis on sustained remission. *Ann Rheum Dis*. (2007) 66:358–63. doi: 10.1136/ard.2006.057497
39. Danks L, Komatsu N, Guerrini MM, Sawa S, Armaka M, Kollias G, et al. RANKL expressed on synovial fibroblasts is primarily responsible for bone erosions during joint inflammation. *Ann Rheum Dis*. (2016) 75:1187–95. doi: 10.1136/annrheumdis-2014-207137
40. Kotake S, Udagawa N, Hakoda M, Mogi M, Yano K, Tsuda E, et al. Activated human T cells directly induce osteoclastogenesis from human monocytes: possible role of T cells in bone destruction in rheumatoid arthritis patients. *Arthritis Rheum*. (2001) 44:1003–12. doi: 10.1002/1529-0131(200105)44:5<1003::AID-ANR179>3.0.CO;2
41. Lubberts E, Oppers-Walgreen B, Pettit AR, Van Den Bersselaar L, Joosten LA, Goldring SR, et al. Increase in expression of receptor activator of nuclear factor kappaB at sites of bone erosion correlates with progression of inflammation in evolving collagen-induced arthritis. *Arthritis Rheum*. (2002) 46:3055–64. doi: 10.1002/art.10607
42. Adamopoulos IE, Suzuki E, Chao CC, Gorman D, Adda S, Maverakis E, et al. IL-17A gene transfer induces bone loss and epidermal hyperplasia associated with psoriatic arthritis. *Ann Rheum Dis*. (2015) 74:1284–92. doi: 10.1136/annrheumdis-2013-204782
43. Bush KA, Farmer KM, Walker JS, Kirkham BW. Reduction of joint inflammation and bone erosion in rat adjuvant arthritis by treatment with interleukin-17 receptor IgG1 Fc fusion protein. *Arthritis Rheum*. (2002) 46:802–5. doi: 10.1002/art.10173
44. McInnes IB, Mease PJ, Kirkham B, Kavanaugh A, Ritchlin CT, Rahman P, et al. Secukinumab, a human anti-interleukin-17A monoclonal antibody, in patients with psoriatic arthritis (FUTURE 2): a randomised, double-blind, placebo-controlled, phase 3 trial. *Lancet*. (2015) 386:1137–46. doi: 10.1016/S0140-6736(15)61134-5
45. Mease PJ, McInnes IB, Kirkham B, Kavanaugh A, Rahman P, van der Heijde D, et al. Secukinumab Inhibition of Interleukin-17A in Patients with Psoriatic Arthritis. *N Engl J Med*. (2015) 373:1329–39. doi: 10.1056/NEJMoa1412679
46. van der Heijde D, Gladman DD, Kishimoto M, Okada M, Rathmann SS, Moriarty SR, et al. Efficacy and Safety of Ixekizumab in Patients with Active Psoriatic Arthritis: 52-week Results from a Phase III Study (SPIRIT-P1). *J Rheumatol*. (2018) 45:367–77doi: 10.3899/jrheum.170429
47. Hueber W, Patel DD, Dryja T, Wright AM, Koroleva I, Bruin G, et al. Effects of AIN457, a fully human antibody to interleukin-17A, on psoriasis, rheumatoid arthritis, and uveitis. *Sci Transl Med*. (2010) 2:52ra72. doi: 10.1126/scitranslmed.3001107
48. Genovese MC, Durez P, Richards HB, Supronik J, Dokoupilova E, Mazurov V, et al. Efficacy and safety of secukinumab in patients with rheumatoid arthritis: a phase II, dose-finding, double-blind, randomised, placebo controlled study. *Ann Rheum Dis*. (2013) 72:863–9. doi: 10.1136/annrheumdis-2012-201601
49. Genovese MC, Fleischmann R, Furst D, Janssen N, Carter J, Dasgupta B, et al. Efficacy and safety of olokizumab in patients with rheumatoid arthritis with an inadequate response to TNF inhibitor therapy: outcomes of a randomised Phase IIb study. *Ann Rheum Dis*. (2014) 73:1607–15. doi: 10.1136/annrheumdis-2013-204760
50. Tlustochowicz W, Rahman P, Seriolo B, Krammer G, Porter B, Widmer A, et al. Efficacy and safety of subcutaneous and intravenous loading dose regimens of secukinumab in patients with active rheumatoid arthritis: results from a randomized phase II study. *J Rheumatol*. (2016) 43:495–503. doi: 10.3899/jrheum.150117
51. Blanco FJ, Moricke R, Dokoupilova E, Codding C, Neal J, Andersson M, et al. Secukinumab in active rheumatoid arthritis: a phase III randomized, double-blind, active comparator- and placebo-controlled study. *Arthritis Rheumatol*. (2017) 69:1144–53. doi: 10.1002/art.40070
52. Sato K, Suematsu A, Okamoto K, Yamaguchi A, Morishita Y, Kadono Y, et al. Th17 functions as an osteoclastogenic helper T cell subset that links T cell activation and bone destruction. *J Exp Med*. (2006) 203:2673–82. doi: 10.1084/jem.20061775
53. Flores-Borja F, Jury EC, Mauri C, Ehrenstein MR. Defects in CTLA-4 are associated with abnormal regulatory T cell function in rheumatoid arthritis. *Proc Natl Acad Sci USA*. (2008) 105:19396–401. doi: 10.1073/pnas.0806855105
54. Sugiyama H, Gyulai R, Toichi E, Garaczi E, Shimada S, Stevens SR, et al. Dysfunctional blood and target tissue CD4+CD25high regulatory T cells in psoriasis: mechanism underlying unrestrained pathogenic effector T cell proliferation. *J Immunol*. (2005) 174:164–73. doi: 10.4049/jimmunol.174.1.164
55. Cao D, van Vollenhoven R, Klareskog L, Trollmo C, Malmstrom V. CD25brightCD4+ regulatory T cells are enriched in inflamed joints of patients with chronic rheumatic disease. *Arthritis Res Ther*. (2004) 6:R335–46. doi: 10.1186/ar1192
56. Bonelli M, Goschl L, Blumel S, Karonitsch T, Hirahara K, Ferner E, et al. Abatacept (CTLA-4Ig) treatment reduces T cell apoptosis and regulatory T cell suppression in patients with rheumatoid arthritis. *Rheumatology*. (2016) 55:710–20. doi: 10.1093/rheumatology/kev403

57. Alvarez-Quiroga C, Abud-Mendoza C, Doniz-Padilla L, Juarez-Reyes A, Monsivais-Urenda A, Baranda L, et al. CTLA-4-Ig therapy diminishes the frequency but enhances the function of Treg cells in patients with rheumatoid arthritis. *J Clin Immunol*. (2011) 31:588–95. doi: 10.1007/s10875-011-9527-5
58. Klareskog L, Stolt P, Lundberg K, Kallberg H, Bengtsson C, Grunewald J, et al. A new model for an etiology of rheumatoid arthritis: smoking may trigger HLA-DR (shared epitope)-restricted immune reactions to autoantigens modified by citrullination. *Arthritis Rheum*. (2006) 54:38–46. doi: 10.1002/art.21575
59. Aletaha D, Neogi T, Silman AJ, Funovits J, Felson DT, Bingham CO, 3rd, et al. 2010 rheumatoid arthritis classification criteria: an American College of Rheumatology/European League Against Rheumatism collaborative initiative. *Ann Rheum Dis*. (2010) 69:1580–8. doi: 10.1136/ard.2010.138461
60. Arkema EV, Goldstein BL, Robinson W, Sokolove J, Wagner CA, Malspeis S, et al. Anti-citrullinated peptide autoantibodies, human leukocyte antigen shared epitope and risk of future rheumatoid arthritis: a nested case-control study. *Arthritis Res Ther*. (2013) 15:R159. doi: 10.1186/ar4342
61. Jilani AA, Mackworth-Young CG. The role of citrullinated protein antibodies in predicting erosive disease in rheumatoid arthritis: a systematic literature review and meta-analysis. *Int J Rheumatol*. (2015) 2015:728610. doi: 10.1155/2015/728610
62. Rantapaa-Dahlqvist S, de Jong BA, Berglin E, Hallmans G, Wadell G, Stenlund H, et al. Antibodies against cyclic citrullinated peptide and IgA rheumatoid factor predict the development of rheumatoid arthritis. *Arthritis Rheum*. (2003) 48:2741–9. doi: 10.1002/art.11223
63. Nielen MM, van Schaardenburg D, Reesink HW, van de Stadt RJ, van der Horst-Bruinsma IE, de Koning MH, et al. Specific autoantibodies precede the symptoms of rheumatoid arthritis: a study of serial measurements in blood donors. *Arthritis Rheum*. (2004) 50:380–6. doi: 10.1002/art.20018
64. Wigerblad G, Bas DB, Fernades-Cerqueira C, Krishnamurthy A, Nandakumar KS, Rogoz K, et al. Autoantibodies to citrullinated proteins induce joint pain independent of inflammation via a chemokine-dependent mechanism. *Ann Rheum Dis*. (2016) 75:730–8. doi: 10.1136/annrheumdis-2015-208094
65. van der Woude D, Rantapaa-Dahlqvist S, Ioan-Facsinay A, Onnekink C, Schwarte CM, Verpoort KN, et al. Epitope spreading of the anti-citrullinated protein antibody response occurs before disease onset and is associated with the disease course of early arthritis. *Ann Rheum Dis*. (2010) 69:1554–61. doi: 10.1136/ard.2009.124537
66. Lu MC, Lai NS, Yu HC, Huang HB, Hsieh SC, Yu CL. Anti-citrullinated protein antibodies bind surface-expressed citrullinated Grp78 on monocyte/macrophages and stimulate tumor necrosis factor alpha production. *Arthritis Rheum*. (2010) 62:1213–23. doi: 10.1002/art.27386
67. Harre U, Lang SC, Pfeifle R, Rombouts Y, Fruhbeisser S, Amara K, et al. Glycosylation of immunoglobulin G determines osteoclast differentiation and bone loss. *Nat Commun*. (2015) 6:6651. doi: 10.1038/ncomms7651
68. Krishnamurthy A, Joshua V, Haj Hensvold A, Jin T, Sun M, Vivar N, et al. Identification of a novel chemokine-dependent molecular mechanism underlying rheumatoid arthritis-associated autoantibody-mediated bone loss. *Ann Rheum Dis*. (2016) 75:721–9. doi: 10.1136/annrheumdis-2015-208093
69. Rombouts Y, Ewing E, van de Stadt LA, Selman MH, Trouw LA, Deelder AM, et al. Anti-citrullinated protein antibodies acquire a pro-inflammatory Fc glycosylation phenotype prior to the onset of rheumatoid arthritis. *Ann Rheum Dis*. (2015) 74:234–41. doi: 10.1136/annrheumdis-2013-203565
70. Pfeifle R, Rothe T, Ipseiz N, Scherer HU, Culemann S, Harre U, et al. Regulation of autoantibody activity by the IL-23-TH17 axis determines the onset of autoimmune disease. *Nat Immunol*. (2017) 18:104–13. doi: 10.1038/ni.3579
71. Wunderlich C, Oliviera I, Figueiredo CP, Rech J, Schett G. Effects of DMARDs on citrullinated peptide autoantibody levels in RA patients-A longitudinal analysis. *Semin Arthritis Rheum*. (2017) 46:709–14. doi: 10.1016/j.semarthrit.2016.09.011
72. Alenius GM, Berglin E, Rantapaa Dahlqvist S. Antibodies against cyclic citrullinated peptide (CCP) in psoriatic patients with or without joint inflammation. *Ann Rheum Dis*. (2006) 65:398–400. doi: 10.1136/ard.2005.040998
73. Perez-Alamino R, Garcia-Valladares I, Cuchacovich R, Iglesias-Gamarra A, Espinoza LR. Are anti-CCP antibodies in psoriatic arthritis patients a biomarker of erosive disease? *Rheumatol Int*. (2014) 34:1211–6. doi: 10.1007/s00296-014-2956-8
74. Rich E, Moreland LW, Alarcon GS. Paucity of radiographic progression in rheumatoid arthritis treated with methotrexate as the first disease modifying antirheumatic drug. *J Rheumatol*. (1999) 26:259–61.
75. Molenaar ET, Voskuyl AE, Dinant HJ, Bezemer PD, Boers M, Dijkmans BA. Progression of radiologic damage in patients with rheumatoid arthritis in clinical remission. *Arthritis Rheum*. (2004) 50:36–42. doi: 10.1002/art.11481
76. Brown AK, Conaghan PG, Karim Z, Quinn MA, Ikeda K, Peterfy CG, et al. An explanation for the apparent dissociation between clinical remission and continued structural deterioration in rheumatoid arthritis. *Arthritis Rheum*. (2008) 58:2958–67. doi: 10.1002/art.23945
77. Keffer J, Probert L, Cazlaris H, Georgopoulos S, Kaslaris E, Kioussis D, et al. Transgenic mice expressing human tumour necrosis factor: a predictive genetic model of arthritis. *EMBO J*. (1991) 10:4025–31.
78. Tunyogi-Csapo M, Kis-Toth K, Radacs M, Farkas B, Jacobs JJ, Finnegan A, et al. Cytokine-controlled RANKL and osteoprotegerin expression by human and mouse synovial fibroblasts: fibroblast-mediated pathologic bone resorption. *Arthritis Rheum*. (2008) 58:2397–408. doi: 10.1002/art.23653
79. Hashizume M, Hayakawa N, Mihara M. IL-6 trans-signalling directly induces RANKL on fibroblast-like synovial cells and is involved in RANKL induction by TNF-alpha and IL-17. *Rheumatology*. (2008) 47:1635–40. doi: 10.1093/rheumatology/ken363
80. Lam J, Takeshita S, Barker JE, Kanagawa O, Ross FP, Teitelbaum SL. TNF-alpha induces osteoclastogenesis by direct stimulation of macrophages exposed to permissive levels of RANK ligand. *J Clin Invest*. (2000) 106:1481–8. doi: 10.1172/JCI11176
81. Yokota K, Sato K, Miyazaki T, Kitaura H, Kayama H, Miyoshi F, et al. Combination of tumor necrosis factor alpha and interleukin-6 induces mouse osteoclast-like cells with bone resorption activity both in vitro and in vivo. *Arthritis Rheumatol*. (2014) 66:121–9. doi: 10.1002/art.38218
82. Yao Z, Li P, Zhang Q, Schwarz EM, Keng P, Arbini A, et al. Tumor necrosis factor-alpha increases circulating osteoclast precursor numbers by promoting their proliferation and differentiation in the bone marrow through up-regulation of c-Fms expression. *J Biol Chem*. (2006) 281:11846–55. doi: 10.1074/jbc.M512624200
83. Wei S, Kitaura H, Zhou P, Ross FP, Teitelbaum SL. IL-1 mediates TNF-induced osteoclastogenesis. *J Clin Invest*. (2005) 115:282–90. doi: 10.1172/JCI23394
84. Nishimoto N, Hashimoto J, Miyasaka N, Yamamoto K, Kawai S, Takeuchi T, et al. Study of active controlled monotherapy used for rheumatoid arthritis, an IL-6 inhibitor (SAMURAI): evidence of clinical and radiographic benefit from an x ray reader-blinded randomised controlled trial of tocilizumab. *Ann Rheum Dis*. (2007) 66:1162–7. doi: 10.1136/ard.2006.068064
85. Jiang Y, Genant HK, Watt I, Cobby M, Bresnihan B, Aitchison R, et al. A multicenter, double-blind, dose-ranging, randomized, placebo-controlled study of recombinant human interleukin-1 receptor antagonist in patients with rheumatoid arthritis: radiologic progression and correlation of Genant and Larsen scores. *Arthritis Rheum*. (2000) 43:1001–9. doi: 10.1002/1529-0131(200005)43:5<1001::AID-ANR7>3.0.CO;2-P
86. Findlay DM, Atkins GJ. TWEAK and TNF regulation of sclerostin: a novel pathway for the regulation of bone remodelling. *Adv Exp Med Biol*. (2011) 691:337–48doi: 10.1007/978-1-4419-6612-4_34
87. Holmen SL, Giambernardi TA, Zylstra CR, Buckner-Berghuis BD, Resau JH, Hess JF, et al. Decreased BMD and limb deformities in mice carrying mutations in both Lrp5 and Lrp6. *J Bone Miner Res*. (2004) 19:2033–40. doi: 10.1359/JBMR.040907
88. Hu H, Hilton MJ, Tu X, Yu K, Ornitz DM, Long F. Sequential roles of Hedgehog and Wnt signaling in osteoblast development. *Development*. (2005) 132:49–60. doi: 10.1242/dev.01564
89. Finzel S, Englbrecht M, Engelke K, Stach C, Schett G. A comparative study of periarticular bone lesions in rheumatoid arthritis and psoriatic arthritis. *Ann Rheum Dis*. (2011) 70:122–7. doi: 10.1136/ard.2010.132423

90. Finzel S, Rech J, Schmidt S, Engelke K, Englbrecht M, Schett G. Interleukin-6 receptor blockade induces limited repair of bone erosions in rheumatoid arthritis: a micro CT study. *Ann Rheum Dis*. (2013) 72:396–400. doi: 10.1136/annrheumdis-2011-201075
91. Matzelle MM, Gallant MA, Condon KW, Walsh NC, Manning CA, Stein GS, et al. Resolution of inflammation induces osteoblast function and regulates the Wnt signaling pathway. *Arthritis Rheum*. (2012) 64:1540–50. doi: 10.1002/art.33504
92. Solomon DH, Kay J, Duryea J, Lu B, Bolster MB, Yood RA, et al. Effects of teriparatide on joint erosions in rheumatoid arthritis: a randomized controlled trial. *Arthritis Rheumatol*. (2017) 69:1741–50. doi: 10.1002/art.40156
93. Redlich K, Gortz B, Hayer S, Zwerina J, Doerr N, Kostenuik P, et al. Repair of local bone erosions and reversal of systemic bone loss upon therapy with anti-tumor necrosis factor in combination with osteoprotegerin or parathyroid hormone in tumor necrosis factor-mediated arthritis. *Am J Pathol*. (2004) 164:543–55. doi: 10.1016/S0002-9440(10)63144-6
94. Ai M, Holmen SL, Van Hul W, Williams BO, Warman ML. Reduced affinity to and inhibition by DKK1 form a common mechanism by which high bone mass-associated missense mutations in LRP5 affect canonical Wnt signaling. *Mol Cell Biol*. (2005) 25:4946–55. doi: 10.1128/MCB.25.12.4946-4955.2005
95. Bourhis E, Wang W, Tam C, Hwang J, Zhang Y, Spittler D, et al. Wnt antagonists bind through a short peptide to the first beta-propeller domain of LRP5/6. *Structure*. (2011) 19:1433–42. doi: 10.1016/j.str.2011.07.005
96. Binnerts ME, Kim KA, Bright JM, Patel SM, Tran K, Zhou M, et al. R-Spondin1 regulates Wnt signaling by inhibiting internalization of LRP6. *Proc Natl Acad Sci USA*. (2007) 104:14700–5. doi: 10.1073/pnas.0702305104
97. Kedlaya R, Veera S, Horan DJ, Moss RE, Ayturk UM, Jacobsen CM, et al. Sclerostin inhibition reverses skeletal fragility in an Lrp5-deficient mouse model of OPPG syndrome. *Sci Transl Med*. (2013) 5:211ra158. doi: 10.1126/scitranslmed.3006627
98. Ma Y, Zhang X, Wang M, Xia Q, Yang J, Wu M, et al. The serum level of Dickkopf-1 in patients with rheumatoid arthritis: a systematic review and meta-analysis. *Int Immunopharmacol*. (2018) 59:227–32. doi: 10.1016/j.intimp.2018.04.019
99. Diarra D, Stolina M, Polzer K, Zwerina J, Ominsky MS, Dwyer D, et al. Dickkopf-1 is a master regulator of joint remodeling. *Nat Med*. (2007) 13:156–63. doi: 10.1038/nm1538
100. Ominsky MS, Vlasseros F, Jolette J, Smith SY, Stouch B, Doellgast G, et al. Two doses of sclerostin antibody in cynomolgus monkeys increases bone formation, bone mineral density, and bone strength. *J Bone Miner Res*. (2010) 25:948–59. doi: 10.1002/jbmr.14
101. Cosman F, Crittenden DB, Adachi JD, Binkley N, Czerwinski E, Ferrari S, et al. Romosozumab Treatment in Postmenopausal Women with Osteoporosis. *N Engl J Med*. (2016) 375:1532–43. doi: 10.1056/NEJMoa1607948
102. Marenzana M, Vugler A, Moore A, Robinson M. Effect of sclerostin-neutralising antibody on periarticular and systemic bone in a murine model of rheumatoid arthritis: a microCT study. *Arthritis Res Ther*. (2013) 15:R125. doi: 10.1186/ar4305
103. Wehmeyer C, Frank S, Beckmann D, Bottcher M, Cromme C, Konig U, et al. Sclerostin inhibition promotes TNF-dependent inflammatory joint destruction. *Sci Transl Med*. (2016) 8:330ra35. doi: 10.1126/scitranslmed.aac4351
104. Chan CKF, Gulati GS, Sinha R, Tompkins JV, Lopez M, Carter AC, et al. Identification of the human skeletal stem cell. *Cell*. (2018) 175:43–56 e21. doi: 10.1016/j.cell.2018.07.029
105. Lee EJ, Lee EJ, Chung YH, Song DH, Hong S, Lee CK, et al. High level of interleukin-32 gamma in the joint of ankylosing spondylitis is associated with osteoblast differentiation. *Arthritis Res Ther*. (2015) 17:350. doi: 10.1186/s13075-015-0870-4
106. Appel H, Ruiz-Heiland G, Listing J, Zwerina J, Herrmann M, Mueller R, et al. Altered skeletal expression of sclerostin and its link to radiographic progression in ankylosing spondylitis. *Arthritis Rheum*. (2009) 60:3257–62. doi: 10.1002/art.24888
107. Fassio A, Idolazzi L, Viapiana O, Benini C, Vantaggiato E, Bertoldo F, et al. In psoriatic arthritis Dkk-1 and PTH are lower than in rheumatoid arthritis and healthy controls. *Clin Rheumatol*. (2017) 36:2377–81. doi: 10.1007/s10067-017-3734-2
108. Shi J, Ying H, Du J, Shen B. Serum sclerostin levels in patients with ankylosing spondylitis and rheumatoid arthritis: a systematic review and meta-analysis. *Biomed Res Int*. (2017) 2017:9295313. doi: 10.1155/2017/9295313
109. Ikebuchi Y, Aoki S, Honma M, Hayashi M, Sugamori Y, Khan M, et al. Coupling of bone resorption and formation by RANKL reverse signalling. *Nature*. (2018) 561:195–200. doi: 10.1038/s41586-018-0482-7

Conflict of Interest Statement: The authors declare that the research was conducted in the absence of any commercial or financial relationships that could be construed as a potential conflict of interest.

frontiers in Immunology

ORIGINAL RESEARCH
published: 05 April 2019
doi: 10.3389/fimmu.2019.00713

Immune Modulation to Enhance Bone Healing—A New Concept to Induce Bone Using Prostacyclin to Locally Modulate Immunity

Sebastian Wendler[1,2†], *Claudia Schlundt*[1,2†], *Christian H. Bucher*[1,2], *Jan Birkigt*[3], *Christian J. Schipp*[1‡], *Hans-Dieter Volk*[2,4], *Georg N. Duda*[1,2,5] *and Katharina Schmidt-Bleek*[1,2*]

[1] Julius Wolff Institute and Center for Musculoskeletal Surgery, Charité–Universitätsmedizin Berlin, Berlin, Germany, [2] Berlin-Brandenburg Center for Regenerative Therapies, Charité–Universitätsmedizin Berlin, Berlin, Germany, [3] Department of Isotope Biogeochemistry, Helmholtz Centre for Environmental Research–UFZ, Leipzig, Germany, [4] Institute of Medical Immunology, Charité–Universitätsmedizin Berlin, Berlin, Germany, [5] Berlin Institute of Health Center for Regenerative Therapies, Berlin, Germany

OPEN ACCESS

Edited by:
Claudine Blin-Wakkach,
UMR7370 Laboratoire de Physio Médecine Moléculaire (LP2M), France

Reviewed by:
Ivan Martin,
Universität Basel, Switzerland
Monica Mattioli-Belmonte,
Polytechnical University of Marche, Italy
Melanie Haffner-Luntzer,
University of Ulm, Germany

***Correspondence:**
Katharina Schmidt-Bleek
katharina.schmidt-bleek@charite.de

[†]These authors shared first authorship

[‡]**Present Address:**
Christian J. Schipp,
Department of Isotope Biogeochemistry, Helmholtz Centre for Environmental Research–UFZ, Leipzig, Germany

Specialty section:
This article was submitted to Inflammation, a section of the journal Frontiers in Immunology

Received: 30 November 2018
Accepted: 15 March 2019
Published: 05 April 2019

Citation:
Wendler S, Schlundt C, Bucher CH, Birkigt J, Schipp CJ, Volk H-D, Duda GN and Schmidt-Bleek K (2019) Immune Modulation to Enhance Bone Healing—A New Concept to Induce Bone Using Prostacyclin to Locally Modulate Immunity. Front. Immunol. 10:713. doi: 10.3389/fimmu.2019.00713

Within an aging population, fracture incidences will rise and with the augmented risks of impaired healing the overall risk of delayed bone regeneration will substantially increase in elderly patients. Thus, new strategies to rescue fracture healing in the elderly are highly warranted. Modulating the initial inflammatory phase toward a reduced pro-inflammation launches new treatment options for delayed or impaired healing specifically in the elderly. Here, we evaluated the capacity of the prostacyclin analog Iloprost to modulate the inflammatory phase toward a pro-regenerative milieu using *in vitro* as well as *in vivo* model systems. *In vitro*, Iloprost administration led to a downregulation of potential unfavorable CD8+ cytotoxic T cells as well as their pro-inflammatory cytokine secretion profile. Furthermore, Iloprost increased the mineralization capacity of osteogenic induced mesenchymal stromal cells through both direct as well as indirect cues. In an *in vivo* approach, Iloprost, embedded in a biphasic fibrin scaffold, decreased the pro-inflammatory and simultaneously enhanced the anti-inflammatory phase thereby improving bone healing outcome. Overall, our presented data confirms a possible strategy to modulate the early inflammatory phase in aged individuals toward a physiological healing by a downregulation of an excessive pro-inflammation that otherwise would impair healing. Further confirmation in phase I/II trials, however, is needed to validate the concept in a broader clinical evaluation.

Keywords: bone healing, immune modulation, prostacyclin analog, T cell, macrophage, immune cell, Iloprost

INTRODUCTION

Bone is one of the few tissues in the human body capable of regenerative, scar-free healing. Thus, a bony injury can result in complete restoration of form and function, a restitutio ad integrum. However, the complex bone healing process consisting of sequential, partly overlapping phases is prone to failure (1–4). Even in today's medical routine 5–10% of fracture patients suffer from delayed healing or a resulting non-union (5–7). Therefore, impaired bone repair after injury is still a clinically relevant problem, which will even further increase in the overall aging population

(8). Thus, a better and deeper understanding of the underlying biological mechanisms under unimpaired healing conditions is necessary for the development of novel therapeutic treatment strategies to improve unsuccessful bone regeneration.

The tight interaction of the immune system and bone healing has been recognized in the emerging research field of osteoimmunology. Especially the early phase of healing, the inflammatory phase seems to be a promising target for immunomodulatory approaches to enhance bone healing (9, 10). The pro-inflammatory reaction following injury (11) is an essential trigger or initiator of the healing process. However, a pronounced or prolonged pro-inflammatory reaction (due to a lack or damped anti-inflammatory phase) will negatively impact the healing process (12–14). Recently, specific subsets of the immune system have been shown to negatively influence bone formation: Effector and effector memory CD8+ T cells are producers of TNFα (tumor necrosis factor alpha) and IFNγ (interferon gamma), highly pro-inflammatory cytokines which have been found to deter osteogenic differentiation (15). Therefore, downregulation of the negative influence of immune cell subsets could potentially enhance bone healing. Anti-inflammatory cytokines such as interleukin (IL) 4/IL-13 further the M2/Th2 response, thus promoting the immune response triggered by tissue injury under a regulatory phenotype rather than a M1/Th1 pro-inflammatory phenotype. A proof of concept study showed that applying IL-4/IL-13 during the initial bone healing phase could indeed enhance bone formation (16). However, a distinct initiation of an anti-inflammation has not been evaluated so far.

Within this study, a prostacyclin (PGI_2) analog was tested as a possible immune modulatory drug to enhance bone formation. PGI_2 is a small molecule derived from arachidonic acid by cyclooxygenase-2 (Cox-2) and prostacyclin synthase. Endogenous PGI_2 is already well-known playing an important role in cardiovascular diseases due its vasodilatory function (17, 18). In recent years, a potential role of PGI_2 as immune modulatory agent was detected by promoting an anti-inflammatory and immunosuppressive effect (19, 20). In particular, the PGI_2 receptor (IP) is present on platelets, medullary thymocytes, neutrophils, dendritic cells, eosinophils, T regulatory cells, and activated T cells (21, 22). Thus, PGI_2 has an impact on both, cells of the innate, and of the adaptive immunity. Due to the strong interconnectivity of the immune system and the skeletal system during bone regeneration, PGI2 could represent a potential and promising agent to further bone fracture healing. In the context of bone injuries, the PGI2 analog Iloprost was already successfully used to treat bone marrow edema and avascular necrosis (23, 24). However, the effect of PGI_2 on the process of bone formation/regeneration was not analyzed by any study so far. In the here presented study, we investigated the immune modulatory effect of PGI_2 in the context of bone regeneration. Since the half-life of endogenous PGI_2 is very short, the PGI_2 analog Iloprost was used. Iloprost is approved as treatment for pulmonary arterial hypertension (25) and peripheral arterial occlusive disease (26), respectively. Within the here presented study, we focused on the immune suppressive capacities of Iloprost, especially on CD8+ T cells and macrophages. Immune modulatory properties were confirmed and the postulated positive osteogenic effect was verified *in vitro*. In a final proof of concept *in vivo* trial, the positive impact of an application of Iloprost during the early bone healing phase was demonstrated in a mouse osteotomy model.

MATERIALS AND METHODS

Animal Model

Female C57BL/6N (Charles River Laboratories, Wilmington, MA, USA) were used for the analysis of the bone healing capacity *in vivo*. All mice were purchased at an age of 8 weeks and mice were housed in small groups in our animal facility. Animals were kept for at least 4 weeks in the non-SPF area of the animal facility (area in the animal facility without filtered air supply for the cages and without additional barrier) to allow a higher environmental pathogen exposure to challenge and to moderately activate the adaptive immune system of the animals. All mice experiments were carried out with the ethical permission according to the principles and policies established by the Animal Welfare Act, the National Institutes of Health Guide for Care and Use of Laboratory Animals, and the National Animal Welfare Guidelines. All animal experiments were approved by the local legal representative animal rights protection authorities (Landesamt for Gesundheit und Soziales Berlin: G0008/12; T0119/14; T0249/11). All results are reported according the ARRIVE guidelines.

Sample Harvesting for the *in vitro* Analysis With Immune Cells

For the immunomodulatory analysis *in vitro*, femora, and humeri were harvested from C57BL/6 N mice. To isolate the bone marrow, the epiphyses were cut off from the bones and the bone marrow was flashed out into RPMI 1640 media (Biochrom, Berlin, Germany). The bone marrow was pushed through a 40 μm cell strainer to get a single cell suspension. Residing erythrocytes were lysed for 4 min at room temperature (RT) in ACK lysing buffer (Gibco Life Technologies GmbH, Darmstadt, Germany). After centrifugation, cells were resuspended in 10 ml RPMI 1640 media and counted.

Isolation of CD8+ T Cells

CD8+ T cells were isolated from bones harvested from C57BL/6N mice. The isolation was performed via the *CD8 S-pluriBeads anti-ms* kit (pluriSelect Life Sciences, Leipzig, Germany). The isolation was carried out following the manufacturer's instructions. Briefly, complete bone marrow cells were resuspended in a 1:2 mixture of the isolation and wash buffer and 40 μl S-pluriBeads were added per 1 x 10^6 target cells and the mixture was incubated for 30 min at RT while continuous slowly shaking (horizontal roller mixer). Cell mixture was washed trough a S-pluriStrainer and target cells remained on the S-pluriStrainer. To detach the CD8+ T cells from the S-pluriBeads, detachment activation buffer D was added to the cells. Detached isolated cells were collected in a new tube, washed, and counted.

The purity of the isolated CD8+ T cells was confirmed by flow cytometry. The following antibodies were used: Life/Dead,

α-CD3 PerCP, α-CD4 AF700, and α-CD8 eF450. The incubation with the antibodies was done on ice for 20 min. After the staining, cells were washed, fixed, and analyzed with a flow cytometer LSR II (Becton Dickinson Bioscience, Heidelberg, Germany).

Study Design for the *in vitro* Analysis of the Osteogenic and Osteoimmunological Effect of Iloprost

The objective of this study was to investigate the potential of the prostacyclin analoque Iloprost to improve bone healing. For this analysis, the osteogenic and osteoimmunological effect of Iloprost was first evaluated *in vitro*. Subsequently, Iloprost was inserted into a fibrin clot in order to confirm the pro-osteogenic potential of Iloprost in an *in vivo* proof of concept approach in a mouse osteotomy model. For the *in vitro* analysis, Iloprost was directly added to the osteogenic differentiation culture of bone marrow mesenchymal stromal cells (BM MSCs) isolated from the femur of C57BL/6N mice (**Figure 1**, left). To investigate an indirect effect of Iloprost on the mineralization capacity of osteogenic induced BM MSCs, all bone marrow cells or isolated CD8+ T cells from the bone marrow were stimulated with α-CD3/α-CD28 and the obtained conditioned media were added to the osteogenic differentiation culture of BM MSCs (**Figure 1**, right). The osteogenic differentiation was quantified based on mineralization by Alizarin Red staining.

Cell Stimulation for the Production of Conditioned Media

Bone marrow and isolated CD8+ T cells were stimulated by an α-CD3/α-CD28 stimulation for 2 days in 96 well-plates. The stimulation was performed in RPMI 1640 media supplemented with 10% fetal bovine serum (FBS), 1% penicillin/streptomycin (P/S), 50 μM β-mercaptoethanol, and 10 ng/ml IL-2. In the respective experimental setup, either PBS or 300 nM or 3 μM Iloprost were added to the culture. 5 x 10^5 cells in 225 μl were plated per well of a 96 well-plate. After the two stimulations, the supernatant was harvested (conditioned media) and stored at −80C.

Isolation and Polarization of Macrophages

1 x 10^6 isolated bone marrow cells were plated per well into a 96 well-plate and incubated for 3 days in RPMI complete media: RPMI 1640 supplemented with 50 ng/ml macrophage colony-stimulating factor (M-CSF), 1% P/S, 10% FBS, and 50 μM β-mercaptoethanol. Subsequently, RPMI complete media was replaced by the respective polarization media and cells were polarized for additional 3 days. For MΦ: RPMI complete media with PBS; M1: RPMI complete media with 20 ng/ml IFNγ and M2: 20 ng/ml IL-4/IL-13. The produced conditioned media was harvested and stored at −80°C. Macrophage monolayers were washed twice with PBS and fixed with 4% PFA/PBS for 10 min. Storage was done in PBS at 4°C for subsequent confirmation of polarization via immunofluorescence.

Immunofluorescence Staining of Polarized Macrophage Subsets

The immunofluorescence staining of polarized macrophages were realized on fixed cellular macrophage monolayers. Cells were shortly washed with PBS, permeabilized in 100 μl PBS supplemented with 0.1% Tween for 30 min and subsequently blocked for 30 min with PBS supplemented with 5% FBS. The following antibodies were used for the staining: α-CD68 FITC, α-CD206 PE, and α-CD80 AF647. Antibodies were incubated for 1 h in the dark at RT. Cells were washed with PBS and cell nuclei were stained with DAPI for 10 min in the dark at RT. Cell monolayers were washed twice with PBS and wells were kept at 4○C in the dark until imaging. Imaging was performed with a standard fluorescence microscope (Axio Observer, Carl Zeiss).

Investigation of the Immunomodulatory Effect of Iloprost

To investigate the immunomodulatory effect of Iloprost on immune cells, ELISA were performed analyzing the secretion of IFNγ, TNFα, and IL-10 as indicated. Frozen conditioned media were thawed and analyzed with respective ELISA kits following the manufacturer's protocol. ELISA was performed with a Mouse IFNγ ELISA Ready-SET-Go!®, Mouse TNFα ELISA Ready-SET-Go!®, and Mouse IL-10 ELISA Ready-SET-Go!® from eBioscience (Affymetrix, Santa Clara, CA USA). The samples were incubated at 4°C overnight. Final staining reactions were stopped with 1 M H_3PO_4 and absorbance values were acquired at 450 nm with a reference wavelength of 570 nm with Tecan Infinite M200 PRO (Tecan, Männedorf, Switzerland) and analyzed with i-control 1.9 software (Tecan, Männedorf, Switzerland).

Isolation and Cultivation of Mesenchymal Stromal Cells

At least 3 x 10^7 isolated bone marrow cells were cultured in expansion media: low glucose DMEM media supplemented with 10% FBS, 1% P/S, and 1% glutamax. Media exchange was performed twice a week to remove non-adherent cells until cultures were confluent. To detach the MSC monolayers, cells were washed once with PBS. TrypLE was added to the monolayer, incubated for 5 min at 37°C. The cell suspension was washed, centrifuged and the passaged cells were plated with increasing surface area.

Osteogenic Differentiation of MSCs and Quantification by Alizarin Red Staining

1.5 x 10^4 MSCs were seeded per well into a 96 well-plate. Cells were cultured in expansion media for 2 days. Subsequently, osteoinductive media was applied to the cells: low glucose DMEM media supplemented with 10% FBS, 100 nM dexamethasone, 10 mM β-glycerol phosphate, 50 μM L-ascorbate-2-phosphate, 1% P/S, and 1% glutamax. Osteogenic differentiation was stopped after 14 days including a media exchange every 3–4 days. When conditioned media of stimulated bone marrow or CD8+ T cells was supplemented, double concentrated osteoinductive media was mixed 1:2 with the respective conditioned media.

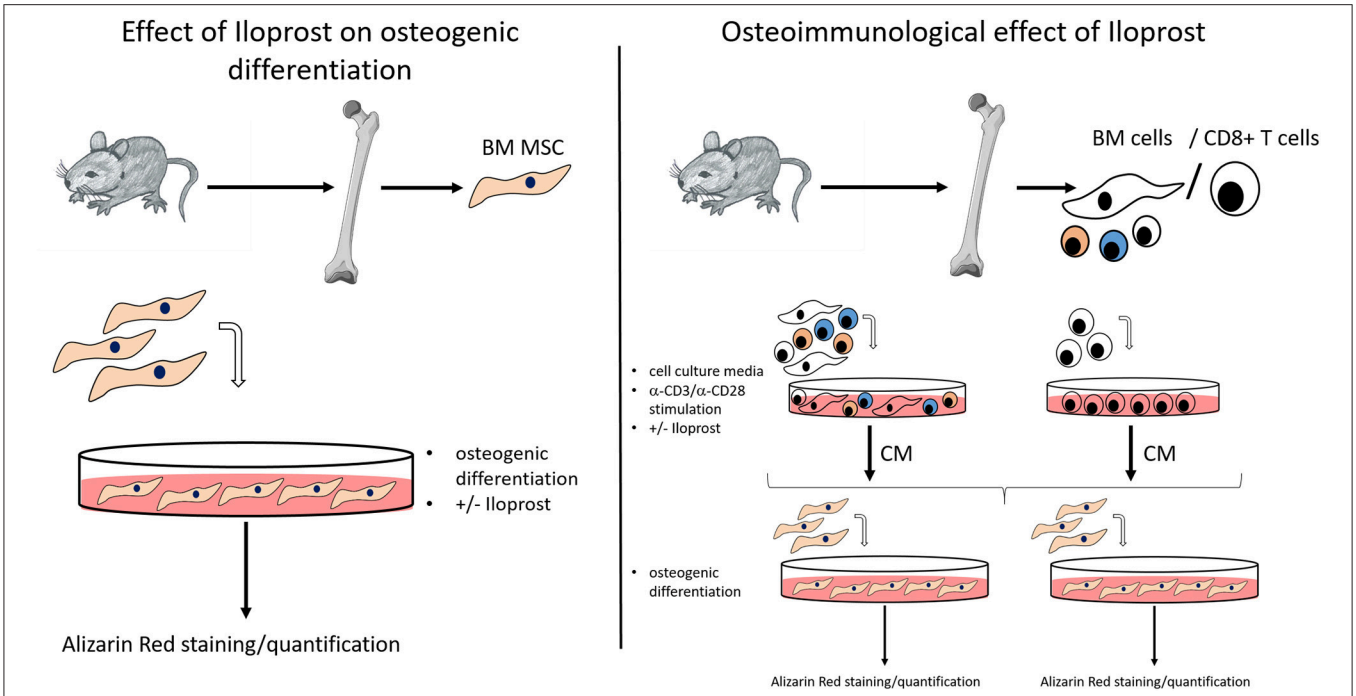

FIGURE 1 | Methodological scheme for the *in vitro* analysis of the osteogenic effect and osteoimmunological effect of Iloprost. BM MSC, bone marrow mesenchymal stromal cells; BM cells ,bone marrow cells; CM, conditioned media.

Alizarin Red staining was applied to quantify the osteogenic differentiation of the cultured MSCs. After a 14 days culture in osteoinductive media, well-plates were washed twice with PBS. Cell layers were fixed for 10 min at RT in 50 µl 4% paraformaldehyde/PBS (PFA/PBS). Cell nuclei were stained for DAPI for 10 min in the dark at RT. Cells were washed in ddH_2O and incubated with 0.5% Alizarin Red for 10 min at RT. Cells were washed five times with ddH_2O and cell layers were dried before imaging. For the quantification, Alizarin Red was detached with 10% cetylpyridinium chloride for 30 min at RT and optical density was measured and quantified with the plate reader Infinite M200 PRO (Tecan, Männedorf, Switzerland).

Chondrogenic Differentiation of MSCs and Quantification by Histomorphometry

3 x 10^5 MSCs were transferred into a 15 ml tube for the chondrogenic differentiation. Cells were centrifuged and chondrogenic induction media was carefully added to the cells without resuspension: high glucose DMEM media supplemented with 100 nM dexamethasone, 50 µg/ml L-ascorbate-2-phosphate, 350 µM L-proline, 2 mM sodium pyruvate, 6.25 µg/ml Insulin-transferrin-sodium selenite media supplement, 1.25 mg/ml bovine serum albumin, 5.35 µg/ml linoleic acid, 10 ng/ml TGF-β1, 10 ng/ml BMP-2, 1% P/S, and 1% glutamax. Pellets were cultured for 21 days under hypoxic conditions. Chondrogenic inductive media was changed twice a week.

For quantification, chondrogenic differentiated cell pellets were paraffin embedded, cut and stained with Alcian Blue (staining of the proteoglycans). Therefore, cell pellets were fixed for 2 h in 4% PFA/PBS, washed twice in PBS and dehydrated in an increasing alcohol series: 30 s in 70% EtOH, 20 min in 80% EtOH, 20 min 96% EtOH and twice 20 min in 100% EtOH. Cell pellets were incubated for 15 min in Xylol and subsequently paraffin embedded. Four micrometer thick sections were cut from three different areas of each pellet. Deparaffinized sections (incubation of the sections twice in Xylol for 10 min each and in a descending alcohol series) were washed in ddH_2O for 2 min, equilibrated in 3% acetic acid for 3 min, stained in 1% Alcian Blue for 45 min, washed in 3% acetic acid, washed in ddH_2O, and stained for cell nuclei in Nuclear Fast Red for 2 min. Pellets were shortly washed in ddH_2O and 70% EtOH. After an ascending alcohol series, pellets were incubated twice in Xylol, 10 min each, and embedded. Acquired images were quantified based on the blue values of bright field images.

Investigation of the Cellular Metabolic Activity by Prestoblue

Using the PrestoBlue Cell Viability Reagent (Thermo Fisher Scientific, Waltham, MA, USA), the metabolic activity of the stimulated cells was investigated after manufacturer's protocol. The reagent was diluted in RPMI complete media (for bone marrow cells) or low glucose DMEM (for MSCs), respectively, and applied to the cultured cells. After a 1 h incubation, the supernatant was collected and fluorescence top reading was performed at 560 nm excitation and 590 nm emission with the plate reader. For background correction, fluorescence values of

no-cell control wells, which contained only reagent solution were averaged and subtracted from values of experimental wells.

Setting of an Osteotomy for the *in vivo* Analysis

The pro-regenerative potential of Iloprost was evaluated in a mouse osteotomy model. Therefore, mice were anesthetised by inhalation of Isoflurane. Before surgery, the animals received subcutaneous injection of the analgesic Buprenorphine (0.03 mg/kg s.c.) and of the antibiotic Clindamycin (0.02 ml s.c.). The operation area of the left femur was shaved and disinfected. The skin was opened by a longitudinal cut from the knee to the hip. The femur was bluntly exposed and stabilized by an external fixator (MouseExFix, RISystem AG, Davos, Switzerland). An osteotomy of 0.7 mm was introduced between the middle pins using a Gigli wire saw (RISystem AG, Davos, Switzerland). A biphasic fibrin clot (loaded with either 3 μM Iloprost or PBS) (Tissucol-kit Immuno, Baxter) was inserted into the osteotomy gap. The skin was closed and sutured. Mice were brought back to the cage and observed until they were fully mobile again. As post-operative analgesia, Tramadol hydrochloride (0.1 mg/ml) was added to the drinking water for 3 days.

Micro-Computed Tomography of Osteotomized Mouse Bones

To evaluate the healing outcome after Iloprost administration, fractured femora were harvested 21 days post-osteotomy and analyzed by μCT. Therefore, mice were euthanized by administering ketamine and xylazine (i.p., ketamine: 120 mg/kg, xylazine: 16 mg/kg) and cervical dislocation in deep anesthesia. After preparation of the femora, they were directly fixed in 4% PFA/PBS for 4 h at 4°C. Subsequently, the bones were dehydrated in an ascending sugar series: 10, 20, and 30%, for 24 h for each at 4°C. The bones were scanned in a μCT Viva 40 (SCANCO Medical AG, Brüttisellen, Switzerland). For the scan, the following parameters were used: 10.5 μm voxel size, 55keVp, and 145 uA. A gray value threshold was defined before analysis in order to be able to distinguish between mineralized and non-mineralized bone tissue (27). The global threshold for defining mineralized bone was set to 242, which corresponds to a mineralization of 369.9 mg hydroxyapatite (HA)/cm^2. The scanned volume of interest (VOI) included 190 slices around the middle of the fracture gap to the distal and proximal part of the femur, respectively. For the quantification of the μCT data, cortical bone was excluded from newly formed mineralized bone.

Histological and Immunohistological Analysis

For histological and immunohistological analysis, fractured bones were cryo embedded. Seven micrometer thick sections were cut and stained either for Movat's Pentachrome (overview staining) or the following cell types (immunofluorescence staining): CD4+ and CD8+ T cells, IFNγ-producing CD8+ T cells, osteoblasts, osteoclasts and differentially polarized macrophages.

The Movat pentachrome staining was done as follows: cryo-sections were thawed for 1 h at RT and fixed for 10 min in 4% PFA/PBS. Sections were washed twice in PBS/Tween-20 for 5 min. Subsequently, sections were incubated for 3 min in 3% acetic acid, for 30 min in 1% Alcian Blue/3% acetic acid, and differentiated for 5 min in 3% acetic acid. After washing in ddH_2O, sections were incubated for 1 h in ethyl alcohol, washed twice in tap water, shortly in ddH_2O and stained in iron hematoxylin (after Weigert) for 10 min. After washing with tap water, sections were incubated for 15 min in brilliant crocein-acid fuchsine. Tissue slides was shortly placed in 0.5% acidic acid, followed by a 20 min incubation in 5% phosphotungstic acid. After 1 min in 0.5% acetic acid, slides were incubated 3x à 5 min in 96% EtOH and stained with Saffron-du-Gatinais for 1 h. Subsequently, they were washed again 3x in 96% EtOH for 2 min each, 2x in Xylol for 10 min each and embedded.

Analysis of the immune cell subsets and osteoblasts, osteoclasts was done by immunofluorescence staining. All steps were performed at RT in a humidified chamber. Thawed cryo-sections were fixed for 20 min in 4% PFA/PBS/Tween-20 and washed twice with PBS/Tween-20. Sections were blocked in 1x TBS supplemented with 7% FBS and 0.05% Tween-20 for 1 h. Blocking buffer was decanted and the primary antibodies were applied to the respective section in the following combinations: (1) CD4+ and CD8+ T cells and osteoblasts: CD4 AF594, CD8 PE, osteocalcin; (2) IFNγ-producing CD8+ T cells: CD8 PE and IFNγ; and (3) differentially polarized macrophages: CD68 FITC, CD206 PE, and CD80 AF647. Tissue sections were washed in 1x TBS and, if necessary, incubated for 2 h with a secondary antibody: anti-rabbit AF647 for osteocalcin or anti-rat AF594 for IFNγ and for CD4. For the staining of osteoclasts, antigen retrieval was performed with ProteinaseK for 15 min on thawed cryo-sections. Sections were washed PBS/Tween-20 and fixed as described above. After washing and blocking, sections were stained for cathepsinK in 3.5% FBS, 0.025% Tween in tris-buffered saline (TBS) for 2 h. Sections were washed and stained for CD68 (FITC) and the secondary antibody for cathepsinK anti-rabbit AF647 in 3.5% FBS, 0.025% Tween in TBS for 2 h. Sections were washed, stained for cell nuclei with DAPI for 10 min and subsequently embedded. Sections were analyzed with a laser scanning microscope LSM 710 (Carl Zeiss AG, Oberkochen, Germany).

Statistics

The statistical evaluation of the presented data was done with the programs Graph Pad Prism and SPSS. Data were presented as dot plot graphs. Statistics were done by using the Mann-Whitney U test and data were statistically significant if $p \leq 0.05$. For comparison of more than two study groups the Bonferroni's *post-hoc* test was used.

RESULTS

Immunomodulatory Effects of Iloprost on Immune Cells

We first tested the immunomodulatory properties of Iloprost on murine immune and mesenchymal stromal cells (MSCs) *in vitro*.

Both, immune cells and MSCs are known to be essential for the early healing phase in bone regeneration.

In a first attempt, two different concentrations of Iloprost were tested on the whole bone marrow cellular composition: 300 nM and 3 μM. As readout, the secretion of the pro-inflammatory cytokines IFNγ and TNFα was analyzed. Both cytokines play an important role as signaling molecules in bone repair, especially in the early fracture healing phase. However, too high amounts of them negatively affect bone repair by diminishing the formation of mineralized matrix by MSCs (15). After a 2-day stimulation of the cells by the different concentrations of Iloprost, the concentration of secreted IFNγ and TNFα was significantly decreased in comparison to the control (PBS supplementation) (IFNγ: ∼130 to ∼55 ng/ml; TNFα: ∼65 to ∼40 pg/ml) (**Figures 2A,B**). Comparing the two different concentrations of Iloprost, the supplementation of the higher one (3 μM) led to an even more pronounced decrease of the secreted cytokines. As expected, non-activated cells showed almost no secretion of IFNγ and TNFα. The metabolic activity of the stimulated bone marrow cells was also downregulated by the supplementation of Iloprost in comparison to the control (**Figure 2C**).

In patients, we already showed that a too high amount of CD8+ T cells, one special subset of the adaptive immunity, negatively regulates successful bone repair (15). CD8+ T cells are one of the main producer of pro-inflammatory cytokines in the early bone repair phase. Therefore, as a next step, we evaluated the immunomodulatory effect of Iloprost on murine CD8+ T cells. CD8+ T cells were isolated via PluriBeads (pluriSelect) from bone marrow and spleen. The purity of the isolated cells was confirmed by flow cytometry after separation as well as after the duration of the *in vitro* stimulation and stayed above 80% (**Figure 3A**). Similar to the stimulation of the whole bone marrow cellular fraction, isolated CD8+ T cells showed a decreased secretion of IFNγ and TNFα under the presence of 3 μM Iloprost in comparison to the control (IFNγ: ∼410 to ∼250 ng/ml; TNFα: ∼275 to ∼180 pg/ml) (**Figures 3B,C**). The metabolic activity was again slightly downregulated by the Iloprost supplementation (**Figure S1**).

Besides cells of the adaptive immunity, also cellular compartments of the innate immune system play a key role in the early fracture healing phase. Macrophages are one of the first cells infiltrating the fracture area and are necessary for (a) the clearance of the cell debris as well as for (b) the recruitment of further cells important for the progression of the healing cascade due to their secreted cytokine profile (16, 28). We already demonstrated the importance of macrophages in bone regeneration using an *in vivo* mouse osteotomy model. After a chemically induced reduction of the macrophage cell population, a disturbed bone healing outcome was observed in comparison to the control group while an induction of the regulatory M2 macrophage phenotype (addition of IL-4/IL-13) lead to a significantly enhanced healing outcome (16). In the here presented study, we further tested whether the supplementation of Iloprost promotes simultaneously the downregulation of pro-inflammatory and the upregulation of anti-inflammatory cytokines by MΦ, M1, or M2 polarized macrophages, respectively (**Figure 4**). Regarding the secretion of TNFα, the supplementation of Iloprost led to a decreased secretion by M*Φ* as well as by pro-inflammatory M1 (∼50 to ∼20 pg/ml) (**Figure 4A**). Whereas, the secretion of the anti-inflammatory cytokine IL-10 was significantly upregulated in the M2 type, but unaffected in the MΦ and M1 macrophages (∼290 to ∼410 pg/ml) (**Figure 4B**). The polarization culture was confirmed by immune fluorescence staining of the stimulated and polarized cells (**Figure 4C**). MΦ macrophages were identified by the marker expression CD68 (green fluorescence signal). M1 were double positive for CD68 and CD80 (CD80: white fluorescence signal) and M2 double positive for CD68 and CD206 (CD206: red fluorescence signal). Cell nuclei were identified by DAPI (blue fluorescence signal).

Effects of Iloprost on the Osteogenic and Chondrogenic Differentiation Capacity of Mesenchymal Stromal Cells

MSCs are the precursor cells for cartilage producing chondrocytes and bone forming osteoblasts. During secondary bone healing, a cartilage template is first build. These chondrocytes further get hypertrophic, mineralize and are subsequently replaced by newly formed woven bone produced by osteoblasts. Thus, a cartilage template is indispensable for successful bone regeneration. Therefore, the osteogenic and chondrogenic differentiation capacity of MSCs was investigated under the influence of Iloprost. We tested again two different concentrations of Iloprost: 300 nM and 3 μM, respectively.

For the osteogenic differentiation, monolayers of MSCs cultured for 14 days in osteoinductive media were stained with Alizarin Red to reveal the calcification of the cells (**Figure 5**). The quantification of the Alizarin Red staining demonstrated that Iloprost had no negative effect on the osteogenic capacity of MSCs (**Figures 5A,B**). The metabolic activity as well as the cell number of the cultured MSCs were also unaffected by the presence of Iloprost in the osteoinductive media (**Figures 5C,D**).

After the demonstration that Iloprost is not affecting the mineralization capacity of MSCs, we evaluated the impact of Iloprost on their capacity to differentiate into the chondrogenic cell lineage. Representative images of Alcian Blue stained paraffin sections of cartilage pellets are presented in **Figure 6A**. The quantification of the Alcian Blue staining revealed no negative effect on the proteoglycan production of chondrogenically induced MSC pellets under the supplementation of Iloprost in comparison to the PBS control (**Figure 6B**).

Osteoimmunological Effect of Iloprost

In the first part of the study, we demonstrated that the supplementation of Iloprost promotes the functionality of immune cells toward both, a reduction of pro-inflammatory signals and an induction of anti-inflammatory ones. We further showed that Iloprost had no negative effect on the osteogenic as well as chondrogenic differentiation capacity of MSCs. Next, we wondered, whether the immune modulatory effect of Iloprost on immune cells is also influencing the osteogenic capacity of MSCs.

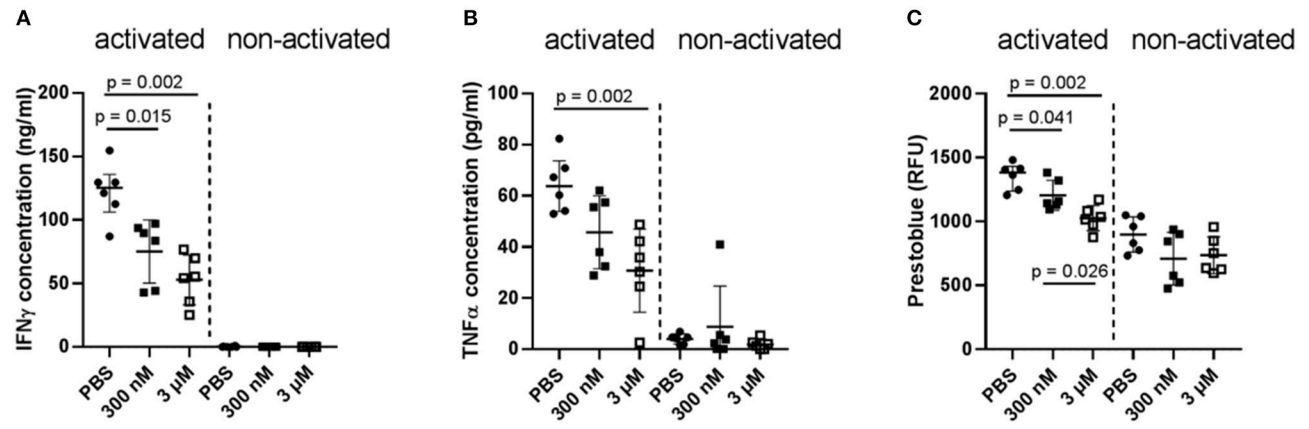

FIGURE 2 | Immunomodulatory effects of Iloprost on bone marrow cells. Bone marrow cells were stimulated for 2 days by α-CD3/α-CD28 in addition to either PBS or two different concentrations of Iloprost (300 nM or 3 µM, respectively). The following secreted cytokine concentrations were evaluated: IFNγ **(A)** and TNFα **(B)**. The metabolic activity of the stimulated bone marrow cells was measured via Prestoblue **(C)**. $n = 6$.

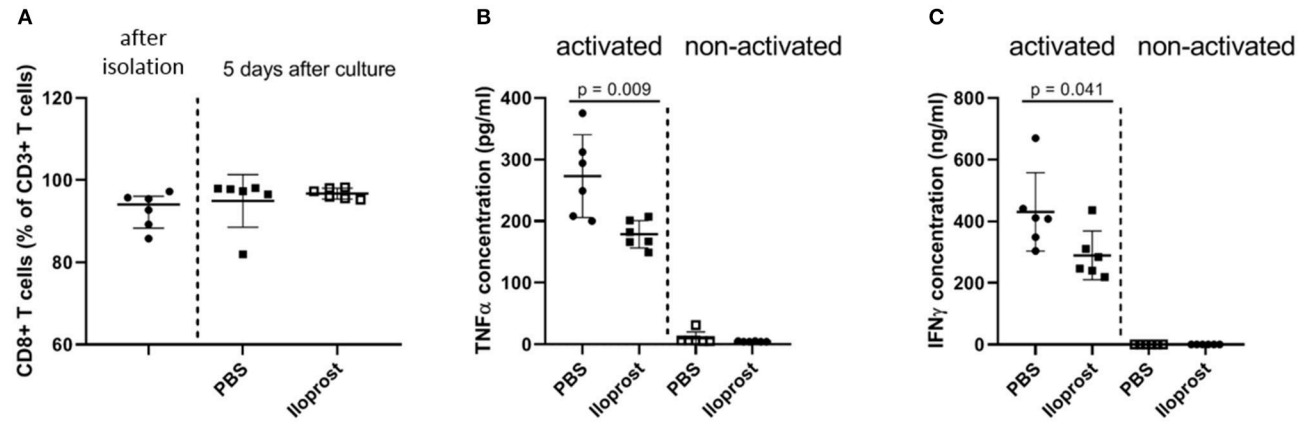

FIGURE 3 | Immunomodulatory effects of Iloprost on isolated CD8+ T cells. The purity of the isolated CD8+ T cells after bead-based separation as well as after *in vitro* stimulation was confirmed by flow cytometry **(A)**. CD8+ T cells were stimulated by α-CD3/α-CD28 in addition to either PBS or 3 µM Iloprost. The following secreted cytokine concentrations were evaluated: TNFα **(B)** and IFNγ **(C)**; $n = 6$.

Therefore, conditioned media (CM) of α-CD3/α-CD28 stimulated and Iloprost treated bone marrow cells and isolated CD8+ T cells, respectively, were added to the osteoinductive culture of MSCs. The CM of activated bone marrow cells significantly decreased the mineralization capacity of MSCs in comparison to the control (cultivated MSCs in osteoinductive media, OM) (**Figures 7A,B**). The supplementation of Iloprost during the α-CD3/α-CD28 stimulation of bone marrow cells was able to compensate partially the negative impact on mineralization induced by the activation (Iloprost, activated). CM of non-activated bone marrow cells had no effect on the mineralization capacity of MSCs (PBS, non-activated).

Repeating the analysis of the osteoimmunological effect of Iloprost on MSCs with isolated CD8+ T cells, similar results were obtained. CM of activated CD8+ T cells led to a significant decrease of mineralized matrix synthesis of cultured MSCs compared to the control (MSCs cultured in OM) (**Figures 8A,B**). Again, the supplementation of Iloprost to the stimulation of CD8+ T cells significantly improved the osteogenic matrix production by MSCs (**Figures 8A,B**; Iloprost, activated). However, this was still significantly lower in comparison to the OM control. CM of non-activated CD8+ T cells had no effect on the mineralization of MSCs (PBS, non-activated).

Summarizing the data from our *in vitro* study, we confirmed the immune modulatory effect of Iloprost on the secreted cytokine profile of immune cells. We also showed that Iloprost had no effect on the cartilage and bone forming capacity of MSCs. Thus, Iloprost is not negatively affecting the pro-regenerative functionality of MSCs. In a next step, we tested the capacity of Iloprost as a bone healing promoting agent in our mouse osteotomy model in a proof of concept *in vivo* approach.

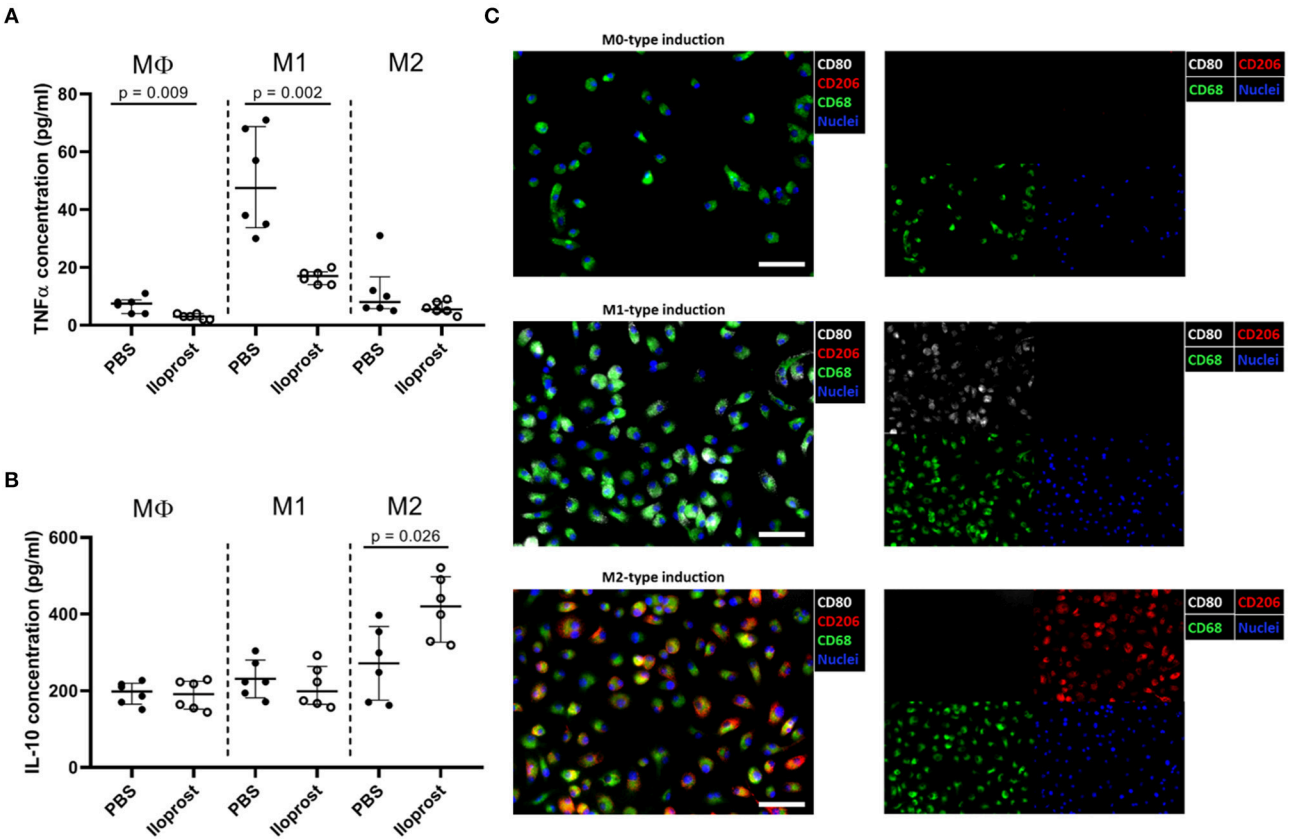

FIGURE 4 | Immunomodulatory effects of Iloprost on polarized bone marrow macrophages. Macrophages were polarized for 3 days toward the M1 or M2 type, supplemented with either PBS or 3 μM Iloprost. **(A,B)** The following secreted cytokine concentrations were evaluated: TNFα **(A)** and IL-10 **(B)** of M1-type induced and M2-type induced polarized macrophages, respectively. **(C)** Representative immune fluorescence images of unpolarised CD68+ MΦ macrophages (on top), CD68+CD80+ M1 macrophages (middle), and CD68+CD206+ M2 macrophages (bottom). Color code of the immune fluorescence images: CD68 = green, CD80 = white, CD206 = red, and cell nuclei = blue (DAPI). Scale bars: 100 μm; $n = 6$.

Iloprost–A Potent Agent to Promote Bone Fracture Healing *in vivo*?

In bone regeneration, a first pro-inflammatory phase is indispensable for the initiation of the healing cascade. Due to the anti-inflammatory effect of Iloprost via its effect on immune cell function shown *in vitro*, we chose an application strategy, where the applied Iloprost will be successively released from a biphasic fibrin scaffold, thus allowing the pro-inflammatory phase to proceed. Fibrous tissue is a component of the classical healing cascade in bone regeneration and thus represents an endogenous material, which is already present in the fracture gap. Furthermore, fibrin is biocompatible and biodegradable. Iloprost embedded in a fibrin clot was inserted during surgery in the osteotomy gap. Due to the biphasic structure of the fibrin scaffold, the included Iloprost would not be directly released in the fracture zone at the onset of the surgery but with a delay. This delay allows the initial pro-inflammatory phase to proceed and to initiate the healing cascade.

The healing outcome was evaluated 21 days post-surgery. The model was chosen to enable detection of healing enhancement–with a gap size of 0.7 mm the healing is not concluded after 21 days (control) (**Figure 9**, PBS). Regarding the Iloprost treated group, μCT analysis 21 days post-surgery showed an improved healing outcome of the mice receiving Iloprost in comparison to the control group (mice with fibrin scaffold, PBS supplementation) (**Figure 9**; Iloprost: mice with Iloprost supplementation; PBS: control group). The quantification of the μCT data confirmed the already visually seen improved healing by a significant increase of bone volume, total callus volume and the ratio of bone volume/total callus volume in the Iloprost treated animals with regard to the control (**Figures 9B–D**).

Next to the μCT evaluation, histological and immunohistological analyses were performed on cryosections of the fractured femora 3 days and 21 days post-osteotomy (**Figures 10**, **11**). Movat Pentachrome staining was performed to evaluate the relative amount of mineralized bone, cartilage, connective tissue and bone marrow (**Figure 10**). In **Figure 10A**, representative Movat Pentachrome pictures are presented to illustrate the tissue formation in and around the osteotomy gap at the respective time point. Three days post-surgery, the fibrin scaffold was still visible within the osteotomy gap in both groups, the control (PBS) and Iloprost treated animals

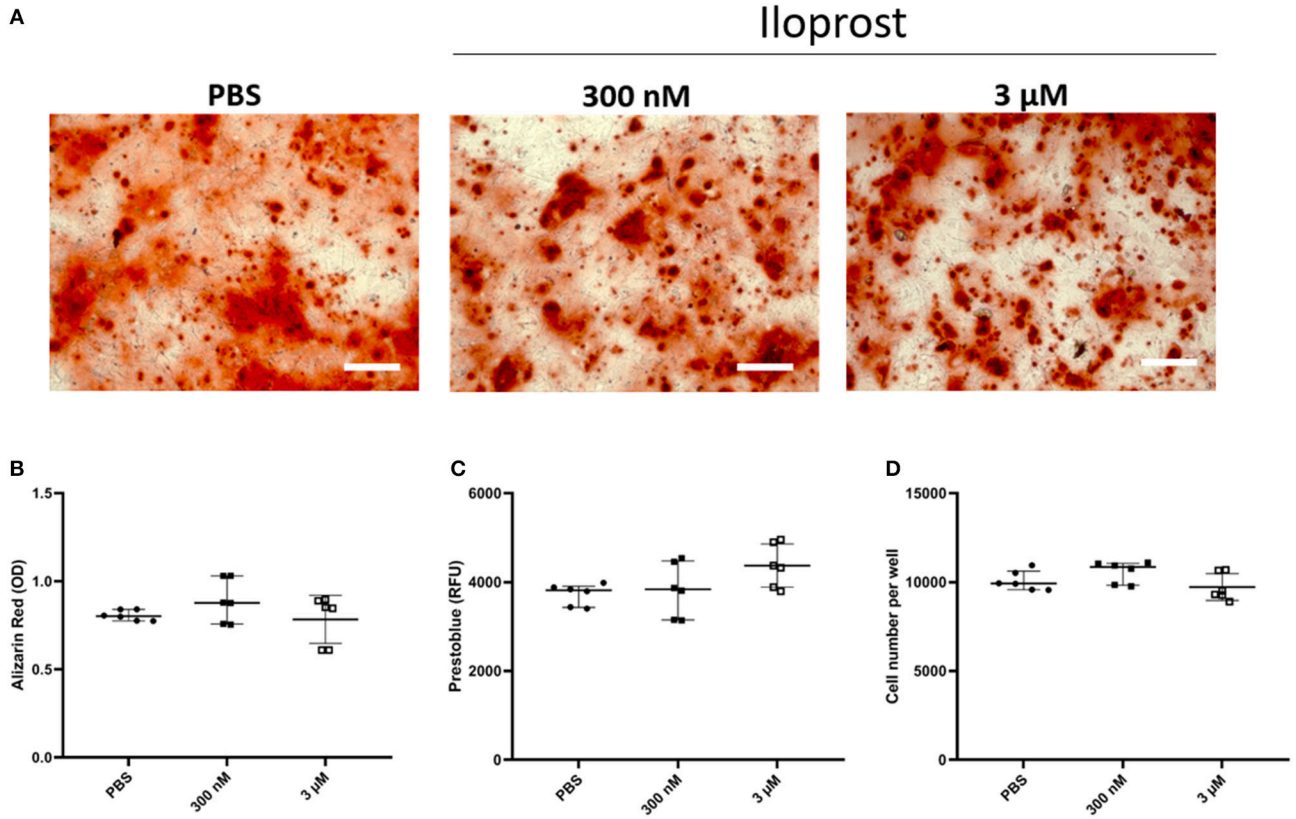

FIGURE 5 | Effect of Iloprost on mineralization capacity of osteogenically induced MSCs. Monolayers of MSCs were stained with Alizarin Red to visualize the formation of mineralized matrix. **(A,B)** Representative images of the Alizarin Red staining of cultured MSCs with osteoinductive media after 14 days of cultivation. Different concentrations of Iloprost were supplemented to the osteoinductive media (300 nM and 3 µM, respectively) **(A)**. Quantification of the Alizarin Red staining **(B)**. The metabolic activity of the cultured MSCs was measured by Prestoblue **(C)**. Determination of the cell number of the cultured MSCs under the different stimuli **(D)**. Scale bars: 200 µm; $n = 6$.

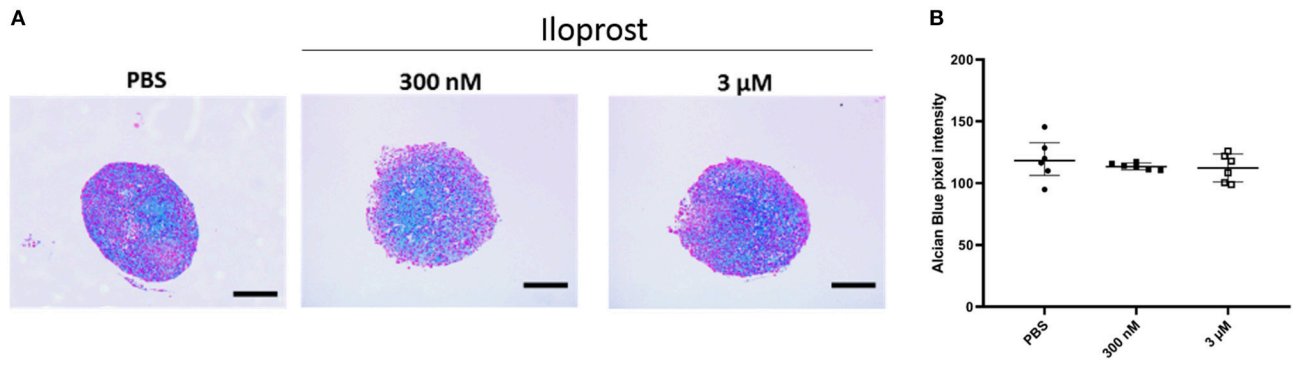

FIGURE 6 | Effect of Iloprost on cartilage formation capacity of chondrogenically induced MSCs. **(A)** Alcian Blue stained paraffin sections of cartilage pellets after 21 days of incubation in chondroinductive media, supplemented with different concentration of Iloprost (300 nM and 3 µM, respectively) or PBS as control. **(B)** Quantification of the Alcian Blue staining. Scale bars: 200 µm; $n = 6$.

(Iloprost), indicated by a red color after Movat's Pentachrome staining (**Figure 10A**, left). After 21 days, no fibrin scaffold was detected anymore in or around the osteotomy area (**Figure 10A**, right). Histomorphometrical analysis of the tissue distribution revealed a significantly higher amount of mineralized bone and cartilage tissue 21 days post-surgery in the Iloprost treated group in comparison to the control animals (**Figure 10B**). Three days post-osteotomy, both groups showed almost no proportion of mineralized bone or cartilage tissue. Both groups showed just slightly differences in the amount of connective tissue at both investigated time points (**Figure 10D**, connective tissue). Regarding the area of bone marrow, the

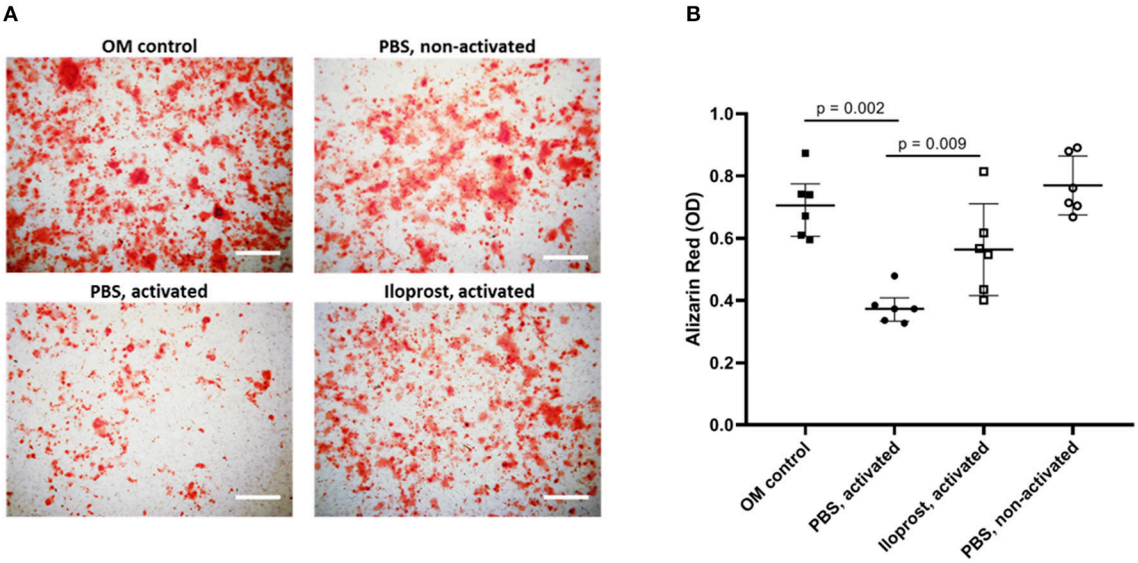

FIGURE 7 | Osteoimmunological effect of Iloprost treated bone marrow cells. α-CD3/α-CD28 activated bone marrow cells were cultured either with Iloprost or PBS as control. Obtained conditioned media was added to an osteogenic differentiation culture of MSCs and the secretion of mineralized matrix was measured by Alizarin Red staining. **(A)** Representative images of the Alizarin Red staining of the different culture conditions. **(B)** Quantification of the Alizarin Red signal. OM, osteoinductive media. Scale bars: 200 μm; $n = 6$.

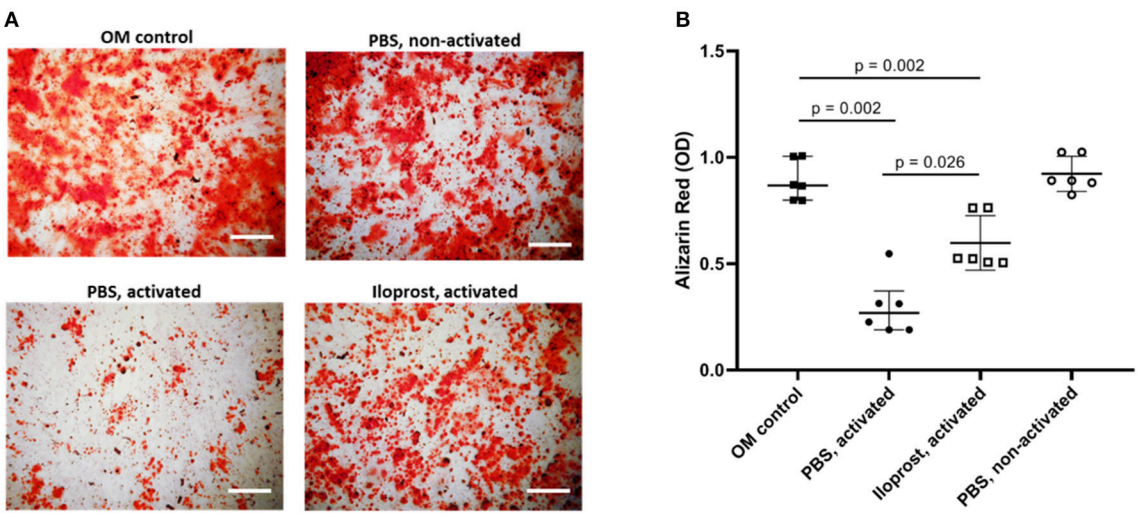

FIGURE 8 | Osteoimmunological effect of Iloprost treated isolated CD8+ T cells. Isolated α-CD3/α-CD28 activate CD8+ T cells were cultured either with Iloprost or PBS as control. Obtained conditioned media was added to an osteogenic differentiation culture of MSCs and the secretion of mineralized matrix was measured by Alizarin Red staining. **(A)** Representative images of the Alizarin Red staining of the different culture conditions. **(B)** Quantification of the Alizarin Red signal. OM, osteoinductive media. Scale bars: 200 μm; $n = 6$.

Iloprost treated mice displayed a slightly higher amount 21 days after surgery.

To better understand the impact and direct influence of Iloprost during the early phase of bone healing, immunohistochemical (IHC) analyses were performed on bone sections of mice sacrificed 3 days post-osteotomy. At this time point, Iloprost conducted its immune modulatory effect as shown below (**Figure 9**). In addition, around 3 days post-osteotomy, the starting shift of the pro-inflammatory into the anti-inflammatory phase is observed in our chosen mouse osteotomy model system.

First, the distribution of CD4+ and CD8+ T cells (identified by CD4 and CD8, respectively), as well as osteoblasts (identified by osteocalcin, OCN) was investigated in a defined region of interest (ROI) in and around the fracture zone (**Figures 11A,B**). Quantification of the analyzed bone sections revealed a

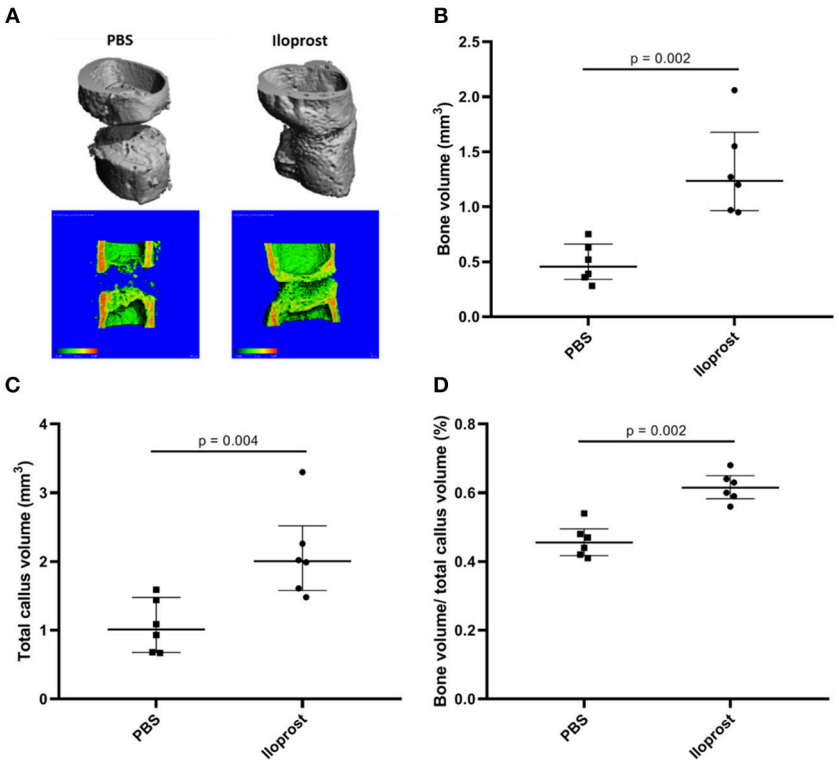

FIGURE 9 | Proof of concept approach of Iloprost to improve bone fracture healing *in vivo*. μCT analysis of the healing outcome 21 days post-osteotomy in a mouse osteotomy model. **(A)** Representative μCT images of the Iloprost treated (right) and control (left, PBS) group. The upper row shows the 3D reconstruction of the μCT measurement. In the lower row, 3D reconstruction was cut in the middle to evaluate the healing progression. The color code indicates the mineralization state, increasing from blue to red. **(B–D)** Quantification of the μCT results; $n = 6$.

significantly reduction of the relative amount of CD4+ and CD8+ T cells in the Iloprost treated mice in comparison to the control. The relative number of osteoblasts was not affected by Iloprost treatment. Next, we were interested in the IFNγ producing CD8+ T cells, which were already shown to be detrimental for successful bone repair. Iloprost treatment led to a clear decrease of IFNγ producing CD8+ T cells with regard to the control group (**Figure 11C**, highlighted by arrows). Next to the T cells, the distribution of MΦ, M1, and M2 type macrophages was also evaluated 3 days post-osteotomy. Corresponding to the chosen marker set for the *in vitro* analysis, CD68 was used as pan-macrophage marker, CD68 and CD80 for M1 and CD68 and CD206 for M2 (**Figure 11D**). Due to the Iloprost administration in the fracture zone, a simultaneous significant decrease of pro-inflammatory M1 and significant increase of anti-inflammatory and pro-regenerative M2 macrophages was detectable. In order to evaluate if Iloprost administration has an impact on bone resorption, osteoclasts were also investigated by IHC. Osteoclasts were identified by the myeloid-lineage marker CD68, the collagen digesting enzyme cathepsinK (CTSK) and presence of multiple nuclei (**Figure 11E**). No significant differences were observed in both groups 3 days post-osteotomy.

Summarizing the data from the proof of concept study in our *in vivo* mouse osteotomy model system, the pro-regenerative effect of Iloprost in bone healing was confirmed. We further revealed underlying changes in the immune cell composition in and around the fracture zone in the early inflammatory phase toward a reduced pro-inflammatory and increased anti-inflammatory cell phenotype caused by the application of Iloprost. Thus, Iloprost is a promising agent to improve bone regeneration by the downregulation of partial unfavorable pro-inflammatory and a simultaneous support of anti-inflammatory and pro-regenerative mediators.

DISCUSSION

Healing is impaired if a prolonged (pro-) inflammatory phase persists and an early anti-inflammatory stimulus is required. Thus, developing strategies that would ensure or even enhance anti-inflammatory stimuli appears mandatory. Iloprost is a well-known drug to treat diseases of the vascular system like pulmonary arterial hypertension and scleroderma (25, 29, 30). Its main function is conducted via vasodilatation (widening of blood vessels). Regarding the bone system, Iloprost is already successfully used to treat bone marrow oedema, partially also in the context of bone injuries (23, 24).

In the here presented study, the immune modulatory effect of the synthetic prostacyclin analog Iloprost was evaluated for

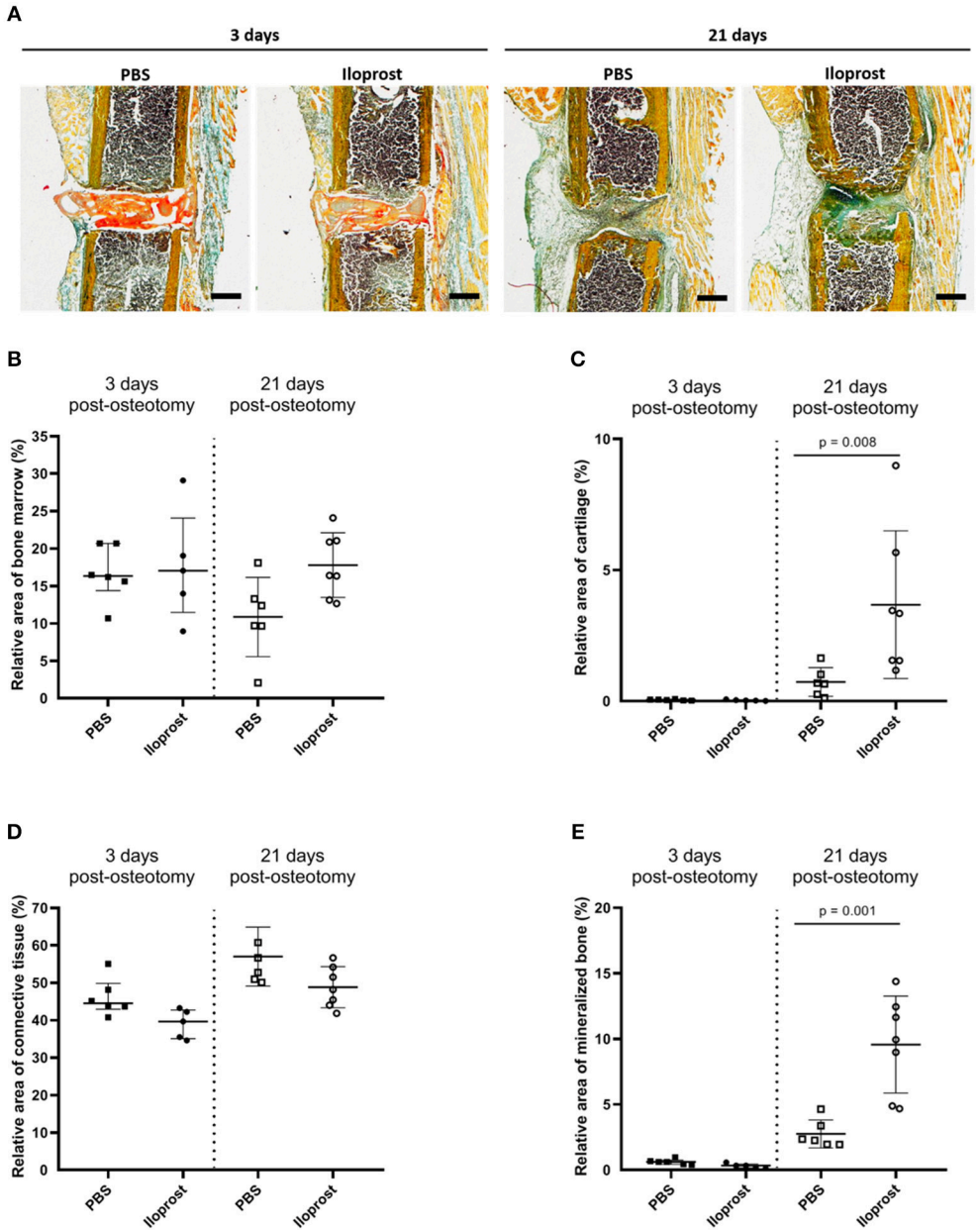

FIGURE 10 | Histological analysis of *in vivo* experiments in mouse osteotomies at days 3 and 21 post-osteotomy. **(A)** Representative Movat's pentachrome pictures are displayed for the respective time point and group. **(B–E)** Histomorphometrical analysis of the Movat Pentachrome stainings: **(B)** bone marrow, **(C)** cartilage tissue, **(D)** connective tissue, and **(E)** mineralized bone tissue. Color coding of the Movat Pentachrome staining: mineralized bone = yellow, cartilage = dark blue-green, connective tissue = light blue-green, muscle fibers = light orange, cell nuclei = purple, fibrin clot = red/orange. Scale bars equal 500 μm, $n = 6$.

bone fracture healing. The impact of Iloprost was investigated on immune cells and MSCs *in vitro* as well as in a well-established mouse osteotomy model *in vivo*. We demonstrated that the supplementation of Iloprost led to a decrease in the expression of pro-inflammatory cytokines by immune cells (T cells and macrophages) and thus promoted a shift in the function of these cells toward the anti-inflammatory path. The metabolic activity of the stimulated immune cells was also downregulated by Iloprost further supporting the observed decrease of the secreted pro-inflammatory cytokine profile. Iloprost had no negative effect on the osteogenic as well as chondrogenic function of MSCs. In an *in vivo* proof of concept approach, the pro-regenerative capacity of Iloprost as potential agent to further bone regeneration was confirmed, evaluated by an improved healing outcome after 21 days. Immunohistochemical analysis of the cellular

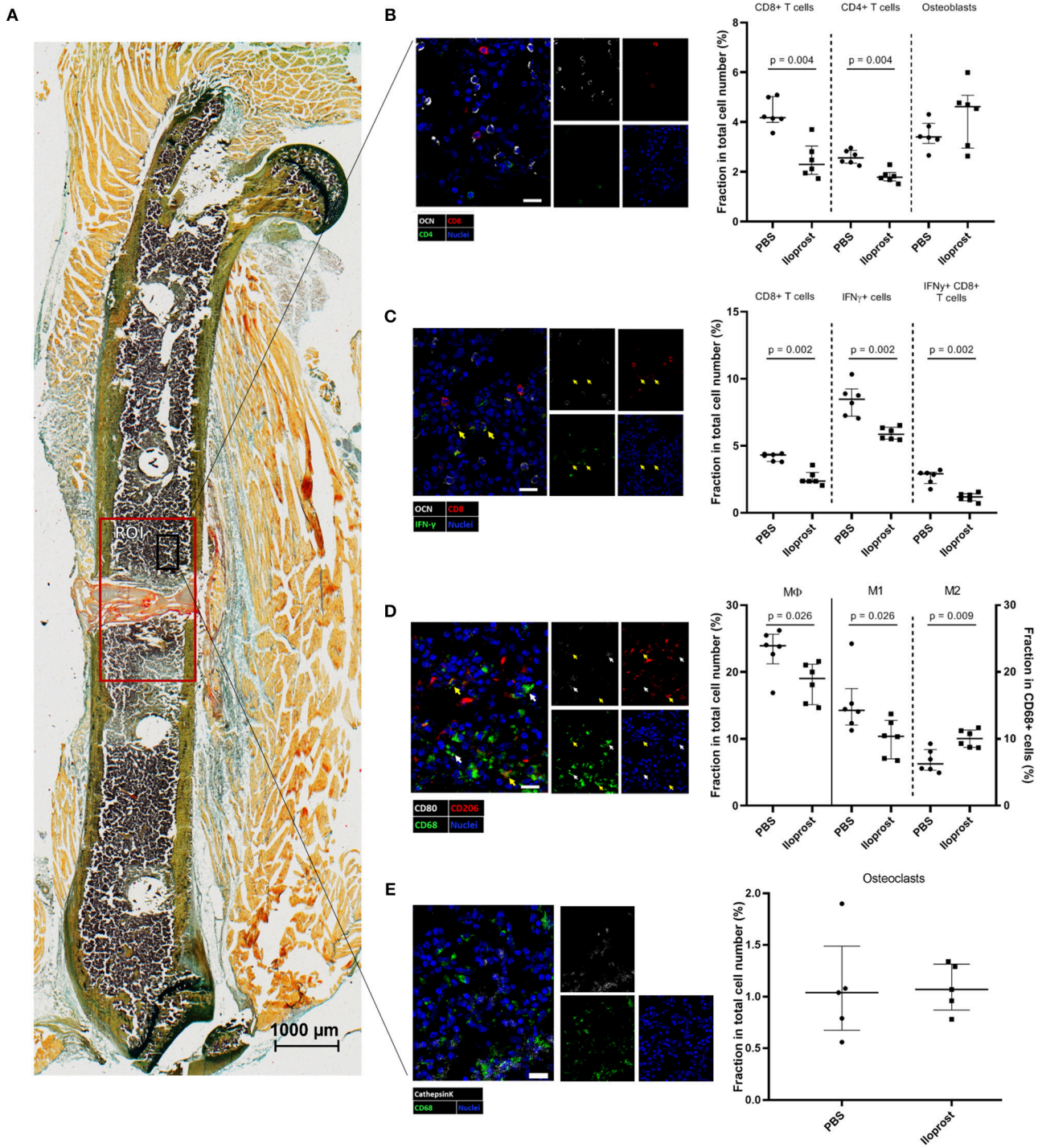

FIGURE 11 | Immunohistochemical (IHC) analysis of the distribution of immune cells in the fracture zone 3 days post-osteotomy. **(A)** A section of a fractured femur from the Iloprost treated group is displayed, Movat Pentachrome staining. The region of interest (ROI) for the quantitative analysis of IHC images is enlarged (red rectangle). The black rectangle represents the region from which the representative examples of the respective IHC staining for **(B)** CD4+ and CD8+ T cells and osteoblasts, **(C)** IFNγ producing CD8+ T cells; CD8+IFNγ+ cells = white indicator, **(D)** macrophages; M1-type macrophages = white indicator; M2-type macrophages = yellow indicator, and **(E)** osteoclasts were taken. The quantification of the cellular distributions are displayed in the corresponding dot plot graphs. Color code: Movat Pentachrome mineralized bone = yellow, cartilage = dark blue-green, connective tissue = light blue-green, muscle fibers = light orange, cell nuclei = purple, fibrin clot = red/orange; **(B)** osteoblasts = white, CD8+ T cells = red, CD4+ T cells = green and cell nuclei = blue; **(C)** osteoblasts = white, CD8+ T cells = red, IFNγ = green, cell nuclei = blue; **(D)** CD68 = green, CD80 = white, CD206 = red; **(E)** osteoclasts: double positive for cathepsinK = white and CD68 = green cell nuclei = blue. Scale bars: 20 µm (IHC) 1,000 µm (Movat Pentachrome); $n = 6$.

distribution in the fracture gap revealed a decrease of potential unfavorable IFNγ producing CD8+ cells as well as an increase of anti-inflammatory M2 macrophages in comparison to the control group due to Iloprost administration concurring with the *in vitro* results. Both are furthering the pro-regenerative pathway.

The signaling receptor for prostacyclin and thus also for Iloprost is found on a variety of different cell types, among others on cells of the innate as well as adaptive immunity. Iloprost signaling leads to an intracellular increase of cyclic adenosine monophosphate (cAMP) via the stimulation of the adenylyl cyclase. cAMP is an anti-inflammatory acting agent that suppresses the effector function of CD4+ and CD8+ T cells (31, 32). Here, we also observed a decrease of the secretion of the pro-inflammatory cytokines TNFα and IFNγ from whole bone marrow cells as well as (IFNγ producing) CD8+ T cells *in vitro* and *in vivo* under the presence of Iloprost. This observation demonstrates the immune modulatory effect of Iloprost on cellular components of the adaptive immunity toward a reduced pro-inflammatory and thus pro-regenerative phenotype. This finding was further confirmed by the increase of the pro-regenerative M2 type macrophages under the influence of Iloprost. The group of Alkhabit also showed an immune modulatory effect of Iloprost on macrophage polarization toward a pro-regenerative phenotype in an *in vivo* model system in rats, supporting our findings (33). Regarding bone fracture healing, possible negative effects of Iloprost on MSCs and bone forming osteoblasts as well as bone resorbing osteoclasts have to be considered. No possible negative effects by Iloprost on the osteogenic and chondrogenic capacities of MSCs were observed *in vitro*, further supporting the local application of Iloprost for bone healing scenarios *in vivo*. In a proof of concept approach, we evaluated the administration of Iloprost in a mouse osteotomy model system. Iloprost was inserted into a fibrin clot delivery system, from which the prostacyclin analog was successively released, which was shown by a downregulation of a pro-inflammatory cellular distribution around the fracture gap 3 days post osteotomy. The *in vivo* study confirmed the positive effect of Iloprost on bone regeneration. Animals treated with Iloprost showed a significantly improved bone healing outcome 21 days post-osteotomy compared to untreated control mice evaluated by μCT as well as histomorphometry after Movat's Pentachrome staining. The observed significantly enhanced bone formation in the Iloprost treated animals can be explained by an earlier starting of the regenerative process due to the down-regulated pro-inflammatory phase at the beginning of the healing cascade in comparison to the PBS treated control mice. Analysis of the cellular distribution of specific immune cells 3 days post-osteotomy in the fractured bones showed a clear tendency toward a reduced pro-inflammatory and increased anti-inflammatory cellular phenotype and cytokine secretion profile, as already observed in the preceding *in vitro* study. Furthermore, no effect on the relative amount of osteoblasts and osteoclasts in and around the fracture gap were detectable after Iloprost treatment 3 days post-osteotomy *in vivo*. *In vitro*, we also showed that the secreted cytokine milieu of activated and either Iloprost or untreated T cells has a significant impact on the osteogenic capacity of MSCs cultured in osteoinductive media. Our results showed a compensatory effect by the Iloprost treatment on the potential anti-regenerative cytokine milieu produced by activated T cells. Thus, the pro-regenerative effect of Iloprost is indirectly mediated on MSCs/osteoblasts by changes in the functionality of (pro-inflammatory) effector T cells participating in the bone regeneration cascade. Next to the effect of Iloprost on CD8+ T cells and macrophages, an influence on other immune cell could further impact bone healing *in vivo*. The early fracture healing phase is characterized by an infiltration of cells of the innate immunity like mast cells and neutrophils. For both, it was already shown, that the administration of prostacyclin analogs led to a reduced recruitment of these cells to the site of injury (34–36). Furthermore, an inhibitory function of Iloprost is reported for the secretion of effector cytokines of bone marrow dendritic cells as well as Th1 and Th2 CD4+ T cells *in vitro* (37). Thus, Iloprost is not only affecting the CD8+, but also the CD4+ T cell compartment in diminishing the (pro-inflammatory) effector cytokine secretion and thus function. One major key element of the potential of Iloprost to improve bone regeneration seems to be the time point of administration during the healing scenario. The group of Dogan reported an inhibitory effect of Iloprost on fracture repair in rats (38). There, Iloprost was administered by a daily injection for 5 days, starting at the time point of surgery. Due to the immune modulatory effect of Iloprost, a too early application of the drug could lead to an inhibition of the indispensable early pro-inflammatory phase initiating the healing cascade. This hypothesis is further supported by the reported effects of Iloprost on mast cells and neutrophils. Both cell types are indispensable for the early fracture healing phase to initiate the healing cascade. If Iloprost is administered directly at the time point of surgery/injury, it will inhibit the crucial recruitment of both cells types and will therefore disturbed the formation of the necessary cellular and cytokine milieu for a correct progression of the regeneration cascade (35, 36). Therefore, we used a fibrin clot for a (1) delayed and (2) successive release of Iloprost into the fracture gap thereby allowing the first pro-inflammatory phase to proceed. The positive impact of Iloprost in bone healing was already demonstrated in a small case study in the clinic for the treatment of subchondral stress fractures of the knee. Patients receiving Iloprost showed an improved healing of the stress fractures in comparison to the control group receiving the opioid analgesic Tramadol (39). Even though Iloprost is beneficial for bone healing applied systemically, this also bears considerable risks which would be circumvented by a local application as we proved in our proof of concept *in vivo* study. Thus, also in the treatment of patients, the possible pro-regenerative effect of Iloprost in bone healing was confirmed further supporting our *in vivo* and *in vitro* results.

CONCLUSION

In the here presented study, the anti-inflammatory impact of Iloprost was confirmed. Cellular components of the immune system play a key role in bone fracture healing. An overwhelming

pro-inflammatory phase in the early fracture healing cascade is correlated with an impaired healing outcome (15). We demonstrated that Iloprost has the potential to compensate the partial unfavorable pro-inflammatory effect of effector T cells and is able to stimulate the formation of an anti-inflammatory and pro-regenerative cellular milieu improving fracture healing. In a consecutive step, this strategy has to be confirmed in clinical phase I/II trials.

AUTHOR CONTRIBUTIONS

SW, KS-B, GD, and H-DV: conceptual idea and design of the study. SW, CS, CB, CJS, and JB: data collection, analysis, and interpretation. SW, CS, CB, KS-B, GD, and H-DV: drafting of the manuscript. All authors revised the manuscript.

ACKNOWLEDGMENTS

We would like to thank Norma Schulz for her excellent technical assistance performing the described experiments. We acknowledge support from the German Research Foundation (DFG) and the Open Access Publication Fund of Charité–Universitätsmedizin Berlin. This work was supported by a grant from the German Research Foundation (FG 2195, DFG SCHM 2977, DU 298/21-1) and the Friede Springer Stiftung.

SUPPLEMENTARY MATERIAL

The Supplementary Material for this article can be found online at: https://www.frontiersin.org/articles/10.3389/fimmu.2019.00713/full#supplementary-material

REFERENCES

1. Marsell R, Einhorn TA. The biology of fracture healing. *Injury*. (2011) 42:551–5. doi: 10.1016/j.injury.2011.03.031
2. Schmidt-Bleek K, Petersen A, Dienelt A, Schwarz C, Duda GN. Initiation and early control of tissue regeneration - bone healing as a model system for tissue regeneration. *Expert Opin Biol Ther*. (2014) 14:247–59. doi: 10.1517/14712598.2014.857653
3. Einhorn TA, Gerstenfeld LC. Fracture healing: mechanisms and interventions. *Nat Rev Rheumatol*. (2015) 11:45–54. doi: 10.1038/nrrheum.2014.164
4. Schmidt-Bleek K, Kwee BJ, Mooney DJ, Duda GN. Boon and bane of inflammation in bone tissue regeneration and its link with angiogenesis. *Tissue Eng Part B Rev*. (2015) 21:354–64. doi: 10.1089/ten.teb.2014.0677
5. Einhorn TA, Lane JM. Significant advances have been made in the way surgeons treat fractures. *Clin Orthop Relat Res*. (1998) 355:S2–3. doi: 10.1097/00003086-199810001-00001
6. Schlundt C, Bucher CH, Tsitsilonis S, Schell H, Duda GN, Schmidt-Bleek K. Clinical and research approaches to treat non-union fracture. *Curr Osteoporos Rep*. (2018) 16:155–68. doi: 10.1007/s11914-018-0432-1
7. Winkler TA, Duda GN, Schmidt-Bleek K. A review of biomaterials in bone defect healing, remaining shortcomings and future opportunities for bone tissue engineering. *Bone Joint Res*. (2018) 7:232–243. doi: 10.1302/2046-3758.73.BJR-2017-0270.R1
8. Gruber R, Koch H, Doll BA, Tegtmeier F, Einhorn TA, Hollinger JO. Fracture healing in the elderly patient. *Exp Gerontol*. (2006) 41:1080–93. doi: 10.1016/j.exger.2006.09.008
9. Bucher CH, Duda GN, Volk H-D, Schmidt-Bleek K. The role of immune reactivity in bone regeneration. In: Zorzi AR, de Miranda JB, editors. *Advanced Techniques in Bone Regeneration*. London: IntechOpen Limited (2016). p. 169–194. doi: 10.5772/62476
10. Schell H, Duda GN, Peters A, Tsitsilonis S, Johnson KA, Schmidt-Bleek K. The haematoma and its role in bone healing. *J Exp Orthop*. (2017) 4:5. doi: 10.1186/s40634-017-0079-3
11. Opal SM. Phylogenetic and functional relationships between coagulation and the innate immune response. *Crit Care Med*. (2000) 28:S77–80. doi: 10.1097/00003246-200009001-00017
12. Lienau J, Schmidt-Bleek K, Peters A, Haschke F, Duda GN, Perka C, et al. Differential regulation of blood vessel formation between standard and delayed bone healing. *J Orthop Res*. (2009) 27:1133–40. doi: 10.1002/jor.20870
13. Schmidt-Bleek K, Schell H, Kolar P, Pfaff M, Perka C, Buttgereit F, et al. Cellular composition of the initial fracture hematoma compared to a muscle hematoma: a study in sheep. *J Orthop Res*. (2009) 27:1147–51. doi: 10.1002/jor.20901
14. Lienau J, Schmidt-Bleek K, Peters A, Weber H, Bail HJ, Duda GN, et al. Insight into the molecular pathophysiology of delayed bone healing in a sheep model. *Tissue Eng Part A*. (2010) 16:191–9. doi: 10.1089/ten.tea.2009.0187
15. Reinke S, Geissler S, Taylor WR, Schmidt-Bleek K, Juelke K, Schwachmeyer V, et al. Terminally differentiated CD8(+) T cells negatively affect bone regeneration in humans. *Sci Transl Med*. (2013) 5:177ra136. doi: 10.1126/scitranslmed.3004754
16. Schlundt C, El Khassawna T, Serra A, Dienelt A, Wendler S, Schell H, et al. Macrophages in bone fracture healing: their essential role in endochondral ossification. *Bone*. (2018) 106:78–89. doi: 10.1016/j.bone.2015.10.019
17. Camacho M, Rodriguez C, Guadall A, Alcolea S, Orriols M, Escudero JR, et al. Hypoxia upregulates PGI-synthase and increases PGI(2) release in human vascular cells exposed to inflammatory stimuli. *J Lipid Res*. (2011) 52:720–31. doi: 10.1194/jlr.M011007
18. Mohite A, Chillar A, So SP, Cervantes V, Ruan KH. Novel mechanism of the vascular protector prostacyclin: regulating microRNA expression. *Biochemistry*. (2011) 50:1691–9. doi: 10.1021/bi101654w
19. Dorris SL, Peebles RS Jr. PGI2 as a regulator of inflammatory diseases. *Mediators Inflamm*. (2012) 2012:926968. doi: 10.1155/2012/926968
20. Muller T, Durk T, Blumenthal B, Herouy Y, Sorichter S, Grimm M, et al. Iloprost has potent anti-inflammatory properties on human monocyte-derived dendritic cells. *Clin Exp Allergy*. (2010) 40:1214–21. doi: 10.1111/j.1365-2222.2010.03558.x
21. Jaffar Z, Wan KS, Roberts K. A key role for prostaglandin I2 in limiting lung mucosal Th2, but not Th1, responses to inhaled allergen. *J Immunol*. (2002) 169:5997–6004. doi: 10.4049/jimmunol.169.10.5997
22. Lovgren AK, Jania LA, Hartney JM, Parsons KK, Audoly LP, Fitzgerald GA, et al. COX-2-derived prostacyclin protects against bleomycin-induced pulmonary fibrosis. *Am J Physiol Lung Cell Mol Physiol*. (2006) 291:L144–156. doi: 10.1152/ajplung.00492.2005
23. Disch AC, Matziolis G, Perka C. The management of necrosis-associated and idiopathic bone-marrow oedema of the proximal femur by intravenous iloprost. *J Bone Joint Surg Br*. (2005) 87:560–4. doi: 10.1302/0301-620X.87B4.15658
24. Jager M, Zilkens C, Bittersohl B, Matheney T, Kozina G, Blondin D, et al. Efficiency of iloprost treatment for osseous malperfusion. *Int Orthop*. (2011) 35:761–5. doi: 10.1007/s00264-010-0998-4
25. Roman A, Barbera JA, Escribano P, Sala ML, Febrer L, Oyaguez I, et al. Cost effectiveness of prostacyclins in pulmonary arterial hypertension. *Appl Health Econ Health Policy*. (2012) 10:175–88. doi: 10.2165/11630780-000000000-00000
26. Riemekasten G, Hoffmann U, Sunderkotter C, Weiss N, Kuhn A, Angiologisch-Dermatologisch-Rheumatologische DUE. [Management of digital ulcers in patients with systemic sclerosis]. *Dtsch Med Wochenschr*. (2012) 137:34–40. doi: 10.1055/s-0031-1298798
27. Bouxsein ML, Boyd SK, Christiansen BA, Guldberg RE, Jepsen KJ, Muller R. Guidelines for assessment of bone microstructure in rodents using micro-computed tomography. *J Bone Miner Res*. (2010) 25:1468–86. doi: 10.1002/jbmr.141

28. Abdelmagid SM, Barbe MF, Safadi FF. Role of inflammation in the aging bones. *Life Sci.* (2015) 123:25–34. doi: 10.1016/j.lfs.2014.11.011
29. Colaci M, Lumetti F, Giuggioli D, Guiducci S, Bellando-Randone S, Fiori G, et al. Long-term treatment of scleroderma-related digital ulcers with iloprost: a cohort study. *Clin Exp Rheumatol.* (2017) 35 (Suppl. 106):179–83.
30. Foti R, Visalli E, Amato G, Benenati A, Converso G, Farina A, et al. Long-term clinical stabilization of scleroderma patients treated with a chronic and intensive IV iloprost regimen. *Rheumatol Int.* (2017) 37:245–9. doi: 10.1007/s00296-016-3582-4
31. Zhou W, Hashimoto K, Goleniewska K, O'neal JF, Ji S, Blackwell TS, et al. Prostaglandin I2 analogs inhibit proinflammatory cytokine production and T cell stimulatory function of dendritic cells. *J Immunol.* (2007) 178:702–10. doi: 10.4049/jimmunol.178.2.702
32. D'amelio P, Cristofaro MA, D'amico L, Veneziano L, Roato I, Sassi F, et al. (2010). Iloprost modulates the immune response in systemic sclerosis. *BMC Immunol.* 11:62. doi: 10.1186/1471-2172-11-62
33. Alkhatib K, Poseno TM, Diaz Perez A, Durdik JM, Stenken JA. Iloprost affects macrophage activation and CCL2 concentrations in a microdialysis model in rats. *Pharm Res.* (2018) 35:20. doi: 10.1007/s11095-017-2277-1
34. Furuta GT, Schmidt-Choudhury A, Wang MY, Wang ZS, Lu L, Furlano RI, et al. Mast cell-dependent tumor necrosis factor alpha production participates in allergic gastric inflammation in mice. *Gastroenterology.* (1997) 113:1560–9. doi: 10.1053/gast.1997.v113.pm9352858
35. Kovtun A, Bergdolt S, Wiegner R, Radermacher P, Huber-Lang M, Ignatius A. The crucial role of neutrophil granulocytes in bone fracture healing. *Eur Cell Mater.* (2016) 32:152–62. doi: 10.22203/eCM.v032a10
36. Kroner J, Kovtun A, Kemmler J, Messmann JJ, Strauss G, Seitz S, et al. Mast cells are critical regulators of bone fracture-induced inflammation and osteoclast formation and activity. *J Bone Miner Res.* (2017) 32:2431–44. doi: 10.1002/jbmr.3234
37. Zhou W, Blackwell TS, Goleniewska K, O'neal JF, Fitzgerald GA, Lucitt M, et al. Prostaglandin I2 analogs inhibit Th1 and Th2 effector cytokine production by CD4 T cells. *J Leukoc Biol.* (2007) 81:809–17. doi: 10.1189/jlb.0606375
38. Dogan A, Duygun F, Kalender AM, Bayram I, Sungur I. Iloprost inhibits fracture repair in rats. *Chin Med J.* (2014) 127:2960–5. doi: 10.3760/cma.j.issn.0366-6999.20132862
39. Mayerhoefer ME, Kramer J, Breitenseher MJ, Norden C, Vakil-Adli A, Hofmann S, et al. MRI-demonstrated outcome of subchondral stress fractures of the knee after treatment with iloprost or tramadol: observations in 14 patients. *Clin J Sport Med.* (2008) 18:358–62. doi: 10.1097/JSM.0b013e31817f3e1c

Conflict of Interest Statement: The authors declare that the research was conducted in the absence of any commercial or financial relationships that could be construed as a potential conflict of interest.

frontiers in Immunology

ORIGINAL RESEARCH
published: 05 April 2019
doi: 10.3389/fimmu.2019.00709

HGMB1 and RAGE as Essential Components of Ti Osseointegration Process in Mice

*Claudia Cristina Biguetti[1], Franco Cavalla[1,2], Elcia Varize Silveira[3], André Petenuci Tabanez[1], Carolina Favaro Francisconi[1], Rumio Taga[1], Ana Paula Campanelli[1], Ana Paula Favaro Trombone[3], Danieli C. Rodrigues[4] and Gustavo Pompermaier Garlet[1]**

[1] Department of Biological Sciences, Bauru School of Dentistry, University of São Paulo, São Paulo, Brazil, [2] Department of Conservative Dentistry, School of Dentistry, University of Chile, Santiago, Chile, [3] Department of Biological and Allied Health Sciences, Universidade Sagrado Coração, Bauru, Brazil, [4] Department of Bioengineering, University of Texas at Dallas, Dallas, TX, United States

OPEN ACCESS

Edited by:
Teun J. De Vries,
VU University Amsterdam,
Netherlands

Reviewed by:
Armando Rojas,
Catholic University of the Maule, Chile
Niamh Fahy,
Erasmus University Rotterdam,
Netherlands

***Correspondence:**
Gustavo Pompermaier Garlet
garletgp@usp.br

Specialty section:
This article was submitted to Inflammation, a section of the journal Frontiers in Immunology

Received: 23 January 2019
Accepted: 15 March 2019
Published: 05 April 2019

Citation:
Biguetti CC, Cavalla F, Silveira EV, Tabanez AP, Francisconi CF, Taga R, Campanelli AP, Trombone APF, Rodrigues DC and Garlet GP (2019) HGMB1 and RAGE as Essential Components of Ti Osseointegration Process in Mice. Front. Immunol. 10:709. doi: 10.3389/fimmu.2019.00709

The release of the prototypic DAMP High Mobility Group Box 1 (HMGB1) into extracellular environment and its binding to the Receptor for Advanced Glycation End Products (RAGE) has been described to trigger sterile inflammation and regulate healing outcome. However, their role on host response to Ti-based biomaterials and in the subsequent osseointegration remains unexplored. In this study, HMGB1 and RAGE inhibition in the Ti-mediated osseointegration were investigated in C57Bl/6 mice. C57Bl/6 mice received a Ti-device implantation (Ti-screw in the edentulous alveolar crest and a Ti-disc in the subcutaneous tissue) and were evaluated by microscopic (microCT [bone] and histology [bone and subcutaneous]) and molecular methods (ELISA, PCR array) during 3, 7, 14, and 21 days. Mice were divided into 4 groups: Control (no treatment); GZA (IP injection of Glycyrrhizic Acid for HMGB1 inhibition, 4 mg/Kg/day); RAP (IP injection of RAGE Antagonistic Peptide, 4 mg/Kg/day), and vehicle controls (1.5% DMSO solution for GZA and 0.9% saline solution for RAP); treatments were given at all experimental time points, starting 1 day before surgeries. HMGB1 was detected in the Ti-implantation sites, adsorbed to the screws/discs. In Control and vehicle groups, osseointegration was characterized by a slight inflammatory response at early time points, followed by a gradual bone apposition and matrix maturation at late time points. The inhibition of HMGB1 or RAGE impaired the osseointegration, affecting the dynamics of mineralized and organic bone matrix, and resulting in a foreign body reaction, with persistence of macrophages, necrotic bone, and foreign body giant cells until later time points. While Control samples were characterized by a balance between M1 and M2-type response in bone and subcutaneous sites of implantation, and also MSC markers, the inhibition of HMGB1 or RAGE caused a higher expression M1 markers and pro-inflammatory cytokines, as well chemokines and receptors for macrophage migration until later time points. In conclusion, HMGB1 and RAGE have a marked role in the osseointegration, evidenced

by their influence on host inflammatory immune response, which includes macrophages migration and M1/M2 response, MSC markers expression, which collectively modulate bone matrix deposition and osseointegration outcome.

Keywords: DAMPs, pre-clinical studies, inflammation, HMGB1, bioengineering, osseointegration, implants, osteoimmunology

INTRODUCTION

Ti-based devices, such as dental implants, are classically used in dentistry, due to their osseointegration capacity that is translated into remarkable clinical success (1–3). However, understanding of the molecular interactions at Ti/host interface, which drive a beneficial equilibrium between immune/inflammatory response and the subsequent bone apposition toward Ti surface remains unclear (3).

A recent study performed an extensive molecular and histological characterization of Ti mediated osseointegration in C57Bl/6 mice, demonstrating a highly orchestrated and transient inflammatory response coordinated with the early stages of osseointegration (4). In view of the dominance of innate immunity elements in the host response that paves the way for osseointegration, in a process where numerous inflammation- and bone healing-related molecules are up-regulated (5, 6), macrophages have been regarded as central determinants of osseointegration outcome (7, 8). Indeed, macrophages can exert key regulatory functions by secreting a range of different mediators (chemokines, cytokines, enzymes, and growth factors) in the inflammatory microenvironment, which consequently influence the intensity and duration of immune response, affecting healing (9, 10). Recent studies suggest macrophages polarization into M1 or M2 phenotypes as a crucial step for determining the success or failure of biomaterial osseointegration, since the dominance of a M1-type response is related to chronic inflammation and fibrous encapsulation of Ti instead of successful osseointegration (7, 9, 11, 12).

Therefore, initial steps of the host inflammatory immune response that will shape macrophages fate in the biomaterial-implantation site seem an essential component for a successful osseointegration outcome. Macrophage polarization around biomaterials begins immediately post-implantation, with biomaterial surface recognition and a transient polarization state, which are influenced by varying microenvironmental cues, some of which are biomaterial-based (9). Thus, it has been supposed that the type and quantity of proteins adsorbed on a biomaterial is influenced by its surface morphological cues and chemistry, which may affect its recognition by macrophages consequently influencing their phenotypic polarization (9, 13).

Considering the candidate proteins for adsorption on Ti surface, damage associated molecular patterns (DAMPs) are a group of endogenous intracellular or extracellular molecules, which are released from their original sites into the microenvironment upon breakage of tissue components caused by trauma or stress, acting as local "danger signals" that trigger host response (14, 15). After their release from damaged tissues, DAMPs are recognized by a number of pattern recognition receptors (PRRs) primarily expressed on macrophages (10, 16, 17). Among several DAMPs/PRRs pathways already described in the literature, the interaction of High Mobility Group Box 1 (HMGB1), the prototypical and most well-characterized DAMP, with the Receptor for Advanced Glycation End Products (RAGE), has been associated with the activation of inflammatory responses and wound healing (18, 19). Indeed, while HMGB1, alone or associated with other molecules, can play pleiotropic functions by activating multiple receptors (TLR4 and TLR2, RAGE, CXCR4) (18, 20, 21). It is also important to mention that HMGB1 is a redox-sensitive molecule and consequently, redox status of its cysteine residues (Cys23, Cys45, and Cys106) is strongly affected by a pro-oxidative and pro-inflammatory environment, since various reactive oxygen species (ROS) are released in inflammatory environments (22, 23). Then, biphasic actions on HMGB1 (pro-inflammatory activity or immune tolerance/healing) may depends on the environment where this molecule is released. In this context, it has been suggested that oxidized or reduced forms of HMGB1 might differently affect the HMGB1 binding into different receptors and induce that biphasic actions (23). For example, oxidized form of HMGB1 accumulates during resolution of inflammation and tissue regeneration in liver, serving as a feedback mechanism to control its proinflammatory activity (22).

RAGE constitute the major receptor for HMGB1 (24–26). Importantly, the axis HMGB1/RAGE is related with several cellular effects which are important to inflammatory and healing outcomes, such as induction of inflammatory response and angiogenesis, tissue remodeling, and stimulation of cellular differentiation for regeneration (19, 27–31). In the context of M1/M2, evidence from *in vivo* studies point that HMGB1 can facilitate M1 macrophage phenotype in certain inflammatory disease models (32, 33), mainly based on HMGB1 interactions with TLR receptors (32). However, other *in vitro* (26) and *in vivo* disease models (34, 35) suggested that HMGB1 can enhance the activity of M2 macrophages, especially in a manner RAGE-dependent (26, 35). Importantly, despite the growing focus on macrophages role in healing, HMGB1/RAGE is a potential trigger of the overall host inflammatory immune response at biomaterials implantation sites, which theoretically can involve other cell besides the macrophages. Indeed, is still unclear how HMGB1/RAGE can trigger and regulate host responses in different inflammatory contexts.

Considering the influence of DAMPs regulating biomaterial incorporation, it has been demonstrated by *in vitro* studies that remaining HMGB1 within xenogeneic biologic scaffolds (after manufacturing processes) affects the response of monocytes/macrophages to the biomaterial and consequently can affect the inflammatory response, such as a bioactive

molecule (36). On the other hand, in metallic and permanent biomaterial incorporation, the molecules driving the host response are theoretically exclusively released by host, such as hypothesized by recent reviews in biomaterials science literature (15, 37). Therefore, DAMPs are suggested to be released from tissue damage immediately after biomaterial implantation, possibly interacting with the surface and influencing the innate inflammatory response in the site of biomaterial implantation (15, 38). However, no previous studies have demonstrated the presence of endogenous DAMPs in biomaterials implantation sites, as well their putative role remains to be demonstrated in a cause-and-effect manner.

In face of all evidences for the role of HMGB1 and its cognate receptor RAGE in modulating inflammatory and healing responses, the release of HMGB1 after Ti implant placement could be a critical step for triggering inflammation and healing outcomes in osseointegration sites. Thus, in this present study, we investigated the role of HMGB1 during Ti-mediated oral osseointegration in C57Bl/6 mice, by means of a cause-effect study of pharmacological inhibition of HMGB1 or its cognate receptor RAGE.

MATERIALS AND METHODS

Material Preparation

Titanium implant screws (titanium-6 aluminum-4 vanadium alloy, NTI-Kahla GmbH Rotary Dental Instruments, Kahla, Thüringen, Germany) of Ø 0.6 mm were cut at a length of 1.5 mm. Also, machined 6AL-4V Tinanium discs (Ti-discs) of Ø 6 and 2 mm thick from commercially pure grade 2 alloy were used for subcutaneous implantation. All material were sterilized by autoclaving before surgical procedures, as previously described for oral osseointegration model in C57Bl/6 mice (4).

Animals

Experimental groups comprised C57Bl/6 male mice (10-weeks-old, 25 g of weight in average), bred and maintained in the animal facilities of University of São Paulo, cared according to the recommendations in the Guide for the Care and Use of Laboratory Animals of the National Institutes of Health (39) were used in this study. The experimental protocols were performed according to ARRIVE guidelines (40) and National Institutes of Health guide for the care and use of Laboratory animals (NIH Publications No. 8023, revised 1978), with approval by the local Institutional Committee for Animal Care and Use (CEEPA-FOB/USP, #012/2014). Mice were provided sterile water *ad libitum* and were fed with sterile standard solid mice chow (Nuvital, Curitiba, PR, Brazil) during all experimental periods of this study, except throughout the first 72 h post-Ti implantation for oral osseointegration model, in which diet was crumbled. Experimental groups for oral osseointegration were comprised by 10 animals per group/time point (3, 7, 14, and 21 days), with 6 animals per group/time point for microscopic analysis (microCT, histological, and birefringence analysis) and 4 for molecular (Real Time PCR array) assays; an additional 1 day time point group with 6 animals per group was used for protein elution and HMGB1 quantification. Experimental groups for subcutaneous Ti disc implantation were comprised by 5 animals per group/time point (3, 7, and 14 days) and Ti-disc was implanted in left and right side of animal dorsa, comprising 10 biological samples for each group/time point: 5 Ti disc samples (Ti discs containing the surrounding tissues) from the left side for microscopic analysis (histological, birefringence analysis, and immunohistochemistry) and 5 Ti disc samples from the right side for molecular analysis (Real Time PCR array) and protein elution (an additional 1 day time point was evaluated for HMGB1 quantification). All experimental groups (oral osseointegration and subcutaneous implantation) were divided according to each treatment: Control (no treatment); GZA, IP injection of glycyrrhizic acid (Sigma Aldrich) 200 mg/Kg/24 h for HMGB1 inhibition; vehicle control for GZA (intraperitoneal [IP] injection of 1.5% DMSO solution); RAP, IP injection of RAGE antagonistic peptide (RAP, Merck Millipore, USA) 4 mg/Kg/24 h as previously described (41, 42); and vehicle control for RAP, IP injection of saline solution 0.9%. Mice received daily IP injections of drugs/vehicle, starting 1 day before the surgical procedure and continuing toward the end of experimental periods. No antibiotics and anti-inflammatory drugs were administered to the animals after implantation surgery, in order to avoid interferences on investigated inflammatory/immunological pathways (4).

Experimental Protocol for Oral Osseointegration Model

The Ti-implant placement in edentulous alveolar crest of the oral cavity of C57Bl/6 mice was performed as previously described (4, 43). Briefly, mice were anesthetized previous to the surgery by ketamine chloride 80 mg/kg (Dopalen, Agribrands Brasil, Paulínia, SP, Brazil) and xylazine chloride 160 mg/kg (Anasedan, Agribrands Brasil, Paulínia, SP, Brazil). Then, the mouse was placed in dorsal decubitus position under a stereomicroscope (DF Vasconcellos, São Paulo, SP, Brazil), and oral mucosa was cleaned using topical chlorhexidine solution for 1 min. An incision of 2 mm width parallel to the palatal crease and 1 mm in front of the left first maxillary molar was made and the subjacent bone was drilled using a Ø 0.50 mm pilot drill (NTI-Kahla GmbH Rotary Dental Instruments, Kahla, Thüringen, Germany) at 600 rpm using a surgical motor (NSK-Nakanishi International, Kanuma,Tochigi, Japan). The Ti-implant was screwed down in the implant bed using a castro viejo micro needle holder (Fine Science Tools, British Columbia, CA, USA). The right edentulous alveolar crest was used as Control side, without implant placement. Importantly, animals with early failure related to the surgical procedure (loss of primary stability upon placement) were immediately detected and were not included in the sample size; being only Ti implantations with complete absence of device mobility included in the sample for subsequent analysis, as previously characterized (4). At the end of experimental periods, mice were euthanized and maxillae were removed for microscopic (microtomographic, histological, histomorphometric) or molecular analysis. Samples selected for microscopic analysis were fixed in PBS-buffered formalin (10%) solution (pH 7.2) for 48 h at room temperature, washed overnight in running water and maintained in alcohol

fixative (70% hydrous ethanol) until the conclusion of the μCT scanning. Then, the specimens were decalcified in 4.13% EDTA (pH 7.2) following histological processing protocols. Samples for molecular analysis were stored in RNA later (Ambion, Austin, TX, USA) solutions following previous protocols (44, 45), samples for HMGB1 quantification were submitted to protein elution protocol and subsequently frozen for posterior protein assay (46, 47).

Experimental Protocol for Ti Implantation on Subcutaneous Tissue

Mice were anesthetized as previous described for oral osseointegration model. Then, a longitudinal incision was performed in the animal dorsa, were one Ti-disc was implanted in each side. Immediately down from Ti implantation, while the control region remained intact. Ti discs containing the surrounding tissues, as well control samples were collected from the left side for microscopic and from the right side for molecular analysis (Real Time PCR array). Samples collected for microscopic analysis were fixed in PBS-buffered formalin (10%) solution (pH 7.2) for 24 h at RT, then washed over-night in running water and processed for routine histology. Samples collected for molecular analysis were stored in RNAlater (Ambion, Austin, TX, USA) solutions for Real Time PCR array. For protein assay (i.e., HMGB1 detection), Ti-screws, and Ti-discs retrieved after implantation were submitted to protein elution protocol for posterior protein assay (46, 47).

ELISA Assay for HMGB1 Detection

Ti-screws (implanted in bone) and Ti-discs (implanted into subcutaneous tissue) were retrieved from implantantion sites at different time points submitted to a protein elution protocol (46, 47). Briefly, Ti devices were subjected to five consecutive washes with 200 μl of double-distilled water and a final wash with 100 mM NaCl in 50 mM Tris-HCl to remove unadsorbed proteins. The absorbed proteins eluate was obtained by three consecutive submersions of the devices in a solution containing 4% SDS, 100 mM DTT, and 0.5 M TEAB, as previously (46, 47). Total protein of the serum was quantified for subsequent normalization (Pierce Protein Assay Kit), and HMGB1 was measured by ELISA according to the protocol recommended by the manufacturer (MyBioSource). The results were expressed as mean values ± standard deviation nanogram (ng) of protein per milligram of tissue, and represent values of duplicates of each sample obtained in two independent experiments.

Micro-Computed Tomography (μCT) Assessment

Mice maxillae containing the Ti-implants were scanned by Skyscan 1176 System (Bruker Microct, Kontich, Belgium) at 80 kV, 300 μA, 180 degrees of rotation, and exposure range of 1 degree. After scanning and previous reconstructions (NRecon software, Bruker Microct, Kontich, Belgium), representative three-dimensional images were obtained by CT-Vox 2.3 software, while quantitative evaluation of bone to implant interface was assessed using CTAn 1.1.4.1 software (Bruker Microct, Kontich, Belgium) based in previous standardization for measuring bone implant contact volume by means of microCT (4). Briefly, for quantification of bone volume proportion (BV/TV, %) at the implant-bone interface area, a cylindrical region of interest (ROI) with a diameter of 700 μm was set and the bone volume quantification was performed only considering bone implant contact region. After binarization and separation between titanium body and bone by the difference of hyperdensities, BV/TV was acquired.

Histomorphometry

The mice maxillae used for microCT scanning were processed for histological analysis following standardized procedures (4, 45, 48). For both, osseointegration model (maxillae) and subcutaneous, semi-serial sections considering the implantation area were cut with 4 μm thickness. A total of six samples (biological replicates) and nine semi-serial sections (technical replicates) from the central region of implantation sites in the maxilla were taken for hematoxylin and eosin [H&E] staining. For subcutaneous sites, a total of five samples (biological replicates) and eight semi-serial sections (technical replicates) were considered for histomorphometry. The histomorphometry was performed by a single calibrated investigator with a binocular microscope (Olympus Optical Co., Tokyo, Honshu, Japan) using a 100x immersion objective. Six histological fields *per* each HE section, comprising the region adjacent to thread spaces (for osseointegration) or Ti disc space (for subcutaneous), were observed under a 100 points grid in a quadrangular area, by using Image J software (Version 1.51, National Institutes of Health, Bethesda, MD, USA). Points were quantified coinciding with the following structures found in the osseointegration sites or in implant failure sites: blood clot, inflammatory cells, blood vessels, fibroblasts and fibers, osteoblasts, osteoclasts, bone matrix, necrotic bone and foreign body giant cells (FBGC), and other elements (empty spaces left by implant space). For subcutaneous, were quantified structures involving inflammatory and healing process surrounding the Ti-disc space (presence of blood clot, inflammatory cells, fibers, fibroblasts, and blood vessels). Results were presented as the mean area density for each structure considered in each examined group.

Birefringence Analysis

A total of six different samples (biological replicates) and four semi-serial sections (technical replicates) for each sample were used for picrosirius red staining and birefringence analysis of the osseointegration model in the maxillae. For each semi-serial section, three histological fields were evaluated comprising the central region of bone to implant contact. In subcutaneous tissue, five samples (biological replicates) and four semi-serial sections (technical replicates) for each sample were analyzed. For each section, six histological fields were analyzed surrounding the Ti disc space. All specimens were analyzed at 40x magnification through polarizing lens coupled to a binocular inverted microscope (Leica DM IRB/E, Leica Microsystems Wetzlar GmbH, Wetzlar, Germany) and images were captured with a Leica Imaging Software (LAX, Leica Microsystems Wetzlar GmbH, Wetzlar, Germany). As previously described (4, 45, 48), green birefringence color indicates thin fibers; yellow and

red colors at birefringence analysis indicate thick collagen fibers. Three fields from each section were analyzed through polarizing lens coupled to a binocular inverted microscope (Leica DM IRB/E, Leica Microsystems Wetzlar GmbH, Wetzlar, Germany), by using 40x magnification immersion objective. Images were captured with a Leica Imaging Software (LAX, Leica Microsystems Wetzlar GmbH, Wetzlar, Germany) and the quantification of birefringence brightness was performed using the software AxioVision 4.8 (Carl Zeiss Microscopy GmbH, Jena, Germany) considering green, yellow, and red spectra pixels2. Mean values of four sections from each animal were calculated and submitted to statistical analysis.

Immunohistochemistry and Quantification of Immunolabeled Inflammatory Cells

A total of five samples (biological replicate) from subcutaneous tissue and three semi-serial sections (technical replicate) of each sample surrounding the Ti implant were used for individual immunodetection of Ly6g-GR1 (sc-168490), F4/80 (a pan marker for murine macrophages, sc-26642), CD80 (M1 macrophage, sc-376012), and CD206 (M2 macrophage, sc-34577), all primary antibodies purchased from Santa Cruz Biotechnology (Santa Cruz Biotechnology, Santa Cruz, CA, USA). Immunohistochemistry protocol was performed as previously described (48). Briefly, histological sections were rehydrated and retrieved the antigens by boiling the histological slides in 10 mM sodium citrate buffer pH 6 for 30 min at 100°C. Subsequently, the sections were pre-incubated with 3% Hydrogen Peroxidase Block (Spring Bioscience Corporation, CA, USA) and subsequently incubated with 7% NFDM to block serum proteins. All primary antibodies were diluted at 1:100 in diluent solution for 1 h at room temperature. Universal immuno-enzyme polymer method was used and sections were incubated in immunohistochemical staining reagent for 30 min at room temperature. The identification of antigen–antibody reaction was performed using 3-3'-diaminobenzidine (DAB) and counterstaining with Mayer's hematoxylin. Positive controls were performed by using mouse spleen for F4/80, CD80, and CD206 macrophages while Ly6g-Gr1+ were directly visualized in the inflamed tissues post-surgical trauma. The analysis of immunolabeled cells (Gr, F4/80, CD80, CD206) was performed by a single calibrated investigator using a 100x magnification, considering six histological fields per section, comprising subcutaneous tissue surrounding the Ti-disc. Three samples (biological replicate) for each experimental period and strains were used for quantitative analysis and a total of three sections of each biological replicate were quantified. A grid image was superimposed on the histological photomicrographs, with 10 parallel lines and 100 points in a quadrangular area, by using Image J software (Version 1.51, National Institutes of Health, Bethesda, MD, USA). Only the points coincident with the immunolabeled cells were considered in cell counting and the mean for each section was obtained for statistical analysis.

Real Time PCR Array Reactions

Maxillae and subcutaneous tissue from all experimental groups and time points were dissected and samples containing only the region of the implant bed were storage in RNA stabilization solution (RNAlater, Thermofisher, Waltham, MA, USA) until Real Time PCR array reactions. Samples from the right side (without implant placement) of maxillae and samples from the down right side of subcutaneous tissue (control region remained intact) were used and a Control. Real Time PCR array reactions were performed as previously described (4, 44, 45), using initially a pool of four samples (biological replicates) from all experimental time-points for each group for maxilla and four samples (biological replicates) for subcutaneous tissue. For all experiments, were performed two technical replicates. Pool analysis were performed in order to select targets in which expression variation presented a significant variation compared to the Control side. Subsequently, upregulated targets were analyzed regarding their kinetics of expression for specific time points (3, 7, 14, and 21days) after implant placement. Briefly, the extraction of total RNA from implantation sites and controls was performed with RNeasy kit (Qiagen Inc, Valencia, CA, USA) according to manufacturers' instructions. The integrity of RNA samples was checked by 2100 Bioanalyzer (Agilent Technologies, Santa Clara, CA, USA), and the complementary DNA was synthesized using 3 μg of RNA through a reverse transcription reaction (QuantiTectRTkit, Qiagen Inc, Valencia, CA, USA) (44). The Real Time PCR array was performed in a Viia7 instrument (LifeTechnologies, Carlsbad, CA, USA) using custom panels for "wound healing" (PAMM-121), "inflammatory cytokines and receptors" (PAMM-011), and "Osteogenesis" (PAMM-026) (SABiosciences, Frederick, MD, USA) for gene expression profiling, followed by data analysis with the RT2 Profiler software (SABiosciences, Frederick, MD, USA) for normalizing the initial geometric mean of three constitutive genes (GAPDH, ACTB, Hprt1), following normalizing the Control group; as previously described (4). Data are expressed as heat map fold change relative to the Control group.

Statistical Analysis

Statistical treatment of quantitative data was performed using GraphPad Prism 5.0 software (GraphPad Software Inc., San Diego, CA, USA). Normally distributed data were analyzed using ANOVA followed by Bonferroni's multiple comparison *post-hoc* tests or student's *t*-test where applicable. For non-normal distributions, data were analyzed by means Kruskal-Wallis test (followed by Dunn's test) and Mann-Whitney test. The statistical significance of the experiment involving Real Time PCR array was evaluated by the Mann-Whitney test, and the values tested for correction of Benjamini and Hochberg (49). Values of $p < 0.05$ were considered statistically significant.

RESULTS

Detection of HMGB1 on Sites of Bone and Subcutaneous Implantation

HMGB1 was found to be present in the protein adsorption layer characteristically formed in biomaterials surface after implantation (**Figure 1**), as demonstrated by the protein elution from both Ti-screws implanted in bone and Ti-discs implanted in subcutaneous tissue. HMGB1 was present in relatively high

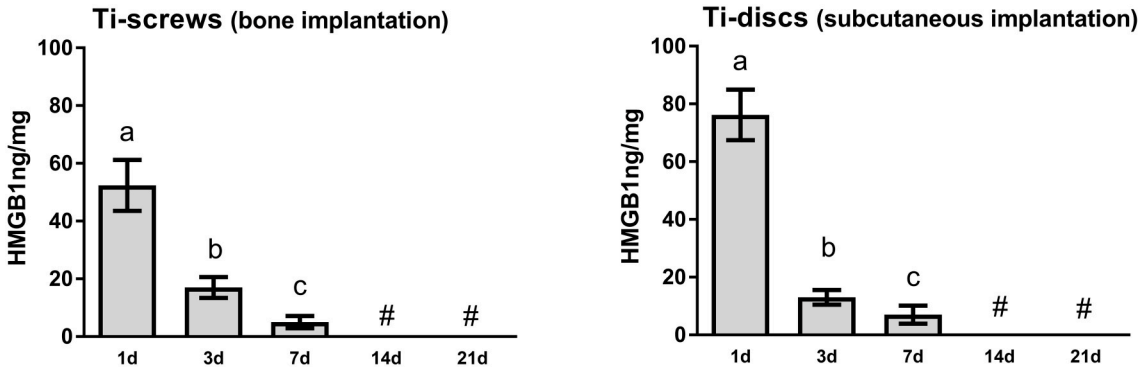

FIGURE 1 | HMGB1 detection in the sites of bone Ti implantation. Ti-screws (implanted in bone) and Ti-discs (implanted into subcutaneous tissue) were retrieved from implantantion sites at 1, 3, 7, 14, and 21 days. Samples were submitted to a protein elution protocol followed by the HMGB1 quantification by ELISA according to the protocol recommended by the manufacturer (MyBioSource). The results were expressed as mean values ± standard deviation nanogram (ng) of protein per milligram of tissue, from a total of five animals/samples (biological replicates) and two technical replicates *per* each group and time point. Different letters indicate significant statistical differences ($p < 0.05$) among time periods in each group, symbol #represent "undectable levels" (Kruskal-Wallis followed by Dunn's test).

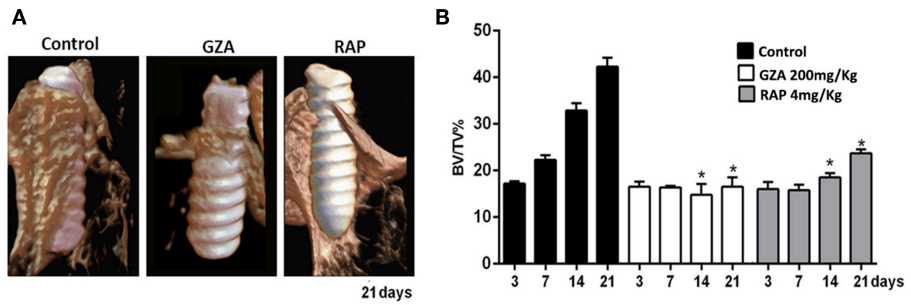

FIGURE 2 | Micro-computed tomography (μCT) analysis of oral osseointegration model in C57Bl/6 mice under HMGB1 or RAGE inhibition. Mice received Ti-screw implantation in the edentulous ridge of maxilla and were divided in according to each treatment: Control (C group, with no treatment); Glycyrrhizic Acid at a dosage of 200 mg/Kg/day (GZA group); or RAGE antagonistic peptide at dosage of 4 mg/Kg/day (RAP group). **(A)** Three-dimensional representative images obtained with the CT-Vox software at 21 days post Ti implantation from Control, GZA, and RAP groups. **(B)** Quantitative analysis of bone volume/tissue volume (BV/TV, %) in the interface bone-Ti along days 3, 7, 14, and 21 post implantation for Control, GZA, and RAP groups. Results are presented as the mean and SD from a total of six biological replicates from each group and time point. Symbol *indicates significant statistical differences ($p < 0.05$) in comparison with control.

concentration in the 1 d time point, followed by a gradual decrease in 3 and 7 days' time points, being non-detectable at the 14 and 21 days' time-points (**Figure 1**), being this pattern similar in bone and subcutaneous implantation sites.

μCT Assessment of Osseointegration

Qualitative and quantitative analyses of mineralized bone matrix revealed a non-significant quantity of bone around Ti threads at 3 days among all groups, whose bone detected around Ti threads characterized the native bone supporting the Ti-implant (**Figures 2A,B**). Detectable, but not statistically significant newly formed bone matrix was observed at 7 days (22.33 ± 1.93) compared to 3 days (17.18 ± 1.11) post Ti-implantation in the Control group, and osseointegration was achieved throughout a gradual and proportion of bone apposition (BV/TV, %) around implant threads at 14 days (32.88 ± 3.16%) and 21 days (42.25 ± 3.86%; **Figure 2B**). On the other hand, the inhibition of HMGB1 and RAGE, in GZA and RAP treated animals, showed a significantly reduced BV/TV around Ti threads at 14 and 21 days compared to the Control group (**Figure 2B**), and DMSO and Saline Solution vehicles treated group as well (data not shown). The mean of BV/TV around implant threads in the GZA treated animals was 14.76 ± 4.06% at 14 days and 16.58 ± 3.40% at 21 days, while in RAP treated animals was 18.53 ± 1.60% at 14 days and 23.69 ± 1.40% at 21 days. The GZA and RAP vehicle control treated groups also achieved osseointegration with no statistical differences compared to the Control (data not shown).

Birefringence of Collagen Fibers on Granulation Tissue and Bone Matrix During Osseointegration

To comprehensively analyze the impact of HGMB1 or RAGE inhibition on organic bone matrix maturation on oral osseointegration in mice, we quantified green, yellow and red spectrum fibers from the bone matrix and initial granulation tissue for all groups (**Figures 3A,B**). All groups showed a negligible quantity of collagen fibers starting at 3 days around the Ti threads, emitting birefringence in the green spectrum (i.e.,

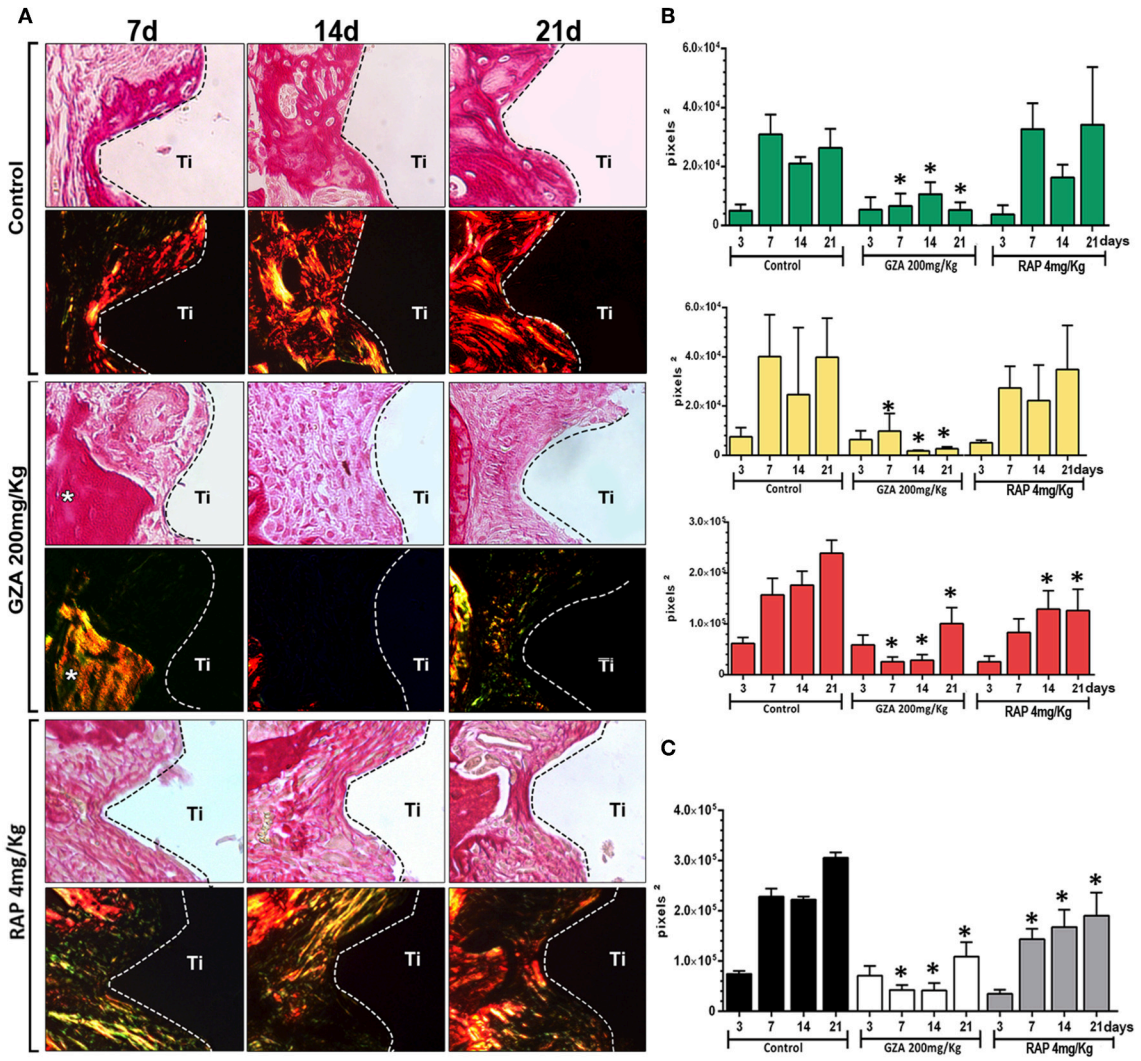

FIGURE 3 | Birefringence analysis of collagen fibers along osseointegration model in C57Bl/6 mice under HMGB1 or RAGE inhibition. Mice received Ti-screw implantation in the edentulous ridge of maxilla and were divided in according to each treatment: Control (C group, with no treatment); Glycyrrhizic Acid at a dosage of 200 mg/Kg/day (GZA group); or RAGE antagonistic peptide at dosage of 4 mg/Kg/day (RAP group). **(A)** Representative sections from oral osseointegration process upon polarized and conventional light, to evaluate collagen fibers maturation along days 3, 7, 14, and 21 post-Ti-screw implantation in the different experimental groups. As visualized upon polarized light, green birefringence color indicates thin fibers; yellow and red colors at birefringence analysis indicate thick collagen fibers. Original magnification 40x. **(B)** Intensity of birefringence measured from Image-analysis software (AxioVision, v. 4.8, CarlZeiss) to identify and quantify area of collagen from each birefringence color (pixels 2) and **(C)** total area of collagen fibers (pixel2) throughout experimental periods. Results are presented as the mean and SD of pixels2 for each color in the birefringence analysis, from a total of six animals/samples (biological replicates) and four technical replicates *per* each group and time point. Symbol *indicates a statistically significant difference vs. control ($p < 0.05$).

immature and thinner fibers). From 7 to 21 days, the Control group showed a significant increase in yellow and red collagen fibers, suggesting organic bone matrix maturation. Conversely, inhibition of HMGB1 in GZA treated mice caused a drastic impairment of bone collagen fibers formation, with significantly reduced amount of all birefringent type of fibers from 7 to 21 days compared to the Control. Under inhibition of RAGE (RAP treated mice), there was also impaired formation and maturation of collagen fibers, with a significantly reduced amount of total fibers at 14 and 21 days compared to the Control. No significant differences were observed in the dynamics of collagen fibers formation and maturation during osseointegration between GZA and RAP Control vehicle treated groups (data not shown).

Histopathological Description and Histomorphometry of Healing Components During Osseointegration

Histopathological analysis revealed osseointegration in the Control group, with intramembranous bone healing following overlapping phases from 3 to 21 days post Ti-implant placement in mice (**Figure 4**). Similar histological dynamics of

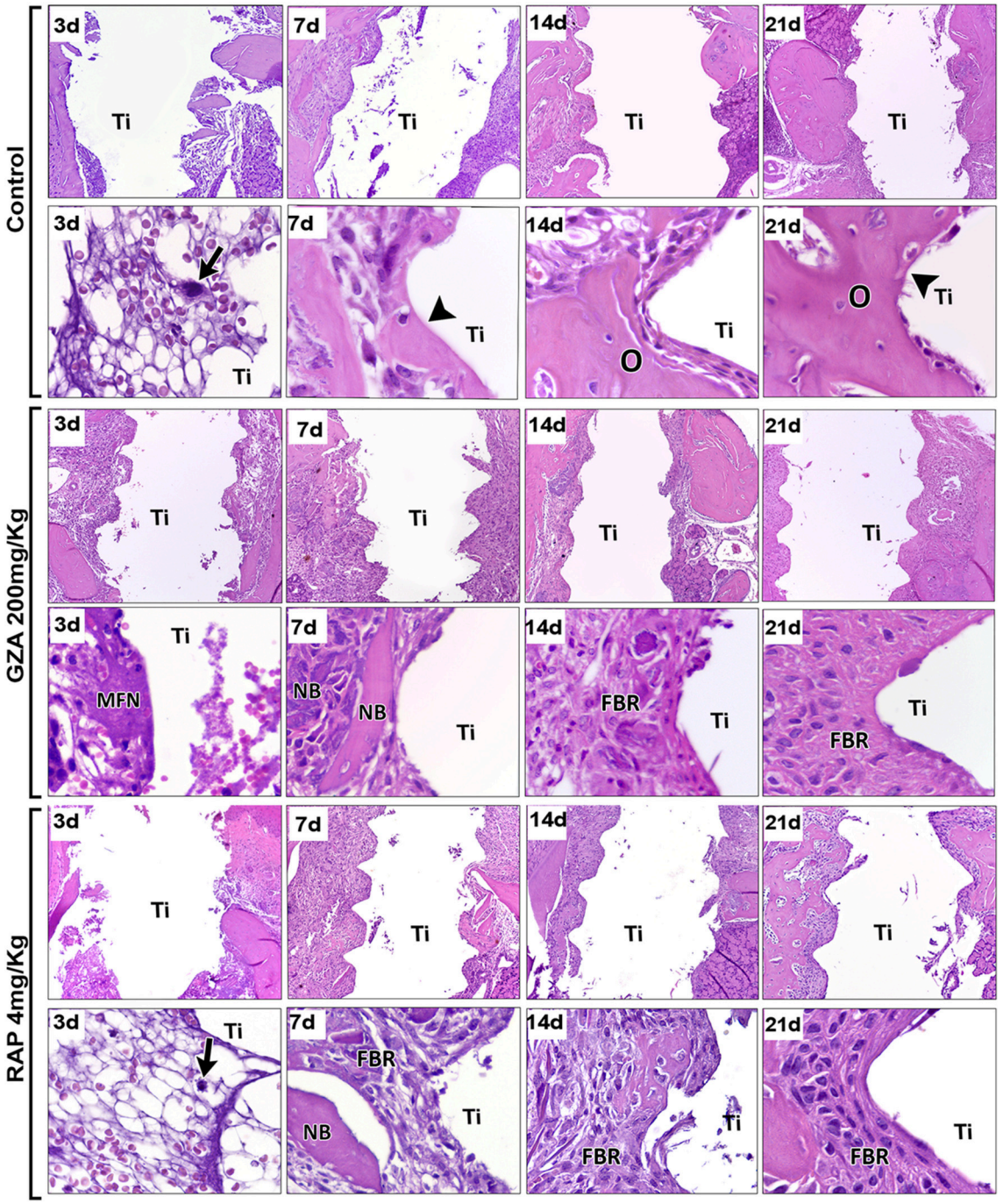

FIGURE 4 | Histopathological analysis along oral osseointegration model in C57Bl/6 mice under HMGB1 or RAGE inhibition. Mice received Ti-screw implantation in the edentulous ridge of maxilla and were divided in according to each treatment: Control (C group, with no treatment); Glycyrrhizic Acid at a dosage of 200 mg/Kg/day (GZA group); or RAGE antagonistic peptide at dosage of 4 mg/Kg/day (RAP group). Chronology of oral osseointegration is observed throughout days 3, 7, 14, and 21 days. Histological slides were stained with H&E and images were captured at 10 and 100x magnification. Ti, Ti screw space; BC, Blood clot; Arrows, fibrin supporting cell migration; Arrowheads, bone/Ti contact region; O, osseointegration; MFN, Malformed fibrin network; NB, Necrotic bone; FBR, Foreign Body Reaction.

osseointegration were observed in the GZA or RAP vehicle treated groups (data not shown). On the other hand, both experimental groups treated with RAP or GZA, exhibited failure of osseointegration, with the typical presence of fibrous connective tissue and foreign body giant cells (FBGC) formation at 14 and 21 days post-Ti implantation. At 3 days, the bone-implant interface in the Control group was filled predominantly by a blood clot (**Figure 5A**) providing support for cell infiltration

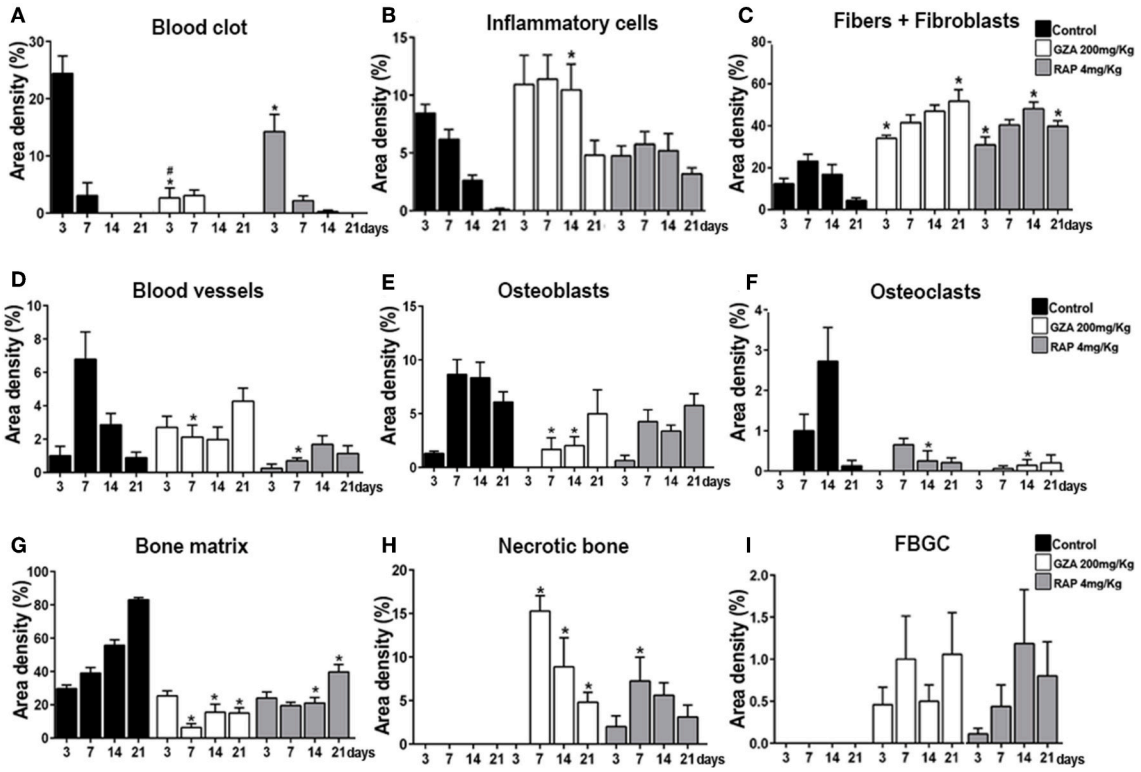

FIGURE 5 | Histomorphometric analysis of healing components along oral osseointegration model in C57Bl/6 mice under HMGB1 or RAGE inhibition. Mice received Ti-screw implantation in the edentulous ridge of maxilla and were divided in according to each treatment: Control (C group, with no treatment); Glycyrrhizic Acid at a dosage of 200 mg/Kg/day (GZA group); or RAGE antagonistic peptide at dosage of 4 mg/Kg/day (RAP group). Results are presented as the means (± SD) of area density for each component related to osseointegration process: **(A)** Blood Clot, **(B)** Inflammatory cells, **(C)** Fibers + Fibroblasts, **(D)** Blood vessels, **(E)** Osteoblasts, **(F)** Osteoclasts, **(G)** Bone matrix, **(H)** Necrotic Bone, and **(I)** FBGC. Results are presented as the mean and SD from a total of six animals/samples (biological replicates) and nine semi-serial sections (technical replicates) *per* each group and time point. Symbol *indicate a statistically significant difference vs. control, #indicate differences between RAP and GZA groups ($p < 0.05$).

(**Figure 4**, arrow). At 7 days, increased quantities of granulation tissue components were observed (blood vessels, fibroblasts, and fibers; **Figures 5C,D**), as well an initial differentiation of osteoblasts and bone matrix from the Ti threads and bone edges (**Figure 4**, arrowheads). At 14 and 21 days, granulation tissue components significantly decreased around Ti threads spaces, followed by an increased quantity of osteoblasts and bone matrix in the same regions (**Figures 4**, **5E,G**) resulting in direct contact between implant and bone (**Figure 4**, arrowheads). Furthermore, Control and vehicle groups exhibited osteoclastic resorption lacunae and a few quantities of osteoclasts found around bone debris and pre-existing bone during 3 and 7 days post Ti implantation, followed by osteoclastic remodeling of newly formed bone at 14 and 21 days.

Comparatively to the osseointegration observed in the Control group, RAP treated mice also showed a suitable blood clot formation the bone-implant interface, but in a slighted reduced number, surrounded by an eosinophilic and slight matrix of fibrin network, with identifiable support for cell migration (**Figure 4**, arrows). On the other hand, the inhibition of HMGB1 in GZA treated mice resulted in a disorganized blood clot, with agglomerated platelets (#) and red blood cells separated from the malformed fibrin networks (MFN) (**Figure 4**, GZA group and **Supplementary Figure 1**) and a drastically reduced area density of this component (**Figure 5A**). Both RAP and GZA treated mice showed necrotic/non-viable bone persisting at 7–21 days post Ti-implantation, as well a foreign body reaction (FBR) with the presence of FBGC (**Figures 4**, **5H,I**). The inhibition of RAGE in RAP group leaded to a negligible higher quantity of osteoblasts and bone formation in scattered areas surrounding Ti thread spaces compared to HMGB1 inhibition in GZA group (**Figures 4**, **5E**). No statistical differences were observed in quantitative results for other elements (empty spaces, artifacts and Ti space; data not shown).

Gene Expression Patterns in Osseointegration Under HGMB1 or RAGE Inhibition

A pool of samples from all periods post-Ti implantation were initially analyzed by means of an exploratory Real Time PCR array (**Figure 6**), considering molecules involved in inflammatory response and bone healing (growth factors; immunological/inflammatory markers; extracellular matrix,

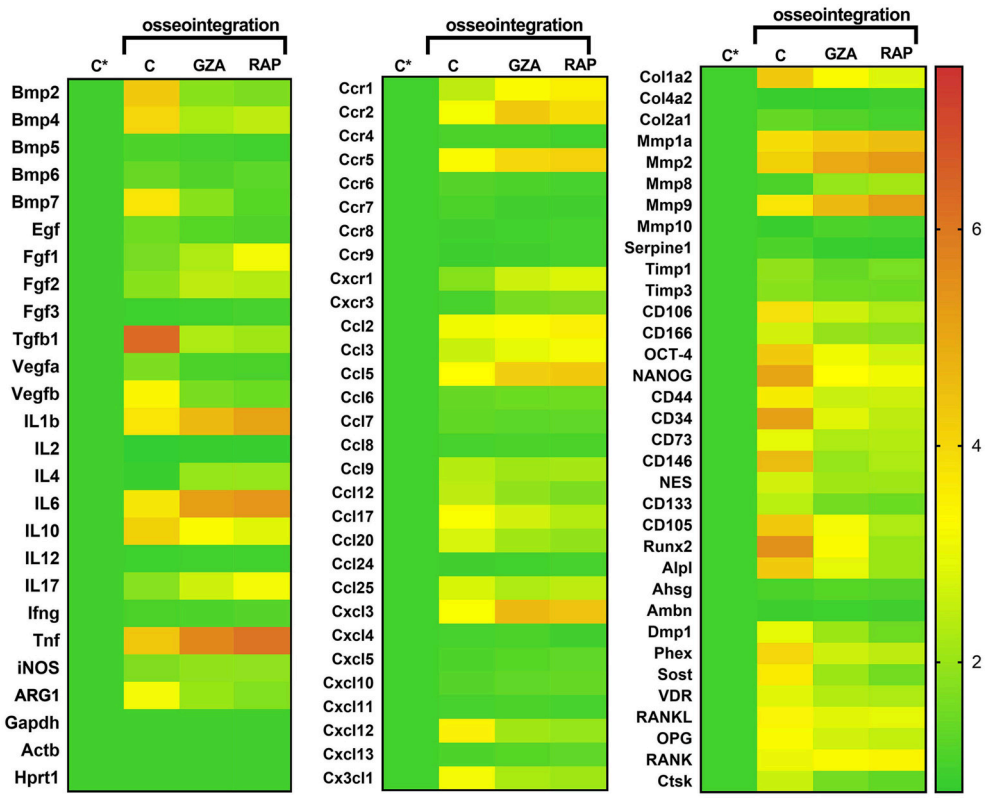

FIGURE 6 | Gene expression patterns in the osseointegration sites under HMGB1 or RAGE inhibition. Mice received Ti-screw implantation in the edentulous ridge of maxilla and were divided in according to each treatment: Control (C group, with no treatment); Glycyrrhizic Acid at a dosage of 200 mg/Kg/day (GZA group); or RAGE antagonistic peptide at dosage of 4 mg/Kg/day (RAP group) Right side without Ti-screw implantation was used as tissue control and represented as **C***. Molecular analysis of the gene expression patterns in the region of Ti screw implantation was comprised of an initial exploratory analysis by Real Time PCR array for each experimental group (Control, RAP and GZA), considering a pool of four samples (biological replicates) and two technical replicates from all the experimental periods (3, 7, 14, 21 days). Real Time PCR array analysis was performed with the VIA7 system (Applied Biosystems Limited, Warrington, Cheshire, UK) using a customized qPCR array comprised of the major targets from the Osteogenesis, Inflammatory Cytokines & Receptors and Wound Healing panels of the PCRarrayRT2 Profiler (SABiosciences/QIAGEN, Gaithersburg, MD, USA). Results are depicted as the fold increase change (and the standard deviation) in mRNA expression from triplicate measurements in relation to the control samples and normalized by internal housekeeping genes (GAPDH, HPRT, β-actin).

MSC, and bone markers). Experimental groups (C, GZA, and RAP) were depicted as the fold increase change in relation to Control samples (C*), which are from the right side of maxilla of C57Bl/6 untreated mice, without surgery. Next, targets with a significant expression significant variation expression in pooled samples were analyzed according to their kinetics of expression during experimental periods (**Figure 7**).

For oral osseointegration model, among growth factors, TGFβ1, and VEGFb were significantly upregulated in C group, such as several MSC putative markers (OCT-4, NANOG, CD44, CD34, CD73, CD146, CD105, CXCL12); while the inhibition of HMGB1 (GZA group) and RAGE (RAP group) resulted in an important reduction in the mRNA levels for all these targets in pooled samples (**Figure 6**). Considering MSC putative markers, mRNA levels peaked at 3 and 7 days at osseointegration Control group and were significantly increased compared to GZA and RAP treated mice, as well TGFb and CXCL12. A slight upregulation for MSC markers were observed in GZA and RAP group compared to Control samples (C*).

Considering bone markers related to osteoblast differentiation (BMP2, BMP4, BMP7, Runx2, ALPL, DMP1, Phex, Sost, VDR) and bone remodeling (RANKL, OPG, CTSK), were positively upregulated in osseointegration Control group, whereas their expressions were drastically reduced in GZA and RAP group, as observed in pooled samples. On the other hand, RAP group presented an upregulation of FGF1 and FGF2 (**Figure 6**). In the osseointegration Control group, the kinetics of BMP2 mRNA levels peaked at 7 days and BMP4 peaked at 14 days. Runx2 and ALPL were upregulated at 7 and 14 days, significantly decreasing at 21 days, while Phex (a osteocyte differentiation marker) was upregulated at 14 days and 21 days (**Figure 7**).

Considering immunological markers for M1/M2 macrophages, a higher expression of ARG1 and IL10, markers for M2 phenotype, was particularly found in the osseointegration process of the Control group compared to the Control tissue (C*), but it was not observed in GZA and RAP treated mice (**Figure 6**). The mRNA levels of these M2 markers peaked at 7 and 14 days, as well TGFb in osseointegration Control group (**Figure 7**). The majority of chemokines and their receptors involved in inflammatory cells migration (CCR1, CCR2, CCR5, CCL2, CCL3, CCL5, CCL9, CCL12, CCL17, CCL20, CCL25, CXCL3, CXC3CL1) were upregulated in osseointegration

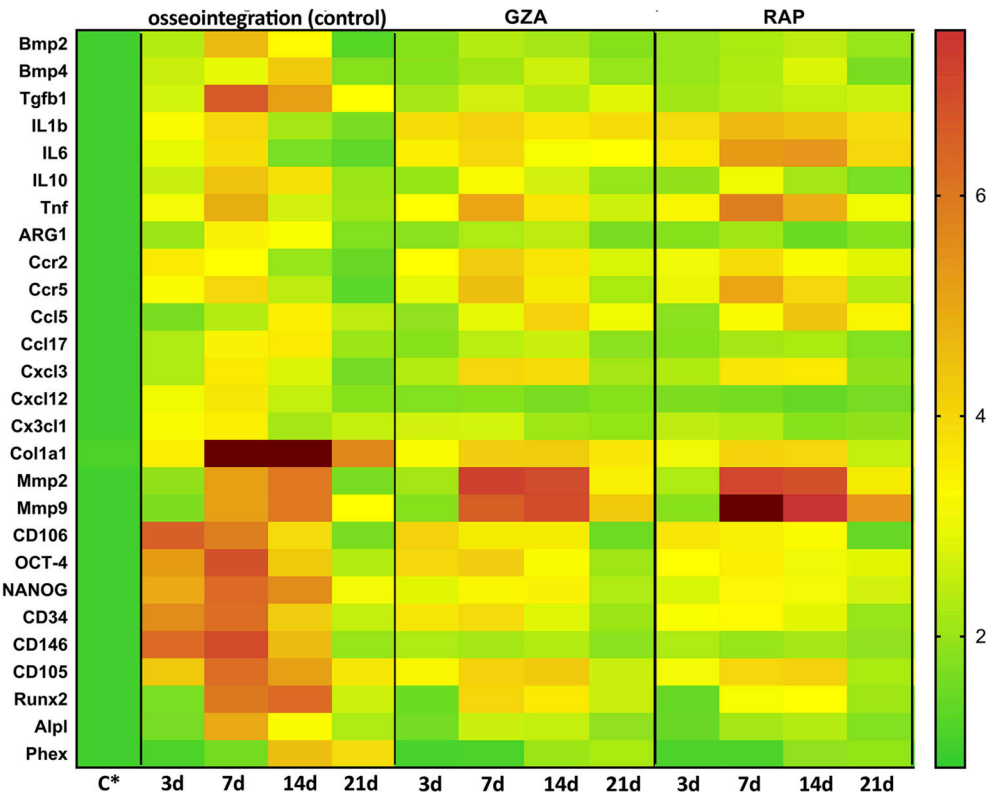

FIGURE 7 | Kinetics of gene expression in the oral osseointegration sites under HMGB1 or RAGE inhibition. Mice received Ti-screw implantation in the edentulous ridge of maxilla and were divided in according to each treatment: Control (C group, with no treatment); Glycyrrhizic Acid at a dosage of 200 mg/Kg/day (GZA group) or RAGE antagonistic peptide at dosage of 4 mg/Kg/day (RAP group). Right side without Ti-screw implantation was used as tissue control and represented as **C***. Molecular analysis of the gene expression in the region of Ti screw implantation was performed following each experimental time point (3, 7, 14, and 21 days), considering four samples (biological replicates) and two technical replicates *per* each group and time point. Targets with a significant expression variation in the previous Real Time PCR array from pooled samples were selected. Real Time PCR array analysis was performed with the VIA7 system (Applied Biosystems Limited, Warrington, Cheshire, UK) using a customized qPCR array comprised of the major targets from the Osteogenesis, Inflammatory Cytokines & Receptors and Wound Healing panels of the PCRarrayRT2 Profiler (SABiosciences/QIAGEN, Gaithersburg, MD, USA). Results are depicted as the fold increase change (and the standard deviation) in mRNA expression from triplicate measurements in relation to the control samples and normalized by internal housekeeping genes (GAPDH, HPRT, β-actin).

sites in the Control group. On the other hand, GZA and RAP treated mice presented a higher expression of CCR2, CCR5, CCL5, and CXCL3 compared to the osseointegration C group in pooled samples (**Figure 6**). Also, pro-inflammatory cytokines were differentially expressed in osseointegration C group compared to the GZA and RAP groups (**Figures 6**, **7**). While pro-inflammatory cytokines (IL1b, IL6, TNF), as well chemokine receptors (CCR2, CCR5) and chemokines (CCL5, CXCL3) were upregulated in early time points (3 and 7 days) in the osseointegration group, their mRNA levels remained upregulated in late time points (14 and 21 days) in GZA and RAP groups.

Finally, among the extracellular matrix markers, Col1a1, MMP2, and MMP9 were upregulated in all experimental groups (**Figure 6**). However, the kinetics of these markers were differently regulated comparing GZA an RAP groups to the osseointegration C group (**Figure 7**). In this way, mRNA levels of Col1a1 were significantly upregulated in the osseointegration Control sites at 7 and 14 days compared to GZA and RAP groups. On the other hand, GZA and RAP treated mice presented higher mRNA levels for MMP2 and MMP9 compared to the Control osseointegration sites (**Figure 7**).

Histomorphometric, Birefringence, Immunohistochemical, and Molecular Analysis of Subcutaneous Healing Under Ti Implantation

Control and both GZA and RAP control vehicle treated mice showed a suitable blood clot formation and a slight inflammatory infiltrate at 3 days, followed by a dense connective tissue formation, containing fibroblasts and negligible quantities of inflammatory cells surrounding region of Ti-disc implantation at 14 days (**Figure 8A**). Also, birefringence analysis revealed a yellow/red spectrum of collagen fibers surrounding the Ti at 14 days (**Figure 8B**). On the other hand, the inhibition of HMGB1 by GZA treatment caused a disruption of blood clot formation at 3 days (arrow, **Figure 8**) and a persistence

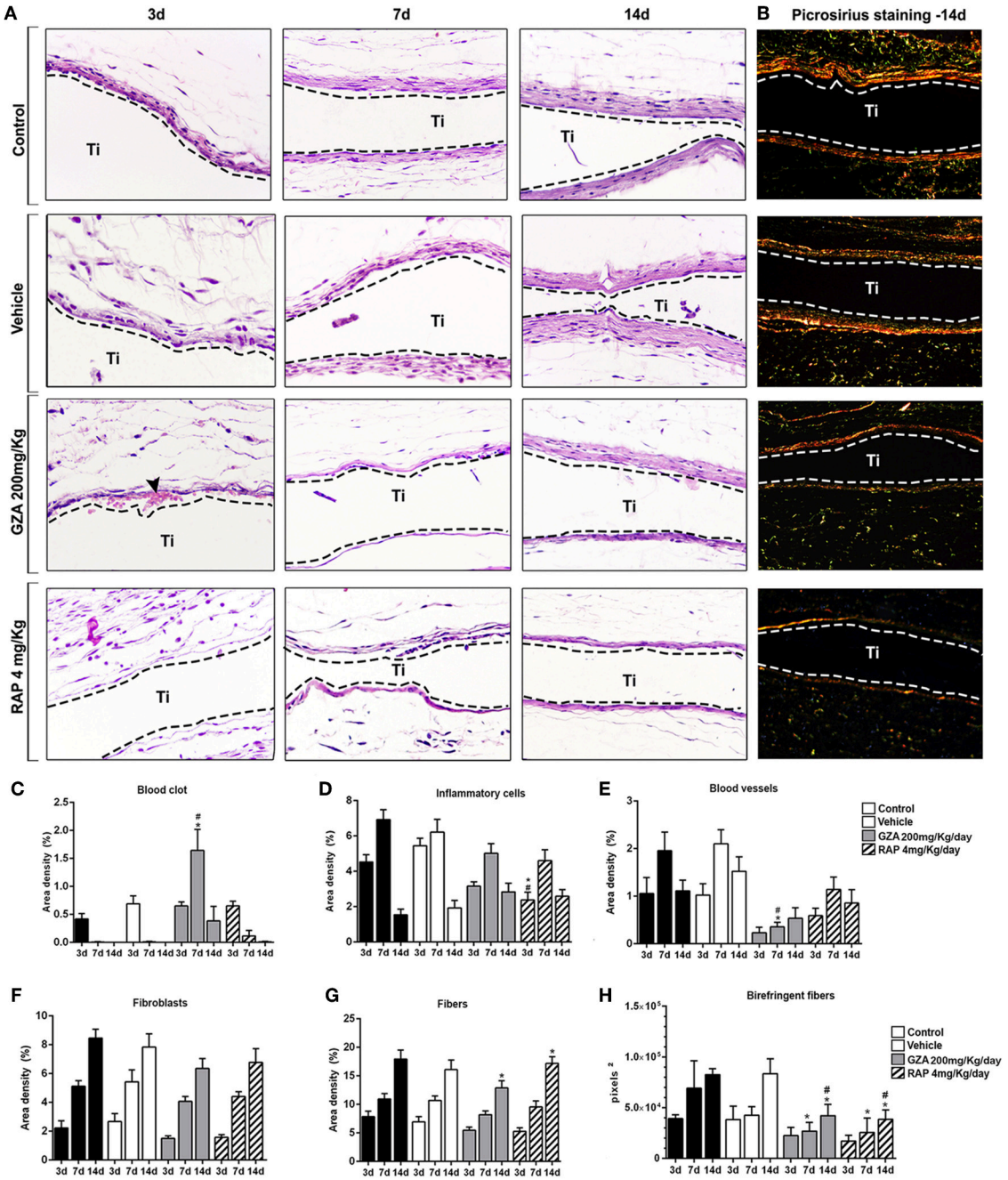

FIGURE 8 | Histophatological, histomorphometric, and birefringence analysis of subcutaneous tissue post implantation of Ti-disc in C57Bl/6 mice under HMGB1 or RAGE inhibition. Mice received Ti-disc implantation in the subcutaneous tissue and were divided in according to each treatment: Control (C group, with no treatment); Vehicle (1.5% DMSO solution); Glycyrrhizic Acid at a dosage of 200 mg/Kg/day (GZA group); or RAGE antagonistic peptide at dosage of 4 mg/Kg/day (RAP group). Vehicle or drugs were administered 1 day before the surgical procedure and were given until the end of experimental periods (3, 7, and 14 days). **(A)** Comparative morphology of the healing phases post Ti disc implantation for each group, stained with H&E (40x magnification) and **(B)** Picrosirius red. **(C–G)** Results from histomorphometry of healing parameters (blood clot, inflammatory cells, fibroblasts, fibers, and blood vessels) are presented as the mean of area density for each structure measured in each examined group. Results are presented as the mean and SD from a total of five animals/samples (biological replicates) and eight semi-serial sections (technical replicates) *per* each group and time point. **(H)** Intensity of birefringence performed using image-analysis software (AxioVision, v. 4.8, CarlZeiss) for total area of birefringent collagen fibers (pixels^2). Results are presented as the mean and SD from a total of five animals/samples (biological replicates) and four semi-serial sections (technical replicates) *per* each group and time point. **(C–H)** Symbols indicate statistically significant difference ($p < 0.05$) between experimental groups (GZA and RAP) vs. Control* and experimental groups vs. Vehicle$^{\#}$ at the same time point.

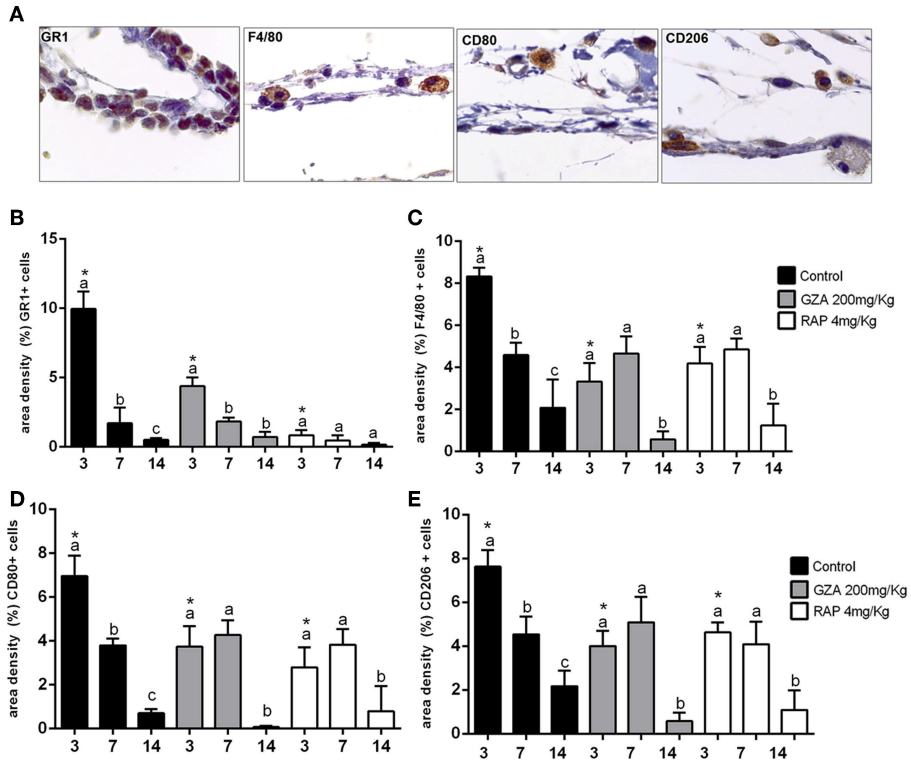

FIGURE 9 | Inflammatory cells recruited to the Ti disc implantation sites in C57Bl/6 mice treated with HMGB1 inhibitor or RAGE antagonist. Mice received Ti-disc implantation in the subcutaneous tissue and were divided in according to each treatment: Control (C group, with no treatment); Vehicle (1.5% DMSO solution); Glycyrrhizic Acid at a dosage of 200 mg/Kg/day (GZA group); or RAGE antagonistic peptide at dosage of 4 mg/Kg/day (RAP group). Vehicles or drugs were administered 1 day before the surgical procedure and were given until the end of experimental periods (3, 7, and 14 days). **(A)** Representative sections of 3 days time point post Ti implantation. Quantitative analysis of **(B)** GR1+, **(C)** F4/80+, **(D)** CD80+cells and **(E)** CD206+ cells was performed for each group at days 3, 7, and 14 days post Ti implantation. Results are presented as the mean and SD from a total of five animals/samples (biological replicates) and three semi-serial sections (technical replicates) *per* each group and time point. Different letters indicate significant differences in each time point ($p < 0.05$); symbol *indicate significant differences between experimental groups (GZA and RAP) vs. control at the same time point.

of blood clot and a decreased area density of blood vessels around Ti disc implantation at 7 days (**Figures 8C,E**). Similarly, both treatments (the inhibition of HMGB1 and the antagonism of RAGE), impaired the host response to the Ti disc by a decreased collagen fiber formation compared to the control and control vehicles, but with no negative effects in the amount of fibroblasts (**Figures 8F,G**). The reduced tissue repair in GZA and RAP could be mainly associated with an ineffective inflammatory response caused by the inhibition of inflammatory signals induced by HMGB1 and RAGE. Immuhistochemistry of GZA and RAP group showed a drastic reduction of GR1+ cells and macrophages (F4/80+ cells, CD80+ cells, CD206+ cells) migration toward the implantation sites at 3 days post Ti implantation compared to the Ti control group (**Figures 9A–E**).

In parallel and in agreement with molecular results for oral osseointegration model, the gene expression patterns in subcutaneous implanted sites on Ti control was also revealed growth factors involved in cell proliferation (FGF1, FGF2, FGF3, TGFb1, EGF) and angiogenesis (VEGFa,b) significantly up-regulated in the Ti Control group compared to the endogenous control (**Supplementary Figure 2**). Consistently, tissue healing and maturation of the ECM was also evidenced in Ti control by a high upregulation of ECM remodeling markers, such as the matrix metalloproteinases (MMP1a, MMP2, MMP9) and their tissue inhibitors TIMPs (TIMP1, TIMP3), as well the protease cathepsin G (CTSG). Among the upregulated cytokines in Ti control samples, CXCL10, CXCL12, CXCL11, IL1β, IL6, TNF were up regulated in the inflammatory phase of healing. Growth factors involved in cell proliferation, mainly for FGF family, were up regulated in GZA and RAP, such as in the Control group, while several ECM formation (Col1a2, Col2a1) and remodeling markers (MMP1a, MMP2, MMP9, TIMP1, TIMP3, CTSG) were down regulated GZA and RAP compared to the control. Importantly, GZA and RAP group presented a downregulation of molecules involved in cell adhesion and migration (CTGF, VTN, ITGA2, ITGA4, ITGA5). All together, these results indicate a role of HMGB1 and RAGE on fibroblasts migration, differentiation, and matrix deposition along tissue repair surrounding a classic biomaterial.

DISCUSSION

Among the several DAMPs and their accompanying PRRs, the interaction of HMGB1 with the receptor RAGE has

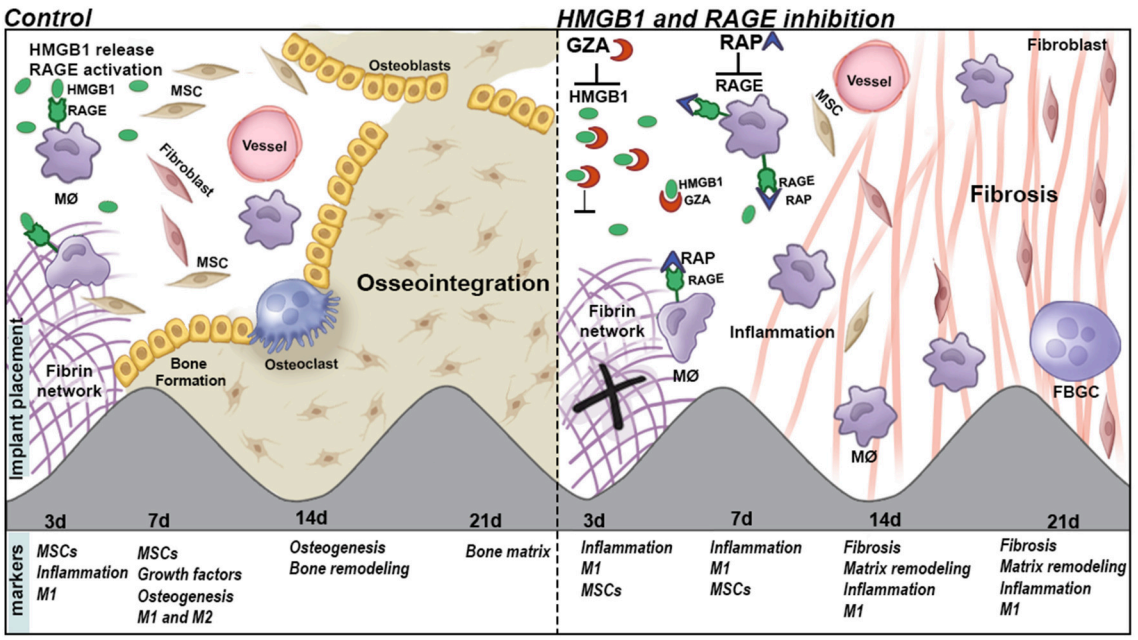

FIGURE 10 | Graphical abstract of proposed roles of HGMB1 and RAGE along oral Ti osseointegration process in mice.

been associated with the activation of inflammatory responses and wound healing, especially in non-infectious environments (18, 19, 22). In this study, the possible involvement of the HMGB1/RAGE pathway in the modulation of host inflammatory immune response at Ti/host interface, and the subsequent influence in the healing and osseointegration processes were investigated. Therefore, to determine the role of HMGB1 and RAGE in the osseointegration process in a cause-and-effect manner, C57Bl/6 mice were subjected to Ti-implant surgical placement in the maxillary edentulous area and were treated with GZA and RAP, respectively, an HMGB1 inhibitor (41) and a RAGE inhibitor (42).

Initially, our results demonstrated that HMGB1 was present in the protein adsorption layer characteristically formed in biomaterials surface after implantation, in both Ti-screws implanted in bone and Ti-discs implanted in subcutaneous tissue (**Figure 1**). Importantly, despite the general assumption that endogenous DAMPs are released upon biomaterials implantation, this is the first actual demonstration that DAMPs (specifically HMGB1) are in fact released and can adsorb to Ti surface. The kinetics of HMGB1 release and adsorption is in agreement with the hypothesis of the injury-triggered release, characterized by high levels in the initial time point followed by a gradual decrease over time (50–52). Also, our results demonstrated that inhibition of both, HMGB1 and RAGE, impaired Ti-mediated osseointegration, as demonstrated by the critical alterations in the dynamics of mineralized and organic bone matrix formation (**Figures 2**, **3**). Accordingly, the inhibition of HMGB1 in a model of tooth extraction in mice significantly delayed the bone healing process, but without inhibiting it completely (21). However, it is crucial to consider that in the present study, the presence of a biomaterial is an important variable in the healing site; which may account for the complete impairment of the osseointegration process in comparison with the partial influence of HMGB1 inhibition described in the socket healing (21). Importantly, no previous studies have described possible associations between RAGE blockade and bone healing or osseointegration. It is also important to mention that HMGB1 and RAGE blockade impair the healing of subcutaneous tissue after the grafting of a Ti-disc, reinforcing the role of HMGB1/RAGE axis in the host response to biomaterials and in the subsequent healing response. While the subcutaneous implantation of Ti-devices obviously does not mimic the osseointegration response, it have been considered a valuable model to study biomaterial/host interaction (53), which can be very useful, especially in mice in the view of the very limited dimensions of the Ti implant used for osseointegration analysis, which limits some experimental approaches.

In order to investigate the mechanisms underlying impaired osseointegration due HMGB1 and RAGE inhibition, a series of histomorphometric, and molecular analysis were performed, comparing unsuccessful and successful osseointegration sites. The process of osseointegration starts with the surgical preparation of the bone niche/defect for implant placement, when coagulation proteins from blood are released and then activated to provide the clot formation and consequently a provisional matrix for cell recruitment and migration (15). Accordingly, in the Control group (which achieved osseointegration), an organized blood clot was evidenced at the host/Ti interface at 3 days post-implantation. However, HMGB1 inhibition resulted in disruption of fibrin network formation and

impairment of the blood clot structure, followed by a significant decrease in blood clot area density when compared to the Control group. Indeed, HMGB1 acts synergistically with thrombin to promote fibrin deposition and accelerate the coagulation *in vivo*, evidencing its role as an organizer in post-injury wound healing (54). Thus, the initial event of osseointegration impairment due to GZA administration seems to be primarily related to the disruption of the blood clot, since the establishment of a fibrin network in association with Ti threads spaces was drastically compromised upon HMGB1 inhibition. Additionally, RAGE inhibition also resulted in a reduction of blood clot area density when compared to the Control group, but without drastic effects over clot organization as observed upon HMGB1 inhibition. Accordingly, while HMBG1 seems to also act in the clotting process directly (i.e., in a RAGE independent way), RAGE expressed on platelets surface is associated with their activation by DAMPs (HMGB1 and S100 proteins) and platelet aggregation (55, 56), which consequently influence the clotting process, but also the release of additional HMGB1 and other pro inflammatory molecules (56, 57).

In addition to the initial interferences in the clotting process, previous studies demonstrated that HMGB1 promotes the secretion of multiple cytokines in the injured sites, strongly activating and driving the acute inflammatory response (58). Also, it is important to consider that HMGB1 is supposed to play also biphasic actions on injured sites (pro-inflammatory activity or immune tolerance/healing) depending of the environment redox state of its three conserved cysteines (Cys23, Cys45 [Box A], and Cys106 [BoxB]) (23). In this context, it has been proposed that during acute inflammatory response, the release of ROS/RNS induce the active and proinflammatory form of HMGB1 (reduced form of HMGB1); while the oxidation of HMGB1 cause immune tolerance, allowing the healing (22, 23). Considering the receptor RAGE, it is important to mention that two extracellular secreted forms of RAGE can be also present in the environment, besides the conventional receptor, they are endogenous secretory (es) and soluble (s) RAGE, have been identified and play active roles on skeletal biology, mainly related to osteoporosis in aged mice (59). It has been supposed that these RAGE isoforms (mainly sRAGE), could also their ligand-binding ability, acting as decoy receptors preventing ligand binding to RAGE. Importantly, while the analysis of redox modulation of HMGB1 activities, as well of a putative role for sRAGE, are beyond the scope of the present study, since our data point to a role for HMGB1 in osseointegration process, future specific studies focused in such elements may provide additional interesting information to the field.

In this study, HMGB1 or RAGE inhibition disturbed the natural course/fate of inflammatory response after Ti implantation. This resulted in the persistence of inflammatory cells around Ti threads until latter time points, comprising primarily macrophages as suggested by the cellular morphology, while Control mice exhibited the resolution of a transient inflammatory response in early time points (**Figure 4**). Accordingly, the molecular analysis demonstrated that HMGB1 or RAGE inhibition resulted in a persistence of high mRNA levels of CCR2, CCR5, CCL5, which are mainly associated with macrophage migration (48, 60), as well as pro-inflammatory cytokines (IL1b, IL-6, and TNF) that characterize M1 activity (61). Thus, our findings suggest a role of HMGB1 and RAGE on the modulation/resolution of chronic inflammatory response post Ti implantation, probably affecting the overall M1/M2 macrophages response. While the reduced size of the Ti-device limits some additional analysis, the subcutaneous implantation of Ti-discs allowed the characterization of the inflammatory changes upon HMGB1 and RAGE blockade, and demonstrate that the total macrophages, M1 and M2 cells counts were reduced in the absence of a functional HMGB1/RAGE axis. Macrophages are considered key elements in the connection between inflammatory and healing events (11). The initial presence of M1 macrophages has been implicated as an essential step for the activation of acute inflammatory response, while the transitory presence of M2 cells in the proliferative/regenerative phase has been suggested as favorable for the regenerative outcome (11). Conversely, a prolonged M1 activity has been associated with negative outcomes of biomaterial implantation, such as chronically inflamed tissue and severe foreign body reaction (FBR) (37). Considering the osseointegration and subcutaneous results, it is possible to suggest that HMGB1/RAGE axis is required for a proper macrophage chemoattraction after Ti implantation, and that both M1 and M2 responses, and the natural M1/M2 switch along the healing, are compromised by HMGB1 and RAGE inhibition. Accordingly, the molecular analysis of the successful Ti-osseointegration sites in the Control group demonstrated an initial M1-type response followed by a M2-type switch, evidenced by upregulation of M2-type markers (ARG1, TGFb, IL10, and CCL17) (62), which were disrupted by HMGB1/RAGE blockade. These observations are in agreement with previous studies (4, 5, 63). In view of that, the provision of environmental cues that govern the phenotype switch of macrophages and different healing outcomes post biomaterial implantation have been usually based on the biomaterial properties, in a perspective where Ti-based devices might modulate or allow a favorable M1/M2 switch (9). However, we demonstrated that inhibition of a DAMP or its receptor (HMGB1 or RAGE) following biomaterial implantation, can also drastically affect the initial microenvironmental signals for triggering osseointegration, even using a gold standard biomaterial such as a Ti-based device. Significantly, the effects of HMGB1 or RAGE inhibition are not limited to macrophages, as demonstrated by the significant reduction of granulocytes (Gr1+ cells) in the Ti disc implantation. While the main of focus in the cellular aspects of osseointegration (and in the biomaterials in general) have been over macrophages (9, 62), granulocytes are essential elements of early host response (64), and consequently can also theoretically impact the subsequent healing and osseointegration.

The lack of favorable biological microenvironment signals in biomaterial implantation sites can result in persistent chronic inflammation, consequently driving the wound healing around the biomaterial into a foreign body response (FBR) (65). In this manner, HMGB1 and RAGE inhibition drastically reduced the expression of MSC markers and bone markers in the sites

of Ti implantation, which was reflected in a fibrotic outcome surrounding Ti threads (**Figures 6**, **7**), with features of FBR, such as differentiation of FBGC surrounding the biomaterial and non-viable bone (**Figure 4**), increased expression of MMPs (**Figure 7**), followed by fibrous tissue formation and consequent biomaterial encapsulation (**Figure 4**). As previously proposed by literature, the modulation of host response for desirable biomaterial incorporation outcome is in part surface-based, depending on beneficial biomaterial properties, but signals provided from biomaterial implantation trauma have also been suggested as crucial cues in this process (9). Accordingly to the Control group results, in the presence of a constructive set of external and endogenous factors, including Ti as the external factor and HMGB1 and RAGE as part of endogenous factors, the inflammatory signals triggered post Ti implantation was linked to upregulation of MSC markers (CD206, OCT-4, NANOG, CD44, CD34, CD73, CD146, CD105) at earlier time points (3 and 7 days), and subsequent bone cells differentiation (Runx2, Alp), bone matrix deposition (Col1a1), remodeling (MMP2 and MMP9) (45), and bone maturation (Phex) (66) (**Figure 7**).

The body of this work suggests the participation of HMGB1 in multiple stages of osseointegration process, as a blood clot organizer and inflammatory/healing molecule (**Figure 10**). Several studies have suggested that HMGB1 can act as a regenerative mediator, by triggering inflammation (20), but also as a healing organizer, promoting the recruitment of MSCs, and platelets activation (20, 58). In this cause-effect study, the inhibition of extracellular HMGB1 following biomaterial implantation caused failure of Ti-mediated osseointegration (**Figures 2**–**5**), which could be associated to its multiple roles acting as a biochemical mediator for clot formation (54, 56, 67), as well as by triggering of signaling inflammatory pathways, which involve the activation of different receptors, such as RAGE. In fact, under the inhibition of RAGE, the immediate extracellular effects of released HMGB1 were maintained, such as confirmed by a suitable blood clot structure in the osseointegration sites at 3 days compared to the HMGB1 inhibition group. However, under the inhibition of RAGE, the HMGB1 cellular effects related to HMGB1/RAGE pathway was blockade, which also resulted in unsuccessful osseointegration.

It is also important to consider the despite the fact that a clear biological effect was observed upon the administration of the RAP and GZA in this study, the dosages used for both inhibitors were based in previous studies carried in C57Bl/6 mice but in different models and kinetics of drug administration (41, 42). Despite the effects observed in our study are compatible with the biological role of HMGB1 and RAGE, confirming the effectiveness of both inhibitions and demonstrating a role for HMGB1 and RAGE in osseointegration process, future studies including a dose-response analysis, may provide additional interesting information to the field. Finally, future studies are required to investigate the inhibition of HMGB1 and/or RAGE only in initial time points during Ti-mediated osseointegration, when these molecules are prevalent and theoretically mainly required, in order to determine their role in each phase of osseointegration.

CONCLUSION

Taken together, our findings suggest that HMGB1 and RAGE actively influence the osseointegration process, by their influence in the balance of host inflammatory immune response, which includes macrophages migration and M1/M2 response, MSC markers expression, and bone deposition (**Figure 10**).

AUTHOR CONTRIBUTIONS

CB and GG contributed to the conception and design, the acquisition, analysis, and interpretation, drafted the manuscript, critically revised the manuscript, gave final approval, and agreed to be accountable for all aspects of work. FC contributed to the acquisition, analysis, and interpretation, drafted the manuscript, critically revised the manuscript, gave final approval, and agreed to be accountable for all aspects of work. ES, APT, and CF contributed to the acquisition, analysis, and interpretation, drafted the manuscript, gave final approval, and agreed to be accountable for all aspects of work. RT, AC, APFT, and DR contributed to the acquisition, analysis, and interpretation, gave final approval, and agreed to be accountable for all aspects of work.

FUNDING

This work was supported by grants #2014/09590-8, #2015/18162-2, #2015/24637-3 from São Paulo Research Foundation (FAPESP), CNPq, and CAPES. DR is supported from the National Institutes of Health (NIH R01 DE026736).

ACKNOWLEDGMENTS

The authors would like to thank Daniele Ceolin, Patricia Germino, and Tania Cestari for their excellent technical assistance.

SUPPLEMENTARY MATERIAL

The Supplementary Material for this article can be found online at: https://www.frontiersin.org/articles/10.3389/fimmu.2019.00709/full#supplementary-material

Supplementary Figure 1 | Histopathological analysis of blood clot in C57Bl/6 mice at 3 days post Ti implantation. Mice received Ti-screw implantation in the edentulous ridge of maxilla and were divided in according to each treatment: Control (C group, with no treatment); Glycyrrhizic Acid at a dosage of 200 mg/Kg/day (GZA group); or RAGE antagonistic peptide at dosage of 4 mg/Kg/day (RAP group). Blood clot is observed throughout days 3, 7, 14, and 21 days. Histological slides were stained with H&E and images were captured at 10 and 100x magnification.

Supplementary Figure 2 | Gene expression patterns post subcutaneous Ti disc implantation in C57Bl/6 mice treated with HMGB1 inhibitor or RAGE antagonist. Mice received Ti-disc implantation in the subcutaneous tissue and were divided in according to each treatment: Control (C group, with no treatment); Glycyrrhizic Acid at a dosage of 200 mg/Kg/day (GZA group); or RAGE antagonistic peptide at dosage of 4 mg/Kg/day (RAP group). Four biological replicates from subcutaneous tissue samples were removed at 3, 7, and 14 days post Ti implantation and a pool of samples from all the experimental time periods in each experimental group was used for a gene expression pattern analysis. Samples of subcutaneous tissue without surgery were used as control. Two technical

replicates were considered for each assay. Gene expression was performed by using exploratory analysis by Real Time PCR array, with the VIA7 system (Applied Biosystems, Warrington, UK) and a customized qPCR array comprised of the major targets (Inflammatory Cytokines & Receptors and Wound Healing panels) of the PCRarrayRT2 Profiler (SABiosciences/QIAGEN). Results are depicted as the fold increase change (and the standard deviation) in mRNA expression from triplicate measurements in relation to the control samples and normalized by internal housekeeping genes (GAPDH, HPRT, β-actin).

REFERENCES

1. Adell R, Lekholm U, Rockler B, Branemark PI. A 15-year study of osseointegrated implants in the treatment of the edentulous jaw. *Int J Oral Surg*. (1981) 10:387–416. doi: 10.1016/S0300-9785(81)80077-4
2. Branemark PI, Hansson BO, Adell R, Breine U, Lindstrom J, Hallen O, et al. Osseointegrated implants in the treatment of the edentulous jaw. Experience from a 10-year period. *Scand J Plast Reconstr Surg Suppl*. (1977) 16:1–132.
3. Albrektsson T, Dahlin C, Jemt T, Sennerby L, Turri A, Wennerberg A. Is marginal bone loss around oral implants the result of a provoked foreign body reaction? *Clin Implant Dent Relat Res*. (2014) 16:155–65. doi: 10.1111/cid.12142
4. Biguetti CC, Cavalla F, Silveira EM, Fonseca AC, Vieira AE, Tabanez AP, et al. Oral implant osseointegration model in C57Bl/6 mice: microtomographic, histological, histomorphometric and molecular characterization. *J Appl Oral Sci*. (2018) 26:e20170601.doi: 10.1590/1678-7757-2017-0601
5. Thalji GN, Nares S, Cooper LF. Early molecular assessment of osseointegration in humans. *Clin Oral Implants Res*. (2014) 25:1273–85. doi: 10.1111/clr.12266
6. Agarwal R, Garcia AJ. Biomaterial strategies for engineering implants for enhanced osseointegration and bone repair. *Adv Drug Deliv Rev*. (2015) 94:53–62. doi: 10.1016/j.addr.2015.03.013
7. Hotchkiss KM, Reddy GB, Hyzy SL, Schwartz Z, Boyan BD, Olivares-Navarrete, R. Titanium surface characteristics, including topography and wettability, alter macrophage activation. *Acta Biomater*. (2016) 31:425–34. doi: 10.1016/j.actbio.2015.12.003
8. Gu Q, Yang H, Shi Q. Macrophages and bone inflammation. *J Orthopaedic Transl*. (2017) 10:86–93. doi: 10.1016/j.jot.2017.05.002
9. Sridharan R, Cameron AR, Kelly DJ, Kearney CJ, O'Brien FJ. Biomaterial based modulation of macrophage polarization: a review and suggested design principles. *Mater Today*. (2015) 18:313–25. doi: 10.1016/j.mattod.2015.01.019
10. Mosser DM, Edwards JP. Exploring the full spectrum of macrophage activation. *Nat Rev Immunol*. (2008) 8:958–69. doi: 10.1038/nri2448
11. Brown BN, Ratner BD, Goodman SB, Amar S, Badylak SF. Macrophage polarization: an opportunity for improved outcomes in biomaterials and regenerative medicine. *Biomaterials*. (2012) 33:3792–802. doi: 10.1016/j.biomaterials.2012.02.034
12. Trindade R, Albrektsson T, Wennerberg A. Current concepts for the biological basis of dental implants: foreign body equilibrium and osseointegration dynamics. *Oral Maxillofacial Surg Clin N Am*. (2015) 27:175–83. doi: 10.1016/j.coms.2015.01.004
13. Corradetti B, Taraballi F, Corbo C, Cabrera F, Pandolfi L, Minardi S, et al. Immune tuning scaffold for the local induction of a pro-regenerative environment. *Sci Rep*. (2017) 7:17030. doi: 10.1038/s41598-017-16895-0
14. Land WG. The role of damage-associated molecular patterns (DAMPs) in human diseases: part II: DAMPs as diagnostics, prognostics and therapeutics in clinical medicine. *Sultan Qaboos Univ Med J*. (2015) 15:e157-70.
15. Vishwakarma A, Bhise NS, Evangelista MB, Rouwkema J, Dokmeci MR, Ghaemmaghami AM, et al. Engineering immunomodulatory biomaterials to tune the inflammatory response. *Trends Biotechnol*. (2016) 34:470–82. doi: 10.1016/j.tibtech.2016.03.009
16. Fukata M, Vamadevan AS, Abreu MT. Toll-like receptors (TLRs) and Nod-like receptors (NLRs) in inflammatory disorders. *Semin Immunol*. (2009) 21:242–53. doi: 10.1016/j.smim.2009.06.005
17. Sims GP, Rowe DC, Rietdijk ST, Herbst R, Coyle AJ. HMGB1 and RAGE in inflammation and cancer. *Ann Rev Immunol*. (2010) 28:367–88. doi: 10.1146/annurev.immunol.021908.132603
18. Kang R, Chen R, Zhang Q, Hou W, Wu S, Cao L, et al. HMGB1 in health and disease. *Mol Aspects Med*. (2014) 40:1–116. doi: 10.1016/j.mam.2014.05.001
19. Tancharoen S, Gando S, Binita S, Nagasato T, Kikuchi K, Nawa Y, et al. HMGB1 promotes intraoral palatal wound healing through RAGE-dependent mechanisms. *Int J Mol Sci*. (2016) 17:11. doi: 10.3390/ijms17111961
20. Schiraldi M, Raucci A, Munoz LM, Livoti E, Celona B, Venereau E, et al. HMGB1 promotes recruitment of inflammatory cells to damaged tissues by forming a complex with CXCL12 and signaling via CXCR4. *J Exp Med*. (2012) 209:551–63. doi: 10.1084/jem.20111739
21. Aoyagi H, Yamashiro K, Hirata-Yoshihara C, Ideguchi H, Yamasaki M, Kawamura M, et al. HMGB1-induced inflammatory response promotes bone healing in murine tooth extraction socket. *J Cell Biochem*. (2018) 27:26710. doi: 10.1002/jcb.26710
22. Yang H, Lundbäck P, Ottosson L, Erlandsson-Harris H, Venereau E, Bianchi ME, et al. Redox modification of cysteine residues regulates the cytokine activity of high mobility group box-1 (HMGB1). *Mol Med*. (2012) 18:250–9. doi: 10.2119/molmed.2011.00389
23. Janko C, Filipović M, Munoz LE, Schorn C, Schett G, Ivanović-Burmazović I, et al.Redox modulation of HMGB1-related signaling. *Antioxid Redox Signal*. (2014) 20:1075–85. doi: 10.1089/ars.2013.5179
24. Kokkola R, Andersson A, Mullins G, Ostberg T, Treutiger CJ, Arnold B, et al. RAGE is the major receptor for the proinflammatory activity of HMGB1 in rodent macrophages. *Scand J Immunol*. (2005) 61:1–9. doi: 10.1111/j.0300-9475.2005.01534.x
25. Rauvala H, Rouhiainen A. RAGE as a receptor of HMGB1 (Amphoterin): roles in health and disease. *Curr Mol Med*. (2007) 7:725–34. doi: 10.2174/156652407783220750
26. Rojas A, Delgado-Lopez F, Perez-Castro R, Gonzalez I, Romero J, Rojas I, et al. HMGB1 enhances the protumoral activities of M2 macrophages by a RAGE-dependent mechanism. *Tumor Biol*. (2016) 37:3321–9. doi: 10.1007/s13277-015-3940-y
27. Luo Y, Li SJ, Yang J, Qiu YZ, Chen FP. HMGB1 induces an inflammatory response in endothelial cells via the RAGE-dependent endoplasmic reticulum stress pathway. *Biochem Biophys Res Commun*. (2013) 438:732–8. doi: 10.1016/j.bbrc.2013.07.098
28. Lei C, Zhang S, Cao T, Tao W, Liu M, Wu, B. HMGB1 may act via RAGE to promote angiogenesis in the later phase after intracerebral hemorrhage. *Neuroscience*. (2015) 295:39–47. doi: 10.1016/j.neuroscience.2015.03.032
29. Tian X, Sun L, Feng D, Sun Q, Dou Y, Liu C, et al. HMGB1 promotes neurovascular remodeling via Rage in the late phase of subarachnoid hemorrhage. *Brain Res*. (2017) 1670:135–45. doi: 10.1016/j.brainres.2017.06.001
30. Su Z, Wang T, Zhu H, Zhang P, Han R, Liu Y, et al. HMGB1 modulates Lewis cell autophagy and promotes cell survival via RAGE-HMGB1-Erk1/2 positive feedback during nutrient depletion. *Immunobiology*. (2015) 220:539–44. doi: 10.1016/j.imbio.2014.12.009
31. Riuzzi F, Sorci G, Sagheddu R, Donato, R. HMGB1-RAGE regulates muscle satellite cell homeostasis through p38-MAPK- and myogenin-dependent repression of Pax7 transcription. *J Cell Sci*. (2012) 125(Pt 6):1440–54. doi: 10.1242/jcs.092163
32. Su Z, Zhang P, Yu Y, Lu H, Liu Y, Ni P, et al. HMGB1 facilitated macrophage reprogramming towards a proinflammatory M1-like phenotype in experimental autoimmune myocarditis development. *Sci Rep*. (2016) 6:21884. doi: 10.1038/srep21884
33. Tian S, Zhang L, Tang J, Guo X, Dong K, Chen SY. HMGB1 exacerbates renal tubulointerstitial fibrosis through facilitating M1 macrophage phenotype at the early stage of obstructive injury. *Am J Physiol Renal Physiol*. (2015) 308:F69–75. doi: 10.1152/ajprenal.00484.2014
34. Son M, Porat A, He M, Suurmond J, Santiago-Schwarz F, Andersson U, et al. C1q and HMGB1 reciprocally regulate human macrophage polarization. *Blood*. (2016) 128:2218–28. doi: 10.1182/blood-2016-05-719757

35. Yang H, Wang H, Levine YA, Gunasekaran MK, Wang Y, Addorisio M, et al. Identification of CD163 as an antiinflammatory receptor for HMGB1-haptoglobin complexes. *JCI Insight*. (2016) 1:7. doi: 10.1172/jci.insight.85375
36. Daly KA, Liu S, Agrawal V, Brown BN, Johnson SA, Medberry CJ, et al. Damage associated molecular patterns within xenogeneic biologic scaffolds and their effects on host remodeling. *Biomaterials*. (2012) 33:91–101. doi: 10.1016/j.biomaterials.2011.09.040
37. Julier Z, Park AJ, Briquez PS, Martino MM. Promoting tissue regeneration by modulating the immune system. *Acta Biomater*. (2017) 53:13–28. doi: 10.1016/j.actbio.2017.01.056
38. Othman Z, Cillero Pastor B, van Rijt S, Habibovic P. Understanding interactions between biomaterials and biological systems using proteomics. *Biomaterials*. (2018) 167:191–204. doi: 10.1016/j.biomaterials.2018.03.020
39. Institute of Laboratory Animal Resources (U.S.). Committee on Care and Use of Laboratory Animals. *Guide for the Care and Use of Laboratory Animals. NIH publication*. Bethesda, MD: U.S. Dept. of Health and Human Services, Public Health Service (2011).
40. Kilkenny C, Browne WJ, Cuthi I, Emerson M, Altman DG. Improving bioscience research reporting: the ARRIVE guidelines for reporting animal research. *Veter Clin Pathol*. (2012) 41:27–31. doi: 10.1371/journal.pbio.1000412
41. Lau A, Wang S, Liu W, Haig A, Zhang ZX, Jevnikar AM. Glycyrrhizic acid ameliorates HMGB1-mediated cell death and inflammation after renal ischemia reperfusion injury. *Am J Nephrol*. (2014) 40:84–95.doi: 10.1159/000364908
42. Arumugam T, Ramachandran V, Gomez SB, Schmidt AM, Logsdon CD. S100P-derived RAGE antagonistic peptide reduces tumor growth and metastasis. *Clin Cancer Res*. (2012) 18:4356–64. doi: 10.1158/1078-0432.CCR-12-0221
43. Mouraret S, Hunter DJ, Bardet C, Brunski JB, Bouchard P, Helms JA. A pre-clinical murine model of oral implant osseointegration. *Bone*. (2014) 58:177–84.doi: 10.1016/j.bone.2013.07.021
44. Araujo-Pires AC, Biguetti CC, Repeke CE, Rodini C Campanelli AP, Trombone AP, et al. Mesenchymal stem cells as active prohealing and immunosuppressive agents in periapical environment: evidence from human and experimental periapical lesions. *J Endodontics*. (2014) 40:1560–5. doi: 10.1016/j.joen.2014.02.012
45. Vieira AE, Repeke CE, Ferreira S Jr., Colavite PM, Biguetti CC, Oliveira RC, et al. Intramembranous bone healing process subsequent to tooth extraction in mice: micro-computed tomography, histomorphometric and molecular characterization. *PLoS ONE*. (2015) 10:e0128021. doi: 10.1371/journal.pone.0128021
46. Romero-Gavilán F, Gomes NC, Ródenas J, Sánchez A, Azkargorta M, Iloro I, et al. Proteome analysis of human serum proteins adsorbed onto different titanium surfaces used in dental implants. *Biofouling*. (2017) 33:98–111. doi: 10.1080/08927014.2016.1259414
47. Kaneko H, Kamiie J, Kawakami H, Anada T, Honda Y, Shiraishi N, et al. Proteome analysis of rat serum proteins adsorbed onto synthetic octacalcium phosphate crystals. *Anal Biochem*. (2011) 418:276–85. doi: 10.1016/j.ab.2011.07.022
48. Biguetti CC, Vieira AE, Cavalla F, Fonseca AC, Colavite PM, Silva RM, et al. CCR2 contributes to F4/80+ cells migration along intramembranous bone healing in Maxilla, but its deficiency does not critically affect the healing outcome. *Front Immunol*. (2018) 9:1804. doi: 10.3389/fimmu.2018.01804
49. Benjamini Y, Hochberg, Y. Controlling the false discovery rate: a practical and powerful approach to multiple testing. *J R Stat Soc Ser B*. (1995) 1:11. doi: 10.1111/j.2517-6161.1995.tb02031.x
50. Liu A, Jin H, Dirsch O, Deng M, Huang H, Bröcker-Preuss M, et al. Release of danger signals during ischemic storage of the liver: a potential marker of organ damage? *Mediators Inflamm*. (2010) 2010:436145. doi: 10.1155/2010/436145
51. Manganelli V, Signore M, Pacini I, Misasi R, Tellan G, Garofalo T, et al. Increased HMGB1 expression and release by mononuclear cells following surgical/anesthesia trauma. *Crit Care*. (2010) 14:R197.doi: 10.1186/cc9316
52. Osoegawa A, Yano T, Yamanaka T, Tagawa T, Shoji F, Yoshino I, et al. Plasma high-mobility group box 1 as an indicator of surgical stress. *Surg Today*. (2011) 41:903–7. doi: 10.1007/s00595-010-4371-4
53. Tilmaciu CM, Mathieu M, Lavigne JP, Toupet K, Guerrero G, Ponche A, et al. *In vitro* and *in vivo* characterization of antibacterial activity and biocompatibility: a study on silver-containing phosphonate monolayers on titanium. *Acta Biomater*. (2015) 15:266–77. doi: 10.1016/j.actbio.2014.12.020
54. Ito T, Kawahara K, Nakamura T, Yamada S, Nakamura T, Abeyama K, et al. High-mobility group box 1 protein promotes development of microvascular thrombosis in rats. *J Thrombosis Haemostasis JTH*. (2007) 5:109–16. doi: 10.1111/j.1538-7836.2006.02255.x
55. Ahrens I, Chen YC, Topcic D, Bode M, Haenel D, Hagemeyer CE, et al. HMGB1 binds to activated platelets via the receptor for advanced glycation end products and is present in platelet rich human coronary artery thrombi. *Thrombosis Haemostasis*. (2015) 114:994–1003. doi: 10.1160/TH14-12-1073
56. Fuentes E, Rojas A, Palomo I. Role of multiligand/RAGE axis in platelet activation. *Thrombosis Res*. (2014) 133:308–14. doi: 10.1016/j.thromres.2013.11.007
57. Fuentes E, Palomo I, Rojas A. Cross-talk between platelet and tumor microenvironment: Role of multiligand/RAGE axis in platelet activation. *Blood Rev*. (2016) 30:213–21. doi: 10.1016/j.blre.2015.11.005
58. Feng L, Xue D, Chen E, Zhang W, Gao X, Yu J, et al. HMGB1 promotes the secretion of multiple cytokines and potentiates the osteogenic differentiation of mesenchymal stem cells through the Ras/MAPK signaling pathway. *Exp Ther Med*. (2016) 12:3941–7.doi: 10.3892/etm.2016.3857
59. Plotkin L, Essex AL, Davis HM. RAGE signaling in skeletal biology. *Curr Osteoporos Rep*. (2019) 17:16–25. doi: 10.1007/s11914-019-00499-w
60. Mack M, Cihak J, Simonis C, Luckow B, Proudfoot AE, Plachy J, et al. Expression and characterization of the chemokine receptors CCR2 and CCR5 in mice. *J Immunol*. (2001) 166:4697–704. doi: 10.4049/jimmunol.166.7.4697
61. Martinez FO, Gordon S. The M1 and M2 paradigm of macrophage activation: time for reassessment. *F1000prime Rep*. (2014) 6:13. doi: 10.12703/P6-13
62. Pajarinen J, Kouri VP, Jamsen E, Li TF, Mandelin J, Konttinen YT. The response of macrophages to titanium particles is determined by macrophage polarization. *Acta Biomater*. (2013) 9:9229–40. doi: 10.1016/j.actbio.2013.06.027
63. Thalji G, Cooper LF. Molecular assessment of osseointegration in vivo: a review of the current literature. *Int J Oral Maxillofac Implants*. (2013) 28:e521–34. doi: 10.11607/jomi.te33
64. Selders GS, Fetz AE, Radic MZ, Bowlin GL. An overview of the role of neutrophils in innate immunity, inflammation and host-biomaterial integration. *Regenerat Biomater*. (2017) 4:55–68. doi: 10.1093/rb/rbw041
65. Anderson JM, Rodriguez A, Chang DT. Foreign body reaction to biomaterials. *Semin Immunol*. (2008) 20:86–100. doi: 10.1016/j.smim.2007.11.004
66. Bonewald LF. The amazing osteocyte. *J Bone Miner Res*. (2011) 26:229–38. doi: 10.1002/jbmr.320
67. Pawlinski R. Platelet HMGB1: the venous clot coordinator. *Blood*. (2016) 128:2376–8. doi: 10.1182/blood-2016-09-738740

Conflict of Interest Statement: The authors declare that the research was conducted in the absence of any commercial or financial relationships that could be construed as a potential conflict of interest.

frontiers in Immunology

ORIGINAL RESEARCH
published: 12 April 2019
doi: 10.3389/fimmu.2019.00797

Experience in the Adaptive Immunity Impacts Bone Homeostasis, Remodeling, and Healing

Christian H. Bucher[1,2], Claudia Schlundt[1,2], Dag Wulsten[1], F. Andrea Sass[1,2], Sebastian Wendler[1,2], Agnes Ellinghaus[1], Tobias Thiele[1], Ricarda Seemann[1], Bettina M. Willie[3], Hans-Dieter Volk[2,4], Georg N. Duda[1,2,5†] and Katharina Schmidt-Bleek[1,2†]*

[1] Julius Wolff Institute and Center for Musculoskeletal Surgery, Charité — Universitätsmedizin Berlin, Berlin, Germany, [2] Berlin-Brandenburg Center for Regenerative Therapies, Charité — Universitätsmedizin Berlin, Berlin, Germany, [3] Department of Pediatric Surgery, Faculty of Medicine, McGill University, Shriners Hospital for Children, Montreal, QC, Canada, [4] Institute of Medical Immunology, Charité — Universitätsmedizin Berlin, Berlin, Germany, [5] Berlin Institute of Health Center for Regenerative Therapies, Berlin, Germany

OPEN ACCESS

Edited by:
Claudine Blin-Wakkach,
UMR7370 Laboratoire de Physio Médecine Moléculaire (LP2M), France

Reviewed by:
Danka Grcevic,
University of Zagreb, Croatia
Kurt David Hankenson,
University of Michigan, United States

***Correspondence:**
Katharina Schmidt-Bleek
katharina.schmidt-bleek@charite.de

[†] These authors have contributed equally to this work

Specialty section:
This article was submitted to Inflammation, a section of the journal Frontiers in Immunology

Received: 30 November 2018
Accepted: 26 March 2019
Published: 12 April 2019

Citation:
Bucher CH, Schlundt C, Wulsten D, Sass FA, Wendler S, Ellinghaus A, Thiele T, Seemann R, Willie BM, Volk H-D, Duda GN and Schmidt-Bleek K (2019) Experience in the Adaptive Immunity Impacts Bone Homeostasis, Remodeling, and Healing. Front. Immunol. 10:797. doi: 10.3389/fimmu.2019.00797

Bone formation as well as bone healing capacity is known to be impaired in the elderly. Although bone formation is outpaced by bone resorption in aged individuals, we hereby present a novel path that considerably impacts bone formation and architecture: Bone formation is substantially reduced in aged individual owing to the experience of the adaptive immunity. Thus, immune-aging in addition to chronological aging is a potential risk factor, with an experienced immune system being recognized as more pro-inflammatory. The role of the aging immune system on bone homeostasis and on the bone healing cascade has so far not been considered. Within this study mice at different age and immunological experience were analyzed toward bone properties. Healing was assessed by introducing an osteotomy, immune cells were adoptively transferred to disclose the difference in biological vs. chronological aging. *In vitro* studies were employed to test the interaction of immune cell products (cytokines) on cells of the musculoskeletal system. In metaphyseal bone, immune-aging affects bone homeostasis by impacting bone formation capacity and thereby influencing mass and microstructure of bone trabeculae leading to an overall reduced mechanical competence as found in bone torsional testing. Furthermore, bone formation is also impacted during bone regeneration in terms of a diminished healing capacity observed in young animals who have an experienced human immune system. We show the impact of an experienced immune system compared to a naïve immune system, demonstrating the substantial differences in the healing capacity and bone homeostasis due to the immune composition. We further showed that *in vivo* mechanical stimulation changed the immune system phenotype in young mice toward a more naïve composition. While this rescue was found to be significant in young individuals, aged mice only showed a trend toward the reconstitution of a more naïve immune phenotype.

Considering the immune system's experience level in an individual, will likely allow one to differentiate (stratify) and treat (immune-modulate) patients more effectively. This work illustrates the relevance of including immune diagnostics when discussing immunomodulatory therapeutic strategies for the progressively aging population of the industrial countries.

Keywords: osteoimmunology, regeneration, bone healing, T cells, adaptive immunity, immune experience, inflamm-aging, biological aging

INTRODUCTION

Beginning in adulthood, age-associated alterations of the musculoskeletal system progress and eventually result in a loss of bone mass (1, 2). With increasing life expectancy, such structural alterations represent a growing clinical challenge: By 2050 people over 60 years will nearly double from about 12 to 22%, to a total of two billion (3). In parallel, trauma and associated bone injuries increase in number and already today represent the second most expensive medical condition (after cardio-vascular diseases) with further increases predicted due to a more active elderly population (4). Bone tissue is, in addition to its role within the musculoskeletal system, the home of major parts of the immune system. Therefore, it is not surprising that recent research acknowledged the significant role of the immune system in bone homeostasis (5).

The interdependency between the immune and skeletal system has gained more and more importance in recent orthopedic research (6–12). Bone cells require positive and negative regulators to maintain homeostasis. Cytokines are involved in the homeostatic and regenerative regulation and communication between the immune system and musculoskeletal system. Cytokines are potent mediators of osteoclast/osteoblast function and differentiation. Classically the cytokine regulation of bone resorption, like tumor necrosis α (TNFα), interleukin 1 α (IL-1α), interferon γ (IFNγ), and interleukin 17A (IL-17A), is discussed and studied but bone forming cells are tightly regulated by cytokines as well (13–15). Subsequent studies have identified several cytokines whose activities inhibit bone resorption and promote bone formation, like the IL-1 receptor antagonist (IL-1Ra), interleukin 4 (IL-4), interleukin 10 (IL-10), interleukin 13 (IL-13), and transforming growth factor β (TGFβ) (16). T and B cells are relevant producers of these inflammatory cytokines but also of cytokines impacting bone homeostasis, like osteoprotegerin (OPG) and RANK ligand (RANKL) (17). With a better understanding of the sequential events of the bone healing cascade, the essential role of the initial pro-inflammatory reaction as an initiator of the healing process has been recognized. Also, the consecutive anti-inflammatory signaling has been acknowledged as essential in order to proceed toward the next healing phase, the revascularization of the fracture zone (18–20). Without reestablishing the supply, the healing will seize. However, immune processes are not only essential during the early healing phase. Recent research showed that immune cells are present throughout the entire healing process with a heightened abundance during the remodeling phase (21) and that T cells are tightly interlinked with the process of collagen I deposition by osteoblasts, thus defining the structure of the newly formed bone tissue (22).

Age-related changes in the immune system have so far not been considered in this context: Specifically, the adaptive immune system is changing with age as a result of repetitive pathogen/ antigen exposure (23). Due to such pathogen/antigen exposures, there is a shift from a more naïve T/B lymphocyte system with a huge polyclonal repertoire of antigen receptors in young individuals toward a well-experienced (memory) T/B lymphocyte system with only a limited antigen receptor repertoire and thus a diminishing naïve lymphocyte pool in aged individuals (24). Such increase in immune experience is not directly linked to the chronological aging of an individual and therefore described as immune-aging. An "aged" adaptive immune system, particularly the T cells, are more pro-inflammatory due to various reasons, including: altered properties of memory/effector T cells in respect to tissue infiltration, lower activation threshold and the associated bystander activation, cytokine memory, and a diminished control by regulatory T cells (25). In consequence, immune-aging is accompanied with an inflamm-aging, a term recently coined in osteoimunological research that refers to an elevated inflammatory state in elderly (26). The heightened pro-inflammatory capacity of an experienced adaptive immune system is further enhanced by its effect on the innate immune response. Pro-inflammatory cytokines such as IFNg produced by T cells elicit a pro-inflammatory reaction through a pattern recognition receptor mediated inflammatory response from the innate immune system (27). Moreover, within an experienced immune system the memory/effector T cell pool forms a self-renewing population of tissue-resident cells which reside within the bone marrow (28, 29). Thus, long-lived memory/effector T cells that are fast pro-inflammatory responders to challenges such as injuries are present in the immediate proximity of a bone fracture and are likely to influence the healing process. We hypothesized that immune-aging impacts bone tissue structural properties directly, in bone homeostasis as well as in healing.

Although adaptive immunity seems to play such a central role in homeostasis and healing, it is surprising that age-associated changes of the immune system are so far rarely considered (30, 31). To overcome this limitation, we present herein a novel approach that includes animal age with and without antigen exposure, to understand the role of adaptive immunity in bone. Thus, the presented study aims at revealing the influence of an experienced immune phenotype in comparison to a

naïve immune phenotype on the tissue formation processes in bone adaptation as well as during bone regeneration to unravel the relevance of immune-aging and inflamm-aging on the bone structure and thereby lay the foundation for a more comprehensive understanding of patient treatment with impaired bone regeneration (11).

MATERIALS AND METHODS

Animals to Study Immune-Aging

Female C57BL/6N mice were purchased from Charles River Laboratories with an age of 8–10 weeks and were used at an age of 12, 52, and 102 weeks, respectively. Animals were imported with a health certificate and kept under obligatory hygiene standards that were monitored according to the FELASA standards. The mice were kept under specific pathogen free (SPF) housing or under non-SPF housing. Food and water was available *ad libitum* and the temperature ($20 \pm 2°C$) controlled with a 12 h light/dark circle. All experiments were carried out with ethical permission according to the policies and principles established by the Animal Welfare Act, the National Institutes of Health Guide for Care and Use of Laboratory Animals, and the National Animal Welfare Guidelines, the ARRIVE guidelines and were approved by the local legal representative animal rights protection authorities (Landesamt für Gesundheit und Soziales Berlin).

Mouse Osteotomy as a Model of Fracture Healing

Bone regeneration was studied by introducing an osteotomy on the left femur. Therefore, the mice were anesthetized with a mixture of isoflurane (Forene) and oxygen (Induction with 2% Isoflurane and maintenance with 1.5%). First line analgesia was done with Bubrenorphine pre surgery, antibiotics with clindamycine and eye ointment to protect the eyes. Post-surgery, tramadol (Tramal) was added to the drinking water for 3 days. The surgical area was shaved and disinfected, and all surgical procedures were performed on a heating pad (37°C). The osteotomy was performed as previously published (32). Shortly, a longitudinal, lateral skin incision and dissection of the fasciae allowed to expose the femur. The *Musculus vastus lateralis* and *Musculus biceps femoris* were dislodged by blunt preparation with protection of the sciatic nerve. Thereafter, serial drilling for pin placement (diameter: 0.45 mm) through the connectors of the external fixator (MouseExFix, RISystem, Davos, Switzerland) was performed, resulting in a fixation of the external fixator construct strictly parallel to the femur. Following rigid fixation, a 0.70 mm osteotomy was performed between the medial pins using a Gigli wire saw (RISystem, Davos, Switzerland). After skin closure, mice were returned to their cages and kept under warming lamps for the period of immediate anesthesia recovery.

Bone Tissue Sample Preparation and Flow Cytometry

Animals were intraperitoneally injected with a mixture of medetomidine and ketamine to induce a deep anesthesia, thereafter euthanized by cervical dislocation. Blood, spleen, and the hind limbs were removed and stored for transportation in ice cold phosphate-buffered saline (PBS). For flow cytometry the spleen was dissected and mashed through a 70 μm mesh to isolate the splenocytes. Erythrocytes were removed by incubation with the RBC Lysis Buffer (BioLegend, San Diego, CA USA). The bone marrow was isolated by cutting open both end of femora or tibia and flushing the bone marrow out of the cavity with a 24G needle and PBS. The single cell suspension was incubated with a fixable live/dead stain (LIVE/DEAD™ Fixable Blue Dead Cell Stain Kit, for UV excitation (Invitrogen™, Waltham, MA USA) and subsequently washed with PBS, 0.5% BSA, and 0.1% NaN_3. Before incubation with the antibodies, the fc receptors were blocked with the TruStain fcX™ (anti-mouse CD16/32) Antibody (BioLegend, San Diego, CA USA). Surface epitopes were stained with fluorochrome coupled antibodies for 20 min on ice. For intracellular staining the surface stained cells were incubated with the eBioscience™ Foxp3/Transcription Factor Staining Buffer Set (Invitrogen™, Waltham, MA USA) according to the manufacture's protocol. Intracellular epitopes were stained for 30 min at room temperature. Stained cells were analyzed on a BD LSRFortessa™ cell analyzer (BD Biosciences, Franklin Lakes, NJ USA). For a list of used antibodies and conjugates please refer to the **Supplementary Table 1**.

Biomechanical Analyses of Femur Tissue Competence

The torsional stiffness, the maximum torque, its corresponding angle and workload were assessed in a torsional load to failure experiment. Following harvesting, the femora were excised and prepared by removing all adjacent muscles and tendons. Subsequently both epiphyses of the femora were embedded with methylmethacrylate (Technovit 3040, Heraeus Kulzer, Hanau, Germany) in custom made molds. Eventually, bones were mounted into a material testing device (Bose ElectroForce LM1, TA Instruments, Eden Prairie, MN USA) and tested by first applying an axially preloaded of 0.3N which remained constant during the following torsional load to failure at a rate of 0.54°/s. Axial displacement, load, torque, and rotation were all acquired at a 100 Hz sample rate. All parameters were calculated by a routine written in MATLAB (The Mathworks, Inc. Natick, MA USA).

3D Structural Analysis of Cortical and Trabecular Bone Using microCT Technology

Following harvesting, structural intact bones were cleaned of excess soft tissue and fixed in buffered formalin and directly loaded on a custom made sample holder and scanned at a nominal resolution of 8 and 1 μm, respectively, with a Bruker SkyScan 1172 high-resolution microCT (Bruker, Kontich, Belgium). A 0.5 mm aluminum filter was employed and an x-ray tube voltage of 70 kV. Camera pixel binning of 2 x 2 was applied and the scan orbit was 180 degrees for 8 μm and 360 degrees for 1 μm, respectively, with a rotation step of 0.2 degree. Reconstruction was carried out with a modified Feldkamp algorithm using the SkyScan NRecon software accelerated by GPU. Gaussian smoothing, ring artifact reduction, misalignment compensation, and beam hardening correction were applied.

The cortical bone was analyzed 4 mm cranial from the knee growth plate and a volume of interest (VOI) of the height of 1.6 mm was extracted. The VOI for the trabecular bone was set 0.4 mm above the growth plate and had a height of 5.2 mm, as this VOI included also the most cranial trabecular structures. The cortical bone region was binarised with a global threshold and for the trabecular bone an adaptive thresholding was applied based on localized analysis of density, to minimize partial volume effect and thickness biasing.

Osteotomized femora were mechanically fixed within a serological pipette (to support integrity of the fractured bone) and the external fixator was removed. Those bones were handled likewise as structural intact bones. Global thresholds were selected by the Otsu algorithm. The same global threshold values were applied to all measured bone samples corresponding to bone mineral density (BMD) value of 590 mg/cm^3 calcium hydroxyapatite (CaHA), calibrated by reference phantoms (Bruker-microCT, Kontich, Belgium) containing 0.25 and 0.75 g/cm^3 CaHA evenly mixed in epoxy resin rods which were of similar diameter to the scanned bones to minimize beam hardening error.

In vitro Assays to Analyze the Osteogenic Differentiation

Murine Cell Culture

Splenocytes and bone marrow cells were isolated from spleen and bone tissue from mice with different ages. The spleen was dissected and mashed through a 70 µm mesh to isolate the splenocytes. Erythrocytes were removed by incubation with the ACK Lysing Buffer (Gibco, Waltham, MA USA). The bone marrow was isolated by cutting open both end of femora or tibia and flushing the bone marrow out of the cavity with a 24G needle and PBS, after filtration through a 40 µm mesh strain, red blood cells were removed with the ACK Lysing Buffer (Gibco, Waltham, MA USA). The splenocytes were activated at a density of 2×10^6 cells/ml with 10 mg/ml plate bound anti-CD3 antibody and soluble 2 mg/ml anti-CD28 (BioLegend, San Diego, CA USA) in RPMI-1640 medium supplemented with 10% heat-inactivated FBS. After 48 h the conditioned medium was collected, pooled, filtered through a 0.22 µm hydrophobic filter (Sartorius) and stored at −80°C. Murine mesenchymal stromal cells were obtained via outgrowth culture from bone marrow cells. The isolated single cells from bone marrow was plated in 25 cm^2 cell culture plates with DMEM low glucose medium (Biochrom, Berlin, Germany) supplemented with 10% FBS (Biochrom, Berlin, Germany), 1% GlutaMAX (Gibco, Waltham, MA USA), and 1% penicillin/streptomycin (Biochrom, Berlin, Germany). After reaching confluency, the cells were detached with TrypLE Express Enzyme (Gibco, Waltham, MA USA) and cultured in passage 1 again in a 25 cm^2 culture flask. By passage 2 the cells were transferred gradually with higher passage number in 75, 150, and 300 cm^2 cell culture flasks. Murine mesenchymal stromal cells (mMSC) were used between passage 5 and 6 for the experiments. Osteogenic differentiation of mMSC was achieved by the supplementation with 100 nM Dexamethasone, 0.05 mM l-ascorbic acid 2-phosphate, and 10 mM β-Glycerolphosphate (33). Conditioned medium was added at a dilution of one to three (1:3). Medium was exchanged every 3–4 days. After 14 days the experiment was stopped and the mineralized extracellular matrix was stained with Alizarin Red S (Sigma-Aldrich, St. Louis, MO USA) and quantification was achieved by resolving the stain with cetylpyridiniumchlorid (Sigma-Aldrich, St. Louis, MO USA). Optical density (OD) was measured with a multimode microplate reader (Tecan Infinite, Männedorf, Switzerland).

Human Cell Culture

Human mesenchymal stromal cells (hMSC) were isolated from bone marrow of patients undergoing total hip replacement (provided by the Center for Musculoskeletal Surgery, Charité - Universitätsmedizin Berlin and distributed by the "Cell and Tissue Harvesting" Core Facility of the BCRT). All protocols were approved by the Charité - Universitätsmedizin Ethics Committee and performed according to the Helsinki Declaration. Human MSC were cultivated with DMEM low glucose medium (Biochrom, Berlin, Germany) supplemented with 10% FBS (Biochrom, Berlin, Germany), 1% GlutaMAX (Gibco, Waltham, MA USA), and 1% penicillin/streptomycin (Biochrom, Berlin, Germany). After three passaging steps, hMSC were characterized by differentiation assays (osteogenic, adipogenic, chondrogenic). Only hMSC that were capable of differentiation in all three lineages were used in the experiment within passage 4–8. Human peripheral blood mononuclear cells (hPBMC) were isolated from buffy coats (provided with ethical approval by DRK, Berlin, Germany) via density gradient centrifugation on Histopaque-1077 (Sigma-Aldrich, St. Louis, MO USA). The buffy coats were separated from blood donor volunteers by the Deutsches Rotes Kreuz (DRK) and fulfilled the criteria of age >30 years old and cytomegalovirus (CMV) positive. Isolation of naïve T cells was achieved with the Naïve T Cell Isolation Kit (Miltenyi Biotec, Bergisch Gladbach, Germany) and CD8+ T cells were isolated via CD8a microbeads (Miltenyi Biotec, Bergisch Gladbach, Germany). The hPBMC were activated at a density of 2×10^6 cells/ml with 10 mg/ml plate bound anti-CD3 antibody and soluble 2 mg/ml anti-CD28 (BioLegend, San Diego, CA USA) in RPMI-1640 medium supplemented with 10% heat-inactivated FBS. After 48 h the conditioned medium was collected, pooled, filtered through a 0.22 µm hydrophobic filter (Sartorius) and stored at −80°C until further use. Osteogenic differentiation of hMSC, under the influence of conditioned medium from hPBMC was developed likewise to murine MSC.

Enzyme-Linked Immunosorbent Assay (ELISA)

Conditioned medium from activated murine splenocytes were harvested as described and processed for enzyme-linked immunosorbent assay (ELISA). ELISA for TNFα (Mouse TNFalpha ELISA ReadySet-Go! 10x #88-7324-86, eBioscience), IFNγ (Mouse IFN gamma ELISA Ready-SET-Go! 10x #88-7314-86, eBioscience), and IL-10 (Mouse IL-10 ELISA Ready-SET-Go! #88-7105-86, eBioscience) was performed according to the manufacturer's instructions in triplicates and optical density was measured with a microplate reader Tecan Infinite (Tecan,

Männedorf, Switzerland). A standard curve was generated with a four parametric logistic curve fit.

Conditioned medium from activated human PBMC were harvested as described and processed for quantitative cytokine detection via ELISA. ELISA for human TNFα (Human TNF alpha Uncoated ELISA, 88-7346, Invitrogen) and human IFNγ (Human IFN gamma Uncoated ELISA, 88-7316, Invitrogen) was performed according to the manufacturer's instructions in triplicates and optical density was measured with a microplate reader Tecan Infinite (Tecan, Männedorf, Switzerland). A standard curve was generated with a four parametric logistic curve fit.

Mechano-Therapeutics: *in vivo* Hind Limb Loading to Analyze Bone Adaptation and Homeostasis

The left tibiae of 10 week (young) and 52 week (aged) old C57Bl/6J mice ($N = 6$/age) underwent *in vivo* cyclic compressive loading, while the right tibia was not loaded and served as an internal control. The flexed knee and the ankle of the mice were placed in our loading device (Bose ElectroForce LM1, TA Instruments, Eden Prairie, MN USA) and axial dynamic compressive loading was applied 5 days/week for 2 weeks while the mice were anesthetized with isoflurane (2.5%). Refer to Willie et al. (34) for further information. Shortly, the loading protocol consisted of 216 cycles applied at 4 Hz, which is the mean mouse locomotory stride frequency (35) delivering a maximum force of −7N for the 10 and −9N for the 52 week old mice, engendering 900 με at the periosteal surface in the tibia mid-diaphysis determined by prior *in vivo* strain gauging studies (36). This strain level equates to about two to three times the strains engendered on the medial tibia when mouse ambulates (37, 38). Mice were sacrificed on day 15, 3 days after the last loading session.

Humanized PBMC Mouse Model to Assess the Osteo-Immune Crosstalk

The humanized peripheral blood mononuclear cell (hPBMC) mouse model is described elsewhere (39–41). Shortly, human PBMC were isolated from venous blood from volunteers via density gradient centrifugation with Histopaque-1077 (Sigma-Aldrich, St. Louis, MO USA). Immune phenotype was characterized with flow cytometry. Cells were incubated with a fixable live/dead stain (LIVE/DEAD™ Fixable Blue Dead Cell Stain Kit, for UV excitation, Invitrogen™, Waltham, MA USA) and subsequently washed with phosphate-buffered saline (PBS), 0.5% BSA, and 0.1% NaN_3. Before incubation with the antibodies, the fc receptors were blocked with the Fc Receptor Blocking Solution (Human TruStain fcX™, BioLegend, San Diego, CA USA). Surface epitopes were stained with fluorochrome coupled antibodies for 20 min. Stained cells were analyzed on a BD LSRFortessa™ cell analyzer (BD Biosciences, Franklin Lakes, NJ USA). For a list of used antibodies and conjugates please refer to the **Supplementary Table 2**. Experience level for stratification was achieved via the CD8+ T_{EMRA} level: 36% [the level was set corresponding to Reinke et al. (42)] and higher were classified as experienced and below 20% as naïve donors. Donor immune phenotype characterization can be found in the **Supplementary Table 3**. Ten million freshly isolated and characterized hPBMCs were transferred at a density of 5×10^6 cells/ml PBS via tail vein injection 1 day before surgery. After 3 or 21 days the organs were harvested and analyzed. An osteotomy was introduced as described in the preceding paragraph. For the analysis 21 days after surgery the callus region of the osteotomized femur was defined as a region of 1.4 mm (double the size of the fracture gap to include the complete callus) around the middle of the fracture gap. The cell transfer has been confirmed by blood sampling and consecutive flow cytometry analysis at day 3 and day 21 after osteotomy surgery.

Statistics

Statistical analysis was carried out with SPSS V.22 and GraphPad Prism V.7 software. All values including animal data are expressed as boxplot distribution giving interquartile ranges, a median, and whiskers representing min and max. All data including *in vitro* studies are expressed with mean ± SD. For animal experiments Mann-Whitney *U* was used as an unpaired, non-parametric test to compare ranks (no normal distribution of the data), for *in vitro* studies an unpaired *t*-test with Welch's correction was employed. Two-tailed and exact *p*-value are calculated with a confidence level of 95%. $P < 0.05$ was considered as statistically significant and marked with an asterisk in all graphics. ROUT test was used to exclude outliers ($Q = 1\%$).

RESULTS

Fracture Healing Deteriorates With Age

While it is frequently discussed that bone healing is impaired in the aged population, it is so far not well-understood how healing is impaired with increased chronological age apart from the age-associated decline in bone mass and quality. It is also recognized that bone fractures tend to heal more effectively in young patients compared to those in elderly (**Figure 1A**). To better understand how bone healing is altered with chronological age, a clinically relevant mouse osteotomy model was employed and bone healing was compared in young, 3 month old and elderly, 24 month old mice. Both groups of mice received a 0.7 mm osteotomy in the left femur which was stabilized by a unilateral external fixator (MouseExFix, RISystem, Davos, Switzerland). To quantify bone healing outcome, mice were analyzed at 21 days post-osteotomy using microcomputed tomography (microCT). 3D structural data analysis revealed a more mature callus in young mice compared to aged mice. The newly formed bone (BV) volume slightly decreased and the total callus volume (TV) showed a trend to be increased, whereas the ratio of bone to total callus volume decreased significantly from 48.5(±5.2) to 38.6(±1.0)%.The number of newly formed trabecular structures (Trabecular number, Tb.N) within the callus decreased significantly from 4.7(±0.5) to 3.6(±0.6)/mm in aged animals (**Figures 1B,C**). Thus, the comparison of young vs. elderly mice clearly demonstrated a diminished healing capacity of bone and matches the casual observations made in elderly patients suffering delays in bone healing.

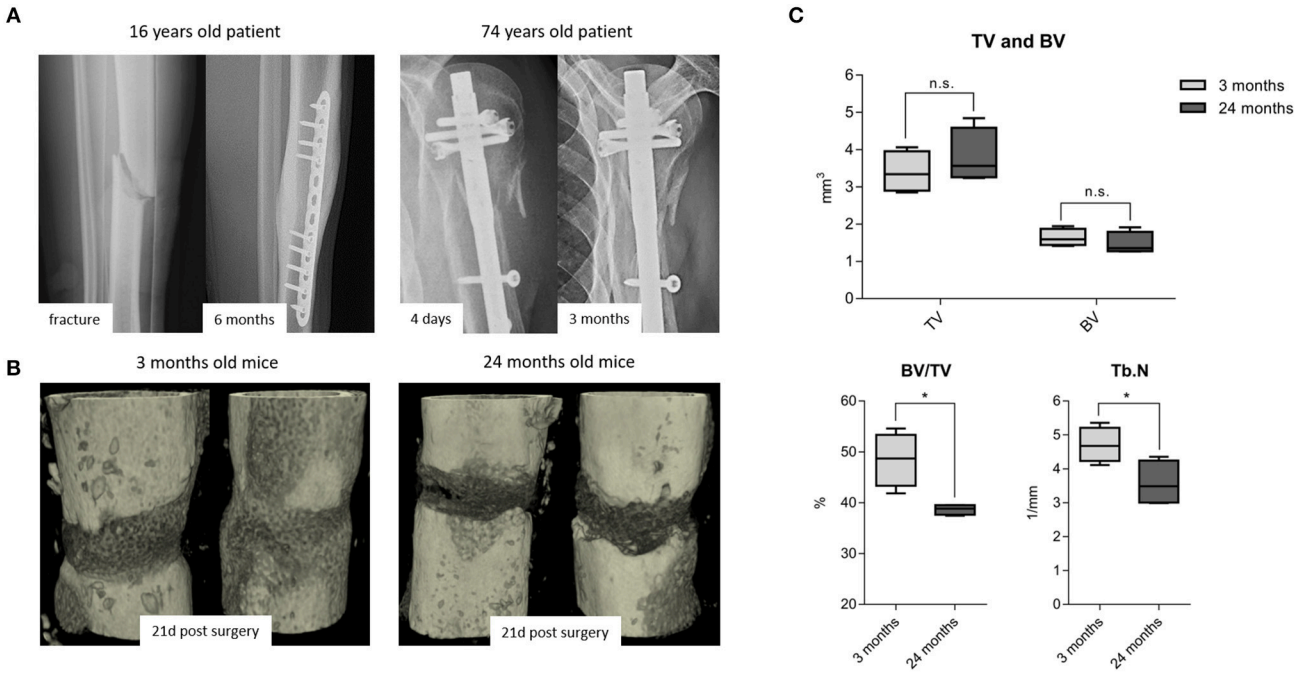

FIGURE 1 | Fracture healing among young and old subjects: (**A** left) X-ray images from a young patient with adequate callus formation after 6 months and (**A** right) from an old patient with no signs of healing after 3 months, leading to delayed fracture healing and revision surgery. This x-ray images are representative images from the clinical routine and depict the need to understand the altered processes within the elderly population. **(B)** 3D rendered x-ray images from 3 to 24 month old mice, respectively, at 21 days post-surgery. Bone healing was delayed in 24 month old compared to the 3 month old mice. **(C)** microCT analysis from the osteotomy gap 21 days post-surgery. Bone volume in total volume (BV/TV) and trabecular number (Tb.N) were diminished in 24 month old fracture callus. TV and BV were not significantly affected by age, but the ratio of newly formed bone in the callus volume was significantly lowered. $N = 6$ animals in the 3 months old group and $N = 5$ in the 24 months old group, boxplot data distribution with median, Mann-Whitney U-test, $^*p < 0.05$.

Antigen Exposure Over Time Alters the Immune Cell Composition

Standard preclinical models use in the majority of cases mice kept under specific pathogen free (SPF) housing conditions—minimizing the exposure to antigens. SPF housing significantly demagnifies the intra-individual variabilities through abolishing the pathogen/antigen exposure. In order to understand the immune-aging process and the development of an immune memory with effector and effector memory cells that are apt to protect the organism from recurrent pathogen exposure, mice were exposed to non-SPF housing conditions. Comparing mice held under SPF conditions with mice that were housed in non-SPF conditions revealed changes within the immune cell composition that mirror the immune-aging that commonly occurs to people while they grow old. These two groups allow one to distinguish between the changes in bone that occur by chronological aging and those changes that are due to the immunological aging. For quantification, the immune composition was characterized by flow cytometry analysis of the spleen from 3, 12, and 24 month old mice, respectively. Antigen exposure primarily influenced the memory compartment of the adaptive immunity over age/time. In both groups, the adaptive immune cell compartment, consisting primary of CD4+ and CD8+ T cells, acquired a more experienced memory phenotype while aging. The naïve cell pool of CD8+ cytotoxic T cells in the SPF mice diminished over time from 90.7(±1.3) to 77.8(±8.3)% within 2 years. However, a more drastic change was observed in the exposed mice: Under non-SPF conditions the memory pool increased to 95.5(±2.4)% of CD8+ T cells whereas the naïve pool was almost completely exhausted with a remnant of 3.0(±1.8)%. Only under non-SPF conditions such nearly complete exhausting of the naïve T cell pool in aged mice could be observed. Similar phenotypical changes could be observed in the CD4+ T helper cell pool (**Figure 2A**).

The memory and effector pool (CD44+) can be distinguished by the CD62L marker into central memory (T_{CM}) and effector memory (T_{EM}) T cells. Both compartments of CD8+ T cells increase with age, but only under non-SPF conditions the inter-individual variance of comparentalization could be seen (see **Figure 2B**). In the CD4+ T cell pool a similar picture could be observed compared to CD8+ T cells with less variance between individual animals. Interestingly, the CD4+ T central memory pool was constant among age and housing condition groups (**Figure 2B**). An increase in memory and effector function of the adaptive immune system was revealed with age and correlated with the housing conditions, which defined the antigen exposure and thus the development of an immune memory.

The classification in T effector/memory (T_{EM}), T central memory (T_{CM}) and T naïve cells in the CD8+ T cell pool describes the compartmentalization, but lacks a description

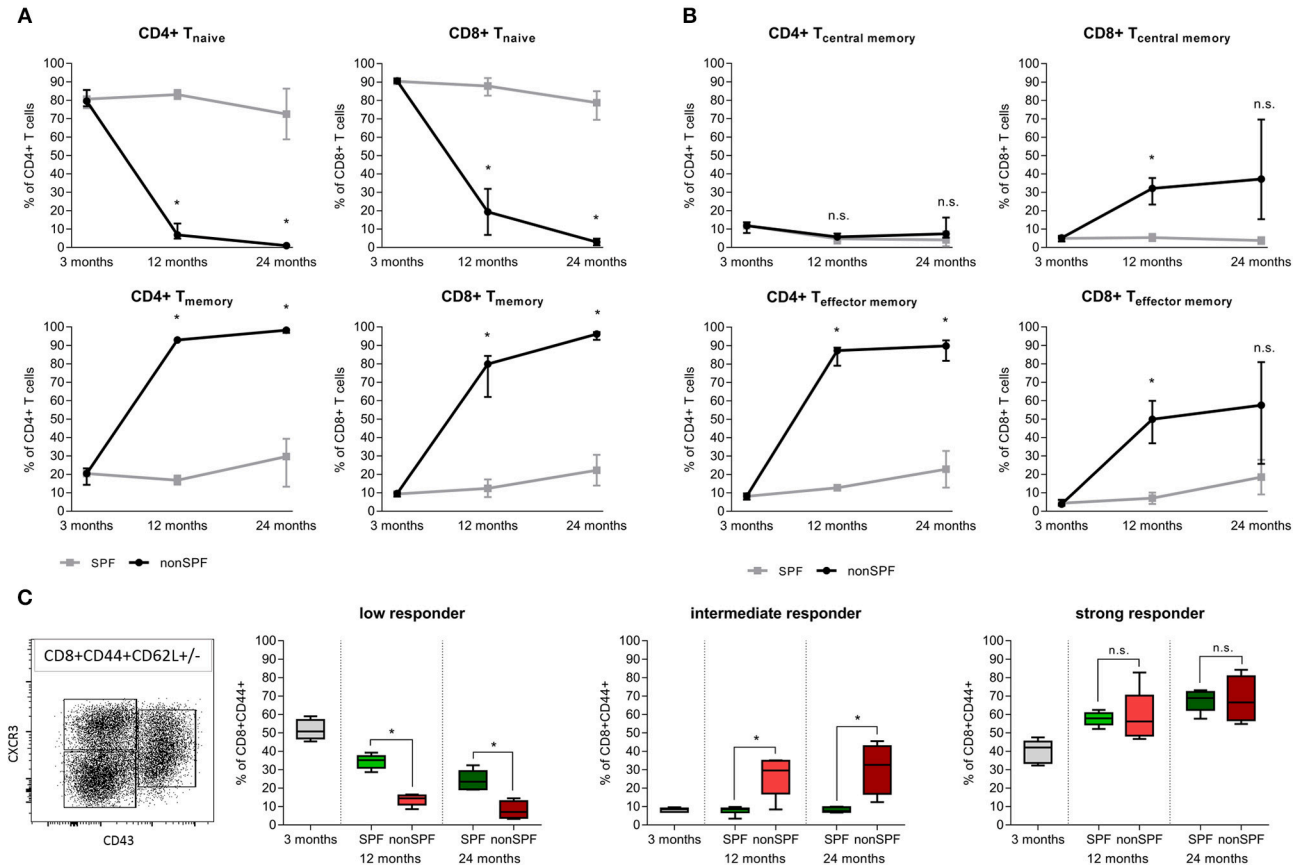

FIGURE 2 | Adaptive immunity changes level of experience among housing conditions (SPF vs. non-SPF) and aging. **(A)** Naïve level of CD4+ and CD8+ T cells diminished and the memory level increased with aging. Exposing the animals to antigens boosts the memory formation significantly. **(B)** Classification of T cells into central memory (T_{CM}) and effector memory (T_{EM}) revealed a different picture for CD4+ and CD8+ T cells: CD8+ T cells increased both compartments under non-SPF conditions, whereas the CD4+ central memory T cells were constant among ages and housing conditions. Keeping mice under SPF conditions oppressed the effect of memory formation. **(C)** CD8+ memory T cells differ in the recall efficiency after antigen encounter. Strong responder CD8+ memory T cells were not affected by non-SPF housing, whereas intermediate responder could only be found under non-SPF conditions (intermediate responder are proven to show fast proliferation and vast cytokine production). The low responder fraction diminished further under non-SPF conditions compared to SPF housing. $N = 6$ animals per age group and housing conditions, **(A,B)** shows median with interquartile range, **(C)** shows boxplot distribution with median, Mann Whitney U-test, $^*p < 0.05$.

of the activation phenotype. Memory CD8+ T cells differ in their capacities to realize a recall response. To quantify the activation potential of immune cells, the spleen of mice under SPF or non-SPF conditions was analyzed in the different age groups. The recall efficiency was classified by surface markers CXCR3 (CD183), CD27, and CD43. CD8+CD44+ memory T cells can be divided in 3 groups of low, intermediate and strong responders. An increase in CXCR3 on the cell surface correlates with an increased proliferative capacity and an increased IL-2 production. Whereas, the low responder characterized by low CXCR3 and CD43 marker show low proliferative capacity and reduced IL-2 production but an increase Granzyme B secretion. Intermediate responder upregulate the CD43 protein on the cell surface and are characterized by a very pronounced proliferation and an elevated secretion of cytokines. The low responder group of CD8+ memory T cells decreased with age and the strong responder increased, almost doubling their population quantity. The increase of strong responder within the memory CD8+ T cells amplifies the earlier finding of an accumulation of memory cells over time. Intermediate responders were almost exclusively found in higher numbers under non-SPF conditions. Under antigen exposure the low responder immune cells decreased over time being replaced by intermediate and strong responder indicating a pronounced inflammatory reaction (**Figure 2C**). Thus, the activation phenotype revealed a higher proliferative and secretory phenotype in mice kept under non-SPF conditions undergoing an immune-aging that consecutively lead to an amplified response capacity upon recall.

Immune-aging (antigen exposure) became further apparent by an in-depth immune phenotyping of these two mice groups kept under different (SPF vs. non-SPF) housing conditions. Strikingly, if mice were kept outside of the SPF housing, a shift occurred from lymphoid toward myeloid immune cells and a shift of the ratio of B and T cells toward T cells (**Figure 3A**). T cells themselves underwent a shift

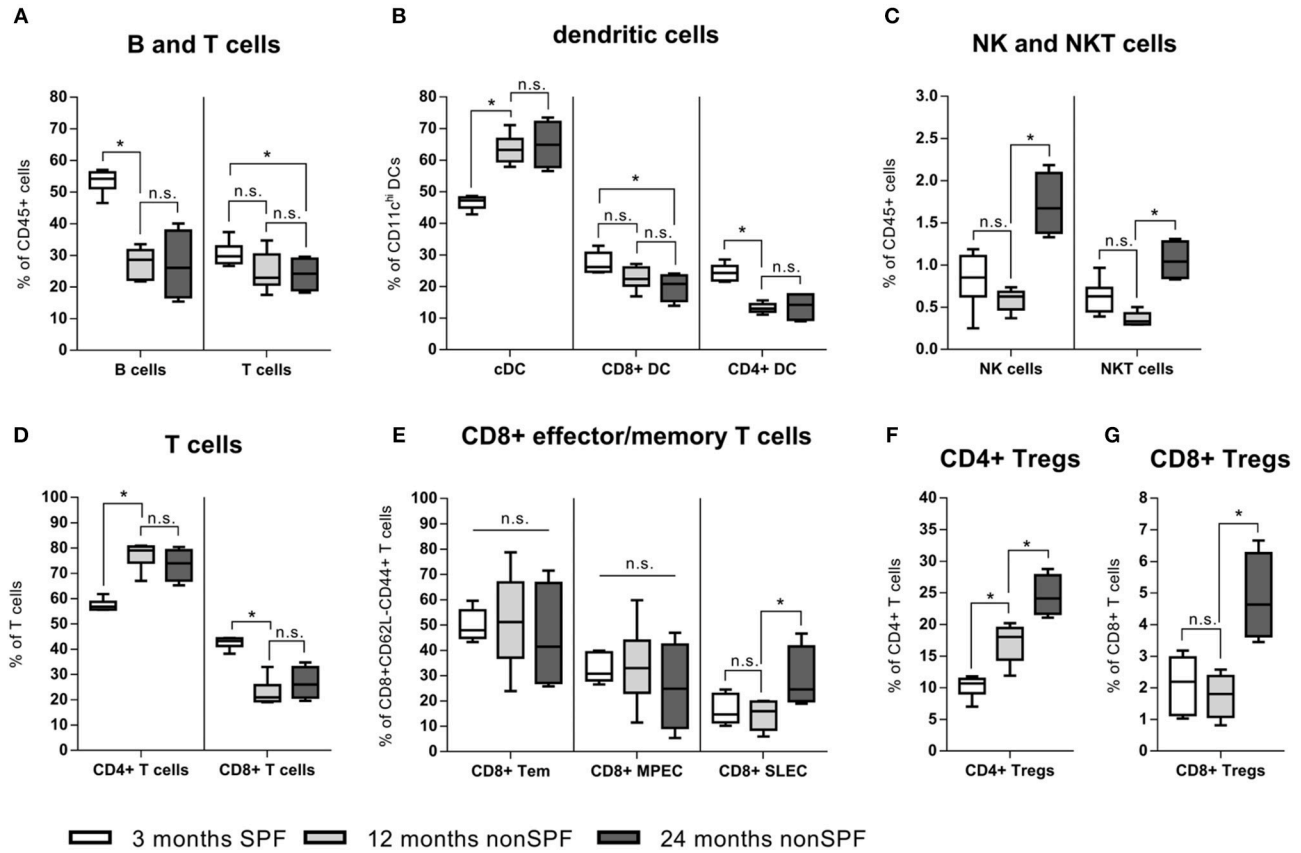

FIGURE 3 | In-depth immune phenotyping showed, that keeping mice under non-SPF conditions significantly changes the immune phenotype with age. **(A)** A shift from lymphoid toward myeloid immune cells could be seen in a lowered B and T cell fraction in the spleen, accompanied by a change of the ratio of B and T cells toward T cells. **(B)** Dendritic cells increased under non-SPF conditions and a shift toward conventional DCs (cDC) occurred. **(C)** Natural killer cells (NK cells) and especially Natural killer T cells (NKT) increased with higher age. **(D)** Under non-SPF conditions a shift from CD8+ T cells toward CD4+ T cells occurred, being stable thereafter throughout aging. **(E)** CD8+ effector memory T cells can further be divided into memory (Tem), memory precursor effector cells (MPEC) and short-lived effector cells (SLEC). The diversity of effector cells increased with age. **(F)** CD4+ T regulatory cells (Treg) increased with age. **(G)** CD8+ T regulatory cells (Treg) are a rare cell population, but could be found in relevant amounts in 24 months old mice. $N = 6$ animals per group, boxplot distribution with median, Mann-Whitney U-test, $^*p < 0.05$.

of the CD4/CD8 ratio toward a more pronounced CD4+ compartment: CD4+ T cells represented ∼70–80% of all CD3+ cells under non-SPF conditions, whereas under SPF conditions the CD4+ T cell pool represented only around 60% of all CD3+ cells (**Figure 3D**). The CD8+ T effector memory pool (CD8+CD44+CD62L-) can further be divided in T effector memory, memory precursor (MPEC), and short-lived effector cells (SLEC) via the markers CD127 and KLRG1. In all three compartments, the inter-individual variance increased with age under non-SPF housing (**Figure 3E**). Within the CD4+ T cell pool the T regulatory cells (Tregs) are of great interest and this immune cell compartment underwent significant changes with age. With 3 month of age 10.2(±1.7)% of CD4+ T cells were Tregs (FoxP3+CD25high), which further increased to 17.1(±3.1)% at 12 and to 23.8(±4.4)% at 24 months (**Figure 3F**). While the proportion of CD8+ Tregs seemed to be stable in the two younger groups, at 24 months the level of CD8+ Tregs increased (**Figure 3G**). As professional antigen presenting cells (APCs) dendritic cells (DCs) are unrivaled in their capability to activate T cells. We found that specifically the dendritic cells underwent a shift from splenic CD8+ and CD4+ DCs toward conventional splenic DCs in non-SPF housing conditions (**Figure 3B**). Regarding the compartments of NK and NKT cells, both cell subpopulations showed a significant increase in the 24-months-aged mice under non-SPF conditions (**Figure 3C**).

In summary, antigen exposure appears to be very crucial for the development of a diversified immune system, especially impacting the development of a specific memory functionality of the immune system.

To distinguish between changes within the bone that occur during chronological aging and those that are caused by the immune-aging, bones of mice with a more naïve immune composition (aged within an SPF surrounding) were compared, using microCT and biomechanical testing, to bones of mice aged with the possibility to develop an immune memory (immune-aging within non-SPF housing).

The Immune Signature Changes the Mechanical Competence of Bone

Biomechanical testing of the femora was conducted with a mechanical testing machine (Bose ElectroForce LM1, TA Instruments, Eden Prairie, MN USA), and loaded to failure in torsion to characterize the mechanical competence of bone under the influence of differently experienced immune phenotypes and in different age groups. Three groups of six animals each were analyzed: 3 month old were considered as young mice without an experienced immune system. Two groups with 12 month old middle age mice were set as aged groups. One group of aged mice was housed under SPF and one group under non-SPF conditions to gain an experience level in the adaptive immunity. Thus, the two aged groups only differed in their immune cell composition and thus any changes of the mechanical competence are due to the difference in the immune phenotype. The stiffness of the femora increased by age from initial 5.4(±0.5) Nmm/deg at 3 months to 7.0(±0.3) Nmm/deg at 12 months. This change was accredited to the chronological aging. The excessive increase to 8.4(±0.9) Nmm/deg seen in animals in non-SPF housing had to be attributed to the more experienced immune system. Torque at the yield point increased with age and was significant higher under non-SPF conditions. The failure torque increased with chronological age, but also showed a further increase with an experienced immune phenotype (however lacking statistical significance): Maximal torque at failure at 3 months of age 20.4(±2.6) Nmm increased to 28.3(±5.3) Nmm at 12 months SPF and 31.2(±6.1) Nmm at 12 months non-SPF, respectively. The post-yield displacement analysis revealed a ductile fracture manner in 3 month old mice and changed to a brittle fracture manner with age and a significant change under non-SPF housing (**Figure 4**). An experienced, immune-aged system, characterized by a higher pro-inflammatory environment resulted in changed biomechanical competences of the bone. To further investigate the underlying structural causes of this difference in mechanical competence, bone structure was analyzed using microCT analysis.

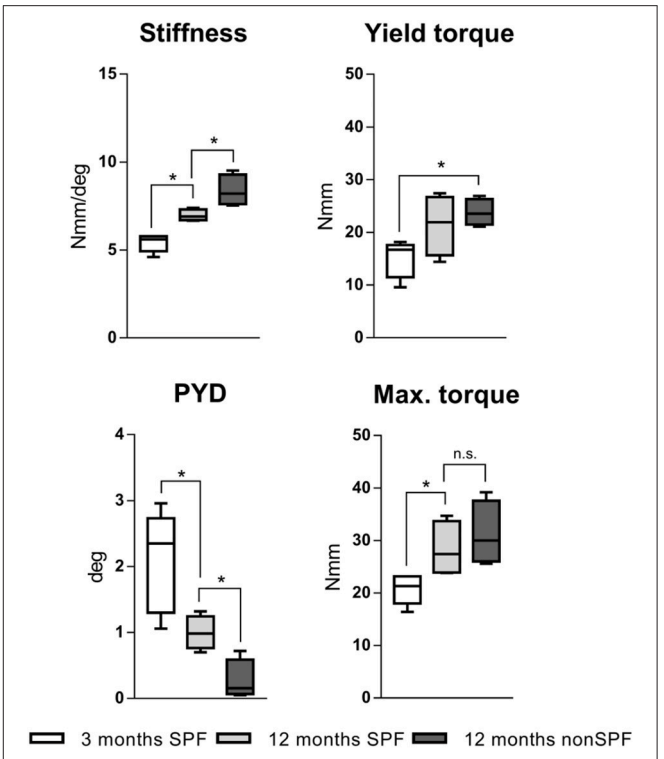

FIGURE 4 | Torsional testing of mouse femora with different immune phenotype. Keeping mouse under non-SPF conditions increased the torsional stiffness compared to 12 months old SPF mice. Yield torque and maximal torque increased by age and was further affected by non-SPF housing. The post-yield displacement (PYD) revelaed a more brittle fracture manner at 12 months under non-SPF compared to 12 months under SPF housing, the 3 month old bone fractured in a more ductile manner. $N = 6$ per group, boxplot distribution with median, Mann-Whitney U-test, $^*p < 0.05$.

The Immune Signature Impacts the Bone Structures

MicroCT analysis was performed on femora of 3 months young mice and two 12 months old groups with one kept under SPF housing (called 12 months SPF) and one kept in non-SPF housing (called 12 months non-SPF) to allow for analyses of chronological aging vs. immune-aging with an increased immunological memory. Both of the old groups showed an aged bone phenotype, additional changes of the bone structure were found within the old mice with an experienced immune phenotype (non-SPF).

Cortical Bone Structure

Total area (Tt.Ar) and bone area (Ct.Ar) increased with age, however both outcome measures were significantly increased in the 12 months non-SPF group compared to the 12 months SPF group. The medullary area (Ma.Ar) did not significantly differ between the groups, leaving the bone marrow canal mostly unaffected. The ratio of bone area inside the tissue area (Ct.Ar/Tt.Ar) was also only different in the aged experienced mouse group, showing an increased ratio of Ct.Ar/Tt.Ar. Strikingly, the total mineral density (TMD) of the cortical bone increased only by age and was not altered by the immune experience (**Figure 5A**). One micrometer resolution scans revealed a periosteal thickness increase with age, specifically on the lateral aspect of the cortex (**Figure 5B**). While in chronological aging, the cortical thickness increased from initial 149(±7) μm at 3 months to 165(±6) μm at 12 months, it increased under the influence of an experienced immune system to 192(±11) μm. Interestingly, this effect was very pronounced on the lateral cortex and demonstrates the general impact of altered immune experience on bone structures such as cortical periosteal perimeter and cortical area.

To judge the mechanical competence of the structure, the mean polar moment of inertia (MMI-polar) was calculated to quantify the bone's capability to resist against rotational loads. The MMI-polar increased with age, reflecting the bone phenotype and age associated adaptation of its mechanical competence like the stiffness of long bones. Surprisingly, this effect of age associated changes in polar moment of inertia were further pronounced in a more experienced immune system.

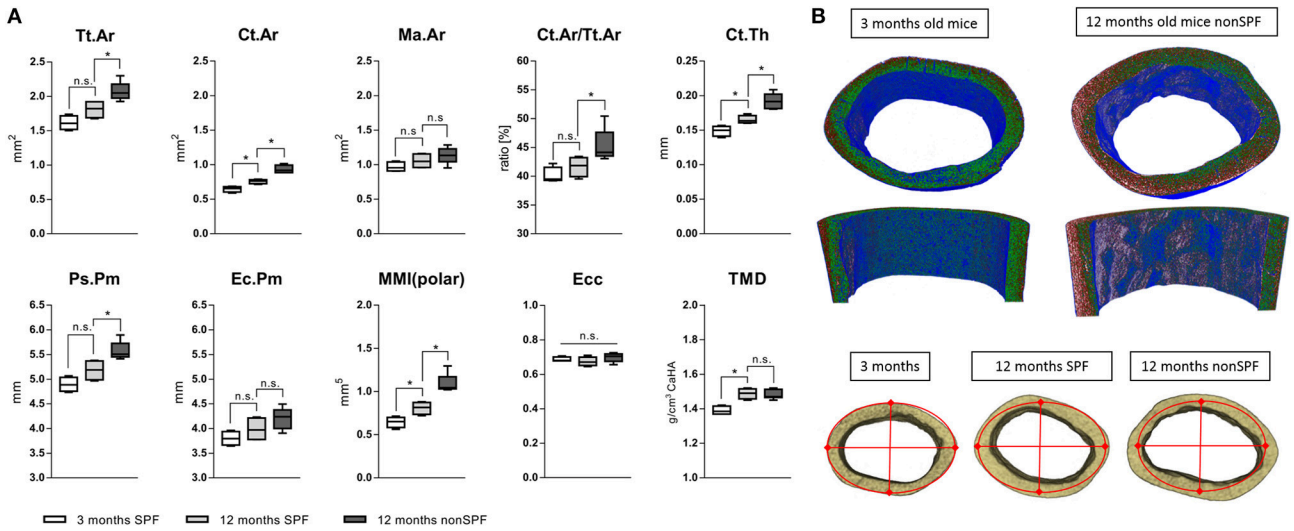

FIGURE 5 | MicroCT analysis of femoral cortical bone. **(A)** Mean total area (Tt.Ar) and cortical area (Ct.Ar) increased under non-SPF conditions compared to SPF conditions. The medullary area (Ma.Ar) and endocortical perimeter (Ec.Pm) are slightly increased, but the periosteal perimeter (Ps.Pm) and cortical thickness (Ct.Th) are significantly increased, demonstrating growth in lateral directions. The ratio of cortical to total area (Ct.Ar/Tt.Ar) was significantly increased in 12 months old mice under non-SPF conditions. Therefore, polar moments of inertia (MMI-polar) were significantly higher under non-SPF conditions. The eccentricity (Ecc) was constant throughout all groups, indicating a constant shape of the cortical femoral bone. Most strikingly the total mineral density (TMD) of the cortical bone was not affected by the housing condition. (**B** top) A density map of the cortical bone comparing a 3 months old mouse with a biologically aged 12 months old mouse. (**B** bottom) Representative images of the cortical bone of a 3 months old mouse compared to 12 months old mice either under SPF or non-SPF conditions. $N = 6$ per group, boxplot distribution with median, Mann-Whitney U-test, $^*p < 0.05$.

Eccentricity (Ecc) is a shape analysis used to define structural deformation of the scanned bones. This parameter was the same for all three analyzed groups indicating that the shape of the cortical bone did not differ among all three groups. The overall mean eccentricity of 0.686(±0.022) indicates a generally elongated, more elliptical object but did not differ neither in chronological nor immunological aged groups (**Figure 5A**).

Trabecular Bone Structure

Bone volume (BV/TV) and trabecular number (Tb.N) decreased with age, independent of the immune experience. However, the trabecular thickness (Tb.Th) was highly effected by the immune cell composition. The trabeculae of 3 month old mice showed a mean thickness of 38(±1) μm and 12 month SPF mice showed an increased thickness to 47(±3) μm, while 12 month non-SPF mice had an even further increased thickness to 53(±5) μm. Trabecular separation indicates the distance between bony structures and revealed that with age the distance increased reflecting the loss of the number of structures, but the two aged groups did not differ. The bone mineral density (BMD) is not affected and the BMD decreases only by age and not by the immune status (**Figures 6A,B**).

The femur length only differed by age, but not with exposure to non-SPF housing conditions. Three months old mice showed a femur length of 14.54 mm ± 0.07, the aged 12 months old mice under SPF conditions showed a femur length of 16.59 mm ± 0.13 comparable to the non-SPF housed mice with 16.86 mm ± 0.27. The weight increased from roughly 22 g at 3 months of age to 27 g in both of the 12 months old group of mice.

In summary, the results show clearly an impact of the immune experience on bone structures but not on bone mineral density. This is a new and so far not reported link between the immune system and the bone structural properties, apparently impacting mechanical competence of bone. The immune experience in 12 month old mice had a significant impact on cortical and trabecular bone microstructure. An experienced immune system led to increases in thickness of the trabecular and cortical bone.

So far, our data illustrate the relevant impact of immune experience on the bone structure. To determine the underlying mechanism, the influence of the immune cell signaling on the osteogenic differentiation of mesenchymal stromal cells had to be investigated. To simulate the immune reaction of an inexperienced vs. an experienced immune system, conditioned medium of activated cells from respective donors was used in osteogenic differentiation assays.

Immune Cells Influence Differentiation and Proliferation of Stromal Cells

To understand why cortical and trabecular microstructure was affected by the adaptive immunity, the interdependency of the immune cells and the bone forming osteoblasts was investigated using mesenchymal stromal cells as an *in vitro* model. To differentiate between the influence of chronological age and experience of the immune system, immune cells from 3 to 12 month old mice were isolated from the spleen, while mesenchymal stromal cells were isolated from bone marrow. Aged mesenchymal stromal cells showed an alleviated ability to differentiate toward the osteogenic lineage: Intensity of the

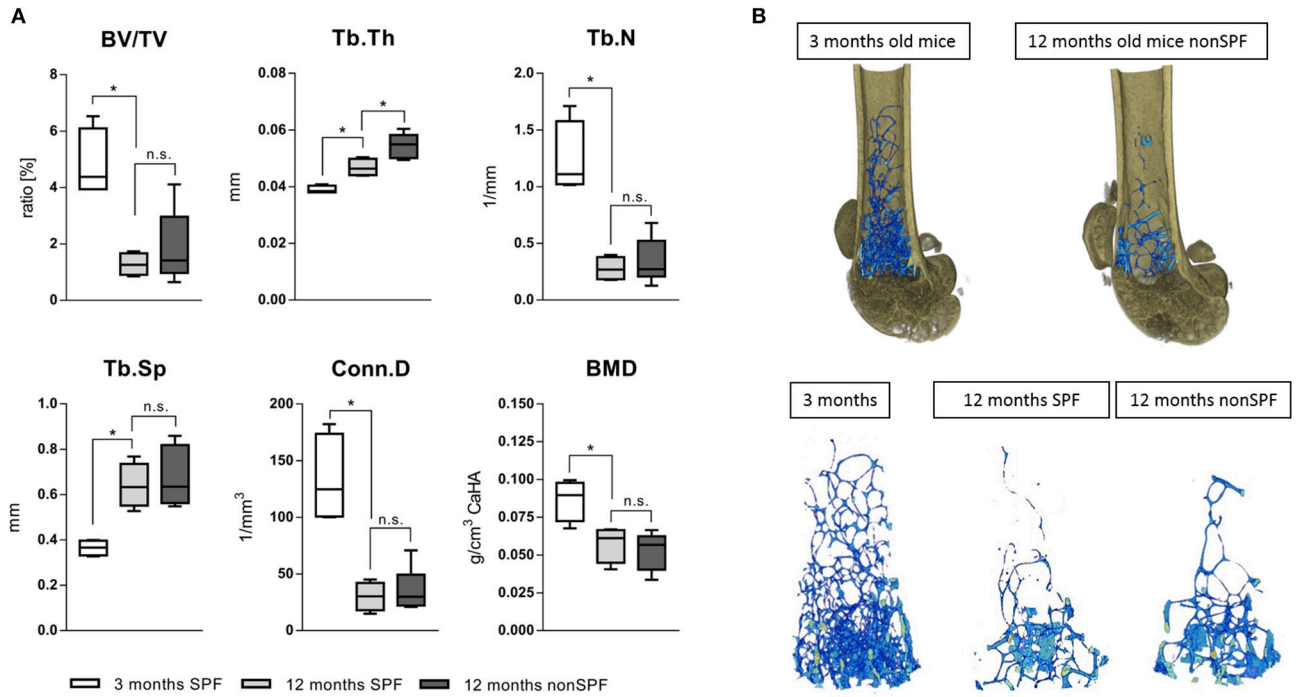

FIGURE 6 | MicroCT analysis of femoral trabecular bone. **(A)** The ratio of bone volume in total volume (BV/TV) and the number of trabecular structures (Tb.N) were both lowered with age, the separation (Tb.Sp) thereafter increased with age. The age dependent loss of trabecular bone was not affected by housing conditions, but the diversity significantly increased under non-SPF conditions. Most strikingly, the trabecular thickness (Tb.Th) not only increased by age but further increased under non-SPF conditions. The connectivity (Conn.D) was not affected by the housing conditions. As seen in the cortical bone analysis the mineral density (BMD) was only affected by age but not by housing conditions. (**B** top) Representative 3D rendered images of trabecular bone comparing a 3 months old mouse with a biologically aged 12 months old mouse. (**B** bottom) Representative images of 3D rendered images of trabecular bone of a 3 months old mouse compared to 12 months old mice either under SPF or non-SPF conditions. $N = 6$ per group, these are the same samples analyzed for the cortical bone parameters (**Figure 5**), boxplot distribution with median, Mann-Whitney *U*-test, $^*p < 0.05$.

Alizarin red S staining of the extracellular matrix decreased with age (**Figure 7**). To represent an immunologically inexperienced immune setting, splenocytes of 3 month old, young mice were stimulated and conditioned medium was harvested. The experienced immune composition was simulated by gaining conditioned medium from splenocytes of 12 month old, immunologically experienced mice. The respective conditioned medium was then added to young or old mesenchymal stromal cells which underwent osteogenic differentiation. As a control conditioned medium from non-activated splenocytes, from both ages was used. Conditioned medium (CM) from activated immune cells decreased the osteogenic differentiation of mMSCs in both age groups compared to non-activated CM and osteogenic medium control (OM). The conditioned medium was either added to 3 months old mMSCs or to the less competent 12 months old mMSCs. In both mMSC groups the conditioned medium gained from the experienced immune cells decreased the osteogenic differentiation significantly **(Figure 7)**. Analyses of the conditioned medium with enzyme-linked immunosorbent assay (ELISA) revealed an increase in pro-inflammatory cytokines like interferon γ (IFNγ) and tumor necrosis factor α (TNFα) (**Figure 7C**). Amazingly, interleukin 10 (IL-10), known to have anti-inflammatory properties, was also increased (**Figure 7C**). These results confirmed that an experienced immune system shows an increased pro-inflammatory capacity—that is negatively affecting the osteogenic potential of MSCs. Hence, osteogenic differentiation of mesenchymal stromal cells is damped under the influence of an aged immune system.

The influence of the immune composition on osteogenic processes further confirm that bone formation, mechanical competence, and structure are dependent on the age/experience of the immune cells. But how would a perturbation alter the interplay of immune and bone system, such as in a homeostatic setting? During bone homeostasis, a key modulator of tissue formation and resorption is the mechanical loading experienced by the bone. Bone adapts to the experienced mechanical loads (43). Is such a mechanically induced bone formation process also affected by the experience of the immune system? A well-established limb-loading model was used in young and aged animals and the changes in the immune cell composition in the bone marrow of loaded bones were monitored.

In vivo Perturbation: Mechanical Loading as a Rescue for Immune Experience?

The bone's capability to adapt its mass and architecture to changes in the mechanical loading environment is a remarkable function. While mechanical loading enhances bone mass in young mice,

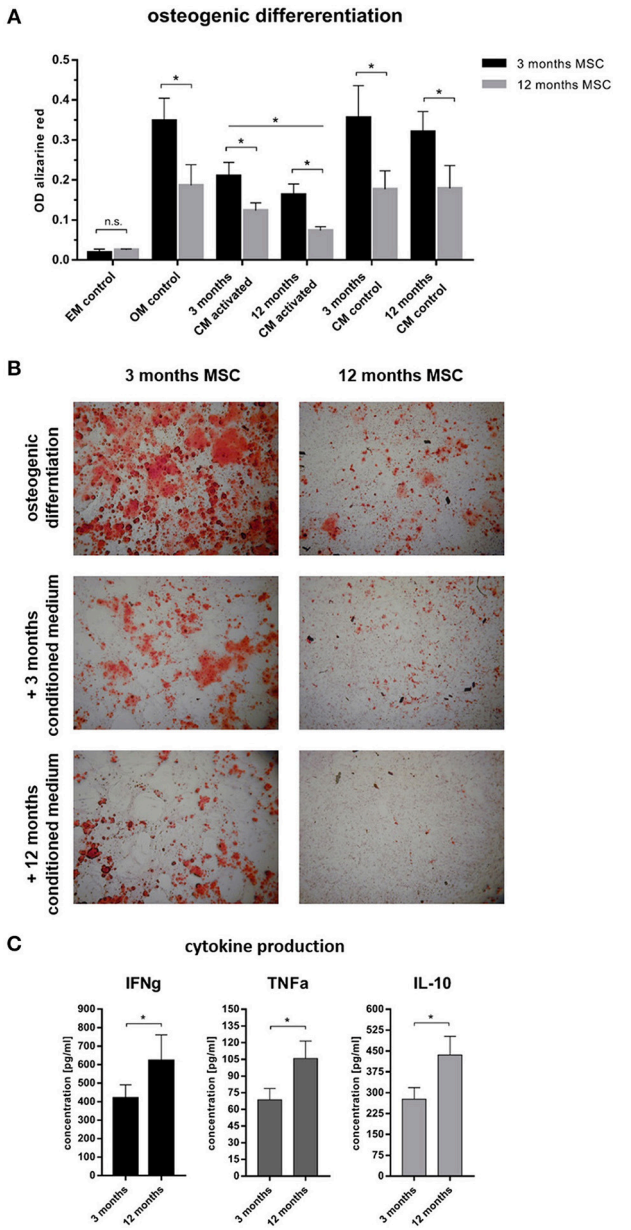

FIGURE 7 | Osteogenic differentiation after 14 days under the influence of conditioned medium from immune cells. **(A)** 3 months old mesenchymal stromal cells (MSC) were compared to 12 months old MSC. The 12 months old MSC showed a reduced osteogenic differentiation potential compared to 3 months old MSC. Adding conditioned medium from immune cells (conditioning for 48 h) that were not activated did not affect the osteogenic differentiation, but adding conditioned medium from activated immune cells lowered the differentiation potential. The conditioned medium from 12 months old mice worsened the ability to differentiate into the osteogenic lineage. **(B)** Representative images of the calcium deposition stained by Alizarin Red S comparing 3 and 12 months old MSC under the influence of different conditioned medium. Twelve months old MSC under the influence of activated 12 months old conditioned medium almost abolished the ability for calcium deposition. **(C)** Analysis of the conditioned medium showed an increase of pro- (IFNγ and TNFα) and anti-inflammatory (IL-10) cytokines from 12 months old immune cells. N = 6 animals per age, conditioned medium was pooled and added at a ratio of 1:3 to the osteogenic differentiation medium, assays were performed in triplicates, mean ± SD, unpaired *t*-test, $^*p < 0.05$.

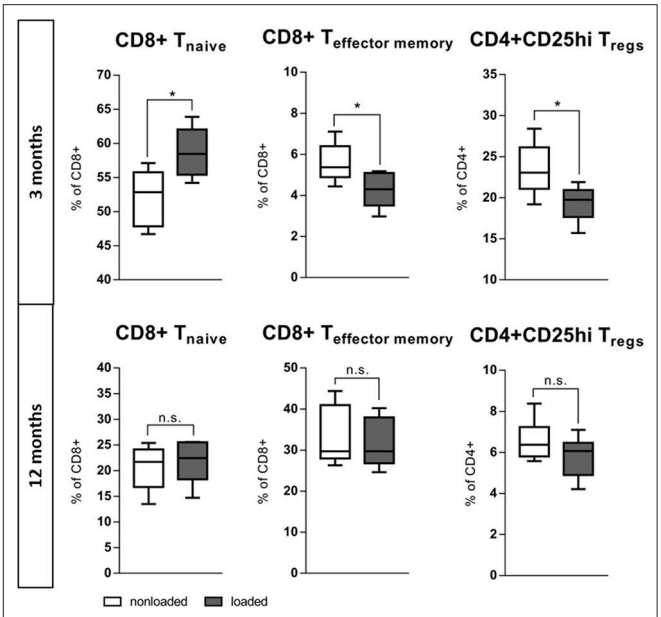

FIGURE 8 | *In vivo* rescue of experience level in the immune system with mechanical loading. The left tibia of 3 and 12 month old mice underwent daily (Monday–Friday) *in vivo* axial compressive cyclic loading for 2 week, thereafter the bone marrow was flow cytometric analyzed. In 3 month old mice the mechanical loading of the tibia increased the population of naïve CD8+ T cells and decreased the effector memory population locally in the bone marrow. CD4+ Tregs decreased comparably to the effector memory T cells. This more naïve immune milieu created under mechanical loading is not viable in 12 months old mice. $N = 6$ animals per age, boxplot distribution with median, Mann-Whitney *U*-test, $^*p < 0.05$.

this effect is reduced in aged individuals (36, 44). The question arose whether this also relates to the immune response involved. The left tibia of 3 and 12 month old mice underwent daily (Monday-Friday) *in vivo* axial compressive cyclic loading for 2 weeks. After 2 weeks, the bone marrow from the loaded and from the non-loaded contralateral tibia was harvested and analyzed with flow cytometry. Strikingly, within the loaded tibia of the young 3 months old mice a more naïve immune phenotype arose when compared to the contralateral non-loaded bone. In the bone marrow of the loaded tibia from the 3 months old mice, the naïve CD8+ T cells increased to 58.7(±3.8)% of all CD8+ T cells compared to 52.2(±4.1)% in the contralateral non-loaded control tibia. In addition, the percentage of CD8+ effector/memory T cells significantly decreased under the influence of loading. This data suggests that a less inflammatory immune cell composition supports bone formation in response to loading of young mice (similar to what we observed in our *in vitro* experiments). This more naïve immune cell milieu did not coincide with loading in the aged, 12 months old mice. CD4+ Tregs, ascribed as potent anti-inflammatory cells, reacted contrariwise to loading with a decrease of their proportion within the bone marrow of the loaded tibia (**Figure 8**). These findings show that the positive effect that mechanical loading had in young mice was absent in the aged animals, and that could indeed be related to differences in the immune response to the mechanical stimulus.

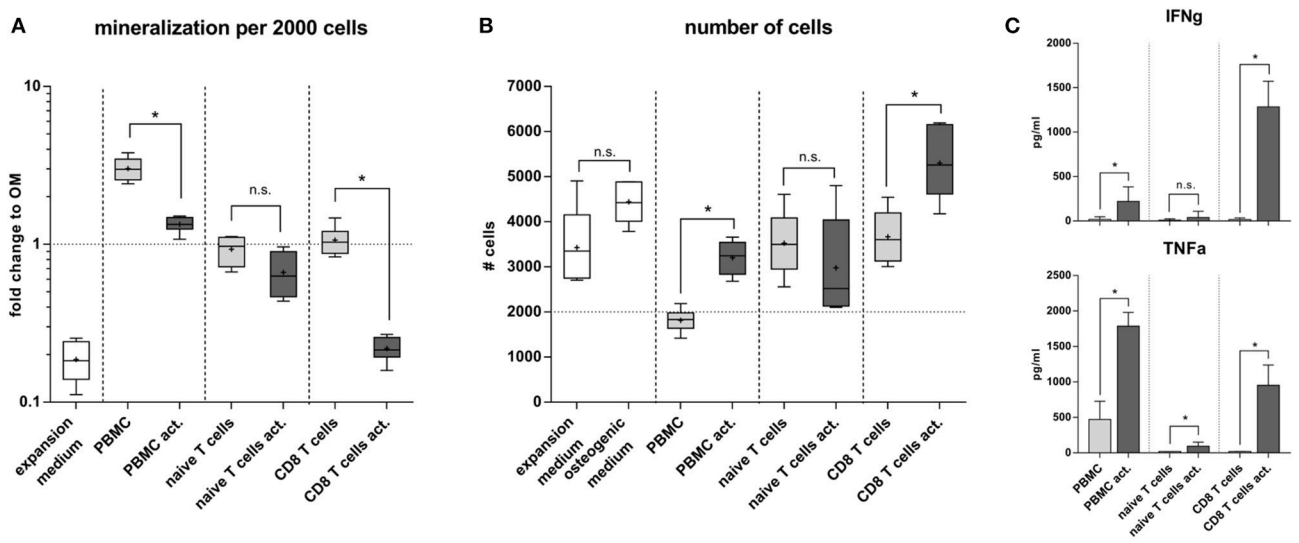

FIGURE 9 | Osteogenic differentiation under the influence of immune cell subsets. **(A)** Naïve T cells compared to CD8+ T cells did not alter the osteogenic differentiation. Activated CD8+ T cells significantly lowered the calcium deposition. Peripheral blood mononuclear cells (hPBMC) increased the mineralization of the extracellular matrix compared to the osteogenic medium without immune cells. This is due to a decreased proliferation **(B)**. Conditioned medium from CD8+ T cells increased proliferation but hindered the osteogenic differentiation of hMSC. **(C)** Cytokine production of activated CD8+ T cells was strong pro-inflammatory, activated PBMC mainly produced TNFα but not IFNγ, whereas activated naïve T cells did not produce significant amounts of IFNγ and TNFα. $N = 3$ immune cell donors, naïve and CD8+ T cell isolation was performed for each donor, $N = 2$ hMSC donors, assay was run in triplicates, boxplot distribution with median, mean depicted with a +, ELISA data shown as mean ± SD, unpaired *t*-test, $^*p < 0.05$.

To further understand the interdependency of an experienced immune system and the osteogenic capacity of mesenchymal stromal cells an *in vitro* "rescue experiment" was performed by analyzing specific cellular subsets in view of their effect on the osteogenic capacity. For this experiment the mouse model where age and immune experience were distinguishable was changed to human cells to model the patient situation more closely *in vitro*.

Naïve and Experienced Human Immune Cell Subsets Differently Affect Osteogenic Differentiation and Proliferation

To further elucidate the interrelation between bone structure and immune experience we selected a more clinically relevant situation by isolating naïve and experienced immune cells directly from human peripheral blood. Distinctly different immune subsets were tested for their influence on the differentiation capacity of human mesenchymal stromal cells (MSC). From density gradient isolated human peripheral blood mononuclear cells (hPBMC) either CD8+ T cells or naïve T cells were isolated and stimulated *in vitro* with CD3 and CD28. Mesenchymal stromal cells were isolated from bone marrow aspirates from patients undergoing hip surgery with written consent. The osteogenic differentiation outcome was calculated per 2000 cells to account for difference between proliferation and differentiation. Our data clearly showed that conditioned medium from naïve T cells did not dampen the osteogenic differentiation ability of MSC, whereas the conditioned medium from CD8+ T cells almost abolished the osteogenic differentiation (**Figure 9A**). Interestingly conditioned medium from activated CD8+ T cells induced proliferation in MSC. In contrast the conditioned medium from whole hPBMC hindered proliferation while supporting osteogenic differentiation (**Figure 9B**). Apparently, signaling patterns from specific immune cell subsets play an important role in distinguishing whether cell proliferation or differentiation is supported and activated. Thus, immune cells appear essential in guiding tissue formation—such as bone formation—and thereby impact the resulting tissue structure. Quantitative cytokine detection revealed an inert cytokine pattern in activated naïve T cells compared to activated CD8+ T cells, which produced a high concentration of IFNγ and TNFα. PBMC already produced a faint milieu of TNFα functionally inhibiting the proliferation of MSCs and therefore promoting the differentiation process as described within other studies (45) (**Figure 9C**).

Determining that the immune cell composition influences the osteogenic potential from mesenchymal stromal cells indicates that the immune signature will also influence the bone healing capacity. Thus, the initial observation that aged patients show a reduced healing capacity (confirmed in a mouse model with an experienced non-SPF immune cell composition) could be related to an experienced immune signature. To further investigate this hypothesis, bone healing was analyzed in a mouse model with a humanized immune system that was either more naive or already more experienced.

In vivo: Bone Regeneration Benefits From a Naïve Immune Milieu

To monitor the behavior of different immune phenotypes on the *in vivo* bone regeneration, a humanized peripheral blood mononuclear cell (hPBMC) mouse model was used: the

humanized PBMC NOD scid gamma (NSG) mice. NOD.Cg-Prkdc^{scid} Il2rg^{tm1Wjl}/SzJ (NSG) mice lack the ability to activate their own immune system and some immune subsets are even completely missing. Human PBMC from different donors were analyzed toward the immune phenotype and an experience level for stratification was achieved via the CD8+ T_{EMRA} level. CD8+ T_{EMRA} cells are known from earlier studies to be predictive for delayed bone healing as published by Reinke et al. (42). Donors with a CD8+ T_{EMRA} level above 30% of total CD8+ T cells were considered as immunologically experienced. NSG mice received intravenously either naïve or experienced hPBMCs from stratified donors and consecutively underwent surgery to introduce a 0.7 mm osteotomy gap stabilized with a unilateral external fixator (MouseExFix, RISystem, Davos, Switzerland). Healing outcome was assessed 21 days post-surgery with microCT. Three groups were analyzed: one group did not receive human immune cells (control), one group received naïve hPBMCs and one group received experienced hPBMCs. The transfection efficacy and accumulation of the human immune cells inside the tissue was verified after 3 and 21 days with flow cytometry (**Figures 10A,B**). The callus 21 days post-surgery showed an increased bone volume fracture (BV/TV) under the influence of naïve hPBMCs compared to the control as well as compared to experienced hPBMC. The bone volume fraction for the group receiving experienced hPBMC did not differ to the control. Quantifying the bone mineral density (BMD) revealed a benefit of immune cells on newly formed bone with an increased mineral density even with experienced immune cells compared to the control. Remarkably, the group with naïve hPBMC showed the highest density of mineralization among all groups. Under the influence of injected hPBMCs newly formed bone revealed a decrease in trabecular numbers while the thickness of those structures significantly increased. The naïve hPBMCs significantly increased the deposition of mineral tissue showing the positive effect of a young/ naïve immune system on the bone healing process (**Figure 10C**). These findings show that bone regeneration benefits from a more naïve immune system.

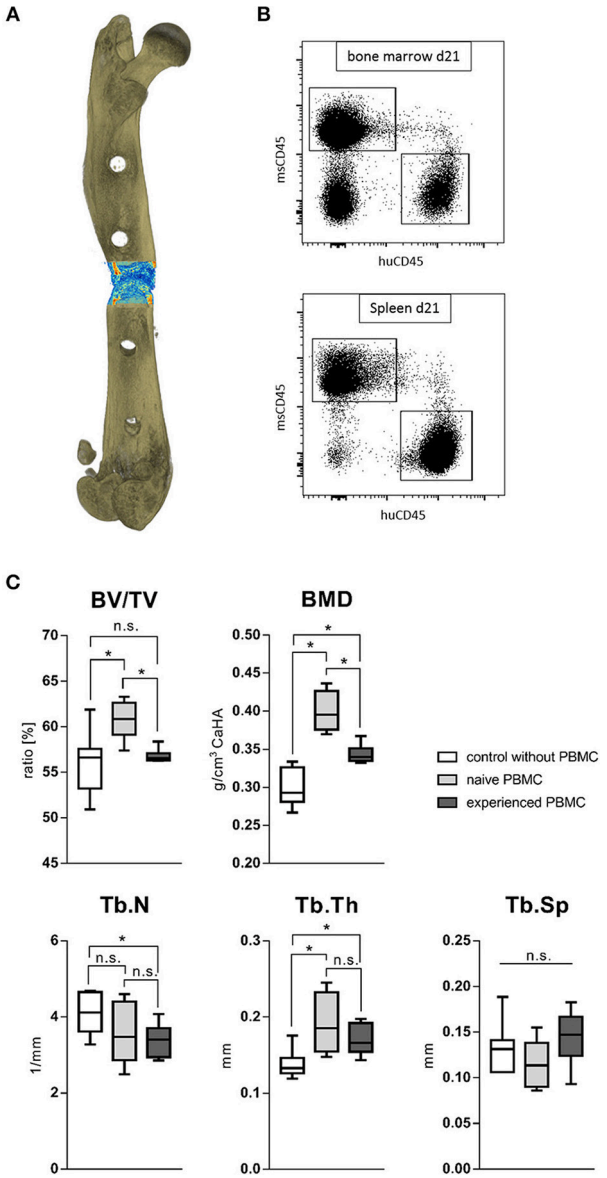

FIGURE 10 | Fracture healing outcome of humanized PBMC mice. **(A)** Representative image of a 21 days old fracture gap. **(B)** Human immune cells settled to spleen and bone marrow in significant levels after transfer. **(C)** Healing under the influence of either experienced or more naïve peripheral blood mononuclear cells (hPBMC) showed a beneficial effect of a more naïve immune phenotype. The bone volume in total volume (BV/TV) was significantly increased under the influence of more naïve hPBMC compared to the control without hPBMC and more experienced hPBMC. The bone mineral density (BMD) and trabecular thickness (Tb.Th) stood to benefit from immune cells. The more naïve hPBMC further increased the mineral density within the fracture gap compared to more experienced hPBMC. The number of newly formed trabecular structures (Tb.N) seemed to decrease under the influence of more experienced hPBMC. $N = 6$ animals in the naïve hPBMC group, $N = 8$ each in control and experienced hPBMC group, boxplot distribution with median, Mann-Whitney U-test, $^*p < 0.05$.

DISCUSSION

Changes within the skeletal system upon aging have been widely acknowledged. This study showed for the first time that not only the chronological age but also the immunological age substantially impacts bone mass and microstructure and should be considered in assessing patient's risk factors and healing potential (42). The immunological age is mostly determined by changes in the adaptive immune system. With increasing antigen exposure, the effector and effector memory pool within the adaptive immunity of an individual increases, while simultaneously the naïve lymphocyte pool diminishes. This process of immune-aging is greatly influenced by time but not *per se* comparable among individuals, specifically if they have seen different immune challenges. This is also mirrored in our data where the immune composition of exposed mice show an increasing standard deviation in the CD8+ T central and effector memory cell population after 2 years of environmental exposure (in a still relatively standardized environment of animal housing). The direction of the immune aging process is comparable among people, however, the pace

with which it proceeds differs due to the living environment and personal habits.

As a first example to illustrate the relevance of the immune experience, we focused on the common assumption that bone healing in the elderly is impaired (46), albeit most studies do not properly document reasons for lack of healing in the aged population (47). There is a paucity of supportive data within the scientific literature on the immune experience or its effect on various biological processes (mainly due to a lack of proper documentation in preclinical studies). Only recently have questionnaires such as the ARRIVE guidelines for preclinical studies included questions related to housing and husbandry that allow one to determine the immunological age of an animal. To analyze the effect of the immune experience on bone homeostasis and healing, immune aging had to be characterized within a mouse model. By dividing mice into two groups and keeping those under specific pathogen free conditions and antigen exposed conditions, respectively, during aging it became possible to distinguish between skeletal changes caused by chronological aging vs. changes that were dependent on the immunological age/state of the animals (biological aging).

Analyzing immune-aging in mice showed an increase in memory and effector function with age. The exposure to antigens in non-SPF housings led to an amplified age-associated phenotype of the immune system, reflecting the changes seen in humans (23). One-year-old non-SPF housed mice appeared to be able to reflect roughly a 40–50 years old human while 2-year-old non-SPF mice reflected humans of around 50–60 years of age. Using such approach, a mouse model was established that allowed the analysis of immune-aging on the bone.

For the analysis of the impact of the immune experience within the study a model was chosen that enabled the investigation of mice of the same age but with a differently developed adaptive immune system due to a difference in housing (SPF vs. non-SPF). While the animals were held as similar as possible in order to determine the immune experience as the source of the changes detected in the bone, additional influences could have had an impact. The influences of the changed immune composition could lead to a change in other cell compartments (e.g., the more pro-inflammatory signaling could induce higher M1 macrophage percentages), epigenetic changes could also occur which were not considered within this study. Also, the microbiota is a potent modulator of the immune system and vice versa, an influence that would offer future research opportunities (9, 48, 49). To overcome this possible bias the humanized PBMC mouse model was applied within this study—these mice were identical up to the day before osteotomy when they received the human immune cells and were kept under identical conditions thereafter for the observation time of 21 days—a time period where the above mentioned changes would not occur in a meaningful way.

It is well-known that biomechanical properties of bone, specifically the energy to mechanical failure decreases with age (50). While our data confirmed the age related changes in biomechanical properties this is the first study to depict that some of these changes are intensified by the immune experience level. This loss in mechanical properties is usually associated with age-related bone microstructural changes in both the cortical and trabecular compartments (51–53) So far, a link between age-related bone loss and adaptive immunity, specifically the experience of the immune system had not been investigated (50–54).

On the other hand, cellular senescence occurring in elderly individuals is a major hallmark of age associated processes representing various types of stress that cause distinct cellular alterations, including major changes in gene expression and metabolism, eventually leading to the development of a pro-inflammatory secretome (55). In accordance with the literature the monocyte-macrophage-osteoclast lineage and the mesenchymal stem cell-osteoblast lineage are affected by increasing age, which is associated with higher baseline levels of inflammatory mediators, and therefore a significant reduction in osteogenic capabilities can be observed (56). This inflamm-aging affects different signaling pathways, gene expression, cellular events like proliferation and differentiation, chemotaxis of precursor cells, expression of growth regulatory factors and the production of bone structural proteins. All these affected processes represent the complex orchestration of interdependent biological events that occur during fracture repair (57).

For the first time, our study clearly illustrates the influence of the experienced immune phenotype on changes in bone mass, microstructure, and mechanical properties that go beyond those attributed to chronological aging. Keeping mice under non-SPF conditions lead to increased cortical thickness. The stiffness and maximal force at failure increased with age due to an increased mineralization density. However, the cortical thickness changed in conjunction with the altered immune composition. The experienced immune signature led to an altered and a more stiff bone structure and a more brittle fracture. Such brittleness increases the risk of fracture upon low-impact loads or injuries—a phenomenon frequently seen in aged patients (58). For the first time, the reduced bone structure and phenotype of an aged bone found in elderly patients can be seen to be even worsened by an immune-aged or inflamm-aged setting. The strong link between immune experience and structural properties makes an immune diagnostic approach to stratify patients according to their immune status a relevant perspective, so far widely ignored in bone treatment and research. Studies from Zhao et al. using a bioinformatics approach revealed likewise significant changes in the inflammatory response during fracture healing upon aging. The inflammatory response was shown to be enriched in the elderly compared to the younger population. In addition changes in the Wnt signaling pathway, vascularization-associated processes, and synaptic-related functions may account for delayed fracture healing in the elderly (59).

The interdependency of the immune and bone compartment has been investigated from different perspectives. Concerning the interplay of osteoclasts and immune cells the pro-inflammatory cytokines TNFα and IFNγ which were analyzed within this study as cytokines delaying the healing/ osteogenesis have been discussed as promoting osteoclastogenesis (60). Bone loss in postmenopausal osteoporosis has been addressed by anti-TNFα treatments (61). This indicates the elevated TNFα levels

could be causative for the postmenopausal bone loss. So far, the immune experience and the higher TNFα levels going hand in hand with higher levels of effector memory T cells has however not yet been considered. That the more pro-inflammatory state of the experienced immune system with high numbers of TNFα producing effector memory T cells could be responsible for reduced bone formation or even bone loss is also mirrored in previous studies where activated T cells have been correlated to bone loss in conditions of inflammation and autoimmune disorders (62, 63), osteoporosis models (64, 65), or even periodontitis and cancer (66–68).

So far, the age-related alteration in mechano-response was solely explained by the mechanical signal losing its specificity to activate osteoblasts or inhibit osteoclasts (69). The here presented data suggest a reprograming of immunity toward a more naïve phenotype and thus a potential rescue mode in young animals. Interestingly, the rescue was only significant in young individuals but showed similar trends in the older animals, suggesting the immune system may play a role in the bones reduced mechano-response with age. The impact of mechanical loading on adaptive immunity illustrates the immune-structure relationship, and thus identifies a re-gain in ones naïve immunity as an additional route that could be exploited therapeutically in the future. In a clinical study moderate intensity exercise in adult subjects revealed a decrease of osteoclastogenic cytokines, showing that biomechanical loading could represent a potential immune modulator (70).

How is bone healing impacted by the immune status? Upon a bone fracture, a cascade of sterile inflammatory reactions are initiated which determine a successful, delayed or failed bone healing (12, 19, 71–73). Earlier studies have shown that a prolonged pro-inflammatory response delays the healing process. Such a prolonged pro-inflammatory cascade could be further enhanced by the here reported immune-aged or inflamm-aged status resulting in a more severe delay of healing. The reported data in the present study demonstrates clearly that a naïve immune system leads to an effective healing while an experienced immunity significantly delays bone formation, as demonstrated by the humanized PBMC mouse models. Again, patient stratification early on would allow for the identification of patients at risk of delayed healing due to an immune-aged status. Preemptive measures could be initiated in these patients to compensate for their healing deficit. A biomarker study is currently ongoing to threshold patients by the level of CD8+ T_{EMRA} cells for a high risk of delayed bone healing (42). As a potential measure to reprogram immunity toward a more naïve phenotype, a mechanical limb loading stimulation such as those experienced in physical exercise was presented. Although a "rescue" toward a more naïve phenotype could clearly be found in young (leading also to an enhanced bone homeostasis) the effect was substantially reduced in a more aged mouse model. Thus, the effect of mechano-therapeutics as measures to reprogram the immune system may alone not be completely sufficient yet. Further in depth understanding of

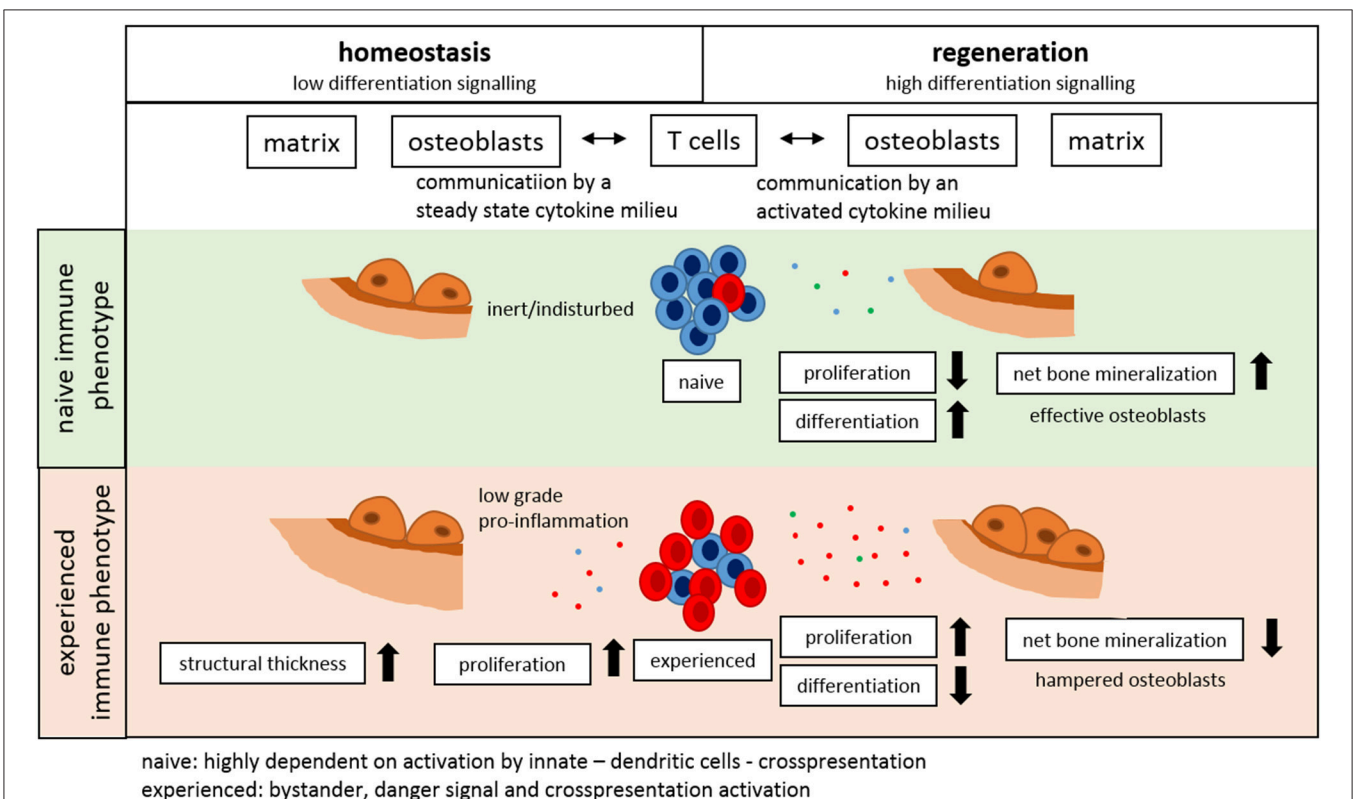

FIGURE 11 | The immune system impacts bone formation.

the processes of re-programming the immune compartment, specifically in inflamm-aged situations seems to be important to further elucidate the therapeutic potential of mechanical loading in the senescent skeleton.

CONCLUSION

In conclusion, our data presented here clearly shows for the first time a distinct link of the immune system to the structural properties of bone as those involved in bone homeostasis, regeneration and adaptation. The experience of the immune system directly impacts bone formation capability and thereby affects structural properties of trabecular and cortical bone as well as overall mechanical competence (**Figure 11**).

ETHICS STATEMENT

This study was carried out in accordance with the recommendations of the ARRIVE and institutional guidelines. The protocol was approved by the Landesamt für Gesundheit und Soziales, LaGeSo, Berlin.

AUTHOR CONTRIBUTIONS

CB, KS-B, GD, BW, and H-DV: conceptual idea and design of the study; CB, CS, SW, DW, FS, and TT: data collection, analysis, and interpretation; CB, KS-B, and AE: animal surgeries; CB, KS-B, CS, GD, H-DV, and BW: drafting of the manuscript; RS: clinical data. All authors revised the manuscript.

FUNDING

This work was supported by a grant from the German Research Foundation (FG 2195: DFG SCHM 2977, DU 298/21-1), the FriedeSpringer Stiftung, the Berlin-Brandenburg Center for Regenerative Therapies, the Berlin-Brandenburg School for Regenerative Therapies and the Einstein Center for Regenerative Therapies.

ACKNOWLEDGMENTS

We would like to acknowledge the Open Access Publication Fund of Charité – Universitätsmedizin Berlin.

We would like to thank Norma Schulz, Anke Dienelt, Christine Figge, Mario Thiele, Anne Seliger and the core unit "Cell and Tissue harvesting."

SUPPLEMENTARY MATERIAL

The Supplementary Material for this article can be found online at: https://www.frontiersin.org/articles/10.3389/fimmu.2019.00797/full#supplementary-material

REFERENCES

1. Manini T. Development of physical disability in older adults. *Curr Aging Sci.* (2011) 4:184–91. doi: 10.2174/1874609811104030184
2. Kiel DP, Rosen CJ, Dempster D. Chapter 20: Age-related bone loss. In: *Primer on the Metabolic Bone Diseases and Disorders of Mineral Metabolism.* Hoboken, NJ: John Wiley & Sons, Inc. (2008) p. 98–102. doi: 10.1002/9780470623992.ch20
3. World Health Organization. *Ageing Heal.* Geneva: Wolrd Health Organization (2018). Available online at: http://www.who.int (accessed February 5, 2018).
4. Bishop JA, Palanca AA, Bellino MJ, Lowenberg DW. Assessment of compromised fracture healing. *J Am Acad Orthop Surg.* (2012) 20:273–82. doi: 10.5435/JAAOS-20-05-273
5. Schmidt-Bleek K, Marcucio R, Duda G. Future treatment strategies for delayed bone healing: an osteoimmunologic approach. *J Am Acad Orthop Surg.* (2016) 24:e134–5. doi: 10.5435/JAAOS-D-16-00513
6. Ono T, Takayanagi H. Osteoimmunology in bone fracture healing. *Curr Osteoporos Rep.* (2017) 15:367–75. doi: 10.1007/s11914-017-0381-0
7. Limmer A, Wirtz D. Osteoimmunology: influence of the immune system on bone regeneration and consumption. *Z Orthop Unfall.* (2017) 155:273–80. doi: 10.1055/s-0043-100100
8. Takayanagi H. New developments in osteoimmunology. *Nat Rev Rheumatol.* (2012) 8:684–9. doi: 10.1038/nrrheum.2012.167
9. Walsh MC, Takegahara N, Kim H, Choi Y. Updating osteoimmunology: regulation of bone cells by innate and adaptive immunity. *Nat Rev Rheumatol.* (2018) 14:146–56. doi: 10.1038/nrrheum.2017.213
10. Ginaldi L, De Martinis M. Osteoimmunology and beyond. *Curr Med Chem.* (2016) 23:3754–74. doi: 10.2174/0929867323666160907162546
11. Schlundt C, Schell H, Goodman SB, Vunjak-Novakovic G, Duda GN, Schmidt-Bleek K. Immune modulation as a therapeutic strategy in bone regeneration. *J Exp Orthop.* (2015) 2:1–10. doi: 10.1186/s40634-014-0017-6
12. Schmidt-Bleek K, Kwee BJ, Mooney DJ, Duda GN. Boon and bane of inflammation in bone tissue regeneration and its link with angiogenesis. *Tissue Eng Part B Rev.* (2015) 21:354–64. doi: 10.1089/ten.teb.2014.0677
13. Schett G. Effects of inflammatory and anti-inflammatory cytokines on the bone. *Eur J Clin Invest.* (2011) 41:1361–6. doi: 10.1111/j.1365-2362.2011.02545.x
14. Pfeilschifter J, Chenu C, Bird A, Mundy GR, Roodman DG. Interleukin-1 and tumor necrosis factor stimulate the formation of human osteoclastlike cells *in vitro*. *J Bone Miner Res.* (2009) 4:113–8. doi: 10.1002/jbmr.5650040116
15. Adamopoulos IE, Bowman EP. Immune regulation of bone loss by Th17 cells. *Arthritis Res Ther.* (2008) 10:225. doi: 10.1186/ar2502
16. Akdis M, Burgler S, Crameri R, Eiwegger T, Fujita H, Gomez E, et al. Interleukins, from 1 to 37, and interferon-γ: receptors, functions, and roles in diseases. *J Allergy Clin Immunol.* (2011) 127:701–21.e70. doi: 10.1016/J.JACI.2010.11.050
17. Li Y, Toraldo G, Li A, Yang X, Zhang H, Qian WP, et al. B cells and T cells are critical for the preservation of bone homeostasis and attainment of peak bone mass *in vivo*. *Blood.* (2007) 109:3839–48. doi: 10.1182/blood-2006-07-037994
18. Schell H, Duda GN, Peters A, Tsitsilonis S, Johnson KA, Schmidt-Bleek K. The haematoma and its role in bone healing. *J Exp Orthop.* (2017) 4:5. doi: 10.1186/s40634-017-0079-3
19. Schmidt-Bleek K, Schell H, Schulz N, Hoff P, Perka C, Buttgereit F, et al. Inflammatory phase of bone healing initiates the regenerative healing cascade. *Cell Tissue Res.* (2012) 347:567–73. doi: 10.1007/s00441-011-1205-7
20. Schmidt-Bleek K, Schell H, Lienau J, Schulz N, Hoff P, Pfaff M, et al. Initial immune reaction and angiogenesis in bone healing. *J Tissue Eng Regen Med.* (2014) 8:120–30. doi: 10.1002/term.1505
21. Könnecke I, Serra A, El Khassawna T, Schlundt C, Schell H, Hauser A, et al. T and B cells participate in bone repair by infiltrating the fracture callus in a two-wave fashion. *Bone.* (2014) 64:155–65. doi: 10.1016/j.bone.2014.03.052

22. El Khassawna T, Serra A, Bucher CH, Petersen A, Schlundt C, Könnecke I, et al. T lymphocytes influence the mineralization process of bone. *Front Immunol.* (2017) 8:562. doi: 10.3389/fimmu.2017.00562
23. Kverneland AH, Streitz M, Geissler E, Hutchinson J, Vogt K, Boës D, et al. Age and gender leucocytes variances and references values generated using the standardized ONE-Study protocol. *Cytometry A.* (2016) 89:543–64. doi: 10.1002/cyto.a.22855
24. Qi Q, Liu Y, Cheng Y, Glanville J, Zhang D, Lee J-Y, et al. Diversity and clonal selection in the human T-cell repertoire. *Proc Natl Acad Sci USA.* (2014) 111:13139–44. doi: 10.1073/pnas.1409155111
25. Weyand CM, Goronzy JJ. Aging of the immune system. Mechanisms and therapeutic targets. *Ann Am Thorac Soc.* (2016) 13:S422–8. doi: 10.1513/AnnalsATS.201602-095AW
26. Clark D, Nakamura M, Miclau T, Marcucio R. Effects of aging on fracture healing. *Curr Osteoporos Rep.* (2017) 15:601–8. doi: 10.1007/s11914-017-0413-9
27. Schoenborn JR, Wilson CB. Regulation of interferon-γ during innate and adaptive immune responses. *Adv Immunol.* (2007) 96:41–101. doi: 10.1016/S0065-2776(07)96002-2
28. Becker TC, Coley SM, Wherry EJ, Ahmed R. Bone marrow is a preferred site for homeostatic proliferation of memory CD8 T cells. *J Immunol.* (2005) 174:1269–73. doi: 10.4049/JIMMUNOL.174.3.1269
29. Di Rosa F, Gebhardt T. Bone marrow T cells and the integrated functions of recirculating and tissue-resident memory T cells. *Front Immunol.* (2016) 7:51. doi: 10.3389/fimmu.2016.00051
30. Badylak S. Perspective: work with, not against, biology. *Nature.* (2016) 540:S55. doi: 10.1038/540S55a
31. Badylak S, Rosenthal N. Regenerative medicine: are we there yet? *npj Regen Med.* (2017) 2:2. doi: 10.1038/s41536-016-0005-9
32. Tsitsilonis S, Seemann R, Misch M, Wichlas F, Haas NP, Schmidt-Bleek K, et al. The effect of traumatic brain injury on bone healing: an experimental study in a novel *in vivo* animal model. *Injury.* (2015) 46:661–5. doi: 10.1016/j.injury.2015.01.044
33. Jaiswal N, Haynesworth SE, Caplan AI, Bruder SP. Osteogenic differentiation of purified, culture-expanded human mesenchymal stem cells *in vitro*. *J Cell Biochem.* (1997) 64:295–312. doi: 10.1002/(SICI)1097-4644(199702)64:2<295::AID-JCB12>3.0.CO;2-I
34. Willie BM, Birkhold AI, Razi H, Thiele T, Aido M, Kruck B, et al. Diminished response to *in vivo* mechanical loading in trabecular and not cortical bone in adulthood of female C57Bl/6 mice coincides with a reduction in deformation to load. *Bone.* (2013) 55:335–46. doi: 10.1016/J.BONE.2013.04.023
35. Clarke K., Still J. Gait analysis in the mouse. *Physiol Behav.* (1999) 66:723–9. doi: 10.1016/S0031-9384(98)00343-6
36. Birkhold AI, Razi H, Duda GN, Weinkamer R, Checa S, Willie BM. Mineralizing surface is the main target of mechanical stimulation independent of age: 3D dynamic *in vivo* morphometry. *Bone.* (2014) 66:15–25. doi: 10.1016/j.bone.2014.05.013
37. De Souza RL, Matsuura M, Eckstein F, Rawlinson SCF, Lanyon LE, Pitsillides AA. Non-invasive axial loading of mouse tibiae increases cortical bone formation and modifies trabecular organization: a new model to study cortical and cancellous compartments in a single loaded element. *Bone.* (2005) 37:810–8. doi: 10.1016/j.bone.2005.07.022
38. Sugiyama T, Meakin LB, Browne WJ, Galea GL, Price JS, Lanyon LE. Bones' adaptive response to mechanical loading is essentially linear between the low strains associated with disuse and the high strains associated with the lamellar/woven bone transition. *J Bone Miner Res.* (2012) 27:1784–93. doi: 10.1002/jbmr.1599
39. Spranger S, Frankenberger B, Schendel DJ. NOD/scid IL-2Rg(null) mice: a preclinical model system to evaluate human dendritic cell-based vaccine strategies *in vivo*. *J Transl Med.* (2012) 10:30. doi: 10.1186/1479-5876-10-30
40. Ishikawa Y, Usui T, Shiomi A, Shimizu M, Murakami K, Mimori T. Functional engraftment of human peripheral T and B cells and sustained production of autoantibodies in NOD/LtSzscid/IL-2Rγ $^{-/-}$ mice. *Eur J Immunol.* (2014) 44:3453–63. doi: 10.1002/eji.201444729
41. King M, Pearson T, Rossini AA, Shultz LD, Greiner DL. Humanized mice for the study of type 1 diabetes and beta cell function. *Ann N Y Acad Sci.* (2008) 1150:46–53. doi: 10.1196/annals.1447.009
42. Reinke S, Geissler S, Taylor WR, Schmidt-Bleek K, Juelke K, Schwachmeyer V, et al. Terminally differentiated CD8^{+} T cells negatively affect bone regeneration in humans. *Sci Transl Med.* (2013) 5:177ra36. doi: 10.1126/scitranslmed.3004754
43. Chen J-H, Liu C, You L, Simmons CA. Boning up on Wolff's Law: mechanical regulation of the cells that make and maintain bone. *J Biomech.* (2010) 43:108–18. doi: 10.1016/J.JBIOMECH.2009.09.016
44. Birkhold AI, Razi H, Duda GN, Weinkamer R, Checa S, Willie BM. The influence of age on adaptive bone formation and bone resorption. *Biomaterials.* (2014) 35:9290–301. doi: 10.1016/j.biomaterials.2014.07.051
45. Mountziaris PM, Spicer PP, Kasper FK, Mikos AG. Harnessing and modulating inflammation in strategies for bone regeneration. *Tissue Eng Part B Rev.* (2011) 17:393–402. doi: 10.1089/ten.TEB.2011.0182
46. Gruber R, Koch H, Doll BA, Tegtmeier F, Einhorn TA, Hollinger JO. Fracture healing in the elderly patient. *Exp Gerontol.* (2006) 41:1080–93. doi: 10.1016/J.EXGER.2006.09.008
47. Goldhahn J, Suhm N, Goldhahn S, Blauth M, Hanson B. Influence of osteoporosis on fracture fixation - a systematic literature review. *Osteoporos Int.* (2008) 19:761–72. doi: 10.1007/s00198-007-0515-9
48. Gibon E, Loi F, Córdova LA, Pajarinen J, Lin T, Lu L, et al. Aging affects bone marrow macrophage polarization: relevance to bone healing. *Regen Eng Transl Med.* (2016) 2:98–104. doi: 10.1007/s40883-016-0016-5
49. Albright JM, Dunn RC, Shults JA, Boe DM, Afshar M, Kovacs EJ. Advanced age alters monocyte and macrophage responses. *Antioxid Redox Signal.* (2016) 25:805–15. doi: 10.1089/ars.2016.6691
50. Willinghamm MD, Brodt MD, Lee KL, Stephens AL, Ye J, Silva MJ. Age-related changes in bone structure and strength in female and male BALB/c Mice. *Calcif Tissue Int.* (2010) 86:470–83. doi: 10.1007/s00223-010-9359-y
51. Ferguson VL, Ayers RA, Bateman TA, Simske SJ. Bone development and age-related bone loss in male C57BL/6J mice. *Bone.* (2003) 33:387–98. doi: 10.1016/S8756-3282(03)00199-6
52. Glatt V, Canalis E, Stadmeyer L, Bouxsein ML. Age-related changes in trabecular architecture differ in female and male C57BL/6J mice. *J Bone Miner Res.* 22:1197–207. doi: 10.1359/jbmr.070507
53. Halloran BP, Ferguson VL, Simske SJ, Burghardt A, Venton LL, Majumdar S. Changes in bone structure and mass with advancing age in the male C57BL/6J mouse. *J Bone Miner Res.* (2002) 17:1044–50. doi: 10.1359/jbmr.2002.17.6.1044
54. Weiss A, Arbell I, Steinhagen-Thiessen E, Silbermann M. Structural changes in aging bone: osteopenia in the proximal femurs of female mice. *Bone.* (1991) 12:165–72. doi: 10.1016/8756-3282(91)90039-L
55. Farr JN, Khosla S. Cellular senescence in bone. *Bone.* (2019) 121:121–33. doi: 10.1016/j.bone.2019.01.015
56. Gibon E, Lu L, Goodman SB. Aging, inflammation, stem cells, and bone healing. *Stem Cell Res Ther.* (2016) 7:44. doi: 10.1186/s13287-016-0300-9
57. Hadjiargyrou M, O'Keefe RJ. The Convergence of fracture repair and stem cells: interplay of genes, aging, environmental factors and disease. *J Bone Miner Res.* (2014) 29:2307–22. doi: 10.1002/jbmr.2373
58. Zimmermann EA, Schaible E, Bale H, Barth HD, Tang SY, Reichert P, et al. Age-related changes in the plasticity and toughness of human cortical bone at multiple length scales. *Proc Natl Acad Sci USA.* (2011) 108:14416–21. doi: 10.1073/pnas.1107966108
59. Zhao S-J, Kong F-Q, Fan J, Chen Y, Zhou S, Xue M-X, et al. Bioinformatics analysis of the molecular mechanism of aging on fracture healing. *Biomed Res Int.* (2018) 2018:7530653. doi: 10.1155/2018/7530653
60. Mori G, D'Amelio P, Faccio R, Brunetti G. The Interplay between the bone and the immune system. *Clin Dev Immunol.* (2013) 2013:720504. doi: 10.1155/2013/720504
61. Charatcharoenwitthaya N, Khosla S, Atkinson EJ, McCready LK, Riggs BL. Effect of blockade of TNF-α and interleukin-1 action on bone resorption in early postmenopausal women. *J Bone Miner Res.* (2007) 22:724–9. doi: 10.1359/jbmr.070207
62. Kong Y-Y, Feige U, Sarosi I, Bolon B, Tafuri A, Morony S, et al. Activated T cells regulate bone loss and joint destruction in adjuvant arthritis through osteoprotegerin ligand. *Nature.* (1999) 402:304–9. doi: 10.1038/46303
63. Colucci S, Brunetti G, Cantatore F, Oranger A, Mori G, Quarta L, et al. Lymphocytes and synovial fluid fibroblasts support osteoclastogenesis

through RANKL, TNFα, and IL-7 in an *in vitro* model derived from human psoriatic arthritis. *J Pathol.* (2007) 212:47–55. doi: 10.1002/path.2153
64. Faienza MF, Brunetti G, Colucci S, Piacente L, Ciccarelli M, Giordani L, et al. Osteoclastogenesis in children with 21-hydroxylase deficiency on long-term glucocorticoid therapy: the role of receptor activator of nuclear factor-κB ligand/osteoprotegerin imbalance. *J Clin Endocrinol Metab.* (2009) 94:2269–76. doi: 10.1210/jc.2008-2446
65. Weitzmann MN, Pacifici R. Estrogen deficiency and bone loss: an inflammatory tale. *J Clin Invest.* (2006) 116:1186–94. doi: 10.1172/JCI28550
66. Tsukasaki M, Komatsu N, Nagashima K, Nitta T, Pluemsakunthai W, Shukunami C, et al. Host defense against oral microbiota by bone-damaging T cells. *Nat Commun.* (2018) 9:701. doi: 10.1038/s41467-018-03147-6
67. Teng YT, Nguyen H, Gao X, Kong YY, Gorczynski RM, Singh B, et al. Functional human T-cell immunity and osteoprotegerin ligand control alveolar bone destruction in periodontal infection. *J Clin Invest.* (2000) 106:R59–67. doi: 10.1172/JCI10763
68. Colucci S, Brunetti G, Rizzi R, Zonno A, Mori G, Colaianni G, et al. T cells support osteoclastogenesis in an *in vitro* model derived from human multiple myeloma bone disease: the role of the OPG/TRAIL interaction. *Blood.* (2004) 104:3722–30. doi: 10.1182/blood-2004-02-0474
69. Razi H, Birkhold AI, Weinkamer R, Duda GN, Willie BM, Checa S. Aging leads to a dysregulation in mechanically driven bone formation and resorption. *J Bone Miner Res.* (2015) 30:1864–73. doi: 10.1002/jbmr.2528
70. Smith JK, Dykes R, Chi DS. The effect of long-term exercise on the production of osteoclastogenic and antiosteoclastogenic cytokines by peripheral blood mononuclear cells and on serum markers of bone metabolism. *J Osteoporos.* (2016) 2016:1–11. doi: 10.1155/2016/5925380
71. Hoff P, Gaber T, Schmidt-Bleek K, Sentürk U, Tran CL, Blankenstein K, et al. Immunologically restricted patients exhibit a pronounced inflammation and inadequate response to hypoxia in fracture hematomas. *Immunol Res.* (2011) 51:116–22. doi: 10.1007/s12026-011-8235-9
72. Schlundt C, El Khassawna T, Serra A, Di-Enelt A, Wendler S, Schell H, et al. Macrophages in bone fracture healing: their essential role in endochondral ossification. *Bone.* (2015) 106:78–89. doi: 10.1016/j.bone.2015.10.019
73. Bucher CH, Lei H, Duda GN, Volk H-D, Schmidt-Bleek K. The role of immune reactivity in bone regeneration. In: *Advanced Techniques in Bone Regeneration* (London: InTech). doi: 10.5772/62476

Conflict of Interest Statement: The authors declare that the research was conducted in the absence of any commercial or financial relationships that could be construed as a potential conflict of interest.

frontiers in Immunology

REVIEW
published: 16 April 2019
doi: 10.3389/fimmu.2019.00798

Mesenchymal Stem Cells Improve Rheumatoid Arthritis Progression by Controlling Memory T Cell Response

Noymar Luque-Campos[1], Rafael A. Contreras-López[1], María Jose Paredes-Martínez[1], Maria Jose Torres[2], Sarah Bahraoui[3], Mingxing Wei[4], Francisco Espinoza[5], Farida Djouad[3], Roberto Javier Elizondo-Vega[6]* and Patricia Luz-Crawford[1]**

[1] Laboratorio de Inmunología Celular y Molecular, Centro de Investigación Biomédica, Facultad de Medicina, Universidad de los Andes, Santiago, Chile, [2] Escuela de Ingeniería Bioquímica, Pontificia Universidad Católica de Valparaíso, Valparaíso, Chile, [3] IRMB, INSERM, Univ Montpellier, Montpellier, France, [4] Cellvax, SAS, Parc BIOCITECH, Romainville, France, [5] Cells for Cells, Universidad de los Andes, Santiago, Chile, [6] Laboratorio de Biología Celular, Departamento de Biología Celular, Facultad de Ciencias Biológicas, Universidad de Concepción, Concepción, Chile

OPEN ACCESS

Edited by:
Teun J. De Vries,
VU University Amsterdam,
Netherlands

Reviewed by:
Akio Morinobu,
Kobe University, Japan
Erik Lubberts,
Erasmus University Rotterdam,
Netherlands

***Correspondence:**
Farida Djouad
farida.djouad@inserm.fr
Roberto Javier Elizondo-Vega
relizondo@udec.cl
Patricia Luz-Crawford
pluz@uandes.cl

Specialty section:
This article was submitted to Inflammation, a section of the journal Frontiers in Immunology

Received: 21 November 2018
Accepted: 26 March 2019
Published: 16 April 2019

Citation:
Luque-Campos N, Contreras-López RA, Paredes-Martínez MJ, Torres MJ, Bahraoui S, Wei M, Espinoza F, Djouad F, Elizondo-Vega RJ and Luz-Crawford P (2019) Mesenchymal Stem Cells Improve Rheumatoid Arthritis Progression by Controlling Memory T Cell Response. Front. Immunol. 10:798. doi: 10.3389/fimmu.2019.00798

In the last years, mesenchymal stem cell (MSC)-based therapies have become an interesting therapeutic opportunity for the treatment of rheumatoid arthritis (RA) due to their capacity to potently modulate the immune response. RA is a chronic autoimmune inflammatory disorder with an incompletely understood etiology. However, it has been well described that peripheral tolerance defects and the subsequent abnormal infiltration and activation of diverse immune cells into the synovial membrane, are critical for RA development and progression. Moreover, the imbalance between the immune response of pro-inflammatory and anti-inflammatory cells, in particular between memory Th17 and memory regulatory T cells (Treg), respectively, is well admitted to be associated to RA immunopathogenesis. In this context, MSCs, which are able to alter the frequency and function of memory lymphocytes including Th17, follicular helper T (Tfh) cells and gamma delta (γδ) T cells while promoting Treg cell generation, have been proposed as a candidate of choice for RA cell therapy. Indeed, given the plasticity of memory $CD4^+$ T cells, it is reasonable to think that MSCs will restore the balance between pro-inflammatory and anti-inflammatory memory T cells populations deregulated in RA leading to prompt their therapeutic function. In the present review, we will discuss the role of memory T cells implicated in RA pathogenesis and the beneficial effects exerted by MSCs on the phenotype and functions of these immune cells abnormally regulated in RA and how this regulation could impact RA progression.

Keywords: mesenchymal stem cells, rheumatoid arthritis, T cell, plasticity, immunomodulatory

INTRODUCTION

Mesenchymal stem cells (MSCs) are multipotent stem cells able to exert immunosuppressive functions on both the innate and the adaptive immune cells (1). They have been isolated from almost all mesodermal tissues including bone marrow, adipose tissue, umbilical cord blood, umbilical cord, placenta, menstrual fluid, and dental pulp (2–5). The International Society for Cellular Therapy (ISCT) has defined minimal criteria for characterizing MSCs that include a fibroblastic-like morphology, the expression of mesodermal markers such as CD90, CD105, and

CD73, the lack of hematopoietic marker expression such as CD45, CD34, CD14, and the capacity to differentiate into adipocytes, chondrocytes and osteoblasts (6). MSCs have been reported as an interesting therapeutic cell candidate for the treatment of autoimmune diseases such as RA, due to their capacity to attenuate the exacerbated pathogenic immune response observed in these patients (7). However, given the complexity of RA disease as well as the mechanisms involved in MSC immunosuppressive functions, it is mandatory to decipher the mechanism by which MSC mediated their immunosuppressive potential on the immune cell subsets associated to RA to improve MSC-based therapy. In this context, one of the main target for MSCs-based therapy are the pathogenic memory T cells due to their critical role in autoimmune disease progression including RA (8). Currently there is no article focusing in discussing the importance of targeting-memory T cells with MSCs-based therapy for autoimmune disease treatment.

Therefore, in this review, we will focus on the effect of MSCs on memory $CD4^+$ T cells subsets and we will discuss about the advantage that this knowledge could render to improve their immunosuppressive properties in order to develop novel MSCs-based therapy for RA treatment. During the development of this review, we will discuss about the role of memory T cells in the evolution of autoimmune disease focusing on RA and we will infer studies between MSCs and their impact in memory T cells and how the regulation of this populations could be a key player on RA improvement.

MSC-BASED THERAPY FOR AUTOIMMUNE DISEASE TREATMENT

MSCs have been largely propose as a therapeutic tool for autoimmune disease treatment due to their potent suppressive activity to inhibit proinflammatory cells from both the innate and adaptive immune system. Indeed, it has been reported that MSCs are able to modulate the differentiation and function of myeloid cells toward immunosuppressive phenotypes. These cells includes monocytes (9, 10), dendritic cells (DCs) (11, 12), macrophages (13), myeloid-derived suppressor cells (MDSCs) (14), and neutrophils (15). Furthermore, MSCs inhibits the proliferation of T cells (16, 17) and B cells (18), as well as their functions. The mechanisms involved in this immunomodulation include cell-cell contacts and the production of soluble factors (19). Besides, MSCs are able to migrate to inflammatory sites in order to interact and modulate proinflammatory immune cells in the site of inflammation (20). For all this reasons, we can currently count a totally of 707 MSC-related clinical trials registered on the NIH Clinical Trial Database (https://clinicaltrials.gov/). These clinical trials mainly tend to evaluate the therapeutic efficacy and safety of MSCs from different sources. Moreover, until December 2018 exists several clinical trials targeting autoimmune disease treatment such as Multiple Sclerosis (MS) ($n = 29$), Crohn's Disease ($n = 7$), systemic lupus erythematous (SLE) ($n = 12$), and RA ($n = 14$). In general, the short-term and long term use of MSCs based therapy give positive effects with no report of serious adverse events besides some immediate type I hypersensitivity (pruritis, rash, fever) in $<$15% of patients (21). For example, Riordan et al. evaluated the safety and efficacy of the intravenous administration of umbilical cord-derived MSCs (UC-MSCs) for the treatment 20 MS patients (22). MS is an inflammatory disorder of the brain and spinal cord in which focal lymphocytic infiltration leads to damage of myelin and axon (23). The authors demonstrated that after 1 year, MRI scans of the brain and the cervical spinal cord showed inactive lesions in 83.3% of the subjects followed (22). In another study, an allogeneic adipose-derived stem cells (ASCs) was used in a phase I/IIa clinical study for Crohn's disease treatment (24). Crohn's disease is a systemic inflammatory chronic disorder that affect the digestive tract (25). ASCs based treatment showed that 69.2% of all the patients had a reduction of the number of draining fistulas after 24 weeks post-injection compared to the placebo group. Moreover, this study demonstrated that eASCs infusion was safe and a beneficial therapy to treat perianal fistula of Crohn's disease patients (24). Finally optimistic results have been obtained for SLE treatment using MSCs (26). SLE is a multisystem autoimmune disease characterized by inflammation of multiple organs owing to in part by loss of tolerance to self-antigens and the production of autoantibodies (27). Wang et al. demonstrated that after 12 months using two intravenous infusions of UC-MSCs in 40 patients with refractory SLE a well-tolerated safety profile with 32.5% (13/40) of patients achieving a major clinical response and a significant decrease in disease-activity (26).

However, despite these results there are still a lot of controversy regarding the positive effects of MSCs based therapy since their effect strongly depends on the etiology of the disease and the degree of inflammation. Thus, it is very important to understand the interaction between MSCs and pathogenic immune cells such as memory T cells since they are main players in the generation, pathogenesis, and progression of autoimmune disease.

MEMORY T CELLS: KEY PLAYER IN THE PATHOGENESIS OF AUTOIMMUNE DISEASE

After infection or immunization, naive T cells undergo a clonal expansion leading to a high frequency of antigen-specific T cells with a rapid effector function. Naïve $CD4^+$ T cells can differentiate into multiple effector T helper (Th) cell subsets such as Th1, Th2, Th17, and T follicular helper (Tfh) cells among others, while naïve $CD8^+$ T cells differentiate into cytotoxic T lymphocytes (CTLs) (28). Once the initial response of the adaptive immune system against an antigen ends, the organism must return to the homeostasis through the contraction of effector T cells. During this period the small amount of cells that survive will eventually become part of the immunological memory: immune cells that are able to respond rapidly to a second round of a specific antigen previously encountered (29). The generation and persistence of memory T cells is an important feature of the adaptive immune system acquired

following antigen exposure that provides lifelong protection against infections (30).

Memory T cells are an heterogeneous population of cells classically distinguished by the expression of the CD45RO isoform and by the absence of the CD45RA ($CD45RO^+CD45RA^-$) (31, 32). Lately, in human, specific subsets of memory $CD4^+$ and $CD8^+$ T cells in peripheral blood mononuclear cells (PBMCs) were identified through the expression of CC-chemokine receptor 7 (CCR7), a chemokine receptor that controls the homing to secondary lymphoid organs (33). CCR7 negative memory T cells were found to produce more effector cytokines, compared to the CCR7 positive subset (34). Based on this finding, two subsets of memory T cells were identified: $CCR7^+$ central memory T cells (T_{CM}) and $CCR7^-$ effector memory T cells (T_{EM}) (33). Several studies have been carried out to characterize the memory cells present in PBMC using an extensive panel of markers. The $CD44^{hi}$, $CD45RO^{hi}$, $CD45RA^{low}$, $CD127^{hi}$, $CD62L^{hi}CCR7^{hi}$ T_{CM} cells are generated and reside in secondary lymphoid tissues in the absence of antigen while $CD44^{hi}$, $CD45RO^{hi}$, $CD45RA^{low}$, $CD127^{hi}$, L-$selectin^{low}$ $CCR7^{low}$ T_{EM} cells, are generated in secondary lymphoid tissues and recirculate between blood and non-lymphoid tissues in the absence of antigen (33).

As mentioned before, the long-lived memory T cells in the presence of secondary antigen exposure expand and develop a more robust and stronger response. In the case of autoimmune diseases memory T cells might become harmful against self-antigens since these memory cells exhibit a potent pathogenic response against self-tissues. Moreover, due to their longevity, they are very difficult to eliminate thus the development of novel therapies directed against these cells are of main importance to control autoimmunity.

In this context, the role of memory T cells in autoimmune diseases has been studied. MS patients have an elevated numbers of memory T cells (35–37), particularly of the T_{EM} subsets (38, 39). Recently it has been reported that memory $CD4^+$ $CCR9^+$ T cells are altered in MS patients and they could be mediate the development of secondary progressive MS progression (40). Also, it has been reported that memory T cells subpopulation are increased in active Crohn's disease patients (41, 42). Indeed, peripheral blood and intestinal mucosa memory T cells from active Crohn's disease patient have an increased intracellular production of TNFα and correlate with the score of the disease (CDAI). In addition, this peripheral blood memory T cells-producing TNFα have an increased migratory profile to extra nodal lymphoid tissues such as the intestinal mucosa (43). Furthermore, there is evidence suggesting an augmentation of $CD4^+$ T_{EM} cells population in SLE pathogenesis (44). Also, the $PD1^+ICOS^+T_{CM}$, and $PD1^+ICOS^+T_{EM}$ subpopulation are increased in SLE patients and T_{EM} positively cells correlated with the severity of the disease (45). Likewise, it has been observed an enrichment of $CD4^+$ T_{EM}-cell associated genes within SLE loci, Crohn's loci and RA loci (46). All this evidence point memory T cell subsets as major contributors of autoimmune pathogenicity.

Role of Memory T Cells in the Development and Progression of RA

RA is an autoimmune disease characterized by the high production of auto-antibodies affecting a wide variety of auto-antigens. Among them, the rheumatoid factor (RF) and anti-citrullinated protein antibodies (ACPAs) have been the most described (47). RA immunopathogenesis is characterized by deficiencies in the immune response with predominance of pro-inflammatory cells and an alteration of the peripheral immune tolerance which involves in particular $CD4^+$ T cells (48, 49). $CD4^+$ T cells of RA patients undergo a premature transition from a naïve to a memory phenotype. The resulting memory $CD4^+$ T cells are hyper-proliferative because of failures in the cell cycle checkpoint which promote their differentiation toward Th1 and Th17 pathogenic T cells (50). This was confirmed in studies demonstrating that RA patients have large numbers of memory CD4 T cells that infiltrate the inflamed synovial membrane (51–55). Moreover, the increased frequency of T_{EM} cell subset was observed in the synovial fluid from RA patients (55). While T_{EM} cells have a short lifetime they possess a potent effector function with a high capacity to secrete pro-inflammatory cytokines allowing them to respond faster to antigens present in the synovial fluid (34). All together, these studies suggest the presence of highly activated and differentiated memory $CD4^+$ T cells with a high capacity to produce pro-inflammatory cytokines in synovial fluid of RA patients.

Conventional Therapy for RA Treatment

A large variety of drugs aiming at reducing the symptoms and gradual progression of the disease are currently available. Among them, synthetic disease-modifying anti-rheumatic drugs (sDMARDs) including methotrexate (MTX), leflunomide, sulfasalazine, and hydroxychloroquine, biologic response modifiers referred as biologics (bDMARDs) and corticosteroids. All these treatments target inflammation and are aimed at improving both the quality of life and prognosis of RA patients (56) through the prevention of structural damage (erosive disease) and control of extra-articular symptoms. Since, RA pathogenesis is associated to alterations of immune cell functions and cytokine secretion produced in part by pro-inflammatory $CD4^+$ T memory responder cells, a wide variety of bDMARDs have been proposed to target the latter cells. For instance, the first bDMARD tested was aimed at reducing the production of tumor necrosis factor alpha (TNF-α) (Infliximab), a pro-inflammatory cytokine highly produced by memory T cells of RA patients (57). Since then, other TNF-targeting agents such as etanercept, adalimumab, certolizumab, and golimumab as well as other biological agents such as anti-IL6 (tocilizumab), anti-CTLA4 (abatacept), and anti-CD20 (Rituximab) were developed (56). However, the treatment of some RA patients with TNF inhibitors did not significantly reduce the frequency of pathogenic Th17 cells revealing that a high range of patients do not respond to this treatment (57). Later, an anti-interleukin 17 (IL-17) antibody (secukinumab) and anti-IL-17RA antibody brodalumab (AMG827) were developed and evaluated in

clinical trials including RA patients with an inadequate response to methotrexate. The phase II clinical study on RA patients demonstrated that the administration of brodalumab did not improve RA progression as revealed by the minimal response criteria set designed by the American College of Rheumatology (ACR) (58). Similar results were observed after secukinumab administration in a phase Ib clinical study that included moderate to severe RA patients (59). Indeed, the administration of these drugs did not reduce the frequency of memory Th17 cells. Interestingly, patients with RA treated with TNF inhibitors, possess pathogenic Th17 cells with a deleterious phenotype because of the high production of granulocyte-macrophage colony-stimulating factor (GM-CSF) (57). Indeed, GM-CSF is indispensable for the differentiation of inflammatory dendritic cells (infDCs) inducing the activation of memory $CD4^+$ T cells producing IL-17 (60, 61). Thus, a monoclonal antibody against GM-CSF has been developed and described to be effective in clinical trial for RA treatment (62). However, despite this promising result, the use of the anti-GM-CSF antibody has not yet been approved (62).

Inhibitors of the Janus kinases (JAKs), such as Tofacitinib and Baricitinib, have also been developed for RA treatment (63, 64). These inhibitors block the activation of signal transducer and activator of transcription (STATs) signaling pathways, which drive the signature of many cytokines including interleukin-7 (IL-7) and interleukin-15 (IL-15) that are important for memory T cells proliferation and survival (64–66). Another approach was the development of drugs that mimic mechanisms naturally produced by our own immune system. For example, Abatacept is a soluble recombinant human fusion protein comprising the extracellular domain of human cytotoxic T-Lymphocyte Antigen 4 (CTLA-4). This protein binds to CD80 and CD86 receptors on the antigen-presenting cells (APCs) and blocks the interaction with T cells through the co-stimulatory molecule CD28 (67). Clinical trials have shown promising results using Abatacept for RA treatment (68). However, a subset of tissue-infiltrating $CD4^+$ T cells from a group of RA patients have been shown to lose the expression of CD28 while starting to express memory markers (54, 69). These latter cells exhibit a high capacity to produce pro-inflammatory cytokines such as interferon-gamma (IFNγ) and TNFα and cytotoxic activity (69–73). Remarkably, the effect of bDMARD administration on memory T cell population has never been addressed.

Although a significant progress has been made with the current state of the art RA treatment for obtaining long-term remission-induction, still between 20 and 30% of patients with moderate-to-severe RA do not positively respond to mono or combinations therapy (plus Methotrexate) with these agents (74) thus the development of novel therapies targeting pathogenic memory T cells seems to be ideal to improve RA progression.

MSC-Based Therapy for RA Treatment

Despite the fact that MSCs based therapy for RA treatment is one of the main autoimmune disease model use to study the mechanism underlying the therapeutic effect of MSCs, nowadays, RA MSCs-based clinical trials has been the least studied within the autoimmune diseases. In this context, exist 14 MSC-based therapy clinical trials for RA. Upon them, it has been reported that the intravenous infusion of allogeneic bone marrow and umbilical cord-derived MSC in a small group of refractory RA patients resistant to the anti-TNF monoclonal antibody therapy, led to a reduced erythrocyte sedimentation rate, improvement on DAS28 clinical score and diminished on the serum anti-cyclic citrullinated peptide (anti-CCP) antibody level, indicating the efficacy of MSC treatment. However, the observed clinical improvement was only partial and temporary because of the short term follow-up (75). In another study, using allogeneic UC-MSCs for RA treatment, the safety and effectiveness was demonstrated in a larger number of patients (76). In this study, MSCs and DMARDs were co-administrated intravenously in 172 patients with active RA inducing a significant increase in the percentage of regulatory $CD4^+$ T cells (Treg) in the blood together with a significant clinical improvement for up to 6 months. Moreover, repeated infusion of MSCs after this period allowed an increased therapeutic efficacy of the cells (76). More recently, in a phase Ib/IIa clinical trial, the intravenous administration of allogeneic expanded adipose-derived stem cells (ASCs) in a study that included 53 patients with a placebo group was shown to be safe and well tolerated in refractory RA patients (77).

Unfortunately at today there is no report that shows an immune-monitoring of RA patients after MSCs infusion that could allow us to compare the immune profile of RA patients treated or not with MSCs with their clinical score before and after MSCs infusion. Indeed, it is mandatory to deepen on how MSCs affect the proinflammatory cells that are deregulated in these patients in particular pathogenic memory T cells. This information will surely help us to understand the mechanism by which MSCs exert their therapeutic function that will allows us to improve MSCs-based therapy.

IMMUNOMODULATORY ROLE OF MSCs ON MEMORY T CELLS: FOCUS ON RA

Despite the significant advances that have been made in the generation of novel therapies against RA, there are still a lot of patients that do not respond to any treatments. Hence it is reasonable to think that the resistance of pathogenic memory T cells could be the main contributor to the absence of a beneficial effect of these immunomodulatory therapies (78, 79). Therefore, it is mandatory for the successfully development of RA therapies to target these specific T cells subsets. In this context, the effect of MSCs on memory T cells have been investigated. For example, Pianta et al. demonstrated that the conditioned medium derived from the mesenchymal layer of the human amniotic membrane (CM-hAMSC) strongly inhibits central memory ($CD45RO^+$ $CD62L^+$) as well as effector memory ($CD45RO^+$ $CD62L^-$) T cell subsets, although the later ones to a lower extent (80). Also, using Peripheral Blood Mononuclear Cells (PBMC) activated with phytohemagglutinin (PHA), it has been shown that MSCs highly inhibit the proliferation of T_{CM}, T_{EM}, and effector $CD4^+$ T cells (81). Moreover, Mareschi et al. observed that MSCs derived from different tissues such as bone marrow and placenta were able to

decrease the proliferation of memory T cells ($CD4^+CD45RO^+$) (82). In particular, PBMC stimulated with PHA were shown to significantly decrease the frequency of $CD4^+$ T_{CM} and T_{EM} cells, that produce TNF-α, IL-2, and IFNγ, when co-cultured with BM-MSCs (83).

Thereby, all these studies aiming at the evaluation of the inhibitory capacity of MSCs on human memory $CD4^+$ T cells, demonstrate a stronger immunomodulatory effect on the T_{CM} cell subset. However, the effect exerted by MSCs on memory T cell subpopulations described to play a key role in RA immunopathogenesis, such as memory Th17 cells, memory Treg cells and memory Tfh cells among others still need to be investigated. Then will be describe the effect of MSCs on particular subpopulations memory T cells that could be related to the RA immunopathogenesis.

Effects of MSCs on Effector Memory Vγ9Vδ2 T Cells

A high frequency of effector memory Vγ9Vδ2 T cells has been found in the peripheral blood and synovial fluid of RA patients. These cells have a potent capacity to secrete inflammatory factors, such as IFNγ and IL-17, and to present antigens (84). MSCs display a potent capacity to suppress the proliferation of γδ T cell, as well as their cytolytic responses and cytokine production (85, 86). This latter effect is mediated by the MSCs release of the COX-2-dependent production of prostaglandin E2 (PGE2) through their receptors, EP2 and EP4, expressed in Vγ9Vδ2 T cells (85, 86). These results suggest that MSCs exert a beneficial effect in RA through their capacity to prevent the immune response dysfunction mediated by γδ T cells via the inhibition of inflammatory cytokine production and the improvement of the anti-inflammatory response.

Interaction Between Pro-inflammatory Memory Tfh Cells and MSCs

The production of auto-antibodies by B cells and thus the production of autoantibodies in RA patients involves in part the cooperation of Tfh cells (87). An association between an increased percentage of $ICOS^+$ blood memory Tfh cells, auto-antibody titer of RA patient sera and the activity and/or severity of RA (88, 89). The differentiation of naïve $CD4^+$T cells isolated from RA patients into Tfh cells was shown to be suppressed by human UC-MSCs in part through the indoleamine 2,3-dioxygenase (IDO) activity of MSC induced by IFNγ produced by Tfh cells (87). In the collagen-induced arthritis (CIA) model, MSC injection prevented arthritis progression in mice by altering both the number and function of Tfh cells (87). These results indicate that MSCs might inhibit the differentiation of Tfh toward the different memory subsets such as Tfh1, Tfh2, and Tfh17 and consequently decrease the auto-reactive B cell number and the production of auto-antibodies, such as anti-CCP.

Effects of MSC on Pro-inflammatory Memory T Cells

Interactions between chemokines and their respective receptors are key mediators of inflammation since they govern the accumulation and homing of memory $CD4^+$ T cells in the synovial membrane of RA patients. Chemokine ligand 3 (CCL3), CCL4, and CCL5 chemokines, which are highly produced by different cell types present in the synovial tissue, bind to various chemokine receptors such as CCR5 expressed at the surface of memory T cells that are (90, 91). CCR5 expression is increased at the surface of synovial tissue and fluid T cells and correlated with IFN-γ expression by synovial memory $CD4^+$ T cells of RA patients (92–94). Synovial memory $CD4^+$ T cells also express *lymphotoxin-alpha* (LT-α) that correlates with CCR6 expression and the presence of lymphocytic aggregates in synovial tissue (95). CCR6 was proposed to play a role in the development of aggregates of $CD4^+$ T cells that are characteristically found in inflamed rheumatoid synovium (94).

As mentioned above, IL-17 plays a critical role in RA inflammatory process. IL-17 enhances the production of chemokines such as CCL20 and the stromal-derived factor 1 (SDF-1) by synoviocytes thus promoting the recruitment of memory T cells to the synovium (96–101). One of the mechanisms associated to the therapeutic effect of MSCs is their capacity to migrate and home into inflamed tissues (19). MSCs are well described to constitutively secrete a variety of different chemokines such as CCL2 (MCP-1), CCL3 (MIP-1α), CCL4 (MIP-1β), CCL5 (RANTES), CCL7 (MCP-3), CCL20 (MIP-3α), CCL26 (eotaxin-3), CXCL1 (GROα), CXCL2 (GROβ), CXCL5 (ENA-78), CXCL8 (IL-8), CXCL10 (IP-10), CXCL11 (i-TAC), CXCL12 (SDF-1), and CX3CL1 (fractalkine) (102–104). Furthermore, BM-MSCs express several chemokine receptors such as CXCR4, CCR1, CCR4, CCR7, CCR10, CCR9, CXCR5, and CXCR6 involved in MSCs migration (105). Thus, such MSCs could potentially migrate into the inflamed synovium and interact with memory T cells, inhibit their proliferation rate or/and alter their pro-inflammatory phenotype and finally reduce inflammation in the synovial membrane.

CXCR4 plays a central role in the homing and retention of $CD4^+$ T cells (96, 106). Interestingly, RA patients with one or more susceptible HLA-DR haplotypes displayed a significantly higher frequency of memory $CXCR4^+CD4^+$ T cells, suggesting that synovial migration and retention of memory $CXCR4^+CD4^+$ T cells is associated with sustained auto-immunity and local inflammation. Moreover, the high frequency of memory $CXCR4^+CD4^+$ T cells correlated with the elevated expression level of HLA-DR on B cells underlying that B cells are important antigen-presenting cells in RA (107). Xie et al. have reported that MSCs exhibit an increased CXCR4 expression level when Notch signaling pathway was inhibited suggesting that notch signaling regulates MSC migration and function (108). Altogether these studies suggest that blocking of Notch pathway might enhance MSC therapeutic effect by increasing their capacity to migrate and home into the synovium where they will interact with memory $CXCR4^+CD4^+$ T cells and control RA pathogenesis.

Effects of MSCs on Th17 and Treg Memory T Cells

Th17 cells express the retinoic acid-related orphan nuclear hormone receptor C (RORC) and secrete IL-17A along with other cytokines, including IL-17F, IL-21, and IL-22. Th17 cells are pro-inflammatory helper cells that protect the

organism against extracellular pathogens, including Gram-negative bacteria, mycobacteria, and fungi (109). However, their deregulation is associated with the generation of autoimmune diseases including RA (109). On the other side, it is well known that human Treg cells play a central role in the maintenance of immune homeostasis and immunological self-tolerance (110). Treg cells exert potent immunosuppressive effects over effector T-cell proliferation and cytokine production through cytokine-independent mechanism requiring cell-to-cell contact. Treg cells are characterized by high expression level of CD25 (also referred as CD25 bright cells) and more specifically, intracellular expression of the transcription factor FoxP3 (111, 112). Moreover, Treg are characterized by a low expression of CD127 (IL-7 receptor alpha-chain) (113), and a down-regulation of CD127 which is associated with regulatory function acquisition (114). The imbalance between Th17 and Treg cells has been largely associated with the RA pathogenesis due to their close differentiation pathways but their completely opposite function. (115, 116). Indeed, Th17 cells are implicated in RA development and progression and high levels of IL-17 have been reported in the synovial fluid of RA patients which is positively correlated with the severity of the disease (117–120). Furthermore, IL-17 is mainly produced by $CD4^+CD45RO^+$ memory T cell (121, 122). Another molecule, the chemokine receptor CCR6, is expressed by memory Th17 cells and associated with their capacity to migrate toward inflammatory joints in response to CCL20 highly produced by T cells and synoviocytes (123, 124). On the other hand, $CD4^+CD25^{high}$ Treg cells are predominantly memory cells in the synovial fluid which is enriched with $CD4^+CD25^+CD127l^{ow}FoxP3^+$ Treg cells in the synovial fluid of RA patients (111, 125, 126). Furthermore, while the percentage of memory Treg cells subsets significantly increased in the synovial fluid of RA patients, it did not change in their peripheral blood, and this increased frequency of memory Treg correlated with the DAS28 (127). However, despite the increased number of Treg in the synovial fluid, inflammation is maintained suggesting an alteration of their functions in RA patients. This was confirmed by a body of studies that has demonstrated by the reduced regulatory functions of Treg derived from the peripheral blood (128–131) and the synovial fluid of RA patients (132). In line with these studies, Treg cells isolated from patients with active RA did not inhibit the secretion of pro-inflammatory cytokine such as IFN-γ and TNFα released by T effector cells (127–130, 133). Notoriously, TNFα can inhibit the suppressive function of Treg (129) suggesting that RA synovial fluid enriched in pro-inflammatory convert memory Treg cells into cells producing pro-inflammatory cytokines such as IL-17 unable to exert regulatory functions (134). An increased percentage of memory $CD45RA^-Foxp3^{low}$ non-regulatory T cells was reported in RA synovial fluid while it did not change in the peripheral blood of patients (55). Memory non-Treg cells produce IL-2, IFN-γ, and IL-17 and express high levels of *RORC* (135, 136).

MSCs are potent inhibitors of $CD4^+$T-bet$^+CD183^+$ (Th1) and $CD4^+RORγt^+CD161^+$ (Th17) cells proliferation and significantly reduce their capacity to produce pro-inflammatory cytokines such as IFN-γ, TNFα, and IL-1β (Th1) and IL-17A and IL-22 (Th17) (80). Indeed, using memory $CD4^+CD45RO^+CCR6^+$ positive cells (Th17 cells), human BM-MSCs have been shown to induce the generation of Th17 cells with regulatory features in an inflammatory environment characterized by a decrease in *RORC* expression, an increase of FoxP3 expression and the acquisition of immunosuppressive functions (137).

Likewise, various studies have shown that MSCs have the capacity to increase the percentage of Treg cells *in vitro* in co-culture in mixed lymphocyte reactions (MLR) (138, 139). MSCs-derived PGE2 and transforming growth factor beta 1 (TGFβ1)

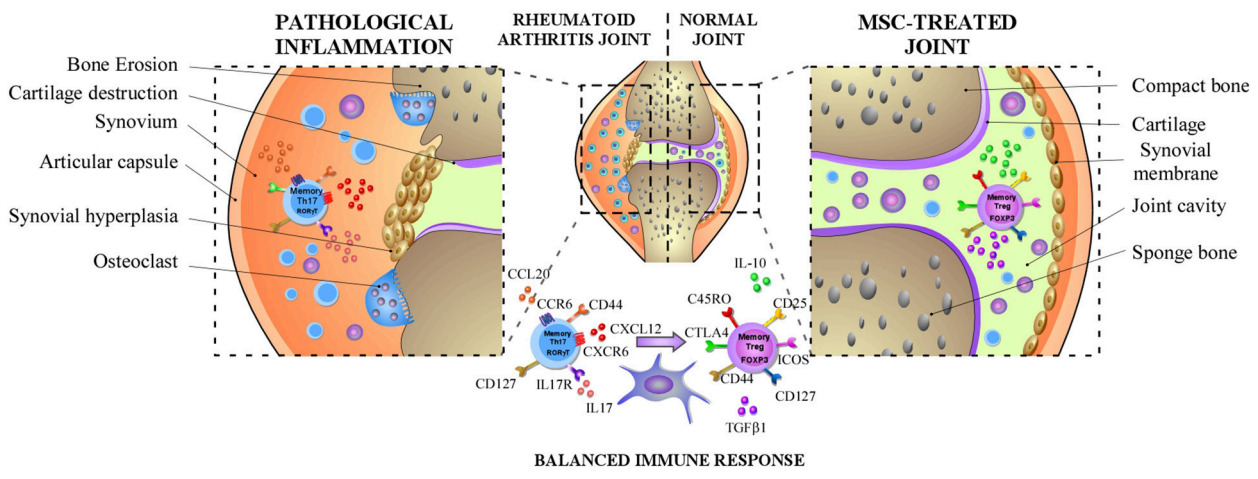

FIGURE 1 | MSCs dampen RA progression through the induction of the balance between memory Th17 and Treg cells. In RA, MSCs can diminish the frequency of pathogenic memory Th17 cells and the production of pro-inflammatory cytokines such as IL-17, IL-22, and GM-CSF and promote their differentiation toward an anti-inflammatory phenotype. In parallel, MSCs might also increase the capacity of memory Treg cells to produce anti-inflammatory cytokines such as IL-10 or TGFβ1 and prolong their immunosuppressive capacity maintaining their anti-inflammatory phenotype.

are not redundant players in this mechanism (140). This was corroborated in a study with human adipose tissue-derived MSCs that were able to reduce IL-17, TNF, and IFN-γ production and to induce IL-10-producing T cells *in vitro* in collagen-specific peripheral blood T cells of RA patients (141). It is well admitted that MSCs co-cultured with purified $CD4^+$ T cells induce the expression of $CD25^{High}$ and $FoxP3^+$ at the surface of these latter T cells in a contact-dependent manner (142, 143). The generation of these $CD4^+CD25^+FoxP3^+$ Treg has been shown to be, in part, dependent on ICOSL expression by MSCs (142). Indeed, ICOS is expressed on activated memory T cells, including Th17 cells, thus through a contact cell-cell mechanism MSCs were proposed to interact with memory Th17 cells and generate memory Treg cells. In another study, it was reported that MSCs were able to recruit both $CD4^+CD25^+CD45RA^+$ and $CD4^+CD25^+CD45RO^+$ Treg cells, but the subpopulation of naïve Treg cells was recruited to a higher extent. Additionally, MSC regulate and maintain the suppressive function of memory Tregs cells over time (144). Therefore, in the context of RA, the regulation of memory Treg cell by MSCs is critical since they are more plastic than naive Treg cell population (136).

Altogether, these studies provide evidence that MSCs do not only increase the generation of Treg cells and the production of IL-10 or TGFβ1 but also extend their immunosuppressive capacity maintaining their phenotype ($FoxP3^+$ $CD127^{low}$) and functions (140, 144). This is a critical function exerted by MSC, considering that Treg from RA patients exhibit an altered functionality. In addition, MSCs by suppressing the secretion of IL17-A by effector-memory Th17 cells decrease the acute or chronic activation of these cells in RA. Thus, MSCs do not only inhibit the IL-17 production but also induce the reprogramming of immunopathogenic memory Th17 cells toward T cells with regulatory phenotype and functions (137) (Summarized on **Figure 1**).

FUTURE PERSPECTIVE

MSCs are multipotent cells with broad immunomodulatory properties, therefore, they have been proposed as the candidate of choice for autoimmune diseases treatment including RA. However, the clinical benefit for RA after 3 months of MSCs administration have shown inconsistent positive effects. Thus, it is necessary to increase the number of patients and studies in order to draw robust conclusions regarding MSC therapeutic effects in RA. Additionally, it is important to highlight that at today, clinical trials using MSCs were injected in patients with severe and refractory RA suggesting that MSCs treatment could be more effective at early stages of the disease (145). Also, the studies only evaluated the short-term efficacy of MSCs, from 3 to 8 months, and therefore the assessment of MSC long-term efficacy still needs to be addressed.

Based on the topics exposed here we believe that further studies needs to be address in order to evaluate the effect of MSC treatment on pathogenic memory T cells derived from RA patients. Since MSCs upon injection will migrate to the site of inflammation were they will find an elevated numbers of proinflammatory memory T cells it is essential to evaluated the effect of MSCs on RA memory T cells that has not been explored. Moreover, it is mandatory to achieve a detailed immune-monitoring of RA patients that analyses the dynamic of pathogenic and non-pathogenic memory T cells upon MSCs infusion.

CONCLUSION

Memory T cells have been largely studied for their pivotal role in the pathogenesis of auto-immune disease such as RA. Although pro-inflammatory memory T cells-exhibit detrimental effect in RA, their potential plasticity offers an approach yet to be explored in order to better control RA progression. In this context, MSCs, potent immunosuppressive cells that are able to inhibit pro-inflammatory T cell proliferation and functions while inducing the generation of regulatory T cells, represent a strong candidate to choose for RA treatment. Thus, deciphering the basis of the crosstalk between MSCs and pathogenic memory T cells in RA will pave the way for developing novel and potent strategies to successfully improve MSC-based therapies.

AUTHOR CONTRIBUTIONS

NL-C, RC-L, FD, RE-V, and PL-C. wrote the manuscript with the input of MP-M, MT, SB, MW, and FE.

FUNDING

This work was supported by Fondo Nacional de Desarrollo Científico y Tecnológico 408 (FONDECYT) Iniciación 11160929, Inserm, the University of Montpellier and the Société Française de Rhumatologie (SFR).

REFERENCES

1. Le Blanc K, Mougiakakos D. Multipotent mesenchymal stromal cells and the innate immune system. *Nat Rev Immunol*. (2012) 12:383–96. doi: 10.1038/nri3209
2. Perry BC, Zhou D, Wu X, Yang F-C, Byers MA, Chu T-MG, et al. Collection, cryopreservation, and characterization of human dental pulp–derived mesenchymal stem cells for banking and clinical use. *Tissue Eng Part C Methods*. (2008) 14:149–56. doi: 10.1089/ten.tec.2008.0031
3. Trivanović D, Mojsilović S, Ilić V, Krstić J, Jauković A, Okić Đorđević I, et al. Immunomodulatory capacity of human mesenchymal stem cells isolated from adipose tissue, dental pulp, peripheral blood and umbilical cord Wharton's jelly. *Centr Eur J Immunol*. (2013) 4:421–9. doi: 10.5114/ceji.2013.39756
4. González PL, Carvajal C, Cuenca J, Alcayaga-Miranda F, Figueroa FE, Bartolucci J, et al. Chorion mesenchymal stem cells show superior differentiation, immunosuppressive, and angiogenic potentials in comparison with haploidentical maternal placental cells: chorion MSCs outmatch other placental cells. *Stem Cells Transl Med*. (2015) 4:1109–21. doi: 10.5966/sctm.2015-0022
5. Luz-Crawford P, Torres MJ, Noël D, Fernandez A, Toupet K, Alcayaga-Miranda F, et al. The immunosuppressive signature of menstrual blood

mesenchymal stem cells entails opposite effects on experimental arthritis and graft versus host diseases: immunosuppresive signature of MenSC. *Stem Cells*. (2016) 34:456–69. doi: 10.1002/stem.2244
6. Dominici M, Le Blanc K, Mueller I, Slaper-Cortenbach I, Marini F, Krause DS, et al. Minimal criteria for defining multipotent mesenchymal stromal cells. The International Society for Cellular Therapy position statement. *Cytotherapy*. (2006) 8:315–7. doi: 10.1080/14653240600855905
7. Tanaka Y. Human mesenchymal stem cells as a tool for joint repair in rheumatoid arthritis. *Clin Exp Rheumatol.* (2015) 33(4 Suppl. 92):S58–62. Available online at: https://www.clinexprheumatol.org/abstract.asp?a=9879
8. Bhargava P, Calabresi PA. Novel therapies for memory cells in autoimmune diseases: novel therapies for memory cells. *Clin Exp Immunol*. (2015) 180:353–60. doi: 10.1111/cei.12602
9. Cutler AJ, Limbani V, Girdlestone J, Navarrete CV. Umbilical Cord-derived mesenchymal stromal cells modulate monocyte function to suppress T cell proliferation. *J Immunol*. (2010) 185:6617–23. doi: 10.4049/jimmunol.1002239
10. Chen P-M, Liu K-J, Hsu P-J, Wei C-F, Bai C-H, Ho L-J, et al. Induction of immunomodulatory monocytes by human mesenchymal stem cell-derived hepatocyte growth factor through ERK1/2. *J Leukoc Biol*. (2014) 96:295–303. doi: 10.1189/jlb.3A0513-242R
11. Jiang X-X. Human mesenchymal stem cells inhibit differentiation and function of monocyte-derived dendritic cells. *Blood*. (2005) 105:4120–6. doi: 10.1182/blood-2004-02-0586
12. Chiesa S, Morbelli S, Morando S, Massollo M, Marini C, Bertoni A, et al. Mesenchymal stem cells impair in vivo T-cell priming by dendritic cells. *Proc Natl Acad Sci USA*. (2011) 108:17384–9. doi: 10.1073/pnas.1103650108
13. Németh K, Leelahavanichkul A, Yuen PST, Mayer B, Parmelee A, Doi K, et al. Bone marrow stromal cells attenuate sepsis via prostaglandin E2–dependent reprogramming of host macrophages to increase their interleukin-10 production. *Nat Med.* (2009) 15:42–9. doi: 10.1038/nm.1905
14. Yen BL, Yen M-L, Hsu P-J, Liu K-J, Wang C-J, Bai C-H, et al. Multipotent human mesenchymal stromal cells mediate expansion of myeloid-derived suppressor cells via hepatocyte growth factor/c-Met and STAT3. *Stem Cell Rep*. (2013) 1:139–51. doi: 10.1016/j.stemcr.2013.06.006
15. Chen C-P, Chen Y-Y, Huang J-P, Wu Y-H. The effect of conditioned medium derived from human placental multipotent mesenchymal stromal cells on neutrophils: possible implications for placental infection. *MHR Basic Sci Reprod Med*. (2014) 20:1117–25. doi: 10.1093/molehr/gau062
16. Di Nicola M. Human bone marrow stromal cells suppress T-lymphocyte proliferation induced by cellular or nonspecific mitogenic stimuli. *Blood*. (2002) 99:3838–43. doi: 10.1182/blood.V99.10.3838
17. Krampera M. Bone marrow mesenchymal stem cells inhibit the response of naive and memory antigen-specific T cells to their cognate peptide. *Blood*. (2003) 101:3722–9. doi: 10.1182/blood-2002-07-2104
18. Corcione A. Human mesenchymal stem cells modulate B-cell functions. *Blood*. (2006) 107:367–72. doi: 10.1182/blood-2005-07-2657
19. Uccelli A, Moretta L, Pistoia V. Mesenchymal stem cells in health and disease. *Nat Rev Immunol*. (2008) 8:726–36. doi: 10.1038/nri2395
20. Griffin MD, Elliman SJ, Cahill E, English K, Ceredig R, Ritter T. Concise review: adult mesenchymal stromal cell therapy for inflammatory diseases: how well are we joining the dots?: MSC therapy for inflammatory diseases. *Stem Cells*. (2013) 31:2033–41. doi: 10.1002/stem.1452
21. Connick P, Kolappan M, Patani R, Scott MA, Crawley C, He X-L, et al. The mesenchymal stem cells in multiple sclerosis (MSCIMS) trial protocol and baseline cohort characteristics: an open-label pre-test: post-test study with blinded outcome assessments. *Trials.* (2011) 12:62. doi: 10.1186/1745-6215-12-62
22. Riordan NH, Morales I, Fernández G, Allen N, Fearnot NE, Leckrone ME, et al. Clinical feasibility of umbilical cord tissue-derived mesenchymal stem cells in the treatment of multiple sclerosis. *J Transl Med*. (2018) 16:57. doi: 10.1186/s12967-018-1433-7
23. Compston A, Coles A. Multiple sclerosis. *Lancet*. (2008) 372:1502–17. doi: 10.1016/S0140-6736(08)61620-7
24. Ibraheim H, Giacomini C, Kassam Z, Dazzi F, Powell N. Advances in mesenchymal stromal cell therapy in the management of Crohn's disease. *Exp Rev Gastroenterol Hepatol.* (2018) 12:141–53. doi: 10.1080/17474124.2018.1393332
25. Lee SH, Kwon JE, Cho M-L. Immunological pathogenesis of inflammatory bowel disease. *Intest Res*. (2018) 16:26–42. doi: 10.5217/ir.2018.16.1.26
26. Wang D, Li J, Zhang Y, Zhang M, Chen J, Li X, et al. Umbilical cord mesenchymal stem cell transplantation in active and refractory systemic lupus erythematosus: a multicenter clinical study. *Arthritis Res Ther*. (2014) 16:R79. doi: 10.1186/ar4520
27. Tsokos GC. Systemic lupus erythematosus. *N Engl J Med*. (2011) 365:2110–21. doi: 10.1056/NEJMra1100359
28. Swain SL, Agrewala JN, Brown DM, Jelley-Gibbs DM, Golech S, Huston G, et al. CD4+ T-cell memory: generation and multi-faceted roles for CD4+ T cells in protective immunity to influenza. *Immunol Rev*. (2006) 211:8–22. doi: 10.1111/j.0105-2896.2006.00388.x
29. Farber DL, Yudanin NA, Restifo NP. Human memory T cells: generation, compartmentalization and homeostasis. *Nat Rev Immunol*. (2014) 14:24–35. doi: 10.1038/nri3567
30. Amsen D, Backer RA, Helbig C. Decisions on the road to memory. In: Katsikis PD, Schoenberger SP, Pulendran B, editors. *Crossroads Between Innate and Adaptive Immunity IV*. New York, NY: Springer New York (2013). p. 107–20. Available online at: http://link.springer.com/10.1007/978-1-4614-6217-0_12 (accessed June 15, 2018).
31. Smith SH, Brown MH, Rowe D, Callard RE, Beverley PC. Functional subsets of human helper-inducer cells defined by a new monoclonal antibody, UCHL1. *Immunology*. (1986) 58:63–70.
32. Sanders ME, Makgoba MW, Sharrow SO, Stephany D, Springer TA, Young HA, et al. Human memory T lymphocytes express increased levels of three cell adhesion molecules (LFA-3, CD2, and LFA-1) and three other molecules (UCHL1, CDw29, and Pgp-1) and have enhanced IFN-gamma production. *J Immunol.* (1988) 140:1401–7.
33. Sallusto F, Lenig D, Förster R, Lipp M, Lanzavecchia A. Two subsets of memory T lymphocytes with distinct homing potentials and effector functions. *Nature.* (1999) 401:708–12.
34. Sallusto F, Geginat J, Lanzavecchia A. Central memory and effector memory T cell subsets: function, generation, and maintenance. *Annu Rev Immunol.* (2004) 22:745–63. doi: 10.1146/annurev.immunol.22.012703.104702
35. Lovett-Racke AE, Trotter JL, Lauber J, Perrin PJ, June CH, Racke MK. Decreased dependence of myelin basic protein-reactive T cells on CD28-mediated costimulation in multiple sclerosis patients. A marker of activated/memory T cells. *J Clin Invest*. (1998) 101:725–30. doi: 10.1172/JCI1528
36. Hedlund G, Sandberg-Wollheim M, Sjögren HO. Increased proportion of CD4+ CDw29+ CD45R– UCHL-1+ lymphocytes in the cerebrospinal fluid of both multiple sclerosis patients and healthy individuals. *Cell Immunol*. (1989) 118:406–12. doi: 10.1016/0008-8749(89)90388-2
37. Muraro PA, Pette M, Bielekova B, McFarland HF, Martin R. Human autoreactive CD4+ T cells from naive CD45RA+ and memory CD45RO+ subsets differ with respect to epitope specificity and functional antigen avidity. *J Immunol.* (2000) 164:5474–81. doi: 10.4049/jimmunol.164.10.5474
38. Mullen KM, Gocke AR, Allie R, Ntranos A, Grishkan IV, Pardo C, et al. Expression of CCR7 and CD45RA in CD4+ and CD8+ subsets in cerebrospinal fluid of 134 patients with inflammatory and non-inflammatory neurological diseases. *J Neuroimmunol*. (2012) 249:86–92. doi: 10.1016/j.jneuroim.2012.04.017
39. Zaffaroni M, Rossini S, Ghezzi A, Parma R, Cazzullo CL. Decrease of CD4+CD45+ T-cells in chronic-progressive multiple sclerosis. *J Neurol.* (1990) 237:1–4. doi: 10.1007/BF00319659
40. Kadowaki A, Saga R, Lin Y, Sato W, Yamamura T. Gut microbiota-dependent CCR9+CD4+ T cells are altered in secondary progressive multiple sclerosis. *Brain.* (2019) 142:916–31. doi: 10.1093/brain/awz012
41. Roman LI, Manzano L, De La Hera A, Abreu L, Rossi I, Alvarez-Mon M. Expanded CD4+CD45RO+ phenotype and defective proliferative response in T lymphocytes from patients with Crohn's disease. *Gastroenterology*. (1996) 110:1008–19. doi: 10.1053/gast.1996.v110.pm8612987
42. De Tena JG, Manzano L, Leal JC, Antonio ES, Sualdea V, Álvarez-Mon M. Active Crohn's disease patients show a distinctive expansion of circulating memory CD4+CD45RO+ CD28- T cells. *J Clin Immunol*. (2004) 24:185–96. doi: 10.1023/B:JOCI.0000019784.20191.7f
43. Tena JGD, Manzano L, Leal JC, Antonio ES, Sualdea V, Álvarez-Mon M. Distinctive pattern of cytokine production and adhesion molecule expression

in peripheral blood memory CD4+ T cells from patients with active Crohn's disease. *J Clin Immunol*. (2006) 26:233–42. doi: 10.1007/s10875-006-9016-4
44. Fritsch RD, Shen X, Illei GG, Yarboro CH, Prussin C, Hathcock KS, et al. Abnormal differentiation of memory T cells in systemic lupus erythematosus. *Arthritis Rheum*. (2006) 54:2184–97. doi: 10.1002/art.21943
45. Zhou H, Hu B, Huang N, Mo X, Li W, Zhang B, et al. Aberrant T cell subsets and cytokines expression profile in systemic lupus erythematosus. *Clin Rheumatol*. (2018) 37:2405–13. doi: 10.1007/s10067-018-4124-0
46. Hu X, Kim H, Stahl E, Plenge R, Daly M, Raychaudhuri S. Integrating autoimmune risk loci with gene-expression data identifies specific pathogenic immune cell subsets. *Am J Hum Genet*. (2011) 89:496–506. doi: 10.1016/j.ajhg.2011.09.002
47. Machold KP, Stamm TA, Nell VPK, Pflugbeil S, Aletaha D, Steiner G, et al. Very recent onset rheumatoid arthritis: clinical and serological patient characteristics associated with radiographic progression over the first years of disease. Rheumatology. (2006) Jul 28;46:342–9.
48. Firestein GS. Evolving concepts of rheumatoid arthritis. *Nature*. (2003) 423:356–61. doi: 10.1038/nature01661
49. Müller-Ladner U, Ospelt C, Gay S, Distler O, Pap T. Cells of the synovium in rheumatoid arthritis. Synovial fibroblasts. *Arthritis Res Ther*. (2007) 9:223. doi: 10.1186/ar2337
50. Yang Z, Shen Y, Oishi H, Matteson EL, Tian L, Goronzy JJ, et al. Restoring oxidant signaling suppresses proarthritogenic T cell effector functions in rheumatoid arthritis. *Sci Transl Med*. (2016) 8:331ra38. doi: 10.1126/scitranslmed.aad7151
51. Thomas R, McIlraith M, Davis LS, Lipsky PE. Rheumatoid synovium is enriched in CD45RBdim mature memory T cells that are potent helpers for B cell differentiation. *Arthritis Rheum*. (1992) 35:1455–65. doi: 10.1002/art.1780351209
52. Kohem CL, Brezinschek RI, Wisbey H, Tortorella C, Lipsky PE, Oppenheimer-Marks N. Enrichment of differentiated CD45RBdim,CD27- memory T cells in the peripheral blood, synovial fluid, and synovial tissue of patients with rheumatoid arthritis. *Arthritis Rheum*. (1996) 39:844–54. doi: 10.1002/art.1780390518
53. Morita Y, Yamamura M, Kawashima M, Harada S, Tsuji K, Shibuya K, et al. Flow cytometric single-cell analysis of cytokine production by CD4+ T cells in synovial tissue and peripheral blood from patients with rheumatoid arthritis. *Arthritis Rheum*. (1998) 41:1669–76. doi: 10.1002/1529-0131(199809)41:9<1669::AID-ART19>3.0.CO;2-G
54. Zhang X, Nakajima T, Goronzy JJ, Weyand CM. Tissue trafficking patterns of effector memory CD4+ T cells in rheumatoid arthritis. *Arthritis Rheum*. (2005) 52:3839–49. doi: 10.1002/art.21482
55. Matsuki F, Saegusa J, Nishimura K, Miura Y, Kurosaka M, Kumagai S, et al. CD45RA–Foxp3low non-regulatory T cells in the CCR7–CD45RA–CD27+CD28+ effector memory subset are increased in synovial fluid from patients with rheumatoid arthritis. *Cell Immunol*. (2014) 290:96–101. doi: 10.1016/j.cellimm.2014.05.011
56. Koenders MI, van den Berg WB. Novel therapeutic targets in rheumatoid arthritis. *Trends Pharmacol Sci*. (2015) 36:189–95. doi: 10.1016/j.tips.2015.02.001
57. Andersson KME, Cavallini NF, Hu D, Brisslert M, Cialic R, Valadi H, et al. Pathogenic transdifferentiation of Th17 cells contribute to perpetuation of rheumatoid arthritis during anti-TNF treatment. *Mol Med*. (2015) 21:536–43. doi: 10.2119/molmed.2015.00057
58. Genovese MC, Durez P, Richards HB, Supronik J, Dokoupilova E, Mazurov V, et al. Efficacy and safety of secukinumab in patients with rheumatoid arthritis: a phase II, dose-finding, double-blind, randomised, placebo controlled study. *Ann Rheum Dis*. (2013) 72:863–9. doi: 10.1136/annrheumdis-2012-201601
59. Martin DA, Churchill M, Flores-Suarez L, Cardiel MH, Wallace D, Martin R, et al. A phase Ib multiple ascending dose study evaluating safety, pharmacokinetics, and early clinical response of brodalumab, a human anti-IL-17R antibody, in methotrexate-resistant rheumatoid arthritis. *Arthritis Res Ther*. (2013) 15:R164. doi: 10.1186/ar4347
60. Greter M, Helft J, Chow A, Hashimoto D, Mortha A, Agudo-Cantero J, et al. GM-CSF controls nonlymphoid tissue dendritic cell homeostasis but is dispensable for the differentiation of inflammatory dendritic cells. *Immunity*. (2012) 36:1031–46. doi: 10.1016/j.immuni.2012.03.027
61. Reynolds G, Gibbon JR, Pratt AG, Wood MJ, Coady D, Raftery G, et al. Synovial CD4+ T-cell-derived GM-CSF supports the differentiation of an inflammatory dendritic cell population in rheumatoid arthritis. *Ann Rheum Dis*. (2016) 75:899–907. doi: 10.1136/annrheumdis-2014-206578
62. Behrens F, Tak PP, Østergaard M, Stoilov R, Wiland P, Huizinga TW, et al. MOR103, a human monoclonal antibody to granulocyte–macrophage colony-stimulating factor, in the treatment of patients with moderate rheumatoid arthritis: results of a phase Ib/IIa randomised, double-blind, placebo-controlled, dose-escalation trial. *Ann Rheum Dis*. (2015) 74:1058–64. doi: 10.1136/annrheumdis-2013-204816
63. Fleischmann R, Kremer J, Cush J, Schulze-Koops H, Connell CA, Bradley JD, et al. Placebo-controlled trial of tofacitinib monotherapy in rheumatoid arthritis. *N Engl J Med*. (2012) 367:495–507. doi: 10.1056/NEJMoa1109071
64. Genovese MC, Kremer J, Zamani O, Ludivico C, Krogulec M, Xie L, et al. Baricitinib in patients with refractory rheumatoid arthritis. *N Engl J Med*. (2016) 374:1243–52. doi: 10.1056/NEJMoa1507247
65. Geginat J, Sallusto F, Lanzavecchia A. Cytokine-driven proliferation and differentiation of human naive, central memory, and effector memory CD4(+) T cells. *J Exp Med*. (2001) 194:1711–9. doi: 10.1084/jem.194.12.1711
66. Boyle DL, Soma K, Hodge J, Kavanaugh A, Mandel D, Mease P, et al. The JAK inhibitor tofacitinib suppresses synovial JAK1-STAT signalling in rheumatoid arthritis. *Ann Rheum Dis*. (2015) 74:1311–6. doi: 10.1136/annrheumdis-2014-206028
67. Hünig T, Beyersdorf N, Kerkau T. CD28 co-stimulation in T-cell homeostasis: a recent perspective. *ImmunoTargets Ther*. (2015) 4:111–22. doi: 10.2147/ITT.S61647
68. Nam JL, Takase-Minegishi K, Ramiro S, Chatzidionysiou K, Smolen JS, van der Heijde D, et al. Efficacy of biological disease-modifying antirheumatic drugs: a systematic literature review informing the (2016) update of the EULAR recommendations for the management of rheumatoid arthritis. *Ann Rheum Dis*. (2017) 76:1113–36. doi: 10.1136/annrheumdis-2016-210713
69. Warrington KJ, Takemura S, Goronzy JJ, Weyand CM. CD4+,CD28- T cells in rheumatoid arthritis patients combine features of the innate and adaptive immune systems. *Arthritis Rheum*. (2001) 44:13–20. doi: 10.1002/1529-0131(200101)44:1<13::AID-ANR3>3.0.CO;2-6
70. Park W, Weyand CM, Schmidt D, Goronzy JJ. Co-stimulatory pathways controlling activation and peripheral tolerance of human CD4+CD28– T cells. *Eur J Immunol*. (1997) 27:1082–90. doi: 10.1002/eji.1830270507
71. Goronzy JJ, Weyand CM. Thymic function and peripheral T-cell homeostasis in rheumatoid arthritis. *Trends Immunol*. (2001) 22:251–5. doi: 10.1016/S1471-4906(00)01841-X
72. Vallejo AN, Bryl E, Klarskov K, Naylor S, Weyand CM, Goronzy JJ. Molecular basis for the loss of CD28 expression in senescent T cells. *J Biol Chem*. (2002) 277:46940–9. doi: 10.1074/jbc.M207352200
73. Appay V, van Lier RAW, Sallusto F, Roederer M. Phenotype and function of human T lymphocyte subsets: consensus and issues: phenotype and function of human T lymphocyte subsets: consensus and issues. *Cytometry Part A*. (2008) 73A:975–83. doi: 10.1002/cyto.a.20643
74. Tayar JH, Suarez-Almazor ME. New understanding and approaches to treatment in rheumatoid arthritis. *Br Med Bull*. (2010) 94:201–14. doi: 10.1093/bmb/ldq007
75. Liang J, Li X, Zhang H, Wang D, Feng X, Wang H, et al. Allogeneic mesenchymal stem cells transplantation in patients with refractory RA. *Clin Rheumatol*. (2012) 31:157–61. doi: 10.1007/s10067-011-1816-0
76. Wang L, Wang L, Cong X, Liu G, Zhou J, Bai B, et al. Human umbilical cord mesenchymal stem cell therapy for patients with active rheumatoid arthritis: safety and efficacy. *Stem Cells Dev*. (2013) 22:3192–202. doi: 10.1089/scd.2013.0023
77. Álvaro-Gracia JM, Jover JA, García-Vicu-a R, Carre-o L, Alonso A, Marsal S, et al. Intravenous administration of expanded allogeneic adipose-derived mesenchymal stem cells in refractory rheumatoid arthritis (Cx611): results of a multicentre, dose escalation, randomised, single-blind, placebo-controlled phase Ib/IIa clinical trial. *Ann Rheum Dis*. (2017) 76:196–202. doi: 10.1136/annrheumdis-2015-208918
78. Yang J, Brook MO, Carvalho-Gaspar M, Zhang J, Ramon HE, Sayegh MH, et al. Allograft rejection mediated by memory T cells is resistant to regulation. *Proc Natl Acad Sci USA*. (2007) 104:19954–9. doi: 10.1073/pnas.0704397104

79. Afzali B, Mitchell PJ, Scottà C, Canavan J, Edozie FC, Fazekasova H, et al. Relative resistance of human CD4+ memory T cells to suppression by CD4+CD25+ regulatory T cells: memory cells as barriers to treg-cell therapy. *Am J Transpl*. (2011) 11:1734–42. doi: 10.1111/j.1600-6143.2011.03635.x
80. Pianta S, Bonassi Signoroni P, Muradore I, Rodrigues MF, Rossi D, Silini A, et al. Amniotic membrane mesenchymal cells-derived factors skew T cell polarization toward treg and downregulate Th1 and Th17 cells subsets. *Stem Cell Rev Rep*. (2015) 11:394–407. doi: 10.1007/s12015-014-9558-4
81. Ribeiro A, Laranjeira P, Mendes S, Velada I, Leite C, Andrade P, et al. Mesenchymal stem cells from umbilical cord matrix, adipose tissue and bone marrow exhibit different capability to suppress peripheral blood B, natural killer and T cells. *Stem Cell Res Ther*. (2013) 4:125. doi: 10.1186/scrt336
82. Mareschi K, Castiglia S, Sanavio F, Rustichelli D, Muraro M, Defedele D, et al. Immunoregulatory effects on T lymphocytes by human mesenchymal stromal cells isolated from bone marrow, amniotic fluid, and placenta. *Exp Hematol*. (2016) 44:138–50.e1. doi: 10.1016/j.exphem.2015.10.009
83. Laranjeira P, Pedrosa M, Pedreiro S, Gomes J, Martinho A, Antunes B, et al. Effect of human bone marrow mesenchymal stromal cells on cytokine production by peripheral blood naive, memory, and effector T cells. *Stem Cell Res Ther*. (2015) 6:3. doi: 10.1186/scrt537
84. Hu C, Qian L, Miao Y, Huang Q, Miao P, Wang P, et al. Antigen-presenting effects of effector memory Vγ9Vδ2 T cells in rheumatoid arthritis. *Cell Mol Immunol*. (2012) 9:245–54. doi: 10.1038/cmi.2011.50
85. Martinet L, Fleury-Cappellesso S, Gadelorge M, Dietrich G, Bourin P, Fournié J-J, et al. A regulatory cross-talk between Vγ9Vδ2 T lymphocytes and mesenchymal stem cells: Immunomodulation. *Eur J Immunol*. (2009) 39:752–62. doi: 10.1002/eji.200838812
86. Liu X, Feng T, Gong T, Shen C, Zhu T, Wu Q, et al. Human umbilical cord mesenchymal stem cells inhibit the function of allogeneic activated V γδ T lymphocytes in vitro. *BioMed Res Int*. (2015) 2015:1–10. doi: 10.1155/2015/317801
87. Liu R, Li X, Zhang Z, Zhou M, Sun Y, Su D, et al. Allogeneic mesenchymal stem cells inhibited T follicular helper cell generation in rheumatoid arthritis. *Sci Rep*. (2015) 5:12777. doi: 10.1038/srep12777
88. Wang J, Shan Y, Jiang Z, Feng J, Li C, Ma L, et al. High frequencies of activated B cells and follicular helper T cells are correlated with disease activity in patients with new onset rheumatoid arthritis: High frequency of TFH and B cells in RA patients. *Clin Exp Immunol*. (2013) 174:212–20. doi: 10.1111/cei.12162
89. Ueno H, Banchereau J, Vinuesa CG. Pathophysiology of T follicular helper cells in humans and mice. *Nat Immunol*. (2015) 16:142–52. doi: 10.1038/ni.3054
90. Akbar AN, Fletcher JM. Memory T cell homeostasis and senescence during aging. *Curr Opin Immunol*. (2005) 17:480–5. doi: 10.1016/j.coi.2005.07.019
91. Ojdana D, Safiejko K, Lipska A, Radziwon P, Dadan J, Tryniszewska E. Effector and memory CD4+ and CD8+ T cells in the chronic infection process. *Folia Histochemica et Cytobiologica*. (2009) 46:413–7. doi: 10.2478/v10042-008-0077-5
92. Qin S, Rottman JB, Myers P, Kassam N, Weinblatt M, Loetscher M, et al. The chemokine receptors CXCR3 and CCR5 mark subsets of T cells associated with certain inflammatory reactions. *J Clin Invest*. (1998) 101:746–54. doi: 10.1172/JCI1422
93. Suzuki N, Nakajima A, Yoshino S, Matsushima K, Yagita H, Okumura K. Selective accumulation of CCR5+ T lymphocytes into inflamed joints of rheumatoid arthritis. *Int Immunol*. (1999) 11:553–9. doi: 10.1093/intimm/11.4.553
94. Nanki T, Lipsky PE. Cytokine, activation marker, and chemokine receptor expression by individual CD4(+) memory T cells in rheumatoid arthritis synovium. *Arthritis Res*. (2000) 2:415–23. doi: 10.1186/ar120
95. Grom AA, Murray KJ, Luyrink L, Emery H, Passo MH, Glass DN, et al. Patterns of expression of tumor necrosis factor alpha, tumor necrosis factor beta, and their receptors in synovia of patients with juvenile rheumatoid arthritis and juvenile spondylarthropathy. *Arthritis Rheum*. (1996) 39:1703–10. doi: 10.1002/art.1780391013
96. Nanki T, Hayashida K, El-Gabalawy HS, Suson S, Shi K, Girschick HJ, et al. Stromal cell-derived factor-1-CXC chemokine receptor 4 interactions play a central role in CD4+ T cell accumulation in rheumatoid arthritis synovium. *J Immunol*. (2000) 165:6590–8. doi: 10.4049/jimmunol.165.11.6590
97. Chabaud M, Page G, Miossec P. Enhancing effect of IL-1, IL-17, and TNF-alpha on macrophage inflammatory protein-3alpha production in rheumatoid arthritis: regulation by soluble receptors and Th2 cytokines. *J Immunol*. (2001) 167:6015–20. doi: 10.4049/jimmunol.167.10.6015
98. Kim K-W, Cho M-L, Kim H-R, Ju J-H, Park M-K, Oh H-J, et al. Up-regulation of stromal cell–derived factor 1 (CXCL12) production in rheumatoid synovial fibroblasts through interactions with T lymphocytes: role of interleukin-17 and CD40L–CD40 interaction. *Arthritis Rheum*. (2007) 56:1076–86. doi: 10.1002/art.22439
99. Kanbe K, Takagishi K, Chen Q. Stimulation of matrix metalloprotease 3 release from human chondrocytes by the interaction of stromal cell-derived factor 1 and CXC chemokine receptor 4. *Arthritis Rheum*. (2002) 46:130–7. doi: 10.1002/1529-0131(200201)46:1<130::AID-ART10020>3.0.CO;2-D
100. Pablos JL, Santiago B, Galindo M, Torres C, Brehmer MT, Blanco FJ, et al. Synoviocyte-derived CXCL12 is displayed on endothelium and induces angiogenesis in rheumatoid arthritis. *J Immunol*. (2003) 170:2147–52. doi: 10.4049/jimmunol.170.4.2147
101. Grassi F, Cristino S, Toneguzzi S, Piacentini A, Facchini A, Lisignoli G. CXCL12 chemokine up-regulates bone resorption and MMP-9 release by human osteoclasts: CXCL12 levels are increased in synovial and bone tissue of rheumatoid arthritis patients. *J Cell Physiol*. (2004) 199:244–51. doi: 10.1002/jcp.10445
102. da Silva Meirelles L, Fontes AM, Covas DT, Caplan AI. Mechanisms involved in the therapeutic properties of mesenchymal stem cells. *Cytokine Growth Factor Rev*. (2009) 20:419–27. doi: 10.1016/j.cytogfr.2009.10.002
103. Ivanova-Todorova E, Bochev I, Dimitrov R, Belemezova K, Mourdjeva M, Kyurkchiev S, et al. Conditioned medium from adipose tissue-derived mesenchymal stem cells induces CD4+FOXP3+ cells and increases IL-10 secretion. *J Biomed Biotechnol*. (2012) 2012:1–8. doi: 10.1155/2012/295167
104. Kyurkchiev D, Ivanova-Todorova E, Bochev I, Mourdjeva M, Kyurkchiev S. Differences between adipose tissue-derived mesenchymal stem cells and bone marrow-derived mesenchymal stem cells as regulators of the immune response. In: Hayat MA, editor. *Stem Cells and Cancer Stem Cells, Vol 10*. Dordrecht: Springer Netherlands (2013). p. 71–84. Available online at: http://link.springer.com/10.1007/978-94-007-6262-6_7 (accessed August 23, 2018).
105. Sohni A, Verfaillie CM. Mesenchymal stem cells migration homing and tracking. *Stem Cells Int*. (2013) 2013:1–8. doi: 10.1155/2013/130763
106. Buckley CD, Amft N, Bradfield PF, Pilling D, Ross E, Arenzana-Seisdedos F, et al. Persistent induction of the chemokine receptor CXCR4 by TGF-beta 1 on synovial T cells contributes to their accumulation within the rheumatoid synovium. *J Immunol*. (2000) 165:3423–9. doi: 10.4049/jimmunol.165.6.3423
107. Nagafuchi Y, Shoda H, Sumitomo S, Nakachi S, Kato R, Tsuchida Y, et al. Immunophenotyping of rheumatoid arthritis reveals a linkage between HLA-DRB1 genotype, CXCR4 expression on memory CD4+ T cells and disease activity. *Sci Rep*. (2016) 6:29338. doi: 10.1038/srep29338
108. Xie J, Wang W, Si J-W, Miao X-Y, Li J-C, Wang Y-C, et al. Notch signaling regulates CXCR4 expression and the migration of mesenchymal stem cells. *Cell Immunol*. (2013) 281:68–75. doi: 10.1016/j.cellimm.2013.02.001
109. Awasthi A, Kuchroo VK. Th17 cells: from precursors to players in inflammation and infection. *Int Immunol*. (2009) 21:489–98. doi: 10.1093/intimm/dxp021
110. Sakaguchi S. Regulatory T cells in the past and for the future. *Eur J Immunol*. (2008) 38:901–37. doi: 10.1002/eji.200890012
111. Baecher-Allan C, Brown JA, Freeman GJ, Hafler DA. CD4+CD25high regulatory cells in human peripheral blood. *J Immunol*. (2001) 167:1245–53. doi: 10.4049/jimmunol.167.3.1245
112. Fontenot JD, Gavin MA, Rudensky AY. Foxp3 programs the development and function of CD4+CD25+ regulatory T cells. *Nat Immunol*. (2003) 4:330–6. doi: 10.1038/ni904
113. Seddiki N, Santner-Nanan B, Martinson J, Zaunders J, Sasson S, Landay A, et al. Expression of interleukin (IL)-2 and IL-7 receptors discriminates between human regulatory and activated T cells. *J Exp Med*. (2006) 203:1693–700. doi: 10.1084/jem.20060468
114. Hartigan-O'Connor DJ, Poon C, Sinclair E, McCune JM. Human CD4+ regulatory T cells express lower levels of the IL-7 receptor alpha chain

(CD127), allowing consistent identification and sorting of live cells. *J Immunol Methods*. (2007) 319:41–52. doi: 10.1016/j.jim.2006.10.008
115. Wang W, Shao S, Jiao Z, Guo M, Xu H, Wang S. The Th17/Treg imbalance and cytokine environment in peripheral blood of patients with rheumatoid arthritis. *Rheumatol Int*. (2012) 32:887–93. doi: 10.1007/s00296-010-1710-0
116. Niu Q, Cai B, Huang Z, Shi Y, Wang L. Disturbed Th17/Treg balance in patients with rheumatoid arthritis. *Rheumatol Int*. (2012) 32:2731–6. doi: 10.1007/s00296-011-1984-x
117. Eggleton P, Bremer E, Tarr JM, de Bruyn M, Helfrich W, Kendall A, et al. Frequency of Th17 CD20+ cells in the peripheral blood of rheumatoid arthritis patients is higher compared to healthy subjects. *Arthritis Res Ther*. (2011) 13:R208. doi: 10.1186/ar3541
118. Metawi SA, Abbas D, Kamal MM, Ibrahim MK. Serum and synovial fluid levels of interleukin-17 in correlation with disease activity in patients with RA. *Clin Rheumatol*. (2011) 30:1201–7. doi: 10.1007/s10067-011-1737-y
119. Kim J, Kang S, Kim J, Kwon G, Koo S. Elevated levels of T helper 17 cells are associated with disease activity in patients with rheumatoid arthritis. *Ann Lab Med*. (2013) 33:52–9. doi: 10.3343/alm.2013.33.1.52
120. Benedetti G, Miossec P. Interleukin 17 contributes to the chronicity of inflammatory diseases such as rheumatoid arthritis: HIGHLIGHTS. *Eur J Immunol*. (2014) 44:339–47. doi: 10.1002/eji.201344184
121. Chabaud M, Durand JM, Buchs N, Fossiez F, Page G, Frappart L, et al. Human interleukin-17: a T cell-derived proinflammatory cytokine produced by the rheumatoid synovium. *Arthritis Rheum*. (1999) 42:963–70. doi: 10.1002/1529-0131(199905)42:5<963::AID-ANR15>3.0.CO;2-E
122. Honorati MC, Meliconi R, Pulsatelli L, Canè S, Frizziero L, Facchini A. High in vivo expression of interleukin-17 receptor in synovial endothelial cells and chondrocytes from arthritis patients. *Rheumatology*. (2001) 40:522–7. doi: 10.1093/rheumatology/40.5.522
123. Hirota K, Yoshitomi H, Hashimoto M, Maeda S, Teradaira S, Sugimoto N, et al. Preferential recruitment of CCR6-expressing Th17 cells to inflamed joints via CCL20 in rheumatoid arthritis and its animal model. *J Exp Med*. (2007) 204:2803–12. doi: 10.1084/jem.20071397
124. Sundrud MS, Trivigno C. Identity crisis of Th17 cells: many forms, many functions, many questions. *Semin Immunol*. (2013) 25:263–72. doi: 10.1016/j.smim.2013.10.021
125. Jiao Z, Wang W, Jia R, Li J, You H, Chen L, et al. Accumulation of FoxP3-expressing CD4+ CD25+ T cells with distinct chemokine receptors in synovial fluid of patients with active rheumatoid arthritis. *Scand J Rheumatol*. (2007) 36:428–33. doi: 10.1080/03009740701482800
126. van Amelsfort JMR, Jacobs KMG, Bijlsma JWJ, Lafeber FPJG, Taams LS. CD4+CD25+ regulatory T cells in rheumatoid arthritis: differences in the presence, phenotype, and function between peripheral blood and synovial fluid. *Arthritis Rheum*. (2004) 50:2775–85. doi: 10.1002/art.20499
127. Walter GJ, Fleskens V, Frederiksen KS, Rajasekhar M, Menon B, Gerwien JG, et al. Phenotypic, functional, and gene expression profiling of peripheral CD45RA+ and CD45RO+ CD4+CD25+CD127 low treg cells in patients with chronic rheumatoid arthritis: peripheral Treg cells in chronic RA. *Arthritis Rheumatol*. (2016) 68:103–16. doi: 10.1002/art.39408
128. Ehrenstein MR, Evans JG, Singh A, Moore S, Warnes G, Isenberg DA, et al. Compromised function of regulatory T cells in rheumatoid arthritis and reversal by anti-TNFα therapy. *J Exp Med*. (2004) 200:277–85. doi: 10.1084/jem.20040165
129. Valencia X. TNF downmodulates the function of human CD4+CD25hi T-regulatory cells. *Blood*. (2006) 108:253–61. doi: 10.1182/blood-2005-11-4567
130. Zanin-Zhorov A, Ding Y, Kumari S, Attur M, Hippen KL, Brown M, et al. Protein kinase C- mediates negative feedback on regulatory T cell function. *Science*. (2010) 328:372–6. doi: 10.1126/science.1186068
131. Nie H, Zheng Y, Li R, Guo TB, He D, Fang L, et al. Phosphorylation of FOXP3 controls regulatory T cell function and is inhibited by TNF-α in rheumatoid arthritis. *Nat Med*. (2013) 19:322–8. doi: 10.1038/nm.3085
132. Westhovens R, Robles M, Ximenes AC, Nayiager S, Wollenhaupt J, Durez P, et al. Clinical efficacy and safety of abatacept in methotrexate-naive patients with early rheumatoid arthritis and poor prognostic factors. *Ann Rheum Dis*. (2009) 68:1870–7. doi: 10.1136/ard.2008.101121
133. Cribbs AP, Kennedy A, Penn H, Read JE, Amjadi P, Green P, et al. Treg cell function in rheumatoid arthritis is compromised by CTLA-4 promoter methylation resulting in a failure to activate the indoleamine 2,3-dioxygenase pathway: defective treg cell function in RA and the IDO pathway. *Arthritis Rheumatol*. (2014) 66:2344–54. doi: 10.1002/art.38715
134. Koenen HJPM, Smeets RL, Vink PM, van Rijssen E, Boots AMH, Joosten I. Human CD25highFoxp3pos regulatory T cells differentiate into IL-17-producing cells. *Blood*. (2008) 112:2340–52. doi: 10.1182/blood-2008-01-133967
135. Ivanov II, McKenzie BS, Zhou L, Tadokoro CE, Lepelley A, Lafaille JJ, et al. The orphan nuclear receptor RORγt directs the differentiation program of proinflammatory IL-17+ T helper cells. *Cell*. (2006) 126:1121–33. doi: 10.1016/j.cell.2006.07.035
136. Miyara M, Yoshioka Y, Kitoh A, Shima T, Wing K, Niwa A, et al. Functional delineation and differentiation dynamics of human CD4+ T cells expressing the FoxP3 transcription factor. *Immunity*. (2009) 30:899–911. doi: 10.1016/j.immuni.2009.03.019
137. Ghannam S, Pene J, Torcy-Moquet G, Jorgensen C, Yssel H. Mesenchymal stem cells inhibit human Th17 cell differentiation and function and induce a T regulatory cell phenotype. *J Immunol*. (2010) 185:302–12. doi: 10.1371/journal.pone.0045272
138. Selmani Z, Naji A, Zidi I, Favier B, Gaiffe E, Obert L, et al. Human leukocyte antigen-G5 secretion by human mesenchymal stem cells is required to suppress T lymphocyte and natural killer function and to induce $CD4^{+}CD25^{high}FOXP3^{+}$ regulatory T cells. *Stem Cells*. (2008) 26:212–22. doi: 10.1634/stemcells.2007-0554
139. Mougiakakos D, Jitschin R, Johansson CC, Okita R, Kiessling R, Le Blanc K. The impact of inflammatory licensing on heme oxygenase-1-mediated induction of regulatory T cells by human mesenchymal stem cells. *Blood*. (2011) 117:4826–35. doi: 10.1182/blood-2010-12-324038
140. English K, Ryan JM, Tobin L, Murphy MJ, Barry FP, Mahon BP. Cell contact, prostaglandin E 2 and transforming growth factor beta 1 play non-redundant roles in human mesenchymal stem cell induction of CD4+ CD25 High forkhead box P3+ regulatory T cells. *Clin Exp Immunol*. (2009) 156:149–60. doi: 10.1111/j.1365-2249.2009.03874.x
141. Gonzalez-Rey E, Gonzalez MA, Varela N, O'Valle F, Hernandez-Cortes P, Rico L, et al. Human adipose-derived mesenchymal stem cells reduce inflammatory and T cell responses and induce regulatory T cells in vitro in rheumatoid arthritis. *Ann Rheum Dis*. (2010) 69:241–8. doi: 10.1136/ard.2008.101881
142. Lee H-J, Kim S-N, Jeon M-S, Yi T, Song SU. ICOSL expression in human bone marrow-derived mesenchymal stem cells promotes induction of regulatory T cells. *Sci Rep*. (2017) Dec 7:44486. doi: 10.1038/srep44486
143. Luz-Crawford P, Espinosa-Carrasco G, Ipseiz N, Contreras R, Tejedor G, Medina DA, et al. Gilz-Activin A as a novel signaling axis orchestrating mesenchymal stem cell and Th17 cell interplay. Theranostics. (2018) 8:846–59. doi: 10.7150/thno.21793
144. Diianni M. Mesenchymal cells recruit and regulate T regulatory cells. *Exp Hematol*. (2008) 36:309–18. doi: 10.1016/j.exphem.2007.11.007
145. Franceschetti T, De Bari C. The potential role of adult stem cells in the management of the rheumatic diseases. *Ther Adv Musculoskel Dis*. (2017) 9:165–79. doi: 10.1177/1759720X17704639

Conflict of Interest Statement: The authors declare that the research was conducted in the absence of any commercial or financial relationships that could be construed as a potential conflict of interest.

frontiers in Immunology

ORIGINAL RESEARCH
published: 30 April 2019
doi: 10.3389/fimmu.2019.00937

Hematopoietic or Osteoclast-Specific Deletion of Syk Leads to Increased Bone Mass in Experimental Mice

*Dániel Csete[1], Edina Simon[1], Ahmad Alatshan[2], Petra Aradi[1,3], Csaba Dobó-Nagy[4], Zoltán Jakus[1,3], Szilvia Benkő[2], Dávid S. Győri[1] and Attila Mócsai[1]**

[1] Department of Physiology, Semmelweis University School of Medicine, Budapest, Hungary, [2] Department of Physiology, Faculty of Medicine, University of Debrecen, Debrecen, Hungary, [3] MTA-SE "Lendület" Lymphatic Physiology Research Group of the Hungarian Academy of Sciences and the Semmelweis University, Budapest, Hungary, [4] Department of Oral Diagnostics, Semmelweis University School of Dentistry, Budapest, Hungary

OPEN ACCESS

Edited by:
Claudine Blin-Wakkach, UMR7370 Laboratoire de Physio Médecine Moléculaire (LP2M), France

Reviewed by:
Irma Machuca-gayet, Centre National de la Recherche Scientifique (CNRS), France
Ari Elson, Weizmann Institute of Science, Israel
Pieter J. M. Leenen, Erasmus University Rotterdam, Netherlands

***Correspondence:**
Attila Mócsai
mocsai.attila@med.semmelweis-univ.hu

Specialty section:
This article was submitted to Inflammation, a section of the journal Frontiers in Immunology

Received: 16 December 2018
Accepted: 11 April 2019
Published: 30 April 2019

Citation:
Csete D, Simon E, Alatshan A, Aradi P, Dobó-Nagy C, Jakus Z, Benkő S, Győri DS and Mócsai A (2019) Hematopoietic or Osteoclast-Specific Deletion of Syk Leads to Increased Bone Mass in Experimental Mice. Front. Immunol. 10:937. doi: 10.3389/fimmu.2019.00937

Syk is a non-receptor tyrosine kinase critically involved in signaling by various immunoreceptors including B-cell-receptors and activating Fc-receptors. We have previously shown that Syk also mediates immunoreceptor-like signals required for the *in vitro* development and function of osteoclasts. However, the perinatal lethality of $Syk^{-/-}$ mice precluded the analysis of the role of Syk in *in vivo* bone metabolism. To overcome that problem, we generated mice with osteoclast-specific ($Syk^{\Delta OC}$) or hematopoietic ($Syk^{\Delta Haemo}$) Syk deficiency by conditional deletion of Syk using Cre recombinase expressed under the control of the Ctsk or Vav1 promoter, respectively. Micro-CT analysis revealed increased bone trabecular density in both $Syk^{\Delta OC}$ and $Syk^{\Delta Haemo}$ mice, although hematopoietic Syk deficiency caused a more severe phenotype than osteoclast-specific Syk deficiency. Osteoclast-specific Syk deficiency reduced, whereas hematopoietic Syk deficiency completely blocked *in vitro* development of osteoclasts. Both interventions inhibited the resorptive activity of osteoclasts and osteoclast-specific gene expression. Kinetic analysis of Syk protein levels, Cre expression and the genomic deletion of the Syk^{flox} allele revealed complete and early deletion of Syk from $Syk^{\Delta Haemo}$ osteoclasts whereas Syk was incompletely deleted at a later stage of osteoclast development from $Syk^{\Delta OC}$ cultures. Those results provide an explanation for the *in vivo* and *in vitro* difference between the $Syk^{\Delta OC}$ and $Syk^{\Delta Haemo}$ mutant strains and suggest late activation of, and incomplete target gene deletion upon, osteoclast-specific Cre expression driven by the Ctsk promoter. Taken together, our results indicate that Syk plays an indispensable role in osteoclast-mediated *in vivo* bone resorption and suggest that Syk-specific inhibitors may provide therapeutic benefit in inflammatory and other diseases characterized by excessive osteoclast-mediated bone resorption.

Keywords: SYK (spleen tyrosine kinase), tyrosine kinase, osteoclasts, Cre-Lox, *in vivo*, mice

INTRODUCTION

Osteoclasts are multinuclear giant cells of hematopoietic origin which develop from myeloid progenitors through a unique biochemical maturation program followed by homotypic fusion (1, 2). Osteoclasts are the sole cell types in the mammalian organism capable of actively resorbing bone tissue and therefore play a critical role in bone homeostasis. Defective osteoclast development or function leads to increased bone mass (osteopetrosis) (3), whereas excessive (pathological) bone resorption occurs during osteoporosis (4), inflammatory joint diseases (e.g., arthritis-induced bone erosions in rheumatoid arthritis) (5, 6) and cancer-induced bone loss (7, 8).

Osteoclast development and function requires a number of extracellular cues including M-CSF, RANKL, as well as integrin-mediated adhesive processes (9). The importance of those pathways is indicated by the severe bone resorption defects in mice lacking M-CSF (10), RANK (11, 12), RANKL (13, 14), or β_3 integrins (15). Culturing myeloid progenitors derived from human blood or mouse bone marrow in the presence of M-CSF and RANKL also leads to formation of osteoclast-like cells with *in vitro* bone resorbing capacity, allowing the analysis of osteoclast development and function in cell culture.

Syk is a non-receptor tyrosine kinase critically involved in various functions of the immune system, as well as certain non-immune-related biological processes (16). Syk is required for B-cell-receptor signaling and therefore the development of B-cells (17, 18). It is a critical component of signaling by a number of activating Fc-receptors such as Fcε-receptors and Fcγ-receptors on neutrophils, macrophages, and mast cells (19–22), as well as the Fc-receptor-related collagen receptor GpVI of platelets (23, 24). Syk also mediates signaling by β_1, β_2, and β_3 integrins in neutrophils, monocytes/macrophages, and platelets (25–27). Syk deficiency causes perinatal lethality (17, 18) likely due to the role of Syk in lymphatic vascular development (28). Most, if not all of those functions of Syk is related to its binding to receptor-associated tyrosine-phosphorylated immunoreceptor tyrosine-based activation motifs (ITAMs) linking immunoreceptors to downstream signaling pathways (16, 29–32). The role of Syk in various immune and inflammatory processes also translates into its role in autoantibody-induced arthritis (24, 33–35) and dermatitis (36, 37) in experimental mice.

We and others have previously shown that the ITAM-containing adapter molecules DAP12 and FcRγ are involved in *in vitro* osteoclast development and function, and that mice lacking both DAP12 and FcRγ show strongly increased mineralized bone mass (38–43). One of the possible mechanisms for those phenotypes could be that, similar to immune cells (16, 29), the ITAM-containing DAP12 and FcRγ adapters would activate the Syk tyrosine kinase in osteoclasts, thus triggering osteoclast development and function. Indeed, Syk-deficient bone marrow cells failed to develop to mature multinucleated osteoclasts or to show resorptive activity in *in vitro* cultures (40, 42, 44, 45), and this *in vitro* phenotype was linked to ITAM signaling by DAP12 and FcRγ (42–44). Those studies provided an unexpected link between immunoreceptor-like signaling and bone homeostasis and therefore provided one of the foundations of the field of osteoimmunology (46, 47). In addition, Syk-mediated pathways have also been linked to integrin signal transduction and the osteoclast cytoskeleton (16, 26, 42, 44, 48). Unfortunately, however, it is at present unclear whether Syk is also involved in bone homeostasis in live animals, as bone morphology of Syk-deficient animals could not be tested because of the perinatal lethality of $Syk^{-/-}$ mice (17, 18).

To overcome the perinatal lethality of $Syk^{-/-}$ animals, we have generated mice with osteoclast-specific or hematopoietic-specific Syk deletion using the Cre-Lox recombination approach. Analysis of the mice with tissue specific Syk deletion revealed strong increase in bone mass upon osteoclast-specific and, particularly, hematopoietic-specific Syk-deficiency, indicating a critical role for Syk in *in vivo* bone homeostasis. Further experiments aimed at understanding the different severities of the bone phenotypes in the two strains indicated that the effect of Syk deficiency on osteoclast development strongly depends on the timing and extent of Cre expression and Cre-mediated inactivation of the *Syk* gene.

MATERIALS AND METHODS

Animals

Mice carrying the $Syk^{tm1.2Tara}$ (referred to as Syk^{flox}) floxed allele of the *Syk* gene (49) were obtained from Alexander Tarakhovsky (Rockefeller University) and were maintained in homozygous ($Syk^{flox/flox}$) form. Mice carrying the $Ctsk^{tm1(cre)Ska}$ (referred to as $Ctsk^{Cre}$) knock-in mutation resulting in the osteoclast-specific expression of the Cre recombinase under the control of the endogenous promoter of the *Ctsk* gene and at the same time inactivating the *Ctsk* gene (50) were obtained from Shigeaki Kato (University of Tokyo) and were maintained in heterozygous form (referred to as Ctsk-Cre) to avoid homozygous inactivation of the *Ctsk* gene. Mice carrying the $Commd10^{Tg(Vav1-icre)A2Kio}$ transgenic insertional mutation expressing the Cre recombinase in the entire haemopoietic lineage from the exogenous Vav1 promoter (51) and at the same time inactivating the *Commd10* gene (52) were obtained from the Jackson Laboratory and were maintained in heterozygous form (referred to as Vav-Cre) to avoid homozygous inactivation of the *Commd10* gene. Mice carrying the $Lyz2^{tm1(cre)Ifo}$ (referred to as $Lyz2^{Cre}$) knock-in mutation expressing the Cre recombinase in the entire myeloid compartment from the endogenous promoter of lysozyme M (53) were purchased from the Jackson Laboratory and were maintained in homozygous form (referred to as LysM-Cre).

Osteoclast-specific deletion of *Syk* was achieved by crossing the Ctsk-Cre and $Syk^{flox/flox}$ mice to obtain $Ctsk^{Cre/+}Syk^{flox/flox}$ (referred to as $Syk^{\Delta OC}$) animals. Deletion of Syk in the entire hematopoietic compartment was achieved by crossing the Vav-Cre and $Syk^{flox/flox}$ mice to obtain $Commd10^{Tg(Vav1-icre)A2Kio/+}Syk^{flox/flox}$ (referred to as $Syk^{\Delta Haemo}$) animals. Myeloid-specific deletion of Syk was achieved by crossing the LysM-Cre and $Syk^{flox/flox}$ mice to obtain $Lyz2^{Cre/Cre}Syk^{flox/flox}$ (referred to as $Syk^{\Delta Myelo}$) animals. The allele obtained by Cre-mediated deletion of the Syk^{flox} allele will be referred to as the Syk^{Δ} allele.

Genotyping of the mice was performed by allele-specific PCR. All mice were on the C57BL/6 genetic background. Wild type C57BL/6 animals were obtained from our breeding colony. The mice were kept in individually sterile ventilated cages (Tecniplast) in a specific pathogen-free facility. All animal experiments were approved by the Animal Experimentation Review Board of Semmelweis University.

Micro-CT Analysis

Mice were sacrificed at 9 weeks of age and their right femurs were subjected to micro-CT analysis by a SkyScan 1172 micro-CT apparatus as described (54, 55). A 70 kV and 124 μA X-ray source with 0.5 mm aluminum filter and a rotation step of 0.5° was used during image acquisition, followed by reconstruction with the SkyScan NRecon software, resulting in an isometric 5 μm voxel size. Volume of interest was selected according to the manufacturer's instructions. Further analysis was performed using the Skyscan CTAn and CTVol software. The lower threshold of binary images was set to an absolute value of 85 throughout the entire study. Our study design did not allow the calculation of absolute bone hydroxyapatite densities.

Quantitative analysis was performed on the trabecular region of the distal femoral metaphysis beginning 50 sections (0.25 mm) from the distal growth plate to an additional 400 sections (2 mm) to the proximal direction, including the entire trabecular area within that range, identified manually by visual inspection. Quantitative parameters included percent bone volume (BV/TV), trabecular number, trabecular thickness and trabecular separation as described (54, 55).

Representative cross sections represent the 200th section (1 mm) from the distal femoral growth plate. 3D images show an axial cylinder of a diameter of 500 μm between sections 150–450 from the distal growth plate.

Histological Procedures and Immunostaining

Femurs isolated from mice at 9 weeks of age were fixed in 4% paraformaldehyde (Sigma-Aldrich) followed by decalcification in Osteomoll (Merck) for 3 weeks. The samples were then dehydrated, and embedded in paraffin (Leica) using a Leica EG1150H embedding station. Eight micrometers of thick sections were obtained using a Thermo Scientific HM340E microtome and were processed for hematoxylin and eosin (Leica) staining, or for immunostaining for the calcitonin receptor using anti-Calcitonin Receptor (Abcam AB11042) and anti-rabbit Alexa Fluor 488 (Life Technologies, A11034) antibodies. Microscopic images were taken by a Nikon ECLIPSE Ni-U microscope connected to a Nikon DS-Ri2 camera.

In vitro Culture and Resorption Assays

In vitro osteoclast cultures were performed essentially as described before (54, 55). Bone marrow cells obtained by flushing the tibia and femur of wild type or mutant mice were cultured in the presence of 10 ng/ml murine M-CSF (Peprotech) for 2 days in α-MEM medium (Sigma) supplemented with 10% FCS (Gibco) and antibiotics. Non-adherent cells were then plated at the concentration of 1.5×10^5 cells/cm^2 and cultured in the presence of 50 ng/ml recombinant murine M-CSF and 50 ng/ml murine RANKL (Peprotech) with medium changes every 2 days. In parallel macrophage cultures, the cells were cultured under identical conditions except that RANKL was omitted.

Cultures were terminated and osteoclast-specific staining was performed using a commercial tartrate-resistant acid phosphatase (TRAP) staining kit (Sigma-Aldrich) at the indicated times after the first addition of RANKL. Photomicrographs were taken using a Leica DMI6000B inverted microscope. The images were then analyzed either manually or by the ImageJ software. Osteoclasts were defined as TRAP-positive cells with 3 or more nuclei.

For *in vitro* resorption assays, osteoclasts were cultured under similar conditions for 7 days on an artificial hydroxyapatite surface (Sigma-Aldrich) followed by washing, imaging by dark field microscopy and further analysis by ImageJ software.

Biochemical Studies

For protein content analysis, osteoclast, or macrophage cultures were washed and then lysed in a Triton-based lysis buffer containing 100 mM NaCl, 30 mM Na-HEPES (pH 7.4), 20 mM NaF, 1 mM Na-EGTA, 1% Triton X-100, 1 mM benzamidine, freshly supplemented with 0.1 U/ml Aprotinin, 1:100 Mammalian Protease Inhibitor Cocktail, 1:100 Phosphatase Inhibitor Cocktail 2, 1 mM PMSF, and 1 mM Na_3VO_4 (all from Sigma-Aldrich). Insoluble material was removed, the lysate supernatants were supplemented with 4× Laemmli's sample buffer and boiled for 10 min. Whole cell lysates were run on SDS-PAGE, electroblotted to nitrocellulose membranes, and then processed for immunoblotting with antibodies against Syk (N19; Santa Cruz) or β-actin (Clone AC-74; Sigma-Aldrich). After incubation with peroxidase-labeled secondary antibodies (GE Healthcare), the signal was developed using the ECL system (GE Healthcare) and exposed to X-ray film. X-ray films were then scanned and processed with Adobe Photoshop.

Quantitative RT-PCR Analysis

To test osteoclast specific and Cre gene expression changes, mouse myeloid progenitors were differentiated into osteoclasts or macrophages in the presence of 50 ng/ml M-CSF with or without 50 ng/ml RANKL for 0–3 days, followed by RNA extraction and reverse transcription as previously described (54–56). For quantitative reverse transcription (RT)-PCR analysis of the osteoclast-specific genes, the following TaqMan assays were used: *Acp5* (TRAP; Taqman Mm00475698_m1), *Ctsk* (cathepsin K; Mm00484039_m1), *Calcr* (Calcitonin receptor; Mm00432271_m1), *Nfatc1* (NFATc1; Mm00479445_m1), and *Tm7sf4* (DC-STAMP; Mm04209235_m1) as previously described (54, 55). For assessment of Cre expression, the 5′- TGACGGTGGGAGAATGTTAATC forward and 5′ GCTACACCAGAGACGGAAATC reverse primers were used. Transcript levels relative to GAPDH were calculated using the comparative Ct method (54, 55).

Sequencing of the Germline *Syk*^{flox} Allele

To determine the exact sequence of the *Syk*^{flox} allele, tail DNA was amplified using the 5′- GCC CGT TCT GTG CCT ACT

GG−3′ forward and 5′- TAG CTA ACC AAA CCC ACG GC−3′ reverse primers spanning the 5′ loxP site, or the 5′- CCA AAG CGG AGT CCT CAC AT−3′ forward and 5′- GTC GGT CCC ATC TTT CC−3′ reverse primers spanning the 3′ loxP site. PCR products were then sent to Microsynth for sequencing and the obtained sequences were aligned with the genomic sequence of the wild type *Syk* gene to obtain the sequence of the Syk^{flox} allele.

Genomic PCR Analysis

Osteoclast cultures were washed at the indicated times after the start of RANKL treatment, followed by isolation of genomic DNA and PCR using standard procedures.

Two different PCR assays were performed on the genomic DNA of osteoclast cultures. In PCR 1, the 5′- GCC CGT TCT GTG CCT ACT GG−3′ forward primer (P fwd) was used along with the 5′- TAG CTA ACC AAA CCC ACG GC−3′ reverse primer (P rev1) to separate the Syk^{+} and Syk^{flox} alleles (234 and 349 bp product length, respectively). In PCR 2, the same P fwd forward primer was used with the 5′- GTC GGT CCC ATC TTT CC−3′ reverse primer (P rev2) to separate the Syk^{+}, Syk^{flox} and Syk^{Δ} alleles (1314, 1560 and 452 bp product length, respectively).

Statistical Analysis

Experiments were performed the indicated number of times. Diagrams show mean and SEM from the indicated number of independent experiments. Micro-CT measurements were analyzed by two-way (factorial) ANOVA with the presence/absence of Cre and the *Syk* genotype as the independent parameters. Other measurements were analyzed by one-way ANOVA followed by Tukey or Unequal n HSD *post hoc* test. In case of the kinetic analysis of osteoclast morphology, statistical analysis was performed on the area under the curve (AUC). *P*-values below 0.05 were considered statistically significant.

RESULTS

The Effect of Osteoclast-Specific Syk Deletion on Trabecular Bone Architecture

The $Syk^{-/-}$ mutation causes perinatal lethality making it technically impossible to analyze the bone morphology of adult $Syk^{-/-}$ mice. We decided to overcome that problem by generating lineage-specific Syk-deficient animals. As a first approach, we crossed mice in which the cDNA of the Cre recombinase has been inserted into the osteoclast-specific Ctsk gene (referred to as $Ctsk^{Cre/+}$ or Ctsk-Cre mice) (50) with mice carrying a floxed *Syk* allele (referred to as $Syk^{flox/flox}$ mice) (49). The resulting $Ctsk^{Cre/+}Syk^{flox/flox}$ (referred to as $Syk^{\Delta OC}$) mice are expected to have defective Syk expression in osteoclasts due to Cre-mediated excision and inactivation of the Syk gene.

We then subjected $Syk^{\Delta OC}$ mice and the appropriate controls to micro-CT analysis of the distal femur. As shown in the longitudinal sections of the femurs of female mice in **Figure 1A**, the $Syk^{\Delta OC}$ mutation strongly increased the density of the trabecular area compared to wild type mice, whereas no dramatic difference could be observed in Ctsk-Cre or $Syk^{flox/flox}$ animals. Analysis of representative cross-sections of male or female mouse femurs also showed increased trabecular density in $Syk^{\Delta OC}$ but not in Ctsk-Cre or $Syk^{flox/flox}$ animals, particularly in the case of female mice (**Figure 1B**). The increased trabecular density was also evident in three-dimensional reconstitution of an axial cylinder within the trabecular area of the femurs (**Figure 1C**).

We also processed micro-CT images for quantitative analysis, incorporating data from the entire trabecular space within a defined distance range from the distal femoral growth plate. As shown in **Figure 2**, the percent bone volume (BV/TV) was strongly increased in $Syk^{\Delta OC}$ mice, whereas no substantial difference could be observed in Ctsk-Cre or $Syk^{flox/flox}$ mice. Male wild type mice had an ∼2.8-fold higher (10.8%) basal percent bone volume (BV/TV) than their female counterparts (3.9%). However, the increase in BV/TV in $Syk^{\Delta OC}$ over wild type mice was more robust in female (4.4-fold) than in male (1.8-fold) animals (**Figure 2**). We have also performed statistical analysis by two-way (factorial) ANOVA which determines the interaction of the two (Ctsk-Cre and $Syk^{flox/flox}$) mutations, i.e., whether the co-existence of the two mutation in the $Syk^{\Delta OC}$ resulted in a statistically significant difference beyond an additive effect. That analysis revealed a significant increase of the BV/TV values both in male ($p = 0.028$) and, especially, in female ($p = 0.00005$) mice.

Further quantitative (**Figure 2**) and statistical (two-way ANOVA) analysis of the trabecular bone revealed a higher trabecular number in $Syk^{\Delta OC}$ mice ($p = 0.0069$ and 0.00001 for males and females, respectively), whereas no consistent change was observed in the trabecular thickness of the same animals ($p =$ 0.85 and 0.87 for males and females, respectively). In agreement with the increased trabecular number, trabecular separation was reduced in $Syk^{\Delta OC}$ mice ($p = 0.00032$ and 0.0011 for males and females, respectively).

Taken together, our results indicate that osteoclast-specific deletion of Syk causes increased bone trabecular mass primarily due to increased bone trabecular number rather than a higher trabecular thickness. However, the phenotype observed in $Syk^{\Delta OC}$ mice (**Figure 2**) appeared to be less dramatic than that reported for $Tyrobp^{-/-}Fcer1g^{-/-}$ double knockout mice lacking both the DAP12 and FcRγ ITAM-containing adapter molecules which were previously proposed to signal through Syk (42, 43, 57).

The Effect of Hematopoietic Deletion of Syk on Trabecular Bone Architecture

The apparently less severe bone phenotype of $Syk^{\Delta OC}$ mice compared to $Tyrobp^{-/-}Fcer1g^{-/-}$ (DAP12/FcRγ double knockout) animals (42, 43, 57) could either be due to a less critical role for Syk in *in vivo* bone homeostasis or the less complete deletion of Syk in $Syk^{\Delta OC}$ animals. To test this latter possibility, we turned to mice with Syk deficiency in the entire hematopoietic compartment due to deletion by the Vav-Cre transgene which causes Cre expression during the early stages of hematopoiesis (51). Accordingly, we subjected Vav-Cre $Syk^{flox/flox}$ (referred to as $Syk^{\Delta Haemo}$) mice and appropriate controls to microCT analysis of the distal femur.

As shown in **Figure 3A**, Syk deletion in the entire hematopoietic compartment by the $Syk^{\Delta Haemo}$ mutation caused a very strong increase in trabecular density in the

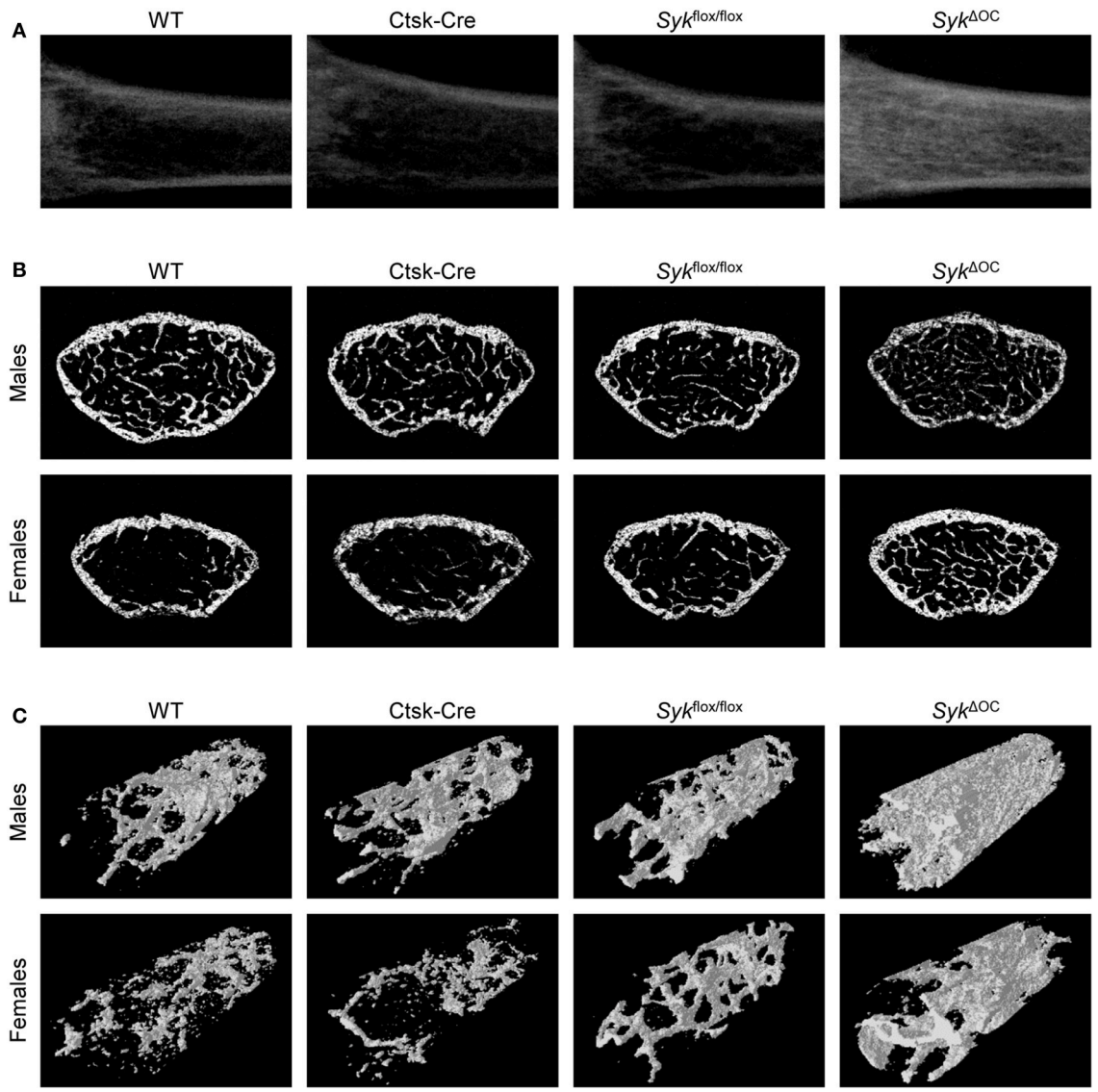

FIGURE 1 | Micro-CT analysis of osteoclast-specific Syk-deficient mice. Representative micro-CT images of the femurs of 9-week-old mice of wild type (WT) and the indicated mutant mice. **(A)** Longitudinal sections of the femur of female mice. **(B)** Cross-sections of the femur of male or female mice. **(C)** 3D reconstitution of an axial cylinder of the trabecular area of the distal metaphysis of femurs of male or female mice. Images are representative of micro-CT analysis of 5 mice per gender and genotype.

longitudinal sections of the femurs of female animals, whereas no substantial changes were observed in Vav-Cre or $Syk^{flox/flox}$ mice. An increased trabecular density in $Syk^{\Delta Haemo}$ mutants could also be observed in cross-sections of the distal femurs of male and, in particular, female mice, whereas no obvious differences could be seen in Vav-Cre or $Syk^{flox/flox}$ animals (**Figure 3B**). Three-dimensional reconstitution of a trabecular area cylinder also showed visible increases in the trabecular density in $Syk^{\Delta Haemo}$ animals (**Figure 3C**).

Further quantitative analysis of the microCT data (**Figure 4**) indicated a strongly increased percent bone volume (BV/TV) in $Syk^{\Delta Haemo}$ mice in both male and female animals. Importantly, BV/TV values in $Syk^{\Delta Haemo}$ mice appeared to be substantially higher than corresponding $Syk^{\Delta OC}$ animals (compare **Figures 2**, **4**). On the other hand, similar to the $Syk^{\Delta OC}$ results, the BV/TV fold increase in $Syk^{\Delta Haemo}$ over wild type animals was higher in females (7.9-fold) than in males (4.0-fold), again primarily due to the higher basal values in male wild type mice. Statistical analysis by two-way ANOVA revealed a highly significant interaction between the effects of the Vav-Cre and $Syk^{flox/flox}$ mutations ($p = 0.00032$ and 0.00003 for males and females, respectively), indicating that Cre-mediated deletion of Syk in $Syk^{\Delta Haemo}$ mice strongly increases trabecular bone mass.

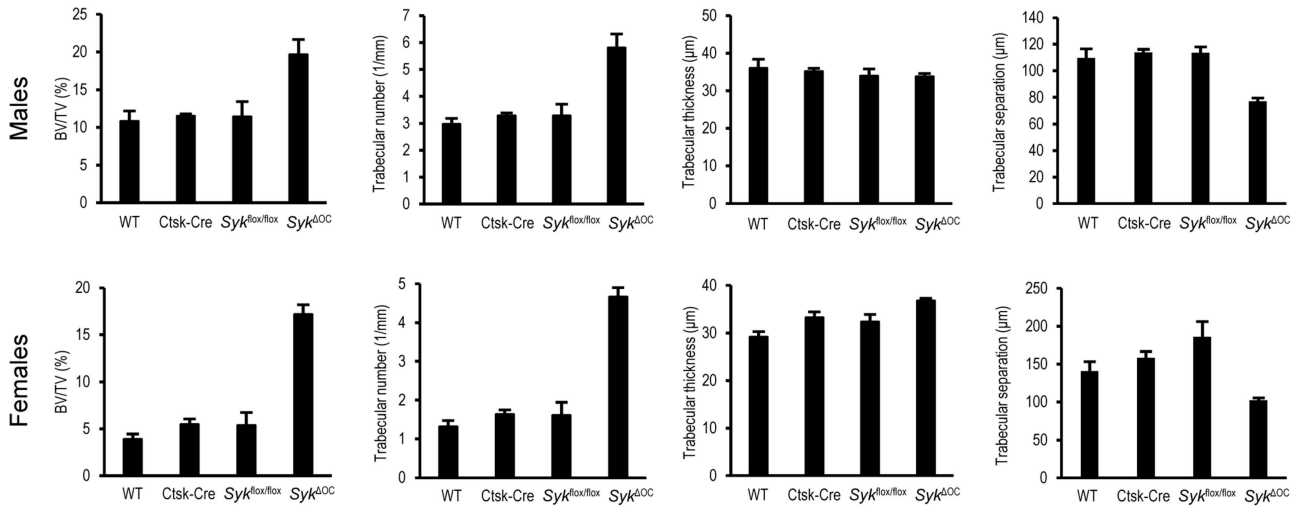

FIGURE 2 | Quantitative micro-CT analysis of osteoclast-specific Syk deficiency. The right femurs of 9-week-old wild type (WT) or the indicated mutant male or female mice were subjected to micro-CT analysis, followed by quantification of percent bone volume (bone volume/total volume, BV/TV), trabecular number, trabecular thickness and trabecular separation. The graphs show mean and SEM of data obtained from 5 mice per gender and genotype.

Further quantitative assessment (**Figure 4**) and statistical analysis (two-way ANOVA) revealed that, similar to the $Syk^{\Delta OC}$ mice, the increased trabecular bone volume was primarily due to an increased trabecular number ($p = 0.0010$ and 0.00001 for males and females, respectively), rather than significant changes in trabecular thickness ($p = 0.31$ and 0.61 for males and females, respectively). Trabecular separation was also reduced in $Syk^{\Delta Haemo}$ mice ($p = 0.0045$ and 0.0071 for males and females, respectively).

Taken together, early deletion of Syk in the entire hematopoietic system results in dramatic increase in the mineralized trabecular bone mass, indicating a critical role for Syk in *in vivo* bone homeostasis. The bone phenotype seen in $Syk^{\Delta Haemo}$ mice is grossly comparable to that reported for $Tyrobp^{-/-}Fcer1g^{-/-}$ (DAP12/FcRγ double knockout) animals (42, 43, 57), raising the possibility that the majority of DAP12/FcRγ signals proceeds through Syk in live mice. However, the 30–45% BV/TV values observed in $Syk^{\Delta Haemo}$ mice are substantially higher than the corresponding values (15–20%) in $Syk^{\Delta OC}$ animals, raising the possibility that the lower values in the latter mutants may be due to incomplete deletion of Syk by Cre expression from the Ctsk-Cre mutation.

Bone Histological Analysis

We have also performed histological analysis of the distal femur of wild type, $Syk^{\Delta OC}$ or $Syk^{\Delta Haemo}$ mice. As shown in **Figure 5A**, a much more dense trabecular network was seen in $Syk^{\Delta OC}$ and, especially, $Syk^{\Delta Haemo}$ mice than in wild type animals. Again, the difference was more pronounced in female mice because of the lower trabecular density in female than in male mice in the wild type cohorts.

To test the presence of mature osteoclasts on the trabecular bone surface, we have performed immunofluorescence staining of bone sections for calcitonin receptor, an osteoclast-specific differentiation marker. As shown in **Figure 5B**, calcitonin receptor signals were evident on the lining of trabecular rods (dark areas) in wild type sections. Similar signals were also seen but at substantially lower numbers in $Syk^{\Delta OC}$ sections, whereas no such signals were seen in $Syk^{\Delta Haemo}$ sections (**Figure 5B**). Those results suggest that the number of calcitonin receptor-positive osteoclasts is reduced in $Syk^{\Delta OC}$ and, especially, in $Syk^{\Delta Haemo}$ mice.

In vitro Osteoclast Development in Lineage-Specific Syk Mutants

We next tested *in vitro* development of osteoclasts from wild type, $Syk^{\Delta OC}$ or $Syk^{\Delta Haemo}$ bone marrow cells in the presence of recombinant M-CSF and RANKL cytokines. Bone marrow cells were first cultured for 2 days in low (10 ng/ml) M-CSF and non-adherent cells (referred to as myeloid progenitors) were then cultured in the presence of 50 ng/ml M-CSF and 50 ng/ml RANKL. Osteoclast development was then tested by assessing cell morphology and positive histochemical staining for the osteoclast-specific TRAP enzyme.

As shown in **Figure 6A**, no TRAP-positive multinuclear cells (osteoclasts) were seen 2 days after addition of RANKL to the cultures. However, osteoclasts started to appear in wild type cultures on day 3 and formed very large multinucleated TRAP-positive cells 3.5 days after the initial RANKL treatment. Some osteoclasts also formed in $Syk^{\Delta OC}$ cultures, though they were much smaller in size and failed to fuse into very large cells even by 3.5 days after RANKL treatment (**Figure 6A**). On the other hand, practically no osteoclasts (multinucleated TRAP-positive cells) could be observed in $Syk^{\Delta Haemo}$ cultures (**Figure 6A**).

We have also quantitated the extent of *in vitro* osteoclast formation. To this end, we have counted the number of osteoclasts (defined as TRAP-positive cells with 3 or more

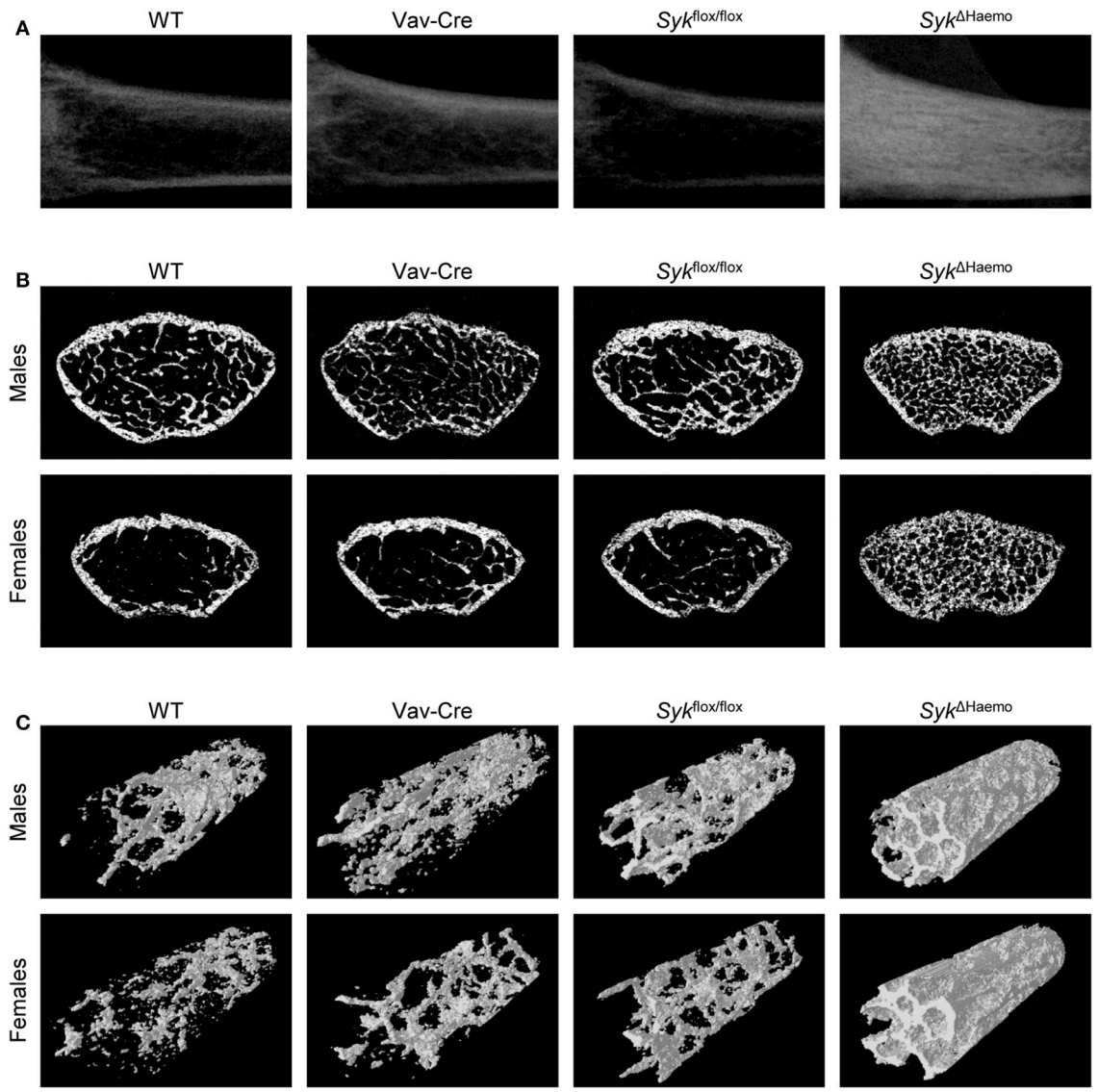

FIGURE 3 | Micro-CT analysis of hematopoietic Syk-deficient mice. Representative micro-CT images of the femurs of 9-week-old mice of wild type (WT) and the indicated mutant mice. **(A)** Longitudinal sections of the femur of female mice. **(B)** Cross-sections of the femur of male or female mice. **(C)** 3D reconstitution of an axial cylinder of the trabecular area of the distal metaphysis of femurs of male or female mice. Images are representative of 5–7 mice per gender and genotype. WT samples are identical to those shown in **Figure 1**.

nuclei; **Figure 6B**) and calculated the percent of the culture area covered by the osteoclasts (**Figure 6C**). Though the two different quantification approaches were related to each other, they also complemented each other, since later stages of osteoclast development may lead to the emergence of very large osteoclasts which occupy large culture areas but are small in numbers (as seen in the last two images in wild type cultures in **Figure 6A**).

As seen in **Figures 6B,C**, there were practically no osteoclasts in any of the cultures 2 days after the initial RANKL addition. However, osteoclasts rapidly emerged afterwards in wild type cultures, reaching a maximum number 1 day later. The area covered by wild type osteoclasts increased further in the next 12 h, even though the number of osteoclasts started to decline, indicating the fusion of the cells into a few very large osteoclasts in this final stage of osteoclast development (**Figures 6B,C**). The number of osteoclasts also increased in $Syk^{\Delta OC}$ cultures and was temporarily even comparable to that of wild type osteoclasts (**Figure 6B**). However, those $Syk^{\Delta OC}$ osteoclasts covered a significantly smaller area than in wild type cultures throughout the experiments (**Figure 6C**), which was in line with the smaller size of $Syk^{\Delta OC}$ osteoclasts in **Figure 6A**. On the other hand, again in agreement with the photomicrographs in **Figure 6A**, practically no osteoclasts could be identified in $Syk^{\Delta Haemo}$ cultures (**Figures 6B,C**).

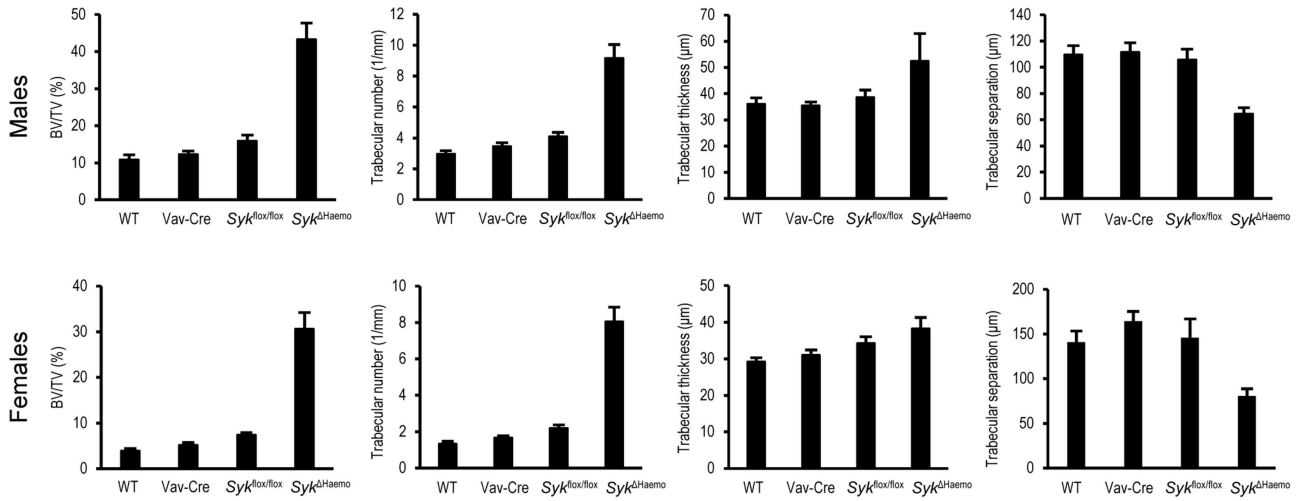

FIGURE 4 | Quantitative micro-CT analysis of hematopoietic Syk deficiency. The right femurs of 9-week-old wild type (WT) or the indicated mutant male or female mice were subjected to micro-CT analysis, followed by quantification of percent bone volume (bone volume/total volume, BV/TV), trabecular number, trabecular thickness and trabecular separation. The graphs show mean and SEM of data obtained from 5–7 mice per gender and genotype. WT values are identical to those shown in **Figure 2**.

We have also performed more detailed statistical analyses (one-way ANOVA) of the area under the curve (AUC) from data presented in **Figures 6B,C**. In case of the number of osteoclasts (**Figure 6B**), no statistical difference was seen between the wild type and $Syk^{\Delta OC}$ cultures ($p = 0.12$), likely reflecting the fact that the osteoclast numbers only declined on the last day in the $Syk^{\Delta OC}$ samples (**Figure 6B**). However, the number of osteoclasts in the $Syk^{\Delta Haemo}$ cultures was statistically highly significantly reduced compared to wild type ones ($p = 0.0013$). The total area covered by osteoclasts was highly significantly reduced both by the $Syk^{\Delta OC}$ ($p = 0.00058$) and the $Syk^{\Delta Haemo}$ ($p = 0.00024$) mutations.

The above results confirm prior studies indicating a critical role for Syk during *in vitro* osteoclast development (40, 42, 44). On the other hand, they also indicate an incomplete osteoclast developmental defect in $Syk^{\Delta OC}$ cultures (as opposed to the complete defect in $Syk^{\Delta Haemo}$ ones), suggesting incomplete deletion of Syk in $Syk^{\Delta OC}$ mutants.

Analysis of the *in vitro* Resorptive Activity of Osteoclasts

We also attempted to test the *in vitro* resorbing capacity of osteoclasts. To this end, myeloid precursors were plated on an artificial hydroxyapatite layer and cultured in the presence of M-CSF and RANKL (50 ng/ml each) for 7 days, followed by assessment of hydroxyapatite resorption by dark field microscopy. It should be noted that this assay measures the combined effect of both osteoclast development and osteoclast-mediated matrix resorption.

As shown in **Figure 7A**, wild type osteoclast cultures were able to resorb substantial areas of the hydroxyapatite layer (resorbed areas show a dark appearance). In contrast, only small areas of resorption could be observed in $Syk^{\Delta OC}$ cultures and no resorption was seen in $Syk^{\Delta Haemo}$ cultures (**Figure 7A**). Quantification of the resorbed area revealed ∼40% resorption in wild type cultures, which was strongly reduced by the $Syk^{\Delta OC}$ and completely eliminated by the $Syk^{\Delta Haemo}$ mutations (**Figure 7B**). Statistical analysis (one-way ANOVA) revealed highly significant reduction of the resorption activity both by the $Syk^{\Delta OC}$ ($p = 0.00040$) and the $Syk^{\Delta Haemo}$ ($p = 0.00038$) mutations.

These results confirm an important role for Syk in the development and/or function of bone-resorbing osteoclasts (42), and also indicate slight differences between the $Syk^{\Delta OC}$ and $Syk^{\Delta Haemo}$ mutations.

Analysis of Osteoclast-Specific Gene Expression

We next tested the changes of osteoclast-specific gene expression in osteoclast cultures from the different genotypes. We have also tested additional control macrophage cultures generated under identical conditions except that RANKL treatment was omitted. As shown in **Figure 8**, the expression of DC-STAMP (encoded by the *Tm7sf4* gene), TRAP (*Acp5*), calcitonin receptor (*Calcr*), NFATc1 (*Nfatc1*) and cathepsin K (*Ctsk*) mRNA strongly increased upon osteoclastic differentiation whereas no such increase could be observed in parallel macrophage cultures. The expression of all those genes were reduced in both the $Syk^{\Delta OC}$ and $Syk^{\Delta Haemo}$ cultures (**Figure 8**), though the defect ranged from a moderate (*Tm7sf4*) to a very strong (*Calcr*) reduction. It should also be noted that the reduced expression of *Ctsk* in $Syk^{\Delta OC}$ samples is likely partially due to the inactivation of one of the two alleles of the *Ctsk* gene by the Ctsk-Cre ($Ctsk^{Cre/+}$) mutation present in those cells. Taken together, gene expression data indicate a role for Syk in regulation of osteoclast-specific gene expression.

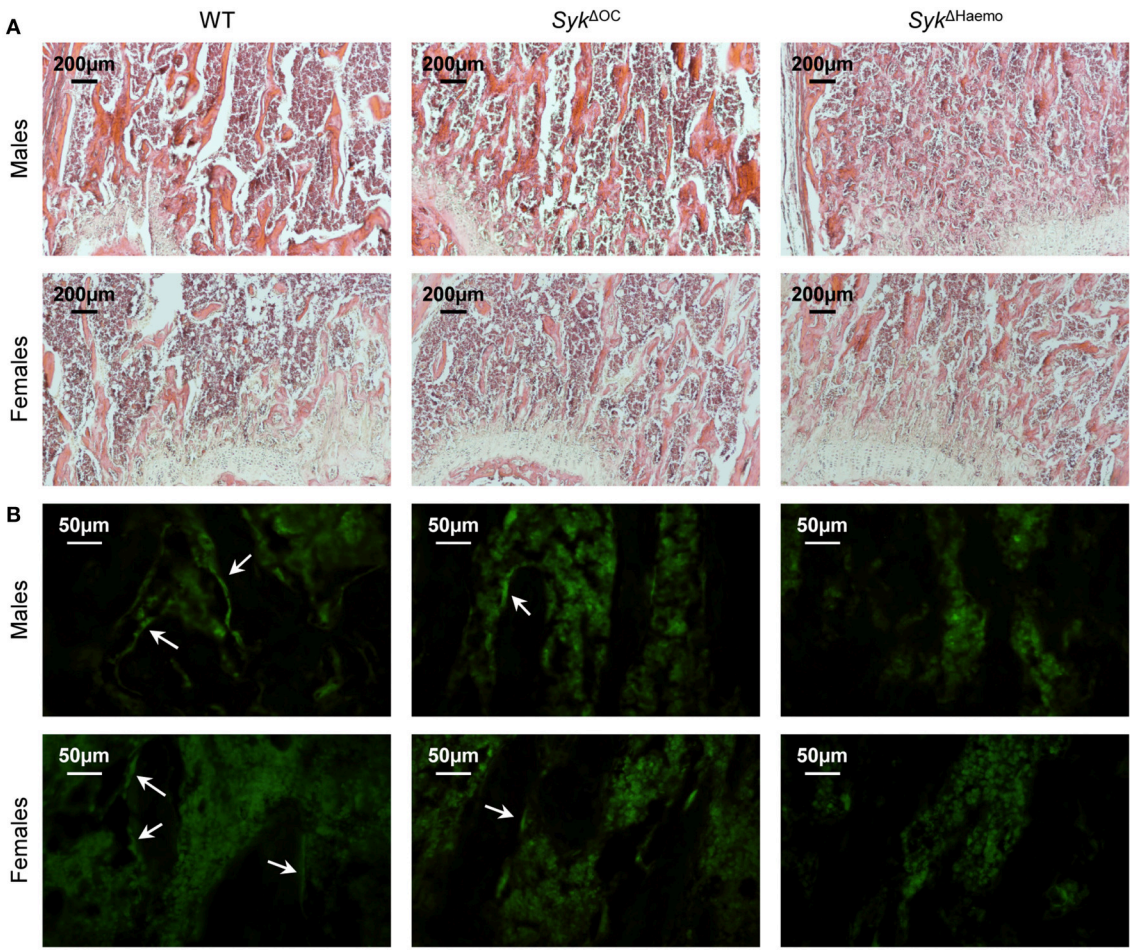

FIGURE 5 | Histological and immunofluorescence analysis of osteoclast-specific and hematopoietic Syk deficiency. Representative photomicrographs of the trabecular area of the femurs of 9-week-old wild type (WT), $Syk^{\Delta OC}$ or $Syk^{\Delta Haemo}$ mice. **(A)** Haematoxylin and eosin staining; original magnification ×10. **(B)** Calcitonin receptor immunostaining; original magnification × 40. Arrows indicate calcitonin receptor-positive bone lining cells (likely osteoclasts). Images are representative of 3 mice per gender and genotype.

Analysis of Syk Protein Levels in Osteoclast Cultures

The different severity of the *in vivo* bone phenotypes (**Figures 1–5**) and *in vitro* osteoclast developmental defect (**Figure 6**) between the $Syk^{\Delta OC}$ and $Syk^{\Delta Haemo}$ mutants raised the possibility that Syk is incompletely deleted from $Syk^{\Delta OC}$ osteoclasts. To test this more specifically, we performed Western Blot analysis of Syk expression during osteoclastic and macrophage differentiation of wild type and mutant bone marrow cells.

As shown in **Figure 9A**, Syk was present in all wild type cultures and its expression slightly even increased during osteoclast differentiation from wild type myeloid progenitors. Importantly, Syk was also present throughout the assessment period in $Syk^{\Delta OC}$ cultures (**Figure 9A**). On the other hand, Syk was completely absent throughout the entire observation period in $Syk^{\Delta Haemo}$ cultures (**Figure 9A**). Semiquantitative analysis of the Western blot samples (**Figure 9B**) confirmed the presence of Syk in all wild type and $Syk^{\Delta OC}$ but not in $Syk^{\Delta Haemo}$ samples. Although there was a tendency of reduced Syk expression in $Syk^{\Delta OC}$ osteoclasts as compared to wild type osteoclasts, this difference was not statistically significant, indicating that the $Syk^{\Delta OC}$ mutation is not able to reduce Syk expression at the overall cell population level.

The above results provided direct evidence supporting our assumption that Syk is incompletely deleted from $Syk^{\Delta OC}$ but it is completely absent from $Syk^{\Delta Haemo}$ osteoclast cultures.

Genetic Analysis of Syk Deletion During Osteoclastogenesis

One of the possible explanations for the observed differences between the $Syk^{\Delta OC}$ and $Syk^{\Delta Haemo}$ mutants is that Cre expression from the Ctsk-Cre mutation occurs at a late stage of osteoclast development which, combined with the potentially long survival of the Syk protein, leads to reduction of Syk protein levels only at a late stage when osteoclast development has already

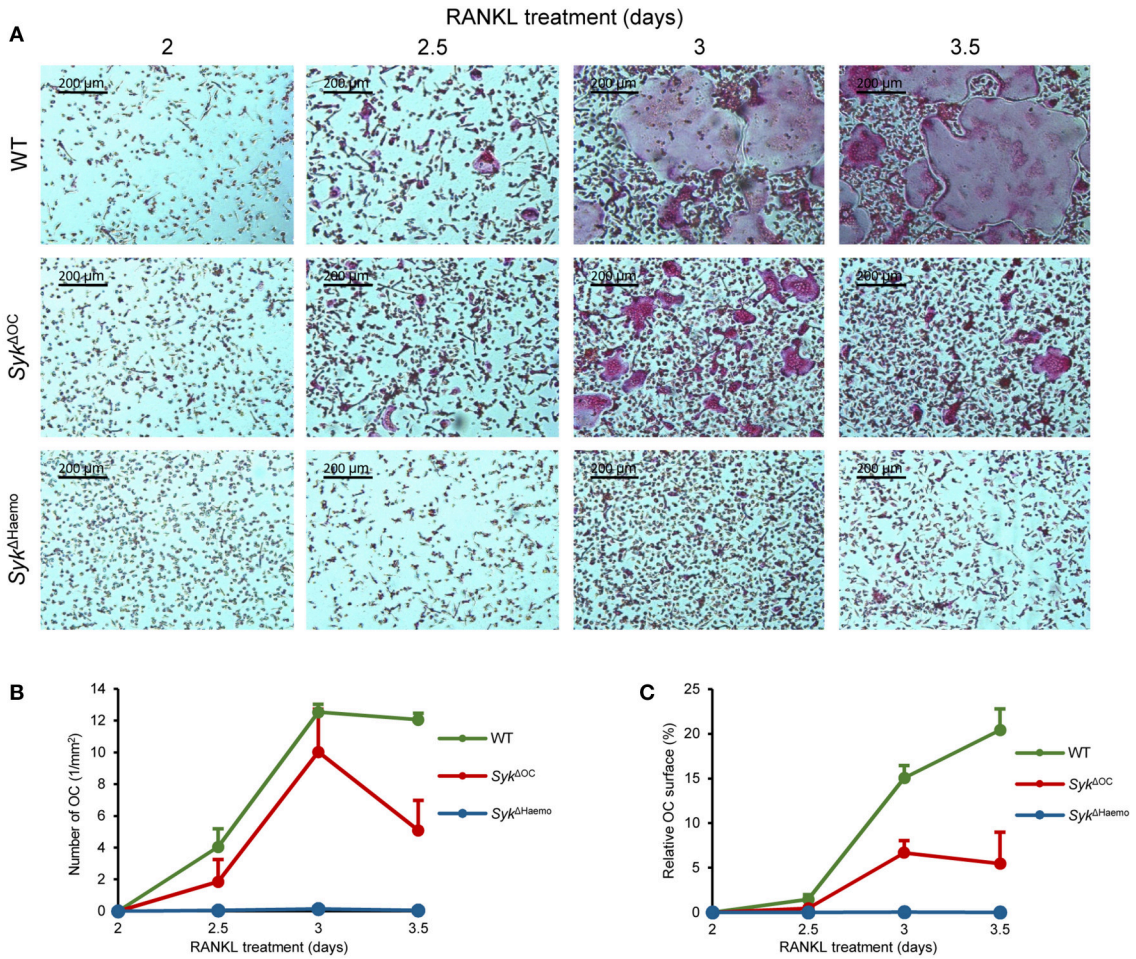

FIGURE 6 | Analysis of *in vitro* osteoclast development. Bone marrow-derived myeloid progenitors from wild type (WT), *Syk*$^{\Delta OC}$ or *Syk*$^{\Delta Haemo}$ mice were cultured in the presence of 50 ng/ml M-CSF and 50 ng/ml RANKL for the indicated times, followed by staining for tartrate-resistant acid phosphatase (TRAP). **(A)** Representative images of TRAP-stained cultures. **(B)** Quantification of the number of osteoclasts (TRAP-positive cells with 3 or more nuclei) in the different cultures. **(C)** The area covered by osteoclasts in the different cultures (in % of the total culture area). Images are representative of, and bar graphs show mean and SEM from, 3 independent experiments.

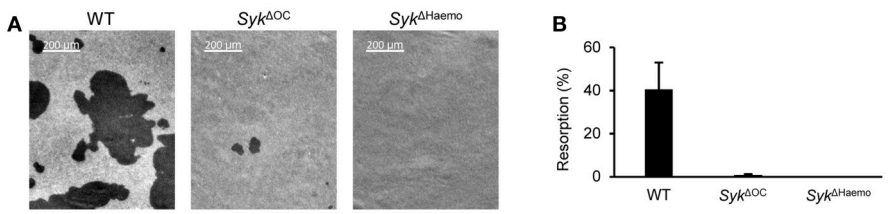

FIGURE 7 | Analysis of the *in vitro* resorptive function of osteoclasts. Bone marrow-derived myeloid progenitors from wild type (WT), *Syk*$^{\Delta OC}$ or *Syk*$^{\Delta Haemo}$ mice were cultured in the presence of 50 ng/ml M-CSF and 50 ng/ml RANKL for 7 days on an artificial hydroxyapatite layer. **(A)** Representative dark-field microscopic images of resorption pits (dark areas). **(B)** Quantification of the resorption area (in percent of the total area). Images are representative of, and bar graphs show mean and SEM from, 3 independent experiments.

occurred. The fact that the substantial expression of the *Ctsk* gene (encoding for cathepsin K) begins at 2 days, and is maximal at 3 days after RANKL treatment (**Figure 8**) (54, 55) would be in line with that possibility.

As a first approach to address the above issue, we performed qPCR-based analysis of the expression the Cre recombinase in osteoclasts and macrophages from the different genotypes (**Figure 10A**). As expected, no Cre expression could be observed

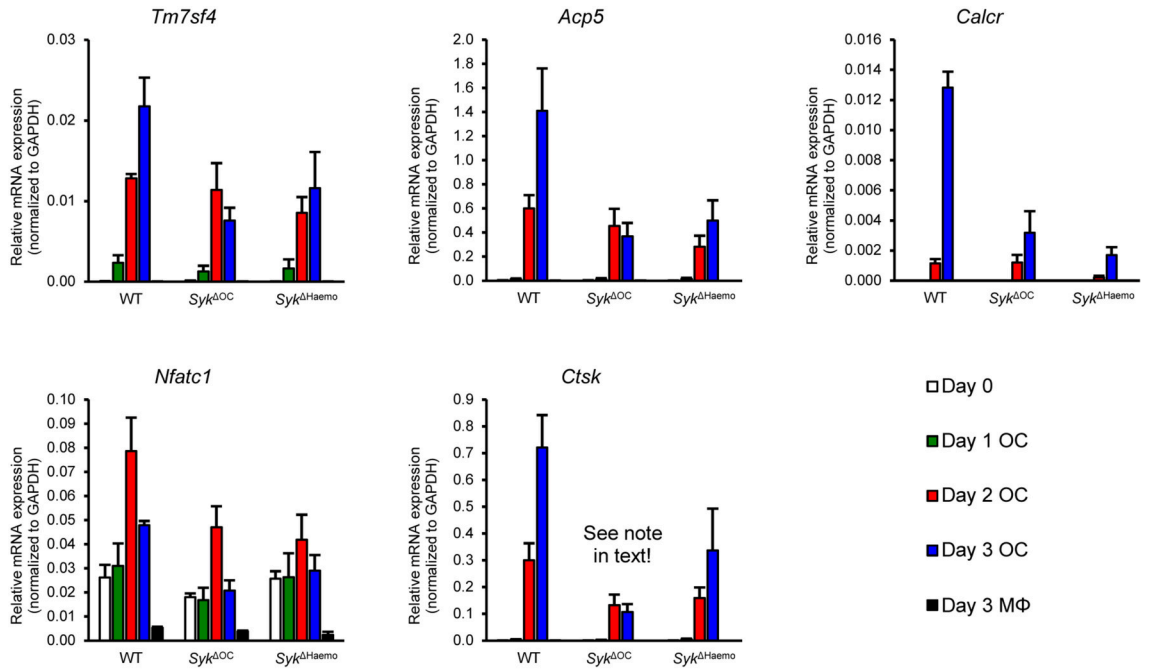

FIGURE 8 | Analysis of osteoclast-specific gene expression. Gene expression in bone marrow-derived cells from wild type (WT), $Syk^{\Delta OC}$ or $Syk^{\Delta Haemo}$ mice cultured for 0–3 days in the presence of 50 ng/ml M-CSF with (osteoclasts; OC) or without (macrophages; MΦ) 50 ng/ml RANKL. The expression of the *Tm7sf4, Acp5, Calcr, Nfatc1,* and *Ctsk* genes (encoding for DC-STAMP, TRAP, Calcitonin receptor, NFATc1, and Cathepsin K, respectively) were determined by quantitative RT-PCR and normalized to *Gapdh*. Bar graphs show mean and SEM from 3 independent experiments.

in wild type cultures. Somewhat surprisingly, no Cre mRNA could be detected in $Syk^{\Delta Haemo}$ cultures either which, together with the complete absence of Syk protein in those cultures (**Figure 9**) suggests that the Vav-Cre transgene is activated at an early stage of hematopoiesis but it is silenced at the stage of myeloid differentiation tested in our experiments. On the other hand, Cre expression could be readily observed in $Syk^{\Delta OC}$ osteoclast but not macrophage cultures (**Figure 10A**). Importantly, substantial Cre expression in $Syk^{\Delta OC}$ osteoclasts was first observed 2 days after the initial RANKL treatment, and continued afterwards. Given that a longer time may be needed to the effective deletion of both *Syk* alleles, the supposedly partial deletion efficacy of the Ctsk-Cre transgene and that the Syk mRNA and protein likely does not immediately disappear after the Cre-mediated inactivation of the *Syk* gene, these results are in line with the continued presence of Syk in $Syk^{\Delta OC}$ osteoclasts beyond 2 days after the initial RANKL administration (**Figure 9**).

As a more direct approach to test Cre-mediated deletion of Syk in our osteoclast cultures, we decided to perform PCR-based analysis of the Syk genomic locus from the cells of our various genotypes. To this end, we first amplified and sequenced the genomic DNA around the two loxP insertion sites, which was used along with the publicly available mouse genomic sequence and the original description of the Syk^{flox} mutation (50) to reconstruct the entire sequence of the Syk^{flox} allele (**Supplementary Figure 1**). The organization of the Syk^{+} (wild type), Syk^{flox} and Syk^{Δ} (result of Cre-mediated deletion) alleles is shown in **Supplementary Figure 2**, indicating the inserted loxP and other sequences, as well as the sites and results of Cre-mediated recombination. Based on this organization, we have designed two PCR protocols (termed PCR 1 and PCR 2) to amplify specific alleles from genomic DNA (**Supplementary Figure 2**). PCR 1 (**Figure 10B** and **Supplementary Figure 2**) was our standard genotyping PCR protocol using the P fwd and P rev1 primer pair, and was able to distinguish between the Syk^{+} and the Syk^{flox} allele, based on the increased length of the PCR product caused by the 115 bp insertion during the generation of the Syk^{flox} allele (49). However, PCR 1 was not able to detect the deleted (Syk^{Δ}) allele because the sequence corresponding to the P rev1 primer was deleted during Cre-mediated excision of the floxed sequences from the Syk^{flox} allele (**Supplementary Figure 2**). Therefore, we designed a novel PCR protocol (PCR 2; **Figure 10C** and **Supplementary Figure 2**) using the same P fwd forward primer along with a new P rev2 reverse primer, spanning the entire floxed sequence, allowing the simultaneous detection of all three (Syk^{+}, Syk^{flox}, and Syk^{Δ}) alleles. We then cultured wild type, $Syk^{\Delta OC}$ and $Syk^{\Delta Haemo}$ bone marrow cells in the presence of M-CSF and RANKL for different periods of time and analyzed their genomic DNA with both the PCR 1 (**Figure 10B**) and PCR 2 (**Figure 10C**) protocols.

Results with PCR 1 are shown in **Figure 10B**. In line with our expectations, the Syk^{+} allele was present throughout the assay period in wild type osteoclast cultures and the Syk^{flox} allele was present in all $Syk^{\Delta OC}$ samples. Though the latter finding indicated the presence of the non-recombined Syk^{flox} allele throughout osteoclast development, it did not exclude

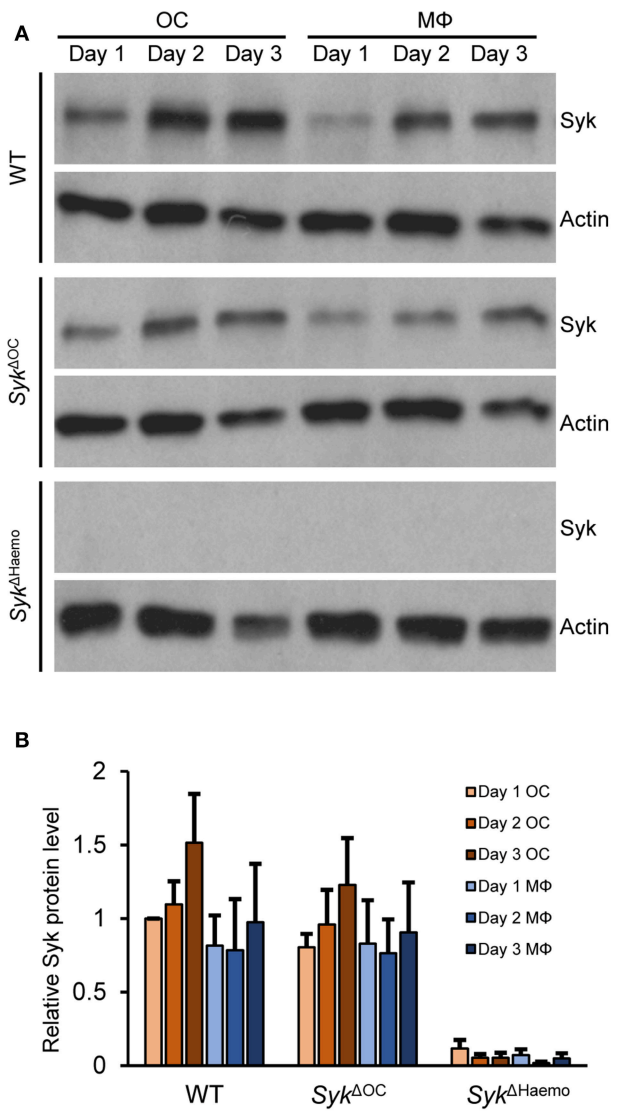

FIGURE 9 | Analysis of the level of Syk protein in osteoclast and macrophage cultures. Bone marrow-derived myeloid progenitors from wild type (WT), $Syk^{\Delta OC}$ or $Syk^{\Delta Haemo}$ mice were cultured in the presence of 50 ng/ml M-CSF with (osteoclasts; OC) or without (macrophages; MΦ) 50 ng/ml RANKL for the indicated times. Whole-cell lysates were then prepared and processed for immunoblotting for Syk, or for actin as a loading control. Representative immunoblots **(A)** or quantification of Syk/actin ratios normalized to Day 1 OC **(B)** are shown. Blots are representative of, and bar graphs show mean and SEM from, 3 to 6 independent experiments.

substantial deletion (reduction) of the Syk^{flox} allele given the tendency of PCR to amplify even small amounts of the target templates when no competing templates are present. In contrast, neither the Syk^{+} nor the Syk^{flox} allele could be amplified from $Syk^{\Delta Haemo}$ cultures (**Figure 10B**), suggesting complete deletion of the Syk^{flox} allele from those cells, likely in an earlier stage of hematopoietic development. Unfortunately, the Syk^{Δ} allele could not be detected with the PCR 1 protocol (**Figure 10B** and **Supplementary Figure 2**).

Results with PCR 2 (which could detect all three alleles including the Syk^{Δ} allele; see **Supplementary Figure 2**) is shown in **Figure 10C**. Those experiments confirmed the expected exclusive presence of the Syk^{+} allele throughout the experiment in wild type cultures, as well as the exclusive presence of the Syk^{Δ} allele throughout the $Syk^{\Delta Haemo}$ samples, indicating complete deletion of the Syk^{flox} allele in the $Syk^{\Delta Haemo}$ cultures. In contrast to the static picture in wild type and $Syk^{\Delta Haemo}$ cultures, the $Syk^{\Delta OC}$ cultures showed dynamic changes in the Syk locus (**Figure 10C**). While only the Syk^{flox} allele was seen 1 day after the initial RANKL treatment, the Syk^{Δ} allele appeared and its amount gradually increased during the next 3 days, parallel to a proportional decline (but not complete disappearance) of the Syk^{flox} allele (**Figure 10C**). It should be noted that the appearance of the smaller-size Syk^{Δ} allele likely had a competitive advantage over the larger-size Syk^{flox} allele in these PCR reactions, leading to a likely underestimation of the amount of the Syk^{flox} allele. Taken together, those results and the time course of the changes indicate that Ctsk-Cre-mediated deletion of the Syk^{flox} allele occurs gradually during 2–4 days after RANKL addition and that only an incomplete genetic deletion of Syk is achieved even until the end of the observation period.

The above results indicate slow and gradual deletion of the Syk^{flox} allele in $Syk^{\Delta OC}$ osteoclast cultures, which is in line with the slow activation of the *Ctsk* gene during *in vitro* osteoclast development (**Figures 8**, **10A**) (54, 55). These results may also explain the less severe *in vivo* phenotypes (**Figures 1**–**5**) and less pronounced *in vitro* osteoclast developmental defect (**Figure 6**), as well as the continuous presence of Syk in osteoclast cultures (**Figure 9**), in the $Syk^{\Delta OC}$ mutants, as compared with the $Syk^{\Delta Haemo}$ mutants which show early and complete deletion of the Syk^{flox} allele from the beginning of the entire osteoclast developmental process.

Analysis of Myeloid-Specific Syk Deletion

Osteoclasts are derived from early myeloid progenitors through a developmental process related to that of macrophages. Therefore, we have also tested certain aspects of osteoclast biology in $Syk^{\Delta Myelo}$ mutants in which Syk is conditionally deleted using the myeloid-specific LysM-Cre knock-in mutation. The $Syk^{\Delta Myelo}$ mutation strongly reduced (but did not completely abrogate) osteoclast development, both in terms of the number of osteoclasts (**Supplementary Figure 3A**) and the area covered by osteoclasts (**Supplementary Figure 3B**). As shown in **Supplementary Figure 3C**, Syk expression was strongly reduced (but did not completely disappear) in both $Syk^{\Delta Myelo}$ osteoclasts and macrophages. The $Syk^{\Delta Myelo}$ mutation also partially reduced osteoclast-specific gene expression, i.e., the upregulation of the mRNA of the *Tm7sf4*, *Acp5*, *Calcr*, *Nfatc1,* and *Ctsk* genes (**Supplementary Figure 3D**). We have also tested Cre expression in wild type and $Syk^{\Delta Myelo}$ cells. As shown in **Supplementary Figure 3D**, Cre mRNA was absent from wild type cells but it was expressed in all $Syk^{\Delta Myelo}$ samples. Interestingly, Cre expression was especially high in early myeloid progenitors (Day 0 samples) and declined afterwards both in osteoclast and macrophage cultures. Taken together, the $Syk^{\Delta Myelo}$ mutation leads to strong but incomplete deletion of

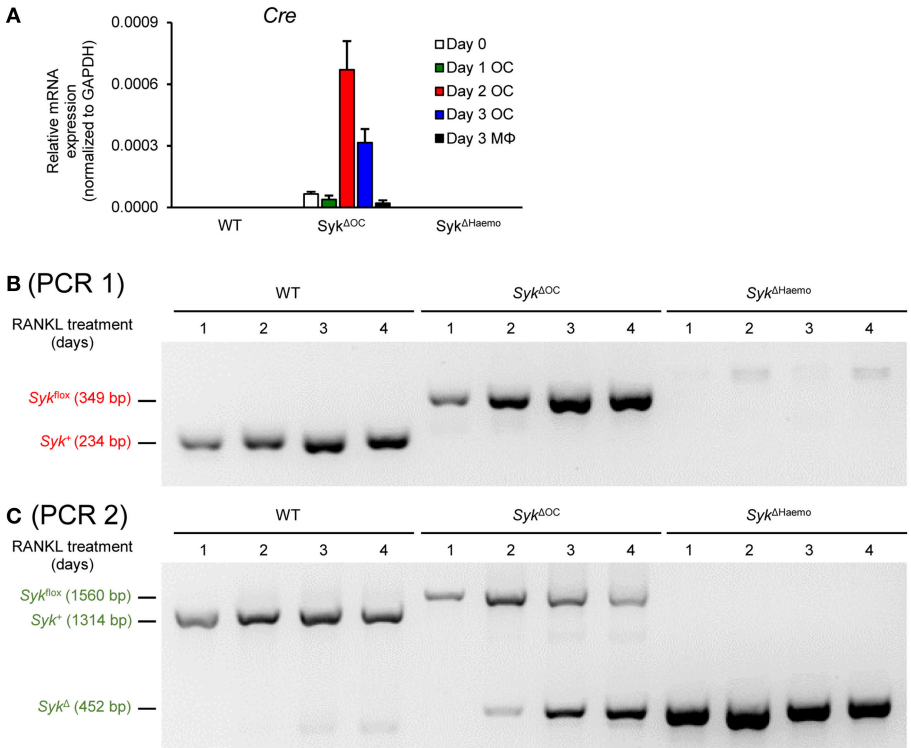

FIGURE 10 | Genetic analysis of Cre expression and Cre-mediated Syk deletion. **(A)** *Cre* expression in wild type (WT), $Syk^{\Delta OC}$ or $Syk^{\Delta Haemo}$ mice bone marrow-derived cells cultured for 0–3 days in the presence of 50 ng/ml M-CSF with (osteoclasts; OC) or without (macrophages; MΦ) 50 ng/ml RANKL. Bar graph shows mean and SEM from 3 independent experiments. **(B,C)** PCR analysis of wild type (WT), $Syk^{\Delta OC}$ or $Syk^{\Delta Haemo}$ osteoclast cultures (differentiated in the presence of 50 ng/ml RANKL and M-CSF for 1–4 days) using PCR 1 (P fwd vs. P rev1 primers; **B**) or PCR 2 (P fwd vs. P rev2 primers; **C**). Images are representative of 4 independent experiments.

Syk during early myeloid differentiation, leading to strongly reduced but not completely abrogated *in vitro* development of osteoclasts.

DISCUSSION

In this manuscript, we provide direct genetic evidence for the role of the Syk tyrosine kinase in normal bone homeostasis in adult mice. The perinatal lethality of $Syk^{-/-}$ mice was overcome by lineage-specific conditional deletion of Syk in osteoclasts ($Syk^{\Delta OC}$ mice) or in the entire hematopoietic system ($Syk^{\Delta Haemo}$ mice). Both osteoclast-specific and hematopoietic Syk deletion led to increased trabecular bone mass and defective *in vitro* osteoclast development and function. However, hematopoietic Syk deletion caused more robust changes than osteoclast-specific Syk deletion both *in vivo* and *in vitro*. Our results suggest that this is due to late and incomplete deletion of Syk in osteoclast-specific Syk mutants, likely caused by late activation and modest activity of Cre expression driven by the *Ctsk* gene promoter during osteoclast development.

We and others have previously shown that Syk plays an important role in *in vitro* osteoclast development and osteoclast-mediated resorptive activity (40, 42, 44). However, the role of Syk in bone homeostasis in live mice could not be tested because of the perinatal lethality of $Syk^{-/-}$ mice (17, 18), although bone density appeared to be increased in third-trimester $Syk^{-/-}$ fetuses (44). Unfortunately, the *in vitro* osteoclast phenotypes cannot be directly extrapolated to the *in vivo* situation since a number of mutations even within the same pathway, such as DAP12 (38, 41–43) or PLCγ2 (54, 58, 59) deficiency, provide examples of practically complete *in vitro* osteoclast defects despite only moderately increased *in vivo* bone mass. Our *in vivo* results, especially those with the $Syk^{\Delta Haemo}$ mice, provide the first direct genetic evidence for a major and critical role of Syk in bone homeostasis in live animals.

The two main models used in this study clarify different aspects of the role of Syk in bone metabolism: the $Syk^{\Delta OC}$ mice provide evidence for an osteoclast-specific role of Syk but it only leads to limited defects, while the $Syk^{\Delta Haemo}$ mice have the widest Syk deletion without embryonic lethality and therefore show the maximum extent of bone resorption defects.

Despite the clear *in vivo* phenotypes of conditional Syk-deficient mice, a number of questions related to the cell type(s) responsible remain open. Our experiments with the $Syk^{\Delta OC}$ mice indicate that the role of Syk in bone metabolism is at least in part mediated by Syk expression in osteoclasts. However, it is at present unclear why $Syk^{\Delta Haemo}$ mice have a more severe phenotype than the $Syk^{\Delta OC}$ animals. A reasonable explanation,

also supported by our *in vitro* findings, is that the $Syk^{\Delta OC}$ mutation only partially deletes Syk in the osteoclast lineage (see further discussion below). However, we cannot exclude the possibility that changes to (a) hematopoietic lineage(s) other than osteoclasts in the $Syk^{\Delta Haemo}$ mice also contribute to the increased bone mass. In addition, it is also possible that Syk deletion in osteoclasts and/or other hematopoietic cells indirectly promote osteoblast-mediated bone production. It should be mentioned that prior studies (44) showed normal bone production by $Syk^{-/-}$ osteoblasts, therefore it is unlikely that Syk deficiency in osteoblasts (e.g., through a leaky Cre expression) contributes to the observed *in vivo* bone phenotypes. It should also be noted that our micro-CT studies indicate increased trabecular number rather than a higher trabecular thickness as the main cause of the *in vivo* bone phenotypes. Unfortunately, different groups have reported different contributions of the changes of trabecular number and trabecular thickness to increased bone mass linked to osteoclast defects (42, 43, 54, 55), making it rather difficult to determine the contribution of osteoclasts and osteoblasts to a bone phenotype based on micro-CT data.

An interesting question arising from this study is why the $Syk^{\Delta OC}$ mutation causes a less severe osteoclast phenotype than the $Syk^{\Delta Haemo}$ mutation. Our results clearly indicate that the $Syk^{\Delta OC}$ mutation is less effective in inactivating the Syk gene in osteoclasts. One possible explanation is the fact that the Ctsk-Cre mutation triggers Cre activation at a relatively later time point (starting at ∼2 days after RANKL treatment) which, combined with the likely continued presence of the preexisting *Syk* mRNA and Syk protein beyond complete deletion of both Syk alleles, may lead to a late disappearance of the Syk protein at a time point where osteoclast development and osteoclast-mediated bone resorption has already occurred. The activation kinetics of the *Ctsk* gene (**Figure 8**) and of the Ctsk-Cre mutation (**Figure 10A**), as well as the late appearance of the Syk^{Δ} allele (**Figure 10C**) all support this explanation. Another possible explanation is that the level of Cre expression from the Ctsk-Cre mutation is too low to provide complete Syk deletion and therefore a significant amount of Syk remains present even after activation of the Ctsk-Cre mutation. In this respect, it is interesting to see that the maximum level of Cre expression in $Syk^{\Delta OC}$ cultures (**Figure 10A**) is at least an order of magnitude less than that in the $Syk^{\Delta Myelo}$ cultures (**Supplementary Figure 3D**). Nevertheless, both scenarios and our own results are consistent with prior reports from the literature showing good specificity but incomplete deletion of target genes (incomplete penetrance) by the Ctsk-Cre mutation (54, 55, 60). Those results also point to the fact that the suitability of Cre-expressing mouse strains for the lineage-specific deletion of floxed alleles depends not only on the specificity of the Cre expression but also on its timing, i.e., whether sufficient time is available for nearly complete deletion of the target gene.

Though the main message of our manuscript is the increased *in vivo* bone mass upon conditional deletion of Syk in live mice, some of our results also address the mechanism of the contribution of Syk to osteoclast development and function. While osteoclast-specific gene expression was reduced in $Syk^{\Delta OC}$ and $Syk^{\Delta Myelo}$ cultures, it was not completely abrogated even in $Syk^{\Delta Myelo}$ cells which practically completely lacked Syk protein expression. Therefore, Syk may not only be involved in osteoclast-specific gene expression but maybe also in later processes such as (pre)osteoclast fusion or the osteoclast-mediated resorption process. It is particularly interesting in this respect that DC-STAMP was only moderately affected by Syk deletion, suggesting that a possible role of Syk in (pre)osteoclast fusion may rely on mechanisms other than DC-STAMP expression. It is also worth noting that practically complete defect of matrix resorption was seen in both $Syk^{\Delta OC}$ and $Syk^{\Delta Myelo}$ cultures (i.e., no substantial difference between the two mutations could be seen in this assay), which, however, is complicated by the fact that this assay measures both osteoclast development and the resorptive activity of the cells, and that the longer culture period could have allowed more complete Syk deletion by the Ctsk-Cre mutation. It is also of interest why the number of osteoclasts are reduced on Day 3.5 in the $Syk^{\Delta OC}$ cultures (**Figure 6**). This may be simply due to the fusion of the cells reducing the number of individual osteoclasts, apoptotic disappearance of osteoclasts during this late stage of culture, and/or active deletion of Syk toward that time period.

We and others have shown that Syk is required for the development of autoantibody-induced arthritis in experimental mice (24, 33–35) and Syk has been proposed as a therapeutic target in human rheumatoid arthritis (61–63). A possible role for Syk in various immune and other cells such as neutrophils, macrophages, mast cells or even platelets (16, 22–24, 26–29, 31, 64–67) may provide an explanation for this observation. Nevertheless, it is important to note that both murine arthritis models (33) and human rheumatoid arthritis (5) are accompanied with bone erosions. Therefore, the role of Syk in osteoclast-mediated *in vivo* bone resorption may also provide an additional cell type beyond immune/inflammatory cells in which Syk inhibitors may have a beneficial therapeutic effect. In addition, Syk-mediated bone resorption may also be a therapeutic target in other diseases characterized by osteoclast-mediated bone resorption such as osteoporosis (4) or osteolytic cancer metastases (7, 8).

Taken together, our results provide direct genetic evidence for the role of Syk in *in vivo* bone metabolism and therefore may contribute to the rationale of developing Syk inhibitors for the treatment of diseases characterized by pathologic bone loss.

ETHICS STATEMENT

All animal experiments were approved by the Animal Experimentation Review Board of the Semmelweis University.

AUTHOR CONTRIBUTIONS

DC, DG, and AM conceived the study, designed the experiments, analyzed, and interpreted the data and wrote the manuscript. DC and ES performed most of the experiments. AA and SB performed the qPCR experiments. PA and ZJ performed the histological studies. CD-N conducted the micro-CT scanning. AM supervised the project.

FUNDING

This work was supported by the Hungarian National Scientific Research Fund (NKFIH-OTKA Grant No. K119653 to AM), the Lendület program of the Hungarian Academy of Sciences (LP2014-4/2018 to ZJ), the Faculty of Medicine of the University of Debrecen (Bridging and Intramural Research Grants to SB) and the Higher Education Institutional Excellence Program of Hungary. SB was a recipient of a János Szodoray Postdoctoral Fellowship from the University of Debrecen. AA held a Stipendium Hungaricum Scholarship from the Government of Hungary.

ACKNOWLEDGMENTS

We thank Nóra Kiss for expert technical assistance, Bence T. Szabó for help with micro-CT scanning, and Shigeaki Kato and Alexander Tarakhovsky for sharing mutant mouse strains.

SUPPLEMENTARY MATERIAL

The Supplementary Material for this article can be found online at: https://www.frontiersin.org/articles/10.3389/fimmu.2019.00937/full#supplementary-material

REFERENCES

1. Boyle WJ, Simonet WS, Lacey DL. Osteoclast differentiation and activation. *Nature*. (2003) 423:337–42. doi: 10.1038/nature01658
2. Ono T, Nakashima T. Recent advances in osteoclast biology. *Histochem Cell Biol*. (2018) 149:325–41. doi: 10.1007/s00418-018-1636-2
3. Sobacchi C, Schulz A, Coxon FP, Villa A, Helfrich MH. Osteopetrosis: genetics, treatment and new insights into osteoclast function. *Nat Rev Endocrinol*. (2013) 9:522–36. doi: 10.1038/nrendo.2013.137
4. Rachner TD, Khosla S, Hofbauer LC. Osteoporosis: now and the future. *Lancet*. (2011) 377:1276–87. doi: 10.1016/S0140-6736(10)62349-5
5. Schett G, Gravallese E. Bone erosion in rheumatoid arthritis: mechanisms, diagnosis and treatment. *Nat Rev Rheumatol*. (2012) 8:656–64. doi: 10.1038/nrrheum.2012.153
6. Le Goff B, Berthelot JM, Maugars Y, Heymann D. Osteoclasts in RA: diverse origins and functions. *Joint Bone Spine*. (2013) 80:586–91. doi: 10.1016/j.jbspin.2013.04.002
7. Clezardin P. Pathophysiology of bone metastases from solid malignancies. *Joint Bone Spine*. (2017) 84:677–84. doi: 10.1016/j.jbspin.2017.05.006
8. Sousa S, Clezardin P. Bone-Targeted Therapies in Cancer-Induced Bone Disease. *Calcif Tissue Int*. (2018) 102:227–50. doi: 10.1007/s00223-017-0353-5
9. Wada T, Nakashima T, Hiroshi N, Penninger JM. RANKL-RANK signaling in osteoclastogenesis and bone disease. *Trends Mol Med*. (2006) 12:17–25. doi: 10.1016/j.molmed.2005.11.007
10. Yoshida H, Hayashi S, Kunisada T, Ogawa M, Nishikawa S, Okamura H, et al. The murine mutation osteopetrosis is in the coding region of the macrophage colony stimulating factor gene. *Nature*. (1990) 345:442–4. doi: 10.1038/345442a0
11. Dougall WC, Glaccum M, Charrier K, Rohrbach K, Brasel K, De Smedt T, et al. RANK is essential for osteoclast and lymph node development. *Genes Dev*. (1999) 13:2412–24. doi: 10.1101/gad.13.18.2412
12. Li J, Sarosi I, Yan XQ, Morony S, Capparelli C, Tan HL, et al. RANK is the intrinsic hematopoietic cell surface receptor that controls osteoclastogenesis and regulation of bone mass and calcium metabolism. *Proc Natl Acad Sci USA*. (2000) 97:1566–71. doi: 10.1073/pnas.97.4.1566
13. Kong YY, Yoshida H, Sarosi I, Tan HL, Timms E, Capparelli C, et al. OPGL is a key regulator of osteoclastogenesis, lymphocyte development and lymph-node organogenesis. *Nature*. (1999) 397:315–23. doi: 10.1038/16852
14. Kim N, Odgren PR, Kim DK, Marks SC, Jr., Choi Y. Diverse roles of the tumor necrosis factor family member TRANCE in skeletal physiology revealed by TRANCE deficiency and partial rescue by a lymphocyte-expressed TRANCE transgene. *Proc Natl Acad Sci USA*. (2000) 97:10905–10. doi: 10.1073/pnas.200294797
15. McHugh KP, Hodivala-Dilke K, Zheng MH, Namba N, Lam J, Novack D, et al. Mice lacking β3 integrins are osteosclerotic because of dysfunctional osteoclasts. *J Clin Invest*. (2000) 105:433–40. doi: 10.1172/JCI8905
16. Mócsai A, Ruland J, Tybulewicz VL. The SYK tyrosine kinase: a crucial player in diverse biological functions. *Nat Rev Immunol*. (2010) 10:387–02. doi: 10.1038/nri2765
17. Turner M, Mee PJ, Costello PS, Williams O, Price AA, Duddy LP, et al. Perinatal lethality and blocked B-cell development in mice lacking the tyrosine kinase Syk. *Nature*. (1995) 378:298–02. doi: 10.1038/378298a0
18. Cheng AM, Rowley B, Pao W, Hayday A, Bolen JB, Pawson T. Syk tyrosine kinase required for mouse viability and B-cell development. *Nature*. (1995) 378:303–6. doi: 10.1038/378303a0
19. Kiefer F, Brumell J, Al-Alawi N, Latour S, Cheng A, Veillette A, et al. The Syk protein tyrosine kinase is essential for Fcγ receptor signaling in macrophages and neutrophils. *Mol Cell Biol*. (1998) 18:4209–20. doi: 10.1128/MCB.18.7.4209
20. Costello PS, Turner M, Walters AE, Cunningham CN, Bauer PH, Downward J, et al. Critical role for the tyrosine kinase Syk in signalling through the high affinity IgE receptor of mast cells. *Oncogene*. (1996) 13:2595–605.
21. Crowley MT, Costello PS, Fitzer-Attas CJ, Turner M, Meng F, Lowell C, et al. A critical role for Syk in signal transduction and phagocytosis mediated by Fcγ receptors on macrophages. *J Exp Med*. (1997) 186:1027–39. doi: 10.1084/jem.186.7.1027
22. Mócsai A, Zhang H, Jakus Z, Kitaura J, Kawakami T, Lowell CA. G-protein-coupled receptor signaling in Syk-deficient neutrophils and mast cells. *Blood*. (2003) 101:4155–63. doi: 10.1182/blood-2002-07-2346
23. Meinders M, Hoogenboezem M, Scheenstra MR, De Cuyper IM, Papadopoulos P, Németh T, et al. Repercussion of megakaryocyte-specific Gata1 loss on megakaryopoiesis and the hematopoietic precursor compartment. *PLoS ONE*. (2016) 11:e0154342. doi: 10.1371/journal.pone.0154342
24. Németh T, Futosi K, Szilveszter K, Vilinovszki O, Kiss-Pápai L, Mócsai A. Lineage-specific analysis of Syk function in autoantibody-induced arthritis. *Front Immunol*. (2018) 9:555. doi: 10.3389/fimmu.2018.00555
25. Vines CM, Potter JW, Xu Y, Geahlen RL, Costello PS, Tybulewicz VL, et al. Inhibition of b2 integrin receptor and Syk kinase signaling in monocytes by the Src family kinase Fgr. *Immunity*. (2001) 15:507–19. doi: 10.1016/S1074-7613(01)00221-7
26. Mócsai A, Zhou M, Meng F, Tybulewicz VL, Lowell CA. Syk is required for integrin signaling in neutrophils. *Immunity*. (2002) 16:547–58. doi: 10.1016/S1074-7613(02)00303-5
27. Obergfell A, Eto K, Mócsai A, Buensuceso C, Moores SL, Brugge JS, et al. Coordinate interactions of Csk, Src, and Syk kinases with αIIbβ3 initiate integrin signaling to the cytoskeleton. *J Cell Biol*. (2002) 157:265–75. doi: 10.1083/jcb.200112113
28. Abtahian F, Guerriero A, Sebzda E, Lu MM, Zhou R, Mócsai A, et al. Regulation of blood and lymphatic vascular separation by signaling proteins SLP-76 and Syk. *Science*. (2003) 299:247–51. doi: 10.1126/science.1079477
29. Mócsai A, Abram CL, Jakus Z, Hu Y, Lanier LL, Lowell CA. Integrin signaling in neutrophils and macrophages uses adaptors containing immunoreceptor tyrosine-based activation motifs. *Nat Immunol*. (2006) 7:1326–33. doi: 10.1038/ni1407
30. Abtahian F, Bezman N, Clemens R, Sebzda E, Cheng L, Shattil SJ, et al. Evidence for the requirement of ITAM domains but not SLP-76/Gads interaction for integrin signaling in hematopoietic cells. *Mol Cell Biol*. (2006) 26:6936–49. doi: 10.1128/MCB.01040-06
31. Fodor S, Jakus Z, Mócsai A. ITAM-based signaling beyond the adaptive immune response. *Immunol Lett*. (2006) 104:29–37. doi: 10.1016/j.imlet.2005.11.001

32. Jakus Z, Fodor S, Abram CL, Lowell CA, Mócsai A. Immunoreceptor-like signaling by β2 and β3 integrins. *Trends Cell Biol*. (2007) 17:493–501. doi: 10.1016/j.tcb.2007.09.001
33. Jakus Z, Simon E, Balázs B, Mócsai A. Genetic deficiency of Syk protects mice from autoantibody-induced arthritis. *Arthritis Rheum*. (2010) 62:1899–910. doi: 10.1002/art.27438
34. Elliott ER, Van Ziffle JA, Scapini P, Sullivan BM, Locksley RM, Lowell CA. Deletion of Syk in neutrophils prevents immune complex arthritis. *J Immunol*. (2011) 187:4319–30. doi: 10.4049/jimmunol.1100341
35. Ozaki N, Suzuki S, Ishida M, Harada Y, Tanaka K, Sato Y, et al. Syk-dependent signaling pathways in neutrophils and macrophages are indispensable in the pathogenesis of anti-collagen antibody-induced arthritis. *Int Immunol*. (2012) 24:539–50. doi: 10.1093/intimm/dxs078
36. Németh T, Virtic O, Sitaru C, Mócsai A. The Syk tyrosine kinase is required for skin inflammation in an *in vivo* mouse model of epidermolysis bullosa acquisita. *J Invest Dermatol*. (2017) 137:2131–9. doi: 10.1016/j.jid.2017.05.017
37. Samavedam UK, Mitschker N, Kasprick A, Bieber K, Schmidt E, Laskay T, et al. Whole-genome expression profiling in skin reveals SYK as a key regulator of inflammation in experimental epidermolysis bullosa acquisita. *Front Immunol*. (2018) 9:249. doi: 10.3389/fimmu.2018.00249
38. Kaifu T, Nakahara J, Inui M, Mishima K, Momiyama T, Kaji M, et al. Osteopetrosis and thalamic hypomyelinosis with synaptic degeneration in DAP12-deficient mice. *J Clin Invest*. (2003) 111:323–32. doi: 10.1172/JCI16923
39. Paloneva J, Mandelin J, Kiialainen A, Bohling T, Prudlo J, Hakola P, et al. DAP12/TREM2 deficiency results in impaired osteoclast differentiation and osteoporotic features. *J Exp Med*. (2003) 198:669–75. doi: 10.1084/jem.20030027
40. Faccio R, Zou W, Colaianni G, Teitelbaum SL, Ross FP. High dose M-CSF partially rescues the Dap12–/– osteoclast phenotype. *J Cell Biochem*. (2003) 90:871–83. doi: 10.1002/jcb.10694
41. Humphrey MB, Ogasawara K, Yao W, Spusta SC, Daws MR, Lane NE, et al. The signaling adapter protein DAP12 regulates multinucleation during osteoclast development. *J Bone Miner Res*. (2004) 19:224–34. doi: 10.1359/JBMR.0301234
42. Mócsai A, Humphrey MB, Van Ziffle JA, Hu Y, Burghardt A, Spusta SC, et al. The immunomodulatory adapter proteins DAP12 and Fc receptor γ-chain (FcRγ) regulate development of functional osteoclasts through the Syk tyrosine kinase. *Proc Natl Acad Sci USA*. (2004) 101:6158–63. doi: 10.1073/pnas.0401602101
43. Koga T, Inui M, Inoue K, Kim S, Suematsu A, Kobayashi E, et al. Costimulatory signals mediated by the ITAM motif cooperate with RANKL for bone homeostasis. *Nature*. (2004) 428:758–63. doi: 10.1038/nature02444
44. Zou W, Kitaura H, Reeve J, Long F, Tybulewicz VL, Shattil SJ, et al. Syk, c-Src, the αVβ3 integrin, and ITAM immunoreceptors, in concert, regulate osteoclastic bone resorption. *J Cell Biol*. (2007) 176:877–88. doi: 10.1083/jcb.200611083
45. Zou W, Croke M, Fukunaga T, Broekelmann TJ, Mecham RP, Teitelbaum SL. Zap70 inhibits Syk-mediated osteoclast function. *J Cell Biochem*. (2013) 114:1871–8. doi: 10.1002/jcb.24531
46. Takayanagi H. Osteoimmunology: shared mechanisms and crosstalk between the immune and bone systems. *Nat Rev Immunol*. (2007) 7:292–304. doi: 10.1038/nri2062
47. Okamoto K, Nakashima T, Shinohara M, Negishi-Koga T, Komatsu N, Terashima A, et al. Osteoimmunology: the conceptual framework unifying the immune and skeletal systems. *Physiol Rev*. (2017) 97:1295–349. doi: 10.1152/physrev.00036.2016
48. Zou W, Reeve JL, Liu Y, Teitelbaum SL, Ross FP. DAP12 Couples c-Fms Activation to the Osteoclast Cytoskeleton by Recruitment of Syk. *Mol Cell*. (2008) 31:422–31. doi: 10.1016/j.molcel.2008.06.023
49. Saijo K, Schmedt C, Su IH, Karasuyama H, Lowell CA, Reth M, et al. Essential role of Src-family protein tyrosine kinases in NF-κB activation during B cell development. *Nat Immunol*. (2003) 4:274–9. doi: 10.1038/ni893
50. Nakamura T, Imai Y, Matsumoto T, Sato S, Takeuchi K, Igarashi K, et al. Estrogen prevents bone loss via estrogen receptor α and induction of Fas ligand in osteoclasts. *Cell*. (2007) 130:811–23. doi: 10.1016/j.cell.2007.07.025
51. de Boer J, Williams A, Skavdis G, Harker N, Coles M, Tolaini M, et al. Transgenic mice with hematopoietic and lymphoid specific expression of Cre. *Eur J Immunol*. (2003) 33:314–25. doi: 10.1002/immu.200310005
52. Goodwin LO, Splinter E, Davis TL, Urban R, He H, Braun RE, et al. Large-scale discovery of mouse transgenic integration sites reveals frequent structural variation and insertional mutagenesis. *bioRxiv*. (2017) 236307. doi: 10.1101/236307
53. Clausen BE, Burkhardt C, Reith W, Renkawitz R, Forster I. Conditional gene targeting in macrophages and granulocytes using LysMcre mice. *Transgenic Res*. (1999) 8:265–77. doi: 10.1023/A:1008942828960
54. Kertész Z, Gyori D, Körmendi S, Fekete T, Kis-Tóth K, Jakus Z, et al. Phospholipase Cγ2 is required for basal but not oestrogen deficiency-induced bone resorption. *Eur J Clin Invest*. (2012) 42:49–60. doi: 10.1111/j.1365-2362.2011.02556.x
55. Gyori D, Csete D, Benko S, Kulkarni S, Mandl P, Dobó-Nagy C, et al. The phosphoinositide 3-kinase isoform PI3Kβ regulates osteoclast-mediated bone resorption in humans and mice. *Arthritis Rheumatol*. (2014) 66:2210–21. doi: 10.1002/art.38660
56. Benko S, Magalhaes JG, Philpott DJ, Girardin SE. NLRC5 limits the activation of inflammatory pathways. *J Immunol*. (2010) 185:1681–91. doi: 10.4049/jimmunol.0903900
57. Wu Y, Torchia J, Yao W, Lane NE, Lanier LL, Nakamura MC, et al. Bone microenvironment specific roles of ITAM adapter signaling during bone remodeling induced by acute estrogen-deficiency. *PLoS ONE*. (2007) 2:e586. doi: 10.1371/journal.pone.0000586
58. Mao D, Epple H, Uthgenannt B, Novack DV, Faccio R. PLCγ2 regulates osteoclastogenesis via its interaction with ITAM proteins and GAB2. *J Clin Invest*. (2006) 116:2869–79. doi: 10.1172/JCI28775
59. Chen Y, Wang X, Di L, Fu G, Bai L, Liu J, et al. Phospholipase Cγ2 mediates RANKL-stimulated lymph node organogenesis and osteoclastogenesis. *J Biol Chem*. (2008) 283:29593–601. doi: 10.1074/jbc.M802493200
60. Okamoto M, Murai J, Imai Y, Ikegami D, Kamiya N, Kato S, et al. Conditional deletion of Bmpr1a in differentiated osteoclasts increases osteoblastic bone formation, increasing volume of remodeling bone in mice. *J Bone Miner Res*. (2011) 26:2511–22. doi: 10.1002/jbmr.477
61. Weinblatt ME, Kavanaugh A, Burgos-Vargas R, Dikranian AH, Medrano-Ramirez G, Morales-Torres JL, et al. Treatment of rheumatoid arthritis with a Syk kinase inhibitor: a twelve-week, randomized, placebo-controlled trial. *Arthritis Rheum*. (2008) 58:3309–18. doi: 10.1002/art.23992
62. Weinblatt ME, Kavanaugh A, Genovese MC, Musser TK, Grossbard EB, Magilavy DB. An oral spleen tyrosine kinase (Syk) inhibitor for rheumatoid arthritis. *N Engl J Med*. (2010) 363:1303–12. doi: 10.1056/NEJMoa1000500
63. Deng GM, Kyttaris VC, Tsokos GC. Targeting Syk in Autoimmune Rheumatic Diseases. *Front Immunol*. (2016) 7:78. doi: 10.3389/fimmu.2016.00078
64. Werninghaus K, Babiak A, Gross O, Holscher C, Dietrich H, Agger EM, et al. Adjuvanticity of a synthetic cord factor analogue for subunit *Mycobacterium tuberculosis* vaccination requires FcRγ-Syk-Card9-dependent innate immune activation. *J Exp Med*. (2009) 206:89–97. doi: 10.1084/jem.20081445
65. Kitaura J, Song J, Tsai M, Asai K, Maeda-Yamamoto M, Mócsai A, et al. Evidence that IgE molecules mediate a spectrum of effects on mast cell survival and activation via aggregation of the FcεRI. *Proc Natl Acad Sci USA*. (2003) 100:12911–6. doi: 10.1073/pnas.1735525100
66. Frommhold D, Mannigel I, Schymeinsky J, Mócsai A, Poeschl J, Walzog B, et al. Spleen tyrosine kinase Syk is critical for sustained leukocyte adhesion during inflammation *in vivo*. *BMC Immunol*. (2007) 8:31. doi: 10.1186/1471-2172-8-31
67. Berton G, Mócsai A, Lowell CA. Src and Syk kinases: key regulators of phagocytic cell activation. *Trends Immunol*. (2005) 26:208–14. doi: 10.1016/j.it.2005.02.002

Conflict of Interest Statement: The authors declare that the research was conducted in the absence of any commercial or financial relationships that could be construed as a potential conflict of interest.

frontiers in Immunology

ORIGINAL RESEARCH
published: 03 May 2019
doi: 10.3389/fimmu.2019.01001

Effects of Sweet Cherry Polyphenols on Enhanced Osteoclastogenesis Associated With Childhood Obesity

Filomena Corbo[1†], Giacomina Brunetti[2†], Pasquale Crupi[3], Sara Bortolotti[4], Giuseppina Storlino[4], Laura Piacente[5], Alessia Carocci[1], Alessia Catalano[1], Gualtiero Milani[1], Graziana Colaianni[4], Silvia Colucci[2], Maria Grano[4], Carlo Franchini[1], Maria Lisa Clodoveo[6], Gabriele D'Amato[7] and Maria Felicia Faienza[5]*

[1] Department of Pharmacy-Drug science, University of Bari Aldo Moro, Bari, Italy, [2] Section of Human Anatomy and Histology, Department of Basic and Medical Sciences, Neurosciences and Sense Organs, University of Bari Aldo Moro, Bari, Italy, [3] CREA-VE, Council for Agricultural Research and Economics–Research Centre for Viticulture and Enology, Turi, Italy, [4] Section of Human Anatomy and Histology, Department of Emergency and Organ Transplantation, University of Bari, Bari, Italy, [5] Paediatric Unit, Department of Biomedical Sciences and Human Oncology, University of Bari Aldo Moro, Bari, Italy, [6] Interdisciplinary Department of Medicine, University of Bari Aldo Moro, Bari, Italy, [7] Neonatal Intensive Care Unit, Di Venere Hospital, Bari, Italy

OPEN ACCESS

Edited by:
Teun J. De Vries,
VU University Amsterdam,
Netherlands

Reviewed by:
Maria Helena Fernandes,
Universidade do Porto, Portugal
Jiankun Xu,
The Chinese University of Hong Kong, China
Ineke Jansen,
VU University Amsterdam,
Netherlands

***Correspondence:**
Giacomina Brunetti
giacomina.brunetti@uniba.it

[†]These authors have contributed equally to this work

Specialty section:
This article was submitted to Inflammation, a section of the journal Frontiers in Immunology

Received: 13 February 2019
Accepted: 18 April 2019
Published: 03 May 2019

Citation:
Corbo F, Brunetti G, Crupi P, Bortolotti S, Storlino G, Piacente L, Carocci A, Catalano A, Milani G, Colaianni G, Colucci S, Grano M, Franchini C, Clodoveo ML, D'Amato G and Faienza MF (2019) Effects of Sweet Cherry Polyphenols on Enhanced Osteoclastogenesis Associated With Childhood Obesity. Front. Immunol. 10:1001. doi: 10.3389/fimmu.2019.01001

Childhood obesity is associated with the development of severe comorbidities, such as diabetes, cardiovascular diseases, and increased risk of osteopenia/osteoporosis and fractures. The status of low-grade inflammation associated to obesity can be reversed through an enhanced physical activity and by consumption of food enrich of anti-inflammatory compounds, such as omega-3 fatty acids and polyphenols. The aim of this study was to deepen the mechanisms of bone impairment in obese children and adolescents through the evaluation of the osteoclastogenic potential of peripheral blood mononuclear cells (PBMCs), and the assessment of the serum levels of RANKL and osteoprotegerin (OPG). Furthermore, we aimed to evaluate the *in vitro* effects of polyphenol cherry extracts on osteoclastogenesis, as possible dietary treatment to improve bone health in obese subjects. High RANKL levels were measured in obese with respect to controls (115.48 ± 35.20 pg/ml vs. 87.18 ± 17.82 pg/ml; $p < 0.01$), while OPG levels were significantly reduced in obese than controls (378.02 ± 61.15 pg/ml vs. 436.75 ± 95.53 pg/ml, respectively, $p < 0.01$). Lower Ad-SoS- and BTT *Z*-scores were measured in obese compared to controls ($p < 0.05$). A significant elevated number of multinucleated TRAP$^+$ osteoclasts (OCs) were observed in the un-stimulated cultures of obese subjects compared to the controls. Interestingly, obese subjects displayed a higher percentage of CD14$^+$/CD16$^+$ than controls. Furthermore, in the mRNA extracts of obese subjects we detected a 2.5- and 2-fold increase of TNFα and RANKL transcripts compared to controls, respectively. Each extract of sweet cherries determined a dose-dependent reduction in the formation of multinucleated TRAP$^+$ OCs. Consistently, 24 h treatment of obese PBMCs with sweet cherry extracts from the three cultivars resulted in a significant reduction of the expression of TNFα. In conclusion, the bone impairment in

obese children and adolescents is sustained by a spontaneous osteoclastogenesis that can be inhibited *in vitro* by the polyphenol content of sweet cherries. Thus, our study opens future perspectives for the use of sweet cherry extracts, appropriately formulated as nutraceutical food, as preventive in healthy children and therapeutic in obese ones.

Keywords: obesity, inflammation, polyphenols, sweet cherry, osteoclastogenesis, CD14+/CD16+ monocytes, osteoporosis, osteopenia

INTRODUCTION

Childhood obesity is one of the major health problems in the western world. It is associated with severe co-morbidities including diabetes, cardiovascular diseases (1, 2), and bone loss, which can occur early in the life (3, 4). It has been reported that the incidence of bone fractures increases in overweight/obese children and adolescents (5). The relationship between childhood obesity and bone impairment has been deepened in animal models. Indeed, Shu et al., found that mice fed with high fat diet (HFD) showed bone loss mainly due to high osteoclastic bone resorption, which is mediated by the increase of pro-osteoclastogenic cytokines and pre-osteoclasts in the bone marrow microenvironment (6).

Osteoclasts (OCs) derive from monocyte precursors which fuse thank to macrophage colony-stimulating factor (MCSF) and receptor activator of nuclear factor kappa-B ligand (RANKL) and become multinucleated cells able to resorb bone. RANKL is mainly produced by cells of the osteoblastic lineage. However, in inflammation also immune cells represent also an important source of the inflammatory cytokines [revised in Dar et al. (7)]. Recently, it has also been reported that bone marrow adipocytes produce RANKL (8), whose action could be inhibited by Osteoprotegerin (OPG), the soluble decoy receptor of RANKL (7). Other cytokines could also support osteoclastogenesis together with RANKL (9), such as TNFα. High levels of this cytokine have been demonstrated in bone diseases as well as in obesity (10–13). This last condition is associated with high levels of pro-inflammatory cytokines, such as interleukins, adipokines, and chemokines, which contribute to the chronic low level of inflammation and oxidative stress which are responsible of the different co-morbidities related to obesity (14, 15). This status of chronic inflammation can be prevented or even reversed by the loss of body weight through a reduction of food intake and enhanced physical activity (16). It has been reported that physical activity directly or indirectly decreased inflammation (17–19). Moreover, eating foods rich in bioactive anti-inflammatory compounds, such as omega-3 fatty acids (FAs) and polyphenols, has been demonstrated to reduce inflammation (20, 21). In particular, the anti-obesity effects of polyphenol-rich diets have been associated to the property of polyphenols to interact with adipose tissues (pre-adipocytes, adipose stem cells, and immune cells).

Sweet cherries are a source of dietary phenolic compounds (∼1,500 mg total phenols per kg fresh weight), including phenolic acids (hydroxycinnamic acids) and flavonoids (anthocyanins, flavan-3-ols and flavonols), which are known for their health benefits and important role in preventing several chronic diseases related to oxidative stress (22, 23). Moreover, they show a low glycemic index respect to other fruits and vegetables and represent a source of vitamins, especially vitamin C and minerals, such as potassium, phosphorus, calcium, and magnesium (24, 25).

Studies *in vitro* and *in vivo* have reported that sweet cherries have anti-inflammatory and anti-carcinogenic activity, and characteristics for prevention of cardiovascular disease and diabetes (26).

In the light of these evidences and of the increasing interest on the polyphenol effects on childhood obesity, the aim of this paper were: (a) to deepen the mechanisms of bone impairment in obese children and adolescents, through the evaluation of the serum levels of RANKL and OPG together with the osteoclastogenic potential of peripheral blood mononuclear cells (PBMCs), and (b) to evaluate *in vitro*, the effects of polyphenols from sweet cherry extracts on osteoclastogenesis, as possible dietary treatment to improve bone health in obesity.

MATERIALS AND METHODS

Subjects

Twenty-five obese children with a mean age of 10.8 ± 2.6 years were enrolled at Endocrinology Unit of Pediatric Hospital Giovanni XXIII, University A. Moro of Bari. Inclusion criteria were body mass index (BMI) ≥95th percentile for age and sex. Exclusion criteria were: type 2 diabetes mellitus, secondary or syndromic forms of obesity, hypothyroidism, Cushing disease, viral hepatitis, metabolic or genetic liver diseases, ongoing therapies for chronic systemic diseases. The control group consisted of 21 normal weight healthy children matched for age and gender, recruited on a voluntary basis in the outpatient clinic, who referred to hospital for minor surgery or electrocardiographic record for minor trauma to head, limbs, or chest pain. All the enrolled patients signed an informed consent form. The local ethic committee approved the study. The study was conducted in accordance to the criteria of the declaration of Helsinki. All subjects were in good general health and were not taking drugs in the last 3 months. Serum levels of (25)OH-vitamin D, osteocalcin, calcium, phosphorus, RANKL, OPG, and alkaline phosphatase were measured as previously reported (10). Bone quality was assessed by QUS measurements, performed with a DBM Sonic 1200 bone profiler (Igea S.r.l., Carpi, MO, Italy) employing a sound frequency of 1.25 MHz, as previously described (27).

Cells and Culture Conditions

PBMCs were isolated by centrifugation of peripheral blood samples over Histopaque 1077 density gradient (Sigma Chemical, St. Louis, MO), and cultured in α-MEM (Life Technologies, Paisley, UK) supplemented with 10% fetal bovine serum, 100 IU/ml penicillin, and 100 μg/ml streptomycin (Life Technologies, Inc. Ltd, Uxbridge, UK). To obtain fully differentiated human OCs, the PBMCs were cultured in the presence or absence of 25 ng/ml recombinant human MCSF and 30 ng/ml RANKL (R&D Systems, Minneapolis, MN) for about 20 days. In some experiments, PBMCs were also cultured in the presence of 75 and 100 μg/ml of polyphenol extracts from Giorgia, Bigarreau, and Ferrovia both for mRNA extraction (24 h), MTT assay (24 h) (28), and for osteoclastogenesis (about 20 days) evaluation. The concentrations of the polyphenol extracts were selected according to literature data (29) and calculated according to a previous *in vitro* study on the effect of quercetin-containing cherry extracts on HepG2 cells (30) by considering 440 dalton as the average molecular weight of the compounds in the extracts; then, they were prepared through vacuum drying of the extracts and re-suspension in a suitable medium for the biological assays. Mature OCs were identified as tartrate-resistant acid phosphatase-positive (TRAP) multinucleated cells (Sigma Aldrich, Milan, Italy) containing three or more nuclei. OC resorbing activity was demonstrated by plating the cells on multiwell slides (4×10^5 cells/well) coated with a calcium phosphate film (Millenium Osteologic; Millenium Biologix Inc, Ontario, Canada). This system incorporates a resorbable artificial bone in the form of submicron calcium phosphate films. The photomicrographs were obtained using a Ellipse E400 microscope (Nikon, Tokyo, Japan) equipped with Nikon Plan Fluor 10×/0.30 dicl. The microscope was connected with a Nikon digital camera DxM 1200; the acquisition software was Lucia G version 4.61 (build 0.64) for Nikon Italy.

Flow Cytometry Analysis

Fresh peripheral blood samples from patients and controls were stained with PerCp-CD14 and FITC-CD16 antibodies (all Beckmann Coulter, Milan, Italy). Events were acquired using C6 flow cytometer (Becton Dickinson Immunocytometry System, Mountain View, CA, USA). The area of positivity was determined using an isotype-matched mAb, a total of 10^6 events for each sample were acquired.

RNA Isolation and Real Time-PCR Amplification

Freshly isolated PBMCs of patients and controls, PBMCs treated for 24 h with polyphenol extracts from sweet cherries as well as OCs cultured in the presence of polyphenol extracts from sweet cherries were subjected to mRNA extraction using spin columns (RNeasy, QIAGEN, Hilden, Germany), and reverse-transcription using iScript Reverse Transcription Supermix (Bio-Rad Laboratories, Hercules, CA). The resulting cDNA was amplified using the SsoFast EvaGreen Supermix (Bio-Rad Laboratories) using the Chromo4 Real-Time PCR Detection System (Bio-Rad Laboratories). The following primer pairs were used for the real-time PCR amplification: RANKL S: CGTTGGATCACAGCACAT, RANKL AS: GCTCCTCTT GGCCAGTC; TNFα S: ATCTACTCCCAGGTCCTC, TNFα AS: GATGCGGCTGATGGTGT; calcitonin receptor (CalcR) S: AACAATAGAGCCCAAGCCATTTC, CalcR AS: CCAGCA CAGCCATCCATCC; Cathepsin K (Cath K) S: GGCTCAAGG TTCTGCTAC, Cath K AS: GCTTCCTGTGGGTCTTCTTCC; RANK S: CAGGATGCTCTCATTGGTCAG, RANK AS: AGA AAGGAGGTGTGGATTGC; GAPDH S: TCATCCCTGCCT CTACTG; AS: TGCTTCACCACCTTCTTG.

Reagents and Standards for Chemical Procedures

Formic acid, LC-MS grade water and acetonitrile were purchased from J.T. Baker (Deventer, Holland). Furulic acid, cyanidin-3-O-glucoside chloride, cyanidin-3-O-rutinoside chloride, delphinidin-3-O-glucoside chloride, quercetin-3-O-rutinoside, quercetin-3-O-glucoside, kaempferol-3-O-glucoside, kaempferol-3-O-rutinoside, isorhamnetin-3-O-glucoside, (+)-catechin, (−)-epicatechin, procyanidins B1 and B2, and epicatechin gallate were purchased from Extrasynthese (Genay, France). Cyanidin-3-O-sophoroside chloride, quercetin-4′-O-glucoside, chlorogenic acid, neochlorogenic acid, and cynarin were purchased from Phytolab (Vestenbergsgreuth, Germany).

Fruit Collection

Three sweet cherry cultivars (cv. Ferrovia, Bigarreau, and Giorgia) grown in Apulia region (Southern Italy) was used in this study. Samples were harvested at commercial maturity (1st decade of May−2nd decade of June), on the basis of total soluble solids (TSS), measured as °Brix using a portable refractometer (Atago PR32, Norfolk, Virginia, USA), and titratable acidity (TA) which was determined in the juice by titration with 0.1 N of NaOH (J.T. Baker, Deventer, Holland) to a pH 7 end point (TSS = ∼ 17 °Brix; TA = ∼ 7 g/L of citric acid equivalents), in 2014 season using 7 years-old sweet cherry trees located in Turi. The trees were trained to a central leader system and planted at a spacing of 4 m × 4 m and were grown under usual conditions of irrigation, fertilization, and pest control (31). Five kg of cherries for each variety were taken on the same day, from four different branches of an individual tree and mixed, then they were frozen in liquid nitrogen and vacuum packed in plastic bags and stored at −80°C for further analysis.

Extraction of Polyphenols From Sweet Cherry and HPLC-MS/MS Analysis

Polyphenols were extracted from cherries and analyzed through a capillary HPLC 1100 coupled with a triple quadrupole QQQ mass detector (Agilent Technologies Palo Alto, CA, U.S.A.), following the procedure proposed in our previous researches (31, 32).

Roughly 100 g of partially defrosted sweet cherry sample were pitted and a homogenate was obtained using an IKA A11—basic homogenizer (IKA—WERKE GMBH & CO.KG—Germany). To avoid compounds degradation, the homogenization was completed in darkness and the sample was placed on ice during the whole procedure (around 5 min). Ten gram of homogenate was put in a glass flask with 10 mL of 1%

hydroxybutyl anisole (BHA) in methanol and 100 μL of ferulic acid internal standard solution (1,000 μg/mL of methanol). Then, the obtained solution was sonicated in an ultrasonic bath of 130 W and 40 kHz (SONICA 2200 EP, SOLTEC, Milano, Italy) for 1 h at 25°C and the liquid phase was separated by filtration under vacuum. The extraction procedure was repeated twice for the solid phase utilizing fresh methanol (10 and 5 mL for 30 min, respectively). Finally, the pooled extracts were concentrated down to 10 mL through a rotavapor Buchi-R-205 under vacuum at 40°C, and stored at −25°C until further analysis.

A Zorbax column SC-C18 (50 × 2.1 mm i.d., particle size 1.8 μm, Agilent Technologies) was used, with the following gradient system: water/formic acid (99:1, v/v) (solvent A) and acetonitrile/formic acid (99:1, v/v) (solvent B), 0.8 min, 95% A−5% B; 2.1 min, 90% A−10% B; 5.6 min, 88% A−12% B; 8 min, 81% A−19% B; 9.2 min 81% A−12% B; 11.2 min 5% A−95% B; 12.8 min 5% A−95%; 13.2 min 95% A−5%; stop time 15 min. The column was kept at 60°C, the flow was maintained at 0.5 mL/min and the sample injection was 1.1 μL. Both positive and negative ESI mode was used for ionization of molecules with capillary voltage at 4,000 V. Nitrogen was used both as drying gas at a flow rate of 8 L/min and as nebulizing gas at a pressure of 30 psi. Temperature of drying gas was 350°C. In the full scan (MS) and product ion (MS/MS) modes, the monitored mass range was from *m/z* 100 to 1,200. Typically, 2 runs were performed during the HPLC-ESI-MS analysis of each sample. First, an MS full-scan acquisition was performed to obtain preliminary information on the predominant *m/z* ratios observed during the elution. An MS/MS full-scan acquisition was then performed: Quadrupole 1 filtered the calculated *m/z* of each compound of interest, while Quadrupole 3 scanned for ions produced by nitrogen collision of these ionized compounds in the chosen range at a scan time of 500 ms/cycle. All data were acquired and processed using Mass Hunter software (version B.01.04; Agilent Technologies). The optimized parameters (fragmentor voltage and collision energy) for each compound together with the mass transitions adopted for multiple reaction monitoring (MRM) are listed in **Table 1S** (Supporting Information). To gauge linearity, calibration curves with five/seven concentration points for each compound were prepared separately. Calibration was performed by linear regression of peak-area ratios of the polyphenols to the relative internal standard vs. the respective standard concentration.

Statistical Analyses

Means and standard deviations of the raw data and regression analysis of calibration samples were carried out using STATISTICA 6.0 software package (StatSoft Inc., Tulsa, OK, U.S.A.).

For statistical analyses of clinical data, the Statistical Package for the Social Sciences (SPSS) for Windows, version 22.0 (SPSS Inc., Chicago, IL, USA) was used. Comparison between groups were performed by *T*-test. Correlations were analyzed with Spearman or Pearson correlation test. The limit of statistical significance was set at 0.05.

TABLE 1 | Characteristics of study population.

	Controls $N = 21$	Obese patients $N = 25$
Gender (male/female)	9/12	9/16
Age (yr)	8.23 ± 3.19	10.8 ± 2.6
Tanner Stage (I, II, III, IV, V)	6,10,4,1,0	8,11,4,2,0
Height SDS	0.36 ± 1.02	0.23 ± 1.48
Weight SDS	0.43 ± 0.87	2.22 ± 0.70**
BMI-SDS	0.25 ± 0.78	2.31 ± 0.41**
Waist circumference (cm)	72.5 ± 7.2	92.04 ± 23.08**
Total cholesterol (mg/dl)	154.8 ± 28.32	164 ± 33.18
HDL (mg/dl)	55.67 ± 9.30	49.08 ± 8.13
LDL (mg/dl)	97.10 ± 21.03	107.54 ± 37.62
Triglycerides (mg/dl)	67.24 ± 19.16	73.00 ± 32.74
Insulin (microU/mL)	9.78 ± 4.50	24.60 ± 12.02**
Glucose (ml/dl)	81.16 ± 7.14	87.22 ± 11.35
HOMA-IR	2.56 ± 0.40	4.93 ± 1.91**
25-OH Vitamin D (ng/ml)	38.64 ± 14.70	29.70 ± 12.89
Osteocalcin (ng/ml)	38.26 ± 19.22	47.44 ± 21.02
PTH (pg/ml)	43.05 ± 15.06	44.07 ± 17.09
Calcium (mg/dl)	9.71 ± 0.40	9.43 ± 0.41
Phosphorus (mg/dl)	4.54 ± 1.4	4.54 ± 0.51
Ad-Sos-Z-score	0.48 ± 0.85	−1.05 ± 1.17*
BTT-Z-score	0.15 ± 0.72	−0.39 ± 1.23*
RANKL (pg/ml)	87.18 ± 17.82	115.48 ± 35.20§
OPG (pg/ml)	436.75 ± 95.53	378.02 ± 61.15§

*SDS, standard deviation score; BMI, body mass index; PTH, parathyroid hormone; Ca, calcium; P, phosphorus; B-ALP, bone alkaline phosphatase; RANKL, receptor activator of nuclear factor kappa-B ligand; OPG, osteoprotegerin. §p < 0.01; *p < 0.05; **p < 0.001.*

RESULTS

Clinical Characteristics

The characteristics of the study population were reported in **Table 1**. Although, in the normal range, lower Ad-SoS- and BTT-*Z*-scores were measured in obese patients compared to controls ($P < 0.05$). The serum levels of 25-OH Vitamin D, calcium, phosphorus, and osteocalcin were comparable to those measured in controls. Interestingly, higher RANKL levels were measured in obese patients with respect to the controls (115.48 ± 35.20 pg/ml vs. 87.18 ± 17.82 pg/ml; $p < 0.01$), while OPG levels were significantly reduced in obese patients than in controls (378.02 ± 61.15 pg/ml vs. 436.75 ± 95.53 pg/ml, respectively, $p < 0.01$). With adjustment for age RANKL levels correlated with waist circumference ($r = 0.144$ $p < 0.022$), and SDS-BMI ($r = 0.129$ $p < 0.038$), whereas OPG levels correlated with waist circumference ($r = -0.348$ $p < 0.0001$), SDS-BMI ($r = -0.381$ $p < 0.0001$), BTT-*Z*-score ($r = 0.208$ $p < 0.002$), HOMA-IR ($r = -0.359$ $p < 0.0001$).

Osteoclastogenesis in Obese Children and Adolescents

OC formation was evaluated in cultures of PBMCs from obese patients and controls. A significant elevated number of multinucleated $TRAP^+$ OCs were counted in the un-stimulated

cultures of obese patients (**Figure 1B**) compared to the controls (**Figure 1A**), as reported in the histogram (**Figure 1C**). The addition of the pro-osteoclastogenic M-CSF and RANKL in the cultures from patients did not affect the OC number, but they appear larger compared those observed in the un-stimulated cultures (**Figure 1E**). Indeed, the number of large OCs (>10 nuclei) was greater in stimulated compared with un-stimulated cultures from obese patients (35 ± 5 vs. 20 ± 6, $p < 0.01$). Conversely, M-CSF and RANKL are necessary to trigger OC formation in cultures from controls (**Figure 1D**), as reported in the histogram (**Figure 1F**).

To investigate the mechanisms of the enhanced osteoclastogenesis in obese we evaluated both the percentage of $CD14^+/CD16^+$ circulating pre-osteoclasts as well as the levels of the pro-osteoclastogenic cytokines RANKL and TNFα in PBMC extracts. Interestingly, patients displayed a high percentage of $CD14^+/CD16^+$, compared to the controls (**Figure 2**). Furthermore, in mRNA extracts of obese patients we detected a 2.5- and 2-fold increase of TNFα and RANKL transcripts compared to controls, respectively (**Figure 3**).

Effect of Polyphenols From Sweet Cherry on the Spontaneous Osteoclastogenesis of Obese Children and Adolescents

Interestingly, we also evaluated *in vitro* the effect of polyphenol cherry extracts on osteoclastogenesis as possible dietary treatment to improve bone health in obesity.

Polyphenols Content in the Cherries Extracts

Table 1S listed the amount of the main flavonoids (anthocyanins, flavan-3-ols, and flavonols) and chlorogenic acids, which were identified as previously described (31, 32), quantified by HPLC-MS/MS analyses in the tested cherries extracts. The content of the phenolic compounds appeared slightly lesser in the extract of Giorgia (1,391 mg/100 g FW) than Bigarreu and Ferrovia (1,820 and 1,768 mg/100 g FW, respectively), even though both the three varieties were principally characterized by anthocyanins, especially cyanidin-3O-rutinoside, accounting for 19–30% of total polyphenols, and chlorogenic acids (particularly, *trans*-3-O-coumaroylquinic acid and *trans*-3-O-caffeoylquinic acid) ranging between 70 and 80% of the total polyphenols (**Table 1S**).

Polyphenols Effect on Osteoclastogenesis of Obese Children and Adolescents

We investigated the effect of polyphenol extracts from Giorgia, Bigarreau, and Ferrovia on PBMC cultures of patients. We demonstrated that each extract determined a dose-dependent reduction in the formation of multinucleated $TRAP^+$ OCs (**Figures 4A–C**). Furthermore, using the highest dose of polyphenol extracts from Giorgia, Bigarreau, and Ferrovia we demonstrated that the treatment also resulted in a significant reduction of resorption activity (**Figure 4D**), together with a significant reduction of the expression of OC marker genes, such as calcitonin receptor, cathepsin K and RANK (**Figure 4E**). Consistently, 24 h treatment of PBMCs from patients with polyphenol extracts from Giorgia, Bigarreau, and Ferrovia resulted in a significant reduction of the expression of TNFα (**Figure 5A**), whereas RANKL levels were unchanged (**Figure 5B**). Furthermore, by MTT we demonstrated that polyphenol extracts did not significantly affect cell viability of PBMCs from patients (**Figure 6**). These results suggested that polyphenols from sweet cherry inhibit osteoclastogenesis through the reduction of pro-osteoclastogenic cytokines, without affecting cell viability.

DISCUSSION

This study demonstrated that in obese children the reduced bone mineral density (BMD) is associated to the decrease of OPG levels, the increase of RANKL levels, enhanced formation of OCs, of circulating pre-osteoclasts, and pro-osteoclastogenic cytokines. Interestingly, the spontaneous osteoclastogenesis is inhibited *in vitro* by sweet cherry polyphenol extracts.

Previous studies demonstrated that obese subjects showed significantly lower OPG levels respect to the controls (33–35); however no correlation has been reported between OPG and BMI (36, 37). Otherwise, few studies measured higher levels of OPG in obese subjects compared with the controls (38, 39). However, all the previous studies correlated the levels of OPG with the altered HOMA-IR, fasting insulin or glucose. Our study, to our knowledge, is the first demonstrating a direct correlation between OPG levels and BTT-Z score in obese children.

It is known that obesity is associated with bone fragility and the reduced OPG levels could contribute to this status. We also found increased RANKL levels which could explain the bone impairment associated with excess of adipose tissue. Interestingly, we found that RANKL levels positively correlated with waist circumference. The correlation between a central obesity parameter, as the waist circumference, and RANKL levels detected in serum and saliva samples has been previously demonstrated (40). Our data confirmed that visceral fat accumulation represents the main parameter which can predict the entity of bone impairment in obese subjects. These findings also suggest to evaluate bone status in obese subjects with a higher waist circumference than normal values. It is known that RANKL and OPG altered levels have been associated to the altered osteoclastogenesis characterizing bone diseases (41–43). Indeed, it has been demonstrated that anti-RANKL antibody is useful in the treatment of osteoporosis (44). The alterations of OPG and RANKL levels together with the increase of $CD14^+/CD16^+$ circulating pre-osteoclasts and TNFα levels are consistent with the spontaneous osteoclastogenesis of our obese patients as well as of other inflammatory diseases associated with bone loss (45). $CD14^+/CD16^+$ cells have been linked with erosive bone diseases, such as psoriatic arthritis and multiple myeloma (46–48). It is known that $CD14^+/CD16^+$ cells display an enhanced pro-osteoclastogenic activity (47, 48) thus supporting the key role of this cells in the alteration of bone health in obesity. Consistently, rodent models of obesity also demonstrated the increase of OC precursors in the bone marrow (49). Consistently, the ongoing theory sustains that weight gain determines local inflammation

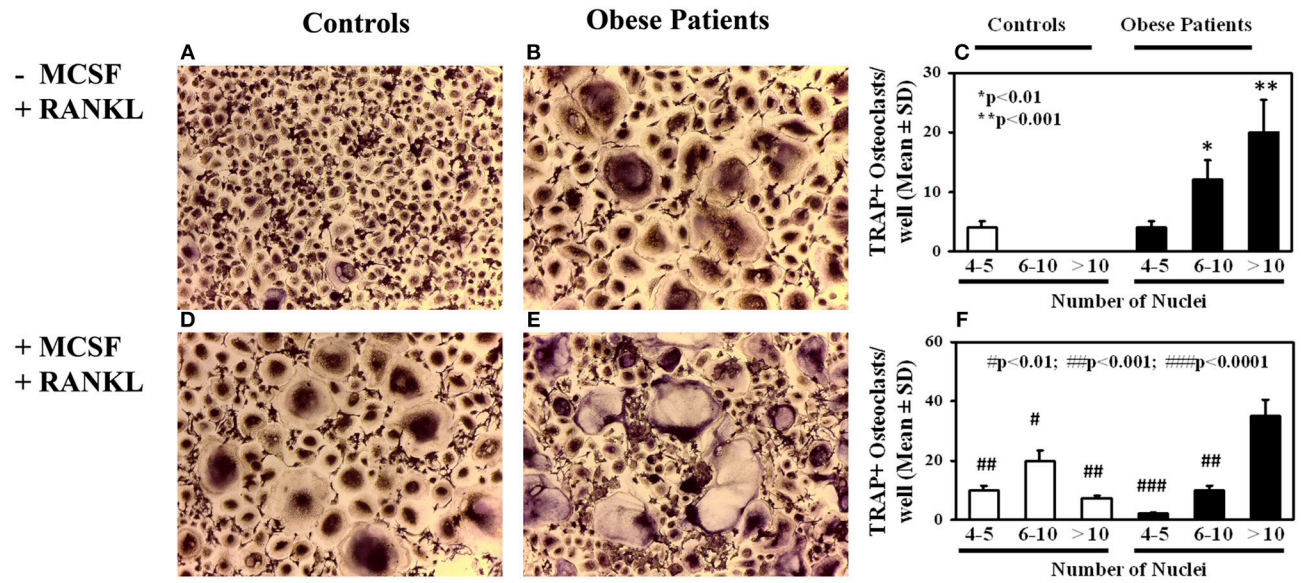

FIGURE 1 | Osteoclastogenesis in obese subjects. Osteoclasts (OCs) identified as tartrate-resistant acid phosphatase-positive ($TRAP^+$) and multinucleated cells with three or more nuclei, differentiated from peripheral blood mononuclear cells (PBMCs) of obese subjects and controls. Few small OCs differentiated in un-stimulated PBMC cultures of a representative control **(A)**, whereas multinucleated $TRAP^+$ OCs differentiated from un-stimulated PBMCs from a representative obese subject **(B)**. The histogram includes OC count deriving from all subjects' cultures, stratified according the number of nuclei per OC **(C)**. In PBMC cultures from the controls, OCs differentiate following MCSF and RANKL addition **(D)**, otherwise in cultures from obese subjects growth factor addition did not further increase osteoclastogenesis **(E)**, compared with the un-stimulated cultures. The histogram reports the results deriving from all the enrolled subjects **(F)**.

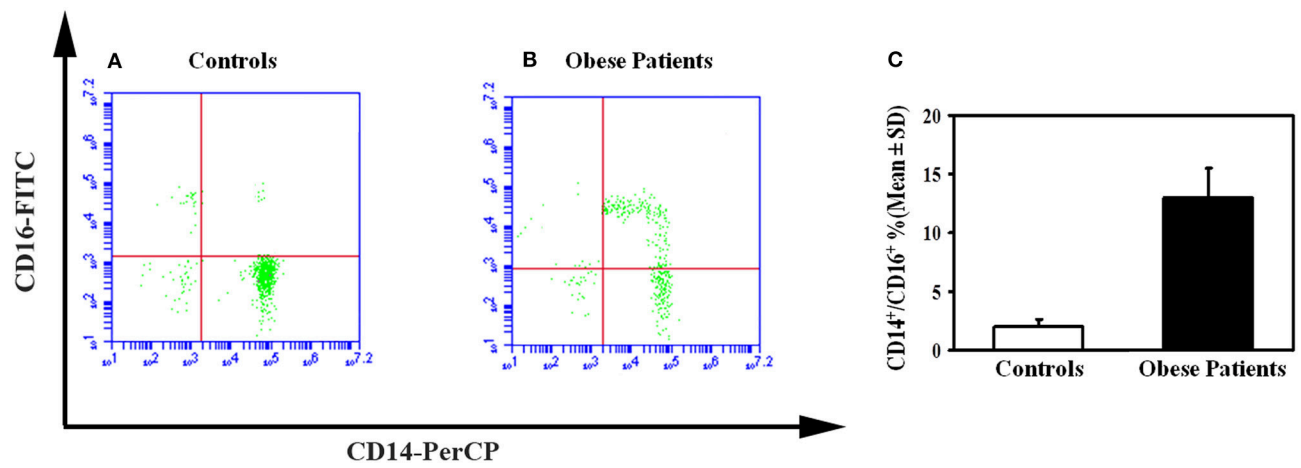

FIGURE 2 | Circulating osteoclast precursors in obese subjects. A representative flow cytometry dot plots displayed the percentage of circulating osteoclast precursors, identified as $CD14^+/16^+$ cells in control **(A)** and obese subjects **(B)**. The histograms represent the percentage of $CD14^+/CD16^+$ cells measured for all enrolled obese and control subjects by flow cytometry **(C)**.

that stimulate the increased recruitment of circulating pro-inflammatory ($Ly6C^{hi}$) monocytes, also capable of differentiate in OCs in bone. Recruited monocytes differentiate into an M1 macrophage phenotype which is responsible of the chronic inflammation and thus organ damage associated to obesity (15).

An increased mRNA levels of pro-osteoclastogenic molecules such as RANKL and TNFα has been found in young mice fed with HFD (6). Interestingly, our results also displayed high mRNA levels of TNFα and RANKL in PBMCs from obese subjects. It has been reported that childhood obesity is associated to a state of chronic low-grade inflammation as well as numerous inflammation-related molecules such as TNFα, interleukin 6 (IL-6), and leptin. High levels of these molecules have been linked to co-morbidities associated to obesity (50–53). Furthermore, consisting with our results, transgenic mouse expressing human TNFα determines the augment of OC precursor percentage (54).

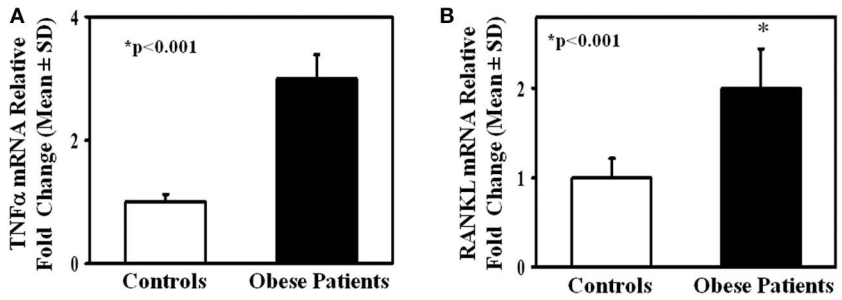

FIGURE 3 | TNFα and RANKL expression in lymphomonocytes from obese subjects. mRNA levels of TNFα **(A)** and RANKL **(B)** in lymphomonocytes from all enrolled controls and obese subjects. Obese subjects expressed higher levels of TNFα and RANKL compared to the controls.

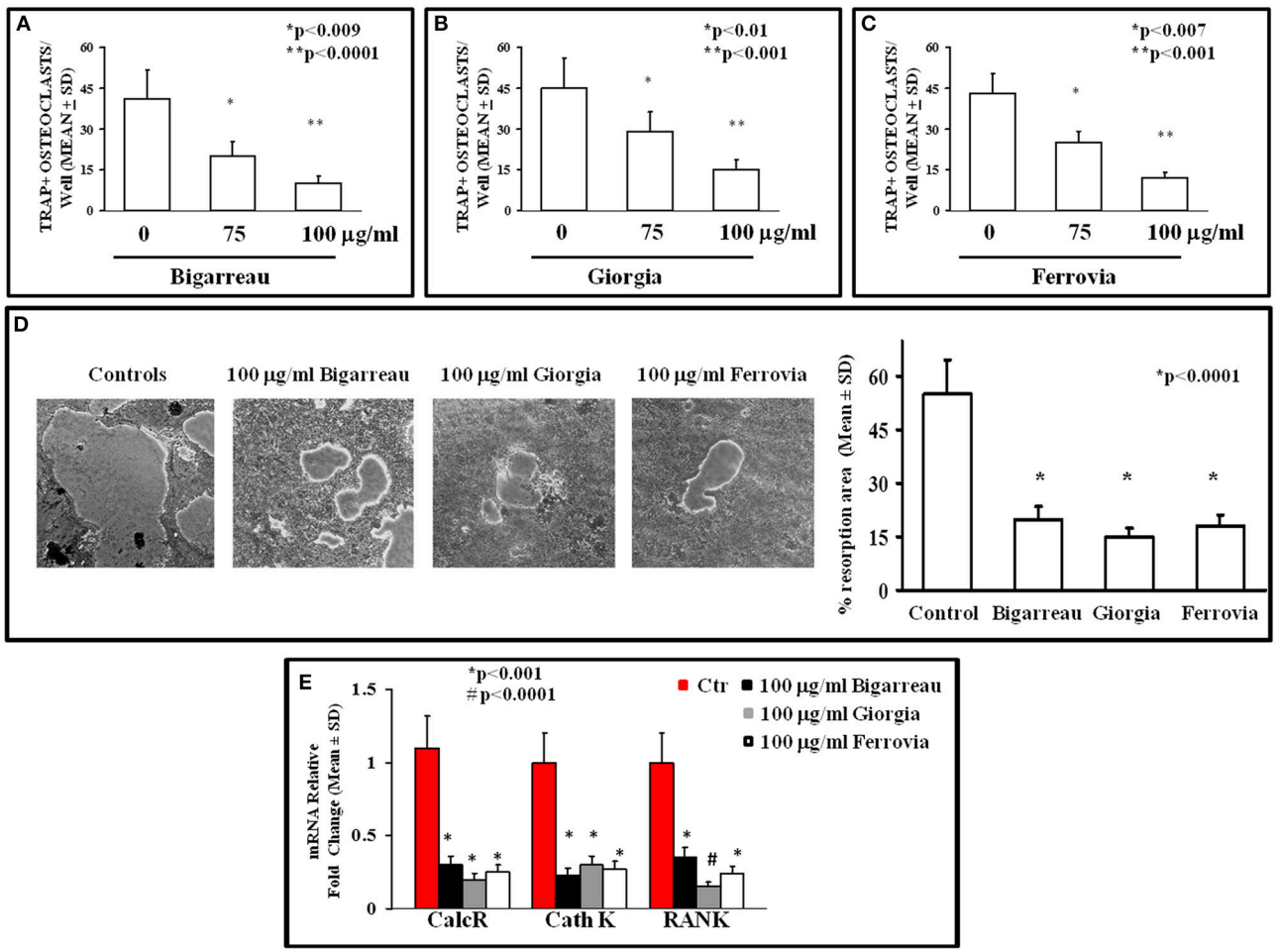

FIGURE 4 | Osteoclastogenesis inhibition by polyphenol extracts from Giorgia, Bigarreau, and Ferrovia. The formation of multinucleated TRAP$^+$ OCs was evaluated in un-stimulated PBMCs from all obese patients cultured in the absence or presence of 75 and 100 µg/ml polyphenol extracts from Bigarreau **(A)**, Giorgia **(B)**, and Ferrovia **(C)**. PBMCs from the patients, cultured on Millenium slides coated with a calcium phosphate film, formed large resorption areas, that were reduced following the treatment with 100 µg/ml polyphenol extracts from Bigarreau, Giorgia, and Ferrovia, as quantified in the histogram **(D)**. The mRNA levels of calcitonin receptor (CalcR), cathepsin K (Cath K), and RANK was evaluated in PBMCs from obese patients cultured in the absence or presence of 100 µg/ml polyphenol extracts from Bigarreau, Giorgia, and Ferrovia **(E)**.

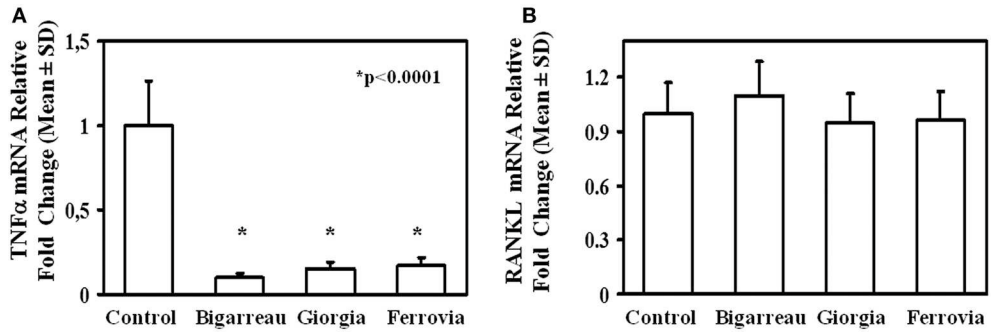

FIGURE 5 | RANKL and TNFα expression in lymphomonocytes from obese subjects. Twenty-four hours treatment of PBMCs from obese subjects with 100 μg/ml polyphenol extracts from Giorgia, Bigarreau, and Ferrovia resulted in a significant reduction of the mRNA levels of TNFα **(A)**, whereas RANKL levels were unchanged **(B)**. The results are referred to all obese subjects.

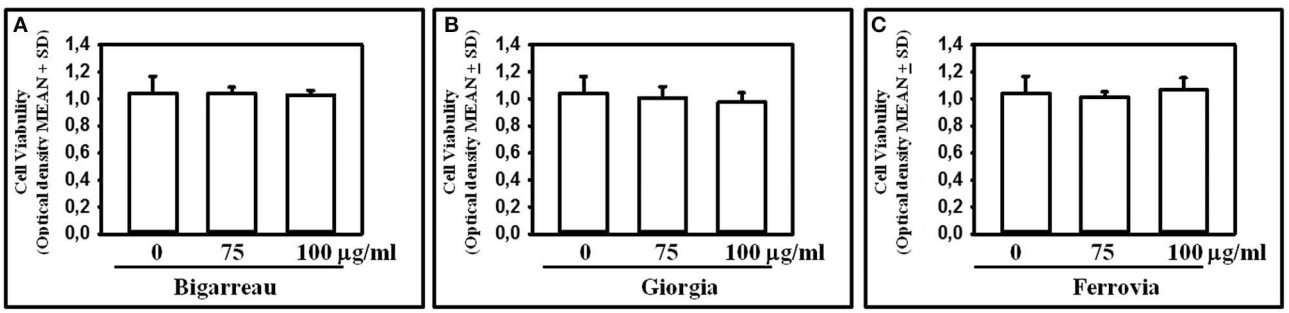

FIGURE 6 | Effect of Polyphenol extracts from Giorgia, Bigarreau, and Ferrovia on PBMC viability. PBMCs were treated for 24 h with 75 and 100 μg/ml polyphenol extracts from Bigarreau **(A)**, Giorgia **(B)**, and Ferrovia **(C)** and analyzed by MTT assay to evaluate cell viability. Results are expressed as mean values of optical density at 570 nm ± standard deviation (SD).

As countermeasure against chronic low-grade inflammation associated to obesity is represented by dietary advice and nutraceuticals (55). Evidences from *in vitro* and experimental models suggest the effects of polyphenols on obesity, obesity-related inflammation, and other metabolic disorders. Their effects include: to induce satiety, to stimulate energy expenditure by inducing thermogenesis in brown adipose tissue, to inhibit adipocyte differentiation and promote adipocyte apoptosis, to modulate lipolysis and activate oxidation (56). Evidence for the effects of polyphenols on obesity and weight control in adult subjects is inconsistent due to the heterogeneity among study populations, intervention period, and polyphenol supplements (57). At the best of our knowledge, there are no studies about the effects of polyphenols extracts on childhood obesity and its comorbidities.

The innovative aspect of this study is related to the inhibition of the spontaneous osteoclastogenesis and reduction of TNFα mRNA levels in PBMC cultures from obese children with the use of polyphenol-rich cherry extracts. This inhibitory effect has been observed with all the three cultivars of sweet cherries, although the content of the phenolic compounds appeared slightly lesser in the extract of Giorgia than Bigarreu and Ferrovia, even though both the three varieties were principally characterized by anthocyanins, especially cyanidin-3O-rutinoside, and chlorogenic acids. These polyphenols' compounds play an important role as antioxidants for bone health, both in young people, in order to favor the formation of peak bone mass, and in the elderly and in menopausal women in order to prevent bone loss. Moreover, the use of these antioxidant compounds has been proposed in anti-resorption therapies considering also that they are able to reduce the OC activity without determining their apoptosis, which is useful to restore physiological bone remodeling (58). Consistently, it has been reported that tea and dried plum polyphenols *in vitro* inhibited osteoclastogenesis (29, 59). Of note, it has also been demonstrated the inhibitory effects of sweet cherry anthocyanins on obesity development in HFD fed mice, by slowing down TNFα and IL-6 levels (60). However, this study did not evaluate the effect on bone, which is known to be negatively affected by obesity as well as by HFD. Conversely, Shen et al., reported that in rats green tea polyphenols improved bone health in HFD-induced obesity by the suppression of bone cell activity (61, 62). Although the positive effect of green tea administration in obese patients has been evaluated in different studies [revised in Suzuki et al. (63)], there were not published data on bone effects. These literature reports together with our findings let us to speculate

that also sweet cherry polyphenols can have a protective effect on bone both in HFD fed mice and obese patients.

CONCLUSIONS

Our study, to our knowledge, is the first demonstrating in obese children a spontaneous osteoclastogenesis inhibited by polyphenols from sweet cherry extracts, through the reduction of TNFα, without affecting cell viability. We also demonstrated that the spontaneous osteoclastogenesis observed in PBMCs from obese children is supported by the high percentage of circulating $CD14^+/CD16^+$ cells and the elevated levels of RANKL and TNFα. Our study opens future perspectives for the use of cherry extracts, appropriately formulated as nutraceuticals as preventive in healthy children and therapeutic in obese ones.

DATA AVAILABILITY

The datasets generated for this study are available on request to the corresponding author.

ETHICS STATEMENT

All the enrolled patients signed an informed consent form. The local ethic committee approved the study. The study was conducted in accordance to the criteria of the declaration of Helsinki.

AUTHOR CONTRIBUTIONS

GB, MF, and FC developed the concept and designed the experiments. GC performed most experiments and analyzed data. LP performed cell cultures and ELISA. SB and GS performed flow cytometry. MF and GD provided patients' samples and clinical data. FC, ACi, ACo, GM, MC, PC, and CF developed the chemical part of the paper. GB, MF, FC, and MC wrote the manuscript and all other authors commented on the manuscript.

FUNDING

This work was supported by EU through the Regione Puglia: Avviso aiuti a sostegno dei Cluster Tecnologici Regionali per l'Innovazione—Progetto: PERFORM TECH (PUGLIA EMERGING FOOD TECHNOLOGY)—La sicurezza alimentare mediante l'impiego di tecnologie emergenti per l'elaborazione di prodotti funzionali, recupero di sostanze nutraceutiche dai sottoprodotti e valorizzazione energetica degli scarti (grant number LPIJ9P2).

SUPPLEMENTARY MATERIAL

The Supplementary Material for this article can be found online at: https://www.frontiersin.org/articles/10.3389/fimmu.2019.01001/full#supplementary-material

REFERENCES

1. Faienza MF, Acquafredda A, Tesse R, Luce V, Ventura A, Maggialetti N, et al. Risk factors for subclinical atherosclerosis in diabetic and obese children. *Int J Med Sci*. (2013) 10:338–43. doi: 10.7150/ijms.5181
2. Styne DM, Arslanian SA, Connor EL, Farooqi IS, Murad MH, Silverstein JH, et al. Pediatric obesity-assessment, treatment, and prevention: an endocrine society clinical practice guideline. *J Clin Endocrinol Metab*. (2017) 102:709–57. doi: 10.1210/jc.2017-00561
3. Cao JJ. Effects of obesity on bone metabolism. *J Orthop Surg Res*. (2011) 6:30. doi: 10.1186/1749-799X-6-30
4. Dimitri P. Fat and bone in children - where are we now? *Ann Pediatr Endocrinol Metab*. (2018) 23:62–9. doi: 10.6065/apem.2018.23.2.62
5. Rana AR, Michalsky MP, Teich S, Groner JI, Caniano DA, Schuster DP. Childhood obesity: a risk factor for injuries observed at a level-1 trauma center. *J Pediatr Surg*. (2009) 44:1601–5. doi: 10.1016/j.jpedsurg.2008.11.060
6. Shu L, Beier E, Sheu T, Zhang H, Zuscik MJ, Puzas EJ. High-fat diet causes bone loss in young mice by promoting osteoclastogenesis through alteration of the bone marrow environment. *Calcif Tissue Int*. (2015) 96:313–23. doi: 10.1007/s00223-015-9954-z
7. Dar HY, Azam Z, Anupam R, Mondal RK, Srivastava RK. Osteoimmunology: the Nexus between bone and immune system. *Front Biosci*. (2018) 23:464–92. doi: 10.2741/4600
8. Fan Y, Hanai JI, Le PT, Bi R, Maridas D, DeMambro V, et al. Parathyroid hormone directs bone marrow mesenchymal cell fate. *Cell Metab*. (2017) 25:661–72. doi: 10.1016/j.cmet.2017.01.001
9. Lam J, Takeshita S, Barker JE, Kanagawa O, Ross FP, Teitelbaum SL. TNF-alpha induces osteoclastogenesis by direct stimulation of macrophages exposed to permissive levels of RANK ligand. *J Clin Invest*. (2000) 106:1481–8. doi: 10.1172/JCI11176
10. Brunetti G, Papadia F, Tummolo A, Fischetto R, Nicastro F, Piacente L, et al. Impaired bone remodeling in children with osteogenesis imperfecta treated and untreated with bisphosphonates: the role of DKK1, RANKL, and TNF-α. *Osteoporos Int*. (2016) 27:2355–65. doi: 10.1007/s00198-016-3501-2
11. D'Amelio P, Grimaldi A, Pescarmona GP, Tamone C, Roato I, Isaia G. Spontaneous osteoclast formation from peripheral blood mononuclear cells in postmenopausal osteoporosis. *FASEB J*. (2005) 19:410–2. doi: 10.1096/fj.04-2214fje
12. Ritchlin CT, Haas-Smith SA, Li P, Hicks DG, Schwarz EM. Mechanisms of TNF-alpha- and RANKL-mediated osteoclastogenesis and bone resorption in psoriatic arthritis. *J Clin Invest*. (2003) 111:821–31. doi: 10.1172/JCI16069
13. Arslan N, Erdur B, Aydin A. Hormones and cytokines in childhood obesity. *Indian Pediatr*. (2010) 47:829–39. doi: 10.1007/s13312-010-0142-y
14. Faienza MF, Francavilla R, Goffredo R, Ventura A, Marzano F, Panzarino G, et al. Oxidative stress in obesity and metabolic syndrome in children and adolescents. *Horm Res Paediatr*. (2012) 78:158–64. doi: 10.1159/000342642
15. Kraakman MJ, Murphy AJ, Jandeleit-Dahm K, Kammoun HL. Macrophage polarization in obesity and type 2 diabetes: weighing down our understanding of macrophage function? *Front Immunol*. (2014) 5:470. doi: 10.3389/fimmu.2014.00470
16. Goran MI, Alderete TL. Targeting adipose tissue inflammation to treat the underlying basis of the metabolic complications of obesity. *Nestle Nutr Inst Work Ser*. (2012) 73:49–60. doi: 10.1159/000341287
17. Abramson JL, Vaccarino V. Relationship between physical activity and inflammation among apparently healthy middle-aged and older US adults. *Arch Intern Med*. (2002) 162:1286–92. doi: 10.1001/archinte.162.11.1286
18. Geffken DF, Cushman M, Burke GL, Polak JF, Sakkinen PA, Tracy RP. Tracy association between physical activity and markers of inflammation in a healthy elderly population. *Am J Epidemiol*. (2001) 153:242–50. doi: 10.1093/aje/153.3.242
19. Pischon T, Hankinson SE, Hotamisligil GS, Rifai N, Rimm EB. Leisure-time physical activity and reduced plasma levels of obesity-related inflammatory markers. *Obes Res*. (2003) 11:1055–64. doi: 10.1038/oby.2003.145

20. Siriwardhana N, Kalupahana NS, Cekanova M, LeMieux M, Greer B, Moustaid-Moussa N. Modulation of adipose tissue inflammation by bioactive food compounds. *J Nutr Biochem*. (2013) 24:613–23. doi: 10.1016/j.jnutbio.2012.12.013
21. Kalupahana NS, Claycombe KJ, Moustaid-Moussa N. (n-3) Fatty acids alleviate adipose tissue inflammation and insulin resistance: mechanistic insights. *Adv Nutr*. (2011) 2:304–16. doi: 10.3945/an.111.000505
22. Picariello G, De Vito V, Ferranti P, Paolucci M, Volpe M. Species- and cultivar-dependent traits of Prunus avium and Prunus cerasus polyphenols. *J Food Comp Anal*. (2016) 40:50–7. doi: 10.1016/j.jfca.2015.10.002
23. Girelli CR, De Pascali SA, Del Coco L, Fanizzi FP. Metabolic profile comparison of fruit juice from certified sweet cherry trees (Prunus avium L.) of Ferrovia and Giorgia cultivars: a preliminary study. *Food Res Int*. (2016) 90:281–7. doi: 10.1016/j.foodres.2016.11.014
24. Yigit D, Baydas E, Güleryüz M. Elemental analysis of various cherry fruits by wavelength dispersive X-ray fluorescence spectrometry. *Asian J Chem*. (2009) 21:2935–42.
25. Schmitz-Eiberger MA, Blanke MM. Bioactive components in forced sweet cherry fruit (Prunus avium L.), antioxidative capacity and allergenic potential as dependent on cultivation under cover. *LWT Food Sci Technol*. (2012) 46:388–92. doi: 10.1016/j.lwt.2011.12.015
26. Kelley DS, Adkins Y, Laugero KD. A review of the health benefits of cherries. *Nutrients*. (2018) 10:E368. doi: 10.3390/nu10030368
27. Faienza MF, Ventura A, Delvecchio M, Fusillo A, Piacente L, Aceto G, et al. High sclerostin and Dickkopf-1 (DKK-1) serum levels in children and adolescents with type 1 diabetes mellitus. *J Clin Endocrinol Metab*. (2017) 102:1174–81. doi: 10.1210/jc.2016-2371
28. Mori G, Brunetti G, Colucci S, Ciccolella F, Coricciati M, Pignataro P, et al. Alteration of activity and survival of osteoblasts obtained from human periodontitis patients: role of TRAIL. *J Biol Regul Homeost Agents*. (2007) 21:105–14.
29. Oka Y, Iwai S, Amano H, Irie Y, Yatomi K, Ryu K, et al. Tea polyphenols inhibit rat osteoclast formation and differentiation. *J Pharmacol Sci*. (2012) 118:55–64. doi: 10.1254/jphs.11082FP
30. Snyder SM, Zhao B, Luo T, Kaiser C, Cavender G, Hamilton-Reeves J, et al. Consumption of quercetin and quercetin-containing apple and cherry extracts affects blood glucose concentration, hepatic metabolism, and gene expression patterns in obese C57BL/6J high fat-fed mice. *J Nutr*. (2016) 146:1001–7. doi: 10.3945/jn.115.228817
31. Crupi P, Genghi R, Antonacci D. In-time and in-space tandem mass spectrometry to determine the metabolic profiling of flavonoids in a typical sweet cherry (Prunus avium L.) cultivar from Southern Italy. *J Mass Spectrom*. (2014) 49:1025–34. doi: 10.1002/jms.3423
32. Crupi P, Bleve G, Tufariello M, Corbo F, Clodoveo ML, Tarricone L. Comprehensive identification and quantification of chlorogenic acids in sweet cherry by tandem mass spectrometry techniques. *J Food Comp Anal*. (2018) 73:103–11. doi: 10.1016/j.jfca.2018.06.013
33. Ugur-Altun B, Altun A, Gerenli M, Tugrul A. The relationship between insulin resistance assessed by HOMA-IR and serum osteoprotegerin levels in obesity. *Diabetes Res Clin Pract*. (2005) 68:217–22. doi: 10.1016/j.diabres.2004.10.011
34. Holecki M, Zahorska-Markiewicz B, Janowska J, Nieszporek T, Wojaczynska-Stanek K, Zak-Golab A, et al. The influence of weight loss on serum osteoprotegerin concentration in obese perimenopausal women. *Obesity*. (2007) 15:1925–9. doi: 10.1038/oby.2007.229
35. Erol M, Bostan Gayret O, Tekin Nacaroglu H, Yigit O, Zengi O, Salih Akkurt M, et al. Association of osteoprotegerin with obesity, insulin resistance and non-alcoholic fatty liver disease in children. *Iran Red Crescent Med J*. (2016) 18:e41873. doi: 10.5812/ircmj.41873
36. Gannage-Yared MH, Fares F, Semaan M, Khalife S, Jambart S. Circulating osteoprotegerin is correlated with lipid profile, insulin sensitivity, adiponectin and sex steroids in an ageing male population. *Clin Endocrinol*. (2006) 64:652–8. doi: 10.1111/j.1365-2265.2006.02522.x
37. Gannagé-Yared MH, Yaghi C, Habre B, Khalife S, Noun R, Germanos-Haddad M, et al. Osteoprotegerin in relation to body weight, lipid parameters insulin sensitivity, adipocytokines, and C-reactive protein in obese and non-obese young individuals: results from both cross-sectional and interventional study. *Eur J Endocrinol*. (2008) 158:353–9. doi: 10.1530/EJE-07-0797
38. Kotanidou EP, Kotanidis CP, Giza S, Serbis A, Tsinopoulou VR, Karalazou P, et al. Osteoprotegerin increases parallel to insulin resistance in obese adolescents. *Endocr Res*. (2018) 44:1–7. doi: 10.1080/07435800.2018.1480630
39. Sulibursk J, Bogdanski P, Gajewska E, Kalmus G, Sobieska M, Samborski W. The association of insulin resistance with serum osteoprotegerin in obese adolescents. *J Physiol Biochem*. (2013) 69:847–53. doi: 10.1007/s13105-013-0261-8
40. Serrano-Piña R, Trujillo-Güiza ML, Scougall Vilchis RJ, Layton-Tovar CF, Mendieta-Zerón H. sRANKL and its correlation with metabolic syndrome parameters in children. *Int J Paediatr Dent*. (2018) 28:633–40. doi: 10.1111/ipd.12422
41. Ventura A, Brunetti G, Colucci S, Oranger A, Ladisa F, Cavallo L, et al. Glucocorticoid-induced osteoporosis in children with 21-hydroxylase deficiency. *Biomed Res Int*. (2013) 2013:250462. doi: 10.1155/2013/250462
42. Brunetti G, Marzano F, Colucci S, Ventura A, Cavallo L, Grano M, et al. Genotype-phenotype correlation in juvenile Paget disease: role of molecular alterations of the TNFRSF11B gene. *Endocrine*. (2012) 42:266–71. doi: 10.1007/s12020-012-9705-0
43. Terpos E, Ntanasis-Stathopoulos I, Gavriatopoulou M, Dimopoulos MA. Pathogenesis of bone disease in multiple myeloma: from bench to bedside. *Blood Cancer J*. (2018) 8:7. doi: 10.1038/s41408-017-0037-4
44. Faienza MF, Chiarito M, D'Amato G, Colaianni G, Colucci S, Grano M, et al. Monoclonal antibodies for treating osteoporosis. *Expert Opin Biol Ther*. (2018) 18:149–57. doi: 10.1080/14712598.2018.1401607
45. de Vries TJ, El Bakkali I, Kamradt T, Schett G, Jansen IDC, D'Amelio P. What are the peripheral blood determinants for increased osteoclast formation in the various inflammatory diseases associated with bone loss? *Front Immunol*. (2019) 10:505. doi: 10.3389/fimmu.2019.00505
46. Wong KL, Yeap WH, Tai JJ, Ong SM, Dang TM, Wong SC. The three human monocyte subsets: implications for health and disease. *Immunol Res*. (2012) 53:41–57. doi: 10.1007/s12026-012-8297-3
47. Chiu YG, Shao T, Feng C, Mensah KA, Thullen M, Schwarz EM, et al. CD16 (FcRgammaIII) as a potential marker of osteoclast precursors in psoriatic arthritis. *Arthritis Res Ther*. (2010) 12:R14. doi: 10.1186/ar2915
48. Bolzoni M, Ronchetti D, Storti P, Donofrio G, Marchica V, Costa F, et al. IL21R expressing CD14+CD16+ monocytes expand in multiple myeloma patients leading to increased osteoclasts. *Haematologica*. (2017) 102:773–84. doi: 10.3324/haematol.2016.153841
49. Ootsuka T, Nakanishi A, Tsukamoto I. Increase in osteoclastogenesis in an obese Otsuka Long-Evans Tokushima fatty rat model. *Mol Med Rep*. (2015) 12:3874–80. doi: 10.3892/mmr.2015.3811
50. Singer K, Lumeng CN. The initiation of metabolic inflammation in childhood obesity. *J Clin Invest*. (2017) 127:65–73. doi: 10.1172/JCI88882
51. Martí A, Marcos A, Martínez JA. Obesity and immune function relationships. *Obes Rev*. (2001) 2:131–40. doi: 10.1046/j.1467-789x.2001.00025.x
52. Dedoussis GV, Kapiri A, Samara A, Dimitriadis D, Lambert D, Pfister M, et al. Expression of inflammatory molecules and associations with BMI in children. *Eur J Clin Invest*. (2010) 40:388–92. doi: 10.1111/j.1365-2362.2010.02277.x
53. Reinehr T, Stoffel-Wagner B, Roth CL, Andler W. High-sensitive C-reactive protein, tumor necrosis factor alpha, and cardiovascular risk factors before and after weight loss in obese children. *Metabolism*. (2005) 54:1155–61. doi: 10.1016/j.metabol.2005.03.022
54. Yao Z, Li P, Zhang Q, Schwarz EM, Keng P, Arbini A, et al. Tumor necrosis factor-alpha increases circulating osteoclast precursor numbers by promoting their proliferation and differentiation in the bone marrow through up-regulation of c-Fms expression. *J Biol Chem*. (2006) 281:11846–55. doi: 10.1074/jbc.M512624200
55. Yarla NS, Polito A, Peluso I. Effects of olive oil on TNF-α and IL-6 in humans: implication in obesity and frailty. *Endocr Metab Immune Disord Drug Targets*. (2018) 18:63–74. doi: 10.2174/1871530317666171120150329
56. Rupasinghe HPV, Sekhon-Loodu S, Mantso T, Panayiotidis MI. Phytochemicals in regulating fatty acids -oxidation: potential underlying mechanisms and their involvement in obesity and weight loss. *Pharmacol Ther*. (2016) 165:153–63. doi: 10.1016/j.pharmthera.2016.06.005
57. Castro-Barquero S, Lamuela-Raventós RM, Doménech M, Estruch R. Relationship between mediterranean dietary polyphenol intake and obesity. *Nutrients*. (2018) 10:1523. doi: 10.3390/nu10101523

58. Domazetovic V, Marcucci G, Iantomasi T, Brandi ML, Vincenzini MT. Oxidative stress in bone remodeling: role of antioxidants. *Clin Cases Miner Bone Metab*. (2017) 14:209–16. doi: 10.11138/ccmbm/2017.14.1.209
59. Bu SY, Lerner M, Stoecker BJ, Boldrin E, Brackett DJ, Lucas EA, et al. Dried plum polyphenols inhibit osteoclastogenesis by downregulating NFATc1 and inflammatory mediators. *Calcif Tissue Int*. (2008) 82:475–88. doi: 10.1007/s00223-008-9139-0
60. Wu T, Tang Q, Yu Z, Gao Z, Hu H, Chen W, et al. Inhibitory effects of sweet cherry anthocyanins on the obesity development in C57BL/6 mice. *Int J Food Sci Nutr*. (2014) 65:351–9. doi: 10.3109/09637486.2013.854749
61. Shen CL, Chyu MC, Cao JJ, Yeh JK. Green tea polyphenols improve bone microarchitecture in high-fat-diet-induced obese female rats through suppressing bone formation and erosion. *J Med Food*. (2013) 16:421–7. doi: 10.1089/jmf.2012.0199
62. Shen CL, Han J, Wang S, Chung E, Chyu MC, Cao JJ. Green tea supplementation benefits body composition and improves bone properties in obese female rats fed with high-fat diet and caloric restricted diet. *Nutr Res*. (2015) 35:1095–105. doi: 10.1016/j.nutres.2015.09.014
63. Suzuki T, Pervin M, Goto S, Isemura M, Nakamura Y. Beneficial effects of tea and the green tea catechin epigallocatechin-3-gallate on obesity. *Molecules*. (2016) 21:E1305. doi: 10.3390/molecules21101305

Conflict of Interest Statement: The authors declare that the research was conducted in the absence of any commercial or financial relationships that could be construed as a potential conflict of interest.

frontiers in Immunology

ORIGINAL RESEARCH
published: 28 May 2019
doi: 10.3389/fimmu.2019.01164

Activation of Shc1 Allows Oncostatin M to Induce RANKL and Osteoclast Formation More Effectively Than Leukemia Inhibitory Factor

Emma Persson[1†‡], Pedro P. C. Souza[2,3†], Thais Floriano-Marcelino[2], Howard Herschel Conaway[4], Petra Henning[5] and Ulf H. Lerner[1,5]*

[1] Department of Molecular Periodontology, Umeå University, Umeå, Sweden, [2] Bone Biology Research Group, Department of Physiology and Pathology, School of Dentistry, São Paulo State University (UNESP), Araraquara, Brazil, [3] School of Dentistry, Federal University of Goiás, Goiânia, Brazil, [4] Department of Physiology and Biophysics, University of Arkansas for Medical Sciences, Little Rock, AR, United States, [5] Department of Internal Medicine and Clinical Nutrition, Centre for Bone and Arthritis Research, Institute for Medicine, Sahlgrenska Academy, University of Gothenburg, Gothenburg, Sweden

Background and Purpose: The gp130 family of cytokines signals through receptors dimerizing with the gp130 subunit. Downstream signaling typically activates STAT3 but also SHP2/Ras/MAPK pathways. Oncostatin M (OSM) is a unique cytokine in this family since the receptor (OSMR) activates a non-redundant signaling pathway by recruitment of the adapter Shc1. We have studied the functional relevance of Shc1 for OSM-induced bone resorption.

Experimental Approach: Osteoblasts were stimulated with OSM and STAT3 and Shc1 activations were studied using real-time PCR and Western blots. The role of STAT3 and Shc1 for OSM-induced RANKL expression and osteoclast formation was studied by silencing their mRNA expressions. Effects of OSM were compared to those of the closely related cytokine leukemia inhibitory factor (LIF).

Key Results: OSM, but not LIF, induced the mRNA and protein expression of Shc1 and activated phosphorylation of Shc1 in the osteoblasts. Silencing of Shc1 decreased OSM-induced activation of STAT3 and RANKL expression. Silencing of STAT3 had no effect on activation of Shc1, but prevented the OSM-mediated increase of RANKL expression. Silencing of either Shc1 or STAT3 in osteoblasts decreased formation of osteoclasts in OSM-stimulated co-cultures of osteoblasts and macrophages. In agreement with these observations, OSM was a more potent and robust stimulator than LIF of RANKL formation and bone resorption in mouse calvariae and osteoclast formation in bone marrow cultures.

Conclusions and Implications: Activation of the Shc1-dependent STAT3 signaling is crucial for OSM-induced osteoclast formation. Inhibition of Shc1 is a potential mechanism to specifically inhibit OSM-induced bone resorption.

Keywords: OSM, LIF, RANKL, Shc1, osteoclast, bone resorption

OPEN ACCESS

Edited by:
Claudine Blin-Wakkach, UMR7370 Laboratoire de Physio Médecine Moléculaire (LP2M), France

Reviewed by:
Julian M. W. Quinn, Garvan Institute of Medical Research, Australia
Kim Henriksen, Nordic Bioscience, Denmark
Nicos Anthony Nicola, Walter and Eliza Hall Institute of Medical Research, Australia

***Correspondence:**
Ulf H. Lerner
ulf.lerner@gu.se

[†] These authors have contributed equally to this work

[‡] Present Address:
Emma Persson, Department of Radiation Sciences, Umeå University, Umeå, Sweden

Specialty section:
This article was submitted to Inflammation, a section of the journal Frontiers in Immunology

Received: *28 February 2019*
Accepted: *08 May 2019*
Published: *28 May 2019*

Citation:
Persson E, Souza PPC, Floriano-Marcelino T, Conaway HH, Henning P and Lerner UH (2019) Activation of Shc1 Allows Oncostatin M to Induce RANKL and Osteoclast Formation More Effectively Than Leukemia Inhibitory Factor. Front. Immunol. 10:1164. doi: 10.3389/fimmu.2019.01164

INTRODUCTION

Oncostatin M (OSM) belongs to the gp130 family of cytokines. It was discovered as a cytokine released from macrophage differentiated U-937 histiocytic lymphoma cells that inhibited proliferation of melanoma cells (1). OSM has also been reported to be expressed in monocytes, dendritic cells, T-cells, neutrophils (2), intestinal stromal cells (3), osteoblasts (4, 5) and osteocytes (5). Several studies have shown that OSM is involved in a wide variety of functions (2, 6), including bone remodeling (7), embryologic development, liver regeneration, haematopoiesis (8), tumorigenic progression and metastasis formation (9, 10), as well as inflammatory processes such as pulmonary fibrosis (11, 12), asthma (13), inflammatory bowel disease (3), periodontal disease (14), rheumatoid arthritis (15) and neurogenic heterotopic ossifications (16).

Cytokines in the gp130 family bind to cell surface receptor (R) subunits, and the ligand-receptor complex interacts with the transmembrane protein gp130 for signal propagation. Activation of the OSMR triggers heterodimerization between the ligand-receptor complex and one gp130 subunit (2). Human OSM can induce signaling through both the OSMR and the receptor for leukemia inhibitory factor (LIF), a closely related cytokine in the gp130 family, whereas mouse OSM acts mainly through the OSMR:gp130 heterodimer (2, 6), although it has been shown that mouse OSM can stimulate bone formation by decreasing sclerostin expression after LIFR-induced activation of STAT3 (5).

OSM stimulates bone resorption in organ cultures (17) and enhances osteoclast formation in crude bone marrow cell cultures (18, 19), effects which are associated with increased expression of receptor activator of NF-κB ligand (RANKL) (17, 18). Interestingly, OSM is more potent and effective than LIF as a stimulator of osteoclast formation in co-cultures of mouse osteoblasts and bone marrow cells (20). The bone phenotype of mice in which the *Osm* gene has been deleted has not been reported, but mice globally deficient in the *Osmr* have increased bone mass and a decreased number of osteoclasts (5), findings which are in agreement with *in vitro* observations showing OSM increasing osteoclast numbers and stimulating bone resorption.

The OSMR has no intrinsic tyrosine kinase activity, but dimerization with gp130 activates the JAK-STAT (Janus kinase and signal transducer and activator of transcription) pathway. JAKs are constitutively connected to the membrane-proximal regions of gp130 and OSMR and, upon activation, JAKs trans-phosphorylate several Tyr residues in the intracellular domains of gp130 and OSMR. In the mouse OSMR, JAK2 is preferentially bound and its activation leads to phosphorylation of Tyr^{917} and Tyr^{945} in the OSMR and subsequent recruitment of the transcription factor STAT3 (21, 22). Recruitment of STAT3 to gp130 is mediated by JAK-dependent phosphorylation of Tyr^{767}/Tyr^{814}/Tyr^{905}/Tyr^{915} (23). Once phosphorylated by JAKs, activated STAT3 dimers translocate to the nucleus and bind to specific DNA sequences in promoter regions of a variety of target genes. JAK-dependent phosphorylation of Tyr^{759} in gp130 results in recruitment and activation of the tyrosine phosphatase SHP-2 [Src homology region 2-containing protein tyrosine phosphatase 2; (24)]. In turn, SHP-2 then forms a complex with Grb2 (growth factor receptor-binding protein 2) and Sos (Son of sevenless), which activates the Ras/Raf/MAPK pathway (25), a hallmark of many haematopoietic cytokine receptors.

A non-redundant signaling pathway distinguishing OSMR from the other receptors in the gp130 family of cytokines is recruitment of the adapter protein Shc1 (Src homology and collagen 1) to Tyr^{861} (26, 27). Shc proteins are phosphotyrosine adapters which link activated transmembrane receptors to downstream signaling cascades (28). Four members of this family have been described, designated Shc1, Shc2, Shc3 and Shc4. Three isoforms of Shc1 protein generated by differential promoter usage (p66) or alternative translational initiation (p46, p52) have been discovered. Shc1 contains both phosphotyrosine binding domains (PTB) and SH2 domains and is able to recruit the Ras/Raf/MAPK adapter Grb2 to the SH2 domain. Phosphorylation of the OSMR on Tyr^{861} allows binding of activated Shc1 to the OSMR, recruitment of Grb2 and subsequent induction of a Ras-dependent kinase cascade, which results in activation of MAPK (26). This is different from the LIF-induced activation of MAPK, where recruitment of SHP-2 to the gp130 subunit in the LIFR mediates activation of MAPK (2). Since OSMR lacks the recruitment motif for SHP-2, activation of Shc1 substitutes for SHP-2 mediated activation of the MAPK caused by the closely related LIFR, but the functional relevance of OSMR-Shc1 in bone has not been investigated. Interestingly, activation of Shc1 has also recently been shown to potentiate STAT3 phosphorylation in breast cancer cells (29), but a role for the OSMR-Shc1-STAT3 axis in osteoblasts has not been assessed.

The aim of the present study was to investigate the importance of the Shc1-STAT3 signaling pathway in OSM-induced RANKL formation in osteoblasts and subsequent osteoclast formation.

Abbreviations: AMV, avian myeloblastosis virus; BMM, bone marrow macrophages; BMC, bone marrow cells; BMP-2, bone morphogenetic protein-2; D3, $1,25(OH)_2$-vitamin D3; EMSA, electrophoretic mobility shift assay; GAPDH, glyceraldehyde-3-phosphate dehydrogenase; gp130, glycoprotein 130; Grb2, Growth factor receptor-binding protein 2; IL, interleukin; JAK, Janus kinase; LIF, leukemia inhibitory factor; LIFR, LIF receptor; MAPK, mitogen-activated protein kinase; M-CSF, macrophage colony-stimulating factor; OPG, osteoprotegerin; OSM, oncostatin M; OSMR, OSM receptor; PTB, phosphotyrosine binding domain; PTH, parathyroid hormone; RANKL, receptor activator of NF-κB ligand; SH2, Src homology 2; Shc, Src homology and collagen; SHP-2, SH2 domain-containing tyrosine phosphatase 2; Sos, Son of sevenless; STAT, signal transducer and activator of transcription; TRAP, tartrate-resistant acid phosphatase; $TRAP^+$MuOCL, $TRAP^+$ multinucleated osteoclasts.

MATERIALS AND METHODS

Materials

Recombinant mouse LIF, mouse OSM, bone morphogenetic protein-2 (BMP-2), macrophage colony-stimulating factor (M-CSF), RANKL (amino acids 158–316; cat. no. 462-TEC) and the ELISA kits for mouse RANKL and mouse OPG were purchased from R&D Systems, Abingdon, UK; bacterial collagenase type I from Worthington Biochemical Corp., Lakewood, NJ, USA; α-MEM, FBS, L-glutamine, and oligonucleotide

primers from Invitrogen, Stockholm, Sweden; RNAqueous®-4PCR RNA isolation kit from Ambion, Inc., Austin TX, USA; 1st strand cDNA synthesis Kit and PCR Core Kit from Roche, Mannheim, Germany; DYEnamic ET terminator cycle sequencing kit from GE Healthcare, Uppsala, Sweden; QIAquick PCR Purification kit was from Qiagen Ltd., Crawley, West Sussex, England; TaqMan Universal PCR Master Mix and TaqMan probes from Applied Biosystems, Foster City, CA, USA; all primary and secondary antibodies used are specified in **Supporting Information Table I**; anti-IgG-HRP secondary antibodies used for Western blot were from Santa Cruz Biotechnology, Inc., Santa Cruz, CA, USA; culture dishes and multi-well plates from Costar, Cambridge, MA, USA, or Nunc International Corp., Naperville, IL, USA. Indomethacin was kindly supplied by Merck, Sharp & Dohme, Haarlem, the Netherlands; the mouse bone marrow stromal cell line ST-2 from Riken BRC Cell Bank (www.brc.riken.go.jp).

Animals

CsA mice from the inbred colony at Umeå University, Swiss mice from the School of Dentistry at Araraquara and C57Bl/6 mice from the University of Gothenburg were used for isolation of calvarial osteoblasts, bone marrow cells or calvarial bone explants. The Institutional Animal Care and Ethics Committees at Umeå University, at the School of Dentistry, Araraquara and at the University of Gothenburg approved all experimental studies. The observation that OSM is a more robust stimulator than LIF of *Tnfsf11* (encoding RANKL) mRNA expression was made in cells from all three genotypes; OSM-induced phosphorylation of Shc1 was assessed in cells from CsA and Swiss mice and found to activate Shc1 in both strains.

Bone Resorption Bioassay

Bone resorption was assessed in organ culture of parietal bones from 6 to 7 days-old mice by analyzing the release of ^{45}Ca from prelabelled bones as previously described (30, 31). Release of isotope was expressed as the percentage release of the initial amount of isotope (calculated as the sum of radioactivity in medium and bone after culture). The data were recalculated and the results expressed as percent of control that was set at 100%, which allowed for accumulation of data from several experiments.

Isolation and Culture of Mouse Calvarial Osteoblasts

Bone cells were isolated from calvariae harvested from 2 to 5 days-old mice using bacterial collagenase in the modified time sequential enzyme-digestion technique (32). Cells from populations 6 to 10, showing an osteoblastic phenotype as assessed by their cyclic AMP-responsiveness to PTH, expression of alkaline phosphatase, osteocalcin and bone sialoprotein, as well as the capacity to form mineralized bone noduli (data not shown), were used. The cells were seeded in culture flasks containing α-MEM supplemented with 10% FBS, L-glutamine and antibiotics at 37°C in humidified air containing 5% CO_2. After 4 days, the cells were sub-cultured in culture dishes or multi-well plates.

Osteoclast Differentiation in Bone Marrow Cell Cultures

Bone marrow cells (BMC) were flushed from femur and tibiae from 6 week-old mice and seeded in 48 multi-well plates containing α-MEM/10% FBS and incubated overnight. The cells were then cultured in the same medium with or without test substances for 7–9 days. Cells staining positive for tartrate-resistant acid phosphatase (TRAP) and containing three or more nuclei were considered osteoclasts and the number of TRAP-positive multinucleated osteoclasts ($TRAP^+$ MuOCL) was counted.

Osteoclast Differentiation in Bone Marrow Macrophage Cultures

Bone marrow cells from 6 to 12 weeks old mice were isolated and incubated in the presence of M-CSF (30 ng/mL) for 3 days in culture dishes, to which stromal cells and lymphoid cells cannot adhere, as previously described (33, 34). The cells adherent to the bottom of the dishes are devoid of phenotypic markers for stromal cells, T- and B-cells, express CD115/c-Fms (75%) and CD11b/Mac-1 (100%), and were used as bone marrow macrophages (BMM). The BMM cells were seeded in 96 multi-well plates and then incubated in M-CSF (30 ng/mL) or M-CSF + RANKL (30 ng/mL + 4 ng/mL) with or without LIF (100 ng/mL) or OSM (100 ng/mL). Cells staining positive for TRAP and containing three or more nuclei were considered osteoclasts and the number of $TRAP^+$ MuOCL was counted.

Stromal Cells

The ST-2 cells were seeded in multi-well plates and incubated in α-MEM/10% FBS overnight. Following incubation, medium with and without test substances was added and the cells incubated for 24 h for subsequent gene expression analysis.

Gene Silencing in Osteoblasts Using Small Interfering RNA

Calvarial osteoblasts were seeded in multi-well plates with α-MEM supplemented with 10% FBS and antibiotics. For co-culture and gene expression experiments, 10^3 cells were seeded per well in 96-well plates, while for protein extraction, 5×10^4 cells/well were seeded in 12-well plates. After overnight attachment, silencing of *Osmr*, *Lifr, Il6st*, *Shc1* or *Stat3* was performed using Lipofectamine RNAiMAX and 30 nM of the appropriate siRNAs listed in **Supporting Information Table II**. Cells treated with a scrambled (siSCR) sequence served as controls. Forty-eight hours after the first silencing, the protocol was repeated. Twenty-four hours after the second silencing, the cells were incubated in medium containing either vehicle, LIF or OSM. At the end of cultures, RNA or protein was extracted. In some experiments, the osteoblasts were co-cultured with BMMs.

Osteoblast and Bone Marrow Macrophage Co-cultures

Following silencing of *Shc1* or *Stat3* in osteoblasts, $2x10^4$ BMMs were added to each well in 96-well plates containing osteoblasts. The co-cultures were exposed to vehicle or OSM (100 ng/mL)

and 3 days later, the cells were fixed with PBS-buffered 4% paraformaldehyde and stained for TRAP. The number of $TRAP^+$ MuOCL was counted in each well.

RNA Isolation and First-Strand cDNA Synthesis

Total RNA was extracted using commercially available RNA isolation kits (Ambion or Qiagen) by following the manufacturer's protocol. For quantitative real-time polymerase chain reactions, RNA was extracted from a single cell culture well, or from individual bones. For semi-quantitative polymerase chain reactions, RNA extracted from three wells was pooled per treatment group. RNA was reverse transcribed into single-stranded cDNA with a commercially available cDNA synthesis kit using.

Semi-quantitative Polymerase Chain Reaction

Polymerase chain reaction analyses were performed using a standard protocol. The reaction conditions were: denaturing at 94°C for 2 min, annealing for 40 s, and elongation at 72°C for 60 s; in subsequent cycles denaturing was performed at 94°C for 40 s. Reaction conditions for OPG and RANKL were as follows: denaturation at 94°C for 35 s, annealing at 65°C for 35 s, and elongation at 72°C for 60 s for 10 cycles. In subsequent cycles, the primer annealing temperature was decreased stepwise by 5°C every 5 cycles from 65 to 45°C. The primer sequences (forward and reverse, given in the 5′-3′ orientation), expected fragment lengths and annealing temperatures used in PCR are listed in **Supporting Information Table III**. The expressions of the target genes were compared at the logarithmic phase of the PCR reaction. No amplification was detected in samples where the RT reaction had been omitted (data not shown). The PCR products were electrophoretically size fractionated in 1.5% agarose gel and visualized using ethidium bromide. The identity of the PCR products was confirmed using a DYEnamic ET terminator cycle sequencing kit with sequences analyzed on an ABI 377 XL DNA Sequencer (PE Applied Biosystems, Foster City, CA).

Quantitative Real-Time Polymerase Chain Reaction

Quantitative real-time PCR analysis was performed using TaqMan kinetics. In each reaction, cDNA was amplified using a TaqMan Universal PCR Master Mix kit, 300 nmol/L of each primer and 100 nmol/L of probe on an ABI Prism 7900 HT Sequence Detection System (Applied Biosystems, Foster City, CA, USA) or predesigned Taqman Assays and Taqman Fast Advance Master Mix on a StepOnePlus Real-Time PCR system. The primers and probes used are listed in **Supporting Information Tables III, IV**. Gapdh (for BMM) or β-actin or 36B4 (for BMC and calvarial osteoblasts) were used as internal standard to correct for differences in starting mRNA concentrations.

Protein Analyses of RANKL and OPG

The protein levels of RANKL and OPG in calvarial bones were analyzed using commercially available ELISA kits. Calvarial cells were lysed using 0.2% Triton X-100 and the extracted samples were analyzed by following the manufacturer's protocol.

Preparation of Total Cell Lysates

Calvarial osteoblasts were seeded in 60 cm^2 dishes at a density of 2×10^4 cells/cm^2. After 3 days of culture with one media change, the cells were incubated in the absence (control) or presence of test substances for different time periods. Following incubation, the cells were washed twice in PBS before addition of lysis buffer (1% Igepal CA-630, 0.1% SDS, 2 mM EDTA, 50 mM NaF, 0.1 mg/mL PMSF, 10 μg/mL leupeptin, 10 μg/mL pepstatin A, in PBS). The dishes were kept on ice for 15 min followed by scraping and collection of cell lysates. Before use in Western blot, cell lysates were concentrated using Microcon centrifugal filter devices according to manufacturer's recommendations. Protein concentration of the cell lysates was measured using the BCA method with bovine albumin as standard.

Western Blot Analysis

For Western blot analysis, cell lysates pooled from three culture dishes were mixed with sample buffer (200 mM Tris-HCl, pH 6.7, 20% glycerol, 10% β-mercaptoethanol, 5% SDS, 0.01% Pyronin Y) and boiled for 3 min. Protein samples were then loaded on 4–12% Tris-HCl polyacrylamide gels and electrophoresis was performed according to the Laemmli method. Electrophoretically separated proteins were then blotted onto a PVDF membrane which was blocked (5% BSA in TBS) overnight. For detection, the membrane was incubated with primary antibody overnight in 1% BSA/PBS in dilutions specified in **Supporting Information Table I**. Three times 10 min of wash in TBS with 0.05% Tween-20 (TBST) was followed by incubation with HRP-conjugated secondary antibody (1:5,000 in 1% BSA, 0.05% Tween-20 in TBS) for 60 min at room temperature. Finally, the membrane was washed extensively with TBST and TBS followed by development using a chemiluminescence detection kit according to manufacturer's protocol.

Preparation of Nuclear Extracts

Calvarial osteoblasts were plated at a density of 2 x 10^4 cells/cm^2 in culture dishes (60 cm^2) containing α-MEM with 10% FBS, L-glutamine and antibiotics. After 4 days with one media change, the cells were incubated in the absence (control) or presence of test substances for 30 min. Following incubation, the cells were washed with ice cold PBS and scraped. Cell suspensions from two culture dishes were pooled and centrifuged briefly and pelleted cells homogenized in lysis buffer A (10 mM HEPES, pH 7.9, 0.1 mM EDTA, 10 mM KCl, 625 μg/mL spermidine, 625 μg/mL spermine, 0.5 mM DTT, 0.5 mM PMSF, 1 μg/mL leupeptin, 1 μg/mL pepstatin A). After 15 min on ice, Igepal CA-630 was added to a final concentration of 0.5%. The nuclei were collected by centrifugation at 12 000 x g for 2 min, and pelleted nuclei were lysed by incubation for 30 min on ice in lysis buffer B (20 mM HEPES, pH 7.9, 0.2 mM EDTA, 0.42 M NaCl, 25% glycerol, 625 μg/mL spermidine, 625 μg/mL spermine, 0.5 mM DTT, 0.5 mM PMSF, 1 μg/mL leupeptin, 1 μg/mL pepstatin A). Supernatants were collected by centrifugation at 16 000 x g for 10 min. The protein concentration of the samples was determined by the

Bradford method and aliquots were stored at −80°C until use in electrophoretic mobility shift assays (EMSAs).

EMSA

Consensus oligonucleotides including an AP-1 site (CGCTTG ATGACTCAGCCGGAA) and a κB site (AGTTGAGGGGAC TTTCCCAGGC) were end-labeled with [γ-^{32}P] ATP using T4 kinase according to manufacturer's instructions. Mutated forms of the AP-1 (CGCTTGATGACTCCGGAA) and NF-κB (AGT TGAGGGACTTTCCCAGGC) oligonucleotides were used in competition studies. Annealing of complementary strands of both labeled and unlabelled oligonucleotides was performed before used in electrophoretic mobility shift assay (EMSA). Reaction mixtures containing 8 μg of nuclear extract, 0.5–1 ng of probe (50 000 cpm), 4 μg poly(dI-dC)•poly(dI-dC), 20 nM DTT, and reaction buffer (50 mM Tris-HCl, pH 7.5, 0.25 M NaCl, 5 mM EDTA, 25% glycerol) were incubated at room temperature for 30 min. In antibody supershifts and competition studies, 2 mg/mL of antibody, or 50- or 100-fold excess of unlabelled probe, was pre-incubated with reaction mixture without probe for 30 min before addition of ^{32}P-labeled probe. After incubation for 30 min at room temperature, samples were loaded onto a non-denaturing polyacrylamide gel and electrophoresed, followed by drying of the gel and autoradiography.

Statistical Analysis

Statistical significance was determined by ANOVA using Levene's homogeneity test and Dunnett's 2-sided, Dunnett's T3 or Tukey's post hoc test. When comparing two groups, non-parametric Mann-Whitney U test, or two-sided Student's *t*-test was used, where applicable. A $P < 0.05$ was considered statistically significant. Statistical significance is presented as follows, $^{*}P < 0.05$, $^{**}P < 0.01$, and $^{***}P < 0.001$. Data are expressed as mean ± SEM. Numerical values are expressed as percent of unstimulated control, with controls presented as 100% or 1-fold, if not otherwise stated. We have used four wells or six bones (^{45}Ca release) per treatment group and then calculated a mean value and standard variation (SEM) for each group, which have been used for statistical analyses and to create the figures. The experiments have then been repeated using the same design and calculations 2–3 times with similar results.

RESULTS

OSM, in Contrast to LIF, Robustly Activates ERK and the AP-1 Complex in Calvarial Osteoblasts

Stimulation of calvarial osteoblasts with OSM (100 ng/mL) resulted in a robust, time-dependent activation of the MAP kinase ERK, as assessed by phosphorylation of Tyr^{204} (**Figure 1A**). OSM treatment also resulted in increased phosphorylation of the MAP kinase JNK on Tyr^{185} and Thr^{183}. In contrast, OSM did not stimulate phosphorylation of the p38 MAPK on Tyr^{182}. Treatment of the osteoblasts with LIF (100 ng/mL) caused a weak, rapidly transient activation of JNK, but did not affect phosphorylation of ERK or p38. Neither OSM nor LIF had any effect on total protein levels of p38, JNK or ERK (**Figure 1A**).

Activation of AP-1 is a consequence of MAPK activation and we, therefore, next studied the effects of OSM on transcriptional control of AP-1 subunits and DNA binding of AP-1, as assessed by semi-quantitative RT-PCR and EMSA, respectively.

OSM (100 ng/mL) increased the mRNA expression in mouse calvarial osteoblasts of *Fos* and *Jun* after 48 h treatment (**Figure 1B**), whereas *Fosb*, *Fosl1*, *Fosl2*, *Junb,* and *Jund* mRNA expressions were unaffected (**Figure 1B**). In contrast, LIF caused a marginal increase of *Fos* mRNA but did not affect the expression of the other AP-1 subunits (**Figure 1B**).

Incubation of calvarial osteoblasts with OSM for 30 min resulted in enhanced DNA binding of AP-1 as assessed by EMSA, whereas LIF had no effect (**Figure 1C**, left top panel). The binding specificity was evident by the complete displacement with a 50-fold excess of unlabelled (cold) homologous oligonucleotide (C), whereas a mutated homologous oligonucleotide (M) and a non-homologous oligonucleotide (NF-κB; NF) had no effect (**Figure 1C**, middle top panel). The antibody shift experiment demonstrated the involvement of both c-Jun (Jun) and c-Fos (Fos) in the AP-1 complex activated by OSM (**Figure 1C**, right top panel). In contrast to the enhanced AP-1 DNA binding activity by OSM, treatment with either OSM or LIF did not result in an effect on NF-κB DNA binding activity (**Figure 1C**, lower panel).

These observations demonstrated clear differences in signaling events downstream the OSM and LIF receptors in primary mouse calvarial osteoblasts, which are in line with observations made in the human osteoblastic MG-63 cell line showing a clear activation of ERK by OSM, but a weaker by LIF (35).

OSM Is a More Robust Activator Than LIF of STAT3 mRNA Expression and Phosphorylation

Stimulation of calvarial osteoblasts with OSM (100 ng/mL) increased expression of *Stat3* mRNA, whereas no such effect was observed after stimulation with LIF (**Figure 2A**).

Western blot analyses indicated that phosphorylation of the transcription factor STAT3 on Tyr^{705}, which is crucial for dimerization of STAT3 and subsequent DNA binding (36), was much greater after treatment with OSM than LIF (**Figure 2B**). No effect on total STAT3 protein by OSM or LIF was observed.

These findings show that OSM robustly activates STAT3, whereas LIF only causes a marginal activation of this transcription factor.

Activation by OSM of the Adapter Protein Shc1 in Calvarial Osteoblasts Is Crucial for STAT3 and ERK Activation

Having observed the differences in MAPK and STAT3 activation in osteoblasts stimulated with OSM and LIF, and knowing that only OSM has been reported to activate the adapter protein Shc1 in several other cell types, we next investigated the role of Shc adapters for the robust activation by OSM of ERK and STAT3 in

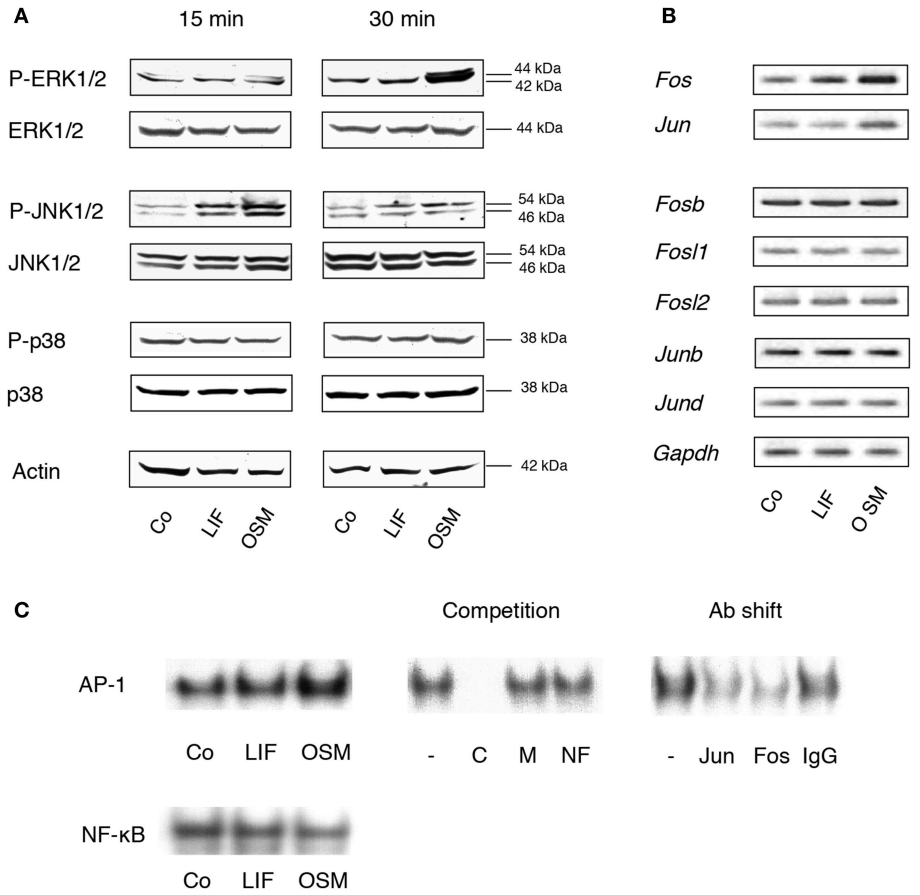

FIGURE 1 | MAP kinases and the AP-1 complex are differentially activated by OSM and LIF. **(A)** Mouse calvarial osteoblasts were cultured in the absence (Co) or presence of LIF or OSM (both at 100 ng/mL) for 15 and 30 min followed by cell lysis and Western blot analysis of total, as well as phosphorylated, ERK, JNK and p38. Actin served as the internal control for protein loading. **(B)** Semi-quantitative PCR analysis of AP-1 subunit mRNA expression after incubation without (Co) or with LIF or OSM (both at 100 ng/mL) for 48 h. *Gapdh* served as loading control. **(C)** EMSA analysis of nuclear extracts from cells incubated for 30 min in the absence (Co) or the presence of LIF or OSM (both at 100 ng/mL). Left upper panel, EMSA for nuclear extracts incubated with AP-1 consensus probe. Middle upper panel, competition studies on nuclear extracts from OSM-stimulated cells. From left: No competitor (–), homologous unlabelled (cold) AP-1 consensus probe (C), mutated AP-1 consensus probe (M), non-homologous probe (NF-κB; NF). Right upper panel, supershifts using antibodies against c-Jun (Jun), c-Fos (Fos), and unspecific IgG (IgG) of nuclear extracts from OSM-stimulated cells. Lower panel, EMSA for nuclear extracts incubated with NF-κB consensus probe.

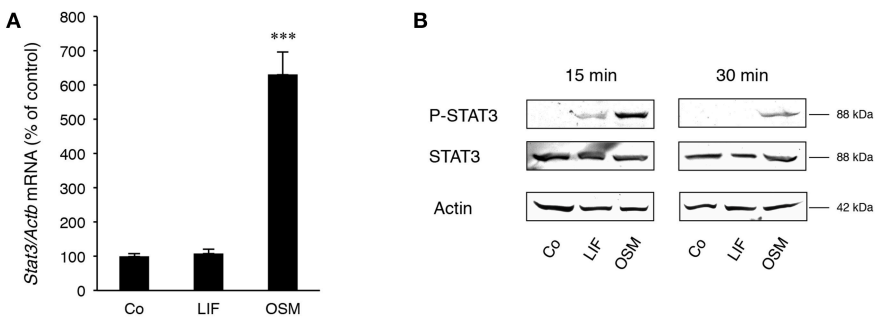

FIGURE 2 | STAT3 is differentially expressed and activated by OSM and LIF. Mouse calvarial osteoblasts were cultured in the absence (Co) or presence of LIF or OSM (both at 100 ng/mL) for 48 h to assess *Stat3* mRNA expression by RT-qPCR **(A)** or for 15 and 30 min to assess phosphorylated and total STAT3 protein levels by Western Blot **(B)**. Values in **(A)** represent means for four wells and SEM is shown as vertical bars. Significant differences compared to untreated cells (Co) is defined as ***$P < 0.001$ analyzed by one-way ANOVA followed by Dunnet's multiple comparison test vs. Co.

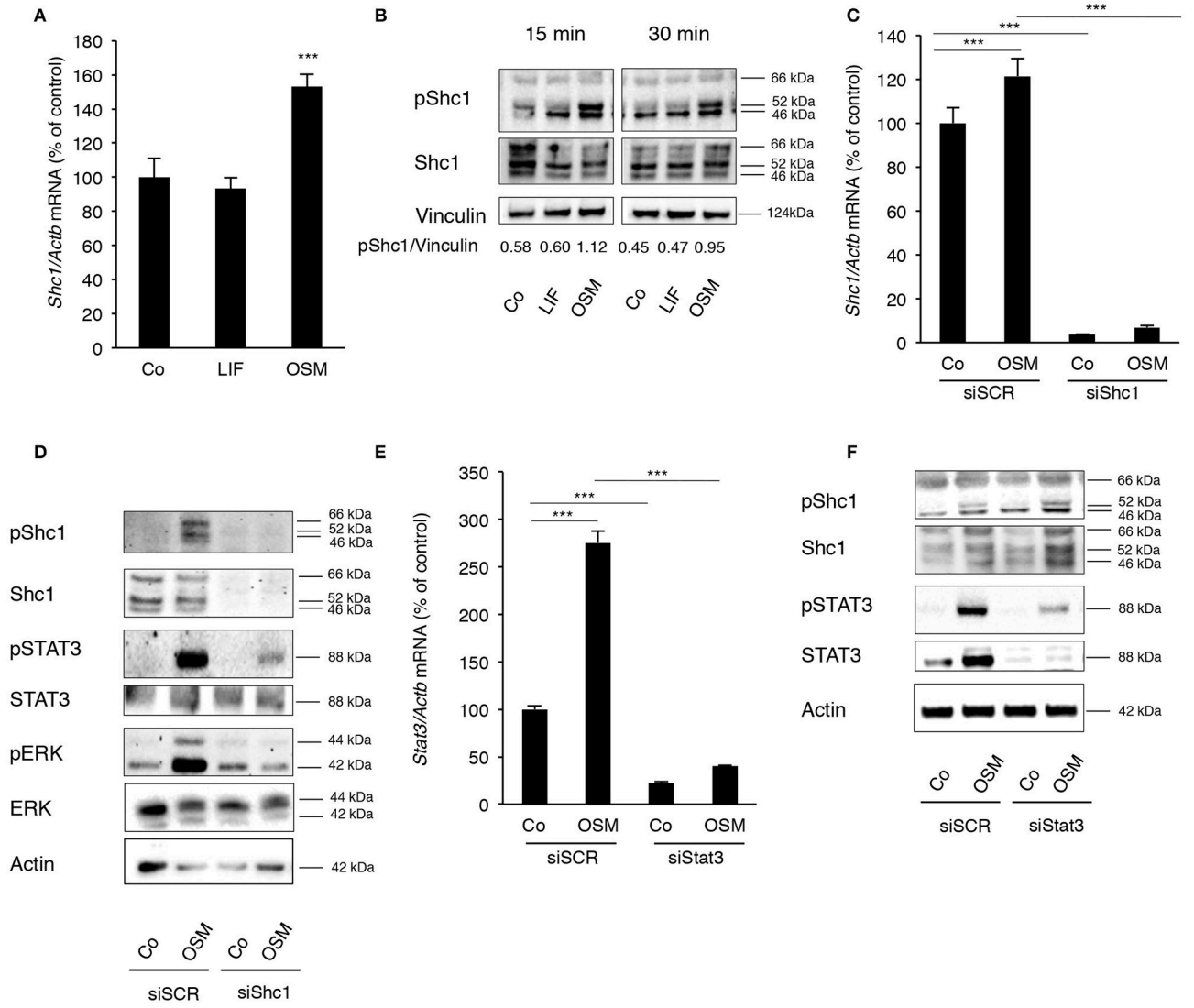

FIGURE 3 | OSM stimulates activation of STAT3 and ERK by phosphorylating the adapter protein Shc1. **(A)** Mouse calvarial osteoblasts were cultured in the absence (Co) or presence of LIF or OSM (both at 100 ng/mL) for 24 h and RNA was extracted for RT-qPCR analysis of *Shc1*mRNA. **(B)** The cells were exposed to LIF or OSM at 100 ng/mL for 15 and 30 min followed by cell lysis and Western blot for phosphorylated Shc1; the bands were quantified and normalized by vinculin. **(C)** Calvarial osteoblasts had the *Shc1* gene silenced by small interfering RNA and were exposed to LIF or OSM (both at 100 ng/mL) for 24 h before RNA extraction and analysis of *Shc1* mRNA expression by RT-qPCR; a scrambled sequence (siSCR) served as control. **(D)** Osteoblasts that had the *Shc1*gene knocked-down by siRNA and control cells exposed to scrambled sequence (siSCR) were exposed to OSM at 100 ng/mL or vehicle for 15 min and proteins were extracted for analysis of the phosphorylation of Shc1, STAT3 and ERK. **(E)** The *Stat3* gene was silenced in calvarial osteoblasts, which were subsequently exposed to OSM at 100 ng/mL or vehicle (Co) for 24 h before analysis of *Stat3* gene expression by RT-qPCR. **(F)** The effect of *Stat3* silencing on phosphorylation of STAT3 and Shc1 was analyzed by Western blot in osteoblasts treated with OSM for 15 min. **(A,C,E)** Values represent means for four wells and SEM is shown as vertical bars. **(A)** Significant differences compared to untreated cells (Co) at each time point are defined as ***$P < 0.001$; analyzed by one-way ANOVA followed by Dunnet's post *hoc-test*. **(C,E)** Significant differences are indicated by horizontal lines where ***$P < 0.001$ two-way ANOVA followed by Tukey post *hoc-test*. The difference in OSM-induced response with and without silencing analyzed by two-way ANOVA was statistically significant [interaction *P*-value in **C** ($P < 0.005$) and in **E** ($P < 0.0001$)]. OSM had no statistically significant effect ($P > 0.05$) on *Shc1* or *Stat3* mRNA expression in cells which had been silenced for *Shc1* or *Stat3*, respectively **(C,E)**.

osteoblasts. The expression of Shc proteins in osteoblasts had not been examined previously and to determine the role of Shc, the expression pattern of Shc proteins in calvarial osteoblasts treated with either OSM or LIF was evaluated.

Calvarial osteoblasts expressed *Shc1* (**Figure 3A**), but not *Shc2*, *Shc3* or *Shc4* mRNA (data not shown). Interestingly, *Shc1* mRNA was upregulated by OSM (**Figure 3A**). All three isoforms of Shc1 protein, p46, p52, and p66, were expressed by the osteoblasts (**Figure 3B**) and activation by OSM stimulated the phosphorylation of Shc1 (**Figure 3B**). OSM activated the phosphorylation of the p52 isoform in all experiments, but phosphorylation of the other isoforms was also observed in some experiments. In contrast to OSM, LIF did not affect *Shc1* mRNA expression or phosphorylation of Shc1 protein (**Figures 3A,B**).

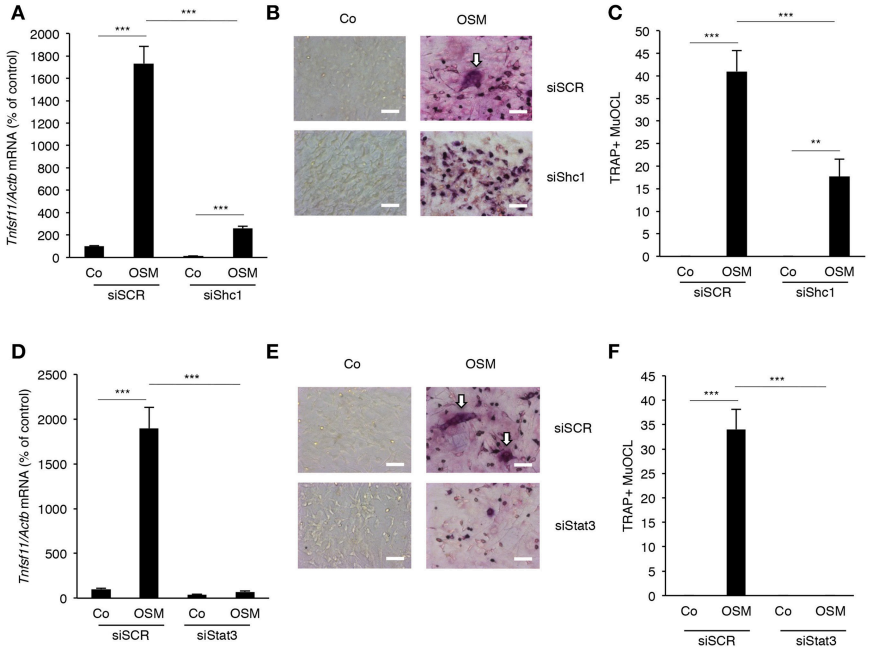

FIGURE 4 | Expression of RANKL in osteoblasts and osteoclastogenesis in co-cultures of bone marrow macrophages and calvarial osteoblasts induced by OSM are dependent on Shc1 and STAT3. Osteoblasts in which the *Shc1* gene **(A)** or the *Stat3* gene **(D)** was knocked-down by siRNA were treated with OSM at 100 ng/mL for 24 h before analysis of *Tnfsf11* gene expression. Osteoblasts transfected with scrambled RNA (siSCR) were similarly treated and analyzed. Osteoblasts in which *Shc1* **(B,C)** or *Stat3* **(E,F)** was knocked down (or siSCR as control) were exposed to OSM (100 ng/mL) or vehicle and co-cultured with BMMs for 3 days before TRAP staining and counting of $TRAP^{+}$MuOCL **(A,C,D,F)**. Values represent means for four wells and SEM is shown as vertical bars. Significant differences are indicated by horizontal lines where $^{**}P < 0.01$; $^{***}P < 0.001$; analyzed by two-way ANOVA followed by Tukey post *hoc-test*. The difference in OSM-induced response with and without silencing analyzed by two-way ANOVA was statistically significant [interaction *P*-value in **A** ($P<0.0001$), **C** ($P<0.005$), **D** ($P<0.0001$) and **F** ($P<0.0001$)]. Scale bar in **(B,E)** is 50 μm.

The importance of Shc1 for OSM-induced STAT3 and ERK activation was then determined by silencing *Shc1* expression in the osteoblasts. The siRNA used decreased the mRNA expression of *Shc1* by 97% in control cells, as well as caused a significant decrease of *Shc1* mRNA in OSM-treated cells (**Figure 3C**). The silencing subsequently resulted in effective reductions of Shc1 protein expression and phosphorylation (**Figure 3D**). Decreased Shc1 activation substantially decreased OSM-induced phosphorylation of STAT3 and ERK, without affecting total protein levels of STAT3 and ERK (**Figure 3D**).

After observing a robust activation of STAT3 by OSM, the role of STAT3 phosphorylation in the OSM-induced activation of Shc1 was evaluated. Treatment of osteoblasts with OSM (100 ng/mL) resulted in a 2.8-fold increase of *Stat3* mRNA expression (**Figure 3E**). Silencing of *Stat3* expression decreased the mRNA expression of *Stat3* in untreated control cells by 80% and significantly decreased OSM-induced upregulation of *Stat3* mRNA (**Figure 3E**). Silencing of *Stat3* resulted in a decrease in STAT3 protein expression and OSM-induced STAT3 phophorylation, as expected, but did not affect phosphorylation of Shc1 (**Figure 3F**). The fact that silencing of *Shc1* resulted in impaired phosphorylation of STAT3 induced by OSM, whereas silencing of *Stat3* did not decrease the OSM-induced activation of Shc1 (**Figure 3F**), indicate that Shc1 activation is upstream of STAT3.

Activation of STAT3 and the Adapter Protein Shc1 by OSM Is Crucial for Stimulation of RANKL Expression and Osteoclastogenesis

Next, the importance of the Shc1-ERK and JAK-STAT3 pathways for stimulation of RANKL expression by OSM was evaluated. Silencing of *Shc1* significantly decreased the OSM-induced mRNA expression of *Tnfsf11* (encoding RANKL) (**Figure 4A**). Importantly, silencing of *Shc1* expression in osteoblasts decreased OSM-induced osteoclast formation in co-cultures of calvarial osteoblasts and BMM (**Figures 4B,C**). Silencing of *Stat3* also resulted in substantially decreased expression of OSM-induced T*nfsf11* mRNA expression (**Figure 4D**), and totally prevented formation of osteoclasts in OSM-stimulated co-cultures of calvarial osteoblasts and BMM (**Figures 4E,F**).

OSM Is a More Robust Stimulator of ^{45}Ca Release and Expression of RANKL in Mouse Calvarial Bones and Calvarial Osteoblasts

Having observed that OSM but not LIF receptors activate Shc1-dependent signaling, we next assessed the importance of this difference for bone resorption, RANKL production and osteoclastogenesis.

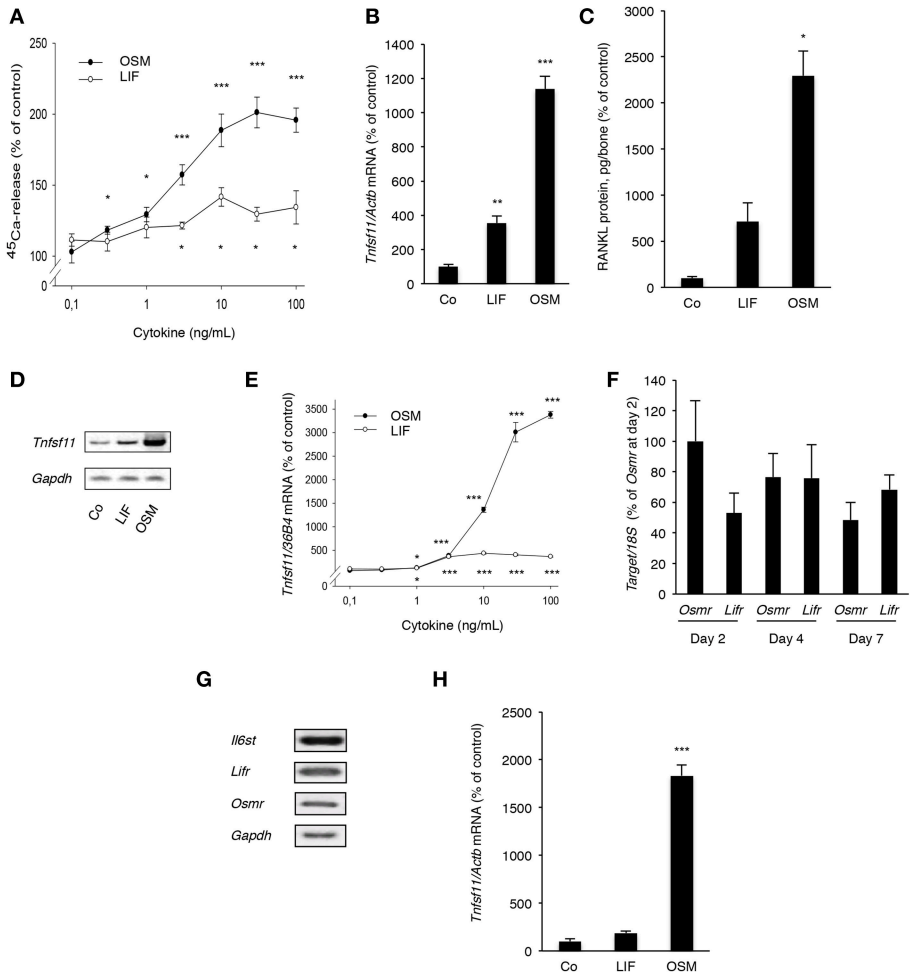

FIGURE 5 | OSM and, to a lesser extent, LIF stimulate bone resorption and RANKL production in calvarial bones, calvarial osteoblasts and stromal cells. **(A)** Mouse calvarial bones were cultured in the absence or the presence of LIF or OSM (both 0.1–100 ng/mL) and bone resorption was assessed by ^{45}Ca release after a 5-day culture period. **(B)** RT-qPCR was performed using mRNA extracted from calvarial bones treated with either LIF or OSM (both at 100 ng/mL) for 24 h to assess the expression of *Tnfsf11*. **(C)** Protein expression of RANKL after 48 h was also analyzed in calvarial bone treated with LIF or OSM (both at 100 ng/L). **(D)** Mouse calvarial osteoblasts were incubated in the absence (Co) or the presence of LIF (100 ng/mL) or OSM (100 ng/mL) for 48 h and expression of *Tnfsf11* was analyzed by semi-quantitative RT-PCR. **(E)** The expression of *Tnfsf11* mRNA in calvarial osteoblasts stimulated by LIF and OSM a different concentrations (0.1-100 ng/mL) was performed using quantitative RT-PCR. **(F)** The mRNA expression of *Osmr* and *Lifr* in osteoblasts was compared at three different time points. **(G)** The receptor components *Il6st, Lifr* and *Osmr* are expressed in ST-2 stromal cells as assessed by RT-PCR. **(H)** The mRNA expression of *Tnfsf11* in ST-2 cells cultured without (Co) or with LIF or OSM (both at 100 ng/mL) for 48 h was analyzed. Values represent means for six bones (calvarial bones) or four wells (cell culture experiments) and SEM is shown as vertical bars. *, **, and ***, indicate significant difference compared to untreated (Co) cells, $^{*}P < 0.05$, $^{**}P < 0.01$, and $^{***}P < 0.001$, respectively. Statistical significance was determined by ANOVA using Levene's homogeneity test followed by Dunnett's T3 *post-hoc* tests vs. Co. In **(F)**, Tukey *post-hoc* test was used to compare all groups and no statistical difference was observed.

Both OSM and LIF stimulated bone resorption, as assessed by ^{45}Ca release from neonatal mouse calvarial bone, in a concentration-dependent manner with OSM being a substantially more effective and potent stimulator than LIF (**Figure 5A**). The effects seen were statistically significant at and above 0.3 ng/mL (10 nM) OSM and 3 ng/mL (140 nM) LIF.

Quantitative PCR analysis revealed that OSM, and to a lesser extent LIF, increased mRNA expression of *Tnfsf11* in the calvarial bones (**Figure 5B**). This was in line with the finding that the protein level of RANKL in the mouse calvarial bones was increased 23-fold by OSM and 7-fold by LIF, respectively (**Figure 5C**).

Calvarial osteoblasts responded to LIF and OSM (both at 100 ng/mL) with enhanced *Tnfsf11* mRNA expression, with OSM clearly being the more effective stimulator (**Figure 5D**). Quantitative real-time PCR analysis showed that the difference in responsiveness between OSM and LIF could be observed over a wide range of concentrations with OSM treatment resulting in a more robust stimulatory effect on *Tnfsf11* mRNA expression (**Figure 5E**). The difference in response seemed not to be due

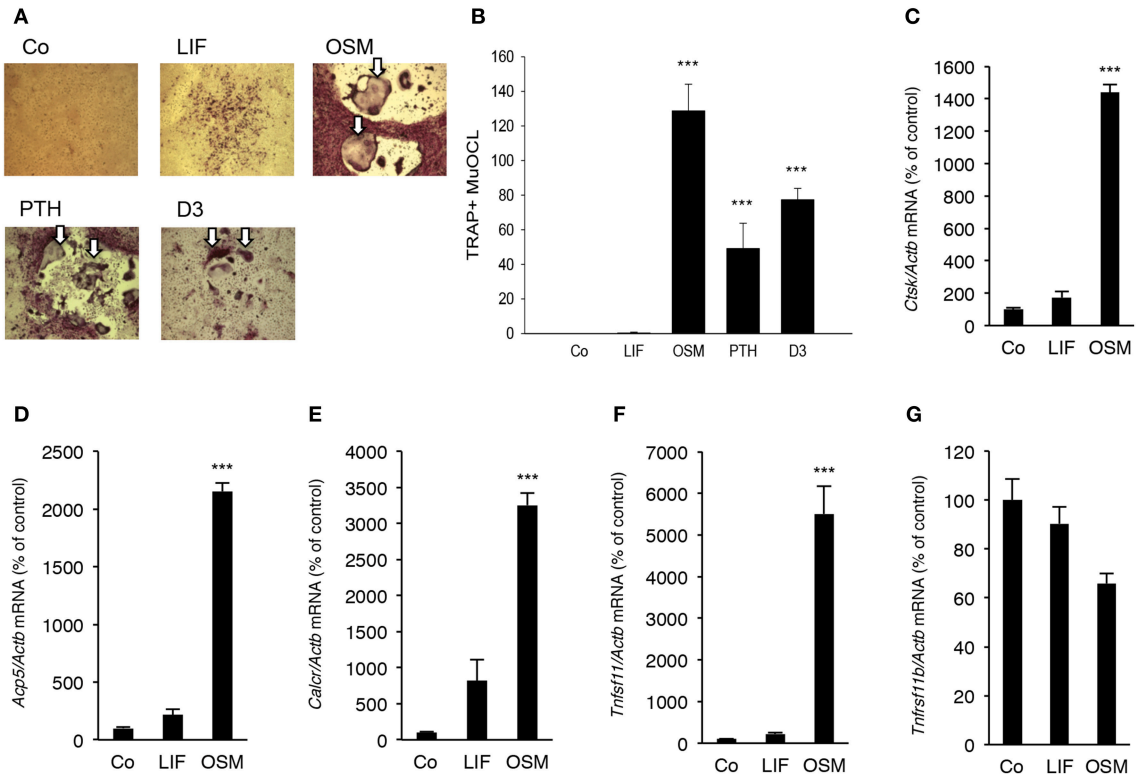

FIGURE 6 | OSM, but not LIF, stimulates osteoclastogenesis in bone marrow cell cultures. Mouse bone marrow cells (BMC) were cultured in the absence (Co) or the presence of LIF, or OSM (both at 100 ng/mL), PTH or 1,25$(OH)_2$-vitamin D3 (D3; both at 10^{-8} M) for 7 days before staining **(A)** and counting **(B)** of tartrate-resistant acid phosphatase (TRAP)-positive multinucleated osteoclasts ($TRAP^+$MuOCL). Quantitative real-time PCR analysis of mRNA expression of cathepsin K (*Ctsk,* **C**), TRAP (*Acp5,* **D**), calcitonin receptor (*Calcr,* **E**) RANKL (*Tnfsf11,* **F**) and OPG (*Tnfsf11b,* **G**) in BMC cultured without (Co) or with LIF or OSM (both at 100 ng/mL) for 7 days. Values represent means for four wells and SEM is shown as vertical bars. ***, indicates significant difference compared to untreated (Co) cells, ***$P < 0.001$. Statistical significance was determined by ANOVA using Levene's homogeneity test followed by Dunnett's 2-sided **(B–F)** or Dunnett's T3 **(G)** *post-hoc* test.

to differences in receptor expression, as assessed by the mRNA expression of *Osmr* and *Lifr* (**Figure 5F**).

The stimulatory effect of OSM on *Tnfsf11* mRNA in the calvarial osteoblasts was dependent on the expression of *Il6st* (encoding gp130) and *Osmr*, but independent of *Lifr* expression, as demonstrated by silencing of the expression of these three receptor components in the calvarial osteoblasts (**Supporting Information Figure S1**). These findings are in agreement with previously reported observations that mouse OSM did not induce *Tnfsf11* mRNA in osteoblasts from $Osmr^{-/-}$ mice (5).

The ST-2 stromal cells expressed mRNA for *Il6st*, *Lifr* and *Osmr* (**Figure 5G**) and responded to OSM with a robust 18-fold increase of *Tnfsf11* mRNA expression, whereas LIF did not cause any significant effect (**Figure 5H**).

OSM but Not LIF Stimulates Osteoclast Formation and Expression of RANKL in Mouse Bone Marrow Cultures

Addition of OSM (100 ng/mL) for 7 days to mouse bone marrow cell (BMC) cultures significantly stimulated the formation of $TRAP^+$ MuOCL (**Figures 6A,B**). The stimulation by OSM was more pronounced than stimulations caused by maximally effective concentrations of parathyroid hormone (PTH) and 1,25$(OH)_2$-vitamin D3. In contrast, treatment with LIF (100 ng/mL) only resulted in formation of a few osteoclasts (**Figures 6A,B**).

It was also found that OSM (100 ng/mL) caused a 14–32 fold enhancement of the mRNA expression of the osteoclastic markers *Ctsk* (encoding cathepsin K), *Acp5* (encoding TRAP, tartrate-resistant acid phosphatase) and *Calcr* (encoding calcitonin receptor), whereas LIF (100 ng/mL) only caused a small 2–8 fold stimulation of the mRNA expression of these genes which was not statistically significant (**Figures 6C–E**).

OSM upregulated *Tnfsf11* mRNA in the BMC cultures 22-fold but did not affect *Tnfrsf11b* mRNA (encoding OPG) (**Figures 6F,G**). No significant effect of LIF on *Tnfsf11* or *Tnfrsf11b* mRNA was observed in the BMC cultures (**Figures 6F,G**).

OSM and LIF Have No Direct Effect on Osteoclastogenesis

Analysis of BMM cultures revealed that neither LIF nor OSM stimulated formation of $TRAP^+$ MuOCL in M-CSF treated BMM

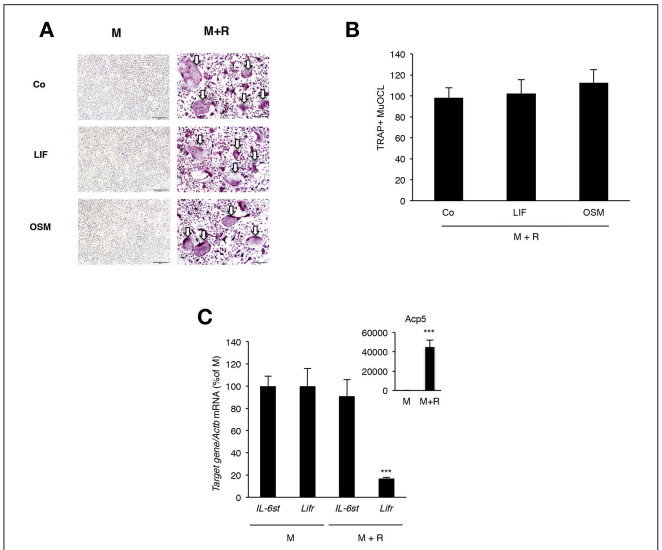

FIGURE 7 | Lack of effect by OSM and LIF on osteoclast formation in bone marrow macrophage cultures. **(A,B)** BMMs were cultured in M-CSF (30 ng/mL) or differentiated to osteoclasts by addition of M-CSF + RANKL (30 and 4 ng/mL, respectively) in the presence or absence of LIF or OSM (both at 100 ng/mL) for 3 days before staining for tartarate-resistant acid phosphatase (TRAP)-positive multinucleated osteoclasts (TRAP^{+}MuOCL), which then were counted. No osteoclasts were formed in the absence of RANKL. **(C)** Quantitative PCR analyses of *Il6st*, *Lifr*, and *Acp5* in BMM cultured for 72 h with M-CSF (30 ng/ml) or M-CSF+RANKL (30 and 4 ng/ml, respectively). Values represent means for four wells and SEM is shown as vertical bars. In **(C)** ***, indicates significant difference compared to cells treated with M-CSF (M), $P < 0.001$. In **(B)** Statistical significance was determined one-way ANOVA followed by Tukey's *post-hoc* test and in **(C)**, Student's *t*-test was used for comparison between M and M + R groups for each gene.

(**Figure 7A**). The cytokines also did not affect osteoclastogenesis when the formation of TRAP^{+} MuOCL in BMM was stimulated by M-CSF and RANKL (**Figures 7A,B**). In M-CSF- and M-CSF+RANKL-stimulated BMM, mRNA of *Il6st* (encoding gp130) and *Lifr* could be detected, but mRNA of *Osmr* was not detected (**Figure 7C**). RANKL-induced differentiation, as demonstrated by time-dependent upregulation of mRNA levels for *Acp5* (encoding TRAP), did not affect the expression of *Il6st* mRNA, but down-regulated *Lifr* mRNA expression (**Figure 7C**).

DISCUSSION

The present study shows that OSM is a more effective stimulator of bone resorption in mouse calvarial bones and a more potent stimulator of osteoclast differentiation and formation in mouse bone marrow cultures than is LIF. These effects were due to indirect effects mediated by osteoblasts/stromal cells rather than due to direct effects on osteoclast progenitor cells. Similarly, Tamura et al. found that LIF was a weaker stimulator of osteoclast formation than OSM in co-cultures of mouse osteoblasts and bone marrow cells (20). Other studies evaluating OSM and LIF have also noted a similar hierarchy of action for the two cytokines using mouse embryonic fibroblasts and rat hepatocytes (37), synovial fibroblasts (38, 39), NIH 3T3 fibroblasts and mouse lung fibroblasts (40). In the present study, we provide evidence that the difference in effects on osteoclastogenesis and bone resorption can be explained by recruitment of the adapter protein Shc1 to the OSMR. This recruitment results in a more robust activation of ERK/STAT3 signaling and expression of RANKL by OSM in comparison to LIFR-mediated signaling.

Heterodimerization of either OSMR:gp130 or LIFR:gp130 results in activation of both JAK/STAT and JAK/SHP-2/Grb2/Sos/Ras/Raf/MAPK signaling through docking of STATs and SHP-2 to different phosphorylated Tyr sites in the gp130 molecule (2, 6, 35, 41). The role of these pathways for bone mass has been assessed in "knock-in" mutant mice, one in which the C-terminal moiety of gp130 has been deleted ($gp130^{\Delta STAT\Delta STAT}$) to reduce STAT1/3 signaling, and another strain of mice in which a point mutation substituting Tyr^{757} (equivalent to Tyr^{759} in human gp130) with Phe^{757} ($gp130^{Y757F/Y757F}$) blocks signaling through the SHP-2/MAPK pathway (42). In a parallel study, mice with a knock-in of gp130 carrying a substitution of Tyr^{759} with Phe^{759} (designated $gp130^{F759/F759}$), which also results in defective SHP-2/MAPK signaling, have been used (43). These studies suggest that SHP-2/MAPK signaling, rather than STAT1/3 signaling, is important for basal bone remodeling and bone mass. However, the activation of downstream signaling pathways by specific cytokines in the gp130 family was not studied in these mice.

The fact that no difference in the mRNA expression of *Osmr* and *Lifr* in osteoblasts was observed indicate that the more robust stimulation of osteoclast formation by OSM is not likely to be due to differences in receptor numbers, but rather explained by differences in downstream signaling.

We found that OSM was a more robust stimulator than LIF of JNK (Tyr^{185}/Thr^{183}) and ERK (Tyr^{204}) in mouse calvarial osteoblasts. This is in agreement with the study by Walker et al. reporting that OSM activates ERK more robustly than LIF in primary osteoblasts. Activation of the transcription factor AP-1 is an important downstream event following MAPK activation and experiments were conducted to determine if OSM affected DNA binding of AP-1 in calvarial osteoblasts (5). In agreement with the activation of ERK by OSM, it was determined with EMSA analysis that increased DNA binding of AP-1 occurred with OSM in calvarial osteoblasts, but not with LIF. Gelshift studies showed that the bound AP-1 heterodimer consisted of c-Fos and c-Jun subunits. In contrast to the increased DNA binding of AP-1 by OSM, EMSA analysis did not show any effect on the DNA binding of NF-κB by OSM or LIF, an observation that is in agreement with EMSA analysis in OSM-stimulated human peritoneal mesothelial cells (44).

Activation of JAK/STAT signaling is a well documented signaling event for cytokines in the IL-6 family. It has previously been reported that OSM and LIF can activate STAT1, STAT3, and STAT5 in osteoblasts, and that signaling through OSMR results in more robust activation of these transcription factors (5). In agreement with these observations, we found that OSM is a more robust activator of STAT3 than LIF, observations which also are in agreement with Itoh et al., who found that OSM caused a more robust and prolonged phosphorylation of STAT3 than LIF in osteoblasts from wild type mice (43). These findings likely

explain why OSM more effectively than LIF enhanced the mRNA and protein expression of RANKL in calvarial bone, calvarial osteoblasts and bone marrow stromal cells. Similarly, O'Brien et al. have demonstrated that OSM-induced *Tnfsf11* mRNA in the UAMS-32 cell line was decreased by transfection with a dominant negative *Stat3* retrovirus (18) and investigators have showed that that silencing of *Stat3* impairs up-regulation of *Tnfsf11* mRNA by OSM in ST2 cells (45, 46). The important role of STAT3 for OSM-induced signaling in osteoblasts has also been demonstrated by the finding that OSM-induced activation of cyclin-dependent kinase inhibitor $p21^{WAF1,CIP1,SD11}$ in the human osteosarcoma cell line MG-63 can be inhibited by transfection with a dominant negative *Stat3* plasmid (47). Furthermore, OSM promotes the binding of STAT3 and RNA polymerase II to 5′ enhancer regions in the *Tnfsf11* promoter shared by PTH and 1,25-dihydroxyvitamin-D3 (48) and to a more distal enhancer region shared by IL-6 (45).

An explanation why OSM is a more robust activator of JAK/STAT and MAPK signaling in the osteoblasts compared to LIF may be that phosphorylated Tyr^{861} in the OSMR acts as a binding site for an SH2 domain in the adapter protein Shc1, which is not recruited to the LIFR:gp130 complex (26). The Shc family of adapter proteins is well known for its role in growth factor signaling, especially the Ras/MAPK pathway, but a role in RANKL expression and osteoclast formation has not been shown previously. Hermanns et al. have shown that mutation of OSMR Tyr^{861} in transfected COS-7 cells not only decreased Shc1 binding to the OSMR, but also decreased phosphorylation of ERK stimulated by OSM without affecting STAT phosphorylation (26). These data suggest that Shc1 plays a unique role in downstream signaling induced by OSM.

In this report, we show for the first time that Shc1 is expressed in osteoblasts and that OSM, but not LIF, upregulates the mRNA expression of *Shc1*. Furthermore, OSM, but not LIF, induced the phosphorylation of Shc1. Furthermore, OSM consistently induced phosphorylation of the p52 isoform, which is the isoform known to be important for activation of the Ras/MAPK pathway. By silencing the expression of *Shc1,* it was found that activations of both STAT3 and ERK elicited by OSM were substantially decreased. Activation of Shc1, however, was not affected by silencing of *Stat3*, indicating that STAT3 is acting downstream of Shc1 in osteoblasts. Although some reports have shown that Shc1 is not upstream of STAT3, a recent study in breast cancer cells expressing *Shc1* mutated in the domain containing Tyr^{239} and Tyr^{240} has also demonstrated that Shc1 is upstream of STAT3 (29). The present observations confirmed previous finding showing that activation of STAT3 is part of the downstream signaling which occurs following LIF and OSM receptor activations, but the more robust activation of STAT3 by OSM and the unique activation of ERK by OSM suggest that these particular effects are dependent on recruitment of Shc1 to the OSMR. In addition, by using the siRNA approach to

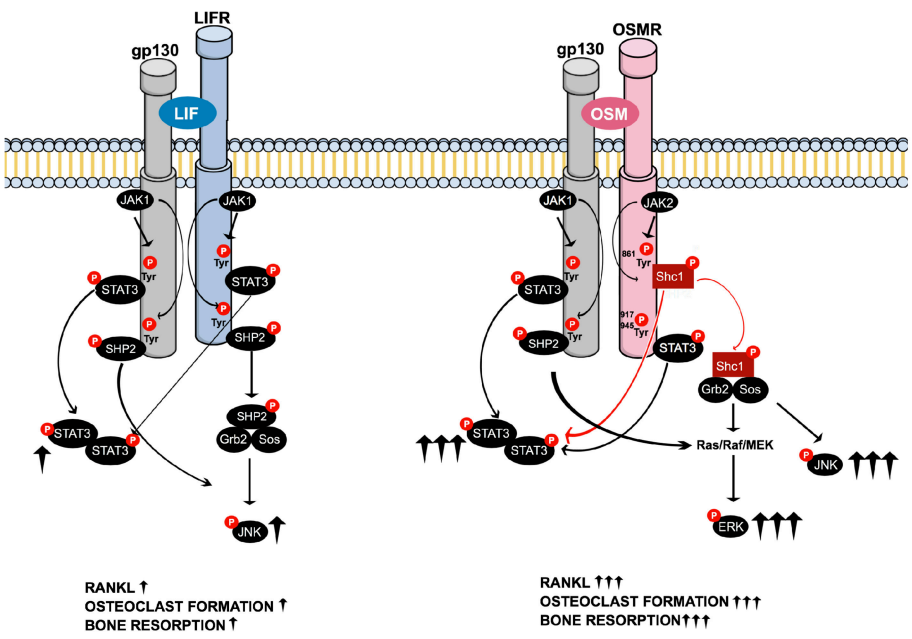

FIGURE 8 | Schematic drawing of the suggested intracellular signaling pathways of LIF and OSM receptors in osteoblasts mediating expression of osteoclastogenic factors, osteoclast formation and bone resorption. Common LIFR/OSMR signaling pathways induced by JAK-mediated phosphorylation of the signal transducer gp130 involve activation of STAT3, as well as activation of JNK through a possible SHP2/Ras/Raf/MAPK cascade **(Left)**. The figure indicates that LIF binds to the LIFR. As discussed in the Introduction section, 2nd paragraph, OSM can also bind to the LIFR to regulate sclerostin expression. In addition to the gp130-mediated pathways common for LIFR and OSMR, the OSM receptor has previously been shown to activate a Shc1-mediated pathway where phosphorylation of the OSMR on Tyr^{861} results in docking and phosphorylation of the adapter molecule Shc1 (26, 27). The activated pShc1 is recruited to the Grb2:SoS complex which in turn induces a Ras/Raf/MAPK cascade that ultimately activates ERK. The Shc1-mediated signaling pathway **(Right)** is suggested to explain the stronger effects by OSM on expression of osteoclastogenic factors, osteoclast formation and bone resorption in comparison to activation of the LIFR:gp130 complex by LIF.

decrease the expression of *Shc1,* it was shown that recruitment of Shc1 to the OSMR was a crucial downstream signaling event in the mechanism by which OSM induces *Tnfsf11* mRNA expression and osteoclast formation. Using the same technique, it was also found that induction of *Tnfsf11* mRNA expression in osteoblasts, and osteoclast formation in co-cultures stimulated by OSM, were critically dependent on the expression of *Stat3* mRNA.

In summary, when compared to LIF, OSM was found to be a more potent stimulator of calvarial bone resorption and osteoclast formation in bone marrow cultures. This was due to greater stimulation of RANKL expression in osteoblasts/stromal cells caused by enhanced activation of STAT3 and JNK by OSM and an ability of OSM to activate ERK that was not shared by LIF. These novel findings in the present study show that the robust and unique stimulatory effects of OSM are dependent on the recruitment of the activated adapter protein Shc1 to the OSMR subunit of the OSMR:gp130 heterodimer, a recruitment that is absent in the LIFR:gp130 complex. From a clinical perspective, inhibition of Shc1 could be a mechanism to decrease OSM-induced bone loss in inflammatory diseases. The suggested differences in signaling downstream of the OSMR and LIFR complexes are summarized in **Figure 8**.

DATA AVAILABILITY

The raw data supporting the conclusions of this manuscript will be made available by the authors, without undue reservation, to any qualified researcher.

ETHICS STATEMENT

This study was carried out in accordance with the recommendations of Institutional Animal Care and Ethics Committees at Umeå University, at the School of Dentistry, Araraquara and at the University of Gothenburg guidelines. The protocol was approved by the Institutional Animal Care and Ethics Committees at Umeå University, at the School of Dentistry, Araraquara and at the University of Gothenburg.

AUTHOR CONTRIBUTIONS

EP and PS contributed equally. EP, PS, and UL designed the study. EP, PS, TF-M, and PH conducted the experiments. EP, PS, TF-M, PH, HC, and UL interpreted the data. EP, PS, and UL wrote the first draft of the manuscript which was edited and approved by all authors.

ACKNOWLEDGMENTS

Anita Lie and Anna Westerlund are acknowledged for excellent technical assistance. This work was supported by the Swedish Research Council, Swedish Rheumatism Association, Royal 80-Year Fund of King Gustav V, COMBINE, the Swedish state under the agreement between the Swedish government and the county councils, the ALF-agreement (#237551), the IngaBritt and Arne Lundberg Foundation, County Council of Västerbotten, grants #2014/05283-3 and 2015/00410-0, São Paulo Research Foundation (FAPESP) and by a scholarship to TF-M from the Coordenação de Aperfeiçoamento de Pessoal de Nível Superior–Brasil (CAPES)–Finance code 001 and grant #061/2013 (PVE080/2012).

SUPPLEMENTARY MATERIAL

The Supplementary Material for this article can be found online at: https://www.frontiersin.org/articles/10.3389/fimmu.2019.01164/full#supplementary-material

REFERENCES

1. Zarling JM, Shoyab M, Marquardt H, Hanson MB, Lioubin MN, Todaro GJ. Oncostatin M: a growth regulator produced by differentiated histiocytic lymphoma cells. *Proc Natl Acad Sci USA.* (1986) 83:9739–43. doi: 10.1073/pnas.83.24.9739
2. Hermanns HM. Oncostatin M and interleukin-31: Cytokines, receptors, signal transduction and physiology. *Cytokine Growth Factor Rev.* (2015) 26:545–58. doi: 10.1016/j.cytogfr.2015.07.006
3. West NR, Hegazy AN, Owens BMJ, Bullers SJ, Linggi B, Buonocore S, et al. Oncostatin M drives intestinal inflammation and predicts response to tumor necrosis factor-neutralizing therapy in patients with inflammatory bowel disease. *Nat Med.* (2017) 23:579–89. doi: 10.1038/nm.4307
4. Su CM, Chiang YC, Huang CY, Hsu CJ, Fong YC, Tang CH. Osteopontin promotes oncostatin m production in human osteoblasts: implication of rheumatoid arthritis therapy. *J Immunol.* (2015) 195:3355–64. doi: 10.4049/jimmunol.1403191
5. Walker EC, McGregor NE, Poulton IJ, Solano M, Pompolo S, Fernandes TJ, et al. Oncostatin M promotes bone formation independently of resorption when signaling through leukemia inhibitory factor receptor in mice. *J Clin Invest.* (2010) 120:582–92. doi: 10.1172/JCI40568
6. Richards CD. The enigmatic cytokine oncostatin m and roles in disease. *ISRN Inflamm.* (2013) 2013:512103. doi: 10.1155/2013/512103
7. Sims NA. Cell-specific paracrine actions of IL-6 family cytokines from bone, marrow and muscle that control bone formation and resorption. *Int J Biochem Cell Biol.* (2016) 79:14–23. doi: 10.1016/j.biocel.2016.08.003
8. Tanaka M, Hirabayashi Y, Sekiguchi T, Inoue T, Katsuki M, Miyajima A. Targeted disruption of oncostatin M receptor results in altered hematopoiesis. *Blood.* (2003) 102:3154–62. doi: 10.1182/blood-2003-02-0367
9. Bolin C, Tawara K, Sutherland C, Redshaw J, Aranda P, Moselhy J, et al. Oncostatin m promotes mammary tumor metastasis to bone and osteolytic bone degradation. *Genes Cancer.* (2012) 3:117–30. doi: 10.1177/1947601912458284
10. Sterbova S, Karlsson T, Persson E. Oncostatin M induces tumorigenic properties in non-transformed human prostate epithelial cells, in part through activation of signal transducer and activator of transcription 3 (STAT3). *Biochem Biophys Res Commun.* (2018) 498:769–74. doi: 10.1016/j.bbrc.2018.03.056
11. Ayaub EA, Dubey A, Imani J, Botelho F, Kolb MRJ, Richards CD, et al. Overexpression of OSM and IL-6 impacts the polarization of pro-fibrotic macrophages and the development of bleomycin-induced lung fibrosis. *Sci Rep.* (2017) 7:13281. doi: 10.1038/s41598-017-13511-z
12. Mozaffarian A, Brewer AW, Trueblood ES, Luzina IG, Todd NW, Atamas SP, et al. Mechanisms of oncostatin M-induced pulmonary inflammation

and fibrosis. *J Immunol.* (2008) 181:7243–53. doi: 10.4049/jimmunol.181.10.7243
13. Simpson JL, Baines KJ, Boyle MJ, Scott RJ, Gibson PG. Oncostatin M (OSM) is increased in asthma with incompletely reversible airflow obstruction. *Experimental Lung Res.* (2009) 35:781–94. doi: 10.3109/01902140902906412
14. Pradeep AR, Garima G, Raju A. Serum levels of oncostatin M (a gp 130 cytokine): an inflammatory biomarker in periodontal disease. *Biomarkers.* (2010) 15:277–82. doi: 10.3109/13547500903573209
15. Lisignoli G, Piacentini A, Toneguzzi S, Grassi F, Cocchini B, Ferruzzi A, et al. Osteoblasts and stromal cells isolated from femora in rheumatoid arthritis (RA) and osteoarthritis (OA) patients express IL-11, leukaemia inhibitory factor and oncostatin M. *Clin Exp Immunol.* (2000) 119:346–53. doi: 10.1046/j.1365-2249.2000.01114.x
16. Torossian F, Guerton B, Anginot A, Alexander KA, Desterke C, Soave, S. et al. Macrophage-derived oncostatin M contributes to human and mouse neurogenic heterotopic ossifications. *JCI Insight.* (2017) 2:96034. doi: 10.1172/jci.insight.96034
17. Palmqvist P, Persson E, Conaway HH, Lerner UH. IL-6, leukemia inhibitory factor, and oncostatin M stimulate bone resorption and regulate the expression of receptor activator of NF-κB ligand, osteoprotegerin, and receptor activator of NF-κB in mouse calvariae. *J Immunol.* (2002) 169:3353–62. doi: 10.4049/jimmunol.169.6.3353
18. O'Brien CA, Gubrij I, Lin SC, Saylors RL, Manolagas SC. STAT3 activation in stromal/osteoblastic cells is required for induction of the receptor activator of NF-kappaB ligand and stimulation of osteoclastogenesis by gp130-utilizing cytokines or interleukin-1 but not 1,25-dihydroxyvitamin D3 or parathyroid hormone. *J Biol Chem.* (1999) 274:19301–8. doi: 10.1074/jbc.274.27.19301
19. Richards CD, Langdon C, Deschamps P, Pennica D, Shaughnessy SG. Stimulation of osteoclast differentiation *in vitro* by mouse oncostatin M, leukaemia inhibitory factor, cardiotrophin-1 and interleukin 6: synergy with dexamethasone. *Cytokine.* (2000) 12:613–21. doi: 10.1006/cyto.1999.0635
20. Tamura T, Udagawa N, Takahashi N, Miyaura C, Tanaka S, Yamada Y, et al. Soluble interleukin-6 receptor triggers osteoclast formation by interleukin 6. *Proc Natl Acad Sci USA.* (1993) 90:11924–8. doi: 10.1073/pnas.90.24.11924
21. Hermanns HM, Radtke S, Haan C, Schmitz-Van de Leur H, Tavernier J, Heinrich PC, et al. Contributions of leukemia inhibitory factor receptor and oncostatin M receptor to signal transduction in heterodimeric complexes with glycoprotein 130. *J Immunol.* (1999) 163:6651–8.
22. Hintzen C, Evers C, Lippok BE, Volkmer R, Heinrich PC, Radtke S, et al. Box 2 region of the oncostatin M receptor determines specificity for recruitment of Janus kinases and STAT5 activation. *J Biol Chem.* (2008) 283:19465–77. doi: 10.1074/jbc.M710157200
23. Schmitz J, Dahmen H, Grimm C, Gendo C, Muller-Newen G, Heinrich PC, et al. The cytoplasmic tyrosine motifs in full-length glycoprotein 130 have different roles in IL-6 signal transduction. *J Immunol.* (2000) 164:848–54. doi: 10.4049/jimmunol.164.2.848
24. Anhuf D, Weissenbach M, Schmitz J, Sobota R, Hermanns HM, Radtke S, et al. Signal transduction of IL-6, leukemia-inhibitory factor, and oncostatin M: structural receptor requirements for signal attenuation. *J Immunol.* (2000) 165:2535–43. doi: 10.4049/jimmunol.165.5.2535
25. Neel BG, Gu H, Pao L. The 'Shp'ing news: SH2 domain-containing tyrosine phosphatases in cell signaling. *Trends Biochem Sci.* (2003) 28:284–93. doi: 10.1016/S0968-0004(03)00091-4
26. Hermanns HM, Radtke S, Schaper F, Heinrich PC, Behrmann I. Non-redundant signal transduction of interleukin-6-type cytokines. The adapter protein Shc is specifically recruited to the oncostatin M receptor. *J Biol Chem.* (2000) 275:40742–8. doi: 10.1074/jbc.M005408200
27. Wang Y, Robledo O, Kinzie E, Blanchard F, Richards C, Miyajima A, et al. Receptor subunit-specific action of oncostatin M in hepatic cells and its modulation by leukemia inhibitory factor. *J Biol Chem.* (2000) 275:25273–85. doi: 10.1074/jbc.M002296200
28. Wills MK, Jones N. Teaching an old dogma new tricks: twenty years of Shc adaptor signalling. *Biochem J.* (2012) 447:1–16. doi: 10.1042/BJ20120769
29. Ahn R, Sabourin V, Bolt AM, Hebert S, Totten S, De Jay N, et al. The Shc1 adaptor simultaneously balances Stat1 and Stat3 activity to promote breast cancer immune suppression. *Nat Commun.* (2017) 8:14638. doi: 10.1038/ncomms14638
30. Lerner UH. Modifications of the mouse calvarial technique improve the responsiveness to stimulators of bone resorption. *J Bone Miner Res.* (1987) 2:375–83. doi: 10.1002/jbmr.5650020504
31. Ljunggren O, Ransjo M, Lerner UH. *In vitro* studies on bone resorption in neonatal mouse calvariae using a modified dissection technique giving four samples of bone from each calvaria. *J Bone Miner Res.* (1991) 6:543–50. doi: 10.1002/jbmr.5650060604
32. Granholm S, Henning P, Lindholm C, Lerner UH. Osteoclast progenitor cells present in significant amounts in mouse calvarial osteoblast isolations and osteoclastogenesis increased by BMP-2. *Bone.* (2013) 52:83–92. doi: 10.1016/j.bone.2012.09.019
33. Granholm S, Lundberg P, Lerner UH. Calcitonin inhibits osteoclast formation in mouse haematopoetic cells independently of transcriptional regulation by receptor activator of NF-{kappa}B and c-Fms. *J Endocrinol.* (2007) 195:415–27. doi: 10.1677/JOE-07-0338
34. Takeshita S, Kaji K, Kudo A. Identification and characterization of the new osteoclast progenitor with macrophage phenotypes being able to differentiate into mature osteoclasts. *J Bone Miner Res.* (2000) 15:1477–88. doi: 10.1359/jbmr.2000.15.8.1477
35. Bellido T, Borba VZ, Roberson P, Manolagas SC. Activation of the Janus kinase/STAT (signal transducer and activator of transcription) signal transduction pathway by interleukin-6-type cytokines promotes osteoblast differentiation. *Endocrinology.* (1997) 138:3666–76. doi: 10.1210/endo.138.9.5364
36. Heinrich PC, Behrmann I, Muller-Newen G, Schaper F, Graeve L. Interleukin-6-type cytokine signalling through the gp130/Jak/STAT pathway. *Biochem J.* (1998) 334:297–314. doi: 10.1042/bj3340297
37. Richards CD, Kerr C, Tanaka M, Hara T, Miyajima A, Pennica D, et al. Regulation of tissue inhibitor of metalloproteinase-1 in fibroblasts and acute phase proteins in hepatocytes *in vitro* by mouse oncostatin M, cardiotrophin-1, and IL-6. *J Immunol.* (1997) 159:2431–7.
38. Langdon C, Kerr C, Hassen M, Hara T, Arsenault AL, Richards CD. Murine oncostatin M stimulates mouse synovial fibroblasts *in vitro* and induces inflammation and destruction in mouse joints *in vivo*. *Am J Pathol.* (2000) 157:1187–96. doi: 10.1016/S0002-9440(10)64634-2
39. Langdon C, Leith J, Smith F, Richards CD. Oncostatin M stimulates monocyte chemoattractant protein-1- and interleukin-1-induced matrix metalloproteinase-1 production by human synovial fibroblasts *in vitro*. *Arthritis Rheumat.* (1997) 40:2139–46. doi: 10.1002/art.1780401207
40. Langdon C, Kerr C, Tong L, Richards CD. Oncostatin M regulates eotaxin expression in fibroblasts and eosinophilic inflammation in C57BL/6 mice. *J Immunol.* (2003) 170:548–55. doi: 10.4049/jimmunol.170.1.548
41. Nicola NA, Babon JJ. Leukemia inhibitory factor (LIF). *Cytokine Growth Factor Rev.* (2015) 26:533–44. doi: 10.1016/j.cytogfr.2015.07.001
42. Sims NA, Jenkins BJ, Quinn JM, Nakamura A, Glatt M, Gillespie MT, et al. Glycoprotein 130 regulates bone turnover and bone size by distinct downstream signaling pathways. *J Clin Invest.* (2004) 113:379–89. doi: 10.1172/JCI19872
43. Itoh S, Udagawa N, Takahashi N, Yoshitake F, Narita H, Ebisu S, et al. A critical role for interleukin-6 family-mediated Stat3 activation in osteoblast differentiation and bone formation. *Bone.* (2006) 39:505–12. doi: 10.1016/j.bone.2006.02.074
44. Hams E, Colmont CS, Dioszeghy V, Hammond VJ, Fielding CA, Williams AS, et al. Oncostatin M receptor-beta signaling limits monocytic cell recruitment in acute inflammation. *J Immunol.* (2008) 181:2174–80. doi: 10.4049/jimmunol.181.3.2174
45. Bishop KA, Meyer MB, Pike JW. A novel distal enhancer mediates cytokine induction of mouse RANKl gene expression. *Mol Endocrinol.* (2009) 23:2095–110. doi: 10.1210/me.2009-0209
46. Onal M, St. John HC, Danielson AL, Markert JW, Riley EM, Pike JW. Unique distal enhancers linked to the mouse Tnfsf11 gene direct tissue-specific and

inflammation-induced expression of RANKL. *Endocrinology*. (2016) 157:482–96. doi: 10.1210/en.2015-1788

47. Bellido T, O'Brien CA, Roberson PK, Manolagas SC. Transcriptional activation of the p21(WAF1,CIP1,SDI1) gene by interleukin-6 type cytokines. A prerequisite for their pro-differentiating and anti-apoptotic effects on human osteoblastic cells. *J Biol Chem.* (1998) 273:21137–44. doi: 10.1074/jbc.273.33.21137
48. Fu Q, Manolagas SC, O'Brien CA. Parathyroid hormone controls receptor activator of NF-κB ligand gene expression via a distant transcriptional enhancer. *Mol Cell Biol.* (2006) 26:6453–68. doi: 10.1128/MCB.00356-06

Conflict of Interest Statement: The authors declare that the research was conducted in the absence of any commercial or financial relationships that could be construed as a potential conflict of interest.

frontiers in Immunology

REVIEW
published: 19 June 2019
doi: 10.3389/fimmu.2019.01408

Immune Function and Diversity of Osteoclasts in Normal and Pathological Conditions

Maria-Bernadette Madel[1,2], *Lidia Ibáñez*[3], *Abdelilah Wakkach*[1,2], *Teun J. de Vries*[4], *Anna Teti*[5], *Florence Apparailly*[6] *and Claudine Blin-Wakkach*[1,2]*

[1] CNRS, Laboratoire de PhysioMédecine Moléculaire, Faculté de Médecine, UMR7370, Nice, France, [2] Faculé de Médecine, Université Côte d'Azur, Nice, France, [3] Department of Pharmacy, Cardenal Herrera-CEU University, València, Spain, [4] Department of Periodontology, Academic Centre of Dentistry Amsterdam, University of Amsterdam and Vrije Univeristeit, Amsterdam, Netherlands, [5] Department of Biotechnological and Applied Clinical Sciences, University of L'Aquila, L'Aquila, Italy, [6] IRMB, INSERM, CHU Montpellier, Université Montpellier, Montpellier, France

Osteoclasts (OCLs) are key players in controlling bone remodeling. Modifications in their differentiation or bone resorbing activity are associated with a number of pathologies ranging from osteopetrosis to osteoporosis, chronic inflammation and cancer, that are all characterized by immunological alterations. Therefore, the 2000s were marked by the emergence of osteoimmunology and by a growing number of studies focused on the control of OCL differentiation and function by the immune system. At the same time, it was discovered that OCLs are much more than bone resorbing cells. As monocytic lineage-derived cells, they belong to a family of cells that displays a wide heterogeneity and plasticity and that is involved in phagocytosis and innate immune responses. However, while OCLs have been extensively studied for their bone resorption capacity, their implication as immune cells was neglected for a long time. In recent years, new evidence pointed out that OCLs play important roles in the modulation of immune responses toward immune suppression or inflammation. They unlocked their capacity to modulate T cell activation, to efficiently process and present antigens as well as their ability to activate T cell responses in an antigen-dependent manner. Moreover, similar to other monocytic lineage cells such as macrophages, monocytes and dendritic cells, OCLs display a phenotypic and functional plasticity participating to their anti-inflammatory or pro-inflammatory effect depending on their cell origin and environment. This review will address this novel vision of the OCL, not only as a phagocyte specialized in bone resorption, but also as innate immune cell participating in the control of immune responses.

Keywords: osteoclast, osteoimmunology, monocyte heterogeneity, inflammation, immune modulation, dendritic cell

OPEN ACCESS

Edited by:
Abbe N. de Vallejo, University of Pittsburgh, United States

Reviewed by:
Julia Charles, Brigham and Women's Hospital and Harvard Medical School, United States
Alejandra Pera, Universidad de Córdoba, Spain

***Correspondence:**
Claudine Blin-Wakkach
blin@unice.fr

Specialty section:
This article was submitted to Inflammation, a section of the journal Frontiers in Immunology

Received: *26 February 2019*
Accepted: *04 June 2019*
Published: *19 June 2019*

Citation:
Madel M-B, Ibáñez L, Wakkach A, de Vries TJ, Teti A, Apparailly F and Blin-Wakkach C (2019) Immune Function and Diversity of Osteoclasts in Normal and Pathological Conditions. Front. Immunol. 10:1408. doi: 10.3389/fimmu.2019.01408

INTRODUCTION

Bone-resorbing osteoclasts (OCLs) were first described 150 years ago (1). Their origin remained unclear for nearly 100 years before they were formally identified as cells of hematopoietic origin. This was evidenced thanks to the analysis of osteopetrotic mice defective in osteoclast function. Hematopoietic cell transfer from normal littermates restored OCL function in *mi/mi* mice and

reciprocal transfer of hematopoietic cells from *mi/mi* mice induced osteopetrosis in normal recipient mice (2). The monocytic origin of OCLs was first demonstrated in colony assays of bone marrow cell fractions (3). From this moment, OCLs have been extensively studied to decipher the mechanisms of bone resorption leading to the identification of key factors required for OCL differentiation, fusion, bone adhesion and bone degradation activity. These studies defined a set of specific properties that cells must fulfill to be defined as *bona fide* OCLs, the most important being multinucleation, the expression of markers such as the tartrate-resistant acid phosphatase (TRAcP) and the capacity to degrade bone and mineralized matrix (4).

Among hematopoietic cells, OCLs belong to the monocytic family. This family of innate immune cells is characterized by its capacity to sense and respond to infections and tissue damage, its phagocytic properties and its high plasticity controlled by the tissue micro-environmental heterogeneity (5–7). Abundant literature addressed the origins and roles of monocytes (MNs), macrophages (Mϕs), and dendritic cells (DCs). Nowadays, it is clearly established that each of these populations includes distinct sub-groups that have specific origin and functional properties ranging from inflammatory to immune suppressive effects (8, 9). However, despite their common origin, the potential implication of OCLs as innate immune cells has been neglected for a long time. The immune face of OCLs emerged only 10 years ago when costimulatory signals mediated by ITAM motifs involved in immune cell activation were shown to be essential for OCL differentiation (10–12). This was further emphasized by the identification of the important link between DCs and OCLs through the ability of DCs to differentiate into bone-resorbing OCLs under pathological conditions (13, 14) (**Table 1**).

In fact, OCLs share many similarities with Mϕs and DCs in their origin and function (**Figure 1**). Like Mϕs in tissues, OCLs are essential to maintain bone homeostasis and remodeling in steady state and to support bone healing after bone damage. Beside bone matrix resorption, they are able to take up apoptotic cells, calcium-phosphate particles or latex beads (27–31). More recently, OCLs have been shown to process, present and cross-present antigens resulting in T cell activation (18, 32, 33). They also produce cytokines and immunomodulatory factors that affect immune responses (34–36), as described below. Moreover, like their monocytic counterparts, OCLs display phenotypic heterogeneity and may arise from different progenitors depending on their environment, the stimuli they receive and their developmental stage (18, 37, 38). In particular, pathological conditions associated to inflammation or cancer provide molecular and cellular signals that stimulate specific monocytic subsets to differentiate into OCLs. Despite this heterogeneity in their origin and environment, OCLs are largely considered as a single population of cells. Consequently, thus far, under pathological conditions OCLs have been investigated for their increased or decreased differentiation and resorptive function but almost never with regard to the implication of different OCL subsets. Moreover, the immunological function of OCLs remains poorly explored. This review addresses the state-of-the-art of this novel vision of the OCL not just as a bone-resorbing cell but also as a cell having immune capacities.

TABLE 1 | Pathological conditions associated with inflammatory osteoclasts differentiated from dendritic cells.

DC origin	Pathological condition	Demonstrated	References
Murine splenic cDCs	Osteopetrosis, high Th17 proportion	*In vivo, in vitro*	(14, 15)
Murine BM-derived DCs	Calvaria induced osteolysis	*In vivo*	(16)
Murine splenic DCs (cell line)	Histiocytosis	*In vivo, in vitro*	(17)
Murine BM-derived DCs	Chronic inflammation	*In vitro*	(18)
Murine Flt3-L-induced BM-derived cDCs	+IL-1β and TNF-α	*In vitro*	(19)
Murine BM-derived DCs and splenic DCs	Periodontitis	*In vitro*	(20)
Human blood-derived MNs	Rheumatoid arthritis	*In vitro*	(13)
Human BM DCs	Multiple myeloma, high level of IL-17	*In vitro*	(21, 22)
Human Langerhans cells*	Langerhans cell histiocytosis	*In vivo*	(23)

**Although Langerhans cells function as DCs, they are related to macrophages in terms of their origin (24–26).*

DIVERSITY IN OSTEOCLAST ORIGIN

Bone Marrow Osteoclast Progenitors

Whereas, MN, Mϕ, and DC origin has been widely explored, the origin of OCLs remained more elusive and OCLs are usually forgotten in hematopoietic lineage trees. However, in adults a common early bone marrow (BM) progenitor for OCLs and other monocytic cells (Mϕ/OCL/DC progenitor, MODP) has been identified downstream of the granulocyte/Mϕ progenitor (GMP) (**Figure 2**) (39, 40). In human, $CD11b^{-}CD34^{+}c\text{-}KIT^{+}FLT3^{+}IL\text{-}3R\alpha^{low}$ BM cells are common progenitors for Mϕs, DCs, OCLs and granulocytes. They give rise to $CD11b^{-}CD34^{+}c\text{-}KIT^{+}FLT3^{+}IL\text{-}3R\alpha^{high}$ cells that are restricted to Mϕ, DC, and OCL differentiation and represent <0.5% of BM cells (39). In mouse, the BM $CD11b^{-/low}c\text{-}kit^{+}CD115^{+}$ fraction contains a common precursor for Mϕs, OCLs, and DCs also representing <0.5% of BM cells (41–44). Within this population, the use of CD27 and Flt3 markers further discriminates subsets of oligopotent progenitors for Mϕ/OCL/DC development ($CD27^{+}Flt3^{+}$) vs. bipotent progenitors for Mϕ/OCL development ($CD27^{low/-}Flt3^{-}$) (40, 45). Moreover, analysis of mouse BM myeloid fractions revealed that early blasts ($CD31^{hi}Ly6C^{-}$), myeloid blasts ($CD31^{+}Ly6C^{+}$) and MNs ($CD31^{-}Ly6C^{hi}$) have different capacity to differentiate into OCLs (46). BM myeloid blasts that express higher CD115 levels differentiate more efficiently and faster than early blats and MNs (46). Indeed, while c-kit is down regulated during murine OCL differentiation, CD115 expression is maintained (44), which is essential for osteoclastogenesis since binding of CD115 to its ligand M-CSF increases the expression of RANK, allowing further differentiation into OCLs under RANKL stimulation (41). Moreover, analysis using BrDU incorporation in mice revealed that quiescent $CD115^{+}$ $RANK^{+}$ progenitors

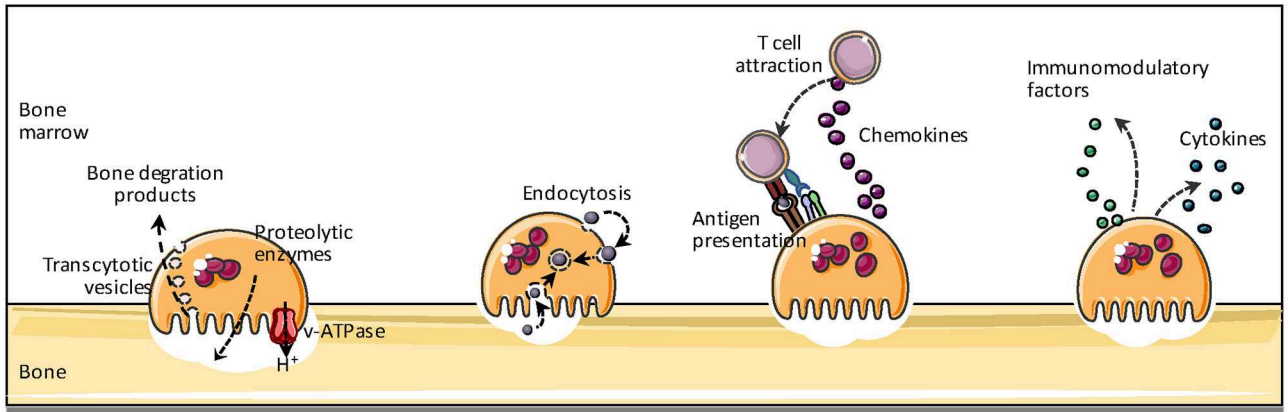

	Bone resorption	Phagocytosis	Antigen presentation and T cell activation	Immune modulation
Physiological Condition	▪ Bone modelling and remodelling ▪ Ca^{2+} homeostasis ▪ Modulation of hematopoiesis ▪ Bone healing	▪ Clearance of apoptotic cells ▪ Self-tolerance	▪ Self tolerance ▪ Secretion of tolerogenic cytokines (e.g. IL10, TGFβ) ▪ Activation of $CD4^+$ and $CD8^+$ regulatory T cells	▪ Immune suppression participating to self tolerance
Pathological Condition	▪ Excessive bone destruction (e.g. osteoporosis, RA, osteolytic metastasis) ▪ Defective OCL differentiation or reduced resorption capacity (e.g. osteopetrosis, pycnodysostosis)	▪ Implant loosening ▪ Inflammation	▪ Inflammatory response ▪ Secretion of inflammatory cytokines (e.g. TNFα, IL1β) ▪ Activation of TNFα-producing $CD4^+$ T cells	▪ Immune suppression participating to cancer progression (e.g. multiple myeloma)

FIGURE 1 | The different immune-related roles of osteoclasts. Besides bone resorption, osteoclasts share many properties with their precursor cells such as phagocytosis, antigen presentation, and immune modulation. These immune-related functions may possess divergent functionalities under physiological and pathological conditions.

represent committed OCL progenitors able to circulate and settle down in the bone (47, 48).

Interestingly, the origin of OCLs from BM HSCs and downstream progenitors appears to be restricted to adults. This was very recently demonstrated by Jacome-Galarza et al. who depleted RANK or CD115 expression in BM-HSC progenitors (using *Csf1r*^{cre} mice) or in BM-HSC and erythro-myeloid progenitors (EMP) (using *Flt3*^{cre} mice). Depletion of these genes in embryonic EMP resulted in osteopetrosis in newborns, whereas only adults were affected by specific depletion in HSC progenitors (38). This study elegantly demonstrated for the first time that OCLs involved in fetal bone formation and tooth eruption are originating from the same progenitors as tissue Mϕs and differ thereby from OCLs arising in adults (**Figures 2A,B**) (38, 49).

Therefore, the interplay between OCLs and other monocytic cells appears much more puzzling than the existence of a common BM progenitor. *In vitro*, OCLs can be generated in the presence of RANKL and M-CSF from hematopoietic cells originating from many tissues. BM in mouse and blood in human are major sources of OCL progenitors, but OCLs can also be obtained from hematopoietic cells from the liver, spleen, thymus and lymph nodes, suggesting a high heterogeneity of potential OCL precursors (3, 50–54). Indeed, in addition to their differentiation from BM progenitors, OCLs can also arise from cells already engaged in the MN or DC pathways (3, 13, 14, 55, 56). As described below, this process is associated with pathological conditions related to bone destruction making OCL differentiation more complex and dynamic than expected. Thus, there is a large variability in OCL precursor cells depending on the signals they receive from their normal or pathological environment. These observations strongly support that OCLs do not represent a single and homogeneous population but that they display the same heterogeneity in their origin and phenotype as other monocytic cells (**Figure 2C**).

Osteoclasts and Monocytes

Monocytes are innate immune cells characterized by a great level of plasticity and found in all tissues. Depending on the environmental cues, they can differentiate into DCs, Mϕs or OCLs. Being involved in both inflammation and bone resorption, MNs represent key regulators of bone tissue

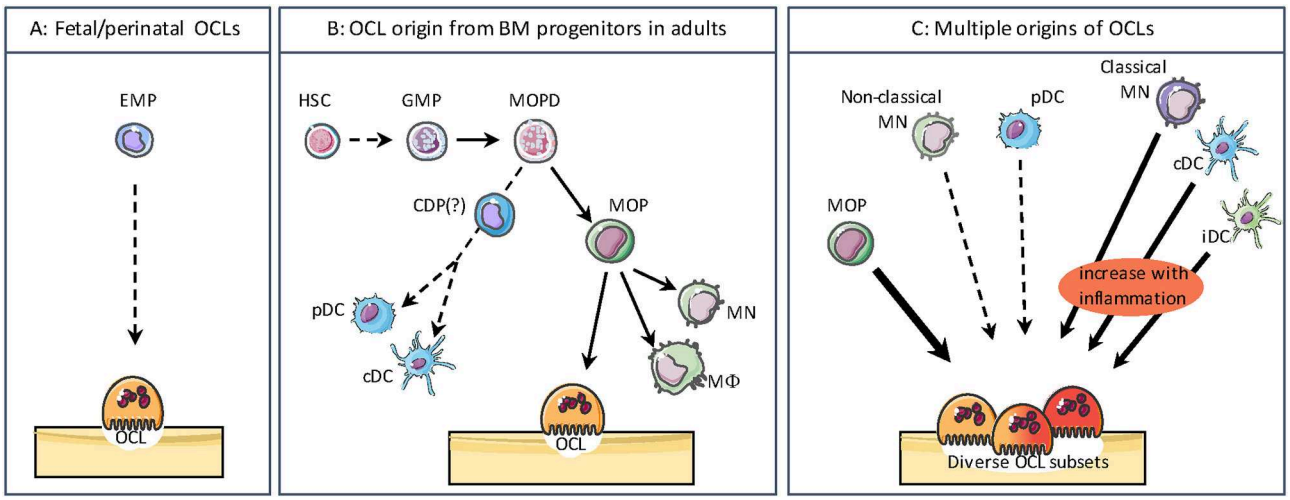

FIGURE 2 | The different origins of osteoclasts. **(A)** During the embryonic and postnatal period, OCLs differentiate from the embryonic erythro-myeloid progenitor (EMP) lineage. **(B)** In adults, bone marrow progenitors for osteoclasts (OCLs) and other monocytic cells such as monocytes (MN), macrophages (MΦ), as well as conventional/classical dendritic cells (cDCs) and plasmacytoid DCs (pDCs) share common progenitors downstream of the granulocyte/MΦ progenitor (GMP). HSC, Hematopoietic Stem Cell; MOPD, MΦ/OCL/DC progenitor; CDP, common DC progenitor; MOP, MΦ/OC progenitor. The divergence of CDP from MODP is not clearly evidenced. **(C)** OCLs have multiple origins depending on their environment. Beside their origin from MOP, in pathological conditions OCLs can also arise from classical MNs, cDCs and inflammatory DCs (iDC). OCLs differentiation from non-classical and pDCs is much less efficient. These different sources of OCLs result in a heterogeneity as observed for other monocytic cells.

homeostasis. Moreover, they are heterogeneous and comprise several subtypes already committed to different functions. Knowledge on MNs has evolved a lot over the past decade thanks to new technologies such as fate mapping and single-cell RNA sequencing (scRNAseq). Historically, they were considered as an intermediate status in the peripheral circulation, between myeloid precursors from the BM and Mϕs in tissues. Now, we know that certain tissue-resident Mϕs are generated independently of MNs during early phases of embryogenesis and that fetal MNs derive from multipotent erythro-myeloid progenitors. Later and throughout life, MNs are generated from the HSC-derived hematopoiesis (49, 57), as described for OCLs (38). In healthy conditions, MNs are present in central (BM) and peripheral (spleen) reservoirs and engrafted into certain resident macrophage pools. They are not only involved in the repopulation of tissue Mϕ and DC compartments but also contribute to the establishment and resolution of local inflammatory reactions and participate in the innate immune surveillance of the organism (58). Under pathological conditions, they are rapidly mobilized in large numbers and recruited to the inflamed tissue where they display both inflammatory and pro-resolving properties to allow tissue repair. This last step must be transient. If monocyte numbers in tissues are not properly regulated and persist overtime, their actions become pathogenic for targeted tissues (59). In particular, massive recruitment of MNs in the BM is associated with increased OCL formation and bone destruction (56, 60).

Two main subsets of MNs exist both in mouse and human (61, 62). In mice, the "classical" monocytes are characterized by the combination of specific surface markers $Ly6C^{high}CCR2^{+}CX3CR1^{low}CD62L^{+}Gr1^{+}$, and were previously named inflammatory monocytes because they can differentiate into inflammatory Mϕs and inflammatory DCs (63, 64). The "non-classical" MNs are characterized by the $Ly6C^{low}CCR2^{low}CX3CR1^{+}CD62L^{-}Gr1^{-}$ surface markers and are also named patrolling MNs because they survey endothelial cells and surrounding tissues for damage or viral infection. Their human counterparts are $CD14^{+}CD16^{-}$ and $CD14^{low}CD16^{+}$, respectively (61, 65). A recent scRNAseq analysis of human blood confirmed that classical and non-classical MN subsets represent two distinct clusters (66). Several genetic mouse models of deletion of transcription factors, cytokines and chemokines, together or not with acute or chronic inflammatory challenges, have been used to delineate functional heterogeneity of the $Ly6C^{high}$ and $Ly6C^{low}$ monocyte subsets *in vivo*. Only few studies however addressed their respective capacity to differentiate into OCLs.

It is now well established that mature mouse $Ly6C^{high}$ MNs differentiate into the BM from unipotent common monocyte progenitors, with an intermediate $Ly6C^{high}CXCR4^{+}$ pre-monocytic step (67). Under steady state conditions, mature $Ly6C^{high}$ MNs constantly egress from the BM in a CCR2-dependent manner (68) following circadian oscillations (69) and circulate for 1 day in the blood. Then, a minority (∼1%) of these MNs convert into non classical $Ly6C^{low}$ MNs that have longer circulating lifespans (∼7 days), while the vast majority (∼99%) of $Ly6C^{high}$ MNs leave the circulation and replenish specific pools of tissue resident Mϕs (70–72). For specific peripheral inflammatory responses to infections or tissue damages, the fate of mouse $Ly6C^{high}$ MNs is identical. Differences rely on the speed and amplitude of the mobilization from BM and spleen to target sites, the kinetic being faster and larger numbers being produced,

leading to blood monocytosis as early as 4 h after endotoxin challenge (73). Additionally, differences also rely on the fraction of blood monocyte-derived Mϕs that replenishes tissue-resident Mϕs after recruitment (71). Mouse Ly6C^{high} MNs are precursors of longer-lived Ly6C^{low} MNs that express higher levels of CX3CR1 (74) and continuously patrol the luminal side of the vasculature in a CX3CR1 and LFA-1/ICAM1-dependent crawling manner (58). Under physiological conditions, Ly6C^{low} MNs are the endothelium housekeepers, playing a key role to control endothelium integrity by scavenging luminal microparticles, recruiting neutrophils for focal necrosis of endothelial cells, phagocytizing cellular debris (75). Upon bacterial infection, Ly6C^{low} MNs secrete IL-10 and are recruited to tissue where they more likely differentiate into alternatively activated Mϕs, contributing to tissue repair. Ly6C^{low} monocytes can also promote tolerance to self-antigens contained in apoptotic cells through a PD-L1-dependent mechanism and thanks to their high capacity to phagocyte apoptotic cells *in vivo* (76). Overall, the multiple capacities of both MN subsets to differentiate into either regulatory or inflammatory mature Mϕs or DCs depend on the inflammatory signal and tissue microenvironment. Interestingly, both mouse MN subsets can go back to the BM thanks to a CXCR4-dependent signal (67). The respective role of Ly6C^{high} and Ly6C^{low} MNs on bone turnover remain yet to be established.

Since MNs constitute a source of OCLs, it is expected that both MN subsets display OCL differentiation potential. Although the culture conditions used *in vitro* to monitor OCL differentiation diverge between studies, it appears that mouse OCLs develop from BM CD11b$^{-/low}$Ly6C^{high} monocytic progenitors (as described above) and from blood CD11b^{high}Ly6C^{high} MNs. In the BM, CD11b$^{-/low}$Ly6C^{high} monocytic progenitors are more prone than CD11b^{+} MNs to differentiate into OCLs (43) because of the negative role of CD11b and β2-integrin signaling on OCL differentiation (77). *In vitro* comparative studies based on BM treatment with various cytokines demonstrated that Ly6C^{high} MNs were far more efficient than Ly6C^{low} monocytes to differentiate into mature OCLs (78). Importantly, the BM CD11b$^{-/low}$Ly6C^{high} population also displays an OCL differentiation capacity *in vivo* and is expanded in inflammatory arthritis models (79). In particular, the CX3CR1^{+} fraction of these cells is highly enriched in OCL precursors (79). In-depth phenotypic characterization allowed to further dissect CD11b$^{-/low}$Ly6C^{high} cells into three different populations with high osteoclastogenic potential based on the expression of the phenotypic marker CD117 (c-Kit) (43).

In the blood, the mouse Ly6C^{high} MN subset also represents the major precursor cell population of OCLs (**Figure 2C**). Indeed, *in vitro* Ly6C^{high} MNs are more efficient than the Ly6C^{low} subset to differentiate into TRAcP positive cells (55). In the context of inflammatory arthritis, disease severity is associated with Ly6C^{high} blood monocytosis, and Ly6C^{high} MNs more specifically migrate to the inflamed joints and contribute to bone erosion due to their excessive differentiation into OCLs (56). Importantly, *in vivo* delivery of therapeutic molecules to Ly6C^{high} MNs, but not to Ly6C^{low} MNs, markedly interferes with pathogenic bone erosion in experimental arthritis, suggesting that the classical subset represents a candidate cell target for anti-osteoclastogenic strategy design (56). In human, OCLs generated from peripheral blood MNs originate from the classical CD14^{+}CD16^{-} subset, and not from the CD16^{+} subset, in an integrin β3-dependent manner (80, 81). Later studies refined this view showing that while the different human MN subsets can differentiate into OCLs when cultured on plastic, OCLs are predominantly formed from classical MNs when cultured on bone slices (82). In the context of inflammatory bone diseases, the distribution of MN subsets is skewed toward a higher proportion of CD14^{+}CD16^{+} MNs (83). Interestingly, it seems that in these pathological conditions, CD14^{+}CD16^{+} MNs are more prone to differentiate into OCLs than in healthy conditions, as demonstrated in psoriatic arthritis patients (84).

The origin of OCLs from MN progenitors or MNs is likely to be dictated by the BM cell environment. Indeed, monocytic OCL precursors show different expression level of cytokines/growth factors leading to different effect of inflammatory cytokines. In human, among the three MN subsets, only the CD14^{high} CD16^{+} intermediate subset responds to IL-17 by forming larger OCLs having higher resorption capacity than in absence of this cytokine (82). In mouse, BM CD31^{high}Ly6C^{-} early blasts, CD31^{+}Ly6C^{+} myeloid blasts and CD31^{-}Ly6C^{high} MNs are differently affected by their environment. When assessing life span, IL-1β enhance OCL formation especially of myeloid blasts, which have rapidly formed and have a short life span, while OCLs derived from CD31^{-}Ly6C^{high} MNs are formed a later stage and have a longer life span (85). Remarkably, M-CSF pretreatment of myeloid blasts or TNFα pretreatment of MNs before addition of RANKL inhibit osteoclast formation from CD31^{-}Ly6C^{high} MNs but not from early blast or myeloid blast despite the expression of RANK (86, 87). These cells were able to regain their osteoclastogenesis capacity when cultured on bone slices, revealing the importance of the bone attachment and signaling in OCL differentiation. This is further supported by the finding that collagen specific motifs are ligands for OSCAR, a costimulatory receptor induced by RANKL and essential for OCL differentiation (88).

Osteoclasts and Dendritic Cells

Dendritic cells have been identified by Steinman and Cohn 45 years ago (89). More than through their phenotype and surface marker expression, DCs are also defined by their functional specificity. Being located in most tissues where they represent 1–5% of the hematopoietic cells, they act as sentinels of the immune system capturing and processing antigens and instructing adaptive immune cells (84). Contrasting with MNs and Mϕs, they have the unique capacity to migrate to the T cell zones of lymphoid organs where they present or cross-present antigens thanks to their expression of major histocompatibility complexes (MHC)-I and -II and activate naive T cells.

As MNs, DCs represent a heterogeneous population of cells. In mouse, DCs that reside in lymphoid organs are composed of CD8^{+} and CD8^{-} conventional/classical DCs (cDC) and IFNα-producing plasmacytoid DCs (pDCs). Equivalent subsets are also present in human, namely CD1c^{+} (BDCA1) and CD141^{+} (BDCA3) cDCs and CD303^{+} (BDCA2) pDCs (90, 91). Plasmacytoid DCs have the capacity to produce high amounts of

IFNα in response to viral and foreign nucleic acids stimulation and to prime naive T cells against viral antigens (92).

In murine non-lymphoid tissues, the two main cDC subsets are $CD11b^+$ and $CD103^+CD11b^-$ (90). These cDCs have a tremendous capacity to permanently sense their environment and uptake antigens in tissues and blood. They express high levels of MHC complexes and the machinery to process and present antigens, they have very high migratory capacity to the lymph nodes mainly governed by the chemokine receptor CCR7 (93) and they are highly efficient in naive T cell activation and polarization. By driving T cell differentiation toward different T helper (Th) subsets or regulatory T (Treg) cells depending on their activation and the cytokine they produce, DCs have the capacity to induce immune responses against foreign antigens or to stimulate self-antigen tolerance (94, 95).

The majority of splenic and lymphoid organ DCs are renewed from BM progenitors (96, 97) and Flt3L play a major role in their homeostasis (98, 99). In human and mouse, cDCs and pDCs arise from BM $Flt3^+CD115^+$c-$kit^{low/int}$ common dendritic progenitors (CDP), downstream from progenitors common to MNs, DCs, Mϕs and OCLs (39, 97, 100, 101). DCs precursors egress from the BM and migrate to lymphoid organs and tissue to differentiate into immature cDCs (102). In contrast, pDCs are generated in the BM and then disseminate to lymphoid tissues (102). Upon inflammation or infection, inflammatory DCs are transiently generated from classical $Ly6C^{high}$ MNs that are recruited into inflamed tissues, and drive T cell activation in the draining lymph nodes (63, 103–105). Contrasting with cDCs, inflammatory DCs are not depend on Flt3L since they are generated in $Flt3L^{-/-}$ mice (106). *In vitro*, inflammatory DCs can be generated from MNs or BM cells in the presence of GM-CSF and IL-4 (105, 107). However, *in vivo* studies in knockout mice identified M-CSF receptor (CD115) as a major factor controlling their development (108). In addition to naive T cells in lymphoid organs, inflammatory DCs can also activate T cells in the inflamed tissues, in particular memory T cells (109). This function appears to be dependent on the antigen dose and the severity of inflammation (105, 106).

Over the past decade, different groups have reported on the capacity of DCs to give rise to OCLs, as described below. This was surprising as DCs are considered as fully differentiated cells and have been described to have a short life (∼1.5 to 3 days) (110, 111). However, more recent data revealed that about 5% of DCs still maintain a proliferation capacity (96, 112–114). DC survival is increased in the presence of lymphotoxin LTα1β2 (112) and RANKL (115, 116). Moreover, mature DCs can undergo further proliferation and differentiation into regulatory DCs when they are in contact with splenic stromal cells (117). These observations support a high plasticity in the fate of DCs depending on their environment.

In regard of the huge number of publications dealing with DCs in secondary organs or even in tissues, very few are focused on mature BM DCs. As in other tissues, DCs represent a small population of BM cells (1–2%) expressing high levels of CD103 (118, 119). They are mainly located in the perivascular region where they form clusters, interact with T cells and provide survival signals to B cells (119). As BM is a major reservoir of memory T cells, the presence of DCs in this organ is thought to contribute to reactivation of these memory T cells (120, 121). In contrast, naive T cell activation is supposed to be restricted to secondary lymphoid organs. However, and surprisingly, BM DCs also have the capacity to present and cross-present antigens to naive $CD4^+$ and $CD8^+$ T cells and to activate them as efficiently as DCs from lymphoid organs (122, 123). This T cell-priming activity of BM DCs is independent of spleen and lymph nodes as it was also observed in mice lacking these organs (122). These observations revealed that the BM is not just a primary lymphoid organ but that it shares some features with secondary lymphoid organs.

The first demonstration of the differentiation of OCLs from DCs was evidenced using human immature DCs generated *in vitro* from blood $CD14^+$ $CD16^{low/-}$ MNs. In response to M-CSF and RANKL, these cells differentiate as efficiently as MNs into bone-resorbing OCLs (13). Human MN-derived DCs differentiate faster than MNs and form OCLs having more nuclei than from MNs (13). This was later confirmed with murine DCs (**Figure 2C**). Splenic cDCs were shown to efficiently differentiate into OCLs in the presence of RANKL and M-CSF and among them the $CD8^-$ subpopulation is the more efficient OCL precursor, whereas OCL differentiation from pDCs is less efficient and takes longer than from cDCs (14). More importantly, this differentiation pathway was also demonstrated *in vivo* using osteopetrotic *oc/oc* mice (14, 15) in which OCLs are abundant but inactive (50). Transfer of cDCs from normal mice into *oc/oc* mice restored bone resorption and improved mice survival demonstrating that OCLs can differentiate from DCs *in vivo* and that osteopetrosis can be treated not only by hematopoietic stem cell transplantation but also by DCs infusion (14, 15). Interestingly, DC-derived OCLs and MN-derived OCLs show an equivalent expression of the main OCL markers (124) and both have the same capacity to resorb bone (13, 14) demonstrating that both populations correspond to *bona fide* OCLs.

As described above for MNs, the differentiation of OCLs from DCs is modulated by their environment. First, this differentiation has been confirmed *in vitro* and *in vivo* in a number of different pathologies related to inflammation or cancer, but never in a healthy context (125) (**Table 1**). Indeed, *in vitro*, TNFα, IL-1α, IL-17 or synovial fluid from arthritic patients enhance the differentiation of human MN-derived DCs into OCLs (13, 19). *In vivo*, the presence of Th17 cells or high levels of RANKL are required to induce the DC-to-OCL differentiation as demonstrated using osteopetrotic *oc/oc* mice or in the context of multiple myeloma (14, 21).

From all these observations, it appears that while adult OCLs differentiate from BM progenitors in steady state, they can also arise from differentiated MNs and DCs in pathological conditions. The origin of OCLs is therefore depending on the developmental stage, the BM environment and the BM recruitment of MNs or DCs. Moreover, OCLs are able to constantly incorporate new nuclei and split off

other groups of nuclei both *in vitro* (126) and *in vivo*[1] (38). Parabiosis experiments between Csf1r^{cre};Rosa26$^{LSL-YFP}$ and Csf1r^{cre};Rosa26$^{LSL-tdTomato}$ mice revealed that 0.5–2% of OCLs acquire new nuclei per day and can persist several weeks *in vivo* (38). Thus, depending on the cells that are present at their vicinity, it is very likely that OCLs are formed by a mix of different OCL progenitors instead of originating from a pure progenitor population, reflecting a high flexibility and the capacity to rapidly adapt to different pathological circumstances.

THE IMMUNE FUNCTION OF OSTEOCLASTS

A number of studies have been conducted on the regulation of OCLs by T cells under inflammatory conditions. Inflammation and bone destruction were observed to occur side by side, as shown for example for rheumatoid arthritis (RA) (127–129), periodontitis (130–133) or inflammatory bowel disease (IBD) (134, 135). During inflammatory states, it has been described that OCL progenitors respond to several interleukins produced by activated CD4$^+$ T cells such as RANKL, TNFα, and IL-17, including in human (52, 116, 136–139). Among CD4$^+$ T cells, only Th17 cells have been shown to induce or enhance OCL differentiation (56, 129, 131, 134–136). During inflammatory conditions, IL-17-expressing Th17 cells were also associated with increased bone destruction and osteoclastogenesis by up regulating RANK in OCL progenitors and by inducing RANKL expression in osteoblasts (60, 137, 140–142). Moreover, they increase the expression of monocyte-attractant chemokines such as MCP1 and MIP1α in osteoblasts and induce *in vivo* the recruitment of OCL monocytic progenitors in the BM (60). In contrast, other T cell-derived cytokines such as IFNγ, IL-4, IL-10, IL-12, and IL-18 as well as regulatory T cells were reported to have a negative effect on osteoclastogenesis (137, 143–146).

Besides numerous studies investigating the potential effect of T cells on OCLs, the reciprocal contribution of OCLs to immune modulation and the understanding of immune responses caused directly by OCLs, as for instance as antigen-presenting cells, remained undiscovered for a long time. Genome-wide expression analysis strengthened the idea that OCLs have an immune function. Indeed, comparative micro-array transcriptomic analysis revealed that *in vitro* differentiated human OCLs are transcriptionally closer to DCs than to MNs (124). Furthermore, during their *in vitro* differentiation process, murine OCLs arising from CD11b$^+$ BM cells up regulate sets of genes involved phagocytosis and immune responses (147). More recently, studies emphasized OCLs as true antigen-presenting cells to regulate and control T cell activation as well as their ability to initiate T cell responses in an antigen-dependent manner (18, 32, 33). Considering OCLs as cells having an immune function besides the classical bone resorption activity is a very new concept that is elaborated in more detail in the following sections.

[1]https://www.armchairmedical.tv/anz-bone-mineral-society/videos/intravital-imaging-of-osteoclasts-in-vivo-reveals-a-novel-cell-fate-mechanism-dr-michelle-mcdonald

Bone Resorption and Phagocytosis

The best-known OCL function is bone resorption and OCLs are regarded as professional phagocytes specially adapted to resorb bone. Contrasting with classical phagocytosis in which internalized material is degraded in intracellular endo-lysosomal vesicles, this unique property of OCLs is accomplished through an extracellular mechanism that makes the OCL a peculiar "giant macrophage" with molecular machinery distinct from any other cell type. After mature OCLs have polarized onto the bone surface, a tight and dynamic seal segregates the underneath extracellular space (later becoming the resorption lacuna) from the rest of the extracellular bone marrow space (148). A massive extracellular proton and enzyme secretion occurs through exocytosis of lysosomes at the most peripheral area of the ruffled border (**Figure 3**) (4, 149). Lysosomal membranes are inserted into this plasma membrane domain, introducing here the vacuolar H^+-ATPase (proton pump) and the ClC7 $2Cl^-/1H^+$ antiporter (chloride channel type 7), while the acidic hydrolases are released into the resorption lacuna microenvironment. Thus, the resorption lacuna has a composition very similar to the one of intracellular endosomes, with low pH, high calcium concentration and abundance of acidic hydrolyses (150, 151). The ruffled border shares membrane characteristics of late endosomes (152). When bone resorption is completed, the resorption lacuna is filled mainly with calcium and phosphate ions as well as small collagen type I fragments. Dynamic studies showed that the inner uptake domain of the ruffled border is specialized in the clathrin-mediated endocytosis of the degraded bone matrix (149, 153, 154) that allows internalization of nanosize particles (155). Then, by a small GTPase-dependent transcytosis trafficking, vacuoles cross the osteoclast cytoplasm to reach the functional secretory zone opposite to the ruffled border (153). Through this domain, the degraded bone products are released in the extracellular microenvironment and taken up by the vascular stream. Finally, although the OCL transcytosis function has been elegantly demonstrated by various groups, this does not exclude that degraded matrix components could leak out from the resorption lacuna when the tight seal of this environment is loosened and the OCL moves away from the previous resorption site to reach a new site where it re-polarizes and starts a new resorption cycle (156).

Beside their specialization in bone resorption, OCLs display the classical phagocytic properties shared by monocytic cells. Phagocytosis is a key form of endocytosis for the clearance of large particles (with few μm range) such as pathogens, microorganisms and abnormal or dead cells and it is essential for tissue repair and modeling, and for fighting against infection (31, 155). Phagocytes express a set phagocytic receptors belonging to non-opsonic receptors (such as scavenger receptors or c-lectin and lectin-like receptors) (157, 158) and to opsonic receptors (such as complement receptors and Fc receptors) (159, 160) able to recognize different microbial components and altered cells. This binding creates a phagocytic synapse and invagination of the cell membrane, activates signaling pathways, and leads to the engulfment of the particles in phagosomes, a process associated with a high dynamic cytoskeleton remodeling (161). The phagosome undergoes maturation and fuses with

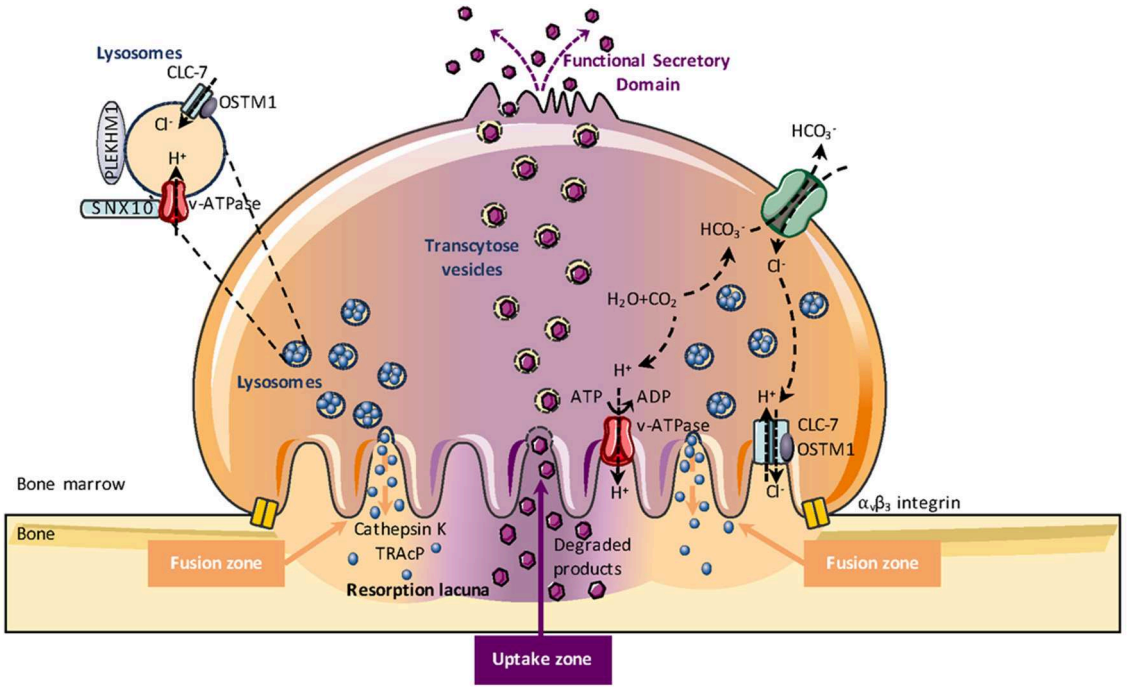

FIGURE 3 | Osteoclast-mediated bone resorption. Bone degradation requires the extracellular secretion of lysosomal enzymes, such as TRAcP (Tartrate-resistant acid phosphatase) and cathepsin K into the resorption lacuna. This exocytosis of lysosomes occurs in the peripheral region of the ruffled border (fusion zone) and is guided by PLEKHM1, OSTM1, and SNX10. Proton pumps (v-ATPase) and the CLC7-antiporter are relocated at the ruffled border plasma membrane of bone-resorbing OCLs and mediate extracellular acidification for bone demineralization during bone resorption. The v-ATPase transports protons obtained by carbohydrase-dependent hydration from CO_2 to H_2CO_3 into the resorption lacuna while HCO_3^+ is excreted via the Cl^-/HCO_3 exchanger. Molecular degradation products generated during bone resorption are released through the central region of the ruffled border (uptake zone). Through transcytosis trading, vacuoles are able to cross the OCL cytoplasm and exit the OCL from the so-called "functional secretory zone" at the basolateral plasma membrane into the vascular space.

lysosomes to form a phagolysosome having the capacity to degrade the ingested particle (31, 161). As the resorption lacuna, the phagolysosome is characterized by a low pH (4.5 to 5) maintained by V-ATPases and ClC family antiporters, and contains hydrolytic enzymes, bactericidal proteins, cationic peptides, and oxidants (162). Depending on the nature of the phagocytic cells, degradation of the ingested particles is different: while proteolysis is extensive in macrophages, it is more partial in DCs to allow the degraded peptides to associate with the MHC complexes for antigen presentation (31).

As other monocytic cells, OCL express a number of factors that play crucial roles in phagocytosis (30, 147). In OCLs, phagocytosis may provide an additional mechanism participating in degradation of calcium-phosphate (CaP) materials together with resorption (29, 163). Indeed, ultrastructural microscopy analysis revealed that OCLs are able to engulf in endophagosomes CaP crystals that undergo intracellular degradation instead of degradation in the resorption lacuna (29). They also internalize other particles such as latex beads or polymethylmethacrylate particles while they maintain their bone resorbing activity (164). This mechanism probably further increases the capacity of OCLs to degrade large particles that are difficult to resorb through classical bone resorption associated with clathrin-dependent endocytosis (29, 165). It can also be involved in implant loosening where phagocytosis of wear particles derived from implants is associated with bone destruction (29, 164).

Interestingly, phagocytosis can occur in glass-seeded OCLs that are not polarized, showing that this process is not necessarily associated with bone resorption (166). This has been demonstrated for phagocytosis of damaged cells. *In vitro*, OCLs have the capacity to recognize and engulf apoptotic bone cells, such as chondrocytes and osteocytes (30, 167, 168) but also other cell types as shown for instance for glutaraldehyde-fixed red blood cells (169) and apoptotic thymocytes, as efficiently as macrophages (30). *In vivo*, this mechanism may participate in regulating inflammation and autoimmunity by clearing apoptotic bone cells that are embedded in a matrix that only OCLs have the unique capacity to resorb (30). These data strongly support that bone resorption is not the sole function of OCLs and that these cells are participating more largely to the immune regulation in the BM.

Osteoclasts and Antigen Presentation

Beside this unique resorption function in bone homeostasis and repair, the close relationship of OCLs with MNs, Mϕs, and DCs raises the question of the potential immune function of OCLs. The fact that OCLs respond to immune signals and that the bone and the immune system are in close proximity to each

other and interact through cellular and molecular exchanges led to the conclusion that OCLs are more than just simple bone resorbing cells (36, 170–172). Indeed, it would not be surprising that OCLs maintain and share similar functions to monocytic cells, in particular DCs that are known to be professional antigen presenting cells (APCs).

Professional APCs are defined as immune cells able to process and present antigens via major histocompatibility complex (MHC), and activate naive T cells through interaction between MHCs and T cell receptors (TCRs), costimulatory signals and cytokine production. Antigens are recognized by T cells in the form of short peptides that have been processed and presented on the APC surface bound to MHC class I or MHC class II molecules (173–175). While MHC-I are ubiquitously expressed on all nucleated cells to present intracellular antigens, MHC-II molecules are constitutively expressed on professional APCs to present exogenous antigens (176, 177). However, only cDCs have the feature to cross-present antigens through MHC-I complexes to prime $CD8^+$ T cells. TCR on $CD8^+$ and $CD4^+$ T cells binds to the MHC-I and MHC-II complexes, respectively, in order to initiate naive T cell activation and to trigger TCR signaling (178, 179). A crucial step in T cell activation is mediated by co-stimulatory molecules such as CD80 (B7.1) and CD86 (B7.2) that determine the functional outcome of the TCR signaling (180, 181). Subsequently, APCs start to secrete cytokines that control the differentiation of activated T cells into effector T cell subsets such as Th1, Th2, or Th17 subsets to promote inflammatory responses or regulatory T cells that regulate immunosuppressive responses (181–184).

In addition to DCs, professional APCs also comprise B cells and Mϕs that have all constitutive expression of MHC-II (173, 185, 186). Other immune cells (including basophils, innate lymphoid cells, neutrophils, mast cells) and non-hematopoietic cells (including endothelial cells, mesenchymal stromal, epithelial cells) have been reported to upregulate MHC-II upon stimulation (187). But the absence of constitutive MHC-II expression, the lack of phagocytic function and a less evident capacity to prime naive T cells in an antigen-dependent manner make these cells atypical APCs (187). Rivollier et al. first showed that human OCLs *in vitro* differentiated from blood MN-derived DCs constitutively express HLA-DR and CD86 (13). This was further confirmed in murine OCLs differentiated *in vitro* from MNs or DCs (18), but also *in vivo* in bone marrow OCLs (18). The assumption that mature OCLs could act as APCs was equally reinforced by others (**Figure 4**). Li et al. observed that similar to DCs, human OCLs express MHC-I and II as well as the co-stimulatory molecules CD80, CD86, and CD40 (33). They also showed that OCLs are able to engulf soluble antigens and to present them on their cell surface demonstrating that OCLs can function as APCs. Additional cytokine assays confirmed that OCLs, similar to DCs, express IL-1β, IL-6, IL-10, transforming growth factor-beta (TGF-β), and TNFα further indicating that they meet the demands as APCs (18, 33). Grassi et al. strengthened this hypothesis by showing that OCLs derived from human monocytic precursors expressed MHC-II and upregulated the expression of CD80 and CD40 during their differentiation (34). Ibáñez et al. have explored this function in murine OCLs using DQ-OVA, a BODIPY-conjugated form of ovalbumin that becomes fluorescent after endolysosomal degradation. They showed that OCLs differentiated *in vitro* from MNs and from DCs both express MHC-II and costimulatory molecules and are able to process and present ovalbumin at least as efficiently as DCs (18). Furthermore, using I-A^bβ-GFP knock-in mice that express a fusion protein between GFP and the I-A^bβ subunit of the MHC-II complex, they demonstrated that OCLs constitutively express MHC-II *in vivo* (18). Lastly, OCLs were also shown to cross-present antigens via MHC-I, a feature considered to be specific for cDCs (32). Interestingly, OCLs process and present antigens even when they are cultured on plastic or when they are not able to resorb bone as shown for OCs from *oc/oc* mice (18). In addition, OCLs that process antigens still retain their bone-resorbing capacity, revealing that antigen presentation and bone resorption are independent functions in OCLs (18). These findings expanded the field of osteoimmunology by directly connecting OCLs to the immune system.

Osteoclasts and T Cell Activation

While T cell activation is usually assumed to take place in secondary lymphoid organs such as the spleen and lymph nodes, naive T cell priming, activation and polarization into effector T cells as well as memory T cell reactivation can also occur in the BM, as described above (120–123). BM T cells represent ∼3–8% of total BM cells and, compared with blood, the BM CD4/CD8 ratio is characteristically decreased (188, 189). Furthermore, in comparison to other lymphoid organs, memory $CD4^+$ T cells specific for previously encountered antigens represent the vast majority of T cells observed in the BM, which includes central memory as well as effector memory T cells (190–192). Therefore, the BM microenvironment is often described as a major reservoir for memory lymphocytes (121, 193–195). Interestingly, T cells are often observed in the close vicinity of OCLs (34, 196–198) or adherent to OCLs (198). Furthermore, OCLs were shown to express chemokines involved in T cell chemotaxis and are able to attract $CD4^+$ and $CD8^+$ T cells *in vitro* as efficiently as DCs (18, 32, 34). Together with their APC function, this supports a contribution of OCLs to the activation of T cells in the bone marrow (**Figure 4**).

Based on transcriptomic analysis showing a high expression of genes related to antigen presentation in mature OCLs (147), Seifert et al. addressed the capacity of OCLs generated from murine BM cells to activate $CD8^+$ T cells (32). Using an antigen-specific system, they reported that OCLs induce $CD8^+$ T cell proliferation and activation by antigen cross-presentation (32), a function unique to DCs that participate in anti-infectious responses and self-tolerance (199). Interestingly, these OCL-primed $CD8^+$ T cells expressed FoxP3, the master gene of regulatory T cells, and have a suppressive effect attested by their capacity to reduce the proliferation of other naive responder $CD8^+$ T cells induced by DCs (32). This study clearly revealed for the first time that OCLs are not only regulated by T cells but can initiate T cell responses themselves, creating a feedback control loop. Indeed, Buchwald et al. (200) showed that the $CD8^+$ Treg

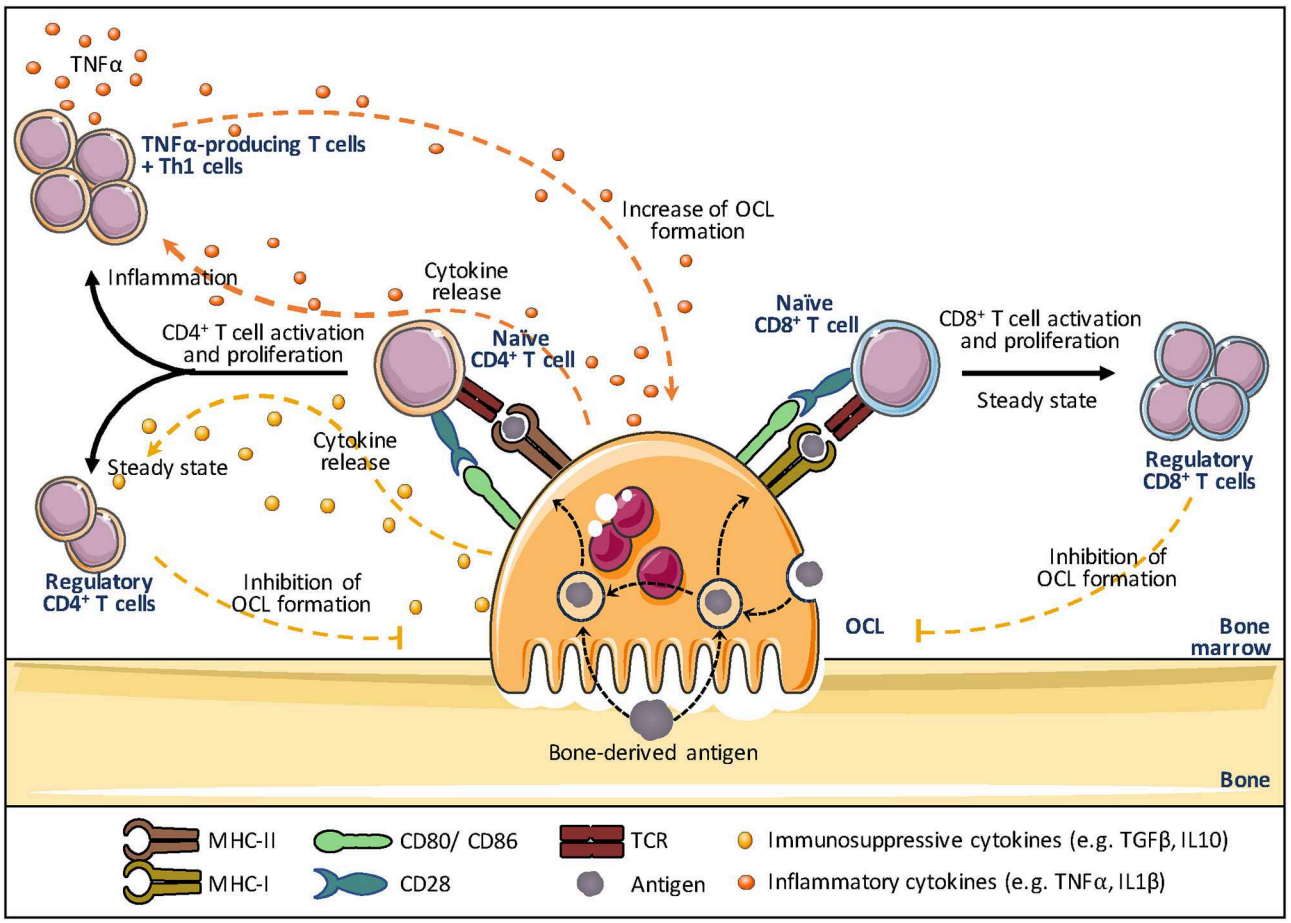

FIGURE 4 | Osteoclasts and antigen presentation. Osteoclasts (OCLs) function as antigen presenting cells (APCs). OCLs process and present antigens (coming from the bone through bone resorption or the bone marrow) in the form of short peptides bound to major histocompatibility complex (MHC)-I or MHC-II molecules. The T cell receptor (TCR) on $CD8^+$ and $CD4^+$ T cells binds to the MHC-I and MHC-II complex, respectively, to initiate T cell activation and to trigger TCR signaling. A key step in T cell activation represents the T cell binding to co-stimulatory molecules (e.g. CD80 and CD86 on OCLs and CD28 on T cells), as they determine the functional outcome of the T cell receptor signaling. Subsequently, OCLs start secreting cytokines that control the differentiation of activated T cells. In steady state, OCLs produce mainly IL-10 and TGFβ and induce regulatory T cells (Treg) that are responsible for immunosuppressive responses and inhibit OCL differentiation, creating a negative feedback down regulating both inflammation and bone resorption. In contrast, in inflammation, OCLs induce effector TNFα-producing T cells that promote inflammation and may stimulate osteoclastogenesis thanks to their TNFα production. The effect of OCLs on $CD8^+$ T cells in inflammatory conditions has not been explored yet.

cells induced by OCLs are in turn able to suppress the resorptive function of OCLs as well as their differentiation.

Besides these findings, OCLs are also able to interact with naive $CD4^+$ T cells. Using a reliable procedure to sort pure OCLs (18, 51), Ibanez et al. (18) demonstrated that OCLs from the BM of healthy mice induced $FoxP3^+$ $CD4^+$ T cells in an antigen-specific manner. These cells were shown to inhibit the activation of $CD4^+$ T cells, confirming that they are immunosuppressive $CD4^+$ Treg cells (18). This capacity was confirmed in human OCLs using T cells from tetanus toxoid (TT)-immunized healthy donors (33). OCLs pulsed with TT activate $CD4^+$ T cells that produce high levels of the immunosuppressive cytokines IL-10 and TGF-β, evoking suppressive T cells (33). OCL-induced immunosuppression has also recently been reported in association with hematologic malignancies (35, 36, 201). In the context of multiple myeloma (MM), OCLs were shown to play a crucial role in the induction of an immunosuppressive microenvironment by upregulating inhibitory checkpoint molecules such as programmed death ligand 1 (PD-L1), CD200 and Galectin-9 as well as immunosuppressive cytokines (**Figure 5**). In addition, OCLs protect MM cells against T cell-mediated cytotoxicity through inhibition of $CD4^+$ and $CD8^+$ T cells and thereby support the development of the malignancy (35).

However, OCLs are not restricted to immunosuppressive function. Indeed, while OCLs derived from healthy mice induce immunosuppressive $CD4^+$ Treg cells, those derived from mice under inflammatory conditions induced TNFα-producing $CD4^+$ T cells, as shown in the context of inflammatory bowel disease (18), a chronic inflammatory disease associated with increased

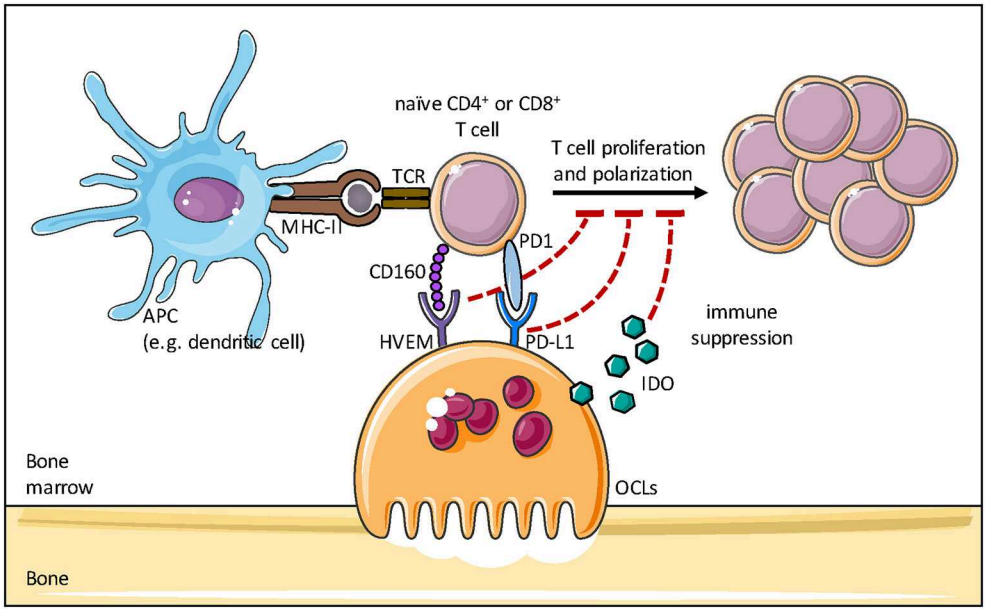

FIGURE 5 | Osteoclasts and immune modulation. Osteoclasts are able to induce an immunosuppressive microenvironment by upregulating inhibitory checkpoint molecules such as programmed death ligand 1 (PD-L1), herpes virus entry mediator (HVEM) and Indoleamine 2,3-dioxygenase (IDO), thereby inhibiting the proliferation and polarization of naive T cells induced by antigen presenting cells (APCs).

OCL differentiation and severe bone destruction (60) (**Figure 4**). As OCLs from healthy mice, MN-derived OCLs induce $CD4^+$ Treg cells and express higher levels of the immunosuppressive cytokine IL-10 than DC-derived OCLs (18). In contrast, as OCLs derived from mice affected by chronic inflammation, DC-derived OCLs very efficiently induce differentiation of $TNF\alpha^+$ $CD4^+$ T cells and express higher levels of inflammatory cytokines (TNFα, IL-1β, IL-6) than MN-derived OCLs (18). These data unveiled for the first time the existence of different OCL subsets having opposite effects on the immune system depending on their context and cell origin. Searching for markers specific for murine OCL subsets, Ibanez et al. identified by flow cytometry the fractalkine receptor CX3CR1 as the first marker specifically expressed in inflammatory OCLs. Admittedly, only about 20% of inflammatory OCLs are positive for CX3CR1 (18) and the role of CX3CR1 in these OCLs as well as the function of $CX3CR1^+$ and $CX3CR1^-$ inflammatory OCLs have not yet been addressed.

Physiological and Clinical Relevance of the Immune Function of Osteoclasts

In the end, the question remains what the biological relevance of antigen presentation by OCLs is. Comparable to APCs, OCLs mainly use clathrin-mediated endocytosis and micropinocytosis to internalize bone degradation products (179, 202). Thus, the physiological significance of the immune function of OCLs may be associated with the sustained release of self-peptides from bone resorption. These self-peptides can be presented by OCLs to inhibit self-responses by producing immunosuppressive cytokines and inducing suppressive Treg cells (18, 32, 200). In addition, OCLs have the ability to engulf and present antigens that are not coming from bone resorption (18, 34). This may also include antigens originating from the periphery such as blood-borne antigens (122, 123) or antigens carried by circulating DCs, neutrophils and B cells (120, 203) that can be presented directly on MHC-II molecules. Interestingly, the proportion of Treg cells among T cells in the BM is higher than in other tissues (204, 205) and they provide the BM with an immune privilege that is required for the maintenance of hematopoietic stem/progenitor cells (205). They also down regulate OCL differentiation participating thereby to the control of bone homeostasis (206–208). Thus, OCLs could therefore be regarded as BM resident APCs participating to maintain the BM immune tolerance under physiological conditions.

Contrary to this, OCL subsets generated under inflammatory conditions are devoid of the capacity to induce Treg cells but instead they induce effector $CD4^+$ T cells that produce TNFα, an inflammatory cytokine that stimulates osteoclastogenesis and promotes inflammation (18). These T cells may also participate in auto-immune responses against bone antigens or in the activation of hematopoietic stem cells. Moreover, the cytokine production profile of OCLs is not only dependent on their physiological or inflammatory environment and cell origin (18) but also on their capacity to respond to bone and bone matrix proteins by secreting high levels of the pro-inflammatory cytokine IL-1β (83, 85, 86, 209). Overall, these data point inflammatory OCLs as major actors in a vicious circle linking bone destruction and inflammation.

This contribution of OCLs not only to bone resorption and homeostasis, but also to immune responses, encompasses the function of classical OCLs and sheds new light on the field of

osteoimmunology. These insights make OCL an important target for anti-inflammatory therapies of chronic inflammatory diseases as well as for influencing the bone environment.

Of note, pathologies related to abnormal OCL activity/differentiation are frequently associated with immune dysfunctions not only in mouse but also in human. In osteopetrotic patients with defective OCL activity or differentiation, bone marrow failure is responsible for extramedullary hematopoiesis and contributes to immune deficiency and increases the risk of infections (210, 211). Besides, genes affected by osteopetrotic defects are not only essential for bone resorption but are also involved in immune responses. Among other examples, deficiency in *Acp5* (encoding TRAcP) induces bone dysplasia but also autoimmunity (212, 213) and deletion or inhibition of *Ctsk* blocks both bone degradation and inflammation (214, 215). In osteoporosis, a number of immune-system related genes are differentially expressed in the BM of post-menopausal osteoporotic patients compared to non-osteoporotic individuals, including cytokines and factors involved in innate immunity (216–218). While such differences in gene expression and immune cell activation are clearly promoting bone destruction, the participation on OCLs in these immune modifications is still not known but cannot be excluded.

The immune function of OCLs emerged only recently, explaining why its contribution to OCL-associated diseases or its modulation by anti-resorption therapies has not yet been explored. A major issue for such investigation is the absence of markers specific for human OCL subsets that are required to identify inflammatory and anti-inflammatory OCLs. Thus, a deeper molecular profiling of human OCL sub-populations and characterization of their immune function remains essential to enable further studies in affected patients.

CONCLUSION

In the last decade, remarkable advances have been made in understanding the interactions between the skeletal and the immune system under both physiological and pathological conditions. In particular, the influence of T cells on OCL formation and activation through complex cytokine interactions including TNFα and RANKL were thoroughly investigated and immune cells were shown to regulate bone cell differentiation and activity. Today however, these interactions are known to be reciprocal, increasing further, the interest for OCLs as immune cells.

Depending on the context, different OCLs are described to derive from distinct progenitor cells. Based on the numerous OCL precursors described, and on the recent identification of an iterative fusion of mature OCLs with circulating monocytic cells[2](38), the possibility of OCL heterogeneity is huge. Additionally, some precursor cells seem to differentiate much more easily than others depending on their context. The existence of heterogeneous OCL populations appears unsurprising when considering that OCL precursors, including MNs and DCs, have been described as phenotypically and functionally heterogeneous for many years. Thus, bone destruction does not rely only on an increase in OCL differentiation and function, but also on the recruitment of OCL subsets that differ from steady state OCLs.

These novel insights in the field of osteoimmunology open new exciting perspectives and emphasize that OCL function is not restricted to bone resorption but expanded to immune cell differentiation and immunomodulation. Based on these observations and according to their immune function, OCLs could act as key players and regulators of the bone immune status in steady state as well as during inflammatory processes and they should not anymore be regarded only as bone-resorbing cells. Therefore, relying only on bone resorption may not be sufficient to block inflammatory bone destruction. New specific anti-resorptive agents targeting inflammatory OCLs and the associated T cell interaction could provide a very novel effective strategy to control inflammatory bone loss and the bone environment without compromising physiological bone remodeling by steady state OCLs.

AUTHOR CONTRIBUTIONS

CB-W conceived the original idea and designed the project. M-BM, LI, TdV, AW, FA, and AT participated in writing the manuscript. M-BM and LI designed the figures. M-BM edited the figures. CB-W edited the manuscript.

FUNDING

This work was supported by the Fondation pour la Recherche Médicale (FRM, ECO20160736019), the Agence Nationale de la Recherche (ANR-16-CE14-0030), the University Côte d'Azur (ANR-15-IDEX-01), the Fondation Arthritis and the Société Française de Biologie des Tissus Minéralisés (SFBTM). Figures have been drawn from pictures from the "Servier Medical Art" gallery, http://smart.servier.com/.

[2]https://www.armchairmedical.tv/anz-bone-mineral-society/videos/intravital-imaging-of-osteoclasts-in-vivo-reveals-a-novel-cell-fate-mechanism-dr-michelle-mcdonald

REFERENCES

1. Kölliker A. *Die normale Resorption des Knochengewebes und Ihre Bedeutung für die Entstehung der Typischen Knochenformen.* (1873). Available online at: https://archive.org/details/b22392610/page/n107
2. Walker DG. Control of bone resorption by hematopoietic tissue. The induction and reversal of congenital osteopetrosis in mice through use of bone marrow and splenic transplants. *J Exp Med.* (1975) 142:651–63. doi: 10.1084/jem.142.3.651
3. Udagawa N, Takahashi N, Akatsu T, Tanaka H, Sasaki T, Nishihara T, et al. Origin of osteoclasts: mature monocytes and macrophages are capable of differentiating into osteoclasts under a suitable microenvironment prepared by bone marrow-derived stromal cells. *Proc Natl Acad Sci USA.* (1990) 87:7260–4. doi: 10.1073/pnas.87.18.7260
4. Cappariello A, Maurizi A, Veeriah V, Teti A. The Great Beauty of the osteoclast. *Arch Biochem Biophys.* (2014) 558:70–8. doi: 10.1016/j.abb.2014.06.017

5. Gordon S, Taylor PR. Monocyte and macrophage heterogeneity. *Nat Rev Immunol.* (2005) 5:953. doi: 10.1038/nri1733
6. Lavin Y, Mortha A, Rahman A, Merad M. Regulation of macrophage development and function in peripheral tissues. *Nat Rev Immunol.* (2015) 15:731–44. doi: 10.1038/nri3920
7. Sprangers S, Vries TJ de, Everts V. Monocyte heterogeneity: consequences for monocyte-derived immune cells. *J Immunol Res.* (2016) 2016:1–10. doi: 10.1155/2016/1475435
8. Guilliams M, Mildner A, Yona S. Developmental and functional heterogeneity of monocytes. *Immunity.* (2018) 49:595–613. doi: 10.1016/j.immuni.2018.10.005
9. Mantovani A, Sica A, Locati M. New vistas on macrophage differentiation and activation. *Eur J Immunol.* (2007) 37:14–6. doi: 10.1002/eji.200636910
10. Mócsai A, Humphrey MB, Van Ziffle JAG, Hu Y, Burghardt A, Spusta SC, et al. The immunomodulatory adapter proteins DAP12 and Fc receptor gamma-chain (FcRgamma) regulate development of functional osteoclasts through the Syk tyrosine kinase. *Proc Natl Acad Sci USA.* (2004) 101:6158–63. doi: 10.1073/pnas.0401602101
11. Koga T, Inui M, Inoue K, Kim S, Suematsu A, Kobayashi E, et al. Costimulatory signals mediated by the ITAM motif cooperate with RANKL for bone homeostasis. *Nature.* (2004) 428:758–63. doi: 10.1038/nature02444
12. Baron R. Arming the osteoclast. *Nat Med.* (2004) 10:458–60. doi: 10.1038/nm0504-458
13. Rivollier A, Mazzorana M, Tebib J, Piperno M, Aitsiselmi T, Rabourdin-Combe C, et al. Immature dendritic cell transdifferentiation into osteoclasts: a novel pathway sustained by the rheumatoid arthritis microenvironment. *Blood.* (2004) 104:4029–37. doi: 10.1182/blood-2004-01-0041
14. Wakkach A, Mansour A, Dacquin R, Coste E, Jurdic P, Carle GF, et al. Bone marrow microenvironment controls the *in vivo* differentiation of murine dendritic cells into osteoclasts. *Blood.* (2008) 112:5074–83. doi: 10.1182/blood-2008-01-132787
15. Mansour A, Abou-Ezzi G, Sitnicka E, Jacobsen SEW, Wakkach A, Blin-Wakkach C. Osteoclasts promote the formation of hematopoietic stem cell niches in the bone marrow. *J Exp Med.* (2012) 209:537–49. doi: 10.1084/jem.20110994
16. Maitra R, Follenzi A, Yaghoobian A, Montagna C, Merlin S, Cannizzo ES, et al. Dendritic cell-mediated *in vivo* bone resorption. *J Immunol.* (2010) 185:1485–91. doi: 10.4049/jimmunol.0903560
17. Grosjean F, Nasi S, Schneider P, Chobaz V, Liu A, Mordasini V, et al. Dendritic cells cause bone lesions in a new mouse model of histiocytosis. *PLoS ONE.* (2015) 10:e0133917. doi: 10.1371/journal.pone.0133917
18. Ibáñez L, Abou-Ezzi G, Ciucci T, Amiot V, Belaïd N, Obino D, et al. Inflammatory osteoclasts prime TNFα-producing CD4(+) T cells and express CX3 CR1. *J Bone Miner Res.* (2016) 31:1899–908. doi: 10.1002/jbmr.2868
19. Speziani C, Rivollier A, Gallois A, Coury F, Mazzorana M, Azocar O, et al. Murine dendritic cell transdifferentiation into osteoclasts is differentially regulated by innate and adaptive cytokines. *Eur J Immunol.* (2007) 37:747–57. doi: 10.1002/eji.200636534
20. Alnaeeli M, Penninger JM, Teng Y-TA. Immune interactions with CD4+ T cells promote the development of functional osteoclasts from murine CD11c+ dendritic cells. *J Immunol.* (2006) 177:3314–26. doi: 10.4049/jimmunol.177.5.3314
21. Tucci M, Stucci S, Savonarola A, Ciavarella S, Cafforio P, Dammacco F, et al. Immature dendritic cells in multiple myeloma are prone to osteoclast-like differentiation through interleukin-17A stimulation. *Br J Haematol.* (2013) 161:821–31. doi: 10.1111/bjh.12333
22. Tucci M, Ciavarella S, Strippoli S, Brunetti O, Dammacco F, Silvestris F. Immature dendritic cells from patients with multiple myeloma are prone to osteoclast differentiation *in vitro*. *Exp Hematol.* (2011) 39:773–83.e1. doi: 10.1016/j.exphem.2011.04.006
23. da Costa CET, Annels NE, Faaij CMJM, Forsyth RG, Hogendoorn PCW, Egeler RM. Presence of osteoclast-like multinucleated giant cells in the bone and nonostotic lesions of Langerhans cell histiocytosis. *J Exp Med.* (2005) 201:687–93. doi: 10.1084/jem.20041785
24. Ginhoux F, Tacke F, Angeli V, Bogunovic M, Loubeau M, Dai X-M, et al. Langerhans cells arise from monocytes *in vivo*. *Nat Immunol.* (2006) 7:265–73. doi: 10.1038/ni1307
25. Hoeffel G, Wang Y, Greter M, See P, Teo P, Malleret B, et al. Adult Langerhans cells derive predominantly from embryonic fetal liver monocytes with a minor contribution of yolk sac-derived macrophages. *J Exp Med.* (2012) 209:1167–81. doi: 10.1084/jem.20120340
26. Kaplan DH. Ontogeny and function of murine epidermal Langerhans cells. *Nat Immunol.* (2017) 18:1068–75. doi: 10.1038/ni.3815
27. Wang W, Ferguson DJ, Quinn JM, Simpson AH, Athanasou NA. Biomaterial particle phagocytosis by bone-resorbing osteoclasts. *J Bone Joint Surg Br.* (1997) 79:849–56. doi: 10.1302/0301-620X.79B5.7780
28. Sakai E, Miyamoto H, Okamoto K, Kato Y, Yamamoto K, Sakai H. Characterization of phagosomal subpopulations along endocytic routes in osteoclasts and macrophages. *J Biochem.* (2001) 130:823–31. doi: 10.1093/oxfordjournals.jbchem.a003054
29. Heymann D, Guicheux J, Rousselle V. Ultrastructural evidence *in vitro* of osteoclast-induced degradation of calcium phosphate ceramic by simultaneous resorption and phagocytosis mechanisms. *Histol Histopathol.* (2001) 16:37–44. doi: 10.14670/HH-16.37
30. Harre U, Keppeler H, Ipseiz N, Derer A, Poller K, Aigner M, et al. Moonlighting osteoclasts as undertakers of apoptotic cells. *Autoimmunity.* (2012) 45:612–9. doi: 10.3109/08916934.2012.719950
31. Gordon S. Phagocytosis: an immunobiologic process. *Immunity.* (2016) 44:463–75. doi: 10.1016/j.immuni.2016.02.026
32. Kiesel JR, Buchwald ZS, Aurora R. Cross-presentation by osteoclasts induces FoxP3 in CD8+ T cells. *J Immunol.* (2009) 182:5477–87. doi: 10.4049/jimmunol.0803897
33. Li H, Hong S, Qian J, Zheng Y, Yang J, Yi Q. Cross talk between the bone and immune systems: osteoclasts function as antigen-presenting cells and activate CD4+ and CD8+ T cells. *Blood.* (2010) 116:210–7. doi: 10.1182/blood-2009-11-255026
34. Grassi F, Manferdini C, Cattini L, Piacentini A, Gabusi E, Facchini A, et al. T cell suppression by osteoclasts *in vitro*. *J Cell Physiol.* (2011) 226:982–90. doi: 10.1002/jcp.22411
35. An G, Acharya C, Feng X, Wen K, Zhong M, Zhang L, et al. Osteoclasts promote immune suppressive microenvironment in multiple myeloma: therapeutic implication. *Blood.* (2016) 128:1590–603. doi: 10.1182/blood-2016-03-707547
36. Mansour A, Wakkach A, Blin-Wakkach C. Emerging roles of osteoclasts in the modulation of bone microenvironment and immune suppression in multiple myeloma. *Front Immunol.* (2017) 8:954. doi: 10.3389/fimmu.2017.00954
37. Everts V, Korper W, Jansen DC, Steinfort J, Lammerse I, Heera S, et al. Functional heterogeneity of osteoclasts: matrix metalloproteinases participate in osteoclastic resorption of calvarial bone but not in resorption of long bone. *FASEB J.* (1999) 13:1219–30. doi: 10.1096/fasebj.13.10.1219
38. Jacome-Galarza CE, Percin GI, Muller JT, Mass E, Lazarov T, Eitler J, et al. Developmental origin, functional maintenance and genetic rescue of osteoclasts. *Nature.* (2019) 568:541–5. doi: 10.1038/s41586-019-1105-7
39. Xiao Y, Zijl S, Wang L, de Groot DC, van Tol MJ, Lankester AC, et al. Identification of the common origins of osteoclasts, macrophages, and dendritic cells in human hematopoiesis. *Stem Cell Rep.* (2015) 4:984–94. doi: 10.1016/j.stemcr.2015.04.012
40. Xiao Y, Palomero J, Grabowska J, Wang L, de Rink I, van Helvert L, et al. Macrophages and osteoclasts stem from a bipotent progenitor downstream of a macrophage/osteoclast/dendritic cell progenitor. *Blood Adv.* (2017) 1:1993–2006. doi: 10.1182/bloodadvances.2017008540
41. Arai F, Miyamoto T, Ohneda O, Inada T, Sudo T, Brasel K, et al. Commitment and differentiation of osteoclast precursor cells by the sequential expression of C-Fms and receptor activator of nuclear factor κb (Rank) receptors. *J Exp Med.* (1999) 190:1741–54. doi: 10.1084/jem.190.12.1741
42. Miyamoto T. Bifurcation of osteoclasts and dendritic cells from common progenitors. *Blood.* (2001) 98:2544–54. doi: 10.1182/blood.V98.8.2544
43. Jacome-Galarza CE, Lee S-K, Lorenzo JA, Aguila HL. Identification, characterization, and isolation of a common progenitor for osteoclasts, macrophages, and dendritic cells from murine bone marrow and periphery. *J Bone Miner Res.* (2013) 28:1203–13. doi: 10.1002/jbmr.1822
44. Jacquin C, Gran DE, Lee SK, Lorenzo JA, Aguila HL. Identification of multiple osteoclast precursor populations in murine bone marrow. *J Bone Miner Res.* (2005) 21:67–77. doi: 10.1359/JBMR.051007

45. Xiao Y, Song J-Y, de Vries TJ, Fatmawati C, Parreira DB, Langenbach GEJ, et al. Osteoclast precursors in murine bone marrow express CD27 and are impeded in osteoclast development by CD70 on activated immune cells. *Proc Natl Acad Sci USA.* (2013) 110:12385–90. doi: 10.1073/pnas.1216082110
46. de Vries TJ, Schoenmaker T, Hooibrink B, Leenen PJM, Everts V. Myeloid blasts are the mouse bone marrow cells prone to differentiate into osteoclasts. *J Leukoc Biol.* (2009) 85:919–27. doi: 10.1189/jlb.0708402
47. Mizoguchi T, Muto A, Udagawa N, Arai A, Yamashita T, Hosoya A, et al. Identification of cell cycle-arrested quiescent osteoclast precursors in vivo. *J Cell Biol.* (2009) 184:541–54. doi: 10.1083/jcb.200806139
48. Muto A, Mizoguchi T, Udagawa N, Ito S, Kawahara I, Abiko Y, et al. Lineage-committed osteoclast precursors circulate in blood and settle down into bone. *J Bone Miner Res.* (2011) 26:2978–90. doi: 10.1002/jbmr.490
49. Gomez Perdiguero E, Klapproth K, Schulz C, Busch K, Azzoni E, Crozet L, et al. Tissue-resident macrophages originate from yolk-sac-derived erythro-myeloid progenitors. *Nature.* (2015) 518:547–51. doi: 10.1038/nature13989
50. Blin-Wakkach C, Wakkach A, Sexton PM, Rochet N, Carle GF. Hematological defects in the oc/oc mouse, a model of infantile malignant osteopetrosis. *Leukemia.* (2004) 18:1505–11. doi: 10.1038/sj.leu.2403449
51. Madel M-B, Ibáñez L, Rouleau M, Wakkach A, Blin-Wakkach C. A novel reliable and efficient procedure for purification of mature osteoclasts allowing functional assays in mouse cells. *Front Immunol.* (2018) 9:2567. doi: 10.3389/fimmu.2018.02567
52. Boyle WJ, Simonet WS, Lacey DL. Osteoclast differentiation and activation. *Nature.* (2003) 423:337–42. doi: 10.1038/nature01658
53. Xing L. Osteoclast fusion and regulation by RANKL-dependent and independent factors. *World J Orthop.* (2012) 3:212. doi: 10.5312/wjo.v3.i12.212
54. Marino S, Logan JG, Mellis D, Capulli M. Generation and culture of osteoclasts. *BoneKEy Rep.* (2014) 3:570. doi: 10.1038/bonekey.2014.65
55. Seeling M, Hillenhoff U, David JP, Schett G, Tuckermann J, Lux A, et al. Inflammatory monocytes and Fcγ receptor IV on osteoclasts are critical for bone destruction during inflammatory arthritis in mice. *Proc Natl Acad Sci USA.* (2013) 110:10729–34. doi: 10.1073/pnas.1301001110
56. Ammari M, Presumey J, Ponsolles C, Roussignol G, Roubert C, Escriou V, et al. Delivery of miR-146a to Ly6C ^{high} monocytes inhibits pathogenic bone erosion in inflammatory arthritis. *Theranostics.* (2018) 8:5972–85. doi: 10.7150/thno.29313
57. Hoeffel G, Ginhoux F. Fetal monocytes and the origins of tissue-resident macrophages. *Cell Immunol.* (2018) 330:5–15. doi: 10.1016/j.cellimm.2018.01.001
58. Auffray C, Fogg D, Garfa M, Elain G, Join-Lambert O, Kayal S, et al. Monitoring of blood vessels and tissues by a population of monocytes with patrolling behavior. *Science.* (2007) 317:666–70. doi: 10.1126/science.1142883
59. Shi C, Pamer EG. Monocyte recruitment during infection and inflammation. *Nat Rev Immunol.* (2011) 11:762–74. doi: 10.1038/nri3070
60. Ciucci T, Ibáñez L, Boucoiran A, Birgy-Barelli E, Pène J, Abou-Ezzi G, et al. Bone marrow Th17 TNFα cells induce osteoclast differentiation, and link bone destruction to IBD. *Gut.* (2015) 64:1072–81. doi: 10.1136/gutjnl-2014-306947
61. Auffray C, Sieweke MH, Geissmann F. Blood monocytes: development, heterogeneity, and relationship with dendritic cells. *Annu Rev Immunol.* (2009) 27:669–92. doi: 10.1146/annurev.immunol.021908.132557
62. Geissmann F, Gordon S, Hume DA, Mowat AM, Randolph GJ. Unravelling mononuclear phagocyte heterogeneity. *Nat Rev Immunol.* (2010) 10:453–60. doi: 10.1038/nri2784
63. Varol C, Landsman L, Fogg DK, Greenshtein L, Gildor B, Margalit R, et al. Monocytes give rise to mucosal, but not splenic, conventional dendritic cells. *J Exp Med.* (2007) 204:171–80. doi: 10.1084/jem.20061011
64. Fogg DK, Sibon C, Miled C, Jung S, Aucouturier P, Littman DR, et al. A clonogenic bone marrow progenitor specific for macrophages and dendritic cells. *Science.* (2006) 311:83–7. doi: 10.1126/science.1117729
65. Cros J, Cagnard N, Woollard K, Patey N, Zhang S-Y, Senechal B, et al. Human CD14dim monocytes patrol and sense nucleic acids and viruses via TLR7 and TLR8 receptors. *Immunity.* (2010) 33:375–86. doi: 10.1016/j.immuni.2010.08.012
66. Villani A-C, Satija R, Reynolds G, Sarkizova S, Shekhar K, Fletcher J, et al. Single-cell RNA-seq reveals new types of human blood dendritic cells, monocytes, and progenitors. *Science.* (2017) 356. doi: 10.1126/science.aah4573
67. Chong SZ, Evrard M, Devi S, Chen J, Lim JY, See P, et al. CXCR4 identifies transitional bone marrow premonocytes that replenish the mature monocyte pool for peripheral responses. *J Exp Med.* (2016) 213:2293–314. doi: 10.1084/jem.20160800
68. Serbina NV, Pamer EG. Monocyte emigration from bone marrow during bacterial infection requires signals mediated by chemokine receptor CCR2. *Nat Immunol.* (2006) 7:311–7. doi: 10.1038/ni1309
69. Nguyen KD, Fentress SJ, Qiu Y, Yun K, Cox JS, Chawla A. Circadian gene Bmal1 regulates diurnal oscillations of Ly6C(hi) inflammatory monocytes. *Science.* (2013) 341:1483–8. doi: 10.1126/science.1240636
70. Patel AA, Zhang Y, Fullerton JN, Boelen L, Rongvaux A, Maini AA, et al. The fate and lifespan of human monocyte subsets in steady state and systemic inflammation. *J Exp Med.* (2017) 214:1913–23. doi: 10.1084/jem.20170355
71. Guilliams M, Scott CL. Does niche competition determine the origin of tissue-resident macrophages? *Nat Rev Immunol.* (2017) 17:451–60. doi: 10.1038/nri.2017.42
72. Yona S, Kim K-W, Wolf Y, Mildner A, Varol D, Breker M, et al. Fate mapping reveals origins and dynamics of monocytes and tissue macrophages under homeostasis. *Immunity.* (2013) 38:79–91. doi: 10.1016/j.immuni.2012.12.001
73. Swirski FK, Nahrendorf M, Etzrodt M, Wildgruber M, Cortez-Retamozo V, Panizzi P, et al. Identification of splenic reservoir monocytes and their deployment to inflammatory sites. *Science.* (2009) 325:612–6. doi: 10.1126/science.1175202
74. Sunderkötter C, Nikolic T, Dillon MJ, Van Rooijen N, Stehling M, Drevets DA, et al. Subpopulations of mouse blood monocytes differ in maturation stage and inflammatory response. *J Immunol.* (2004) 172:4410–7. doi: 10.4049/jimmunol.172.7.4410
75. Carlin LM, Stamatiades EG, Auffray C, Hanna RN, Glover L, Vizcay-Barrena G, et al. Nr4a1-dependent Ly6C(low) monocytes monitor endothelial cells and orchestrate their disposal. *Cell.* (2013) 153:362–75. doi: 10.1016/j.cell.2013.03.010
76. Peng Y, Latchman Y, Elkon KB. Ly6C(low) monocytes differentiate into dendritic cells and cross-tolerize T cells through PDL-1. *J Immunol.* (2009) 182:2777–85. doi: 10.4049/jimmunol.0803172
77. Park-Min K-H, Lee EY, Moskowitz NK, Lim E, Lee S-K, Lorenzo JA, et al. Negative regulation of osteoclast precursor differentiation by CD11b and β 2 integrin-B-cell lymphoma 6 signaling. *J Bone Miner Res.* (2013) 28:135–49. doi: 10.1002/jbmr.1739
78. Zhao Z, Hou X, Yin X, Li Y, Duan R, Boyce BF, et al. TNF induction of NF-κB RelB enhances RANKL-induced osteoclastogenesis by promoting inflammatory macrophage differentiation but also limits it through suppression of NFATc1 expression. *PLoS ONE.* (2015) 10:e0135728. doi: 10.1371/journal.pone.0135728
79. Charles JF, Hsu L-Y, Niemi EC, Weiss A, Aliprantis AO, Nakamura MC. Inflammatory arthritis increases mouse osteoclast precursors with myeloid suppressor function. *J Clin Invest.* (2012) 122:4592–605. doi: 10.1172/JCI60920
80. Komano Y, Nanki T, Hayashida K, Taniguchi K, Miyasaka N. Identification of a human peripheral blood monocyte subset that differentiates into osteoclasts. *Arthritis Res Ther.* (2006) 8:R152. doi: 10.1186/ar2046
81. Geissmann F, Jung S, Littman DR. Blood monocytes consist of two principal subsets with distinct migratory properties. *Immunity.* (2003) 19:71–82. doi: 10.1016/S1074-7613(03)00174-2
82. Sprangers S, Schoenmaker T, Cao Y, Everts V, de Vries TJ. Different blood-borne human osteoclast precursors respond in distinct ways to IL-17A. *J Cell Physiol.* (2016) 231:1249–60. doi: 10.1002/jcp.25220
83. De Vries TJ, el Bakkali I, Schett GA, Kamradt T, Jansen ID, D'Amelio P. What are the peripheral blood determinants for increased osteoclast formation in the various inflammatory diseases associated with bone loss? *Front Immunol.* (2019) 10:505. doi: 10.3389/fimmu.2019.00505
84. Chiu YG, Shao T, Feng C, Mensah KA, Thullen M, Schwarz EM, et al. CD16 (FcRγIII) as a potential marker of osteoclast precursors in psoriatic arthritis. *Arthritis Res Ther.* (2010) 12:R14. doi: 10.1186/ar2915

85. Cao Y, Jansen IDC, Sprangers S, Stap J, Leenen PJM, Everts V, et al. IL-1β differently stimulates proliferation and multinucleation of distinct mouse bone marrow osteoclast precursor subsets. *J Leukoc Biol.* (2016) 100:513–23. doi: 10.1189/jlb.1A1215-543R
86. de Vries TJ, Schoenmaker T, Aerts D, Grevers LC, Souza PPC, Nazmi K, et al. M-CSF priming of osteoclast precursors can cause osteoclastogenesis-insensitivity, which can be prevented and overcome on bone: bone activates osteoclast precursors. *J Cell Physiol.* (2015) 230:210–25. doi: 10.1002/jcp.24702
87. Cao Y, Jansen IDC, Sprangers S, de Vries TJ, Everts V. TNF-α has both stimulatory and inhibitory effects on mouse monocyte-derived osteoclastogenesis. *J Cell Physiol.* (2017) 232:3273–85. doi: 10.1002/jcp.26024
88. Barrow AD, Raynal N, Andersen TL, Slatter DA, Bihan D, Pugh N, et al. OSCAR is a collagen receptor that costimulates osteoclastogenesis in DAP12-deficient humans and mice. *J Clin Invest.* (2011) 121:3505–16. doi: 10.1172/JCI45913
89. Steinman RM, Cohn ZA. Identification of a novel cell type in peripheral lymphoid organs of mice. I. Morphology, quantitation, tissue distribution. *J Exp Med.* (1973) 137:1142–62. doi: 10.1084/jem.137.5.1142
90. Merad M, Sathe P, Helft J, Miller J, Mortha A. The dendritic cell lineage: ontogeny and function of dendritic cells and their subsets in the steady state and the inflamed setting. *Annu Rev Immunol.* (2013) 31:563–604. doi: 10.1146/annurev-immunol-020711-074950
91. Schlitzer A, McGovern N, Ginhoux F. Dendritic cells and monocyte-derived cells: two complementary and integrated functional systems. *Semin Cell Dev Biol.* (2015) 41:9–22. doi: 10.1016/j.semcdb.2015.03.011
92. Reizis B, Bunin A, Ghosh HS, Lewis KL, Sisirak V. Plasmacytoid dendritic cells: recent progress and open questions. *Annu Rev Immunol.* (2011) 29:163–83. doi: 10.1146/annurev-immunol-031210-101345
93. Ohl L, Mohaupt M, Czeloth N, Hintzen G, Kiafard Z, Zwirner J, et al. CCR7 governs skin dendritic cell migration under inflammatory and steady-state conditions. *Immunity.* (2004) 21:279–88. doi: 10.1016/j.immuni.2004.06.014
94. Walsh KP, Mills KHG. Dendritic cells and other innate determinants of T helper cell polarisation. *Trends Immunol.* (2013) 34:521–30. doi: 10.1016/j.it.2013.07.006
95. Wakkach A, Fournier N, Brun V, Breittmayer J-P, Cottrez F, Groux H. Characterization of dendritic cells that induce tolerance and T regulatory 1 cell differentiation *in vivo*. *Immunity.* (2003) 18:605–17. doi: 10.1016/S1074-7613(03)00113-4
96. Liu K, Waskow C, Liu X, Yao K, Hoh J, Nussenzweig M. Origin of dendritic cells in peripheral lymphoid organs of mice. *Nat Immunol.* (2007) 8:578–83. doi: 10.1038/ni1462
97. Liu K, Nussenzweig MC. Origin and development of dendritic cells. *Immunol Rev.* (2010) 234:45–54. doi: 10.1111/j.0105-2896.2009.00879.x
98. McKenna HJ, Stocking KL, Miller RE, Brasel K, De Smedt T, Maraskovsky E, et al. Mice lacking flt3 ligand have deficient hematopoiesis affecting hematopoietic progenitor cells, dendritic cells, and natural killer cells. *Blood.* (2000) 95:3489–97.
99. Shurin MR, Pandharipande PP, Zorina TD, Haluszczak C, Subbotin VM, Hunter O, et al. FLT3 ligand induces the generation of functionally active dendritic cells in mice. *Cell Immunol.* (1997) 179:174–84. doi: 10.1006/cimm.1997.1152
100. Lee J, Breton G, Oliveira TYK, Zhou YJ, Aljoufi A, Puhr S, et al. Restricted dendritic cell and monocyte progenitors in human cord blood and bone marrow. *J Exp Med.* (2015) 212:385–99. doi: 10.1084/jem.20141442
101. Hettinger J, Richards DM, Hansson J, Barra MM, Joschko A-C, Krijgsveld J, et al. Origin of monocytes and macrophages in a committed progenitor. *Nat Immunol.* (2013) 14:821–30. doi: 10.1038/ni.2638
102. Shortman K, Naik SH. Steady-state and inflammatory dendritic-cell development. *Nat Rev Immunol.* (2007) 7:19–30. doi: 10.1038/nri1996
103. Randolph GJ, Inaba K, Robbiani DF, Steinman RM, Muller WA. Differentiation of phagocytic monocytes into lymph node dendritic cells *in vivo*. *Immunity.* (1999) 11:753–61. doi: 10.1016/S1074-7613(00)80149-1
104. Domínguez PM, Ardavín C. Differentiation and function of mouse monocyte-derived dendritic cells in steady state and inflammation. *Immunol Rev.* (2010) 234:90–104. doi: 10.1111/j.0105-2896.2009.00876.x
105. Segura E, Amigorena S. Inflammatory dendritic cells in mice and humans. *Trends Immunol.* (2013) 34:440–5. doi: 10.1016/j.it.2013.06.001
106. Plantinga M, Guilliams M, Vanheerswynghels M, Deswarte K, Branco-Madeira F, Toussaint W, et al. Conventional and monocyte-derived CD11b+ dendritic cells initiate and maintain T helper 2 cell-mediated immunity to house dust mite allergen. *Immunity.* (2013) 38:322–35. doi: 10.1016/j.immuni.2012.10.016
107. Xu Y, Zhan Y, Lew AM, Naik SH, Kershaw MH. Differential development of murine dendritic cells by GM-CSF versus Flt3 ligand has implications for inflammation and trafficking. *J Immunol.* (2007) 179:7577–84. doi: 10.4049/jimmunol.179.11.7577
108. Greter M, Helft J, Chow A, Hashimoto D, Mortha A, Agudo-Cantero J, et al. GM-CSF controls nonlymphoid tissue dendritic cell homeostasis but is dispensable for the differentiation of inflammatory dendritic cells. *Immunity.* (2012) 36:1031–46. doi: 10.1016/j.immuni.2012.03.027
109. Wakim LM, Waithman J, van Rooijen N, Heath WR, Carbone FR. Dendritic cell-induced memory T cell activation in nonlymphoid tissues. *Science.* (2008) 319:198–202. doi: 10.1126/science.1151869
110. Kamath AT, Pooley J, O'Keeffe MA, Vremec D, Zhan Y, Lew AM, et al. The development, maturation, and turnover rate of mouse spleen dendritic cell populations. *J Immunol.* (2000) 165:6762–70. doi: 10.4049/jimmunol.165.12.6762
111. Kamath AT, Henri S, Battye F, Tough DF, Shortman K. Developmental kinetics and lifespan of dendritic cells in mouse lymphoid organs. *Blood.* (2002) 100:1734–41.
112. Kabashima K, Banks TA, Ansel KM, Lu TT, Ware CF, Cyster JG. Intrinsic lymphotoxin-beta receptor requirement for homeostasis of lymphoid tissue dendritic cells. *Immunity.* (2005) 22:439–50. doi: 10.1016/j.immuni.2005.02.007
113. Bogunovic M, Ginhoux F, Wagers A, Loubeau M, Isola LM, Lubrano L, et al. Identification of a radio-resistant and cycling dermal dendritic cell population in mice and men. *J Exp Med.* (2006) 203:2627–38. doi: 10.1084/jem.20060667
114. Merad M, Manz MG, Karsunky H, Wagers A, Peters W, Charo I, et al. Langerhans cells renew in the skin throughout life under steady-state conditions. *Nat Immunol.* (2002) 3:1135–41. doi: 10.1038/ni852
115. Josien R, Li HL, Ingulli E, Sarma S, Wong BR, Vologodskaia M, et al. TRANCE, a tumor necrosis factor family member, enhances the longevity and adjuvant properties of dendritic cells *in vivo*. *J Exp Med.* (2000) 191:495–502. doi: 10.1084/jem.191.3.495
116. Wong BR, Josien R, Lee SY, Sauter B, Li HL, Steinman RM, et al. TRANCE (tumor necrosis factor [TNF]-related activation-induced cytokine), a new TNF family member predominantly expressed in T cells, is a dendritic cell-specific survival factor. *J Exp Med.* (1997) 186:2075–80. doi: 10.1084/jem.186.12.2075
117. Zhang M, Tang H, Guo Z, An H, Zhu X, Song W, et al. Splenic stroma drives mature dendritic cells to differentiate into regulatory dendritic cells. *Nat Immunol.* (2004) 5:1124–33. doi: 10.1038/ni1130
118. Schirrmacher V. Cancer-reactive memory T cells from bone marrow: spontaneous induction and therapeutic potential (Review). *Int J Oncol.* (2015) 47:2005–16. doi: 10.3892/ijo.2015.3197
119. Sapoznikov A, Pewzner-Jung Y, Kalchenko V, Krauthgamer R, Shachar I, Jung S. Perivascular clusters of dendritic cells provide critical survival signals to B cells in bone marrow niches. *Nat Immunol.* (2008) 9:388–95. doi: 10.1038/ni1571
120. Cavanagh LL, Bonasio R, Mazo IB, Halin C, Cheng G, van der Velden AWM, et al. Activation of bone marrow-resident memory T cells by circulating, antigen-bearing dendritic cells. *Nat Immunol.* (2005) 6:1029–37. doi: 10.1038/ni1249
121. Mazo IB, Honczarenko M, Leung H, Cavanagh LL, Bonasio R, Weninger W, et al. Bone marrow is a major reservoir and site of recruitment for central memory CD8+ T cells. *Immunity.* (2005) 22:259–70. doi: 10.1016/j.immuni.2005.01.008
122. Feuerer M, Beckhove P, Garbi N, Mahnke Y, Limmer A, Hommel M, et al. Bone marrow as a priming site for T-cell responses to blood-borne antigen. *Nat Med.* (2003) 9:1151–7. doi: 10.1038/nm914
123. Milo I, Sapoznikov A, Kalchenko V, Tal O, Krauthgamer R, van Rooijen N, et al. Dynamic imaging reveals promiscuous crosspresentation of blood-borne antigens to naive CD8+ T cells in the bone marrow. *Blood.* (2013) 122:193–208. doi: 10.1182/blood-2012-01-401265

124. Gallois A, Lachuer J, Yvert G, Wierinckx A, Brunet F, Rabourdin-Combe C, et al. Genome-wide expression analyses establish dendritic cells as a new osteoclast precursor able to generate bone-resorbing cells more efficiently than monocytes. *J Bone Miner Res.* (2010) 25:661–72. doi: 10.1359/jbmr.090829
125. Laperine O, Blin-Wakkach C, Guicheux J, Beck-Cormier S, Lesclous P. Dendritic-cell-derived osteoclasts: a new game changer in bone-resorption-associated diseases. *Drug Discov Today.* (2016) 21:1345–54. doi: 10.1016/j.drudis.2016.04.022
126. Jansen IDC, Vermeer JAF, Bloemen V, Stap J, Everts V. Osteoclast fusion and fission. *Calcif Tissue Int.* (2012) 90:515–22. doi: 10.1007/s00223-012-9600-y
127. Gravallese EM, Manning C, Tsay A, Naito A, Pan C, Amento E, et al. Synovial tissue in rheumatoid arthritis is a source of osteoclast differentiation factor. *Arthritis Rheum.* (2000) 43:250. doi: 10.1002/1529-0131(200002)43:2<250::AID-ANR3>3.0.CO;2-P
128. Gravallese EM. Bone destruction in arthritis. *Ann Rheum Dis.* (2002) 61(Suppl 2):ii84–6. doi: 10.1136/ard.61.suppl_2.ii84
129. Jung SM, Kim KW, Yang C-W, Park S-H, Ju JH. Cytokine-mediated bone destruction in rheumatoid arthritis. *J Immunol Res.* (2014) 2014:1–15. doi: 10.1155/2014/263625
130. Baker PJ, Dixon M, Evans RT, Dufour L, Johnson E, Roopenian DC. CD4(+) T cells and the proinflammatory cytokines gamma interferon and interleukin-6 contribute to alveolar bone loss in mice. *Infect Immun.* (1999) 67:2804–9.
131. Taubman MA, Kawai T. Involvement of T-lymphocytes in periodontal disease and in direct and indirect induction of bone resorption. *Crit Rev Oral Biol Med.* (2001) 12:125–35. doi: 10.1177/10454411010120020301
132. Lerner UH. Inflammation-induced bone remodeling in periodontal disease and the influence of post-menopausal osteoporosis. *J Dent Res.* (2006) 85:596–607. doi: 10.1177/154405910608500704
133. de Vries TJ, Andreotta S, Loos BG, Nicu EA. Genes critical for developing periodontitis: lessons from mouse models. *Front Immunol.* (2017) 8:1395. doi: 10.3389/fimmu.2017.01395
134. Ali T, Lam D, Bronze MS, Humphrey MB. Osteoporosis in inflammatory bowel disease. *Am J Med.* (2009) 122:599–604. doi: 10.1016/j.amjmed.2009.01.022
135. Wakkach A, Rouleau M, Blin-Wakkach C. Osteoimmune interactions in inflammatory bowel disease: central role of bone marrow Th17 TNFα cells in osteoclastogenesis. *Front Immunol.* (2015) 6:640. doi: 10.3389/fimmu.2015.00640
136. Kong Y-Y, Feige U, Sarosi I, Bolon B, Tafuri A, Morony S, et al. Activated T cells regulate bone loss and joint destruction in adjuvant arthritis through osteoprotegerin ligand. *Nature.* (1999) 402:304–9. doi: 10.1038/46303
137. Sato K, Suematsu A, Okamoto K, Yamaguchi A, Morishita Y, Kadono Y, et al. Th17 functions as an osteoclastogenic helper T cell subset that links T cell activation and bone destruction. *J Exp Med.* (2006) 203:2673–82. doi: 10.1084/jem.20061775
138. Oostlander AE, Everts V, Schoenmaker T, Bravenboer N, van Vliet SJ, van Bodegraven AA, et al. T cell-mediated increased osteoclast formation from peripheral blood as a mechanism for Crohn's disease-associated bone loss. *J Cell Biochem.* (2012) 113:260–8. doi: 10.1002/jcb.23352
139. D'Amelio P, Grimaldi A, Di Bella S, Brianza SZM, Cristofaro MA, Tamone C, et al. Estrogen deficiency increases osteoclastogenesis up-regulating T cells activity: a key mechanism in osteoporosis. *Bone.* (2008) 43:92–100. doi: 10.1016/j.bone.2008.02.017
140. Adamopoulos IE, Chao C, Geissler R, Laface D, Blumenschein W, Iwakura Y, et al. Interleukin-17A upregulates receptor activator of NF-κB on osteoclast precursors. *Arthritis Res Ther.* (2010) 12:R29. doi: 10.1186/ar2936
141. Kotake S, Udagawa N, Takahashi N, Matsuzaki K, Itoh K, Ishiyama S, et al. IL-17 in synovial fluids from patients with rheumatoid arthritis is a potent stimulator of osteoclastogenesis. *J Clin Invest.* (1999) 103:1345–52. doi: 10.1172/JCI5703
142. Lubberts E, van den Bersselaar L, Oppers-Walgreen B, Schwarzenberger P, Coenen-de Roo CJJ, Kolls JK, et al. IL-17 promotes bone erosion in murine collagen-induced arthritis through loss of the receptor activator of NF-kappa B ligand/osteoprotegerin balance. *J Immunol.* (2003) 170:2655–62. doi: 10.4049/jimmunol.170.5.2655
143. Takahashi N, Mundy GR, Roodman GD. Recombinant human interferon-gamma inhibits formation of human osteoclast-like cells. *J Immunol.* (1986) 137:3544–49.
144. Moreno JL. IL-4 suppresses osteoclast development and mature osteoclast function by a STAT6-dependent mechanism: irreversible inhibition of the differentiation program activated by RANKL. *Blood.* (2003) 102:1078–86. doi: 10.1182/blood-2002-11-3437
145. Hong MH, Williams H, Jin CH, Pike JW. The inhibitory effect of interleukin-10 on mouse osteoclast formation involves novel tyrosine-phosphorylated proteins. *J Bone Miner Res.* (2000) 15:911–8. doi: 10.1359/jbmr.2000.15.5.911
146. Udagawa N, Horwood NJ, Elliott J, Mackay A, Owens J, Okamura H, et al. Interleukin-18 (interferon-gamma-inducing factor) is produced by osteoblasts and acts via granulocyte/macrophage colony-stimulating factor and not via interferon-gamma to inhibit osteoclast formation. *J Exp Med.* (1997) 185:1005–12. doi: 10.1084/jem.185.6.1005
147. Kiesel J, Miller C, Abu-Amer Y, Aurora R. Systems level analysis of osteoclastogenesis reveals intrinsic and extrinsic regulatory interactions. *Dev Dyn.* (2007) 236:2181–97. doi: 10.1002/dvdy.21206
148. Saltel F, Chabadel A, Bonnelye E, Jurdic P. Actin cytoskeletal organisation in osteoclasts: a model to decipher transmigration and matrix degradation. *Eur J Cell Biol.* (2008) 87:459–68. doi: 10.1016/j.ejcb.2008.01.001
149. Mulari MTK, Zhao H, Lakkakorpi PT, Väänänen HK. Osteoclast ruffled border has distinct subdomains for secretion and degraded matrix uptake: membrane turnover at osteoclast ruffled border. *Traffic.* (2003) 4:113–25. doi: 10.1034/j.1600-0854.2003.40206.x
150. Scott CC, Gruenberg J. Ion flux and the function of endosomes and lysosomes: pH is just the start: The flux of ions across endosomal membranes influences endosome function not only through regulation of the luminal pH. *BioEssays.* (2011) 33:103–10. doi: 10.1002/bies.201000108
151. Palokangas H, Mulari M, Väänänen HK. Endocytic pathway from the basal plasma membrane to the ruffled border membrane in bone-resorbing osteoclasts. *J Cell Sci.* (1997) 110:1767–80.
152. Baron R. Polarity and membrane transport in osteoclasts. *Connect Tissue Res.* (1989) 20:109–20. doi: 10.3109/03008208909023879
153. Mulari M, Vääräniemi J, Väänänen HK. Intracellular membrane trafficking in bone resorbing osteoclasts: membrane trafficking in osteoclasts. *Microsc Res Tech.* (2003) 61:496–503. doi: 10.1002/jemt.10371
154. Akisaka T, Yoshida H, Suzuki R. The ruffled border and attachment regions of the apposing membrane of resorbing osteoclasts as visualized from the cytoplasmic face of the membrane. *J Electron Microsc.* (2006) 55:53–61. doi: 10.1093/jmicro/dfl012
155. El-Sayed A, Harashima H. Endocytosis of gene delivery vectors: from clathrin-dependent to lipid raft-mediated endocytosis. *Mol Ther.* (2013) 21:1118–30. doi: 10.1038/mt.2013.54
156. Teti A, Marchisio PC, Zallone AZ. Clear zone in osteoclast function: role of podosomes in regulation of bone-resorbing activity. *Am J Physiol-Cell Physiol.* (1991) 261:C1–7. doi: 10.1152/ajpcell.1991.261.1.C1
157. Canton J, Neculai D, Grinstein S. Scavenger receptors in homeostasis and immunity. *Nat Rev Immunol.* (2013) 13:621–34. doi: 10.1038/nri3515
158. Dambuza IM, Brown GD. C-type lectins in immunity: recent developments. *Curr Opin Immunol.* (2015) 32:21–7. doi: 10.1016/j.coi.2014.12.002
159. Bakema JE, van Egmond M. The human immunoglobulin A Fc receptor FcαRI: a multifaceted regulator of mucosal immunity. *Mucosal Immunol.* (2011) 4:612–24. doi: 10.1038/mi.2011.36
160. van Lookeren Campagne M, Wiesmann C, Brown EJ. Macrophage complement receptors and pathogen clearance. *Cell Microbiol.* (2007) 9:2095–102. doi: 10.1111/j.1462-5822.2007.00981.x
161. Rosales C, Uribe-Querol E. Phagocytosis: a fundamental process in immunity. *BioMed Res Int.* (2017) 2017:1–18. doi: 10.1155/2017/9042851
162. Flannagan RS, Jaumouillé V, Grinstein S. The cell biology of phagocytosis. *Annu Rev Pathol.* (2012) 7:61–98. doi: 10.1146/annurev-pathol-011811-132445
163. Pierce AM. Attachment to and phagocytosis of mineral by alveolar bone osteoclasts. *J Submicrosc Cytol Pathol.* (1989) 21:63–71.
164. Wang W, Ferguson DJ, Quinn JM, Simpson AH, Athanasou NA. Osteoclasts are capable of particle

phagocytosis and bone resorption. *J Pathol.* (1997) 182:92–8. doi: 10.1002/(SICI)1096-9896(199705)182:1<92::AID-PATH813>3.0.CO;2-E
165. Stenbeck G, Horton MA. Endocytic trafficking in actively resorbing osteoclasts. *J Cell Sci.* (2004) 117:827–36. doi: 10.1242/jcs.00935
166. Stenbeck G, Horton MA. Cell-matrix interaction in resorbing osteoclasts. *J Cell Sci.* (2000) 113:1577–87.
167. Boabaid F, Cerri PS, Katchburian E. Apoptotic bone cells may be engulfed by osteoclasts during alveolar bone resorption in young rats. *Tissue Cell.* (2001) 33:318–25. doi: 10.1054/tice.2001.0179
168. Soskolne WA. Phagocytosis of osteocytes by osteoclasts in femora of two week-old rabbits. *Cell Tissue Res.* (1978) 195:557–64. doi: 10.1007/BF00233897
169. Chambers TJ. Phagocytosis and trypsin-resistant glass adhesion by osteoclasts in culture. *J Pathol.* (1979) 127:55–60. doi: 10.1002/path.1711270202
170. Boyce BF, Yao Z, Xing L. Osteoclasts have multiple roles in bone in addition to bone resorption. *Crit Rev Eukaryot Gene Expr.* (2009) 19:171–80. doi: 10.1615/CritRevEukarGeneExpr.v19.i3.10
171. Lee S-H, Kim T-S, Choi Y, Lorenzo J. Osteoimmunology: cytokines and the skeletal system. *BMB Rep.* (2008) 41:495–510. doi: 10.5483/BMBRep.2008.41.7.495
172. Mansour A, Wakkach A, Blin-Wakkach C. Role of osteoclasts in the hematopoietic stem cell niche formation. *Cell Cycle Georget Tex.* (2012) 11:2045–6. doi: 10.4161/cc.20534
173. Steinman RM, Inaba K. The binding of antigen presenting cells to T lymphocytes. *Adv Exp Med Biol.* (1988) 237:31–41. doi: 10.1007/978-1-4684-5535-9_4
174. Jensen PE. Recent advances in antigen processing and presentation. *Nat Immunol.* (2007) 8:1041–8. doi: 10.1038/ni1516
175. Trombetta ES, Mellman I. Cell biology of antigen processing *in vitro* and *in vivo*. *Annu Rev Immunol.* (2005) 23:975–1028. doi: 10.1146/annurev.immunol.22.012703.104538
176. ten Broeke T, Wubbolts R, Stoorvogel W. MHC class II antigen presentation by dendritic cells regulated through endosomal sorting. *Cold Spring Harb Perspect Biol.* (2013) 5:a016873. doi: 10.1101/cshperspect.a016873
177. van den Elsen PJ. Expression regulation of major histocompatibility complex class I and class II encoding genes. *Front Immunol.* (2011) 2:48. doi: 10.3389/fimmu.2011.00048
178. Neefjes J, Jongsma MLM, Paul P, Bakke O. Towards a systems understanding of MHC class I and MHC class II antigen presentation. *Nat Rev Immunol.* (2011) 11:823–36. doi: 10.1038/nri3084
179. Blum JS, Wearsch PA, Cresswell P. Pathways of antigen processing. *Annu Rev Immunol.* (2013) 31:443–73. doi: 10.1146/annurev-immunol-032712-095910
180. Harding FA, McArthur JG, Gross JA, Raulet DH, Allison JP. CD28-mediated signalling co-stimulates murine T cells and prevents induction of anergy in T-cell clones. *Nature.* (1992) 356:607–9. doi: 10.1038/356607a0
181. Gutcher I, Becher B. APC-derived cytokines and T cell polarization in autoimmune inflammation. *J Clin Invest.* (2007) 117:1119–27. doi: 10.1172/JCI31720
182. Abbas AK, Murphy KM, Sher A. Functional diversity of helper T lymphocytes. *Nature.* (1996) 383:787–93. doi: 10.1038/383787a0
183. Sakaguchi S, Yamaguchi T, Nomura T, Ono M. Regulatory T cells and immune tolerance. *Cell.* (2008) 133:775–87. doi: 10.1016/j.cell.2008.05.009
184. Neurath MF, Finotto S, Glimcher LH. The role of Th1/Th2 polarization in mucosal immunity. *Nat Med.* (2002) 8:567–73. doi: 10.1038/nm0602-567
185. Banchereau J, Steinman RM. Dendritic cells and the control of immunity. *Nature.* (1998) 392:245–52. doi: 10.1038/32588
186. Unanue E, Allen P. The basis for the immunoregulatory role of macrophages and other accessory cells. *Science.* (1987) 236:551–7. doi: 10.1126/science.2437650
187. Kambayashi T, Laufer TM. Atypical MHC class II-expressing antigen-presenting cells: can anything replace a dendritic cell? *Nat Rev Immunol.* (2014) 14:719–30. doi: 10.1038/nri3754
188. Di Rosa F, Pabst R. The bone marrow: a nest for migratory memory T cells. *Trends Immunol.* (2005) 26:360–6. doi: 10.1016/j.it.2005.04.011
189. Westermann J, Pabst R. Distribution of lymphocyte subsets and natural killer cells in the human body. *Clin Investig.* (1992) 70:539–44. doi: 10.1007/BF00184787
190. Di Rosa F, Santoni A. Memory T-cell competition for bone marrow seeding. *Immunology.* (2003) 108:296–304. doi: 10.1046/j.1365-2567.2003.01593.x
191. Herndler-Brandstetter D, Landgraf K, Tzankov A, Jenewein B, Brunauer R, Laschober GT, et al. The impact of aging on memory T cell phenotype and function in the human bone marrow. *J Leukoc Biol.* (2012) 91:197–205. doi: 10.1189/jlb.0611299
192. Price PW, Cerny J. Characterization of CD4+ T cells in mouse bone marrow. I. Increased activated/memory phenotype and altered TCR Vbeta repertoire. *Eur J Immunol.* (1999) 29:1051–6. doi: 10.1002/(SICI)1521-4141(199903)29:03<1051::AID-IMMU1051>3.3.CO;2-P
193. Akatsuka Y, Torikai H, Inamoto Y, Tsujimura K, Morishima Y, Kodera Y, et al. Bone marrow may be a reservoir of long-lived memory T cells specific for minor histocompatibility antigen. *Br J Haematol.* (2006) 135:413–4. doi: 10.1111/j.1365-2141.2006.06313.x
194. Sabbagh L, Snell LM, Watts TH. TNF family ligands define niches for T cell memory. *Trends Immunol.* (2007) 28:333–9. doi: 10.1016/j.it.2007.06.001
195. Tokoyoda K, Zehentmeier S, Hegazy AN, Albrecht I, Grün JR, Löhning M, et al. Professional memory CD4+ T lymphocytes preferentially reside and rest in the bone marrow. *Immunity.* (2009) 30:721–30. doi: 10.1016/j.immuni.2009.03.015
196. Kikuta J, Wada Y, Kowada T, Wang Z, Sun-Wada G-H, Nishiyama I, et al. Dynamic visualization of RANKL and Th17-mediated osteoclast function. *J Clin Invest.* (2013) 123:866–73. doi: 10.1172/JCI65054
197. Pöllinger B, Junt T, Metzler B, Walker UA, Tyndall A, Allard C, et al. Th17 cells, not IL-17+ γδ T cells, drive arthritic bone destruction in mice and humans. *J Immunol.* (2011) 186:2602–12. doi: 10.4049/jimmunol.1003370
198. Moonen CGJ, Alders ST, Bontkes HJ, Schoenmaker T, Nicu EA, Loos BG, et al. Survival, retention, and selective proliferation of lymphocytes is mediated by gingival fibroblasts. *Front Immunol.* (2018) 9:1725. doi: 10.3389/fimmu.2018.01725
199. Heath WR, Carbone FR. Cross-presentation in viral immunity and self-tolerance. *Nat Rev Immunol.* (2001) 1:126–34. doi: 10.1038/35100512
200. Buchwald ZS, Kiesel JR, DiPaolo R, Pagadala MS, Aurora R. Osteoclast activated FoxP3+ CD8+ T-cells suppress bone resorption *in vitro*. *PLoS ONE.* (2012) 7:e38199. doi: 10.1371/journal.pone.0038199
201. Tai Y-T, Cho S-F, Anderson KC. Osteoclast immunosuppressive effects in multiple myeloma: role of programmed cell death ligand 1. *Front Immunol.* (2018) 9:1822. doi: 10.3389/fimmu.2018.01822
202. Zhao H. Membrane trafficking in osteoblasts and osteoclasts: new avenues for understanding and treating skeletal diseases. *Traffic Cph Den.* (2012) 13:1307–14. doi: 10.1111/j.1600-0854.2012.01395.x
203. Tacke F, Ginhoux F, Jakubzick C, van Rooijen N, Merad M, Randolph GJ. Immature monocytes acquire antigens from other cells in the bone marrow and present them to T cells after maturing in the periphery. *J Exp Med.* (2006) 203:583–97. doi: 10.1084/jem.20052119
204. Zou L, Barnett B, Safah H, Larussa VF, Evdemon-Hogan M, Mottram P, et al. Bone marrow is a reservoir for CD4+CD25+ regulatory T cells that traffic through CXCL12/CXCR4 signals. *Cancer Res.* (2004) 64:8451–5. doi: 10.1158/0008-5472.CAN-04-1987
205. Fujisaki J, Wu J, Carlson AL, Silberstein L, Putheti P, Larocca R, et al. *In vivo* imaging of Treg cells providing immune privilege to the haematopoietic stem-cell niche. *Nature.* (2011) 474:216–9. doi: 10.1038/nature10160
206. Buchwald ZS, Kiesel JR, Yang C, DiPaolo R, Novack DV, Aurora R. Osteoclast-induced Foxp3+ CD8 T-cells limit bone loss in mice. *Bone.* (2013) 56:163–73. doi: 10.1016/j.bone.2013.05.024
207. Zaiss MM, Frey B, Hess A, Zwerina J, Luther J, Nimmerjahn F, et al. Regulatory T cells protect from local and systemic bone destruction in arthritis. *J Immunol.* (2010) 184:7238–46. doi: 10.4049/jimmunol.0903841
208. Kelchtermans H, Geboes L, Mitera T, Huskens D, Leclercq G, Matthys P. Activated CD4+CD25+ regulatory T cells inhibit osteoclastogenesis and collagen-induced arthritis. *Ann Rheum Dis.* (2009) 68:744–50. doi: 10.1136/ard.2007.086066
209. Yao Z, Xing L, Qin C, Schwarz EM, Boyce BF. Osteoclast precursor interaction with bone matrix induces osteoclast formation directly by an interleukin-1-mediated autocrine mechanism. *J Biol Chem.* (2008) 283:9917–24. doi: 10.1074/jbc.M706415200

210. Villa A, Vezzoni P, Frattini A. Osteopetroses and immunodeficiencies in humans. *Curr Opin Allergy Clin Immunol.* (2006) 6:421–7. doi: 10.1097/01.all.0000246620.26623.5b
211. Stark Z, Savarirayan R. Osteopetrosis. *Orphanet J Rare Dis.* (2009) 4:5. doi: 10.1186/1750-1172-4-5
212. Briggs TA, Rice GI, Daly S, Urquhart J, Gornall H, Bader-Meunier B, et al. Tartrate-resistant acid phosphatase deficiency causes a bone dysplasia with autoimmunity and a type I interferon expression signature. *Nat Genet.* (2011) 43:127–31. doi: 10.1038/ng.748
213. Lausch E, Janecke A, Bros M, Trojandt S, Alanay Y, De Laet C, et al. Genetic deficiency of tartrate-resistant acid phosphatase associated with skeletal dysplasia, cerebral calcifications and autoimmunity. *Nat Genet.* (2011) 43:132–7. doi: 10.1038/ng.749
214. Hao L, Zhu G, Lu Y, Wang M, Jules J, Zhou X, et al. Deficiency of cathepsin K prevents inflammation and bone erosion in rheumatoid arthritis and periodontitis and reveals its shared osteoimmune role. *FEBS Lett.* (2015) 589:1331–9. doi: 10.1016/j.febslet.2015.04.008
215. Hao L, Chen J, Zhu Z, Reddy MS, Mountz JD, Chen W, et al. Odanacatib, a cathepsin K-specific inhibitor, inhibits inflammation and bone loss caused by periodontal diseases. *J Periodontol.* (2015) 86:972–83. doi: 10.1902/jop.2015.140643
216. Balla B, Kósa JP, Kiss J, Podani J, Takács I, Lazáry Á, et al. Transcriptional profiling of immune system-related genes in postmenopausal osteoporotic versus non-osteoporotic human bone tissue. *Clin Immunol.* (2009) 131:354–9. doi: 10.1016/j.clim.2009.01.004
217. Pineda B, Serna E, Laguna-Fernández A, Noguera I, Panach L, Hermenegildo C, et al. Gene expression profile induced by ovariectomy in bone marrow of mice: a functional approach to identify new candidate genes associated to osteoporosis risk in women. *Bone.* (2014) 65:33–41. doi: 10.1016/j.bone.2014.05.001
218. Pietschmann P, Mechtcheriakova D, Meshcheryakova A, Föger-Samwald U, Ellinger I. Immunology of osteoporosis: a mini-review. *Gerontology.* (2016) 62:128–37. doi: 10.1159/000431091

Conflict of Interest Statement: The authors declare that the research was conducted in the absence of any commercial or financial relationships that could be construed as a potential conflict of interest.

frontiers in Immunology

REVIEW
published: 25 June 2019
doi: 10.3389/fimmu.2019.01409

S1P-S1PR1 Signaling: the "Sphinx" in Osteoimmunology

Lan Xiao [1,2†], Yinghong Zhou [1,2,3†], Thor Friis [1], Kenneth Beagley [1,2] and Yin Xiao [1,2,3]*

[1] Institute of Health and Biomedical Innovation, Queensland University of Technology, Brisbane, QLD, Australia, [2] The Australia-China Centre for Tissue Engineering and Regenerative Medicine, Queensland University of Technology, Brisbane, QLD, Australia, [3] Key Laboratory of Oral Medicine, Guangzhou Institute of Oral Disease, Stomatology Hospital of Guangzhou Medical University, Guangzhou, China

The fundamental interaction between the immune and skeletal systems, termed as osteoimmunology, has been demonstrated to play indispensable roles in the maintenance of balance between bone resorption and formation. The pleiotropic sphingolipid metabolite, sphingosine 1-phosphate (S1P), together with its cognate receptor, sphingosine-1-phosphate receptor-1 (S1PR1), are known as key players in osteoimmunology due to the regulation on both immune system and bone remodeling. The role of S1P-S1PR1 signaling in bone remodeling can be directly targeting both osteoclastogenesis and osteogenesis. Meanwhile, inflammatory cell function and polarization in both adaptive immune (T cell subsets) and innate immune cells (macrophages) are also regulated by this signaling axis, suggesting that S1P-S1PR1 signaling could aslo indirectly regulate bone remodeling *via* modulating the immune system. Therefore, it could be likely that S1P-S1PR1 signaling might take part in the maintenance of continuous bone turnover under physiological conditions, while lead to the pathogenesis of bone deformities during inflammation. In this review, we summarized the immunological regulation of S1P-S1PR1 signal axis during bone remodeling with an emphasis on how osteo-immune regulators are affected by inflammation, an issue with relevance to chronical bone disorders such as rheumatoid arthritis, spondyloarthritis and periodontitis.

Keywords: osteoimmunology, sphingosine 1-phosphate (S1P), sphingosine 1-phosphate receptor-1 (S1PR1), bone remodeling, immunomodulation

OPEN ACCESS

Edited by:
Teun J. De Vries,
VU University
Amsterdam, Netherlands

Reviewed by:
Markus Gräler,
Friedrich Schiller University
Jena, Germany
Leyre BM,
UMR5246 Institut de Chimie et
Biochimie Moléculaires et
Supramoléculaires (ICBMS), France

***Correspondence:**
Yin Xiao
yin.xiao@qut.edu.au

† These authors have contributed equally to this work

Specialty section:
This article was submitted to Inflammation, a section of the journal Frontiers in Immunology

Received: *11 February 2019*
Accepted: *04 June 2019*
Published: *25 June 2019*

Citation:
Xiao L, Zhou Y, Friis T, Beagley K and Xiao Y (2019) S1P-S1PR1 Signaling: the "Sphinx" in Osteoimmunology. Front. Immunol. 10:1409. doi: 10.3389/fimmu.2019.01409

INTRODUCTION

Skeletal bone undergoes a life-long and continuous renovation termed "bone remodeling," a process that is necessary for bone homeostasis and consists of osteoclasts-driven bone resorption and osteoblasts-driven bone formation (1). Osteoclasts and osteoblasts—derived from immune progenitor cells and mesenchymal stem cells (MSCs), respectively—are linked *via* immune modulators and are the fundamental cell types of these two interconnected systems. Osteoimmunology, a term first coined at the beginning of this century (2), was identified over forty years ago (3), and describes the interaction between cells from the immune and skeletal systems. The realm of osteoimmunology has revealed a complex system of mutual regulation existing between immune cells and bone cells. This relationship sees the immune response greatly affecting osteoclast-osteoblast coupling, thus mediating the balance between bone resorption and formation, whereas, at another level, cells from the skeletal system have a profound effect on the differentiation and function of immune cells.

Sphingosine is one of the most important sphingolipid metabolites (4–6). It is named after the Sphinx, a mythical creature of Greek mythology famed for its mysterious features (7). Phosphorylation of sphingosine forms the pleiotropic and bioactive lipid sphingosine-1-phosphate (S1P) (8). S1P is produced by various cell types, which acts not only as an intracellular second messenger, but also an extracellular first messenger in both an autocrine and paracrine manner. It does this by binding with a class of G-protein-coupled receptors, known as sphingosine-1-phosphate receptors (S1PRs), of which there are currently five known subtypes, S1PR1 through to S1PR5 (9). Of these receptors, S1PR1 is expressed in most mammalian cell types and considered to be multifunctional in many biological processes. S1P-S1PR1 signaling has long been addressed as a key regulator of the immune response, due to its involvement in the chemotaxis, activation, differentiation, and function of immune cells (9–13). The elevated concentration of S1P, coupled with an up-regulation of S1PR1 expression locally within inflammatory tissues in many diseases, as well as the therapeutic effects of S1PR1 modulators, is an indication of the important role of S1P-S1PR1 signaling in inflammation (8, 13).

S1P-S1PR1 signaling is primarily thought to be a catalyst of inflammation and thereby inducing osteoclastogenesis; however, the fact that this pathway is also active during bone regeneration suggests an enigmatic and rather intriguing role in bone remodeling (14, 15). In this review, we will seek to highlight the interactions between the immune and skeletal systems, how these interactions affect bone remodeling, and what is known about the role of S1P-S1PR1 signaling in the emerging field of osteoimmunology.

THE FUNCTION OF S1P AND ITS RECEPTOR S1PR1

Sphingolipids are a key component of mammalian cell membranes and are metabolized in response to certain stimuli (4, 5). Sphingolipids are *de novo* biosynthesized from serine and palmitate in the endoplasmic reticulum (ER) (4, 5, 16, 17). The condensation of sphingolipids (*via* the action of serine palmitoyl transferase, SPT) forms 3-keto-dihydrosphingosine (16, 17), which is reduced to dihydrosphingosine, then subsequently acylated by (dihydro)-ceramide synthase (also known as Lass or CerS) to form dihydroceramide (18). The desaturation of dihydroceramide forms ceramides (19), the central player in sphingolipid metabolism (20), which could be deacylated by ceramidases (CERase) to produce sphingosines (21, 22). Sphingosine could be salvaged through reacylation, a process termed as "salvage pathway" which leading to ceramide regeneration; or it can be phosphorylated to form the multifunctional bioactive lipid S1P, which mediates a number of cellular processes, such as cell proliferation, survival, differentiation, migration, as well as cytokine and chemokine production (4, 5, 20, 23). S1P can be reversibly dephosphorylated to sphingosine by intracellular S1P phosphatases (SPPs) and extracellular lipid phosphate phosphatases, or irreversibly degraded by S1P lyase (SPL) (20, 24–27). In most mammalian cells, S1P levels are held in check by the actions of SPL and SPPs. SPL inhibition *via* both genetic and pharmacological tools results in tissue S1P accumulation *in vivo* (28). The exception is platelets, which lack SPL (29), and erythrocytes, which lack both SPL and SPPs (30). This absence explains why, under normal physiological conditions, circulating S1P levels are significantly higher (μM range) in peripheral blood than in solid tissues. S1P is also maintained at relatively high levels (>100 nM) in the lymphatic circulation, which is mainly due to the presence of lymphatic endothelial cells (31–33). Cells from the macrophage-monocyte lineage are also important producers of S1P (34).

The phosphorylation of sphingosine is performed by sphingosine kinases 1 and 2 (SPHK1 and SPHK2) (35). SPHK1 is mainly present in the cytoplasm which, after being activated by certain stimuli, is translocated to the cell membrane where it catalyzes sphingosine phosphoration (36). On the other hand, SPHK2 distributes not only in cell membrane, but also in organelles such as the ER, mitochondria, as well as in nucleus, which providing S1P for essential cellular processes, such as respiration, histone acetylation, and gene expression (37–39). For example, S1P is reported to regulate gene expression through modulating HDAC1 and HDAC2 activity (38, 40). Intracellular S1P also plays an essential part in tumor-necrosis factor-α (TNF-α) triggered NF-κB signaling *via* targeting TNF receptor-associated factor 2 (TRAF2), therefore participating the inflammatory, anti-apoptotic and immune processes (41). Once S1P is generated, it could be transported to activate its receptors, therefore functioning in a paracrine and/or autocrine manner (42, 43). This "inside-out relocation" of S1P is indispensable of special transports, as the polar head group in S1P makes it unable to move through the hydrophobic mammalian cell membranes (44). Transports such as the ATP-binding cassette (ABC) transporters family members have been demonstrated to facilitate S1P transporting in erythrocytes, platelets, and mammalian cells in an ATP-dependent manner (42, 45–49). Another transport, major facilitator superfamily transporter 2b (Mfsd2b) has also been found to play essential roles in exporting S1P in erythrocytes and platelets (50, 51). Especially, the transport spinster homolog 2 (SPNS2) is considered as a major regulator in S1P secretion in mammalian cells in a non-ATP dependent manner, which therefore playing essential roles in immune cell development and trafficking, as well as bone homeostasis (43, 52–57). Under inflammatory conditions, SPHK1 is abnormally activated to produce high levels of S1P, which is released into the local microenvironment. Inflammatory cytokines such as TNF-α, IL-1β, and interferon-γ (IFN-γ), have been shown to induce SPHK1 in an extracellular signal regulated kinase (ERK) signaling-dependent manner (38, 41, 58–60), and this partially explains the high S1P levels in the inflammatory tissues (61). Furthermore, inflammation is accompanied by vascular leakage, which may allow S1P to permeate from blood to tissues thereby raising the S1P concentrations within the inflammatory tissues (62).

The secreted S1P regulates pleiotropic biological functions by binding with its receptors (63). Upon activation, the S1P receptors couple with diverse heterotrimeric G-protein subunits (known as Gαi, Gαq/11, and Gα12/13), thereby directing

different downstream signaling pathways (64). S1PR1 is the most widely expressed S1P receptor in most tissues, such as the lungs, brain, and especially immune organs (65–67). Following activation by S1P, S1PR1 interacts with Gαi, which then regulates the downstream signaling molecules (**Figure 1**), such as phospholipase C (PLC), phosphoinositide 3-kinase (PI3K), Ras guanosine triphosphatase (GTPase) and adenylyl cyclase (AC) (9, 68). These molecules subsequently activate their downstream signaling pathways (**Figure 1**), including Rac GTPase, mitogen-activated protein kinase (MAPK), Akt, and mammalian target of rapamycin (mTOR) (6, 9, 68, 69).

S1PR1 has a key role in the development of the vascular system and is highly expressed in differentiating endothelial cells (70). It is required to maintain the integrity of endothelial cell barrier and thus regulates vascular permeability responses, especially under inflammatory conditions (71). When SPHK1 is induced by inflammation, it enhances S1P production in endothelial cells, which then acts in a feed-forward manner to stimulate more S1PR1 expression, counteracting the increased permeability caused by pro-inflammatory mediators e.g., lipopolysaccharides (LPS), thereby preventing otherwise lethal cell-leakage in response to inflammation. The indispensable role of S1PR1 in vascular network stability has been further demonstrated by global *S1pr1* gene deletion, which results in defective vascular maturation and then embryonic lethality (70). Specific *S1pr1* deletion in endothelial cells results in deformities in the primary vascular plexus (angiogenic hypersprouting), limited blood flow, and vascular leakage (72–75). In epithelial cells, S1PR1 maintains cell barrier integrity and initiates the immune defense against the invading pathogens (76). S1PR1 is expressed in MSCs and regulates cell migration, proliferation, differentiation, and survival (77), whereas in osteoclast- and osteoblast-precursor cells S1PR1 expression is associated with their differentiation (78), further testament to its role in bone remodeling.

THE REGULATORY ROLES OF S1P-S1PR1 SIGNALING IN BONE REMODELING

Bone Remodeling and Osteoclast-Osteoblast Coupling

Osteoclasts and osteoblasts are the major players in the bone remodeling process. The hematopoietic stem cells (HSCs)-derived osteoclasts are considered as the major type of cells responsible for bone resorption (79). Osteoclastogenesis depends on receptor activator of nuclear factor-kappa B ligand (RANKL), a cytokine in the TNF family (80). RANKL activates its cognate receptor, receptor activator of nuclear factor-kappa B (RANK), initiating osteoclastogenic signals (**Figure S1**). The RANKL-RANK axis, together with the downstream NF-κB signaling pathway, is indispensable in osteoclastogenesis (81, 82). Another key factor in osteoclast formation is macrophage colony-stimulating factor (M-CSF), which is critical in regulating survival and proliferation of osteoclast precursors (83).

Osteoblasts are the major producer of RANKL and M-CSF (84), indicating that osteoclasts and osteoblasts are related "coupling" cells that link osteoclastogenesis to osteogenesis. Osteoblasts are derived from MSCs and are the main cell type responsible for bone formation (79). Factors such as alkaline phosphatase (ALP), runt-related transcription factor 2 (RUNX2), osteocalcin (OCN), and the Wnt/β-catenin and TGF-β signaling pathways, as well as the signal transducer and activator of transcription 3 (STAT3) signaling, are considered to be crucial in osteogenesis (85–89). Besides RANKL and M-CSF, osteoblasts also produce osteoprotegerin (OPG), which, conversely, acts as a decoy receptor of RANKL and thereby impeding osteoclastogenesis (90). Hence, osteoclasts and osteoblasts are interconnected by the RANKL/RANK/OPG axis, with the ratio of RANKL to OPG determining the balance between bone resorption and formation.

Bone remodeling is a strictly regulated process that must maintain bone formation at a rate equal to that of bone resorption (2). Skeletal pathologies arise when this balance is disrupted. The most common one of such disorders is when bone remodeling is skewed toward resorption—that is, when osteoclastogenesis is aberrantly stimulated so the rate of bone resorption exceeds bone formation, resulting in a net bone loss, as seen in inflammatory diseases, such as rheumatoid arthritis (RA) (91),periodontitis (92), and apical periodontitis (93).

The Roles of S1P-S1PR1 in Bone Remodeling

S1P has been found to induce both osteoclastogenesis and osteogenesis, a dual role that makes S1P-S1PR1 signaling more intriguing.

S1P-S1PR1 Signaling in Osteoclastogenesis

Together with its ligand S1P, S1PR1 directs chemotactic migration of osteoclast precursors *in vitro* and *in vivo*. S1P-S1PR1 signaling is thought to regulate osteoclast precursor trafficking to and from bone surface, where the precursor cells fuse and differentiate into osteoclasts, a process which dynamically regulates bone mineral homeostasis and osteoclastogenesis (78). S1PR1-dependent chemo-attraction is only activated when S1P concentration is comparably low. High concentrations of S1P activates the S1PR2 on the precursor cells and triggers an S1PR2-dependent chemo repulsion (94). This mechanism partially explains how these precursor cells are retained in bone marrow, where lower levels of S1P are found than in the peripheral blood. S1PR1 and S1PR2 act in a concerted manner to regulate osteoclast precursors egressing from bone marrow into circulation, depending on the relative concentrations of S1P. It is also found that the active form of vitamin D, 1,25-D, and its clinically used analog, eldecalcitol (ELD), effectively reduce bone resorption *via* inhibiting S1PR2 in circulating osteoclast precursors, as S1PR2-blockage directs the migration of osteoclast precursors from bone surface to blood. This study reveals the pharmacologic effect of vitamin D analog in therapy against osteoporosis (95), suggesting that the "S1PR1-S1PR2 concert" should be considered as a therapeutic target for diseases with bone loss. During RANKL-mediated osteoclast differentiation, the activity of SPHK1 is significantly enhanced and increases production of S1P by the precursor cells. Conversely, inhibition of SPHK1 leads to suppression of osteoclastogenesis (34).

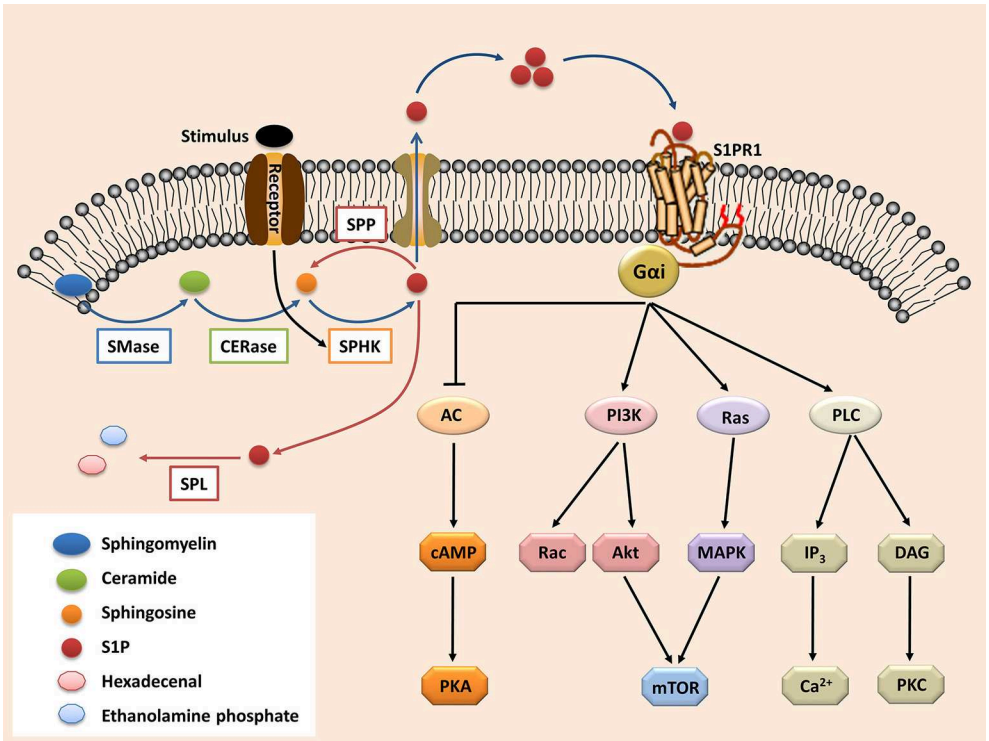

FIGURE 1 | The S1P-S1PR1 signaling. Sphingolipid (derived from cell membrane) is cleaved (by sphingomyelinases, SMase) to ceramide. Ceramide is then deacylated by ceramidases (CERase) to produce sphingosine. S1P is produced by phosphorylation of sphingosine, which is mediated by SPHKs (SPHK1 and SPHK2, which can be activated by certain stimulus). S1P can be reversibly degraded by S1P phosphatases (SPPs), or irreversibly degraded by S1P lyase (SPL). On the other hand, S1P can be transported outside the cells and acts in the autocrine or paracrine manners to activate its receptor S1PR1. The S1PR1 then activates its down-stream signal cascades and therefore regulates diverse cell activities. S1P, sphingosine-1-phosphate; S1PR1, sphingosine-1-phosphate receptor 1; PLC, phospholipase C; PI3K, phosphoinositide 3-kinase; AC, adenylyl cyclase; Ras, Ras GTPase; Rac, Rac GTPase; MAPK, mitogen-activated protein kinase; cAMP, cyclic adenosine monophosphate; mTOR, mammalian target of rapamycin; PKA, protein kinase A; PKC, protein kinase C; DAG, diacylglycerol; IP_3, Inositol trisphosphate.

S1P-S1PR1 Signaling in Osteogenesis

Although S1P is found to induce osteoclastogenesis, it also plays a positive role in osteogenesis. In the process of BMP-2-mediated osteoblast differentiation, S1P significantly induces ALP activity and the expressions of key bone formation markers, such as OCN and RUNX2. Enhanced BMP-2/SMAD signaling is the result of MEK (mitogen-activated protein kinase kinase) 1/2-ERK1/2 pathway activation (14). Another study indicates that S1P-S1PR1 signaling activation in osteoblasts mediates the activation of PI3K/Akt signaling and therefore inhibits glycogen synthase kinase-3β (GSK-3β), which leads to induced nuclear translocation of β-catenin, a key process in osteogenesis (96). S1P has also been found to induce RUNX2 expression in osteoblasts and thereby improve osteogenesis *in vitro* and *in vivo*, which is achieved through S1PR2-dependent activation of Smad1/5/8 signaling (97). Conditioned medium from osteoclasts can induce osteogenesis and is thought to be due to Wnt10b, BMP-6, and S1P secreted into the medium. And whereas S1P and BMP-6 can trigger the migration of pre-osteoblasts toward bone resorption sites, S1P can also induce osteogenic differentiation of the same cells by activating S1PR1, a finding that becomes apparent when S1PR1 is blocked (15). These properties of S1P-S1PR1 signaling to some degree explain how bone formation is initiated following bone resorption. Accordingly, hormone calcitonin (CT) has been found to block S1P secretion of osteoclast *via* SPNS2 inhibition, which consequently results in decreased bone formation *in vivo* in a S1PR3-dependent manner (55). In a more recent study, induced expression and activity of SPHK1 and SPHK2 have been observed during the *in vitro* osteoblast differentiation, accompanied with enhanced *Spns2* gene level, as well as increased S1P secretion. Blockage of SPHK1 or SPHK2 results in retarded osteogenic differentiation and mineralization, suggesting the indispensable role of S1P signaling in osteogenesis (54).

S1P-S1PR1 Signaling in Osteoclast-Osteoblast Coupling

Interestingly, intracellular S1P, which is produced during osteoclastogenesis, also inhibits this process, by suppressing p38-MAPK signaling, a key signaling pathway downstream of RANK (**Figure S1**). This is in contrast with extracellular S1P which has no effect on osteoclast differentiation, suggesting S1P can target cells other than osteoclasts, e.g., the coupling osteoblasts (34). S1P activates p38-MAPK and ERK signaling in osteoblasts, resulting in increased levels of cyclooxygenase-2 (COX2). COX2 induces the expression of prostaglandin E2 (PGE2), which prompts the production of RANKL by osteoblasts. RANKL binds to its receptor RANK on osteoclast precursors which promotes

osteoclast differentiation and S1P secretion, thereby setting up a feed-forward loop for osteoclastogenesis.

Cathepsin K (CSTK) is an enzyme that is involved in bone degradation which, when specifically deleted in osteoclast lineage by targeted *in vivo* gene modification, results in a condition characterized by an increased number of osteoblasts and bone formation, as well as an increased number of dysfunctional osteoclasts and impaired bone resorption (98). The *in vitro* analysis of primary osteoblasts showed enhanced ALP activity and osteogenic potential, as well as increased RANKL/OPG ratio. Osteoclasts from *CSTK*-knockout mice presented with up-regulated expression of SPHK1 and increased S1P production leading to a higher RANKL/OPG ratio of the primary osteoblasts, which in turn increased the number of osteoclasts. The antagonist of S1PR1 and S1PR3 reduced the osteogenic ability of osteoblasts induced by the conditioned medium of *CSTK*-deficient osteoclasts, suggesting the enhanced *in vivo* osteogenesis was due to the activation of S1PR1 and S1PR3 (98).

In a more recent study, S1P degradation was blocked *via* SPL inhibition (through both genetic and pharmacological means) *in vivo*, and this resulted in increased bone mass and enhanced bone strength, accompanied with induced OPG expression and reduced osteoclastogenesis in mice (28). Further research revealed the role of S1P-S1PR2 under this phenomenon. In osteoblast, S1P-S1PR2 signaling played a significant role in bone remodeling, which not only promoting the osteogenic differentiation, but also inducing OPG production *via* p38–GSK3β-β-catenin and Wnt5A–LRP5 pathways, suggesting S1P-S1PR2 signaling should improve bone formation while limiting bone resorption. Accordingly, SPL inhibition ameliorated osteoporosis in OPG-deficient mice through inducing the activity and mineralization of osteoblast while reducing osteoclastogenesis. In addition, S1PR2-deficience resulted in osteopenia in mice, accompanied with reduced OPG expression and retarded differentiation of osteoblast (28). These results indicate that similar to S1PR1, S1P-S1PR2 signaling also acts as a coupling factor between osteoclast and osteoblast. However, S1PR2 activation leads to increased OPG production, which possibly neutralizing S1PR1-mediated RANKL expression and hence osteoclastogenesis. It is presumed that S1PR1-S1PR2 may act in a balanced way to maintain physiological bone remodeling, while this balance might be destroyed under pathological conditions such as inflammation, which needs further investigation. From these studies, it could be concluded that S1P acts as a coordinator between bone resorption and formation, which, in combination with its positive effects in both osteoclastogenesis and osteogenesis, suggesting a complicated role of this signaling in bone remodeling.

THE IMMUNOMODULATORY ROLE OF S1P-S1PR1 SIGNALING IN OSTEOIMMUNOLOGY

The balance of bone remodeling is maintained by the immune system, which, therefore, links the skeletal, and immune systems together. As a key regulator of the immune system, the S1P-S1PR1 signaling could be postulated to indirectly impact bone remodeling by the immunomodulation, indicating its enigmatic role in osteoimmunology.

Osteoimmunology

Evidence of the relationship between the immune and skeletal systems became apparent with the finding that IL-1, secreted by antigen-stimulated immune cells, plays a positive role in osteoclastogenesis (99). Since then, many more studies have demonstrated the role of immune system on bone remodeling (**Figure 2**) (100). Furthermore, cells derived from skeletal system, such as MSCs, are capable of regulating immune responses (101). Such findings gave birth to osteoimmunology, a field that is concerned with interactions between immune and skeletal systems, within which the cells from each system are correlated through a variety of factors and signaling pathways such as S1P-S1PR1.

Regulation of Bone Remodeling by Immune System

The adaptive immune cells—T-helper cells—play a critical role in bone remodeling by producing RANKL, the key factor in osteoclastogenesis, and also other factors that regulate bone metabolism. Cytokines derived from type 1 helper T (Th1) cells, such as IFNγ and granulocyte-macrophage colony-stimulating factor (GM-CSF), suppress osteoclastogenesis by interrupting the RANK signaling (**Figure 2**) (102–105). However, it is also reported that GM-CSF facilitates the fusion of pre-osteoclasts into multinucleated osteoclasts, suggesting a fundamental role of GM-CSF in the function of osteoclasts (106, 107). In addition, GM-CSF derived from breast tumor cells has been found as responsible for osteolytic bone metastasis *in vivo* (107). Other cytokines derived from type 2 helper T (Th2) cells, such as interleukin-4 (IL-4) and IL-10, also inhibit RANK signaling and osteoclast differentiation (108–110). IL-6, which is produced by Th2 cells and M1 macrophages, triggers osteoclastogenesis by promoting RANKL production, as well as stimulating IL-1 production, which amplifies the inflammatory response (111–113). IL-6 also induces the differentiation of type 17 helper T (Th17) cells, which secrete the pro-inflammatory cytokine IL-17 (114, 115), and in turn promote RANKL secretion and osteoclastogenesis (116, 117). The immune-suppressive regulatory T (Treg) cells (118), inhibit osteoclastogenesis in a direct cell-to-cell contact-dependent manner, by binding of cytotoxic T-lymphocyte-associated protein 4 (CTLA-4) on Treg cells with CD80 and CD86 on osteoclast precursors; Treg cells also reduce osteoclastogenesis by secreting IL-4 and IL-10 (119). Another Treg cell-derived factor, TGF-β, has pleiotropic effects on osteoclastogenesis. On one hand, TGF-β can induce osteoclast differentiation by promoting RANK expression and regulate activator protein 1 (AP-1) signaling (120, 121), a key downstream effector of RANK (**Figure S1**). However, in osteoclast-osteoblast co-cultures, TGF-β can also suppress RANKL expression in osteoblasts, effectively applying the brakes on osteoclastogenesis (120).

Cells from the innate immune system also contribute to the regulation of osteoclastogenesis. Macrophages, the

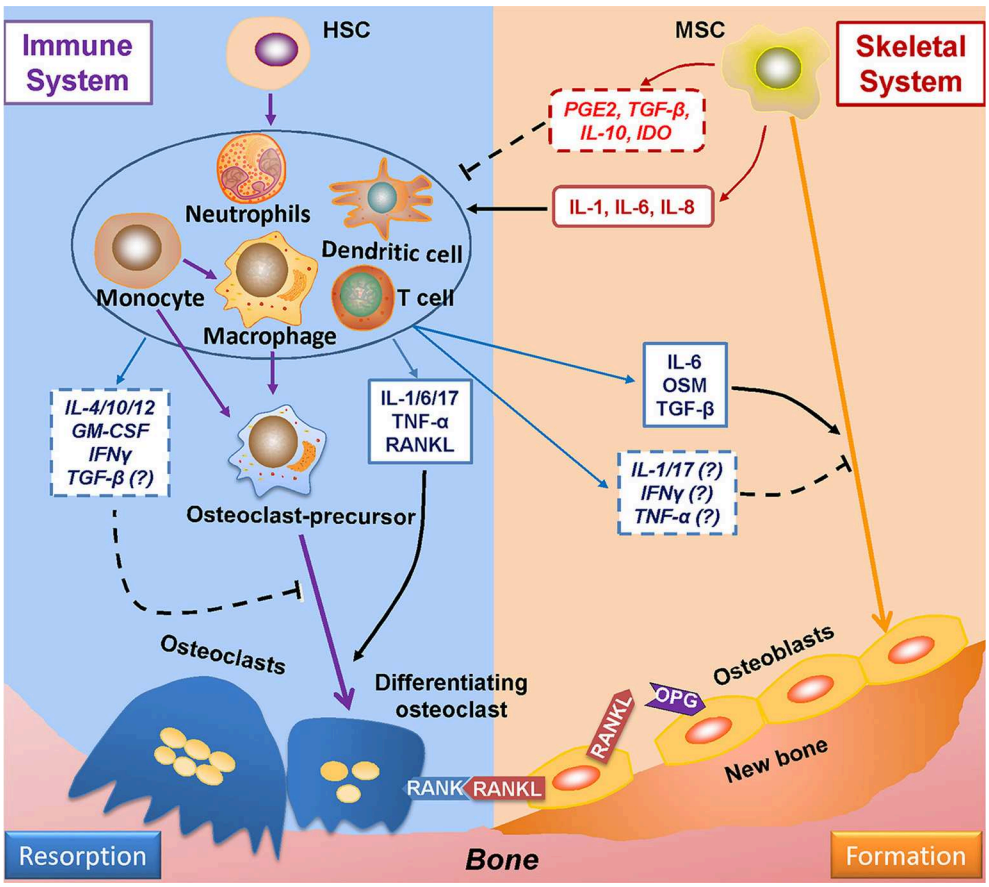

FIGURE 2 | Mutual regulations between the immune and skeletal systems. The two major players in bone remodeling—osteoclasts and osteoblasts are coupled through the RANKL-RANK-OPG axis: osteoblasts-derived RANKL combines with its ligand RANK in osteoclasts and plays an indispensable role in osteoclastogenesis; OPG (which is also derived from osteoblasts) reduces osteoclastogenesis by impairing the RANKL-RANK signaling. The immune system greatly takes part in osteoclastogenesis by producing RANKL; also, the immune-related factors either affect pre-osteoclasts, or interacts with osteoblasts to induce RANKL production to regulate osteoclastogenesis. The immune-derived regulators also affect the process of osteogenesis. On the other hand, the progenitor cells of the skeleton system—MSCs suppress immune response either by cell to cell intact or by secreting functional regulators; whereas under certain conditions, MSCs upon TLR4 stimulation secret factors which induce immune response. RANKL, receptor activator of nuclear factor factor-kappa B ligand; RANK, receptor activator of nuclear factor-kappa B; OPG, osteoprotegerin.

major components of innate immunity, constitute three subpopulations of cells: (1) non-activated M0 macrophages; (2) pro-inflammatory M1 macrophages, which are classically activated by LPS or Th1 cell cytokines such as IFNγ; and (3) M2 macrophages, which is alternatively activated by Th2 cell cytokines, such as IL-4 or IL-13, and are classified as anti-inflammatory macrophages (122–125). Macrophages are precursors of osteoclasts (126) and secrete factors that actively affect osteoclastogenesis. M1 macrophages express IL-1α and IL-1β which activates RANK signaling thereby inducing osteoclastogenesis, under both physiological and pathological conditions (127, 128). M1 macrophages also express TNF-α, which stimulates osteoclast differentiation by activating the NF-κB signaling (129, 130). Moreover, TNF-α promotes RANKL expression of osteoblasts to induce osteoclastogenesis (131, 132). On the contrary, M2 macrophages-derived IL-10 (133) is a negative regulator of osteoclastogenesis (110).

These immune-derived factors also participate in the regulation of osteogenic process. Originated from Treg cells and M2 macrophages, TGF-β has been identified as a crucial factor in osteoblast differentiation and mineralization (134). M2 macrophages also recruit MSCs (osteoblast precursors) by producing the transmembrane glycoprotein Osteoactivin (OA)/Glycoprotein non-metastatic melanoma protein B (GPNMB) (135). Interestingly, some pro-inflammatory factors, known as osteoclastogenic promoters, have also been found to induce osteogenesis. For instance, IL-6 can enhance ALP activity *in vivo via* STAT3 signaling, a further indication of the ability of IL-6 to affect osteogenesis (136–140). Originated from M1 macrophages, oncostatin M (OSM) facilitates osteogenesis by activating RUNX2 *via* STAT3 signaling pathway. Studies with OSM or OSM receptor (OSMR) deficient mice show reduced bone healing, evidence for its critical role in osteogenesis (141, 142). There are studies indicate that IL-1 (143, 144),

TABLE 1 | Effects of immune cells on bone remodeling.

Immune cells	Main functional factors	Effects on osteoclastogenesis	Effects on osteogenesis
M1 macrophages	IL-1	Activation (127, 128)	Activation (143, 144)/Inhibition (148, 149)
	TNF-α	Activation (129–132)	Activation (147, 150)/Inhibition (148, 149)
	OSM	Activation (151, 152)	Activation (141, 142)
M2 macrophages	IL-10	Inhibition (110)	Activation (153)/Inhibition (154, 155)
	TGF-β	Dural (120, 121)	Activation (134)
Th1 cells	IFNγ	Inhibition (105)	Activation (156, 157)/Inhibition (238)
	GM-CSF	Activation(106, 107)/Inhibition (102–104)	Activation (158)
Th2 cells	IL-4	Inhibition (108, 109)	Inhibition (159)
	IL-6	Activation (111–113)	Activation (136–140)
Th17 cells	IL-17	Activation (114, 115)	Activation (145, 146)/Inhibition (160)
Treg cells	CTLA-4	Inhibition (119)	–

CTLA-4, cytotoxic T-lymphocyte-associated protein 4; GM-CSF, granulocyte-macrophage colony-stimulating factor; IFNγ, interferon-γ; IL, interleukin; OSM, oncostatin M; TGF-β, transforming growth factor-β; Th, T helper; TNF-α: tumor necrosis factor α; Treg, regulatory T.

IL-17 (145, 146), and TNF-α (147) play positive roles in bone formation *in vitro* and *in vivo*, however, conflicting results exist (**Table 1**).

Accumulating evidences indicate that macrophages play an indispensable role in bone formation. The bone residential macrophages are required in osteogenesis and are, more importantly, also needed for the maintenance of bone-forming surfaces. Both M1 and M2-derived secreted factors are found to promote osteogenesis, especially M1-derived OSM (142). Interestingly, RANKL is found to induce a M1-like macrophage phenotype; this M1-like macrophage infiltration appears during the early stage of bone repair and is identified to facilitate osteogenesis (167). Furthermore, the conversion of M1 to M2 macrophages significantly improves mineralization of the co-cultured osteoblasts *in vitro* (168). This is consistent with the *in vivo* macrophage polarization during bone healing, that the infiltration of M1-like macrophages during the early inflammatory phase is indispensable for bone healing, while the M2-like macrophage infiltration becomes dominant in the later stage of bone repair (167). It can be presumed that the transient activation of M1 macrophages are essential for the early osteoblast activation, while M2 macrophages are indispensable for the later mineralization. Especially, cells from the macrophage—monocyte lineage are considered as important source of S1P (28), a crucial regulator in bone remodeling as discussed above, suggesting that macrophage-derived modulation on bone remodeling might also due to S1P-S1PR1 signaling, which needs further study in the future.

Immune-Regulation Mediated by Cells From Skeletal System

The skeletal system exerts a regulatory effect on the immune system *via* the actions of MSCs, which are capable of suppressing the differentiation and function of effector immune cells, such as Th1, Th17, and M1. MSCs can inhibit differentiation of M0 macrophages to dendritic cells (DCs) and suppress their maturation and function. MSCs also induce macrophage polarization to the M2 phenotype and interfere with T cell proliferation, cytokine production and polarization, in particular the promotion of Treg cell differentiation (101, 169–172). The immune-suppressing functions of MSCs are achieved either through direct cell-cell contact or secretion of soluble immune-modulators, some of which are produced constitutively while others are produced in response to inflammatory factors or activated immune cells (173). Direct cell-cell contact suppression is achieved through the programmed death 1 (PD-1) pathway (174), whereas immune suppressive factors include prostaglandin E2 (PGE2), TGF-β, IL-10, leukemia inhibitory factor (LIF), IL-1 receptor antagonist (IL-1RA) (173, 175). Of these factors, PGE2 is considered to be one of the most potent in MSCs' immunosuppressive arsenal, especially in term of macrophage polarization (101, 176). MSCs secrete PGE2 in response to pro-inflammatory factors, such as IFNγ or LPS (171, 177) and convert M1 macrophages to M2 phenotype (178). This process, which depends on PGE2, induces the production of immune suppressive cytokines (such as IL-10), while impeding the secretion of pro-inflammatory cytokines (such as TNF-α and IL-6), resulting in a microenvironment more suitable for tissue regeneration (171, 179). These effects of PGE2 directly affect the immune response and acts as a coupling factor between macrophages and MSCs/pre-osteoblasts in a way that facilitates osteogenesis (180).

However, when toll-like receptors (TLRs) are activated by LPS, IFN-α/γ, or TNF-α, MSCs can respond by producing pro-inflammatory cytokines (173) such as IL-1β and IL-6 and the chemokine IL-8, which attract the migration of neutrophils and augment the inflammatory response (181). It has emerged that similar to macrophages, human MSCs also polarizes into two distinct phenotypes: pro-inflammatory MSC1 and immunosuppressive MSC2 (182). TLR signaling plays an active role in this polarization, in which acute and low-level activation of TLR4 directs MSCs toward the MSC1 phenotype, whereas the TLR3 activation induces an MSC2 phenotype. The MSC1 phenotype can also be induced by IFNs or direct contact with certain pro-inflammatory cells. Polarized MSCs

TABLE 2 | Possible effects of S1P-derived immune-regulation on bone remodeling.

Cell type	Immune-regulation of S1P	Possible effects on bone remodeling	
		Osteoclasto-genesis	Osteogenesis
M1 macrophages	Differentiation↓ (161)	↓	↑
M2 macrophages	Differentiation↑ (161)	↓	↑
Th1 cells	Response↓ (162)	↓	↑
Th2 cells	Response↑ (163)	↓	↑
Th17 cells	Differentiation↑ (164, 165) Response↑ (164, 165)	↑	↑(?)
Treg cells	Differentiation↓ (165, 166)	↑	-

Th, T helper; Treg, regulatory T.

are thought to play roles similar to that of M1 and M2 macrophages in tissue repair (183), with MSC1s contributing to early stage inflammation and MSC2s contributing to late tissue regeneration. Of note, a recent study has found that macrophage-derived inflammatory factors could induce the RANKL production of bone marrow stromal cells through the SPHK1-S1PR1 axis (184), suggesting that S1P-S1PR1 signaling might participate in MSC polarization and therefore in turn regulate immune response.

Roles of S1P-S1PR1 in Osteoimmunology

When S1P binds with S1PR1, it forms a complex that governs a diverse range of immune cell activities, such as cell migration, proliferation, and differentiation (185). This immunomodulatory effect is thought to be pivotal for bone remodeling (**Figure 3**).

S1P-S1PR1 signaling plays a decisive role in regulating the traffic and egression of immune cells, such as HSCs, DCs, macrophages (monocytes), neutrophils, mast cells, T and B lymphocytes, natural killer T (NKT) cells (78, 186–193). Under both homeostatic and pathological conditions, S1P-S1PR1 signaling is required for mature thymocytes to egress from the thymus, as are T/B cells from secondary lymphoid tissues into blood or lymph (188, 194–196). S1PR1 deficiency results in blocked lymphocyte egression, a condition known as lymphopenia (196), suggesting a vital role for S1PR1 in the timely and appropriate distribution of immune cells, a process that aids homeostasis of the immune system. During inflammation, there is a spike of the local concentration of S1P, results in activated S1PR1 and the recruitment of immune cells—such as effector T cells—to the inflamed tissues and their *in situ* retention (61), which therefore promotes the inflammatory response—a process that induces bone resorption (100).

S1P-S1PR1 signaling is also an essential modulator of immune cell differentiation and function. S1P is required for the maturation and function of DCs, which further affects the activation and polarization of $CD4^+$T cells (197, 198). S1P regulates the function and especially the polarization of $CD4^+$T cell subsets. S1PR1 activation in $CD4^+$T cells impairs the production of IFNγ by Th1 cells, while enhance the production of Th2 cells-derived effector cytokine IL-4, thereby downregulating the Th1 cell response while upregulating that of Th2 cells (162, 163, 199, 200). On the other hand, S1P can induce the differentiation and activation of Th17 cells, as well as the production of IL-17 *in vitro* (**Table 2**)—both of which promote osteoclastogenesis (201). This is accompanied by reduced production of Th1 and Th2 cell-derived cytokines, a process that is considered to be S1PR1-dependent (164, 165). Furthermore, signaling through S1PR1 impedes the differentiation and function of Treg cells, the vital suppressor in immune response and osteoclast differentiation (118), by activating the downstream Akt-mTOR signaling pathway (166, 202), thereby exacerbating bone resorption (**Table 2**). More importantly, by enhancing RANKL production in $CD4^+$T cells S1P contributes to osteoclastogenesis (203).

However, in macrophage polarization, S1P-S1PR1 signaling tends to favor differentiation to an anti-inflammatory phenotype, inducing a conversion of the M1 to M2 subset (161). The S1P-derived induction of Th2 response and IL-4 secretion may indirectly affect this process. The shift from M1 toward the M2 subset (161) could be considered as reducing osteoclastogenesis, since the M1 macrophage-derived cytokines are recognized as inducers for osteoclast differentiation (**Table 1**). A similar shift may also take place in osteogenesis in which M1 macrophages, indispensable during the early stages of bone repair, shift toward the M2 phenotype that is required in the later stages of bone formation (142, 168). Therefore, in contrast to its immune-inductive role in $CD4^+$ T cell polarization, S1P-S1PR1 signaling has an immune-suppressive role in determining macrophage polarization, which complicates its role in bone remodeling (**Table 2**).

From these studies, a picture emerges of how S1P modulate osteoimmunology (**Figure 4**). Under physiological conditions, S1P secreted from osteoclasts during normal bone resorption may initiate bone formation. S1P prompts the migration and subsequent differentiation of MSCs to the resorption pits and also promotes the secretion of PGE2. The combined effect of S1P and PGE2 determines macrophage phenotype and creates a microenvironment suitable for bone regeneration. On the other hand, S1P and PGE2 induce the RANKL expression of osteoblasts. Osteoclast-precursors, which are also recruited by S1P, migrate to the resorption site where they are exposed to osteoblast-derived RANKL, which promotes their differentiation into mature osteoclasts, thus underpinning the continuous process of bone remodeling. Under pathological conditions, such as inflammation, the effects of S1P and PGE2 on macrophages are counteracted by inflammatory cytokines, which interfere with the conversion of M1 to M2 macrophages, resulting in a microenvironment that is unfavorable to osteogenesis. This is further exacerbated once the MSCs stop being immunosuppressive and exhibit a pro-inflammatory phenotype. T cells are also activated by S1P, which infiltrate in the site of resorption and secrete more RANKL into the local microenvironment. The high concentration of RANKL and inflammatory cytokines leads to a catabolic

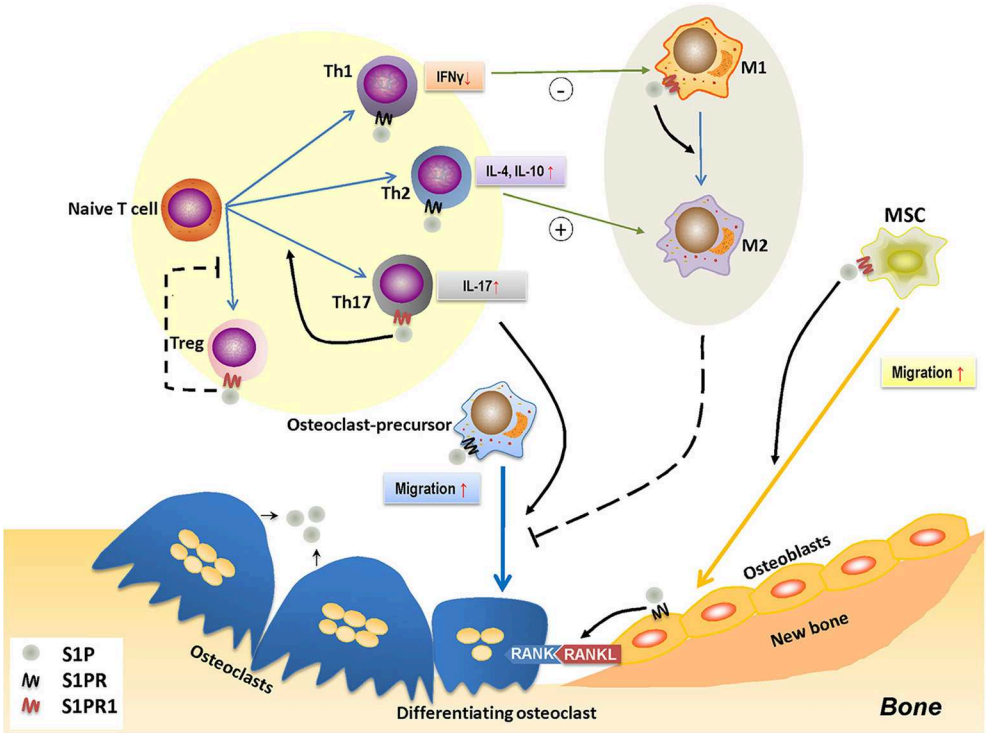

FIGURE 3 | The role of S1P-S1PR1 signaling in osteoimmunology. S1P-S1PR1 signaling is greatly involved in the interaction between immune system and bone remodeling. On one hand, S1PR1 directly affects osteoclastogenesis by inducing the migration of osteoclast-precursors. The direct effect of S1P on osteoclast-precursors results in reduced osteoclastogenesis; however, it induces RANKL production of osteoblasts and facilitating the RANKL-RANK mediated osteoclastogenesis. S1P also induces the migration of MSCs and osteogenesis by activating S1PR1. On the other hand, S1P-S1PR1 signaling participates in immune regulation, which affects the polarization and function of T-helper cells. S1P-S1PR1 signaling induces the differentiation and function of Th17 cells (known as inducing osteoclastogenesis) while impedes that of Treg cells (known as reducing osteoclastogenesis); therefore facilitating osteoclastogenesis. S1P also induces the function of Th2 cells while reduces that of Th1 cells, which affects the macrophage phenotype; also, S1P directly induces the transition of M1 to M2 phenotype by activating S1PR1. This conversion of pro-inflammatory M1 macrophages to tissue-engineering M2 macrophages therefore impedes osteoclastogenesis, which might also affect osteogenesis. S1P, sphingosine-1-phosphate; S1PR, sphingosine-1-phosphate receptor(s); S1PR1, sphingosine-1-phosphate receptor 1; MSC, mesenchymal stem cell; Th1/2/17, type 1/2/17 helper T cell; M1/M2, M1/M2 macrophage; Treg, regulatory T cell; IFNγ, interferon-γ; IL-4/10/17, interleukin-4/10/17.

imbalance that favors bone resorption. Of note, it is still unclear whether S1P signaling leads to "normal" or "abnormal" bone formation, as elevated S1P has also been found in diseases with unwanted excessive bone formation such as spondyloarthritis (54, 204).

Taken together, the weight of evidence all points to S1P-S1PR1 signaling having a pivotal role in osteoimmunology. At one level there is a direct link between S1P-S1PR1 and osteoclast-osteoblast coupling; however, there is also an indirect link that affects bone remodeling *via* S1P-S1PR1 regulation of immune response. Under certain pathological conditions, this finely tuned system is thrown into disequilibrium resulting in an overactive immune environment where bone resorption outstrips formation.

S1P-S1PR1 SIGNALING IN BONE DISEASES

Abnormally activated S1P-S1PR1 signaling has been observed in many diseases, such as RA, multiple sclerosis and cancer (205–207). The importance of S1P-S1PR1 signaling in osteoimmunology highlights the need to assess its roles in the pathogenesis of bone diseases. In addition, S1P regulation *via* SPL inhibition has been demonstrated to enhance bone mass and strength in a S1PR2-dependant manner *in vivo*, which also effectively ameliorating osteoporosis in S1PR2-deficient mice, suggesting S1P is a potential therapeutic target for bone diseases (28).

RA is an autoimmune disorder of the joints characterized by excessive osteoclastogenesis—the result of inflammatory immune response (206). Activated S1P-S1PR1 signaling is found in the synovial tissues of RA joints (206), which is considered to promote RANKL production of $CD4^+$T cells and synoviocytes in a COX-2-dependant manner (203). The joint and bone destruction is significantly alleviated in *Sphk1*-deficient mice: the reduced circulating S1P leads to limited COX-2 expression and Th17 differentiation, with a resulting inhibition of osteoclastogenesis in inflammatory joints (208). Fingolimod, also known as FTY720, is a sphingosine analog that acts as a modulator of S1P-S1PR1 signaling, which has been clinically used in treatment against multiple sclerosis

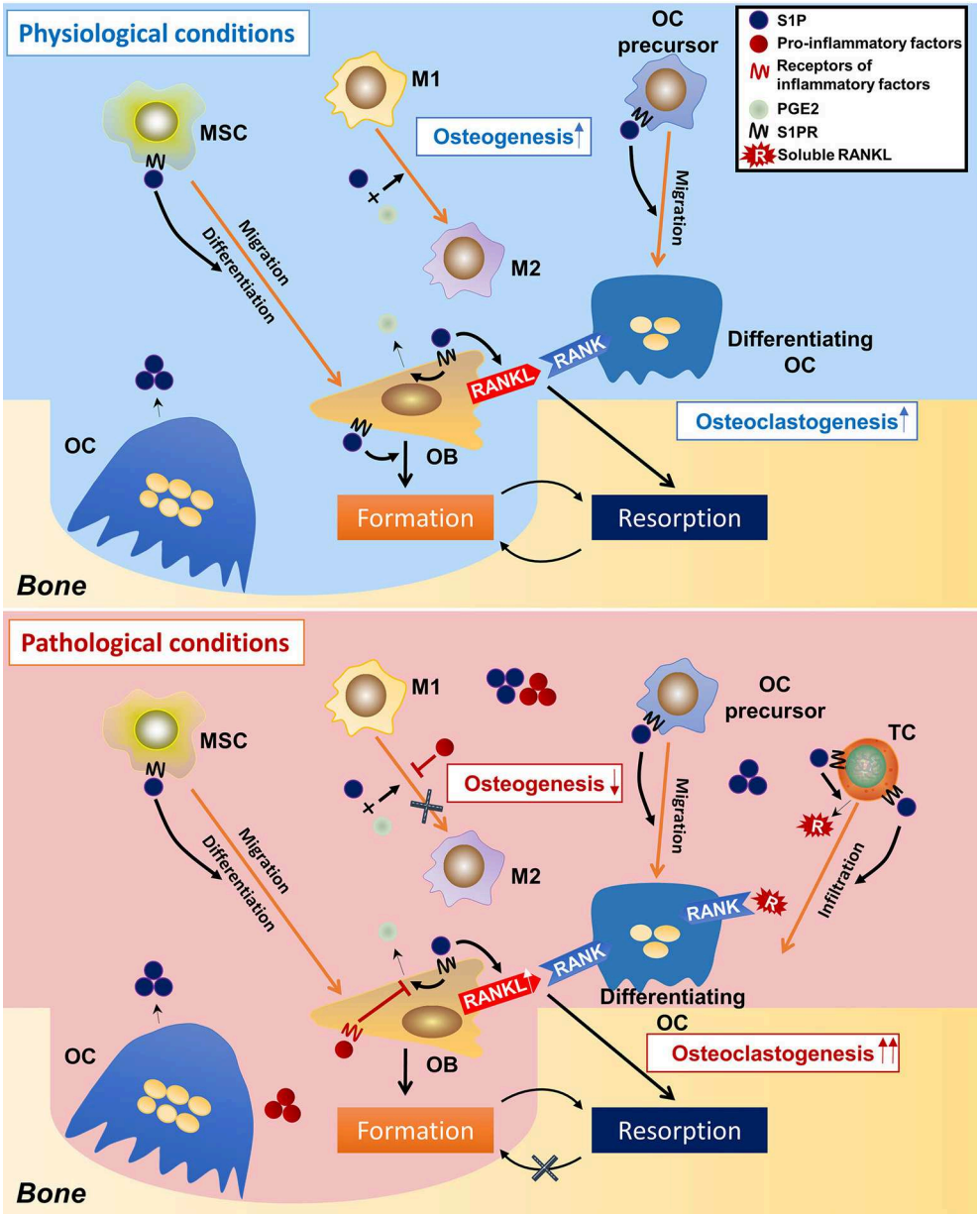

FIGURE 4 | Speculations on the regulatory roles of S1P on osteoimmunology under physiological and pathological conditions. In the physiological condition, osteoclast-derived S1P initiates bone formation by triggering MSCs migration to the resorption cite and by inducing osteoblasts differentiation. During the osteogenic process, S1P also induces the production of PGE2, which, together with S1P, leads the polarization of macrophages toward the M2 phenotype, thereby facilitating bone formation. S1P also induces RANKL production of osteoblasts, as well as the migration of osteoclast-precursors, initiating a new round of osteoclastogenesis. This makes the constant remodeling and bone metastasis. However, in the pathological condition (inflammation), the over-accumulated S1P results in infiltration of inflammatory cells (i.e., T-helper cells), which not only secret large amounts of pro-inflammatory cytokines, but also produce a lot of RANKL (in stimulation of S1P), which greatly induces osteoclastogenesis. On the other hand, the pro-inflammatory factors neutralize the immune-suppressive function of S1P and PGE2 on macrophages, result in failed conversion from M1 to M2 phenotype–an unsuitable circumstance for osteogenesis. This eventually makes to the imbalance between bone resorption and formation and thereby bone loss. S1P, sphingosine-1-phosphate; S1PR, sphingosine-1-phosphate receptor(s); MSC, mesenchymal stem cell; M1/M2, M1/M2 macrophage; OC, osteoclast; OB, osteoblast; TC, T cell; PGE2, prostaglandin E2.

(209). FTY720 is phosphorylated by SPHK2 (FTY720-P) *in vivo* to gain high affinity to S1PR1 (210, 211). Although both S1P and FTY720-P induce S1PR1 internalization (212, 213), the endocytosed S1PR1 following S1P binding is eventually recycled back to cell surface (212); while the endocytosed S1PR1 induced by FTY720-P is then irreversibly degraded (184, 213–217), resulting a pharmacologic deletion of S1PR1 from cell surface (218). FTY720 has been demonstrated

to be effective in a mouse RA model, which inhibited the infiltration of effector $CD4^+$T cells and reduced IL-6 and TNF-α expression in synovial fibroblast cells (219). Similar results have been found in adjuvant-induced arthritis (AA) and collagen-induced arthritis (CIA) rodent models, which were achieved *via* modulating the migration of T cells and DCs, as well as regulating T cell polarization (220–222), suggesting that S1PR1-deletion could be a pharmacological strategy for RA. Interestingly, strategies to increase S1P also showed therapeutic effects in RA animal models. SPL inhibitors, (E)-1-(4-((1R, 2S,3R)-1,2,3,4-Tetrahydroxybutyl)-1H-imidazol-2-yl)ethanone Oxime (LX2931) and (1R,2S,3R)-1-(2-(Isoxazol-3-yl)-1H-imidazol-4-yl)butane-1,2,3,4-tetraol (LX2932) have been found to reduce symptoms and pathological changes in the RA mice model, which could dose-dependently decrease the numbers of circulating lymphocytes by sequestrating them in the thymus (223). In phase I clinical trial, LX2931 administration effectively decreased peripheral lymphocyte counts, suggesting it could potentially reduce local inflammation in RA patient (223). The similar effects between S1P induction and S1PR1 reduction indicate that other S1PRs such as S1PR2, which has demonstrated effects against S1PR1 (28, 94), should also be considered as therapeutic target for RA in the future.

Besides RA, S1P signaling might also participate in the pathogenesis of other arthritis such as spondyloarthritis. Spondyloarthritis (SpA) is a group of several inner-related disorders: psoriatic arthritis, arthritis related to inflammatory bowel disease, reactive arthritis, a subgroup of juvenile idiopathic arthritis, as well as ankylosing spondylitis (the prototypic subtype) (224). Spondyloarthritis is characterized by enthesopathy—inflammation at the cites (named as enthesis) where ligaments and tendons attach to the bone through fibrocartilage connections (54, 224). SpA at later stage usually results in abnormities at enthesis such as excessive bone formation, increased mineralization and fusion of bone, as well as ankyloses (54). A recent study has found that the S1P levels in serum from SpA patients are significantly induced, as compared with those from healthy donors (54, 204). S1P has also been found to induce the mineralization of primary chondrocytes and osteoblasts originated from enthesis (54). This suggests the accumulation of S1P may result in the excessive ossification in SpA, which still needs further verification (54).

S1P is also strongly associated with the pathogenesis of infection-related inflammatory bone loss, as seen in periodontitis and periapical lesions: an inflammatory condition caused by teeth-related bacterial infections that erodes alveolar bone. In a mouse periodontitis model, the ablation of SPHK1 can significantly attenuate alveolar bone loss and is accompanied by a reduction in the numbers of leukocytes and osteoclasts in the periodontal tissues (225). S1P-S1PR1 signaling is also linked to periapical lesions: an upregulation of S1PR1 positively correlates with RANKL and osteoclast expression and negatively with the number of Treg cells during the pathogenesis of periapical bone destruction (226). Further research into this phenomenon indicates that infection-induced M1 macrophages interact with osteoblast—precursors to enhance the production of S1P, which acts in an autocrine manner to activate S1PR1 on osteoblast-precursors. The activation of S1P-S1PR1 signaling results in induced RANKL production, which is partially achieved through the mTOR signaling-dependent inhibition of autophagy in osteoblast-precursors (184). These studies suggest modulation of S1P-S1PR1 signaling could be a novel therapeutic strategy for infection-induced inflammatory bone diseases.

FUTURE DIRECTIONS AND CONCLUSION

Although S1P has been studied for years, many questions still remain un-resolved regarding its role in bone remodeling. For instance, the actual outcome of S1P-S1PR1 signaling-derived modulation on bone remodeling is unknown, since it is found to induce both osteoclastogenesis and osteogenesis. The role of S1P-S1PR1 signaling in osteoimmunology is even more complicated, as its downstream signaling pathway, mTOR, has a dual role in immune system, that in Th cells it directs the polarization toward inflammatory phenotype, while in macrophages it directs the anti-inflammatory M2 polarization (125, 227–229). Until now the detailed cross-talk between immune and skeletal systems over bone regeneration remains unclear, further investigation on different types of infiltrating immune cells, as well as their mutual-regulations during bone regeneration, would help to understand the ultimate role of S1P-S1PR1 signaling in osteoimmunology. It could be presumed that this signaling takes part in the maintenance of the balance between bone resorption and formation under physiological conditions. Especially under inflammatory conditions, a question arises about whether the activated S1P-S1PR1 signaling would trigger osteogenesis in osteoblast-precursors, and it could be proposed that this signaling plays a role in the pathogenesis of inflammation-related bone sclerosis lesions, such as bone spurs in arthritis or sequestrum in osteomyelitis. Another question lies in the mechanism and outcome of S1P-S1PR1 mediated osteogenesis: it has been proved that S1P-S1PR1 leads to induced Wnt-β-catenin signaling pathway to improve osteoblast differentiation (96); however, if β-catenin induction continues, it would result in interrupted Notch signaling and therefore should interfere the terminal differentiation toward osteocytes, as it has been identified that Wnt and Notch pathways are mutually exclusive during osteogenesis; and the up-regulated Notch signaling plays indispensable roles in osteocyte differentiation, while Wnt signaling is more dominant during osteoblast differentiation (230). Also, S1P-S1PR1 activation will leads to the activation of mTOR signaling (166, 202). Although mTOR has been found to play decisive roles in the transition from pre-osteoblasts to osteoblasts (231–233), however, it acts as an inhibitor in the autophagy—an indispensable process in extracellular calcium deposition during mineralization (234–239). It could be presumed that S1P-S1PR1-Akt-mTOR signaling pathway should play positive roles during early stage osteoblast differentiation, however, the later stage osteocyte differentiation as well as mineralization

might be affected; also, the quality of such mineralization might be abnormal or even pathological, as compared with the physiological ones.

In summary, S1P, a key coupling factor for osteoclasts and osteoblasts, plays a complex role in bone remodeling by targeting both osteoclastogenesis and osteogenesis. The immunomodulatory feature of S1P-S1PR1 signaling further indicates that favors the inflammatory cell phenotypes in the adaptive immune system (T cell subsets), while induces macrophage polarization toward the anti-inflammatory phenotype. This dual role in immune system indicates that S1P-S1PR1 signaling might take part in the maintenance of continuous bone turnover under physiological conditions, while lead to the pathogenesis of bone deformities during inflammation. Further investigation of the S1P-S1PR1 signaling pathway should help to get a better understanding about osteoimmunology and therefore benefit the clinical approach for inflammatory bone disorders.

AUTHOR CONTRIBUTIONS

All authors listed have made a substantial, direct and intellectual contribution to the work, and approved it for publication. LX involved in the concept and design of the article, wrote the manuscript. YZ involved in the conception and design of the article, reviewed the manuscript. TF assisted with manuscript preparation. KB reviewed the manuscript. YX involved in the conception and design of the article, and reviewed the manuscript.

FUNDING

This study was provided by the National Natural Science Foundation of China (NSFC, Grant No. 31771025), the National Natural Science Foundation of China (NSFC) Young Scientists Fund (Grant No. 81700969), the National Health and Medical Research Council (NHMRC) Early Career Fellowship (Grant No. 1105035).

ACKNOWLEDGMENTS

This study includes content from LX's thesis Dissecting the role of sphingosine 1-phosphate sphingosine 1-phosphate receptor 1 in inflammatory bone remodeling (240). This study has only appeared in this thesis, and the inclusion is in line with the policy of Queensland University of Technology.

SUPPLEMENTARY MATERIAL

The Supplementary Material for this article can be found online at: https://www.frontiersin.org/articles/10.3389/fimmu.2019.01409/full#supplementary-material

Figure S1 | The RANKL-RANK axis mediated osteoclastogenic signals. RANK is activated when combining with its ligand RANKL. Activated RANK then triggers the down-stream osteoclastogenic signaling cascades. Activated TRAF6 induces the MAPK, IKK, and NF-κB signaling, which eventually result in activation of NFATc1 and osteoclastogenesis. RANKL: receptor activator of nuclear factor factor-kappa B ligand. RANK, receptor activator of nuclear factor-kappa B; TRAF6, tumor-necrosis factor (TNF) receptor-associated factor 6; IKK, inhibitor of nuclear factor kappa-B kinase; MAPK, mitogen-activated protein kinase; NF-κB, nuclear factor kappa B; AP-1, activator protein1; ERK, extracellular signal regulated kinase; JNK, c-Jun N-terminal kinase; NFATc1, nuclear factor of activated T-cells, cytoplasmic 1.

REFERENCES

1. Raggatt LJ, Partridge NC. Cellular and molecular mechanisms of bone remodeling. *J Biol Chem.* (2010) 285:25103–8. doi: 10.1074/jbc.R109.041087
2. Arron JR, Choi Y. Osteoimmunology: bone versus immune system. *Nature.* (2000) 408:535–6. doi: 10.1038/35046196
3. Horton JE, Raisz LG, Simmons HA, Oppenheim JJ, Mergenhagen SE. Bone resorbing activity in supernatant fluid from cultured human peripheral blood leukocytes. *Science.* (1972) 177:793–5. doi: 10.1126/science.177.4051.793
4. Gault CR, Obeid LM, Hannun YA. An overview of sphingolipid metabolism: from synthesis to breakdown. *Sphingolipids Signal Regulat Molecules.* (2010) 688:1–23. doi: 10.1007/978-1-4419-6741-1_1
5. Hannun YA, Obeid LM. Sphingolipids and their metabolism in physiology and disease. *Nat Rev Molecul Cell Biol.* (2018) 19:175–91. doi: 10.1038/nrm.2017.107
6. Takabe K, Paugh SW, Milstien S, Spiegel S. "Inside-out" signaling of sphingosine-1-phosphate: therapeutic targets. *Pharmacol Rev.* (2008) 60:181–95. doi: 10.1124/pr.107.07113
7. Thudichum JLW. *A Treatise on the Chemical Constitution of the Brain.* London: Archon Books (1962).
8. Maceyka M, Harikumar KB, Milstien S, Spiegel S. Sphingosine-1-phosphate signaling and its role in disease. *Trends Cell Biol.* (2012) 22:50–60. doi: 10.1016/j.tcb.2011.09.003
9. Kihara Y, Maceyka M, Spiegel S, Chun J. Lysophospholipid receptor nomenclature review: IUPHAR Review 8. *Br J Pharmacol.* (2014) 171:3575–94. doi: 10.1111/bph.12678
10. Yanagida K, Hla T. Vascular and immunobiology of the circulatory sphingosine 1-phosphate gradient. *Annu Rev Physiol.* (2017) 79:67–91. doi: 10.1146/annurev-physiol-021014-071635
11. Obinata H, Hla T. Sphingosine 1-phosphate and inflammation. *Int Immunol.* (2019) 2019:dxz037. doi: 10.1093/intimm/dxz037
12. Mendoza A, Fang V, Chen C, Serasinghe M, Verma A, Muller J, et al. Lymphatic endothelial S1P promotes mitochondrial function and survival in naive T cells. *Nature.* (2017) 546:158. doi: 10.1038/nature22352
13. Aoki M, Aoki H, Ramanathan R, Hait NC, Takabe K. Sphingosine-1-phosphate signaling in immune cells and inflammation: roles and therapeutic potential. *Mediat Inflamm.* (2016) 2016:8606878. doi: 10.1155/2016/8606878
14. Sato C, Iwasaki T, Kitano S, Tsunemi S, Sano H. Sphingosine 1-phosphate receptor activation enhances BMP-2-induced osteoblast differentiation. *Biochem Biophys Res Commun.* (2012) 423:200–5. doi: 10.1016/j.bbrc.2012.05.130
15. Pederson L, Ruan M, Westendorf JJ, Khosla S, Oursler MJ. Regulation of bone formation by osteoclasts involves Wnt/BMP signaling and the chemokine sphingosine-1-phosphate. *Proc Natl Acad Sci USA.* (2008) 105:20764–9. doi: 10.1073/pnas.0805133106
16. Hannun YA, Obeid LM. The ceramide-centric universe of lipid-mediated cell regulation: stress encounters of the lipid kind. *J Biol Chem.* (2002) 277:25847–50. doi: 10.1074/jbc.R200008200
17. Linn S, Kim H, Keane E, Andras L, Wang E, Merrill A. Regulation of *de novo* sphingolipid biosynthesis and the toxic consequences of its disruption. *Biochem Soc Trans.* (2001) 29(Pt 6):831–5. doi: 10.1042/0300-5127:0290831

18. Pewzner-Jung Y, Ben-Dor S, Futerman AH. When do Lasses (longevity assurance genes) become CerS (ceramide synthases)? Insights into the regulation of ceramide synthesis. *J Biol Chem.* (2006) 281:25001–5. doi: 10.1074/jbc.R600010200
19. Causeret C, Geeraert L, Van der Hoeven G, Mannaerts GP, Van Veldhoven PP. Further characterization of rat dihydroceramide desaturase: tissue distribution, subcellular localization, and substrate specificity. *Lipids.* (2000) 35:1117–25. doi: 10.1007/s11745-000-0627-6
20. Hannun YA, Obeid LM. Principles of bioactive lipid signalling: lessons from sphingolipids. *Nat Rev Molecul Cell Biol.* (2008) 9:139–50. doi: 10.1038/nrm2329
21. Xu R, Jin J, Hu W, Sun W, Bielawski J, Szulc Z, et al. Golgi alkaline ceramidase regulates cell proliferation and survival by controlling levels of sphingosine and S1P. *FASEB J.* (2006) 20:1813–25. doi: 10.1096/fj.05-5689com
22. Galadari S, Wu BX, Mao C, Roddy P, El Bawab S, Hannun YA. Identification of a novel amidase motif in neutral ceramidase. *Biochem J.* (2006) 393:687–95. doi: 10.1042/BJ20050682
23. Spiegel S, Milstien S. The outs and the ins of sphingosine-1-phosphate in immunity. *Nat Rev Immunol.* (2011) 11:403–15. doi: 10.1038/nri2974
24. Mechtcheriakova D, Wlachos A, Sobanov J, Kopp T, Reuschel R, Bornancin F, et al. Sphingosine 1-phosphate phosphatase 2 is induced during inflammatory responses. *Cell Signal.* (2007) 19:748–60. doi: 10.1016/j.cellsig.2006.09.004
25. Peest U, Sensken SC, Andréani P, Hänel P, Van Veldhoven PP, Gräler MH. S1P-lyase independent clearance of extracellular sphingosine 1-phosphate after dephosphorylation and cellular uptake. *J Cell Biochem.* (2008) 104:756–72. doi: 10.1002/jcb.21665
26. Johnson KR, Johnson KY, Becker KP, Bielawski J, Mao C, Obeid LM. Role of human sphingosine-1-phosphate phosphatase 1 in the regulation of intra- and extracellular sphingosine-1-phosphate levels and cell viability. *J Biol Chem.* (2003) 278:34541–7. doi: 10.1074/jbc.M301741200
27. Sigal YJ, Mcdermott MI, Morris AJ. Integral membrane lipid phosphatases/phosphotransferases: common structure and diverse functions. *Biochem J.* (2005) 387:281–93. doi: 10.1042/BJ20041771
28. Weske S, Vaidya M, Reese A, Lipinski KV, Keul P, Bayer JK, et al. Targeting sphingosine-1-phosphate lyase as an anabolic therapy for bone loss. *Nat Med.* (2018) 24:667–8. doi: 10.1038/s41591-018-0005-y
29. Ito K, Anada Y, Tani M, Ikeda M, Sano T, Kihara A, et al. Lack of sphingosine 1-phosphate-degrading enzymes in erythrocytes. *Biochem Biophys Res Commun.* (2007) 357:212–7. doi: 10.1016/j.bbrc.2007.03.123
30. Rosen H, Gonzalez-Cabrera PJ, Sanna MG, Brown S. Sphingosine 1-phosphate receptor signaling. *Annual Rev Biochem.* (2009) 78:743–68. doi: 10.1146/annurev.biochem.78.072407.103733
31. Pappu R, Schwab SR, Cornelissen I, Pereira JP, Regard JB, Xu Y, et al. Promotion of lymphocyte egress into blood and lymph by distinct sources of sphingosine-1-phosphate. *Science.* (2007) 316:295–8. doi: 10.1126/science.1139221
32. Schwab SR, Pereira JP, Matloubian M, Xu Y, Huang Y, Cyster JG. Lymphocyte sequestration through S1P lyase inhibition and disruption of S1P gradients. *Science.* (2005) 309:1735–9. doi: 10.1126/science.1113640
33. Venkataraman K, Lee YM, Michaud J, Thangada S, Ai Y, Bonkovsky HL, et al. Vascular endothelium as a contributor of plasma sphingosine 1-phosphate. *Circul Res.* (2008) 102:669–76. doi: 10.1161/CIRCRESAHA.107.165845
34. Ryu J, Kim HJ, Chang EJ, Huang H, Banno Y, Kim HH. Sphingosine 1-phosphate as a regulator of osteoclast differentiation and osteoclast–osteoblast coupling. *EMBO J.* (2006) 25:5840–51. doi: 10.1038/sj.emboj.7601430
35. Hait NC, Oskeritzian CA, Paugh SW, Milstien S, Spiegel S. Sphingosine kinases, sphingosine 1-phosphate, apoptosis and diseases. *Biochim Biophys Acta.* (2006) 1758:2016–26. doi: 10.1016/j.bbamem.2006.08.007
36. Pitson SM. Regulation of sphingosine kinase and sphingolipid signaling. *Trends Biochem Sci.* (2011) 36:97–107. doi: 10.1016/j.tibs.2010.08.001
37. Strub GM, Paillard M, Liang J, Gomez L, Allegood JC, Hait NC, et al. Sphingosine-1-phosphate produced by sphingosine kinase 2 in mitochondria interacts with prohibitin 2 to regulate complex IV assembly and respiration. *FASEB J.* (2011) 25:600–12. doi: 10.1096/fj.10-167502
38. Hait NC, Allegood J, Maceyka M, Strub GM, Harikumar KB, Singh SK, et al. Regulation of histone acetylation in the nucleus by sphingosine-1-phosphate. *Science.* (2009) 325:1254–7.
39. Selvam SP, De Palma RM, Oaks JJ, Oleinik N, Peterson YK, Stahelin RV, et al. Binding of the sphingolipid S1P to hTERT stabilizes telomerase at the nuclear periphery by allosterically mimicking protein phosphorylation. *Sci Signal.* (2015) 8:ARTN ra58. doi: 10.1126/scisignal.aaa4998
40. Riccio A. New endogenous regulators of class I histone deacetylases. *Sci Signal.* (2010) 3:ARTN pe1. doi: 10.1126/scisignal.3103pe1
41. Alvarez SE, Harikumar KB, Hait NC, Allegood J, Strub GM, Kim EY, et al. Sphingosine-1-phosphate is a missing cofactor for the E3 ubiquitin ligase TRAF2. *Nature.* (2010) 465:1084–8. doi: 10.1038/nature09128
42. Nishi T, Kobayashi N, Hisano Y, Kawahara A, Yamaguchi A. Molecular and physiological functions of sphingosine 1-phosphate transporters. *Bba-Mol Cell Biol L.* (2014) 1841:759–65. doi: 10.1016/j.bbalip.2013.07.012
43. Spiegel S, Maczis MA, Maceyka M, Milstien S. New insights into functions of the sphingosine-1-phosphate transporter SPNS2. *J Lipid Res.* (2019) 60:484–9. doi: 10.1194/jlr.S091959
44. Kim RH, Takabe K, Milstien S, Spiegel S. Export and functions of sphingosine-1-phosphate. *Bba-Mol Cell Biol L.* (2009) 1791:692–6. doi: 10.1016/j.bbalip.2009.02.011
45. Kobayashi N, Kobayashi N, Yamaguchi A, Nishi T. Characterization of the ATP-dependent Sphingosine 1-phosphate transporter in rat erythrocytes. *J Biol Chem.* (2009) 284:21192–200. doi: 10.1074/jbc.M109.006163
46. Kobayashi N, Nishi T, Hirata T, Kihara A, Sano T, Igarashi Y, et al. Sphingosine 1-phosphate is released from the cytosol of rat platelets in a carrier-mediated manner. *J Lipid Res.* (2006) 47:614–21. doi: 10.1194/jlr.M500468-JLR200
47. Nieuwenhuis B, Luth A, Jakobi M, Kleuser B. Involvement of the Abc-Transporter Abcc1 and the Sphingosine 1-Phosphate Receptor Subtype S1p3 in the cytoprotection of human fibroblasts by the glucocorticoid dexamethasone. *Naunyn Schmiedebergs Arch. Pharmacol.* (2010) 382:21. doi: 10.1007/s00109-009-0468-x
48. Takabe K, Kim RH, Allegood JC, Mitra P, Ramachandran S, Nagahashi M, et al. Estradiol induces export of sphingosine 1-phosphate from breast cancer cells via ABCC1 and ABCG2. *J Biol Chem.* (2010) 285:10477–86. doi: 10.1074/jbc.M109.064162
49. Tanfin Z, Serrano-Sanchez M, Leiber D. ATP-binding cassette ABCC1 is involved in the release of sphingosine 1-phosphate from rat uterine leiomyoma ELT3 cells and late pregnant rat myometrium. *Cell Signal.* (2011) 23:1997–2004. doi: 10.1016/j.cellsig.2011.07.010
50. Vu TM, Ishizu AN, Foo JC, Toh XR, Zhang FY, Whee DM, et al. Mfsd2b is essential for the sphingosine-1-phosphate export in erythrocytes and platelets. *Nature.* (2017) 550:524–8. doi: 10.1038/nature24053
51. Kobayashi N, Kawasaki-Nishi S, Otsuka M, Hisano Y, Yamaguchi A, Nishi T. MFSD2B is a sphingosine 1-phosphate transporter in erythroid cells. *Sci Rep.* (2018) 8:ARTN4969. doi: 10.1038/s41598-018-23300-x
52. Kawahara A, Nishi T, Hisano Y, Fukui H, Yamaguchi A, Mochizuki N. The Sphingolipid Transporter Spns2 Functions in Migration of Zebrafish Myocardial Precursors. *Science.* (2009) 323:524–7. doi: 10.1126/science.1167449
53. Hisano Y, Kobayashi N, Kawahara A, Yamaguchi A, Nishi T. The Sphingosine 1-phosphate transporter, SPNS2, functions as a transporter of the phosphorylated form of the immunomodulating agent FTY720. *J Biol Chem.* (2011) 286:1758–66. doi: 10.1074/jbc.M110.171116
54. Bougault C, El Jamal A, Briolay A, Mebarek S, Boutet MA, Garraud T, et al. Involvement of sphingosine kinase/sphingosine 1-phosphate metabolic pathway in spondyloarthritis. *Bone.* (2017) 103:150–8. doi: 10.1016/j.bone.2017.07.002
55. Keller J, Catala-Lehnen P, Huebner AK, Jeschke A, Heckt T, Lueth A, et al. Calcitonin controls bone formation by inhibiting the release of sphingosine 1-phosphate from osteoclasts. *Nat Commun.* (2014) 5:5215 doi: 10.1038/ncomms6215
56. Fukuhara S, Simmons S, Kawamura S, Inoue A, Orba Y, Tokudome T, et al. The sphingosine-1-phosphate transporter Spns2 expressed on endothelial cells regulates lymphocyte trafficking in mice. *J Clin Invest.* (2012) 122:1416–26. doi: 10.1172/JCI60746

57. Nijnik A, Clare S, Hale C, Chen J, Raisen C, Mottram L, et al. The role of sphingosine-1-phosphate transporter Spns2 in immune system function. *J Immunol.* (2012) 189:102–11. doi: 10.4049/jimmunol.1200282
58. Pettus BJ, Bielawski J, Porcelli AM, Reames DL, Johnson KR, Morrow J, et al. The sphingosine kinase 1/sphingosine-1-phosphate pathway mediates COX-2 induction and PGE2 production in response to TNF-α. *FASEB J.* (2003) 17:1411–21. doi: 10.1096/fj.02-1038com
59. Park ES, Choi S, Shin B, Yu J, Yu J, Hwang J M, et al. Tumor necrosis factor (TNF) receptor-associated factor (TRAF)-interacting protein (TRIP) negatively regulates the TRAF2 ubiquitin-dependent pathway by suppressing the TRAF2-sphingosine 1-phosphate (S1P) interaction. *J Biol Chem.* (2015) 290:9660–73. doi: 10.1074/jbc.M114.609685
60. Harikumar KB, Yester JW, Surace MJ, Oyeniran C, Price MM, Huang WC, et al. K63-linked polyubiquitination of transcription factor IRF1 is essential for IL-1-induced production of chemokines CXCL10 and CCL5. *Nat Immunol.* (2014) 15:231–8. doi: 10.1038/ni.2810
61. Ledgerwood LG, Lal G, Zhang N, Garin A, Esses SJ, Ginhoux F, et al. The sphingosine 1-phosphate receptor 1 causes tissue retention by inhibiting the entry of peripheral tissue T lymphocytes into afferent lymphatics. *Nat Immunol.* (2008) 9:42–53. doi: 10.1038/ni1534
62. Kono M, Proia RL. Imaging S1P1 activation *in vivo*. *Exp Cell Res.* (2015) 333:178–82. doi: 10.1016/j.yexcr.2014.11.023
63. Sanchez T, Hla T. Structural and functional characteristics of S1P receptors. *J Cell Biochem.* (2004) 92:913–22. doi: 10.1002/jcb.20127
64. Davis MD, Kehrl JH. The influence of sphingosine-1-phosphate receptor signaling on lymphocyte trafficking: how a bioactive lipid mediator grew up from an "immature" vascular maturation factor to a "mature" mediator of lymphocyte behavior and function. *Immunol Res.* (2009) 43:187–97. doi: 10.1007/s12026-008-8066-5
65. Cahalan SM, Gonzalez-Cabrera PJ, Sarkisyan G, Nguyen N, Schaeffer MT, Huang L, et al. Actions of a picomolar short-acting S1P1 agonist in S1P1-eGFP knock-in mice. *Nat Chem Biol.* (2011) 7:254–6. doi: 10.1038/nchembio.547
66. Chae SS, Proia RL, Hla T. Constitutive expression of the S1P 1 receptor in adult tissues. *Prostagland Other Lipid Med.* (2004) 73:141–50. doi: 10.1016/j.prostaglandins.2004.01.006
67. Kono M, Tucker AE, Tran J, Bergner JB, Turner EM, Proia RL. Sphingosine-1-phosphate receptor 1 reporter mice reveal receptor activation sites *in vivo*. *J Clin Invest.* (2014) 124:2076–86. doi: 10.1172/JCI71194
68. Cuvillier O. Sphingosine 1-phosphate receptors: from biology to physiopathology. *Med Sci.* (2012) 28:951–7. doi: 10.1051/medsci/20122811013
69. Nayak D, Huo Y, Kwang W, Pushparaj P, Kumar S, Ling EA, et al. Sphingosine kinase 1 regulates the expression of proinflammatory cytokines and nitric oxide in activated microglia. *Neuroscience.* (2010) 166:132–44. doi: 10.1016/j.neuroscience.2009.12.020
70. Liu Y, Wada R, Yamashita T, Mi Y, Deng CX, Hobson JP, et al. Edg-1, the G protein–coupled receptor for sphingosine-1-phosphate, is essential for vascular maturation. *J Clin Invest.* (2000) 106:951–61. doi: 10.1172/JCI10905
71. Camerer E, Regard JB, Cornelissen I, Srinivasan Y, Duong DN, Palmer D, et al. Sphingosine-1-phosphate in the plasma compartment regulates basal and inflammation-induced vascular leak in mice. *J Clin Invest.* (2009) 119:1871–9. doi: 10.1172/JCI38575
72. Shoham AB, Malkinson G, Krief S, Shwartz Y, Ely Y, Ferrara N, et al. S1P1 inhibits sprouting angiogenesis during vascular development. *Development.* (2012) 139:3859–69. doi: 10.1242/dev.078550
73. Gaengel K, Niaudet C, Hagikura K, Laviña B, Muhl L, Hofmann JJ, et al. The sphingosine-1-phosphate receptor S1PR1 restricts sprouting angiogenesis by regulating the interplay between VE-cadherin and VEGFR2. *Dev Cell.* (2012) 23:587–99. doi: 10.1016/j.devcel.2012.08.005
74. Jung B, Obinata H, Galvani S, Mendelson K, Ding BS, Skoura A, et al. Flow-regulated endothelial S1P receptor-1 signaling sustains vascular development. *Dev Cell.* (2012) 23:600–10. doi: 10.1016/j.devcel.2012.07.015
75. Mendelson K, Evans T, Hla T. Sphingosine 1-phosphate signalling. *Development.* (2014) 141:5–9. doi: 10.1242/dev.094805
76. Eskan MA, Rose BG, Benakanakere MR, Zeng Q, Fujioka D, Martin MH, et al. TLR4 and S1P receptors cooperate to enhance inflammatory cytokine production in human gingival epithelial cells. *Eur J Immunol.* (2008) 38:1138–47. doi: 10.1002/eji.200737898
77. Pitson SM, Pébay A. Regulation of stem cell pluripotency and neural differentiation by lysophospholipids. *Neurosignals.* (2009) 17:242–54. doi: 10.1159/000231891
78. Ishii M, Egen JG, Klauschen F, Meier-Schellersheim M, Saeki Y, Vacher J, et al. Sphingosine-1-phosphate mobilizes osteoclast precursors and regulates bone homeostasis. *Nature.* (2009) 458:524–8. doi: 10.1038/nature07713
79. Kini U, Nandeesh B. Physiology of bone formation, remodeling, and metabolism. In: Fogelman I, Gnanasegaran G, van der Wall H, editors. *Radionuclide and Hybrid Bone Imaging*. Berlin; Heidelberg: Springer (2012). p. 29–57. doi: 10.1007/978-3-642-02400-9_2
80. Lacey D, Timms E, Tan HL, Kelley M, Dunstan C, Burgess T, et al. Osteoprotegerin ligand is a cytokine that regulates osteoclast differentiation and activation. *Cell.* (1998) 93:165–76. doi: 10.1016/S0092-8674(00)81569-X
81. Theill LE, Boyle WJ, Penninger JM. RANK-L and RANK: T cells, bone loss, and mammalian evolution. *Annu Rev Immunol.* (2002) 20:795–823. doi: 10.1146/annurev.immunol.20.100301.064753
82. Kong YY, Yoshida H, Sarosi I, Tan HL, Timms E, Capparelli C, et al. OPGL is a key regulator of osteoclastogenesis, lymphocyte development and lymph-node organogenesis. *Nature.* (1999) 397:315–23. doi: 10.1038/16852
83. Yoshida H, Hayashi SI, Kunisada T, Ogawa M, Nishikawa S, Okamura H, et al. The murine mutation osteopetrosis is in the coding region of the macrophage colony stimulating factor gene. *Nature.* (1990) 345:442–4. doi: 10.1038/345442a0
84. Udagawa N, Takahashi N, Akatsu T, Tanaka H, Sasaki T, Nishihara T, et al. Origin of osteoclasts: mature monocytes and macrophages are capable of differentiating into osteoclasts under a suitable microenvironment prepared by bone marrow-derived stromal cells. *Proc Natl Acad Sci USA.* (1990) 87:7260–4. doi: 10.1073/pnas.87.18.7260
85. Komori T. Signaling networks in RUNX2-dependent bone development. *J Cell Biochem.* (2011) 112:750–5. doi: 10.1002/jcb.22994
86. Cai T, Sun D, Duan Y, Wen P, Dai C, Yang J, et al. WNT/β-catenin signaling promotes VSMCs to osteogenic transdifferentiation and calcification through directly modulating Runx2 gene expression. *Exp Cell Res.* (2016) 345:206–17. doi: 10.1016/j.yexcr.2016.06.007
87. Wu M, Chen G, Li YP. TGF-β and BMP signaling in osteoblast, skeletal development, and bone formation, homeostasis and disease. *Bone Res.* (2016) 4:16009. doi: 10.1038/boneres.2016.9
88. Potier E, Ferreira E, Andriamanalijaona R, Pujol JP, Oudina K, Logeart-Avramoglou D, et al. Hypoxia affects mesenchymal stromal cell osteogenic differentiation and angiogenic factor expression. *Bone.* (2007) 40:1078–87. doi: 10.1016/j.bone.2006.11.024
89. Yue R, Zhou BO, Shimada IS, Zhao Z, Morrison SJ. Leptin receptor promotes adipogenesis and reduces osteogenesis by regulating mesenchymal stromal cells in adult bone marrow. *Cell Stem Cell.* (2016) 18:782–96. doi: 10.1016/j.stem.2016.02.015
90. Simonet W, Lacey D, Dunstan C, Kelley M, Chang MS, Lüthy R, et al. Osteoprotegerin: a novel secreted protein involved in the regulation of bone density. *Cell.* (1997) 89:309–19. doi: 10.1016/S0092-8674(00)80209-3
91. Rodan GA, Martin TJ. Therapeutic approaches to bone diseases. *Science.* (2000) 289:1508–14. doi: 10.1126/science.289.5484.1508
92. Taubman MA, Valverde P, Han X, Kawai T. Immune response: the key to bone resorption in periodontal disease. *J Periodontol.* (2005) 76:2033–41. doi: 10.1902/jop.2005.76.11-S.2033
93. Wang CY, Stashenko P. Characterization of bone-resorbing activity in human periapical lesions. *J Endodont.* (1993) 19:107–11. doi: 10.1016/S0099-2399(06)80503-0
94. Ishii M, Kikuta J, Shimazu Y, Meier-Schellersheim M, Germain RN. Chemorepulsion by blood S1P regulates osteoclast precursor mobilization and bone remodeling *in vivo*. *J Exp Med.* (2010) 207:2793–8. doi: 10.1084/jem.20101474
95. Kikuta J, Kawamura S, Okiji F, Shirazaki M, Sakai S, Saito H, et al. Sphingosine-1-phosphate-mediated osteoclast precursor monocyte migration is a critical point of control in antibone-resorptive action

of active vitamin D. *Proc Natl Acad Sci USA.* (2013) 110:7009–13. doi: 10.1073/pnas.1218799110

96. Matsuzaki E, Hiratsuka S, Hamachi T, Takahashi-Yanaga F, Hashimoto Y, Higashi K, et al. Sphingosine-1-phosphate promotes the nuclear translocation of β-catenin and thereby induces osteoprotegerin gene expression in osteoblast-like cell lines. *Bone.* (2013) 55:315–24. doi: 10.1016/j.bone.2013.04.008
97. Higashi K, Matsuzaki E, Hashimoto Y, Takahashi-Yanaga F, Takano A, Anan H, et al. Sphingosine-1-phosphate/S1PR2-mediated signaling triggers Smad1/5/8 phosphorylation and thereby induces Runx2 expression in osteoblasts. *Bone.* (2016) 93:1–11. doi: 10.1016/j.bone.2016.09.003
98. Lotinun S, Kiviranta R, Matsubara T, Alzate JA, Neff L, Lüth A, et al. Osteoclast-specific cathepsin K deletion stimulates S1P-dependent bone formation. *J Clin Invest.* (2013) 123:666–81. doi: 10.1172/JCI64840
99. Dewhirst FE, Stashenko PP, Mole JE, Tsurumachi T. Purification and partial sequence of human osteoclast-activating factor: identity with interleukin 1 beta. *J Immunol.* (1985) 135:2562–8. Available online at: http://www.jimmunol.org/content/135/4/2562
100. Takayanagi H. Osteoimmunology: shared mechanisms and crosstalk between the immune and bone systems. *Nat Rev Immunol.* (2007) 7:292–304. doi: 10.1038/nri2062
101. Nauta AJ, Fibbe WE. Immunomodulatory properties of mesenchymal stromal cells. *Blood.* (2007) 110:3499–506. doi: 10.1182/blood-2007-02-069716
102. Kim MS, Day CJ, Morrison NA. MCP-1 is induced by RANKL, promotes osteoclast fusion and rescues GM-CSF suppression of osteoclast formation. *J Biol Chem.* (2005) 280:16163–9. doi: 10.1074/jbc.M412713200
103. Miyamoto T, Ohneda O, Arai F, Iwamoto K, Okada S, Takagi K, et al. Bifurcation of osteoclasts and dendritic cells from common progenitors. *Blood.* (2001) 98:2544–54. doi: 10.1182/blood.V98.8.2544
104. Lari R, Fleetwood AJ, Kitchener PD, Cook AD, Pavasovic D, Hertzog PJ, et al. Macrophage lineage phenotypes and osteoclastogenesis—Complexity in the control by GM-CSF and TGF-β. *Bone.* (2007) 40:323–36. doi: 10.1016/j.bone.2006.09.003
105. Takayanagi H, Ogasawara K, Hida S, Chiba T, Murata S, Sato K, et al. T-cell-mediated regulation of osteoclastogenesis by signalling cross-talk between RANKL and IFN-γ. *Nature.* (2000) 408:600–5. doi: 10.1038/35046102
106. Lee MS, Kim HS, Yeon JT, Choi SW, Chun CH, Kwak HB, et al. GM-CSF regulates fusion of mononuclear osteoclasts into bone-resorbing osteoclasts by activating the Ras/ERK pathway. *J Immunol.* (2009) 183:3390–9. doi: 10.4049/jimmunol.0804314
107. Park BK, Zhang H, Zeng Q, Dai J, Keller ET, Giordano T, et al. NF-κB in breast cancer cells promotes osteolytic bone metastasis by inducing osteoclastogenesis via GM-CSF. *Nat Med.* (2007) 13:62–9. doi: 10.1038/nm1519
108. Abu-Amer Y. IL-4 abrogates osteoclastogenesis through STAT6-dependent inhibition of NF-κB. *J Clin Invest.* (2001) 107:1375–85. doi: 10.1172/JCI10530
109. Moreno JL, Kaczmarek M, Keegan AD, Tondravi M. IL-4 suppresses osteoclast development and mature osteoclast function by a STAT6-dependent mechanism: irreversible inhibition of the differentiation program activated by RANKL. *Blood.* (2003) 102:1078–86. doi: 10.1182/blood-2002-11-3437
110. Park-Min KH, Ji JD, Antoniv T, Reid AC, Silver RB, Humphrey MB, et al. IL-10 suppresses calcium-mediated costimulation of receptor activator NF-κB signaling during human osteoclast differentiation by inhibiting TREM-2 expression. *J Immunol.* (2009) 183:2444–55. doi: 10.4049/jimmunol.0804165
111. Kudo O, Sabokbar A, Pocock A, Itonaga I, Fujikawa Y, Athanasou N. Interleukin-6 and interleukin-11 support human osteoclast formation by a RANKL-independent mechanism. *Bone.* (2003) 32:1–7. doi: 10.1016/S8756-3282(02)00915-8
112. Hashizume M, Hayakawa N, Mihara M. IL-6 trans-signalling directly induces RANKL on fibroblast-like synovial cells and is involved in RANKL induction by TNF-α and IL-17. *Rheumatology.* (2008) 47:1635–40. doi: 10.1093/rheumatology/ken363
113. Kurihara N, Bertolini D, Suda T, Akiyama Y, Roodman GD. IL-6 stimulates osteoclast-like multinucleated cell formation in long term human marrow cultures by inducing IL-1 release. *J Immunol.* (1990) 144:4226–30.
114. Korn T, Mitsdoerffer M, Croxford AL, Awasthi A, DardalhonVA, Galileos G, et al. IL-6 controls Th17 immunity in vivo by inhibiting the conversion of conventional T cells into Foxp3+ regulatory T cells. *Proc Natl Acad Sci USA.* (2008) 105:18460–5. doi: 10.1073/pnas.0809850105
115. Kimura A, Naka T, Kishimoto T. IL-6-dependent and-independent pathways in the development of interleukin 17-producing T helper cells. *Proc Natl Acad Sci USA.* (2007) 104:12099–104. doi: 10.1073/pnas.0705268104
116. Lubberts E, van den Bersselaar L, Oppers-Walgreen B, Schwarzenberger P, Coenen-de Roo CJ, Kolls JK, et al. IL-17 promotes bone erosion in murine collagen-induced arthritis through loss of the receptor activator of NF-κB ligand/osteoprotegerin balance. *J Immunol.* (2003) 170:2655–62. doi: 10.4049/jimmunol.170.5.2655
117. Van Den Berg WB, Miossec P. IL-17 as a future therapeutic target for rheumatoid arthritis. *Nat Rev Rheumatol.* (2009) 5:549–53. doi: 10.1038/nrrheum.2009.179
118. Sakaguchi S, Yamaguchi T, Nomura T, Ono M. Regulatory T cells and immune tolerance. *Cell.* (2008) 133:775–87. doi: 10.1016/j.cell.2008.05.009
119. Zaiss MM, Axmann R, Zwerina J, Polzer K, Gückel E, Skapenko A, et al. Treg cells suppress osteoclast formation: a new link between the immune system and bone. *Arthrit Rheumat.* (2007) 56:4104–12. doi: 10.1002/art.23138
120. Quinn JM, Itoh K, Udagawa N, Häusler K, Yasuda H, Shima N, et al. Transforming growth factor β affects osteoclast differentiation via direct and indirect actions. *J BoneMineral Res.* (2001) 16:1787–94. doi: 10.1359/jbmr.2001.16.10.1787
121. Galvin RJS, Gatlin CL, Horn JW, Fuson TR. TGF-β enhances osteoclast differentiation in hematopoietic cell cultures stimulated with RANKL and M-CSF. *Biochem Biophys Res Commun.* (1999) 265:233–9. doi: 10.1006/bbrc.1999.1632
122. Mills CD, Kincaid K, Alt JM, Heilman MJ, Hill A. M. M-1/M-2 macrophages and the Th1/Th2 paradigm. *J Immunol.* (2000) 164:6166–73. doi: 10.4049/jimmunol.164.12.6166
123. Horwood NJ. Macrophage polarization and bone formation: a review. *Clin Rev Allergy Immunol.* (2016) 51:79–86. doi: 10.1007/s12016-015-8519-2
124. Mantovani A, Sica A, Sozzani S, Allavena P, Vecchi A, Locati M. The chemokine system in diverse forms of macrophage activation and polarization. *Trends Immunol.* (2004) 25:677–86. doi: 10.1016/j.it.2004.09.015
125. Murray PJ, Allen JE, Biswas SK, Fisher EA, Gilroy DW, Goerdt S, et al. Macrophage activation and polarization: nomenclature and experimental guidelines. *Immunity.* (2014) 41:14–20. doi: 10.1016/j.immuni.2014.06.008
126. Takeshita S, Kaji K, Kudo A. Identification and characterization of the new osteoclast progenitor with macrophage phenotypes being able to differentiate into mature osteoclasts. *J Bone Mineral Res.* (2000) 15:1477–88. doi: 10.1359/jbmr.2000.15.8.1477
127. Wei S, Kitaura H, Zhou P, Ross FP, Teitelbaum SL. IL-1 mediates TNF-induced osteoclastogenesis. *J Clin Invest.* (2005) 115:282–90. doi: 10.1172/JCI200523394
128. Zwerina J, Redlich K, Polzer K, Joosten L, Krönke G, Distler J, et al. TNF-induced structural joint damage is mediated by IL-1. *Proc Natl Acad Sci USA.* (2007) 104:11742–7. doi: 10.1073/pnas.0610812104
129. Lam J, Takeshita S, Barker JE, Kanagawa O, Ross FP, Teitelbaum SL. TNF-α induces osteoclastogenesis by direct stimulation of macrophages exposed to permissive levels of RANK ligand. *J Clin Invest.* (2000) 106:1481–8. doi: 10.1172/JCI11176
130. Kobayashi K, Takahashi N, Jimi E, Udagawa N, Takami M, Kotake S, et al. Tumor necrosis factor α stimulates osteoclast differentiation by a mechanism independent of the ODF/RANKL–RANK interaction. *J Exp Med.* (2000) 191:275–86. doi: 10.1084/jem.191.2.275
131. Kitaura H, Sands MS, Aya K, Zhou P, Hirayama T, Uthgenannt B, et al. Marrow stromal cells and osteoclast precursors differentially contribute to TNF-α-induced osteoclastogenesis *in vivo*. *J Immunol.* (2004) 173:4838–46. doi: 10.4049/jimmunol.173.8.4838
132. Zou W, Hakim I, Tschoep K, Endres S, Bar-Shavit Z, Tumor necrosis factor-α mediates RANK ligand stimulation of osteoclast differentiation by an autocrine mechanism. *J Cell Biochem.* (2001) 83:70–83. doi: 10.1002/jcb.1202

133. Ho VW, Sly LM. Derivation and characterization of murine alternatively activated (M2) macrophages. *Methods Mol Biol.* (2009) 531:173–85. doi: 10.1007/978-1-59745-396-7_12
134. Bonewald L, Dallas S. Role of active and latent transforming growth factor β in bone formation. *J Cell Biochem.* (1994) 55:350–7. doi: 10.1002/jcb.240550312
135. Wu B, Sondag G, Malcuit C, Kim MH, Safadi FF. Macrophage-associated osteoactivin/GPNMB mediates mesenchymal stem cell survival, proliferation, and migration via a CD44-dependent mechanism. *J Cellul Biochem.* (2015) 117:1511–21. doi: 10.1002/jcb.25394
136. Cho TJ, Kim J, Chung C, Yoo W, Gerstenfeld L, Einhorn T, et al. Expression and role of interleukin-6 in distraction osteogenesis. *Calcified Tissue Int.* (2007) 80:192–200. doi: 10.1007/s00223-006-0240-y
137. Sammons J, Ahmed N, El-Sheemy M, Hassan H. The role of BMP-6, IL-6, and BMP-4 in mesenchymal stem cell-dependent bone development: effects on osteoblastic differentiation induced by parathyroid hormone and vitamin D3. *Stem Cells Dev.* (2004) 13:273–80. doi: 10.1089/154732804323099208
138. Blanchard F, Duplomb L, Baud'huin M, Brounais B. The dual role of IL-6-type cytokines on bone remodeling and bone tumors. *Cytokine Growth Factor Rev.* (2009) 20:19–28. doi: 10.1016/j.cytogfr.2008.11.004
139. Itoh S, Udagawa N, Takahashi N, Yoshitake F, Narita H, Ebisu S, et al. A critical role for interleukin-6 family-mediated Stat3 activation in osteoblast differentiation and bone formation. *Bone.* (2006) 39:505–12. doi: 10.1016/j.bone.2006.02.074
140. Bellido T, Borba VZ, Roberson P, Manolagas SC. Activation of the janus kinase/STAT (Signal Transducer and Activator of Transcription) signal transduction pathway by interleukin-6-type cytokines promotes osteoblast differentiation 1. *Endocrinology.* (1997) 138:3666–76. doi: 10.1210/en.138.9.3666
141. Song HY, Jeon ES, Kim JI, Jung JS, Kim JH. Oncostatin M promotes osteogenesis and suppresses adipogenic differentiation of human adipose tissue-derived mesenchymal stem cells. *J Cell Biochem.* (2007) 101:1238–51. doi: 10.1002/jcb.21245
142. Guihard P, Danger Y, Brounais B, David E, Brion R, Delecrin J, et al. Induction of osteogenesis in mesenchymal stem cells by activated monocytes/macrophages depends on oncostatin M signaling. *Stem Cells.* (2012) 30:762–72. doi: 10.1002/stem.1040
143. Sonomoto K, Yamaoka K, Oshita K, Fukuyo S, Zhang X, Nakano K, et al. Interleukin-1β induces differentiation of human mesenchymal stem cells into osteoblasts via the Wnt-5a/receptor tyrosine kinase–like orphan receptor 2 pathway. *Arthr Rheum.* (2012) 64:3355–63. doi: 10.1002/art.34555
144. Ma T, Miyanishi K, Trindade MC, Genovese M, Regula D, Smith RL, et al. Interleukin 1 receptor antagonist inhibits localized bone formation *in vivo*. *J Rheumatol.* (2003) 30:2547–52.
145. Huang H, Kim H, Chang E, Lee Z, Hwang S, Kim H, et al. IL-17 stimulates the proliferation and differentiation of human mesenchymal stem cells: implications for bone remodeling. *Cell Death Differen.* (2009) 16:1332–43. doi: 10.1038/cdd.2009.74
146. Ono T, Okamoto K, Nakashima T, Nitta T, Hori S, Iwakura Y, et al. IL-17-producing γδ T cells enhance bone regeneration. *Nat Commun.* (2016) 7:10928. doi: 10.1038/ncomms10928
147. Hess K, Ushmorov A, Fiedler J, Brenner RE, Wirth T. TNFα promotes osteogenic differentiation of human mesenchymal stem cells by triggering the NF-κB signaling pathway. *Bone.* (2009) 45:367–76. doi: 10.1016/j.bone.2009.04.252
148. Nanes MS. Tumor necrosis factor-α: molecular and cellular mechanisms in skeletal pathology. *Gene.* (2003) 321:1–15. doi: 10.1016/S0378-1119(03)00841-2
149. Perrien DS, Brown EC, Fletcher TW, Irby DJ, Aronson J, Gao GG, et al. Interleukin-1 and tumor necrosis factor antagonists attenuate ethanol-induced inhibition of bone formation in a rat model of distraction osteogenesis. *J Pharmacol Exp Therapeut.* (2002) 303:904–8. doi: 10.1124/jpet.102.039636
150. Ding J, Ghali O, Lencel P, Broux O, Chauveau C, Devedjian J, et al. TNF-α and IL-1β inhibit RUNX2 and collagen expression but increase alkaline phosphatase activity and mineralization in human mesenchymal stem cells. *Life Sci.* (2009) 84:499–504. doi: 10.1016/j.lfs.2009.01.013
151. Bozec A, Bakiri L, Hoebertz A, Eferl R, Schilling AF, Komnenovic V, et al. Osteoclast size is controlled by Fra-2 through LIF/LIF-receptor signalling and hypoxia. *Nature.* (2008) 454:221–5. doi: 10.1038/nature07019
152. Richards CD, Langdon C, Deschamps P, Pennica D, Shaughnessy SG. Stimulation of osteoclast differentiation in vitro by mouse oncostatin M, leukaemia inhibitory factor, cardiotrophin-1 and interleukin 6: synergy with dexamethasone. *Cytokine.* (2000) 12:613–21. doi: 10.1006/cyto.1999.0635
153. Dresner-Pollak R, Gelb N, Rachmilewitz D, Karmeli F, Weinreb M. Interleukin 10-deficient mice develop osteopenia, decreased bone formation, and mechanical fragility of long bones. *Gastroenterology.* (2004) 127:792–801. doi: 10.1053/j.gastro.2004.06.013
154. Van Vlasselaer P, Borremans B, Van Den Heuvel R, Van Gorp U, de Waal Malefyt R. Interleukin-10 inhibits the osteogenic activity of mouse bone marrow. *Blood.* (1993) 82:2361–70.
155. Van Vlasselaer P, Borremans B, Van Gorp U, Dasch J, De Waal-Malefyt R. Interleukin 10 inhibits transforming growth factor-beta (TGF-beta) synthesis required for osteogenic commitment of mouse bone marrow cells. *J Cell Biol.* (1994) 124:569–77. doi: 10.1083/jcb.124.4.569
156. Croes M, Öner FC, van Neerven D, Sabir E, Kruyt MC, Blokhuis TJ, et al. Proinflammatory T cells and IL-17 stimulate osteoblast differentiation. *Bone.* (2016) 84:262–70. doi: 10.1016/j.bone.2016.01.010
157. Duque G, Huang DC, Macoritto M, Rivas D, Yang XF, Ste-Marie LG, et al. Autocrine regulation of interferon γ in mesenchymal stem cells plays a role in early osteoblastogenesis. *Stem Cells.* (2009) 27:550–8. doi: 10.1634/stemcells.2008-0886
158. Postiglione L, Di Domenico G, Montagnani S, Di Spigna G, Salzano S, Castaldo C, et al. Granulocyte-macrophage colony-stimulating factor (GM-CSF) induces the osteoblastic differentiation of the human osteosarcoma cell line SaOS-2. *Calcified Tissue Int.* (2003) 72:85–97. doi: 10.1007/s00223-001-2088-5
159. Liu Y, Wang L, Kikuiri T, Akiyama K, Chen C, Xu X, et al. Mesenchymal stem cell-based tissue regeneration is governed by recipient T lymphocytes via IFN-γ and TNF-α. *Nat Med.* (2011) 17:1594–601.
160. Kim YG, Park JW, Lee JM, Suh JY, Lee JK, Chang BS, et al. IL-17 inhibits osteoblast differentiation and bone regeneration in rat. *Arch Oral Biol.* (2014) 59:897–905. doi: 10.1016/j.archoralbio.2014.05.009
161. Hughes JE, Srinivasan S, Lynch KR, Proia RL, Ferdek P, Hedrick CC. Sphingosine-1-phosphate induces an antiinflammatory phenotype in macrophages. *Circul Res.* (2008) 102:950–8. doi: 10.1161/CIRCRESAHA.107.170779
162. Dorsam G, Graeler MH, Seroogy C, Kong Y, Voice JK, Goetzl EJ. Transduction of multiple effects of sphingosine 1-phosphate (S1P) on T cell functions by the S1P1 G protein-coupled receptor. *J Immunol.* (2003) 171:3500–7. doi: 10.4049/jimmunol.171.7.3500
163. Wang W, Huang MC, Goetzl EJ. Type 1 sphingosine 1-phosphate G protein-coupled receptor (S1P1) mediation of enhanced IL-4 generation by CD4 T cells from S1P1 transgenic mice. *J Immunol.* (2007) 178:4885–90. doi: 10.4049/jimmunol.178.8.4885
164. Huang MC, Watson SR, Liao JJ, Goetzl EJ. Th17 augmentation in OTII TCR plus T cell-selective type 1 sphingosine 1-phosphate receptor double transgenic mice. *J Immunol.* (2007) 178:6806–13. doi: 10.4049/jimmunol.178.11.6806
165. Liao JJ, Huang MC, Goetzl EJ. Cutting edge: alternative signaling of Th17 cell development by sphingosine 1-phosphate. *J Immunol.* (2007) 178:5425–8. doi: 10.4049/jimmunol.178.9.5425
166. Liu G, Yang K, Burns S, Shrestha S, Chi H. The S1P1-mTOR axis directs the reciprocal differentiation of TH1 and Treg cells. *Nat Immunol.* (2010) 11:1047–56. doi: 10.1038/ni.1939
167. Huang R, Wang X, Zhou Y, Xiao Y. RANKL-induced M1 macrophages are involved in bone formation. *Bone Res.* (2017) 5:17019. doi: 10.1038/boneres.2017.19
168. Loi F, Córdova LA, Zhang R, Pajarinen J, Lin TH, Goodman SB, et al. The effects of immunomodulation by macrophage subsets on osteogenesis *in vitro*. *Stem Cell Res Ther.* (2016) 7:15. doi: 10.1186/s13287-016-0276-5
169. Aggarwal S, Pittenger MF. Human mesenchymal stem cells modulate allogeneic immune cell responses. *Blood.* (2005) 105:1815–22. doi: 10.1182/blood-2004-04-1559

170. Gur-Wahnon D, Borovsky Z, Beyth S, Liebergall M, Rachmilewitz J. Contact-dependent induction of regulatory antigen-presenting cells by human mesenchymal stem cells is mediated via STAT3 signaling. *Exp Hematol.* (2007) 35:426–33. doi: 10.1016/j.exphem.2006.11.001
171. Németh K, Leelahavanichkul A, Yuen PS, Mayer B, Parmelee A, Doi K, et al. Bone marrow stromal cells attenuate sepsis via prostaglandin E2–dependent reprogramming of host macrophages to increase their interleukin-10 production. *Nat Med.* (2009) 15:42–9. doi: 10.1038/nm.1905
172. Fibbe WE, Nauta AJ, Roelofs H. Modulation of immune responses by mesenchymal stem cells. *Annals N Y Acad Sci.* (2007) 1106:272–8. doi: 10.1196/annals.1392.025
173. Bunnell BA, Betancourt AM, Sullivan DE. New concepts on the immune modulation mediated by mesenchymal stem cells. *Stem Cell Res Ther.* (2010) 1:34. doi: 10.1186/scrt34
174. Augello A, Tasso R, Negrini SM, Amateis A, Indiveri F, Cancedda R, et al. Bone marrow mesenchymal progenitor cells inhibit lymphocyte proliferation by activation of the programmed death 1 pathway. *Eur J Immunol.* (2005) 35:1482–90. doi: 10.1002/eji.200425405
175. Auletta JJ, Deans RJ, Bartholomew AM. Emerging roles for multipotent, bone marrow–derived stromal cells in host defense. *Blood.* (2012) 119:1801–9. doi: 10.1182/blood-2011-10-384354
176. Bianco P, Robey PG, Simmons PJ. Mesenchymal stem cells: revisiting history, concepts, and assays. *Cell Stem Cell.* (2008) 2:313–9. doi: 10.1016/j.stem.2008.03.002
177. Chen K, Wang D, Du WT, Han ZB, Ren H, Chi Y, et al. Human umbilical cord mesenchymal stem cells hUC-MSCs exert immunosuppressive activities through a PGE 2-dependent mechanism. *Clin Immunol.* (2010) 135:448–58. doi: 10.1016/j.clim.2010.01.015
178. Maggini J, Mirkin G, Bognanni I, Holmberg J, Piazzón IM, Nepomnaschy I, et al. Mouse bone marrow-derived mesenchymal stromal cells turn activated macrophages into a regulatory-like profile. *PLoS ONE.* (2010) 5:e9252. doi: 10.1371/journal.pone.0009252
179. MacKenzie KF, Clark K, Naqvi S, McGuire VA, Nöehren G, Kristariyanto Y, et al. PGE2 induces macrophage IL-10 production and a regulatory-like phenotype via a protein kinase A–SIK–CRTC3 pathway. *J Immunol.* (2013) 190:565–77. doi: 10.4049/jimmunol.1202462
180. Chyun YS, Raisz LG. Stimulation of bone formation by prostaglandin E2. *Prostaglandins.* (1984) 27:97–103. doi: 10.1016/0090-6980(84)90223-5
181. Raicevic G, Rouas R, Najar M, Stordeur P, Boufker HI, Bron D, et al. Inflammation modifies the pattern and the function of Toll-like receptors expressed by human mesenchymal stromal cells. *Hum Immunol.* (2010) 71:235–44. doi: 10.1016/j.humimm.2009.12.005
182. Waterman RS, Tomchuck SL, Henkle SL, Betancourt AM. A new mesenchymal stem cell (MSC) paradigm: polarization into a pro-inflammatory MSC1 or an Immunosuppressive MSC2 phenotype. *PLoS ONE.* (2010) 5:e10088. doi: 10.1371/journal.pone.0010088
183. Verreck FA, de Boer T, Langenberg DM, van der Zanden L, Ottenhoff TH. Phenotypic and functional profiling of human proinflammatory type-1 and anti-inflammatory type-2 macrophages in response to microbial antigens and IFN-γ-and CD40L-mediated costimulation. *J Leukocyte Biol.* (2006) 79:285–93. doi: 10.1189/jlb.0105015
184. Xiao L, Zhou Y, Zhu L, Yang S, Huang R, Shi W, et al. SPHK1-S1PR1-RANKL axis regulates the interactions between macrophages and BMSCs in inflammatory bone loss. *J Bone Miner Res.* (2018) 3:1090–104. doi: 10.1002/jbmr.3396
185. Rivera J, Proia RL, Olivera A. The alliance of sphingosine-1-phosphate and its receptors in immunity. *Nat Rev Immunol.* (2008) 8:753–63. doi: 10.1038/nri2400
186. Wang F, Van Brocklyn JR, Hobson JP, Movafagh S, Zukowska-Grojec Z, Milstien S, et al. Sphingosine 1-phosphate stimulates cell migration through a Gi-coupled cell surface receptor potential involvement in angiogenesis. *J Biol Chem.* (1999) 274:35343–50. doi: 10.1074/jbc.274.50.35343
187. Schwab SR, Cyster JG. Finding a way out: lymphocyte egress from lymphoid organs. *Nat Immunol.* (2007) 8:1295–301. doi: 10.1038/ni1545
188. Zachariah MA, Cyster JG. Neural crest–derived pericytes promote egress of mature thymocytes at the corticomedullary junction. *Science.* (2010) 328:1129–35. doi: 10.1126/science.1188222
189. Cinamon G, Zachariah MA, Lam OM, Foss FW, Cyster JG. Follicular shuttling of marginal zone B cells facilitates antigen transport. *Nat Immunol.* (2008) 9:54–62. doi: 10.1038/ni1542
190. Jenne CN, Enders A, Rivera R, Watson SR, Bankovich AJ, Pereira JP, et al. T-bet–dependent S1P5 expression in NK cells promotes egress from lymph nodes and bone marrow. *J Exp Med.* (2009) 206:2469–81. doi: 10.1084/jem.20090525
191. Rathinasamy A, Czeloth N, Pabst O, Förster R, Bernhardt G. The origin and maturity of dendritic cells determine the pattern of sphingosine 1-phosphate receptors expressed and required for efficient migration. *J Immunol.* (2010) 185:4072–81. doi: 10.4049/jimmunol.1000568
192. König K, Diehl L, Rommerscheidt-Fuss U, Golletz C, Quast T, Kahl P, et al. Four-and-a-half LIM domain protein 2 is a novel regulator of sphingosine 1-phosphate receptor 1 in CCL19-induced dendritic cell migration. *J Immunol.* (2010) 185:1466–75. doi: 10.4049/jimmunol.0903449
193. Jolly PS, Bektas M, Olivera A, Gonzalez-Espinosa C, Proia RL, Rivera J, et al. Transactivation of sphingosine-1–phosphate receptors by FcεRI triggering is required for normal mast cell degranulation and chemotaxis. *J Exp Med.* (2004) 199:959–70. doi: 10.1084/jem.20030680
194. Zhang L, Orban M, Lorenz M, Barocke V, Braun D, Urtz N, et al. A novel role of sphingosine 1-phosphate receptor S1pr1 in mouse thrombopoiesis. *J Exp Med.* (2012) 209:2165–81. doi: 10.1084/jem.20121090
195. Allende ML, Tuymetova G, Lee BG, Bonifacino E, Wu YP, Proia RL. S1P1 receptor directs the release of immature B cells from bone marrow into blood. *J Exp\ Med.* (2010) 207:1113–24. doi: 10.1084/jem.20092210
196. Sinha RK, Park C, Hwang IY, Davis MD, Kehrl JH. B lymphocytes exit lymph nodes through cortical lymphatic sinusoids by a mechanism independent of sphingosine-1-phosphate-mediated chemotaxis. *Immunity.* (2009) 30:434–46. doi: 10.1016/j.immuni.2008.12.018
197. Czeloth N, Schippers A, Wagner N, Müller W, Küster B, Bernhardt G, et al. Sphingosine-1 phosphate signaling regulates positioning of dendritic cells within the spleen. *J Immunol.* (2007) 179:5855–63. doi: 10.4049/jimmunol.179.9.5855
198. Maeda Y, Matsuyuki H, Shimano K, Kataoka H, Sugahara K, Chiba K. Migration of CD4 T cells and dendritic cells toward sphingosine 1-phosphate (S1P) is mediated by different receptor subtypes: S1P regulates the functions of murine mature dendritic cells via S1P receptor type *J Immunol.* (2007) 178:3437–46. doi: 10.4049/jimmunol.178.6.3437
199. Gräler MH, Huang MC, Watson S, Goetzl EJ. Immunological effects of transgenic constitutive expression of the type 1 sphingosine 1-phosphate receptor by mouse lymphocytes. *J Immunol.* (2005) 174:1997–2003. doi: 10.4049/jimmunol.174.4.1997
200. Song J, Matsuda C, Kai Y, Nishida T, Nakajima K, Mizushima T, et al. A novel sphingosine 1-phosphate receptor agonist, 2-amino-2-propanediol hydrochloride (KRP-203), regulates chronic colitis in interleukin-10 gene-deficient mice. *J Pharmacol Exp Therapeut.* (2008) 324:276–83. doi: 10.1124/jpet.106.119172
201. Sato K, Suematsu A, Okamoto K, Yamaguchi A, Morishita Y, Kadono Y, et al. Th17 functions as an osteoclastogenic helper T cell subset that links T cell activation and bone destruction. *J Exp Med.* (2006) 203:2673–82. doi: 10.1084/jem.20061775
202. Liu G, Burns S, Huang G, Boyd K, Proia RL, Flavell RA, et al. The receptor S1P1 overrides regulatory T cell–mediated immune suppression through Akt-mTOR. *Nat Immunol.* (2009) 10:769–77. doi: 10.1038/ni.1743
203. Takeshita H, Kitano M, Iwasaki T, Kitano S, Tsunemi S, Sato C, et al. Sphingosine 1-phosphate (S1P)/S1P receptor 1 signaling regulates receptor activator of NF-κB ligand (RANKL) expression in rheumatoid arthritis. *Biochem Biophys Res Commun.* (2012) 419:154–9. doi: 10.1016/j.bbrc.2012.01.103
204. Barra G, Lepore A, Gagliardi M, Somma D, Matarazzo MR, Costabile F, et al. Sphingosine Kinases promote IL-17 expression in human T lymphocytes. *Sci Rep.* (2018) 8:13233. doi: 10.1038/s41598-018-31666-1
205. Choi JW, Gardell SE, Herr DR, Rivera R, Lee CW, Noguchi K, et al. FTY720 (fingolimod) efficacy in an animal model of multiple sclerosis requires astrocyte sphingosine 1-phosphate receptor 1 (S1P1) modulation. *Proc Natl Acad Sci USA.* (2011) 108:751–6. doi: 10.1073/pnas.1014154108
206. Kitano M, Hla T, Sekiguchi M, Kawahito Y, Yoshimura R, Miyazawa K, et al. Sphingosine 1-phosphate/sphingosine 1-phosphate receptor

1 signaling in rheumatoid synovium: Regulation of synovial proliferation and inflammatory gene expression. *Arthr Rheum.* (2006) 54:742–53. doi: 10.1002/art.21668
207. Ogretmen B. Sphingolipid metabolism in cancer signalling and therapy. *Nat Rev Cancer.* (2018) 18:33–50. doi: 10.1038/nrc.2017.96
208. Baker DA, Barth J, Chang R, Obeid LM, Gilkeson GS. Genetic sphingosine kinase 1 deficiency significantly decreases synovial inflammation and joint erosions in murine TNF-α-induced arthritis. *J Immunol.* (2010) 185:2570–9. doi: 10.4049/jimmunol.1000644
209. Kappos L, Antel J, Comi G, Montalban X, O'Connor P, Polman CH, et al. Oral fingolimod (FTY720) for relapsing multiple sclerosis. *N Engl J Med.* (2006) 355:1124–40. doi: 10.1056/NEJMoa052643
210. Sanchez T, Estrada-Hernandez T, Paik JH, Wu MT, Venkataraman K, Brinkmann V, et al. Phosphorylation and action of the immunomodulator FTY720 inhibits vascular endothelial cell growth factor-induced vascular permeability. *J Biol Chem.* (2003) 278:47281–90. doi: 10.1074/jbc.M306896200
211. Kharel Y, Lee S, Snyder AH, Sheasley-O'Neill SL, Morris MA, Setiady Y, et al. Sphingosine kinase 2 is required for modulation of lymphocyte traffic by FTY. *J Biol Chem.* (2005) 280:36865–72. doi: 10.1074/jbc.M506293200
212. Liu CH, Thangada S, Lee MJ, Van Brocklyn JR, Spiegel S, Hla T. Ligand-induced trafficking of the sphingosine-1-phosphate receptor EDG. *Molecul Biol Cell.* (1999) 10:1179–90. doi: 10.1091/mbc.10.4.1179
213. Gräler MH, Goetzl EJ. The immunosuppressant FTY720 down-regulates sphingosine 1-phosphate G-protein-coupled receptors. *FASEB J.* (2004) 18:551–3. doi: 10.1096/fj.03-0910fje
214. Jo E, Sanna MG, Gonzalez-Cabrera PJ, Thangada S, Tigyi G, Osborne DA, et al. S1P 1-selective in vivo-active agonists from high-throughput screening: off-the-shelf chemical probes of receptor interactions, signaling, and fate. *Chem Biol.* (2005) 12:703–15. doi: 10.1016/j.chembiol.2005.04.019
215. Oo ML, Thangada S, Wu MT, Liu CH, Macdonald TL, Lynch KR, et al. Immunosuppressive and anti-angiogenic sphingosine 1-phosphate receptor-1 agonists induce ubiquitinylation and proteasomal degradation of the receptor. *J Biol Chem/.* (2007) 282:9082–9. doi: 10.1074/jbc.M610318200
216. Oo ML, Chang SH, Thangada S, Wu MT, Rezaul K, Blaho V, et al. Engagement of S1P1-degradative mechanisms leads to vascular leak in mice. *J Clin Invest.* (2011) 121:2290–300. doi: 10.1172/JCI45403
217. Gonzalez-Cabrera PJ, Hla T, Rosen H. Mapping pathways downstream of sphingosine 1-phosphate subtype 1 by differential chemical perturbation and proteomics. *J Biol Chem.* (2007) 282:7254–64. doi: 10.1074/jbc.M610581200
218. Dyckman AJ. Modulators of Sphingosine-1-phosphate pathway biology: recent advances of sphingosine-1-phosphate Receptor 1 (S1P1) agonists and future perspectives. *J Med Chem.* (2017) 60:5267–89. doi: 10.1021/acs.jmedchem.6b01575
219. Tsunemi S, Iwasaki T, Kitano S, Imado T, Miyazawa K, Sano H. Effects of the novel immunosuppressant FTY720 in a murine rheumatoid arthritis model. *Clin Immunol.* (2010) 136:197–204. doi: 10.1016/j.clim.2010.03.428
220. Matsuura M, Imayoshi T, Okumoto T. Effect of FTY720, a novel immunosuppressant, on adjuvant- and collagen-induced arthritis in rats. *Int J Immunopharmacol.* (2000) 22:323–31. doi: 10.1016/S0192-0561(99)00088-0
221. Han YP, Li X, Zhou QY, Jie HY, Lao XB, Han JC, et al. FTY720 Abrogates collagen-induced arthritis by hindering dendritic cell migration to local lymph nodes. *J Immunol.* (2015) 195:4126–35. doi: 10.4049/jimmunol.1401842
222. Miller DC, Whittington KB, Brand DD, Hasty KA, Rosloniec EF. The CII-specific autoimmune T-cell response develops in the presence of FTY720 but is regulated by enhanced Treg cells that inhibit the development of autoimmune arthritis. *Arthrit Res Ther.* (2016) 18:ARTN8. doi: 10.1186/s13075-015-0909-6
223. Bagdanoff JT, Donoviel MS, Nouraldeen A, Carlsen M, Jessop TC, Tarver J, et al. Inhibition of Sphingosine 1-Phosphate Lyase for the treatment of rheumatoid arthritis: discovery of (E)-1-(4((1R,2S,3R)-1,2,3,4-Tetrahydroxybutyl)-1H-imidazol-2-yl)ethanone Oxime (LX2931) and (1R,2S,3R)-1-(2-(Isoxazol-3-yl)-1H-imidazol-4-yl)butane-1,2,3,4-tetraol (LX2932). *J Med Chem.* (2010) 53:8650–62. doi: 10.1021/jm101183p
224. Dougados M, Baeten D. Spondyloarthritis. *Lancet.* (2011) 377:2127–37. doi: 10.1016/S0140-6736(11)60071-8
225. Yu H, Sun C, Argraves K. Periodontal inflammation and alveolar bone loss induced by Aggregatibacter actinomycetemcomitans is attenuated in sphingosine kinase 1-deficient mice. *J Periodontal Res.* (2016) 51:38–49. doi: 10.1111/jre.12276
226. Xiao L, Zhu L, Yang S, Lei D, Xiao Y, Peng B. Different correlation of sphingosine-1-phosphate receptor 1 with receptor activator of nuclear factor Kappa B ligand and regulatory T cells in rat periapical lesions. *J Endodont.* (2015) 41:479–86. doi: 10.1016/j.joen.2014.10.010
227. Byles V, Covarrubias AJ, Ben-Sahra I, Lamming DW, Sabatini DM, Manning, BD, et al. The TSC-mTOR pathway regulates macrophage polarization. *Nat Commun.* (2013) 4:2834. doi: 10.1038/ncomms3834
228. Gulen MF, Kang Z, Bulek K, Youzhong W, Kim TW, Chen Y, et al. The receptor SIGIRR suppresses Th17 cell proliferation via inhibition of the interleukin-1 receptor pathway and mTOR kinase activation. *Immunity.* (2010) 32:54–66. doi: 10.1016/j.immuni.2009.12.003
229. Zhu L, Yang T, Li L, Sun L, Hou Y, Hu X, et al. TSC1 controls macrophage polarization to prevent inflammatory disease. *Nat Commun.* (2014) 5:4696. doi: 10.1038/ncomms5696
230. Shao J, Zhou Y, Xiao Y. The regulatory roles of Notch in osteocyte differentiation via the crosstalk with canonical Wnt pathways during the transition of osteoblasts to osteocytes. *Bone.* (2018) 108:165–78. doi: 10.1016/j.bone.2018.01.010
231. Chen J, Long F. mTORC1 signaling promotes osteoblast differentiation from preosteoblasts. *PLoS ONE.* (2015) 10:e0130627. doi: 10.1371/journal.pone.0130627
232. Fitter S, Matthews MP, Martin SK, Xie J, Ooi SS, Walkley CR, et al. mTORC1 plays an important role in skeletal development by controlling preosteoblast differentiation. *Mol Cell Biol.* (2017) 37:e00668–16. doi: 10.1128/MCB.00668-16
233. Chen J, Long F. mTOR signaling in skeletal development and disease. *Bone Res.* (2018) 6:1. doi: 10.1038/s41413-017-0004-5
234. Nollet M, Santucci-Darmanin S, Breuil V, Al-Sahlanee R, Cros C, Topi M, et al. Autophagy in osteoblasts is involved in mineralization and bone homeostasis. *Autophagy.* (2014) 10:1965–77. doi: 10.4161/auto.36182
235. Ravikumar B, Vacher C, Berger Z, Davies JE, Luo S, Oroz LG, et al. Inhibition of mTOR induces autophagy and reduces toxicity of polyglutamine expansions in fly and mouse models of Huntington disease. *Nat Genet.* (2004) 36:585–95. doi: 10.1038/ng1362
236. Ching JK, Weihl CC. Rapamycin-induced autophagy aggravates pathology and weakness in a mouse model of VCP-associated myopathy. *Autophagy.* (2013) 9:799–800. doi: 10.4161/auto.23958
237. Kim J, Kundu M, Viollet B, Guan KL. AMPK and mTOR regulate autophagy through direct phosphorylation of Ulk. *Nat Cell Biol.* (2011) 13:132–41. doi: 10.1038/ncb2152
238. Noda T, Ohsumi Y. Tor, a phosphatidylinositol kinase homologue, controls autophagy in yeast. *J Biol Chem.* (1998) 273:3963–6. doi: 10.1074/jbc.273.7.3963
239. Schmelzle T, Hall MN. TOR, a central controller of cell growth. *Cell.* (2000) 103:253–62. doi: 10.1016/S0092-8674(00)00117-3
240. Xiao L. *Dissecting the Role of Sphingosine 1-Phosphate-Sphingosine 1-Phosphate Receptor 1 in Inflammatory Bone Remodelling.* Brisbane: Queensland University of Technology (2017).

Conflict of Interest Statement: The authors declare that the research was conducted in the absence of any commercial or financial relationships that could be construed as a potential conflict of interest.

frontiers in Immunology

REVIEW
published: 03 July 2019
doi: 10.3389/fimmu.2019.01483

How Autoantibodies Regulate Osteoclast Induced Bone Loss in Rheumatoid Arthritis

Ulrike Steffen[†], *Georg Schett*[*‡] *and Aline Bozec*[*‡]

Department of Internal Medicine 3, University of Erlangen-Nuremberg, Erlangen, Germany

Rheumatoid arthritis (RA) is a chronic inflammatory disease, characterized by autoimmunity that triggers joint inflammation and tissue destruction. Traditional concepts of RA pathogenesis have strongly been focused on inflammation. However, more recent evidence suggests that autoimmunity *per se* modulates the disease and in particular bone destruction during the course of RA. RA-associated bone loss is caused by increased osteoclast differentiation and activity leading to rapid bone resorption. Autoimmunity in RA is based on autoantibodies such as rheumatoid factor (RF) and autoantibodies against citrullinated proteins (ACPA). These autoantibodies exert effector functions on immune cells and on bone resorbing osteoclasts, thereby facilitating bone loss. This review summarizes potential pathways involved in increased destruction of bone tissue in RA, particularly focusing on the direct and indirect actions of autoantibodies on osteoclast generation and function.

Keywords: rheumatoid factor (RF), autoantibodies against citrullinated proteins (ACPA), osteoclasts, rheumatoid arthritis, cytokines

OPEN ACCESS

Edited by:
Claudine Blin-Wakkach, UMR7370 Laboratoire de Physio Médecine Moléculaire (LP2M), France

Reviewed by:
Diane Van Der Woude, Leiden University Medical Center, Netherlands
Hannie Westra, University of Groningen, Netherlands

***Correspondence:**
Georg Schett
georg.schett@uk-erlangen.de
Aline Bozec
aline.bozec@uk-erlangen.de

[†]*Former name: Ulrike Harre*

[‡]*These authors have contributed equally to this work*

Specialty section:
This article was submitted to Inflammation, a section of the journal Frontiers in Immunology

Received: *27 January 2019*
Accepted: *13 June 2019*
Published: *03 July 2019*

Citation:
Steffen U, Schett G and Bozec A (2019) How Autoantibodies Regulate Osteoclast Induced Bone Loss in Rheumatoid Arthritis. Front. Immunol. 10:1483. doi: 10.3389/fimmu.2019.01483

INTRODUCTION

Skeletal homeostasis is maintained by continuous removal and replacement of bone throughout life. This process is controlled by the coordinated activity of specific bone cells. Osteoclasts are highly specialized multinucleated cells derived from hematopoietic precursors of the myeloid lineage with the capacity to resorb bone [reviewed in Tanaka et al. (1)]. Osteoclast formation is controlled by the action of soluble mediators, such as receptor activator of nuclear factor-κB ligand (RANKL; also known as TNFSF11), macrophage colony-stimulating factor 1 (M-CSF), and negative regulators, such as the decoy receptor for RANKL, osteoprotegerin (OPG). These cytokines are provided by cells of the osteoblast lineage and immune cells located within the bone microenvironment [reviewed in Schett (2)]. Bone resorption also liberates growth factors deposited in bone, which can act locally on osteoblasts and immune cells.

In parallel to osteoclast-mediated bone resorption, bone formation results from the proliferation of skeletal stem cells and their differentiation into osteoblast. Their fate is to either stay as bone lining cells or to be embedded into the bone matrix as osteocytes [reviewed in Bonewald (3)]. The osteoblast cell lineage includes osteoblast precursors, bone lining cells and osteocytes. Each of them express specific signals that regulate resident cells within the bone marrow. In addition to the crosstalk between different types of bone cells, there is a tight interaction between bone and immune cells, which is still not fully characterized. The importance of this interaction is reflected by diseases, such as rheumatoid arthritis (RA), in which immune activation is linked to bone loss.

RA is a chronic systemic autoimmune disease affecting about 1% of the population worldwide [reviewed in McInnes and Schett (4)]. It is associated with pain, joint swelling, progressive disability and systemic comorbidity. One of the major consequences of RA is the degradation of cartilage and bone tissue. This process results in joint destruction, which leads to significant loss of life quality for the patients. RA-associated bone loss is characterized by three different manifestations: (i) local erosions in the inflamed joints, where bone and cartilage are in direct contact with the inflamed synovium, (ii) periarticular bone loss of trabecular and cortical bone close to sites of inflammation, and (iii) systemic osteopenia and osteoporosis [reviewed in Zerbini et al. (5)]. All three forms of bone loss are caused by altered bone homeostasis with increased osteoclast generation and activity resulting in accelerated bone resorption, while osteoblast-mediated bone formation is suppressed. The reasons for enhanced osteoclast activity have been in the focus of extensive research. Aside from direct inter-cellular interactions and systemic effects of inflammatory cytokines, autoantibodies have been found to play a major role both via directly influencing osteoclasts, as well as, through the induction of inflammatory cytokines released by macrophages.

In this review, we will summarize the current knowledge on autoantibody-mediated bone loss in RA. We will focus on the direct effects of autoantibodies on osteoclasts and pre-osteoclasts as well as indirect effects via cytokines released by activated macrophages. In addition, we will discuss the implications of antibody glycosylation.

THE REGULATION OF OSTEOCLAST ACTIVITY AND DIFFERENTIATION BY AUTOANTIBODIES

Autoantibodies in RA

Although the causes of RA are diverse and not completely understood, it is clear that disease specific autoantibodies constitute an important trigger. The main autoantibodies associated with RA are the rheumatoid factor (RF) and autoantibodies against citrullinated proteins (ACPA). RF is directed against the Fc part of IgG and mainly occurs as IgM. However, to a smaller extent, RF can also be detected as IgG or IgA. Up to 70% of RA patients are RF positive. Of note, RF is also found in a subset of healthy people, especially in the elderly, in patients with other rheumatic diseases (e.g., Sjögren's syndrome or systemic lupus erythematosus) or in patients with viral infections like hepatitis C (6, 7). Although RF is positively associated with increased bone erosion, especially in ACPA positive patients (8, 9), there are no data available about its direct effects on cytokine production or osteoclastogenesis. As RF is directed against IgG, it might lead to a constant basal inflammation by the formation of random IgG complexes or enhance the size of existing immune complexes formed by other autoantibodies. Indeed, the addition of monoclonal IgM-RF increased the production of the pro-inflammatory cytokine TNF-α by macrophages after treatment with ACPA-containing IgG from RA patients (10), suggesting a synergistic interaction of ACPA and RF.

In contrast to RF, ACPA are highly specific for RA with a very low prevalence in healthy people (11, 12). ACPA provide diagnostic value in predicting disease severity and the likelihood to develop bone erosions in RA patients (13). ACPA are detectable up to 10 years before clinical onset of RA (14). Some months before the occurrence of clinical symptoms, ACPA broaden their epitope recognition and isotype usage profile and change their glycosylation toward a more inflammatory phenotype (14–16). In 2010, ACPA have been included into the diagnostic criteria for RA by the American College of Rheumatology (ACR) and European League Against Rheumatism (EULAR) (17). ACPA recognize a variety of citrullinated proteins with citrullinated vimentin, α-enolase, fibrinogen and collagen being the most prominent antigens. Citrullination is a post-translational modification of a positively charged arginine residue into a partially negatively charged citrulline residue. As this process changes the net charge of a protein, neo epitopes appear, that can be recognized by the immune system resulting in autoantibody formation. Citrullination is performed by enzymes of the peptidylarginine deiminase (PAD) family and occuring physiologically during the formation of neutrophil extracellular traps (NETs), apoptosis and skin keratinization [reviewed in Baka et al. (18)]. In addition, the bacterium *Porphyromonas gingivalis* (which is involved in periodontitis) releases PAD (19). Bacterial PAD is suspected to contribute to protein citrullination and ACPA formation, but more research is needed to truly confirm a relationship between periodontitis and RA [reviewed in Araujo et al. (20) and Potempa et al. (21)]. Another trigger of citrullination, especially in the lung, is smoking [reviewed in Klareskog et al. (22)].

Apart from ACPA, a couple of other autoantibodies against posttranslational modifications (AMPA) have been found in the last years, such as autoantibodies against carbamylated proteins (anti-CarP) (23) or autoantibodies against acetylated proteins (24). All groups of autoantibodies can be detected independently of each other in patients with RA. According to a meta-analysis evaluating 25 studies, ACPA are present in 47–88% of RA patients (13). Anti-CarP could be detected in 39–58% of RA patients and in 8–16% of RA patients that are ACPA negative (23, 25, 26), but also in about 7% of osteoarthritis patients and 3,6% of healthy controls (11).

Epidemiological Evidence for Autoantibody-Mediated Bone Loss in RA

Bone loss is strongly associated with ACPA positivity in RA patients (27–29). Higher ACPA titers correlate with increased systemic osteopenia, indicating that ACPA might contribute to bone loss, either directly or via increased systemic inflammation. In the last years, several studies tried to disentangle direct ACPA-mediated effects from inflammation with inconclusive results. Llorente et al. described that the presence of ACPA was associated with baseline bone mass independently of disease activity in a cohort of early RA patients (30), suggesting direct effects of ACPA on the bone. This was further confirmed by studies describing that ACPA positive individuals without clinical signs of RA

display signs of bone loss in metacarpal joints (31, 32). However, subclinical inflammation can't be fully excluded in these studies. Ten Brinck et al. reported that ACPA positive RA patients only exhibited bone resorption in the presence of local inflammation (33). However, general inflammation alone seems insufficient to induce bone loss, since patients with ACPA positive RA displayed the most severe form of bone loss when compared to patients suffering from other inflammatory diseases like seronegative RA, psoriatic arthritis or inflammatory bowel disease (34). These studies indicate that an interplay of direct and indirect effects of ACPA on bone homeostasis leads to local and systemic bone loss. We will discuss the mechanisms by which ACPA affect bone later in this review.

Like ACPA, anti-CarP are associated with higher disease severity and increased bone erosion (23, 26, 35), but more research is needed to elucidate its underlying mechanisms. The fact that ACPA fine specificity does not seem to correlate with disease progression and bone erosion (36, 37) strongly suggests common mechanisms for all AMPA to mediate bone loss, most likely via the conserved Fc part of IgG.

FcγR Signaling in Immune Cells and in Osteoclasts

Humans possess five classical FcγR: FcγRI, FcγRIIA, FcγRIIB FcγRIIIA, and FcγRIIIB that differ in their IgG binding capacity and downstream signaling pathways [reviewed in Nimmerjahn and Ravetch (38), Ghazizadeh (39), Nimmerjahn and Ravetch (40), and Ono (41)]. FcγRI is the only known high-affinity FcγR that is able to bind uncomplexed IgG while all other FcγR need the crosslinking effects of immune complexes to become activated. Activation of FcγRI, FcγRIIA and FcγRIIIA results in the phosphorylation of either an intrinsic immunoreceptor tyrosine-based activation motif (ITAM) domain (as for FcγRIIA) or an ITAM domain supplied by accessory proteins, typically the Fc-receptor common γ-chain (FcRγ-chain) (**Figure 1A**). This phosphorylation leads to the recruitment and activation of spleen tyrosine kinase (Syk) and its downstream targets. The most important events after FcγR activation are calcium influx and the engagement of the rat sarcoma (RAS)- rapidly accelerated fibrosarcoma (RAF)- mitogen-activated protein kinase (MAPK) pathway, resulting in antigen uptake, phagocytosis, cellular activation, and the release of pro-inflammatory cytokines by immune cells. Activating FcγRs have one potent inhibitory opponent: FcγRIIB, which contains an intrinsic immunoreceptor tyrosine-based inhibition motif (ITIM) domain. The ITIM domain interferes with ITAM signaling through engagement of src homology 2-containing inositol phosphatase (SHIP) or src homology 2 domain-containing protein tyrosine phosphatases (SHPs) that inhibit calcium influx by hydrolyzing phosphoinositide intermediates. FcγRIIIB, expressed on neutrophils, has a glycosylphosphatidylinositol (GPI) anchor without a signaling domain (44). The mechanisms by which FcγRIIIB transduces signals are still unknown.

Osteoclasts belong to the myeloid cell lineage and share many features with macrophages. Like macrophages, osteoclasts and their precursors express FcγR (45–47) with FcγRI, FcγRIIB and FcγRIIIA being significantly upregulated during human *ex vivo* osteoclastogenesis (46). It is not clear whether FcγR possess a role in bone homeostasis. However, activation of FcγR with crosslinked antibodies enhanced osteoclastogenesis from murine bone marrow cells (47). This suggests that FcγR regulate osteoclast activity and bone resorption. Of

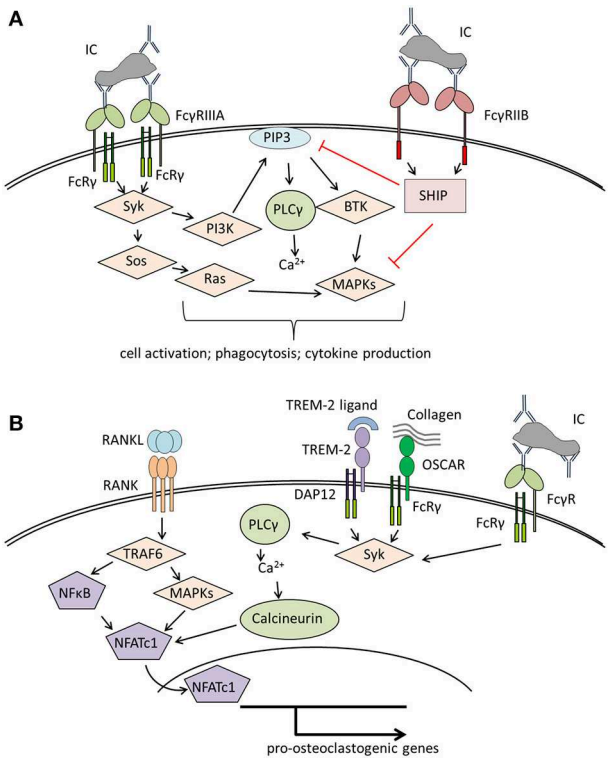

FIGURE 1 | Overview of signaling pathways of **(A)** Fcγ receptors (FcγRs) on immune cells and **(B)** co-stimulatory molecules involved in osteoclastogenesis. **(A)** Crosslinking of activating FcγR (here FcγRIIIA) results in Syk activation starting various signaling pathways that lead to immune cell activation and effector functions like phagocytosis or cytokine production. The distinct signaling pathways have been reviewed in detail in Nimmerjahn and Ravetch (40), Rosales (42). **(B)** Binding of RANKL to RANK leads to the activation of TRAF6, NFκB, and several MAP kinases resulting in the activation of NFATc1, the master transcription factor for pro-osteoclastogenic genes. For a stable NFATc1 activation, costimulatory signals provided by several receptors associated to the accessory molecules DAP12 or FcRγ, like TREM-2 or OSCAR are needed [reviewed in detail in Humphrey and Nakamura (43)]. These receptors lead to Syk activation with subsequent calcium influx enhancing NFATc1 activation. In a similar way, binding of immune complexes to FcγR initiates co-stimulatory signals, thereby enhancing osteoclastogenesis. BTK, Bruton's tyrosin kinase; DAP12, DNAX activation protein of 12kDa; FcRγ, Fc receptor gamma chain; IC, immune complex; MAPKs, mitogen-activated protein kinases; NFATc1, nuclear factor of activated T cells cytoplasmic 1; NFκB, nuclear factor kappa-light-chain-enhancer of activated B cells; OSCAR, Osteoclast-associated immunoglobulin-like receptor; PI3K, phosphatidylinositol-3 kinase; PIP3, phosphatidylinositol 3,4,5-trisphosphate; PLCγ, phospholipase Cγ; SHIP, SH2 domain-containing inositol 5'-phosphatase; Syk, spleen tyrosine kinase; Sos, son of Sevenless; TRAF6, TNF receptor associated factor 6; TREM-2, triggering receptor expressed on myeloid cells 2.

note, osteoclast development is strongly dependent on co-stimulatory signals provided by the accessory protein FcRγ-chain (that is also used by FcγR) and its functional analog DNAX activation protein of 12 kDa (DAP12) (**Figure 1B**). Mice lacking both proteins display a severe osteopetrotic phenotype with impaired osteoclast function (48, 49). FcRγ-chain is likely involved in osteoblast-osteoclast and osteoclast-matrix interactions as it is associated with paired immunoglobulin-like receptor A (PIR-A) and osteoclast-associated receptor (OSCAR) (48, 50). DAP12 associates with TREM-2 and signal-regulatory protein b1 (SIRPb1), which seems to be necessary for the communication between osteoclast precursors (48, 51). Both accessory proteins might enhance the effects of RANKL-signaling by amplifying calcium influx required for the activation of the pro-osteoclastogenic transcription factor, NFATc1 (48).

Direct Actions of ACPA on Osteoclastogenesis

The described positive effects of FcγR signaling on osteoclastogenesis suggest that autoantibodies or autoimmune complexes could directly enhance osteoclast development and hence osteoclast-mediated bone loss in patients with RA. Indeed, we found that affinity-purified autoantibodies against citrullinated vimentin from RA patients, but not ACPA-depleted serum IgG were able to enhance osteoclastogenesis and bone resorption in *ex vivo* osteoclastogenesis assays as well as in recombination activation gene 1 (RAG1)-deficient mice (52). This effect was based on direct binding of autoantibodies to osteoclasts and their precursors resulting in the release of the pro-inflammatory cytokine TNF-α. In later studies, Krishnamurthy and colleagues suggested similar pro-osteoclastogenic effects of ACPA using polyclonal ACPA, purified with a cyclic citrullinated peptide (CCP)-column as well as monoclonal ACPA (53). While the results with polyclonal anti-CCP antibodies confirmed the original findings with polyclonal antibodies against citrullinated vimentin, the monoclonal antibody preparations were later demonstrated to not recognize citrullinated proteins and therefore have to be viewed with caution.

In a murine model of antigen-induced arthritis, immunization against and subsequent challenge with citrullinated vimentin induced stronger periarticular bone loss than immunization against and challenge with methylated bovine serum albumin (mBSA) (54). This effect was independent from inflammation, as mBSA induced more severe synovitis. Similarly, mice immunized with autologous citrullinated type II mouse collagen developed arthritis and bone loss correlating with serum ACPA levels (55).

Together, these studies indicate a direct effect of ACPA on osteoclastogenesis and bone loss. Whether this pro-osteoclastic effect is indeed based on antigen-antibody binding or is preferentially mediated by FcγR remains to be determined.

Impact of Immune Complexes on Osteoclastogenesis

Recently, we found that under certain circumstances not only ACPA, but basically any kind of IgG containing immune complex can increase osteoclast number and bone resorption *in vitro* as well as *in vivo* via binding to FcγR (46, 56). In a murine model of inflammatory arthritis, the osteoclast specific deletion of FcγRIV resulted in a protection from aberrant osteoclast generation and bone erosion in inflamed joints, while inflammation itself was not affected, indicating that inflammatory cytokines alone are not sufficient to induce bone loss in inflammatory arthritis (47). Mice with a global deletion of the inhibitory FcγRIIB exhibit an osteoporotic phenotype even under steady state conditions due to an increase in osteoclast number (57). FcγRIIB is an important regulator of B cells and its deletion leads to a massive induction of autoantibodies (58) that could enhance osteoclastogenesis. Indeed, despite no difference in osteoclast numbers generated *ex vivo* from wildtype and FcγRIIB deficient bone marrow, the addition of sera from FcγRIIB-deficient mice resulted in an increased osteoclastogenesis. This effect could be blocked by IgG depletion or deletion of FcγRIII.

Indirect Effects of Autoantibodies on Osteoclastogenesis by Induction of Proinflammatory Cytokines

In addition to the direct action of autoantibodies on osteoclastogenesis, the release of inflammatory cytokines by macrophages upon autoantibody stimulation has been identified to enhance osteoclast differentiation and function (**Figure 2**). The disequilibrium between pro- and anti-inflammatory cytokine activities facilitates the induction of chronic inflammation and joint damage. It is less known though, how cytokines are organized within a hierarchical regulatory network. Macrophages are considered to play a seminal part in cytokine production in the joints of patients with RA and represent a major source for most of the prominent mediators of disease, such as tumor necrosis factor (TNF)-α and interleukin (IL)-6, but also other cytokines and chemokines involved in the disease process, such as IL-1β, IL-8, and chemokine (C-C motif) ligand 2 (CCL2) (59).

Autoantibodies and their immune complexes may play a central role in shaping a pro-inflammatory environment. Indeed, complexes of ACPA and RF induce robust cytokine production from human macrophages (60–62). This effect is mediated by FcγR signaling on macrophages inducing a strong activation signal for cytokine release (63). In particular, macrophages pre-exposed to M-CSF are sensitive to immune complex-mediated cytokine production. In the synovial membrane of RA patients, M-CSF is present in large amounts (64). We recently showed that treatment of human monocytes with ACPA antibodies or RF leads to the production of the cytokines TNF-α, IL-1β, IL-6, and IL-8 (65). This induction of pro-inflammatory cytokines can enhance osteoclast differentiation (**Figure 2**).

TNF-α is among the most potent cytokines to stimulate osteoclastogenesis. On one hand, TNF-α can induce TRAP positive cells in the absence of RANKL through the induction of the NF-κB pathway (66). On the other hand, TNF-α induces RANK expression by osteoclast precursors (67). In addition, TNF-α and RANKL cooperate to induce osteoclast formation in a TRAF-6 independent pathway through TRAF-3 signaling (68). In addition, TNF-α can indirectly regulate osteoclasts through various stimuli of the stromal cells, for examples by production of RANKL or other cytokines (69).

Like TNF-α, IL-6 is a powerful molecule to induce osteoclast differentiation (70). IL-6 binds the IL-6 receptor, comprising

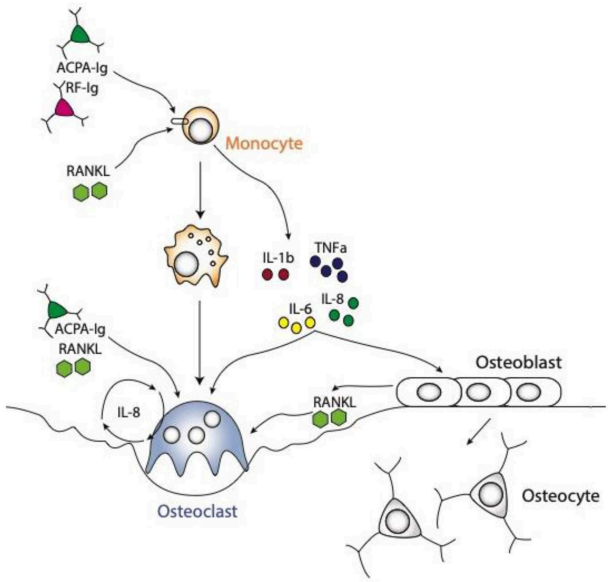

FIGURE 2 | Schematic representations of osteoclast differentiation regulated by ACPA or RF antibodies induced cytokines produced by the monocytic lineages. The cytokines, like TNFa, IL1b, IL6, and IL8 are produced by monocyte lineage challenge with ACPA or RF autoantibodies. All these cytokines are directly able to enhance osteoclast formation. Moreover, they can also regulate stromal cells to secrete RANKL, which in turn will induce osteoclast differentiation. It is also well-known that ACPA can influence IL8 secretion by osteoclasts them-selves which will enhance osteoclastogenesis in an autocrine manner.

the subunit gp130 that is also required for other cytokines. IL-6R induction leads to STAT3 phosphorylation, followed by JAK, which finally induces osteoclast markers (70). Its role is quite contradictory, because one report described that IL-6 inhibits RANKL-induced osteoclastogenesis. It is likely that IL-6 independently regulates different pathways such as NF-κB, ERK or JNK, leading to alternative regulation of osteoclastogenesis (71, 72). In the treatment of human RA, TNF-α, and IL-6 antagonists ameliorate RA equally, indicating that both cytokines are key drivers of synovitis. Of note, the T cell costimulation inhibitor abatacept (cytotoxic T-lymphocyte associated antigen 4 (CTLA4) is most effective in patients with high ACPA and RF autoantibodies (73, 74). Tanaka et al. showed that immune complexes increased CD80/86 expression on monocyte lineages, rendering them sensitive to abatacept (75) which might explain the strong efficacy of abatacept in ACPA positive RA patients. Interestingly, abatacept treatment not only regulates monocytes but also osteoclast differentiation (76).

Implications of Antibody Glycosylation

IgG has one conserved Fc-glycosylation site located at asparagine-297 in the CH2 domain of the heavy chain (**Figure 3**). This glycosylation is critical for the correct conformation of the Fc part and regulates the binding affinity of IgG to FcγR [reviewed in Arnold et al. (77)]. Elimination of the glycan either by enzymatic deglycosylation or by mutation of asparagine-297 to alanine results in a loss of FcγR binding and hence effector functions (78–80). The glycan core structure is strongly conserved and consists of a heptamer of mannose and N-acetyl glucosamine residues. This core structure can be extended by galactose, terminal sialic acid, bisecting N-acetylglucosamine, and core fucose, resulting in a huge variety of theoretically possible glycoforms [reviewed in Zauner et al. (81)]. The exact composition of the Fc glycan determines whether IgG exerts rather pro- or anti-inflammatory effects on immune cells. Especially galactose and terminal sialic acid have been shown to render IgG more anti-inflammatory. 35–45% of random serum IgG from healthy donors is monogalactosylated and 16–27% is bigalactosylated (82). Galactosylation decreases with age (83). During pregnancy, galactosylation is increased and correlates with pregnancy-induced remission of RA (84–86). Only about 10–20% of human serum IgG is sialylated (87, 88), but this low percentage seems to be enough to sustain an anti-inflammatory environment under healthy conditions. It is believed that sialylated IgG actively suppresses immune cells via receptors of the C-type lectin superfamily, such as dendritic cell specific ICAM-grabbing non-integrin (DC-SIGN) (with the murine ortholog SIGNR-1) and the dendritic cell immunoreceptor (DCIR) (89, 90). In addition to Fc glycosylation, about 15–25% of IgG contain Fab glycosylation sites [reviewed in Zauner et al. (81)]. These sites emerge during somatic hypermutation. So far it is unclear if Fab glycosylation has a functional role.

Of note, ACPA display less terminal sialic acid compared to total IgG. ACPA from synovial fluid are even less sialylated (91). The low sialic acid content of ACPA and probably also of other autoantibodies seems to play a key role for the development of clinical disease and bone erosion. In a murine model of collagen induced arthritis, we found that mice fed with sialic acid precursor N-acetylmannosamine did not only display higher sialylation of IgG1, but also have a lower incidence, lower arthritis scores and less bone destruction (46). In addition, it was shown that mice lacking IL-23 do not develop collagen-induced arthritis despite the induction of collagen autoantibodies (92). Autoantibody titers and affinity were not changed compared to wildtype mice, but autoantibodies from IL-23 deficient mice contained more sialic acid. Enzymatic removal of terminal sialic acid resulted in higher arthritis scores, demonstrating the importance of antibody glycosylation for IgG activity. The importance of glycosylation for autoantibody-mediated bone loss is further demonstrated by the fact that even pooled serum IgG from healthy donors is able to enhance osteoclastogenesis and bone resorption after complexation and enzymatic removal of sialic acid (46).

So far it is not completely understood how antibody glycosylation is regulated. The IL-23-T_H17 axis seems to play a crucial role in autoantibody sialylation by the regulation of the enzyme ST6 beta-galactoside α-2,6-sialyltransferase 1 (St6Gal1) that attaches sialic acid to terminal galactose residues (92). Also estrogen positively regulates St6Gal1 expression and postmenopausal women with RA receiving hormone replacement therapy displayed significantly increased Fc sialylation of IgG (93).

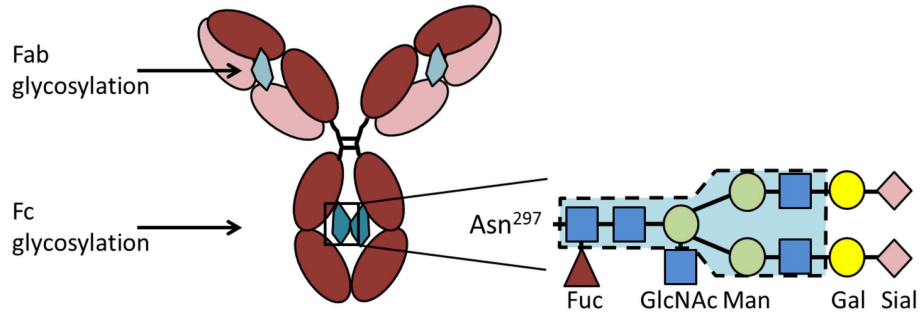

FIGURE 3 | IgG glycosylation. IgG contains a conserved glycosylation site at the asparagine (Asn)^{297} in the CH2 domain of the heavy chain. The Fc glycan (depicted in petrol) consists of a conserved heptamer (shaded in blue) that can be extended by various additional sugar residues. Here we show a fully processed glycan containing all sugar residues possible. In addition to the Fc glycan, some IgG molecules contain a glycosylation site in the Fab region (depicted in light petrol) that occurs stochastically due to the introduction of a new glycosylation site during somatic hypermutation. Asn, asparagine; Gal, galactose; GlcNAc, N-acetylglucosamine; Fuc, fucose; Man, mannose; Sial, sialic acid.

Conclusions and Future Research Agenda

Within the last years, evidence emerged that disease-associated autoantibodies play an important role in the development of bone loss in RA. Especially ACPA have been shown to contribute to aberrant osteoclast formation and activation either by direct stimulation of osteoclast precursors or the induction of a cytokine storm mainly by macrophages. Furthermore, low Fc sialylation of ACPA contributes to their inflammatory and pro-osteoclastogenic phenotype.

The majority of studies addressing autoantibody-mediated bone loss has been performed in mice or *in vitro* models and might incompletely reflect the human situation. There are interesting human studies suggesting that ACPA induce bone loss in the absence of inflammation. However, additional human studies are needed to clarify to what extent ACPA contribute to bone loss in RA patients.

Furthermore, beside the hyperactivation of osteoclasts, an impairment of osteoblast development and function is found in RA patients that aggravates bone loss. To date there is no report showing a direct action of ACPA or RF autoantibodies on osteoblast differentiation or activity, although the FcγRs have been shown to be expressed by stromal cells (47). It would be essential to further develop *in vivo* and *in vitro* experiments delineating the molecular actions of autoantibodies on bone formation.

Beside ACPA, a variety of antibodies directed against modified proteins (AMPA) have been discovered in the last years. Most prominent are anti-CarP, but also antibodies against proteins that have undergone acetylation, oxidation, or malondialdehyde-acetaldehyde addition have been described in RA patients [reviewed in Chang and Nigrovic (94)]. It is likely that other autoantibodies against posttranslational modifications, such as anti-CarP affect osteoclastogenesis and bone loss as well. However, there are no mechanistic data available so far. In addition, there are other autoantibodies known that act via completely different mechanisms than the ones described in this article. For example autoantibodies against OPG function as enhancers of osteoclastogenesis by neutralizing OPG [reviewed in Hauser and Harre (95)]. These autoantibodies are found in autoimmune diseases, such as RA and celiac disease and seem to be a feature that is independent of the original disease drivers. Nevertheless, it might be important to check for the presence of these autoantibodies, especially in patients that are not responding to the current therapies.

Based on the fact that ACPA are associated with increased bone loss in RA, one would wish to control autoimmunity in RA and to induce seroconversion or at least lowering of ACPA levels by treatment. Such approaches are for instance B cell depletion by rituximab or inhibition of T cell co-stimulation with abatacept, which are approved therapies in RA and which significantly lower ACPA levels (96). However, whether modifying autoantibody levels has clinical value in controlling disease, remains to be determined. Aside from antibody reduction, the triggers promoting the induction of effector function of autoantibodies are also targets for future interventions. Given the fact that Fc glycosylation (and especially sialylation) controls the pathogenicity of autoantibodies, it will be interesting to know whether one can control IgG sialylation in RA patients. This might be an important step toward tolerance induction and disease cure.

In addition, in the last years, more attention has been laid on the role of the mucosal immune system during RA initiation and propagation [reviewed in Caminer et al. (97) and Wells et al. (98)]. Dysregulations of microbiota and the gut barrier function might trigger the series of events that deregulate T and B cell responses resulting in autoimmunity in RA patients.

AUTHOR CONTRIBUTIONS

All authors listed have made a substantial, direct and intellectual contribution to the work, and approved it for publication.

ACKNOWLEDGMENTS

This study was supported by the Deutsche Forschungsgemeinschaft: DFG BO-3811/5-1; BO-3811/6-1; CRC1181 project A01; HA 8163/1-1; FOR2886 (TP2, TP3, and TP4); the SPP2084 μBone; the Interdisciplinary Center for Clinical Research (IZKF) grant D23.

REFERENCES

1. Tanaka Y, Nakayamada S, Okada Y. Osteoblasts and osteoclasts in bone remodeling and inflammation. *Curr Drug Targets Inflamm Allergy.* (2005) 4:325–8. doi: 10.2174/1568010054022015
2. Schett G. Osteoimmunology in rheumatic diseases. *Arthritis Res Ther.* (2009) 11:210. doi: 10.1186/ar2571
3. Bonewald LF. The role of the osteocyte in bone and nonbone disease. *Endocrinol Metab Clin North Am.* (2017) 46:1–18. doi: 10.1016/j.ecl.2016.09.003
4. McInnes IB, Schett G. The pathogenesis of rheumatoid arthritis. *N Engl J Med.* (2011) 365:2205–19. doi: 10.1056/NEJMra1004965
5. Zerbini CAF, Clark P, Mendez-Sanchez L, Pereira RMR, Messina OD, Una CR, et al. Biologic therapies and bone loss in rheumatoid arthritis. *Osteopor Int.* (2017) 28:429–446. doi: 10.1007/s00198-016-3769-2
6. Nakken B, Papp G, Bosnes V, Zeher M, Nagy G, Szodoray P. Biomarkers for rheumatoid arthritis: from molecular processes to diagnostic applications-current concepts and future perspectives. *Immunol Lett.* (2017) 189:13–18. doi: 10.1016/j.imlet.2017.05.010
7. Palazzi C, Buskila D, D'Angelo S, D'Amico E, Olivieri I. Autoantibodies in patients with chronic hepatitis C virus infection: pitfalls for the diagnosis of rheumatic diseases. *Autoimmun Rev.* (2012) 11:659–63. doi: 10.1016/j.autrev.2011.11.011
8. Aletaha D, Alasti F, Smolen JS. Rheumatoid factor determines structural progression of rheumatoid arthritis dependent and independent of disease activity. *Ann Rheum Dis.* (2013) 72:875–80. doi: 10.1136/annrheumdis-2012-201517
9. Hecht C, Englbrecht M, Rech J, Schmidt S, Araujo E, Engelke K, et al. Additive effect of anti-citrullinated protein antibodies and rheumatoid factor on bone erosions in patients with RA. *Ann Rheum Dis.* (2015) 74:2151–6. doi: 10.1136/annrheumdis-2014-205428
10. Sokolove J, Johnson DS, Lahey LJ, Wagner CA, Cheng D, Thiele GM, et al. Rheumatoid factor as a potentiator of anti-citrullinated protein antibody-mediated inflammation in rheumatoid arthritis. *Arthritis Rheumatol.* (2014) 66:813–21. doi: 10.1002/art.38307
11. van Delft MAM, van Beest S, Kloppenburg M, Trouw LA, Ioan-Facsinay A. Presence of autoantibodies in erosive hand osteoarthritis and association with clinical presentation. *J Rheumatol.* (2018) 46:101–5. doi: 10.3899/jrheum.180256
12. Wegner N, Lundberg K, Kinloch A, Fisher B, Malmstrom V, Feldmann M, et al. Autoimmunity to specific citrullinated proteins gives the first clues to the etiology of rheumatoid arthritis. *Immunol Rev.* (2010) 233:34–54. doi: 10.1111/j.0105-2896.2009.00850.x
13. Jilani AA, Mackworth-Young CG. The role of citrullinated protein antibodies in predicting erosive disease in rheumatoid arthritis: a systematic literature review and meta-analysis. *Int J Rheumatol.* (2015) 2015:728610. doi: 10.1155/2015/728610
14. Kokkonen H, Mullazehi M, Berglin E, Hallmans G, Wadell G, Ronnelid J, et al. Antibodies of IgG, IgA and IgM isotypes against cyclic citrullinated peptide precede the development of rheumatoid arthritis. *Arthritis Res Ther.* (2011) 13:R13. doi: 10.1186/ar3237
15. Suwannalai P, van de Stadt LA, Radner H, Steiner G, El-Gabalawy HS, Zijde CM, et al. Avidity maturation of anti-citrullinated protein antibodies in rheumatoid arthritis. *Arthritis Rheum.* (2012) 64:1323–8. doi: 10.1002/art.33489
16. van der Woude D, Rantapaa-Dahlqvist S, Ioan-Facsinay A, Onnekink C, Schwarte CM, Verpoort KN, et al. Epitope spreading of the anti-citrullinated protein antibody response occurs before disease onset and is associated with the disease course of early arthritis. *Ann Rheum Dis.* (2010) 69:1554–61. doi: 10.1136/ard.2009.124537
17. Aletaha D, Neogi T, Silman AJ, Funovits J, Felson DT, Bingham CO III, et al. 2010 rheumatoid arthritis classification criteria: an American College of Rheumatology/European League Against Rheumatism collaborative initiative. *Ann Rheum Dis.* (2010) 69:1580–8. doi: 10.1002/art.27584
18. Baka Z, Gyorgy B, Geher P, Buzas EI, Falus A, Nagy G. Citrullination under physiological and pathological conditions. *Joint Bone Spine.* (2012) 79:431–6. doi: 10.1016/j.jbspin.2012.01.008
19. McGraw WT, Potempa J, Farley D, Travis J. Purification, characterization, and sequence analysis of a potential virulence factor from Porphyromonas gingivalis, peptidylarginine deiminase. *Infect Immun.* (1999) 67:3248–56.
20. Araujo VM, Melo IM, Lima V. Relationship between periodontitis and rheumatoid arthritis: review of the literature. *Mediators Inflamm.* (2015) 2015:259074. doi: 10.1155/2015/259074
21. Potempa J, Mydel P, Koziel J. The case for periodontitis in the pathogenesis of rheumatoid arthritis. *Nat Rev Rheumatol.* (2017) 13:606–20. doi: 10.1038/nrrheum.2017.132
22. Klareskog L, Malmstrom V, Lundberg K, Padyukov L, Alfredsson L. Smoking, citrullination and genetic variability in the immunopathogenesis of rheumatoid arthritis. *Semin Immunol.* (2011) 23:92–8. doi: 10.1016/j.smim.2011.01.014
23. Shi J, Knevel R, Suwannalai P, van der Linden MP, Janssen GM, van Veelen PA, et al. Autoantibodies recognizing carbamylated proteins are present in sera of patients with rheumatoid arthritis and predict joint damage. *Proc Natl Acad Sci USA.* (2011) 108:17372–7. doi: 10.1073/pnas.1114465108
24. Juarez M, Bang H, Hammar F, Reimer U, Dyke B, Sahbudin I, et al. Identification of novel antiacetylated vimentin antibodies in patients with early inflammatory arthritis. *Ann Rheum Dis.* (2016) 75:1099–107. doi: 10.1136/annrheumdis-2014-206785
25. Ospelt C, Bang H, Feist E, Camici G, Keller S, Detert J, et al. Carbamylation of vimentin is inducible by smoking and represents an independent autoantigen in rheumatoid arthritis. *Ann Rheum Dis.* (2017) 76:1176–83. doi: 10.1136/annrheumdis-2016-210059
26. Montes A, Regueiro C, Perez-Pampin E, Boveda MD, Gomez-Reino JJ, Gonzalez A. Anti-carbamylated protein antibodies as a reproducible independent type of rheumatoid arthritis autoantibodies. *PLoS ONE.* (2016) 11:e0161141. doi: 10.1371/journal.pone.0161141
27. Hafstrom I, Ajeganova S, Forslind K, Svensson B. Anti-citrullinated protein antibodies are associated with osteopenia but not with pain at diagnosis of rheumatoid arthritis: data from the BARFOT cohort. *Arthritis Res Ther.* (2019) 21:45. doi: 10.1186/s13075-019-1833-y
28. Orsolini G, Caimmi C, Viapiana O, Idolazzi L, Fracassi E, Gatti D, et al. Titer-dependent effect of anti-citrullinated protein antibodies on systemic bone mass in rheumatoid arthritis patients. *Calcif Tissue Int.* (2017) 101:17–23. doi: 10.1007/s00223-017-0253-8
29. Sargin G, Kose R, Senturk T. Relationship between bone mineral density and anti-citrullinated protein antibody and rheumatoid factor in patients with rheumatoid arthritis. *Eur J Rheumatol.* (2019) 6:29–33. doi: 10.5152/eurjrheum.2018.18099
30. Llorente I, Merino L, Ortiz AM, Escolano E, Gonzalez-Ortega S, Garcia-Vicuna R, et al. Anti-citrullinated protein antibodies are associated with decreased bone mineral density: baseline data from a register of early arthritis patients. *Rheumatol Int.* (2017) 37:799–806. doi: 10.1007/s00296-017-3674-9
31. Keller KK, Thomsen JS, Stengaard-Pedersen K, Nielsen AW, Schiottz-Christensen B, Svendsen L, et al. Local bone loss in patients with anti-citrullinated peptide antibody and arthralgia, evaluated with high-resolution peripheral quantitative computed tomography. *Scand J Rheumatol.* (2018) 47:110–116. doi: 10.1080/03009742.2017.1333629
32. Kleyer A, Finzel S, Rech J, Manger B, Krieter M, Faustini F, et al. Bone loss before the clinical onset of rheumatoid arthritis in subjects with anticitrullinated protein antibodies. *Ann Rheum Dis.* (2014) 73:854–60. doi: 10.1136/annrheumdis-2012-202958
33. Ten Brinck RM, Toes REM, van der Helm-van Mil AHM. Inflammation functions as a key mediator in the link between ACPA and erosion development: an association study in Clinically Suspect Arthralgia. *Arthritis Res Ther.* (2018) 20:89. doi: 10.1186/s13075-018-1574-3
34. Simon D, Kleyer A, Englbrecht M, Stemmler F, Simon C, Berlin A, et al. A comparative analysis of articular bone in large cohort of patients with chronic inflammatory diseases of the joints, the gut and the skin. *Bone.* (2018) 116:87–93. doi: 10.1016/j.bone.2018.07.017
35. Ceccarelli F, Perricone C, Colasanti T, Massaro L, Cipriano E, Pendolino M, et al. Anti-carbamylated protein antibodies as a new biomarker of erosive joint damage in systemic lupus erythematosus. *Arthritis Res Ther.* (2018) 20:126. doi: 10.1186/s13075-018-1622-z
36. Scherer HU, van der Woude D, Willemze A, Trouw LA, Knevel R, Syversen SW, et al. Distinct ACPA fine specificities, formed under the

influence of HLA shared epitope alleles, have no effect on radiographic joint damage in rheumatoid arthritis. *Ann Rheum Dis.* (2011) 70:1461–4. doi: 10.1136/ard.2010.146506
37. van Beers JJ, Willemze A, Jansen JJ, Engbers GH, Salden M, Raats J, et al. ACPA fine-specificity profiles in early rheumatoid arthritis patients do not correlate with clinical features at baseline or with disease progression. *Arthritis Res Ther.* (2013) 15:R140. doi: 10.1186/ar4322
38. Nimmerjahn F, Ravetch JV. Antibody-mediated modulation of immune responses. *Immunol Rev.* (2010) 236:265–75. doi: 10.1111/j.1600-065X.2010.00910.x
39. Ghazizadeh S, Bolen JB, Fleit HB. Tyrosine phosphorylation and association of Syk with Fc gamma RII in monocytic THP-1 cells. *Biochem J.* (1995) 305(Pt 2):669–74. doi: 10.1042/bj3050669
40. Nimmerjahn F, Ravetch JV. Fcgamma receptors as regulators of immune responses. *Nat Rev Immunol.* (2008) 8:34–47. doi: 10.1038/nri2206
41. Ono M, Bolland S, Tempst P, Ravetch JV. Role of the inositol phosphatase SHIP in negative regulation of the immune system by the receptor Fc(gamma)RIIB. *Nature.* (1996) 383:263–6. doi: 10.1038/383263a0
42. Rosales C. Fcgamma receptor heterogeneity in leukocyte functional responses. *Front Immunol.* (2017) 8:280. doi: 10.3389/fimmu.2017.00280
43. Humphrey MB, Nakamura MC. A comprehensive review of immunoreceptor regulation of osteoclasts. *Clin Rev Allergy Immunol.* (2016) 51:48–58. doi: 10.1007/s12016-015-8521-8
44. Selvaraj P, Rosse WF, Silber R, Springer TA. The major Fc receptor in blood has a phosphatidylinositol anchor and is deficient in paroxysmal nocturnal haemoglobinuria. *Nature.* (1988) 333:565–7. doi: 10.1038/333565a0
45. Harre U, Keppeler H, Ipseiz N, Derer A, Poller K, Aigner M, et al. Moonlighting osteoclasts as undertakers of apoptotic cells. *Autoimmunity.* (2012) 45:612–9. doi: 10.3109/08916934.2012.719950
46. Harre U, Lang SC, Pfeifle R, Rombouts Y, Fruhbeisser S, Amara K, et al. Glycosylation of immunoglobulin G determines osteoclast differentiation and bone loss. *Nat Commun.* (2015) 6:6651. doi: 10.1038/ncomms7651
47. Seeling M, Hillenhoff U, David JP, Schett G, Tuckermann J, Lux A, et al. Inflammatory monocytes and Fcgamma receptor IV on osteoclasts are critical for bone destruction during inflammatory arthritis in mice. *Proc Natl Acad Sci USA.* (2013) 110:10729–34. doi: 10.1073/pnas.1301001110
48. Koga T, Inui M, Inoue K, Kim S, Suematsu A, Kobayashi E, et al. Costimulatory signals mediated by the ITAM motif cooperate with RANKL for bone homeostasis. *Nature.* (2004) 428:758–63. doi: 10.1038/nature02444
49. Kaifu T, Nakahara J, Inui M, Mishima K, Momiyama T, Kaji M, et al. Osteopetrosis and thalamic hypomyelinosis with synaptic degeneration in DAP12-deficient mice. *J Clin Invest.* (2003) 111:323–32. doi: 10.1172/JCI200316923
50. Kim N, Takami M, Rho J, Josien R, Choi Y. A novel member of the leukocyte receptor complex regulates osteoclast differentiation. *J Exp Med.* (2002) 195:201–9. doi: 10.1084/jem.20011681
51. Paradowska-Gorycka A, Jurkowska M. Structure, expression pattern and biological activity of molecular complex TREM-2/DAP12. *Hum Immunol.* (2013) 74:730–7. doi: 10.1016/j.humimm.2013.02.003
52. Harre U, Georgess D, Bang H, Bozec A, Axmann R, Ossipova E, et al. Induction of osteoclastogenesis and bone loss by human autoantibodies against citrullinated vimentin. *J Clin Invest.* (2012) 122:1791–802. doi: 10.1172/JCI60975
53. Krishnamurthy A, Joshua V, Haj Hensvold A, Jin T, Sun M, Vivar N, et al. Identification of a novel chemokine-dependent molecular mechanism underlying rheumatoid arthritis-associated autoantibody-mediated bone loss. *Ann Rheum Dis.* (2016) 75:721–9. doi: 10.1136/annrheumdis-2015-208093
54. Engdahl C, Bang H, Dietel K, Lang SC, Harre U, Schett G. Periarticular bone loss in arthritis is induced by autoantibodies against citrullinated vimentin. *J Bone Mineral Res.* (2017) 32:1681–91. doi: 10.1002/jbmr.3158
55. Dusad A, Duryee MJ, Shaw AT, Klassen LW, Anderson DR, Wang D, et al. Induction of bone loss in DBA/1J mice immunized with citrullinated autologous mouse type II collagen in the absence of adjuvant. *Immunol Res.* (2014) 58:51–60. doi: 10.1007/s12026-013-8479-7
56. Grotsch B, Lux A, Rombouts Y, Hoffmann AC, Andreev D, Nimmerjahn F, et al. Fra1 controls rheumatoid factor autoantibody production by bone marrow plasma cells and the development of autoimmune bone loss. *J Bone Miner Res.* (2019) 2019:e3705. doi: 10.1002/jbmr.3705
57. Negishi-Koga T, Gober HJ, Sumiya E, Komatsu N, Okamoto K, Sawa S, et al. Immune complexes regulate bone metabolism through FcRgamma signalling. *Nat Commun.* (2015) 6:6637. doi: 10.1038/ncomms7637
58. Bolland S, Ravetch JV. Spontaneous autoimmune disease in Fc(gamma)RIIB-deficient mice results from strain-specific epistasis. *Immunity.* (2000) 13:277–85. doi: 10.1016/S1074-7613(00)00027-3
59. Haringman JJ, Gerlag DM, Zwinderman AH, Smeets TJ, Kraan MC, Baeten D, et al. Synovial tissue macrophages: a sensitive biomarker for response to treatment in patients with rheumatoid arthritis. *Ann Rheum Dis.* (2005) 64:834–8. doi: 10.1136/ard.2004.029751
60. Anquetil F, Clavel C, Offer G, Serre G, Sebbag M. IgM and IgA rheumatoid factors purified from rheumatoid arthritis sera boost the Fc receptor- and complement-dependent effector functions of the disease-specific anti-citrullinated protein autoantibodies. *J Immunol.* (2015) 194:3664–74. doi: 10.4049/jimmunol.1402334
61. Clavel C, Ceccato L, Anquetil F, Serre G, Sebbag M. Among human macrophages polarised to different phenotypes, the M-CSF-oriented cells present the highest pro-inflammatory response to the rheumatoid arthritis-specific immune complexes containing ACPA. *Ann Rheum Dis.* (2016) 75:2184–91. doi: 10.1136/annrheumdis-2015-208887
62. Laurent L, Clavel C, Lemaire O, Anquetil F, Cornillet M, Zabraniecki L, et al. Fcgamma receptor profile of monocytes and macrophages from rheumatoid arthritis patients and their response to immune complexes formed with autoantibodies to citrullinated proteins. *Ann Rheum Dis.* (2011) 70:1052–9. doi: 10.1136/ard.2010.142091
63. Clavel C, Nogueira L, Laurent L, Iobagiu C, Vincent C, Sebbag M, et al. Induction of macrophage secretion of tumor necrosis factor alpha through Fcgamma receptor IIa engagement by rheumatoid arthritis-specific autoantibodies to citrullinated proteins complexed with fibrinogen. *Arthritis Rheum.* (2008) 58:678–88. doi: 10.1002/art.23284
64. Firestein GS, Xu WD, Townsend K, Broide D, Alvaro-Gracia J, Glasebrook A, et al. Cytokines in chronic inflammatory arthritis. I. Failure to detect T cell lymphokines (interleukin 2 and interleukin 3) and presence of macrophage colony-stimulating factor (CSF-1) and a novel mast cell growth factor in rheumatoid synovitis. *J Exp Med.* (1988) 168:1573–86. doi: 10.1084/jem.168.5.1573
65. Bozec A, Luo Y, Engdahl C, Figueiredo C, Bang H, Schett G. Abatacept blocks anti-citrullinated protein antibody and rheumatoid factor mediated cytokine production in human macrophages in IDO-dependent manner. *Arthritis Res Ther.* (2018) 20:24. doi: 10.1186/s13075-018-1527-x
66. Azuma Y, Kaji K, Katogi R, Takeshita S, Kudo A. Tumor necrosis factor-alpha induces differentiation of and bone resorption by osteoclasts. *J Biol Chem.* (2000) 275:4858–64. doi: 10.1074/jbc.275.7.4858
67. Komine M, Kukita A, Kukita T, Ogata Y, Hotokebuchi T, Kohashi O. Tumor necrosis factor-alpha cooperates with receptor activator of nuclear factor kappaB ligand in generation of osteoclasts in stromal cell-depleted rat bone marrow cell culture. *Bone.* (2001) 28:474–83. doi: 10.1016/S8756-3282(01)00420-3
68. Yao Z, Lei W, Duan R, Li Y, Luo L, Boyce BF. RANKL cytokine enhances TNF-induced osteoclastogenesis independently of TNF receptor associated factor (TRAF) 6 by degrading TRAF3 in osteoclast precursors. *J Biol Chem.* (2017) 292:10169–79. doi: 10.1074/jbc.M116.771816
69. Kitaura H, Zhou P, Kim HJ, Novack DV, Ross FP, Teitelbaum SL. M-CSF mediates TNF-induced inflammatory osteolysis. *J Clin Invest.* (2005) 115:3418–27. doi: 10.1172/JCI26132
70. Kudo O, Sabokbar A, Pocock A, Itonaga I, Fujikawa Y, Athanasou NA. Interleukin-6 and interleukin-11 support human osteoclast formation by a RANKL-independent mechanism. *Bone.* (2003) 32:1–7. doi: 10.1016/S8756-3282(02)00915-8
71. Feng W, Liu H, Luo T, Liu D, Du J, Sun J, et al. Combination of IL-6 and sIL-6R differentially regulate varying levels of RANKL-induced osteoclastogenesis through NF-kappaB, ERK and JNK signaling pathways. *Sci Rep.* (2017) 7:41411. doi: 10.1038/srep41411
72. Yoshitake F, Itoh S, Narita H, Ishihara K, Ebisu S. Interleukin-6 directly inhibits osteoclast differentiation by suppressing receptor activator of NF-kappaB signaling pathways. *J Biol Chem.* (2008) 283:11535–40. doi: 10.1074/jbc.M607999200

73. Pers YM, Fortunet C, Constant E, Lambert J, Godfrin-Valnet M, De Jong A, et al. Predictors of response and remission in a large cohort of rheumatoid arthritis patients treated with tocilizumab in clinical practice. *Rheumatology.* (2014) 53:76–84. doi: 10.1093/rheumatology/ket301
74. Alten R, Nusslein HG, Mariette X, Galeazzi M, Lorenz HM, Cantagrel A, et al. Baseline autoantibodies preferentially impact abatacept efficacy in patients with rheumatoid arthritis who are biologic naive: 6-month results from a real-world, international, prospective study. *RMD Open.* (2017) 3:e000345. doi: 10.1136/rmdopen-2016-000345
75. Tanaka M, Krutzik SR, Sieling PA, Lee DJ, Rea TH, Modlin RL. Activation of Fc gamma RI on monocytes triggers differentiation into immature dendritic cells that induce autoreactive T cell responses. *J Immunol.* (2009) 183:2349–55. doi: 10.4049/jimmunol.0801683
76. Bozec A, Zaiss MM, Kagwiria R, Voll R, Rauh M, Chen Z, et al. T cell costimulation molecules CD80/86 inhibit osteoclast differentiation by inducing the IDO/tryptophan pathway. *Sci Transl Med.* (2014) 6:235ra60. doi: 10.1126/scitranslmed.3007764
77. Arnold JN, Wormald MR, Sim RB, Rudd PM, Dwek RA. The impact of glycosylation on the biological function and structure of human immunoglobulins. *Annu Rev Immunol.* (2007) 25, 21–50. doi: 10.1146/annurev.immunol.25.022106.141702
78. Collin M, Shannon O, Bjorck L. IgG glycan hydrolysis by a bacterial enzyme as a therapy against autoimmune conditions. *Proc Natl Acad Sci USA.* (2008) 105:4265–70. doi: 10.1073/pnas.0711271105
79. Kao D, Danzer H, Collin M, Gross A, Eichler J, Stambuk J, et al. A Monosaccharide residue is sufficient to maintain mouse and human IgG subclass activity and directs IgG effector functions to cellular Fc receptors. *Cell Rep.* (2015) 13:2376–85. doi: 10.1016/j.celrep.2015.11.027
80. Lux A, Yu X, Scanlan CN, Nimmerjahn F. Impact of immune complex size and glycosylation on IgG binding to human FcgammaRs. *J Immunol.* (2013) 190:4315–23. doi: 10.4049/jimmunol.1200501
81. Zauner G, Selman MH, Bondt A, Rombouts Y, Blank D, Deelder AM, et al. Glycoproteomic analysis of antibodies. *Mol Cell Proteomics.* (2013) 12:856–65. doi: 10.1074/mcp.R112.026005
82. Kaneko Y, Nimmerjahn F, Ravetch JV. Anti-inflammatory activity of immunoglobulin G resulting from Fc sialylation. *Science.* (2006) 313:670–3. doi: 10.1126/science.1129594
83. Parekh R, Roitt I, Isenberg D, Dwek R, Rademacher T. Age-related galactosylation of the N-linked oligosaccharides of human serum IgG. *J Exp Med.* (1988) 167:1731–6. doi: 10.1084/jem.167.5.1731
84. Bondt A, Selman MH, Deelder AM, Hazes JM, Willemsen SP, Wuhrer M, et al. Association between galactosylation of immunoglobulin G and improvement of rheumatoid arthritis during pregnancy is independent of sialylation. *J Proteome Res.* (2013) 12:4522–31. doi: 10.1021/pr400589m
85. Rook GA, Steele J, Brealey R, Whyte A, Isenberg D, Sumar N, et al. Changes in IgG glycoform levels are associated with remission of arthritis during pregnancy. *J Autoimmun.* (1991) 4:779–94. doi: 10.1016/0896-8411(91)90173-A
86. van de Geijn FE, Wuhrer M, Selman MH, Willemsen SP, de Man YA, Deelder AM, et al. Immunoglobulin G galactosylation and sialylation are associated with pregnancy-induced improvement of rheumatoid arthritis and the postpartum flare: results from a large prospective cohort study. *Arthritis Res Ther.* (2009) 11:R193. doi: 10.1186/ar2892
87. Selman MH, Derks RJ, Bondt A, Palmblad M, Schoenmaker B, Koeleman CA, et al. Fc specific IgG glycosylation profiling by robust nano-reverse phase HPLC-MS using a sheath-flow ESI sprayer interface. *J Proteomics.* (2012) 75:1318–29. doi: 10.1016/j.jprot.2011.11.003
88. Anumula KR. Quantitative glycan profiling of normal human plasma derived immunoglobulin and its fragments Fab and Fc. *J Immunol Methods.* (2012) 382:167–76. doi: 10.1016/j.jim.2012.05.022
89. Anthony RM, Wermeling F, Karlsson MC, Ravetch JV. Identification of a receptor required for the anti-inflammatory activity of IVIG. *Proc Natl Acad Sci USA.* (2008) 105:19571–8. doi: 10.1073/pnas.0810163105
90. Massoud AH, Yona M, Xue D, Chouiali F, Alturaihi H, Ablona A, et al. Dendritic cell immunoreceptor: a novel receptor for intravenous immunoglobulin mediates induction of regulatory T cells. *J Allergy Clin Immunol.* (2014) 133:853–63e5. doi: 10.1016/j.jaci.2013.09.029
91. Scherer HU, van der Woude D, Ioan-Facsinay A, el Bannoudi H, Trouw LA, Wang J, et al. Glycan profiling of anti-citrullinated protein antibodies isolated from human serum and synovial fluid. *Arthritis Rheum.* (2010) 62:1620–9. doi: 10.1002/art.27414
92. Pfeifle R, Rothe T, Ipseiz N, Scherer HU, Culemann S, Harre U, et al. Regulation of autoantibody activity by the IL-23-TH17 axis determines the onset of autoimmune disease. *Nat Immunol.* (2017) 18:104–13. doi: 10.1038/ni.3579
93. Engdahl C, Bondt A, Harre U, Raufer J, Pfeifle R, Camponeschi A, et al. Estrogen induces St6gal1 expression and increases IgG sialylation in mice and patients with rheumatoid arthritis: a potential explanation for the increased risk of rheumatoid arthritis in postmenopausal women. *Arthritis Res Ther.* (2018) 20:84. doi: 10.1186/s13075-018-1586-z
94. Chang MH, Nigrovic PA. Antibody-dependent and -independent mechanisms of inflammatory arthritis. *JCI Insight.* (2019) 4:278. doi: 10.1172/jci.insight.125278
95. Hauser B, Harre U. The role of autoantibodies in bone metabolism and bone loss. *Calcif Tissue Int.* (2018) 102:522–32. doi: 10.1007/s00223-017-0370-4
96. Wunderlich C, Oliviera I, Figueiredo CP, Rech J, Schett G. Effects of DMARDs on citrullinated peptide autoantibody levels in RA patients-A longitudinal analysis. *Semin Arthritis Rheum.* (2017) 46:709–14. doi: 10.1016/j.semarthrit.2016.09.011
97. Caminer AC, Haberman R, Scher JU. Human microbiome, infections, and rheumatic disease. *Clin Rheumatol.* (2017) 36:2645–53. doi: 10.1007/s10067-017-3875-3
98. Wells PM, Williams FMK, Matey-Hernandez ML, Menni C, Steves CJ. 'RA and the microbiome: do host genetic factors provide the link? *J Autoimmun.* (2019) 99:104–15. doi: 10.1016/j.jaut.2019.02.004

Conflict of Interest Statement: The authors declare that the research was conducted in the absence of any commercial or financial relationships that could be construed as a potential conflict of interest.

frontiers in Immunology

REVIEW
published: 17 July 2019
doi: 10.3389/fimmu.2019.01663

Finding a Toll on the Route: The Fate of Osteoclast Progenitors After Toll-Like Receptor Activation

Pedro P. C. Souza[1] *and Ulf H. Lerner*[2]*

[1] Faculty of Dentistry, Federal University of Goiás, Goiânia, Brazil, [2] Centre for Bone and Arthritis Research at Department of Internal Medicine and Clinical Nutrition, Institute for Medicine, Sahlgrenska Academy at University of Gothenburg, Gothenburg, Sweden

M-CSF and RANKL are two crucial cytokines stimulating differentiation of mature, bone resorbing, multinucleated osteoclasts from mononucleated progenitor cells in the monocyte/macrophage lineage. In addition to the receptors for M-CSF and RANKL, osteoclast progenitor cells express receptors for several other pro- and anti-osteoclastogenic cytokines, which also regulate osteoclast formation by affecting signaling downstream M-CSF and RANKL receptors. Similar to many other cells originating from myeloid hematopoetic stem cells, also osteoclast progenitors express toll-like receptors (TLRs). Nine murine TLRs are expressed in the progenitors and all, with the exception of TLR2 and TLR4, are downregulated during osteoclastogenesis. Activation of TLR2, TLR4, and TLR9, but not TLR5, in osteoclast progenitors stimulated with M-CSF and RANKL arrests differentiation along the osteoclastic lineage and keeps the cells at a macrophage stage. When the progenitors are primed with M-CSF/RANKL and then stimulated with agonists for TLR2, TLR4, or TLR9 in the presence of M-CSF, but in the absence of RANKL, the cells differentiate to mature, bone resorbing osteoclasts. TLR 2, 4, 5, and 9 are also expressed on osteoblasts and their activation increases osteoclast differentiation by an indirect mechanism through stimulation of RANKL. In mice, treatment with agonists for TLR2, 4, and 5 results in osteoclast formation and extensive bone loss. It remains to be shown the relative importance of inhibitory and stimulatory effects by TLRs on osteoclast progenitors and the role of RANKL produced by TLR stimulated osteoblasts, for the bone resorbing effects *in vivo*.

Keywords: toll-like receptors, osteoclast, lipopolysaccharide, RANKL, bone resorption

OPEN ACCESS

Edited by:
Claudine Blin-Wakkach, UMR7370 Laboratoire de Physio Médecine Moléculaire (LP2M), France

Reviewed by:
Frédéric Velard, Université de Reims Champagne-Ardenne, France
Anne Blangy, UMR5237 Centre de Recherche en Biologie cellulaire de Montpellier (CRBM), France

***Correspondence:**
Ulf H. Lerner
ulf.lerner@gu.se

Specialty section:
This article was submitted to Inflammation, a section of the journal Frontiers in Immunology

Received: *28 February 2019*
Accepted: *03 July 2019*
Published: *17 July 2019*

Citation:
Souza PPC and Lerner UH (2019) Finding a Toll on the Route: The Fate of Osteoclast Progenitors After Toll-Like Receptor Activation. Front. Immunol. 10:1663. doi: 10.3389/fimmu.2019.01663

INTRODUCTION

Human body is constantly exposed to microorganisms. In addition to our own cells, humans host a vast community of microbes, with an estimation of the number of bacteria exceeding the number of host cells by a factor of 1.3 (1, 2). The majority of these microorganisms populate the gastrointestinal tract and regulate processing and absorption of nutrients and vitamin biosynthesis, which impacts the development and remodeling of multiple organs, including bone (3). Recently, it has been demonstrated that disturbances in normal microbial population are associated with effects on bone, not only due to impaired uptake of nutrients, but also due to the activation of pattern-recognition receptors (PRRs) expressed in immune cells by microbe-associated molecular patterns

(MAMPs) released by microorganisms (4–6). The intestinal microbiota modulates unexpected events distant to the mucosal surface, such as sex steroid deficiency induced bone loss (7). In contrast to wild type mice, sex steroid-depleted germ-free mice, fail to increase osteoclastogenic cytokines and, consequently, bone resorption is not increased and bone mass is preserved. Microbial recolonization restores the capacity of sex steroid depletion to induce trabecular bone loss. Interestingly, a shift in the normal microbial population by supplementation with probiotics protects mice from sex steroid depletion-induced bone loss. Corroborating these observations in mice, a double blind, placebo-controlled clinical trial demonstrated that daily intake of *Lactobacillus reuteri* for 12 months reduces the loss of volumetric bone mineral density (BMD) in 75–80 year old women who had low BMD (8).

The effect of MAMPs in bone metabolism becomes evident in infectious diseases close to the skeleton. In periodontitis, a highly prevalent inflammatory disease afflicting more than two thirds of Americans aging more than 65 years, bone loss is clinically observed due to infection by pathogenic bacteria and their recognition by the host immune system (9). Bacteria-induced bone loss is also involved in the pathogenesis of osteomyelitis (10). Bone resorption due to excessive osteoclast formation is also observed in *Staphylococcus aureus* septic arthritis (11, 12), an uncommon, but not rare disease affecting 2–10 patients of 100,000 in the general population (13). Not only MAMPs can activate PRRs since these receptors recognize also endogenously produced molecules such as danger-associated molecular patterns (DAMPs).

To study the interactions between bone and immune cells, the field of osteoimmunology emerged almost 50 years ago. In 1970, a breakthrough publication by Haussman et al. reported that endotoxin from the microorganism commonly found in the gingival sulcus, *Bacteroides melaninogenicus*, was as potent as parathyroid hormone in its ability to induce osteoclastogenesis and bone resorption (14). Two years later, Horton et al. described a factor released by leucocytes exposed to dental plaque that stimulated bone resorption in organ cultures of fetal rat radii by increasing the number of osteoclasts (15). These were the first evidence that bacterial components could indirectly affect bone metabolism through activation of inflammatory cells. Since then, the mechanisms underlying the interactions between inflammatory cells and bone cells have been extensively studied, particularly the role of cytokines in inflammatory bone loss (16).

A great advance in the field of osteoimmunology became possible after the breakthrough discoveries in late 1990's related to the characterization of Toll-like receptors. Toll protein, primarily related to dorso-ventral embryo patterning of *Drosophila melanogaster* (17), was identified in 1996 as a critical molecule for the response against the fungus *Aspergillus fumigatus* (18). Its homologous in humans, once called hToll and now Toll-like receptor 4 (TLR4), was shown 1 year later to be linked also to cytokine production in human monocytes (19). The identification of a mutation in the *Tlr4* gene in mice that render them resistant to endotoxin confirmed the participation of TLRs in innate immunity (20).

Not surprisingly, osteoclasts, which are derived from the hematopoietic stem cells, express TLRs and respond to MAMPs (21). Thus, the effect of TLR activation in osteoclasts and their precursors is an important aspect in the pathogenesis of inflammation-induced bone remodeling. In this review, we aim to dissect the molecular mechanisms underlying the effects of TLRs in osteoclast biology.

OSTEOCLASTS, BONE CELLS EMERGING FROM THE IMMUNE SYSTEM

The clinical observation of local and systemic bone loss in a variety of inflammatory diseases demonstrates the influence of inflammation on bone metabolism (22). These diseases include rheumatoid arthritis, psoariatric arthritis, ankylosing spondylitis, septic arthritis, periodontitis, inflammatory bowel disease, osteomyelitis and loosening of joint prosthesis, and dental implants. The effect by the inflammatory process is most often locally in joints or jaw bones, but rheumatoid arthritis and inflammatory bowel disease also cause systemic bone loss, so called secondary osteoporosis. In periodontitis, failed dental implants and septic arthritis, bone loss is associated with infections by bacteria known to activate TLRs, but these receptors can also be activated by endogenous substances produced by cells in the inflamed joint in patients with rheumatoid arthritis. The expansion of the knowledge in the osteoimmunology field has helped us to understand how bacteria and tissue-produced ligands can regulate bone remodeling by activating TLRs.

Mouse monocytes and macrophages from different origins, such as bone marrow, spleen, thymus and peripheral blood, are capable of differentiating to mature osteoclasts when co-cultured with stromal cells in the presence of 1,25-dihydroxyvitamin D3 (23). The common origin with inflammatory cells might explain why osteoclast-induced bone resorption is triggered by proinflammatory cytokines such as IL-1β, TNF-α, OSM, IL-6, IL-11, and IL-17 (16). The mechanism underlying the action of proinflammatory cytokines in bone loss is quite intricate and involves direct mechanisms through binding of cytokines to cytokine receptors expressed by osteoclast precursors, and indirect mechanisms through production of osteoclastogenic factors by inflammatory and resident cells.

Macrophages and osteoclasts share the same progenitor cells, and differentiation of both cells is affected by a loss-of-function mutation in the macrophage-colony stimulating factor (M-CSF) gene (24). The essential role of M-CSF in osteoclastogenesis is also evidenced in mice lacking its receptor c-FMS, encoded by the *Csfr1* gene, which develop severe osteopetrosis (25). The skeletal phenotype caused by deficient M-CSF signaling is due to the essential role of M-CSF on proliferation and survival of osteoclast progenitors (26).

Among the cytokine receptors affecting osteoclastogenesis, a crucial molecule is the receptor RANK (receptor activator of nuclear factor (NF)-κB) (**Figure 1**). Mice deficient in *Tnfrsf11a* (the gene encoding RANK) have impaired osteoclastogenesis and display severe osteopetrosis (27). RANKL (the ligand for RANK), a cytokine belonging to the tumor-necrosis factor

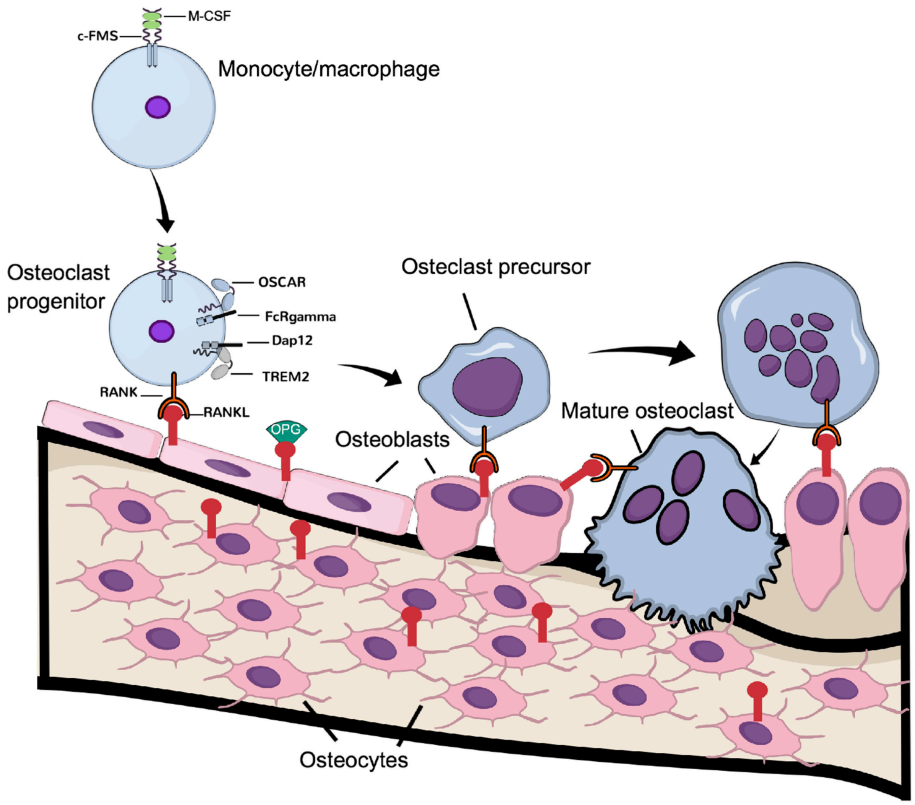

FIGURE 1 | Physiological osteoclast differentiation. Osteoclast progenitors, express c-FMS, the receptor for M-CSF. Upon M-CSF binding to c-Fms, these cells express RANK, which is activated by RANKL expressed by osteoblasts and osteocytes. Binding of RANKL to RANK, in cooperation with the signaling from costimulatory receptors OSCAR/FcRgamma and TREM-2/Dap12, induce differentiation of the progenitor cells to osteoclast precursors, which eventually fuse to latent, multinucleated osteoclasts. Continuous signaling by RANK induces their activation to mature, bone resorbing osteoclasts.

(TNF) superfamily, is expressed by resident bone cells such as osteoblasts and osteocytes (16), and also by different T cells (28), again indicating the active influence of the immune system in osteoclastogenesis. Deletion of the *Tnfsf11* (the gene encoding RANKL) results in mice phenocopying *Tnfrsf11a*$^{-/-}$ mice. Both the formation and activity of mature osteoclasts are stimulated by ligation of RANKL to RANK *in vitro* (29–31). To counteract RANKL action, a decoy receptor lacking a transmembrane domain, osteoprotegerin (OPG), competes with RANK for RANKL binding and blocks osteoclast differentiation and activation (32, 33).

Not only immune cells require costimulatory signals for activation but also osteoclasts require these signals for their activation, in addition to the signaling induced by M-CSF and RANKL (**Figure 1**). In fact, the immunoreceptor tyrosine-based activation motif (ITAM)-harboring adaptors, Fc receptor common gamma subunit (FcRγ), and DNAX-activating protein (DAP)12 are essential for osteoclast terminal differentiation, as demonstrated in osteopetrotic mice lacking these receptors (34). In osteoclasts, the immunoglobulin-like receptors associated with FcRγ and DAP12 are osteoclast-associated receptor (OSCAR) and the triggering receptor expressed in myeloid cells 2 (TREM-2), respectively (26). Although FcRγ/DAP12 are crucial for osteoclastogenesis to occur, the ligands activating the receptors in osteoclast progenitors are not known. Recently, it was demonstrated that downstream of kinase-3 (DOK3), a protein known to physically interact with DAP12 in macrophages to inhibit TLR signaling (35), is an important negative regulator of osteoclast formation. The mechanism involves inhibition of M-CSF and RANKL-induced activation of Syk and ERK. *In vivo*, *DOK3*$^{-/-}$ mice have reduced trabecular bone mass and increased number of TRAP^{+} osteoclasts (36).

Since osteoclasts derive from hematopoietic precursors, it is not surprising that TLRs affect osteoclast biology. Being a highly specialized cell, however, activation of TLRs in osteoclasts and their progenitor cells leads to complex outcomes that will be further explored in this review.

THE TOLL-LIKE RECEPTOR FAMILY IN OSTEOCLASTS

The TLR family is composed of 13 members in mammals, 10 of which are identified in humans (TLR1-10), among which nine are expressed by osteoclast progenitors (TLR1-9) (37). The members of this family are homologous of the Drosophila Toll protein and consist of integral membrane glycoproteins with extracellular domains of leucine-rich repeats (LRRs), a single

transmembrane domain and a C-terminal intracellular domain homologous to the intracellular domain of Interleukin-1 receptor (IL1R), referred to as Toll/IL-1R domain (TIR domain) (38, 39).

Despite the conserved extracellular LRR domain, TLRs can sense a broad range of MAMPs expressed by invading microbes and danger-associated molecular patterns (DAMPs) expressed by the host, probably by insertions of specific amino acids conferring ligand specificity (40) (**Figure 2**). Interestingly, different ligands can bind to the same TLR (**Figure 2**). Thus, TLR4, as an example, can recognize MAMPs such as lipopolysaccharide LPS (41) and lipid A (42), as well as DAMPs such as serum amyloid A (43), S100A8/S100A9 (44), oxidized low-density lipoprotein and amyloid β (45), in addition to several other MAMPs and DAMPs. The capacity to recognize different structures by the TLRs explains why endogenous TLR ligands, such as DAMPs secreted by necrotic cells and extracellular matrix (ECM) in response to tissue damage or injury, as well as MAMPs, such as LPS, lipopeptides, CpG oligodeoxynucleotides, and flagellin, among others, affect osteoclastogenesis. The effects and mechanism of action of MAMPs and DAMPs in osteoclasts is summarized in **Table S1** and will be further addressed below.

For signaling, DAMPs and MAMPs associate with TLRs mainly as homo and heterodimers (46). In the case of TLR4, recognition of LPS requires binding to the accessory proteins LPS-binding protein and CD14 before being transferred to the TLR4/MD2 protein complex (47). In addition to TLR4; TLR2, TLR5, and TLR9 are responsible for recognition of bacterial components. TLR2, in association with either TLR1 or TLR6, recognizes various bacterial cell wall components, such as lipoteicoic acid (48) and lipoproteins/lipopeptides (49, 50), while TLR5 mediates the response to flagellin (51) (**Figure 2**). Similarly to TLR4, and in accordance with their functions, TLR2 and TLR5 are membrane bound. Among the intracellular TLRs, TLR9 recognizes bacterial DNA through CpG motifs (52). The cell response to viruses is manly triggered by the recognition of viral components by the intracellular receptors TLR3, 7, and 8 (53), although it is reported that TLR4 can also recognize viral proteins (54). TLR7 can also be targeted by the synthetic compound imiquimod, used for topical treatment of skin cancers and other cutaneous disorders (55).

Since the cloning of TLR4, it has been shown that TLR4 signals through NF-κB pathway to induce cytokine production (19). Later, several molecules were identified as adapter proteins upstream the activation of NF-κB and other signaling pathways, such as MAPKs, as extensively reviewed elsewhere (56–59).

To induce effector gene expression, upstream of NF-κB, TLRs use the canonical myeloid differentiation factor 88 (Myd88) pathway and the non-canonical Myd88-independent, TIR-domain-containing adapter-inducing interferon-β (TRIF) pathway (**Figure 3**). With exception of TLR3, all TLRs activate the Myd88-dependent pathway, while the Myd88-independent pathway can also be activated by TLR3, TLR4, and TLR5 (**Figure 3**).

Upon agonist binding, a hallmark of TLRs activation is the production of cytokines, including interferons. Activation of the Myd88 pathway leads mainly to the production of pro-inflammatory cytokines, while engagement of TRIF triggers interferon production (60). Since both pro-inflammatory cytokines and interferons are known to affect bone metabolism (16, 61), activation of TLRs can indirectly interfere with osteoclast function.

TLR ACTIVATION IN OSTEOCLASTS, FRIEND OR FOE?

Since the pioneering observation showing that LPS from *Bacteroides melaninogenicus* (those days called endotoxin) present in the biofilm in tooth pockets, as well as LPS from *Escherichia coli* and *Salmonella typhii,* could stimulate osteoclast formation, mineral release, and bone matrix degradation in organ cultured fetal rat long bones (14), it has been shown by several groups that LPS from different species of bacteria can stimulate bone resorption *ex vivo* (62–64) and *in vivo* (65–67). Following the discovery of TLRs, it has been found that LPS from several bacteria stimulates osteoclast formation and bone resorption *in vivo* through activation of TLR4 (68, 69), whereas *P. gingivalis* LPS utilizes TLR2 to induce osteoclastogenesis (70, 71). It cannot, however, be determined in these experimental systems if LPS increases osteoclastogenesis by targeting osteoclast progenitor cells, or if osteoclast-supporting cells mediate the effect. The fact that mouse bone marrow macrophages express TLRs (TLR1-TLR9) (72), and that both TLR and RANK recruit TRAF6 to the cytoplasmic tail of the receptors and activate NF-κB, suggests that TLR agonists may, similar to RANKL, stimulate osteoclastogenesis through TLRs present in osteoclast progenitor cells. Using purified bone marrow macrophages/osteoclast progenitors, however, it has been shown that LPS can both inhibit and stimulate osteoclastogenesis dependent on the differentiation level of the progenitors (73). Other studies have demonstrated that LPS can stimulate osteoclast formation also indirectly through enhancing RANKL formation by targeting osteoclast-supporting cells (see further below).

TLR ACTIVATION INHIBITS OSTEOCLASTOGENESIS STIMULATED BY RANKL

As mentioned above, mouse bone marrow macrophages express TLR1-TLR9, but when these cells are induced to differentiate to mature osteoclasts with RANKL, all receptors, with the exception of TLR2 and TLR4, are downregulated (72). This observation indicates that osteoclast progenitors in bone marrow could be responsive to a variety of TLR agonists. However, despite the fact that the TLR2 agonist *P. gingivalis* activates ERK1/2, p38, JNK, and NF-κB in mouse bone marrow macrophages, similar to RANKL, treatment of the macrophages with M-CSF and *P. gingivalis* does not result in formation of osteoclasts (74). Similar observation has been made by adding either *E. coli* LPS or CpG-ODN to M-CSF-stimulated macrophages to activate TLR4 and TLR9, respectively (75, 76). Interestingly, activation of TLR9 induced the formation of $TRAP^{+}$ mononucleated cells, but no mature osteoclasts were formed. In contrast to RANKL,

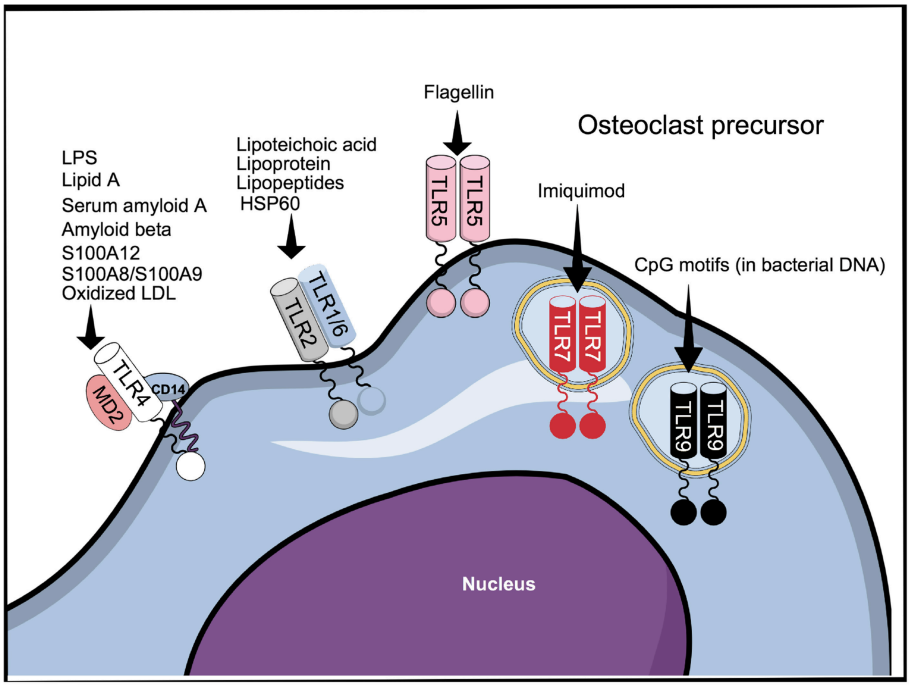

FIGURE 2 | TLR1-9 are expressed by cells belonging to the osteoclast lineage, of which TLR2, 4, 5, 7, and 9 have been shown to be functional. The figure represents all the TLRs that have been described to be expressed in cells belonging to the osteoclast lineage and some of their ligands.

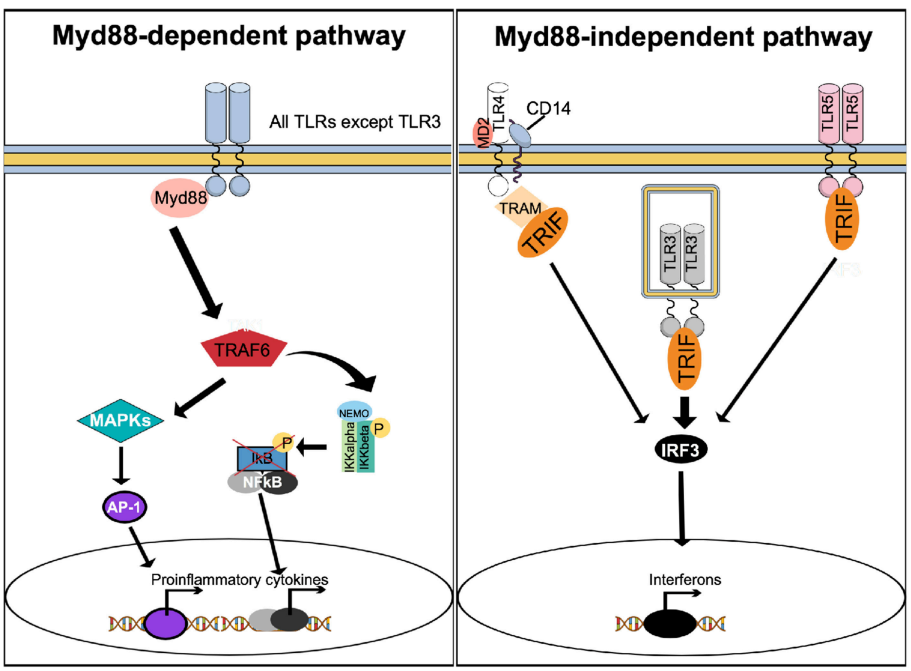

FIGURE 3 | Stimulation of TLRs activates multiple signaling pathways. With exception of TLR3, activation of TLRs results in recruitment of Myd88 to activate the Myd88-dependent canonical pathway. Myd88 activates TRAF6 to form a protein complex capable of phosphorylating the IKK complex, resulting in NF-κB activation. In parallel, the Myd88-dependent pathway results in activation of MAPK and AP-1. The Myd88-dependent pathway results in increased expression of proinflammatory cytokines. The Myd88-independent, non-canonical pathway can be activated by TLR4, TLR3, and TLR5, causing recruitment of TRIF. Unlike TLR3 and TLR5, which recruit TRIF directly to their TIR domain, TLR4 uses TRAM as an adapter protein. TRIF activates IRF3, which translocate to the nucleus to trigger expression of interferon.

activation of TLR2 with *P. gingivalis* stimulation did not induce activation of c-Fos or Nfatc1. Given the crucial role of these transcription factors for osteoclast formation, as demonstrated by the lack of osteoclasts and the osteopetrotic skeleton seen in mice with genetic deletion of *Fos* (77) or *Nfatc1* (78), it is apparent that this difference in signaling downstream RANK and TLR2 is the reason why TLR2 activation does not induce osteoclastogenesis. In contrast to these observations, it has recently been reported that the synthetic TLR7 agonist imiquimod stimulated osteoclast formation in M-CSF treated human $CD14^+$ monocytes cultured for 21 days, an effect associated with enhanced expression of *Nfatc1* (79).

Surprisingly, activation of TLR in bone marrow macrophages, simultaneously stimulated with RANKL, abolishes osteoclast formation (**Figure 4A**). Thus, addition of either peptidoglycan from *S. aureus*, *S. aureus* bacteria, lipoteichoic acid from *S. aureus*, *P. gingivalis* bacteria, or *P. gingivalis* LPS, which all activate TLR2, or addition of the synthetic TLR2 agonist $Pam2CSK_4$ (Pam2), to RANKL-stimulated macrophages, completely blocks osteoclast formation (72, 74, 80–83). Also addition of poly(I:c) dsRNA activating TLR3, *E. coli* LPS activating TLR4, or CpG motif of unmethylated DNA (Cpg-ODN) activating TLR9, blocks RANKL-induced osteoclastogenesis in M-CSF-treated mouse bone marrow macrophage cultures (72, 75, 76, 84). M-CSF/RANKL-stimulated macrophages lose their capacity to phagocyte zymosan, but when co-treated with the TLR agonists, the cells still can phagocyte these particles, demonstrating that they are arrested at the macrophage stage (72). Activation of these four TLRs, also inhibits osteoclast formation in RANKL-stimulated human peripheral blood monocyte cell cultures (72). In agreement with these findings, activation of TLR2 with Pam_3CSK_4 (Pam3), or TLR4 with *E. coli* LPS, inhibits osteoclast formation using human $CD14^+$ monocytes as progenitor cells, an effect associated with decreased expression of RANK and TREM (84). The TLR2-induced inhibition is dependent on MyD88, but not on TRIF signaling (74). In contrast to activation of TLR2, TLR3, TLR4, and TLR9, activation of TLR5 using flagellin from two different bacteria does not inhibit RANKL-induced osteoclast formation in mouse macrophages expressing TLR5 mRNA and protein (85).

Since osteoclast progenitor cells might be challenged by several agonists activating different TLRs during infectious diseases, the interactions between different TLR agonists have been assessed. Thus, synergistic inhibitory effects on osteoclast formation have been observed when mouse macrophages have been treated with TLR3 together with TLR4, or with TLR4 together with TLR9 (86). These synergistic inhibitions were partially explained by decreased protein expression of the receptor for M-CSF.

RANKL-Induced Signaling Pathways Are Affected by Activation of TLRs

Similar to RANKL, peptidoglycan from *S. aureus,* poly(I:c) dsRNA, *E. coli* LPS and Cpg-ODN activate NF-κB in mouse macrophages (72), an observation also made in macrophages stimulated with *P. gingivalis* (74). Also similar to RANKL, this bacterium activates ERK1/2, p38 and JNK, both when added alone and when added together with RANKL (74), indicating that inhibition of osteoclastogenesis by TLR2 is not due to decreased phosphorylation of MAPKs. Similarly, *P. gingivalis* did not affect RANKL-induced activation of NF-κB (74). Nor does stimulation of TLR4 with *E. coli* LPS affect RANKL-induced activation of NF-κB, ERK1/2 or p38 (76). Importantly, however, activation of TLR2 with *P. gingivalis,* or TLR4 with *E. coli* LPS, inhibits RANKL-induced activation of Nfatc1, which explains why these TLRs block osteoclastogenesis (74, 76). Activation of TLR2 also inhibited c-Fos induction by RANKL, which is an additional mechanism by which osteoclast formation is decreased. Since c-Fos is a transcription factor upstream of Nfatc1 (87), it is likely that regulation of c-Fos is the reason why Nfatc1 is decreased. Also activation of TLR9 inhibits RANKL-induced c-Fos, by a mechanism due to increased degradation of both c-Fos mRNA and protein (88). This might be due to that the activation of ERK1/2 by CpG-ODN is transient, whereas RANKL causes a sustained activation of ERK1/2, a difference which is explained by the finding that CpG-ODN, but not RANKL, induces the expression of the phosphatase PP2A (88).

Serum amyloid A is a circulating, danger-associated, liver protein which is upregulated by inflammatory processes and which binds to TLR2 (89). This protein also inhibits RANKL-stimulated osteoclast formation in mouse bone marrow macrophage (BMM) cultures (90). The inhibition is associated with decreased expression of RANKL-induced *Fos* and *Nfatc1* mRNA expression, increased expression of the macrophage transcription factors *Mafb* and *Irf8*, as well as with decreased expression of c-Fms protein on the surface of the progenitor cells due to enhanced ectodomain shedding.

Cytokines Involved in TLR-Induced Inhibition of Osteoclastogenesis

In agreement with the fact that increased formation of inflammatory cytokines is a well-known, Myd88-dependent, phenomenon in macrophages stimulated by TLR agonist, it has been observed that activation of BMMs with peptidoglycan, poly(I:c)dsRNA, *E. coli* LPS, CpG-ODN results in increased expression of TNF-α (72, 75). The expression of *Tnfsf2* (encoding TNF-α), as well as the mRNA expression of *Il6*, and *Il12p40*, is upregulated after stimulation with *P. gingivalis*, whereas RANKL does not affect the expression of any of these cytokines (74). The expression of *Il12p40* mRNA and IL-12 protein is increased also by CpG-ODN (91). Since neutralization of IL-12 partially rescued the inhibitory effect by CpG-ODN on osteoclast formation, and since IL-12 is an inhibitor of osteoclast differentiation (92), it seems induction of anti-osteoclastogenic cytokines by TLR9 might partially explain the inhibitory effect on osteoclastogenesis.

Not only inflammatory cytokines are induced by TLR signaling, but also type I interferons are induced through the TRIF-mediated pathway (**Figure 3**). Since IFN-β is a negative feedback regulator of RANKL-induced osteoclast formation due to decreased expression of c-Fos protein (93), the possibility

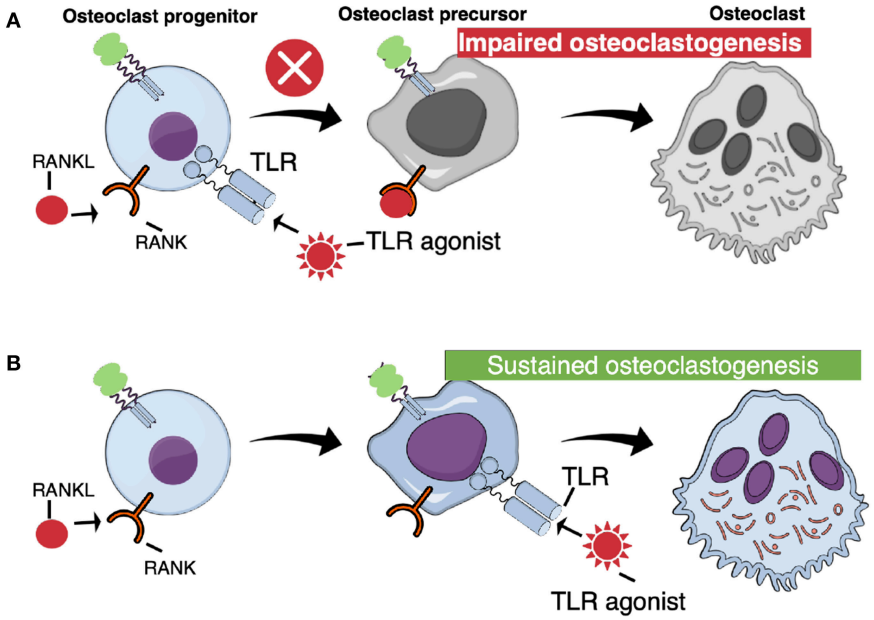

FIGURE 4 | TLR activation at different stages of osteoclast differentiation results in different outcomes. **(A)** When TLR agonists are added at early stages of osteoclast differentiation, concomitant with RANKL, osteoclastogenesis is arrested. **(B)** Committed osteoclast precursors primed with RANKL are capable to differentiate to mature, functional osteoclasts when challenged with TLR agonists in the absence of RANKL.

exists that IFN-β may be important for decreased osteoclast formation caused by activation of TLR2 and TLR4. The observations showing that TLR2- and TLR4-induced inhibition of *RANK* expression and human osteoclast formation is independent of IFN-β (84) and that TLR2-induced inhibition of human osteoclastogenesis is dependent on Myd88, but not TRIF, argues for that IFN-β is not involved in the decreased osteoclast formation caused by activation of TLR2 or TLR4. Most recently, however, it has been reported that haptoglobin decreased osteoclast formation *in vivo* and *in vitro* through activation of TLR4 and induction of IFN-β (94). Thus, haptoglobin deficient mice have low trabecular bone mass and increased numbers of osteoclasts, with no effect on osteoblast numbers. Treatment of mice locally with haptoglobin results in decreased osteoclast formation in mice co-stimulated by RANKL injections. In mouse BMM cultures, haptoglobin decreases osteoclast formation by a mechanism dependent on TLR4, but not on TLR2 or TLR7, and associated with increased mRNA and protein expression of IFN-β. The inhibitory effect was abolished by antibodies neutralizing IFN-β. Similar to previous findings (93) increased IFN-β and decreased osteoclast formation was associated with unaffected mRNA expression of *Fos* but decreased c-Fos protein expression. It was, however, surprising that haptoglobin did not induce phosphorylation of IRF-3, which is a well-known inducer of IFN-β in the TRIF pathway activated by TLRs (**Figure 3**). It, therefore, remains to be understood why TLRs and haptoglobin induce IFN-β by seemingly different mechanisms in osteoclast progenitor cells. It also remains to be understood why TLR-induced inhibition of osteoclast differentiation in human osteoclast progenitors is independent of IFN-β, whereas activation of TLR4 by haptoglobin in mouse osteoclast progenitors is dependent.

IL-1 receptors, similar to TLRs, have a cytosolic TIR domain, and also share several common downstream signaling pathways. It has, therefore, been investigated how activation of IL-1 receptors affect RANKL-induced osteoclast formation. Lee et al., using human $CD14^+$ monocytes, found that IL-1β also inhibited RANKL-stimulated osteoclast formation, when the cells were co-stimulated with the two cytokines (95). In contrast, Chen et al., using mouse bone marrow macrophages, found that IL-1α, in contrast to *P. gingivalis* LPS, enhanced osteoclast formation induced by RANKL (81). IL-1α-induced stimulation was observed with both stimulatory and permissive concentrations of RANKL. Both the inhibitory effect by *P. gingivalis* LPS and the stimulatory by IL-1α were dependent on Myd88. The diverse responses were explained by the observation that LPS abrogated the RANKL-induced expression of *Blimp1*, a transcriptional repressor of the anti-osteoclastogenic transcription factors IRF8 and MafB, whereas IL-1α potentiated RANKL-induced expression of *Blimp1*.

Comparison of Effects by TLRs on Osteoclast Formation *in vitro* and *in vivo*

The inhibitory effects by activation of TLRs on osteoclast formation does not explain why infections with *E. coli*, *S. aureus*, or *P. gingivalis* result in increased formation of osteoclasts and bone resorption (96). It has been suggested, however, that the inhibition of osteoclast formation by TLR may be part of a homeostatic mechanism limiting bone resorption during infection and inflammation (84). It might also be possible

that the inhibitory effect is a mechanism to increase the number of macrophages involved in the defense against the bacterial infections.

The inhibition of osteoclastogenesis by TLR agonists seems to be specific to un-committed purified mouse bone marrow macrophages and human peripheral blood monocytes, since *P. gingivalis* LPS, *S. aureus* and Pam2 do not inhibit bone resorption in RANKL-stimulated mouse calvarial bones *ex vivo* (82, 83). Nor do these agonists inhibit osteoclast formation in RANKL-stimulated calvarial periosteal cell cultures containing osteoclast progenitors. This may be of particular interest since formation of mature osteoclasts only takes place on bone surfaces, not in bone marrow. The reason why the osteoclast progenitors in the periosteum is not inhibited by TLR agonists is not known, but may be due that these cells do not express TLRs, or that these cells are committed osteoclast progenitors, or that surrounding non-osteoclastic cells make the osteoclast progenitors insensitive to TLR-induced inhibition.

TLR ACTIVATION INDUCES OSTEOCLASTOGENESIS IN RANKL-PRIMED CELLS

In contrast to the inhibition of un-committed osteoclast progenitors in bone marrow or peripheral blood, activation of TLR in RANKL-committed osteoclast progenitors from bone marrow results in stimulation of osteoclastogenesis (**Figure 4B**). Zou et al. were the first to show that mouse bone marrow macrophages primed with M-CSF/RANKL, and then treated with *E. coli* LPS and M-CSF, in the absence of RANKL, differentiate to mature osteoclasts (97). Under these conditions, LPS induced the expression of IL-1β and TNF-α, and addition of antibodies neutralizing TNF-α inhibited osteoclast stimulation by LPS, in agreement with previous studies showing that the stimulatory effect of LPS *in vivo* on the numbers of osteoclast progenitors in bone marrow is inhibited in mice deficient of the *p55* TNF receptor (67). In contrast, inhibition of IL-1β with the IL-1 receptor antagonist did not affect LPS-induced stimulation of osteoclast formation in RANKL-primed cells. The effect of commitment by RANKL is long-lasting and *E. coli* LPS is able to induce osteoclastogenesis several days after priming (76). Under these conditions, LPS does not decrease the expression of Nfatc1, in contrast to the inhibition seen when LPS is added together with RANKL to non-committed cells. Also addition of *P. gingivalis* to RANKL-primed cells results in osteoclast formation (74). Similar induction of osteoclast formation is obtained by adding other TLR2 agonists, such as formaldehyde-inactivated *S. aureus*, Pam2 and Pam3 (83, 98). At variance, Kassem et al. found that UV-light inactivated *S. aureus*, *P. gingivalis* LPS and heat-killed *Listeria monocytogenes* cause increased numbers of $TRAP^+$ mononucleated cells in RANKL-primed bone marrow macrophage cultures. These cells expressed enhanced mRNA levels of *Acp5* (encoding TRAP), *Ctsk* (encoding cathepsin K), *c-Fos,* and *Nfatc1*, but did not form multinucleated osteoclasts. In contrast, Pam2 and Pam3 robustly stimulated formation of multinucleated osteoclasts. Activation of TLR9 with CpG-ODN in RANKL-primed cells also results in formation of multinucleated osteoclasts and, similar to activation of TLR4, activation by CpG-ODN is dependent on TNF-α (75). Synergistic stimulation of osteoclastogenesis in RANKL-primed cells by co-treatment with either TLR3/TLR9 agonists, or TLR4/TLR9 agonists, has also been observed (86).

Since TLR2 and TLR4 are not downregulated during osteoclastogenesis (72), the role of these receptors in mature osteoclasts has been assessed. Three studies have demonstrated that activation of TLR2 with peptidoglycan from *S. aureus,* or of TLR4 with *E. coli* LPS, increases the survival of mature osteoclasts (72, 76, 99), an observation not seen by adding agonists activating TLR3 or TLR9.

It is apparent that TLRs have dual effects on osteoclastogenesis dependent on the differentiation status of osteoclasts or their progenitors. The exact molecular mechanisms causing osteoclast progenitors to respond to TLR agonists with enhanced differentiation along the osteoclastic lineage, provided the cells are primed with RANKL, and then exposed to TLR agonists in the absence of RANKL remains to be shown. Another important issue is if the dual actions also are occurring *in vivo*. It is well-documented in several experimental systems that LPS induces osteoclast formation and bone loss *in vivo*, which means that the overall effect is that of a stimulation of osteoclastogenesis.

Indirect Activation of Osteoclastogenesis by TLRs

One mechanism by which TLR activation induces osteoclast formation *in vivo* may be through the above-described mechanism, where TLR agonists directly enhance osteoclastogenesis in committed osteoclasts. Another mechanism may be due to increased expression of osteoclast-stimulating cytokines (16). These cytokines induce osteoclast formation indirectly by increasing the expression of production of RANKL in osteoblasts/osteocytes (**Figure 5**, left part). The possibility also exists that TLR agonists enhance osteoclast differentiation indirectly by regulating the production of RANKL and OPG in osteoblasts (**Figure 5**, right part). The fact that osteoblasts express TLR2, TLR4, TLR5, TLR6, and TLR9 further support such a possibility (82, 85, 100, 101).

Stimulation of TLR4 with LPS from either *E. coli* or *Actinobacillus actinomycetemcomitans* increases the mRNA expression of *Tnfsf11* in mouse calvarial osteoblasts, the osteoblastic cell line MC-3T3E1 and the stromal cell line ST-2 (100). This effect was independent of TNF-α. In contrast to activation of TLR4, activation of TLR9 with CpG-ODN does not induce *Tnfsf11* mRNA in osteoblasts, although both *E. coli* LPS and CpG-ODN stimulated the expression of TNF-α and activated NF-κB, ERK1/2 and p38 (101). Using co-cultures of osteoblasts and bone marrow macrophages from wild type mice and mice deficient in either *Tlr4* or *Tlr9*, it has been shown that both LPS and CpG-ODN stimulate osteoclast differentiation, but that the effect of CpG-ODN is more dependent on TLR9 receptors in

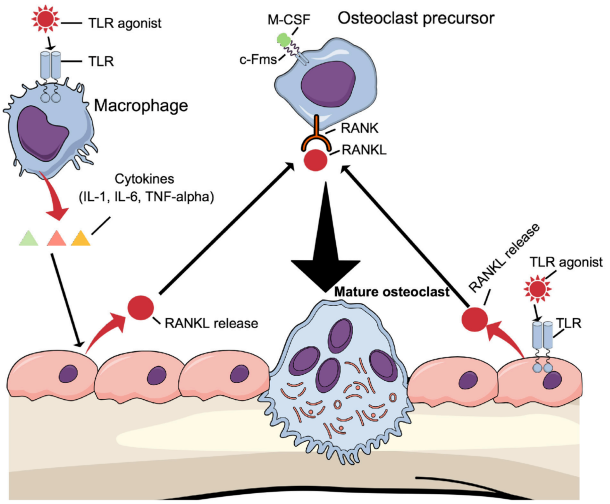

FIGURE 5 | Osteoclastogenesis can be induced indirectly by TLR agonists TLR agonists induce the expression of proinflammatory, pro-osteoclastogenic cytokines such as IL-1β, IL-6, and TNF-α by macrophages, which will bind to cytokine receptors expressed in osteoblasts causing induction of RANKL expression. Alternatively, TLR agonists bind to TLRs expressed by osteoblasts to induce RANKL expression. In both cases, RANKL will induce differentiation of osteoclast precursors to mature osteoclasts.

macrophages than those in osteoblasts (102). In contrast, the effect of LPS was dependent on TLR4 in osteoblasts.

Activation of TLR2 in mouse calvarial osteoblasts by a variety of agonists (*P. gingivalis* LPS, *S. aureus*, Pam2, Pam3, heat-killed *Listeria monocytogenes,* and lipoprotein from *Mycoplasma salivarium*) increases *Tnfsf11* mRNA expression, depending on Myd88, but independent of IL-1β, IL-6 or TNF-α, without affecting the mRNA expression of *Tnfrsf11b* (encoding OPG) (82, 83). The agonists activated NF-κB and the effect on *Tnfsf11* expression could be inhibited by Celastrol, an inhibitor of IκB kinase. A similar stimulation of *Tnfsf11* mRNA and RANKL protein, with no effect on *Tnfrsf11b* mRNA and OPG protein, was observed in mouse calvarial bones *ex vivo* stimulated by *P. gingivalis* LPS, *S. aureus* and Pam2, which resulted in increased osteoclast formation and bone resorption in the calvarial bones, independent of the IL-1β, IL-6 and TNF-α (82, 83). Treatment of mice *in vivo* with *P. gingivalis* LPS or Pam2 also resulted in increased mRNA expression of *Tnfsf11*, no effect on *Tnfrsf11b* mRNA, enhanced osteoclast formation and bone loss, effects which were absent in *Tlr2*$^{-/-}$ mice (82). Increased mRNA expression of *Tnfsf11* and soluble RANKL protein has also been observed in synovial fibroblasts from patients with rheumatoid arthritis (79).

Further support for a TLR-dependent indirect mechanism stimulating osteoclast formation comes from experiments showing that LPS, stimulating TLR4, and diacyl lipopeptide, stimulating TLR2, enhances osteoclast formation in cocultures of mouse osteoblasts and bone marrow macrophages (103). The effect on both LPS and diacyl lipopeptide, but not osteoclast formation induced by 1,25$(OH)_2$-vitamin D3, was dependent on Myd88, but not TRIF, and associated with increased mRNA expression of *Tnfsf11*, which most likely was the reason for the stimulatory effect on osteoclast formation although not formally shown.

Activation of TLR5 in mouse calvarial osteoblasts with flagellin from two different bacteria also results in increased mRNA expression of *Tnfsf11*, but, in contrast to activation of TLR2, flagellin decreases *Tnfrsf11b* mRNA in the osteoblasts (85). Stimulation of *Tnfsf11* mRNA by flagellin was dependent on Myd88, but independent on IL-1β, IL-6, and TNF-α. Similar to activation of TLR2, flagellin activated NF-κB and stimulation of *Tnfsf11* mRNA was inhibited by two different IκB kinase inhibitors. Increased *Tnfsf11* mRNA and RANKL protein, and decreased *Tnfrsf11b* mRNA and OPG protein, was also observed in mouse calvarial bones *ex vivo*, and treatment with flagellin increased osteoclast formation and bone resorption in the calvaria. A similar increase of *Tnfsf11* mRNA and decrease of *Opg* mRNA can be seen in mice treated with flagellin, causing increased osteoclast formation and extensive bone loss in wild type, but not in *Tlr5*$^{-/-}$ mice (85).

Another indirect mechanism by which TLRs can stimulate osteoclastogenesis is through TLR2-induced upregulation of the chemokine CXCL10 (104). Stimulation of mouse calvarial osteoblasts with Pam3 results in increased mRNA expression of *Cxcl10* and CXCL10 protein. When supernatants from Pam3-stimulated osteoblasts were added to RANKL-stimulated cultures of the RAW264.7 cell line it was observed that the supernatants potentiated the osteoclastogenic effect of RANKL by a mechanism that could be inhibited by antibodies neutralizing CXCL10.

CONCLUSION

Altogether, observations on osteoclast progenitors and osteoblasts, as well as findings in organ cultures and *in vivo*, demonstrate that TLRs can increase osteoclast formation and bone resorption by several mechanisms. In cell cultures, TLRs also can arrest osteoclast differentiation when acting on un-committed progenitors cells by interfering with RANKL-induced signaling. The importance of TLRs in osteoblasts and osteoclast progenitors *in vivo* must await studies using mice with cell specific deletions of different TLRs in these bone cells.

AUTHOR CONTRIBUTIONS

PS and UL wrote the manuscript and approved it for publication.

ACKNOWLEDGMENTS

The studies performed in the author's laboratory have been supported by the Swedish Research Council, the Swedish Foundation for Strategic Research, COMBINE, the ALF/LUA research grant in Gothenburg, the Lundberg Foundation, the Torsten and Ragnar Söderberg's Foundation, the Swedish

Rheumatism Association, the Royal 80 Year Fund of King Gustav V; Conselho Nacional de Desenvolvimento Científico e Tecnológico (CNPq), Science Without Borders Program (Grant #080/2012) and Sao Paulo Research Foundation (FAPESP) (Grant #2014/05283-3).

SUPPLEMENTARY MATERIAL

The Supplementary Material for this article can be found online at: https://www.frontiersin.org/articles/10.3389/fimmu.2019.01663/full#supplementary-material

REFERENCES

1. Sender R, Fuchs S, Milo R. Are we really vastly outnumbered? Revisiting the ratio of bacterial to host cells in humans. *Cell.* (2016) 164:337–40. doi: 10.1016/j.cell.2016.01.013
2. Sender R, Fuchs S, Milo R. Revised estimates for the number of human and bacteria cells in the body. *PLoS Biol.* (2016) 14:e1002533. doi: 10.1371/journal.pbio.1002533
3. Kau AL, Ahern PP, Griffin NW, Goodman AL, Gordon JI. Human nutrition, the gut microbiome and the immune system. *Nature.* (2011) 474:327–36. doi: 10.1038/nature10213
4. Sjogren K, Engdahl C, Henning P, Lerner UH, Tremaroli V, Lagerquist MK, et al. The gut microbiota regulates bone mass in mice. *J Bone Miner Res.* (2012) 27:1357–67. doi: 10.1002/jbmr.1588
5. Ohlsson C, Sjogren K. Effects of the gut microbiota on bone mass. *Trends Endocrinol Metab.* (2015) 26:69–74. doi: 10.1016/j.tem.2014.11.004
6. Hernandez CJ, Guss JD, Luna M, Goldring SR. Links between the microbiome and bone. *J Bone Miner Res.* (2016) 31:1638–46. doi: 10.1002/jbmr.2887
7. Li JY, Chassaing B, Tyagi AM, Vaccaro C, Luo T, Adams J, et al. Sex steroid deficiency-associated bone loss is microbiota dependent and prevented by probiotics. *J Clin Invest.* (2016) 126:2049–63. doi: 10.1172/JCI86062
8. Nilsson AG, Sundh D, Backhed F, Lorentzon M. *Lactobacillus reuteri* reduces bone loss in older women with low bone mineral density: a randomized, placebo-controlled, double-blind, clinical trial. *J Intern Med.* (2018) 284:307–17. doi: 10.1111/joim.12805
9. Eke PI, Wei L, Borgnakke WS, Thornton-Evans G, Zhang X, Lu H, et al. Periodontitis prevalence in adults ≥ 65 years of age, in the USA. *Periodontol 2000.* (2016). **72**:76–95. doi: 10.1111/prd.12145
10. Putnam NE, Fulbright LE, Curry JM, Ford CA, Petronglo JR, Hendrix AS, et al. MyD88 and IL-1R signaling drive antibacterial immunity and osteoclast-driven bone loss during *Staphylococcus aureus* osteomyelitis. *PLoS Pathog.* (2019) 15:e1007744. doi: 10.1371/journal.ppat.1007744
11. Verdrengh M, Carlsten H, Ohlsson C, Tarkowski A. Addition of bisphosphonate to antibiotic and anti-inflammatory treatment reduces bone resorption in experimental *Staphylococcus aureus*-induced arthritis. *J Orthop Res.* (2007) 25:304–10. doi: 10.1002/jor.20317
12. Verdrengh M, Bokarewa M, Ohlsson C, Stolina M, Tarkowski A. RANKL-targeted therapy inhibits bone resorption in experimental *Staphylococcus aureus*-induced arthritis. *Bone.* (2010) 46:752–8. doi: 10.1016/j.bone.2009.10.028
13. Wright JA, Nair SP. Interaction of staphylococci with bone. *Int J Med Microbiol.* (2010) 300:193–204. doi: 10.1016/j.ijmm.2009.10.003
14. Hausmann E, Raisz LG, Miller WA. Endotoxin: stimulation of bone resorption in tissue culture. *Science.* (1970) 168:862–4. doi: 10.1126/science.168.3933.862
15. Horton JE, Raisz LG, Simmons HA, Oppenheim JJ, Mergenhagen SE. Bone resorbing activity in supernatant fluid from cultured human peripheral blood leukocytes. *Science.* (1972) 177:793–5. doi: 10.1126/science.177.4051.793
16. Souza PP, Lerner UH. The role of cytokines in inflammatory bone loss. *Immunol Invest.* (2013) 42:555–622. doi: 10.3109/08820139.2013.822766
17. Hashimoto C, Hudson KL, Anderson KV. The toll gene of Drosophila, required for dorsal-ventral embryonic polarity, appears to encode a transmembrane protein. *Cell.* (1988) 52:269–79. doi: 10.1016/0092-8674(88)90516-8
18. Lemaitre B, Nicolas E, Michaut L, Reichhart JM, Hoffmann JA. The dorsoventral regulatory gene cassette spatzle/Toll/cactus controls the potent antifungal response in Drosophila adults. *Cell.* (1996) 86:973–83. doi: 10.1016/S0092-8674(00)80172-5
19. Medzhitov R, Preston-Hurlburt P, Janeway CAJr. A human homologue of the Drosophila Toll protein signals activation of adaptive immunity. *Nature.* (1997) 388:394–7. doi: 10.1038/41131
20. Poltorak A, He X, Smirnova I, Liu MY, Van Huffel C, Du X, et al. Defective LPS signaling in C3H/HeJ and C57BL/10ScCr mice: mutations in Tlr4 gene. *Science.* (1998) 282:2085–8. doi: 10.1126/science.282.5396.2085
21. Hayashi S, Yamada T, Tsuneto M, Yamane T, Takahashi M, Shultz LD, et al. Distinct osteoclast precursors in the bone marrow and extramedullary organs characterized by responsiveness to Toll-like receptor ligands and TNF-alpha. *J Immunol.* (2003) 171:5130–9. doi: 10.4049/jimmunol.171.10.5130
22. Liu YC, Lerner UH, Teng YT. Cytokine responses against periodontal infection: protective and destructive roles. *Periodontol 2000.* (2010) 52:163–206. doi: 10.1111/j.1600-0757.2009.00321.x
23. Udagawa N, Takahashi N, Akatsu T, Tanaka H, Sasaki T, Nishihara T, et al. Origin of osteoclasts: mature monocytes and macrophages are capable of differentiating into osteoclasts under a suitable microenvironment prepared by bone marrow-derived stromal cells. *Proc Natl Acad Sci USA.* (1990) 87:7260–4. doi: 10.1073/pnas.87.18.7260
24. Yoshida H, Hayashi S, Kunisada T, Ogawa M, Nishikawa S, Okamura H, et al. The murine mutation osteopetrosis is in the coding region of the macrophage colony stimulating factor gene. *Nature.* (1990) 345:442–4. doi: 10.1038/345442a0
25. Dai XM, Ryan GR, Hapel AJ, Dominguez MG, Russell RG, Kapp S, et al. Targeted disruption of the mouse colony-stimulating factor 1 receptor gene results in osteopetrosis, mononuclear phagocyte deficiency, increased primitive progenitor cell frequencies, and reproductive defects. *Blood.* (2002) 99:111–20. doi: 10.1182/blood.V99.1.111
26. Nakashima T, Hayashi M, Takayanagi H. New insights into osteoclastogenic signaling mechanisms. *Trends Endocrinol Metab.* (2012) 23:582–90. doi: 10.1016/j.tem.2012.05.005
27. Dougall WC, Glaccum M, Charrier K, Rohrbach K, Brasel K, De Smedt T, et al. RANK is essential for osteoclast and lymph node development. *Genes Dev.* (1999) 13:2412–24. doi: 10.1101/gad.13.18.2412
28. Theill LE, Boyle WJ, Penninger JM. RANK-L and RANK: T cells, bone loss, and mammalian evolution. *Annu Rev Immunol.* (2002) 20:795–823. doi: 10.1146/annurev.immunol.20.100301.064753
29. Nakagawa N, Kinosaki M, Yamaguchi K, Shima N, Yasuda H, Yano K, et al. RANK is the essential signaling receptor for osteoclast differentiation factor in osteoclastogenesis. *Biochem Biophys Res Commun.* (1998) 253:395–400. doi: 10.1006/bbrc.1998.9788
30. Burgess TL, Qian Y, Kaufman S, Ring BD, Van G, Capparelli C, et al. The ligand for osteoprotegerin (OPGL) directly activates mature osteoclasts. *J Cell Biol.* (1999) 145:527–38. doi: 10.1083/jcb.145.3.527
31. Hsu H, Lacey DL, Dunstan CR, Solovyev I, Colombero A, Timms E, et al. Tumor necrosis factor receptor family member RANK mediates osteoclast differentiation and activation induced by osteoprotegerin ligand. *Proc Natl Acad Sci USA.* (1999) 96:3540–5. doi: 10.1073/pnas.96.7.3540
32. Bucay N, Sarosi I, Dunstan CR, Morony S, Tarpley J, Capparelli C, et al. osteoprotegerin-deficient mice develop early onset osteoporosis and arterial calcification. *Genes Dev.* (1998) 12:1260–8. doi: 10.1101/gad.12.9.1260
33. Yasuda H, Shima N, Nakagawa N, Mochizuki SI, Yano K, Fujise N, et al. Identity of osteoclastogenesis inhibitory factor (OCIF) and osteoprotegerin (OPG): a mechanism by which OPG/OCIF inhibits osteoclastogenesis *in vitro*. *Endocrinology.* (1998) 139:1329–37. doi: 10.1210/endo.139.3.5837
34. Koga T, Inui M, Inoue K, Kim S, Suematsu A, Kobayashi E, et al. Costimulatory signals mediated by the ITAM motif cooperate with RANKL for bone homeostasis. *Nature.* (2004) 428:758–63. doi: 10.1038/nature02444
35. Peng Q, Long CL, Malhotra S, Humphrey MB. A physical interaction between the adaptor proteins DOK3 and DAP12 is required to inhibit

lipopolysaccharide signaling in macrophages. *Sci Signal.* (2013) 6:ra72. doi: 10.1126/scisignal.2003801
36. Cai X, Xing J, Long CL, Peng Q, Humphrey MB. DOK3 modulates bone remodeling by negatively regulating osteoclastogenesis and positively regulating osteoblastogenesis. *J Bone Miner Res.* (2017) 32:2207–18. doi: 10.1002/jbmr.3205
37. Satoh T, Akira S. Toll-like receptor signaling and its inducible proteins. *Microbiol Spectr.* (2016) 4. doi: 10.1128/microbiolspec.MCHD-0040-2016
38. Gay NJ, Keith FJ. Drosophila Toll and IL-1 receptor. *Nature.* (1991) 351:355–6. doi: 10.1038/351355b0
39. Kang JY, Lee JO. Structural biology of the Toll-like receptor family. *Annu Rev Biochem.* (2011) 80:917–41. doi: 10.1146/annurev-biochem-052909-141507
40. Bell JK, Mullen GE, Leifer CA, Mazzoni A, Davies DR, Segal DM. Leucine-rich repeats and pathogen recognition in Toll-like receptors. *Trends Immunol.* (2003) 24:528–33. doi: 10.1016/S1471-4906(03)00242-4
41. Chow JC, Young DW, Golenbock DT, Christ WJ, Gusovsky F. Toll-like receptor-4 mediates lipopolysaccharide-induced signal transduction. *J Biol Chem.* (1999) 274:10689–92. doi: 10.1074/jbc.274.16.10689
42. Maeshima N, Fernandez RC. Recognition of lipid A variants by the TLR4-MD-2 receptor complex. *Front Cell Infect Microbiol.* (2013) 3:3. doi: 10.3389/fcimb.2013.00003
43. Sandri S, Rodriguez D, Gomes E, Monteiro HP, Russo M, Campa A. Is serum amyloid A an endogenous TLR4 agonist? *J Leukoc Biol.* (2008) 83:1174–80. doi: 10.1189/jlb.0407203
44. Vogl T, Tenbrock K, Ludwig S, Leukert N, Ehrhardt C, Van Zoelen MA, et al. Mrp8 and Mrp14 are endogenous activators of Toll-like receptor 4, promoting lethal, endotoxin-induced shock. *Nat Med.* (2007) 13:1042–9. doi: 10.1038/nm1638
45. Stewart CR, Stuart LM, Wilkinson K, Van Gils JM, Deng J, Halle A, et al. CD36 ligands promote sterile inflammation through assembly of a Toll-like receptor 4 and 6 heterodimer. *Nat Immunol.* (2010) 11:155–61. doi: 10.1038/ni.1836
46. Botos I, Segal DM, Davies DR. The structural biology of Toll-like receptors. *Structure.* (2011) 19:447–59. doi: 10.1016/j.str.2011.02.004
47. Kim SJ, Kim HM. Dynamic lipopolysaccharide transfer cascade to TLR4/MD2 complex via LBP and CD14. *BMB Rep.* (2017) 50:55–7. doi: 10.5483/BMBRep.2017.50.2.011
48. Schroder NW, Morath S, Alexander C, Hamann L, Hartung T, Zahringer U, et al. Lipoteichoic acid (LTA) of *Streptococcus pneumoniae* and *Staphylococcus aureus* activates immune cells via Toll-like receptor (TLR)-2, lipopolysaccharide-binding protein (LBP), and CD14, whereas TLR-4 and MD-2 are not involved. *J Biol Chem.* (2003) 278:15587–94. doi: 10.1074/jbc.M212829200
49. Aliprantis AO, Yang RB, Mark MR, Suggett S, Devaux B, Radolf JD, et al. Cell activation and apoptosis by bacterial lipoproteins through toll-like receptor-2. *Science.* (1999) 285:736–9. doi: 10.1126/science.285.5428.736
50. Lien E, Sellati TJ, Yoshimura A, Flo TH, Rawadi G, Finberg RW, et al. Toll-like receptor 2 functions as a pattern recognition receptor for diverse bacterial products. *J Biol Chem.* (1999) 274:33419–25. doi: 10.1074/jbc.274.47.33419
51. Hayashi F, Smith KD, Ozinsky A, Hawn TR, Yi EC, Goodlett DR, et al. The innate immune response to bacterial flagellin is mediated by Toll-like receptor 5. *Nature.* (2001) 410:1099–103. doi: 10.1038/35074106
52. Hemmi H, Takeuchi O, Kawai T, Kaisho T, Sato S, Sanjo H, et al. A Toll-like receptor recognizes bacterial DNA. *Nature.* (2000) 408:740–5. doi: 10.1038/35047123
53. Chen N, Xia P, Li S, Zhang T, Wang TT, Zhu J. RNA sensors of the innate immune system and their detection of pathogens. *IUBMB Life.* (2017) 69:297–304. doi: 10.1002/iub.1625
54. Kurt-Jones EA, Popova L, Kwinn L, Haynes LM, Jones LP, Tripp RA, et al. Pattern recognition receptors TLR4 and CD14 mediate response to respiratory syncytial virus. *Nat Immunol.* (2000) 1:398–401. doi: 10.1038/80833
55. Chi H, Li C, Zhao FS, Zhang L, Ng TB, Jin G, et al. Anti-tumor activity of toll-like receptor 7 agonists. *Front Pharmacol.* (2017) 8:304. doi: 10.3389/fphar.2017.00304
56. Akira S, Takeda K. Toll-like receptor signalling. *Nat Rev Immunol.* (2004) 4:499–511. doi: 10.1038/nri1391
57. Takeda K, Akira S. TLR signaling pathways. *Semin Immunol.* (2004) 16:3–9. doi: 10.1016/j.smim.2003.10.003
58. West AP, Koblansky AA, Ghosh S. Recognition and signaling by toll-like receptors. *Annu Rev Cell Dev Biol.* (2006) 22:409–37. doi: 10.1146/annurev.cellbio.21.122303.115827
59. Kawai T, Akira S. Signaling to NF-kappaB by Toll-like receptors. *Trends Mol Med.* (2007) 13:460–9. doi: 10.1016/j.molmed.2007.09.002
60. Akira S, Uematsu S, Takeuchi O. Pathogen recognition and innate immunity. *Cell.* (2006) 124:783–801. doi: 10.1016/j.cell.2006.02.015
61. Tang M, Tian L, Luo G, Yu X. Interferon-gamma-mediated osteoimmunology. *Front Immunol.* (2018) 9:1508. doi: 10.3389/fimmu.2018.01508
62. Iino Y, Hopps RM. The bone-resorbing activities in tissue culture of lipopolysaccharides from the bacteria *Actinobacillus* actinomycetemcomitans, Bacteroides gingivalis and *Capnocytophaga* ochracea isolated from human mouths. *Arch Oral Biol.* (1984) 29:59–63. doi: 10.1016/0003-9969(84)90043-8
63. Ishihara Y, Nishihara T, Maki E, Noguchi T, Koga T. Role of interleukin-1 and prostaglandin in *in vitro* bone resorption induced by *Actinobacillus* actinomycetemcomitans lipopolysaccharide. *J Periodontal Res.* (1991) 26:155–60. doi: 10.1111/j.1600-0765.1991.tb01639.x
64. Amano S, Kawakami K, Iwahashi H, Kitano S, Hanazawa S. Functional role of endogenous CD14 in lipopolysaccharide-stimulated bone resorption. *J Cell Physiol.* (1997) 173:301–9.
65. Umezu A, Kaneko N, Toyama Y, Watanabe Y, Itoh H. Appearance of osteoclasts by injections of lipopolysaccharides in rat periodontal tissue. *J Periodontal Res.* (1989) 24:378–83. doi: 10.1111/j.1600-0765.1989.tb00886.x
66. Orcel P, Feuga M, Bielakoff J, De Vernejoul MC. Local bone injections of LPS and M-CSF increase bone resorption by different pathways *in vivo* in rats. *Am J Physiol.* (1993) 264:E391–7. doi: 10.1152/ajpendo.1993.264.3.E391
67. Abu-Amer Y, Ross FP, Edwards J, Teitelbaum SL. Lipopolysaccharide-stimulated osteoclastogenesis is mediated by tumor necrosis factor via its P55 receptor. *J Clin Invest.* (1997) 100:1557–65. doi: 10.1172/JCI119679
68. Hou L, Sasaki H, Stashenko P. Toll-like receptor 4-deficient mice have reduced bone destruction following mixed anaerobic infection. *Infect Immun.* (2000) 68:4681–7. doi: 10.1128/IAI.68.8.4681-4687.2000
69. Nakamura H, Fukusaki Y, Yoshimura A, Shiraishi C, Kishimoto M, Kaneko T, et al. Lack of Toll-like receptor 4 decreases lipopolysaccharide-induced bone resorption in C3H/HeJ mice in vivo. *Oral Microbiol Immunol.* (2008) 23:190–5. doi: 10.1111/j.1399-302X.2007.00410.x
70. Burns E, Bachrach G, Shapira L, Nussbaum G. Cutting edge: TLR2 is required for the innate response to *Porphyromonas gingivalis*: activation leads to bacterial persistence and TLR2 deficiency attenuates induced alveolar bone resorption. *J Immunol.* (2006) 177:8296–300. doi: 10.4049/jimmunol.177.12.8296
71. Lin J, Bi L, Yu X, Kawai T, Taubman MA, Shen B, et al. *Porphyromonas gingivalis* exacerbates ligature-induced, RANKL-dependent alveolar bone resorption via differential regulation of Toll-like receptor 2 (TLR2) and TLR4. *Infect Immun.* (2014) 82:4127–34. doi: 10.1128/IAI.02084-14
72. Takami M, Kim N, Rho J, Choi Y. Stimulation by toll-like receptors inhibits osteoclast differentiation. *J Immunol.* (2002) 169:1516–23. doi: 10.4049/jimmunol.169.3.1516
73. Bar-Shavit Z. Taking a toll on the bones: regulation of bone metabolism by innate immune regulators. *Autoimmunity.* (2008) 41:195–203. doi: 10.1080/08916930701694469
74. Zhang P, Liu J, Xu Q, Harber G, Feng X, Michalek SM, et al. TLR2-dependent modulation of osteoclastogenesis by *Porphyromonas gingivalis* through differential induction of NFATc1 and NF-kappaB. *J Biol Chem.* (2011) 286:24159–69. doi: 10.1074/jbc.M110.198085
75. Zou W, Schwartz H, Endres S, Hartmann G, Bar-Shavit Z. CpG oligonucleotides: novel regulators of osteoclast differentiation. *FASEB J.* (2002) 16:274–82. doi: 10.1096/fj.01-0586com
76. Liu J, Wang S, Zhang P, Said-Al-Naief N, Michalek SM, Feng X. Molecular mechanism of the bifunctional role of lipopolysaccharide in osteoclastogenesis. *J Biol Chem.* (2009) 284:12512–23. doi: 10.1074/jbc.M809789200
77. Grigoriadis AE, Wang ZQ, Cecchini MG, Hofstetter W, Felix R, Fleisch HA, et al. c-Fos: a key regulator of osteoclast-macrophage

lineage determination and bone remodeling. *Science.* (1994) 266:443–8. doi: 10.1126/science.7939685
78. Asagiri M, Sato K, Usami T, Ochi S, Nishina H, Yoshida H, et al. Autoamplification of NFATc1 expression determines its essential role in bone homeostasis. *J Exp Med.* (2005) 202:1261–9. doi: 10.1084/jem.20051150
79. Kim KW, Kim BM, Won JY, Lee KA, Kim HR, Lee SH. Toll-like receptor 7 regulates osteoclastogenesis in rheumatoid arthritis. *J Biochem.* (2019). doi: 10.1093/jb/mvz033. [Epub ahead of print].
80. Yang J, Ryu YH, Yun CH, Han SH. Impaired osteoclastogenesis by staphylococcal lipoteichoic acid through Toll-like receptor 2 with partial involvement of MyD88. *J Leukoc Biol.* (2009) 86:823–31. doi: 10.1189/jlb.0309206
81. Chen Z, Su L, Xu Q, Katz J, Michalek SM, Fan M, et al. IL-1R/TLR2 through MyD88 divergently modulates osteoclastogenesis through regulation of nuclear factor of activated T Cells c1 (NFATc1) and B lymphocyte-induced maturation protein-1 (Blimp1). *J Biol Chem.* (2015) 290:30163–74. doi: 10.1074/jbc.M115.663518
82. Kassem A, Henning P, Lundberg P, Souza PP, Lindholm C, Lerner UH. *Porphyromonas gingivalis* stimulates bone resorption by enhancing RANKL (receptor activator of NF-kappaB ligand) through activation of toll-like receptor 2 in osteoblasts. *J Biol Chem.* (2015) 290:20147–58. doi: 10.1074/jbc.M115.655787
83. Kassem A, Lindholm C, Lerner UH. Toll-like receptor 2 stimulation of osteoblasts mediates *Staphylococcus aureus* induced bone resorption and osteoclastogenesis through enhanced RANKL. *PLoS ONE.* (2016) 11:e0156708. doi: 10.1371/journal.pone.0156708
84. Ji JD, Park-Min KH, Shen Z, Fajardo RJ, Goldring SR, Mchugh KP, et al. Inhibition of RANK expression and osteoclastogenesis by TLRs and IFN-gamma in human osteoclast precursors. *J Immunol.* (2009) 183:7223–33. doi: 10.4049/jimmunol.0900072
85. Kassem A, Henning P, Kindlund B, Lindholm C, Lerner UH. TLR5, a novel mediator of innate immunity-induced osteoclastogenesis and bone loss. *FASEB J.* (2015) 29:4449–60. doi: 10.1096/fj.15-272559
86. Krisher T, Bar-Shavit Z. Regulation of osteoclastogenesis by integrated signals from toll-like receptors. *J Cell Biochem.* (2014) 115:2146–54. doi: 10.1002/jcb.24891
87. Okamoto K, Nakashima T, Shinohara M, Negishi-Koga T, Komatsu N, Terashima A, et al. Osteoimmunology: the conceptual framework unifying the immune and skeletal systems. *Physiol Rev.* (2017) 97:1295–349. doi: 10.1152/physrev.00036.2016
88. Amcheslavsky A, Bar-Shavit Z. Toll-like receptor 9 ligand blocks osteoclast differentiation through induction of phosphatase. *J Bone Miner Res.* (2007) 22:1301–10. doi: 10.1359/jbmr.070501
89. Cheng N, He R, Tian J, Ye PP, Ye RD. Cutting edge: TLR2 is a functional receptor for acute-phase serum amyloid A. *J Immunol.* (2008) 181:22–6. doi: 10.4049/jimmunol.181.1.22
90. Oh E, Lee HY, Kim HJ, Park YJ, Seo JK, Park JS, et al. Serum amyloid A inhibits RANKL-induced osteoclast formation. *Exp Mol Med.* (2015) 47:e194. doi: 10.1038/emm.2015.83
91. Amcheslavsky A, Bar-Shavit Z. Interleukin (IL)-12 mediates the anti-osteoclastogenic activity of CpG-oligodeoxynucleotides. *J Cell Physiol.* (2006) 207:244–50. doi: 10.1002/jcp.20563
92. Horwood NJ, Elliott J, Martin TJ, Gillespie MT. IL-12 alone and in synergy with IL-18 inhibits osteoclast formation *in vitro*. *J Immunol.* (2001) 166:4915–21. doi: 10.4049/jimmunol.166.8.4915
93. Takayanagi H, Kim S, Matsuo K, Suzuki H, Suzuki T, Sato K, et al. RANKL maintains bone homeostasis through c-Fos-dependent induction of interferon-beta. *Nature.* (2002) 416:744–9. doi: 10.1038/416744a
94. Kwon JO, Jin WJ, Kim B, Ha H, Kim HH, Lee ZH. Haptoglobin acts as a TLR4 ligand to suppress osteoclastogenesis via the TLR4-IFN-beta axis. *J Immunol.* (2019) 202:3359–69. doi: 10.4049/jimmunol.1800661
95. Lee B, Kim TH, Jun JB, Yoo DH, Woo JH, Choi SJ, et al. Direct inhibition of human RANK+ osteoclast precursors identifies a homeostatic function of IL-1beta. *J Immunol.* (2010) 185:5926–34. doi: 10.4049/jimmunol.1001591
96. Nair SP, Meghji S, Wilson M, Reddi K, White P, Henderson B. Bacterially induced bone destruction: mechanisms and misconceptions. *Infect Immun.* (1996) 64:2371–80.
97. Zou W, Bar-Shavit Z. Dual modulation of osteoclast differentiation by lipopolysaccharide. *J Bone Miner Res.* (2002) 17:1211–8. doi: 10.1359/jbmr.2002.17.7.1211
98. Kim J, Yang J, Park OJ, Kang SS, Kim WS, Kurokawa K, et al. Lipoproteins are an important bacterial component responsible for bone destruction through the induction of osteoclast differentiation and activation. *J Bone Miner Res.* (2013) 28:2381–91. doi: 10.1002/jbmr.1973
99. Itoh K, Udagawa N, Kobayashi K, Suda K, Li X, Takami M, et al. Lipopolysaccharide promotes the survival of osteoclasts via Toll-like receptor 4, but cytokine production of osteoclasts in response to lipopolysaccharide is different from that of macrophages. *J Immunol.* (2003) 170:3688–95. doi: 10.4049/jimmunol.170.7.3688
100. Kikuchi T, Matsuguchi T, Tsuboi N, Mitani A, Tanaka S, Matsuoka M, et al. Gene expression of osteoclast differentiation factor is induced by lipopolysaccharide in mouse osteoblasts via Toll-like receptors. *J Immunol.* (2001) 166:3574–9. doi: 10.4049/jimmunol.166.5.3574
101. Zou W, Amcheslavsky A, Bar-Shavit Z. CpG oligodeoxynucleotides modulate the osteoclastogenic activity of osteoblasts via Toll-like receptor 9. *J Biol Chem.* (2003) 278:16732–40. doi: 10.1074/jbc.M212473200
102. Amcheslavsky A, Hemmi H, Akira S, Bar-Shavit Z. Differential contribution of osteoclast- and osteoblast-lineage cells to CpG-oligodeoxynucleotide (CpG-ODN) modulation of osteoclastogenesis. *J Bone Miner Res.* (2005) 20:1692–9. doi: 10.1359/JBMR.050515
103. Sato N, Takahashi N, Suda K, Nakamura M, Yamaki M, Ninomiya T, et al. MyD88 but not TRIF is essential for osteoclastogenesis induced by lipopolysaccharide, diacyl lipopeptide, and IL-1alpha. *J Exp Med.* (2004) 200:601–11. doi: 10.1084/jem.20040689
104. Modinger Y, Rapp A, Pazmandi J, Vikman A, Holzmann K, Haffner-Luntzer M, et al. C5aR1 interacts with TLR2 in osteoblasts and stimulates the osteoclast-inducing chemokine CXCL10. *J Cell Mol Med.* (2018) 22:6002–14. doi: 10.1111/jcmm.13873

Conflict of Interest Statement: The authors declare that the research was conducted in the absence of any commercial or financial relationships that could be construed as a potential conflict of interest.

frontiers in Immunology

REVIEW
published: 18 July 2019
doi: 10.3389/fimmu.2019.01664

Osteoimmunology of Oral and Maxillofacial Diseases: Translational Applications Based on Biological Mechanisms

*Carla Alvarez[1,2], Gustavo Monasterio[2], Franco Cavalla[3], Luis A. Córdova[4], Marcela Hernández[2], Dominique Heymann[5], Gustavo P. Garlet[6], Timo Sorsa[7,8], Pirjo Pärnänen[7], Hsi-Ming Lee[9], Lorne M. Golub[9], Rolando Vernal[2,10] and Alpdogan Kantarci[1]**

[1] Forsyth Institute, Cambridge, MA, United States, [2] Periodontal Biology Laboratory, Faculty of Dentistry, Universidad de Chile, Santiago, Chile, [3] Department of Conservative Dentistry, Faculty of Dentistry, Universidad de Chile, Santiago, Chile, [4] Department of Oral and Maxillofacial Surgery, Faculty of Dentistry, San Jose's Hospital and Clínica Las Condes, Universidad de Chile, Santiago, Chile, [5] INSERM, UMR 1232, LabCT, CRCINA, Institut de Cancérologie de l'Ouest, Université de Nantes, Université d'Angers, Saint-Herblain, France, [6] Department of Biological Sciences, Bauru School of Dentistry, University of São Paulo, Bauru, Brazil, [7] Department of Oral and Maxillofacial Diseases, University of Helsinki, Helsinki University Hospital, Helsinki, Finland, [8] Department of Oral Diseases, Karolinska Institutet, Stockholm, Sweden, [9] Department of Oral Biology and Pathology, School of Dental Medicine, Stony Brook University, Stony Brook, NY, United States, [10] Dentistry Unit, Faculty of Health Sciences, Universidad Autónoma de Chile, Santiago, Chile

OPEN ACCESS

Edited by:
Teun J. De Vries, VU University Amsterdam, Netherlands

Reviewed by:
Dana T. Graves, University of Pennsylvania, United States
Jérôme Bouchet, Université Paris Descartes, France

***Correspondence:**
Alpdogan Kantarci
akantarci@forsyth.org

Specialty section:
This article was submitted to Inflammation, a section of the journal Frontiers in Immunology

Received: *27 December 2018*
Accepted: *03 July 2019*
Published: *18 July 2019*

Citation:
Alvarez C, Monasterio G, Cavalla F, Córdova LA, Hernández M, Heymann D, Garlet GP, Sorsa T, Pärnänen P, Lee H-M, Golub LM, Vernal R and Kantarci A (2019) Osteoimmunology of Oral and Maxillofacial Diseases: Translational Applications Based on Biological Mechanisms. Front. Immunol. 10:1664. doi: 10.3389/fimmu.2019.01664

The maxillofacial skeleton is highly dynamic and requires a constant equilibrium between the bone resorption and bone formation. The field of osteoimmunology explores the interactions between bone metabolism and the immune response, providing a context to study the complex cellular and molecular networks involved in oro-maxillofacial osteolytic diseases. In this review, we present a framework for understanding the potential mechanisms underlying the immuno-pathobiology in etiologically-diverse diseases that affect the oral and maxillofacial region and share bone destruction as their common clinical outcome. These otherwise different pathologies share similar inflammatory pathways mediated by central cellular players, such as macrophages, T and B cells, that promote the differentiation and activation of osteoclasts, ineffective or insufficient bone apposition by osteoblasts, and the continuous production of osteoclastogenic signals by immune and local stromal cells. We also present the potential translational applications of this knowledge based on the biological mechanisms involved in the inflammation-induced bone destruction. Such applications can be the development of immune-based therapies that promote bone healing/regeneration, the identification of host-derived inflammatory/collagenolytic biomarkers as diagnostics tools, the assessment of links between oral and systemic diseases; and the characterization of genetic polymorphisms in immune or bone-related genes that will help diagnosis of susceptible individuals.

Keywords: osteoimmunology, oral, maxillofacial, periodontal disease, biomarkers

INTRODUCTION

The maxillofacial skeletal structure has a complex geometry, adapted to the high mechanical requirements of the masticatory function. In this complex system, the alveolar bone accommodates the teeth and periodontal tissues while the basal bone provides support and insertion of masticatory muscles. Also, the mandible has two bilateral vertical rami that articulate with the base of the skull to form the temporomandibular joint (TMJ). Under physiological conditions, the bone undergoes continuous remodeling in a dynamic equilibrium of bone resorption by osteoclasts and bone formation by osteoblasts, at anatomically discrete sites known as basic multicellular units (BMUs) (1). Tight control of bone remodeling at the BMUs level is necessary to conserve structural integrity as the formation component needs to replace the exact amount removed by resorption. The strict synchronization of bone resorption and formation is referred to as coupling, a term that applies to each BMUs along with the skeleton (2). Bone coupling is controlled through a complex cellular communication network regulated by the signaling between osteoblasts, their mesenchymal pre-osteoblastic precursors, osteocytes, and osteoclasts and their monocytic precursors (1). Although circulating hormones, including PTH and 1,25-dihydroxyvitamin-D3, are considered to be the critical regulators of bone remodeling, it has become clear that locally generated cytokines are the key modulators of bone-cells communication and function (2).

The field of osteoimmunology has provided insight into the mechanics of osteoclast differentiation and activation during inflammation by immune cells and their soluble products. This process is fundamentally regulated by a triad of proteins of the tumor necrosis factor/tumor necrosis factor receptor family namely the receptor activator of nuclear factor κB ligand (RANKL), its functional receptor (RANK), and its soluble decoy receptor osteoprotegerin (OPG). Both soluble and membrane-bound RANKL can induce osteoclastogenesis through RANK in osteoclast precursors. Meanwhile, OPG inhibits the interaction between RANKL and RANK, and arrests osteoclastogenesis (3, 4). Under homeostatic conditions, RANKL is produced mainly by osteocytes, which have a higher capacity to support osteoclastogenesis than osteoblasts and are essentials for bone remodeling (5, 6). Interestingly, osteoblasts also produce RANKL which acts as an acceptor for vesicular RANK produced by mature osteoclasts. The osteoblastic RANKL-RANK cross-linking triggers RANKL reverse signaling, which promotes bone formation through the increased expression of early regulators of osteoblast differentiation (7). Under inflammatory conditions, however, the sources of RANKL are increased; immune cells such as particular subtypes of T cells and B cells can also produce RANKL (8). In addition, the local secretion of pro-inflammatory cytokines, such as IL-17 can induce the production of RANKL by osteoblasts and fibroblasts with osteoclastogenic capacity (9) suggesting a highly complex network of cellular origins of RANKL activity in tissues induced by inflammation.

In addition to osteoclast differentiation, inflammation impacts bone formation. Anabolic bone apposition is generally sustained by the expression of different growth factors such as fibroblast growth factors (FGFs), platelet-derived growth factors (PDGFs), insulin-like growth factors (IGFs), tumor growth factor β (TGF-β), bone morphogenetic proteins (BMPs), and Wnt proteins, released from the bone matrix or produced locally by different cell types (10–14). In particular, the Wnt/β-catenin and Bmp/Runx2 signaling pathways are essential for bone mass maintenance by regulating the differentiation and anabolic bone-formation activity of osteoblasts and osteocytes (15, 16). However, during inflammation, the activation of the classical (or canonical) NF-κB pathway inhibits the production of bone matrix proteins by decreasing the Bmp2-stimulated Runx2 and Wnt-stimulated β-catenin binding to osteocalcin and bone sialoprotein promoters (12). Inflammation also induces the production of the Wnt/β-catenin pathway inhibitors Dickkopf factor-1 (DKK1) and sclerotin (17, 18). The decline of inflammation restores the osteoblast functions by activating the canonical Wnt/β-catenin pathway (19), which has been shown to up-regulate OPG expression and inhibit osteoclast differentiation (20). Accumulating evidence, therefore, points to the failure of endogenous inflammation-resolution pathways as an underlying factor in the initiation and progression of chronic osteolytic inflammatory diseases and their relationship with systemic diseases.

In osteolytic inflammatory diseases such as periodontal disease, apical periodontitis, maxillofacial bone sarcomas and osteoarthritis of the TMJ, inflammation results in tissue destruction by the continuous release of osteoclastogenic mediators that counteract the production of bone-coupling signals. These otherwise different diseases share similar inflammatory pathways mediated by central cellular players, such as macrophages, T and B cells, that promote the differentiation and activation of osteoclasts, ineffective or insufficient bone apposition by osteoblasts, and the continuous production of osteoclastogenic signals by immune and local stromal cells. In the present review, we focused on the immune pathways that lead to the clinical signs of bone loss in different oro-maxillofacial diseases and possible translational applications of this knowledge.

PERIODONTAL DISEASE

Definition and Pathogenesis of the Periodontal Disease

Among the osteolytic chronic inflammatory disorders of the jaws, periodontitis is the most well-defined and studied. The mechanisms underlying the pathogenesis of periodontitis are complex as periodontitis is a multifactorial disease that requires the combination of both a susceptible host and a dysbiotic polymicrobial community (21). Periodontitis is a significant public health problem due to its high prevalence, its cause of tooth loss, and its association with systemic diseases (22). Host susceptibility to periodontal diseases is the combination of genetic, epigenetic, behavioral, and environmental factors that modulate the immune response and the conditions of maintenance of the microbial community that colonizes the pathogenic biofilm (23, 24). The periodontitis-associated

microbial communities not only stimulate but also exploit inflammation as a way to obtain nutrients for growth and persistence. The virulence factors of the bacteria can inhibit the antimicrobial functions and promote the pro-inflammatory and tissue-destructive properties of the host immune response to escape annihilation; consequently exacerbating and perpetuating the disease (21, 25). Thus, the interactions between the host and the microorganisms in periodontal disease are not only complex but also evolving.

Cellular and the Molecular Immune Basis of the Periodontal Disease

The immune response during periodontitis involves different elements of innate and adaptive immunity. One of the first responders during the pathogenesis of periodontitis is the complement system, first recognized in early clinical studies that associated the disease with the presence of activated complement fragments in the gingival crevicular fluid (GCF) (26, 27). The use of animal models helped to clarify the role of complement-related mechanisms during periodontitis and alveolar bone loss (26, 28). These studies have highlighted the synergistic cross-talk of the complement with TLR pathways. For example, the activation of both C5aR1 and TLR2 by specific agonists resulted in the induction of significantly higher levels of pro-inflammatory cytokines in the gingiva (28). Mice lacking C5aR1 are resistant to bone-destructive diseases such as periodontitis and arthritis (29, 30), attributed to the critical role of the anaphylatoxin receptors in initiating neutrophils and macrophages adhesion and recruitment, necessary for the induction of bone resorption (31). Also, *P. gingivalis* targets C5aR to promote its adaptive fitness by manipulating the activation of TLR2 via the C5a-C5aR axis, allowing it to escape the IL-12p70-dependent immune clearance. This C5aR1-dependent evasion mechanism is crucial for the induction of microbial dysbiosis (29, 32).

Periodontal health is particularly sensitive to neutrophil functions and dysfunctions. Both hyper- and hypo-responsiveness of neutrophils have been associated with dysregulated inflammatory response and bone loss (33). Rare diseases related to defective extravasation of circulating neutrophils (LAD-1 deficiency) or neutrophil functionality (Papillon-Lefèvre syndrome) display a severe and fast-progressive form of periodontitis (34). If neutrophils cannot reach the gingiva, there is an overproduction of IL-23, IL-17, and G-CSF in the periodontium, attributed to macrophages, which in turn induces further inflammation and osteoclastogenesis (35). *P. gingivalis* possesses virulence factors that disrupt the neutrophil responses. For example, the LPS-induced TLR2 activation and cross-talk with C5aR inhibits the Myd88 but activates the Mal-PI3K pathway; this abolishes the antimicrobial response and PI3K-mediated phagocytosis while triggering the Mal-dependent inflammation (36). *P. gingivalis* can inhibit opsonization and phagocytosis, enhance neutrophil recruitment and respiratory burst, thus incrementing the neutrophil-associated inflammation and tissue damage (37). Neutrophils may also possess a hyper-inflammatory phenotype characterized by the over-expression of reactive oxygen species and pro-inflammatory cytokines (IL-1β, IL-6, IL-8, and TNF-α), which along with their other defective functions such as phagocytosis and chemotaxis, contribute to additional tissue-damage and comorbidity with other inflammatory diseases (38, 39). In the context of osteoimmunological regulation of periodontal diseases, neutrophils display heterotypic adhesion to osteoblast and modulate their function (40) and possess a regulatory role during microbial infection by secreting the anti-inflammatory cytokine IL-10 (41). Neutrophils acquire regulatory functions by direct cell-to-cell contact with regulatory T (Treg) cells or by exogenous IL-10 stimuli. The IL-10-producing neutrophils have been found in the purulent exudate collected from periodontal pockets in patients with chronic periodontitis; their role in the resolution of periodontal inflammation still needs to be investigated (42).

Even though macrophages are in low quantities in periodontal tissues (43), they participate in the pathogenesis of periodontitis as central players by initiating or resolving inflammation, contributing to tissue repair, activating lymphocyte-mediated adaptive immunity and mediating alveolar bone resorption and apposition (44). During inflammation, tissue-resident macrophages are expanded, and circulating monocytes are recruited to be differentiated into macrophage-like cells (45). Macrophages are divided into two functionally different subtypes: M1 classically-activated macrophages, produced in response to IFN-γ, TNF-α, IL-1β, and IL-6, with pro-inflammatory, antibacterial and antiviral functions; M2 alternatively-activated macrophages, produced in response to IL-4 and IL-13, with anti-inflammatory and tissue-repair/regeneration functions that expresses high levels of IL-10 (46–48). While these classes are clearly defined in mice; in humans, macrophages represent a continuum of highly plastic effector cells, resembling a spectrum of diverse phenotype states (47). Both M1 and M2 macrophages are increased in periodontitis compared to controls, yet the M1/M2 ratio is higher in periodontitis and is associated with increased expression of M1-related molecules such as IL-1β, IL-6 and matrix metalloproteinase (MMP)-9 (48, 49). Circulating monocytes/macrophages are affected by experimental periodontitis and display an M1 phenotype by overexpressing TNF-α and IL-6 (50). The temporal analysis of inflammation to healing osteolytic periodontal lesions showed a shift in the macrophage activation from inflammatory (CD80 and TNF-α expression) to resolving (CD206 expression) phenotype, which correlated to bone loss (51).

Lymphocytes are the majority of all $CD45^+$ hematopoietic-origin cells within the normal gingival mucosa (43) and play a key role in osteoimmunology. The $CD3^+$ T cell compartment is the dominant population in both health and disease, reflecting a 10-fold increase in total inflammatory cells (43). The analysis of alveolar bone resorption during *P. gingivalis*-induced experimental periodontitis in MHC-I or MHC-II deficient mice showed the destructive role for $CD4^+$ T cells (52); yet effector-memory $CD8^+$ T cells are present in normal gingival mucosa (43) suggesting a protective role for $CD8^+$ T cells during periodontitis possibly due their ability to suppress osteoclastogenesis (53). Upon activation by

the APCs, $CD4^+$ T cells are polarized into distinct effector phenotypes depending on the nature of the antigen, co-stimulatory signals, and the local cytokine milieu (22). These phenotypes are Th1, Th2, Th9, Th17, Th22, and Treg, each with a particular transcription factor, often called a master switch, that modulates the phenotypic differentiation and particular effector-functions making these phenotypes highly plastic (54). Each phenotype has different involvement in the pathogenesis of periodontitis. They can be broadly classified in two axes: (1) Th1/Th17 pro-inflammatory and osteoclastogenic and (2) Th2/Treg mechanistically implied in the arrest of the disease and progression (55). Th9 and Th22, which are relatively new-subsets, have been scantily characterized in periodontal disease. Th22 cells were increased in gingival biopsies in periodontitis, associated with the increased osteoclastic activity, and triggered upon stimulation with the periodontal pathogen *Aggregatibacter actinomycetemcomitans* (56, 57).

Th1 cells produce pro-inflammatory cytokines such as IFN-γ, IL-12, IL-1β, and TNF-α, under the control of the transcription factor T-bet (22). The Th1-type of response, mediated by the production of IFN-γ, is necessary for both the control of microbial invasion and bone loss. The induction of periodontitis with *A. actinomycetemcomitans* in IFN-γ-deficient mice resulted in a less severe bone loss but impaired host defense against the microbial challenge, followed by a disseminated bacterial infection and mice death (58). *P. gingivalis* promotes the expression of type-1 interferons by disrupting innate immunological functions through degradation of Myd88, resulting in a constitutively priming of $CD4^+$ T-cells by dendritic cells and leading to elevated IFN-γ and RANKL expression associated with increased alveolar bone loss. Blocking type-I IFN signaling prevented the destructive Th1 immune response and alveolar bone loss (59).

Th17 cells are the most osteoclastogenic type of T-cells, directly expressing and inducing RANKL expression on resident cells through IL-17 production, and necessary to sustain the host defense against the dysbiotic microbial community. Th17 cells produce IL-17A, IL-17F, and IL-22, under the control of the master switch RORγ, and the critical participation of the transcription factor STAT3 (60). In healthy individuals, Th17 cells naturally accumulate in the gingival mucosa with age and promote barrier defense. This growth depends on mechanical stimulation, such as chewing, which induces the production of IL-6 in epithelial cells, and is independent of commensal bacteria (61). The expansion of the Th17 cells during periodontitis, on the other hand, is dependent on microbial dysbiosis and requires both IL-6 and IL-23 production (62). These are predominantly resident memory Th17 cells, capable of quick responses and the primary producers of IL-17. A recent study in mice confirmed that IL-17 producing Th17 cells rather than γδT cells are involved in bone damage during periodontitis. IL-17 production is necessary for host defense against the invasion of oral bacteria (9). Also, a significant proportion of the IL-17 producing Th17 cells were exFoxp3Th17, cells that expressed high amounts of membrane-bound RANKL, suggesting that at some point, these cells might have had regulatory functions (9). Accordingly, patients with autosomal-dominant STAT3 deficiency (AD-HIES), are less susceptible to periodontitis (62).

The Th2 and Treg type of responses are implicated in the resolution of periodontitis (63). Th2 cells produce IL-4, IL-5, and IL-13, and mediate humoral immunity and mast cell activation in allergic reactions (22). Treg cells produce IL-10 and TGF-β and are crucial for the maintenance of immune homeostasis and tissue repair under the control of the master switch Foxp3 (64). Tregs inhibit osteoclast differentiation and their bone resorptive activity through the interaction of CTLA-4 with CD80/86 on osteoclasts and their precursors (29). Both Th2 and Treg cells express the chemokine receptor CCR4. The induction of periodontitis in $CCR4^{-/-}$ mice presented a significant deficiency of Treg migration, associated with increased inflammatory alveolar bone loss (63).

B cells are practically not present in normal gingival mucosa (43), but they dramatically increase as the disease progresses, making it a distinct feature of the established periodontal lesion (22). During periodontitis, stromal cells and immune cells express different cytokines and chemokines such as IL-4, IL6, IL-5, CXCL13, and APRIL that induce B cell migration and support their survival in the periodontium (65, 66). Patients with periodontitis have a significantly higher percentage of $CD19^+CD27^+CD382^-$ memory B cells and $CD138^+HLA\text{-}DR^{low}$ plasma cells while B1 cells, which have been previously described as a regulatory type of B cell ($CD20^+CD69^-CD43^+CD27^+CD11b^+$) are decreased (67, 68). B cells/plasma cells are well-known for their humoral immunity. However, periodontitis progresses despite the presence of B cells and the induction of humoral responses against periodontal bacteria. The B cell-mediated IgG-dominant immune response might contribute to the pathogenesis of periodontitis (65, 68). Most infiltrating B cells present during periodontitis produce RANKL, suggesting that they can directly induce osteoclastogenesis (8). Indeed, the induction of experimental periodontitis in B cell-deficient mice showed significantly less bone loss (65). Latest data demonstrated the existence of a regulatory B cell subtype (Bregs) that can inhibit inflammation and support Treg differentiation through their production of IL-10. Bregs cells in humans have been identified as both $CD19^+CD24^{hi}CD38^{hi}CD1d^{hi}$ and $CD19^+CD24^{hi}CD27^+$ cells (69). In mice, the functional IL-10-producing subset of Bregs, B10, have bone protective roles during periodontitis (70).

Osteoimmunological Processes in the Periodontal Disease

The periodontium offers a unique environment to understand the interactions between the immune system and bone since it combines mucosal and skeletal tissues and the interaction between the host and the oral microbiota (21). The alveolar bone is susceptible to different types of mechanical stress and is continuously remodeled by the coupled action of osteoclasts and osteoblasts within the bone surface (3, 71). As reviewed above, the immune response caused by the dysbiotic microbiota during periodontitis dramatically enhances the production of

local RANKL by different immune cell types such as Th17 and B cells. However, recent studies with specific cell type-depleted animals have highlighted the impact of RANKL production by osteocytes, osteoblasts, and periodontal ligament cells on osteoclast differentiation and alveolar bone loss (72). Osteocytes respond to inflammation, specifically to IL-6 and IL-17, by producing RANKL and increasing their osteoclastogenesis (73, 74). In a *P. gingivalis* and *Fusobacterium nucleatum*-induced periodontitis model, the genetic depletion of RANKL in osteocytes decreased the alveolar bone destruction and osteoclast differentiation (75). Osteocytes react to *P. gingivalis* LPS by producing sclerostin, which reduces osteoblastic bone formation by inhibiting the Wnt/β catenin signaling pathway (76).

Osteoblasts and periodontal ligament cells also respond to IL-17, producing RANKL, and decreasing OPG production (77). The osteoblastic inflammatory-mediated RANKL production depends on the activation of the classical NF-κB pathway. The inhibition of NF-κB activation in osteoblastic lineage cells in mice reduces osteoclast numbers and RANKL expression induced by periodontal infection (72). Specific genetic depletion of RANKL production in osteoblasts and periodontal ligament cells during ligature-induced periodontitis reduces the alveolar bone resorption in an even greater extent that the RANKL depletion on $CD4^+$ cells (9). Osteocytes, osteoblasts, and periodontal ligament cells significantly contribute to osteoclastogenesis during periodontitis by translating inflammatory signals into RANKL overexpression, often paired with OPG downregulation. This process results in the disruption of the coupling of bone resorption and apposition (**Figure 1**) (77). A recent study further demonstrated that bone matrix-derived products activate the NLRP3 inflammasome and stimulate osteoclast differentiation (78). The intracellular multi-protein complex known as the inflammasome functions as a molecular platform that triggers the activation of caspase-1, necessary to proteolytically process the biologically inactive form of IL-1β and IL-18 into mature cytokines. This conversion is key since RANKL acts in concert with TNF-α or IL-1β to regulate osteoclastogenesis (79).

Translational Applications

Systematic approaches to control inflammation through immune modulation have been applied in different animal models of periodontal disease with the potential for translational applications. For instance, the blockade of the complement cascade at an earlier level, by the inhibition of C3 with AMY-101 (Cp40), is effective in a non-human primate model of periodontitis (80). This model is significantly more predictive of drug efficacy in a clinical setting since complement blockage inhibits inflammation in naturally occurring periodontitis (81). In murine models, the local delivery of CCL2 by control-delivered microparticles promoted the recruitment and differentiation of M2 macrophages, which in turn prevented alveolar bone loss (82). Similarly, the administration of CCL22-releasing microparticles prevented inflammatory bone loss by inducing the selective chemo-attraction of Treg in both murine and canine models of periodontitis (63). Rosiglitazone, a peroxisome proliferator-activated receptor (PPAR)-γ agonist, induced resolving macrophages with an M2-like phenotype that reduce bone resorption and enhance bone formation (51). The treatment with all-trans-retinoic acid or the synthetic retinoic acid receptor (RAR) agonist tamibarotene (Am80) improved the Th17/Treg balance and decreased the alveolar bone loss during periodontitis (83, 84). The treatment with RvD2 (a resolution agonist) prevented alveolar bone loss by inhibiting the systemic and gingival Th1-type of response in *P. gingivalis*-induced periodontitis (85). *In vivo* inhibition of Th17 differentiation by knocking *Stat3* or pharmaceutically inhibiting *Rorc* in $CD4^+$ T cells led to significantly reduced alveolar-bone loss (up to 70%), reflecting their critical role in the induction of bone resorption by producing IL-17 and expressing RANKL (9). The antibody-mediated neutralization of APRIL or BLyS substantially diminished the number of infiltrating B-cells and reduced bone loss during the experimental periodontitis (65). The adoptive transfer of B10 cells, previously cultured with *P. gingivalis* LPS and cytosine-phospho-guanine (CpG) oligodeoxynucleotides, into mice with *P. gingivalis* and ligature-induced periodontitis, showed a significant reduction of bone loss and gingival inflammation, associated with increased local IL-10 production (70). Also, the gingival application of an optimized combination of CD40L, IL-21, anti-Tim1, which *in vitro* induces IL-10 production on B10 cells, inhibited bone loss in ligature-induced experimental periodontitis (86). Thus, the development of immune-based therapies has been proven effective in the prevention of bone destruction during experimental periodontitis *in vivo*. Current approaches to drug delivery and local applications of these therapeutic strategies in humans are being tested.

APICAL PERIODONTITIS

Definition and Pathogenesis of the Periapical Periodontitis

The infection of periodontal tissues in the periapical area following the bacterial invasion of pulp in the root canal system leads to the inflammatory destruction of the periodontal ligament, radicular cement and alveolar bone, which are the clinical hallmarks of apical periodontitis. Interestingly, the pathogenesis underlying the clinical presentation of apical periodontitis possesses outstanding parallels with that of periodontitis (87–89). Both conditions are initiated by an infectious stimulus and share pathological mechanisms of tissue destruction (chronic and exacerbated immune response that uncouples tissue balance) as well as the susceptibility traits and the treatment approach (eradication of the infecting microorganisms) (87, 90). Indeed, epidemiological data suggest that there is a correlation between the occurrence of apical periodontitis and marginal bone loss characteristic of periodontitis (91), reinforcing the existence of a common susceptibility profile.

Cellular and Molecular Basis of the Periapical Periodontitis

Although microorganisms are essential for disease initiation, their presence is not sufficient to explain the pathologic

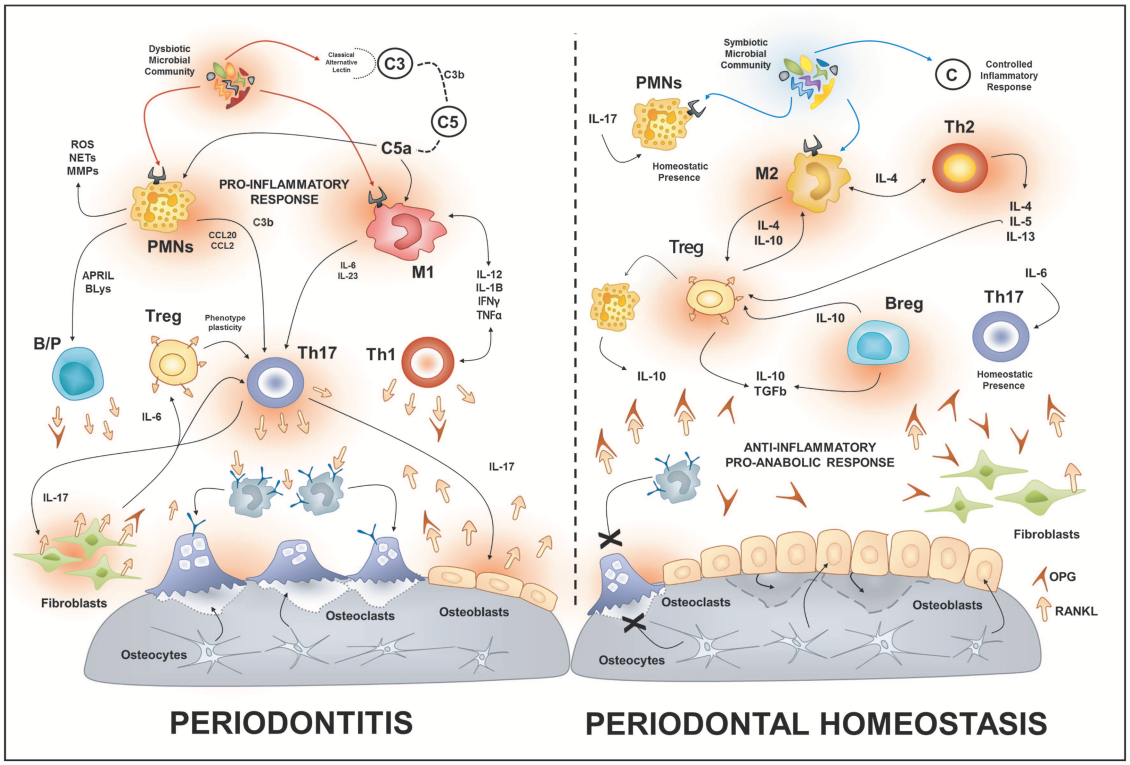

FIGURE 1 | Osteoimmunology of periodontal disease. During periodontitis, the immune response induced by the dysbiotic microbiota enhances the production of local RANKL by different immune cells types such as Th1, Th17, B cells. Additionally, the increased gingival levels of IL-17 stimulate the membrane-bound expression of RANKL in osteoblasts and periodontal ligament fibroblasts; this provokes the activation of osteoclast and bone-loss. On the contrary, in health, different immune cells such as Tregs, Bregs, M2, and Th2 cells promote an anti-inflammatory and pro-anabolic state that sustain the alveolar-bone homeostasis. PMNs, polymorph nuclear neutrophil; B/P, B and plasma cell.

phenomena that generate inflammatory destruction of the apical periodontium (92). The presence of a protected reservoir of microorganisms inside the root canal system precludes their eradication by immune defense mechanisms, generating a loop of constant activation and amplification of the immune response. Without active regulatory or suppressive signals, this amplification loop of the immune response results in a constant and exacerbated response, which causes the progressive destruction of periodontal support (87). This exacerbated immune response tampers with the normal turnover mechanisms of periodontal tissue, particularly bone, uncoupling bone formation from bone resorption leading to a net bone loss. Conversely, immunoregulatory mechanisms can provide a fine tune to immune effector mechanisms, resulting in a response that can control the spread of the infection outside the root canal system, while limiting the pathological tissue destruction. The balance shift toward deficient or excessive response can allow for infection spreading or uncontrolled periapical tissue resorption (93).

The treatment of apical periodontitis requires the disinfection of the root canal system and its obliteration with a biomaterial capable of maintaining a sterile environment and, in some refractory cases, the surgical elimination of periapical tissues (94, 95). The absence of reliable means to know in advance if the endodontic treatment will be successful or not is a critical weakness in endodontic therapy. Once the apical lesion has developed, there are no highly sensitive clinical or radiographic tools to predict if a lesion will acquire an activated phenotype -and continue to expand to the surrounding tissues- or will attain an inactive phenotype, resulting in the arrest of its progression or even remission and healing. Since not all subjects suffering from an infection of the root canal will develop apical periodontitis, it is logical to propose that a susceptibility profile is necessary for the occurrence of the disease The identification of putative genetic and molecular markers potentially responsible for the periapical immune-balance might help to discriminate susceptible or resistant subjects to improve the treatment outcome prediction (96). Additionally, periapical lesion development does not follow a linear pattern, alternating active and inactive phases, like the "bursts" progression model, described for periodontitis (97, 98). Therefore, the understanding of host response elements responsible for the switch from activity to inactivity can also contribute to elucidate the basis of susceptibility/resistance to lesions development.

From the genetic viewpoint, the overall hypothesis is that polymorphic variations in critical genes could contribute to

increased risk to suffer from apical periodontitis. That possibility is investigated using a case-control approach, based on the comparison of a group of diseased subjects (i.e., cases) to an unaffected group of individuals (i.e., controls). However, in the context of periapical lesions, the use of a healthy population as control group disregards the classic case-control study definition, which states that a case-control study is designed to determine if exposure is associated with an outcome (99). The absence of the exposure (bacterial invasion of the pulp in the root canal system) disqualifies the healthy controls to be compared with susceptible individuals that develop periapical lesions upon the "exposure." The study design, therefore, should comprise groups exposed to the same causal agent required for periapical lesions development, but with distinct clinical outcomes. The inclusion of theoretically resistant individuals (i.e., presenting deep caries without periapical lesions) have been found to improve the odds of identifying genetic factors that potentially contribute to increasing the risk to periapical lesions development (100, 101). A similar approach has been used in chronic periodontitis, with the use of chronic gingivitis subjects as a theoretically resistant population (99, 102).

Despite the inherent complexity to genetic association case-control studies, another useful approach to unravel the potential influence of genetic variants in apical periodontitis pathogenesis is to perform correlation analysis between the different genotypes/alleles and host response markers. For instance, MMP1-1607 polymorphism (rs1799750) is associated with increased expression of MMP-1 mRNA. MMPs are a family of collagenolytic enzymes responsible for the degradation and remodeling of the extracellular matrix. An increase in the expression or activation of MMPs without a parallel increase in their tissue inhibitors mediate numerous pathological processes, including apical periodontitis (103). In a sample of 326 subjects, the alternative variant of MMP-1 rs1799750 was associated with increased risk to suffer from apical periodontitis. Additionally, the cytokines TNFα, IL-21, IL-17A, and IFN-γ were associated with augmented transcriptional activity of MMP-1 in apical periodontitis, favoring its development (104).

Wnt/β-catenin signaling plays an essential role in bone biology, especially in the differentiation of osteoblasts and the suppression of bone resorption (105). The Wnt family in humans consists of 19 highly conserved genes that regulate gene expression, cell behavior, cell adhesion, and cell polarity (106). The polymorphic variations on the genes WNT3 and WNT3A were associated with increased susceptibility to apical periodontitis, specifically an intronic SNP in WNT3 (rs9890413) and a promoter SNP in WNT3A (rs1745420). The WNT3 (rs9890413) SNP is in an intronic region and to this date has no known function, so its putative mechanism of action to regulate apical periodontitis susceptibility is indefinite. On the other hand, a functional assays showed that the alternate allele G in the associated WNT3A (rs1745420), located in the gene promoter, increased promoter activity by 1.5-fold in comparison to the ancestral allele C. These findings suggested that this SNP may have a regulatory role in WNT3A expression and function (data not published).

The comparison of the gene expression signatures of periapical lesions with periapical tissues known to experience bone resorption or bone formation (i.e., in pressure and tension sides of teeth submitted to orthodontic forces) may allow for the discrimination of osteolytic activity status. Using this approach, it was possible to categorize apical granulomas in "active" or "inactive" according to their molecular profile of RANKL/OPG mRNA expression (107). Once the activity of the lesion was defined, it was possible to discriminate host response patterns associated with each subset. In this context, the inflammatory signature of 110 apical granulomas (persisting apical lesion after a technically adequate endodontic treatment, requiring surgery) and 26 healthy periapical tissues as controls were characterized (108). The apical granulomas were categorized as "active" or "inactive" according to the molecular profile of RANKL/OPG mRNA expression (107). The inflammatory signature was investigated by the expression of Th1, Th2, Th9, Th17, Th22, Thf, Tr1, and Tregs cytokines/markers. The cluster analysis revealed that "active" apical lesions were characterized by increased expression of TNF-α, IFN-γ, IL-17A, and IL-21, whereas "inactive" lesions expressed increased levels of IL-4, IL-9, IL-10, IL-22, and Foxp3. Interestingly, distinct patterns of IFNγ and IL-17 expression were described in periapical lesions. Lesions presenting a high RANKL/OPG ratio (active) overexpress IFNγ and IL-17 compared with inactive lesions. Additionally, active lesions can be clustered in groups presenting distinct patterns of IFNγ and IL-17 expression, suggesting that Th1/Th17 cytokines can drive apical periodontitis development independently (108). Accordingly, different studies describe that Th1 and Th17 responses can be mutually inhibitory (109). However, the Th1/Th17 interplay seems to be way more complicated than the mutually inhibitory activity, suggesting that collaborative and inhibitory phases may coexist in different disease stages. Also, cells presenting features of both Th17 and Th1 subsets, including Tbet and IFNγ expression, have been described in inflammatory and osteolytic conditions (110).

Therefore, the activity status of apical periodontitis may be determined by the relative enrichment of different Th subsets. Indeed, leukocytes subsets such as Th2, Tregs, and MSCs mediate a natural immunoregulatory response that suppresses apical periodontitis development. IL-4 (the prototypical Th2 cytokine) was described to induce the expression of CCL22, a main chemoattractant of Tregs (63). It is noteworthy that Tregs hallmark products, such as IL-10 and TGF-β, are described to boost MSCs immunosuppressive properties (111). Therefore, while all the details regarding the potential Th2, Tregs and MSCs cooperation remain to be unraveled, the existence of a protective/regulatory cellular network in inflamed periapical tissues seems feasible (89, 108).

Impact of Osteoimmunology in the Periapical Disease

A recent study points to an unexpected potential trigger of a protective immunoregulatory response (112). While RANKL has a well-characterized role in the control of

bone homeostasis, it can also play critical roles in the regulation of the immune system. Indeed, while anti-RANKL administration resulted in the arrest of periapical bone loss, it led to an unremitting pro-inflammatory response and impaired immunoregulation, restored by Tregs adoptive transfer (113). Therefore, RANKL seems to be responsible for trigger immunoregulatory feedback via Tregs induction, which in turn acts as suppressive elements (113). Notably, RANKL seems to play a fundamental role in linking the immune system with bone metabolism. Infiltrating immune cells are an important source of RANKL, but also resident bone osteoblast produce and secrete RANKL, most of the time under the regulatory influence of osteocytes following mechanical or endocrine stimulus (73, 75).

Despite the lymphocyte-centered paradigm of the most studies into apical periodontitis pathogenesis in the last decade, other leukocyte subsets (such as granulocytes) also can play significant roles in periapical lesion pathogenesis. For example, we determined that CXCL12 levels increase significantly in apical periodontitis. CXC ligand 12 (CXCL12 a.k.a. SDF-1) is a pleiotropic chemokine that regulates the influx of leukocytes to inflamed sites. In apical periodontitis, CXCL12 proved to be the primary molecular signal responsible for the recruitment of mast cells into the periapical inflammatory infiltrate during lesion development (114). This CXCL12/mast cell axis is significant as mast cells can secrete a variety of molecular signals and regulate many diseases (115, 116).

Another major cellular player during the first stages of the immune response in the pathogenesis of apical periodontitis is the neutrophil. These cells invade the apical periodontium in vast numbers and are in the front line of contention of bacterial infection. Despite being mainly associated with the direct killing of bacteria and tissue necrosis, neutrophils are also capable of releasing molecular mediators into the extracellular compartment and influencing the later stages of the response (117, 118). Accordingly, a significant increase in heat shock protein 27 (HSP27) and Serpin Family B member 1 (SERPINB1) protein levels were identified in apical periodontitis compared to healthy tissues (119). HSP27 belongs to the heat shock protein gene family and has an essential role in the inhibition of apoptosis in thermal and chemical stress, protecting the cells from injury in hostile environments (120). SERPINB1 is a potent inhibitor of neutrophil serine proteases and plays crucial roles in protecting PMN and other cells from apoptosis (121). The role of another Serpin family member (SERPINE1) has been demonstrated in the stabilization of apical lesions (122), thus pointing to a molecular pathway of Serpin family proteins regulating PMN functions and periodontal destruction in apical periodontitis. Importantly, this increased expression of HSP27 and SERPINB1 was compartmentalized to epithelial cells and infiltrating neutrophils in the inflammatory front (119). The expression of HSP27 and SERPINB1 was inversely correlated with markers of acute inflammation and markedly increased in apical lesion characterized as "stable/inactive." This evidence suggests that HSP27 and SERPINB1 could be putative markers of lesion regression and useful to follow the outcome of endodontic treatment

Ultimately, most osteoclastogenic signals are controlled by osteocytes, whether directly by secreting osteoclastogenic signals or indirectly by entering apoptosis (123–125). The inflammatory milieu characteristic of apical periodontitis creates the necessary environment to favor pro-osteoclastogenic signaling and net bone loss (72). The communication network established between osteocytes and osteoblast is capable of sensing delicate environmental changes and react to favoring the bone formation and resorption (126). The exacerbated and unrelenting immune response characteristic of apical periodontitis provides plenty of pro-resorptive signals that tilt the balance in favor of bone resorption (127, 128).

Taken together, recent findings point to a complex and multilevel regulatory network that underlies the clinical presentation of apical periodontitis (**Figure 2**). Infecting agents and immune defense mechanisms are in opposing trenches in an all-out war leading to apical lesion formation or regression. As in many other diseases characterized by inflammatory tissue destruction, the regulatory features of the immune system have a disproportionally important role in the progress and outcome of the disease. Despite extensive efforts, there is still much to be investigated and learned before we can develop a comprehensive molecular model capable of guiding changes in clinical conducts leading to improved clinical outcomes in the treatment and management of apical periodontitis.

BIOLOGICALLY-BASED DIAGNOSTICS AND THERAPEUTICS TO MANAGE ORAL AND SYSTEMIC HEALTH IN PERIODONTITIS PATIENTS

Marginal periodontitis and periapical periodontitis are the most common oral diseases involving alveolar bone loss (129). Substantial research supports the positive association between periodontitis and several systemic diseases such as cardiovascular diseases and diabetes, while growing evidence is unveiling an analog connection with periapical lesions. Recently, periodontitis has also been associated with the onset and development of oral and extraoral cancers, and their fatal outcome (130–132).

The result of periodontitis forms is a prolonged release of both host-derived inflammatory/collagenolytic mediators (e.g., arachidonic acid metabolites, cytokines, nitric oxide [NO], reactive oxygen species [ROS] and MMPs), and virulence factors generated by the dysbiotic perio-pathogens and/or endodontic pathogens in the etiologic microbial biofilm. Though this response is intended to restrain dissemination, this toxic "brew" impairs the host's immune response. The proposed mechanisms linking periodontitis and extraoral diseases involve the spread of bacteria from the oral cavity causing damage to other organs, the increase in inflammatory systemic burden, or an autoimmune response triggered by oral bacterial species (133–138).

Albeit clinical and radiographic examinations are the gold standard for the diagnosis of periodontal and periapical diseases, variations in the inflammatory profile might impact disease susceptibility and severity at both local and systemic levels (129, 139). Oral fluids (gingival crevicular fluid/GCF, mouth

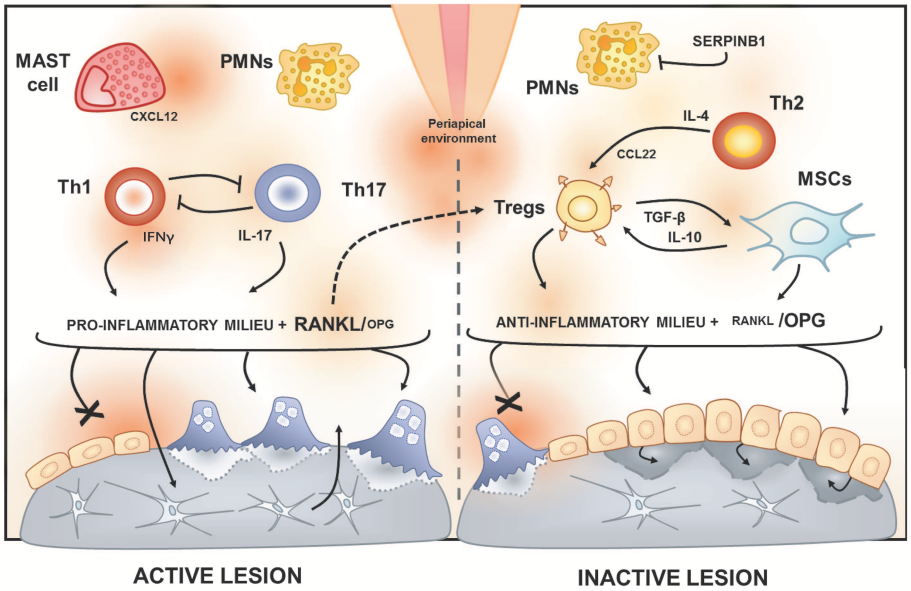

FIGURE 2 | Immunological features of active and inactive periapical lesions. In the periapical environment, the presence of endodontic pathogens and its products (such as LPS) triggers the host inflammatory immune response. The analysis of gene expression signatures of periapical lesions allows for the discrimination of osteolytic activity status in "active" or "inactive" according to RANKL/OPG expression ratio. Active periapical lesions are characterized by high RANKL/OPG ratio is an association with a pro-inflammatory milieu, which includes a high level of IFN-g and IL-17. Distinct patterns of IFNg and IL-17 expression were described in periapical lesions, suggesting that Th1 and Th17 subsets, described to be mutually inhibitory, can drive apical periodontitis development independently. The presence of PMNs and mast cells also have been associated with lesion activity. Conversely, inactive lesions are characterized by a low RANKL/OPG ratio is an association with an anti-inflammatory milieu, which is supposed to involve a cooperative immunoregulatory network composed by Th2 and Tregs subsets, as well by MSCs. The prototypical Th2 cytokine IL-4 is described to induce the expression of CCL22, a main chemoattractant of Tregs. Noteworthy, Tregs hallmark products, such as IL-10 and TGF-β, are described to boost MSCs immunosuppressive properties. Interestingly, a recent study points to RANKL as an unexpected immunoregulatory feedback trigger via Tregs induction.

rinse, and saliva samples) obtained non-invasively from the oral cavity are critical sources for factors and/or biomarkers related to the metabolic activity of periodontal tissues. Quantitative point of care (PoC)/chair-side technologies are emerging as available tools to monitor periodontal conditions, including orthodontic tooth movement, periodontitis, apical periodontitis, and peri-implantitis, whereas key inflammatory mediators can be targeted for therapeutic purposes. Complementary salivary/oral fluid MMP-8 determinations aid to identify periodontal loss and inflammation in line with clinically deepened periodontal pockets, bleeding on probing, and radiographic alveolar bone loss (140–144). MMP-8, MMP-9, TRAP-5, and MPO demonstrates very high diagnostic accuracy in GCF for discriminating periodontitis, apical periodontitis, gingivitis and/or healthy periodontium, supporting their usefulness for PoC diagnostics (129, 142). Of interest, oral fluid biomarker analysis has shown usefulness in extraoral conditions or diseases (141, 142), whereas GCF placental and inflammatory markers proved the diagnostic potential for preeclampsia (145) and gestational diabetes mellitus in pre-symptomatic women (146), revealing new emerging spectra for oral fluid applications.

Up to now, several studies have explored the associations between tooth loss, oral infections, CVD and diabetes, and it is widely accepted that low-grade systemic inflammation, as measured by CRP and other biomarkers, influences their development and progression. Currently, there is substantial evidence supporting that marginal periodontitis imparts increased risk for future atherosclerotic cardiovascular disease, in which the exacerbated inflammatory burden favors atheroma formation, maturation, and exacerbation. Periodontal treatment can reduce systemic inflammation as evidenced by a reduction in C-reactive protein (CRP), reduce the levels of oral fluid and systemic (serum) proinflammatory biomarkers of tissue destruction and improve endothelial function and subclinical atherosclerosis, but the evidence is not yet conclusive (131, 147). Periodontitis also associates with elevated risk for dysglycaemia and insulin resistance, as well as incident type 2 diabetes, whereas the latter is also an essential modifying factor for periodontitis. Evidence supports that periodontal therapy seems to improve glycemic control, although studies involving long-term follow-up are also inconclusive (133). Despite the associations between endodontic infections, CVD and diabetes have not been thoroughly explored; emerging evidence sustains an analogous link (134).

Most available mechanistic studies seeking for an association between apical periodontitis and the systemic inflammatory burden lacks adequate control for confounders. Often, a clinically heterogeneous mixture of acute and chronic forms of apical periodontitis is included, and participants are older

than the main risk group, resulting in overall inconclusive evidence for hsCRP. Few recent studies accounting for these variables reported early endothelial dysfunction and up-regulation of pro-inflammatory cytokines, including IL-1, IL-2, IL-6, reactive oxygen species, as well as asymmetrical dimethylarginine in serum from young adults with CAP compared to healthy volunteers (148). Recently our group demonstrated an association between apical lesions and cardiovascular risk based on CRP serum levels concentrations (135), but the systemic effects of endodontic treatment are yet unknown (134).

Recently periodontitis was proposed as an independent risk factor for cancer development, such as digestive tract cancer, pancreatic, lung, prostate, breast, uteri, lymphoma, and hematological cancer. Moreover, in population-based studies, periodontitis was strongly linked to cancer mortality, especially in patients with pancreatic cancer (130, 149, 150). Studies demonstrate a role of microorganisms such as Human Papillomavirus (HPV), Epstein-Barr virus (EBV) and *P. gingivalis* that could be detected in inflamed periodontal tissues and might favor cancer initiation at the oral cavity or distant tissues (151–153). Recently, *Treponema denticola*, a virulent proteolytic periodontopathogen, was found to promote the onset of oro-digestive cancers (154, 155). Besides oral pathogens, the local and systemic inflammatory responses associated with periodontitis can represent an indirect mechanism that could promote cancer development (130).

Periodontitis derived-systemic low-grade inflammation can also be readily monitored in serum samples, by measuring acute-phase proteins such as C-reactive protein, to further diagnostically assess the risk. hsCRP measurement is especially recommended in subjects at intermediate cardiovascular risk to determine the need for treatment (156); hsCRP levels are also used to evaluate the success of an intervention such as the metalloproteinase inhibition with sub-antimicrobial doses of doxycycline to prevent acute coronary syndromes (MIDAS) (157, 158). In this way, biomarker's utility becomes clinically practical with the current availability of PoC chair-side biomarker analysis of oral fluids & serum, and host-modulation therapies such as non-antimicrobial doxycycline medications (Periostat®, now generic; and Oracea®) as pleiotropic MMP-inhibitors, and others such as omega-3 fatty acid derivatives (e.g., docosahexaenoic acid), i.e., the resolvins (**Figure 3**) (159–161). Thus, recently-developed strategies of personalizing the use of "host-modulation therapy," when indicated by modern PoC chair-side diagnostic tests (140, 144), may significantly enhance the beneficial outcome of both the commonly-used oral therapy (scaling & root planing, and oral hygiene instruction) and its impact on the overall medical health of the patient. Further evidence of the need for modern, biologically-based diagnostics and therapeutics to manage the oral/systemic health of the patient is continuously emerging. These findings reinforce the view that modern, biologically-based oral-systemic health management requires a "two-pronged strategy" including diagnostic monitoring in oral fluids biomarkers, and optimally therapeutic suppressing these mediators with "host-modulation therapy" combined with microbial biofilm management. Both strategies are currently available to the dental clinician as the result of long-term and substantial basic and translational research.

BONE SARCOMAS (BS) AFFECTING THE MAXILLOFACIAL REGION

Definition and Epidemiological Impact of Bone Sarcomas

Bone Sarcomas (BS) are rare primary mesenchymal bone tumors (<0.2% of malignant tumors of EUROCARE database), including osteosarcoma (OS), Ewing sarcoma (ES) and chondrosarcoma (CS) (162). BS affects more frequently the appendicular skeleton (lower limbs) than the craniomaxillofacial skeleton. In this area, maxilla and mandible are more affected bones over cranial bones (163). Thus, maxillofacial (MF) OS (MFOS), ES (MFES), and CS (MFCS) are considered malignant tumors of the maxillofacial region according to the 4th edition of the World Health Organization Classification of head and neck tumors (164). Here, we will focus specifically on MFOS, MFES, and MFCS, highlighting the role of immune response on their pathophysiology and, also, revising experimental approaches for therapy.

Maxillofacial Osteosarcoma (MFOS)

MFOS represent <10% of the total OS (165). Compared with the appendicular OS, which peaks in the 2nd and sixth decade, MFOS peaks in the 3rd decade (162, 163, 165). Typically, MFOS arise from the cancellous compartment rather than bony surfaces. MFOS affects the alveolar ridge of the mandible and posterior area of the maxilla (163, 166). MFOS can be categorized according to the predominant matrix as an osteoblastic, fibroblastic, chondroblastic, telangiectatic, or osteoclastic type (163, 165). At the X-ray imaging, MFOS appear as either as the osteolytic form with undefined margins or, the osteoblastic form, showing a sclerotic and sunburst structure caused by radiated bone spiculae (163).

Maxillofacial Ewing Sarcoma (MFES)

MFES is 1–4% of all ES which peak in both the first and second decades mainly in white Caucasian people, affecting equally both sexes (163). MFES is an aggressive, hemorrhagic, and rapidly metastatic malignant tumor affecting naso-orbital bones. MFES are characterized by an irregular lesion combining sclerosis and lucent zones compromising cortical bone. MFES also show the characteristic onion peel appearance and sunburst new bone formation, which correspond to periosteal osteogenic reaction (163).

Maxillofacial Chondrosarcoma (MFCS)

It accounts for 2% of all CS with a peak incidence during the 4th to fifth decades with a male predilection (ratio 2.4:1). It affects mostly the skull base, maxilla, and less frequent the orbit and, cartilage of the nasal septum. MFCS can be observed after malignant and benign diseases such as OS, fibrosarcoma, Paget disease, and fibrous dysplasia (163, 167).

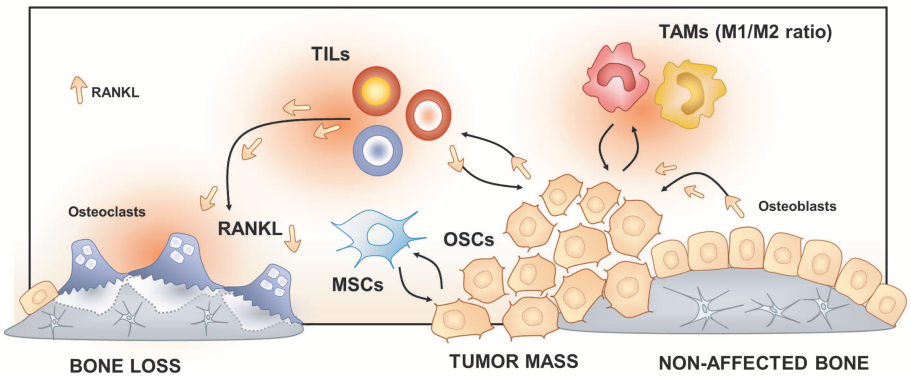

FIGURE 3 | Osteoimmunology at the osteosarcoma (OS) niche. Tumor-Associated Macrophages (TAMs), Tumor-Infiltrating Lymphocytes (TILs) and Mesenchymal Stem cells (MSCs) regulate osteosarcoma cells (OSCs) proliferation, tumor mass progression, and metastasis. The RANK/RANKL signaling leads to both OSCs progression and increased osteoclast activation and bone loss in the OS niche.

Histologically, chondrosarcoma of the craniofacial region can be divided into (a) the conventional subtype with myxoid and/or hyaline components, the most common form, is slow growing, and rarely metastatic; (b) the aggressive mesenchymal and dedifferentiated subtype, more aggressive and tends to metastasize and; the clear cell subtype, extremely rare (163). High-grade CS can induce metastasis, but local recurrence of curettage is a common feature of such tumors. Since the vast majority of literature describing the pathophysiology of BS focus on the non-maxillofacial OS, we will base our work upon these recent findings.

These three entities result from the disruption of differentiation of Mesenchymal Stem Cells (MSCs) into bone and cartilage cell lineages (168). In bone homeostasis, MSCs differentiate into stromal cells, which will contribute to both the hematopoietic and the skeletal niches (168, 169). At the skeletal niche level, stromal cells will activate transcription factors such as Runx2 to follow the osteogenic path to become functional osteoblasts or, Sox9 to follow the chondrogenic pathway to become cartilage cells (168) (**Figure 3**).

BS results from the interaction of both OS cells (OSCs), cancer stem cells, and their niche. OSCs are the malignant counterpart of osteoblasts. OSCs are mesenchymal-derived cells subjected to an initial oncogenic event altering the commitment from a mesenchymal cell toward an osteoblast by a mutation (e.g., *p53* and *Rb*) and/or aberrant Hedgehog and Notch signaling (168, 170). Within the tumor mass, cells exhibit high heterogeneous profiling that can be partly explained by the presence of cancer stem-like cells (CSCs), the clonal evolution of OSCs and the high heterogeneity of the local tumor microenvironment (168, 170). These cells are characterized by its self-renewing property, and they are proposed as responsible for tumor progression, resistance to chemotherapy, and initiate metastasis (168, 171). Based on the "seed and soil' theory of Paget, it is now well-recognized that OS, like other cancers, requires an adequate local microenvironment for its development (168, 171). This specialized microenvironment provides all metabolites and regulates the self-renewal process of CSCs (171). Interactions between OSCs, CSCs, and its niche may determine OS progression or dormancy and, potential drug resistance (171, 172).

Cellular and the Molecular Immune Basis of Bone Sarcomas

Some clinical studies correlate survival rates of OS patients with both immune markers and the immune cell (lymphocyte/macrophage) ratio (173, 174). However, the role of the immune system in OS development remains still misunderstood. The relationship among OS niche and immune response may be explained by the fact that OSCs (and also, bone cells) are surrounded by bone marrow cells occupying the same bone marrow space. Within this space, hematopoietic precursors give rise to the immune cell population, lymphoid, myeloid cells, and mast cells. These cells will regulate both innate and acquired immune responses (173). Consistently; an immune infiltrates composed by monocyte/macrophages/dendritic cells and T-lymphocytes have been identified in OS tissues (173, 174). Although B-lymphocyte and mast cells are less represented in the OS tumor mass, they are far more distributed in the interface bone-tumor. Both lymphocytes and mast cells are essential sources of RANKL, becoming key players in the activation of osteoclasts, and then contributing to the osteolytic feature of OS (173, 174).

Macrophages are essential cells participating in bone homeostasis (173, 174). Macrophages, located in the vicinity of the tumor, are known as Tumor-Associated Macrophages (TAMs) (168). TAMs control local immunity, angiogenesis, and regulate tumor cell migration and invasion (168). Also, TAMs participate in the seating of cancer cells at the metastatic site by modeling the permissiveness of the host-tissues (168). TAMs are composed by a large variety of subpopulations which have been classified initially in M1 and M2 subtypes according to their differentiation and activities. M1, the pro-inflammatory macrophage subset, are classified as anti-tumor cells and associated with excellent survival rates, and M2, the

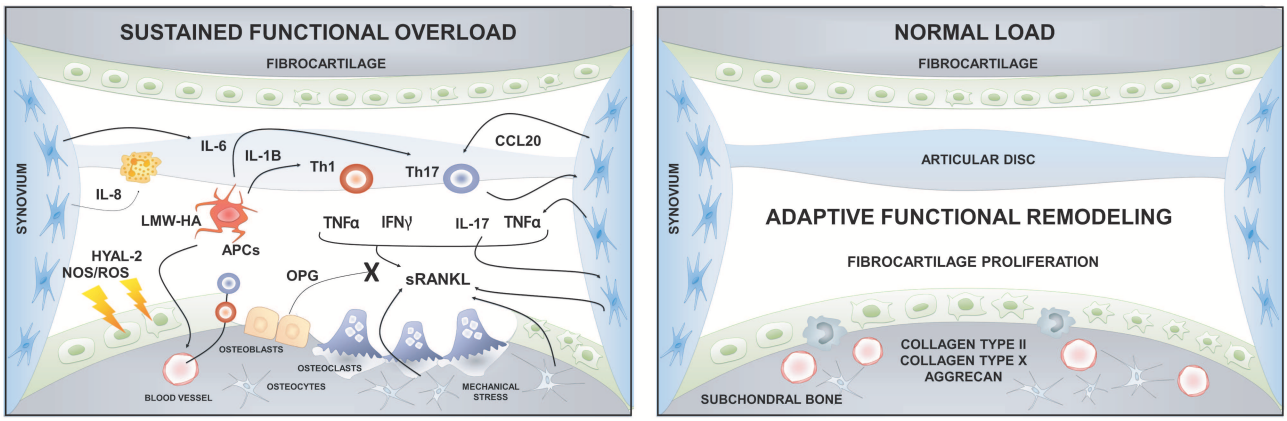

FIGURE 4 | Immune response and bone crosstalk during temporomandibular joint osteoarthritis. The sustained functional overload that exceeds the joint adaptive capacity can induce dysfunctional remodeling. This dysfunctional remodeling is characterized by increased oxidative stress, due to hypoxia/reperfusion effect, and higher levels of catabolic enzymes that degrade the fibrocartilage extracellular matrix and induce chondrocyte apoptosis. The molecular products derived from cartilage breakdown (e.g., LMW-HA or PG) can trigger the immuno-inflammatory response by interacting with APCs and finally resulting in the activation of Th17 lymphocytes and the RANK/RANKL/OPG axis, leading to subchondral bone resorption. The normal joint load of the TMJ, such as static loading during swallowing or teeth clenching, induces an adaptive functional remodeling of joint tissues and promotes fibrocartilage healing. HYAL, hyaluronidase; LMW-HA, low molecular weight hyaluronan; NOS, nitric oxide; OPG, osteoprotegerin; ROS, reactive oxygen species; sRANKL; soluble receptor activator of nuclear factor-kappa B ligand; APCs, Antigen presenting cells.

anti-inflammatory macrophage subset, as pro-tumor regulators (168, 173, 174). Thus, in OS patients, a TAM-M1 predominant ratio over TAM-M2 was associated with better survival rates and the opposite, with poor prognosis (168, 173, 174). These associations may be explained by an immunosuppressive effect on intra-tumor T-lymphocytes, and pro-angiogenic effect exerted by TAM-M2 observed both preclinical models of OS and metastatic patients (168, 173, 174).

T-infiltrating Lymphocytes (TILs) are the second more prevalent infiltrated cell type in OS tissues and OS metastasis (174). Studies showed that selected subpopulations of T-cells ($CD8^+/FOXP3^+$) exhibit high reactivity again tumor cells compared with non-infiltrating lymphocytes (175). Thus, OS patients with elevated $CD8^+/FOXP3^+$ -ratio had better survival rates confirming the immunosuppressive role of TIL in OS pathogenesis (175, 176). TILs have higher cytotoxic properties again OS cells compared with circulating T-cells; however, OSCs secrete immunosuppressive molecules preventing the activation of TILs on the tumor site (175).

Beside immune cells, Mesenchymal Stem Cells (MSCs) have been reported as an essential regulator of OS behavior (177). Indeed, both bone and the bone marrow niche are rich in MSCs that are closely located to OS cells (178). Several studies demonstrated that MSCs establish active crosstalk with OSCs controlling OS progression and/metastasis (178). MSCs and early developed pre-osteoblasts communicate with OSCs by secreted vesicles containing mRNA, proteins, and miRNA modulating OSCs proliferation and stemness (e.g., ability to form sarcospheres, expression of stem-associated genes) (179). Reciprocally, OSCs are able to educate MSCs by tumor-secreted extracellular vesicles turning MSCs into OS extracellular vesicle-educated MSCs. These cells promote tumor progression and/or metastasis via secretion of IL-6, TGF-β and IFN-γ and by inhibiting T, B and NK cell proliferation (173, 174).

Impact of Osteoimmunology in Bone Sarcomas

Bone remodeling is controlled by osteoblasts and osteoclasts, which are responsible for bone formation and resorption, respectively. Bone remodeling is regulated by the RANKL/RANK/OPG triad (180). RANKL expressed as a membranous or secreted form by stromal and osteoblastic cells which binds to RANK, a transmembranous receptor expressed by pre-osteoclast. Their interaction leads to the activation of pro-osteoclastic genes (e.g., *NFATc1*, *cathepsin K*, *TRAP*), osteoclast differentiation (osteoclastogenesis) and then, bone resorption (180, 181). OPG is secreted by stromal and osteoblastic cells acting as a soluble decoy receptor for RANKL, leading to the inhibition of osteoclastogenesis and bone loss (180, 181).

In the OS context, the fact that RANK usually is not expressed by osteoblastic cells and the recognition of $RANK^+$ OSCs have been long debated. However, human data and most of established OSC lines confirm the expression of RANK by OSC, proposing the interaction of RANK with its ligand (RANKL) as a critical contributor in OS pathogenesis (181). In this line, a preclinical genetic model of aggressive OS in a RANKL invalidated mice showed the complete blocking of OS development, confirming the critical role of RANK/RANKL signaling into OS progression (182). Moreover, human data analyzing OS tissues from patients with or without metastatic status showed that RANK is expressed in both groups, meaning that RANK expression is not related with the metastatic status, becoming a potential predisposing factor. However, the overexpression of RANKL and the lower

OPG/RANK ratio in tumors from metastatic patients lead to hypothesize that the RANKL available in the OS niche is a significant driver to tumor progression and metastasis in OS patients (181). Taken these findings together, strongly support the use of RANKL blockers as a therapeutic approach for OS progression to a metastatic status (181).

On the other hand, the RANKL/RANK/OPG triad has been associated with the pathogenesis of OS by regulating both the osteoclastic activity and, immunoregulatory effects (180, 181). However, the real contribution of osteoclasts to the pathogenesis of OS remains still controversial. Some authors propose that the RANKL-activated osteoclasts might exert a pro-tumoral function in the early stage and on the contrary, a pro-bone remodeling/anti-tumoral effect in the later stage of OS (180, 181). Moreover, osteoclasts may modulate immune response promoting an immunogenic $CD4^+$ T cell response upon inflammation. Taken together, osteoclasts can be considered as essential regulators of OS growth and progression through either their resorptive or their immune functions (180, 181).

Bone Sarcomas and Immune-Based Therapeutic Approaches

In contrast to CS for which the conventional therapy is based on surgery with adequate margins, current treatments of ES and OS associate chemotherapy and surgery. Chemotherapy lines combined a minimum of three cytotoxic agents among doxorubicin, cisplatin, methotrexate, and ifosfamide (168). Unfortunately, most conventional therapies used results in limited therapeutic responses, and new approaches are urgently needed explaining the high number of clinical trials with new drugs for rare cancers including immune modulators, check-point inhibitors and tyrosine-kinase inhibitors (168, 174, 183, 184). Among immune regulators, an activator of macrophages such as muramyl tripeptide phosphatidylethanolamine (MTPPE) showed therapeutic efficacy in the metastatic OS. Trabectedin, a cytotoxic agent, could be attractive to treat sarcomas thanks its effect on macrophage differentiation toward M1 subtypes and targeting of PD1/PDL1 may be promising therapy by disrupting the communications between cancer cells and immune protagonists (183, 184). However, future therapeutic development will require a better characterization of the critical molecular network involved in the differentiation of BS cells and their microenvironment that should lead to the identification of new therapeutic targets and will allow better stratification of the patients enrolled in clinical trials (183, 184).

OSTEOARTHRITIS OF THE TEMPOROMANDIBULAR JOINT

Definition and Pathogenesis of the Osteoarthritis of the Temporomandibular Joint

Degenerative joint disease (DJD) is characterized by the progressive breakdown of articular cartilage, variable degrees of synovial inflammation, and pathological remodeling of subchondral bone (185, 186). Osteoarthritis (OA) is considered the most common form of DJD, affecting approximately 15% of the world population, and a leading cause of pain and disability (187, 188). Although, it mainly affects load-bearing synovial joints, such as the knee, hip, spine, and finger, other joints such as the shoulder or temporomandibular joint (TMJ) could also be affected (189). The TMJ is an exceptional synovial joint that connects the jawbone to the skull and, compared to the knee joint, it is exposed only to limited load-bearing forces (189). It has different morphological, functional, biomechanical, and biological features in comparison to other synovial joints (190). In the knee joint, hyaline cartilage covers articular surfaces, while in the TMJ, the articular lining is covered by fibrocartilage, which is surrounded by an angiogenic microenvironment and is softer than hyaline cartilage (186, 191). Thus, TMJ osteoarthritis (TMJ-OA) should not be considered as a common joint disease, but rather a unique one.

Although different factors such as systemic illnesses, developmental abnormalities, disc displacement, micro-trauma, and parafunction have been associated with the etiology of TMJ-OA, functional overload has been described as its main etiologic factor (28, 189, 192, 193). Articular remodeling is an essential biological process that responds to normal functional loading and ensures the joint's homeostasis (189). However, excessive or unbalanced mechanical loading in the TMJ can induce dysfunctional articular remodeling, leading to degenerative changes (189). Two kinds of mechanical loading occur in the TMJ: Static loading, which occurs during teeth clenching, jaw bracing, and swallowing; and dynamic loading, which occurs during tooth grinding, jaw thrusting, talking, and chewing (194). For instance, the static loading applied during forced mouth opening for 1 day increases the expression of Dickkopf factor-3 (Dkkf-3), an antagonistic non-canonical member of the Wnt family, in the cartilage surface and induces the synthesis of type II and type X collagen in the inner fibrocartilage layers; thus, promoting anabolic effects over the mineralized and unmineralized condylar cartilage (195). Nevertheless, when the same force was applied for 1 week, catabolic effects and several degenerative lesions were observed in the TMJs (196, 197).

Similarly, *in vitro* experiments demonstrated that the effects of loading forces are time-dependent. After 24 h of dynamic compressive loading over condylar chondrocytes, the expression levels of aggrecan, type I and type II collagen increased, possibly as an adaptation attempt; though, after 48 h these expression levels decreased significantly, showing a catabolic effect of prolonged loading (198). Furthermore, compressive forces also promote osteoclastogenesis through the increased expression of RANKL in synovial cells (199). In brief, light forces induced with a mouth opening protocol demonstrated an anabolic effect over TMJ, while massive forces induced a catabolic effect over joint tissues (200). Dynamic overloading forces in a TMJ-OA mice model disrupted the metabolism of hyaluronan (HA), one of the central extracellular matrix (ECM) glycosaminoglycans (GAGs) of the TMJ fibrocartilage (200). In this study, the sustained loading forces significantly decreased the expression levels of hyaluronan synthase (HAS) 2 and 3 and increased the expression levels of hyaluronidase (HYAL) 2 and KIAA1199,

an HA binding protein that facilitates the degradation of HA in articular cartilage (200). Interestingly, low-molecular-weight fragments of HA (LMW-HA) can act as a damage-associated molecular pattern (DAMPs), activating antigen presenting cells and initiating the immuno-inflammatory response (201, 202).

Cellular and the Molecular Immune Basis of the Osteoarthritis of the Temporomandibular Joint

Many contributing factors have been described in the progression of bone changes during TMJ-OA, including genetic factors, female hormones, catabolic enzymes, and inflammatory mediators (203). Although inflammation has considerable importance in the progression of TMJ-OA, it is classified as a "low-inflammatory arthritic condition" as opposed to rheumatoid arthritis (RA), which is considered as a "high-inflammatory condition" (204). Recent studies suggest that OA is an inflammatory disease, at least in certain patients, and that synovial inflammation is accompanied by immune cells infiltration, similarly to RA (205–207). Of these immune cells, macrophages and T lymphocytes are the most abundant cell types that infiltrate the synovia during TMJ-OA, representing approximately 65% and 22% of the total immune cells, respectively (208). Furthermore, several inflammatory cytokines and mediators are increased in the synovial fluid of TMJ-OA affected patients, such as IL-1β, IL-6, IL-17, IFN-γ, TNF-α, prostaglandin E2 (PGE2), and chemerin, suggesting a role of the immuno-inflammatory response during the pathogenesis of the TMJ-OA (209–213). In addition to metabolic or mechanical factors, chronic inflammation induces early damage of the cartilage and consequently initiates biomechanical changes in hard and soft tissues of the joint (214). Thus, the low-grade inflammation present in OA is a result of the interactions between the immune response and local factors, such as tissue breakdown and metabolic dysfunction (215).

The inflammatory response to trauma, hypoxia-reperfusion injury, or chemical-provoked wound typically occurs in the absence of microorganisms; therefore, it has been called "sterile inflammation" (216). The first step of sterile inflammation requires the presence of endogenous molecules released during tissue or cellular injury, which can act as DAMPs able to trigger the immuno-inflammatory response (216). DAMPs can be molecules derived from necrotic cell death, such as high-mobility group box 1 (HMGB1), heat shock proteins (HSPs), or purine-derived metabolites (e.g., ATP); or fragments of molecules derived from the breakdown of the ECM, such as fragments of heparan sulfate, byglican, or HA (e.g., LMW-HA) (215). At initial stages of TMJ-OA, increased local oxidative stress induces the fragmentation of HA in the synovial fluid and fibrocartilage (217–219). The oxidative stress could increase due to direct mechanical trauma, by homolytic fission, or due to hypoxia-reperfusion, and the following non-enzymatic release of reactive oxygen species (ROS) (217, 218). The molecular weight of HA decreases and LMW-HA accumulates within the joint milieu as the disease progresses leading to an increase of joint friction due to the reduction of the chondroprotective and boundary lubrication originally provided by HA (219, 220). Furthermore, LMW-HA can trigger the immune response by interacting with the toll-like receptor (TLR)-2 or TLR-4 expressed in antigen presenting cells (221). TLR activation during OA has been associated with the development of synovitis, cartilage degeneration, and disease susceptibility (222). Using an animal model of TMJ-OA, Kong et al. demonstrated that synovial inflammation changes are related to increased TLR-4 activation and enhanced IL-1β production (223). This synovial inflammatory reaction characterized by the increased levels of IL-1β induced by TLR-4 stimulation depends on the phosphorylation of p38 during the mitogen-activated protein kinase (MAPK) signaling cascade and culminates in the activation of nuclear factor-κB (NF-κB) or nuclear transcription factor activation protein-1 (AP-1) (224). Synovitis is frequently observed during the progression of TMJ-OA (225, 226). The lining layer of synovium is mainly composed of fibroblast-like cells and macrophage-like cells (227). These resident cells play a vital role in the immuno-inflammatory response and bone metabolism during OA by producing several inflammatory mediators that enhance the breakdown of joint tissues (228, 229). Synovial fibroblasts (SF) have the ability to transduce IL-17 signals by expressing different variants of the IL-17 receptor (IL-17R) (227). In response to IL-17A, SFs of the TMJ up-regulate the expression levels of the chemokines CXCL1, IL-8, and CCL20, a specific chemoattractant of Th17 lymphocytes (227). IL-17A also induces increased production of IL-6 by SFs of the TMJ (227), and IL-6 favors the Th17 cell differentiation and promotes osteoclastogenesis and bone resorption (230, 231). Thus, the increased levels of Th17-related chemokines and cytokines produced by SFs of the TMJ stimulated by IL-17A could be related to bone loss and OA progression (227).

In other synovial joints, RANKL is highly expressed on SFs (232), while in TMJ synovium, RANKL is detected in the cytoplasm of synovial lining cells, endothelial cells, and SFs (233). A recent study using Tnfsf11flox/Δ Lck-Cre mice, which lack RANKL expression in T lymphocytes, demonstrated that the absence of RANKL-producing T cells does not protect against osteoclastogenesis and bone resorption (234). On the other hand, the deletion of RANKL on SFs using Tnfsf11flox/Δ Col6a1-Cre mice was protective against osteoclastogenesis and bone loss, thus demonstrating that SFs are the primary RANKL-expressing cells, and responsible for the osteoclast formation and bone resorption during joint inflammation (234). Interestingly, TMJ chondrocytes affected by chondral degradation, may also promote osteoclastogenesis by increasing the RANKL:OPG ratio, ultimately resulting in a subchondral bone loss (235).

LMW-HA is a potent activator of APCs, in particular, dendritic cells (DCs), through the interaction with the complex TLR-4/Cluster of differentiation (CD)44/Myeloid differentiation protein (MD)-2 (236, 237). LMW-HA induces an immuno-phenotypic maturation of DCs through the up-regulation of CD44, CD83, CD80/86, intercellular adhesion molecule-1 (ICAM-1), and the major histocompatibility complex (MHC) II (238). Furthermore, DCs exposed to LMW-HA increase their capacity to stimulate alloreactive T lymphocytes to secrete IL-12, IL-1β, and TNF-α (238). Apart from that, LMW-HA could act as a co-stimulatory molecule during antigen presentation by

interacting with CD44 and could also promote the activation and polarization of T lymphocytes (239). The stimulatory effects of LMW-HA over DCs are mediated by the TLR-4 complex signaling pathway, including the phosphorylation of p38 and p42/p44 MAPK and the consequent nuclear translocation of NF-κB (237). LMW-HA also increases the migratory capacity of DCs and stimulates its trafficking toward the draining lymph nodes (240). Moreover, LMW-HA can induce the polarization of DCs to conventional type 1 (cDC1) and type 2 (cDC2) subsets, by increasing the expression levels of their specific transcription factors interferon regulatory factor 4 (IRF4), neurogenic locus notch homolog protein 2 (NOTCH2), and basic leucine zipper ATF-like transcription factor 3 (BATF3) (241). Thus, cDC1 produces TNF-α and cDC2 produces IL-6 and IL-23, inducing the selective differentiation and activation of Th1 and Th17 lymphocytes (242, 243).

Peripheral Th lymphocytes are involved in the pathogenesis of OA (244). T lymphocytes from OA patients can recognize peptides presented by APCs such as the amino acid regions 16–39 and 263–282 located in the G1 domain of human cartilage proteoglycan aggrecan (PG) (245). The recognition of these PG epitopes enhances the proliferation of OA-derived T lymphocytes and increases the production of cytokines, IL-1β, IL-6, IFN-γ, and TNF-α, and CC-chemokines, CCL-2, and CCL-3 (245). Increased expression of the Th1/Th17/Th22 cytokines IL-1β, IL-17, and IL-22, chemokines CCL5, and CCL20, and chemokines receptors CCR5 and CCR7 have been detected in synovial cells of TMJ-OA affected patients (212, 246). Further, the increased levels of IL-1β, IL-17, and IL-22 significantly correlate with the enhanced RANKL expression and immunological signs of bone degeneration (246). Moreover, the synovial fluid obtained from TMJ-OA affected patients induces significantly more osteoclast maturation and activity in comparison to synovial fluid obtained from controls (246).

Although both Th1 and Th17 cells are involved in the etiology of OA, it has been reported that the IL-23/IL-17 axis is more critical than the IL-12/IFN-γ axis in the onset of the disease (247–249). Analyses of blood samples obtained from OA affected patients, and healthy donors showed a significantly higher percentage of activated CD4+ T cells and Th17 lymphocytes in the OA group, while there were no differences between the percentages of Th1 and Th2 lymphocytes among the studied groups (250). Further, increased numbers of Th17 cells have also been detected in the OA synovial membrane (251). An osteoarthritic joint milieu with low levels of TGF-β but high levels of IL-12 induces the plasticity of Th17 lymphocytes to an intermediate phenotype between Th1 and Th17 lymphocytes known as Th17/1 cells. These cells are characterized by an increased expression of the transcription factors retinoic acid-related orphan receptor C2 (RORC2), and T-box expressed in T cells (T-bet) and production of the cytokines IFN-γ and IL-17 (252). Indeed, in OA patients, both peripheral blood and synovial fluid frequencies of Th17/1 cells are significantly increased in comparison to healthy subjects or even rheumatoid arthritis patients (253). Additionally, the enrichment of Th17/1 cells in OA patients is higher in synovial fluid than serum (253). These findings suggest that Th17/1 cells could be a Th subset with a particular role during OA and; thus, need to be further evaluated in TMJ-OA.

Higher expression levels of IL-17 have been reported in either synovial membranes or synovial fluid of TMJ-OA affected patients (212, 246, 254, 255). IL-6, a key cytokine involved in Th17 polarization, is also increased in the TMJ-OA affected patients (256). *In vitro* experiments have demonstrated that IL-17A promotes synovial hyperplasia, synoviocyte invasion, cartilage breakdown, and angiogenesis (257–260). Using SFs isolated from patients with TMJ disorders, Hattori et al. determined that IL-17A upregulates the expression of IL-6, CXCL1, IL-8, and CCL20, in a dose- and time-dependent manner, promoting T lymphocyte chemoattraction toward the TMJ synovial tissues (227). However, the central role of the Th17 lymphocytes during the pathogenesis of the joint disorders is related to its RANKL-producing osteoclastogenic function (261).

Impact of Osteoimmunology in the Osteoarthritis of the Temporomandibular Joint

Different types of cells orchestrate the physiological remodeling process within the TMJ bone microenvironment. As mentioned before, osteoclasts and osteoblasts are the primary effector cells involved in the bone resorption and formation, respectively, in the articular subchondral bone. In this molecular-and-cellular-regulated process, however, the contribution of other cell types, such as osteocytes, has been considered. Osteocytes are a group of cells which differentiate from osteoblasts, that during the formation of mineralized tissues are left embedded within the bone matrix, and further contribute to the regulation of bone metabolism (262). Even though, under physiological conditions, osteoblasts are considered as the primary source of RANKL for the RANKL-induced osteoclastogenesis and consequent osteoclast-mediated subchondral bone remodeling; osteocyte-specific RANKL-deficient mice (*Tnfsf11*$^{flox/\Delta}$ *Dmp1-Cre* or *Tnfsf11*$^{flox/flox}$ *Sost-Cre* mice) present a similar osteopetrotic phenotype than RANKL-null mice; thus, demonstrating the importance of osteocytes as a primary source of RANKL (5, 263). Moreover, by using a high-purity isolation method for osteocytes and osteoblasts, Nakashima et al. evidenced that osteocytes have a stronger ability to induce and support osteoclastogenesis than osteoblasts, through higher *Tnfsf11* (encoding RANKL) mRNA expression and RANKL production (5). Apart from that, the authors demonstrated that the absence of RANKL in T cells is not critical for bone metabolism in physiological conditions (5).

Osteocytes also actively release RANKL in response to mechanical stress (5). Indeed, osteocytes contact osteoclast precursor cells and mature osteoclasts through long dendrites that reach the bone surface, which enable direct cell-cell interaction by membrane-expressed factors released in response to load forces, such as RANKL (264). A mechanical stress experiment with MLO-Y4 osteocyte-like cells revealed that *Tnfsf11* expression is remarkably induced by mechanical strength (5). In fact, during the application of orthodontic forces for bone remodeling-dependent tooth movement, osteocytes were

the primary source of RANKL in response to compressive forces, thus promoting osteoclastogenesis and bone resorption (265). Conversely, increased loading forces during mastication induced by a hard diet in mice showed an increase in the osteocyte-mediated bone formation, through an increment of the levels of insulin-like growth factor (IGF)-1 and thus, promoting osteoblastogenesis (266). Therefore, the osteocyte response to mechanical load could drastically differ between the physiological context and the pathological scenario during TMJ-OA. Indeed, osteocytes adjacent to sites of bone microdamage, as occurs in subchondral bone during the advanced stage of TMJ-OA, undergo apoptosis; whereas osteocytes adjacent to this apoptotic cells upregulate the expression of osteoclastogenic and immunogenic signaling molecules, such as ATP, membrane-derived peptides, chemokines, vascular endothelial cell growth factor A (VEGFA), and RANKL (262). Besides, osteocytes exposed to extra-cellular matrix molecules derived from TMJ-OA subchondral bone osteoblasts showed decreased levels of maturation and increased levels of apoptosis due to a decrease in the integrin-β1 expression, in comparison with extra-cellular matrix molecules derived from normal subchondral bone osteoblasts (267). This suggests that the pathological behavior of osteocytes in response to the mechanical overload during the progression of TMJ-OA could be due to molecular and cellular changes occurring in the joint microenvironment.

The RANKL:OPG ratio is increased in synovial fluid obtained from TMJ-OA patients, mainly due to the increased levels of RANKL together with the decreased levels of OPG detected in the joint microenvironment (212, 268). The secretion of IL-17 by Th17 lymphocytes enhances the RANKL production by osteoblasts, osteocytes, and SFs and activates the production of other osteoclastogenic cytokines, such as TNF-α, IL-1β, and IL-6 by synovial macrophages (269). Thus, the accumulation of Th17 lymphocytes in synovial tissues may contribute to subchondral bone resorption by stimulating the RANKL-mediated osteoclast activity (270). Kikuta et al. using intravital multiphoton microscopy, have demonstrated that Th17 but not Th1 lymphocytes preferentially adhere to mature osteoclasts and that low levels of RANKL secreted by mature osteoclast-adhered Th17 lymphocytes could induce the rapid conversion from moving-non-resorptive to static-bone-resorptive osteoclast phenotype in bone (271). Besides, using a mice model of primary hyperparathyroidism, it was described that the osteocyte-mediated RANKL production induced by Th17-derived IL17A/IL17RA interaction is critical for the bone catabolic activity, revealing another potential mechanism of subchondral bone loss induction by Th17 cells during TMJ-OA (74). Altogether, these studies demonstrated a pivotal role for Th17 lymphocytes in the osteoimmunology of the TMJ-OA, through the modulation of the osteoblast/osteocyte/osteoclast activity (**Figure 4**).

Overall, the evidence presented above shows that TMJ-OA could be considered a chronic mechanically induced and immuno-inflammatory-mediated disease, mainly due to the continuous production of DAMPs during joint tissues destruction, particularly LMW-HA, the activation of a Th17-pattern of immune response and the consequent RANKL-mediated and osteoclast-induced bone resorption.

Translational Applications

For the diagnosis of the TMJ-OA, four criteria are usually used: Joint noises, chronic joint pain, joint cramping during movements of the jaw, and degenerative bone deterioration detected through imaging (111, 214, 272). However, these criteria are only observable when the disease has been established, and tissue damage has occurred; so these gold-standard criteria do not allow early symptoms detection to prevent or stop the progression of TMJ-OA. In addition, when the diagnosis has been made, the analysis of treatment success is based on exactly the same criteria and, in older adults, these criteria are unreliable, due to the subjective component of clinical symptoms and the involuntary movements that many individuals present, which diminish the sharpness of the images and in some cases making their contribution, as a complement to the diagnosis, uncertain (273).

Several research groups have proposed to incorporate competing molecular strategies that could allow the early diagnosis of TMJ-OA and the evaluation of its therapeutic success (256, 273–281). In this sense, the determination of molecular mediators associated with the inflammatory and destructive articular tissue processes characteristic of TMJ-OA is convenient; however, nowadays, there are no registered initiatives focused on the development of an alternative solution complementary to the current standards for the diagnosis of the disease.

In this sense, the validation of a diagnostic strategy based on the identification of a panel of detectable biomarkers in the synovial fluid of the TMJ and complementary to the traditional clinical-imaging methods of diagnosis of TMJ-OA is feasible. An ideal diagnostic panel should incorporate osteoimmunology markers. In this way, the identification of molecular mediators associated with the differentiation and activity of osteoblasts, osteoclasts and/or osteocytes, as well as cytokines (IL-1β, IL-6, IL-17, IL-12, and TNF-α), MMPs (MMP-8 and MMP-9), and RANKL, could be proposed as potentially sensitive and specific biomarkers to detect early degenerative changes in the TMJ.

CONCLUSIONS

The understanding of the immune-mediated bone destruction during periodontal diseases, periapical infections, maxillary bone-sarcomas, and temporomandibular joint osteoarthritis require a detailed analysis of a wide array of pathways. While each disease in the oral and maxillofacial milieu has a distinct etiological basis, recent work has demonstrated that several mechanistic aspects could share common cellular and molecular processes that are unique to the oral and maxillofacial structures. In this work, we have reviewed the cutting-edge literature in an attempt to identify the most current knowledge in the oral osteoimmunology to provide new therapeutic approaches in otherwise difficult to treat bone lesions. The characterization of the different molecules involved in immune-mediated tissue destruction has been identified to provide biomarkers that would

be useful to comprehend the link between bone-destructive oral diseases, such as periodontal disease and apical periodontitis, with systemic diseases. Collectively, the work represents a unique attempt to tackle common pathways of osteoimmunology and osteoinflammation of the oral cavity, which presents a highly unique environment colonized by the highest number of bacterial species in the mammalian body and regulated by highly functional biomechanical forces created by occlusion. Thus, successful prevention and treatment of oral diseases require recognition of this complexity to design specialized therapeutic approaches and maintain the treatment outcomes.

AUTHOR CONTRIBUTIONS

CA, RV, and AK conceived the original idea and designed the manuscript. TS, PP, H-ML, LG, and MH provided the data. CA, FC, LC, GM, and MH designed the figures. GG edited the figures. All authors participated in manuscript writing and critically reviewed the manuscript. AK edited the manuscript and supervised the project.

FUNDING

This work was financially supported by grants TYH 2016251, TYH 2017251, TYH 2018229, Y1014SL017, and Y1014SL018 from the Helsinki University Hospital Research Foundation, Finland; The Finnish Dental Association Apollonia; The Karolinska Institutet, Stockholm, Sweden; NIDCR grants R01 DE012872 and R01 DE25020 NIH; and grants FONDECYT 1140904, 1160741, and 1181780 from Comisión Nacional de Investigación Científica y Tecnológica (CONICYT) from the Chilean Government. AK is supported by NIH grant AG062496.

REFERENCES

1. Furuya M, Kikuta J, Fujimori S, Seno S, Maeda H, Shirazaki M, et al. Direct cell–cell contact between mature osteoblasts and osteoclasts dynamically controls their functions *in vivo*. *Nat Commun*. (2018) 9:300. doi: 10.1038/s41467-017-02541-w
2. Sims NA, Martin TJ. Coupling the activities of bone formation and resorption: a multitude of signals within the basic multicellular unit. *BoneKEy Rep*. (2014) 3:481. doi: 10.1038/bonekey.2013.215
3. Graves DT, Li J, Cochran DL. Inflammation and uncoupling as mechanisms of periodontal bone loss. *J Dental Res*. (2011) 90:143–53. doi: 10.1177/0022034510385236
4. Takayanagi H. Inflammatory bone destruction and osteoimmunology. *J Periodontal Res*. (2005) 40:287–93. doi: 10.1111/j.1600-0765.2005.00814.x
5. Nakashima T, Hayashi M, Fukunaga T, Kurata K, Oh-Hora M, Feng JQ, et al. Evidence for osteocyte regulation of bone homeostasis through RANKL expression. *Nat Med*. (2011) 17:1231–4. doi: 10.1038/nm.2452
6. Xiong J, Onal M, Jilka RL, Weinstein RS, Manolagas SC, O'Brien CA. Matrix-embedded cells control osteoclast formation. *Nat Med*. (2011) 17:1235–41. doi: 10.1038/nm.2448
7. Ikebuchi Y, Aoki S, Honma M, Hayashi M, Sugamori Y, Khan M, et al. Coupling of bone resorption and formation by RANKL reverse signalling. *Nature*. (2018) 561:195–200. doi: 10.1038/s41586-018-0482-7
8. Kawai T, Matsuyama T, Hosokawa Y, Makihira S, Seki M, Karimbux NY, et al. B and T lymphocytes are the primary sources of RANKL in the bone resorptive lesion of periodontal disease. *Am J Pathol*. (2006) 169:987–98. doi: 10.2353/ajpath.2006.060180
9. Tsukasaki M, Komatsu N, Nagashima K, Nitta T, Pluemsakunthai W, Shukunami C, et al. Host defense against oral microbiota by bone-damaging T cells. *Nat Commun*. (2018) 9:701. doi: 10.1038/s41467-018-03147-6
10. Takei Y, Minamizaki T, Yoshiko Y. Functional diversity of fibroblast growth factors in bone formation. *Int J Endocrinol*. (2015) 2015:729352. doi: 10.1155/2015/729352
11. Davies OG, Grover LM, Lewis MP, Liu Y. PDGF is a potent initiator of bone formation in a tissue engineered model of pathological ossification. *J Tissue Eng Regenerat Med*. (2018) 12:e355-e67. doi: 10.1002/term.2320
12. Yakar S, Rosen CJ, Beamer WG, Ackert-Bicknell CL, Wu Y, Liu J-L, et al. Circulating levels of IGF-1 directly regulate bone growth and density. *J Clin Invest*. (2002) 110:771–81. doi: 10.1172/JCI0215463
13. Wu M, Chen G, Li Y-P. TGF-β and BMP signaling in osteoblast, skeletal development, and bone formation, homeostasis and disease. *Bone Res*. (2016) 4:16009. doi: 10.1038/boneres.2016.9
14. Chen Y, Alman BA. Wnt pathway, an essential role in bone regeneration. *J Cell Biochem*. (2009) 106:353–62. doi: 10.1002/jcb.22020
15. Tu X, Delgado-Calle J, Condon KW, Maycas M, Zhang H, Carlesso N, et al. Osteocytes mediate the anabolic actions of canonical Wnt/beta-catenin signaling in bone. *Proc Natl Acad Sci USA*. (2015) 112:E478-86. doi: 10.1073/pnas.1409857112
16. Phimphilai M, Zhao Z, Boules H, Roca H, Franceschi RT. BMP signaling is required for RUNX2-dependent induction of the osteoblast phenotype. *J Bone Mineral Res*. (2006) 21:637–46. doi: 10.1359/jbmr.060109
17. Ruaro B, Casabella A, Paolino S, Pizzorni C, Ghio M, Seriolo C, et al. Dickkopf-1 (Dkk-1) serum levels in systemic sclerosis and rheumatoid arthritis patients: correlation with the Trabecular Bone Score (TBS). *Clin Rheumatol*. (2018) 37:3057–62. doi: 10.1007/s10067-018-4322-9
18. Napimoga MH, Nametala C, da Silva FL, Miranda TS, Bossonaro JP, Demasi AP, et al. Involvement of the Wnt-beta-catenin signalling antagonists, sclerostin and dickkopf-related protein 1, in chronic periodontitis. *J Clin Periodontol*. (2014) 41:550–7. doi: 10.1111/jcpe.12245
19. Matzelle MM, Gallant MA, Condon KW, Walsh NC, Manning CA, Stein GS, et al. Resolution of inflammation induces osteoblast function and regulates the Wnt signaling pathway. *Arthritis Rheumat*. (2012) 64:1540–50. doi: 10.1002/art.33504
20. Glass DA II, Bialek P, Ahn JD, Starbuck M, Patel MS, Clevers H, et al. Canonical Wnt signaling in differentiated osteoblasts controls osteoclast differentiation. *Dev Cell*. (2005) 8:751-64. doi: 10.1016/j.devcel.2005.02.017
21. Hajishengallis G. Periodontitis: from microbial immune subversion to systemic inflammation. *Nat Rev Immunol*. (2015) 15:30-44. doi: 10.1038/nri3785
22. Hajishengallis G, Korostoff JM. Revisiting the Page & Schroeder model: the good, the bad and the unknowns in the periodontal host response 40 years later. *Periodontology 2000*. (2017) 75:116–51. doi: 10.1111/prd.12181
23. Papapanou PN, Sanz M, Buduneli N, Dietrich T, Feres M, Fine DH, et al. Periodontitis: Consensus report of workgroup 2 of the 2017 world workshop on the classification of periodontal and peri-implant diseases and conditions. *J Periodontol*. (2018) 45:S162–S70. doi: 10.1111/jcpe.12946
24. Kurgan S, Kantarci A. Molecular basis for immunohistochemical and inflammatory changes during progression of gingivitis to periodontitis. *Periodontology 2000*. (2018) 76:51–67. doi: 10.1111/prd.12146
25. Hajishengallis G. The inflammophilic character of the periodontitis-associated microbiota. *Mol Oral Microbiol*. (2014) 29:248-57. doi: 10.1111/omi.12065
26. Hajishengallis G. Complement and periodontitis. *Biochem Pharmacol*. (2010) 80:1992–2001. doi: 10.1016/j.bcp.2010.06.017
27. Schenkein HA, Genco RJ. Gingival fluid and serum in periodontal diseases. II. Evidence for cleavage of complement components C3, C3 proactivator

(factor B) and C4 in gingival fluid. *J Periodontol*. (1977) 48:778–84. doi: 10.1902/jop.1977.48.12.778
28. Hajishengallis G, Hajishengallis E, Kajikawa T, Wang B, Yancopoulou D, Ricklin D, et al. Complement inhibition in pre-clinical models of periodontitis and prospects for clinical application. *Semi Immunol*. (2016) 28:285–91. doi: 10.1016/j.smim.2016.03.006
29. Liang S, Krauss JL, Domon H, McIntosh ML, Hosur KB, Qu H, et al. The C5a receptor impairs IL-12-dependent clearance of Porphyromonas gingivalis and is required for induction of periodontal bone loss. *J Immunol*. (2011) 186:869–77. doi: 10.4049/jimmunol.1003252
30. Grant EP, Picarella D, Burwell T, Delaney T, Croci A, Avitahl N, et al. Essential role for the C5a receptor in regulating the effector phase of synovial infiltration and joint destruction in experimental arthritis. *J Exp Med*. (2002) 196:1461–71. doi: 10.1084/jem.20020205
31. Modinger Y, Loffler B, Huber-Lang M, Ignatius A. Complement involvement in bone homeostasis and bone disorders. *Sem Immunol*. (2018) 37:53–65. doi: 10.1016/j.smim.2018.01.001
32. Olsen I, Lambris JD, Hajishengallis G. Porphyromonas gingivalis disturbs host-commensal homeostasis by changing complement function. *J Oral Microbiol*. (2017) 9:1340085. doi: 10.1080/20002297.2017.1340085
33. Hajishengallis E, Hajishengallis G. Neutrophil homeostasis and periodontal health in children and adults. *J Dental Res*. (2014) 93:231–7. doi: 10.1177/0022034513507956
34. Hajishengallis G, Moutsopoulos NM, Hajishengallis E, Chavakis T. Immune and regulatory functions of neutrophils in inflammatory bone loss. *Semi Immunol*. (2016) 28:146–58. doi: 10.1016/j.smim.2016.02.002
35. Moutsopoulos NM, Konkel J, Sarmadi M, Eskan MA, Wild T, Dutzan N, et al. Defective neutrophil recruitment in leukocyte adhesion deficiency type I disease causes local IL-17-driven inflammatory bone loss. *Sci Transl Med*. (2014) 6:229ra40-ra40. doi: 10.1126/scitranslmed.3007696
36. Sochalska M, Potempa J. Manipulation of neutrophils by *Porphyromonas gingivalis* in the development of periodontitis. *Front Cell Infect Microbiol*. (2017) 7:197. doi: 10.3389/fcimb.2017.00197
37. Maekawa T, Krauss JL, Abe T, Jotwani R, Triantafilou M, Triantafilou K, et al. *Porphyromonas gingivalis* manipulates complement and TLR signaling to uncouple bacterial clearance from inflammation and promote dysbiosis. *Cell Host Microbe*. (2014) 15:768–78. doi: 10.1016/j.chom.2014.05.012
38. Ling MR, Chapple IL, Matthews JB. Peripheral blood neutrophil cytokine hyper-reactivity in chronic periodontitis. *Innate Immunity*. (2015) 21:714–25. doi: 10.1177/1753425915589387
39. Kantarci A, Oyaizu K, Van Dyke TE. Neutrophil-mediated tissue injury in periodontal disease pathogenesis: findings from localized aggressive periodontitis. *J Periodontol*. (2003) 74:66–75. doi: 10.1902/jop.2003.74.1.66
40. Allaeys I, Rusu D, Picard S, Pouliot M, Borgeat P, Poubelle PE. Osteoblast retraction induced by adherent neutrophils promotes osteoclast bone resorption: implication for altered bone remodeling in chronic gout. *Lab Invest.* (2011) 91:905–20. doi: 10.1038/labinvest.2011.46
41. Zhang N, Schroppel B, Lal G, Jakubzick C, Mao X, Chen D, et al. Regulatory T cells sequentially migrate from inflamed tissues to draining lymph nodes to suppress the alloimmune response. *Immunity*. (2009) 30:458–69. doi: 10.1016/j.immuni.2008.12.022
42. Lewkowicz N, Mycko MP, Przygodzka P, ćwiklińska H, Cichalewska M, Matysiak M, et al. Induction of human IL-10-producing neutrophils by LPS-stimulated Treg cells and IL-10. *Mucosal Immunol*. (2015) 9:364. doi: 10.1038/mi.2015.66
43. Dutzan N, Konkel JE, Greenwell-Wild T, Moutsopoulos NM. Characterization of the human immune cell network at the gingival barrier. *Mucosal Immunol*. (2016) 9:1163–72. doi: 10.1038/mi.2015.136
44. Hasturk H, Kantarci A, Van Dyke TE. Oral inflammatory diseases and systemic inflammation: role of the macrophage. *Front Immunol*. (2012) 3:118. doi: 10.3389/fimmu.2012.00118
45. Lavin Y, Mortha A, Rahman A, Merad M. Regulation of macrophage development and function in peripheral tissues. *Nat Rev Immunol*. (2015) 15:731–44. doi: 10.1038/nri3920
46. Murray PJ, Wynn TA. Protective and pathogenic functions of macrophage subsets. *Nat Rev Immunol*. (2011) 11:723-37. doi: 10.1038/nri3073
47. Sima C, Glogauer M. Macrophage subsets and osteoimmunology: tuning of the immunological recognition and effector systems that maintain alveolar bone. *Periodontology 2000*. (2013) 63:80–101. doi: 10.1111/prd.12032
48. Yang J, Zhu Y, Duan D, Wang P, Xin Y, Bai L, et al. Enhanced activity of macrophage M1/M2 phenotypes in periodontitis. *Arch Oral Biol*. (2018) 96:234–42. doi: 10.1016/j.archoralbio.2017.03.006
49. Yu T, Zhao L, Huang X, Ma C, Wang Y, Zhang J, et al. Enhanced activity of the macrophage M1/M2 phenotypes and phenotypic switch to M1 in periodontal infection. *J Periodontol*. (2016) 87:1092–102. doi: 10.1902/jop.2016.160081
50. Miyajima S, Naruse K, Kobayashi Y, Nakamura N, Nishikawa T, Adachi K, et al. Periodontitis-activated monocytes/macrophages cause aortic inflammation. *Sci Rep*. (2014) 4:5171. doi: 10.1038/srep05171
51. Viniegra A, Goldberg H, Cil C, Fine N, Sheikh Z, Galli M, et al. Resolving macrophages counter osteolysis by anabolic actions on bone cells. *J Dental Res*. (2018) 97:1160–9. doi: 10.1177/0022034518777973
52. Baker PJ, Dixon M, Evans RT, Dufour L, Johnson E, Roopenian DC. CD4(+) T cells and the proinflammatory cytokines gamma interferon and interleukin-6 contribute to alveolar bone loss in mice. *Infect Immunity*. (1999) 67:2804-9.
53. Cardoso EM, Arosa FA. CD8(+) T cells in chronic periodontitis: roles and rules. *Front Immunol*. (2017) 8:145. doi: 10.3389/fimmu.2017.00145
54. Bluestone JA, Mackay CR, O'Shea JJ, Stockinger B. The functional plasticity of T cell subsets. *Nat Rev Immunol*. (2009) 9:811. doi: 10.1038/nri2654
55. Garlet GP, Giannobile WV. Macrophages: the bridge between inflammation resolution and tissue repair? *J Dental Res*. (2018) 97:1079–81. doi: 10.1177/0022034518785857
56. Diaz-Zuniga J, Melgar-Rodriguez S, Rojas L, Alvarez C, Monasterio G, Carvajal P, et al. Increased levels of the T-helper 22-associated cytokine (interleukin-22) and transcription factor (aryl hydrocarbon receptor) in patients with periodontitis are associated with osteoclast resorptive activity and severity of the disease. *J Periodontal Res*. (2017) 52:893–902. doi: 10.1111/jre.12461
57. Diaz-Zuniga J, Melgar-Rodriguez S, Monasterio G, Pujol M, Rojas L, Alvarez C, et al. Differential human Th22-lymphocyte response triggered by Aggregatibacter actinomycetemcomitans serotypes. *Arch Oral Biol*. (2017) 78:26–33. doi: 10.1016/j.archoralbio.2017.02.008
58. Garlet GP, Cardoso CR, Campanelli AP, Garlet TP, Avila-Campos MJ, Cunha FQ, et al. The essential role of IFN-gamma in the control of lethal Aggregatibacter actinomycetemcomitans infection in mice. *Microb Infect*. (2008) 10:489–96. doi: 10.1016/j.micinf.2008.01.010
59. Mizraji G, Nassar M, Segev H, Sharawi H, Eli-Berchoer L, Capucha T, et al. Porphyromonas gingivalis promotes unrestrained Type I interferon production by dysregulating TAM signaling via MYD88 degradation. *Cell Rep*. (2017) 18:419–31. doi: 10.1016/j.celrep.2016.12.047
60. Yang XO, Pappu BP, Nurieva R, Akimzhanov A, Kang HS, Chung Y, et al. T helper 17 lineage differentiation is programmed by orphan nuclear receptors ROR alpha and ROR gamma. *Immunity*. (2008) 28:29–39. doi: 10.1016/j.immuni.2007.11.016
61. Dutzan N, Abusleme L, Bridgeman H, Greenwell-Wild T, Zangerle-Murray T, Fife ME, et al. On-going mechanical damage from mastication drives homeostatic Th17 cell responses at the oral barrier. *Immunity*. (2017) 46:133–47. doi: 10.1016/j.immuni.2016.12.010
62. Dutzan N, Kajikawa T, Abusleme L, Greenwell-Wild T, Zuazo CE, Ikeuchi T, et al. A dysbiotic microbiome triggers Th17 cells to mediate oral mucosal immunopathology in mice and humans. *Sci Transl Med*. (2018) 10:eaat0797. doi: 10.1126/scitranslmed.aat0797
63. Araujo-Pires AC, Vieira AE, Francisconi CF, Biguetti CC, Glowacki A, Yoshizawa S, et al. IL-4/CCL22/CCR4 axis controls regulatory T-cell migration that suppresses inflammatory bone loss in murine experimental periodontitis. *J Bone Mineral Res*. (2015) 30:412-22. doi: 10.1002/jbmr.2376
64. Alvarez C, Rojas C, Rojas L, Cafferata EA, Monasterio G, Vernal R. Regulatory T lymphocytes in periodontitis: a translational view. *Medi Inflamm*. (2018) 2018:7806912. doi: 10.1155/2018/7806912
65. Abe T, AlSarhan M, Benakanakere MR, Maekawa T, Kinane DF, Cancro MP, et al. The B cell-stimulatory cytokines BLyS and APRIL are elevated in human periodontitis and are required for B cell-dependent bone loss

in experimental murine periodontitis. *J Immunol*. (2015) 195:1427–35. doi: 10.4049/jimmunol.1500496
66. Nakajima T, Amanuma R, Ueki-Maruyama K, Oda T, Honda T, Ito H, et al. CXCL13 expression and follicular dendritic cells in relation to B-cell infiltration in periodontal disease tissues. *J Periodontal Res*. (2008) 43:635–41. doi: 10.1111/j.1600-0765.2008.01042.x
67. Demoersman J, Pochard P, Framery C, Simon Q, Boisrame S, Soueidan A, et al. B cell subset distribution is altered in patients with severe periodontitis. *PLoS ONE*. (2018) 13:e0192986. doi: 10.1371/journal.pone.0192986
68. Mahanonda R, Champaiboon C, Subbalekha K, Sa-Ard-Iam N, Rattanathammatada W, Thawanaphong S, et al. Human memory B cells in healthy gingiva, gingivitis, and periodontitis. *J Immunol*. (2016) 197:715–25. doi: 10.4049/jimmunol.1600540
69. Rosser Elizabeth C, Mauri C. Regulatory B cells: origin, phenotype, and function. *Immunity*. (2015) 42:607–12. doi: 10.1016/j.immuni.2015.04.005
70. Wang Y, Yu X, Lin J, Hu Y, Zhao Q, Kawai T, et al. B10 cells alleviate periodontal bone loss in experimental periodontitis. *Infect Immunity*. (2017) 85:e00335-17. doi: 10.1128/IAI.00335-17
71. Jonasson G, Skoglund I, Rythen M. The rise and fall of the alveolar process: dependency of teeth and metabolic aspects. *Arch Oral Biol*. (2018) 96:195–200. doi: 10.1016/j.archoralbio.2018.09.016
72. Pacios S, Xiao W, Mattos M, Lim J, Tarapore RS, Alsadun S, et al. Osteoblast lineage cells play an essential role in periodontal bone loss through activation of nuclear factor-kappa B. *Sci Rep*. (2015) 5:16694. doi: 10.1038/srep16694
73. Wu Q, Zhou X, Huang D, Ji Y, Kang F. IL-6 enhances osteocyte-mediated osteoclastogenesis by promoting JAK2 and RANKL activity *in vitro*. *Cell Physiol Biochem*. (2017) 41:1360–9. doi: 10.1159/000465455
74. Li J-Y, Yu M, Tyagi AM, Vaccaro C, Hsu E, Adams J, et al. IL-17 receptor signaling in osteoblasts/osteocytes mediates PTH-induced bone loss and enhances osteocytic RANKL production. *J Bone Mineral Res*. (2019) 34:349–60. doi: 10.1002/jbmr.3600
75. Graves DT, Alshabab A, Albiero ML, Mattos M, Corrêa JD, Chen S, et al. Osteocytes play an important role in experimental periodontitis in healthy and diabetic mice through expression of RANKL. *J Clin Periodontol*. (2018) 45:285–92. doi: 10.1111/jcpe.12851
76. Sakamoto E, Kido J-i, Takagi R, Inagaki Y, Naruishi K, Nagata T, et al. Advanced glycation end-product 2 and Porphyromonas gingivalis lipopolysaccharide increase sclerostin expression in mouse osteocyte-like cells. *Bone*. (2019) 122:22–30. doi: 10.1016/j.bone.2019.02.001
77. Lin D, Li L, Sun Y, Wang W, Wang X, Ye Y, et al. IL-17 regulates the expressions of RANKL and OPG in human periodontal ligament cells via TRAF6/TBK1-JNK/NF-κB pathways. *Immunology*. (2014) 144:472–85. doi: 10.1111/imm.12395
78. Alippe Y, Wang C, Ricci B, Xiao J, Qu C, Zou W, et al. Bone matrix components activate the NLRP3 inflammasome and promote osteoclast differentiation. *Sci Rep*. (2017) 7:6630. doi: 10.1038/s41598-017-07014-0
79. Wei S, Kitaura H, Zhou P, Ross FP, Teitelbaum SL. IL-1 mediates TNF-induced osteoclastogenesis. *J Clin Invest*. (2005) 115:282–90. doi: 10.1172/JCI200523394
80. Kajikawa T, Briones RA, Resuello RRG, Tuplano JV, Reis ES, Hajishengallis E, et al. Safety and efficacy of the complement inhibitor AMY-101 in a natural model of periodontitis in non-human primates. *Mol Therapy Methods Clin Dev*. (2017) 6:207–15. doi: 10.1016/j.omtm.2017.08.001
81. Maekawa T, Briones RA, Resuello RR, Tuplano JV, Hajishengallis E, Kajikawa T, et al. Inhibition of pre-existing natural periodontitis in non-human primates by a locally administered peptide inhibitor of complement C3. *J Clin Periodontol*. (2016) 43:238–49. doi: 10.1111/jcpe.12507
82. Zhuang Z, Yoshizawa-Smith S, Glowacki A, Maltos K, Pacheco C, Shehabeldin M, et al. Induction of M2 macrophages prevents bone loss in murine periodontitis models. *J Dental Res*. (2018) 98:200–8. doi: 10.1177/0022034518805984
83. Jin Y, Wang L, Liu D, Lin X. Tamibarotene modulates the local immune response in experimental periodontitis. *Int Immunopharmacol*. (2014) 23:537–45. doi: 10.1016/j.intimp.2014.10.003
84. Wang L, Wang J, Jin Y, Gao H, Lin X. Oral administration of all-trans retinoic acid suppresses experimental periodontitis by modulating the Th17/treg imbalance. *J Periodontol*. (2014) 85:740–50. doi: 10.1902/jop.2013.130132
85. Mizraji G, Heyman O, Van Dyke TE, Wilensky A. Resolvin D2 restrains Th1 immunity and prevents alveolar bone loss in murine periodontitis. *Front Immunol*. (2018) 9:785. doi: 10.3389/fimmu.2018.00785
86. Hu Y, Yu P, Yu X, Hu X, Kawai T, Han X. IL-21/anti-Tim1/CD40 ligand promotes B10 activity in vitro and alleviates bone loss in experimental periodontitis *in vivo*. *Biochim et Biophy Acta Mol Basis Dis*. (2017) 1863:2149–57. doi: 10.1016/j.bbadis.2017.06.001
87. Cavalla F, Araujo-Pires AC, Biguetti CC, Garlet GP. Cytokine networks regulating inflammation and immune defense in the oral cavity. *Curr Oral Health Rep*. (2014) 1:104-13. doi: 10.1007/s40496-014-0016-9
88. Cavalla F, Biguetti CC, Garlet T, Trombone A, Garlet GP. Inflammatory *Pathways of Bone Resorption in Periodontitis, in Pathogenesis of Periodontal Diseases Biological Concepts for Clinicians*. Switzerland: Springer International Publishing AG. (2018) 59-86. doi: 10.1007/978-3-319-53737-5_6
89. Francisconi CF, Vieira AE, Biguetti CC, Glowacki AJ, Trombone AP, Letra A, et al. Characterization of the protective role of regulatory T cells in experimental periapical lesion development and their chemoattraction manipulation as a therapeutic tool. *J Endodont*. (2016) 42:120–6. doi: 10.1016/j.joen.2015.09.022
90. Garlet GP. Destructive and protective roles of cytokines in periodontitis: a re-appraisal from host defense and tissue destruction viewpoints. *J Dental Res*. (2010) 89:1349-63. doi: 10.1177/0022034510376402
91. Jansson L. Relationship between apical periodontitis and marginal bone loss at individual level from a general population. *Int Dental J*. (2015) 65:71–6. doi: 10.1111/idj.12143
92. Silva N, Abusleme L, Bravo D, Dutzan N, Garcia-Sesnich J, Vernal R, et al. Host response mechanisms in periodontal diseases. *J Appl Oral Sci*. (2015) 23:329–55. doi: 10.1590/1678-775720140259
93. Repeke CE, Ferreira SB Jr, Vieira AE, Silveira EM, Avila-Campos MJ, da Silva JS, et al. Dose-response met-RANTES treatment of experimental periodontitis: a narrow edge between the disease severity attenuation and infection control. *PLoS ONE*. (2011) 6:e22526. doi: 10.1371/journal.pone.0022526
94. Tomson PL, Simon SR. Contemporary cleaning and shaping of the root canal system. *Primary Dental J*. (2016) 5:46–53. doi: 10.1308/205016816819304196
95. Darcey J, Roudsari RV, Jawad S, Taylor C, Hunter M. Modern endodontic principles. part 5: obturation. *Dental Update*. (2016) 43:114–6. doi: 10.12968/denu.2016.43.2.114
96. Menezes-Silva R, Khaliq S, Deeley K, Letra A, Vieira AR. Genetic susceptibility to periapical disease: conditional contribution of MMP2 and MMP3 genes to the development of periapical lesions and healing response. *J Endodont*. (2012) 38:604–7. doi: 10.1016/j.joen.2012.02.009
97. Hernandez M, Dutzan N, Garcia-Sesnich J, Abusleme L, Dezerega A, Silva N, et al. Host-pathogen interactions in progressive chronic periodontitis. *J Dental Res*. (2011) 90:1164–70. doi: 10.1177/0022034511401405
98. Provenzano JC, Antunes HS, Alves FR, Rocas IN, Alves WS, Silva MR, et al. Host-bacterial interactions in post-treatment apical periodontitis: a metaproteome analysis. *J Endodont*. (2016) 42:880–5. doi: 10.1016/j.joen.2016.02.013
99. Garlet GP, Trombone AP, Menezes R, Letra A, Repeke CE, Vieira AE, et al. The use of chronic gingivitis as reference status increases the power and odds of periodontitis genetic studies: a proposal based in the exposure concept and clearer resistance and susceptibility phenotypes definition. *J Clin Periodontol*. (2012) 39:323–32. doi: 10.1111/j.1600-051X.2012.01859.x
100. Dill A, Letra A, Chaves de Souza L, Yadlapati M, Biguetti CC, Garlet GP, et al. Analysis of multiple cytokine polymorphisms in individuals with untreated deep carious lesions reveals IL1B (rs1143643) as a susceptibility factor for periapical lesion development. *J Endodont*. (2015) 41:197–200. doi: 10.1016/j.joen.2014.10.016
101. Maheshwari K, Silva RM, Guajardo-Morales L, Garlet GP, Vieira AR, Letra A. Heat shock 70 protein genes and genetic susceptibility to apical periodontitis. *J Endodont*. (2016) 42:1467–71. doi: 10.1016/j.joen.2016.07.010
102. Cavalla F, Biguetti CC, Dionisio TJ, Azevedo MCS, Martins W Jr, Santos CF, et al. CCR5Delta32 (rs333) polymorphism is associated with decreased risk of chronic and aggressive periodontitis: A case-control analysis based in disease resistance and susceptibility phenotypes. *Cytokine*. (2018) 103:142–9. doi: 10.1016/j.cyto.2017.09.022

103. Cavalla F, Hernández-Ríos P, Sorsa T, Biguetti C, Hernández M. Matrix metalloproteinases as regulators of periodontal inflammation. *Int J Mol Sci*. (2017) 18:440. doi: 10.3390/ijms18020440
104. Trombone AP, Cavalla F, Silveira EM, Andreo CB, Franciscone CF, Fonseca AC, et al. MMP1-1607 polymorphism increases the risk for periapical lesion development through the upregulation MMP-1 expression in association with pro-inflammatory milieu elements. *J Appl Oral Sci*. (2016) 24:366–75. doi: 10.1590/1678-775720160112
105. Lerner UH, Ohlsson C. The WNT system: background and its role in bone. *J Int Med*. (2015) 277:630–49. doi: 10.1111/joim.12368
106. Tan Z, Ding N, Lu H, Kessler JA, Kan L. Wnt signaling in physiological and pathological bone formation. *Histol Histopathol*. (2018) 34:18062. doi: 10.14670/HH-18-062
107. Menezes R, Garlet TP, Letra A, Bramante CM, Campanelli AP, Figueira Rde C, et al. Differential patterns of receptor activator of nuclear factor kappa B ligand/osteoprotegerin expression in human periapical granulomas: possible association with progressive or stable nature of the lesions. *J Endodont*. (2008) 34:932–8. doi: 10.1016/j.joen.2008.05.002
108. Araujo-Pires AC, Francisconi CF, Biguetti CC, Cavalla F, Aranha AM, Letra A, et al. Simultaneous analysis of T helper subsets (Th1, Th2, Th9, Th17, Th22, Tfh, Tr1 and Tregs) markers expression in periapical lesions reveals multiple cytokine clusters accountable for lesions activity and inactivity status. *J Appl Oral Sci*. (2014) 22:336–46. doi: 10.1590/1678-775720140140
109. Hu X, Ivashkiv LB. Cross-regulation of signaling pathways by interferon-gamma: implications for immune responses and autoimmune diseases. *Immunity*. (2009) 31:539–50. doi: 10.1016/j.immuni.2009.09.002
110. van Hamburg JP, Tas SW. Molecular mechanisms underpinning T helper 17 cell heterogeneity and functions in rheumatoid arthritis. *J Autoimmunity*. (2018) 87:69–81. doi: 10.1016/j.jaut.2017.12.006
111. Wang L, Zhao Y, Shi S. Interplay between mesenchymal stem cells and lymphocytes: implications for immunotherapy and tissue regeneration. *J Dental Res*. (2012) 91:1003–10. doi: 10.1177/0022034512460404
112. Francisconi CF, Vieira AE, Azevedo MCS, Tabanez AP, Fonseca AC, Trombone APF, et al. RANKL triggers treg-mediated immunoregulation in inflammatory osteolysis. *J Dental Res*. (2018) 97:917–27. doi: 10.1177/0022034518759302
113. Lin J, Yang L, Silva HM, Trzeciak A, Choi Y, Schwab SR, et al. Increased generation of Foxp3(+) regulatory T cells by manipulating antigen presentation in the thymus. *Nat Commun*. (2016) 7:10562. doi: 10.1038/ncomms10562
114. Cavalla F, Reyes M, Vernal R, Alvarez C, Paredes R, Garcia-Sesnich J, et al. High levels of CXC ligand 12/stromal cell-derived factor 1 in apical lesions of endodontic origin associated with mast cell infiltration. *J Endodont*. (2013) 39:1234–9. doi: 10.1016/j.joen.2013.06.020
115. Rivellese F, Mauro D, Nerviani A, Pagani S, Fossati-Jimack L, Messemaker T, et al. Mast cells in early rheumatoid arthritis associate with disease severity and support B cell autoantibody production. *Ann Rheumat Dis*. (2018) 77:1773–81. doi: 10.1136/annrheumdis-2018-213418
116. Cardamone C, Parente R, Feo GD, Triggiani M. Mast cells as effector cells of innate immunity and regulators of adaptive immunity. *Immunol Lett*. (2016) 178:10–4. doi: 10.1016/j.imlet.2016.07.003
117. Dallenga T, Schaible UE. Neutrophils in tuberculosis–first line of defence or booster of disease and targets for host-directed therapy? *Pathog Dis*. (2016) 74:ftw012. doi: 10.1093/femspd/ftw012
118. Pechous RD. With friends like these: the complex role of neutrophils in the progression of severe pneumonia. *Front Cell Infect Microbiol*. (2017) 7:160. doi: 10.3389/fcimb.2017.00160
119. Cavalla F, Biguetti C, Jain S, Johnson C, Letra A, Garlet GP, et al. Proteomic profiling and differential messenger RNA expression correlate HSP27 and serpin family B member 1 to apical periodontitis outcomes. *J Endodont*. (2017) 43:1486–93. doi: 10.1016/j.joen.2017.03.014
120. Singh MK, Sharma B, Tiwari PK. The small heat shock protein Hsp27: present understanding and future prospects. *J Therm Biol*. (2017) 69:149–54. doi: 10.1016/j.jtherbio.2017.06.004
121. Baumann M, Pham CT, Benarafa C. SerpinB1 is critical for neutrophil survival through cell-autonomous inhibition of cathepsin G. *Blood*. (2013) 121:3900–7. doi: 10.1182/blood-2012-09-455022
122. Garlet GP, Horwat R, Ray HL Jr, Garlet TP, Silveira EM, Campanelli AP, et al. Expression analysis of wound healing genes in human periapical granulomas of progressive and stable nature. *J Endodont*. (2012) 38:185–90. doi: 10.1016/j.joen.2011.09.011
123. Al-Dujaili SA, Lau E, Al-Dujaili H, Tsang K, Guenther A, You L. Apoptotic osteocytes regulate osteoclast precursor recruitment and differentiation *in vitro*. *J Cell Biochem*. (2011) 112:2412–23. doi: 10.1002/jcb.23164
124. Hayashida C, Ito J, Nakayachi M, Okayasu M, Ohyama Y, Hakeda Y, et al. Osteocytes produce interferon-beta as a negative regulator of osteoclastogenesis. *J Biol Chem*. (2014) 289:11545–55. doi: 10.1074/jbc.M113.523811
125. Zhao S, Zhang YK, Harris S, Ahuja SS, Bonewald LF. MLO-Y4 osteocyte-like cells support osteoclast formation and activation. *J Bone Mineral Res*. (2002) 17:2068–79. doi: 10.1359/jbmr.2002.17.11.2068
126. Buenzli PR, Sims NA. Quantifying the osteocyte network in the human skeleton. *Bone*. (2015) 75:144–50. doi: 10.1016/j.bone.2015.02.016
127. Ito N, Wijenayaka AR, Prideaux M, Kogawa M, Ormsby RT, Evdokiou A, et al. Regulation of FGF23 expression in IDG-SW3 osteocytes and human bone by pro-inflammatory stimuli. *Mol Cell Endocrinol*. (2015) 399:208–18. doi: 10.1016/j.mce.2014.10.007
128. Algate K, Haynes DR, Bartold PM, Crotti TN, Cantley MD. The effects of tumour necrosis factor-alpha on bone cells involved in periodontal alveolar bone loss; osteoclasts, osteoblasts and osteocytes. *J Periodontal Res*. (2016) 51:549–66. doi: 10.1111/jre.12339
129. Baeza M, Garrido M, Hernandez-Rios P, Dezerega A, Garcia-Sesnich J, Strauss F, et al. Diagnostic accuracy for apical and chronic periodontitis biomarkers in gingival crevicular fluid: an exploratory study. *J Clin Periodontol*. (2016) 43:34–45. doi: 10.1111/jcpe.12479
130. Corbella S, Veronesi P, Galimberti V, Weinstein R, Del Fabbro M, Francetti L. Is periodontitis a risk indicator for cancer? A meta-analysis. *PLoS ONE*. (2018) 13:e0195683. doi: 10.1371/journal.pone.0195683
131. Tonetti MS, Van Dyke TE. Periodontitis and atherosclerotic cardiovascular disease: consensus report of the Joint EFP/AAPWorkshop on Periodontitis and Systemic Diseases. *J Periodontol*. (2013) 84 (Suppl 4S):S24-s9. doi: 10.1902/jop.2013.1340019
132. Periodontal manifestations of systemic diseases and developmental and acquired conditions: Consensus report of workgroup 3 of the 2017 World Workshop on the Classification of Periodontal and Peri-Implant Diseases and Conditions. *Br Dental J*. (2018) 225:141. doi: 10.1038/sj.bdj.2018.616
133. Sanz M, Ceriello A, Buysschaert M, Chapple I, Demmer RT, Graziani F, et al. Scientific evidence on the links between periodontal diseases and diabetes: consensus report and guidelines of the joint workshop on periodontal diseases and diabetes by the International Diabetes Federation and the European Federation of Periodontology. *J Clin Periodontol*. (2018) 45:138–49. doi: 10.1111/jcpe.12808
134. Gomes MS, Blattner TC, Sant'Ana Filho M, Grecca FS, Hugo FN, Fouad AF, et al. Can apical periodontitis modify systemic levels of inflammatory markers? A systematic review and meta-analysis. *J Endodont*. (2013) 39:1205–17. doi: 10.1016/j.joen.2013.06.014
135. Garrido M, Cardenas AM, Astorga J, Quinlan F, Valdes M, Chaparro A, et al. Elevated systemic inflammatory burden and cardiovascular risk in young adults with endodontic apical lesions. *J Endodont*. (2019) 45:111–5. doi: 10.1016/j.joen.2018.11.014
136. Schenkein HA, Loos BG. Inflammatory mechanisms linking periodontal diseases to cardiovascular diseases. *J Clin Periodontol*. (2013) 40(Suppl 14):S51–69. doi: 10.1111/jcpe.12060
137. Garrido M, Dezerega A, Bordagaray MJ, Reyes M, Vernal R, Melgar-Rodriguez S, et al. C-reactive protein expression is up-regulated in apical lesions of endodontic origin in association with interleukin-6. *J Endodont*. (2015) 41:464–9. doi: 10.1016/j.joen.2014.12.021
138. Hernandez-Rios P, Pussinen PJ, Vernal R, Hernandez M. Oxidative stress in the local and systemic events of apical periodontitis. *Front Physiol*. (2017) 8:869. doi: 10.3389/fphys.2017.00869
139. Buduneli N, Kinane DF. Host-derived diagnostic markers related to soft tissue destruction and bone degradation in periodontitis. *J Clin Periodontol*. (2011) 38(Suppl 11):85–105. doi: 10.1111/j.1600-051X.2010.01670.x
140. Sorsa T, Gursoy UK, Nwhator S, Hernandez M, Tervahartiala T, Leppilahti J, et al. Analysis of matrix metalloproteinases, especially MMP-8, in gingival

creviclular fluid, mouthrinse and saliva for monitoring periodontal diseases. *Periodontology 2000*. (2016) 70:142–63. doi: 10.1111/prd.12101
141. Rathnayake N, Gieselmann DR, Heikkinen AM, Tervahartiala T, Sorsa T. Salivary Diagnostics-point-of-care diagnostics of MMP-8 in dentistry and medicine. *Diagnostics*. (2017) 7:E7 doi: 10.3390/diagnostics7010007
142. Leppilahti JM, Harjunmaa U, Jarnstedt J, Mangani C, Hernandez M, Tervahartiala T, et al. Diagnosis of newly delivered mothers for periodontitis with a novel oral-rinse aMMP-8 point-of-care test in a rural malawian population. *Diagnostics*. (2018) 8:E67. doi: 10.3390/diagnostics8030067
143. Alassiri S, Parnanen P, Rathnayake N, Johannsen G, Heikkinen AM, Lazzara R, et al. The ability of quantitative, specific, and sensitive point-of-care/chair-side oral fluid immunotests for aMMP-8 to detect periodontal and peri-implant diseases. *Dis Mark*. (2018) 2018:1306396. doi: 10.1155/2018/1306396
144. Sorsa T, Gieselmann D, Arweiler NB, Hernandez M. A quantitative point-of-care test for periodontal and dental peri-implant diseases. *Nat Rev Dis Primers*. (2017) 3:17069. doi: 10.1038/nrdp.2017.69
145. Chaparro A, Sanz A, Quintero A, Inostroza C, Ramirez V, Carrion F, et al. Increased inflammatory biomarkers in early pregnancy is associated with the development of pre-eclampsia in patients with periodontitis: a case control study. *J Periodontal Res*. (2013) 48:302–7. doi: 10.1111/jre.12008
146. Chaparro A, Zuniga E, Varas-Godoy M, Albers D, Ramirez V, Hernandez M, et al. Periodontitis and placental growth factor in oral fluids are early pregnancy predictors of gestational diabetes mellitus. *J Periodontol*. (2018) 89:1052–60. doi: 10.1002/JPER.17-0497
147. Payne JB, Golub LM, Stoner JA, Lee HM, Reinhardt RA, Sorsa T, et al. The effect of subantimicrobial-dose-doxycycline periodontal therapy on serum biomarkers of systemic inflammation: a randomized, double-masked, placebo-controlled clinical trial. *J Am Dental Assoc*. (2011) 142:262–73. doi: 10.14219/jada.archive.2011.0165
148. Cotti E, Dessi C, Piras A, Flore G, Deidda M, Madeddu C, et al. Association of endodontic infection with detection of an initial lesion to the cardiovascular system. *J Endodont*. (2011) 37:1624–9. doi: 10.1016/j.joen.2011.09.006
149. Heikkila P, But A, Sorsa T, Haukka J. Periodontitis and cancer mortality: Register-based cohort study of 68,273 adults in 10-year follow-up. *Int J Cancer*. (2018) 142:2244–53. doi: 10.1002/ijc.31254
150. Damle SG. Health consequences of poor oral health? *Contemp Clin Dent*. (2018) 9:1. doi: 10.4103/ccd.ccd_106_18
151. Hormia M, Willberg J, Ruokonen H, Syrjanen S. Marginal periodontium as a potential reservoir of human papillomavirus in oral mucosa. *J Periodontol*. (2005) 76:358–63. doi: 10.1902/jop.2005.76.3.358
152. Saygun I, Kubar A, Ozdemir A, Slots J. Periodontitis lesions are a source of salivary cytomegalovirus and Epstein-Barr virus. *J Periodontal Res*. (2005) 40:187–91. doi: 10.1111/j.1600-0765.2005.00790.x
153. Katz J, Onate MD, Pauley KM, Bhattacharyya I, Cha S. Presence of *Porphyromonas gingivalis* in gingival squamous cell carcinoma. *Int J Oral Sci*. (2011) 3:209–15. doi: 10.4248/IJOS11075
154. Nieminen MT, Listyarifah D, Hagstrom J, Haglund C, Grenier D, Nordstrom D, et al. Treponema denticola chymotrypsin-like proteinase may contribute to orodigestive carcinogenesis through immunomodulation. *Br J Cancer*. (2018) 118:428–34. doi: 10.1038/bjc.2017.409
155. Kylma AK, Jouhi L, Listyarifah D, Mohamed H, Makitie A, Remes SM, et al. Treponema denticola chymotrypsin-like protease as associated with HPV-negative oropharyngeal squamous cell carcinoma. *Br J Cancer*. (2018) 119:89–95. doi: 10.1038/s41416-018-0143-5
156. Pearson TA, Mensah GA, Alexander RW, Anderson JL, Cannon RO III, Criqui M, et al. Markers of inflammation and cardiovascular disease: application to clinical and public health practice: a statement for healthcare professionals from the Centers for Disease Control and Prevention and the American Heart Association. *Circulation*. (2003) 107:499–511. doi: 10.1161/01.CIR.0000052939.59093.45
157. Brown DL, Desai KK, Vakili BA, Nouneh C, Lee HM, Golub LM. Clinical and biochemical results of the metalloproteinase inhibition with subantimicrobial doses of doxycycline to prevent acute coronary syndromes (MIDAS) pilot trial. *Arterioscler Thromb Vasc Biol*. (2004) 24:733–8. doi: 10.1161/01.ATV.0000121571.78696.dc
158. Bench TJ, Jeremias A, Brown DL. Matrix metalloproteinase inhibition with tetracyclines for the treatment of coronary artery disease. *Pharmacol Res*. (2011) 64:561–6. doi: 10.1016/j.phrs.2011.05.002
159. Golub LM, Evans RT, McNamara TF, Lee HM, Ramamurthy NS. A non-antimicrobial tetracycline inhibits gingival matrix metalloproteinases and bone loss in Porphyromonas gingivalis-induced periodontitis in rats. *Ann NY Acad Sci*. (1994) 732:96–111. doi: 10.1111/j.1749-6632.1994.tb24728.x
160. Golub LM, Lee HM, Stoner JA, Sorsa T, Reinhardt RA, Wolff MS, et al. Subantimicrobial-dose doxycycline modulates gingival crevicular fluid biomarkers of periodontitis in postmenopausal osteopenic women. *J Periodontol*. (2008) 79:1409–18. doi: 10.1902/jop.2008.070623
161. Hamilton JA, Hasturk H, Kantarci A, Serhan CN, Van Dyke T. Atherosclerosis, periodontal disease, and treatment with resolvins. *Curr Atheroscl Rep*. (2017) 19:57. doi: 10.1007/s11883-017-0696-4
162. The EESNWG. Bone sarcomas: ESMO clinical practice guidelines for diagnosis, treatment and follow-up †. *Ann Oncol*. (2012) 23(suppl_7):vii100-vii9. doi: 10.1093/annonc/mds254
163. Razek AA. Imaging appearance of bone tumors of the maxillofacial region. *World J Radiol*. (2011) 3:125–34. doi: 10.4329/wjr.v3.i5.125
164. Wright JM, Vered M. Update from the 4th edition of the World Health Organization classification of head and neck tumours: odontogenic and maxillofacial bone tumors. *Head Neck Pathol*. (2017) 11:68–77. doi: 10.1007/s12105-017-0794-1
165. Bertin H, Guilho R, Brion R, Amiaud J, Battaglia S, Moreau A, et al. Jaw osteosarcoma models in mice: first description. *J Transl Med*. (2019) 17:56. doi: 10.1186/s12967-019-1807-5
166. Park YK, Ryu KN, Park HR, Kim DW. Low-grade osteosarcoma of the maxillary sinus. *Skeletal Radiol*. (2003) 32:161-4. doi: 10.1007/s00256-002-0577-x
167. David E, Blanchard F, Heymann MF, De Pinieux G, Gouin F, Redini F, et al. The bone niche of chondrosarcoma: a sanctuary for drug resistance, tumour growth and also a source of new therapeutic targets. *Sarcoma*. (2011) 2011:932451. doi: 10.1155/2011/932451
168. Brown HK, Schiavone K, Gouin F, Heymann MF, Heymann D. Biology of bone sarcomas and new therapeutic developments. *Calci Tiss Int*. (2018) 102:174–95. doi: 10.1007/s00223-017-0372-2
169. Chan CKF, Gulati GS, Sinha R, Tompkins JV, Lopez M, Carter AC, et al. Identification of the human skeletal stem cell. *Cell*. (2018) 175:43–56.e21. doi: 10.1016/j.cell.2018.07.029
170. Gambera S, Abarrategi A, Gonzalez-Camacho F, Morales-Molina A, Roma J, Alfranca A, et al. Clonal dynamics in osteosarcoma defined by RGB marking. *Nat Commun*. (2018) 9:3994. doi: 10.1038/s41467-018-06401-z
171. Brown HK, Tellez-Gabriel M, Heymann D. Cancer stem cells in osteosarcoma. *Cancer Lett*. (2017) 386:189–95. doi: 10.1016/j.canlet.2016.11.019
172. Vallette FM, Olivier C, Lezot F, Oliver L, Cochonneau D, Lalier L, et al. Dormant, quiescent, tolerant and persister cells: four synonyms for the same target in cancer. *Biochem Pharmacol*. (2018) 162:169–76 doi: 10.1016/j.bcp.2018.11.004
173. Dumars C, Ngyuen JM, Gaultier A, Lanel R, Corradini N, Gouin F, et al. Dysregulation of macrophage polarization is associated with the metastatic process in osteosarcoma. *Oncotarget*. (2016) 7:78343–54. doi: 10.18632/oncotarget.13055
174. Heymann MF, Lezot F, Heymann D. The contribution of immune infiltrates and the local microenvironment in the pathogenesis of osteosarcoma. *Cell Immunol*. (2017). doi: 10.1016/j.cellimm.2017.10.011
175. Koirala P, Roth ME, Gill J, Piperdi S, Chinai JM, Geller DS, et al. Immune infiltration and PD-L1 expression in the tumor microenvironment are prognostic in osteosarcoma. *Sci Rep*. (2016) 6:30093. doi: 10.1038/srep30093
176. Fritzsching B, Fellenberg J, Moskovszky L, Sapi Z, Krenacs T, Machado I, et al. CD8(+)/FOXP3(+)-ratio in osteosarcoma microenvironment separates survivors from non-survivors: a multicenter validated retrospective study. *Oncoimmunology*. (2015) 4:e990800. doi: 10.4161/2162402X.2014.990800
177. Stamatopoulos A, Stamatopoulos T, Gamie Z, Kenanidis E, Ribeiro RDC, Rankin KS, et al. Mesenchymal stromal cells for bone sarcoma treatment: Roadmap to clinical practice. *J Bone Oncol*. (2019) 16:100231. doi: 10.1016/j.jbo.2019.100231
178. Baglio SR, Lagerweij T, Perez-Lanzon M, Ho XD, Leveille N, Melo SA, et al. Blocking tumor-educated MSC paracrine activity halts

osteosarcoma progression. *Clin Cancer Res*. (2017) 23:3721–33. doi: 10.1158/1078-0432.CCR-16-2726
179. Avnet S, Di Pompo G, Chano T, Errani C, Ibrahim-Hashim A, Gillies RJ, et al. Cancer-associated mesenchymal stroma fosters the stemness of osteosarcoma cells in response to intratumoral acidosis via NF-kappaB activation. *Int J Cancer*. (2017) 140:1331–45. doi: 10.1002/ijc.30540
180. Renema N, Navet B, Heymann MF, Lezot F, Heymann D. RANK-RANKL signalling in cancer. *Biosci Rep*. (2016) 36:e00366. doi: 10.1042/BSR20160150
181. Navet B, Ando K, Vargas-Franco JW, Brion R, Amiaud J, Mori K, et al. The intrinsic and extrinsic implications of RANKL/RANK signaling in osteosarcoma: from tumor initiation to lung metastases. *Cancers*. (2018) 10:E398. doi: 10.3390/cancers10110398
182. Chen Y, Di Grappa MA, Molyneux SD, McKee TD, Waterhouse P, Penninger JM, et al. RANKL blockade prevents and treats aggressive osteosarcomas. *Sci Transl Med*. (2015) 7:317ra197. doi: 10.1126/scitranslmed.aad0295
183. Heymann MF, Brown HK, Heymann D. Drugs in early clinical development for the treatment of osteosarcoma. *Expert Opin Investigat Drugs*. (2016) 25:1265–80. doi: 10.1080/13543784.2016.1237503
184. Heymann D. Metastatic osteosarcoma challenged by regorafenib. *Lancet Oncol*. (2018) 20:12–4. doi: 10.1016/S1470-2045(18)30821-0
185. Loeser RF, Goldring SR, Scanzello CR, Goldring MB. Osteoarthritis: a disease of the joint as an organ. *Arthritis Rheum*. (2012) 64:1697–707. doi: 10.1002/art.34453
186. Vos LM, Kuijer R, Huddleston Slater JJ, Bulstra SK, Stegenga B. Inflammation is more distinct in temporomandibular joint osteoarthritis compared to the knee joint. *J Oral Maxillofac Surg*. (2014) 72:35–40. doi: 10.1016/j.joms.2013.08.022
187. Allen KD, Golightly YM. State of the evidence. *Curr Opin Rheumatol*. (2015) 27:276–83. doi: 10.1097/BOR.0000000000000161
188. Johnson VL, Hunter DJ. The epidemiology of osteoarthritis. *Best Pract Res Clin Rheumatol*. (2014) 28:5–15. doi: 10.1016/j.berh.2014.01.004
189. Tanaka E, Detamore MS, Mercuri LG. Degenerative disorders of the temporomandibular joint: etiology, diagnosis, and treatment. *J Dental Res*. (2008) 87:296–307. doi: 10.1177/154405910808700406
190. Embree MC, Kilts TM, Ono M, Inkson CA, Syed-Picard F, Karsdal MA, et al. Biglycan and fibromodulin have essential roles in regulating chondrogenesis and extracellular matrix turnover in temporomandibular joint osteoarthritis. *Am J Pathol*. (2010) 176:812–26. doi: 10.2353/ajpath.2010.090450
191. Yee G, Yu Y, Walsh WR, Lindeman R, Poole MD. The immunolocalisation of VEGF in the articular cartilage of sheep mandibular condyles. *J Craniomaxillofac Surg*. (2003) 31:244–51. doi: 10.1016/S1010-5182(03)00040-4
192. Matsumoto R, Ioi H, Goto TK, Hara A, Nakata S, Nakasima A, et al. Relationship between the unilateral TMJ osteoarthritis/osteoarthrosis, mandibular asymmetry and the EMG activity of the masticatory muscles: a retrospective study. *J Oral Rehabil*. (2010) 37:85–92. doi: 10.1111/j.1365-2842.2009.02026.x
193. Krisjane Z, Urtane I, Krumina G, Neimane L, Ragovska I. The prevalence of TMJ osteoarthritis in asymptomatic patients with dentofacial deformities: a cone-beam CT study. *Int J Oral Maxillofacial Surg*. (2012) 41:690–5. doi: 10.1016/j.ijom.2012.03.006
194. Betti BF, Everts V, Ket JCF, Tabeian H, Bakker AD, Langenbach GE, et al. Effect of mechanical loading on the metabolic activity of cells in the temporomandibular joint: a systematic review. *Clin Oral Investig*. (2018) 22:57–67. doi: 10.1007/s00784-017-2189-9
195. Utreja A, Dyment NA, Yadav S, Villa MM, Li Y, Jiang X, et al. Cell and matrix response of temporomandibular cartilage to mechanical loading. *Osteoarthr Cartilage*. (2016) 24:335-44. doi: 10.1016/j.joca.2015.08.010
196. Fujisawa T, Kuboki T, Kasai T, Sonoyama W, Kojima S, Uehara J, et al. A repetitive, steady mouth opening induced an osteoarthritis-like lesion in the rabbit temporomandibular joint. *J Dental Res*. (2003) 82:731–5. doi: 10.1177/154405910308200914
197. Sobue T, Yeh WC, Chhibber A, Utreja A, Diaz-Doran V, Adams D, et al. Murine TMJ loading causes increased proliferation and chondrocyte maturation. *J Dental Res*. (2011) 90:512–6. doi: 10.1177/0022034510390810
198. Nicodemus GD, Villanueva I, Bryant SJ. Mechanical stimulation of TMJ condylar chondrocytes encapsulated in PEG hydrogels. *J Biomed Mater Res A*. (2007) 83:323–31. doi: 10.1002/jbm.a.31251
199. Ichimiya H, Takahashi T, Ariyoshi W, Takano H, Matayoshi T, Nishihara T. Compressive mechanical stress promotes osteoclast formation through RANKL expression on synovial cells. *Oral Surg Oral Med Oral Pathol Oral Radiol Endod*. (2007) 103:334–41. doi: 10.1016/j.tripleo.2006.05.026
200. Shinohara T, Izawa T, Mino-Oka A, Mori H, Iwasa A, Inubushi T, et al. Hyaluronan metabolism in overloaded temporomandibular joint. *J Oral Rehabil*. (2016) 43:921–8. doi: 10.1111/joor.12443
201. Petrey AC, de la Motte CA. Hyaluronan, a crucial regulator of inflammation. *Front Immunol*. (2014) 5:101. doi: 10.3389/fimmu.2014.00101
202. Scheibner KA, Lutz MA, Boodoo S, Fenton MJ, Powell JD, Horton MR. Hyaluronan fragments act as an endogenous danger signal by engaging TLR2. *J Immunol*. (2006) 177:1272-81. doi: 10.4049/jimmunol.177.2.1272
203. Wang XD, Zhang JN, Gan YH, Zhou YH. Current understanding of pathogenesis and treatment of TMJ osteoarthritis. *J Dental Res*. (2015) 94:666–73. doi: 10.1177/0022034515574770
204. de Souza RF, Lovato da Silva CH, Nasser M, Fedorowicz Z, Al-Muharraqi MA. Interventions for the management of temporomandibular joint osteoarthritis. *Cochrane Database Syst Rev*. (2012) 2012:CD007261. doi: 10.1002/14651858.CD007261.pub2
205. Sakkas LI, Platsoucas CD. The role of T cells in the pathogenesis of osteoarthritis. *Arthritis Rheum*. (2007) 56:409–24. doi: 10.1002/art.22369
206. de Lange-Brokaar BJ, Ioan-Facsinay A, van Osch GJ, Zuurmond AM, Schoones J, Toes RE, et al. Synovial inflammation, immune cells and their cytokines in osteoarthritis: a review. *Osteoarthr Cartilage*. (2012) 20:1484–99. doi: 10.1016/j.joca.2012.08.027
207. Ponchel F, Burska AN, Hensor EM, Raja R, Campbell M, Emery P, et al. Changes in peripheral blood immune cell composition in osteoarthritis. *Osteoarthr Cartilage*. (2015) 23:1870-8. doi: 10.1016/j.joca.2015.06.018
208. Pessler F, Chen LX, Dai L, Gomez-Vaquero C, Diaz-Torne C, Paessler ME, et al. A histomorphometric analysis of synovial biopsies from individuals with Gulf War Veterans' Illness and joint pain compared to normal and osteoarthritis synovium. *Clin Rheumatol*. (2008) 27:1127-34. doi: 10.1007/s10067-008-0878-0
209. Kaneyama K, Segami N, Nishimura M, Suzuki T, Sato J. Importance of proinflammatory cytokines in synovial fluid from 121 joints with temporomandibular disorders. *Br J Oral Maxillofac Surg*. (2002) 40:418–23. doi: 10.1016/S0266-4356(02)00215-2
210. Kellesarian SV, Malignaggi VR, Abduljabbar T, Vohra F, Malmstrom H, Romanos GE, et al. Efficacy of scaling and root planing with and without adjunct antimicrobial photodynamic therapy on the expression of cytokines in the gingival crevicular fluid of patients with periodontitis: a systematic review. *Photodiagnosis Photodyn Ther*. (2016) 16:76–84. doi: 10.1016/j.pdpdt.2016.08.009
211. Lim WH, Toothman J, Miller JH, Tallents RH, Brouxhon SM, Olschowka ME, et al. IL-1beta inhibits TGFbeta in the temporomandibular joint. *J Dental Res*. (2009) 88:557–62. doi: 10.1177/0022034509336823
212. Vernal R, Velasquez E, Gamonal J, Garcia-Sanz JA, Silva A, Sanz M. Expression of proinflammatory cytokines in osteoarthritis of the temporomandibular joint. *Arch Oral Biol*. (2008) 53:910–5. doi: 10.1016/j.archoralbio.2008.04.004
213. Simsek Kaya G, Yapici Yavuz G, Kiziltunc A. Expression of chemerin in the synovial fluid of patients with temporomandibular joint disorders. *J Oral Rehabil*. (2018) 45:289–94 doi: 10.1111/joor.12608
214. Kalladka M, Quek S, Heir G, Eliav E, Mupparapu M, Viswanath A. Temporomandibular joint osteoarthritis: diagnosis and long-term conservative management: a topic review. *J Indian Prosthodont Soc*. (2014) 14:6–15. doi: 10.1007/s13191-013-0321-3
215. Robinson WH, Lepus CM, Wang Q, Raghu H, Mao R, Lindstrom TM, et al. Low-grade inflammation as a key mediator of the pathogenesis of osteoarthritis. *Nat Rev Rheumatol*. (2016) 12:580-92. doi: 10.1038/nrrheum.2016.136
216. Chen GY, Nunez G. Sterile inflammation: sensing and reacting to damage. *Nat Rev Immunol*. (2010) 10:826–37. doi: 10.1038/nri2873
217. Milam SB. Pathogenesis of degenerative temporomandibular joint arthritides. *Odontology*. (2005) 93:7–15. doi: 10.1007/s10266-005-0056-7
218. Milam SB, Zardeneta G, Schmitz JP. Oxidative stress and degenerative temporomandibular joint disease: a proposed hypothesis. *J Oral Maxillofac Surg*. (1998) 56:214–23. doi: 10.1016/S0278-2391(98)90872-2

219. Wei L, Xiong H, Li B, Gong Z, Li J, Cai H, et al. Change of HA molecular size and boundary lubrication in synovial fluid of patients with temporomandibular disorders. *J Oral Rehabil*. (2010) 37:271–7. doi: 10.1111/j.1365-2842.2009.02048.x
220. Takahashi T, Tominaga K, Takano H, Ariyoshi W, Habu M, Fukuda J, et al. A decrease in the molecular weight of hyaluronic acid in synovial fluid from patients with temporomandibular disorders. *J Oral Pathol Med*. (2004) 33:224–9. doi: 10.1111/j.0904-2512.2004.00024.x
221. Jiang D, Liang J, Fan J, Yu S, Chen S, Luo Y, et al. Regulation of lung injury and repair by Toll-like receptors and hyaluronan. *Nature Med*. (2005) 11:1173–9. doi: 10.1038/nm1315
222. Scanzello CR, Goldring SR. The role of synovitis in osteoarthritis pathogenesis. *Bone*. (2012) 51:249–57. doi: 10.1016/j.bone.2012.02.012
223. Kong J, Yang Y, Sun S, Xie J, Lin X, Ji P. Effect of toll-like receptor 4 on synovial injury of temporomandibular joint in rats caused by occlusal interference. *Medi Inflamm*. (2016) 2016:7694921. doi: 10.1155/2016/7694921
224. Lin X, Xie J, Sun S, Ren X, Kong J, Ji P. Toll-Like Receptor 4 (TLR4) stimulates synovial injury of temporomandibular joint in rats through the activation of p38 mitogen-activated protein kinase (MAPK) signaling pathway. *Med Sci Monit*. (2018) 24:4405–12. doi: 10.12659/MSM.908526
225. Israel HA, Diamond B, Saed-Nejad F, Ratcliffe A. Osteoarthritis and synovitis as major pathoses of the temporomandibular joint: comparison of clinical diagnosis with arthroscopic morphology. *J Oral Maxillofac Surg*. (1998) 56:1023–7. doi: 10.1016/S0278-2391(98)90246-4
226. Israel HA, Langevin CJ, Singer MD, Behrman DA. The relationship between temporomandibular joint synovitis and adhesions: pathogenic mechanisms and clinical implications for surgical management. *J Oral Maxillofac Surg*. (2006) 64:1066–74. doi: 10.1016/j.joms.2006.03.012
227. Hattori T, Ogura N, Akutsu M, Kawashima M, Watanabe S, Ito K, et al. Gene expression profiling of IL-17A-treated synovial fibroblasts from the human temporomandibular joint. *Medi Inflamm*. (2015) 2015:436067. doi: 10.1155/2015/436067
228. Chang SK, Gu Z, Brenner MB. Fibroblast-like synoviocytes in inflammatory arthritis pathology: the emerging role of cadherin-11. *Immunol Rev*. (2010) 233:256–66. doi: 10.1111/j.0105-2896.2009.00854.x
229. Buckley CD, Gilroy DW, Serhan CN. Proresolving lipid mediators and mechanisms in the resolution of acute inflammation. *Immunity*. (2014) 40:315–27. doi: 10.1016/j.immuni.2014.02.009
230. Axmann R, Bohm C, Kronke G, Zwerina J, Smolen J, Schett G. Inhibition of interleukin-6 receptor directly blocks osteoclast formation *in vitro* and *in vivo*. *Arthritis Rheum*. (2009) 60:2747–56. doi: 10.1002/art.24781
231. Kimura A, Kishimoto T. IL-6: regulator of Treg/Th17 balance. *Eur J Immunol*. (2010) 40:1830–5. doi: 10.1002/eji.201040391
232. Takayanagi H, Iizuka H, Juji T, Nakagawa T, Yamamoto A, Miyazaki T, et al. Involvement of receptor activator of nuclear factor kappaB ligand/osteoclast differentiation factor in osteoclastogenesis from synoviocytes in rheumatoid arthritis. *Arthritis Rheum*. (2000) 43:259-69. doi: 10.1002/1529-0131(200002)43:2<259::AID-ANR4>3.0.CO;2-W
233. Kaneyama K, Segami N, Sato J, Yoshimura H, Nishiura R. Expression of receptor activator of nuclear factor-kappaB ligand in synovial tissue: comparison with degradation of articular cartilage in temporomandibular joint disorders. *Oral Surg Oral Med Oral Pathol Oral Radiol Endod*. (2007) 104:e12-7. doi: 10.1016/j.tripleo.2007.02.016
234. Danks L, Komatsu N, Guerrini MM, Sawa S, Armaka M, Kollias G, et al. RANKL expressed on synovial fibroblasts is primarily responsible for bone erosions during joint inflammation. *Ann Rheumat Dis*. (2016) 75:1187–95. doi: 10.1136/annrheumdis-2014-207137
235. Jiao K, Niu LN, Wang MQ, Dai J, Yu SB, Liu XD, et al. Subchondral bone loss following orthodontically induced cartilage degradation in the mandibular condyles of rats. *Bone*. (2011) 48:362–71. doi: 10.1016/j.bone.2010.09.010
236. Taylor KR, Yamasaki K, Radek KA, Di Nardo A, Goodarzi H, Golenbock D, et al. Recognition of hyaluronan released in sterile injury involves a unique receptor complex dependent on Toll-like receptor 4, CD44, and MD-2. *J Biol Chem*. (2007) 282:18265–75. doi: 10.1074/jbc.M606352200
237. Termeer C, Benedix F, Sleeman J, Fieber C, Voith U, Ahrens T, et al. Oligosaccharides of Hyaluronan activate dendritic cells via toll-like receptor 4. *J Exp Med*. (2002) 195:99–111. doi: 10.1084/jem.20001858
238. Termeer CC, Hennies J, Voith U, Ahrens T, Weiss JM, Prehm P, et al. Oligosaccharides of hyaluronan are potent activators of dendritic cells. *J Immunol*. (2000) 165:1863–70. doi: 10.4049/jimmunol.165.4.1863
239. Galandrini R, Galluzzo E, Albi N, Grossi CE, Velardi A. Hyaluronate is costimulatory for human T cell effector functions and binds to CD44 on activated T cells. *J Immunol*. (1994) 153:21–31.
240. Rizzo M, Bayo J, Piccioni F, Malvicini M, Fiore E, Peixoto E, et al. Low molecular weight hyaluronan-pulsed human dendritic cells showed increased migration capacity and induced resistance to tumor chemoattraction. *PLoS ONE*. (2014) 9:e107944. doi: 10.1371/journal.pone.0107944
241. Monasterio G, Guevara J, Ibarra JP, Castillo F, Diaz-Zuniga J, Alvarez C, et al. Immunostimulatory activity of low-molecular-weight hyaluronan on dendritic cells stimulated with Aggregatibacter actinomycetemcomitans or *Porphyromonas gingivalis*. *Clin Invest*. (2019) 23:1887–94. doi: 10.1007/s00784-018-2641-5
242. Tussiwand R, Gautier EL. Transcriptional regulation of mononuclear phagocyte development. *Front Immunol*. (2015) 6:533. doi: 10.3389/fimmu.2015.00533
243. Persson EK, Uronen-Hansson H, Semmrich M, Rivollier A, Hagerbrand K, Marsal J, et al. IRF4 transcription-factor-dependent CD103(+)CD11b(+) dendritic cells drive mucosal T helper 17 cell differentiation. *Immunity*. (2013) 38:958–69. doi: 10.1016/j.immuni.2013.03.009
244. Symons JA, McCulloch JF, Wood NC, Duff GW. Soluble CD4 in patients with rheumatoid arthritis and osteoarthritis. *Clin Immunol Immunopathol*. (1991) 60:72–82. doi: 10.1016/0090-1229(91)90113-O
245. de Jong H, Berlo SE, Hombrink P, Otten HG, van Eden W, Lafeber FP, et al. Cartilage proteoglycan aggrecan epitopes induce proinflammatory autoreactive T-cell responses in rheumatoid arthritis and osteoarthritis. *Ann Rheumat Dis*. (2010) 69:255–62. doi: 10.1136/ard.2008.103978
246. Monasterio G, Castillo F, Rojas L, Cafferata EA, Alvarez C, Carvajal P, et al. Th1/Th17/Th22 immune response and their association with joint pain, imagenological bone loss, RANKL expression and osteoclast activity in temporomandibular joint osteoarthritis: a preliminary report. *J Oral Rehabil*. (2018) 45:589–97. doi: 10.1111/joor.12649
247. Murphy CA, Langrish CL, Chen Y, Blumenschein W, McClanahan T, Kastelein RA, et al. Divergent pro- and antiinflammatory roles for IL-23 and IL-12 in joint autoimmune inflammation. *J Exp Med*. (2003) 198:1951–7. doi: 10.1084/jem.20030896
248. Nakae S, Nambu A, Sudo K, Iwakura Y. Suppression of immune induction of collagen-induced arthritis in IL-17-deficient mice. *J Immunol*. (2003) 171:6173–7. doi: 10.4049/jimmunol.171.11.6173
249. Nakae S, Saijo S, Horai R, Sudo K, Mori S, Iwakura Y. IL-17 production from activated T cells is required for the spontaneous development of destructive arthritis in mice deficient in IL-1 receptor antagonist. *Proc Natl Acad Sci USA*. (2003) 100:5986–90. doi: 10.1073/pnas.1035999100
250. Lurati A, Laria A, Gatti A, Brando B, Scarpellini M. Different T cells' distribution and activation degree of Th17 CD4+ cells in peripheral blood in patients with osteoarthritis, rheumatoid arthritis, and healthy donors: preliminary results of the MAGENTA CLICAO study. *Open Access Rheumatol*. (2015) 7:63–8. doi: 10.2147/OARRR.S81905
251. Yamada H, Nakashima Y, Okazaki K, Mawatari T, Fukushi J, Oyamada A, et al. Preferential accumulation of activated Th1 cells not only in rheumatoid arthritis but also in osteoarthritis joints. *J Rheumatol*. (2011) 38:1569–75. doi: 10.3899/jrheum.101355
252. Nistala K, Adams S, Cambrook H, Ursu S, Olivito B, de Jager W, et al. Th17 plasticity in human autoimmune arthritis is driven by the inflammatory environment. *Proc Natl Acad Sci USA*. (2010) 107:14751-6. doi: 10.1073/pnas.1003852107
253. Penatti A, Facciotti F, De Matteis R, Larghi P, Paroni M, Murgo A, et al. Differences in serum and synovial CD4+ T cells and cytokine profiles to stratify patients with inflammatory osteoarthritis and rheumatoid arthritis. *Arthritis Res Ther*. (2017) 19:103. doi: 10.1186/s13075-017-1305-1
254. Hussein MR, Fathi NA, El-Din AM, Hassan HI, Abdullah F, Al-Hakeem E, et al. Alterations of the CD4(+), CD8 (+) T cell subsets, interleukins-1beta, IL-10, IL-17, tumor necrosis factor-alpha and soluble intercellular adhesion molecule-1 in rheumatoid arthritis and

osteoarthritis: preliminary observations. *Pathol Oncol Res*. (2008) 14:321–8. doi: 10.1007/s12253-008-9016-1
255. Sarkar S, Justa S, Brucks M, Endres J, Fox DA, Zhou X, et al. Interleukin (IL)-17A, F and AF in inflammation: a study in collagen-induced arthritis and rheumatoid arthritis. *Clin Exp Immunol*. (2014) 177:652–61. doi: 10.1111/cei.12376
256. Kaneyama K, Segami N, Sato J, Nishimura M, Yoshimura H. Interleukin-6 family of cytokines as biochemical markers of osseous changes in the temporomandibular joint disorders. *Br J Oral Maxillofac Surg*. (2004) 42:246–50. doi: 10.1016/S0266-4356(03)00258-4
257. Moran EM, Mullan R, McCormick J, Connolly M, Sullivan O, Fitzgerald O, et al. Human rheumatoid arthritis tissue production of IL-17A drives matrix and cartilage degradation: synergy with tumour necrosis factor-alpha, Oncostatin M and response to biologic therapies. *Arthritis Res Ther*. (2009) 11:R113. doi: 10.1186/ar2772
258. Toh ML, Gonzales G, Koenders MI, Tournadre A, Boyle D, Lubberts E, et al. Role of interleukin 17 in arthritis chronicity through survival of synoviocytes via regulation of synoviolin expression. *PLoS ONE*. (2010) 5:e13416. doi: 10.1371/journal.pone.0013416
259. Li GQ, Zhang Y, Liu D, Qian YY, Zhang H, Guo SY, et al. Celastrol inhibits interleukin-17A-stimulated rheumatoid fibroblast-like synoviocyte migration and invasion through suppression of NF-kappaB-mediated matrix metalloproteinase-9 expression. *Int Immunopharmacol*. (2012) 14:422–31. doi: 10.1016/j.intimp.2012.08.016
260. Chen Y, Zhong M, Liang L, Gu F, Peng H. Interleukin-17 induces angiogenesis in human choroidal endothelial cells *in vitro*. *Invest Ophthalmol Vis Sci*. (2014) 55:6968–75. doi: 10.1167/iovs.14-15029
261. Sato K, Suematsu A, Okamoto K, Yamaguchi A, Morishita Y, Kadono Y, et al. Th17 functions as an osteoclastogenic helper T cell subset that links T cell activation and bone destruction. *J Exp Med*. (2006) 203:2673–82. doi: 10.1084/jem.20061775
262. Schaffler MB, Cheung WY, Majeska R, Kennedy O. Osteocytes: master orchestrators of bone. *Calcif Tissue Int*. (2014) 94:5–24. doi: 10.1007/s00223-013-9790-y
263. Xiong J, Piemontese M, Onal M, Campbell J, Goellner JJ, Dusevich V, et al. Osteocytes, not osteoblasts or lining cells, are the main source of the RANKL required for osteoclast formation in remodeling bone. *PLoS ONE*. (2015) 10:e0138189. doi: 10.1371/journal.pone.0138189
264. Kramer I, Halleux C, Keller H, Pegurri M, Gooi JH, Weber PB, et al. Osteocyte Wnt/beta-catenin signaling is required for normal bone homeostasis. *Mol Cell Biol*. (2010) 30:3071–85. doi: 10.1128/MCB.01428-09
265. Shoji-Matsunaga A, Ono T, Hayashi M, Takayanagi H, Moriyama K, Nakashima T. Osteocyte regulation of orthodontic force-mediated tooth movement via RANKL expression. *Sci Rep*. (2017) 7:8753. doi: 10.1038/s41598-017-09326-7
266. Inoue M, Ono T, Kameo Y, Sasaki F, Ono T, Adachi T, et al. Forceful mastication activates osteocytes and builds a stout jawbone. *Sci Rep*. (2019) 9:4404. doi: 10.1038/s41598-019-40463-3
267. Prasadam I, Farnaghi S, Feng JQ, Gu W, Perry S, Crawford R, et al. Impact of extracellular matrix derived from osteoarthritis subchondral bone osteoblasts on osteocytes: role of integrinbeta1 and focal adhesion kinase signaling cues. *Arthritis Res Ther*. (2013) 15:R150. doi: 10.1186/ar4333
268. Wakita T, Mogi M, Kurita K, Kuzushima M, Togari A. Increase in RANKL: OPG ratio in synovia of patients with temporomandibular joint disorder. *J Dental Res*. (2006) 85:627–32. doi: 10.1177/154405910608500709
269. Takayanagi H. Osteoimmunology: shared mechanisms and crosstalk between the immune and bone systems. *Nat Rev Immunol*. (2007) 7:292–304. doi: 10.1038/nri2062
270. Takayanagi H. Osteoimmunology and the effects of the immune system on bone. *Nat Rev Rheumatol*. (2009) 5:667–76. doi: 10.1038/nrrheum.2009.217
271. Kikuta J, Wada Y, Kowada T, Wang Z, Sun-Wada GH, Nishiyama I, et al. Dynamic visualization of RANKL and Th17-mediated osteoclast function. *J Clin Invest*. (2013) 123:866–73. doi: 10.1172/JCI65054
272. Schiffman E, Ohrbach R, Truelove E, Look J, Anderson G, Goulet JP, et al. Diagnostic criteria for temporomandibular disorders (DC/TMD) for clinical and research applications: recommendations of the international RDC/TMD Consortium Network* and orofacial pain special interest groupdagger. *J Oral & Facial Pain Headache*. (2014) 28:6–27. doi: 10.11607/jop.1151
273. Kim YK, Kim SG, Kim BS, Lee JY, Yun PY, Bae JH, et al. Analysis of the cytokine profiles of the synovial fluid in a normal temporomandibular joint: preliminary study. *J Craniomaxillofac Surg*. (2012) 40:e337-41. doi: 10.1016/j.jcms.2012.02.002
274. Takahashi T, Kondoh T, Fukuda M, Yamazaki Y, Toyosaki T, Suzuki R. Proinflammatory cytokines detectable in synovial fluids from patients with temporomandibular disorders. *Oral Surg Oral Med Oral Pathol Oral Radiol Endod*. (1998) 85:135–41. doi: 10.1016/S1079-2104(98)90415-2
275. Kotake S, Udagawa N, Takahashi N, Matsuzaki K, Itoh K, Ishiyama S, et al. IL-17 in synovial fluids from patients with rheumatoid arthritis is a potent stimulator of osteoclastogenesis. The Journal of clinical investigation. (1999) 103:1345-52. doi: 10.1172/JCI5703
276. Tanimoto K, Suzuki A, Ohno S, Honda K, Tanaka N, Doi T, et al. Effects of TGF-beta on hyaluronan anabolism in fibroblasts derived from the synovial membrane of the rabbit temporomandibular joint. *J Dental Res*. (2004) 83:40–4. doi: 10.1177/154405910408300108
277. Kuroda S, Tanimoto K, Izawa T, Fujihara S, Koolstra JH, Tanaka E. Biomechanical and biochemical characteristics of the mandibular condylar cartilage. *Osteoarthr Cartilage*. (2009) 17:1408–15. doi: 10.1016/j.joca.2009.04.025
278. Nakano T, Scott PG. Changes in the chemical composition of the bovine temporomandibular joint disc with age. *Arch Oral Biol*. (1996) 41:845–53. doi: 10.1016/S0003-9969(96)00040-4
279. Jibiki M, Shimoda S, Nakagawa Y, Kawasaki K, Asada K, Ishibashi K. Calcifications of the disc of the temporomandibular joint. *J Oral Pathol Med*. (1999) 28:413–9. doi: 10.1111/j.1600-0714.1999.tb02113.x
280. Takano Y, Moriwake Y, Tohno Y, Minami T, Tohno S, Utsumi M, et al. Age-related changes of elements in the human articular disk of the temporomandibular joint. *Biol Trace Element Res*. (1999) 67:269–76. doi: 10.1007/BF02784426
281. Pufe T, Harde V, Petersen W, Goldring MB, Tillmann B, Mentlein R. Vascular endothelial growth factor (VEGF) induces matrix metalloproteinase expression in immortalized chondrocytes. *J Pathol*. (2004) 202:367–74. doi: 10.1002/path.1527

Conflict of Interest Statement: TS is an inventor of US-patent 5652223, 5736341, 5866432, 6143476, 20170023571/A1, and patent 127416. LG and H-ML are listed on patents on the medications/compounds described in this paper, which have been fully assigned to their institution, Stony Brook University, State University of New York and financially supported by NIDCR/NIH, R37-DE03987, K16DE-00275, K11DE00363, R01DE012872, 1R41DE024946, R42-DE024964, and additional support from U.S. Dept. of Defense (DoD); Johnson & Johnson, Collagenex Pharma., Inc., Galderma R&D, Kroc Foundation for Medical Res., Traverse Biosciences, Inc., N.Y. State Diabetes Assoc., Stony Brook University Center for Advanced Biotechnology.

The remaining authors declare that the research was conducted in the absence of any commercial or financial relationships that could be construed as a potential conflict of interest.

frontiers in Immunology

REVIEW
published: 23 July 2019
doi: 10.3389/fimmu.2019.01724

Chronic Implant-Related Bone Infections—Can Immune Modulation be a Therapeutic Strategy?

Elisabeth Seebach and Katharina F. Kubatzky**

Department of Infectious Diseases, Medical Microbiology and Hygiene, Heidelberg University Hospital, Heidelberg, Germany

Chronic implant-related bone infections are a major problem in orthopedic and trauma-related surgery with severe consequences for the affected patients. As antibiotic resistance increases in general and because most antibiotics have poor effectiveness against biofilm-embedded bacteria in particular, there is a need for alternative and innovative treatment approaches. Recently, the immune system has moved into focus as the key player in infection defense and bone homeostasis, and the targeted modulation of the host response is becoming an emerging field of interest. The aim of this review was to summarize the current knowledge of impaired endogenous defense mechanisms that are unable to prevent chronicity of bone infections associated with a prosthetic or osteosynthetic device. The presence of foreign material adversely affects the immune system by generating a local immune-compromised environment where spontaneous clearance of planktonic bacteria does not take place. Furthermore, the surface structure of the implant facilitates the transition of bacteria from the planktonic to the biofilm stage. Biofilm formation on the implant surface is closely linked to the development of a chronic infection, and a misled adaption of the immune system makes it impossible to effectively eliminate biofilm infections. The interaction between the immune system and bone cells, especially osteoclasts, is extensively studied in the field of osteoimmunology and this crosstalk further aggravates the course of bone infection by shifting bone homeostasis in favor of bone resorption. T cells play a major role in various chronic diseases and in this review a special focus was therefore set on what is known about an ineffective T cell response. Myeloid-derived suppressor cells (MDSCs), anti-inflammatory macrophages, regulatory T cells (T_{reg}s) as well as osteoclasts all suppress immune defense mechanisms and negatively regulate T cell-mediated immunity. Thus, these cells are considered to be potential targets for immune therapy. The success of immune checkpoint inhibition in cancer treatment encourages the transfer of such immunological approaches into treatment strategies of other chronic diseases. Here, we discuss whether immune modulation can be a therapeutic tool for the treatment of chronic implant-related bone infections.

Keywords: chronic implant-related bone infection, osteomyelitis, bacterial infection, biofilm, immune modulation, MDSCs, T cells, immune checkpoint molecules

OPEN ACCESS

Edited by:
Teun J. De Vries,
VU University
Amsterdam, Netherlands

Reviewed by:
Jim Cassat,
Vanderbilt University Medical Center,
United States
Ryan Trombetta,
United States Army Institute of
Surgical Research, United States

****Correspondence:***
Elisabeth Seebach
elisabeth.seebach@
med.uni-heidelberg.de
Katharina F. Kubatzky
kubatzky@uni-heidelberg.de

Specialty section:
This article was submitted to
Microbial Immunology,
a section of the journal
Frontiers in Immunology

Received: *25 March 2019*
Accepted: *09 July 2019*
Published: *23 July 2019*

Citation:
Seebach E and Kubatzky KF (2019)
Chronic Implant-Related Bone
Infections—Can Immune Modulation
be a Therapeutic Strategy?
Front. Immunol. 10:1724.
doi: 10.3389/fimmu.2019.01724

INTRODUCTION

Primary hip and knee arthroplasties belong to the most successful surgeries of this century (>1,000,000/year in the U.S.) and the numbers of surgeries are rising due to demographical changes (1). Concomitantly, the number of revision surgeries and associated complications is increasing. Prosthetic joint infections (PJIs) are one of the most feared complications that often result in revision of the artificial joint with serious consequences for the patients and high costs for the respective health systems (1, 2). For primary arthroplasty the incidence of infection ranges between 1 and 2% depending on the register (1, 3). A current study states the risk of re-infection after PJI-induced revision surgery at around 8% for hips (4) and knees (5), but also much higher values (up to 57.1%) are published (6, 7). In trauma-related bone reconstructions (2,000,000/year in the U.S.), fracture-related infections (FRIs) associated with osteosynthetic stabilization are a major problem as the surgery field is often contaminated due to bacterial access through open wounds and broken bone that penetrates the skin (open fractures). This leads to an infection risk ranging from 10% (8, 9) to 50% depending on the fracture type (10). Thus, chronic implant-related bone infections are a serious burden in current and future health care.

Homeostasis of Bone

Bone is a dynamic organ undergoing constant remodeling in order to maintain homeostasis of bone formation and degradation, and to preserve bone mass. Bone remodeling is organized by the interplay between bone forming osteoblasts (OBs) and bone resorbing osteoclasts (OCs). OBs differentiate from mesenchymal stromal cells (MSCs) that reside within the bone marrow, whereas OCs develop from myeloid precursor cells. Osteoclastogenesis is regulated through the osteoprotegerin (OPG)/receptor activator of NF-κB (RANK)/RANK-Ligand (RANKL) pathway. OPG serves as a negative regulator of osteoclastogenesis that inhibits the RANK—RANKL interaction via binding of RANKL [reviewed in (11, 12)]. Bone homeostasis depends on the local cytokine milieu. While inflammation is necessary to induce physiological bone healing (13), it can lead to increased bone resorption under pathological situations such as bone infections (14).

Definition of Bone Infections

Osteomyelitis is an infection of the bone that is characterized by an inflammatory reaction and destruction of bone due to bacterial colonization of the bone itself, the bone marrow and the surrounding tissue. Osteomyelitis can occur by local spread of bacteria from an adjacent, contaminating source caused by trauma or bone surgery; or secondary to a vascular undersupply as it is mostly the case in diabetic foot ulcers. Hematogenous osteomyelitis is caused by bacteria, which come from a source of infection localized somewhere else in the body (e.g., a dental infection) and enter the bone via the blood stream (15, 16). PJIs caused by hematogenous seeding of the prosthesis often appear a long time after bone surgery (late bone infection: >2 years after surgery), whereas contamination during implantation of the medical device or during hospitalization before the wound has closed usually leads to early (<3 months after surgery) or delayed post-operative infections (3 months−2 years after surgery) (2). Zimmerli and Sendi further suggest a clinically more relevant classification that is used as a guide for surgical management. Here, PJIs are defined as early post-operative when symptoms occur within 1 month and are called chronic when diagnosed later than 1 month after surgery. Hematogenous PJIs are classified as acute when symptoms occur <3 weeks after a former uneventful post-operative period and chronic when symptoms persist for over 3 weeks (17). The predominantly isolated bacteria are part of the physiological skin microflora, such as *Staphylococcus aureus (S. aureus)*, coagulase-negative staphylococci and enterococci (1, 18). Early and acute symptoms of infection, such as pain, warming and swelling of the site of infection and fever, are mostly associated with highly virulent bacteria like *S. aureus*; whereas less virulent bacteria, such as *Staphylococcus epidermidis (S. epidermidis)*, cause more subtle symptoms typical for a low-grade inflammation that often are not diagnosed before infection chronicity (2). FRIs are mostly caused by inoculation of bacteria through an open wound/penetrated skin or through the surgical access needed for osteosynthetic bone reconstruction with *S. aureus* being the primary causative agent (19). At present, they are defined as early when occurring <2 weeks, delayed at 3–10 weeks and late >10 weeks after implantation of the osteosynthetic device (17, 20). However, the criteria for FRIs that can be used as guidelines for clinical management as they are established for PJIs are still under discussion (21). The early and acute states of osteomyelitis are characterized by bacterial colonization of the bone, pus formation, vascular undersupply and a strong inflammatory immune response associated with fever, pain and swelling (15, 16). The resulting increased levels of pro-inflammatory cytokines, such as tumor necrosis factor alpha (TNF-α), interleukin-1 beta (IL-1β) and IL-6, induce tissue destruction and a shift toward osteoclastogenesis and bone resorption (14). At this stage, a prompt and aggressive antibiotic and surgical treatment is generally sufficient to clear the infection. Unsuccessful treatment however results in the manifestation of a chronic bone infection, which is characterized by persistence of bacteria, areas of dead bone, so-called sequestra, periosteal new bone formation, fistula and low-grade inflammation. The recurrence of infection with fever is a clear sign for a chronic progression of the disease (15, 16) and depends on different bacteria reservoirs. *S. aureus* is known to survive intracellularly within non-professional phagocytes such as osteoblasts (22), an immune evasion mechanism still controversially discussed for *S. epidermidis* (23–25). A current study showed that *S. aureus* colonizes the canaliculi and osteocyte lacunae of living cortical bone (26). Furthermore, many bacteria are able to form sessile communities; referred to as biofilms, which preferentially colonize dead bone and foreign devices (17, 27). Biofilms evade bacterial clearance through the immune system and antibiotic treatment and therefore are one key characteristic of chronic implant-related bone infections and a major cause for bacterial persistence (28, 29). Current

treatment strategies aim to eradicate biofilms to reduce the risk of re-infection.

Current Treatment Concepts

Current treatment concepts are based on the surgical removal of the infected tissue and strict antibiotic treatment to reduce bacterial burden as much as possible (17). Antibiotic regimens depend on the result of susceptibility testing of isolated cultures and should be administered for a total duration of 6–12 weeks. In the case of Staphylococcus subspecies, treatment guidelines recommend the use of rifampin, which is effective against biofilm-embedded bacteria, in combination with an intravenously administrable antibiotic for 2 weeks followed by an oral antibiotic therapy. For Methicillin-resistant strains, the combination of rifampin with vancomycin is recommended (20, 30). Surgical treatment of PJIs includes debridement with implant retention and one- or two-stage exchanges with placement of an antibiotic-laden spacer between the explantation and re-implantation of the prosthesis for up to 8 weeks. The procedure applied mainly relies on the time-point, when an implant-related bone infection is diagnosed. In early/acute infections the biofilm is still immature and the infection can be eradicated with retention of the implant. The success rate of this procedure is >80% when the implant is stable and the causative pathogen is susceptible to antibiotic treatment. Otherwise, in the case of Methicillin-resistant *S. aureus* (MRSA) or after chronic manifestation of infection associated with mature biofilm, for example, the foreign device has to be exchanged (30, 31). In FRIs, the decision for retention, exchange or removal of the implant mainly depends on the onset of infection (early-delayed-late), the type of fixation device and fracture consolidation. Here, infection clearance can be achieved because the foreign material can be removed after bone bridging has occurred. Until then, the stability of the bone fracture needs to be preserved meaning that after extensive debridement, external fixation and bone reconstruction may be required. Local delivery of antibiotics either by non-resorbable bone cement or degradable bone graft materials can be beneficial (19, 20). All of these approaches are associated with tremendous consequences for the patients with long hospital stays, repeated surgeries and an impairment of limb function between explantation and re-implantation of the devices. Due to the enhanced tolerance of biofilm-embedded bacteria against most antibiotics and the existence of dormant cells within biofilms, bone niches and/or host cells, treatment approaches often do not end in complete clearance of the pathogen and re-infection occurs frequently (32, 33). As a last consequence, this can lead to non-healing bone defects (non-union), stiffening of the affected joint or even amputation of the infected limb (20, 34).

Role of the Implant and Biofilm Formation

The implant itself represents a major risk factor for the initial development and chronic progression of osteomyelitis and recurrence of infection. In a tissue cage model in guinea pigs, the presence of a foreign material decreased the required infection dose from $>10^8$ CFUs *S. aureus* to 10^2 CFUs (35). Also in rats, infection doses as low as 10^2 CFUs *S. aureus* were sufficient to induce implant-associated bone infections without any further promoter such as soft tissue trauma or bone injury (36). One reason for this increased susceptibility is that the implant adversely affects the immune system by activating neutrophils, phagocytic cells, and the complement system. This results in an inflammatory and cytotoxic local environment that causes cell death and tissue damage (37). In this immune-compromised environment, successful clearance of bacteria by the host defense does not take place. Bacteria additionally profit from the foreign material as their surface structures serve as an attractive source for bacterial attachment that facilitate the transition from the planktonic to the biofilm stage (38). The concept of "race to the surface" describes the balance between tissue integration and bacterial colonization of an implant. The success of its implantation depends on the immediate interaction with host cells and the integration within the respective tissue (osseointegration in case of orthopedic devices), which prevents bacterial adhesion and biofilm formation. If bacterial colonization occurs first, tissue integration is impaired and bacteria can persist by forming biofilms (39, 40).

In the presence of a medical device, biofilm formation starts with the adhesion of planktonic bacteria to the implant surface, a process mediated by hydrophobic, electrostatic and van der Waals interactions that allows unspecific attachment (**Figure 1**). Directly after insertion into the body, the implant is coated with serum and tissue proteins. This allows specific attachment of bacteria by bacterial adhesion molecules (microbial surface components recognizing adhesive matrix molecules, MSCRAMMs) that bind to host proteins such as collagen and fibronectin (41). After the initial colonization, bacteria begin to produce a biofilm consisting of exopolysaccharides, proteins, lipids and nucleic acids that form a protective, slimy layer around them (extracellular polymeric substance, EPS). This effectively shields the included bacteria from immune cells and antibiotics (28, 38). Polysaccharide intercellular adhesin (PIA), for example, is a glycosaminoglycan of the EPS that mediates cell-cell adhesion and aggregation of bacteria in staphylococci biofilms (42). Immature biofilms are found in early post-operative and acute hematogenous infections (30). Biofilm maturation is characterized by biofilm growth, bacterial multiplication and production of additional virulence factors (28). Mature biofilms have a high bacterial density and are a constant source of bacterial spreading (43). They are associated with chronic infections (30). Biofilm formation and maturation, production of virulence factors and release of bacteria by mature biofilm are mediated by quorum sensing (QS) signaling systems (28, 44, 45). QS allows cell-to-cell communication between bacteria due to the release of small molecules called "autoinducers". By this, bacteria are able to determine their population density and react on environmental changes in a population-wide manner (46, 47). Within the hostile environment of mature biofilms, bacteria differentiate into a non-growing phenotype called "persister cells". This dormant cell population is highly tolerant to antibiotics and contributes to the chronicity and the risk of re-infection of implants (41, 48). Another bacteria

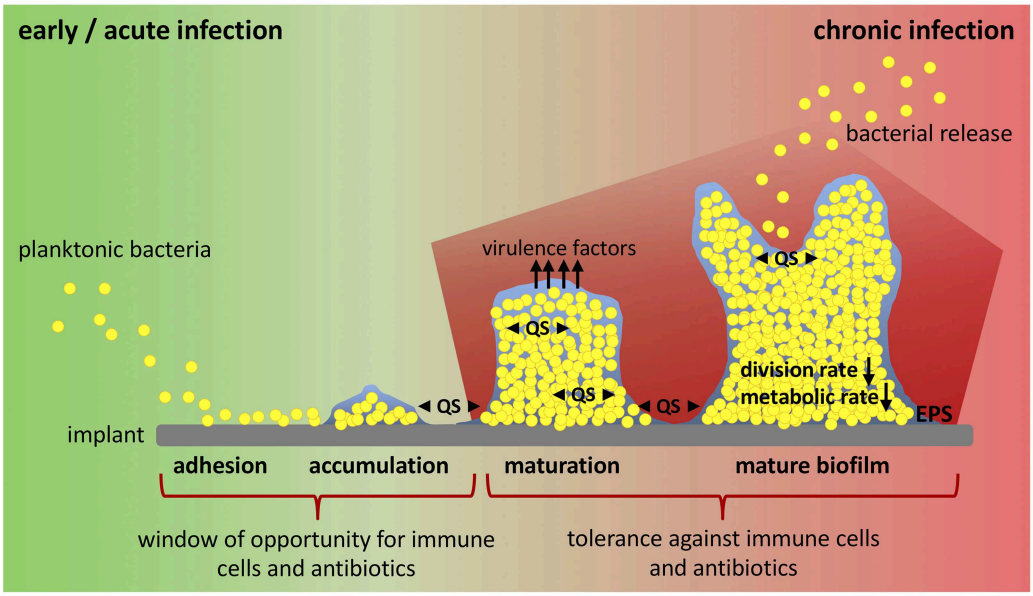

FIGURE 1 | Biofilm formation and window of opportunity for an effective clearance of bacteria. Implant-related bone infections are defined as early and chronic post-operative or acute and chronic hematogenous depending on the time interval between implantation of the medical device and onset of symptoms. Early and acute infections are associated with immature biofilms, whereas mature biofilms play a role in chronic situations. Biofilm formation starts when planktonic bacteria adhere to the implant surface. Attached bacteria then accumulate and start to produce biofilm. During biofilm maturation bacteria strongly multiply, build up further biofilm, and release virulence factors. Mature biofilm shows a high bacterial density with low division rate and decreased metabolic activity (persister cells). Release of planktonic bacteria by biofilm disassembly can lead to recurrence of infection. All these steps are mediated by an intercellular signaling system referred to as quorum sensing (QS). There is only a small window of opportunity for immune cells and antibiotic treatment to successfully clear bacteria and prevent biofilm formation and infection persistence. Biofilm maturation however is characterized by increasing tolerance against immune cells and antibiotics and leads to chronicity of infection. EPS, extracellular polymeric substance; QS, quorum sensing.

phenotype associated with recurrent bone infections are small colony variants (SCVs). SCVs are a metabolically inactive and slow-growing form of bacteria that forms due to defects in electron transport and thymidine biosynthesis (49). Mainly, SCVs are related to intracellular persistence of bacteria as they survive within host cells, but their contribution to biofilm formation and antibiotic tolerance is also discussed (50, 51). In addition to its function as a physical barrier and environment for SCV and persister cell formation, it is hypothesized that biofilm and embedded bacteria affect the local immunological environment in favor of decreased bacterial killing and enhanced persistence (37, 52, 53). The interaction between the foreign device, bacteria and biofilm dampens the host immune response and is one major reason for the ineffective elimination and chronicity of implant-related bone infections (37). Thus, the investigation of endogenous defense mechanisms has moved into focus and the possibility to modulate a misdirected host immune response might provide an attractive target for innovative therapeutic strategies against chronic implant-related bone infections.

The aim of this review is 2-fold: First to summarize the immune response against implant-related bone infections highlighting the transition from acute to chronic infection defined by the presence of biofilm. Secondly, to examine immune modulatory interventions that have been applied for the treatment of other chronic diseases and discuss their feasibility and application for treating chronic implant-related osteomyelitis.

IMMUNE RESPONSE AGAINST CHRONIC IMPLANT-RELATED BONE INFECTIONS

In the presence of planktonic bacteria, polymorphonuclear neutrophils (PMNs) and macrophages (Mϕs) infiltrate the site of infection. Here, they are activated via binding of pathogen-associated molecular patterns (PAMPs) to the respective pattern recognition receptors (PRRs) such as toll-like receptors (TLRs), which results in the activation of transcription factors such as the nuclear factor "kappa-light-chain-enhancer" of activated B-cells (NF-κB) [reviewed in (54, 55)]. As a consequence, the cells generate an inflammatory environment by secretion of pro-inflammatory cytokines and contribute to bacterial killing by release of antimicrobial peptides, generation of reactive oxygen (ROS) and nitrogen species (NOS) and phagocytosis. Furthermore, PMNs form extracellular fibril matrices consisting of granule proteins and DNA that helps to trap bacteria for further degradation (neutrophil extracellular traps, NETs) [reviewed in (52)]. Thus, in the absence of foreign materials, the innate immune system is usually able to control infection at the planktonic stage leading to bacterial clearance and effective prevention of infection progression.

In the case of implant-related infections, the implant is recognized as a foreign body that induces an innate immune reaction. The release of anti-microbial peptides, ROS, NOS, and NETs and "frustrated" phagocytosis of the non-phagocytosable material leads to cell exhaustion, cell death, and tissue damage. Thus, an immune compromised environment with reduced bacterial killing is established around the implant [reviewed in (37, 41, 56)]. Additionally, the implant creates a niche for bacteria to evade the host defense by hiding in structural pores of the surface that are inaccessible for the larger immune cells (41). So, the foreign material makes clearance of planktonic bacteria ineffective, which ultimately results in bacterial persistence and chronicity of infection.

In a mouse model of chronic implant-associated *S. aureus* osteomyelitis, it was shown that biofilm formation on contaminated implants already started on the first day after surgery. Between days 3 and 7, a strong proliferation of bacteria and biofilm growth took place, and the maturation of biofilm reached its maximum around day 14, when proliferation declined, and bacterial dispersal became apparent. The biofilm then stayed stable over the remaining study period for up to 56 days (57). This means that the planktonic window in which an effective bacterial clearance could take place is rather small and that during the course of implant-related bone infections, the immune system is almost entirely confronted with biofilm (**Figure 1**). The following findings explain at least in part the immune privileged nature of mature biofilms (**Figure 2**).

The biofilm itself plays an important role in shielding the embedded bacteria against the immune cells and protects the bacteria from immune cell recognition. Mature biofilm consists of a dense extracellular polymeric matrix, which is difficult to penetrate and engulf by phagocytes (58). On the other hand, the EPS contains PAMPs, which normally induce a pro-inflammatory immune response through TLR signaling. However, in the context of biofilms, exopolysaccharides such as PIA, which represent the main matrix component, are associated with immune evasion and protection against innate defense mechanisms (52, 59). Extracellular DNA (eDNA) is an EPS component that consists of eukaryotic DNA from host cells (e.g., through NET formation by PMNs) as well as prokaryotic DNA released by QS-controlled autolysis of bacteria. eDNA has an important role in stabilizing the biofilm matrix and in horizontal gene transfer (52, 60). Bacterial DNA is highly immunogenic and can be recognized by TLR9 (61). For *S. aureus* biofilms however, it was shown that biofilms evade TLR2 and TLR9 recognition. Possible explanations are that the exposure of PAMPs due to the biofilm-shielded bacteria is reduced, and polysaccharides of the biofilm EPS may interfere with TLR-ligand engagement (58, 62). In *Pseudomonas aeruginosa* biofilms, eDNA seems to induce a pro-inflammatory and anti-microbial neutrophil response, as neutrophil activity against *in vitro* biofilms is reduced after DNase treatment (63). However, eDNA also induces increased tolerance against anti-microbial peptides (64). Besides physical and chemical protection, biofilm formation leads to an acidic, hypoxic and nutrient-deprived local environment, which alters immune cell metabolism and activation (65). The release of toxins by the biofilm embedded bacteria further impairs immune cell function and induces cell death (66, 67).

Biofilm is not completely protected against recognition by phagocytic cells (68). *In vitro* data indicate that leukocytes are able to adhere to biofilms and penetrate them under laminar-shear conditions. This is followed by the production of pro-inflammatory cytokines in response to young and mature biofilms; however, the cells were not able to phagocytose the biofilm-embedded bacteria (69). In samples of patients with implant-associated bone infections, Wagner et al. isolated highly activated PMNs, which showed a reduced ability to migrate and a high production of superoxides. The authors concluded that like in planktonic infections, PMNs infiltrate the site of infection and get locally activated but then are unable to effectively clear the biofilm embedded bacteria. Instead, PMNs remain at the site of infection where they release cytotoxic products that contribute to host tissue destruction but do not effectively control the infection (70, 71). Other *in vitro* experiments confirmed the release of granule proteins and DNA by PMNs as a response to biofilm exposure, but in contrast to the study of Leid et al., they could also observe phagocytosis of biofilm bacteria (72). Effective phagocytosis normally depends on the opsonization of bacteria by antibodies and complement factors (73). In contrast to planktonic bacteria, phagocytosis of biofilm by PMNs seems to be independent of opsonization as serum treatment of biofilms did not enhance bacterial uptake. However, reduced deposition of IgG and C3b on biofilm-embedded bacteria contributes to their ineffective killing by PMNs, which may be due to other mechanisms such as a decreased ROS production (74, 75). The biofilm destruction by PMNs was dependent on its maturation stage: whereas immature biofilm (day 2 and 6) was infiltrated and cleared by PMNs at least *in vitro*, mature biofilm (day 15) was shown to be more tolerant against the host immune response (76). This can be explained by the increased biofilm mass making it more difficult for the immune cells to penetrate and engulf the biofilm, but also by an altered gene expression profile of the biofilm embedded bacteria as a reaction to attacking phagocytic cells. Up-regulation for example of the accessory gene regulator (*agr*) locus, which encodes for a staphylococci QS system that activates multiple pathogenicity factors, leads to increased tolerance against immune cell killing and phagocytosis (77, 78). Data from a mouse post-arthroplasty infection model revealed that the recruitment of neutrophils to the site of infection depends on IL-1β. Moreover, the respective knock-out mice showed decreased numbers of neutrophils with more biofilm formation indicating that neutrophils reduce biofilm burden at least to some extent (62). Consistent with these findings, IL-1β expression was decreased during biofilm infection in a mouse catheter-biofilm model (58). Macrophages can either be activated via the classical route which results in a more pro-inflammatory subtype (M1) related to bacterial killing, or via the alternative route which induces a more anti-inflammatory/regulatory and pro-fibrotic subtype (M2) (79). In the mouse catheter-biofilm model, it was shown that biofilm skews infiltrating macrophages from the M1 toward the M2 subtype, as evidenced by a decrease in inducible nitric oxide synthases (iNOS) and an increase in arginase-1 (Arg-1) production. Ultimately, this induced an

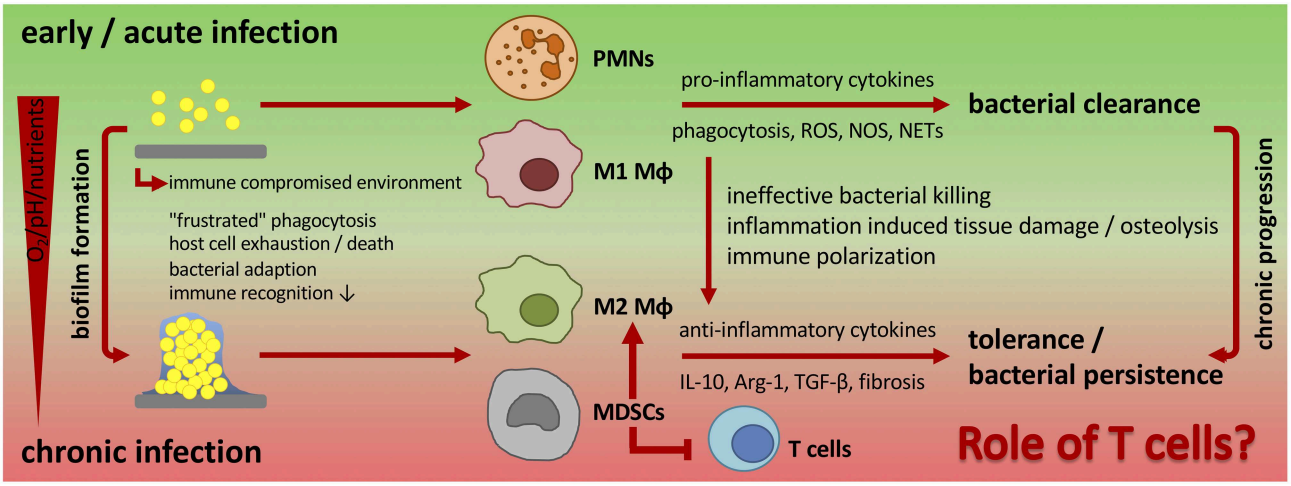

FIGURE 2 | Changing immune response during biofilm formation and chronic progression of implant-related bone infections. Planktonic infections are usually spontaneously cleared by the innate immune system. Neutrophils and classically activated (M1) macrophages are the pre-dominant cell populations that induce a pro-inflammatory cytokine milieu, release antimicrobial products, and phagocytose bacteria. In implant-associated infections the foreign material itself induces an immune reaction. As a result, an immune compromised environment around the implanted device is established that is characterized by an ineffective immune response against the non-phagocytosable material, dysfunction of immune cells and immune cell death. Bacteria take advantage of the foreign material and the impaired immune reaction and start to colonize the implant and form a biofilm. Biofilm-embedded bacteria can adapt to the host defense mechanisms, which results in a decreased immune recognition and enhanced bacterial survival and persistence. The unresolved inflammation is then associated with tissue damage and in the case of bone infections with osteolysis. Additionally, biofilm formation influences the local environment and induces a hypoxic, nutrient-deprived and acidic milieu that further impairs immune cell function. As a consequence, biofilms skew the immune system toward an anti-inflammatory response with a pre-dominantly alternative (M2) macrophage polarization and a high number of immune suppressive MDSCs that are known to inhibit T cell immunity and to induce immune tolerance. Ultimately, this leads to chronicity of infection. The role of T cells in the defense against chronic implant-associated infections is not fully understood and only a few studies focus on this topic. PMNs, polymorphonuclear neutrophils; Mϕ, macrophage; MDSCs, myeloid-derived suppressor cells; ROS, reactive oxygen species; NOS, nitrogen species; NETs, neutrophil extracellular traps; IL-10, interleukin-10; Arg-1, arginase-1; TGF-β, transforming growth factor-beta.

anti-inflammatory and more pro-fibrotic response preventing effective phagocytosis and bacterial killing (58). The deposition of a fibrotic matrix around the biofilm associated with an alternative macrophage response prevented immune cells from infiltrating the site of infection, which further promoted bacterial persistence. This biofilm-mediated immune suppression was overcome by an early administration of classically activated (M1) macrophages or the treatment with the C5a receptor agonist EP67, which induces a pro-inflammatory macrophage phenotype and indeed resulted in reduced biofilm formation (80). The mechanistic details of how biofilms can polarize macrophages are not completely understood, but one explanation can be an altered immunometabolism. Planktonic bacteria predominantly induce aerobic glycolysis, which provides necessary intermediates for anabolic processing of pro-inflammatory effector molecules such as ROS and NO. Biofilms instead lead to a more anti-inflammatory response, which is generally associated with oxidative phosphorylation (OxPhos). Biofilm formation changes the environmental conditions, which alters the metabolic profiles of macrophages toward OxPhos and anti-inflammation [reviewed in (65)].

Myeloid-derived suppressor cells (MDSCs) are described as a heterogeneous cell population consisting of immature monocytes (M-MDSCs) and granulocytes (G-MDSCs) initially found to suppress T cell activation (81). Typically, these cells differentiate into neutrophils, Mϕs and dendritic cells (DCs) at the site of inflammation, but under chronic conditions such as cancer or chronic infections, respectively, MDSCs arrest in an immature state and promote a negative regulation of the immune system (82). By this, MDSCs have an important role in keeping the balance between long-lasting inflammation and tissue damage, but also contribute to disease chronicity. The mechanisms behind biofilm-mediated MDSC accumulation and arrest have not been determined yet and are important aspects of future research. The group of Tammy Kielian found a remarkable presence of MDSCs in a mouse orthopedic biofilm model (83) as well as in samples from patients with prosthetic joint infections that underwent revision surgery (84, 85). MDSC levels increased continuously after the onset of biofilm formation and then stabilized after chronic progression of infection (85). MDSCs are known to inhibit the pro-inflammatory activation of macrophages. Antibody-mediated depletion of MDSCs within the mouse model therefore resulted in improved bacterial clearance (83). Enhanced numbers of MDSCs and M2 macrophages were also found in a rat PJI model. Additionally, *in vitro* experiments showed that the biofilm was able to induce the differentiation of M-MDSCs into anti-inflammatory M2-like macrophages (86). Using knock-out models for IL-12 or IL-10, the group of Tammy Kielian showed that the presence of IL-12 was required for the recruitment of MDSCs to the site of infection (85), but that the immune suppressive action of MDSCs was mediated by release of IL-10, a cytokine known to shift macrophage polarization toward

an anti-inflammatory phenotype (87). The loss of IL-12 or IL-10 resulted in lower numbers of MDSCs, enhanced presence of pro-inflammatory monocytes, increased bacterial clearance and decreased biofilm burden. Adoptive transfer of wild-type MDSCs restored MDSC influx and immune suppressive action with aggravated disease outcome (85, 87). MDSC-derived Arg-1 only showed a minimal effect on biofilm growth. Instead, Arg-1 seemed to play a role in host immune cell activity against planktonic bacteria, which again confirmed the divergent immune responses against planktonic and biofilm infections (88).

The last step of the biofilm lifecycle is the release of bacteria back into their planktonic stage. By this, the bacteria become re-accessible for antibiotics and host defense mechanisms; however, this can also be linked to the spreading of infection and sepsis (43, 89). Furthermore, there is evidence that bacteria released from mature biofilms induce an increased pro-inflammatory reaction when compared to their planktonic counterparts that further supports inflammation-associated tissue destruction and infection relapse (90).

Role of T Cells

T cells belong to the adaptive immunity and mediate the specific immune response. They can be divided into cluster of differentiation (CD)4-positive helper T cells and CD8-positive cytotoxic T cells. Cytotoxic CD8 T cells directly eliminate infected cells through the release of cytotoxic proteins. CD4 helper T cells need to get activated by professional antigen presenting cells (APCs) in order to support a cellular and humoral immune response. T cell activation occurs after binding of an antigen- major histocompatibility complex (MHC)-complex to a T cell receptor (TCR) and further requires costimulation by binding of CD28 present on T cells to CD80/86. Depending on the cytokine environment, CD4 helper T cells differentiate into Th1, Th2, and Th17 subtypes as well as regulatory T cells (T_{reg}s) (91). The contribution of T cells during the immune response against chronic implant-related bone infections is not fully determined and there are some contradictory data about the presence, effector function and inhibition of T cells at the site of biofilm infections that will be addressed in the following section (**Tables 1A,B**).

Studies using human tissue samples indicate that CD4 and CD8 T cells are present at the site of implant-related biofilm infections (92, 93). T cells isolated from the infectious samples showed a high proportion of $CD28^-/CD11b^+$ cells that indicates terminally differentiated T effector cells. These cells further produced high levels of perforin and IFN-γ typical for cytotoxic T cells which are classically associated with virus infections (**Table 1A**) (93–95). Whether this T cell response participates in infection defense or contributes to bone destruction by promoting osteoclastogenesis is yet unknown and has to be addressed in future studies. Mouse models showed that chronic implant-related bone infections can have a pronounced pro-inflammatory Th1 and Th17 response that is unable to clear infections at an early stage (**Table 1B**) (97, 99). Indeed, an early induction of a Th2/T_{reg} based response was able to prevent chronicity of infection (98). Heim et al. found only low numbers of T cells at the site of orthopedic biofilm infections in human samples (**Table 1A**) (84, 85) as well as in the corresponding mouse model (**Table 1B**) (83). The authors explain this with a high presence of MDSCs in their samples (see section above) (83) and they showed that the MDSCs, in particular G-MDSCs, suppressed T cell proliferation throughout the course of infection (83, 96). This fits with the finding of Kumar et al. who reported a reduced T cell proliferation in patient samples from chronic prosthesis infection (93). Along with inhibiting local T cell proliferation, MDSCs were associated with decreased T cell homing to the site of infection by down-regulated L-selectin (CD62L) expression (100), which might additionally explain the low numbers of T cell infiltrates. The mediators behind MDSC-derived T cell suppression are not clear yet, but this seems to be independent of IL-10 and IL-12 (85, 87). Besides that, Heim et al. found that the effects of MDSC-mediated immune suppression were more obvious on phagocytic cells (monocytes and neutrophils) than on T cells. The absence of MDSC action in the orthopedic biofilm mouse model led to an increased influx of monocytes and neutrophils and restored pro-inflammatory activity of these cells and resulted in decreased bacterial burden (83, 85, 87). Interestingly, in the same mouse model, PMNs as well as monocytes also exhibited suppressive activity on T cell proliferation after biofilm had developed (96). Besides playing a major role in innate immunity against pathogens, PMNs are discussed to directly interact with T cells. They are assumed to be able to activate T cells through MHC class II–mediated antigen-presentation as well as to exert an immune suppressive action on T cells by depletion of L-arginine via Arg-1 thereby exhibiting a more MDSC-like phenotype (101). This indicates that biofilm maturation potentially changes the initial pro-inflammatory PMN function toward a more anti-inflammatory action, which might then have an additional impact on the T cell response during infection progression.

Brady et al. compared the immune response in subcutaneous mouse models of acute and chronic implant-related biofilm *S. aureus* infection. By analyzing cytokine and chemokine levels of respective tissues using proteomic arrays, they found increased cytokine levels indicating a promoted pro-inflammatory Th1/Th17 response in their biofilm model. This was associated with down-regulated chemokine levels and decreased T cell homing to the site of infection, creating a strong pro-inflammatory reaction with low T cell infiltration (102). Interestingly, by comparing early (day 7) with late (day 21) biofilm infection in their chronic infection model, they found a similar cytokine response during the course of infection, which did not show any remarkable changes, but simply decreased when the infection become chronic. This is explained partly by the fact that at this time most bacteria are metabolically inactive and production of virulence factors and pro-inflammatory mediators has declined. Further research is needed to investigate possible additional factors that play a role in the dampened response after biofilm formation and chronicity of infection.

The activation of naïve T cells by APCs is an essential step of the T cell response. It is therefore conceivable that an altered APC function can lead to an ineffective T cell immunity against biofilms. Likely, APCs are already impaired by the implant and contribute to the immune

TABLE 1A | T cell response against implant-related bone infections—human studies.

Research question	Approach	Major findings	References
Characterization of leukocyte infiltrates and cytokine expression in PJI samples compared to aseptic loosening.	• Samples from endoprosthesis patients with PJI or aseptic loosening were analyzed for leukocyte counts and subtypes (FACS) and cytokines (Multiplex Assay).	â Higher leukocyte numbers in infected vs. aseptic samples. â Higher numbers of G-MDSCs in infected vs. aseptic samples (no difference in neutrophils or monocytes). â Reduced T cell numbers in infected vs. aseptic samples (non-significant). â Increased levels of IL-10, IL-6 and CXCL-1 in infected vs. aseptic samples. â **Accumulation of immune suppressive G-MDSCs in PJIs prevents activation of antimicrobial effector mechanisms by this leading to infection persistence.**	(84)
Characterization of leukocyte infiltrates and cytokine expression in PJI and aseptic human samples for comparison with data from a mouse orthopedic infection model.	• Samples from endoprosthesis patients with PJI or aseptic loosening were analyzed for leukocyte counts and subtypes (FACS) and cytokines (qPCR, Multiplex Assay).	â Increased MDSC-like and reduced T cell numbers with elevated pro-inflammatory cytokine levels in infected compared to aseptic human samples. â **Comparable immune response during orthopedic biofilm infection between mouse and human system.**	(85)
Analysis of T cell activity in human tissue samples after infectious vs. aseptic implant loosening.	• FACS, histological and gene expression analysis of T cell infiltrates in tissue samples from patients undergoing infectious or aseptic revision surgery.	â Increased numbers of $CD28^{-}CD11b^{+}$ (activated) CD4 or CD8 T cells in infected samples vs. aseptic samples. â Increased expression of T cell marker CD3 and no differences of monocyte marker CD14 and osteoclast marker cathepsin K in infected vs. aseptic samples. â **Enhanced numbers of activated T cells in implant-associated infection.**	(92)
Characterization of T cell phenotype in chronically infected vs. non-infected bone samples.	• Analysis of cortical bone samples from patients undergoing primary prosthetic surgery (non-infected) and samples from patients undergoing revision surgery (chronically infected) by multiparametric FACS.	â Presence of CD4 and CD8 T cells in both samples, increased HLA-DR expression on T cells and reduced T cell proliferation in infected vs. non-infected samples, no T_{reg}s or T cell apoptosis in infected samples. â Increase of $CD28^{-}$ CD4 T cells and $CD80^{+}$, $CD40^{+}$ and $CD40L^{+}$ CD4 and CD8 T cells in infected vs. non infected samples. â Increased perforin and CD11b and decreased CD7 expression in $CD28^{-}$ T cells. â Increased number of (long-term activated) cytotoxic $CD28^{-}$ CD4 T cells with reduced proliferation capacity in chronically infected bones.	(93)
Analysis of systemic and local T cell activation in patients with implant-associated bone infections.	• Blood and lavage from site of infection were taken from patients with implant-associated bone infections and analyzed by FACS for T cell activation markers.	â Upregulation of CD11b and loss of CD28 on CD4 T cells in blood samples of infected patients compared to healthy donors. â Increased expression of TLR1,2,4 associated with $CD11b^{+}CD28^{-}$ CD4 T cells in blood samples of infected patients. â Accumulation of $CD11b^{+}CD28^{-}$ CD4 T cells and $CD57^{+}$ CD8 T cells at site of infection. â Increased IFN-γ expression by T cells from site of infection. â **Recruitment and activation of CD4 and CD8 effector T cells in patients with implant-associated bone infections.**	(94)
Analysis of T cell infiltration in patients with implant-associated bone infections compared to patients with sterile joint inflammation.	• Blood and lavage from site of infection were taken from patients with implant-associated bone infections and analyzed by FACS for T cell markers. • As control synovial fluid from patients with rheumatoid arthritis (RA) was used.	â Loss of CD62L expression by T cells isolated from the infection or inflammation site compared to respective blood sample. â Shift of local CD4/CD8 ratio toward CD8 in infected and CD4 in RA patients. â Perforin and granzyme B expression by CD8 T cells at site of infection. â Detection of $CD28^{+}$ and $CD28^{-}$ subpopulation in lavage with increased CD11b and CD57 expression on $CD28^{-}$ CD8 T cells. â **Expansion and infiltration of cytotoxic CD8 effector T cells in patients with implant-associated bone infections.**	(95)

Bold text indicates key finding of the respective study.

TABLE 1B | T cell response against implant-related bone infections—mouse models.

Research question	Approach	Major findings	References
Characterization of invading MDSC subpopulations in a mouse orthopedic biofilm infection model.	• Insertion of a K-wire in femora of C57BL/6 mice and inoculation of 10^3 CFU *S. aureus* (SA) at the implant tip. • Analysis of infiltrating leukocyte populations by FACS, cytospin, *in vivo* proliferation assay, *in vitro* T cell activation capacity and RNA sequencing on days 3, 7, 14, and 28.	â Identification of $CD11b^{high}$ granulocytic MDSCs and $CD11b^{low}$ PMNs. â **G-MDSCs proliferate at the site of biofilm infection and suppress T cell response over the whole course of infection (planktonic and biofilm phase), whereas PMNs show immune suppressive activity only after biofilm development.**	(96)
Monitoring of the immune reaction during sterile or infected bone healing in an implant-stabilized mouse fracture model.	• Fixation of a SA pre-incubated osteosynthetic device (9×10^5 CFU/implant) and creation of an osteotomy in femora of C57BL/6 mice. • Quantitative microbiology and analysis of immune response by histology, FACS, qPCR, and Multiplex Cytokine Assay over 35 days.	â Positive cultures over whole period with highest bacterial loads on days 1–3. â Complete bone healing in non-infected controls by day 35, non-union with osteolysis in infected animals. â Minimal inflammatory cell infiltration in controls on day 3 with signs of tissue healing on day 7, increased invasion of inflammatory cells in infected animals on day 3 with strong inflammation/osteolysis on day 7. â Increased cell numbers in lymph nodes and spleen of infected animals. â Increased IL-4 and late IFN-γ expression in controls and increased IL-17, TNF-α, IL-1β, and IL-10 expression in infected animals. â **Bone healing is associated with sustained Th2 and late Th1 and bone infection with a central Th17 and pro-inflammatory response unable to control infection (with decrease in bone healing markers TGF-β and PDGF).**	(97)
Role of MDSC-derived IL-10 in MDSC-mediated immune suppression in orthopedic biofilm infections.	• Insertion of a K-wire in femora of C57BL/6 wt and IL-10 ko mice and inoculation of 10^3 CFU SA at the implant tip. • Adoptive transfer experiments of wt MDSCs in IL-10 ko mice. • Analysis of bacterial burden by SA recovery, MDSC and monocyte/Mϕ invasion and cytokine profile by ELISA, FACS, cytokine array and qPCR on days 3, 7, and 14 and analysis of *in vitro*-derived wt and IL-10 ko MDSC activity by T cell proliferation assay.	â Infiltrating MDSCs are the main source of increased IL-10 levels in orthopedic implant biofilm infections. â Decreased MDSCs and increased monocyte/Mϕ recruitment in IL-10 ko mice on day 14 with enhanced pro-inflammatory activity of monocytes/Mϕ and decreased bacterial burden. Partly reversible by adoptive transfer of wt MDSCs. No changes in neutrophil and T cell infiltrates in IL-10 ko mice. â Inhibition of T cell proliferation by biofilm-associated MDSCs is independent of IL-10. â **MDSC-derived IL-10 induces an anti-inflammatory monocyte phenotype at the site of biofilm infection that promotes bacterial persistence, but has no direct effect on T cell proliferation.**	(87)
Role of IL-12 in MDSC recruitment and MDSC-mediated immune suppression in orthopedic biofilm infections.	• Insertion of a K-wire in femora of C57BL/6 wt and IL-12 ko mice and inoculation of 10^3 CFU SA at the implant tip. • Adoptive transfer experiments of wt MDSCs in IL-12 ko mice. • Analysis of bacterial burden by SA recovery, MDSC and monocyte/Mϕ invasion and cytokine profile by ELISA, FACS, cytokine array and qPCR on days 7, 14, 21, and 28, CT and histology and analysis of MDSC activity isolated from site of infection of wt and IL-12 ko mice by T cell proliferation assay. • Comparison of data with human samples of PJIs.	â Detection of bacteria during the whole period with strong inflammation of infected tissue and bone destruction. â Increased cytokine (IL-12, IL-1β, TNF-α, and G-CSF) and chemokine levels in infected animals, associated with increased MDSC and neutrophil and reduced monocyte/Mϕ and early T cell invasion compared to aseptic samples. â IL-12 ko mice show decreased MDSC recruitment and decreased cytokine levels with enhanced monocyte and neutrophil infiltration and decreased bacterial burden compared to wt mice. â Adoptive transfer of wt MDSCs in IL-12 ko mice reduces monocyte and neutrophil invasion and leads to increased bacterial burden compared to wt mice. â MDSC isolated from site of infection in IL-12 ko mice are able to inhibit T cell proliferation like MDSC from wt mice. â **IL-12 promotes MDSC accumulation at the site of infection, causing a MDCS-mediated reduction of monocyte and neutrophil invasion. No direct role of IL-12 in activation of immune suppressive MDSC function and T cell proliferation.**	(85)

(Continued)

TABLE 1B | Continued

Research question	Approach	Major findings	References
Role of MDSCs and MDSC-mediated T cell suppression in orthopedic biofilm infections.	• Insertion of a K-wire in femora of C57BL/6 mice and inoculation of 10^3 CFU SA at the implant tip. • Antibody-mediated depletion of MDSC *in vivo*. • Histological, Multiplex cytokine array, FACS and qPCR analysis of tissue samples, T cell proliferation assay and monocyte co-culture experiments.	â Increased numbers of MDSCs in samples of infected animals vs. non-infected controls on day 7. â MDSCs isolated from infected tissue inhibit T cell proliferation and cytokine secretion. â MDSC depletion reduce biofilm burden (mainly by restoring pro-inflammatory activity of monocyte). â **Biofilm-associated MDSCs inhibit T cell response.**	(83)
Prevention of chronicity of an implant-associated biofilm infection through a Th1↓/Th2↑ polarized immune reaction.	• Implantation of SA pre-treated pins (3×10^5 CFU/pin) in tibiae of Th1-biased C57BL/6, Th2-biased Balb/c and STAT6 ko Balb/c mice. • Treg depletion in Balb/c with anti-CD25 and Th1 suppression in C57BL/6 with anti-IL12p40 treatment. • Analysis of bacterial clearance, Treg frequency and local cytokine profile on days 7 and 21.	â Spontaneous bacterial clearance in ∼75% of Balb/c mice. â Higher levels of IL-4 and IL-10 and T_{reg} frequency in Balb/c and increased neutrophil infiltration in C57BL/6 mice. â STAT6 ko and T_{reg} depletion lead to loss of protection in Balb/c mice. â Anti-IL12p40 treatment induces bacterial clearance in ∼40% of C57BL/6 mice. â **Early induction of Th2/T_{reg} and suppression of Th1/Th17 response protects from chronicity.**	(98)
Investigation of immune response during chronic progression of an implant-associated biofilm infection.	• Implantation of SA pre-treated pins (2×10^5 CFU/pin) in tibiae of C57BL/6 mice. • Analysis of activated immune cells, antibody production and local cytokine up to day 28.	â Activation of a CD4 T cell response, early production of Th1-IgG subtype IgG2b and local pro-inflammatory cytokine profile in infected animals. â **An early Th1 and Th17 and reduced T_{reg} immune response is ineffective to prevent infection and leads to chronicity.**	(99)

Bold text indicates key finding of the respective study.

compromised environment and increased bacterial colonization. Two biodegradable and biocompatible materials that are known to provoke a normal foreign body response were tested for DC activation and subsequent DC-mediated T cell proliferation and polarization in the presence or absence of *S. aureus* and *S. epidermidis*, respectively (103). The authors found that the biomaterials alone did not induce DC activation and subsequent DC-mediated T cell activation, but in combination with bacteria, DCs had a slightly changed cytokine secretion profile. However, these changes were too small to affect subsequent T cell activation. Thus, the presence of a foreign material does not impair APC-mediated T-cell activation upon bacterial exposure. The altered cytokine secretion by DCs stimulated by bacteria in the presence of a biomaterial could still have an impact on other immune cells like PMNs and macrophages which can promote bacterial survival. In this study only planktonic bacteria were used to stimulate DCs in the presence of a biomaterial. Therefore, the influence of biofilm formed on the biomaterial and potential changes in DC and subsequent T cell activation remain to be investigated.

So far, there are only a few studies that address the T cell response in chronic implant-associated bone infections and results argue for the presence of activated cytotoxic T cells at the site of biofilm formation and an early pro-inflammatory Th1/Th17 response. However, the decreased homing to the site of biofilm infection and a reduced T cell proliferation and potentially impaired function might trigger the formation of biofilm-associated suppressive immune cells.

It has to be taken into consideration that mouse studies that investigate the immune response against implant-related bone infections usually use *S. aureus* to induce biofilm-infections (**Table 1B**). However, *S. aureus* is a highly virulent pathogen that causes a strong pro-inflammatory Th1 immune response in planktonic infections (102) and early and acute bone infections (30). It needs to be investigated whether the findings also apply for less virulent bacteria like *S. epidermidis* that is associated with less symptomatic but chronic implant-infections. A recent study compared *S. aureus* and *S. epidermidis* -induced implant-associated osteomyelitis in mice (104). This study revealed that *S. aureus* caused osteolysis, reactive bone formation and abscess formation, whereas this was not apparent in *S. epidermidis* infection. Both bacteria colonized the implant and formed biofilm. The findings underline the different roles of *S. aureus* and *S. epidermidis* in chronic implant-related bone infections. In human studies, the cohorts include patients with implant-related bone infections caused by different bacteria and the time point of revision surgery and immune analysis might depend on the virulence of the respective bacteria. So, it is possible that different stages of biofilm infection are within the same cohort. This might explain the apparently conflicting findings in T cell quantities between the different studies (84, 92). Investigations of T cells in implant-related bone infections have been restricted to the evaluation of numbers and types of T cells present at the site of biofilms. The functionality of biofilm-associated T cells and the mechanisms behind the T cell response have not been examined yet. Apparently, there is a need for further research to investigate the insufficient T cell response during

biofilm formation and chronic progression of implant-related bone infections in more detail.

Humoral Immune Response

The identification of a protective humoral immunity (105) and biofilm-associated antigens raised the hope for vaccination strategies (106). Indeed, administration of a multicomponent and protein-based vaccine before bacterial challenge with subsequent antibiotic treatment significantly reduced the risk for infection in a biofilm model of osteomyelitis in rabbits (107). Passive immunization against implant-related osteomyelitis in mice with neutralizing antibodies associated with protective immunity in orthopedic infections led to reduced bacterial burden, osteolysis, and abscess formation, respectively, due to increased opsonophagocytosis of bacterial megaclusters by recruited macrophages (108, 109). A current study showed that a combinatory approach using passive immunization together with antibiotic and surgical treatment was capable of reducing re-infection in a mouse model of MRSA-induced implant-related osteomyelitis, thereby enabling osseointegration and bone healing (110). Despite this promising animal data, unfortunately, attempts to develop an effective vaccination strategy for humans have been unsuccessful so far (111).

Role of the Bone Environment

Due to the crosstalk between bone and immune cells, cells of the bone environment (OBs, OCs, MSCs) are also involved in the course of bone infection. A pro-inflammatory immune cell environment induces a shift in bone homeostasis toward increased osteoclastogenesis and bone resorption, which is further supported by local osteoblasts that can release pro-inflammatory proteins in response to bacteria (112, 113). Dapunt et al. showed that expression of pro-inflammatory proteins by osteoblasts is not only induced by planktonic bacteria but also by biofilm components. This indicates that OBs not only play a role in the host response against biofilm-associated infections, but also enhance osteolysis associated with these infections (114, 115). Besides an increased osteoclastogenesis, new bone deposition by osteoblasts is reduced as the infectious environment and bacterial internalization lead to decreased mineralization and increased apoptosis of osteoblastic cells (116). Release of internalized bacteria and dying osteoblasts might further impair the immune response against the bacteria.

In the case of osteosynthetically stabilized fractures, implant-associated bone infections impair the healing process and can lead to non-unions. During bone regeneration, the host response against bacteria and biofilm seems to interfere with the naturally occurring immune reaction required to induce the healing cascade. This unresolved pro-inflammatory environment is ineffective to clear the infection and at the same time is detrimental to bone regeneration (97, 117). MSCs as osteogenic precursor cells have an important role in bone healing (118). They are also known to have immune modulatory activity and exert an immune suppressive effect on T cells (119), which might impact the development and progression of bone infections. Indeed, in a rat plate-stabilized ostectomy-model, local implantation of MSCs to improve bone regeneration aggravated implant-associated bone infections (120).

These data indicate that implant-associated bone infections and septic non-unions are characterized by a complex interplay between bacteria, cells of the immune system, and cells of the bone environment.

Osteoclasts as Immune Competent Cells

Besides being the main players in bone resorption, osteoclasts are part of the immune system and interact with immune cells, especially with T cells [reviewed in (121, 122)]. Interactions are ambilateral with T cells influencing osteoclastogenesis and OCs having an impact on T cell activity. Activated T cells express RANKL which stimulates the differentiation of human monocytes into mature osteoclasts (123). Th17 helper cells and their cytokine IL-17 are shown to enhance osteoclastogenesis, while the Th1 and Th2 cytokines IFN-γ and IL-4 are associated with an anti-osteoclastogenic potential (124, 125). T_{reg}s were proven to have an inhibitory effect on osteoclast generation [reviewed in (126)]. In addition to the anti-osteoclastogenic effects of T_{reg}-derived cytokines IL-10 and TGF-β, direct cell-cell contact through binding of cytotoxic T-lymphocyte-associated protein-4 (CTLA-4) to CD80/86 on osteoclast precursors inhibits osteoclastogenesis (127) (more information on this are provided in the following section about immune modulation). OCs can function as antigen presenting cells that can activate T cells upon antigen exposure (128). However, a suppressive effect of OCs on the *in vitro* T cell response via the induction of indoleamine 2,3-dioxygenase (IDO) was also described (129, 130). Furthermore, OCs can prime CD8 T cells toward a regulatory phenotype (OC-iTc_{reg}) which then again has a suppressive effect on T cell activation and inhibit osteoclastogenesis [reviewed in (131)]. Taken together, it can be said that osteoclast precursors share many of the immune suppressive characteristics that have been associated with MDSCs (121, 132).

So far, research investigating the immunological function of osteoclasts has been done under sterile conditions either in *in vitro* experiments or in animal models of sterile bone loss, such as inflammatory arthritis or osteoporosis. Whether similar findings can be obtained in an infectious setting such as implant-associated bone infections need further investigations.

In summary, the implant as a foreign material as well as the bacteria, especially in form of a biofilm, lead to a dysregulation of the immune response and misbalance of bone homeostasis in favor of bacterial persistence, bone destruction and infection chronicity. We suggest that this impaired osteoimmunological environment represents an attractive target for modulation, making immune therapy an interesting approach for the treatment of chronic implant-related bone infections.

MODULATION OF THE IMMUNE RESPONSE DURING CHRONIC IMPLANT-RELATED BONE INFECTIONS

Enormous effort has been put into the development of new antibiotics, anti-microbial coatings of the implant, vaccination

strategies as well as interruption of the QS system to avoid biofilm formation and chronicity of implant-related bone infections, yet with limited success (32). Modulation of the immune system is a promising field in treating chronic diseases and offers the potential to combine current therapeutic and surgical strategies while strengthening endogenous defense mechanisms. Especially the success of immune therapy in cancer treatment encourages to take a broader view and transfer novel approaches into other diseases. The following section will address what is known about immune therapy in other chronic diseases and discuss whether there are targets for immune modulation that might allow treating chronic implant-related bone infections (**Figure 3** and **Table 2**).

Immune Regulation During Chronic Diseases

Immune responses are tightly regulated to prevent an unresolved immune reaction, which would lead to long-lasting inflammation and tissue damage. The regulation of this process is mediated by cells of the innate and adaptive immune system including immune suppressive MDSCs, anti-inflammatory (M2) Mϕ and regulatory T_{reg}s that help to generate an immune microenvironment characterized by high levels of IL-10, Arg-1 and TGF-β (133). In general, this limits the pro-inflammatory effector phase, which ends with antigen clearance, resolution of inflammation and the induction of an immunological memory. In contrast, disease continuation and long-term exposure to antigens, as it occurs in tumors or chronic infections, induce an enhanced up-regulation of inhibitory molecules by immune cells. Ultimately, this leads to immune cell dysfunction associated with ineffective control and persistence of disease. Upon long-term stimulation, T cells increasingly express inhibitory receptors, known as "immune checkpoint molecules," of which CTLA-4 and programmed cell death protein-1 (PD-1) are the most prominent members. Binding of their respective ligands expressed on immune and non-immune cells leads to T cells with low or diminished effector functions that are called anergic or exhausted T cells. T cell dysfunction has moved into the focus of interest as it can be reversed by the use of immune checkpoint inhibitors (ICIs), which makes them an attractive target for re-stimulation of the immune response [reviewed in (134)]. Blockade of immune checkpoints has been successfully introduced into certain cancer treatments (135) and is discussed as a treatment option for infectious diseases such as malaria, HIV (136) and sepsis (137). Furthermore, Fc-fusion proteins of immune checkpoint molecules are currently being investigated for their use as immune suppressive therapy e.g., in autoimmune disorders (138). Immune therapy therefore includes immune activating and immune suppressing approaches, both of which represent attractive targets for treatment of chronic infections depending on the local immune environment.

Immune Activation or Suppression in Chronic Implant-Related Bone Infections

Long-lasting interactions of bacteria, biofilm components, and host cells that occur in chronic implant-related bone infections severely impair the immune response. Thus, immune therapy can be an interesting tool to restore appropriate immune function. As suggested by the literature, chronic implant-related bone infections initially provoke a more pro-inflammatory immunity. This is then dampened to a more anti-inflammatory and immune tolerant response during the chronic course of infection, which prevents tissue damage but also contributes to bacterial persistence. However, pro- and anti-inflammation cannot be simply attributed to different stages of the disease as they occur simultaneously throughout the course of infection. Favoring one above the other would risk to further aggravate immune pathology. The immune reaction during the early planktonic phase is additionally impaired by the presence of the implant, whose influence has to be considered in immune therapeutic intervention. Furthermore, the type of bacteria plays an important role in the induced immune response; highly virulent strains like *S. aureus* cause strong pro-inflammatory immune reactions, whereas more benign strains such as *S. epidermidis* induce rather moderate and subtle immune responses. All this has to be considered when an immune therapeutic approach is suggested because non-specific boosting of the immune system might end in hyper-inflammation causing tissue damage, while immune inhibition might lead to increased bacterial burden, bacteremia and/or secondary infections. To avoid such conceivable scenarios, we should learn from the lessons already made in sepsis immune-stimulatory therapy which has so far failed to reliably and safely improve patient outcome (139, 140), before introducing immune modulation in the treatment of chronic implant-related bone infections: (1) The immune response is changing throughout the infection, therefore correct timing of therapeutic intervention is indispensable to ensure immune stimulation or inhibition. (2) The immune status of leukocytes can differ depending on the location (lymphoid organs, peripheral blood or site of infection). Systemic immune stimulation/inhibition might not be appropriate and a more tissue/infection site-specific approach should be preferred. Specification can be provided by targeting immune molecules depending on the cell subsets they are preferentially expressed, anatomic prevalence of their expression and/or their distinguished function (141). (3) The immune profile can be highly heterogeneous between patients. Personalized immune therapy should be provided to optimize individual outcome and predictive immune biomarkers should be included in the decision-making for the respective therapeutic target to guarantee responsiveness and minimize adverse effects (135). As the targets of immune modulation have unique functions, combinatory approaches can improve efficacy of immune therapeutic treatment (142). The combination of modulators of innate immune defense with classical ICI targeting adaptive immunity and/or cell-based therapeutic vaccination would allow treatment at multiple levels. However, to ensure optimum patient outcome and safety, immune therapeutics can only be used as medication in addition to current antibiotic and surgical treatment options.

Targeting Immune Checkpoint Molecules

The first ICI approved for therapy of advanced melanoma was an antibody against CTLA-4 (ipilimumab) in 2011 (143, 144). CTLA-4 is a homologous but antagonistic and competitive receptor for CD28 that has a higher affinity for binding

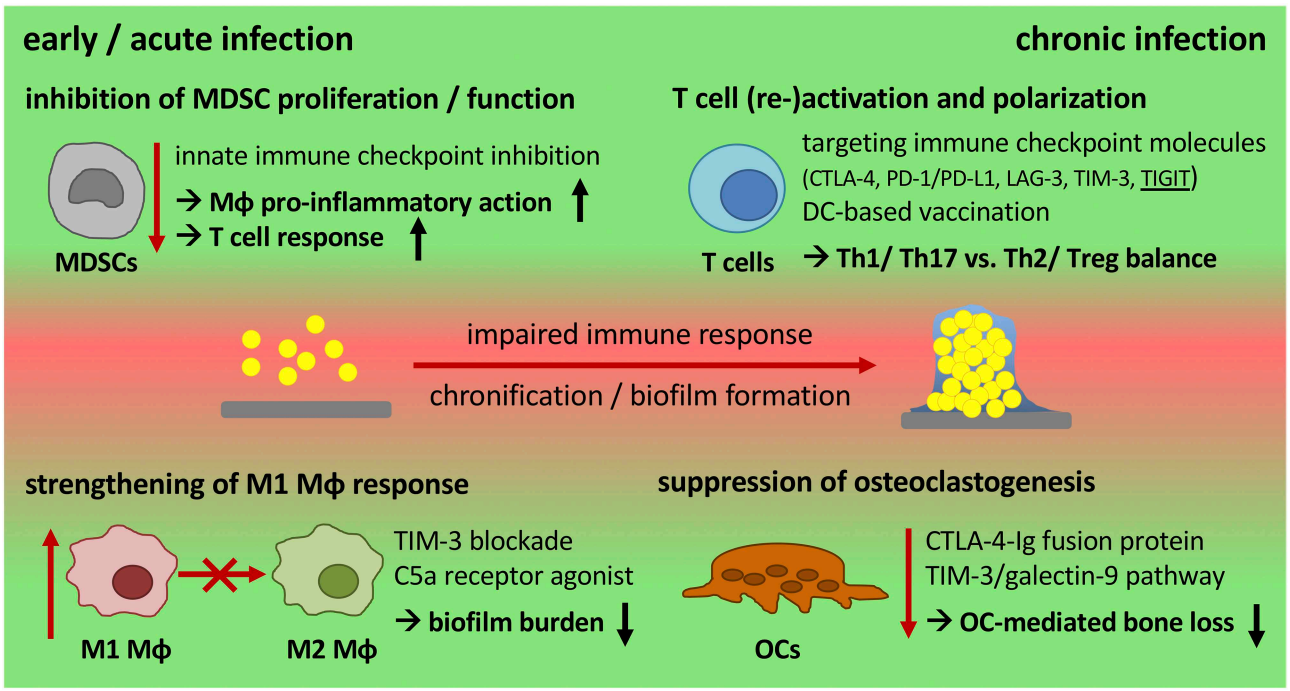

FIGURE 3 | Potential targets for immune modulation during chronic progression of implant-related bone infections. Biofilm formation skews the immune response toward an anti-inflammatory, immune inhibitory and tolerant environment that is associated with high numbers of MDSCs, M2 macrophages, and an ineffective T cell response. Immune modulation by therapeutic intervention offers the possibility to generate a more effective immune response that supports bacterial killing and the reduction of biofilm burden. An early inhibition of MDSC activity and the induction of a more pro-inflammatory (M1) Mϕ response are potential targets to strengthen innate defense mechanisms. Re-stimulation of T cell effector functions by targeting immune checkpoint molecules can overcome T cell dysfunction caused by chronic disease progression and might prevent re-infection after revision surgery. Targeting TIGIT as well as using DC-based vaccination strategies may provide the opportunity to direct T cell polarization toward Th1 or Th2 -dominated responses. When boosting the immune system, its impact on inflammatory tissue destruction has to be considered as a balance between anti-bacterial activity and cytotoxicity is required. CTLA-4 and the TIM-3/galectin-9 pathway are important immune regulators that can also be used as checkpoints to control osteoclast numbers as a means to reduce bone resorption. MDSCs, myeloid-derived suppressor cells; Mϕ, macrophage; DC, dendritic cell; OCs, osteoclasts; ICI, immune checkpoint inhibitor; CTLA-4, cytotoxic T-lymphocyte-associated protein-4; PD-1/PD-L1, programmed cell death protein-1/PD ligand-1; LAG-3, lymphocyte activation gene-3; TIM-3, T cell immunoglobulin and mucin-domain containing protein-3; TIGIT, T cell immunoglobulin and ITIM domain.

CD80/86 than CD28. Binding of CTL-4 to CD80/86 results in transendocytosis of CD80/86 and inhibition of T cell co-stimulation. Under physiological conditions, CTLA-4 plays an important role in ensuring self-tolerance. The administration of anti-CTLA-4 antibodies proved to be efficient in tumor control but at the same time showed a high incidence of adverse effects and autoimmunity. Activation of this pathway can therefore be a promising approach to treat autoimmune disorders [reviewed in (145)]. Treatment with a soluble CTLA-4-Ig fusion protein (abatacept), which links the extracellular domain of human CTLA-4 to a fragment of the Fc part of human IgG1 (146), was successful in reducing the symptoms of rheumatoid arthritis (RA) (147). However, it aggravated the course of septic arthritis in a mouse model (148). To our knowledge, nothing is known about a potential role of CTLA-4-mediated inhibition of CD28 in chronic implant-related bone infections. Most T cells isolated from blood and tissue of patients undergoing infection-induced revision surgery were shown to be $CD28^-$ (92, 93), which might indicate that in chronicity, the majority of effector T cells would not respond to CTLA-4 based therapy. Interestingly, it was shown that binding of CTLA-4 to CD80/86 expressed on the surface of murine bone marrow leukocytes and human blood monocytes directly inhibited RANKL and TNF-mediated differentiation of these cells into osteoclasts *in vitro* and reduced osteoclast formation and bone resorption in an arthritic joint model in mice (149). This suggests that CTLA-4 can be considered as an anti-osteoclastogenic molecule. The inhibitory effect of CD80/86 engagement by CTLA-4 on osteoclastogenesis was further investigated by Bozec et al., who found that induction of apoptosis in osteoclast precursor cells via the IDO/tryptophan pathway was responsible for the reduced osteoclast formation. As expected, the CTLA-4-Ig fusion protein abatacept led to reduced numbers of osteoclast precursor cells and osteoclasts in RA patients and in cell culture experiments. Blocking CTLA-4 with the neutralizing antibody ipilimumab increased the osteoclastogenic potential in humans (150). These data indicate that targeting checkpoint molecules like CTLA-4 provide the opportunity to control osteoclast numbers and bone homeostasis. Still, it has to be considered that in an

TABLE 2 | Potential targets for immune modulation during chronic implant-related bone infections.

		Target	Mechanism	Potential benefit for chronic implant-related bone infections
T cell immunity		CTLA-4	Competitive binding of CD80/86 and inhibition of T cell co-stimulation. Anti-CTLA-4 antibodies restore T cell activation.	Isolated T cells from chronic implant-related bone infections are mostly $CD28^{-}$. Usefulness of CTLA-4 to re-activate T cells after chronicity of infection is therefore questionable.
		PD-1/PD-L1	Induction of effector T cell exhaustion. Blocking this pathway by antibodies restores T cell function.	Role of exhausted T cells in chronicity of bone infections is unclear. Cells of the bone environment (MSCs, OCs) express PD-L1 upon inflammation, therefore inhibition of this pathway might decrease bone cell-mediated T cell suppression.
		LAG-3/TIM-3/TIGIT	Inhibition of APC-mediated T cell activation and Th1/Th17 -mediated T cell response.	Blood T cells from patients with chronic osteomyelitis show increased expression of LAG-3 and impaired proliferation/function. Hence, LAG-3 blockade can increase T cell activation in chronic implant-related bone infections. An early Th2/T_{reg} immunity was shown to prevent biofilm formation and chronicity in a murine orthopedic implant infection model. TIGIT treatment at an early time point can be supportive to clear infections via induction of a Th2-based T cell response.
Innate immunity	MDSCs	Innate IC molecules	Controlling MDSC proliferation and function.	MDSCs are associated with an anti-inflammatory environment in chronic implant-related bone infections. Eliminating MDSCs can prevent unwanted immune suppression and strengthen pro-inflammatory immune reactions.
	Mϕ	TIM-3	Inhibitory receptor on Mϕs, by this suppressing a pro-inflammatory response.	Chronic implant-related bone infections are associated with a shift toward an anti-inflammatory (M2) Mϕ phenotype which supports bacterial persistence. Blockade of TIM-3 can strengthen a pro-inflammatory (M1) Mϕ response and enhance bacterial killing.
		C5a receptor	Binding of C5a receptor influences Mϕ polarization.	Targeting Mϕ polarization via C5a receptor ligands can prevent formation of anti-inflammatory (M2) Mϕs associated with chronic infection. Early treatment with a C5a receptor agonist induces a pro-inflammatory (M1) Mϕ response which leads to reduced biofilm burden in a mouse implant-infection model (80).
	DCs	Antigen presentation	Induction of an antigen-specific T cell immunity and desired T cell differentiation.	The role of DCs in chronic implant-related bone infections is unclear, but DC therapy could allow the generation of biofilm-specific DCs and the induction of a more effective host immune response.
Osteoclastogenesis		CTLA-4	Inhibition of osteoclastogenesis through binding to CD80/86 on monocytes. Administration of a CTLA-4-Ig fusion protein reduces osteoclast numbers.	Bone infections are associated with high numbers of osteoclasts and increased bone resorption, CTLA-4 treatment can reduce inflammation-induced bone destruction.
		TIM-3/galectin-9	Binding of galectin-9 to TIM-3 expressed on osteoclast precursors suppresses osteoclastogenesis.	Targeting the TIM-3/galectin-9 pathway can reduce osteoclast formation and bone loss in chronic implant-related bone infections.

auto-inflammatory environment, treatment with CTLA-4 is beneficial in reducing osteoclastogenesis, but under infectious conditions it might suppress necessary immune activity and by this potentially aggravate disease progression. Thus, immune checkpoint-mediated inhibition of osteoclastogenesis can be a promising target to decrease inflammation-induced bone resorption and reduce bacterial colonization of damaged tissue, but additional impairment of the immune response has to be excluded.

The best studied immune checkpoint molecule is PD-1 and its ligands PD-L1 and PD-L2, which are targeted to treat T cell dysfunction in cancer and chronic infectious diseases. Compared to CTLA-4, which acts at the level of T cell activation, PD-1 is up-regulated on effector T cells after continuous stimulation. Thus, the PD-1/PD-L1 pathway suppresses activity and function of effector T cells and induces T cell exhaustion (144). Several antibodies targeting the PD-1/PD-L1 pathway have been approved for the treatment of specific cancers and new therapeutics as well as new applications are currently investigated in clinical trials (135). Antibodies against PD-1/PD-L1 have also been transferred into treatment approaches for chronic virus diseases and malaria to improve CD4 and CD8 effector T cell function (136). Additionally, they were shown to have the potential to reverse sepsis-induced immune

suppression (137). Negative side effects of PD-1/PD-L1 blockade seem to be less frequent when compared to CTLA-4 treatment. However, nearly half of the patients do not respond to PD-1 blockade alone (136) and combinatory therapy was shown to be more effective, albeit more toxic (151). The role of PD-L2 has not yet been fully clarified: initially, PD-L2 was described as a second ligand for PD-1 that negatively influences T cell immunity (152, 153). A costimulatory function of PD-L2 and the initiation of a Th1 response is also discussed (154). PD-L2 is furthermore suggested to counteract PD-1/PD-L1-mediated T cell exhaustion making a soluble PD-L2 fusion protein an attractive candidate to block the PD-1/PD-L1 pathway (136, 155). In an *in vitro* setting with *S. epidermidis* strains isolated from patients with orthopedic implant loosening, it was shown that after phagocytic uptake SCVs trigger an anti-inflammatory macrophage response with up-regulated PD-L1/L2 expression so that they are able to survive intracellularly without damaging the host cell (156). Whether this also applies to biofilm embedded bacteria has not been investigated yet. Furthermore, MSCs, which are in close contact to the site of bone infections, up-regulate PD-L1/L2 expression and secretion upon stimulation with pro-inflammatory cytokines (157, 158) or induce PD-L1 expression in DCs after exposure to LPS (159). By this, they directly and indirectly inhibit T cell proliferation and function. It can be speculated that the PD-1/PD-L1 pathway might play a role in the persistence of implant-related bone infections. Until now, to our knowledge there is nothing described about an up-regulation of PD-1 on T cells and PD-L1/L2 on host cells associated with biofilm formation during chronic progression of implant-related bone infections. As chronic implant-related bone infections were linked to high numbers of $CD28^-$ T cells (92–94) and as it was shown recently that CD28 is indispensable for effectiveness of PD-1 blockade (160, 161), it remains to be seen whether these patients would indeed profit from a PD-1/PD-L1 targeted therapy. OCs were found to mediate their immune suppressive action through galectin-9 and PD-L1 expression and induction of PD-L1 expression on tumor cells in multiple myeloma (162, 163). As OCs are highly present at the site of bone infection, PD-L1 antibodies that can decrease OC-mediated T cell inhibition might enhance T cell immunity in chronic implant-related bone infections.

Lymphocyte activation gene-3 (LAG-3), T cell immunoglobulin and mucin-domain containing protein-3 (TIM-3) and T cell immunoglobulin and ITIM domain (TIGIT) are other immune checkpoint molecules that are currently explored as targets for immune therapy. LAG-3 is up-regulated on CD4 and CD8 T cells as well as on natural killer cells (NK cells). It affects effector T cell function and T_{reg} suppressive activity by binding to MHC class II with higher affinity than CD4 or LSECtin (liver and lymph node sinusoidal endothelial cell C-type lectin). Since LSECtin is involved in antigen uptake (164) and MHC class II is essential for antigen presentation, LAG-3 is suggested to impair the antigen-specific signal in T cell activation [reviewed in (141, 142)]. Indeed, an increased expression of LAG-3 was found on T cells in blood samples of patients suffering from chronic osteomyelitis and was associated with impaired T cell proliferation and function (165). This gives a hint that LAG-3 blockade could be a potential approach for treating chronic implant-associated bone infections. Furthermore, a soluble Lag-3-Ig fusion protein (IMP321) has been shown to lead to APC activation via MHC class II, thus being a candidate to support APC-mediated immunity (166, 167). TIM-3 is expressed on DCs and Mϕs as well as on activated CD4 T cells, predominantly of the Th1 type, CD8 T cells and NK cells [reviewed in (142)]. Via interaction with galectin-9, TIM-3 plays a protective role in autoimmunity by regulating the Th1 response and subsequent macrophage activation (168), triggering cell death (169), and increasing MDSC expansion (170). In cancer and chronic virus infections, high TIM-3 expression was linked to T cell dysfunction. Co-blockade of PD-1 and TIM-3 is superior at improving anti-tumor and anti-viral effector function than PD-1 inhibition alone [reviewed in (141)]. In line with this, TIM-3 expressing T_{reg}s showed an increased expression of suppressive molecules and were highly effective in inhibiting Th1/Th17 immune responses (171). Furthermore, high expression levels of TIM-3 on Mϕs are associated either with a quiescent state or an anti-inflammatory (M2) phenotype. Blockade of the TIM-3 pathway therefore may result in a more efficient pro-inflammatory (M1) macrophage response (172) which was shown to reduce biofilm burden in a catheter-associated biofilm infection model in mice (80). Binding of galectin-9 to TIM-3 expressed on osteoclast precursor cells suppressed osteoclast formation and thereby attenuated inflammatory bone loss in adjuvant-induced arthritis (173) indicating a further therapeutic application of the TIM-3/galectin-9 system next to modulating the immune response. TIGIT is a co-inhibitory receptor present on activated T cells, NK cells and T_{reg}s and competes with its stimulatory counterpart CD226 for binding of CD155 expressed on APCs, T cells and non-immune cells. CD226 predominantly promotes a Th1/Th17 response with high levels of IFN-γ and IL-17, whereas binding of TIGIT induces a shift toward a Th2 and IL-10 dominated immunity. Therefore, TIGIT interacts with APCs, effector T cells as well as T_{reg}s to dampen pro-inflammatory immune responses at multiple levels in favor of a more tolerogenic immune environment [reviewed in (141)]. Prabhakara et al. showed that an early shift from a Th1/Th17 response toward a Th2/T_{reg} immunity was capable of preventing biofilm formation and chronicity of an orthopedic implant infection in mice (98). TIGIT treatment to strengthen a Th2 dominated response might therefore be a supportive strategy in clearing implant-related bone infections at an early stage.

Lag-3, TIM-3, and TIGIT are suggested to regulate immune function at the site of tissue inflammation to inhibit immune pathology, whereas CTLA-4 and PD-1 act more systemically. Because their primary role is to maintain immune homeostasis and self-tolerance in the healthy organism, the first three are predicted to be less toxic (141). Furthermore, due to their specialized roles either at the stage of T cell activation or T cell effector function, molecules from these two groups might exert synergistic effects and provide a more efficient therapeutic outcome when used in combination (142).

Targeting Innate Immunity

Next to directly improving T cell immunity, another approach is to target innate immune cells and modulate the immune response in a more general way. High MDSC activation and accumulation are found in various cancers where they inhibit T cell proliferation and function, leading to tumor tolerance (174). MDSCs are associated with inflammation-induced tumor progression, as they are activated by pro-inflammatory IL-1β that subsequently induces a tumor-promoting IL-10-dominated environment and an anti-inflammatory (M2) macrophage response (175, 176). Heim et al. showed that MDSC-derived IL-10 is responsible for the anti-inflammatory monocyte response and bacterial persistence in an orthopedic biofilm infection model (87). This indicates that there are some common characteristics between these two chronic diseases. Furthermore, MDSCs express ICI ligands that can directly impair T cell function (177) and also reduce the efficacy of immune checkpoint inhibitors in cancer therapy (178). Therefore, targeting MDSCs in combination with ICI is a promising approach to improve patient outcome (179). Next to the application of approved therapeutics that are effective in reducing MDSC numbers and/or function (e.g., all-trans retinoic acid), the investigation of new drugs that eliminate MDSCs is of high interest. An innate immune checkpoint inhibitor that targets MDSC proliferation and function is currently being investigated in a phase 1 clinical trial (INB_{03}) (180). MDSCs contribute to the immune compromised environment in implant-related bone infections and to the chronicity of infection. An early inhibition of MDSC function could be a possible approach to circumvent unwanted immune suppression directly at the onset of infection. In combination with a strict antibiotic treatment this might be able to clear the infection before biofilm manifestation and might prevent bacterial persistence.

Another approach is to directly target macrophage polarization. As tumors and chronic infections are associated with an environment favoring an anti-inflammatory (M2) macrophage response and immune suppression, shifting the balance toward the more pro-inflammatory (M1) macrophage subtype might increase the ability to kill tumor cells and bacteria (181).

Hanke et al. used a cell transfer of exogenously M1-activated Mϕs or administration of a C5a receptor agonist (EP67) in a catheter-associated infection model in mice, which resulted in a pronounced pro-inflammatory Mϕ response and in a reduction of biofilm burden (80). M1 Mϕ not only prevented biofilm formation when injected at an early time point of infection, but were also capable of reducing established biofilms, whereas antibiotic treatment had no effect. This indicates that redirection toward a pro-inflammatory milieu can attenuate mature biofilms. DCs are antigen-presenting cells that activate T cells and induce adaptive defense mechanisms (91). This makes them an attractive tool for immune stimulatory treatment of chronic diseases. Different strategies have been reported and include vaccination strategies with autologous and *ex vivo*-generated DCs that had been stimulated with tumor antigens. After re-injection, these cells can induce an effective anti-cancer immunity through priming of a Th1 and specific cytotoxic T cell response. However, *ex vivo* manipulation is expensive and includes a high risk of infection. The *in vivo* targeting of DCs by antibodies coupled with the respective antigens specifically binding to DC receptors involved in antigen presentation is an attractive alternative [reviewed in (182)]. The role of DCs in the unsuccessful immune response against implant-related bone infections and a potential contribution to biofilm formation has not been investigated so far. Targeting DCs offers the possibility to control the type of T cell response and to induce a biofilm-specific T cell immunity by loading them with biofilm-antigens. Therefore, DC therapy might be an attractive approach to improve a specific host immune defense against implant-related bone infections.

In summary, immune modulation can be a promising approach to restore a desired immune microenvironment during the course of chronic implant-related bone infections: an early immune modulatory intervention might be able to inhibit biofilm formation and inflammation-associated tissue destruction, and might allow the elimination of infection at its onset. After chronic progression of the infection, a comprehensive approach combining surgical removal of infectious tissue, antibiotic treatment and strengthening of the host immune response might improve therapeutic outcome. The combination of rifampin and immune re-activation might be a strategy to eliminate mature biofilms that can increase the chance for surgical regimes with implant retention. After implant exchange, strengthening the specific immunity against the initial infection can help provide an immune response that is able to eliminate potentially remaining bacteria (persister cells) and prevent re-infection. It needs to be clarified in future studies whether the activation of a biofilm-specific immune response by immune therapy is sufficient to combat mature biofilm and other sources of bacterial persistence (SCVs, canalicular propagation) independent of surgical and antibiotic treatment. However, more basic research is needed to address whether an immune modulatory intervention can be a useful treatment strategy in implant-related osteomyelitis. As immune therapy is associated with adverse immune reactions, a safe and beneficial application has to be ensured before applying immune therapeutic approaches into patients with chronic implant-related bone infections.

CONCLUDING REMARKS

Chronic implant-related bone infections are a major problem in orthopedic and trauma surgery. As numbers of joint replacements are rising, complications such as bone infections also increase. Current treatment options are associated with severe consequences for patients and often fail to eliminate the infection. The high risk of chronicity for such infections is due to successful evasion strategies of bacteria with biofilm formation being one major mechanism behind bacterial persistence. The presence of a foreign material facilitates biofilm formation and further supports the persistence of an infection. Thus, there is a high interest to clear infections already at the planktonic

stage before biofilm transition occurs and to prevent reinfection after antibiotic and surgical treatment. For this, however, novel therapeutic strategies are required. Immune therapy shows promising results in the treatment of different chronic diseases and strengthening endogenous defense mechanisms could be an attractive new approach for chronic implant-related bone infections. So far, investigations of the immune response against chronic implant-related bone infections demonstrate a discrepancy between a strong pro-inflammatory immune reaction that is associated with osteoclastogenesis and bone destruction, and an immune suppression that potentially impairs successful bacterial killing. Future treatment strategies involving the immune system have to consider this two-sided immune response to avoid adverse reactions. Since the amount of information is limited, the success of immune therapeutic intervention in chronic implant-related bone infections mostly remains speculative and further research is needed to investigate appropriate and safe targets. Furthermore, it has to be clarified if an immune modulatory approach is also capable of targeting bacterial persistence e.g., within biofilms. Immune modulation can serve as an additional and required medical treatment option to restore an effective host response. It is to be hoped that the combination of antibiotic and surgical treatment with immune therapeutic intervention may lead to the successful management of chronic implant-related bone infections in the future.

AUTHOR CONTRIBUTIONS

ES reviewed the relevant literature and wrote the manuscript. KK critically revised the manuscript. Both authors have read and approved the manuscript.

FUNDING

ES was funded by the Physician Scientist Program of the Medical Faculty of Heidelberg. We acknowledge the financial support of the Deutsche Forschungsgemeinschaft (DFG) and the Ruprecht-Karls-Universität Heidelberg within the funding program Open Access Publishing.

ACKNOWLEDGMENTS

We thank Nikolas Stevens for technical support and Christy Yu for critically proofreading the manuscript.

REFERENCES

1. Tande AJ, Patel R. Prosthetic joint infection. *Clin Microbiol Rev.* (2014) 27:302–45. doi: 10.1128/CMR.00111-13
2. Zimmerli W, Trampuz A, Ochsner PE. Prosthetic-joint infections. *N Engl J Med.* (2004) 351:1645–54. doi: 10.1056/NEJMra040181
3. Kurtz SM, Lau E, Watson H, Schmier JK, Parvizi J. Economic burden of periprosthetic joint infection in the United States. *J Arthroplasty.* (2012) 27:61–5 e1. doi: 10.1016/j.arth.2012.02.022
4. Kunutsor SK, Whitehouse MR, Blom AW, Beswick AD, Team I. Re-infection outcomes following one- and two-stage surgical revision of infected hip prosthesis: a systematic review and meta-analysis. *PLoS ONE.* (2015) 10:e0139166. doi: 10.1371/journal.pone.0139166
5. Kunutsor SK, Whitehouse MR, Lenguerrand E, Blom AW, Beswick AD, Team I. Re-infection outcomes following one- and two-stage surgical revision of infected knee prosthesis: a systematic review and meta-analysis. *PLoS ONE.* (2016) 11:e0151537. doi: 10.1371/journal.pone.0151537
6. Marculescu CE, Berbari EF, Hanssen AD, Steckelberg JM, Harmsen SW, Mandrekar JN, et al. Outcome of prosthetic joint infections treated with debridement and retention of components. *Clin Infect Dis.* (2006) 42:471–8. doi: 10.1086/499234
7. Lee J, Kang CI, Lee JH, Joung M, Moon S, Wi YM, et al. Risk factors for treatment failure in patients with prosthetic joint infections. *J Hosp Infect.* (2010) 75:273–6. doi: 10.1016/j.jhin.2010.03.012
8. Spencer J, Smith A, Woods D. The effect of time delay on infection in open long-bone fractures: a 5-year prospective audit from a district general hospital. *Ann R Coll Surg Engl.* (2004) 86:108–12. doi: 10.1308/003588404322827491
9. Darouiche RO. Treatment of infections associated with surgical implants. *N Engl J Med.* (2004) 350:1422–9. doi: 10.1056/NEJMra035415
10. Okike K, Bhattacharyya T. Trends in the management of open fractures. A critical analysis. *J Bone Joint Surg Am.* (2006) 88:2739–48. doi: 10.2106/00004623-200612000-00025
11. Khosla S. Minireview: the OPG/RANKL/RANK system. *Endocrinology.* (2001) 142:5050–5. doi: 10.1210/endo.142.12.8536
12. Raggatt LJ, Partridge NC. Cellular and molecular mechanisms of bone remodeling. *J Biol Chem.* (2010) 285:25103–8. doi: 10.1074/jbc.R109.041087
13. Kolar P, Schmidt-Bleek K, Schell H, Gaber T, Toben D, Schmidmaier G, et al. The early fracture hematoma and its potential role in fracture healing. *Tissue Eng Part B Rev.* (2010) 16:427–34. doi: 10.1089/ten.teb.2009.0687
14. Wright JA, Nair SP. Interaction of staphylococci with bone. *Int J Med Microbiol.* (2010) 300:193–204. doi: 10.1016/j.ijmm.2009.10.003
15. Lazzarini L, Mader JT, Calhoun JH. Osteomyelitis in long bones. *J Bone Joint Surg Am.* (2004) 86-A:2305–18. doi: 10.2106/00004623-200410000-00028
16. Lew DP, Waldvogel FA. Osteomyelitis. *Lancet.* (2004) 364:369–79. doi: 10.1016/S0140-6736(04)16727-5
17. Zimmerli W, Sendi P. Orthopaedic biofilm infections. *APMIS.* (2017) 125:353–64. doi: 10.1111/apm.12687
18. Schierholz JM, Beuth J. Implant infections: a haven for opportunistic bacteria. *J Hosp Infect.* (2001) 49:87–93. doi: 10.1053/jhin.2001.1052
19. Trampuz A, Zimmerli W. Diagnosis and treatment of infections associated with fracture-fixation devices. *Injury.* (2006) 37(Suppl 2):S59–66. doi: 10.1016/j.injury.2006.04.010
20. Metsemakers WJ, Kuehl R, Moriarty TF, Richards RG, Verhofstad MHJ, Borens O, et al. Infection after fracture fixation: current surgical and microbiological concepts. *Injury.* (2018) 49:511–22. doi: 10.1016/j.injury.2016.09.019
21. Metsemakers WJ, Morgenstern M, McNally MA, Moriarty TF, McFadyen I, Scarborough M, et al. Fracture-related infection: a consensus on definition from an international expert group. *Injury.* (2018) 49:505–10. doi: 10.1016/j.injury.2017.08.040
22. Loffler B, Tuchscherr L, Niemann S, Peters G. Staphylococcus aureus persistence in non-professional phagocytes. *Int J Med Microbiol.* (2014) 304:170–6. doi: 10.1016/j.ijmm.2013.11.011
23. Khalil H, Williams RJ, Stenbeck G, Henderson B, Meghji S, Nair SP. Invasion of bone cells by Staphylococcus epidermidis. *Microbes Infect.* (2007) 9:460–5. doi: 10.1016/j.micinf.2007.01.002
24. Valour F, Trouillet-Assant S, Rasigade JP, Lustig S, Chanard E, Meugnier H, et al. Staphylococcus epidermidis in orthopedic device infections: the role of bacterial internalization in human osteoblasts and biofilm formation. *PLoS ONE.* (2013) 8:e67240. doi: 10.1371/journal.pone.0067240
25. Campoccia D, Testoni F, Ravaioli S, Cangini I, Maso A, Speziale P, et al. Orthopedic implant infections: incompetence of *Staphylococcus epidermidis*, *Staphylococcus lugdunensis*, and *Enterococcus faecalis* to invade osteoblasts. *J Biomed Mater Res A.* (2016) 104:788–801. doi: 10.1002/jbm.a.35564

26. de Mesy Bentley KL, Trombetta R, Nishitani K, Bello-Irizarry SN, Ninomiya M, Zhang L, et al. Evidence of *Staphylococcus aureus* deformation, proliferation, and migration in canaliculi of live cortical bone in murine models of osteomyelitis. *J Bone Miner Res.* (2017) 32:985–90. doi: 10.1002/jbmr.3055
27. Costerton JW, Stewart PS, Greenberg EP. Bacterial biofilms: a common cause of persistent infections. *Science.* (1999) 284:1318–22. doi: 10.1126/science.284.5418.1318
28. Hoiby N, Ciofu O, Johansen HK, Song ZJ, Moser C, Jensen PO, et al. The clinical impact of bacterial biofilms. *Int J Oral Sci.* (2011) 3:55–65. doi: 10.4248/IJOS11026
29. Leid JG. Bacterial biofilms resist key host defenses. *Microbe.* (2009) 4:66–70.
30. Li C, Renz N, Trampuz A. Management of periprosthetic joint infection. *Hip Pelvis.* (2018) 30:138–46. doi: 10.5371/hp.2018.30.3.138
31. Zimmerli W, Moser C. Pathogenesis and treatment concepts of orthopaedic biofilm infections. *FEMS Immunol Med Microbiol.* (2012) 65:158–68. doi: 10.1111/j.1574-695X.2012.00938.x
32. Moriarty TF, Kuehl R, Coenye T, Metsemakers WJ, Morgenstern M, Schwarz EM, et al. Orthopaedic device-related infection: current and future interventions for improved prevention and treatment. *EFORT Open Rev.* (2016) 1:89–99. doi: 10.1302/2058-5241.1.000037
33. Lebeaux D, Ghigo JM, Beloin C. Biofilm-related infections: bridging the gap between clinical management and fundamental aspects of recalcitrance toward antibiotics. *Microbiol Mol Biol Rev.* (2014) 78:510–43. doi: 10.1128/MMBR.00013-14
34. Jones RE, Russell RD, Huo MH. Alternatives to revision total knee arthroplasty. *J Bone Joint Surg Br.* (2012) 94:137–40. doi: 10.1302/0301-620X.94B11.30620
35. Zimmerli W, Waldvogel FA, Vaudaux P, Nydegger UE. Pathogenesis of foreign body infection: description and characteristics of an animal model. *J Infect Dis.* (1982) 146:487–97. doi: 10.1093/infdis/146.4.487
36. Lucke M, Schmidmaier G, Sadoni S, Wildemann B, Schiller R, Stemberger A, et al. A new model of implant-related osteomyelitis in rats. *J Biomed Mater Res B Appl Biomater.* (2003) 67:593–602. doi: 10.1002/jbm.b.10051
37. Zimmerli W, Sendi P. Pathogenesis of implant-associated infection: the role of the host. *Semin Immunopathol.* (2011) 33:295–306. doi: 10.1007/s00281-011-0275-7
38. Arciola CR, Campoccia D, Speziale P, Montanaro L, Costerton JW. Biofilm formation in Staphylococcus implant infections. A review of molecular mechanisms and implications for biofilm-resistant materials. *Biomaterials.* (2012) 33:5967–82. doi: 10.1016/j.biomaterials.2012.05.031
39. Gristina AG. Biomaterial-centered infection: microbial adhesion versus tissue integration. *Science.* (1987) 237:1588–95. doi: 10.1126/science.3629258
40. Busscher HJ, van der Mei HC, Subbiahdoss G, Jutte PC, van den Dungen JJ, Zaat SA, et al. Biomaterial-associated infection: locating the finish line in the race for the surface. *Sci Transl Med.* (2012) 4:153rv10. doi: 10.1126/scitranslmed.3004528
41. Arciola CR, Campoccia D, Montanaro L. Implant infections: adhesion, biofilm formation and immune evasion. *Nat Rev Microbiol.* (2018) 16:397–409. doi: 10.1038/s41579-018-0019-y
42. Otto M. Staphylococcal biofilms. *Curr Top Microbiol Immunol.* (2008) 322:207–28. doi: 10.1007/978-3-540-75418-3_10
43. Boles BR, Horswill AR. Staphylococcal biofilm disassembly. *Trends Microbiol.* (2011) 19:449–55. doi: 10.1016/j.tim.2011.06.004
44. Kong KF, Vuong C, Otto M. Staphylococcus quorum sensing in biofilm formation and infection. *Int J Med Microbiol.* (2006) 296:133–9. doi: 10.1016/j.ijmm.2006.01.042
45. Yarwood JM, Schlievert PM. Quorum sensing in Staphylococcus infections. *J Clin Invest.* (2003) 112:1620–5. doi: 10.1172/JCI20442
46. Henke JM, Bassler BL. Bacterial social engagements. *Trends Cell Biol.* (2004) 14:648–56. doi: 10.1016/j.tcb.2004.09.012
47. Kaufmann GF, Park J, Janda KD. Bacterial quorum sensing: a new target for anti-infective immunotherapy. *Expert Opin Biol Ther.* (2008) 8:719–24. doi: 10.1517/14712598.8.6.719
48. del Pozo JL, Patel R. The challenge of treating biofilm-associated bacterial infections. *Clin Pharmacol Ther.* (2007) 82:204–9. doi: 10.1038/sj.clpt.6100247
49. Proctor RA, von Eiff C, Kahl BC, Becker K, McNamara P, Herrmann M, et al. Small colony variants: a pathogenic form of bacteria that facilitates persistent and recurrent infections. *Nat Rev Microbiol.* (2006) 4:295–305. doi: 10.1038/nrmicro1384
50. Singh R, Ray P, Das A, Sharma M. Role of persisters and small-colony variants in antibiotic resistance of planktonic and biofilm-associated *Staphylococcus aureus*: an *in vitro* study. *J Med Microbiol.* (2009) 58:1067–73. doi: 10.1099/jmm.0.009720-0
51. Garcia LG, Lemaire S, Kahl BC, Becker K, Proctor RA, Denis O, et al. Antibiotic activity against small-colony variants of *Staphylococcus aureus*: review of *in vitro*, animal and clinical data. *J Antimicrob Chemother.* (2013) 68:1455–64. doi: 10.1093/jac/dkt072
52. Watters C, Fleming D, Bishop D, Rumbaugh KP. Host responses to biofilm. *Prog Mol Biol Transl Sci.* (2016) 142:193–239. doi: 10.1016/bs.pmbts.2016.05.007
53. Gries CM, Kielian T. Staphylococcal biofilms and immune polarization during prosthetic joint infection. *J Am Acad Orthop Surg.* (2017) 25(Suppl. 1):S20–4. doi: 10.5435/JAAOS-D-16-00636
54. Janeway CA Jr, Medzhitov R. Innate immune recognition. *Annu Rev Immunol.* (2002) 20:197–216. doi: 10.1146/annurev.immunol.20.083001.084359
55. Kawai T, Akira S. The role of pattern-recognition receptors in innate immunity: update on Toll-like receptors. *Nat Immunol.* (2010) 11:373–84. doi: 10.1038/ni.1863
56. Franz S, Rammelt S, Scharnweber D, Simon JC. Immune responses to implants - a review of the implications for the design of immunomodulatory biomaterials. *Biomaterials.* (2011) 32:6692–709. doi: 10.1016/j.biomaterials.2011.05.078
57. Nishitani K, Sutipornpalangkul W, de Mesy Bentley KL, Varrone JJ, Bello-Irizarry SN, Ito H, et al. Quantifying the natural history of biofilm formation *in vivo* during the establishment of chronic implant-associated *Staphylococcus aureus* osteomyelitis in mice to identify critical pathogen and host factors. *J Orthop Res.* (2015) 33:1311–9. doi: 10.1002/jor.22907
58. Thurlow LR, Hanke ML, Fritz T, Angle A, Aldrich A, Williams SH, et al. *Staphylococcus aureus* biofilms prevent macrophage phagocytosis and attenuate inflammation *in vivo*. *J Immunol.* (2011) 186:6585–96. doi: 10.4049/jimmunol.1002794
59. Vuong C, Voyich JM, Fischer ER, Braughton KR, Whitney AR, DeLeo FR, et al. Polysaccharide intercellular adhesin (PIA) protects Staphylococcus epidermidis against major components of the human innate immune system. *Cell Microbiol.* (2004) 6:269–75. doi: 10.1046/j.1462-5822.2004.00367.x
60. Montanaro L, Poggi A, Visai L, Ravaioli S, Campoccia D, Speziale P, et al. Extracellular DNA in biofilms. *Int J Artif Organs.* (2011) 34:824–31. doi: 10.5301/ijao.5000051
61. Dalpke A, Zimmermann S, Heeg K. CpG DNA in the prevention and treatment of infections. *Biodrugs.* (2002) 16:419–31. doi: 10.2165/00063030-200216060-00003
62. Bernthal NM, Pribaz JR, Stavrakis AI, Billi F, Cho JS, Ramos RI, et al. Protective role of IL-1beta against post-arthroplasty Staphylococcus aureus infection. *J Orthop Res.* (2011) 29:1621–6. doi: 10.1002/jor.21414
63. Fuxman Bass JI, Russo DM, Gabelloni ML, Geffner JR, Giordano M, Catalano M, et al. Extracellular DNA: a major proinflammatory component of *Pseudomonas aeruginosa* biofilms. *J Immunol.* (2010) 184:6386–95. doi: 10.4049/jimmunol.0901640
64. Lewenza S. Extracellular DNA-induced antimicrobial peptide resistance mechanisms in *Pseudomonas aeruginosa*. *Front Microbiol.* (2013) 4:21. doi: 10.3389/fmicb.2013.00021
65. Yamada KJ, Kielian T. Biofilm-leukocyte cross-talk: impact on immune polarization and immunometabolism. *J Innate Immun.* (2018): 11:280–8. doi: 10.1159/000492680
66. Scherr TD, Hanke ML, Huang O, James DB, Horswill AR, Bayles KW, et al. *Staphylococcus aureus* biofilms induce macrophage dysfunction through leukocidin AB and alpha-toxin. *MBio.* (2015) 6:e01021-15. doi: 10.1128/mBio.01021-15
67. Scherr TD, Heim CE, Morrison JM, Kielian T. Hiding in plain sight: interplay between staphylococcal biofilms and host immunity. *Front Immunol.* (2014) 5:37. doi: 10.3389/fimmu.2014.00037
68. Dapunt U, Hansch GM, Arciola CR. Innate immune response in implant-associated infections: neutrophils against biofilms. *Materials.* (2016) 9:E387. doi: 10.3390/ma9050387

69. Leid JG, Shirtliff ME, Costerton JW, Stoodley P. Human leukocytes adhere to, penetrate, and respond to *Staphylococcus aureus* biofilms. *Infect Immun.* (2002) 70:6339–45. doi: 10.1128/IAI.70.11.6339-6345.2002
70. Wagner C, Kaksa A, Muller W, Denefleh B, Heppert V, Wentzensen A, et al. Polymorphonuclear neutrophils in posttraumatic osteomyelitis: cells recovered from the inflamed site lack chemotactic activity but generate superoxides. *Shock.* (2004) 22:108–15. doi: 10.1097/01.shk.0000132488.71875.15
71. Wagner C, Kondella K, Bernschneider T, Heppert V, Wentzensen A, Hansch GM. Post-traumatic osteomyelitis: analysis of inflammatory cells recruited into the site of infection. *Shock.* (2003) 20:503–10. doi: 10.1097/01.shk.0000093542.78705.e3
72. Meyle E, Stroh P, Gunther F, Hoppy-Tichy T, Wagner C, Hansch GM. Destruction of bacterial biofilms by polymorphonuclear neutrophils: relative contribution of phagocytosis, DNA release, and degranulation. *Int J Artif Organs.* (2010) 33:608–20. doi: 10.1177/039139881003300906
73. van Kessel KP, Bestebroer J, van Strijp JA. Neutrophil-mediated phagocytosis of *Staphylococcus aureus*. *Front Immunol.* (2014) 5:467. doi: 10.3389/fimmu.2014.00467
74. Stroh P, Gunther F, Meyle E, Prior B, Wagner C, Hansch GM. Host defence against Staphylococcus aureus biofilms by polymorphonuclear neutrophils: oxygen radical production but not phagocytosis depends on opsonisation with immunoglobulin G. *Immunobiology.* (2011) 216:351–7. doi: 10.1016/j.imbio.2010.07.009
75. Kristian SA, Birkenstock TA, Sauder U, Mack D, Gotz F, Landmann R. Biofilm formation induces C3a release and protects *Staphylococcus epidermidis* from IgG and complement deposition and from neutrophil-dependent killing. *J Infect Dis.* (2008) 197:1028–35. doi: 10.1086/528992
76. Gunther F, Wabnitz GH, Stroh P, Prior B, Obst U, Samstag Y, et al. Host defence against Staphylococcus aureus biofilms infection: phagocytosis of biofilms by polymorphonuclear neutrophils (PMN). *Mol Immunol.* (2009) 46:1805–13. doi: 10.1016/j.molimm.2009.01.020
77. Scherr TD, Roux CM, Hanke ML, Angle A, Dunman PM, Kielian T. Global transcriptome analysis of Staphylococcus aureus biofilms in response to innate immune cells. *Infect Immun.* (2013) 81:4363–76. doi: 10.1128/IAI.00819-13
78. Ricciardi BF, Muthukrishnan G, Masters E, Ninomiya M, Lee CC, Schwarz EM. *Staphylococcus aureus* evasion of host immunity in the setting of prosthetic joint infection: biofilm and beyond. *Curr Rev Musculoskelet Med.* (2018) 11:389–400. doi: 10.1007/s12178-018-9501-4
79. Benoit M, Desnues B, Mege JL. Macrophage polarization in bacterial infections. *J Immunol.* (2008) 181:3733–9. doi: 10.4049/jimmunol.181.6.3733
80. Hanke ML, Heim CE, Angle A, Sanderson SD, Kielian T. Targeting macrophage activation for the prevention and treatment of Staphylococcus aureus biofilm infections. *J Immunol.* (2013) 190:2159–68. doi: 10.4049/jimmunol.1202348
81. Gabrilovich DI, Nagaraj S. Myeloid-derived suppressor cells as regulators of the immune system. *Nat Rev Immunol.* (2009) 9:162–74. doi: 10.1038/nri2506
82. Veglia F, Perego M, Gabrilovich D. Myeloid-derived suppressor cells coming of age. *Nat Immunol.* (2018) 19:108–19. doi: 10.1038/s41590-017-0022-x
83. Heim CE, Vidlak D, Scherr TD, Kozel JA, Holzapfel M, Muirhead DE, et al. Myeloid-derived suppressor cells contribute to *Staphylococcus aureus* orthopedic biofilm infection. *J Immunol.* (2014) 192:3778–92. doi: 10.4049/jimmunol.1303408
84. Heim CE, Vidlak D, Odvody J, Hartman CW, Garvin KL, Kielian T. Human prosthetic joint infections are associated with myeloid-derived suppressor cells (MDSCs): implications for infection persistence. *J Orthop Res.* (2018) 36:1605–13. doi: 10.1002/jor.23806
85. Heim CE, Vidlak D, Scherr TD, Hartman CW, Garvin KL, Kielian T. IL-12 promotes myeloid-derived suppressor cell recruitment and bacterial persistence during *Staphylococcus aureus* orthopedic implant infection. *J Immunol.* (2015) 194:3861–72. doi: 10.4049/jimmunol.1402689
86. Peng KT, Hsieh CC, Huang TY, Chen PC, Shih HN, Lee MS, et al. *Staphylococcus aureus* biofilm elicits the expansion, activation and polarization of myeloid-derived suppressor cells *in vivo* and *in vitro*. *PLoS ONE.* (2017) 12:e0183271. doi: 10.1371/journal.pone.0183271
87. Heim CE, Vidlak D, Kielian T. Interleukin-10 production by myeloid-derived suppressor cells contributes to bacterial persistence during Staphylococcus aureus orthopedic biofilm infection. *J Leukoc Biol.* (2015) 98:1003–13. doi: 10.1189/jlb.4VMA0315-125RR
88. Yamada KJ, Heim CE, Aldrich AL, Gries CM, Staudacher AG, Kielian T. Arginase-1 expression in myeloid cells regulates *Staphylococcus aureus* planktonic but not biofilm infection. *Infect Immun.* (2018) 86:IAI.00206-18. doi: 10.1128/IAI.00206-18
89. Otto M. Staphylococcal infections: mechanisms of biofilm maturation and detachment as critical determinants of pathogenicity. *Annu Rev Med.* (2013) 64:175–88. doi: 10.1146/annurev-med-042711-140023
90. Franca A, Perez-Cabezas B, Correia A, Pier GB, Cerca N, Vilanova M. *Staphylococcus epidermidis* biofilm-released cells induce a prompt and more marked *in vivo* inflammatory-type response than planktonic or biofilm cells. *Front Microbiol.* (2016) 7:1530. doi: 10.3389/fmicb.2016.01530
91. Pennock ND, White JT, Cross EW, Cheney EE, Tamburini BA, Kedl RM. T cell responses: naive to memory and everything in between. *Adv Physiol Educ.* (2013) 37:273–83. doi: 10.1152/advan.00066.2013
92. Dapunt U, Giese T, Prior B, Gaida MM, Hansch GM. Infectious versus non-infectious loosening of implants: activation of T lymphocytes differentiates between the two entities. *Int Orthop.* (2014) 38:1291–6. doi: 10.1007/s00264-014-2310-5
93. Kumar G, Roger PM, Ticchioni M, Trojani C, Bernard de Dompsur R, Bronsard N, et al. T cells from chronic bone infection show reduced proliferation and a high proportion of CD28(-) CD4 T cells. *Clin Exp Immunol.* (2014) 176:49–57. doi: 10.1111/cei.12245
94. Kotsougiani D, Pioch M, Prior B, Heppert V, Hansch GM, Wagner C. Activation of T lymphocytes in response to persistent bacterial infection: induction of CD11b and of toll-like receptors on T cells. *Int J Inflam.* (2010) 2010:526740. doi: 10.4061/2010/526740
95. Wagner C, Heck D, Lautenschlager K, Iking-Konert C, Heppert V, Wentzensen A, et al. T lymphocytes in implant-associated posttraumatic osteomyelitis: identification of cytotoxic T effector cells at the site of infection. *Shock.* (2006) 25:241–6. doi: 10.1097/01.shk.0000192119.68295.14
96. Heim CE, West SC, Ali H, Kielian T. Heterogeneity of Ly6G(+) Ly6C(+) myeloid-derived suppressor cell infiltrates during *Staphylococcus aureus* biofilm infection. *Infect Immun.* (2018) 86:e00684-18. doi: 10.1128/IAI.00684-18
97. Rochford ETJ, Sabate Bresco M, Zeiter S, Kluge K, Poulsson A, Ziegler M, et al. Monitoring immune responses in a mouse model of fracture fixation with and without Staphylococcus aureus osteomyelitis. *Bone.* (2016) 83:82–92. doi: 10.1016/j.bone.2015.10.014
98. Prabhakara R, Harro JM, Leid JG, Keegan AD, Prior ML, Shirtliff ME. Suppression of the inflammatory immune response prevents the development of chronic biofilm infection due to methicillin-resistant *Staphylococcus aureus*. *Infect Immun.* (2011) 79:5010–8. doi: 10.1128/IAI.05571-11
99. Prabhakara R, Harro JM, Leid JG, Harris M, Shirtliff ME. Murine immune response to a chronic *Staphylococcus aureus* biofilm infection. *Infect Immun.* (2011) 79:1789–96. doi: 10.1128/IAI.01386-10
100. Hanson EM, Clements VK, Sinha P, Ilkovitch D, Ostrand-Rosenberg S. Myeloid-derived suppressor cells down-regulate L-selectin expression on CD4+ and CD8+ T cells. *J Immunol.* (2009) 183:937–44. doi: 10.4049/jimmunol.0804253
101. Muller I, Munder M, Kropf P, Hansch GM. Polymorphonuclear neutrophils and T lymphocytes: strange bedfellows or brothers in arms? *Trends Immunol.* (2009) 30:522–30. doi: 10.1016/j.it.2009.07.007
102. Brady RA, Mocca CP, Plaut RD, Takeda K, Burns DL. Comparison of the immune response during acute and chronic *Staphylococcus aureus* infection. *PLoS ONE.* (2018) 13:e0195342. doi: 10.1371/journal.pone.0195342
103. Balraadjsing PP, de Jong EC, Grijpma DW, Tanck MW, Zaat SA. Poly(trimethylene carbonate) and poly(D,L-lactic acid) modify human dendritic cell responses to staphylococci but do not affect Th1 and Th2 cell development. *Eur Cell Mater.* (2018) 35:103–16. doi: 10.22203/eCM.v035a08
104. Nishitani K, Ishikawa M, de Mesy Bentley K, Ito H, Matsuda S, Daiss J, et al. Evidence of *Staphylococcus epidermidis* biofilm infection in the absence of abscess formation or osteolysis in a murine implant-associated osteomyelitis model. *Orthopaed Proc.* (2018) 100-B(SuppL. 3):56.

105. Li D, Gromov K, Soballe K, Puzas JE, O'Keefe RJ, Awad H, et al. Quantitative mouse model of implant-associated osteomyelitis and the kinetics of microbial growth, osteolysis, and humoral immunity. *J Orthop Res.* (2008) 26:96–105. doi: 10.1002/jor.20452
106. Brady RA, Leid JG, Camper AK, Costerton JW, Shirtliff ME. Identification of Staphylococcus aureus proteins recognized by the antibody-mediated immune response to a biofilm infection. *Infect Immun.* (2006) 74:3415–26. doi: 10.1128/IAI.00392-06
107. Brady RA, O'May GA, Leid JG, Prior ML, Costerton JW, Shirtliff ME. Resolution of Staphylococcus aureus biofilm infection using vaccination and antibiotic treatment. *Infect Immun.* (2011) 79:1797–803. doi: 10.1128/IAI.00451-10
108. Gedbjerg N, LaRosa R, Hunter JG, Varrone JJ, Kates SL, Schwarz EM, et al. Anti-glucosaminidase IgG in sera as a biomarker of host immunity against Staphylococcus aureus in orthopaedic surgery patients. *J Bone Joint Surg Am.* (2013) 95:e171. doi: 10.2106/JBJS.L.01654
109. Varrone JJ, de Mesy Bentley KL, Bello-Irizarry SN, Nishitani K, Mack S, Hunter JG, et al. Passive immunization with anti-glucosaminidase monoclonal antibodies protects mice from implant-associated osteomyelitis by mediating opsonophagocytosis of Staphylococcus aureus megaclusters. *J Orthop Res.* (2014) 32:1389–96. doi: 10.1002/jor.22672
110. Yokogawa N, Ishikawa M, Nishitani K, Beck CA, Tsuchiya H, Mesfin A, et al. Immunotherapy synergizes with debridement and antibiotic therapy in a murine 1-stage exchange model of MRSA implant-associated osteomyelitis. *J Orthop Res.* (2018) 36:1590–8. doi: 10.1002/jor.23801
111. Proctor RA. Recent developments for Staphylococcus aureus vaccines: clinical and basic science challenges. *Eur Cell Mater.* (2015) 30:315–26. doi: 10.22203/eCM.v030a22
112. Kubatzky KF, Uhle F, Eigenbrod T. From macrophage to osteoclast - How metabolism determines function and activity. *Cytokine.* (2018) 112:102–15. doi: 10.1016/j.cyto.2018.06.013
113. Josse J, Velard F, Gangloff SC. *Staphylococcus aureus* vs. osteoblast: relationship and consequences in osteomyelitis. *Front Cell Infect Microbiol.* (2015) 5:85. doi: 10.3389/fcimb.2015.00085
114. Dapunt U, Giese T, Stegmaier S, Moghaddam A, Hansch GM. The osteoblast as an inflammatory cell: production of cytokines in response to bacteria and components of bacterial biofilms. *BMC Musculoskelet Disord.* (2016) 17:243. doi: 10.1186/s12891-016-1091-y
115. Dapunt U, Maurer S, Giese T, Gaida MM, Hansch GM. The macrophage inflammatory proteins MIP1alpha (CCL3) and MIP2alpha (CXCL2) in implant-associated osteomyelitis: linking inflammation to bone degradation. *Mediat Inflamm.* (2014) 2014:728619. doi: 10.1155/2014/728619
116. Marriott I. Apoptosis-associated uncoupling of bone formation and resorption in osteomyelitis. *Front Cell Infect Microbiol.* (2013) 3:101. doi: 10.3389/fcimb.2013.00101
117. Blanchette KA, Prabhakara R, Shirtliff ME, Wenke JC. Inhibition of fracture healing in the presence of contamination by Staphylococcus aureus: effects of growth state and immune response. *J Orthop Res.* (2017) 35:1845–54. doi: 10.1002/jor.23573
118. Bruder SP, Fink DJ, Caplan AI. Mesenchymal stem cells in bone development, bone repair, and skeletal regeneration therapy. *J Cell Biochem.* (1994) 56:283–94. doi: 10.1002/jcb.240560303
119. Bunnell BA, Betancourt AM, Sullivan DE. New concepts on the immune modulation mediated by mesenchymal stem cells. *Stem Cell Res Ther.* (2010) 1:34. doi: 10.1186/scrt34
120. Seebach E, Holschbach J, Buchta N, Bitsch RG, Kleinschmidt K, Richter W. Mesenchymal stromal cell implantation for stimulation of long bone healing aggravates Staphylococcus aureus induced osteomyelitis. *Acta Biomater.* (2015) 21:165–77. doi: 10.1016/j.actbio.2015.03.019
121. Charles JF, Aliprantis AO. Osteoclasts: more than 'bone eaters'. *Trends Mol Med.* (2014) 20:449–59. doi: 10.1016/j.molmed.2014.06.001
122. Takayanagi H. New immune connections in osteoclast formation. *Ann N Y Acad Sci.* (2010) 1192:117–23. doi: 10.1111/j.1749-6632.2009.05303.x
123. Kotake S, Udagawa N, Hakoda M, Mogi M, Yano K, Tsuda E, et al. Activated human T cells directly induce osteoclastogenesis from human monocytes: possible role of T cells in bone destruction in rheumatoid arthritis patients. *Arthritis Rheum.* (2001) 44:1003–12. doi: 10.1002/1529-0131(200105)44:5<1003::AID-ANR179>3.3.CO;2-R
124. Sato K, Suematsu A, Okamoto K, Yamaguchi A, Morishita Y, Kadono Y, et al. Th17 functions as an osteoclastogenic helper T cell subset that links T cell activation and bone destruction. *J Exp Med.* (2006) 203:2673–82. doi: 10.1084/jem.20061775
125. Takayanagi H, Ogasawara K, Hida S, Chiba T, Murata S, Sato K, et al. T-cell-mediated regulation of osteoclastogenesis by signalling cross-talk between RANKL and IFN-gamma. *Nature.* (2000) 408:600–5. doi: 10.1038/35046102
126. Bozec A, Zaiss MM. T regulatory cells in bone remodelling. *Curr Osteoporos Rep.* (2017) 15:121–5. doi: 10.1007/s11914-017-0356-1
127. Zaiss MM, Axmann R, Zwerina J, Polzer K, Guckel E, Skapenko A, et al. Treg cells suppress osteoclast formation: a new link between the immune system and bone. *Arthritis Rheum.* (2007) 56:4104–12. doi: 10.1002/art.23138
128. Li H, Hong S, Qian J, Zheng Y, Yang J, Yi Q. Cross talk between the bone and immune systems: osteoclasts function as antigen-presenting cells and activate CD4+ and CD8+ T cells. *Blood.* (2010) 116:210–7. doi: 10.1182/blood-2009-11-255026
129. Grassi F, Manferdini C, Cattini L, Piacentini A, Gabusi E, Facchini A, et al. T cell suppression by osteoclasts *in vitro*. *J Cell Physiol.* (2011) 226:982–90. doi: 10.1002/jcp.22411
130. Li H, Lu Y, Qian J, Zheng Y, Zhang M, Bi E, et al. Human osteoclasts are inducible immunosuppressive cells in response to T cell-derived IFN-gamma and CD40 ligand *in vitro*. *J Bone Miner Res.* (2014) 29:2666–75. doi: 10.1002/jbmr.2294
131. Buchwald ZS, Aurora R. Osteoclasts and CD8 T cells form a negative feedback loop that contributes to homeostasis of both the skeletal and immune systems. *Clin Dev Immunol.* (2013) 2013:429373. doi: 10.1155/2013/429373
132. Charles JF, Hsu LY, Niemi EC, Weiss A, Aliprantis AO, Nakamura MC. Inflammatory arthritis increases mouse osteoclast precursors with myeloid suppressor function. *J Clin Invest.* (2012) 122:4592–605. doi: 10.1172/JCI60920
133. Ortega-Gomez A, Perretti M, Soehnlein O. Resolution of inflammation: an integrated view. *EMBO Mol Med.* (2013) 5:661–74. doi: 10.1002/emmm.201202382
134. Wherry EJ, Kurachi M. Molecular and cellular insights into T cell exhaustion. *Nat Rev Immunol.* (2015) 15:486–99. doi: 10.1038/nri3862
135. Darvin P, Toor SM, Sasidharan Nair V, Elkord E. Immune checkpoint inhibitors: recent progress and potential biomarkers. *Exp Mol Med.* (2018) 50:165. doi: 10.1038/s12276-018-0191-1
136. Wykes MN, Lewin SR. Immune checkpoint blockade in infectious diseases. *Nat Rev Immunol.* (2018) 18:91–104. doi: 10.1038/nri.2017.112
137. Patil NK, Guo Y, Luan L, Sherwood ER. Targeting immune cell checkpoints during sepsis. *Int J Mol Sci.* (2017) 18:2413. doi: 10.3390/ijms18112413
138. Paluch C, Santos AM, Anzilotti C, Cornall RJ, Davis SJ. Immune checkpoints as therapeutic targets in autoimmunity. *Front Immunol.* (2018) 9:2306. doi: 10.3389/fimmu.2018.02306
139. Cavaillon JM, Eisen D, Annane D. Is boosting the immune system in sepsis appropriate? *Crit Care.* (2014) 18:216. doi: 10.1186/cc13787
140. Davies R, O'Dea K, Gordon A. Immune therapy in sepsis: are we ready to try again? *J Intensive Care Soc.* (2018) 19:326–44. doi: 10.1177/1751143718765407
141. Anderson AC, Joller N, Kuchroo VK. Lag-3, Tim-3, and TIGIT: co-inhibitory receptors with specialized functions in immune regulation. *Immunity.* (2016) 44:989–1004. doi: 10.1016/j.immuni.2016.05.001
142. De Sousa Linhares A, Leitner J, Grabmeier-Pfistershammer K, Steinberger P. Not all immune checkpoints are created equal. *Front Immunol.* (2018) 9:1909. doi: 10.3389/fimmu.2018.01909
143. Hodi FS, O'Day SJ, McDermott DF, Weber RW, Sosman JA, Haanen JB, et al. Improved survival with ipilimumab in patients with metastatic melanoma. *N Engl J Med.* (2010) 363:711–23. doi: 10.1056/NEJMoa1003466
144. Dyck L, Mills KHG. Immune checkpoints and their inhibition in cancer and infectious diseases. *Eur J Immunol.* (2017) 47:765–79. doi: 10.1002/eji.201646875
145. Rowshanravan B, Halliday N, Sansom DM. CTLA-4: a moving target in immunotherapy. *Blood.* (2018) 131:58–67. doi: 10.1182/blood-2017-06-741033

146. Linsley PS, Brady W, Urnes M, Grosmaire LS, Damle NK, Ledbetter JA. CTLA-4 is a second receptor for the B cell activation antigen B7. *J Exp Med.* (1991) 174:561–9. doi: 10.1084/jem.174.3.561
147. Genovese MC, Becker JC, Schiff M, Luggen M, Sherrer Y, Kremer J, et al. Abatacept for rheumatoid arthritis refractory to tumor necrosis factor alpha inhibition. *N Engl J Med.* (2005) 353:1114–23. doi: 10.1056/NEJMoa050524
148. Ali A, Welin A, Schwarze JC, Svensson MN, Na M, Jarneborn A, et al. CTLA4 immunoglobulin but not anti-tumor necrosis factor therapy promotes staphylococcal septic arthritis in mice. *J Infect Dis.* (2015) 212:1308–16. doi: 10.1093/infdis/jiv212
149. Axmann R, Herman S, Zaiss M, Franz S, Polzer K, Zwerina J, et al. CTLA-4 directly inhibits osteoclast formation. *Ann Rheum Dis.* (2008) 67:1603–9. doi: 10.1136/ard.2007.080713
150. Bozec A, Zaiss MM, Kagwiria R, Voll R, Rauh M, Chen Z, et al. T cell costimulation molecules CD80/86 inhibit osteoclast differentiation by inducing the IDO/tryptophan pathway. *Sci Transl Med.* (2014) 6:235ra60. doi: 10.1126/scitranslmed.3007764
151. Boutros C, Tarhini A, Routier E, Lambotte O, Ladurie FL, Carbonnel F, et al. Safety profiles of anti-CTLA-4 and anti-PD-1 antibodies alone and in combination. *Nat Rev Clin Oncol.* (2016) 13:473–86. doi: 10.1038/nrclinonc.2016.58
152. Latchman Y, Wood CR, Chernova T, Chaudhary D, Borde M, Chernova I, et al. PD-L2 is a second ligand for PD-1 and inhibits T cell activation. *Nat Immunol.* (2001) 2:261–8. doi: 10.1038/85330
153. Zhang Y, Chung Y, Bishop C, Daugherty B, Chute H, Holst P, et al. Regulation of T cell activation and tolerance by PDL2. *Proc Natl Acad Sci USA.* (2006) 103:11695–700. doi: 10.1073/pnas.0601347103
154. Tseng SY, Otsuji M, Gorski K, Huang X, Slansky JE, Pai SI, et al. B7-DC, a new dendritic cell molecule with potent costimulatory properties for T cells. *J Exp Med.* (2001) 193:839–46. doi: 10.1084/jem.193.7.839
155. Karunarathne DS, Horne-Debets JM, Huang JX, Faleiro R, Leow CY, Amante F, et al. Programmed death-1 ligand 2-mediated regulation of the PD-L1 to PD-1 axis is essential for establishing CD4(+) T cell immunity. *Immunity.* (2016) 45:333–45. doi: 10.1016/j.immuni.2016.07.017
156. Magrys A, Paluch-Oles J, Bogut A, Kielbus M, Plewik D, Koziol-Montewka M. The role of programmed death ligand 1 pathway in persistent biomaterial-associated infections. *J Microbiol.* (2015) 53:544–52. doi: 10.1007/s12275-015-5022-7
157. Davies LC, Heldring N, Kadri N, Le Blanc K. Mesenchymal stromal cell secretion of programmed death-1 ligands regulates T cell mediated immunosuppression. *Stem Cells.* (2017) 35:766–76. doi: 10.1002/stem.2509
158. Pennesi G. PD1-mediated mesenchymal stem cells immunemodulation: the two sides of the coin. *Int Clin Pathol J.* (2018) 6:164–5 doi: 10.15406/icpjl.2018.06.00179
159. Moravej A, Karimi MH, Geramizadeh B, Azarpira N, Zarnani AH, Yaghobi R, et al. Mesenchymal stem cells upregulate the expression of PD-L1 but not VDR in dendritic cells. *Immunol Invest.* (2017) 46:80–96. doi: 10.1080/08820139.2016.1225757
160. Hui E, Cheung J, Zhu J, Su X, Taylor MJ, Wallweber HA, et al. T cell costimulatory receptor CD28 is a primary target for PD-1-mediated inhibition. *Science.* (2017) 355:1428–33. doi: 10.1126/science.aaf1292
161. Kamphorst AO, Wieland A, Nasti T, Yang S, Zhang R, Barber DL, et al. Rescue of exhausted CD8 T cells by PD-1-targeted therapies is CD28-dependent. *Science.* (2017) 355:1423–7. doi: 10.1126/science.aaf0683
162. An G, Acharya C, Feng X, Wen K, Zhong M, Zhang L, et al. Osteoclasts promote immune suppressive microenvironment in multiple myeloma: therapeutic implication. *Blood.* (2016) 128:1590–603. doi: 10.1182/blood-2016-03-707547
163. Tai YT, Cho SF, Anderson KC. Osteoclast immunosuppressive effects in multiple myeloma: role of programmed cell death ligand 1. *Front Immunol.* (2018) 9:1822. doi: 10.3389/fimmu.2018.01822
164. Dominguez-Soto A, Aragoneses-Fenoll L, Martin-Gayo E, Martinez-Prats L, Colmenares M, Naranjo-Gomez M, et al. The DC-SIGN-related lectin LSECtin mediates antigen capture and pathogen binding by human myeloid cells. *Blood.* (2007) 109:5337–45. doi: 10.1182/blood-2006-09-048058
165. Wang Y, Wang J, Meng J, Jiang H, Zhao J, Qian H, et al. Epigenetic modification mediates the increase of LAG-3(+) T cells in chronic osteomyelitis. *Inflammation.* (2017) 40:414–21. doi: 10.1007/s10753-016-0486-0
166. Triebel F. LAG-3: a regulator of T-cell and DC responses and its use in therapeutic vaccination. *Trends Immunol.* (2003) 24:619–22. doi: 10.1016/j.it.2003.10.001
167. Sierro S, Romero P, Speiser DE. The CD4-like molecule LAG-3, biology and therapeutic applications. *Expert Opin Ther Targets.* (2011) 15:91–101. doi: 10.1517/14712598.2011.540563
168. Monney L, Sabatos CA, Gaglia JL, Ryu A, Waldner H, Chernova T, et al. Th1-specific cell surface protein Tim-3 regulates macrophage activation and severity of an autoimmune disease. *Nature.* (2002) 415:536–41. doi: 10.1038/415536a
169. Zhu C, Anderson AC, Schubart A, Xiong H, Imitola J, Khoury SJ, et al. The Tim-3 ligand galectin-9 negatively regulates T helper type 1 immunity. *Nat Immunol.* (2005) 6:1245–52. doi: 10.1038/ni1271
170. Dardalhon V, Anderson AC, Karman J, Apetoh L, Chandwaskar R, Lee DH, et al. Tim-3/galectin-9 pathway: regulation of Th1 immunity through promotion of CD11b+Ly-6G+ myeloid cells. *J Immunol.* (2010) 185:1383–92. doi: 10.4049/jimmunol.0903275
171. Gautron AS, Dominguez-Villar M, de Marcken M, Hafler DA. Enhanced suppressor function of TIM-3+ FoxP3+ regulatory T cells. *Eur J Immunol.* (2014) 44:2703–11. doi: 10.1002/eji.201344392
172. Ocana-Guzman R, Torre-Bouscoulet L, Sada-Ovalle I. TIM-3 regulates distinct functions in macrophages. *Front Immunol.* (2016) 7:229. doi: 10.3389/fimmu.2016.00229
173. Moriyama K, Kukita A, Li YJ, Uehara N, Zhang JQ, Takahashi I, et al. Regulation of osteoclastogenesis through Tim-3: possible involvement of the Tim-3/galectin-9 system in the modulation of inflammatory bone destruction. *Lab Invest.* (2014) 94:1200–11. doi: 10.1038/labinvest.2014.107
174. Tamadaho RSE, Hoerauf A, Layland LE. Immunomodulatory effects of myeloid-derived suppressor cells in diseases: role in cancer and infections. *Immunobiology.* (2018) 223:432–42. doi: 10.1016/j.imbio.2017.07.001
175. Bunt SK, Clements VK, Hanson EM, Sinha P, Ostrand-Rosenberg S. Inflammation enhances myeloid-derived suppressor cell cross-talk by signaling through Toll-like receptor 4. *J Leukoc Biol.* (2009) 85:996–1004. doi: 10.1189/jlb.0708446
176. Ostrand-Rosenberg S, Sinha P, Beury DW, Clements VK. Cross-talk between myeloid-derived suppressor cells (MDSC), macrophages, and dendritic cells enhances tumor-induced immune suppression. *Semin Cancer Biol.* (2012) 22:275–81. doi: 10.1016/j.semcancer.2012.01.011
177. Ballbach M, Dannert A, Singh A, Siegmund DM, Handgretinger R, Piali L, et al. Expression of checkpoint molecules on myeloid-derived suppressor cells. *Immunol Lett.* (2017) 192:1–6. doi: 10.1016/j.imlet.2017.10.001
178. Weber R, Fleming V, Hu X, Nagibin V, Groth C, Altevogt P, et al. Myeloid-derived suppressor cells hinder the anti-cancer activity of immune checkpoint inhibitors. *Front Immunol.* (2018) 9:1310. doi: 10.3389/fimmu.2018.01310
179. Toor SM, Elkord E. Therapeutic prospects of targeting myeloid-derived suppressor cells and immune checkpoints in cancer. *Immunol Cell Biol.* (2018) 96:888–97. doi: 10.1111/imcb.12054
180. Tesi RJ. MDSC; the most important cell you have never heard of. *Trends Pharmacol Sci.* (2019) 40:4–7. doi: 10.1016/j.tips.2018.10.008
181. Labonte AC, Tosello-Trampont AC, Hahn YS. The role of macrophage polarization in infectious and inflammatory diseases. *Mol Cells.* (2014) 37:275–85. doi: 10.14348/molcells.2014.2374
182. Freitas-Silva R, Brelaz-de-Castro MC, Pereira VR. Dendritic cell-based approaches in the fight against diseases. *Front Immunol.* (2014) 5:78. doi: 10.3389/fimmu.2014.00078

Conflict of Interest Statement: The authors declare that the research was conducted in the absence of any commercial or financial relationships that could be construed as a potential conflict of interest.

frontiers in Immunology

REVIEW
published: 08 August 2019
doi: 10.3389/fimmu.2019.01901

Macrophage-Derived Extracellular Vesicles as Carriers of Alarmins and Their Potential Involvement in Bone Homeostasis

*Bartijn C. H. Pieters[1], Alfredo Cappariello[2], Martijn H. J. van den Bosch[1], Peter L. E. M. van Lent[1], Anna Teti[3] and Fons A. J. van de Loo[1]**

[1] Experimental Rheumatology, Radboud University Medical Center, Nijmegen, Netherlands, [2] Research Laboratories - Department of Oncohematology IRCCS Bambino Gesù Children's Hospital, Rome, Italy, [3] Department of Biotechnological and Applied Clinical Sciences, University of L'Aquila, L'Aquila, Italy

Extracellular vesicles are a heterogeneous group of cell-derived membranous structures, which facilitate intercellular communication. Recent studies have highlighted the importance of extracellular vesicles in bone homeostasis, as mediators of crosstalk between different bone-resident cells. Osteoblasts and osteoclasts are capable of releasing various types of extracellular vesicles that promote both osteogenesis, as well as, osteoclastogenesis, maintaining bone homeostasis. However, the contribution of immune cell-derived extracellular vesicles in bone homeostasis remains largely unknown. Recent proteomic studies showed that alarmins are abundantly present in/on macrophage-derived EVs. In this review we will describe these alarmins in the context of bone matrix regulation and discuss the potential contribution macrophage-derived EVs may have in this process.

Keywords: alarmins, bone homeostasis, extracellular vesicles, exosomes, macrophages

OPEN ACCESS

Edited by:
Daniela Bosisio, University of Brescia, Italy

Reviewed by:
David Stephen Pisetsky, Duke University, United States
Joost Joe Oppenheim, National Cancer Institute at Frederick, United States

****Correspondence:***
Fons A. J. van de Loo
fons.vandeloo@radboudumc.nl

Specialty section:
This article was submitted to Inflammation, a section of the journal Frontiers in Immunology

Received: *26 February 2019*
Accepted: *26 July 2019*
Published: *08 August 2019*

Citation:
Pieters BCH, Cappariello A, van den Bosch MHJ, van Lent PLEM, Teti A and van de Loo FAJ (2019) Macrophage-Derived Extracellular Vesicles as Carriers of Alarmins and Their Potential Involvement in Bone Homeostasis. Front. Immunol. 10:1901. doi: 10.3389/fimmu.2019.01901

INTRODUCTION

Intercellular communication is an important biological process which allows cells to coordinate their response to physiological changes, environmental triggers and pathogenic invaders in a spatial and temporal fashion. A new addition to the intercellular communication system are extracellular vesicles (EVs) (1). EVs are small cell membrane-derived phospholipid bilayer structures that range in diameter from 30 to 2000 nm. Previously, they were considered to be merely cellular waste products, nowadays EVs are recognized as regulatory structures, produced and released by an actively regulated intracellular and energy dependent process as a means to shuttle complex cargo and deliver biological information to recipient cell/tissues. A distinction can be made between three different subtypes of vesicles based on their biogenesis and size: exosomes (30–150 nm diameter) released by exocytosis, microvesicles or microparticles (100–1,500 nm diameter) formed by budding from the plasma membrane (shedding vesicles, matrix vesicles) and apoptotic bodies (500–2,000 nm diameter) released from apoptotic cells (2). While the latter are the specific products of the complex processes of cells undergoing programmed cell death, all other EV subtypes are not phenotypically linked to cell death.

Upon release, EVs can interact with recipient cells in a number of ways. Host receptor activation can be induced via the interaction of vesicle membrane proteins either in a juxtacrine fashion or by paracrine signaling after being cleaved and released from EVs. EVs can also fuse with the cell membrane, mediating membrane receptor transfer and releasing its cargo intracellularly. Finally, EVs can be taken up by cells via endocytosis, delivering their cargo inside endocytic vacuoles (3). EV-mediated transfer of protein, genetic information (DNA, RNA and predominately small non-coding RNA and microRNA) is shown to be very efficient and intravesicular cargo is protected from degradation in the intercellular environment by their lipid bilayer membrane (4).

The involvement of EVs in bone homeostasis was previously thought to be primarily via matrix vesicles, a specific subgroup of EVs that consist of small membrane particles (20–200 nm), which bud off from the plasma membrane of mineralizing cells, such as osteoblasts and chondrocytes, prior to the onset of matrix mineralization [reviewed in (5)]. Ultrastructural studies in the late 1960's have shown that cartilage calcification starts in and around matrix vesicles, and matrix vesicles have since been implicated to play a role in the calcification of bone, cartilage, and dentin. However, more recent studies show the importance of bone cell-derived EVs as mediators of intercellular communication and their function in bone homeostasis and remodeling [reviewed in (6)]. In this review we will briefly summarize the communication between bone cells via EVs and thereafter focus on the potential role of macrophage-derived EVs carrying alarmins as contributors of bone remodeling.

THE FUNCTION OF EVs IN BONE REMODELING EXTENDS THAT OF BEING MATRIX PARTICLES

The skeleton physiology is not exempt from the participation of EVs in biological processes. In fact, the skeleton houses a complex microenvironment that hosts a great diversity of cells, such as osteoblasts, osteoclasts, osteocytes, and other myeloid cells of the bone marrow, including macrophages. All of these cells are known to release EVs which can regulate each other's function.

Osteoblasts

Osteoblasts are specialized mesenchymal cells that are responsible for bone matrix synthesis and mineralization during both initial bone formation and later bone remodeling. These cells were first recognized to promote mineralization, releasing matrix vesicles able to initiate nucleation of hydroxyapatite crystals (7). Across the years, further investigations deeply characterized the cargo and functions of matrix vesicles derived from osteoblasts and osteoblast-like cells, identifying alkaline phosphatase, the pyrophosphate generating enzyme PC1 and the pyrophosphate channel ANK as key mechanisms causing pyrophosphate production and influx into these EVs by hydroxyapatite nucleation.

Primary osteoblasts and their EVs share a similar gene profile, which included the expression of *atf4, alp, runx2, osx, col1a1* (8). A deeper proteomic characterization of exosomes derived from osteoblastic cell line (MC3T3) revealed many proteins related to the osteogenic pathways, such as mTOR, integrins, and eukaryotic initiation factor-2 signaling (9). Transcriptomic profiling performed in mineralizing MC3T3 revealed EVs containing osteogenic miRNAs (10). Exposure of mouse bone marrow-derived stromal ST2 cells to MC3T3-derived EVs, induced their osteogenic differentiation, manifested by the up-regulation of osteogenic markers, such as runt-related transcription factor 2 (RUNX2) and alkaline phosphatase, and enhancing matrix mineralization through the modulation of calcium, Wnt, insulin, and TGF-β signaling pathways.

van Leeuwen et al. studied the molecular profile of EVs from human osteoblasts, both in naïve and mineralizing conditions (11, 12). Comparing the cellular and EV mRNAs of osteoblasts, they showed that EVs were enriched with mRNAs related to protein translation, RNA processing and cell-to-cell communication, in particular with osteoclasts (NFKBIB, PGF), adipocytes (FGF1) and hematopoietic stem cells (FLT3LG, IL18) (11). Taken together, these findings suggest that osteoblasts release EVs capable of enhancing osteogenic differentiation, thereby contributing to bone formation and mineralization.

Osteoclasts

Osteoclasts are unique in their ability to resorb bone and play an important role in bone turnover. A tight crosstalk with osteoblasts and osteocytes, which influence osteoclastogenesis by the factors they produce, is crucial to synchronize the activities in homeostatic bone remodeling (13, 14). Osteoclasts differentiate from myeloid progenitor cells under the influence of macrophage colony-stimulating factor (M-CSF) and receptor activator of nuclear factor kappa-B ligand (RANKL) (15, 16). Next to RANKL signaling, a co-stimulatory signal is required for osteoclastogenesis. After full differentiation, mature multinucleated osteoclasts can start to secrete acids and lytic enzymes that together resorb the bony tissues (14).

A recent study reported that osteoclast precursors are capable of releasing exosomes that could directly promote the osteogenic differentiation of the recipient mesenchymal stem cells (17). On the other hand, Liu and colleagues showed that mature osteoclast-derived exosomes were internalized by osteoblasts leading to a miR-214-3p-dependent inhibition of osteoblast activity and bone formation (18).

Interestingly, osteoclast EVs seemed to be involved in their own maturation. Holliday's group showed that pre-osteoclast EVs promoted osteoclastogenesis in whole bone marrow stromal cell cultures upon Vitamin D_3 treatment, while mature osteoclast EVs inhibited osteoclastogenesis in the same culture conditions (19). This effect was demonstrated to be due to RANK expressed by EVs only from mature osteoclasts, presumably able to bind competitively RANKL in the microenvironment, similarly to

Abbreviations: DAMP, damage-associated molecular pattern; EV, extracellular vesicle; HSP, heat shock protein; M-CSF, macrophage colony-stimulating factor; MSC, mesenchymal stem cell; NF-κB, activating nuclear factor-κB; RAGE, receptor for advanced glycosylation end products; RANKL, receptor activator of nuclear factor kappa-B ligand; RUNX2, runt-related transcription factor 2; TLR, toll-like receptor.

osteoprotegerin (OPG). Furthermore, EVs from osteoclasts have been shown to transfer osteoclast-osteoblast coupling factors. RANK-expressing EVs from mature osteoclasts bind RANKL on osteoblasts, activating the reverse signaling and inducing RUNX2 activity in osteoblasts and bone formation (20). The idea of EV-based osteoclast-to-osteoblast coupling is strengthened by the paper of Sun et al. showing that EVs from osteoclasts express EphrinA2, which binds the Eph receptor expressed by osteoblasts, inhibiting bone formation (21, 22). These findings highlight the importance of EVs in the communication between osteoclasts and osteoblasts, but it is yet to be determined what the relative contribution of the vesicles is compared to the total secretome of these cells.

Osteocytes

Osteocytes, the end stage of osteoblast differentiation, are matrix-embedded cells mainly involved in the regulation of bone remodeling and in the adaptation to mechanical forces (23). Morrel et al. found that mechanical stimulation activated osteocyte network inducing Ca^{2+}-dependent contractions and enhancing the production and release of EVs containing RANKL, OPG and sclerostin (SOST) (24).

In comparison to osteoblast- and osteoclast-derived EVs much less is known about osteocyte-derived EVs. Osteocytes produce a unique EV population, described by Sato et al. in the osteocyte-ablated mouse model. They characterized circulating EVs of osteocyte-less mice and found 12 downregulated miRNAs in plasma. Furthermore, they described that this pool of miRNAs was enriched in EVs from osteocyte-like MLO-Y4 cells compared to non-osteocytic ST2 cells (25). Among the osteocyte miRNAs is miR-218 which could be taken up by osteoblasts, resulting in downregulation of SOST leading to osteogenic activity (26).

Other Bone Interacting Cells

The balanced interplay between these three bone cell types is also under control of immune cells like macrophages and T-cells and often during inflammation the homeostatic situation is turned into accelerated bone loss. These immune cells produce cytokines that steer the differentiation of progenitor cells into osteoblasts or osteoclasts thereby influencing bone regeneration.

Interestingly, the biogenesis of EVs is controlled by intracellular Ca^{2+} concentrations in the EV-producing cells and, furthermore, EVs are often carriers of calcium ions contributing to calcification of tissues (27). As bone regulates calcium homeostasis in the body, it may indirectly influence EV biogenesis as well. Moreover, cytokines and growth factors can alter intracellular Ca^{2+} levels by depleting calcium from the endoplasmic reticulum and by increasing calcium influx from the extracellular space. Hence, inflammation can regulate both the extra- and intracellular Ca^{2+} levels and thereby regulate EV biogenesis although many other intracellular mechanisms are involved as well. In the next paragraphs we will discuss how EVs derived from innate immune cells might communicate with bone cells and regulate bone homeostasis via alarmins.

MACROPHAGES AS A SOURCE FOR EVs CARRYING ALARMINS

Macrophages are a highly heterogenous population derived from the myeloid linage that can reside in bone either as resident cells or as a result of recruited myeloid precursors, mainly monocytes, that differentiate in the tissue. The interplay between macrophages and bone cells is critical to bone formation and repair. Osteal macrophages, also known as osteomacs, are one of these resident macrophages located in close proximity to the bone surface and do not express TRAP (28). However, they colocalize with TRAP positive osteoclasts and are found immediately adjacent or near to giant osteoclasts at catabolic sites (29). Osteomacs are also tightly associated with osteoblasts in the endosteal and the periosteal surface. When osteoblasts undergo apoptosis they are phagocytosed together with the debris by neighboring osteomacs (28). Osteomacs have also been shown to support bone formation and osteoblast mineralization *in vitro* and *in vivo* using a mouse model in which macrophages were ablated (MaFIA, macrophage Fas-induced apoptosis mouse) (28).

Apart from being crucial in homeostasis of normal bone, macrophages also play a critical role in inflammation-driven bone diseases (30). Tissue damage elicited by external (injuries, chemicals, infection) and internal triggers (DNA damage, immunological reactions) or by shortage (nutrients, oxygen) or excess (sugar, cholesterol) of factors can induce macrophage activation that disturbs bone homeostasis and causes bone destruction. Most of the damage associated factors are first sensed by resident macrophages that become stressed and upon activation recruit more macrophages. Resident and recruited macrophages respond to their local environment and activate specific transcriptional programs that drive them to a spectrum of different phenotypes ranging from pro-inflammatory M-1 like to anti-inflammatory M-2 like macrophages (31). When macrophages become stressed, pro- and anti-inflammatory mediators are released into the micro milieu that regulate innate and adaptive immune cells and may cause disbalanced bone homeostasis (32).

The majority of pro-inflammatory factors that are released by macrophages are rapidly suppressed by many feedback mechanisms. However, EVs are able to deliver pro-inflammatory factors to other cells in a protected way (33). Nevertheless, not all secreted proteins detected in the medium are also present in the EVs since packaging of the biomolecular cargo within the macrophage EVs is a regulated process (34). LPS stimulated macrophages release interleukins in the medium that were absent in their exosomes (35). On the other hand, many alarmins, damage-associated molecular patterns (DAMPs), are present in macrophage-derived EVs. For example, New et al. showed that macrophage-derived EVs are enriched in S100A9 and Anx5 and contribute to microcalcifications observed in atherosclerotic plagues (36). Using gain- and loss-of-function experiments the authors reveal the critical role for Anx5-S100A9 complexes in this process, highlighting the functional activity of EV-carried alarmins.

Alarmins

Alarmins are endogenous molecules that are constitutively available and released upon cellular stress and activate the immune system, causing inflammation *in vivo*. Many alarmins are intracellular proteins that are both passively and actively secreted. Passive release is often associated with cell injury or death, whereas active release is regulated by mechanisms independent of ER-Golgi routes, such as degranulation or pyroptosis. Upon release, alarmins can bind a range of receptors among which toll-like receptors (TLRs) and receptors for advanced glycosylation end products (RAGE) are the most studied (37).

Proteomic studies on both monocyte- and macrophage-derived EVs show the presence of a large variety of alarmins, including annexins, galectins, heat-shock proteins and S100-alarmins (38–47). An overview of EV-associated alarmins is presented in **Table 1**. Within these studies different EV-populations were studied, ranging from exosomes to microparticles. Differential ultracentrifugation protocols were used for most studies, either in combination with density gradient or precipitation techniques. Most alarmins were present in the majority of the studies, including HSP-90, annexins, and several S100-proteins. Simultaneously, part of the alarmins were only found in a limited number of studies. These observed differences could be due to the different isolation methods, EV-subtypes investigated or sensitivity of the proteomic analysis.

Recruitment of alarmins into EVs seems to be partially dependent on the macrophage activation state. Stimulation of macrophages with curdlan, a bacterial β-glucan, increased vesicle-mediated protein secretion, and specifically increased the amount of alarmins found in their EVs (38). Similarly, infection of macrophages with influenza A virus, resulted in an increase in alarmins found in their produced EVs (39). It remains to be investigated whether polarization of macrophages also changes alarmin expression of their EVs, it has however been shown that microvesicles produced by M1 and M2 macrophages contain different mRNAs that can identify the macrophage phenotype (48).

From these proteomic studies it is not possible to determine which of these alarmins are surface-accessible. As most receptors recognizing alarmins (TLRs, RAGE) sense the extracellular milieu it is important which of these alarmins are carried on the surface of EVs. A recent study by Cvjetkovic et al. presented a novel work-flow designed to identify proteins localized on the surface of EVs (49). Using a multiple proteomics approach, combining proteinase treatment and biotin tagging, they were able to identify many proteins of cytosolic origin that were localized on the surface of mast cell-derived EVs. Among the identified proteins were a number of alarmins, including nucleolin, S100-A9, -A10, -A13, galectin-1, and several heat shock proteins. Interestingly, all annexins (A1-A7, A11, and A13) were absent from the surface, and were instead present intravesicularly (49). In contrast, Stewart, et al. showed that annexin-2 is localized on the surface of EVs (50). These discrepancies could be due to the different cell types used and the different sub-groups of EVs investigated. Microvesicles seem to more predominant in their surface expression of annexin-V

TABLE 1 | List of alarmins found by proteomic analysis of monocyte and macrophage-derived EVs.

	Vesicle subtype	References
Heat-shock proteins		
Heat shock conjugate 71 kDa	Exosomes, microparticle, microvesicles	(38, 39, 41, 42, 44–47)
HSP-β1	Exosomes, microparticle	(38, 39, 43–45, 47)
HSP-70 (protein 1A)	Exosomes, microparticle	(38, 39, 41, 43–45, 47)
HSP-70 (protein 4)	Exosomes, microparticle	(39–42, 44, 45, 47)
HSP-70 (protein 13)	Exosomes	(39, 41, 42)
HSP-75, mitochondrial	Exosomes, microparticle	(39, 41, 43, 44, 47)
HSP-90α	Exosomes, microparticle, microvesicles	(38–42, 44–47)
HSP-90β	Exosomes, microparticle, microvesicles	(38–47)
HSP-105	Exosomes, microparticle	(39, 41–47)
10 kDa heat shock protein	Exosomes, microparticle	(38, 39, 41, 42, 44, 45, 47)
60 kDa heat shock protein	Exosomes, microparticle	(39, 41–47)
Annexins		
Annexin A1	Exosomes, microparticle	(38–45, 47)
Annexin A2	Exosomes, microparticle	(38–45, 47)
Annexin A3	Exosomes, microparticle	(39–42)
Annexin A4	Exosomes, microparticle	(38–43, 45, 47)
Annexin A5	Exosomes, microparticle, microvesicles	(38, 39, 41–47)
Annexin A6	Exosomes, microparticle, microvesicles	(38–41, 43–47)
Annexin A7	Exosomes, microparticle	(38, 39, 41–45, 47)
Annexin A11	Exosomes, microparticle	(38–41, 43–45, 47)
Galectins		
Galectins-1	Exosomes, microparticle	(38, 39, 41, 42, 45, 47)
Galectin-3	Exosomes, microparticle	(39, 41, 42, 45, 47)
Galectin-7	Exosomes, microparticle	(38, 39, 44, 47)
Galectin-9	Exosomes, microparticle	(38, 39, 47)
Galectin-9B	Exosomes, microparticle	(39, 45)
S100-alarmins		
S100-A4	Exosomes, microparticle	(38, 39, 41, 42, 45, 47)
S100-A6	Exosomes, microparticle	(38, 39, 41, 42, 45, 47)
S100-A8	Exosomes, microparticle	(38, 39, 45, 47)
S100-A9	Exosomes, microparticle	(39, 45, 47)
S100-A10	Exosomes, microparticle	(38, 39, 41, 42, 45, 47)
S100-A11	Exosomes, microparticle	(38, 39, 41, 42, 45, 47)
S100-P	Exosomes	(39)
Miscellaneous		
Cathelicidin	Exosomes	(39)
Defensin α3	Exosomes	(39)
Endoplasmin	Exosomes, microparticle	(38, 39, 41–45, 47)
Fibronectin	Exosomes, microparticle	(38, 39, 42, 43, 45–47)
HMGB1	Exosomes, microparticle	(41, 43, 45)
Nucleolin	Exosomes, microparticle	(39, 41–45, 47)
Thymosin β4	Exosomes, microparticle	(39, 42, 45)
78 kDa glycoseregulated protein	Exosomes	(42)

compared to exosomes, as demonstrated by Heijnen et al. (51). The sorting mechanism responsible for protein localization remains to be identified.

THE EFFECT OF ALARMINS ON OSTEOBLASTS AND OSTEOCLASTS

Alarmins play wide roles in different cell types. Multiple studies described the profound involvement of families of alarmins in osteocyte, osteoblast and osteoclast differentiation and function, including annexins, galactins, heat shock proteins, S100-proteins and various other proteins, although detailed studies for many of the individual family members are still lacking.

Annexins

Annexins are autocrine/paracrine factors secreted by several cell types. Among them, Annexin 2 (AnxII) was demonstrated to increase bone resorption (52). This effect was shown to be due to activation of bone marrow stromal cells with the overexpression of GM-CSF and RANKL, both being pro-osteoclastogenic factors (53). Additionally, a previous study showed that overexpression of AnxII stimulated osteoclast formation (54). Another study poses that AnxII is only involved in the proliferation of osteoclast precursors, probably via stimulation of GM-CSF production, but not in the later multinucleation stages of osteoclast differentiation (52). The receptor that mediates these effects remains to be elucidated. However, most studies described an autocrine effect of osteoclast-produced AnxII, leaving the importance of macrophage-derived AnxII in the stimulation of osteoclasts unknown.

Galectins

Galectins are a class of proteins that bind specifically to β-galactoside sugars, consisting of 15 members, of which 9 are known in humans and 11 in mice. These soluble proteins have both intra- and extracellular functions (55).

Galectin-1 (Gal-1) has been proposed to mediate cell-to-cell and cell-to-matrix adhesion (55). Furthermore, galectin-1 has been found both to promote and inhibit cell proliferation of a number of cells. In particular, Gal-1 was demonstrated to decrease differentiation of bone marrow stromal cells (56).

Galectin 3 (Gal-3) is another member of the galectin family found to affect both osteoblast and osteoclast differentiation. It has been demonstrated that exogenous recombinant Gal-3 inhibited terminal differentiation of a human pre-osteoblast cell line (57). Weilner et al. found that Gal-3 affected osteogenic differentiation of mesenchymal stem cells (MSCs) and, interestingly, that Gal-3 can be detected in EVs from plasma. Administration of Gal-3-EVs to MCSs increased osteoblastogenesis, preventing β-catenin degradation (58). On the other hand, Gal-3 strongly decreased osteoclast formation from precursors by suppressing nuclear factor of activated T-cells c1 (NFATc1), whereas Gal-3-deficient bone marrow cells had an increased osteoclastogenic potential. Moreover, addition to mature osteoclasts inhibited their resorptive capacity (59, 60). Likewise, Gal-9 markedly decreased osteoclast formation from cell lines and bone marrow cells, probably via binding to its receptor T-cell immunoglobin- and mucin-domain-containing molecule 3 (Tim-3) (61).

Heat Shock Proteins

Heat shock proteins (HSPs) are among the most well-studied alarmins. Under physiological conditions they act as intracellular chaperone proteins, but some members are secreted upon stress. Stress factors such as IL-1β and TNFα have been shown to increase HSP60 secretion. These increased HSP60 levels were shown to promote osteoclast formation and activity *via* potentiation of RANK-RANKL signaling. The same study showed that this effect runs *via* binding of HSP60 to TLR2 (62). The finding that HSP60 is an agonist for the triggering receptor expressed in myeloid cells (TREM)2 receptor, which is part of the co-stimulatory signaling that is needed for osteoclastogenesis, might give an additional mechanism of how HSP60 might increase osteoclastogenesis (63).

In contrast, the HSP70 family member heat-shock 70-kDA protein-8 binds to the ubiquitin-like protein monoclonal non-specific suppressor factor β and double knockdown of these factors inhibited RANKL-induced osteoclastogenesis (64). The effects of HSP90 on osteoclastogenesis are more controversial. Whereas, its inhibition with SNX-2112 potently inhibited osteoclast formation (65), the effects of HSP90 inhibition with 17-allylamino-17-demethoxygeldanamycin (17-AAG) on osteoclast formation was shown to be cell-type dependent (66–68).

S100 Family Proteins

S100 proteins are low molecular weight proteins that belong to the family of calcium binding proteins. Extracellular S100A4 binds to cell surface receptors, such as the RAGE, activating nuclear factor-κB (NF-κB) (69). On mature murine osteoblasts, S100A4 was shown to inhibit mineralization activity and the expression of late-stage osteoblast markers via activation of the NF-κB pathway (70). Additionally, S100A4 has been shown to stimulate osteoclast formation (71). Moreover, although *in vitro* osteoclast cultures with S100A4-deficient bone marrow resulted in more TRAP+ cells compared to wild type cells, the formed osteoclasts were much smaller with less nuclei, underlining the importance for S100A4 in osteoclast formation (72). Finally, binding of S100A4 to extracellular annexins has been shown to regulate the fusogenic activity of osteoclasts (73). The most well-studied S100 proteins in the context of inflammatory bone diseases are S100A8 and S100A9, however data about their direct function on osteoblasts and osteoclasts is rather limited. A previous study showed that stimulation of mature murine osteoclasts with S100A8 enhances their further fusion and resorbing activity *via* binding to TLR4 (74). Another study showed that S100A9 directly stimulates osteoclast formation from monocytes in the context of osteomyelitis in the absence of RANKL (75). However, addition of S100A9 to human monocytes strongly inhibits osteoclast differentiation (76).

High Mobility Group box Protein 1

High mobility group box protein 1 (HMGB1) is a non-histone nuclear protein that acts as an alarmin extracellularly. TLR2/4/9 and RAGE have been implicated as receptors of

extracellular HMGB1. HMGB1 release occurs during tissue injury or microbial invasion via two major pathways, one passive and the other active. Passive release is associated with necrotic cell death, whereas during active release HMGB1 is first shuttled to the cytoplasm, in a JAK-STAT dependent manner, and is thereafter either released into the extracellular space during pyroptosis or alternatively via exocytosis of secretory lysosomes (77, 78). HMGB1 has also been found in EVs. For lymphocytes it is primarily associated with apoptotic vesicles (79), whereas, for macrophages it has also been shown in vesicles released in response to TLR-activation (80). A function for HMGB1 in bone homeostasis has been described, where it can stimulate osteoclastogenesis. HMGB1-RAGE signaling was shown to be important in regulating actin cytoskeleton reorganization, thereby contributing to RANKL-induced and integrin-dependent osteoclastogenesis (81).

Other Alarmins

Fibronectin also plays a crucial role in the differentiation of osteoblasts (82). Fibronectin is a heterodimeric extracellular matrix glycoprotein that has several cell- and matrix-binding domains (83). Normal human and murine osteoblasts express fibronectin receptors α3β1, α4β1, α5β1, αvβ3, and αvβ5 integrins (84–86). Fibronectin was shown to induce osteoblast differentiation, since perturbation of binding between fibronectin and osteoblasts suppressed nodule formation and maturation, as well as alkaline phosphatase and osteocalcin expression (82). Moreover, fibronectin also displayed pro-survival effect on mature osteoblasts (87). In contrast, fibronectin inhibits the formation of osteoclasts but stimulates the activity of mature osteoclasts *via* nitric oxide and IL-1β-mediated pathways (88). Finally, the antimicrobial peptide of the cathelicidin family LL-37 inhibits osteoclastogenesis by inhibiting the calcineurin activity (89) and the actin-sequestering protein thymosin β4 suppresses osteoclast differentiation (90).

SUMMARY AND PERSPECTIVE

The function of soluble alarmins has widely been studied, and it is clear there is a profound involvement of alarmins in bone-resident cell differentiation and function. A number of these alarmins have also been identified on EVs derived from monocytes/macrophages, and make up a sizable portion of the vesicle cargo. We hypothesize that vesicle-carried alarmins can have similar effects to soluble alarmins on osteoblast and osteoclast differentiation and function and thereby contribute to bone homeostasis (schematic cartoon in **Figure 1**).

The composition and relative quantities of alarmins on monocyte/macrophage-derived EVs will ultimately determine their function. Although functional studies are limited, as focus is often on the vesicle as a whole rather than individual proteins carried by the EV, a delicate study by New et al. revealed a critical role of the alarmins Anx5 and S100A9 present on macrophage-derived EVs in microcalcifications in atherosclerotic plaques (36). An additional study, by Nair et al. has shown that LPS stimulated macrophages release microvesicles coated with histones, a different type of alarmin. These histones can interact with TLR4 promoting inflammatory responses (91). On that note, it is important to understand where alarmins are expressed, either on the membrane surface or intravesicularly. Surface bound alarmins can interact with membrane bound receptors on the bone cells, such as TLRs or RAGE, whereas intravesicular alarmins can only interact with intracellular receptors. The mode of uptake is also important in this regard, as a portion of engulfed vesicles are immediately degraded in the lysosome of the recipient cell and therefore will not have to chance to release their alarmins intravesicular.

EVs also contain different molecules such as lipids, polymers of nucleotides, sugars, and other cell metabolites, and when EVs are taken up these molecules will have an impact on the bone cells as well. Nevertheless, alarmins on EVs mediate their first direct contact with bone cells *via* membrane receptor recognition and this interaction could be an effective target to treat bone destruction. Secondly it might be possible to steer either the expression of alarmins in monocytes/macrophages or the EV-loading mechanism toward EVs that possess an anti-inflammatory and bone inducing phenotype. EVs are quite sturdy and can be transportation *via* the circulation, which makes alarmin-EVs important messengers in the local bone remodeling process also when monocytes/macrophages are not in close proximity with the bone cells. An important feature of EVs which enables this distal communication is the ability to integrate with extracellular matrix. Besides carrying alarmins, EVs carry an abundance of adhesion molecules and can bind various matrix molecules allowing interaction with bone (92). This makes EVs uniquely equipped to function as a long-distance alarmin-delivery system to osteoclasts and osteoblasts at the bone site.

Our understanding of extracellular vesicles and alarmins as regulators of bone homeostasis have greatly increased over the past decade, however a role for alarmins on/in extracellular vesicles is often overlooked. Clearly macrophages play a role in bone remodeling and are a source of vesicle-carried alarmins. Future studies should be directed to determine the contribution macrophage-derived EVs have, and identify the alarmin that causes the deregulation of bone homeostasis under inflammatory conditions.

OUTSTANDING QUESTIONS

By reviewing the involvement of alarmins in/on EVs in bone homeostasis, we realized how many questions in this field of research remain unanswered. Below, we highlight a couple of these questions that require further investigation to move this research field forward.

1) How are alarmins associated with EVs, intravesicular or present on the outside of the vesicle membrane? And is there preferential loading for certain types of alarmins?

   Using multiple proteomics approaches, combining proteinase treatment and biotin tagging [method published by Cvjetkovic et al. (49)], it would be possible to delineate

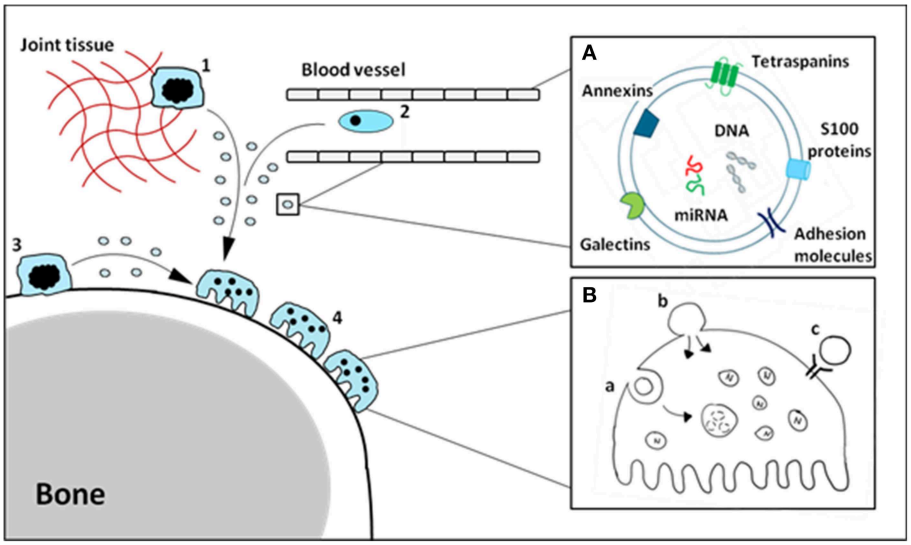

FIGURE 1 | Schematic cartoon of macrophage-derived EVs carrying alarmins impacting osteoclasts. Tissue-resident (1), circulating (2) and osteal macrophages (3) can secrete EVs carrying alarmins **(A)**. These vesicles can interact with bone cells, including osteoclasts (4), in a number of different ways **(B)**. Vesicles can be internalized (a), fuse with the cell membrane (b) or ligands present on the outer membrane of the vesicle can interact with receptors on the cellular membrane (c). The composition and relative quantities of alarmins on macrophage-derived EVs will determine their functional effects.

which alarmins are present on the outer membrane versus intravesicular.

2) Are alarmins associated with EVs functionally active? And how does this activity relate to soluble alarmins?

   In vitro separation of EVs from soluble alarmins derived from macrophages can be difficult, as this heavily depends on the isolation techniques used. If sufficient separation can be achieved, it will be possible to determine how effective each fraction is.

3) In the setting of bone homeostasis, how large is the contribution of EV-associated alarmins compared to soluble alarmins?

   To delineate the contribution of particle-bound versus soluble alarmins we could utilize macrophage-specific knockdown/inhibition of EV-secretion or EV-loading mechanisms, preventing secretion of alarmin-carrying EVs specifically for macrophages.

4) Is there a difference in alarmin content between osteomacs and circulating macrophages? And where are alarmin-carrying EVs produced primarily?

   Comparing the cargo of osteomac- and macrophage-derived EVs using proteomics will shed light on how the EVs differ in alarmin content. It will however remain difficult to trace back the cellular origin of EVs *in vivo* without prior labeling of the producing cells.

AUTHOR CONTRIBUTIONS

BP, AC, and MvdB wrote sections of the manuscript. PvL, AT, and FvdL critically revised the manuscript. All authors contributed to manuscript revision, read, and approved the submitted version.

REFERENCES

1. Théry C. Exosomes: secreted vesicles and intercellular communications. *F1000 Biol Rep*. (2011) 3:15. doi: 10.3410/B3-15
2. Colombo M, Raposo GC. Théry, Biogenesis, secretion, and intercellular interactions of exosomes and other extracellular vesicles. *Annu Rev Cell Dev Biol*. (2014) 30:255–89. doi: 10.1146/annurev-cellbio-101512-122326
3. Mathivanan S, Ji H, Simpson RJ. Exosomes: extracellular organelles important in intercellular communication. *J Proteomics*. (2010) 73:1907–20. doi: 10.1016/j.jprot.2010.06.006
4. Valadi H, Ekström K, Bossios A, Sjöstrand M, Lee JJ, Lötvall JO. Exosome-mediated transfer of mRNAs and microRNAs is a novel mechanism of genetic exchange between cells. *Nat Cell Biol*. (2007) 9:654. doi: 10.1038/ncb1596
5. Golub EE. Biomineralization and matrix vesicles in biology and pathology. *Semin Immunopathol*. (2011) 33:409–17. doi: 10.1007/s00281-010-0230-z
6. Gao M, Gao W, Papadimitriou JM, Zhang C, Gao J, Zheng M, et al. Exosomes—the enigmatic regulators of bone homeostasis. *Bone Res*. (2018) 6:36. doi: 10.1038/s41413-018-0039-2
7. Bonucci E. Fine structure of early cartilage calcification. *J Ultrastruct Res*. (1967) 20:33–50. doi: 10.1016/S0022-5320(67)80034-0
8. Cappariello A, Loftus A, Muraca M, Maurizi A, Rucci N, Teti A. Osteoblast-derived extracellular vesicles are biological tools for the delivery of active molecules to bone. *J Bone Miner Res*. (2018) 33:517–33. doi: 10.1002/jbmr.3332
9. Ge M, Ke R, Cai T, Yang J, Mu X. Identification and proteomic analysis of osteoblast-derived exosomes. *Biochem Biophys Res Commun*. (2015) 467:27–32. doi: 10.1016/j.bbrc.2015.09.135
10. Cui Y, Luan J, Li H, Zhou X, Han J. Exosomes derived from mineralizing osteoblasts promote ST2 cell osteogenic differentiation by alteration of microRNA expression. *FEBS Lett*. (2016) 590:185–92. doi: 10.1002/1873-3468.12024

11. Morhayim J, van de Peppel J, Dudakovic A, Chiba H, van Wijnen AJ, van Leeuwen JP. Molecular characterization of human osteoblast-derived extracellular vesicle mRNA using next-generation sequencing. *Biochim Biophys Acta Mol Cell Res*. (2017) 1864:1133–41. doi: 10.1016/j.bbamcr.2017.03.011
12. Morhayim J, van de Peppel J, Demmers JA, Kocer G, Nigg AL, van Driel M. Proteomic signatures of extracellular vesicles secreted by nonmineralizing and mineralizing human osteoblasts and stimulation of tumor cell growth. *FASEB J*. (2014) 29:274–85. doi: 10.1096/fj.14-261404
13. Lacey DL, Timms E, Tan HL, Kelley MJ, Dunstan CR, Burgess T, et al. Osteoprotegerin ligand is a cytokine that regulates osteoclast differentiation and activation. *Cell*. (1998) 93:165–76. doi: 10.1016/S0092-8674(00)81569-X
14. Teitelbaum SL. Osteoclasts: what do they do and how do they do it? *Am J Pathol*. (2007) 170:427–35. doi: 10.2353/ajpath.2007.060834
15. Kodama H, Nose M, Niida S, Yamasaki A. Essential role of macrophage colony-stimulating factor in the osteoclast differentiation supported by stromal cells. *J Exp Med*. (1991) 173:1291–4. doi: 10.1084/jem.173.5.1291
16. Odgren PR, Kim N, MacKay CA, Mason-Savas A, Choi Y, Marks SC Jr. The role of RANKL (TRANCE/TNFSF11), a tumor necrosis factor family member, in skeletal development: effects of gene knockout and transgenic rescue. *Connect Tissue Res*. (2003) 44:264–71. doi: 10.1080/03008200390181753
17. Ekström K, Omar O, Granéli C, Wang X, Vazirisani F, Thomsen P. Monocyte exosomes stimulate the osteogenic gene expression of mesenchymal stem cells. *PLoS ONE*. (2013) 8:e75227. doi: 10.1371/journal.pone.0075227
18. Liu J, Liang C, Guo B, Wu X, Li D, Zhang Z, et al. Increased PLEKHO1 within osteoblasts suppresses Smad-dependent BMP signaling to inhibit bone formation during aging. *Aging Cell*. (2017) 16:360–76. doi: 10.1111/acel.12566
19. Huynh N, VonMoss L, Smith D, Rahman I, Felemban MF, Zuo J, et al. Characterization of regulatory extracellular vesicles from osteoclasts. *J Dental Res*. (2016) 95:673–9. doi: 10.1177/0022034516633189
20. Ikebuchi Y, Aoki S, Honma M, Hayashi M, Sugamori Y, Khan M, et al. Coupling of bone resorption and formation by RANKL reverse signalling. *Nature*. (2018) 561:195. doi: 10.1038/s41586-018-0482-7
21. Irie N, Takada Y, Watanabe Y, Matsuzaki Y, Naruse C, Asano M, et al. Bidirectional signaling through ephrinA2-EphA2 enhances osteoclastogenesis and suppresses osteoblastogenesis. *J Biol Chem*. (2009) 284:14637–44. doi: 10.1074/jbc.M807598200
22. Sun W, Zhao C, Li Y, Wang L, Nie G, Peng J, et al. Osteoclast-derived microRNA-containing exosomes selectively inhibit osteoblast activity. *Cell Discov*. (2016) 2:16015. doi: 10.1038/celldisc.2016.15
23. Bonewald LF. The amazing osteocyte. *J Bone Miner Res*. (2011) 26:229–38. doi: 10.1002/jbmr.320
24. Morrell AE, Brown GN, Robinson ST, Sattler RL, Baik AD, Zhen G, et al. Mechanically induced Ca^{2+} oscillations in osteocytes release extracellular vesicles and enhance bone formation. *Bone Res*. (2018) 6:6. doi: 10.1038/s41413-018-0007-x
25. Sato M, Suzuki T, Kawano M, Tamura M. Circulating osteocyte-derived exosomes contain miRNAs which are enriched in exosomes from MLO-Y4 cells. *Biomed Rep*. (2017) 6:223–31. doi: 10.3892/br.2016.824
26. Qin Y, Peng Y, Zhao W, Pan J, Ksiezak-Reding H, Cardozo C. Myostatin inhibits osteoblastic differentiation by suppressing osteocyte-derived exosomal microRNA-218: a novel mechanism in muscle-bone communication. *J Biol Chem*. (2017) 292:11021–33. doi: 10.1074/jbc.M116.770941
27. Savina A, Furlán M, Vidal M, Colombo MI. Exosome release is regulated by a calcium-dependent mechanism in K562 cells. *J Biol Chem*. (2003) 278:20083–90. doi: 10.1074/jbc.M301642200
28. Chang MK, Raggatt LJ, Alexander KA, Kuliwaba JS, Fazzalari NL, Schroder K, et al. Osteal tissue macrophages are intercalated throughout human and mouse bone lining tissues and regulate osteoblast function *in vitro* and *in vivo*. *J Immunol*. (2008) 181:1232–1244. doi: 10.4049/jimmunol.181.2.1232
29. Wu AC, Raggatt LJ, Alexander KA, Pettit AR. Unraveling macrophage contributions to bone repair. *BoneKEy Rep*. (2013) 2:373. doi: 10.1038/bonekey.2013.107
30. Fujiwara N, Kobayashi K. Macrophages in inflammation. *Curr Drug Targets Inflamm Allergy*. (2005) 4:281–6. doi: 10.2174/1568010054022024
31. Xue J, Schmidt SV, Sander J, Draffehn A, Krebs W, Quester I, et al. Transcriptome-based network analysis reveals a spectrum model of human macrophage activation. *Immunity*. (2014) 40:274–88. doi: 10.1016/j.immuni.2014.01.006
32. Välimäki E, Cypryk W, Virkanen J, Nurmi K, Turunen PM, Eklund KK, et al. Calpain activity is essential for ATP-driven unconventional vesicle-mediated protein secretion and inflammasome activation in human macrophages. *J Immunol*. (2016) 197:3315–25. doi: 10.4049/jimmunol.1501840
33. Fitzgerald W, Freeman ML, Lederman MM, Vasilieva E, Romero R, Margolis L. A system of cytokines encapsulated in extracellular vesicles. *Sci Rep*. (2018) 8:8973. doi: 10.1038/s41598-018-27190-x
34. Urbanelli L, Magini A, Buratta S, Brozzi A, Sagini K, Polchi A, et al. Signaling pathways in exosomes biogenesis, secretion and fate. *Genes*. (2013) 4:152–170. doi: 10.3390/genes4020152
35. McDonald MK, Tian Y, Qureshi RA, Gormley M, Ertel A, Gao R, et al. Functional significance of macrophage-derived exosomes in inflammation and pain. *Pain*. (2014) 155:1527–39. doi: 10.1016/j.pain.2014.04.029
36. New SE, Goettsch C, Aikawa M, Marchini JF, Shibasaki M, Yabusaki K, et al. Macrophage-derived matrix vesicles: an alternative novel mechanism for microcalcification in atherosclerotic plaques. *Circ Res*. (2013) 113:72–7. doi: 10.1161/CIRCRESAHA.113.301036
37. Yang D, Han Z, Oppenheim JJ. Alarmins and immunity. *Immunol Rev*. (2017) 280:41–56. doi: 10.1111/imr.12577
38. Cypryk W, Ohman T, Eskelinen EL, Matikainen S, Nyman TA. Quantitative proteomics of extracellular vesicles released from human monocyte-derived macrophages upon β-glucan stimulation. *J Proteome Res*. (2014) 13:2468–477. doi: 10.1021/pr4012552
39. Cypryk W, Lorey M, Puustinen A, Nyman TA, Matikainen S. Proteomic and bioinformatic characterization of extracellular vesicles released from human macrophages upon influenza A virus infection. *J Proteome Res*. (2016) 16:217–27. doi: 10.1021/acs.jproteome.6b00596
40. Hassani K, Olivier M. Immunomodulatory impact of Leishmania-induced macrophage exosomes: a comparative proteomic and functional analysis. *PLoS Negl Trop Dis*. (2013) 7:e2185. doi: 10.1371/journal.pntd.0002185
41. Zhu Y, Chen X, Pan Q, Wang Y, Su S, Jiang C. A comprehensive proteomics analysis reveals a secretory path-and status-dependent signature of exosomes released from tumor-associated macrophages. *J Proteome Res*. (2015) 14:4319–31. doi: 10.1021/acs.jproteome.5b00770
42. Niu C, Wang X, Zhao M, Cai T, Liu P, Li J, et al. Macrophage foam cell–derived extracellular vesicles promote vascular smooth muscle cell migration and adhesion. *J Am Heart Assoc*. (2016) 5:e004099. doi: 10.1161/JAHA.116.004099
43. Reales-Calderón JA, Vaz C, Monteoliva L, Molero G, Gil C. Candida albicans modifies the protein composition and size distribution of THP-1 macrophage-derived extracellular vesicles. *J Proteome Res*. (2016) 16:87–105. doi: 10.1021/acs.jproteome.6b00605
44. Bernimoulin M, Waters EK, Foy M, Steele BM, Sullivan M, Falet H, et al. Differential stimulation of monocytic cells results in distinct populations of microparticles. *J Thrombosis Haemostasis*. (2009) 7:1019–28. doi: 10.1111/j.1538-7836.2009.03434.x
45. Hare NJ, Chan B, Chan E, Kaufman KL, Britton WJ, Saunders BM. Microparticles released from *Mycobacterium tuberculosis*-infected human macrophages contain increased levels of the type I interferon inducible proteins including ISG15. *Proteomics*. (2015) 15:3020–9. doi: 10.1002/pmic.201400610
46. Ramirez MI, Deolindo P, de Messias-Reason IJ, Arigi EA, Choi H, Almeida IC, et al. Dynamic flux of microvesicles modulate parasite–host cell interaction of Trypanosoma cruzi in eukaryotic cells. *Cell Microbiol*. (2017) 19:e12672. doi: 10.1111/cmi.12672
47. Hare NJ, Lee LY, Loke I, Britton WJ, Saunders BM, Thaysen-Andersen M. *Mycobacterium tuberculosis* infection manipulates the glycosylation machinery and the N-glycoproteome of human macrophages and their microparticles. *J Proteome Res*. (2016) 16:247–63. doi: 10.1021/acs.jproteome.6b00685
48. Garzetti L, Menon R, Finardi A, Bergami A, Sica A, Martino G, et al. Activated macrophages release microvesicles containing polarized M1 or M2 mRNAs. *J Leukocyte Biol*. (2014) 95:817–25. doi: 10.1189/jlb.0913485
49. Cvjetkovic A, Jang SC, Konečná B, Höög JL, Sihlbom C, Lässer C, et al. Detailed analysis of protein topology of extracellular vesicles–evidence of unconventional membrane protein orientation. *Sci Rep*. (2016) 6:36338. doi: 10.1038/srep36338

50. Stewart S, Gessler F, Pluchino S, Moreau K. Inside-out: unpredicted Annexin A2 localisation on the surface of extracellular vesicles. *Matters*. (2016) 2:e201602000015. doi: 10.19185/matters.201602000015
51. Heijnen HF, Schiel AE, Fijnheer R, Geuze HJ, Sixma JJ. Activated platelets release two types of membrane vesicles: microvesicles by surface shedding and exosomes derived from exocytosis of multivesicular bodies and-granules. *Blood*. (1999) 94:3791–9.
52. Menaa C, Devlin RD, Reddy SV, Gazitt Y, Choi SJ, Roodman GD. Annexin II increases osteoclast formation by stimulating the proliferation of osteoclast precursors in human marrow cultures. *J Clin Investig*. (1999) 103:1605–13. doi: 10.1172/JCI6374
53. Li F, Chung H, Reddy SV, Lu G, Kurihara N, Zhao AZ, et al. Annexin II stimulates RANKL expression through MAPK. *J Bone Miner Res*. (2005) 20:1161–7. doi: 10.1359/JBMR.050207
54. Takahashi S, Reddy SV, Chirgwin JM, Devlin R, Haipek C, Anderson J, et al. Cloning and identification of annexin II as an autocrine/paracrine factor that increases osteoclast formation and bone resorption. *J Biol Chem*. (1994) 269:28696–701.
55. Barondes SH, Cooper DN, Gitt MA, Leffler H. Galectins. Structure and function of a large family of animal lectins. *J Biol Chem*. (1994) 269:20807.
56. Andersen H, Jensen ON, Moiseeva EP, Eriksen EF. A proteome study of secreted prostatic factors affecting osteoblastic activity: Galectin-1 is involved in differentiation of human bone marrow stromal cells. *J Bone Miner Res*. (2003) 18:195–203. doi: 10.1359/jbmr.2003.18.2.195
57. Nakajima K, Kho DH, Yanagawa T, Harazono Y, Gao X, Hogan V, et al. Galectin-3 inhibits osteoblast differentiation through notch signaling. *Neoplasia*. (2014) 16:939–49. doi: 10.1016/j.neo.2014.09.005
58. Weilner S, Keider V, Winter M, Harreither E, Salzer B, Weiss F, et al. Vesicular Galectin-3 levels decrease with donor age and contribute to the reduced osteo-inductive potential of human plasma derived extracellular vesicles. *Aging*. (2016) 8:16. doi: 10.18632/aging.100865
59. Li YJ, Kukita A, Teramachi J, Nagata K, Wu Z, Akamine A, et al. A possible suppressive role of galectin-3 in upregulated osteoclastogenesis accompanying adjuvant-induced arthritis in rats. *Lab Invest*. (2009) 89:26. doi: 10.1038/labinvest.2008.111
60. Simon D, Derer A, Andes FT, Lezuo P, Bozec A, Schett G, et al. Galectin-3 as a novel regulator of osteoblast-osteoclast interaction and bone homeostasis. *Bone*. (2017) 105:35–41. doi: 10.1016/j.bone.2017.08.013
61. Moriyama K, Kukita A, Li YJ, Uehara N, Zhang JQ, Takahashi I, et al. Regulation of osteoclastogenesis through Tim-3: possible involvement of the Tim-3/galectin-9 system in the modulation of inflammatory bone destruction. *Lab Invest*. (2014) 94:1200. doi: 10.1038/labinvest.2014.107
62. Koh JM, Lee YS, Kim YS, Park SH, Lee SH, Kim HH, et al. Heat shock protein 60 causes osteoclastic bone resorption via toll-like receptor-2 in estrogen deficiency. *Bone*. (2009) 45:650–60. doi: 10.1016/j.bone.2009.06.007
63. Stefano L, Racchetti G, Bianco F, Passini N, Gupta RS, Panina Bordignon P, et al. The surface-exposed chaperone, Hsp60, is an agonist of the microglial TREM2 receptor. *J Neurochem*. (2009) 110:284–94. doi: 10.1111/j.1471-4159.2009.06130.x
64. Notsu K, Nakagawa M, Nakamura M. Ubiquitin-like protein MNSFβ noncovalently binds to molecular chaperone HSPA8 and regulates osteoclastogenesis. *Mol Cell Biochem*. (2016) 421:149–56. doi: 10.1007/s11010-016-2795-x
65. Okawa Y, Hideshima T, Steed P, Vallet S, Hall S, Huang K, et al. SNX-2112, a selective Hsp90 inhibitor, potently inhibits tumor cell growth, angiogenesis, and osteoclastogenesis in multiple myeloma and other hematologic tumors by abrogating signaling via Akt and ERK. *Blood*. (2009) 113:846–55. doi: 10.1182/blood-2008-04-151928
66. Francis LK, Alsayed Y, Leleu X, Jia X, Singha UK, Anderson J, et al. Combination mammalian target of rapamycin inhibitor rapamycin and HSP90 inhibitor 17-allylamino-17-demethoxygeldanamycin has synergistic activity in multiple myeloma. *Clin Cancer Res*. (2006) 12:6826–35. doi: 10.1158/1078-0432.CCR-06-1331
67. Price JT, Quinn JM, Sims NA, Vieusseux J, Waldeck K, Docherty SE, et al. The heat shock protein 90 inhibitor, 17-allylamino-17-demethoxygeldanamycin, enhances osteoclast formation and potentiates bone metastasis of a human breast cancer cell line. *Cancer Res*. (2005) 65:4929–38. doi: 10.1158/0008-5472.CAN-04-4458
68. van der Kraan AG, Chai RC, Singh PP, Lang BJ, Xu J, Gillespie MT, et al. HSP90 inhibitors enhance differentiation and MITF (microphthalmia transcription factor) activity in osteoclast progenitors. *Biochem J*. (2013) 451:235–44. doi: 10.1042/BJ20121626
69. Boye K, Maelandsmo GM. S100A4 and metastasis: a small actor playing many roles. *Am J Pathol*. (2010) 176:528–35. doi: 10.2353/ajpath.2010.090526
70. Kim H, Lee YD, Kim MK, Kwon JO, Song MK, Lee ZH, et al. Extracellular S100A4 negatively regulates osteoblast function by activating the NF-κB pathway. *BMB Rep*. (2017) 50:97. doi: 10.5483/BMBRep.2017.50.2.170
71. Mah SJ, Lee J, Kim H, Kang YG, Baek SH, Kim HH, et al. Induction of S100A4 in periodontal ligament cells enhances osteoclast formation. *Arch Oral Biol*. (2015) 60:1215–21. doi: 10.1016/j.archoralbio.2015.05.014
72. Erlandsson MC, Svensson MD, Jonsson IM, Bian L, Ambartsumian N, Andersson S, et al. Expression of metastasin S100A4 is essential for bone resorption and regulates osteoclast function. *Biochim Biophys Acta Mol Cell Res*. (2013) 1833:2653–63. doi: 10.1016/j.bbamcr.2013.06.020
73. Verma SK, Leikina E, Melikov K, Gebert C, Kram V, Young MF, et al. Cell-surface phosphatidylserine regulates osteoclast precursor fusion. *J Biol Chem*. (2018) 293:254–70. doi: 10.1074/jbc.M117.809681
74. Grevers LC, de Vries TJ, Vogl T, Abdollahi-Roodsaz S, Sloetjes AW, Leenen PJ, et al. S100A8 enhances osteoclastic bone resorption *in vitro* through activation of Toll-like receptor 4: implications for bone destruction in murine antigen-induced arthritis. *Arth Rheum*. (2011) 63:1365–75. doi: 10.1002/art.30290
75. Dapunt U, Giese T, Maurer S, Stegmaier S, Prior B, Hänsch GM, et al. Neutrophil-derived MRP-14 is up-regulated in infectious osteomyelitis and stimulates osteoclast generation. *J Leukocyte Biol*. (2015) 98:575–82. doi: 10.1189/jlb.3VMA1014-482R
76. Di Ceglie I, Blom AB, Davar R, Logie C, Martens JHA, Habibi E, et al. The alarmin S100A9 hampers osteoclast differentiation from human circulating precursors by reducing the expression of RANK. *FASEB J*. (2019) doi: 10.1096/fj.201802691RR. [Epub ahead of print].
77. Lu B, Antoine DJ, Kwan K, Lundbäck P, Wähämaa H, Schierbeck H, et al. JAK/STAT1 signaling promotes HMGB1 hyperacetylation and nuclear translocation. *Proc Natl Acad Sci USA*. (2014) 111:3068–73. doi: 10.1073/pnas.1316925111
78. Gardella S, Andrei C, Ferrera D, Lotti LV, Torrisi MR, Bianchi ME, et al. The nuclear protein HMGB1 is secreted by monocytes via a non-classical, vesicle-mediated secretory pathway. *EMBO Rep*. (2002) 3:995–1001. doi: 10.1093/embo-reports/kvf198
79. Tucher C, Bode K, Schiller P, Claßen L, Birr C, Souto-Carneiro MM, et al. Extracellular vesicle subtypes released from activated or apoptotic T-lymphocytes carry a specific and stimulus-dependent protein cargo. *Front Immunol*. (2018) 9:534. doi: 10.3389/fimmu.2018.00534
80. Jiang W, Pisetsky DS. The role of IFN-α and nitric oxide in the release of HMGB1 by RAW 264.7 cells stimulated with polyinosinic-polycytidylic acid or lipopolysaccharide. *J Immunol*. (2006) 177:3337–43. doi: 10.4049/jimmunol.177.5.3337
81. Zhou Z, Han JY, Xi CX, Xie JX, Feng X, Wang CY, et al. HMGB1 regulates RANKL-induced osteoclastogenesis in a manner dependent on RAGE. *J Bone Miner Res*. (2008) 23:1084–96. doi: 10.1359/jbmr.080234
82. Moursi AM, Damsky CH, Lull J, Zimmerman D, Doty SB, Aota S, et al. Fibronectin regulates calvarial osteoblast differentiation. *J Cell Sci*. (1996) 109:1369–80.
83. Hynes RO. Integrins: versatility, modulation, and signaling in cell adhesion. *Cell*. (1992) 69:11–25. doi: 10.1016/0092-8674(92)90115-S
84. Clover J, Dodds R, Gowen M. Integrin subunit expression by human osteoblasts and osteoclasts in situ and in culture. *J Cell Sci*. (1992) 103:267–71.
85. Grzesik WJ, Robey PG. Bone matrix RGD glycoproteins: immunolocalization and interaction with human primary osteoblastic bone cells *in vitro*. *J Bone Miner Res*. (1994) 9:487–96. doi: 10.1002/jbmr.5650090408
86. Saito T, Albelda SM, Brighton CT. Identification of integrin receptors on cultured human bone cells. *J Orthop Res*. (1994) 12:384–94. doi: 10.1002/jor.1100120311
87. Globus RK, Doty SB, Lull JC, Holmuhamedov E, Humphries MJ, Damsky CH. Fibronectin is a survival factor for differentiated osteoblasts. *J Cell Sci*. (1998) 111:1385–93.

88. Gramoun A, Azizi N, Sodek J, Heersche JN, Nakchbandi I, Manolson MF. Fibronectin inhibits osteoclastogenesis while enhancing osteoclast activity via nitric oxide and interleukin-1β-mediated signaling pathways. *J Cell Biochem*. (2010) 111:1020–34. doi: 10.1002/jcb.22791
89. Supanchart C, Thawanaphong S, Makeudom A, Bolscher JG, Nazmi K, Kornak U, et al. The antimicrobial peptide, LL-37, inhibits *in vitro* osteoclastogenesis. *J Dental Res*. (2012) 91:1071–7. doi: 10.1177/0022034512460402
90. Lee SI, Yi JK, Bae WJ, Lee S, Cha HJ, Kim EC. Thymosin beta-4 suppresses osteoclastic differentiation and inflammatory responses in human periodontal ligament cells. *PLoS ONE*. (2016) 11:e0146708. doi: 10.1371/journal.pone.0146708
91. Nair RR, Mazza D, Brambilla F, Gorzanelli A, Agresti A, Bianchi ME. LPS-challenged macrophages release microvesicles coated with histones. *Front Immunol*. (2018) 9:1463. doi: 10.3389/fimmu.2018.01463
92. Rilla K, Mustonen AM, Arasu UT, Härkönen K, Matilainen J, Nieminen P, et al. Extracellular vesicles are integral and functional components of the extracellular matrix. *Matrix Biol*. (2017). 75:201–19. doi: 10.1016/j.matbio.2017.10.003

Conflict of Interest Statement: The authors declare that the research was conducted in the absence of any commercial or financial relationships that could be construed as a potential conflict of interest.

Advantages of publishing in Frontiers

OPEN ACCESS
Articles are free to read for greatest visibility and readership

FAST PUBLICATION
Around 90 days from submission to decision

HIGH QUALITY PEER-REVIEW
Rigorous, collaborative, and constructive peer-review

TRANSPARENT PEER-REVIEW
Editors and reviewers acknowledged by name on published articles

Frontiers
Avenue du Tribunal-Fédéral 34
1005 Lausanne | Switzerland

Visit us: www.frontiersin.org
Contact us: info@frontiersin.org | +41 21 510 17 00

REPRODUCIBILITY OF RESEARCH
Support open data and methods to enhance research reproducibility

DIGITAL PUBLISHING
Articles designed for optimal readership across devices

FOLLOW US
@frontiersin

IMPACT METRICS
Advanced article metrics track visibility across digital media

EXTENSIVE PROMOTION
Marketing and promotion of impactful research

LOOP RESEARCH NETWORK
Our network increases your article's readership